WHAT YOU CAN DO FOR *STAR*

All users of this abstract service are urged to forward reports to be considered for announcement in *STAR*. This will aid NASA in its efforts to provide the fullest possible coverage of all scientific and technical publications that might support aeronautics and space research and development. If you have prepared relevant reports (other than those that you will transmit to NASA, DoD, or DOE through the usual contract- or grant-reporting channels), please send them for consideration to the NASA Scientific and Technical Information Facility, P.O. Box 8757, BWI Airport, Maryland 21240.

Reprints of journal articles, book chapters, and conference papers are also welcome. These will be considered for announcement in *STAR's* companion journal, *International Aerospace Abstracts*.

You may specify a particular source to be included in a report announcement if you wish; otherwise the report will be placed on public sale at the National Technical Information Service. Copyrighted publications will be announced but not distributed or sold.

PURCHASE OF *STAR*

The semimonthly issues are available to registered users on annual subscription for $99.00 from the NASA Scientific and Technical Information Facility, ATTN: Registration Services, P.O. Box 8757, BWI Airport, MD 21240. *STAR* is publically available on annual subscription for $99.00 from the Superintendent of Documents, U.S. Government Printing Office, Washington, DC 20402.

PUBLISHED BY:

UNITED STATES GOVERNMENT
NATIONAL AERONAUTICS AND SPACE ADMINISTRATION
SCIENTIFIC AND TECHNICAL INFORMATION DIVISION
Scientific and Technical Aerospace Reports, Volume 27, is prepared by the NASA Scientific and Technical Information Facility operated for the National Aeronautics and Space Administration by RMS Associates.

The Administrator of the National Aeronautics and Space Administration has determined that the publication of this periodical is necessary in the transaction of the public business required by law of this Agency. Use of funds for printing this periodical has been approved by the Director of the Office of Management and Budget through March 22, 1989.

US ISSN 0036-8741

WHAT YOU CAN DO FOR *STAR*

All users of this abstract service are urged to forward reports to be considered for announcement in *STAR*. This will aid NASA in its efforts to provide the fullest possible coverage of all scientific and technical publications that might support aeronautics and space research and development. If you have prepared relevant reports (other than those that you will transmit to NASA, DoD, or DOE through the usual contract- or grant-reporting channels), please send them for consideration to the NASA Scientific and Technical Information Facility, P.O. Box 8757, BWI Airport, Maryland 21240.

Reprints of journal articles, book chapters, and conference papers are also welcome. These will be considered for announcement in *STAR's* companion journal, *International Aerospace Abstracts*.

You may specify a particular source to be included in a report announcement if you wish; otherwise the report will be placed on public sale at the National Technical Information Service. Copyrighted publications will be announced but not distributed or sold.

PURCHASE OF *STAR*

The semimonthly issues are available to registered users on annual subscription for $99.00 from the NASA Scientific and Technical Information Facility, ATTN: Registration Services, P.O. Box 8757, BWI Airport, MD 21240. *STAR* is publically available on annual subscription for $99.00 from the Superintendent of Documents, U.S. Government Printing Office, Washington, DC 20402.

PUBLISHED BY:

UNITED STATES GOVERNMENT
NATIONAL AERONAUTICS AND SPACE ADMINISTRATION
SCIENTIFIC AND TECHNICAL INFORMATION DIVISION
Scientific and Technical Aerospace Reports, Volume 27, is prepared by the NASA Scientific and Technical Information Facility operated for the National Aeronautics and Space Administration by RMS Associates.

The Administrator of the National Aeronautics and Space Administration has determined that the publication of this periodical is necessary in the transaction of the public business required by law of this Agency. Use of funds for printing this periodical has been approved by the Director of the Office of Management and Budget through March 22, 1989.

US ISSN 0036-8741

Scientific and Technical Aerospace Reports (STAR) is a major component of a comprehensive National Aeronautics and Space Administration information system covering aeronautics, space, and supporting disciplines. *STAR* is issued on the 8th and 23rd of each month and announces current publications of the following types:

- NASA, NASA contractor, and NASA grantee reports
- Reports issued by other U.S. Government Agencies, domestic and foreign institutions, universities, and private firms
- Translations in report form
- NASA-owned patents and patent applications
- Other U.S. Government Agency patents and patent applications
- Foreign patents and patent applications
- Domestic dissertations and theses
- Foreign dissertations and theses

Journal, book, and conference literature, cover-to-cover journal translations, and certain foreign dissertations are announced in a companion journal, *International Aerospace Abstracts (IAA),* available on subscription from the American Institute of Aeronautics and Astronautics, Technical Information Service, 555 West 57th Street, 12th Floor, New York, New York 10019.

SUBJECT SCOPE

Subject scope of *STAR,* and *IAA* includes all aspects of aeronautics and space research and development, supporting basic and applied research, and applications. Aerospace aspects of earth resources, energy development, conservation, oceanography, environmental protection, urban transportation, and other topics of high national priority are also covered.

OTHER NASA PUBLICATIONS

Other NASA publications and information services are described in the publication, *The NASA Scientific and Technical Information System ... and How to Use It,* available without charge from the NASA Scientific and Technical Information Facility, P.O. Box 8757, BWI Airport, Maryland 21240.

HOW TO USE *STAR* SUBJECT CATEGORIES

STAR is categorized by 10 major subject divisions divided into 76 specific subject categories and one general category/division. The major subject divisions are listed in the Table of Contents, together with a note for each that defines its scope and provides any cross-references. For example:

AERONAUTICS

Includes aeronautics (general); aerodynamics; air transportation and safety; aircraft communications and navigation; aircraft design, testing and performance; aircraft instrumentation; aircraft propulsion and power; aircraft stability and control; and research and support facilities (air).

For related information see also *Astronautics.*

Each major division is further divided into as many as nine specific categories, which are identified by category numbers.

Abstracts in *STAR* are grouped by specific category, the categories appearing in sequential order. Category breaks in the abstract section are identified by the category number and title, and a scope note. Cross-references to other categories are provided as appropriate. For example:

02 AERODYNAMICS

Includes aerodynamics of bodies, combinations, wings, rotors, and control surfaces; and internal flow in ducts and turbomachinery.

For related information see also *34 Fluid Mechanics and Heat Transfer.*

CROSS-REFERENCES

Individual *STAR* abstracts are not ordinarily cross-referenced, except for certain conference reports or book translations that have had separate abstracts written for their component papers or chapters. Citations and abstracts of the components follow immediately after those of the parent document. When the subject content of a component differs sufficiently from the general content of the parent, a cross-reference citation also is printed at the end of the category to which it normally would have been assigned if it were independent.

DOCUMENTS ON MICROFICHE

Documents on microfiche[1] are designated by a pound sign (#) following the accession number. The pound sign is used without regard to the source or quality of the microfiche.

AVAILABILITIES

One or more sources from which a document announced in *STAR* is available to the public is given in each citation. The most commonly indicated sources and their acronyms or abbreviations are listed below. If the publication is available from a source other than those listed, the publisher and his address will be displayed on the availability line or in combination with the corporate source line.

Avail: NTIS. Sold by the National Technical Information Service. Prices for hard copy (HC) and microfiche (MF) are indicated by a price code following the letters HC or MF in the *STAR* citation. Current values for the price codes are given in the tables on page vii.

Initially distributed microfiche under the NTIS SRIM (Selected Research in Microfiche) is available at greatly reduced unit prices. For this service and for information concerning subscription to NASA printed reports, consult the NTIS Subscription Section, Springfield, Va. 22161.

NOTE ON ORDERING DOCUMENTS: When ordering NASA publications (those followed by the * symbol), use the N accession number. NASA patent applications (only the specifications are offered) should be ordered by the US-Patent-Appl-SN number. Non-NASA publications (no asterisk) should be ordered by the AD, PB, or other *report number* shown on the last line of the citation, not by the N accession number. It is also advisable to cite the title and other bibliographic identification.

Avail: SOD (or GPO). Sold by the Superintendent of Documents, U.S. Government Printing Office, in hard copy. The current price and order number are given following the availability line. (NTIS will fill microfiche requests, as indicated above, for those documents identified by a # symbol.)

(1) A microfiche is a transparent sheet of film, 105 by 148 mm in size, containing as many as 60 to 98 pages of information reduced to micro images (not to exceed 26:1 reduction).

Avail: BLL (formerly NLL): British Library Lending Division, Boston Spa, Wetherby, Yorkshire, England. Photocopies available from this organization at the price shown. (If none is given, inquiry should be addressed to the BLL.)

Avail: DOE Depository Libraries. Organizations in U.S. cities and abroad that maintain collections of Department of Energy reports, usually in microfiche form, are listed in *Energy Research Abstracts*. Services available from the DOE and its depositories are described in a booklet, *DOE Technical Information Center - Its Functions and Services* (TID-4660), which may be obtained without charge from the DOE Technical Information Center.

Avail: ESDU. Pricing information on specific data, computer programs, and details on ESDU topic categories can be obtained from ESDU International Ltd. Requesters in North America should use the Virginia address while all other requesters should use the London address, both of which are on page vi.

Avail: Fachinformationszentrum, Karlsruhe. Sold by the Fachinformationszentrum Energie, Physik, Mathematik GMBH, Eggenstein Leopoldshafen, Federal Republic of Germany, at the price shown in deutschmarks (DM).

Avail: HMSO. Publications of Her Majesty's Stationery Office are sold in the U.S. by Pendragon House, Inc. (PHI), Redwood City, California. The U.S. price (including a service and mailing charge) is given, or a conversion table may be obtained from PHI.

Avail: NASA Public Document Rooms. Documents so indicated may be examined at or purchased from the National Aeronautics and Space Administration, Public Documents Room (Room 126), 600 Independence Ave., S.W., Washington, D.C. 20546, or public document rooms located at each of the NASA research centers, the NASA Space Technology Laboratories, and the NASA Pasadena Office at the Jet Propulsion Laboratory.

Avail: Univ. Microfilms. Documents so indicated are dissertations selected from *Dissertation Abstracts* and are sold by University Microfilms as xerographic copy (HC) and microfilm. All requests should cite the author and the Order Number as they appear in the citation.

Avail: US Patent and Trademark Office. Sold by Commissioner of Patents and Trademarks, U.S. Patent and Trademark Office, at the standard price of $1.50 each, postage free. (See discussion of NASA patents and patent applications below.)

Avail: (US Sales Only). These foreign documents are available to users within the United States from the National Technical Information Service (NTIS). They are available to users outside the United States through the International Nuclear Information Service (INIS) representative in their country, or by applying directly to the issuing organization.

Avail: USGS. Originals of many reports from the U.S. Geological Survey, which may contain color illustrations, or otherwise may not have the quality of illustrations preserved in the microfiche or facsimile reproduction, may be examined by the public at the libraries of the USGS field offices whose addresses are listed in this Introduction. The libraries may be queried concerning the availability of specific documents and the possible utilization of local copying services, such as color reproduction.

Avail: Issuing Activity, or Corporate Author, or no indication of availability. Inquiries as to the availability of these documents should be addressed to the organization shown in the citation as the corporate author of the document.

NASA PATENTS AND PATENT APPLICATIONS

Patents and patent applications owned by NASA are announced in *STAR* under appropriate subject categories and are referenced in the *STAR* indexes. In the Report/Accession Number Index, patents are indexed by the NASA Case Number (which appears in lieu of the report number in other indexes), the U.S. Patent Number, the U.S. Patent Application Serial Number, and the U.S. Patent Class. Patent applications for which patents have not yet been issued are indexed by the NASA Case Number and the U.S. Patent Application Serial Number.

NASA *patent application specifications* are sold in paper copy by the National Technical Information Service at price code A02. Microfiche are sold at price code A01. The US-Patent-Appl-SN- number should be used in ordering either paper copy or microfiche from NTIS. Printed copies of *patents* (which are not microfiched) are available for purchase at $1.50 per copy from:

Commissioner of Patents and Trademarks
U.S. Patent and Trademark Office
Washington, D.C. 20231

When ordering patents, the U.S. Patent Number should be used, and payment must be remitted in advance, preferably by money order or check payable to the Commissioner of Patents and Trademarks. Prepaid purchase coupons for ordering are also available from the Patent and Trademark Office. The patents and patent applications announced in *STAR* are owned by NASA and are available for royalty-free licensing. Requests for licensing terms and further information should be addressed to:

Associate General Counsel for Intellectual Property/Code GP
National Aeronautics and Space Administration
Washington, D.C. 20546

ELIGIBILITY AND REGISTRATION FOR NASA INFORMATION PRODUCTS AND SERVICES

A variety of services is available to organizations of the following types that have registered with NASA to receive specific services or products:

1. NASA offices, research centers, contractors, subcontractors, grantees, and consultants;
2. Other U.S. Government agencies and their contractors;
3. Libraries in the United States that have arrangements with NASA to maintain collections of NASA documents for public reference;
4. Other organizations in the United States having a need for NASA documents in work related to aeronautics and space research;
5. Organizations abroad that have established reciprocal document exchange arrangements with NASA.

Only the central service points or central points of document acquisition and control within qualified organizations are eligible to register for NASA products and services. Domestic organizations that may be eligible to receive various classes of NASA publications and services should address their requests for registration or for further information to:

NASA Scientific and Technical Information Facility
ATTN: Registration Services
Post Office Box 8757
BWI Airport, Maryland 21240

Organizations abroad should direct requests to the same address, but to the attention of: International Exchange Program.

AVAILABILITY OF *STAR* ABSTRACTS ON MICROFICHE

Microfiche of the abstract sections of this issue and other issues of *STAR* are available on annual subscription from NTIS as PB89-911300, Attn: Subscriptions, 5285 Port Royal Road, Springfield, Virginia 22161. Annual subscription rates are $70.00 North America; $140.00 foreign. Abstract sections for previous years retroactive to 1964 are available at the current rates. Microfiche for individual *STAR* issue abstract sections are not available.

PUBLIC COLLECTIONS OF NASA DOCUMENTS

DOMESTIC: NASA and NASA-sponsored documents and a large number of aerospace publications are available to the public for reference purposes at the library maintained by the American Institute of Aeronautics and Astronautics, Technical Information Service, 555 West 57th Street, 12th Floor, New York, New York 10019

EUROPEAN: An extensive collection of NASA and NASA-sponsored publications is maintained by the British Library Lending Division, Boston Spa, Wetherby, Yorkshire, England for public access. The British Library Lending Division also has available many of the non-NASA publications cited in *STAR*. European requesters may purchase facsimile copy or microfiche of NASA and NASA-sponsored documents, those identified by both the symbols # and * from ESA - Information Retrieval Service European Space Agency, 8-10 rue Mario-Nikis, 75738 Paris CEDEX 15, France.

FEDERAL DEPOSITORY LIBRARY PROGRAM

In order to provide the general public with greater access to U.S. Government publications, Congress established the Federal Depository Library Program under the Government Printing Office (GPO), with 50 regional depositories responsible for permanent retention of material, inter-library loan, and reference services. At least one copy of nearly every NASA and NASA-sponsored publication, either in printed or microfiche format, is received and retained by the 50 regional depositories. A list of the regional GPO libraries, arranged alphabetically by state, appears on the inside back cover. These libraries are *not* sales outlets. A local library can contact a Regional Depository to help locate specific reports, or direct contact may be made by an individual.

ADDRESSES OF ORGANIZATIONS

American Institute of Aeronautics and Astronautics
Technical Information Service
555 West 57th Street, 12th Floor
New York, New York 10019

British Library Lending Division,
Boston Spa, Wetherby, Yorkshire,
England

Commissioner of Patents and Trademarks
U.S. Patent and Trademark Office
Washington, D.C. 20231

Department of Energy
Technical Information Center
P.O. Box 62
Oak Ridge, Tennessee 37830

ESA-Information Retrieval Service
ESRIN
Via Galileo Galilei
00044 Frascati (Rome) Italy

ESDU International
P.O. Box 1633
Manassas, Virginia 22110

ESDU International, Ltd.
251-259 Regent Street
London, W1R 7AD, England

Fachinformationszentrum Energie, Physik, Mathematik GMBH
7514 Eggenstein Leopoldshafen
Federal Republic of Germany

Her Majesty's Stationery Office
P.O. Box 569, S.E. 1
London, England

NASA Scientific and Technical Information Facility
P.O. Box 8757
B.W.I. Airport, Maryland 21240

National Aeronautics and Space Administration
Scientific and Technical Information Division (NTT)
Washington, D.C. 20546

National Technical Information Service
5285 Port Royal Road
Springfield, Virginia 22161

Pendragon House, Inc.
899 Broadway Avenue
Redwood City, California 94063

Superintendent of Documents
U.S. Government Printing Office
Washington, D.C. 20402

University Microfilms
A Xerox Company
300 North Zeeb Road
Ann Arbor, Michigan 48106

University Microfilms, Ltd.
Tylers Green
London, England

U.S. Geological Survey Library
National Center - MS 950
12201 Sunrise Valley Drive
Reston, Virginia 22092

U.S. Geological Survey Library
2255 North Gemini Drive
Flagstaff, Arizona 86001

U.S. Geological Survey
345 Middlefield Road
Menlo Park, California 94025

U.S. Geological Survey Library
Box 25046
Denver Federal Center, MS914
Denver, Colorado 80225

NTIS PRICE SCHEDULES

(Effective January 1, 1989)

Schedule A
STANDARD PRICE DOCUMENTS AND MICROFICHE

PRICE CODE	NORTH AMERICAN PRICE	FOREIGN PRICE
A01	$ 6.95	$13.90
A02	10.95	21.90
A03	13.95	27.90
A04-A05	15.95	31.90
A06-A09	21.95	43.90
A10-A13	28.95	57.90
A14-A17	36.95	73.90
A18-A21	42.95	85.90
A22-A25	49.95	99.90
A99	*	*
NO1	55.00	70.00
NO2	55.00	80.00

Schedule E
EXCEPTION PRICE DOCUMENTS AND MICROFICHE

PRICE CODE	NORTH AMERICAN PRICE	FOREIGN PRICE
E01	$ 9.00	18.00
E02	11.50	23.00
E03	13.00	26.00
E04	15.50	31.00
E05	17.50	35.00
E06	20.50	41.00
E07	23.00	46.00
E08	25.50	51.00
E09	28.00	56.00
E10	31.00	62.00
E11	33.50	67.00
E12	36.50	73.00
E13	39.00	78.00
E14	42.50	85.00
E15	46.00	92.00
E16	50.50	101.00
E17	54.50	109.00
E18	59.00	118.00
E19	65.50	131.00
E20	76.00	152.00
E99	*	*

*Contact NTIS for price quote.

IMPORTANT NOTICE

NTIS Shipping and Handling Charges
U.S., Canada, Mexico — ADD $3.00 per TOTAL ORDER
All Other Countries — ADD $4.00 per TOTAL ORDER

Exceptions — Does NOT apply to:
ORDERS REQUESTING NTIS RUSH HANDLING
ORDERS FOR SUBSCRIPTION OR STANDING ORDER PRODUCTS *ONLY*

NOTE: Each additional delivery address on an order requires a separate shipping and handling charge.

VOLUME 27 NUMBER 1 / JANUARY 8, 1989

TABLE OF CONTENTS

AERONAUTICS

Includes aeronautics (general); aerodynamics; air transportation and safety; aircraft communications and navigation; aircraft design, testing and performance; aircraft instrumentation; aircraft propulsion and power; aircraft stability and control; and research and support facilities (air).

For related information see also *Astronautics.*

01 AERONAUTICS (GENERAL) 1

02 AERODYNAMICS 1

Includes aerodynamics of bodies, combinations, wings, rotors, and control surfaces; and internal flow in ducts and turbomachinery.

For related information see also *34 Fluid Mechanics and Heat Transfer*

03 AIR TRANSPORTATION AND SAFETY 6

Includes passenger and cargo air transport operations; and aircraft accidents.

For related information see also *16 Space Transportation* and *85 Urban Technology and Transportation.*

04 AIRCRAFT COMMUNICATIONS AND NAVIGATION 8

Includes digital and voice communication with aircraft; air navigation systems (satellite and ground based); and air traffic control.

For related information see also *17 Space Communications, Spacecraft Communications, Command and Tracking* and *32 Communications and Radar.*

05 AIRCRAFT DESIGN, TESTING AND PERFORMANCE 8

Includes aircraft simulation technology.

For related information see also *18 Spacecraft Design, Testing and Performance* and *39 Structural Mechanics.* For land transportation vehicles see *85 Urban Technology and Transportation.*

06 AIRCRAFT INSTRUMENTATION N.A.

Includes cockpit and cabin display devices; and flight instruments.

For related information see also *19 Spacecraft Instrumentation* and *35 Instrumentation and Photography.*

07 AIRCRAFT PROPULSION AND POWER 9

Includes prime propulsion systems and systems components, e.g., gas turbine engines and compressors; and onboard auxiliary power plants for aircraft.

For related information see also *20 Spacecraft Propulsion and Power, 28 Propellants and Fuels,* and *44 Energy Production and Conversion.*

08 AIRCRAFT STABILITY AND CONTROL 10

Includes aircraft handling qualities; piloting; flight controls; and autopilots.

For related information see also *05 Aircraft Design, Testing and Performance.*

09 RESEARCH AND SUPPORT FACILITIES (AIR) 12

Includes airports, hangars and runways; aircraft repair and overhaul facilities; wind tunnels; shock tubes; and aircraft engine test stands.

For related information see also *14 Ground Support Systems and Facilities (Space).*

ASTRONAUTICS

Includes astronautics (general); astrodynamics; ground support systems and facilities (space); launch vehicles and space vehicles; space transportation; space communications, spacecraft communications, command and tracking; spacecraft design, testing and performance; spacecraft instrumentation; and spacecraft propulsion and power.

For related information see also *Aeronautics*

12 ASTRONAUTICS (GENERAL) 13

For extraterrestrial exploration see *91 Lunar and Planetary Exploration.*

13 ASTRODYNAMICS 21

Includes powered and free-flight trajectories; and orbital and launching dynamics.

14 GROUND SUPPORT SYSTEMS AND FACILITIES (SPACE) N.A.

Includes launch complexes, research and production facilities; ground support equipment, e.g., mobile transporters; and simulators.

For related information see also *09 Research and Support Facilities (Air).*

15 LAUNCH VEHICLES AND SPACE VEHICLES 21

Includes boosters; operating problems of launch/space vehicle systems; and reusable vehicles.

For related information see also *20 Spacecraft Propulsion and Power.*

16 SPACE TRANSPORTATION 21

Includes passenger and cargo space transportation, e.g., shuttle operations; and space rescue techniques.

For related information see also *03 Air Transportation and Safety* and *18 Spacecraft Design, Testing and Performance.* For space suits see *54 Man/System Technology and Life Support.*

17 SPACE COMMUNICATIONS, SPACECRAFT COMMUNICATIONS, COMMAND AND TRACKING N.A.

Includes telemetry; space communications networks; astronavigation and guidance; and radio blackout.

For related information see also *04 Aircraft Communications and Navigation* and *32 Communications and Radar.*

18 SPACECRAFT DESIGN, TESTING AND PERFORMANCE 22

Includes satellites; space platforms; space stations; spacecraft systems and components such as thermal and environmental controls; and attitude controls.

For life support systems see *54 Man/System Technology and Life Support.* For related information see also *05 Aircraft Design, Testing and Performance, 39 Structural Mechanics,* and *16 Space Transportation.*

19 SPACECRAFT INSTRUMENTATION N.A.

For related information see also *06 Aircraft Instrumentation* and *35 Instrumentation and Photography.*

20 SPACECRAFT PROPULSION AND POWER 23

Includes main propulsion systems and components, e.g. rocket engines; and spacecraft auxiliary power sources.

For related information see also *07 Aircraft Propulsion and Power, 28 Propellants and Fuels, 44 Energy Production and Conversion,* and *15 Launch Vehicles and Space Vehicles.*

CHEMISTRY AND MATERIALS

Includes chemistry and materials (general); composite materials; inorganic and physical chemistry; metallic materials; nonmetallic materials; propellants and fuels; and materials processing.

23 CHEMISTRY AND MATERIALS (GENERAL) 25

24 COMPOSITE MATERIALS 25

Includes physical, chemical, and mechanical properties of laminates and other composite materials.

For ceramic materials see *27 Nonmetallic Materials.*

25 INORGANIC AND PHYSICAL CHEMISTRY 27

Includes chemical analysis, e.g., chromatography; combustion theory; electrochemistry; and photochemistry.

For related information see also *77 Thermodynamics and Statistical Physics.*

26 METALLIC MATERIALS 30

Includes physical, chemical, and mechanical properties of metals, e.g., corrosion; and metallurgy.

27 NONMETALLIC MATERIALS 32

Includes physical, chemical, and mechanical properties of plastics, elastomers, lubricants, polymers, textiles, adhesives, and ceramic materials.

For composite materials see *24 Composite Materials.*

28 PROPELLANTS AND FUELS 34

Includes rocket propellants, igniters and oxidizers; their storage and handling procedures; and aircraft fuels.

For related information see also *07 Aircraft Propulsion and Power, 20 Spacecraft Propulsion and Power,* and *44 Energy Production and Conversion.*

29 MATERIALS PROCESSING 35

Includes space-based development of products and processes for commercial application.

For biological materials see *55 Space Biology.*

ENGINEERING

Includes engineering (general); communications and radar; electronics and electrical engineering; fluid mechanics and heat transfer; instrumentation and photography; lasers and masers; mechanical engineering; quality assurance and reliability; and structural mechanics.

For related information see also *Physics.*

31 ENGINEERING (GENERAL) 35

Includes vacuum technology; control engineering; display engineering; cryogenics; and fire prevention.

32 COMMUNICATIONS AND RADAR 36

Includes radar; land and global communications; communications theory; and optical communications.

For related information see also *04 Aircraft Communications and Navigation* and *17 Space Communications, Spacecraft Communications, Command and Tracking.* For search and rescue see *03 Air Transportation and Safety,* and *16 Space Transportation.*

33 ELECTRONICS AND ELECTRICAL ENGINEERING 42

Includes test equipment and maintainability; components, e.g., tunnel diodes and transistors; microminiaturization; and integrated circuitry.

For related information see also *60 Computer Operations and Hardware* and *76 Solid-State Physics.*

34 FLUID MECHANICS AND HEAT TRANSFER 44

Includes boundary layers; hydrodynamics; fluidics; mass transfer and ablation cooling.

For related information see also *02 Aerodynamics* and *77 Thermodynamics and Statistical Physics.*

35 INSTRUMENTATION AND PHOTOGRAPHY 48

Includes remote sensors; measuring instruments and gages; detectors; cameras and photographic supplies; and holography.

For aerial photography see *43 Earth Resources and Remote Sensing.* For related information see also *06 Aircraft Instrumentation* and *19 Spacecraft Instrumentation.*

36 LASERS AND MASERS 50

Includes parametric amplifiers.

For related information see also *76 Solid-State Physics.*

37 MECHANICAL ENGINEERING 52

Includes auxiliary systems (nonpower); machine elements and processes; and mechanical equipment.

38 QUALITY ASSURANCE AND RELIABILITY N.A.

Includes product sampling procedures and techniques; and quality control.

39 STRUCTURAL MECHANICS 53

Includes structural element design and weight analysis; fatigue; and thermal stress.

For applications see *05 Aircraft Design, Testing and Performance* and *18 Spacecraft Design, Testing and Performance.*

GEOSCIENCES

Includes geosciences (general); earth resources and remote sensing; energy production and conversion; environment pollution; geophysics; meteorology and climatology; and oceanography.

For related information see also *Space Sciences.*

42 GEOSCIENCES (GENERAL) N.A.

43 EARTH RESOURCES AND REMOTE SENSING 56

Includes remote sensing of earth resources by aircraft and spacecraft; photogrammetry; and aerial photography.

For instrumentation see *35 Instrumentation and Photography.*

44 ENERGY PRODUCTION AND CONVERSION 72

Includes specific energy conversion systems, e.g., fuel cells; global sources of energy; geophysical conversion; and windpower.

For related information see also *07 Aircraft Propulsion and Power, 20 Spacecraft Propulsion and Power,* and *28 Propellants and Fuels.*

45 ENVIRONMENT POLLUTION 74

Includes atmospheric, noise, thermal, and water pollution.

46 GEOPHYSICS 75

Includes aeronomy; upper and lower atmosphere studies; ionospheric and magnetospheric physics; and geomagnetism.

For space radiation see *93 Space Radiation.*

47 METEOROLOGY AND CLIMATOLOGY 76

Includes weather forecasting and modification.

48 OCEANOGRAPHY 89

Includes biological, dynamic, and physical oceanography; and marine resources.

For related information see also *43 Earth Resources and Remote Sensing.*

LIFE SCIENCES

Includes life sciences (general); aerospace medicine; behavioral sciences; man/system technology and life support; and space biology.

51 LIFE SCIENCES (GENERAL) 90

52 AEROSPACE MEDICINE 90

Includes physiological factors; biological effects of radiation; and effects of weightlessness on man and animals.

53 BEHAVIORAL SCIENCES 91

Includes psychological factors; individual and group behavior; crew training and evaluation; and psychiatric research.

54 MAN/SYSTEM TECHNOLOGY AND LIFE SUPPORT 91

Includes human engineering; biotechnology; and space suits and protective clothing.

For related information see also *16 Space Transportation.*

55 SPACE BIOLOGY N.A.

Includes exobiology; planetary biology; and extraterrestrial life.

MATHEMATICAL AND COMPUTER SCIENCES

Includes mathematical and computer sciences (general); computer operations and hardware; computer programming and software; computer systems; cybernetics; numerical analysis; statistics and probability; systems analysis; and theoretical mathematics.

59 MATHEMATICAL AND COMPUTER SCIENCES (GENERAL) N.A.

60 COMPUTER OPERATIONS AND HARDWARE 92

Includes hardware for computer graphics, firmware, and data processing.

For components see *33 Electronics and Electrical Engineering.*

61 COMPUTER PROGRAMMING AND SOFTWARE 93

Includes computer programs, routines, algorithms, and specific applications, e.g., CAD/CAM.

62 COMPUTER SYSTEMS 99

Includes computer networks and special application computer systems.

63 CYBERNETICS 101

Includes feedback and control theory, artificial intelligence, robotics and expert systems.

For related information see also *54 Man/System Technology and Life Support.*

64 NUMERICAL ANALYSIS 101

Includes iteration, difference equations, and numerical approximation.

65 STATISTICS AND PROBABILITY 103

Includes data sampling and smoothing; Monte Carlo method; and stochastic processes.

66 SYSTEMS ANALYSIS 104

Includes mathematical modeling; network analysis; and operations research.

67 THEORETICAL MATHEMATICS 105

Includes topology and number theory.

PHYSICS

Includes physics (general); acoustics; atomic and molecular physics; nuclear and high-energy physics; optics; plasma physics; solid-state physics; and thermodynamics and statistical physics.

For related information see also *Engineering.*

70 PHYSICS (GENERAL) N.A.

For precision time and time interval (PTTI) see *35 Instrumentation and Photography;* for geophysics, astrophysics or solar physics see *46 Geophysics, 90 Astrophysics,* or *92 Solar Physics.*

71 ACOUSTICS 105
Includes sound generation, transmission, and attenuation.
For noise pollution see *45 Environment Pollution.*

72 ATOMIC AND MOLECULAR PHYSICS 106
Includes atomic structure, electron properties, and molecular spectra.

73 NUCLEAR AND HIGH-ENERGY PHYSICS 107
Includes elementary and nuclear particles; and reactor theory.
For space radiation see *93 Space Radiation.*

74 OPTICS 107
Includes light phenomena and optical devices.
For lasers see *36 Lasers and Masers.*

75 PLASMA PHYSICS 109
Includes magnetohydrodynamics and plasma fusion.
For ionospheric plasmas see *46 Geophysics.* For space plasmas see *90 Astrophysics.*

76 SOLID-STATE PHYSICS 112
Includes superconductivity.
For related information see also *33 Electronics and Electrical Engineering* and *36 Lasers and Masers.*

77 THERMODYNAMICS AND STATISTICAL PHYSICS 114
Includes quantum mechanics; theoretical physics; and Bose and Fermi statistics.
For related information see also *25 Inorganic and Physical Chemistry* and *34 Fluid Mechanics and Heat Transfer.*

SOCIAL SCIENCES

Includes social sciences (general); administration and management; documentation and information science; economics and cost analysis; law, political science, and space policy; and urban technology and transportation.

80 SOCIAL SCIENCES (GENERAL) N.A.
Includes educational matters.

81 ADMINISTRATION AND MANAGEMENT 115
Includes management planning and research.

82 DOCUMENTATION AND INFORMATION SCIENCE 116
Includes information management; information storage and retrieval technology; technical writing; graphic arts; and micrography.
For computer documentation see *61 Computer Programming and Software.*

83 ECONOMICS AND COST ANALYSIS N.A.
Includes cost effectiveness studies.

84 LAW, POLITICAL SCIENCE AND SPACE POLICY N.A.
Includes NASA appropriation hearings; aviation law; space law and policy; international law; international cooperation; and patent policy.

85 URBAN TECHNOLOGY AND TRANSPORTATION 118
Includes applications of space technology to urban problems; technology transfer; technology assessment; and surface and mass transportation.
For related information see *03 Air Transportation and Safety, 16 Space Transportation,* and *44 Energy Production and Conversion.*

SPACE SCIENCES

Includes space sciences (general); astronomy; astrophysics; lunar and planetary exploration; solar physics; and space radiation.
For related information see also *Geosciences.*

88 SPACE SCIENCES (GENERAL) 119

89 ASTRONOMY 119
Includes radio, gamma-ray, and infrared astronomy; and astrometry.

90 ASTROPHYSICS 133
Includes cosmology; celestial mechanics; space plasmas; and interstellar and interplanetary gases and dust.
For related information see also *75 Plasma Physics.*

91 LUNAR AND PLANETARY EXPLORATION 134
Includes planetology; and manned and unmanned flights.
For spacecraft design or space stations see *18 Spacecraft Design, Testing and Performance.*

92 SOLAR PHYSICS 141
Includes solar activity, solar flares, solar radiation and sunspots.
For related information see *93 Space Radiation.*

93 SPACE RADIATION N.A.
Includes cosmic radiation; and inner and outer earth's radiation belts.
For biological effects of radiation see *52 Aerospace Medicine.* For theory see *73 Nuclear and High-Energy Physics.*

GENERAL

Includes aeronautical, astronautical, and space science related histories, biographies, and pertinent reports too broad for categorization; histories or broad overviews of NASA programs.

99 GENERAL N.A.

Note: N.A. means that no abstracts were assigned to this category for this issue.

SUBJECT INDEX I-1
PERSONAL AUTHOR INDEX I-47
CORPORATE SOURCE INDEX I-55
CONTRACT NUMBER INDEX I-65
REPORT/ACCESSION NUMBER INDEX I-67

TYPICAL CITATION AND ABSTRACT

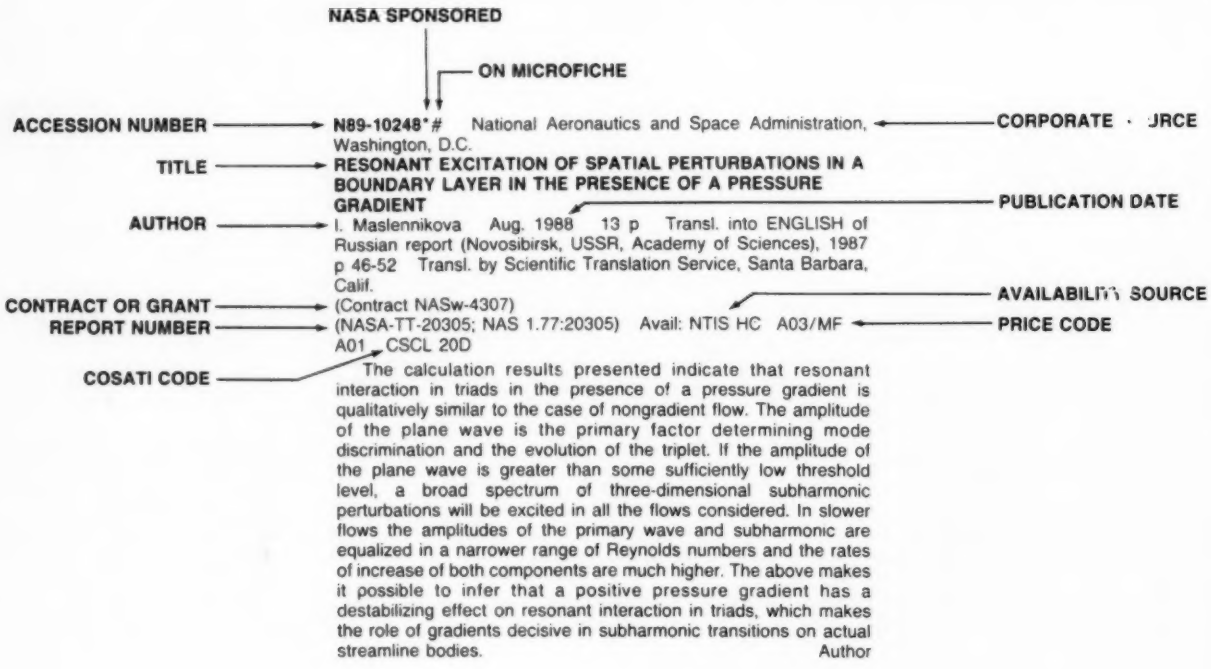
NASA SPONSORED
ON MICROFICHE
ACCESSION NUMBER
N89-10248*# National Aeronautics and Space Administration, Washington, D.C.
CORPORATE SOURCE
TITLE
RESONANT EXCITATION OF SPATIAL PERTURBATIONS IN A BOUNDARY LAYER IN THE PRESENCE OF A PRESSURE GRADIENT
AUTHOR
I. Maslennikova Aug. 1988 13 p Transl. into ENGLISH of Russian report (Novosibirsk, USSR, Academy of Sciences), 1987 p 46-52 Transl. by Scientific Translation Service, Santa Barbara, Calif.
PUBLICATION DATE
CONTRACT OR GRANT
(Contract NASw-4307)
AVAILABILITY SOURCE
REPORT NUMBER
(NASA-TT-20305; NAS 1.77:20305) Avail: NTIS HC A03/MF A01 CSCL 20D
PRICE CODE
COSATI CODE
The calculation results presented indicate that resonant interaction in triads in the presence of a pressure gradient is qualitatively similar to the case of nongradient flow. The amplitude of the plane wave is the primary factor determining mode discrimination and the evolution of the triplet. If the amplitude of the plane wave is greater than some sufficiently low threshold level, a broad spectrum of three-dimensional subharmonic perturbations will be excited in all the flows considered. In slower flows the amplitudes of the primary wave and subharmonic are equalized in a narrower range of Reynolds numbers and the rates of increase of both components are much higher. The above makes it possible to infer that a positive pressure gradient has a destabilizing effect on resonant interaction in triads, which makes the role of gradients decisive in subharmonic transitions on actual streamline bodies. Author

VOLUME 27 NUMBER 1 / JANUARY 8, 1989

Scientific and Technical Aerospace Reports

A Semimonthly Publication of the National Aeronautics and Space Administration

01 AERONAUTICS (GENERAL)

N89-10001# Advisory Group for Aerospace Research and Development, Neuilly-Sur-Seine (France). Flight Mechanics Panel.
TECHNICAL EVALUATION REPORT ON THE FLIGHT MECHANICS PANEL SYMPOSIUM ON FLIGHT VEHICLE DEVELOPMENT TIME AND COST REDUCTION
Gerald G. Kayten (Kayten, Gerald G., Chevy Chase, Md) 1988 16 p Symposium held in Toulouse, France, 11-14 May 1987
(AGARD-AR-244; ISBN-92-835-0473-9) Copyright Avail: NTIS HC A03/MF A01

There is a current perception that time and especially the cost of the new systems are increasing at an ever accelerating rate greater than that for improvement of the capabilities of the machines. The purpose of this symposium was to provide a forum to identify and discuss the elements contributing to the increased time and cost development, and to explore the question of what can be done to arrest and reverse the trend. Another aim of this symposium was to encourage others in the nontechnical area to join with the technical people in attacking these problems resolutely. It is considered that the meeting was successful in focusing attention on this situation, showing what technologies can do to reduce development time and cost growth, and by highlighting key areas that must be addressed to reverse the trend. Author

N89-10002* National Aeronautics and Space Administration, Washington, D.C.
AERONAUTICAL ENGINEERING: A CONTINUING BIBLIOGRAPHY WITH INDEXES (SUPPLEMENT 231)
Oct. 1988 132 p
(NASA-SP-7037(231); NAS 1.21:7037(231)) Avail: NTIS HC A07; NTIS standing order as PB88-914100. $8.50 domestic, $17.00 foreign CSCL 01A

This bibliography lists 469 reports, articles, and other documents introduced into the NASA scientific and technical information system in September, 1988. Author

N89-10003# Royal Aerospace Establishment, Farnborough (England).
AEROSPACE SYSTEMS AND TECHNOLOGY: THE ROLE OF THE RAE
G. G. Pope Jun. 1988 38 p Presented at RAE Handley Page Memorial Lecture, London, United Kingdom, 21 Apr. 1988 Original contains color illustrations
(RAE-TR-88042; RAE-DR/55/07; ETN-88-93140) Copyright Avail: NTIS HC A03/MF A01; Defence Research Information Centre, 65 Brown Street, Glasgow, G2 8EX, United Kingdom

The evolution and role of the U.K. Royal Aerospace Establishment are reviewed and research in night and all-weather operations, flight control systems for ASTOVL aircraft, computational fluid dynamics, airframe materials, weapon aim-point refinement, remote sensing, and systems assessment is summarized. ESA

02 AERODYNAMICS

Includes aerodynamics of bodies, combinations, wings, rotors, and control surfaces; and internal flow in ducts and turbomachinery.

For related information see also *34 Fluid Mechanics and Heat Transfer.*

N89-10004# National Aerospace Lab., Tokyo (Japan).
MEASUREMENT OF AERODYNAMIC CHARACTERISTICS OF A HANG-GLIDER-WING BY GROUND RUN TESTS USING A TEST VEHICLE
Koki Hozumi, Masaki Komoda, Takatsugu Ono, and Yukichi Tsukano 1987 29 p In JAPANESE; ENGLISH summary
(NAL-TR-953; ISSN-0389-4010) Avail: NTIS HC A03/MF A01

In order to investigate longitudinal force and moment characteristics of a hang-glider-wing, ground run tests were conducted using a test vehicle. A hang-glider-wing was installed on a test vehicle using a six-components-balance for wing tunnel use. Aerodynamic force and moment were measured during the vehicle run at various constant speeds. Geometrical twist distribution along the wing span was recorded as well. Measured force and moment data were corrected for possible ground effect and upwash effect due to movement of the vehicle. The lift curve slope was about 23 percent smaller than that predicted by theory for a rigid wing of the same geometry. An abrupt increase in the pitching moment was measured as C sub L decreased from positive to negative. These particular features indicate that aeroelastic deformations affect the aerodynamic characteristics of hang-gliders and/or motor-hang-gliders are mandatory for their flight safety. Using the Moriya method, aeroelastic camber variations at typical spanwise stations were estimated for each combination of dynamic pressure and section angle of attack. Applying the Weissinger method, lift and pitching moment characteristics were analyzed twist distributions. By comparing these analysis with the measured data, geometrical deformations of the flexible wing were elucidated. Author

N89-10005# Aeronautical Research Labs., Melbourne (Australia).
A POTENTIAL THEORY FOR THE STEADY SEPARATED FLOW ABOUT AN AEROFOIL SECTION
Tran-Cong Ton Feb. 1988 31 p
(ARL-AERO-R-176; AR-004-596) Copyright Avail: NTIS HC A03/MF A01

An incompressible potential flow theory is used to determine the steady separated flow about an airfoil. The theory permits a continuous variation from fully-attached (Joukowski) flow to fully-separated (Helmholtz) flow, with the Kutta condition always satisfied at the trailing edge, and with the position of the separation point as an assignable parameter to determine the flow configuration. The method is also applicable to other flows such as that about a flat plate with a rear free-stream flap. Author

N89-10006# Advisory Group for Aerospace Research and Development, Neuilly-Sur-Seine (France). Propulsion and Energetics Panel.
AGARD MANUAL ON AEROELASTICITY IN AXIAL-FLOW TURBOMACHINES. VOLUME 2: STRUCTURAL DYNAMICS AND AEROELASTICITY

Max F. Platzer, ed. and Franklin O. Carta, ed. (United Technologies Research Center, East Hartford, Conn.) Jun. 1988 266 p (AGARD-AG-298-Vol-2; ISBN-92-835-0467-4) Copyright Avail: NTIS HC A12/MF A01

An overview of structural dynamics characteristics and analysis methods applicable to single blades and bladed assemblies is presented. The blade fatigue problem and its assessment methods, and life-time predictions are considered. Aeroelastic topics covered include: the problem of blade-disc shroud aeroelastic coupling, formulations and solutions for tuned and mistuned rotors, and instrumentation on test procedures to perform a fan flutter test. The effect of stagnation temperature and pressure on flutter is demonstrated and currently available forced vibration and flutter design methodology is reviewed. For individual titles, see N89-10007 through N89-10016.

N89-10007# Imperial Coll. of Science and Technology, London (England). Dept. of Mechanical Engineering.

BASIC STRUCTURAL DYNAMICS **c39**

D. J. Ewins *In* AGARD, AGARD Manual on Aeroelasticity in Axial-Flow Turbo Machines. Volume 2: Structural Dynamics and Aeroelasticity Jun. 1988 14 p (For primary document see N89-10006 01-02)

Copyright Avail: NTIS HC A12/MF A01

Concepts are introduced which are dynamics aspects and the properties of interest as well as summarizing the appropriate analysis method, available for deriving the required information in specific cases. The task of formulating a suitable mathematical model is discussed. The use of finite element methods for this modeling task is examined. Some of the special analysis methods which are especially appropriate for dealing with the particular structural forms common in bladed assemblies are outlined. Author

N89-10008# Imperial Coll. of Science and Technology, London (England).

STRUCTURAL DYNAMIC CHARACTERISTICS OF INDIVIDUAL BLADES **c07**

D. J. Ewins and R. Henry (Institut National des Sciences Appliquees, Lyon, France) *In* AGARD, AGARD Manual on Aeroelasticity in Axial-Flow Turbo Machines. Volume 2: Structural Dynamics and Aeroelasticity Jun. 1988 27 p (For primary document see N89-10006 01-02)

Copyright Avail: NTIS HC A12/MF A01

The basic characteristics of blade vibration properties are outlined. The design features are identified which have an influence on the IR values. Simple models of blades were used, then the methods were applied to calculation of the structural dynamic properties of real blades. The natural frequencies and mode shapes of a blade in its operational environment may differ considerably from those calculated for the same blade as an isolated component. These differences are examined. Author

N89-10009# Imperial Coll. of Science and Technology, London (England). Dept. of Mechanical Engineering.

STRUCTURAL DYNAMIC CHARACTERISTICS OF BLADED ASSEMBLIES **c07**

D. J. Ewins *In* AGARD, AGARD Manual on Aeroelasticity in Axial-Flow Turbo Machines. Volume 2: Structural Dynamics and Aeroelasticity Jun. 1988 37 p (For primary document see N89-10006 01-02)

Copyright Avail: NTIS HC A12/MF A01

Considerable efforts were expended in order to make accurate predictions for the essential structural dynamic properties of typical turbomachine blades. In the pursuit of accuracy in these predictions, the effect of the coupling between one blade and its neighbors via the structure connections which exist, was neglected. The patterns of both natural frequencies and mode shapes for various assemblies are illustrated and the major controlling factors in each case identified. Simplified mathematical models of a bladed assembly are used that permit detailed parametric studies necessary to determine the patterns of behavior. Author

N89-10010# Rolls-Royce Ltd., Bristol (England).

FATIGUE AND ASSESSMENT METHODS OF BLADE VIBRATION **c07**

E. K. Armstrong *In* AGARD, AGARD Manual on Aeroelasticity in Axial-Flow Turbo Machines. Volume 2: Structural Dynamics and Aeroelasticity Jun. 1988 34 p (For primary document see N89-10006 01-02)

Copyright Avail: NTIS HC A12/MF A01

Fatigue is the failure mode of a metal which was subjected to a large number of applications of stress. In a fatigue failure a component suffers the development of a crack, which propagates very quickly across the section of the component. In the majority of the cases this stress is a result of the vibration of the blades, compressor, or turbine, at a significant amplitude. It is necessary to appreciate the major factors controlling the fatigue of blading which are encountered in the actual operation of gas turbines and the practical steps which can be taken to assess the levels of vibration which are present, to ensure as far as possible that blade failures due to this cause are minimized. Author

N89-10011# Office National d'Etudes et de Recherches Aeronautiques, Paris (France).

LIFE TIME PREDICTION: SYNTHESIS ON ONERA's RESEARCH IN VISCOPLASTICITY AND CONTINUOUS DAMAGE MECHANICS, APPLIED TO ENGINE MATERIALS AND STRUCTURES **c07**

R. Labourdette *In* AGARD, AGARD Manual on Aeroelasticity in Axial-Flow Turbo Machines. Volume 2: Structural Dynamics and Aeroelasticity Jun. 1988 15 p (For primary document see N89-10006 01-02)

Copyright Avail: NTIS HC A12/MF A01

Improvements in the metallurgy of superalloy materials make it possible to use them at higher temperatures. However, it follows from the increase in temperature that more severe thermomechanical problems are encountered when dealing with the design and life prediction of turbine blades. Roughly speaking, two phenomena are to be described for such a prediction: creep and fatigue. The main steps for the method of life prediction developed at ONERA are: behavior of the macroscopic volume element; damage accumulation under creep-fatigue conditions; and numerical methods of stress and damage calculation in complex structures undergoing thermomechanical loading. The steps are described in detail. Author

N89-10012# United Technologies Research Center, East Hartford, Conn.

AEROELASTIC COUPLING: AN ELEMENTARY APPROACH **c07**

Franklin O. Carta *In* AGARD, AGARD Manual on Aeroelasticity in Axial-Flow Turbo Machines. Volume 2: Structural Dynamics and Aeroelasticity Jun. 1988 16 p (For primary document see N89-10006 01-02)

Copyright Avail: NTIS HC A12/MF A01

It was shown in the original 1967 paper that the energy method, using unsteady isolated airfoil theory, and applied to actual multiblade rotors, yielded results that were remarkably accurate. This fortuitous agreement was sufficiently encouraging to foster a continuing development of the technique and its constituent aerodynamic and structural dynamic components. As shown in these two volumes and in the several citations to advanced analyses, current practice has gone well beyond the relatively simplistic view of the early paper. The aerodynamic input now encompasses multiblade systems subjected to compressible flows, and structures are modeled to include nonlinearities and mistuning. Nevertheless, the paper has served its purpose well. In its original form it set the stage for the continual improvement of engine flutter prediction methods, and in this manual it provides the reader with a vehicle for coordinating the separate disciplines which, together, represent the modern approach to flutter prediction of turbomachinery blade rows. Author

N89-10013# Massachusetts Inst. of Tech., Cambridge. Gas Turbine Lab.
AEROELASTIC FORMULATION FOR TUNED AND MISTUNED ROTORS **c07**
Edward F. Crawley *In* AGARD, AGARD Manual on Aeroelasticity in Axial-Flow Turbo Machines. Volume 2: Structural Dynamics and Aeroelasticity Jun. 1988 24 p (For primary document see N89-10006 01-02)
Copyright Avail: NTIS HC A12/MF A01

The topics to be addressed are: the formulation of the aeroelastic problem, including a summary of the relations necessary to transform various diverse structural and aerodynamic models to a consistent notation; a brief review of the solution techniques applicable; the trends in aeroelastic stability for tuned rotors; and the effects of mistuning on stability. Author

N89-10014# Pratt and Whitney Aircraft, East Hartford, Conn.
FAN FLUTTER TEST **c07**
Hans Stargardter *In* AGARD, AGARD Manual on Aeroelasticity in Axial-Flow Turbo Machines. Volume 2: Structural Dynamics and Aeroelasticity Jun. 1988 35 p (For primary document see N89-10006 01-02)
Copyright Avail: NTIS HC A12/MF A01

The objective is to describe an aeroelastic investigation of fan flutter. Discussion includes test procedures for flutter evaluation, data acquisition and reduction, safety, and instrumentation. Some data contents are included, but are not the primary concern. Initially, a complete sequence of preparation, testing, and analysis of an ideal fan flutter test is presented. This is followed by identification of dangerous blade vibrations, a case history of a NASA/Pratt and Whitney Subsonic/Transonic Flutter Study, and a discussion and analysis of the program results. Lastly, a summary relating this test to the overall discussion of fan flutter testing is presented. It will be noted that many of the steps in the ideal test situation were omitted in the actual case history. Most of these differences are in the test preparation area because the case history used a previously tested design in which much of the preliminary work and safety screening was already accomplished. Author

N89-10015# Jeffers (James D., III), Tampa, Fla.
AEROELASTIC THERMAL EFFECTS **c07**
James D. Jeffers, III *In* AGARD, AGARD Manual on Aeroelasticity in Axial-Flow Turbo Machines. Volume 2: Structural Dynamics and Aeroelasticity Jun. 1988 6 p (For primary document see N89-10006 01-02)
Copyright Avail: NTIS HC A12/MF A01

The adverse effect of increasing temperature on the stability of turbomachinery airfoils was long recognized but remains today one that is not fully understood. The quantitative effect on the reduced frequency parameter, k = omega c/V, which was experimentally and analytically shown to be one of the most influential stability parameters, is readily calculated. The effects of increasing temperature on the parameters that comprise reduced frequency are well known. Unfortunately, the resulting effect on aeroelastic stability, particularly for stall flutter, is not. This inability to completely assess thermal effects, among others, was dramatically underscored by an occurrence of subsonic stall flutter in the first stage fan rotor of the F100 turbofan engine early in the development program. The severity of the problem prompted an intensive experimental test program and analysis to first determine a solution and, further, to assess the design techniques used to avoid the problem. As a result, a decade of extensive analytical and experimental research was conducted at the Government Products Division of Pratt and Whitney Aircraft, the United Technologies Research Center, and the NASA Lewis Research Center. The following is a summary of some of the findings of these investigations. Author

N89-10016# Detroit Diesel Allison, Indianapolis, Ind.
FORCED VIBRATION AND FLUTTER DESIGN METHODOLOGY **c39**
Lynn E. Snyder and Donald W. Burns *In* AGARD, AGARD Manual on Aeroelasticity in Axial-Flow Turbo Machines. Volume 2: Structural Dynamics and Aeroelasticity Jun. 1988 28 p (For primary document see N89-10006 01-02)
Copyright Avail: NTIS HC A12/MF A01

The aeroelastic principles and considerations of designing blades, disks, and vanes to avoid high cycle fatigue failure is covered. Two types of vibration that can cause high cycle fatigue, flutter, and forced vibration, will first be defined and the basic governing equations discussed. Next, under forced vibration design the areas of source definition, types of components, vibratory mode shape definitions, and basic steps in design for adequate high cycle fatigue life will be presented. For clarification a forced vibration design example will be shown using a high performance turbine blade/disk component. Finally, types of flutter, dominant flutter parameters, and flutter procedures and design parameters will be discussed. The overall emphasis is on application to initial design of blades, disks, and vanes of aeroelastic criteria to prevent high cycle fatigue failures. Author

N89-10017*# National Aeronautics and Space Administration. Ames Research Center, Moffett Field, Calif.
WAVE DRAG AND HIGH-SPEED PERFORMANCE OF SUPERSONIC STOVL FIGHTER CONFIGURATION
Donald A. Durston and Ronald K. Stonum Jan. 1988 19 p Presented at the International Powered Life Conference in Santa Clara, Calif., 7-10 Dec. 1987
(NASA-TM-100061; A-88072; NAS 1.15:100061) Avail: NTIS HC A03/MF A01 CSCL 01A

A supersonic STOVL fighter aircraft aerodynamic research program is under way at NASA Ames Research Center. The research focuses on technology development for this type of aircraft and includes generating an extensive aerodynamic database and resolving particular aerodynamic uncertainties for various twin- and single-engine aircraft concepts. Highlights of the results from this program are presented. The highlights include propulsion-induced effects on the aircraft drag, prediction capabilities, volume integration for minimizing drag, and wave drag and aerodynamic efficiency comparisons. Results indicate that estimated STOVL fighter performance is roughly comparable to the performance of modern conventional fighters in terms of wave drag and aerodynamic efficiency. Author

N89-10018# Instituto de Pesquisas Espaciais, Sao Jose dos Campos (Brazil). Dept. of Astrophysics.
SCIENTIFIC BALLOONING IN BRAZIL
Ricardo VarelaCorrea Jun. 1988 6 p Presented at the 6th Simposio Nipo-Brasileiro de Ciencia e Tecnologia, Sao Jose dos Campos, Brazil
(INPE-4602-PRE/1325) Avail: NTIS HC A02/MF A01

Scientific ballooning is being increased in the world because of the possibility of the use of up-to-date detectors and applied electronics. After the burst of the SN1987A, several institutions from several countries have shown interest in using the balloon for stratospheric balloon launching in the Southern Hemisphere. Several places in the countryside have good airports in low population density areas, ideal for balloon launching. Depending on stratospheric wind speed, flights over 25 hours are possible. Flights during turn-around and boomerang may increase flight duration. At the balloon base, only west direction flights are possible, with up to 15 hours at ceiling. With the increasing users, demands for lighter instruments and safer flights are providing new ideas for power and weight reductions. The telemetry is being improved with transmission in L band and new command system. The tracking antennas at the balloon base and at the down range station will provide location of the balloon, backing up the OMEGA system. The OMEGA system in the Southern Hemisphere is reliable and suitable for balloon trajectory. A new onboard filter is providing OMEGA data with more the three stations locked at the receiver, during the worse time of day (sunrise and sunset). Author

N89-10019*# Chrysler Corp., New Orleans, La. Military Public Electronic Systems.
SPACE SHUTTLE PHASE B WIND TUNNEL MODEL AND TEST INFORMATION. VOLUME 3: LAUNCH CONFIGURATION

J. L. Glynn and D. E. Poucher Jul. 1988 444 p
(Contract NAS1-18276)
(NASA-CR-178416-Vol-3-Pt-1; NAS 1.26:178416-Vol-3-Pt-1; DMS-DB-02-Vol-3-Pt-1) Avail: NTIS HC A19/MF A01 CSCL 01A

Archived wind tunnel test data are available for flyback booster or other alternate recoverable configuration as well as reusable orbiters studied during initial development (Phase B) of the Space Shuttle, including contractor data for an extensive variety of configurations with an array of wing and body planforms. The test data have been compiled into a database and are available for application to current winged flyback or recoverable booster aerodynamic studies. The Space Shuttle Phase B Wind Tunnel Database is structured by vehicle component and configuration. Basic components include booster, orbiter, and launch vehicle. Booster configuration types include straight and delta wings, canard, cylindrical, retroglide and twin body. Orbiter configurations include straight and delta wings, lifting body, drop tanks and double delta wings. Launch configurations include booster and orbiter components in various stacked and tandem combinations. The digital database consists of 220 files containing basic tunnel data. Database structure is documented in a series of reports which include configuration sketches for the various planforms tested. This is Volume 3 -- launch configurations. Author

N89-10020*# National Aeronautics and Space Administration. Langley Research Center, Hampton, Va.
WEAK-WAVE ANALYSIS OF SHOCK INTERACTION WITH A SLIPSTREAM
Raymond L. Barger Nov. 1988 20 p
(NASA-TP-2848; L-16469; NAS 1.60:2848) Avail: NTIS HC A03/MF A01 CSCL 01A

A weak wave analysis of shock interaction with a slipstream is presented. The theory is compared to that for the acoustic case and to the exact nonlinear analysis. Sample calculations indicate that the weak wave theory yields a good approximation to the exact solution when the shock waves are sufficiently weak that the associated entropy increase is negligible. A qualitative discussion of the case of counterflowing streams is also included. Author

N89-10021# National Aerospace Lab., Tokyo (Japan).
NORMAL FORCE COEFFICIENT OF SUPERSONIC FLOWS OVER CONICAL FLARE, CONE-CYLINDER AND CONICAL BOATTAILS
Kunio Nomizo Oct. 1987 21 p In JAPANESE; ENGLISH summary
(NAL-TR-949; ISSN-0389-4010) Avail: NTIS HC A03/MF A01

A numerical calculation of the supersonic flow of a perfect gas over conical flares, cone-cylinder, and conical boattail at a small angle of attack was performed. The Allen E. Pluckett method was found to be useful for predicting the flow field about conical flares with slope abnormalities. The relationship of the normal force distribution between linearized theory and the present method is shown. The normal force distribution calculated by the present method was found to be smaller than that of linearized theory as a whole. Linearized theory estimates the density of gas to be thicker than that of present theory. The present method was simplified by eliminating the density terms. According to the linearized theory, the normal force coefficient is determined by the area ratio of a flare or boattail and is constant along the flare or boattail surface. However, the present method shows that the normal force coefficient decreases downstream, since the density of a gas decreases as it flows downstream. Even if the Mach number varies, linearized theory shows that normal force is constant. But present theory shows that normal force decreases as Mach number increases for flare and boattails an exact analytical solution is obtained for supersonic flow along with a slightly inclined circular cone. The governing equations are simplified by eliminating the density terms, and the after-body of a cone cylinder was calculated by the present method. Also investigated were overexpanded sonic jets through axisymmetric conical nozzles and the effects fo the pressure and Mach number of supersonic jets . Author

N89-10022*# National Aeronautics and Space Administration. Ames Research Center, Moffett Field, Calif.
NAVIER-STOKES SIMULATION OF TRANSONIC WING FLOW FIELDS USING A ZONAL GRID APPROACH
Neal M. Chaderjian Jan. 1988 26 p
(NASA-TM-100039; A-88020; NAS 1.15:100039) Avail: NTIS HC A03/MF A01 CSCL 01A

The transonic Navier-Stokes code was used to simulate flow fields about isolated wings for workshop wind-tunnel and free-air cases using the thin-layer Reynolds-averaged Navier-Stokes equations. An implicit finite-difference scheme based on a diagonal version of the Beam-Warming algorithm was used to integrate the governing equations. A zonal grid approach was used to allow efficient grid refinement near the wing surface. The flow field was sensitive to the turbulent transition model, and flow unsteadiness was observed for a wind-tunnel case but not for the corresponding free-air case. The specification of experimental pressure at the wind-tunnel exit plane is the primary reason for the difference of these two numerical solutions. Author

N89-10023# National Aerospace Lab., Tokyo (Japan).
ESTIMATION OF UP-WASH DISTRIBUTION AROUND AN AUTOMOBILE BY THREE-DIMENSIONAL SMOKE WIND TUNNEL TEST
Koki Hozumi Dec. 1986 11 p In JAPANESE; ENGLISH summary
(NAL-TR-921; ISSN-0389-4010) Avail: NTIS HC A03/MF A01

In an aerodynamic experiment with a hang glider wing mounted on a running automobile, it is necessary to correct the effects of the up-wash flow field induced by the automobile itself since they significantly deteriorate the measurement accuracy. Streamlines around an automobile model were observed in a three-dimensional smoke wind tunnel. The up-wash distribution was estimated from the shape of the streamlines. The measured up-wash distribution was found to be well approximated by that of an equivalent Rankine Oval, so that the oval, as a whole, could replace the automobile's wake shape. By selecting appropriate Rankine Ovals, up-wash distributions can easily be estimated at arbitrary positions around an automobile, except in the separated flow region. The amount of side wall correction is also described. Author

N89-10024*# National Aeronautics and Space Administration. Langley Research Center, Hampton, Va.
VALIDATION OF A PAIR OF COMPUTER CODES FOR ESTIMATION AND OPTIMIZATION OF SUBSONIC AERODYNAMIC PERFORMANCE OF SIMPLE HINGED-FLAP SYSTEMS FOR THIN SWEPT WINGS
Harry W. Carlson (PRC Systems Services Co., Hampton, Va.) and Christine M. Darden Washington Nov. 1988 118 p
(NASA-TP-2828; L-16428; NAS 1.60:2828) Avail: NTIS HC A06/MF A01 CSCL 01A

Extensive correlations of computer code results with experimental data are employed to illustrate the use of linearized theory attached flow methods for the estimation and optimization of the aerodynamic performance of simple hinged flap systems. Use of attached flow methods is based on the premise that high levels of aerodynamic efficiency require a flow that is as nearly attached as circumstances permit. A variety of swept wing configurations are considered ranging from fighters to supersonic transports, all with leading- and trailing-edge flaps for enhancement of subsonic aerodynamic efficiency. The results indicate that linearized theory attached flow computer code methods provide a rational basis for the estimation and optimization of flap system aerodynamic performance at subsonic speeds. The analysis also indicates that vortex flap design is not an opposing approach but is closely related to attached flow design concepts. The successful vortex flap design actually suppresses the formation of detached vortices to produce a small vortex which is restricted almost entirely to the leading edge flap itself. Author

N89-10025*# Pratt and Whitney Aircraft, East Hartford, Conn.
TURBOFAN FORCED MIXER LOBE FLOW MODELING. PART 3: APPLICATION TO AUGMENT ENGINES Final Report
T. Barber, G. C. Moore, and J. R. Blatt Washington NASA Oct. 1988 32 p
(Contract NAS3-23039)
(NASA-CR-4147; E-4085; NAS 1.26:4147) Avail: NTIS HC A03/MF A01 CSCL 01A

Military engines frequently need large quantities of thrust for short periods of time. The addition of an augmentor can provide such thrust increases but with a penalty of increased duct length and engine weight. The addition of a forced mixer to the augmentor improves performance and reduces the penalty, as well as providing a method for siting the required flame holders. In this report two augmentor concepts are investigated: a swirl-mixer augmentor and a mixer-flameholder augmentor. Several designs for each concept are included and an experimental assessment of one of the swirl-mixer augmentors is presented. Author

N89-10026# Office National d'Etudes et de Recherches Aerospatiales, Paris (France).
LA RECHERCHE AEROSPATIALE, BIMONTHLY BULLETIN, NUMBER 1987-4, 239/JULY-AUGUST
ESA Jun. 1988 74 p Transl. into ENGLISH of La Recherche Aerospatiale, Bulletin Bimestriel (Paris, France, ONERA), no. 1987-4, 239/Jul.-Aug., 1987
(ESA-TT-1088; ETN-88-93051) Avail: NTIS HC A04/MF A01

Particle approximation of the two-dimensional Navier-Stokes equations; infrared system evaluation apparatus; strong coupling between inviscid fluid and boundary layer for airfoils with sharp leading edge (two-dimensional incompressible steady case); continuum damage mechanics and its applicaton to structural lifetime predictions; unsteady three-dimensional stall on a rectangular wing; and Fourier condition in integral methods: application to thin bodies, are discussed. For individual titles, see N89-10027 through N89-10027.

N89-10027# Office National d'Etudes et de Recherches Aerospatiales, Paris (France).
UNSTEADY THREE-DIMENSIONAL STALL ON A RECTANGULAR WING
J. J. Costes *In its* La Recherche Aerospatiale, Bimonthly Bulletin, Number 1987-4, 239/July-August Jun. 1988 p 55-69 Transl. into ENGLISH from La Recherche Aerospatiale, Bimestriel (Paris, France, ONERA), no. 1987-4, 239/Jul.-Aug., 1987 (For primary document see N89-10026 01-02)
Avail: NTIS HC A04/MF A01

Steady and unsteady stall are studied on a rectangular wing in normal flow. The wing is allowed to oscillate in pitch around the fore quarter chord. Experiments performed at the S 2 wind-tunnel in Chalais-Meudon with a rectangular wing and a wind velocity of 95 m/s are in good agreement with the results obtained from the theory developed. Author

N89-10028*# De Havilland Aircraft Co. of Canada Ltd., Downsview (Ontario).
PHASE 4 STATIC TESTS OF THE J-97 POWERED, EXTERNAL AUGMENTOR V/STOL MODEL AT THE NASA, AMES RESEARCH CENTER, NOVEMBER 1983
D. B. Garland Dec. 1985 87 p
(Contract NASw-2797)
(NASA-CR-177395; NAS 1.26:177395) Avail: NTIS HC A05/MF A01 CSCL 01A

A large-scale, ejector-lift V/STOL Model, powered by a J-97 engine, was tested at the NASA Ames Research Center Outdoor Aerodynamics Research Facility. The model incorporated the external augmentor concept developed by DHC. Since the first test at Ames in 1979, the fuselage augmentor nozzle array has been redesigned with a larger pitch and notched nozzles instead of plain slot nozzles. Thrust augmentation of the ejector as measured at Ames Research Center was lower than that measured in the DHC laboratory. It is believed that this difference is due to the high temperature of the primary jet flow as compared to the DHC blown-down rig. An ejector-lift/vectored thrust configuration was also included in the recent tests. This is an arrangement where the fuselage augmentor is shortened in the chordwise direction and the extra thrust is generated with a vectorable, ventral nozzle. In free air the shortened fuselage augmentor produced the same augmentation as the long augmentor. In ground proximity, at a height of 27 in, and with zero pitch angle, a negative ground effect was measured equal to 6.5 percent of the free-air lift.
Author

N89-10029*# North Carolina State Univ., Raleigh. Dept. of Mechanical and Aerospace Engineering.
A TRANSONIC INTERACTIVE BOUNDARY-LAYER THEORY FOR LAMINAR AND TURBULENT FLOW OVER SWEPT WINGS Final Report
Shawn H. Woodson and Fred R. DeJarnette Washington Oct. 1988 82 p
(Contract NCC1-22)
(NASA-CR-4185; NAS 1.26:4185) Avail: NTIS HC A05/MF A01 CSCL 01A

A 3-D laminar and turbulent boundary-layer method is developed for compressible flow over swept wings. The governing equations and curvature terms are derived in detail for a nonorthogonal, curvilinear coordinate system. Reynolds shear-stress terms are modeled by the Cebeci-Smith eddy-viscosity formulation. The governing equations are descretized using the second-order accurate, predictor-corrector finite-difference technique of Matsuno, which has the advantage that the crossflow difference formulas are formed independent of the sign of the crossflow velocity component. The method is coupled with a full potential wing/body inviscid code (FLO-30) and the inviscid-viscous interaction is performed by updating the original wing surface with the viscous displacement surface calculated by the boundary-layer code. The number of these global iterations ranged from five to twelve depending on Mach number, sweep angle, and angle of attack. Several test cases are computed by this method and the results are compared with another inviscid-viscous interaction method (TAWFIVE) and with experimental data. Author

N89-10030# Office National d'Etudes et de Recherches Aerospatiales, Paris (France).
LA RECHERCHE AEROSPATIALE, BIMONTHLY BULLETIN, NUMBER 1987-6, 241/NOVEMBER-DECEMBER
ESA Jun. 1988 62 p Transl. into ENGLISH of La Recherche Aerospatiale, Bulletin Bimestriel (Paris, France, ONERA), no. 1987-6, 241/Nov.-Dec., 1987
(ESA-TT-1102; ETN-88-93056) Avail: NTIS HC A04/MF A01

Triaxial electrostatic accelerometers; numerical model of axisymmetrical turbulent reactive flows with tangential velocity; supersonic missile air intake design and development critieria; parallelization of a spectral influence matrix method for the numerical solution of the Navier-Stokes equations; and study of damage initiation in the matrix of a composite material by a homogenization method are discussed. For individual titles, see N89-10031 through N89-10031.

N89-10031# Office National d'Etudes et de Recherches Aerospatiales, Paris (France).
SUPERSONIC MISSILE AIR INTAKES: DESIGN AND DEVELOPMENT CRITERIA
G. Laruelle *In its* La Recherche Aerospatiale, Bimonthly Bulletin, Number 1987-6, 241/November-December Jun. 1988 p 23-34 Transl. into ENGLISH from La Recherche Aerospatiale, Bulletin Bimestriel (Paris, France, ONERA), no. 1987-6, 241/Nov.-Dec., 1987 (For primary document see N89-10030 01-02)
Avail: NTIS HC A04/MF A01

The first missiles powered by ramjets were built essentially for the purposes of checking the flight performance of this type engine. They generally had just one air intake in the nose, which is the optimum position, aerodynamically speaking. Thanks to technological advances, the ramjet is now becoming an engine of great interest for military applications, which have imposed constraints on the shape and location of the air intakes on the

missile. Knowing the flow around an ogival cylindrical body at incidence, it is possible to specify the position for the air intakes and to design their frontal section. For the coming generation of ramjet missiles, performance must be increased. At the present time, this means high maneuverability and long range. New design criteria were taken into account for this, not the least of which are the constraints to reduce the radar cross section. High maneuverability means the air intakes have to function well in the very distorted flow fields occurring at high angle of attack, where the integration of the air intakes with the body is essential. Long range flight can be achieved at high altitude and high Mach number. A compromise must be found between maximum performance in cruising flight and the requirements for climbing and final descent. For this, air intakes with movable parts are being studied, as well as noncircular cross-sections of fuselage giving optimum lift-to-dray ratios. Author

N89-10032# Helsinki Univ. Technology, Otaniemi (Finland). Lab. of Aerodynamics.
COMPARISON OF EULER ALGORITHMS FOR TWO-DIMENSIONAL SHOCK CALCULATIONS
Timo Siikonen and Tuomo Saarinen 1988 39 p
(PB88-210372; Rept-B-12; ISBN-951-754-458-8) Avail: NTIS HC A03/MF A01 CSCL 01A

The suitability of three compressible flow algorithms for two-dimensional shock calculations has been tested. The algorithms are MacCormack's explicit and implicit methods, a central difference method and a flux vector splitting method. All the methods are applied in a conservative finite-volume form. They are compared by calculating a two-dimensional shock reflection problem. The performance is evaluated through the number of iteration cycles and through the computation times on different computers, including a vector computer. GRA

N89-10033*# Mississippi State Univ., Mississippi State. Dept. of Chemical Engineering.
STANDARDIZATION OF THE CARBON-PHENOLIC MATERIALS AND PROCESSES. VOL. 2: TEST METHODS AND SPECIFICATIONS Final Report, 1 Sep. 1985 - 31 Aug. 1988
William B. Hall 31 Aug. 1988 282 p
(Grant NAG8-545)
(NASA-CR-183227; NAS 1.26:183227) Avail: NTIS HC A13/MF A01 CSCL 01A

Carbon-phenolic composite materials are used in the ablation process in the nozzles of the Space Shuttle Main Engine. The nozzle is lined with carbon cloth-phenolic resin composites. The extreme heat and erosion of the burning propellant are controlled by the carbon-phenolic composite by means of ablation, a heat and mass transfer process in which a large amount of heat is dissipated by sacrificailly removing material from a surface. Phenolic materials ablate with the initial formation of a char. The depth of the char is a function of the heat conduction coefficient of the composite. The char layer is a poor conductor so it protects the underlying phenolic composite from the high heat of the burning propellant. The nozzle component ablative liners (carbon cloth-phenolic resin composites) are tape wrapped, hydroclave and/or autoclave cured, machined and assembled. The tape consists of prepreg broadcloth. The materials flow sheet for the nozzle ablative liners is given. The prepreg is a three component system: phenolic resin, carbon cloth, and carbon filler. This is Volume 2 of the report, Test Methods and Specifications. F.M.R.

N89-10034*# National Aeronautics and Space Administration. Langley Research Center, Hampton, Va.
THE PROS AND CONS OF CODE VALIDATION
Percy J. Bobbitt Jul. 1988 49 p Presented at the 6th AIAA Applied Aerodynamic Conference, Williamsburg, Va., 6-8 Jun. 1988 Previously announced in IAA as A88-42125
(NASA-TM-100657; NAS 1.15:100657; AIAA-Paper-88-2535)
Avail: NTIS HC A03/MF A01 CSCL 01A

Computational and wind tunnel error sources are examined and quantified using specific calculations of experimental data, and a substantial comparison of theoretical and experimental results, or a code validation, is discussed. Wind tunnel error sources considered include wall interference, sting effects, Reynolds number effects, flow quality and transition, and instrumentation such as strain gage balances, electronically scanned pressure systems, hot film gages, hot wire anemometers, and laser velocimeters. Computational error sources include math model equation sets, the solution algorithm, artificial viscosity/dissipation, boundary conditions, the uniqueness of solutions, grid resolution, turbulence modeling, and Reynolds number effects. It is concluded that, although improvements in theory are being made more quickly than in experiments, wind tunnel research has the advantage of the more realistic transition process of a right turbulence model in a free-transition test. Author

03 AIR TRANSPORTATION AND SAFETY

Includes passenger and cargo air transport operations; and aircraft accidents.

For related information see also *16 Space Transportation* and *85 Urban Technology and Transportation.*

N89-10035# National Transportation Safety Board, Washington, D. C. Bureau of Field Operations.
AIRCRAFT ACCIDENT REPORTS, BRIEF FORMAT, US CIVIL AND FOREIGN AVIATION, ISSUE NUMBER 10 OF 1987 ACCIDENTS
30 Mar. 1988 403 p
(PB88-916905; NTSB/AAB-88/05) Avail: NTIS HC A18/MF A01; also available on subscription, North American Continent HC $185.00/year; all others write for quote CSCL 01C

The publication contains selected aircraft accident reports in Brief Format occuring in U.S. civil and foreign aviation operations during 1987. Approximately 200 General Aviation and Air Carrier accidents presented represent a random selection. The publication is issued irregularly, normally 18 times each year. The Brief Format presents the facts, conditions, circumstances and probable causes for each accident. GRA

N89-10036# National Transportation Safety Board, Washington, D. C. Bureau of Field Operations.
AIRCRAFT ACCIDENT REPORTS, BRIEF FORMAT, US CIVIL AND FOREIGN AVIATION, ISSUE NUMBER 12 OF 1986 ACCIDENTS
25 Apr. 1988 414 p
(PB88-916903; NTSB/AAB-88/03) Avail: NTIS HC A18/MF A01; also available on subscription, North American continent HC $185.00/year; all others write for quote CSCL 01C

Selected aircraft accident reports in Brief Format occuring in the U.S. civil and foreign aviation operations during 1986 are presented. Approximately 200 General Aviation and Air Carrier accidents presented represent a random selection. The publication is issueo irregularly, normally eighteen times each year. The Brief Format represents the facts, conditions, circumstances and probable causes for each accident. GRA

N89-10037*# National Aeronautics and Space Administration. Ames Research Center, Moffett Field, Calif.
USING FULL-MISSION SIMULATION FOR HUMAN FACTORS RESEARCH IN AIR TRANSPORT OPERATIONS
Harry W. Orlady, Robert W. Hennessy, Richard Obermayer, Donald Vreuls (Vreuls Research Corp., Thousand Oaks, Calif.), and Miles R. Murphy Jul. 1988 85 p
(NASA-TM-88330; A-86320; NAS 1.15:88330) Avail: NTIS HC A05/MF A01 CSCL 05H

This study examined state-of-the-art mission oriented simulation and its use in human factors research. Guidelines were developed for doing full-mission human factors research on crew member behavior during simulated air transport operations. The existing literature was reviewed. However, interviews with experienced investigators provided the most useful information. The fundamental scientific and practical issues of behavioral research in a simulation

environment are discussed. Guidelines are presented for planning, scenario development, and the execution of behavioral research using full-mission simulation in the context of air transport flight operations . Research is recommended to enhance the validity and productivity of full-mission research by: (1) validating the need for high-fidelity simulation of all major elements in the operational environment, (2) improving methods for conducting full-mission research, and (3) examining part-task research on specific problems through the use of vehicles which contain higher levels of abstraction (and lower fidelity) of the operational environment.
Author

N89-10450# Office National d'Etudes et de Recherches Aeronautiques, Paris (France).
ANALYSIS OF RECENT IN-FLIGHT LIGHTNING MEASUREMENTS ON DIFFERENT AIRCRAFT
J. L. Boulay, J. P. Moreau, A. Asselineau, and P. L. Rustan (Defense Nuclear Agency, Washington, D.C.) *In* NOAA, International Aerospace and Ground Conference on Lightning and Static Electricity Apr. 1988 p 136-14 (For primary document see N89-10429 01-47)
Avail: NTIS HC A23/MF A01 CSCL 01C

N89-10451*# Electro Magnetic Applications, Inc., Lakewood, Colo.
LINEAR AND NONLINEAR INTERPRETATION OF CV-580 LIGHTNING DATA
Poh H. Ng, Terence H. Rudolph, and Rodney A. Perala *In* NOAA, International Aerospace and Ground Conference on Lightning and Static Electricity Apr. 1988 p 145-15 Sponsored in part by FAA, Atlantic City, N.J. (For primary document see N89-10429 01-47)
(Contract NAS1-17748)
Avail: NTIS HC A23/MF A01 CSCL 01C

N89-10452# Boeing Advanced Systems Co., Seattle, Wash.
LIGHTNING TESTS ON AN ALL-COMPOSITE HELICOPTER
David B. Walen *In* NOAA, International Aerospace and Ground Conference on Lightning and Static Electricity Apr. 1988 p 152-15 (For primary document see N89-10429 01-47)
Avail: NTIS HC A23/MF A01 CSCL 01C

N89-10454*# Electro Magnetic Applications, Inc., Huntsville, Ala.
ESTIMATING ELECTRIC FIELD ENHANCEMENT FACTORS ON AN AIRCRAFT UTILIZING A SMALL SCALE MODEL: A METHOD EVALUATION
Calvin C. Easterbrook, Terence Rudolph, and Kevin Easterbrook *In* NOAA, International Aerospace and Ground Conference on Lightning and Static Electricity Apr. 1988 p 171-17 (For primary document see N89-10429 01-47)
(Contract NAS1-17748)
Avail: NTIS HC A23/MF A01 CSCL 01C

N89-10455# AIRO, Inc., Colorado Springs, Colo.
A CHRONOLOGY OF IN-CLOUD ELECTRIC FIELD AND LIGHTNING STRIKES ON AN INSTRUMENTED RESEARCH AIRCRAFT
J. William Bullock and J. J. Jones (New Mexico State Bureau of Mines and Mineral Resources, Socorro.) *In* NOAA, International Aerospace and Ground Conference on Lightning and Static Electricity Apr. 1988 p 175-18 (For primary document see N89-10429 01-47)
Avail: NTIS HC A23/MF A01 CSCL 04B

N89-10456*# National Severe Storms Lab., Norman, Okla.
LIGHTNING INITIATION ON AIRCRAFT IN THUNDERSTORMS
Vladislav Mazur *In* NOAA, International Aerospace and Ground Conference on Lightning and Static Electricity Apr. 1988 p 181-19 Previously announced as A88-22289 Sponsored in part by NASA (For primary document see N89-10429 01-47)
Avail: NTIS HC A23/MF A01 CSCL 01C

N89-10457# De Havilland Aircraft Co. of Canada Ltd., Downsview (Ontario).
LIGHTNING TESTS TO MEASURE THE BULK CURRENT LEVELS ASSOCIATED WITH THE ELECTRONIC ENGINE CONTROL OF A TURBOPROP COMMUTER TRANSPORT
Peter Bootsma *In* NOAA, International Aerospace and Ground Conference on Lightning and Static Electricity Apr. 1988 p 192-19 (For primary document see N89-10429 01-47)
Avail: NTIS HC A23/MF A01 CSCL 01C

N89-10459# Electro Magnetic Applications, Inc., Lakewood, Colo.
INTERFERENCE OF PRECIPITATION STATIC DISCHARGES WITH AIRCRAFT NAVIGATIONAL SYSTEMS
Gregory J. Rigden *In* NOAA, International Aerospace and Ground Conference on Lightning and Static Electricity Apr. 1988 p 205-21 Sponsored in part by FAA, Atlantic City, N.J.; Lightning and Transients Research Inst., St. Paul, Minn. (For primary document see N89-10429 01-47)
(Contract DTFA03-84-C-00066)
Avail: NTIS HC A23/MF A01 CSCL 01C

N89-10460# New Mexico Inst. of Mining and Technology, Socorro.
ELECTRIFICATION OF HOVERING HELICOPTERS
C. B. Moore, Marx Brock, and Clyde N. Richards (Atmospheric Physics, Inc., Peralta, N. Mex.) *In* NOAA, International Aerospace and Ground Conference on Lightning and Static Electricity Apr. 1988 p 213-21 (For primary document see N89-10429 01-47)
Avail: NTIS HC A23/MF A01 CSCL 01C

N89-10461# Naval Research Lab., Washington, D.C. Plasma Physics Div.
MEASUREMENT OF THE ELECTROSTATIC CHARGING ON LARGE HELICOPTERS AND CONTROL OF THE SHOCK HAZARD
R. E. Pechacek, D. P. Murphy, and J. R. Greig (G-T Devices, Inc., Springfield, Va.) *In* NOAA, International Aerospace and Ground Conference on Lightning and Static Electricity Apr. 1988 p 218-22 (For primary document see N89-10429 01-47)
Avail: NTIS HC A23/MF A01 CSCL 01C

N89-10478*# National Aeronautics and Space Administration. Langley Research Center, Hampton, Va.
IMPLICATIONS OF A RECENT LIGHTNING STRIKE TO A NASA JET TRAINER
Bruce D. Fisher, Ralph J. Taeuber, and Keith E. Crouch (Lightning Technologies, Inc., Pittsfield, Mass.) *In* NOAA, International Aerospace and Ground Conference on Lightning and Static Electricity Apr. 1988 p 360-36 Previously announced in IAA as A88-22291 (For primary document see N89-10429 01-47)
Avail: NTIS HC A23/MF A01 CSCL 01C

N89-10483# Saab-Scania, Linkoping (Sweden).
FINITE DIFFERENCE ANALYSIS OF EXTERNAL AND INTERNAL LIGHTNING RESPONSE OF THE JAS39 CFC WING
Bo I. Wahlgren and Jonas W. Rosen *In* NOAA, International Aerospace and Ground Conference on Lightning and Static Electricity Apr. 1988 p 396-40 (For primary document see N89-10429 01-47)
Avail: NTIS HC A23/MF A01 CSCL 01C

N89-10485# Societe Nationale Industrielle Aerospatiale, Toulouse (France).
MODELLING OF COMMON MODE COUPLING BETWEEN AN AIRCRAFT WING TRAVERSED BY A LIGHTNING CURRENT AND WIRING INSTALLED IN THAT WING
Michel Crokaert *In* NOAA, International Aerospace and Ground Conference on Lightning and Static Electricity Apr. 1988 p 408-42 (For primary document see N89-10429 01-47)
Avail: NTIS HC A23/MF A01 CSCL 01C

N89-10492# Messerschmitt-Boelkow-Blohm G.m.b.H., Munich (West Germany).
INDIRECT EFFECTS ON ELECTRONIC AND MECHANICAL SYSTEMS INSTALLED IN CARBON FIBRE COMPOUND AIRCRAFT STRUCTURES
Rainer Strauss *In* NOAA, International Aerospace and Ground Conference on Lightning and Static Electricity Apr. 1988 p 470-48 (For primary document see N89-10429 01-47)
Avail: NTIS HC A23/MF A01 CSCL 01C

04 AIRCRAFT COMMUNICATIONS AND NAVIGATION

Includes digital and voice communication with aircraft; air navigation systems (satellite and ground based); and air traffic control.

For related information see also *17 Space Communications, Spacecraft Communications, Command and Tracking* and *Communications and Radar.*

N89-10038# Federal Aviation Administration, Washington, D.C. Advanced System Design Service.
TERMINAL CONTROL AREA DESIGN AND AIR TRAFFIC LOADINGS Final Report
Thomas H. Higgins Aug. 1988 34 p
(DOT/FAA/DS-88/11) Avail: NTIS HC A03/MF A01

The response probability density function (pdf) technique adapted here uses the pdf's of the variables governing both the air traffic loadings of stress and the terminal airspace design configurations sensitivty or strengths. This technique is proposed as a method which may be used to predict the relative level of safety and collision risk for TCA design configurations and air traffic loadings. For the first time, a strong relationship was found between near midair collision reports and midair collisions for annual operations within the fifty states. Operations, airports, and airspace area were found to relate to these criteria of safety and provide useful interactive predictor equations. Author

05 AIRCRAFT DESIGN, TESTING AND PERFORMANCE

Includes aircraft simulation technology.

For related information see also *18 Spacecraft Design, Testing and Performance* and *39 Structural Mechanics.* For land transportation vehicles see *85 Urban Technology and Transportation.*

N89-10039# Naval Postgraduate School, Monterey, Calif.
UNMANNED AIR VEHICLES - REAL TIME INTELLIGENCE WITHOUT THE RISK M.S. Thesis
James B. Miller Mar. 1988 77 p
(AD-A195199) Avail: NTIS HC A05/MF A01 CSCL 01C

Unmanned Air Vehicles (UAVs) are capable of supporting the officer in tactical command (OTC) by gathering intelligence in real- or near real-time. UAVs now under development will be able to collect high-resolution imagery, and thus provide the OTC with the option of gathering tactical intelligence without using manned reconnaissance platforms. This thesis asserts that UAVs should be used to supplement existing intelligence sensors, particularly in those cases where current sources are too ambiguous, slow, dangerous or take resources away from their primary duties. GRA

N89-10040# Materials Research Labs., Melbourne (Australia).
CONTAMINATION OF ENVIRONMENTAL CONTROL SYSTEMS IN HERCULES AIRCRAFT
A. G. Kelso, J. M. Charlesworth, and G. G. McVea Apr. 1988 27 p
(MRL-R-1116; AR-005-230) Copyright Avail: NTIS HC A03/MF A01

The assistance of MRL was requested by RAAF in determining the origins of contamination of turboprop bleed air used for environmental control in Hercules C-130 transport aircraft. Air sampling in the interior of affected planes was performed in-flight and on the ground, together with laboratory sampling of vapor from all suspect contaminating fluids. Gas chromatographic (GC) and GC/mass spectrometric (MS) analysis of collected samples confirmed that aviation turbine fuel leakage produces a continuous background of hydrocarbon vapor around 0.1 to 0.5 ppm in affected aircraft. Positive indications of turbine oil vapors were found in filter bags taken from the air-duct system of suspect aircraft. Some traces of organophosphorus compounds, particularly the tricresyl phosphate additive in the oil, were found in the air filter bags. However, at present there is no evidence to support a hypothesis that neurotoxic bicyclophosphorous compounds derived from the oil additive are present. It is strongly recommended that in addition to normal maintenance of turbine oil seals and fuel nozzles, the use of charcoal cloth filters in the air ducting system be investigated as a means of absorbing the noxious odors. Author

N89-10041# Lockheed Aeronautical Systems Co., Burbank, Calif.
WHEEL PERFORMANCE EVALUATION. PHASE 1: ANALYSIS Final Report
P. C. Durup, T. R. Brussat, and L. Bakow Sep. 1988 107 p
(DOT/FAA/CT-88/16) Avail: NTIS HC A06/MF A01

The procedures of analysis and dynamometer testing that may be used to develop data and supporting technology for improving aircraft wheel performance are described. As related to current wheel standards and in-service inspection procedures, load/test spectra which characterize wheel operating environments (associated with long, medium, and short haul aircraft) are defined. These spectra may be applied as a basis for effective dynamometer testing and to the verification of wheel service limits taking into account stress corrosion and crack growth conditions. Author

N89-10042# Technische Hogeschool, Delft (Netherlands). Dept. of Aerospace Engineering.
DESIGN AND EVALUATION OF DYNAMIC FLIGHT TEST MANOEUVERES
J. A. Mulder Oct. 1986 305 p
(PB88-210760; LR-497) Avail: NTIS HC A14/MF A01 CSCL 01C

Analysis of dynamic flight test data, in the sense of estimating stability and control derivaties from measurements of the dynamic response of the aircraft to control input signals, can be formulated in the theoretical frame work of maximum likelihood estimation theory. It is shown that, if certain conditions concerning accuracy and type of the variables measured in flight are met, the original maximum likelihood estimation problem can be decomposed into two separate estimation problems which are much easier to solve than the original estimation problem. A new technique for the calculation of optimal input signals was developed. The technique is based on the description of input singals by linear combinations of elements of finite sets of orthonormal functions. A flight test program was carried out with a DeHaviland DHC-2 Beaver experimental aircraft, equiped with an automatic control system. The system allowed precise implementation in real time of quite arbitrary elevator, aileron and rudder control input signals. Also a high accuracy flight test measurement system was installed in the aircraft. Author

N89-10056# Societe Nationale Industrielle Aerospatiale, Paris (France). Tactical Missile Div.
SIMULATION WITH REAL ELEMENTS OF EXOCET ANTI-SHIP MISSILES [SIMULATION AVEC ELEMENTS REELS DES MISSILES ANTI-NAVIRES EXOCET]
Christiane Renon, Guy leGallo, and Gerard Selince *In* AGARD, Guidance and Control Systems Simulation and Validation Techniques Jul. 1988 9 p In FRENCH (For primary document see N89-10048 01-08)
Copyright Avail: NTIS HC A07/MF A01

N89-10057# Rockwell International Corp., Columbus, Ohio.
HELLFIRE SYSTEM MODEL VALIDATION
R. V. Hupp *In* AGARD, Guidance and Control Systems Simulation and Validation Techniques Jul. 1988 13 p (For primary document see N89-10048 01-08)
Copyright Avail: NTIS HC A07/MF A01

06 AIRCRAFT INSTRUMENTATION

Includes cockpit and cabin display devices; and flight instruments.

For related information see also *19 Spacecraft Instrumentation* and *35 Instrumentation and Photography.*

No abstracts in this category.

07 AIRCRAFT PROPULSION AND POWER

Includes prime propulsion systems and systems components, e.g., gas turbine engines and compressors; and onboard auxilliary power plants for aircraft.

For related information see also *20 Spacecraft Propulsion and Power, 28 Propellants and Fuels,* and *44 Energy Production and Conversion.*

N89-10043*# National Aeronautics and Space Administration. Lewis Research Center, Cleveland, Ohio.
VIBRATION, PERFORMANCE, FLUTTER AND FORCED RESPONSE CHARACTERISTICS OF A LARGE-SCALE PROPFAN AND ITS AEROELASTIC MODEL
Richard August (Sverdrup Technology, Inc., Cleveland, Ohio.) and Krishna Rao V. Kaza 1988 28 p Presented at the 24th Joint Propulsion Conference, Boston, Mass., 11-13 Jul. 1988; sponsored by AIAA, ASME, SAE and ASEE
(NASA-TM-101322; E-4260; NAS 1.15:101322; AIAA-88-3155) Avail: NTIS HC A03/MF A01 CSCL 21E

An investigation of the vibration, performance, flutter, and forced response of the large-scale propfan, SR7L, and its aeroelastic model, SR7A, has been performed by applying available structural and aeroelastic analytical codes and then correlating measured and calculated results. Finite element models of the blades were used to obtain modal frequencies, displacements, stresses and strains. These values were then used in conjunction with a 3-D, unsteady, lifting surface aerodynamic theory for the subsequent aeroelastic analyses of the blades. The agreement between measured and calculated frequencies and mode shapes for both models is very good. Calculated power coefficients correlate well with those measured for low advance ratios. Flutter results show that both propfans are stable at their respective design points. There is also good agreement between calculated and measured blade vibratory strains due to excitation resulting from yawed flow for the SR7A propfan. The similarity of structural and aeroelastic results show that the SR7A propfan simulates the SR7L characteristics. Author

N89-10044# Air Force Wright Aeronautical Labs., Wright-Patterson AFB, Ohio.
A COMPARATIVE EVALUATION OF RPD (ROTARY PARTICLE DEPOSITOR) AND FERROGRAPHIC DIAGNOSTIC METHODS FOR TURBINE ENGINE LUBRICANT SAMPLES Final Report, 12 May - 30 Sep. 1987
Robert L. Wright Mar. 1988 28 p
(AD-A196207; AFWAL-TR-88-2020) Avail: NTIS HC A03/MF A01 CSCL 11H

A Rotary Particle Depositor (RPD) was evaluated and compared to analytical (AF) and direct reading (DR) ferrographs to ascertain if the RPD is better suited for analysis of wear debris in turbine engine lubricant samples than the AF and DR. Experimentally, sieved iron particles were added to synthetic turbine engine lubricants at various concentrations and analyzed by RPD and ferrographic methods and compared. Also, lubricant samples containing a fine test dust were analyzed by RPD and AF to determine the effectiveness of the RPD's centripetal acceleration and the AF's gravity flow in eliminating non-ferrous contamination from the sample. Finally, actual lubricant samples from a turbine engine simulator were analyzed by RPD and ferrographic methods and compared. For lubricant samples with relatively small amounts of non-ferrous contamination or samples where non-ferrous particles are important in machine health condition assessment, the AF and DR ferrographs are equal or superior to RPD for lubricant analyses. GRA

N89-10045*# Queensland Univ., St. Lucia (Australia). Dept. of M. E.
SHOCK TUNNEL STUDIES OF SCRAMJET PHENOMENA Final Report
R. G. Morgan, A. Paull, R. J. Stalker, P. Jacobs, N. Morris, I. Stringer, and C. Brescianini Sep. 1988 16 p
(Grant NAGw-674)
(NASA-CR-181721; NAS 1.26:181721) Avail: NTIS HC A03/MF A01 CSCL 21E

Commissioning of the new T4 shock tunnel at the University of Queensland implied that it was no longer necessary to focus the work of the research group about an annual test series conducted in the T3 shock tunnel in Canberra. Therefore, it has been possible to organize a group for work to proceed along lines such that particular personnel are associated with particular project areas. The format of this report consists of a series of reports on specific project areas, with a brief general introduction commenting on each report. The introduction is structured by project areas, with the title of the relevant report stated under the project area heading. The reports themselves follow in the order of the project area headings. Author

N89-10008# Imperial Coll. of Science and Technology, London (England).
STRUCTURAL DYNAMIC CHARACTERISTICS OF INDIVIDUAL BLADES
D. J. Ewins and R. Henry (Institut National des Sciences Appliquees, Lyon, France) *In* AGARD, AGARD Manual on Aeroelasticity in Axial-Flow Turbo Machines. Volume 2: Structural Dynamics and Aeroelasticity Jun. 1988 27 p (For primary document see N89-10006 01-02)
Copyright Avail: NTIS HC A12/MF A01

N89-10009# Imperial Coll. of Science and Technology, London (England). Dept. of Mechanical Engineering.
STRUCTURAL DYNAMIC CHARACTERISTICS OF BLADED ASSEMBLIES
D. J. Ewins *In* AGARD, AGARD Manual on Aeroelasticity in Axial-Flow Turbo Machines. Volume 2: Structural Dynamics and Aeroelasticity Jun. 1988 37 p (For primary document see N89-10006 01-02)
Copyright Avail: NTIS HC A12/MF A01

N89-10010# Rolls-Royce Ltd., Bristol (England).
FATIGUE AND ASSESSMENT METHODS OF BLADE VIBRATION
E. K. Armstrong *In* AGARD, AGARD Manual on Aeroelasticity in Axial-Flow Turbo Machines. Volume 2: Structural Dynamics and Aeroelasticity Jun. 1988 34 p (For primary document see N89-10006 01-02)
Copyright Avail: NTIS HC A12/MF A01

N89-10011# Office National d'Etudes et de Recherches Aeronautiques, Paris (France).
LIFE TIME PREDICTION: SYNTHESIS ON ONERA's RESEARCH IN VISCOPLASTICITY AND CONTINUOUS DAMAGE MECHANICS, APPLIED TO ENGINE MATERIALS AND STRUCTURES

R. Labourdette *In* AGARD, AGARD Manual on Aeroelasticity in Axial-Flow Turbo Machines. Volume 2: Structural Dynamics and Aeroelasticity Jun. 1988 15 p (For primary document see N89-10006 01-02)
Copyright Avail: NTIS HC A12/MF A01

N89-10012# United Technologies Research Center, East Hartford, Conn.
AEROELASTIC COUPLING: AN ELEMENTARY APPROACH
Franklin O. Carta *In* AGARD, AGARD Manual on Aeroelasticity in Axial-Flow Turbo Machines. Volume 2: Structural Dynamics and Aeroelasticity Jun. 1988 16 p (For primary document see N89-10006 01-02)
Copyright Avail: NTIS HC A12/MF A01

N89-10013# Massachusetts Inst. of Tech., Cambridge. Gas Turbine Lab.
AEROELASTIC FORMULATION FOR TUNED AND MISTUNED ROTORS
Edward F. Crawley *In* AGARD, AGARD Manual on Aeroelasticity in Axial-Flow Turbo Machines. Volume 2: Structural Dynamics and Aeroelasticity Jun. 1988 24 p (For primary document see N89-10006 01-02)
Copyright Avail: NTIS HC A12/MF A01

N89-10014# Pratt and Whitney Aircraft, East Hartford, Conn.
FAN FLUTTER TEST
Hans Stargardter *In* AGARD, AGARD Manual on Aeroelasticity in Axial-Flow Turbo Machines. Volume 2: Structural Dynamics and Aeroelasticity Jun. 1988 35 p (For primary document see N89-10006 01-02)
Copyright Avail: NTIS HC A12/MF A01

N89-10015# Jeffers (James D., III), Tampa, Fla.
AEROELASTIC THERMAL EFFECTS
James D. Jeffers, III *In* AGARD, AGARD Manual on Aeroelasticity in Axial-Flow Turbo Machines. Volume 2: Structural Dynamics and Aeroelasticity Jun. 1988 6 p (For primary document see N89-10006 01-02)
Copyright Avail: NTIS HC A12/MF A01

08 AIRCRAFT STABILITY AND CONTROL

Includes aircraft handling qualities; piloting; flight controls; and autopilots.

For related information see also *05 Aircraft Design, Testing and Performance.*

N89-10046*# Manudyne Systems, Inc., Los Altos, Calif.
HELICOPTER ROLL CONTROL EFFECTIVENESS CRITERIA PROGRAM SUMMARY Final Contractor Report, Jul. 1983 - Jul. 1987
Robert K. Heffley, Simon M. Bourne, and Marc A. Mnich Apr. 1988 103 p Prepared for Army Research and Technology Labs., Moffett Field, Calif.
(Contract NAS2-11665)
(NASA-CR-177477; NAS 1.26:177477; USAAVSCOM-TR-87-A-13) Avail: NTIS HC A06/MF A01 CSCL 01C

A study of helicopter roll control effectiveness is summarized for the purpose of defining military helicopter handling qualities requirements. The study is based on an analysis of pilot-in-the-loop task performance of several basic maneuvers. This is extended by a series of piloted simulations using the NASA Ames Vertical Motion Simulator and selected flight data. The main results cover roll control power and short-term response characteristics. In general the handling qualities requirements recommended are set in conjunction with desired levels of flight task and maneuver response which can be directly observed in actual flight. An important aspect of this, however, is that vehicle handling qualities need to be set with regard to some quantitative aspect of mission performance. Specific examples of how this can be accomplished include a lateral unmask/remask maneuver in the presence of a threat and an air tracking maneuver which recognizes the kill probability enhancement connected with decreasing the range to the target. Conclusions and recommendations address not only the handling qualities recommendations, but also the general use of flight simulators and the dependence of mission performance on handling qualities. Author

N89-10047# National Aerospace Lab., Tokyo (Japan).
FUNCTIONAL MOCK-UP TESTS OF THE FLIGHT CONTROL SYSTEM OF THE NAL QSTOL RESEARCH AIRCRAFT: PLANNING AND MECHANICAL SYSTEM TEST
Sep. 1987 56 p In JAPANESE; ENGLISH summary
(NAL-TR-944; ISSN-0389-4010) Avail: NTIS HC A04/MF A01

The control system of the National Aerospace Laboratory Quiet-STOL Research Aircraft has a mechanical control system and a triplex digital Stability and Control Augmentation System (SCAS). The mechanical system is responsible for the safety control system, while the digital SCAS system was to be evaluated through experiments. Functional mock-up tests were carried out to check safety and performance of the total control system using actual system component hardware and simulating aerodynamic and mechanical environmental conditions. The mechanical system dynamics test and the total plan for the functional mock-up test are described as the fundamental process to ensure minimum safety requirements of the system component matching. The static and dynamic characteristics of the mechanical control system showed good agreement with the specifications of Japanese Airworthiness Standards (equivalent to FAR25) and MIL. Author

N89-10048# Advisory Group for Aerospace Research and Development, Neuilly-Sur-Seine (France). Guidance and Control Panel.
GUIDANCE AND CONTROL SYSTEMS SIMULATION AND VALIDATION TECHNIQUES
William P. Albritton, Jr., ed. (Amtec, Inc., Athens, Ala.) Jul. 1988 133 p In ENGLISH and FRENCH
(AGARD-AG-273; ISBN-92-835-0472-0) Copyright Avail: NTIS HC A07/MF A01

This AGARDograph addresses simulation and validation techniques for guidance and control systems of tactical guided weapons. Many developments have taken place over the last few years. In particular, physical simulation using hybrid, hardware-in-the-loop techniques has assumed much more importance. The chapter on digital simulation techniques provides descriptions of digital simulation techniques for application to some of the more difficult aspects of tactical guided weapon guidance and control systems. Concerning hardware-in-the-loop (HITL) simulation techniques, descriptions are provided of facility design techniques for performing HITL simulation and particular information on radar simulation techniques. System Simulation and Validation Experience presenting lessons learned type information from some of the major programs are examined. The application of the techniques to guided weapon developments is presented. For individual titles, see N89-10049 through N89-10057.

N89-10049# Raytheon Co., Bedford, Mass. Missile Systems Div.
COMPARISON OF STATISTICAL DIGITAL SIMULATION METHODS **c61**
Paul Zarchan *In* AGARD, Guidance and Control Systems Simulation and Validation Techniques Jul. 1988 16 p (For primary document see N89-10048 01-08)
Copyright Avail: NTIS HC A07/MF A01

The various statistical digital simulation methods used in the preliminary analysis and synthesis of a homing missile guidance system are compared. A unifying example is used to illustrate the advantages and computer costs of each of the methods. Author

N89-10050# Dynetics, Inc., Huntsville, Ala.
A GENERIC SEEKER SIMULATION FOR THE EVALUATION OF ACTIVE RF GUIDANCE SYSTEMS **c61**
Frank T. Campos *In* AGARD, Guidance and Control Systems

Simulation and Validation Techniques Jul. 1988 9 p (For primary document see N89-10048 01-08)
(Contract F08635-83-C-0123)
Copyright Avail: NTIS HC A07/MF A01

The essential features of a generic simulation of an active radio frequency (RF) air-to-air missile seeker is described. The concept of generic simulations is supported by the need for a common test-bed of system models and simulation technology capable of supporting advanced seeker development programs. An extensive library of target, environment, and RF seeker models was incorporated within a modular program structure featuring tri-level hierarchy of program control that allows the selective management of program options for specifying the fidelity and functional implementation of models used at the component, subsystem, and system levels. The Generic Seeker Simulation offers considerable flexibility for simulating a broad range of RF seeker configurations and has a significant potential for supporting the evaluation of competitive designs and advanced seeker technologies. Author

N89-10051# Magnavox Electronic Systems Co., Fort Wayne, Ind. Control Systems Operation.
DIGITAL SIMULATION TECHNIQUES FOR END GAME PHENOMENA **c61**
Martin E. Tanenhaus and Duane J. Cart *In* AGARD, Guidance and Control Systems Simulation and Validation Techniques Jul. 1988 37 p (For primary document see N89-10048 01-08)
Copyright Avail: NTIS HC A07/MF A01

This report is based on efforts to develop a color graphics based analytical methodology for determining end game performance of smart sensors on missiles and projectiles. These sensor systems defend against present and future target threats. The development of a computer based methodology to define and test weapon system sensor performance requirements, predict end game sensor and fuze burst point distributions, assess weapon system effectiveness, and evaluate advanced weapons design concepts is presented. A graphics driven target modeling methodology is presented, together with verification, correlation, and validation techniques. A complex radar target model with detailed graphics, radar cross section (RCS), glint, imagery analysis, and target Doppler signature output was developed. A sensor system signal processor model is developed and exercised with the target model to provide system performance assessments. Verifiable correlation between system model performance and real hardware was obtained. End game system function results are utilized in a weapons effectiveness simulation and appraisal. Author

N89-10052# Raytheon Co., Bedford, Mass.
DESIGN CRITERIA FOR HARDWARE-IN-THE-LOOP SIMULATION FACILITIES **c61**
S. J. Powers and M. E. Sisle *In* AGARD, Guidance and Control Systems Simulation and Validation Techniques Jul. 1988 10 p (For primary document see N89-10048 01-08)
Copyright Avail: NTIS HC A07/MF A01

The criteria used in the design of a Hardware-in-the-Loop (HIL) simulation facility are outlined. Although dealing with a missile interceptor facility, the criteria are directly applicable to any electronic weapon system simulation facility. The first step in the process is defining the role that the facility will play in the development cycle. Facility requirements which drive the model and data requirements are then defined and the facility design follows from the requirements. Following completion of the facility development is the conduct of system integration tests. Verification/validation criteria are established and met, the process is complete, allowing the facility operation to begin. Facility operation and maintenance become ongoing functions. Author

N89-10053# Boeing Aerospace Co., Seattle, Wash.
COST EFFECTIVE SIMULATION FOR MILLIMETER WAVE GUIDANCE SYSTEMS
Vance H. Maples and George A. Eastman *In* AGARD, Guidance and Control Systems Simulation and Validation Techniques Jul. 1988 7 p (For primary document see N89-10048 01-08)
Copyright Avail: NTIS HC A07/MF A01

The introduction of millimeter wave (MMw) active-passive, air-to-surface missile seeker systems to counter the European armor threat has increased the need for simulators to evaluate the performance of this class of seeker. Existing simulation techniques have not proved to be cost effective, and are generally unable to obtain sufficient target spatial position control at millimeter wave frequencies to ensure high fidelity simulations. The conventional approach to simulating a target for seeker testing is to build a transponder which receives the transmitted signal to the seeker, delays it to represent range, modulates it to simulate the intended target signal, and retransmits it through an antenna array which positions the target spatially. Target modeling and position control are implemented using simulation components at the radar frequency. A concept for target simulation for FM/WC modulated radar sensors, uses the signal from the seeker transmitted to illuminate an array of target antennas. This radar scene simulation technique provides a lower cost simulation method for evaluating FM/WC modulated millimeter wave seekers. This technique is equally effective for pulse modulated seeker simulation when a millimeter wave illuminating source is added to the system. In either case, it significantly reduces the high-cost/marginal-performance millimeter wave hardware required in the simulator and can be applied to evaluation of both active and passive seeker modes. Author

N89-10054# Boeing Aerospace Co., Seattle, Wash.
RANGE DELAY TECHNIQUES FOR RADAR TARGET SIMULATORS **c09**
Leland C. Buse *In* AGARD, Guidance and Control Systems Simulation and Validation Techniques Jul. 1988 9 p (For primary document see N89-10048 01-08)
Copyright Avail: NTIS HC A07/MF A01

It was recognized that the Radar Guided Seeker and countermeasure development using flight tests as a primary evaluation tool is costly and insecure from interception of signal and telemetry emenations. Radar Target Simulators were developed which provide the capability both to evaluate actual radar guided seeker hardware and software and to evaluate countermeasures against the actual seeker hardware in a secure environment. Experience with these simulators has demonstrated that with adequate simulator hardware, valid closed-loop performance evaluations can be conducted which will accurately reflect flight test performance. A critical issue in the implementation of such systems is the simulation of radar pulse range delay. This must be accomplished with sufficient fidelity to represent a range-delayed target of ECM signal credible to modern seeker signal processors. Various range delay techniques as applied to Radar Target Simulators are presented. In particular, a digital approach to the solution of the range delay problem is developed from basic concepts through actual hardware implementation. Author

N89-10055# Raytheon Co., Bedford, Mass.
SIMULATION VALIDATION EXPERIENCE: PATRIOT GUIDANCE SYSTEM
William C. Morton *In* AGARD, Guidance and Control Systems Simulation and Validation Techniques Jul. 1988 11 p (For primary document see N89-10048 01-08)
Copyright Avail: NTIS HC A07/MF A01

The increased use of sophisticated simulations as performance prediction tools during the development of guided missiles has placed greater emphasis on comprehensive validation of the models used. Validation of several simulations was accomplished by Raytheon Company while developing the Army's PATRIOT air defense system. The validation experience is presented for two large-scale guidance simulations; the Hybrid Guidance System Simulation and the Guidance Test and Simulation Facility. Examples of the data collected are presented in the course of discussing the approach to validating all mathematical as well as

hardware-in-the-loop simulations. Conclusions are drawn as to the most effective methods and the value of the validation process to the overall system development. Author

N89-10056# Societe Nationale Industrielle Aerospatiale, Paris (France). Tactical Missile Div.
SIMULATION WITH REAL ELEMENTS OF EXOCET ANTI-SHIP MISSILES [SIMULATION AVEC ELEMENTS REELS DES MISSILES ANTI-NAVIRES EXOCET] **c05**
Christiane Renon, Guy leGallo, and Gerard Selince *In* AGARD, Guidance and Control Systems Simulation and Validation Techniques Jul. 1988 9 p In FRENCH (For primary document see N89-10048 01-08)
Copyright Avail: NTIS HC A07/MF A01

Simulation results gained on the first 1500 production anti-ship missiles of the EXOCET family (MM 38, MM 40, AM 39, SM 39) are presented. After describing the simulation facilities of the tactical missile division of Aerospatiale and in particular Subdray facility located near Bourges in France, the role of simulation is shown from the beginning of the project, through development up to the production of the missiles. The advantage of such simulation during the production phase is emphasized. It is used to improve the quality of missiles, to gain knowledge useful for the development of new versions and as a quality insurance method during production. Author

N89-10057# Rockwell International Corp., Columbus, Ohio.
HELLFIRE SYSTEM MODEL VALIDATION **c05**
R. V. Hupp *In* AGARD, Guidance and Control Systems Simulation and Validation Techniques Jul. 1988 13 p (For primary document see N89-10048 01-08)
Copyright Avail: NTIS HC A07/MF A01

The hybrid simulation facilities, system modeling, and validation process for a U.S. Army missile development program are discussed. Two fundamental problems in missile system design and development require an accurate, valid, proven computer simulation; analysis of errors and performance verification. The classical approach to error analysis is by Monte Carlo simulation. System performance over the entire spectrum of operating conditions cannot be verified by field tests alone due to economic constraints; it must be verified by simulation. Verification of total system performance was a major analytical effort in the development program. A complete hybrid computing facility was procured and dedicated to this end. Two independent system simulations were developed; a hybrid simulation and an all digital simulation. The development program was very successful. The computer simulation equipment procured for this effort was found to be quite adequate for the task and cost effective. Author

N89-10058*# Lockheed-Georgia Co., Marietta.
QUADRUPLEX DIGITAL FLIGHT CONTROL SYSTEM ASSESSMENT Final Report
D. B. Mulcare, L. E. Downing, and M. K. Smith Jul. 1988 68 p (Contract NAS2-11853)
(NASA-CR-182741; NAS 1.26:182741; DOT/FAA/CT-86/30-Rev) Avail: NTIS HC A04/MF A01 CSCL 01C

Described are the development and validation of a double fail-operational digital flight control system architecture for critical pitch axis functions. Architectural tradeoffs are assessed, system simulator modifications are described, and demonstration testing results are critiqued. Assessment tools and their application are also illustrated. Ultimately, the vital role of system simulation, tailored to digital mechanization attributes, is shown to be essential to validating the airworthiness of full-time critical functions such as augmented fly-by-wire systems for relaxed static stability airplanes. Author

N89-10059*# National Aeronautics and Space Administration. Langley Research Center, Hampton, Va.
DEVELOPMENT IN HELICOPTER TAIL BOOM STRAKE APPLICATIONS IN THE US
John C. Wilson, Henry L. Kelley, Cynthia C. Donahue, and Kenneth R. Yenni Oct. 1988 19 p Prepared for presentation at the International Conference on Helicopter Handling Qualities and Control, London, England, 15-17 Nov. 1988
(NASA-TM-101496; NAS 1.15:101496; AVSCOM-TM-88-B-014) Avail: NTIS HC A03/MF A01 CSCL 01C

The use of a strake or spoiler on a helicopter tail boom to beneficially change helicopter tail boom air loads was suggested in the United States in 1975. The anticipated benefits were a change of tail boom loads to reduce required tail rotor thrust and power and improve directional control. High tail boom air loads experienced by the YAH-64 and described in 1978 led to a wind tunnel investigation of the usefullness of strakes in altering such loads on the AH-64, UH-60, and UH-1 helicopters. The wind tunnel tests of 2-D cross sections of the tail boom of each demonstrated that a strake or strakes would be effective. Several limited test programs with the U.S. Army's OH-58A, AH-64, and UH-60A were conducted which showed the effects of strakes were modest for those helicopters. The most recent flight test program, with a Bell 204B, disclosed that for the 204B the tail boom strake or strakes would provide more than a modest improvement in directional control and reduction in tail rotor power. Author

09 RESEARCH AND SUPPORT FACILITIES (AIR)

Includes airports, hangars and runways; aircraft repair and overhaul facilities; wind tunnels; shock tubes; and aircraft engine test stands.

For related information see also *14 Ground Support Systems and Facilities (Space).*

N89-10060*# National Aeronautics and Space Administration. Langley Research Center, Hampton, Va.
HIGHLIGHTS OF EXPERIENCE WITH A FLEXIBLE WALLED TEST SECTION IN THE NASA LANGLEY 0.3-METER TRANSONIC CRYOGENIC TUNNEL
Stephen W. D. Wolf (Vigyan Research Associates, Inc., Hampton, Va.) and Edward J. Ray Sep. 1988 12 p Previously announced in IAA as A88-37938
(NASA-TM-101491; NAS 1.15:101491) Avail: NTIS HC A03/MF A01 CSCL 14B

The unique combination of adaptive wall technology with a contonuous flow cryogenic wind tunnel is described. This powerful combination allows wind tunnel users to carry out 2-D tests at flight Reynolds numbers with wall interference essentially eliminated. Validation testing was conducted to support this claim using well tested symmetrical and cambered airfoils at transonic speeds and high Reynolds numbers. The test section hardware has four solid walls, with the floor and ceiling flexible. The method of adapting/shaping the floor and ceiling to eliminate top and bottom wall interference at its source is outlined. Data comparisons for different size models tested and others in several sophisticated 2-D wind tunnels are made. In addition, the effects of Reynolds number, testing at high lift with associated large flexible wall movements, the uniqueness of the adapted wall shapes, and the effects of sidewall boundary layer control are examined. The 0.3-m TCT is now the most advanced 2-D research facility anywhere. Author

N89-10061*# Southampton Univ. (England). Dept. of Aeronautics and Astronautics.
AN INVESTIGATION INTO FORCE-MOMENT CALIBRATION TECHNIQUES APPLICABLE TO A MAGNETIC SUSPENSION AND BALANCE SYSTEM M.S. Thesis
Jonathan Eskins Aug. 1988 207 p
(Grant NsG-7523)
(NASA-CR-181695; NAS 1.26:181695; AASU-88/4) Avail: NTIS HC A10/MF A01 CSCL 14B

The problem of determining the forces and moments acting on a wind tunnel model suspended in a Magnetic Suspension and Balance System is addressed. Two calibration methods were investigated for three types of model cores, i.e., Alnico, Samarium-Cobalt, and a superconducting solenoid. Both methods

involve calibrating the currents in the electromagnetic array against known forces and moments. The first is a static calibration method using calibration weights and a system of pulleys. The other method, dynamic calibration, involves oscillating the model and using its inertia to provide calibration forces and moments. Static calibration data, found to produce the most reliable results, is presented for three degrees of freedom at 0, 15, and -10 deg angle of attack. Theoretical calculations are hampered by the inability to represent iron-cored electromagnets. Dynamic calibrations, despite being quicker and easier to perform, are not as accurate as static calibrations. Data for dynamic calibrations at 0 and 15 deg is compared with the relevant static data acquired. Distortion of oscillation traces is cited as a major source of error in dynamic calibrations. Author

N89-10062# Sandia National Labs., Albuquerque, N. Mex.
THE RADIATION-HARDENED INTEGRATED CIRCUIT (RHIC) LABORATORY: PURSUIT OF CLASS 1
M. DeWitte 1988 12 p Presented at the 9th Annual International Symposium on Contamination Control, Los Angeles, Calif., 26 Sep. 1988
(Contract DE-AC04-76DP-00789)
(DE88-006640; SAND-88-0545C; CONF-880933-1) Avail: NTIS HC A03/MF A01

The Radiation-Hardened Integrated Circuit (RHIC) Laboratory is a research and development facility operated by Sandia National Laboratories for the Department of Energy. This report describes the features of the laboratory in detail. The facility is operated by the Center for Radiation-Hardened Microelectronics (CRM) and supports government clients with the rapid development and pilot production of radiation-hardened ULSI microelectronics. More than 25 years after Sandia's Willis Whitfield invented the first vertical laminar flow clean room, Sandia National Laboratories has once again taken the lead in clean room technology with the design and construction of the RHIC facility. The building was designed to support wafer fabrication of ULSI integrated circuits through the 1990's. The facility consists of 12,000 s.f. (net) Ultra-Clean Room in a bay and chase configuration. The 174,000 s.f. building houses the majority of the Sandia CRM with 62,000 s.f. dedicated to office and light laboratory, 46,000 s.f. allocated for the clean room bay, chase and equipment repair/service area with the remaining 66,000 s.f. required for central plant and process support space. DOE

N89-10054# Boeing Aerospace Co., Seattle, Wash.
RANGE DELAY TECHNIQUES FOR RADAR TARGET SIMULATORS
Leland C. Buse *In* AGARD, Guidance and Control Systems Simulation and Validation Techniques Jul. 1988 9 p (For primary document see N89-10048 01-08)
Copyright Avail: NTIS HC A07/MF A01

12 ASTRONAUTICS (GENERAL)

For extraterrestrial exploration see *91 Lunar and Planetary Exploration.*

N89-10063*# National Aeronautics and Space Administration. Goddard Space Flight Center, Greenbelt, Md.
PROCEEDINGS OF 1987 GODDARD CONFERENCE ON SPACE APPLICATIONS OF ARTIFICIAL INTELLIGENCE (AI) AND ROBOTICS
Ellen G. Stolarik, ed., Ronald G. Littlefield, ed., and David S. Beyer, ed. 1987 718 p Conference held in Greenbelt, Md., 13-14 May 1987
(NASA-TM-89663; NAS 1.15:89663) Avail: NTIS HC A99/MF E03 CSCL 22A

Topics addressed include: planning/scheduling expert systems; fault isolation/diagnosis expert systems; data processing/analysis expert systems; expert system tools/techniques; and robotics. For individual titles, see N89-10064 through N89-10105.

N89-10064*# National Aeronautics and Space Administration. Ames Research Center, Moffett Field, Calif.
MAINTAINING AN EXPERT SYSTEM FOR THE HUBBLE SPACE TELESCOPE GROUND SUPPORT c89
Kelly Lindenmayer, Shon Vick (Space Telescope Science Inst., Baltimore, Md.), and Don Rosenthal *In* NASA, Goddard Space Flight Center, Proceedings of 1987 Goddard Conference on Space Applications of Artificial Intelligence (AI) and Robotics 1987 p 1-1 (For primary document see N89-10063 01-12)
Avail: NTIS HC A99/MF E03 CSCL 03A

The transformation portion of the Hubble Space Telescope (HST) Proposal Entry Processor System converts astronomer-oriented description of a scientific observing program into a detailed description of the parameters needed for planning and scheduling. The transformation system is one of a very few rulebased expert systems that has ever entered an operational phase. The day to day operations of the system and its rulebase are no longer the responsibility of the original developer. As a result, software engineering properties of the rulebased approach become more important. Maintenance issues associated with the coupling of rules within a rulebased system are discussed and a method is offered for partitioning a rulebase so that the amount of knowledge needed to modify the rulebase is minimized. This method is also used to develop a measure of the coupling strength of the rulebase. Author

N89-10065*# Bendix Field Engineering Corp., Lanham, Md.
AN EXPERT SYSTEM FOR SCHEDULING REQUESTS FOR COMMUNICATIONS LINKS BETWEEN TDRSS AND ERBS c32
David R. McLean, Ronald G. Littlefield, and David S. Beyer *In* NASA, Goddard Space Flight Center, Proceedings of 1987 Goddard Conference on Space Applications of Artificial Intelligence (AI) and Robotics 1987 16 p Previously announced in IAA as A88-20485 (For primary document see N89-10063 01-12)
Avail: NTIS HC A99/MF E03 CSCL 17B

An ERBS-TDRSS Contact Planning System (ERBS-TDRSS CPS) is described which uses a graphics interface and the NASA Transportable Interference Engine. The procedure involves transfer of the ERBS-TDRSS Ground Track Orbit Prediction data to the ERBS flight operations area, where the ERBS-TDRSS CPS automatically generates requests for TDRSS service. As requested events are rejected, alternative context sensitive strategies are employed to generate new requested events until a schedule is completed. A report generator builds schedule requests for separate ERBS-TDRSS contacts. IAA

N89-10066*# Ford Aerospace and Communications Corp., College Park, Md. Space Station Programs.
THE MISSION OPERATIONS PLANNING ASSISTANT c81
James G. Schuetzle *In* NASA, Goddard Space Flight Center, Proceedings of 1987 Goddard Conference on Space Applications of Artificial Intelligence (AI) and Robotics 1987 16 p Previously announced in IAA as A88-20484 (For primary document see N89-10063 01-12)
Avail: NTIS HC A99/MF E03 CSCL 05A

The Mission Operations Planning Assistant (MOPA) is a knowledge-based system developed to support the planning and scheduling of instrument activities on the Upper Atmospheric Research Satellite (UARS). The MOPA system represents and maintains instrument plans at two levels of abstraction in order to keep plans comprehensible to both UARS Prinicpal Investigators and Command Management personnel. The hierarchical representation of plans also allows MOPA to automatically create detailed instrument activity plans from which spacecraft command loads may be generated. The MOPA system was developed on a Symbolics 3640 computer using the ZETALISP and ART languages. MOPA's features include a textual and graphical interface for plan inspection and modification, recognition of instrument operational constraint violations during the planning process, and consistency maintenance between the different planning levels. This paper describes the current MOPA system. IAA

N89-10067*# National Aeronautics and Space Administration. Langley Research Center, Hampton, Va.
AUTOPLAN: A PC-BASED AUTOMATED MISSION PLANNING TOOL
Frank C. Paterra, Marc S. Allen (Computer Technology Associates, Inc., Newport News, Va.), and George F. Lawrence *In* NASA, Goddard Space Flight Center, Proceedings of 1987 Goddard Conference on Space Applications of Artificial Intelligence (AI) and Robotics 1987 16 p Previously announced in IAA as A88-20486 (For primary document see N89-10063 01-12)
Avail: NTIS HC A99/MF E03 CSCL 22A

A PC-based automated mission and resource planning tool, AUTOPLAN, is described, with application to small-scale planning and scheduling systems in the Space Station program. The input is a proposed mission profile, including mission duration, number of allowable slip periods, and requirement profiles for one or more resources as a function of time. A corresponding availability profile is also entered for each resource over the whole time interval under study. AUTOPLAN determines all integrated schedules which do not require more than the available resources. IAA

N89-10068*# Jet Propulsion Lab., California Inst. of Tech., Pasadena.
PLAN-IT: SCHEDULING ASSISTANT FOR SOLAR SYSTEM EXPLORATION
William C. Dias (ITT Federal Electric Corp., Vandenberg AFB, Calif.), Julia A. Henricks, and Jennifer C. Wong *In* NASA, Goddard Space Flight Center, Proceedings of 1987 Goddard Conference on Space Applications of Artificial Intelligence (AI) and Robotics 1987 16 p Previously announced in IAA as A88-20487 (For primary document see N89-10063 01-12)
Avail: NTIS HC A99/MF E03 CSCL 22A

A frame-based expert scheduling system shell, PLAN-IT, is developed for spacecraft scheduling in the Request Integration Phase, using the Comet Rendezvous Asteroid Flyby (CRAF) mission as a development base. Basic, structured, and expert scheduling techniques are reviewed. Data elements such as activity representation and resource conflict representation are discussed. Resource constraints include minimum and maximum separation times between activities, percentage of time pointed at specific targets, and separation time between targeted intervals of a given activity. The different scheduling technique categories and the rationale for their selection are also considered. IAA

N89-10069*# Contel Federal Systems, Inc., Gaithersburg, Md.
AN EXPERT SYSTEM THAT PERFORMS A SATELLITE STATION KEEPIMG MANEUVER **c81**
M. Kate LinesBrowning and John L. Stone, Jr. *In* NASA, Goddard Space Flight Center, Proceedings of 1987 Goddard Conference on Space Applications of Artificial Intelligence (AI) and Robotics 1987 13 p Previously announced in IAA as A88-20488 (For primary document see N89-10063 01-12)
Avail: NTIS HC A99/MF E03 CSCL 05A

The development and characteristics of a prototype expert system, Expert System for Satellite Orbit Control (ESSOC), capable of providing real-time spacecraft system analysis and command generation for a geostationary satellite are described. The ESSOC recommends appropriate commands that reflect both the changing spacecraft condition and previous procedural action. An internal knowledge base stores satellite status information and is updated with processed spacecraft telemetry. Procedural structure data are encoded in production rules. Structural methods of knowledge acquisition and the design and performance-enhancing techniques that enable ESSOC to operate in real time are also considered. IAA

N89-10070*# Jet Propulsion Lab., California Inst. of Tech., Pasadena.
DEEP SPACE NETWORK RESOURCE SCHEDULING APPROACH AND APPLICATION **c81**
William C. Eggemeyer and Alan Bowling *In* NASA, Goddard Space Flight Center, Proceedings of 1987 Goddard Conference on Space Applications of Artificial Intelligence (AI) and Robotics 1987 9 p (For primary document see N89-10063 01-12)
Avail: NTIS HC A99/MF E03 CSCL 05A

Deep Space Network (DSN) resource scheduling is the process of distributing ground-based facilities to track multiple spacecraft. The Jet Propulsion Laboratory has carried out extensive research to find ways of automating this process in an effort to reduce time and manpower costs. This paper presents a resource-scheduling system entitled PLAN-IT with a description of its design philosophy. The PLAN-IT's current on-line usage and limitations in scheduling the resources of the DSN are discussed, along with potential enhancements for DSN application. Author

N89-10071*# Computer Sciences Corp., Beltsville, Md. System Sciences Div.
SPACE STATION PLATFORM MANAGEMENT SYSTEM (PMS) REPLANNING USING RESOURCE ENVELOPES **c81**
Joy Lee Bush, Anna Critchfield, and Audrey Loomis *In* NASA, Goddard Space Flight Center, Proceedings of 1987 Goddard Conference on Space Applications of Artificial Intelligence (AI) and Robotics 1987 17 p (For primary document see N89-10063 01-12)
Avail: NTIS HC A99/MF E03 CSCL 05A

One of the responsibilities of the Space Station Platform Management System (PMS) is to maintain constraint-free, short-term plans for platform and free-flyer activities. Both the replanning function and the associated constraint-checking function are viewed as potentially requiring expert system assistance. The PMS Resource Envelope Scheduling System (PRESS) expert system, which is currently under development, is described. The PRESS capabilities will include the following: plan, replan, and perform constraint checking using resource envelopes resembling those required for telescience; initialize itself using the results fo a previous run; infer the replanning needs associated with a change in resource availability; allow the user to determine the level of interaction (including an advisory capability) with the system during execution; and generate both a graphic timeline and a report as output. The PRESS is being developed on an IBM PC/AT using TeKnowledge, Inc.'s M.1 expert system shell. The PRESS activity definitions and constraints are based on those defined for the Cosmic Background Explorer (COBE) mission scheduled for launch in early 1989. Author

N89-10072*# National Aeronautics and Space Administration. Goddard Space Flight Center, Greenbelt, Md.
CLEAR: COMMUNICATIONS LINK EXPERT ASSISTANCE RESOURCE **c81**
Larry G. Hull and Peter M. Hughes *In its* Proceedings of 1987 Goddard Conference on Space Applications of Artificial Intelligence (AI) and Robotics 1987 12 p (For primary document see N89-10063 01-12)
Avail: NTIS HC A99/MF E03 CSCL 05A

Communications Link Expert Assistance Resource (CLEAR) is a real time, fault diagnosis expert system for the Cosmic Background Explorer (COBE) Mission Operations Room (MOR). The CLEAR expert system is an operational prototype which assists the MOR operator/analyst by isolating and diagnosing faults in the spacecraft communication link with the Tracking and Data Relay Satellite (TDRS) during periods of realtime data acquisition. The mission domain, user requirements, hardware configuration, expert system concept, tool selection, development approach, and system design were discussed. Development approach and system implementation are emphasized. Also discussed are system architecture, tool selection, operation, and future plans. Author

N89-10073*# National Aeronautics and Space Administration. Goddard Space Flight Center, Greenbelt, Md.
THE LOAD SHEDDING ADVISOR: AN EXAMPLE OF A CRISIS-RESPONSE EXPERT SYSTEM **c81**
Terry B. Bollinger, Eric Lightner, John Laverty (Bendix Field Engineering Corp., Greenbelt, Md.), and Edward Ambrose *In its* Proceedings of 1987 Goddard Conference on Space Applications

of Artificial Intelligence (AI) and Robotics 1987 11 p (For primary document see N89-10063 01-12)
Avail: NTIS HC A99/MF E03 CSCL 05A

A Prolog-based prototype expert system is described that was implemented by the Network Operations Branch of the NASA Goddard Space Flight Center. The purpose of the prototype was to test whether a small, inexpensive computer system could be used to host a load shedding advisor, a system which would monitor major physical environment parameters in a computer facility, then recommend appropriate operator reponses whenever a serious condition was detected. The resulting prototype performed significantly to efficiency gains achieved by replacing a purely rule-based design methodology with a hybrid approach that combined procedural, entity-relationship, and rule-based methods. Author

N89-10074*# National Aeronautics and Space Administration. Goddard Space Flight Center, Greenbelt, Md.
A LOCAL AREA COMPUTER NETWORK EXPERT SYSTEM FRAMEWORK **c62**
Robert Dominy *In its* Proceedings of 1987 Goddard Conference on Space Applications of Artificial Intelligence (AI) and Robotics 1987 5 p Prepared in cooperation with Bendix Field Engineering Corp., Greebelt, Md. (For primary document see N89-10063 01-12)
Avail: NTiS HC A99/MF E03 CSCL 09B

Over the past years an expert system called LANES designed to detect and isolate faults in the Goddard-wide Hybrid Local Area Computer Network (LACN) was developed. As a result, the need for developing a more generic LACN fault isolation expert system has become apparent. An object oriented approach was explored to create a set of generic classes, objects, rules, and methods that would be necessary to meet this need. The object classes provide a convenient mechanism for separating high level information from low level network specific information. This approach yeilds a framework which can be applied to different network configurations and be easily expanded to meet new needs. Author

N89-10075*# National Aeronautics and Space Administration. Goddard Space Flight Center, Greenbelt, Md.
FIESTA: AN OPERATIONAL DECISION AID FOR SPACE NETWORK FAULT ISOLATION **c81**
Dawn Lowe, Bob Quillin, Nadine Matteson, Bill Wilkinson, and Steve Miksell (Stanford Telecommunications, Inc., McLean, Va.) *In its* Proceedings of 1987 Goddard Conference on Space Applications of Artificial Intelligence (AI) and Robotics 1987 21 p Prepared in cooperation with Bendix Field Engineering Corp., Greenbelt, Md. (For primary document see N89-10063 01-12)
(Contract NAS5-27600)
Avail: NTIS HC A99/MF E03 CSCL 05A

The Fault Tolerance Expert System for Tracking and Data Relay Satellite System (TDRSS) Applications (FIESTA) is a fault detection and fault diagnosis expert system being developed as a decision aid to support operations in the Network Control Center (NCC) for NASA's Space Network. The operational objectives which influenced FIESTA development are presented and an overview of the architecture used to achieve these goals are provided. The approach to the knowledge engineering effort and the methodology employed are also presented and illustrated with examples drawn from the FIESTA domain. Author

N89-10076*# National Aeronautics and Space Administration. Goddard Space Flight Center, Greenbelt, Md.
EXPERT SYSTEM SUPPORT FOR HST OPERATIONS **c81**
Bryant Cruse (Lockheed Missiles and Space Co., Greenbelt, Md.) and Charles Wende *In its* Proceedings of 1987 Goddard Conference on Space Applications of Artificial Intelligence (AI) and Robotics 1987 11 p (For primary document see N89-10063 01-12)
Avail: NTIS HC A99/MF E03 CSCL 05A

An expert system is being developed to support vehicle anomaly diagnosis for the Hubble Space Telescope (HST). Following a study of safemode entry analyses, a prototype system was developed which reads engineering telemetry formats, and when a safemode event is detected, extracts telemetry from the downlink and writes it into a knowledge base for more detailed analyses. The prototype then summarizes vehicle events (limits exceeded, specific failures). This prototype, the Telemetry Analysis Logic for Operations Support (TALOS) uses the Lockheed Expert System (LES) shell, and includes over 1600 facts, 230 rules, and 27 goals. Although considered a prototype, it is already an operationally useful system. The history leading into the TALOS prototype will be discussed, an overview of the present TALOS system will be presented, and the role of the TALOS system in contingency planning will be delineated. Author

N89-10077*# Stanford Telecommunications, Inc., McLean, Va.
A HIERARCHICALLY DISTRIBUTED ARCHITECTURE FOR FAULT ISOLATION EXPERT SYSTEMS ON THE SPACE STATION **c81**
Steve Miksell and Sue Coffer *In* NASA, Goddard Space Flight Center, Proceedings of 1987 Goddard Conference on Space Applications of Artificial Intelligence (AI) and Robotics 1987 9 p (For primary document see N89-10063 01-12)
(Contract NAS5-29280)
Avail: NTIS HC A99/MF E03 CSCL 05A

The Space Station Axiomatic Fault Isolating Expert Systems (SAFTIES) system deals with the hierarchical distribution of control and knowledge among independent expert systems doing fault isolation and scheduling of Space Station subsystems. On its lower level, fault isolation is performed on individual subsystems. These fault isolation expert systems contain knowledge about the performance requirements of their particular subsystem and corrective procedures which may be involved in repsonse to certain performance errors. They can control the functions of equipment in their system and coordinate system task schedules. On a higher level, the Executive contains knowledge of all resources, task schedules for all systems, and the relative priority of all resources and tasks. The executive can override any subsystem task schedule in order to resolve use conflicts or resolve errors that require resources from multiple subsystems. Interprocessor communication is implemented using the SAFTIES Communications Interface (SCI). The SCI is an application layer protocol which supports the SAFTIES distributed multi-level architecture. Author

N89-10078*# National Aeronautics and Space Administration. Goddard Space Flight Center, Greenbelt, Md.
AUTOMATION OF SPACECRAFT CONTROL CENTERS **c81**
Robert Dutilly *In its* Proceedings of 1987 Goddard Conference on Space Applications of Artificial Intelligence (AI) and Robotics 1987 9 p (For primary document see N89-10063 01-12)
Avail: NTIS HC A99/MF E03 CSCL 05A

The objective is to describe the further automation of the Payload Operations Control Centers, specifically the Mission Operations Room, by using a series of expert systems interconnected together. The feasibility of using expert systems in the Mission Operations Room is presently being determined. The expert system under development is called the Communications Link Expert Assistance Resource (CLEAR) project. It is the first control center expert system being designed and implemented at Goddard. It will demonstrate the feasibility and practicality of expert systems in a real-time control center environment. There is a two-fold purpose. First is to briefly describe the present effort of the CLEAR expert system under development. The second is to describe how a series of interacting expert systems could be developed to almost totally automate the Mission Operations Room within the control center. How these expert systems would be put together and what functions they could perform in the control center is described. These efforts will provide a great deal of applicability toward the automation of the space station. Author

N89-10079*# National Aeronautics and Space Administration. Goddard Space Flight Center, Greenbelt, Md.
SPACELAB DATA PROCESSING FACILITY (SLDPF) QUALITY ASSURANCE EXPERT SYSTEMS DEVELOPMENT c81
Angelita C. Kelly, Lisa Basile, Troy Ames, Janice Watson, and William Dallam (Lockheed Missiles and Space Co., Greenbelt, Md.) *In* NASA, Goddard Space Flight Center, Proceedings of 1987 Goddard Conference on Space Applications of Artificial Intelligence (AI) and Robotics 1987 23 p Previously announced in IAA as A88-20490 (For primary document see N89-10063 01-12)
Avail: NTIS HC A99/MF E03 CSCL 05A

Spacelab Data Processing Facility (SLDPF) expert system prototypes were developed to assist in the quality assurance of Spacelab and/or Attached Shuttle Payload (ASP) processed telemetry data. The SLDPF functions include the capturing, quality monitoring, processing, accounting, and forwarding of mission data to various user facilities. Prototypes for the two SLDPF functional elements, the Spacelab Output Processing System and the Spacelab Input Processing Element, are described. The prototypes have produced beneficial results including an increase in analyst productivity, a decrease in the burden of tedious analyses, the consistent evaluation of data, and the providing of concise historical records. IAA

N89-10080*# Space Telescope Science Inst., Baltimore, Md.
AN EXPERT SYSTEM APPROACH TO ASTRONOMICAL DATA ANALYSIS c82
Mark D. Johnston *In* NASA, Goddard Space Flight Center, Proceedings of 1987 Goddard Conference on Space Applications of Artificial Intelligence (AI) and Robotics 1987 17 p (For primary document see N89-10063 01-12)
Avail: NTIS HC A99/MF E03 CSCL 05B

Expert systems technology has much to offer to the problem of astronomical data analysis, where large data volumes and sophisticated analysis goals have caused a variety of interesting problems to arise. The construction of a prototype expert system whose target domain is CCD image calibration, is reported. The prototype is designed to be extensible to different and more complex problems in a straighforward way, and to be largely independent of the details of the specific data analysis system which executes the plan it generates. Author

N89-10081*# National Aeronautics and Space Administration. Ames Research Center, Moffett Field, Calif.
EXPERT SYSTEMS TOOLS FOR HUBBLE SPACE TELESCOPE OBSERVATION SCHEDULING c81
Glenn Miller, Don Rosenthal, William Cohen, and Mark Johnston (Space Telescope Science Inst., Baltimore, Md.) *In* NASA, Goddard Space Flight Center, Proceedings of 1987 Goddard Conference on Space Applications of Artificial Intelligence (AI) and Robotics 1987 13 p Previously announced in IAA as A88-20489 (For primary document see N89-10063 01-12)
Avail: NTIS HC A99/MF E03 CSCL 05A

The utility of expert systems techniques for the Hubble Space Telescope (HST) planning and scheduling is discussed and a plan for development of expert system tools which will augment the existing ground system is described. Additional capabilities provided by these tools will include graphics-oriented plan evaluation, long-range analysis of the observation pool, analysis of optimal scheduling time intervals, constructing sequences of spacecraft activities which minimize operational overhead, and optimization of linkages between observations. Initial prototyping of a scheduler used the Automated Reasoning Tool running on a LISP workstation. IAA

N89-10082*# George Washington Univ., Washington, D.C. Inst. for Artificial Intelligence.
TOWARD AN EXPERT PROJECT MANAGEMENT SYSTEM c81
Barry G. Silverman, Arthur Murray, Coty Diakite (Intellitek, Inc., Rockville, Md.), and Kostas Feggos *In* NASA, Goddard Space Flight Center, Proceedings of 1987 Goddard Conference on Space Applications of Artificial Intelligence (AI) and Robotics 1987 18 p (For primary document see N89-10063 01-12)
Avail: NTIS HC A99/MF E03 CSCL 05A

The purpose of the research effort is to prescribe a generic reusable shell that any project office can install and customize for the purposes of advising, guiding, and supporting project managers in that office. The prescribed shell is intended to provide both: a component that generates prescriptive guidance for project planning and monitoring activities, and an analogy (intuition) component that generates descriptive insights of previous experience of successful project managers. The latter component is especially significant in that it has the potential to: retrieve insights, not just data, and provide a vehicle for expert PMs to easily transcribe their current experiences in the course of each new project managed. Author

N89-10083*# Computer Sciences Corp., Baltimore, Md. Astronomy Programs.
A NATURAL LANGUAGE QUERY SYSTEM FOR HUBBLE SPACE TELESCOPE PROPOSAL SELECTION c61
Thomas Hornick, William Cohen, and Glenn Miller *In* NASA, Goddard Space Flight Center, Proceedings of 1987 Goddard Conference on SpaceApplications o f Artificial Intelligence (AI) and Robotics 1987 17 p Prepared in cooperation with Space Telescope Science Inst., Baltimore, Md. (For primary document see N89-10063 01-12)
Avail: NTIS HC A99/MF E03 CSCL 09B

The proposal selection process for the Hubble Space Telescope is assisted by a robust and easy to use query program (TACOS). The system parses an English subset language sentence regardless of the order of the keyword phases, allowing the user a greater flexibility than a standard command query language. Capabilities for macro and procedure definition are also integrated. The system was designed for flexibility in both use and maintenance. In addition, TACOS can be applied to any knowledge domain that can be expressed in terms of a single reaction. The system was implemented mostly in Common LISP. The TACOS design is described in detail, with particular attention given to the implementation methods of sentence processing. Author

N89-10084*# Ford Aerospace and Communications Corp., College Park, Md. Space Missions Div.
MAINTAINING CONSISTENCY BETWEEN PLANNING HIERARCHIES: TECHNIQUES AND APPLICATIONS c81
David R. Zoch *In* NASA, Goddard Space Flight Center, Proceedings of 1987 Goddard Conference on Space Applications of Artificial Intelligence (AI) and Robotics 1987 18 p (For primary document see N89-10063 01-12)
Avail: NTIS HC A99/MF E03 CSCL 05A

In many planning and scheduling environments, it is desirable to be able to view and manipulate plans at different levels of abstraction, allowing the users the option of viewing and manipulating either a very detailed representation of the plan or a high-level more abstract version of the plan. Generating a detailed plan from a more abstract plan requires domain-specific planning/scheduling knowledge; the reverse process of generating a high-level plan from a detailed plan Reverse Plan Maintenance, or RPM) requires having the system remember the actions it took based on its domain-specific knowledge and its reasons for taking those actions. This reverse plan maintenance process is described as implemented in a specific planning and scheduling tool, The Mission Operations Planning Assistant (MOPA), as well as the applications of RPM to other planning and scheduling problems; emphasizing the knowledge that is needed to maintain the correspondence between the different hierarchical planning levels. Author

N89-10085*# Ford Aerospace and Communications Corp., College Park, Md.
A LISP-Ada CONNECTION c61
Allan Jaworski, David Lavallee, and David Zoch *In* NASA, Goddard Space Flight Center, Proceedings of 1987 Goddard Conference

on Space Applications of Artificial Intelligence (AI) and Robotics 1987 14 p (For primary document see N89-10063 01-12)
Avail: NTIS HC A99/MF E03 CSCL 09B

The prototype demonstrates the feasibility of using Ada for expert systems and the implementation of an expert-friendly interface which supports knowledge entry. In the Ford LISP-Ada Connection (FLAC) system LISP and Ada are used in ways which complement their respective capabilities. Future investigation will concentrate on the enhancement of the expert knowledge entry/debugging interface and on the issues associated with multitasking and real-time expert systems implementation in Ada.
Author

N89-10086*# Computer Sciences Corp., Baltimore, Md. Astronomy Programs.
EXPERT SYSTEMS BUILT BY THE EXPERT: AN EVALUATION OF OPS5 **c61**
Robert Jackson *In* NASA, Goddard Space Flight Center, Proceedings of 1987 Goddard Conference on Space Applications of Artificial Intelligence (AI) and Robotics 1987 14 p Prepared in cooperation with Space Telescope Science Inst., Baltimore, Md. (For primary document see N89-10063 01-12)
Avail: NTIS HC A99/MF E03 CSCL 09B

Two expert systems were written in OPS5 by the expert, a Ph.D. astronomer with no prior experience in artificial intelligence or expert systems, without the use of a knowledge engineer. The first system was built from scratch and uses 146 rules to check for duplication of scientific information within a pool of prospective observations. The second system was grafted onto another expert system and uses 149 additional rules to estimate the spacecraft and ground resources consumed by a set of prospective observations. The small vocabulary, the IF this occurs THEN do that logical structure of OPS5, and the ability to follow program execution allowed the expert to design and implement these systems with only the data structures and rules of another OPS5 system as an example. The modularity of the rules in OPS5 allowed the second system to modify the rulebase of the system onto which it was grafted without changing the code or the operation of that system. These experiences show that experts are able to develop their own expert systems due to the ease of programming and code reusability in OPS5.
Author

N89-10087*# National Aeronautics and Space Administration. Langley Research Center, Hampton, Va.
SPACE TRUSS ASSEMBLY USING TELEOPERATED MANIPULATORS **c18**
Walter W. Hankins, III, Randolph W. Mixon, Howard C. Jones, and Thomas W. Burgess (Oak Ridge National Lab., Tenn.) *In* NASA, Goddard Space Flight Center, Proceedings of 1987 Goddard Conference on Space Applications of Artificial Intelligence (AI) and Robotics 1987 18 p (For primary document see N89-10063 01-12)
Avail: NTIS HC A99/MF E03 CSCL 22B

Teleoperator experiments were conducted which have demonstrated that a realistic, complex task, typical of those accomplished on-orbit by EVA astronauts, can be done in a smooth, timely manner with manipulators remotely controlled by humans. The real concerns were: (1) do manipulators have sufficient dexterity for these tasks, (2) can sufficient information from the remote site be provided to permit adequate teleoperator control, (3) can reasonable times relative to EVA times be achieved, (4) can the task be completed without frequent and/or damaging impacts among the task components and the manipulators? Positive answers were found to all of these concerns. Tasks times, operator fatigue, and smoothness of operation could be improved by designing the task components and the manipulators for greater compatibility. The data recorded supplements a data base of performance metrics for the same task done in the water immersion training facility as well as space flight and provides management with an objective basis for deciding how and where to apply manipulators in space.
Author

N89-10088*# California Univ., Berkeley. Telerobotics Unit.
A UNIVERSITY TEACHING SIMULATION FACILITY **c54**
Lawrence Stark, Won-Soo Kim, Frank Tendick, Mitchell Tyler, Blake Hannaford, Wissam Barakat, Olaf Bergengruen, Louis Braddi, Joseph Eisenberg, and Stephen Ellis et al. *In* NASA, Goddard Space Flight Center, Proceedings of 1987 Goddard Conference on Space Applications of Artificial Intelligence (AI) and Robotics 1987 30 p (For primary document see N89-10063 01-12)
Avail: NTIS HC A99/MF E03 CSCL 05H

An experimental telerobotics (TR) simulation is described suitable for studying human operator (HO) performance. Simple manipulator pick-and-place and tracking tasks allowed quantitative comparison of a number of calligraphic display viewing conditions. A number of control modes could be compared in this TR simulation, including displacement, rate, and acceleratory control using position and force joysticks. A homeomorphic controller turned out to be no better than joysticks; the adaptive properties of the HO can apparently permit quite good control over a variety of controller configurations and control modes. Training by optimal control example seemed helpful in preliminary experiments.
Author

N89-10089*# Grumman Aerospace Corp., Bethpage, N.Y.
OPEN CONTROL/DISPLAY SYSTEM FOR A TELEROBOTICS WORK STATION **c54**
Saul Keslowitz *In* NASA, Goddard Space Flight Center, Proceedings of 1987 Goddard Conference on Space Applications of Artificial Intelligence (AI) and Robotics 1987 21 p (For primary document see N89-10063 01-12)
Avail: NTIS HC A99/MF E03 CSCL 05H

A working Advanced Space Cockpit was developed that integrated advanced control and display devices into a state-of-the-art multimicroprocessor hardware configuration, using window graphics and running under an object-oriented, multitasking real-time operating system environment. This Open Control/Display System supports the idea that the operator should be able to interactively monitor, select, control, and display information about many payloads aboard the Space Station using sets of I/O devices with a single, software-reconfigurable workstation. This is done while maintaining system consistency, yet the system is completely open to accept new additions and advances in hardware and software. The Advanced Space Cockpit, linked to Grumman's Hybrid Computing Facility and Large Amplitude Space Simulator (LASS), was used to test the Open Control/Display System via full-scale simulation of the following tasks: telerobotic truss assembly, RCS and thermal bus servicing, CMG changeout, RMS constrained motion and space constructible radiator assembly, HPA coordinated control, and OMV docking and tumbling satellite retrieval. The proposed man-machine interface standard discussed has evolved through many iterations of the tasks, and is based on feedback from NASA and Air Force personnel who performed those tasks in the LASS.
Author

N89-10090*# Human Machine Interfaces, Inc., Knoxville, Tenn. Fuel Recycle Div.
CONSOLIDATED FUEL REPROSSING PROGRAM: THE IMPLICATIONS OF FORCE REFLECTION FOR TELEOPERATION IN SPACE **c54**
John V. Draper, Joseph N. Herndon, and Wendy E. Moore *In* NASA, Goddard Space Flight Center, Proceedings of 1987 Goddard Conference on Space Applications of Artificial Intelligence (AI) and Robotics 1987 16 p Previously announced as N87-27402 Prepared in cooperation with Martin Marietta Aerospace, Denver, Colo. (For primary document see N89-10063 01-12)
(Contract DE-AC05-84OR-21400)
Avail: NTIS HC A99/MF E03 CSCL 05H

Previous research on teleoperator force feedback is reviewed and results of a testing program which assessed the impact of force reflection on teleoperator task performance are reported. Force relection is a type of force feedback in which the forces acting on the remote portion of the teleoperator are displayed to the operator by back-driving the master controller. The testing program compared three force reflection levels: 4 to 1 (four units

of force on the slave produce one unit of force at the master controller), 1 to 1, and infinity to 1 (no force reflection). Time required to complete tasks, rate of occurrence of errors, the maximum force applied to tasks components, and variability in forces applied to components during completion of representative remote handling tasks were used as dependent variables. Operators exhibited lower error rates, lower peak forces, and more consistent application of forces using force relection than they did without it. These data support the hypothesis that force reflection provides useful information for teleoperator users. The earlier literature and the results of the experiment are discussed in terms of their implications for space based teleoperator systems. The discussion described the impact of force reflection on task completion performance and task strategies, as suggested by the literature. It is important to understand the trade-offs involved in using telerobotic systems with and without force reflection.
Author

N89-10091*# Martin Marietta Aerospace, Denver, Colo.
ISSUES, CONCERNS, AND INITIAL IMPLEMENTATION RESULTS FOR SPACE BASED TELEROBOTIC CONTROL **c54**
D. A. Lawrence, J. D. Chapel, and T. M. Depkovich *In* NASA, Goddard Space Flight Center, Proceedings of 1987 Goddard Conference on Space Applications of Artificial Intelligence (AI) and Robotics 1987 18 p (For primary document see N89-10063 01-12)
Avail: NTIS HC A99/MF E03 CSCL 05H

Telerobotic control for space based assembly and servicing tasks presents many problems in system design. Traditional force reflection teleoperation schemes are not well suited to this application, and the approaches to compliance control via computer algorithms have yet to see significant testing and comparison. These observations are discussed in detail, as well as the concerns they raise for imminent design and testing of space robotic systems. As an example of the detailed technical work yet to be done before such systems can be specified, a particular approach to providing manipulator compliance is examined experimentally and through modeling and analysis. This yields some initial insight into the limitations and design trade-offs for this class of manipulator control schemes. Implications of this investigation for space based telerobots are discussed in detail.
Author

N89-10092*# RCA Advanced Technology Labs., Moorestown, N.J.
A SHARED POSITION/FORCE CONTROL METHODOLOGY FOR TELEOPERATION **c54**
Jin S. Lee *In* NASA, Goddard Space Flight Center, Proceedings of 1987 Goddard Conference on Space Applications of Artificial Intelligence (AI) and Robotics 1987 12 p (For primary document see N89-10063 01-12)
Avail: NTIS HC A99/MF E03 CSCL 05H

A flexible and computationally efficient shared position/force control concept and its implementation in the Robot Control C Library (RCCL) are presented form the point of teleoperation. This methodology enables certain degrees of freedom to be position-controlled through real time manual inputs and the remaining degrees of freedom to be force-controlled by computer. Functionally, it is a hybrid control scheme in that certain degrees of freedom are designated to be under position control, and the remaining degrees of freedom to be under force control. However, the methodology is also a shared control scheme because some degrees of freedom can be put under manual control and the other degrees of freedom put under computer control. Unlike other hybrid control schemes, which process position and force commands independently, this scheme provides a force control loop built on top of a position control inner loop. This feature minimizes the computational burden and increases disturbance rejection. A simple implementation is achieved partly because the joint control servos that are part of most robots can be used to provide the position control inner loop. Along with this control scheme, several menus were implemented for the convenience of the user. The implemented control scheme was successfully demonstrated for the tasks of hinged-panel opening and peg-in-hole insertion.
Author

N89-10093*# Jet Propulsion Lab., California Inst. of Tech., Pasadena.
MULTIPLE SENSOR SMART ROBOT HAND WITH FORCE CONTROL **c54**
Richard R. Killion, Lee R. Robinson, and Antal Bejczy *In* NASA, Goddard Space Flight Center, Proceedings of 1987 Goddard Conference on Space Applications of Artificial Intelligence (AI) and Robotics 1987 20 p (For primary document see N89-10063 01-12)
Avail: NTIS HC A99/MF E03 CSCL 05H

A smart robot hand developed at JPL for the Protoflight Manipulator Arm (PFMA) is described. The development of this smart hand was based on an integrated design and subsystem architecture by considering mechanism, electronics, sensing, control, display, and operator interface in an integrated design approach. The mechanical details of this smart hand and the overall subsystem are described elsewhere. The sensing and electronics components of the JPL/PFMA smart hand are summarized and it is described in some detail in control capabilities.
Author

N89-10094*# McDonnell-Douglas Astronautics Co., Houston, Tex. Engineering Services.
AN OPTIMAL RESOLVED RATE LAW FOR KINDEMATICALLY REDUNDANT MANIPULATORS **c54**
B. J. Bourgeois *In* NASA, Goddard Space Flight Center, Proceedings of 1987 Goddard Conference on Space Applications of Artificial Intelligence (AI) and Robotics 1987 20 p Previously announced as N88-17268 (For primary document see N89-10063 01-12)
Avail: NTIS HC A99/MF E03 CSCL 05H

The resolved rate law for a manipulator provides the instantaneous joint rates required to satisfy a given instantaneous hand motion. When the joint space has more degrees of freedom than the task space, the manipulator is kinematically redundant and the kinematic rate equations are underdetermined. These equations can be locally optimized, but the resulting pseudo-inverse solution was found to cause large joint rates in some case. A weighting matrix in the locally optimized (pseudo-inverse) solution is dynamically adjusted to control the joint motion as desired. Joint reach limit avoidance is demonstrated in a kinematically redundant planar arm model. The treatment is applicable to redundant manipulators with any number of revolute joints and to nonplanar manipulators.
Author

N89-10095*# Maryland Univ., College Park. Robotics Lab.
AN ADAPTIVE CONTROL SCHEME FOR A FLEXIBLE MANIPULATOR **c54**
T. C. Yang, J. C. S. Yang, and P. Kudva (Advanced Technology and Research, Inc., Burtonsville, Md.) *In* NASA, Goddard Space Flight Center, Proceedings of 1987 Goddard Conference on Space Applications of Artificial Intelligence (AI) and Robotics 1987 14 p (For primary document see N89-10063 01-12)
Avail: NTIS HC A99/MF E03 CSCL 05H

The problem of controlling a single link flexible manipulator is considered. A self-tuning adaptive control scheme is proposed which consists of a least squares on-line parameter identification of an equivalent linear model followed by a tuning of the gains of a pole placement controller using the parameter estimates. Since the initial parameter values for this model are assumed unknown, the use of arbitrarily chosen initial parameter estimates in the adaptive controller would result in undesirable transient effects. Hence, the initial stage control is carried out with a PID controller. Once the identified parameters have converged, control is transferred to the adaptive controller. Naturally, the relevant issues in this scheme are tests for parameter convergence and minimization of overshoots during control switch-over. To demonstrate the effectiveness of the proposed scheme, simulation results are presented with an analytical nonlinear dynamic model of a single link flexible manipulator.
Author

N89-10096*# National Aeronautics and Space Administration. Ames Research Center, Moffett Field, Calif.
ADVANCED DATA MANAGEMENT DESIGN FOR AUTONOMOUS TELEROBOTIC SYSTEMS IN SPACE USING SPACEBORNE SYMBOLIC PROCESSORS **c60**
Andre Goforth *In* NASA, Goddard Space Flight Center, Proceedings of 1987 Goddard Conference on Space Applications of Artificial Intelligence (AI) and Robotics 1987 19 p (For primary document see N89-10063 01-12)
Avail: NTIS HC A99/MF E03 CSCL 09B

The use of computers in autonomous telerobots is reaching the point where advanced distributed processing concepts and techniques are needed to support the functioning of Space Station era telerobotic systems. Three major issues that have impact on the design of data management functions in a telerobot are covered. It also presents a design concept that incorporates an intelligent systems manager (ISM) running on a spaceborne symbolic processor (SSP), to address these issues. The first issue is the support of a system-wide control architecture or control philosophy. Salient features of two candidates are presented that impose constraints on data management design. The second issue is the role of data management in terms of system integration. This referes to providing shared or coordinated data processing and storage resources to a variety of telerobotic components such as vision, mechanical sensing, real-time coordinated multiple limb and end effector control, and planning and reasoning. The third issue is hardware that supports symbolic processing in conjunction with standard data I/O and numeric processing. A SSP that currently is seen to be technologically feasible and is being developed is described and used as a baseline in the design concept. Author

N89-10097*# Little (Arthur D.), Inc., Cambridge, Mass.
ROBOT HANDS AND EXTRAVEHICULAR ACTIVITY **c16**
Beth Marcus *In* NASA, Goddard Space Flight Center, Proceedings of 1987 Goddard Conference on Space Applications of Artificial Intelligence (AI) and Robotics 1987 16 p (For primary document see N89-10063 01-12)
Avail: NTIS HC A99/MF E03 CSCL 22B

Extravehicular activity (EVA) is crucial to the success of both current and future space operations. As space operations have evolved in complexity so has the demand placed on the EVA crewman. In addition, some NASA requirements for human capabilities at remote or hazardous sites were identified. One of the keys to performing useful EVA tasks is the ability to manipulate objects accurately, quickly and without early or excessive fatigue. The current suit employs a glove which enables the crewman to perform grasping tasks, use tools, turn switches, and perform other tasks for short periods of time. However, the glove's bulk and resistance to motion ultimately causes fatigue. Due to this limitation it may not be possible to meet the productivity requirements that will be placed on the EVA crewman of the future with the current or developmental Extravehicular Mobility Unit (EMU) hardware. In addition, this hardware will not meet the requirements for remote or hazardous operations. In an effort to develop ways for improving crew productivity, a contract was awarded to develop a prototype anthromorphic robotic hand (ARH) for use with an extravehicular space suit. The first step in this program was to perform a a design study which investigated the basic technology required for the development of an ARH to enhance crew performance and productivity. The design study phase of the contract and some additional development work is summarized. Author

N89-10098*# Oak Ridge National Lab., Tenn. Center for Engineering Systems Advanced Research.
DYNAMIC TASK ALLOCATION FOR A MAN-MACHINE SYMBIOTIC SYSTEM **c54**
L. E. Parker and F. G. Pin *In* NASA, Goddard Space Flight Center, Proceedings of 1987 Goddard Conference on Space Applications of Artificial Intelligence (AI) and Robotics 1987 19 p Previously announced as N87-30070 Submitted for publication (For primary document see N89-10063 01-12)
(Contract DE-AC05-84OR-21400)
Avail: NTIS HC A99/MF E03 CSCL 05H

This report presents a methodological approach to the dynamic allocation of tasks in a man-machine symbiotic system in the context of dexterous manipulation and teleoperation. This report addresses a symbiotic system containing two symbiotic partners which work toward controlling a single manipulator arm for the execution of a series of sequential manipulation tasks. It is proposed that an automated task allocator use knowledge about the constraints/criteria of the problem, the available resources, the tasks to be performed, and the environment to dynamically allocate task recommendations for the man and the machine. The presentation of the methodology includes discussions concerning the interaction of the knowledge areas, the flow of control, the necessary communication links, and the replanning of the task allocation. Examples of task allocation are presented to illustrate the results of this methodolgy. DOE

N89-10099*# National Bureau of Standards, Gaithersburg, Md. Robot Systems Div.
NASREN: STANDARD REFERENCE MODEL FOR TELEROBOT CONTROL **c60**
J. S. Albus, R. Lumia, and H. McCain *In* NASA, Goddard Space Flight Center, Proceedings of 1987 Goddard Conference on Space Applications of Artificial Intelligence (AI) and Robotics 1987 19 p (For primary document see N89-10063 01-12)
Avail: NTIS HC A99/MF E03 CSCL 09B

A hierarchical architecture is described which supports space station telerobots in a variety of modes. The system is divided into three hierarchies: task decomposition, world model, and sensory processing. Goals at each level of the task dedomposition heirarchy are divided both spatially and temporally into simpler commands for the next lower level. This decomposition is repreated until, at the lowest level, the drive signals to the robot actuators are generated. To accomplish its goals, task decomposition modules must often use information stored it the world model. The purpose of the sensory system is to update the world model as rapidly as possible to keep the model in registration with the physical world. The architecture of the entire control system hierarch is described and how it can be applied to space telerobot applications. Author

N89-10100*# RCA Astro-Electronics Div., Princeton, N. J. Space Div.
KINEMATIC STUDY OF FLIGHT TELEROBOTIC SERVICER CONFIGURATION ISSUES **c18**
R. H. Lewis, R. D. Scott, and W. S. Howard *In* NASA, Goddard Space Flight Center, Proceedings of 1987 Goddard Conference on Space Applications of Artificial Intelligence (AI) and Robotics 1987 17 p (For primary document see N89-10063 01-12)
Avail: NTIS HC A99/MF E03 CSCL 22B

Several factors, such as body size and shape, and the number of arms and their placement, will influence how well the Flight Telerobotic Servicer (FTS) is suited to its potential duties for the Space Station Program. In order to examine the implications of these configuration options, eight specific 2, 3, and 4 armed FTS configuration were simulated and used to perform a Space Station Orbital Replacement Unit (ORU) exchange. The strengths and weaknesses of each configuration were evaluated. Although most of the configurations examined were able to perform the exchange, several of the 3 and 4 arm configurations had operational advantages. The results obtained form these simulations are specific to the assumptions associated with the ORU exchange scenario examined. However, they do illustrate the general interrelationships and sensitivities which need to be understood. Author

N89-10101*# Martin Marietta Aerospace, Denver, Colo. Advance Automation Technology (Robotics) Group.
ACTUATORS FOR A SPACE MANIPULATOR **c54**
W. Chun and P. Brunson *In* NASA, Goddard Space Flight Center, Proceedings of 1987 Goddard Conference on Space

Applications of Artificial Intelligence (AI) and Robotics 1987 20 p (For primary document see N89-10063 01-12)
Avail: NTIS HC A99/MF E03 CSCL 05H

The robotic manipulator can be decomposed into distinct subsytems. One particular area of interest of mechanical subsystems is electromechanical actuators (or drives). A drive is defined as a motor with an appropriate transmission. An overview is given of existing, as well as state-of-the-art drive systems. The scope is limited to space applications. A design philosophy and adequate requirements are the initial steps in designing a space-qualified actuator. The focus is on the d-c motor in conjunction with several types of transmissions (harmonic, tendon, traction, and gear systems). The various transmissions will be evaluated and key performance parameters will be addressed in detail. Included in the assessment is a shuttle RMS joint and a MSFC drive of the Prototype Manipulator Arm. Compound joints are also investigated. Space imposes a set of requirements for designing a high-performance drive assembly. Its inaccessibility and cryogenic conditions warrant special considerations. Some guidelines concerning these conditions are present. The goal is to gain a better understanding in designing a space actuator.
Author

N89-10102*# National Aeronautics and Space Administration. Goddard Space Flight Center, Greenbelt, Md.
CABLE APPLICATIONS IN ROBOT COMPLIANT DEVICES **c54**
James J. Kerley *In its* Proceedings of 1987 Goddard Conference on Space Applications of Artificial Intelligence (AI) and Robotics 1987 11 p (For primary document see N89-10063 01-12)
Avail: NTIS HC A99/MF E03 CSCL 05H

Robotic systems need compliance to connect the robot to the work object. The cable system illustrated offers compliance for mating but can be changed in space to become quite stiff. Thus the same system can do both tasks, even in environments where the work object or robot are moving at different frequencies and different amplitudes. The adjustment can be made in all six degrees of freedom, translated in or rotated in any plane and still make a good contact and control.
Author

N89-10103*# National Aeronautics and Space Administration. John F. Kennedy Space Center, Cocoa Beach, Fla.
COMPUTER HARDWARE AND SOFTWARE FOR ROBOTIC CONTROL **c60**
Virgil Leon Davis *In* NASA, Goddard Space Flight Center, Proceedings of 1987 Goddard Conference on Space Applications of Artificial Intelligence (AI) and Robotics 1987 19 p (For primary document see N89-10063 01-12)
Avail: NTIS HC A99/MF E03 CSCL 09B

The KSC has implemented an integrated system that coordinates state-of-the-art robotic subsystems. It is a sensor based real-time robotic control system performing operations beyond the capability of an off-the-shelf robot. The integrated system provides real-time closed loop adaptive path control of position and orientation of all six axes of a large robot; enables the implementation of a highly configurable, expandable testbed for sensor system development; and makes several smart distributed control subsystems (robot arm controller, process controller, graphics display, and vision tracking) appear as intelligent peripherals to a supervisory computer coordinating the overall systems.
Author

N89-10104*# Jet Propulsion Lab., California Inst. of Tech., Pasadena.
TELEOPERATED POSITION CONTROL OF A PUMA ROBOT **c54**
Edmund Austin and Chung P. Fong *In* NASA, Goddard Space Flight Center, Proceedings of 1987 Goddard Conference on Space Applications of Artificial Intelligence (AI) and Robotics 1987 19 p (For primary document see N89-10063 01-12)
Avail: NTIS HC A99/MF E03 CSCL 05H

A laboratory distributed computer control teleoperator system is developed to support NASA's future space telerobotic operation. This teleoperator system uses a universal force-reflecting hand controller in the local iste as the operator's input device. In the remote site, a PUMA controller recieves the Cartesian position commands and implements PID control laws to position the PUMA robot. The local site uses two microprocessors while the remote site uses three. The processors communicate with each other through shared memory. The PUMA robot controller was interfaced through custom made electronics to bypass VAL. The development status of this teleoperator system is reported. The execution time of each processor is analyzed, and the overall system throughput rate is reported. Methods to improve the efficiency and performance are discussed.
Author

N89-10105*# Advanced Technology and Research, Inc., Burtonsville, Md.
PERFORMANCE IMPROVEMENT OF ROBOTS USING A LEARNING CONTROL SCHEME **c63**
Ramuhalli Krishna, Pen-Tai Chiang, and Jackson C. S. Yang (Maryland Univ., College Park.) *In* NASA, Goddard Space Flight Center, Proceedings of 1987 Goddard Conference on Space Applications of Artificial Intelligence (AI) and Robotics 1987 20 p (For primary document see N89-10063 01-12)
Avail: NTIS HC A99/MF E03 CSCL 09B

Many applications of robots require that the same task be repeated a number of times. In such applications, the errors associated with one cycle are also repeated every cycle of the operation. An off-line learning control scheme is used here to modify the command function which would result in smaller errors in the next operation. The learning scheme is based on a knowledge of the errors and error rates associated with each cycle. Necessary conditions for the iterative scheme to converge to zero errors are derived analytically considering a second order servosystem model. Computer simulations show that the errors are reduced at a faster rate if the error rate is included in the iteration scheme. The results also indicate that the scheme may increase the magnitude of errors if the rate information is not included in the iteration scheme. Modification of the command input using a phase and gain adjustment is also proposed to reduce the errors with one attempt. The scheme is then applied to a computer model of a robot system similar to PUMA 560. Improved performance of the robot is shown by considering various cases of trajectory tracing. The scheme can be successfully used to improve the performance of actual robots within the limitations of the repeatability and noise characteristics of the robot.
Author

N89-10106# Edgerton, Germeshausen and Grier, Inc., Idaho Falls, Idaho.
MULTIMEGAWATT POWER SOURCES FOR COMMERCIAL SPACE OPERATIONS
John A. Dearien and John S. Martinell 1988 8 p Presented at the 25th Space Congress, Cocoa Beach, Fla., 26 Apr. 1988 (Contract DE-AC07-76ID-01570)
(DE88-015119; EGG-M-88088; CONF-8804176-1) Avail: NTIS HC A02/MF A01

There is a great deal of interest in commercial operation in space today, but very little consideration of where the power to run such an operation is to come from. For any commercial operation in space, the power source, especially those involving kilowatts and megawatts of power, must be considered at the very onset of the venture. The Multimegawatt Space Reactor Program at the Idaho National Engineering Laboratory is working this problem in conjunction with the development of Strategic Defense Initiative needs. The same type of up-front power development program needs to be considered in all discussions associated with commercial development in space. A system developed for a commercial operation in space will most likely be a hybrid system utilizing both electrical and thermal energy. Even if the commercial process consists totally of high power thermal energy usage, there will be a certain amount of electricity required for controls, mass transport, environmental control (if manned), and communications. The optimum system will thus require a great deal of planning and coordination with the development of the commercial process.
DOE

13 ASTRODYNAMICS

Includes powered and free-flight trajectories; and orbital and launching dynamics.

N89-10107# Centre National d'Etudes Spatiales, Toulouse (France). Dept. d'Analyse et Evaluation en Mecanique Spatiale.
PRIMORB: PRELIMINARY ORBIT WITH TWO POSITIONS [PRIMORB: UNE PREMIERE ORBITE AVEC 2 POSITIONS]
M. Vincent, C. Aubert, and F. Nouel 27 Mar. 1986 29 p In FRENCH; ENGLISH summary
(CNES-CT/DTI/MS/AE/072; ETN-88-93085) Avail: NTIS HC A03/MF A01

A program which allows satellite orbit computation from two positions measured at two different times is described. The computation method uses iterative corrections on semimajor axis as proposed by Taff and Randall (1985). The program is adapted for microcomputers and useful for first orbit determination before accurate determination with tracking data. Numerical results for SPOT circular polar orbit and GRANAT high excentric orbit are presented. ESA

N89-10108# Centre National d'Etudes Spatiales, Toulouse (France). Centre Spatial.
CARTEL: A METHOD TO CALIBRATE S-BAND RANGES WITH GEOSTATIONARY SATELLITES. RESULTS OF ORBIT DETERMINATION
A. Guitart and B. Mesnard 20 May 1986 229 p In FRENCH; ENGLISH summary
(CNES-CT/DTI/MS/AE/124; ETN-88-93086) Avail: NTIS HC A11/MF A01

A satellite tracking campaign was organized, with 4 S-band stations, for 1 wk. The relative geometry of the network with respect to the satellites was an opportunity to show how the most precise orbit can be computed with the operational software. This precise orbit served as a reference to evaluate what can be achieved with one station with range and angular measurements, a typical configuration used for stationkeeping of geostationary satellites. Orbit computation implied numerical integration with gravitational (Earth, Moon, and Sun) and solar radiation pressure forces acting on the satellite. Arc lengths of 2 days gave initial state vectors which were compared every day. Precision of 10 m is achieved. However, an analysis of the influence of parameters in the orbit computations reveals that the absolute accuracy is of the order of 100 m, since modeling perturbations were neglected in the operational software (e.g., polar motion). In a relative sense, the reference orbit allows estimation of systematic errors for other tracking antennas. ESA

N89-10109# Centre National d'Etudes Spatiales, Toulouse (France).
ZOOM ORBITOGRAPHY SOFTWARE: ON THE GIVENS METHOD. PRESENTATION AND SOFTWARE IMPLEMENTATION EVALUATION FOR LEAST SQUARE PROBLEMS
Nadia Biad 28 Aug. 1986 92 p In FRENCH; ENGLISH summary
(CNES-CT/DTI/MS/AE/219; ETN-88-93087) Avail: NTIS HC A05/MF A01

The mathematical description of the orbit restitution problem is discussed. The least squares problem is solved with the Givens method. Numerical studies were performed to show the behavior of the software. The method simplifies and improves calculations, but it is stressed that care must be taken to ensure that the values of the Givens matrices R bar, D are accurate, and the calculation methods used to obtain them stable. ESA

N89-10188*# Jet Propulsion Lab., California Inst. of Tech., Pasadena.
PRECISE ORBIT DETERMINATION FOR NASA'S EARTH OBSERVING SYSTEM USING GPS (GLOBAL POSITIONING SYSTEM)
B. G. Williams *In its* The Telecommunications and Data Acquisition Report 15 Aug. 1988 p 16-27 (For primary document see N89-10186 01-32)
Avail: NTIS HC A14/MF A01 CSCL 22A

N89-10189*# Jet Propulsion Lab., California Inst. of Tech., Pasadena.
PSA: A PROGRAM TO STREAMLINE ORBIT DETERMINATION FOR LAUNCH SUPPORT OPERATIONS
V. N. Legerton and N. A. Mottinger *In its* The Telecommunications and Data Acquisition Report 15 Aug. 1988 p 28-41 (For primary document see N89-10186 01-32)
Avail: NTIS HC A14/MF A01 CSCL 22A

14 GROUND SUPPORT SYSTEMS AND FACILITIES (SPACE)

Includes launch complexes, research and production facilities; ground support equipment, e.g., mobile transporters; and simulators.

For related information see also *09 Research and Support Facilities (Air).*

N89-10211*# Jet Propulsion Lab., California Inst. of Tech., Pasadena.
SUMMARY OF DSN (DEEP SPACE NETWORK) REIMBURSABLE LAUNCH SUPPORT
N. A. Fanelli and M. E. Wyatt *In its* The Telecommunications and Data Acquisition Report 15 Aug. 1988 p 301-306 (For primary document see N89-10186 01-32)
Avail: NTIS HC A14/MF A01 CSCL 14B

15 LAUNCH VEHICLES AND SPACE VEHICLES

Includes boosters; operating problems of launch/space vehicle systems; and reusable vehicles.

For related information see also *20 Spacecraft Propulsion and Power.*

N89-10110# Societe Europeenne de Propulsion, Vernon (France).
MEANS FOR TESTING AEROSPACE LAUNCHER STRUCTURES [MOYENS D'ESSAIS DES STRUCTURES DE LANCEURS AEROSPATIAUX]
Jean-Claude Vinot and Robert Gazave 1987 3 p In FRENCH Presented at the 8th Congres Francais de Mecanique, Nantes, France, 1 Sep. 1988
(ETN-88-93082) Avail: NTIS HC A02/MF A01

Testing of Ariane type launcher structures, particularly the propulsion system, is reviewed. Vibration and acoustic tests are introduced. The need for theoretical approaches to pass from low level to high level results, other than by extrapolation, taking into account the nonlinearities of the structure, is stressed. ESA

16 SPACE TRANSPORTATION

Includes passenger and cargo space transportation, e.g., shuttle operations; and space rescue techniques.

For related information see also *03 Air Transportation and Safety* and *18 Spacecraft Design, Testing and Performance.* For space suits see *54 Man/System Technology and Life Support.*

N89-10111*# National Aeronautics and Space Administration. Lewis Research Center, Cleveland, Ohio.
FIRE BEHAVIOR AND RISK ANALYSIS IN SPACECRAFT
Robert Friedman and Kurt R. Sacksteder [1988] 14 p Prepared for presentation at the Winter Annual Meeting of the American Society of Mechanical Engineers, Chicago, Ill., 28 Nov. - 3 Dec.

1988
(NASA-TM-100944; E-4232; NAS 1.15:100944) Avail: NTIS HC A03/MF A01 CSCL 22B

Practical risk management for present and future spacecraft, including space stations, involves the optimization of residual risks balanced by the spacecraft operational, technological, and economic limitations. Spacecraft fire safety is approached through three strategies, in order of risk: (1) control of fire-causing elements, through exclusion of flammable materials for example; (2) response to incipient fires through detection and alarm; and (3) recovery of normal conditions through extinguishment and cleanup. Present understanding of combustion in low gravity is that, compared to normal gravity behavior, fire hazards may be reduced by the absence of buoyant gas flows yet at the same time increased by ventilation flows and hot particle expulsion. This paper discusses the application of low-gravity combustion knowledge and appropriate aircraft analogies to fire detection, fire fighting, and fire-safety decisions for eventual fire-risk management and optimization in spacecraft. Author

N89-10097*# Little (Arthur D.), Inc., Cambridge, Mass.
ROBOT HANDS AND EXTRAVEHICULAR ACTIVITY
Beth Marcus *In* NASA, Goddard Space Flight Center, Proceedings of 1987 Goddard Conference on Space Applications of Artificial Intelligence (AI) and Robotics 1987 16 p (For primary document see N89-10063 01-12)
Avail: NTIS HC A99/MF E03 CSCL 22B

17 SPACE COMM., SPACECRAFT COMM., COMMAND & TRACKING

Includes telemetry; space communications networks; astronavigation and guidance; and radio blackout.

For related information see also *04 Aircraft Communications and Navigation* and *32 Communications and Radar.*

N89-10207*# Jet Propulsion Lab., California Inst. of Tech., Pasadena.
PHASING THE ANTENNAS OF THE VERY LARGE ARRAY (VLA) FOR RECEPTION OF TELEMETRY FROM VOYAGER 2 AT NEPTUNE ENCOUNTER
J. S. Ulvestad *In its* The Telecommunications and Data Acquisition Report 15 Aug. 1988 p 257-273 (For primary document see N89-10186 01-32)
Avail: NTIS HC A14/MF A01 CSCL 09F

18 SPACECRAFT DESIGN, TESTING AND PERFORMANCE

Includes satellites; space platforms; space stations; spacecraft systems and components such as thermal and environmental controls; and attitude controls.

For life support systems see *54 Man/System Technology and Life Support.* For related information see also *05 Aircraft Design, Testing and Performance, 39 Structural Mechanics,* and *16 Space Transportation.*

N89-10112# Aerospace Corp., El Segundo, Calif. Chemistry and Physics Lab.
SULFIDE CORROSION OF SILVER CONTACTS DURING SATELLITE STORAGE
Reinhold Bauer 25 Mar. 1988 12 p
(Contract F04701-85-C-0086)
(AD-A196217; TR-0086A(2945-03)-7; SD-TR-88-53) Avail: NTIS HC A03/MF A01 CSCL 11F

Delays in satellite launchings may require satellites to be stored on the ground for up to 6 years, and, in some instances, electrical scratchy noise on pure silver electrical connectors may develop in as little as 6 months. This problem has been attributed to the growth of silver sulfide, Ag2S, a semiconductor, on the silver contact surfaces. We offer suggestions that could improve storage specifications for satellites where Ag2S might be reduced to a level (thickness) where it does not pose a problem. This review of Ag2S growth might also be applicable to other satellite components where silver Ag is present, e.g., mirrors. GRA

N89-10113# National Aerospace Lab., Tokyo (Japan).
A DIGITAL SIMULATION METHOD OF CUMULATIVE FATIGUE DAMAGE EVALUATION FOR SPACECRAFT COMPONENTS
1987 16 p In JAPANESE; ENGLISH summary
(NAL-TR-957; ISSN-0389-4010) Avail: NTIS HC A03/MF A01

Prior to launching of a satellite, several certification tests are carried out for satellite and rocket on-board components. The ground test requirements are strictly specified to verify their reliability and ability to accomplish mission objectives. But it is not easy to define ground test parameters such as load patterns, levels, and duration times in the earlier stages of whole system development. Test parameters after being fully integrated in the spacecraft would differ in general from those expected in the preliminary design stage. This work is concerned with the effect of various load patterns on the fatigue strength of mission equipment. A method of evaluating fatigue damage by using a fatigue damage accumulation (FDA) ratio is proposed, then the FDA ratios are computed for different types of load patterns. Random load time history, which has a given power spectrum density function, was generated by digital computer simulation. Two-dimensional cycle counting by an advanced type of the range-pair-mean methods was adapted. Miner's rule was applied to calculate cumulative fatigue damage. This work concentrates on FDA characteristics of various random load patterns which have the same power level. Simulation results showed that load patterns with predominant frequencies have about the same FDA ratio as patterns without predominant frequencies if both of them have the same frequency band width. The relationship between irregularity factors and FDA ratios is also discussed. Author

N89-10114 Virginia Polytechnic Inst. and State Univ., Blacksburg.
SOLUTION OF TWO-POINT BOUNDARY VALUE PROBLEMS IN OPTIMAL MANEUVERS OF FLEXIBLE VEHICLES Ph.D. Thesis
Roger Clifton Thompson 1988 172 p
Avail: Univ. Microfilms Order No. DA8804435

Obtaining solutions to nonlinear two point boundary value problems is often a formidable task that is effectively restricted to a relatively small number of numerical methods. An asymptotic perturbation method that can be applied to a large class of nonlinear two point boundary value problems is presented and compared with some of the classical numerical methods available. Simple examples are included to illustrate the application of the perturbation method. Two distinct types of optimal maneuvers of flexible vehicles are examined. An optimal control problem for three dimensional attitude acquisition of a rigid and a flexible spacecraft is formulated, and the perturbation method is used to determine the solution for each problem. For the rigid body attitude maneuvers, large angle solutions are generated. However, the flexible spacecraft optimal maneuvers are solved only for small angular motions and small flexural amplitudes. In the second type of problem, single axis, time optimal maneuvers of a flexible body are considered. A sub-optimal problem is developed, and numerical simulations for controlling multiple modes are presented. The solutions are then parameterized. Dissert. Abstr.

N89-10115*# National Aeronautics and Space Administration. Goddard Space Flight Center, Greenbelt, Md.
EFFECTS OF SWITCH LEAKAGES UPON NIMBUS-7 SMMR CALIBRATION
Daesoo Han and Seung T. Kim (ST Systems Corp., Lanham, Md.) Jun. 1988 15 p
(Contract NAS5-29386)
(NASA-CR-180792; NAS 1.26:180792) Avail: NTIS HC A03/MF A01 CSCL 22B

A calibration model for the Nimbus-7 Scanning Multichannel

Microwave Radiometer (SMMR) is studied. This model not only removes major drawbacks of the current calibration model but also helps us understand the performance degradation of the aging instrument. The current Nimbus-7 SMMR calibration algorithm was derived without considering the interference effect between the two orthogonally polarized signals merging at a ferrite polarization selector switch. The resulting calibrated brightness temperatures, considered as a function of scan angle phi, are not symmetric around phi=0. However, neither the origin of the asymmetry nor the manner in which the two orthogonal components are mixed is fully understood. The proposed calibration model incorporates all the leakage factors associated with the ferrite switches along the signal paths. The resulting calibration equations clarify how the orthogonal components of surface brightness are coupled at radiometers. As a consequence, the origin of the asymmetry is clearly identified and explained. In addition, the feasibility of absolute calibration using in-orbit data is discussed. Author

N89-10116# Instituto de Investigacion Tecnologia, Madrid (Spain).
STUDY ON CONCEPTUAL DESIGN OF SPACECRAFT USING COMPUTER-AIDED ENGINEERING TECHNIQUES Final Report
I. J. Perez-Arriaga, J. J. Alba, F. Cuadra, J. J. SanGil, M. Angulo, and N. Balteas Paris, France ESA Dec. 1987 138 p
(Contract ESTEC-6886/85-NL-PP)
(ESA-CR(P)-2615; ETN-88-93149) Avail: NTIS HC A07/MF A01

A formal characterization of the process of conceptual design of spacecraft was derived, and the basic functions and requirements for a Conceptual Design of Spacecraft Tool (CDST) were defined. The major building blocks needed in the CDST were individually analyzed, including: knowledge acquisition procedures; knowledge representation techniques; automatic design approach suitable for computer implementation; decision-making logic adapted to a multiobjective environment; and design process control logic relying on existing artificial intelligence techniques. A possible hardware and software configuration based on existing resources was derived, and a mock-up of a simplified CDST was developed and implemented so that hands-on experience on each major aspect can be obtained. A working plan for a phased/expandable development of the CDST was produced. ESA

N89-10117*# National Aeronautics and Space Administration. Lewis Research Center, Cleveland, Ohio.
THE SOLAR DYNAMIC RADIATOR WITH A HISTORICAL PERSPECTIVE
K. L. McLallin, M. L. Fleming, F. W. Hoehn, and R. L. Howerton (Rockwell International Corp., Canoga Park, Calif.) Aug. 1988 12 p Presented at the 23rd Intersociety Energy Conversion Engineering Conference, Denver Colo., 31 Jul. - 5 Aug. 1988; sponsored in part by ASME, AIAA, ANS, SAE, IEEE, ACS, and AIChE
(NASA-TM-100972; E-4265; NAS 1.15:100972) Avail: NTIS HC A03/MF A01 CSCL 22B

A historical perspective on pumped-fluid loop space radiators provides a basis for the design of the Space Station Solar Dynamic (SD) power module radiator. SD power modules, capable of generating 25 kW (electrical) each, are planned for growth in Station power requirements. The Brayton cycle SD module configuration incorporates a pumped-fluid loop radiator that must reject up to 99 kW (thermal). The thermal/hydraulic design conditions in combination with required radiator orientation and packaging envelope form a unique set of constraints as compared to previous pumped-fluid loop radiator systems. Nevertheless, past program successes have demonstrated a technology base that can be applied to the SD radiator development program to ensure a low risk, low cost system. Author

N89-10087*# National Aeronautics and Space Administration. Langley Research Center, Hampton, Va.
SPACE TRUSS ASSEMBLY USING TELEOPERATED MANIPULATORS
Walter W. Hankins, III, Randolph W. Mixon, Howard C. Jones, and Thomas W. Burgess (Oak Ridge National Lab., Tenn.) *In* NASA, Goddard Space Flight Center, Proceedings of 1987 Goddard Conference on Space Applications of Artificial Intelligence (AI) and Robotics 1987 18 p (For primary document see N89-10063 01-12)
Avail: NTIS HC A99/MF E03 CSCL 22B

N89-10100*# RCA Astro-Electronics Div., Princeton, N. J. Space Div.
KINEMATIC STUDY OF FLIGHT TELEROBOTIC SERVICER CONFIGURATION ISSUES
R. H. Lewis, R. D. Scott, and W. S. Howard *In* NASA, Goddard Space Flight Center, Proceedings of 1987 Goddard Conference on Space Applications of Artificial Intelligence (AI) and Robotics 1987 17 p (For primary document see N89-10063 01-12)
Avail: NTIS HC A99/MF E03 CSCL 22B

19 SPACECRAFT INSTRUMENTATION

For related information see also *06 Aircraft Instrumentation* and *35 Instrumentation and Photography.*

No abstracts in this category.

20 SPACECRAFT PROPULSION AND POWER

Includes main propulsion systems and components, e.g., rocket engines; and spacecraft auxilliary power sources.

For related information see also *07 Aircraft Propulsion and Power, 28 Propellants and Fuels, 44 Energy Production and Conversion,* and *15 Launch Vehicles and Space Vehicles.*

N89-10118# National Aerospace Lab., Tokyo (Japan).
FABRICATION AND TEST OF A CARBON-CARBON COMPOSITE COMBUSTION CHAMBER FOR A LOW THRUST STORABLE ENGINE
Kazuo Kusaka, Shuichi Ueda, Noboru Abe, Hiroshi Miyajima, Takuo Kuwahara, Katsuaki Kosaka, and Ryuichi Nagashima Oct. 1987 32 p In JAPANESE; ENGLISH summary
(NAL-TR-946; ISSN-0389-4010) Avail: NTIS HC A03/MF A01

One possible approach to obtaining a high specific impulse in a low thrust bipropellant engine is to reduce the film cooling requirement by constructing a combustion chamber with a temperature resistant yet-to-be-developed carbon/carbon (C/C) composite material whose high temperature specific strength is very high, is described. A preliminary effort to develop a C/C composite chamber, as well as an injector for a low thrust storable engine, is described. Performance tests of injectors for a 2000 N class, fuel film cooled, NTO/MMH propellant engine were conducted at sea level with a workhorse combustion chamber. It was shown that a graphite nozzle insert could be used repeatedly for performance evaluation at a firing duration of 7 seconds. A C/C composite chamber with SiC coating on the inner wall and organic silicide coating over the carbon CVD layer on the outer wall was selected for the firing test. Two sea level tests, of 30 and 60 s durations, at a chamber pressure of 0.85 MPa were demonstrated on a single C/C composite chamber. It was shown that the basic C/C composite material had sufficient high-temperature strength and that the SiC coating on the inner wall was durable at the operating conditions. The outside carbon CVD coating seemed to be effective in shutting off the permeability of the combustion gases from the inside of the chamber. However, the organic silicide coatings applied to protect the carbon CVD layer from oxidizing atmosphere in the sea level tests were not sufficiently effective. Author

N89-10119*# Rockwell International Corp., Canoga Park, Calif. Rocketdyne Div.
ORBIT TRANSFER ROCKET ENGINE TECHNOLOGY PROGRAM. PHASE 2: ADVANCED ENGINE STUDY Interim Report
C. Erickson, A. Martinez, and B. Hines Feb. 1987 85 p
(Contract NAS3-23773)
(NASA-CR-179602; NAS 1.26:179602; RI/RD-87-126) Avail: NTIS HC A05/MF A01 CSCL 21H

In Phase 2 of the Advanced Engine Study, the Failure Modes and Effects Analysis (FMEA) maintenance-driven engine design, preliminary maintenance plan, and concept for space operable disconnects generated in Phase 1 were further developed. Based on the results of the vehicle contractors Orbit Transfer Vehicle (OTV) Concept Definition and System Analysis Phase A studies, minor revisions to the engine design were made. Additional refinements in the engine design were identified through further engine concept studies. These included an updated engine balance incorporating experimental heat transfer data from the Enhanced Heat Load Thrust Chamber Study and a Rao optimum nozzle contour. The preliminary maintenance plan of Phase 1 was further developed through additional studies. These included a compilation of critical component lives and life limiters and a review of the Space Shuttle Main Engine (SSME) operations and maintenance manual in order to begin outlining the overall maintenance procedures for the Orbit Transfer Vehicle Engine and identifying technology requirements for streamlining space-based operations. Phase 2 efforts also provided further definition to the advanced fluid coupling devices including the selection and preliminary design of a preferred concept and a preliminary test plan for its further development. Author

N89-10120 Georgia Inst. of Tech., Atlanta.
INVESTIGATION OF THE FLAME-ACOUSTIC WAVE INTERACTION DURING AXIAL SOLID ROCKET INSTABILITIES Ph.D. Thesis
Subramanian V. Sankar 1987 213 p
Avail: Univ. Microfilms Order No. DA8803712

The mechanisms responsible for the driving of axial mode instabilities in solid propellant rocket motors are investigated. Since experimental investigation of actual solid propellant flames is presently not possible because of the extremely small dimensions of their combustion zones, this research has investigated the driving properties of simulated solid propellant flames which are amenable to experimental probing. Specifically, the behavior of laminar, premixed, flat flames, stabilized on the porous side wall of a rectangular duct and subjected to axial acoustic oscillations was investigated. The oscillatory behavior of the flames were experimentally investigated with the help of pressure sensors, high speed schlieren/shadowgraph cine photography, photomultipliers and a Laser Doppler Velocimeter. These studies reveal that the flames drive the acoustic waves through a combined dipole-monopole mechanism. Furthermore, the driving/damping properties of the investigated flames are dependent on their location with respect to the standing acoustic wave in the duct, the flame structure, the frequency of the acoustic oscillation and the acoustic admittance of the burner surface. Dissert. Abstr.

N89-10121# National Aerospace Lab., Tokyo (Japan).
MEASUREMENT OF INFRARED HORIZON PROFILES FROM TT-500A SOUNDING ROCKET
Isao Yamaguchi, Yoshiaki Ohkami, Osamu Okamoto, Takashi Kida, Toshio Akimoto, and Yasuhumi Wakabayashi Oct. 1987 106 p In JAPANESE; ENGLISH summary
(NAL-TR-947; ISSN-0389-4010) Avail: NTIS HC A06/MF A01

An earth sensor utilizing infrared (IR) horizon radiation is one of the fundamental attitude sensors for three-axis attitude stabilized spacecraft. The attitude measurement accuracy of this type of sensor greatly depends on the variation of the IR radiation magnitude and characteristics, which are determined by upper atmosphere meteorological conditions. The IR radiation measurements from the TT-500A sounding rocket performed in August, 1983, is presented together with the results of the preliminary study. Author

N89-10122*# National Aeronautics and Space Administration. Lewis Research Center, Cleveland, Ohio.
PHOTOVOLTAICS FOR HIGH CAPACITY SPACE POWER SYSTEMS
Dennis J. Flood Oct. 1988 16 p Presented at the 39th Annual Astronautical Congress of the International Astronautical Federation, Bangalore, India, 8-15 Oct. 1988
(NASA-TM-101341; E-4360; NAS 1.15:101341) Avail: NTIS HC A03/MF A01 CSCL 10B

The anticipated energy requirements of future space missions will grow by factors approaching 100 or more, particularly as a permanent manned presence is established in space. The advances that can be expected in solar array performance and lifetime, when coupled with advanced, high energy density storage batteries and/or fuel cells, will continue to make photovoltaic energy conversion a viable power generating option for the large systems of the future. The specific technologies required to satisfy any particular set of power requirements will vary from mission to mission. Nonetheless, in almost all cases the technology push will be toward lighter weight and higher efficiency, whether of solar arrays or storage devices. This paper will describe the content and direction of the current NASA program in space photovoltaic technology. The paper will also discuss projected system level capabilities of photovoltaic power systems in the context of some of the new mission opportunities under study by NASA, such as a manned lunar base, and a manned visit to Mars. Author

N89-10123*# National Aeronautics and Space Administration. Lewis Research Center, Cleveland, Ohio.
TECHNOLOGY ISSUES ASSOCIATED WITH FUELING THE NATIONAL AEROSPACE PLANE WITH SLUSH HYDROGEN
Ned P. Hannum [1988] 9 p Prepared for presentation at the 7th Joint Intersociety Cryogenic Conference Symposium, Houston, Tex., 22-26 Jan. 1989; sponsored in part by ASME, AIChE and IIR
(NASA-TM-101386; E-4445; NAS 1.15:101386) Avail: NTIS HC A02/MF A01 CSCL 21H

The National Aerospace Plane is a horizontal takeoff and landing, single stage-to-orbit vehicle using hydrogen fuel. The first flights are planned for the mid 1990's. The success of this important national program requires advances in virtually every discipline associated with both airbreathing and space flight. The high heating value, cooling capacity, and combustion properties make hydrogen the fuel of choice, but low density results in a large vehicle. Both fuel cooling capacity and density are increased with the use of slush hydrogen and result in significant reductions in vehicle size. A national program to advance this technology and to find engineering solutions to the many design issues is now under way. The program uses the expertise of the cryogenics production and services industry, the instrumentation industry, universities and governments. The program will be discussed to highlight the major issues and display progress to date. Author

N89-10440*# Electro Magnetic Applications, Inc., Lakewood, Colo.
TRANSFER IMPEDANCE MEASUREMENTS OF THE SPACE SHUTTLE SOLID ROCKET MOTOR (SRM) JOINTS, WIRE MESHES AND A CARBON GRAPHITE MOTOR CASE
Peter B. Papazian, Rodney A. Perala, John D. Curry, Alan B. Lankford, and J. David Keller *In* NOAA, International Aerospace and Ground Conference on Lightning and Static Electricity Apr. 1988 p 68-77 Sponsored in part by NASA Langley Research Center, and by Morton Thiokol, Inc., Brigham City, Utah (For primary document see N89-10429 01-47)
(Contract NAS8-30490)
Avail: NTIS HC A23/MF A01 CSCL 04B

23 CHEMISTRY AND MATERIALS (GENERAL)

N89-10124*# National Aeronautics and Space Administration. Lewis Research Center, Cleveland, Ohio.
THE EFFECT OF Al2O3, CaO, Cr2O3 AND MgO ON DEVITRIFICATION OF SILICA
Isidor Zaplatynsky Oct. 1988 14 p
(NASA-TM-101335; E-4350; NAS 1.15:101335) Avail: NTIS HC A03/MF A01 CSCL 07A

The effect of doping on devitrification of vitreous silica was studied at 1100, 1200, and 1300 C. Dispersion of dopants on a molecular scale was accomplished via a sol-gel technique. All dopants accelerated the devitrification of silica but to different degrees. The most active was CaO followed by MgO, Al2O3, and Cr2O3. Pure silica and silica containing Cr2O3 and Al2O3 devitrified to alpha-cristobalite only, whereas silica doped with CaO and MgO produced alpha-quartz and alpha-cristobalite. It appears that prolonged heat treatment would cause alpha-quartz to transform to alpha-cristobalite. Author

24 COMPOSITE MATERIALS

Includes physical, chemical, and mechanical properties of laminates and other composite materials.
For ceramic materials see *27 Nonmetallic Materials.*

N89-10125*# Clemson Univ., S.C. Dept. of Mechanical Engineering.
FRACTURE CRITERIA FOR DISCONTINUOUSLY REINFORCED METAL MATRIX COMPOSITES Semiannual Report, 16 Feb. - 15 Aug. 1988
H. J. Rack, J. G. Goree, J. Albritton, and P. Ratnaparkhi 21 Oct. 1988 152 p
(Grant NAG1-724)
(NASA-CR-181175; NAS 1.26:181175) Avail: NTIS HC A08/MF A01 CSCL 11D

Summarized is the progress achieved during the period September 16, 1987 to August 15, l988 on NASA Grant NAG1-724, Fracture Criteria for Discontinuously Reinforced Metal Matrix Composites. Appended are copies of three manuscripts prepared under NASA funding during the performance period. Author

N89-10126# Sandia National Labs., Albuquerque, N. Mex.
EVALUATION AND CONTROL OF RESIDUAL STATES IN CURVED, COMPOSITE PANELS
R. C. Reuter, Jr. 1988 11 p Presented at the 4th Japan-US Conference on Composite Panels, Washington, D.C., 27 Jun. 1988
(Contract DE-AC04-76DP-00789)
(DE88-012103; SAND-87-2294C; CONF-8806164-1) Avail: NTIS HC A03

Analytical techniques were employed to characterize residual effects induced in laminated, curved, composite panels during fabrication processing. The analysis was utilized to predict the radius of a mold upon which panels could be fabricated so that they deform, upon release from the mold, to a predetermined radius of curvature. Sample panels were fabricated which provided experimental data and partial verification of the analytical methods developed. DOE

N89-10127*# Mississippi State Univ., Mississippi State. Dept. of Chemical Engineering.
STANDARDIZATION OF THE CARBON-PHENOLIC MATERIALS AND PROCESSES. VOL. 1: EXPERIMENTAL STUDIES Final Report, 1 Sep. 1985 - 31 Aug. 1988
William B. Hall 31 Aug. 1988 180 p
(Grant NAG8-545)
(NASA-CR-183226; NAS 1.26:183226) Avail: NTIS HC A09/MF A01 CSCL 11D

Carbon-phenolic composite materials are used as ablative material in the solid rocket motor nozzle of the Space Shuttle. The nozzle is lined with carbon cloth-phenolic resin composites. The nominal effects of the completely consumed solid propellant on the carbon-phenolic material are given. The extreme heat and erosion of the burning propellant are controlled by the carbon-phenolic composite by ablation, the heat and mass transfer process in which a large amount of heat is absorbed by sacrificially removing material from the nozzle surface. Phenolic materials ablate with the initial formation of a char. The depth of the char is a function of the heat conduction coefficient of the composite. The char layer is a very poor heat conductor so it protects the underlying phenolic composite from the high heat of the burning propellant. The nozzle component ablative liners (carbon cloth-phenolic composites) are tape wrapped, hydroclave and/or autoclave cured, machined, and assembled. The tape consists of a prepreg broadcloth. The materials flow sheet for the nozzle ablative liners is shown. The prepreg is a three component system: phenolic resin, carbon cloth, and carbon filler. This is Volume 1 of two, Experimental Studies. F.M.R.

N89-10128*# Case Western Reserve Univ., Cleveland, Ohio.
THERMODYNAMIC ANALYSIS OF COMPATIBILITY OF SEVERAL REINFORCEMENT MATERIALS WITH FeAl ALLOYS
Ajay K. Misra Washington NASA Oct. 1988 30 p
(Contract NCC3-43)
(NASA-CR-4172; NAS 1.26:4172) Avail: NTIS HC A03/MF A01 CSCL 11D

Chemical compatibility of several reinforcement materials with FeAl alloys within the concentration range 40 to 50 at pct Al have been analyzed from thermodynamic considerations at 1173 and 1273 K. The reinforcement materials considered in this study include carbides, borides, oxides, nitrides, and silicides. Although several chemically compatible reinforcement materials are identified, the coefficients of thermal expansion for none of these materials match closely with that of FeAl alloys and this might pose serious problems in the design of composite systems based on FeAl alloys. Author

N89-10129*# Washington Univ., St. Louis, Mo. Lab. for Ultrasonics.
PHYSICAL PRINCIPLES OF ULTRASONIC NON-DESTRUCTIVE EVALUATION OF ADVANCED COMPOSITES Semiannual Progress Report, 15 Mar. - 14 Sep. 1988
James G. Miller Sep. 1988 19 p
(Grant NsG-1601)
(NASA-CR-180225; NAS 1.26:180225) Avail: NTIS HC A03/MF A01 CSCL 11D

Results are presented from the continued investigations into the use of ultrasonic measurement techniques for the detection and characterization of porosity. The effects that bleeder cloth impressions (left after the cure process) have on the capability of polar backscatter to interrogate volume effects such as porosity are described. Some preliminary data regarding a comparison of phase sensitive and phase insensitivie detection for materials characterization is presented. Author

N89-10130*# National Aeronautics and Space Administration. Lewis Research Center, Cleveland, Ohio.
PROPERTIES OF SILICON CARBIDE FIBER-REINFORCED SILICON NITRIDE MATRIX COMPOSITES
Ramakrishna T. Bhatt (Army Aviation Systems Command, Cleveland, Ohio.) Jun. 1988 17 p Presented at the International Conference on Whisker- and Fiber-Toughened Ceramics, Oak Ridge, Tenn., 6-9, Jun. 1988; sponsored by American Society for Metals
(NASA-TM-101356; E-4386; NAS 1.15:101356; AVSCOM-TR-88-C-027) Avail: NTIS HC A03/MF A01 CSCL 11D

The mechanical properties of NASA Lewis developed SiC/RBSN composites and their thermal and environmental stability havd been studied. The composites consist of nearly 30 vol pct of aligned 142 micron diameter chemically vapor-deposited SiC

fibers in a relatively porous silicon nitride matrix. In the as-fabricated condition, the unidirectional and 2-D composites exhibited metal-like stress-strain behavior, graceful failure, and showed improved properties when compared with unreinforced matrix of comparable density. Furthermore, the measured room temperature tensile properties were relativley independent of tested volume and were unaffected by artifical notches normal to the loading direction or by thermal shocking from temperatures up to 800 C. The four-point bend strength data measured as a function of temperature to 1400 C in air showed that as-fabricated strength was maintained to 1200 C. At 1400 C, however, nearly 15 pct loss in strength was observed. Measurement of room temperature tensile strength after 100 hr exposure at temperatures to 1400 C in a nitrogen environment indicated no loss from the as-fabricated composite strength. On the other hand, after 100 hr exposure in flowing oxygen at 1200 and 1400 C, the composites showed approximately 40 pct loss from their as-fabricated ultimate tensile strength. Those exposed between 400 to 1200 C showed nearly 60 pct strength loss. Oxidation of the fiber/matrix interface as well as internal oxidation of the porous Si3N4 matrix are likely mechanisms for strength degradation. The excellent strength reproducibility, notch insensitivity, and high temperature strength of the composite makes it an ideal candidate for advanced heat engine applications provided coating or densification methods are developed to avoid internal oxidation attack. Author

N89-10131*# Case Western Reserve Univ., Cleveland, Ohio.
THERMODYNAMIC ANALYSIS OF COMPATIBILITY OF SEVERAL REINFORCEMENT MATERIALS WITH BETA PHASE NiAl ALLOYS Final Report
Ajay K. Misra Washington NASA Nov. 1988 60 p
(Contract NCC3-43)
(NASA-CR-4171; E-4299; NAS 1.26:4171) Avail: NTIS HC A04/MF A01 CSCL 11D

Chemical compatibility of several reinforcement materials with beta phase NiAl alloys within the concentration range 40 to 50 at. percent Al have been analyzed from thermodynamic considerations at 1373 and 1573 K. The reinforcement materials considered in this study include carbides, borides, oxides, nitrides, beryllides, and silicides. Thermodynamic data for NiAl alloys have been reviewed and activity of Ni and Al in the beta phase have been derived at 1373 and 1573 K. Criteria for chemical compatibility between the reinforcement material and the matrix have been defined and several chemically compatible reinforcement materials have been defined. Author

N89-10132*# PRC Systems Services Co., Hampton, Va.
CHEMOVISCOSITY MODELING FOR THERMOSETTING RESIN SYSTEMS, PART 3
T. H. Hou and J. M. Bai Aug. 1988 42 p
(Contract NAS1-18000)
(NASA-CR-181718; NAS 1.26:181718) Avail: NTIS HC A03/MF A01 CSCL 11D

A new analytical model for simulating chemoviscosity resin has been formulated. The model is developed by modifying the well established Williams-Landel-Ferry (WLF) theory in polymer rheology for thermoplastic materials. By introducing a relationship between the glass transition temperature (T sub g (t)) and the degree of cure alpha(t) of the resin system under cure, the WLF theory can be modified to account for the factor of reaction time. Temperature-dependent functions of the modified WLF theory parameters C sub 1 (T) and C sub 2 (T) were determined from the isothermal cure data. Theoretical predictions of the model for the resin under dynamic heating cure cycles were shown to compare favorably with the experimental data. This work represents a progress toward establishing a chemoviscosity model which is capable of not only describing viscosity profiles accurately under various cure cycles, but also correlating viscosity data to the changes of physical properties associated with the structural transformations of the thermosetting resin systems during cure. Author

N89-10133# Sandia National Labs., Albuquerque, N. Mex.
FLEXURAL FATIGUE OF A 2-D CARBON/CARBON COMPOSITE MATERIAL
T. R. Guess 1988 15 p Presented at the 20th International Conference of the Society for the Advancement of Materials and Process Engineering, Minneapolis, Minn., 27 Sep. 1988
(Contract DE-AC04-76DP-00789)
(DE88-010501; SAND-87-3040C; CONF-880909-1) Avail: NTIS HC A03/MF A01

An experimental study of the static and cyclic fatigue response of a quasi-isotropic carbon/carbon composite was conducted. This 16-ply carbon fabric/carbon matrix composite is a candidate material for use as RF antenna shield limiters in the Tokamak Fusion Test Reactor, Princeton, N.J. In this application, the material will be subjected to bending loads and must withstand 100,000 cycles without failure. The experimental approach was to use the four-point flexural test to evaluate both static and fatigue properties of the material at room temperature. For the static tests, beam specimens were strain gaged on both the tension and compression sides and loaded to failure. This composite had identical moduli in tension and compression (9.4 million psi) and an apparent flexural strength of about 27.6 ksi; specimen yielding began between 17 and 19 ksi. Cyclic fatigue tests were conducted under sinusoidal load control at different levels of stress amplitude. Each cyclic test was continued until either fatigue failure occurred or 100,000 cycles were reached. Those specimens reaching 100,000 cycles without failure were subsequently loaded to failure for measurement of residual flexural strength. The experimental fatigue data appear to be linear when plotted as an S-N curve (flexural stress vs. log N), where N is the number of cycles to failure. When the maximum flexural stress was less than about 70 percent of the static flexural strength, the carbon/carbon composite had a fatigue life greater than 100,000 cycles. Also, it was found that those specimens which did not fail in the first 100,00 cycles had residual strengths equal to specimens loaded to failure on the first cycle. DOE

N89-10134*# National Aeronautics and Space Administration. Lewis Research Center, Cleveland, Ohio.
THERMAL EFFECTS ON THE MECHANICAL PROPERTIES OF SiC FIBER REINFORCED REACTION BONDED SILICON NITRIDE MATRIX (SiC/RBSN) COMPOSITES
R. T. Bhatt and R. E. Phillips (Sverdrup Technology, Inc., Cleveland, Ohio.) Oct. 1988 17 p Submitted for publication
(NASA-TM-101348; E-4375; NAS 1.15:101348; AVSCOM-TR-88-C-028) Avail: NTIS HC A03/MF A01 CSCL 11D

The elevated temperature four-point flexural strength and the room temperature tensile and flexural strength properties after thermal shock were measured for ceramic composites consisting of 30 vol pct uniaxially aligned 142 micron diameter SiC fibers in a reaction bonded Si3N4 matrix. The elevated temperature strengths were measured after 15 min of exposure in air at temperatures to 1400 C. Thermal shock treatment was accomplished by heating the composite in air for 15 min at temperatures to 1200 C and then quenching in water at 25 C. The results indicate no significant loss in strength properties either at temperature or after thermal shock when compared with the strength data for composites in the as-fabricated condition. Author

N89-10135 British Petroleum Co. Ltd., London (England).
GRADED STRUCTURE COMPOSITES Patent Application
Alan Robert Begg, Colin William Brown, and Neil Edward Seth Charman 23 Mar. 1988 6 p Filed 4 Sep. 1987 Priority 18 Sep. 1986 GB 8622464
(EP-Patent-0-260-850-A2; EP-Patent-Appl-87307826.5; Int-Patent-Class-B22F-7/02; ETN-88-93126) Avail: UK Patent Office, 25 Southampton Buildings, London WC2A 1AY, United Kingdom

Tough, wear resistant tungsten carbide steel graded structure composite, a process for preparing it, and tools and products fabricated from it are described. The composites have a surface layer, e.g., of WC and a binder; an interface layer, e.g., which is a

stepwise transition from the surface layer whereby the binder content thereof gradually increases; a substrate layer which is a combination of, e.g., an initial high carbon steel layer; and a base layer of bainitic steel. The composites are substantially nonporous and can be used to fabricate components such as drill bits, wear plates, pump components, machine tools, seals, washers, and bearings. ESA

N89-10136 British Petroleum Co. Ltd., London (England).
LEAF SPRING Patent Application
Stephen Alexander Hope 20 Jan. 1988 7 p Filed 9 Jul. 1987 Priority 17 Jul. 1986 GB 8617540
(EP-Patent-0-253-574-A1; EP-Patent-Appl-87306071.9; Int-Patent-Class-F16F-1/36; ETN-88-93128) Avail: UK Patent Office, 25 Southampton Buildings, London WC2A 1AY, United Kingdom

A leaf spring of fiber reinforced composite material comprising a longitudinal cross section having a thickened central zone, adjacent tapered zones, and end zones is described. The tapered zones have curved surfaces comprising convex and concave portions, the convex portions being adjacent to the central zones and the concave portions being adjacent to the end zones. Each convex and concave portion is a segment of a curve defined by the equation (X/A) sup C + (Y/B) sup D = 1. ESA

N89-10137 British Petroleum Co. Ltd., London (England).
POLYMER COMPOSITES Patent Application
Paul Davison Calvert and Raymond Mario Ellul 12 Aug. 1987 15 p Filed 29 Jan. 1987 Priority 30 Jan. 1986 GB 8602318; 20 May 1986 GB 8612283
(EP-Patent-0-232-138-A2; EP-Patent-Appl-87300809.8; Int-Patent-Class-C-08-K-3/00; ETN-88-93130) Avail: UK Patent Office, 25 Southampton Buildings, London WC2A 1AY, United Kingdom

Polymer composites comprising polymeric matrices in which crystallites of organic or inorganic compounds are grown in-situ is presented. Four growth techniques are suggested. The specific technique chosen depends on factors such as the nature of the polymer matrix, the crystals desired, the solubility of the components in any given solvent, the thickness of the polymer, or the crystal density of the composite. Whichever technique is used to grow the non-centrosymmetrical crystals in the polymer matrix, it is also highly desirable to orient the crystals grown in the polymer matrix so that all the crystals are substantially in parallel alignment. This is essential if the composite is to act as a single crystal with respect to its electro-optical properties. ESA

N89-10479# Office National d'Etudes et de Recherches Aeronautiques, Paris (France).
ELECTROMAGNETIC COUPLING THROUGH COMPOSITE MATERIALS
V. Gobin, G. Labaune, and F. Issac *In* NOAA, International Aerospace and Ground Conference on Lightning and Static Electricity Apr. 1988 p 370-37 Sponsored in part by DRET (Direction des Recherches, Etudes et Techniques), and AMD/BA (Avions Marcel Dassault Breguet Aviation) (For primary document see N89-10429 01-47)
Avail: NTIS HC A23/MF A01 CSCL 11D

25 INORGANIC AND PHYSICAL CHEMISTRY

Includes chemical analysis, e.g., chromatography; combustion theory; electrochemistry; and photochemistry.

For related information see also *77 Thermodynamics and Statistical Physics.*.

N89-10138# California Univ., Berkeley. Lawrence Berkeley Lab. Materials and Chemical Science Div.
TWO-DIMENSIONAL SPATIALLY RESOLVED RAMAN SPECTROSCOPY OF SOLID MATERIALS
D. K. Veirs, G. M. Rosenblatt, R. H. Dauskardt, and R. O. Ritchie Mar. 1988 9 p Presented at the MAS/EMSA Microbeam Analysis Conference, Milwaukee, Wis., 7 Aug. 1988
(Contract DE-AC03-76SF-00098)
(DE88-014867; LBL-24971; CONF-880841-18) Avail: NTIS HC A02/MF A01

Chemical compositional analysis of solid materials often is based on vibrational spectroscopy, either infrared or Raman. Vibrational analysis is particularly valuable. The development of mutichannel detection systems for Raman spectroscopy coupled with microscopic techniques has resulted in a number of commercial Raman microprobes (from Spex Industries, Jobin-Yvon ISA, Dilor, for example) capable of probing areas on the order of 100 sq microns routinely. For macroscopic samples, with dimensions of thousands of microns on a side, an instrument which multiplexes both the spatial domain and wavelength would enhance the capability of Raman spectroscopy. We report on the development of such a Raman instrument and describe, as an example, its application to the investigation of the phase transformation accompanying crack growth in partially stabilized zirconia (PSZ). DOE

N89-10139# Los Alamos National Lab., N. Mex.
AB INITIO STUDIES OF TRANSITION-METAL DIHYDROGEN CHEMISTRY
Edward M. Kober and P. Jeffrey Hay 1988 19 p Presented at the Symposium on Computational Chemistry: The Challenge of D and F Electrons, Toronto, Ontario, 6 Jun. 1988
(Contract W-7405-eng-36)
(DE88-014467; LA-UR-88-1791; CONF-8806182-1) Avail: NTIS HC A03/MF A01

Examples of transition metal complexes containing dihydrogen ligands are investigated using ab initio electronic structure calculations employing effective core potentials. Calculated geometrical structures and relative energies of various forms of WL5(H2) complexes (L = CO, PR3) are reported, and the influence of the ligand on the relative stabilities of the dihydrogen and dihydride forms is studied. The possible intramolecular mechanisms for H/D scrambling are investigated in another d sup 6 complex, Cr(CO)4(H2)2, where various polyhydride intermediates are possible. DOE

N89-10140# California Univ., Berkeley. Lawrence Berkeley Lab. National Center for Electron Microscopy.
BACKGROUND MODELLING ALTERNATIVES IN ELECTRON ENERGY-LOSS SPECTROSCOPY AND THEIR IMPLICATIONS ON MICROANALYSIS
Kannan M. Krishnan and M. T. Stampfer Apr. 1988 4 p Presented at the MAS/EMSA Microbeam Analysis Conference, Milwaukee, Wis., 7 Aug. 1988
(Contract DE-AC03-76SF-00098)
(DE88-010361; LBL-25203; CONF-880841-14) Avail: NTIS HC A02/MF A01

With the advent of parallel detectors, electron energy-loss spectroscopy (EELS) is expected to be employed increasingly in the routine microanalysis of light elements. The quantitation formulae that are used are relatively simple and straightforward and require only a measurement of the integrated core-loss intensity over a particular energy window beyond the ionization edge and most often, a calculated ionization cross-section. Even though the hydrogenic cross-sections that are used routinely for microanalysis can be a source of error, it is observed that the procedure that largely determines the accuracy of quantification is the removal of the contribution of the background below the ionization edge. DOE

N89-10141*# National Aeronautics and Space Administration, Washington, D.C.
A NEW METHOD OF DETERMINING ACID BASE STRENGTH DISTRIBUTION AND A NEW ACIDITY-BASICITY SCALE FOR SOLID CATALYSTS: THE STRONGEST POINT, HO
T. Yamanaka and K. Tanabe Aug. 1988 19 p Transl. into ENGLISH from Sekiyo Gakkai Shi (Japan), v. 20, no. 12, 1977 p 1122-1125 Transl. by SCITRAN, Inc., Santa Barbara, Calif.

Original document was prepared by Takasago Perfumery Co., Ltd, Tokyo, Japan, and by Hokkaido Univ., Sapporo, Japan
(Contract NASw-4307)
(NASA-TT-20334; NAS 1.77:20334) Avail: NTIS HC A03/MF A01 CSCL 07D

The use of the strongest H sub 0 as an acid-base scale is illustrated. It is concluded that the catalytic activity arises from carbonium ions for solid catalysts whose strongest point values are less than 2, from carbanions for solid catalysts whose strongest point values are larger than 10, and from both acid and base points for those which have the H sub 0 value of 4 to 8. Further, from correlation between selectivity of o-isopropyl compounds and their strongest point H sub 0, it was found that the ortho selectivity increased as the basicity of the solid surface increased. Author

N89-10142# SRI International Corp., Menlo Park, Calif.
BASIC RESEARCH ON NATURAL GAS COMBUSTION PHENOMENA-CATALYTIC COMBUSTION Annual Report, 1987
M. A. Quinlan, H. Wise, and J. G. McCarty Mar. 1988 73 p
(Contract GRI-5086-260-1245)
(PB88-214606; GRI-88/0096) Avail: NTIS HC A04/MF A01 CSCL 21B

The intrinsic methane combustion activity of a series of metal oxide catalysts representing several structural classes was determined by temperature programmed reaction and stationary state order of reaction experiments. The oxide catalysts examined thus far include: (1) a series of lanthanum based transition metal 1,1 perovskites; (2) a layered perovskite, La2NiO4; (3) YBa2Cu3O7, the superconducting perovskite; (4) several alumina spinels; and (5) simple binary oxides of disparate structure. These metal oxide catalysts were typically prepared by conventional precipitation and calcination methods and characterized by X-ray diffraction, BET surface area, and the temperature programmed evolution of oxygen. When normalized for surface area, the specific methane combustion activity of transition metal oxides correlates inversely with their thermochemical stability. The performance of the oxide catalysts was greatly influenced by sintering at elevated temperatures. The most stable oxide was the lanthanum-alumina perovskite, LaAlO3, which was stable up to 1473 K. The kinetics of catalytic methane combustion were examined in detail for selected catalysts.
Author

N89-10143# Pacific Northwest Labs., Richland, Wash. Chemical Methods and Separations Group.
ELECTROSPRAY IONIZATION PHENOMENA AND THE INTERFACE OF CAPILLARY ELECTROPHORESIS AND MASS SPECTROMETRY
Richard D. Smith, Charles J. Barinaga, and Harold R. Udseth Jun. 1988 4 p Presented at the 36th Annual Conference on Mass Spectrometry and Allied Topics, San Francisco, Calif., 6 Jun. 1988
(Contract DE-AC06-76RL-01830)
(DE88-014080; PNL-SA-15664; CONF-8806199-4) Avail: NTIS HC A02/MF A01

Recently a new electrospray ionization interface for capillary electrophoresis-mass spectroscopy (CE-MS) has been developed. The interface uses a sheath flow of liquid to make electrical contact at the CZE terminus, thus defining both the CZE and electrospray field gradients. Ions created by the ESI process are sampled through a 1 mm nozzle into a region mechanically pumped at 50 L/s using a single-stage roots blower. The ions entering this region are sampled through a 2 mm dia skimmer orifice located 0.5 cm behind the nozzle orifice. Ions passing through the skimmer enter a radio frequency focusing quadrupole. This region is pumped by a cryopump. A mixture of four quaternary phosphonium salts is used to illustrate capillary electrophoresis separations with mass spectroscopy and their uses. DOE

N89-10144# National Aerospace Lab., Tokyo (Japan).
STUDY ON TWIN VALVELESS PULSE BURNER: COMBUSTION STABILITY AND MIXING PATTERNS
1987 16 p In JAPANESE; ENGLISH summary
(NAL-TR-955; ISSN-0389-4010) Avail: NTIS HC A03/MF A01

Ensemble-averaged heat release rates and pressures inside the combustion chambers were measured to better understand the operating characteristics of a twin valveless pulse burner. The combustion flows were also visualized using a high-speed laser schlieren photography. A measurement system of OH chemiluminescence intensity and pressure transducers were used as diagnostic tools. Based on the well-known Rayleigh's criterion, the effects on the combustion stabilities of varying the equivalence ratio and the mass flux are discussed. Results show that the phase difference between heat release rate and pressure contributes significantly to the pulse combustion stability. In addition, the phase difference does not depend on the mass flux but on the equivalence ratio, indicating that the fuel/air mixing is a determinant factor in the phase relationship. This mixing process was successfully visualized on the schlieren photographs.
Author

N89-10145# Cornell Univ., Ithaca, N.Y. Lab. of Atomic and Solid State Physics.
PHYSICS AND TECHNOLOGY FOR THE IN-SITU INVESTIGATION OF PROPERTIES OF MATERIALS Annual Report, 15 Jan. 1987 - 14 Jan. 1988
J. M. Parpia and R. C. Richardson 12 May 1988 9 p
(Grant AF-AFOSR-0148-87; AF Proj. 2306)
(AD-A195498; AFOSR-88-0611TR) Avail: NTIS HC A02/MF A01 CSCL 07D

The progress report is broken up into four sections, the first detailing the apparatus constructed, the second, results on CoSi2, and third, very recent results on free standing Aluminium films and wires. In addition, results on Arsenic doped Silicon are proceeding and are described briefly. Samples can be inserted into our Oxford 200 top loading dilution refrigerator cryostat which has been modified to include a 7T magnet mounted on the mixing chamber. We also have a small independently operated solenoid which is used to ramp the magnetic field slowly, and to provide a zero field environment, by nulling out trapped fields in the main solenoid. This apparatus allows us to carry out transport measurements down below 20 mK (5 mK in zero field), provided that the sample holders are properly heat sunk. We have carried out measurements on several samples of Cobalt Silicate (CoSi2). The first was on a 170 Angstrom thick layer where we observed that the material had a resistance ration of approximately 5.5, with a superconducting transition at approximately 1K (mid point 0.75K), (see figure 1a), and a critical field of approximately 100 G. In this sample, we have observed a shallow minimum in resistance at 4.5 K (figure 1b) with a log T low temperature resistance in the normal state. GRA

N89-10146# Utah State Univ., Bedford, Mass. Radiance Lab.
HIGH RESOLUTION INFRARED SPECTROSCOPY OF CARBON DIOXIDE AND NITROUS OXIDE AT ELEVATED TEMPERATURES Environmental Research Papers, Oct. 1985 - 31 Dec. 1987
Mark P. Esplin, William M. Barowy, Ronald J. Huppi, Laurence S. Rothman, and George A. Vanasse 11 Mar. 1988 69 p
(Contract F19628-83-C-0056)
(AD-A196317; AFGL-TR-88-0067; AFGL-ERP-999) Avail: NTIS HC A04/MF A01 CSCL 07B

Although both Carbon Dioxide and Nitrous Oxide are minor constituents of the terrestrial atmosphere, they play leading roles in several current atmospheric problems. Both CO2 and N2O are greenhouse gases, and while it is known that the atmospheric concentrations of both gases is increasing, the impact of these trends on global temperature is not yet adequately understood. In addition to being a greenhouse gas, N2O plays an indirect part in ozone chemistry. Heating a molecule makes possible the observations of molecular transitions originating from highly excited rotation-vibration states. Heating a molecule makes possible the observations of molecular transitions originating from highly excited rotation-vibration states. These observations can then be used to characterize the shape of the molecular potential function at increasing distances from the minimum of the potential function. The infrared spectra of linear molecules like CO2 and N2O are

composed of vibration bands made up of a number of nearly equally spaced rotation lines. A Fourier Spectrometer is ideally suited to the study of high temperature gases since it meets both of these needs by providing high resolution over a wide spectral region. GRA

N89-10147# Rice Univ., Houston, Tex. Dept. of Chemical Engineering.
REPORTS OF INVESTIGATIONS ON: DERIVATION OF AN INFINITE-DILUTION ACTIVITY COEFFICIENT MODEL AND APPLICATION TO TWO-COMPONENT VAPOR/LIQUID EQUILIBRIA DATA Final Report
Vaughan P. Roper and Riki Kobayashi Feb. 1988 325 p
(Contract DE-FG22-83PC-60037)
(DE88-007517; DOE/PC-60037/T8) Avail: NTIS HC A14/MF A01

Infinite-dilution fugacity coefficients were obtained for the system fluorene/phenanthrene at thirteen temperatures by fitting total pressure across the entire mole fraction range by a computer routine. A thermodynamically consistent routine, that allowed for both positive and negative pressure deviations from the ideal values, was used to correlate data over the full mole fraction range from 0 to 1. The four-suffix Margules activity coefficient model without modification essentially served this purpose since total pressures and total pressure derivatives with respect to mole fraction were negligible compared to pressure measurement precision. The water/ethanol system and binary systems comprised of aniline, chlorobenzene, acetonitrile and other polar compounds were fit for total pressure across the entire mole fraction range for binary Vapor-Liquid-Equilibria (VLE) using the rigorous, thermodynamically consistent Gibbs-Duhem Relation derived by Ibl and Dodge. Data correlation was performed using a computer least squares procedure. Infinite-dilution fugacity coefficients were obtained using a modified Margules activity coefficient model. DOE

N89-10148# Pacific Northwest Labs., Richland, Wash. Chemical Methods and Separations Group.
AN IMPROVED INTERFACE FOR CAPILLARY ZONE ELECTROPHORESIS-MASS SPECTROMETRY
R. D. Smith, J. A. Loo, C. J. Barinaga, and H. R. Udseth Jun. 1988 4 p Presented at the 36th Annual Conference on Mass Spectrometry and Allied Topics, San Francisco, Calif., 6 Jun. 1988
(Contract DE-AC06-76RL-01830)
(DE88-014079; PNL-SA-15730; CONF-8806199-5) Avail: NTIS HC A02/MF A01

We have recently developed an improved electrospray ionization interface for capillary electrophoresis mass-spectrometry (CZE-MS). Our initial interface employed a vacuum deposited metal film at the exit of the capillary to make an electrical contact with the eluting buffer and establish the electrospray field gradient. This interface did, however, impose significant limitations on the range of Capillary Electrophoretic (CE) separations that could be performed. To circumvent these limitations, an interface that does not require a metalized tip was designed and developed. In the new approach, the electrical contact at the column exit is made through a flowing liquid sheath. The principal advantage of this interface is that it allows operation with a much broader range of electrophoresis conditions. The sheath flow can be readily varied in both composition and volume. DOE

N89-10149# Flow Research, Inc., Kent, Wash.
DIRECT NUMERICAL SIMULATIONS (DNS) OF AN UNPREMIXED TURBULENT JET FLAME Annual Technical Report, 16 Feb. 1985 - 16 Feb. 1988
P. Givi, W.-H. Jou, P. A. McMurtry, and R. W. Metcalfe Mar. 1988 197 p
(Contract F49620-85-C-0067)
(AD-A196128; FLOW-RR-440; AFOSR-88-0646TR) Avail: NTIS HC A09/MF A01 CSCL 20D

Direct numerical simulations (DNS) have been performed to study the phenomenon of mixing and its effects on chemical reactions in an unpremixed turbulent reactive flow. The type of flows considered were: (1) two-dimensional temporally developing mixing layers, (2) two- and three-dimensional spatially evolving mixing layers, and (3) three-dimensional homogeneous turbulent flows. The emphasis of the simulations for the first two types of flows was the local flame extinction caused by the high rate of strain in a chemically nonequilibrium turbulent flow. It was shown that flame extinction occurs in the high strain region of the braids of the coherent structures. Preliminary investigation of the three-dimensional flow shows a highly contorted flame sheet caused by the combination of the two-dimensional coherent structures and the longitudinal (streamwise) vortices. The homogeneous turbulence simulations were performed to test Toor's hypothesis. The results of the simulations suggested a revision to the hypothesis. During the course of the research, a three-dimensional spectral-element code was developed for the three-dimensional flows. The code combined the accuracy of a pseudospectral code with the flexibility of a finite element code. Scalar transport equations are included for simulations of mixing and chemical reaction in a complex three-dimensional turbulent flow. GRA

N89-10150# Lawrence Livermore National Lab., Calif.
PULSE COMBUSTOR MODELING: ONE DIMENSIONAL WAVE-DYNAMIC MODEL UTILIZING DYNAMIC INJECTION AND ENERGY RELEASE SUBMODELS
P. K. Barr, J. O. Keller, T. T. Bramlette, and C. K. Westbrook 11 Jan. 1988 21 p Presented at the 22nd International Symposium on Combustion, Seattle, Wash., 14 Aug. 1988
(Contract W-7405-eng-48)
(DE88-005369; UCRL-98039; CONF-880802-1) Avail: NTIS HC A03/MF A01

A numerical model of a pulse combustor has been developed to simulate the dynamic interactions among major physical processes that control the combustor's operation. In the model the nonlinear wave motion is driven by the periodic injection and combustion processes. This model is fully coupled because these driving processes are related to the pressure and temperature in the combustion chamber, as well as to each other. The dynamic wave pattern is determined by integrating the unsteady, one-dimensional, variable-area equations of continuity, momentum and energy, including losses due to friction and heat transfer. The injection model assumes the reactant flow rate is driven by the calculated pressure drop across a flapper valve. The combustion submodel uses a two-step process to determine the cyclic-varying energy release profile from the injection profile. This submodel first estimates the rate at which the cold reactants mix with the hot products from previous cycles. It then translates this rate of mixing to a rate of energy release based on chemical kinetics calculations. The combination of the submodels for injection and combustion produces a pulse combustor model that is dynamic in nature in that it fully couples the injection and mixing processes to the acoustic waves. DOE

N89-10151# Sandia National Labs., Albuquerque, N. Mex.
SEMICONDUCTOR BRIDGE (SCB): A NEW METHOD FOR THE IGNITION OF EXPLOSIVES AND PYROTECHNICS
R. W. Bickes, Jr. 1988 13 p Presented at the 1st IFAC Workshop on Advances in Automation, Quebec, Canada, 12 Sep. 1988
(Contract DE-AC04-76DP-00789)
(DE88-011246; SAND-88-0679C; CONF-880976-1) Avail: NTIS HC A03/MF A01

Small metal bridgewires (hot wires) are often used to ignite energetic powders such as propellants, pyrotechnics and explosive powders. We have developed a new means for ignition of such powders using a semiconductor bridge or SCB which is heavily doped polysilicon film 100 micron long by 380 micron wide by 2 micron thick. When driven by a short (less than 20 microsec), low energy (less than 3.5 mJ) current pulse, the SCB produces a hot plasma that ignites the explosive material pressed against it. SCB explosive devices function in a few tens of microseconds and operate at one-tenth the input energy of conventional hot-wire

devices. Despite the low energy for ignition, tests have revealed the SCB devices to be electrostatic discharge safe and less sensitive to no-fire current levels than hot-wire components. We report in this paper data obtained comparing a pyrotechnic SCB actuator with its hot-wire analog, a comparison of an SCB thruster with its hot-wire equivalent and test results for a prototype SCB lead azide detonator. In addition, because the SCB is compatible with digital circuitry, we are developing smart components which will incorporate the SCB into a single thumb size package (containing the SCB and firing set) which is controlled by digital signals. Thus programmed firing (such as accurate delay sequences) of SCB devices is easily achieved. We describe in this paper a prototype delay device and a sequential firing experiment in which twenty actuators were fired in a programmed sequence. DOE

N89-10465# United Kingdom Atomic Energy Authority, Culham (England). Lightning Studies Unit.
FACTORS INFLUENCING THE DETECTION OF VOLTAGE SPARKS BY FLAMMABLE GAS AND OPTICAL TECHNIQUES
S. J. Haigh, R. E. Baldwin, and C. R. Banks *In* NOAA, International Aerospace and Ground Conference on Lightning and Static Electricity Apr. 1988 p 272-28 (For primary document see N89-10429 01-47)
Avail: NTIS HC A23/MF A01 CSCL 21B

26 METALLIC MATERIALS

Includes physical, chemical, and mechanical properties of metals, e.g., corrosion; and metallurgy.

N89-10152# Los Alamos National Lab., N. Mex.
THEORETICAL STUDIES OF GRAIN BOUNDARIES IN Ni, Al AND Ni3Al WITH AND WITHOUT BORON
S. P. Chen, A. F. Voter, R. C. Albers, A. M. Boring, and P. J. Hay 1988 8 p Presented at the Spring Meeting of the Materials Research Society, Reno, Nev., 4 Apr. 1988
(Contract W-7405-eng-36)
(DE88-014323; LA-UR-88-2260; CONF-880408-34) Avail: NTIS HC A02/MF A01

Atomistic simulations of (001) symmetric tilt grain boundaries in Ni, Al, and Ni3Al are presented. The atomistic structures of the simulated grain boundaries have been analyzed in terms of the structural unit model, which is found to be of limited utility for intermetallics. Simulation results show that boron segregates more strongly to grain boundaries than to free surfaces, and strengthens the grain boundary. Good cohesive properties of the grain boundaries occur when both boron and some segregated Ni are present. The Ni and B are found to co-segregate to the Ni3Al boundary with an energy advantage of approximately 0.5 eV. DOE

N89-10153# California Univ., Berkeley. Lawrence Berkeley Lab. Center for Advanced Materials.
TENSILE PROPERTIES OF COMMERCIAL ALUMINUM-LITHIUM ALLOYS AT CRYOGENIC TEMPERATURES
J. Glazer and J. W. Morris, Jr. Mar. 1988 12 p Presented at the Aluminum-Lithium Symposium, Los Angeles, Calif., 22 Mar. 1988
(Contract DE-AC03-76SF-00098)
(DE88-014857; LBL-24987; CONF-8803135-1) Avail: NTIS HC A03/MF A01

The mechanical properties of commercially available aluminum alloys at cryogenic temperatures have attracted increasing interest in the past few years because of the large number of potential aerospace applications, primarily in tankage for cryogenic fuels. Aluminum-lithium alloys are of particular interest because of their low density and the extremely good low temperature properties that have been measured to date. This paper compares the behavior of AA 2090-T81 plate and AA 2091-T8 plate, which has not previously been surveyed. The 2090 data include new results at 200 K that indicate that property trends are not monotonic with temperature. The 2091 results show a peak in properties between 77 K and 200 K. These data point to the hazards of doing property screening at 77 K rather than 4 K. They also suggest some avenues for further exploration of the mechanisms that control elongation and fracture toughness. DOE

N89-10154# Army Materials Research Agency, Watertown, Mass.
STRUCTURE OF GRAIN BOUNDARIES IN IRON
Ralph J. Harrison, Frans Spaepen, Arthur Ford Voter, and Shao-Ping Chen (Los Alamos National Lab., N. Mex.) 1988 26 p Presented at the 34th Sagamore Army Materials Research, Lake George, N.Y., 31 Aug. 1987
(Contract W-7405-eng-36)
(DE88-014412; LA-UR-88-2128; CONF-8708268-1) Avail: NTIS HC A03/MF A01

The present research has been carried out as part of the Steel Research Group's program to improve the properties of ultra-high-strength steels. It is an investigation of the mechanism of cohesion at grain boundaries as a step toward the design of alloy steel with improved resistance against boundary decohesion under stress corrosion conditions. This research involves a theoretical study of grain boundaries in iron alloys, examining the mechanism of cohesion as affected by structure including imperfections, by the average alloy composition and by segregation at the boundaries. This paper summarizes what we have done to date in obtaining approximate grain boundary structures. We have tested the approximate interatomic potential for iron which we have obtained by using it to compute the interplanar spacings at the surface and then comparing the computed results with experimental observations. Results are discussed. DOE

N89-10155# Oak Ridge National Lab., Tenn. Metals and Ceramics Div.
RECENT DEVELOPMENTS IN ALUMINIDES AND SILICIDES
C. T. Liu, W. C. Oliver, C. G. McKamey, W. D. Porter, and E. P. George 1988 16 p Presented at the 2nd International SAMPE Metals and Metals Processing Conference, Dayton, Ohio, 2 Aug. 1988
(Contract DE-AC05-84OR-21400)
(DE88-012926; CONF-880855-4) Avail: NTIS HC A03

This paper summarizes recent alloy development in Ni3Al, Ni3Si, Fe3Al, and Al3Ti alloys at ORNL. Micro-alloying with boron suppresses brittle intergranular fracture and dramatically improves ductilities of Ni3Al and Ni3Si with hypostoichiometric compositions. Chromium additions reduce environmental embrittlement and increase the ductility of the alloys at elevated temperatures. Alloying with chromium also reduces brittle cleavage fracture and enhances tensile ductility in Fe3Al, alloys. Hardness measurements reveal that Al3Ti alloys with the LI2 structure, stabilized by Ni, Fe, and Cu, retain their strength at high temperatures. Ductile nickel and iron aluminides and silicides developed at ORNL have the potential to be used as new engineering materials for elevated-temperature structural use. DOE

N89-10156*# National Aeronautics and Space Administration. Lewis Research Center, Cleveland, Ohio.
T55-L-712 TURBINE ENGINE COMPRESSOR HOUSING REFURBISHMENT-PLASMA SPRAY PROJECT
George W. Leissler and John S. Yuhas (Army Aviation Systems Command, Cleveland, Ohio.) Oct. 1988 44 p
(DA Proj. 1L1-62209-AH-76)
(NASA-TM-101310; E-4301; NAS 1.15:101310) Avail: NTIS HC A03/MF A01 CSCL 11F

A study was conducted to assess the feasibility of reclaiming T55-L-712 turbine engine compressor housings with an 88 wt percent aluminum to 12 wt percent silicon alloy applied by a plasma spray process. Tensile strength testing was conducted on as-sprayed and thermally cycled test specimens which were plasma sprayed with 0.020 to 0.100 in. coating thicknesses. Satisfactory tensile strength values were observed in the as-sprayed tensile specimens. There was essentially no decrease in tensile strength

after thermally cycling the tensile specimens. Furthermore, compressor housings were plasma sprayed and thermally cycled in a 150-hr engine test and a 200-hr actual flight test during which the turbine engine was operated at a variety of loads, speeds and torques. The plasma sprayed coating system showed no evidence of degradation or delamination from the compressor housings. As a result of these tests, a procedure was designed and developed for the application of an aluminum-silicon alloy in order to reclaim T55-L-712 turbine engine compressor housings.
Author

N89-10157# Cameron Iron Works, Inc., Houston, Tex.
APPLICATIONS OF PROCESS MODELLING TO HEAT TREATMENT OF SUPERALLOYS
Arthur B. Shapiro (Lawrence Livermore National Lab., Calif.) and R. Wallis Jul. 1988 24 p Presented at the Metal Forming Modeling Subgroup of IMOG, Los Alamos, N. Mex., 23 Feb. 1988
(Contract W-7405-eng-48)
(DE88-015445; UCRL-98126; CONF-880259-2) Avail: NTIS HC A03/MF A01

Finite element models using the LLNL TOPAZ and NIKE codes have been used to determine the quenching media required to give the cooling rates necessary to meet the property specifications for superalloy components. They have also been used, qualitatively, to reduce the residual stresses developed during quenching with a subsequent reduction in distortion problems during machining. A further application has been the elimination of cracking during the quenching of crack-sensitive alloys. DOE

N89-10158# Los Alamos National Lab., N. Mex.
THE INFLUENCE OF TEXTURE ON STRAIN HARDENING
U. F. Kocks, M. G. Stout, and A. D. Rollett 1988 11 p Presented at the 8th International Conference on Strength of Metals and Alloys, Tampere, Finland, 22 Aug. 1988
(Contract W-7405-eng-36)
(DE88-009157; LA-UR-88-1168; CONF-880844-2) Avail: NTIS HC A03/MF A01

It is well known that the strain hardening behavior of metals is not the same in tension, compression, torsion and rolling, for example. We report on a new set of experiments, comprising wire-drawing interrupted by tensile tests, free compression, channel-die compression, and short-tube torsion in aluminum, an Al-Mg alloy, copper, silver, and 70:30 brass. The texture was measured before straining and at vonMises strain levels of roughly 1.0 and 2.0. Computer simulations of the deformation starting from a set of random grains weighted by observed initial texture, predicted deformation textures in qualitative agreement with the observed ones in most cases. Quantitatively, the simulations yielded the Taylor factors as a function of strain for all paths and, with an assumed hardening law for the representative grain, the macroscopic stress/strain curves. The grain hardening rate as a function of resolved shear stress was described in tabular form such as to match one of the macroscopic curves, and then used to predict the others. The eventual fit was quite good; we will describe what judgments needed to be made to achieve this result. The conclusion is that the strain-path dependence of work hardening can be explained simply as a consequence of texture development. DOE

N89-10159# Oak Ridge National Lab., Tenn.
MICROMECHANISMS OF DEFORMATION AND FRACTURE IN ORDERED INTERMETALLIC ALLOYS. 1: STRENGTHENING MECHANISMS
M. H. Yoo, J. A. Horton, and C. T. Liu Jul. 1988 58 p
(Contract DE-AC05-84OR-21400)
(DE88-015382; ORNL/TM-10709-Pt-1) Avail: NTIS HC A04/MF A01

The stability and mobility of active slip and twin modes in superlattice structures, for both cubic and noncubic crystals, are theoretically investigated based on the energetics and kinetics of dislocation dissociations. The main concept of the force couplet model for the positive temperature dependence of yield and flow stresses is introduced. Two sources of the glide resistance in ordered lattices are the fault dragging mechanism and the cross-slip pinning mechanism. The effective fault energy consists of two terms related to the chemical and mechanical instability of a shear fault (antiphase boundary, superlattice intrinsic stacking fault, or microtwin). Dependence of the yield stress on the orientation and the sense of applied stress stems from the signs and magnitudes of the glide and nonglide stresses. As the effective fault energy is altered by solute segregation and/or high nonglide stress, the two glide resistance mechanisms are affected differently. In Ni sub 3 Al and Beta-CuZn, the major aspects of anomalous yield strength, strain rate sensitivity, in situ deformation transmission electron microscopy observations, microtwinning, and non-stoichiometry effect are discussed in view of the present model.
DOE

N89-10160# Lawrence Livermore National Lab., Calif. Chemistry and Materials Science Dept.
PREMARTENSITIC MICROSTRUCTURES AS SEEN IN THE HIGH-RESOLUTION ELECTRON MICROSCOPE: A STUDY OF A NIAl ALLOY
D. Schryvers, L. Tanner, and G. VanTendeloo (Universitaire Instelling Antwerpen, Wilrijk, Belgium) 12 Feb. 1988 5 p Presented at the NATO Advanced Study Institute on Alloy Phase Stability, Crete, Greece, 14 Jun. 1987 Prepared in cooperation with Lawrence Berkeley Lab., Calif.
(Contract W-7405-eng-48)
(DE88-008042; UCRL-98231; CONF-8706103-9) Avail: NTIS HC A02/MF A01

The present study indicates that the B2 beta-phase in quenched Ni(62.5)Al(37.5) is distorted by displacement waves involving a planar shuffling of atoms resembling the final 7R martensite structure and with wavelengths of the order of 1.3 nm. The appearance of a group of zone axes (110) (110) modulation with the indicated periodicity corresponds well with recent inelastic neutron scattering results which reveal nonlinear behavior in the TA group of zone axes (110) phonon dispersion curve around the same wavelengths indicating a partial lattice softening for such waves. In bulk material all six equivalent wave-vectors are equally present. These distortional modulations are configured in some form of three-dimensional assembly. Following the interpretation given above, it can be concluded that a one-dimensional domain structure along one of six group of zone axes (110) directions may exist. However, the beating of six displacement waves with apparently uncorrelated phase and wavelengths rules out the existence of a conventional three-dimensional domain structure. For this reason it is uncertain whether much more information can be gained from such image simulations. There are now numerous indications that the underlying structure to the tweed contrast in this alloy is a precursor effect of the martensitic transformation. However, a detailed description of the effective correlation between the distorted parent phase and the martensitic product phase has yet to be developed. Recent HREM results reveal the existence of a sequence of different structures in the transition region between the modulated beta-phase and the martensitic phase, depending on parameters such as the local composition and stress. Such transition structures include modulated Beta-phase in which only one (110) modulation is preferred or in which the periodicity differs from the above described 1.3 nm and the FCT L1(sub o) martensite with single shear defects. DOE

N89-10161# Massachusetts Inst. of Tech., Cambridge. Dept. of Materials Science and Engineering.
A STUDY OF THE FATIGUE BEHAVIOR OF SMALL CRACKS IN NICKEL-BASE SUPERALLOYS Final Report, 1 Jan. 1984 - 1 Aug. 1987
Regis M. Pelloux, Jun Feng, and Glenn Romanoski 24 Feb. 1988 153 p
(Grant AF AFOSR-0075-84; AF Proj. 2306)
(AD-A195489; AFOSR-88-0457TR) Avail: NTIS HC A08/MF A01 CSCL 11F

The fatigue of behavior of short cracks was investigated in five wrought nickel-base superalloys currently used for aircraft

turbine disks. Cracks were initiated at artificial defects and at persistent slip bands. Test frequencies ranged from 20Hz to 10cpm. Fatigue crack growth rates were measured over crack lengths ranging from 10 um to 1mm. Most of the testing was performed in load control with stress ranges approaching the cyclic yield strengths of alloys. Strain controlled tests were performed on IN100 under elastic-plastic cycling conditions. GRA

N89-10162# Los Alamos National Lab., N. Mex.
CHARACTERIZATION OF DYNAMIC FRACTURE IN COPPER UNDER UNIAXIAL STRESS AND UNIAXIAL STRAIN
A. K. Zurek, J. N. Johnson, and C. E. Frantz 1988 9 p Presented at the 2nd International Conference on Mechanical and Physical Behavior of Materials Under Dynamic Loading, Ajaccio, France, 19 Sep. 1988
(Contract W-7405-eng-36)
(DE88-007824; LA-UR-88-1001; CONF-880940-1) Avail: NTIS HC A02

We have characterized fracture modes in copper under conditions of dynamic uniaxial tension (expanding ring tests) and dynamic uniaxial strain (spall tests). The spall strength in copper was measured as a function of grain size, purity and initial porosity. A unified model for ductile fracture is developed, and a qualitative prediction of the relative magnitudes of porosity and plastic deformational strain for spall and uniaxial tension tests is presented. DOE

N89-10163# Los Alamos National Lab., N. Mex.
METASTABLE ALLOY PHASES PREPARED BY SOLID STATE REACTIONS AND BALL MILLING
R. B. Schwarz 1988 20 p Presented at the 8th International Conference on Strength of Metals and Alloys, Tampere, Finland, 22 Aug. 1988
(Contract W-7405-eng-36)
(DE88-009156; LA-UR-88-1167; CONF-880844-3) Avail: NTIS HC A03/MF A01

The main methods of synthesis of amorphous metallic alloys are based on: (1) the rapid solidification of alloys from the liquid or vapor phase, (2) solid state interdiffusion reactions between pure metals having negative heats of mixing, and (3) mechanical attrition of crystalline intermetallics. We describe methods (2) and (3), developed around 1983, and we discuss recent advances in the understanding of the glass forming ranges for the three methods of synthesis. DOE

N89-10164# Oak Ridge National Lab., Tenn.
ENGINEERING PROCESSING AND PROPERTIES OF NICKEL ALUMINIDES
V. K. Sikka 1988 15 p Presented at the 2nd International SAMPE Metals and Metals Processing Conference, Dayton, Ohio, 2 Aug. 1988
(Contract DE-AC05-84OR-21400)
(DE88-011019; CONF-880855-3) Avail: NTIS HC A03/MF A01

Ordered intermetallic compounds of iron, nickel, and titanium are materials recently under development for structural applications. Among these, Ni3Al has been made reasonably ductile by the addition of small amounts of boron. Further additions of zirconium and chromium have been utilized for enhancement of high temperature strength and intermediate temperature ductility. Nickel aluminide alloys based on Ni3Al are near commercialization. This paper describes the melting, processing, mechanical properties, physical properties, corrosion, and weldability of these alloys. Applications for nickel aluminides have been identified. Potential suppliers who have recently licensed the nickel aluminide technology from Oak Ridge National Laboratory (ORNL) are also listed. DOE

N89-10165*# National Aeronautics and Space Administration. Langley Research Center, Hampton, Va.
A COMPENDIUM OF SOURCES OF FRACTURE TOUGHNESS AND FATIGUE CRACK GROWTH DATA FOR METALLIC ALLOYS, PART 3
C. Michael Hudson and Sue K. Seward Sep. 1988 32 p
(NASA-TM-100675; NAS 1.15:100675) Avail: NTIS HC A03/MF A01 CSCL 11F

This Technical Memorandum presents sources of fracture toughness and fatigue crack growth data for metallic alloys. This is Part 3 of a three volume report. Author

27 NONMETALLIC MATERIALS

Includes physical, chemical, and mechanical properties of plastics, elastomers, lubricants, polymers, textiles, adhesives, and ceramic materials.

For composite materials see *24 Composite Materials.*

N89-10166*# National Aeronautics and Space Administration. Lewis Research Center, Cleveland, Ohio.
A SINTERING MODEL FOR SiC(SUB)w/Si3N4 COMPOSITES
Marc R. Freedman, James D. Kiser, and William A. Sanders 1988 19 p Presented at the 90th Annual Meeting of the American Ceramic Society, Cincinnati, Ohio, 1-5 May 1988
(NASA-TM-101336; E-4354; NAS 1.15:101336) Avail: NTIS HC A03/MF A01 CSCL 11C

Presented is a model which suggests that it should be possible to pressureless sinter a SiC(sub w)/ Si3N4 composite to theoretical density. Prior failure to achieve complete densification by sintering is attributed to the use of compositions which result in a glass deficit. There is one basic premise for this model. The ratio of glass amount to surface area of nonglass constituents must be the same for both composite and sinterable monolithic Si3N4. This model suggests that whisker and grain sizes and whisker loading influence the glass amount necessary for successful sintering of composites. According to the model, a large glass amount will be necessary for successful sintering of these composites. However, grain boundary thicknesses in the composite will be less than those in the analogous monolithic materials. This suggests that good high temperature strength may still be attained. A recent report supports the predictions of the model. Author

N89-10167# Lawrence Livermore National Lab., Calif.
DIRECTIONAL SPECTRAL EMISSIVITY MEASUREMENTS ON A CERAMIC MOLD MATERIAL
Mark A. Havstad and William McLean Apr. 1988 17 p
(Contract W-7405-eng-48)
(DE88-015407; UCID-21385) Avail: NTIS HC A03/MF A01

This document describes directional spectral emittance measurements made on a ceramic mold material that is to be used to cast high- temperature turbine rotors. The work was performed at approximately 700 K and 5 x 10 to the -9 Torr in an emissivity measurement apparatus. The results, which show low scatter and conform to expectations derived from both theoretical relations and published ceramic data, give a total hemispherical emissivity of 0.42 + or - 0.04 when integrated over wavelength and direction at 1000 K. DOE

N89-10168# Garrett Corp., Torrance, Calif.
DEVELOPMENT OF CERAMIC MATRIX COMPOSITES FOR APPLICATION IN THE CERAMIC TECHNOLOGY FOR ADVANCED HEAT ENGINES Final Report
H. C. Yeh, J. Schienle, K. Karasek, and S. Bradley Jun. 1988 177 p Prepared for ORNL, Tenn.
(Contract DE-AC05-84OR-21400)
(DE88-015329; ORNL/Sub-85-22008/1) Avail: NTIS HC A09/MF A01

A technology base for fabrication of SiC whisker-reinforced Si3N4 composites was developed. The feasibility of fabricating near-netshape SiC-Si3N4 using procedures amenable to production was demonstrated. Green composite parts containing up to 40 percent SiC whiskers were prepared by slip casting and were densified to greater than 3.2 gm/cc using both metal and glass encapsulation HIP processing. Improvements in both strength and fracture toughness were achieved in Si3N4 through SiC whisker

reinforcement. The strength, toughness, and elastic and thermal properties were correlated with whisker chemistry, whisker loading, processing parameters, and microstructure. DOE

N89-10169*# National Aeronautics and Space Administration, Washington, D.C.
NEW DIAMOND
M. Kitabatake and K. Wasa Sep. 1988 13 p Transl. into ENGLISH from Kagaku, Zoken (Kyoro, Japan), v. 112, 1987 p 155-161 Transl. by Scientific Translation Service, Santa Barbara, Calif.
(Contract NASw-4307)
(NASA-TT-20325; NAS 1.77:20325) Avail: NTIS HC A03/MF A01 CSCL 11C

Gas-phase growth technologies for diamond synthesis are examined, which lead to wide applications as an important industrial material. Applications derived for new investigations are presented. Author

N89-10170# Georgia Inst. of Tech., Atlanta. School of Mechanical Engineering
DEVELOPMENT OF A THEORY OF WEAR OF CERAMICS Final Report
W. O. Winer and B.-Y. Ting Jul. 1988 49 p
(Contracts DE-AC05-84OR-21400; ORNL-19B-07802C)
(DE88-015327; ORNL/Sub-84-7802/1) Avail: NTIS HC A03/MF A01

This report covers the first three years of the contract entitled, Development of a Theory of Wear of Ceramics, (DOE--ORNL Project Authorization 19x-15, Basic Agreement No. 7802). The research work carried out during this period includes: (1) the exploration of the hotspots and the triboluminescence generated by a sliding contact between a sapphire disk and ceramic pins, (2) the use of an infrared scanning system (AGA Thermovision 750) to measure the contact temperature between a sappphire disk and ceramic pins, (3) installing a new infrared scanning system (Inframetrics model 525) with a digital video processor (Quantex DS50) and a computer for temperature measurement, (4) preliminary wear measurements under a controlled environment for a PSZ pin sliding against a sapphire disk, (5) measurements of mean wear depth of hotspots of Si3N4 sliding against sapphire, and (6) developing a thermomechanical wear theory. These topics are discussed. DOE

N89-10171# Illinois Univ., Urbana.
TIME-DEPENDENT MECHANICAL BEHAVIOR OF PARTIALLY STABILIZED ZIRCONIA FOR DIESEL ENGINE APPLICATIONS Final Report
M. K. Ferber and T. Hine Jul. 1988 61 p Prepared for ORNL, Tenn.
(Contract DE-AC05-84OR-21400)
(DE88-015330; ORNL/Sub-85-27416/1) Avail: NTIS HC A04/MF A01

Recently there has been considerable interest in utilizing ceramic materials in diesel engine applications. And as a result of this interest, the fatigue behavior of several commercially-available MgO partially stabilized zirconias (Mg-PSZ) was studied by measuring the strength (S sub f as a function of time (t), temperature (T), and applied stress level (sigma). The two Mg-PSZ types included TS PSZ (thermal shock grade) and MS PSZ (maximum strength grade/1983 vintage). Both 1983 and 1984 vintages of the TS PSZ (designated TS(83) and TS(84)) were examined. The strength was determined using an interrupted fatigue (I.F.) test in which flexure samples were exposed at temperatures between 500 and 1000 C for times up to 1000 h. During testing, the applied stress was maintained at a percentage of the short-term S sub f value measured at the same T. Specific stress levels included 0, 60, 70, and 80 percent. The following techniques were used to characterize both the as-received and tested I.F. specimens: (1) SEM, (2) TEM, (3) optical microscopy, (4) X-ray diffraction, (5) micro-Raman spectroscopy, and (6) dilatometry. SEM allowed for routine examination of the microstructures and fracture surfaces. Changes in the primary phase assemblage resulting from the high-temperature exposure were monitored using X-ray diffraction, Raman spectroscopy, and standard optical phase analysis. The hysteresis characteristics which were determined from dilational measurements provided insights into the nature of the tetragonal (t) to monoclinic (m) transformation and thus the stability of the (t) precipitates. Finally, TEM was used to study the influence of stress, time, and temperature upon the microstructure of the I.F. samples. DOE

N89-10172# Los Alamos National Lab., N. Mex.
COMPARISON OF SURFACE MODIFICATIONS OF POLY(ETHER URETHANES) BY CHEMICAL INFUSION AND GRAFT POLYMERIZATION
D. A. Wrobleski, D. L. Cash, and R. E. Hermes 1988 5 p Presented at the 196th American Chemical Society National Meeting, Los Angeles, Calif., 25 Sep. 1988
(Contract W-7405-eng-36)
(DE88-007887; LA-UR-88-869; CONF-880912-1) Avail: NTIS HC A02/MF A01

Our approach to surface modification uses the chemical infusion process to introduce materials into the outermost layer of the polymeric material, thereby altering the surface without changing the bulk properties of the polymer. The infused materials may slowly diffuse out of the infusion layer if they are volatile or highly mobile. However, if polymeric infusant materials are employed, they may become chain entangled with the host polymer and result in a permanently modified surface. A second approach utilizes photo-initiated graft polymerization of poly(ether urethanes) with an appropriate monomer. We have explored both of these methods by examining the infusion of polyvinylpyrrolidone (PVP) and poly(ethylene glycol) (PEG) into commercially available poly(ether urethanes) and the graft polymerization of N-vinyl pyrrolidone onto poly(ether urethanes). Results are presented here. DOE

N89-10173# Societe Europeenne de Propulsion, Vernon (France). Lab. de la Qualite des Approvisionnements.
CHOICE OF COATING AND SURFACE BEHAVIOR OF THE HYDROGEN TURBOPUMP OF THE VULCAIN ENGINE [CHOIX DES REVETEMENTS ET COMPORTEMENTS DES SURFACES DE LA TURBOPOMPE A HYDROGENE DU MOTEUR VULCAIN]
J. C. Sylvestre 1988 24 p In FRENCH Presented at Journee Surfair 7, Cannes, France, 27 May 1988
(ETN-88-93084) Avail: NTIS HC A03/MF A01

Surface coatings for the hydrogen turbopump of the main engine of the Ariane 5 launch vehicle are discussed. The operating conditions, materials selection, and tribology of the engine are summarized. Test rigs and instrumentation are described. Austenitic alloys are preferred, except for bearings, where martensitic alloys are chosen. Characterization of the surface coatings in cold conditions and microgeometric surface characterization are outlined. Coatings based on electrolytic deposition, vapor phase depositing, and ionic nitruration were studied. ESA

N89-10174 British Petroleum Co. Ltd., London (England).
ADHESIVE BLENDS AND MULTI-LAYERED STRUCTURES COMPRISING THE ADHESIVE BLENDS Patent Application
Philip Stephen Hope and Peter John Malley 30 Jul. 1986 12 p Filed 23 Jul. 1987 Priority 30 Jul. 1986 GB 8618587
(EP-Patent-0-258-990-A1; EP-Patent-Appl-87306543.7; Int-Patent-Class-C08L-23/10; ETN-88-93127) Avail: UK Patent Office, 25 Southampton Buildings, London WC2A 1AY, United Kingdom

A polyolefin-containing adhesive blend comprising: (1) 10 to 30 parts by weight of a graft copolymer of a polypropylene backbone grafted with 0.001 to 30 percent by weight of at least 1 polymerizable ethylenically unsaturated carboxylic acid or derivative thereof; (2) 10 to 50 parts by weight of a linear low density polyethylene; and (3) 20 to 80 parts by weight of polypropylene, the sum of (1) (2) and (3) being 100 parts by weight is presented. The adhesive blend is suitable for bonding polypropylene to polar materials such as ethylene-vinyl alcohol copolymers and nylon. The invention includes multilayered structures produced using the polyolefin-containing adhesive blend. ESA

28 PROPELLANTS AND FUELS

Includes rocket propellants, igniters, and oxidizers; their storage and handling procedures; and aircraft fuels.

For related information see also *07 Aircraft Propulsion and Power, 20 Spacecraft Propulsion and Power,* and *44 Energy Production and Conversion.*

N89-10175# Federal Aviation Agency, Atlantic City, N.J.
THE PERFORMANCE OF ALTERNATE FUELS IN GENERAL AVIATION AIRCRAFT Final Report
Augusto M. Ferrara and Richard Wares (IIT Research Inst., Bartlesville, Okla.) Jul. 1988 47 p
(DOT/FAA/CT-88/13) Avail: NTIS HC A03/MF A01

The results of a study which measured the effects of pressure altitude on fuel weathering are described. Samples of unleaded automobile gasoline were exposed to varying pressure altitudes, and the effects of this exposure on aircraft performance and volatility were measured. The composition of the fuel, aircraft configuration, and the initial temperature of the fuel when transferred to the tank were varied to determine the extent these variables affected the aircraft performance. Experiments were conducted which demonstrated that the use of 100 F fuel during aircraft certification will provide the greatest margin of safety. In addition, the suitability of methyl-tertiary-butyl ether as an acceptable fuel for use in general aviation aircraft was demonstrated. Several different oxygenated fuels (including gasolines containing alcohols) were aged in ground-based tests. The results are presented. Author

N89-10176# Southwest Research Inst., San Antonio, Tex. Fuels and Lubricants Research Facility.
FINAL REVIEW OF US ARMY FIRE-RESISTANT FUEL PROGRAM Interim Report, Oct. 1984 - Dec. 1987
Dernard R. Wright, Mike D. Kanakia, George E. Fodor, and Lee G. Dodge Dec. 1987 66 p
(Contracts DAAK70-87-C-0043; DAAK70-85-C-0007; DA Proj. 1L7-62733-AH-20)
(AD-A194304; BFLRF-244) Avail: NTIS HC A04/MF A01
CSCL 21D

Extensive research has been conducted by the U.S. Army on means for making hydrocarbon fuels resistant to unwanted fires. An approach to developing a fire-resistant fuel (FRF) for use with diesel- and gas turbine-powered armored combat vehicles has been identified. This approach comprises the addition of water and emulsifier to diesel fuel with simple mixing. The resulting FRF is a clear-to-hazy microemulsion. The fuel enhances fuel fire safety by decreasing ignition susceptibility, by retarding flame spread rates, and by self-extinguishing if ignited when spilled. However, it burns readily when atomized, and diesel engines and turbines combustors start, idle, and run satisfactorily on FRF. The thrust of this program was to address the problems associated with utilization of the current formula in the field. The main problem areas addressed included the production and storage of FRF at reduced temperatures; the vehicular fuel systems effects, e.g., fuel filter plugging, resulting from the use of the water-containing emulsions; and the effects of transportability and possible fuel-handling system contamination by the FRF constituents. As a result of this program, additional work was not recommended because of several requirements that could not easily be solved in field applications. GRA

N89-10177# Materials Research Labs., Melbourne (Australia).
NUMERICAL SIMULATION OF THE EXPLOSIVES EFFECTS OF TWO CLOSELY SPACED PYROTECHNIC PODS
J. A. Waschl Nov. 1987 21 p
(MRL-R-1095; AR-005-191) Avail: NTIS HC A03/MF A01

Described are some computer simulations to study the effects of two pyrotechnic noise-generating pods which deflagrate in close proximity, at, or nearly at, the same time. Some modifications to the computer code HULL, to improve the efficiency of the calculations, are described. The calculations show that though there is reinforcement of the shock wave between adjacent pods, the increased effect on nearby personnel is small. The effect of non-synchronous deflagrations is less than synchronous ones. The overall conclusion is that the problem of multiple pods can be treated as one of single pods as far as hazard is concerned, though with more pods in a confined space there is an increased chance of a person being located in a hazard region. Author

N89-10178# Commission of the European Communities, Ispra (Italy). Joint Research Centre.
HYDROGEN SUPPLY OVER LONG DISTANCES USING CHEMICALS DESCRIPTION AND EVALUATION OF A TECHNICAL SYSTEM
G. Giacomazzi 1987 30 p
(DE88-012630; EUR-11329) Avail: NTIS (US Sales Only) HC A03

The problem of the transport of hydrogen has been studied. The basic concept was the following: where electricity is available at low cost as compared to European costs, it is possible to produce hydrogen by electrolysis, also at low cost; if it is possible to transport the hydrogen in Europe at costs which are not prohibitive, one would thus have in Europe a low-cost energy vector. That electricity is available at low cost true only in certain parts of the world which are either a long way from Europe and/or geographically and climatically difficult. In fact, it can be transmitted by pipeline in gaseous form but it cannot be transported in bulk by sea in liquid form (LH2) at normal pressure such as, for example, the liquefied natural gas, because of lack, at the present state of technology, of suitable ships. Also the transportation in relatively small tanks by special ships should be excluded because of the physical characteristics of hydrogen. These facts exclude sites of hydrogen production which are separated from the sites of use by the sea. Economics and some conclusions of hydrogen transport are presented. DOE

N89-10179# Federal Aviation Agency, Atlantic City, N.J.
ALTERNATE FUELS FOR GENERAL AVIATION AIRCRAFT WITH SPARK IGNITION ENGINES Final Report
Augusto M. Ferrara Jun. 1988 81 p
(DOT/FAA/CT-88/05) Avail: NTIS HC A05/MF A01

Described are the results of a study into the behavior of several alternate fuels under consideration for use in general aviation aircraft engines. The study consists of a literature search and engine tests using a dynamometer. The literature search identifies material compatibility problems and possible solutions. For the engine tests, a number of gasoline/alcohol blends were prepared using both ethanol and methanol in varying concentrations and the vapor lock behavior was identified. The engine oil was analyzed during the study with the intent of detecting accelerated wear. Based on the results of the study, a number of considerations pertaining to the use of these alternate fuels in general aviation aircraft are identified. Author

N89-10180# Ballistic Research Labs., Aberdeen Proving Ground, Md.
HAN (HYDROXYLAMMONIUM NITRATE DENSITY)-BASED LIQUID GUN PROPELLANTS: PHYSICAL PROPERTIES Final Technical Report
Madelyn M. Decker, Nathan Klein, Eli Freedman, Charles S. Leveritt, and Josephine Q. Wojciechowski Nov. 1987 63 p
(AD-A195246; BRL-TR-2864) Avail: NTIS HC A04/MF A01
CSCL 19A

Mixtures of hydroxylammonium nitrate (HAN), water, and the nitrate salt of an aliphatic amine (AAN), are being actively considered as propellants for use in a liquid propellant gun. A number of such AAN salts have been considered for this application; the preferred one is triethanolammonium nitrate (TEAN), which is used in propellants LGP 1845 and 1846, the current prime candidates for the gun now under development. The physical properties of the propellants and of their components must fall within acceptable ranges for practical applications. The low temperature properties of LGP 1845 and 1846 and of HAN-water and TEAN-water mixtures have been investigated. The results for LGP 1845 and 1846 show only transitions from homogeneous liquid to homogeneous glass at -90C and -100C,

respectively, with no indication of crystallization or component separation over wide concentration ranges. Results for HAN-water and TEAN-water mixtures are complex; crystallization, phase separation, and glass transitions are seen. GRA

N89-10181# Mitre Corp., McLean, Va.
DIRECT METHANE CONVERSION: AN ASSESSMENT
D. Gray, G. Tomlinson, and J. Shen (Department of Energy, Washington, D. C.) 1988 6 p Presented at the 196th American Chemical Society National Meeting, Los Angeles, Calif., 25 Sep. 1988 Prepared in cooperation with USDOE, Washington, D.C.
(Contract DE-AC04-76DP-00789)
(DE88-010225; SAND-88-7092C; CONF-880912-6) Avail: NTIS HC A02/MF A01

If it were possible to convert methane directly to methanol or higher hydrocarbons with high conversion and selectivity, both the steam reforming and methanol synthesis steps could be eliminated. This direct conversion approach has the potential for considerable savings in cost if technically sound processes can be developed. Interest in direct methane or natural gas conversion has recently intensified worldwide. Several approaches to this are being researched at oil companies and in programs funded by the Department of Energy or the Gas Research Institute. The more technically advanced processes are those that operate in the temperature range 600 to 800 C. This paper assesses the technical potential of some of these high temperature direct methane conversion approaches being researched by various groups. These new approaches are then compared to the conventional technology for converting methane to gasoline by utilizing steam reforming, methanol synthesis and Mobil's Methanol-To-Gasoline (MTG) technology. The direct methane conversion approaches analyzed in this report are Oxidative Coupling, partial oxidation, and Oxyhydrochlorination. Table 1 summarizes the known process parameters and calculated conversion efficiencies for the new direct methane conversion approaches and the baseline technology considered in this analysis. Using the preliminary data available, the computer simulations of the new approaches all show overall system efficiencies that are not greatly different from the conventional technology. DOE

N89-10182# Los Alamos National Lab., N. Mex.
SINGLE CRYSTAL ORIENTATION EFFECTS IN SHOCK INITIATION OF PETN EXPLOSIVE
J. J. Dick 1988 4 p Presented at the Shock Wave Symposium, Pullman, Wash., 1 Sep. 1988
(Contract W-7405-eng-36)
(DE88-014406; LA-UR-88-2523; CONF-8809109-1) Avail: NTIS HC A02/MF A01

Over the past nine years in Los Alamos we have studied shock initiation of detonation in single crystals of PETN explosive. We have demonstrated the effects of point defects and crystal orientation on shock sensitivity. Here we report recent work on orientation effects and anomalous detonation in (110) orientation at 4 GPa. DOE

N89-10467# New Mexico Inst. of Mining and Technology, Socorro. Geophysical Research Center.
LIGHTNING PROTECTION FOR HIGH EXPLOSIVES AND INSTRUMENTATION USING A FIELD MILL SYSTEM
William Rison and Gerald P. Chapman (Mission Research Corp., Albuquerque, N. Mex.) *In* NOAA, International Aerospace and Ground Conference on Lightning and Static Electricity Apr. 1988 p 289-29 (For primary document see N89-10429 01-47)
Avail: NTIS HC A23/MF A01 CSCL 21I

29 MATERIALS PROCESSING

Includes space-based development of products and processes for commercial applications.
For biological materials see *55 Space Biology.*

N89-10183# Instituto de Pesquisas Espaciais, Sao Jose dos Campos (Brazil).
THEORETICAL MODEL FOR THE SOLUTE DISTRIBUTION OF A PbSnTe GROWTH BY VMS IN MICROGRAVITY ENVIRONMENT
Mauricio Fabbri, Iraja N. Bandeira, and Luiz C. M. Miranda Aug. 1988 8 p Presented at the 39th Congress of the International Astronautical Federation, Bangalore, India, 8-15 Oct. 1988 Submitted for presentation
(INPE-4664-PRE/1365) Avail: NTIS HC A02/MF A01

The basic mechanism occurring in a diffusion-controlled growth of a Pb(1-x)Sn(x)Te crystal by the Vapor Melt Solid (VMS) technique is investigated. A physical model for the mass transfer by the vapor and liquid phases without parasitory convection is stated and solved with an accurate implicit moving-boundary finite-difference scheme. It is shown that growth by VMS in microgravity is expected to yield very good-quality PbSnTe crystals, due to a mechanical stabilization of the liquid layer and enhancement of the streaming effect in the vapor phase. More accurate results concerning Bridgman growth of PbSnTe in the diffusion-controlled regime were also obtained. These preliminary investigations are intended to support an experiment being devised in cooperation with the Laboratory of Materials Science in Space of the USSR Space Research Institute to grow a PbSnTe crystal at MIR facilities. Author

31 ENGINEERING (GENERAL)

Includes vacuum technology; control engineering; display engineering; cryogenics; and fire prevention.

N89-10184*# National Aeronautics and Space Administration. Marshall Space Flight Center, Huntsville, Ala.
RECHARGEABLE METAL HYDRIDES FOR SPACECRAFT APPLICATION
J. L. Perry Sep. 1988 37 p
(NASA-TM-4076; M-598; NAS 1.15:4076) Avail: NTIS HC A03/MF A01 CSCL 21I

Storing hydrogen on board the Space Station presents both safety and logistics problems. Conventional storage using pressurized bottles requires large masses, pressures, and volumes to handle the hydrogen to be used in experiments in the U.S. Laboratory Module and residual hydrogen generated by the ECLSS. Rechargeable metal hydrides may be competitive with conventional storage techniques. The basic theory of hydride behavior is presented and the engineering properties of LaNi5 are discussed to gain a clear understanding of the potential of metal hydrides for handling spacecraft hydrogen resources. Applications to Space Station and the safety of metal hydrides are presented and compared to conventional hydride storage. This comparison indicates that metal hydrides may be safer and require lower pressures, less volume, and less mass to store an equivalent mass of hydrogen. Author

N89-10185# Midwest Research Inst., Golden, Colo. Solar Energy Research Inst.
IMPACTS OF ADVANCED REFRIGERATOR INSULATION
T. F. Potter, D. K. Benson, and L. K. Smith Jul. 1988 14 p Presented at the Summer Study on Energy Efficiency in Buildings, Pacific Grove, Calif., 28 Aug. 1988
(Contract DE-AC02-83CH-10093)
(DE88-001180; SERI/TP-254-3380; CONF-880814-5) Avail: NTIS HC A03/MF A01

Recent developments in advanced insulations, such as powders under a soft vacuum (R = 20 per inch), and hard-vacuum insulation with spacers (R = 15 per 0.1 inch), merit evaluating their practical uses. Refrigerator/freezers (R/Fs) are well-suited for incorporating

the new insulations for the following reasons: the energy consumption of R/Fs must be reduced to comply with the National Appliance Energy Conservation Act (NAECA) standards; the Montreal Protocol to Control Ozone-Depleting Substances calls for a reduction in chlorofluorocarbons (CFCs) that are now used in the insulative foams in R/F sidewalls; and both high R-values to minimize heat gain through the walls, and thin walls to maximize the interior volume, are desirable. We selected two different R/F base-cases for this analysis; one had the typically used CFC foam (R = 7.7 per inch), while the other featured non-CFC foam (R = 5.3 per inch) in the exterior walls and doors. (In keeping with industry practice, both refrigerator doors were insulated with fiberglass.) Two simulated modifications of both of the base cases, based on the DOE closed-door test, included replacing part of the wall and door insulation with either 1 inch of powder or a 0.1 inch layer of hard vacuum/spacer insulation. Both of these modifications met the standard, even when the non-CFC foam base case was simulated. DOE

N89-10474# Stringfellow and Associates, Atlanta, Ga.
LIGHTNING AND SURGE PROTECTION OF LARGE GROUND FACILITIES
Michael F. Stringfellow *In* NOAA, International Aerospace and Ground Conference on Lightning and Static Electricity Apr. 1988 p 328-33 (For primary document see N89-10429 01-47)
Avail: NTIS HC A23/MF A01 CSCL 13B

N89-10477# Electro Magnetic Applications, Inc., Lakewood, Colo.
MODEL RESULTS FOR A PROPOSED TACTICAL MISSILE TRAINING SITE LIGHTNING PROTECTION SYSTEM
John D. Curry *In* NOAA, International Aerospace and Ground Conference on Lightning and Static Electricity Apr. 1988 p 353-35 (For primary document see N89-10429 01-47)
(Contract DAAH01-85-D-A015)
Avail: NTIS HC A23/MF A01 CSCL 13B

N89-10481# Office National d'Etudes et de Recherches Aeronautiques, Paris (France).
THE SAFIR LIGHTNING MONITORING AND WARNING SYSTEM, APPLICATIONS TO AEROSPACE ACTIVITIES
P. Richard, A. Soulage, P. Laroche, and J. Appel *In* NOAA, International Aerospace and Ground Conference on Lightning and Static Electricity Apr. 1988 p 383-39 (For primary document see N89-10429 01-47)
Avail: NTIS HC A23/MF A01 CSCL 13B

N89-10482# Electricity Council Research Centre, Capenhurst (England).
A LIGHTNING LOCATION SYSTEM FOR THE UK ELECTRICITY SUPPLY INDUSTRY
Laura Scott *In* NOAA, International Aerospace and Ground Conference on Lightning and Static Electricity Apr. 1988 p 391-39 (For primary document see N89-10429 01-47)
Avail: NTIS HC A23/MF A01 CSCL 13B

N89-10495# SRI International Corp., Menlo Park, Calif.
GROUNDING FOR SAFETY AND COMPATIBILITY
Edward F. Vance and Werner Graf *In* NOAA, International Aerospace and Ground Conference on Lightning and Static Electricity Apr. 1988 p 494-49 (For primary document see N89-10429 01-47)
Avail: NTIS HC A23/MF A01 CSCL 13B

32 COMMUNICATIONS AND RADAR

Includes radar; land and global communications; communications theory; and optical communications.

For related information see also *04 Aircraft Communications and Navigation* and *17 Space Communications, Spacecraft Communications, Command and Tracking.* For search and rescue see *03 Air Transportation and Safety,* and *16 Space Transportation.*

N89-10186*# Jet Propulsion Lab., California Inst. of Tech., Pasadena.
THE TELECOMMUNICATIONS AND DATA ACQUISITION REPORT Progress Report, Apr. - Jun. 1988
E. C. Posner, ed. 15 Aug. 1988 312 p
(NASA-CR-183243; JPL-TDA-PR-42-94; NAS 1.26:183243) Avail: NTIS HC A14/MF A01 CSCL 17B

In space communications, radio navigation, radio science, and ground based radio and radar astronomy, activities of the Deep Space Network and its associated Ground Communications Facility in planning, in supporting research and technology, in implementation, and in operations are reported. Also included is TDA funded activity at JPL on data and information systems and reimbursable DSN work performed for other space agencies through NASA. For individual titles, see N89-10187 through N89-10211.

N89-10187*# Jet Propulsion Lab., California Inst. of Tech., Pasadena.
DEEP SPACE TRACKING IN LOCAL REFERENCE FRAMES
R. N. Treuhaft *In its* The Telecommunications and Data Acquisition Report 15 Aug. 1988 p 1-15 (For primary document see N89-10186 01-32)
Avail: NTIS HC A14/MF A01 CSCL 17B

A self-calibrating deep space tracking technique is described which can potentially produce two nanoradian angular spacecraft determinations. The technique uses very long base interferometric observations of a spacecraft and several radio sources. The currently employed single source technique is described as a parameter estimation procedure. Then, the number of parameters and observations leads to the proposed local reference frame technique. Station clock, Earth rotation, and tropospheric parameters are estimated along with spacecraft position from the multisource observation sequence. The contributions to spacecraft angular uncertainty from system noise, tropospheric fluctuations, and uncalibrated radio source structure are evaluated. Of these experimental errors, radio source structure dominates the determination of the spacecraft position in the radio reference frame. It is shown, however, that the sensitivity of relative spacecraft position accuracies to time-invariant radio source structure effects may be on the order of 2 nanoradians. Author

N89-10188*# Jet Propulsion Lab., California Inst. of Tech., Pasadena.
PRECISE ORBIT DETERMINATION FOR NASA'S EARTH OBSERVING SYSTEM USING GPS (GLOBAL POSITIONING SYSTEM) **c13**
B. G. Williams *In its* The Telecommunications and Data Acquisition Report 15 Aug. 1988 p 16-27 (For primary document see N89-10186 01-32)
Avail: NTIS HC A14/MF A01 CSCL 22A

An application of a precision orbit determination technique for NASA's Earth Observing System (EOS) using the Global Positioning System (GPS) is described. This technique allows the geometric information from measurements of GPS carrier phase and P-code pseudo-range to be exploited while minimizing requirements for precision dynamical modeling. The method combines geometric and dynamic information to determine the spacecraft trajectory; the weight on the dynamic information is controlled by adjusting fictitious spacecraft accelerations in three dimensions which are treated as first order exponentially time correlated stochastic processes. By varying the time correlation and uncertainty of the stochastic accelerations, the technique can range from purely geometric to purely dynamic. Performance estimates for this

technique as applied to the orbit geometry planned for the EOS platforms indicate that decimeter accuracies for EOS orbit position may be obtainable. The sensitivity of the predicted orbit uncertainties to model errors for station locations, nongravitational platform accelerations, and Earth gravity is also presented.
Author

N89-10189*# Jet Propulsion Lab., California Inst. of Tech., Pasadena.
PSA: A PROGRAM TO STREAMLINE ORBIT DETERMINATION FOR LAUNCH SUPPORT OPERATIONS **c13**
V. N. Legerton and N. A. Mottinger *In its* The Telecommunications and Data Acquisition Report 15 Aug. 1988 p 28-41 (For primary document see N89-10186 01-32)
Avail: NTIS HC A14/MF A01 CSCL 22A

An interactive, menu driven computer program was written to streamline the orbit determination process during the critical launch support phase of a mission. Residing on a virtual memory minicomputer, this program retains the quantities in-core needed to obtain a least squares estimate of the spacecraft trajectory with interactive displays to assist in rapid radio metric data evaluation. Menu-driven displays allow real time filter and data strategy development. Graphical and tabular displays can be sent to a laser printer for analysis without exiting the program. Products generated by this program feed back to the main orbit determination program in order to further refine the estimate of the trajectory. The final estimate provides a spacecraft ephemeris which is transmitted to the mission control center and used for antenna pointing and frequency predict generation by the Deep Space Network. The development and implementation process of this program differs from that used for most other navigation software by allowing the users to check important operating features during development and have changes made as needed. Author

N89-10190*# Jet Propulsion Lab., California Inst. of Tech., Pasadena.
SPAIN 31-GHz OBSERVATIONS OF SKY BRIGHTNESS TEMPERATURES **c46**
B. L. Gary *In its* The Telecommunications and Data Acquisition Report 15 Aug. 1988 p 42-60 (For primary document see N89-10186 01-32)
Avail: NTIS HC A14/MF A01 CSCL 04A

A water vapor radiometer was deployed at DSS 63 for 3 months of sky brightness temperature measurements at 31 GHz. An exceedance plot was derived from this data showing the fraction of time that 31 GHz 30 degree elevation angle brightness temperature exceeds specified values. The 5 percent exceedance statistics occurs at 75 K, compared with 70 K in Australia.
Author

N89-10191*# Jet Propulsion Lab., California Inst. of Tech., Pasadena.
AUSTRALIA 31-GHz BRIGHTNESS TEMPERATURE EXCEEDANCE STATISTICS **c46**
B. L. Gary *In its* The Telecommunications and Data Acquisition Report 15 Aug. 1988 p 61-74 (For primary document see N89-10186 01-32)
Avail: NTIS HC A14/MF A01 CSCL 04A

Water vapor radiometer measurements were made at DSS 43 during an 18 month period. Brightness temperatures at 31 GHz were subjected to a statistical analysis which included correction for the effects of occasional water on the radiometer radome. An exceedance plot was constructed, and the 1 percent exceedance statistics occurs at 120 K. The 5 percent exceedance statistics occurs at 70 K, compared with 75 K in Spain. These values are valid for all of the three month groupings that were studied.
Author

N89-10192*# Jet Propulsion Lab., California Inst. of Tech., Pasadena.
GRAVITATIONAL WAVE SEARCHES USING THE DSN (DEEP SPACE NETWORK) **c46**
S. J. Nelson and J. W. Armstrong *In its* The Telecommunications and Data Acquisition Report 15 Aug. 1988 p 75-85 (For primary document see N89-10186 01-32)
Avail: NTIS HC A14/MF A01 CSCL 04A

The Deep Space Network Doppler spacecraft link is currently the only method available for broadband gravitational wave searches in the 0.01 to 0.001 Hz frequency range. The DSN's role in the worldwide search for gravitational waves is described by first summarizing from the literature current theoretical estimates of gravitational wave strengths and time scales from various astrophysical sources. Current and future detection schemes for ground based and space based detectors are then discussed. Past, present, and future planned or proposed gravitational wave experiments using DSN Doppler tracking are described. Lastly, some major technical challenges to improve gravitational wave sensitivities using the DSN are discussed. Author

N89-10193*# Jet Propulsion Lab., California Inst. of Tech., Pasadena.
EVALUATION OF THE CHARACTERISTICS OF A FIELD EMISSION CATHODE FOR USE IN A MERCURY ION TRAP FREQUENCY STANDARD **c33**
J. M. Christman *In its* The Telecommunications and Data Acquisition Report 15 Aug. 1988 p 86-92 (For primary document see N89-10186 01-32)
Avail: NTIS HC A14/MF A01 CSCL 09A

The performance is reported of a field emission array characterized for the purpose of replacing the filament in a trapped ion frequency standard. This dark electron emitter eliminates the need for the interference filter currently used in the trapped ion standard. While reducing the filament's unwanted light, this filter causes a significant reduction in the signal. The magnetic field associated with the filament is also eliminated, thus potentially improving the present stability of the trapped ion standard. The operation of the filament in the present system is described, as well as the associated concerns. The cathode considered for the filament's replacement is then described along with the experimental system. Experimental results, observations, and conclusions are presented. Author

N89-10194*# Jet Propulsion Lab., California Inst. of Tech., Pasadena.
SIMULTANEOUS S- AND X-BAND UPLINK-DOWNLINK PERFORMANCE AT DSS 13
A. J. Freiley *In its* The Telecommunications and Data Acquisition Report 15 Aug. 1988 p 93-101 (For primary document see N89-10186 01-32)
Avail: NTIS HC A14/MF A01 CSCL 20N

The Deep Space Station 13 26-meter antenna with the second generation S/X feedcone was tested to determine the dual S- and X-band (2.1 to 2.3 GHz and 7.1 to 8.5 GHz) transmit and receive performance. Measurements were conducted using the 20 kW transmitters at S- and X-band while simultaneously receiving S- and X-band. This system proved to be very quiet compared with the other DSN antennas. Under normal tracking configurations, no noise burst or intermodulation product (IMP) activity was detectable to the -175 dBm level. To prove the instrumentation's ability to detect such phenomena, an IMP generator was introduced onto the system with positive, verifiable results. The IMP occurred at the -162 dBm level, accompanied by moderate noise burst activity, and was readily repeatable. The measurement also showed the possible need for additional fourth channel filtering in the system to reduce the effect of the transmitter power on the low noise amplifiers. Author

N89-10195*# Jet Propulsion Lab., California Inst. of Tech., Pasadena.
X/X/Ka-BAND PRIME FOCUS FEED ANTENNA FOR THE MARS OBSERVER BEACON SPACECRAFT
P. Stanton, H. Reilly, and M. Esquivel *In its* The Telecommunications and Data Acquisition Report 15 Aug. 1988 p 103-109 (For primary document see N89-10186 01-32)
Avail: NTIS HC A14/MF A01 CSCL 20N

The results of an X/X/Ka-band feed design concept

demonstration are presented. The purpose is to show the feasibility of adding a Ka-band beacon to the Mars Observer spacecraft. Scale model radiation patterns were made and analyzed. Author

N89-10196*# Jet Propulsion Lab., California Inst. of Tech., Pasadena.
DUAL PASSBAND DICHROIC PLATE FOR X-BAND
T. Y. Otoshi and M. M. Franco *In its* The Telecommunications and Data Acquisition Report 15 Aug. 1988 p 110-134 (For primary document see N89-10186 01-32)
Avail: NTIS HC A14/MF A01 CSCL 20N

A need arose in the Deep Space Network for a dichroic plate that would simultaneously pass two desired frequency bands in the X-band region. In addition, the plate must be totally reflective for S-band frequencies. A dielectrically loaded dichroic plate is described that was developed to meet this need. The unique microwave properties that the new dichroic plate had to possess were: (1) insertion losses of less than 0.04 dB for X-band uplink frequencies centered at 7167 MHz and for X-band downlink frequencies centered at about 8425 MHz; (2) insertion losses that met the low loss requirements at 30 deg incidence angle simultaneously for both parallel and perpendicular polarizations; (3) total reflectivity at S-band frequencies; and (4) ability to maintain these electrical characteristics while passing 100 kW of CW power at X-band or while reflecting 100 kW of CW power at S-band. The dual passband dichroic plate is a thick metallic plate having an array of periodic round holes filled with Teflon plugs. Test results on an experimental prototype plate indicate that it is technically possible to design a dielectrically filled dichroic plate that meets all of the technical requirements. Author

N89-10197*# Jet Propulsion Lab., California Inst. of Tech., Pasadena.
ANTENNA POINTING COMPENSATION BASED ON PRECISION OPTICAL MEASUREMENT TECHNIQUES
L. L. Schumacher and H. C. Vivian *In its* The Telecommunications and Data Acquisition Report 15 Aug. 1988 p 135-144 (For primary document see N89-10186 01-32)
Avail: NTIS HC A14/MF A01 CSCL 20N

The pointing control loops of the Deep Space Network 70 meter antennas extend only to the Intermediate Reference Structure (IRS). Thus, distortion of the structure forward of the IRS due to unpredictable environmental loads can result in uncompensated boresight shifts which degrade blind pointing accuracy. A system is described which can provide real time bias commands to the pointing control system to compensate for environmental effects on blind pointing performance. The bias commands are computed in real time based on optical ranging measurements of the structure from the IRS to a number of selected points on the primary and secondary reflectors. Author

N89-10198*# Jet Propulsion Lab., California Inst. of Tech., Pasadena.
A 32-GHz REFLECTED-WAVE MASER AMPLIFIER WITH WIDE INSTANTANEOUS BANDWIDTH
J. Shell and D. Neff *In its* The Telecommunications and Data Acquisition Report 15 Aug. 1988 p 145-162 (For primary document see N89-10186 01-32)
Avail: NTIS HC A14/MF A01 CSCL 20N

An eight stage, 32 GHz reflected wave ruby maser was built. The maser operates in a 3 watt closed cycle refrigerator at 4.5 K and is capable of 21 dB of net gain with an instantaneous bandwidth of 400 MHz. The input noise temperature referred to the room temperature flange is approximately 21 K. Author

N89-10199*# Jet Propulsion Lab., California Inst. of Tech., Pasadena.
AN 8.4-GHz CRYOGENICALLY COOLED HEMT AMPLIFIER FOR DSS 13 **c33**
L. Tanida *In its* The Telecommunications and Data Acquisition Report 15 Aug. 1988 p 163-169 (For primary document see N89-10186 01-32)
Avail: NTIS HC A14/MF A01 CSCL 09A

A prototype 8.4 GHz (X-band) high electron mobility transistor (HEMT) amplifier/closed cycle refrigerator system was installed in the Deep Space Station 13 feedcone in August 1987. The amplifier is cryogenically cooled to a physical temperature of 12 K and provides 31 K antenna noise temperature (zenith) and 35 dB of gain at a frequency of 8.2 to 8.6 GHz. Antenna system noise temperature is less than 50 K from 7.2 to 9.4 MHz. The low noise HEMT amplifier system is intended for use as a radio astronomy or space communications receiver front end. Author

N89-10200*# Jet Propulsion Lab., California Inst. of Tech., Pasadena.
DESIGN OF AN OPTICAL PPM COMMUNICATION LINK IN THE PRESENCE OF COMPONENT TOLERANCES
C.-C. Chen *In its* The Telecommunications and Data Acquisition Report 15 Aug. 1988 p 170-179 (For primary document see N89-10186 01-32)
Avail: NTIS HC A14/MF A01 CSCL 17B

A systematic approach is described for estimating the performance of an optical direct detection pulse position modulation (PPM) communication link in the presence of parameter tolerances. This approach was incorporated into the JPL optical link analysis program to provide a useful tool for optical link design. Given a set of system parameters and their tolerance specifications, the program will calculate the nominal performance margin and its standard deviation. Through use of these values, the optical link can be designed to perform adequately even under adverse operating conditions. Author

N89-10201*# Jet Propulsion Lab., California Inst. of Tech., Pasadena.
ATMOSPHERIC PROPAGATION EFFECTS RELEVANT TO OPTICAL COMMUNICATIONS
K. S. Shaik *In its* The Telecommunications and Data Acquisition Report 15 Aug. 1988 p 180-200 (For primary document see N89-10186 01-32)
Avail: NTIS HC A14/MF A01 CSCL 17B

A number of atmospheric phenomena affect the propagation of light. The effects of clear air turbulence are reviewed as well as atmospheric turbidity on optical communications. Among the phenomena considered are astronomical and random refraction, scintillation, beam broadening, spatial coherence, angle of arrival, aperture averaging, absorption and scattering, and the effect of opaque clouds. An extensive reference list is also provided for further study. Useful information on the atmospheric propagation of light in relation to optical deep space communications to an earth based receiving station is available, however, further data must be generated before such a link can be designed with committed performance. Author

N89-10202*# Jet Propulsion Lab., California Inst. of Tech., Pasadena.
NODE SYNCHRONIZATION OF VITERBI DECODERS USING STATE METRICS **c61**
U. Cheng *In its* The Telecommunications and Data Acquisition Report 15 Aug. 1988 p 201-209 (For primary document see N89-10186 01-32)
Avail: NTIS HC A14/MF A01 CSCL 09B

The concept of node synchronization using state metrics is investigated. The branch metrics are integrated over a fixed time interval and the results are compared to the detection threshold. If the threshold is exceeded, the out-of-sync hypothesis is accepted; otherwise, the in-sync hypothesis is accepted. It is shown that the detection threshold can be chosen independent of any particular convolutional code with fixed code rate and constant length if the code has reasonably good bit error rate performance. Three node synchronization schemes are compared: (1) a scheme using the syndrome; (2) a scheme using the frame-sync patterns; and (3) a scheme using the state metrics. At very low signal to noise ratios (SNR), scheme 2 can be faster than scheme 1. For Voyager's rate 1/2 and constraint length 7 convolutional code, this happens for SNRs of less than 0.7 dB. This result is obtained by assuming that the code frame-sync pattern has good aperiodic autocorrelation

properties. For a fixed false alarm probability, the sequential detection scheme based on the syndrome is faster than scheme 3 with fixed integration time. A sequential detection technique is needed to improve the speed of scheme 3. Author

N89-10203*# Jet Propulsion Lab., California Inst. of Tech., Pasadena.
A SOFTWARE SIMULATION STUDY OF THE LONG CONSTRAINT LENGTH VLSI VITERBI DECODER c61
S. Arnold and F. Pollara *In its* The Telecommunications and Data Acquisition Report 15 Aug. 1988 p 210-221 (For primary document see N89-10186 01-32)
Avail: NTIS HC A14/MF A01 CSCL 09B

A software simulation of long constraint length Viterbi decoders was developed. This software closely follows the hardware architecture that was chosen for the Very Large Scale Integration implementation. The program is used to validate the design of the decoder and to generate test vectors for the VLSI circuits. Author

N89-10204*# Jet Propulsion Lab., California Inst. of Tech., Pasadena.
AN AUTOMATIC FREQUENCY CONTROL LOOP USING OVERLAPPING DFTs (DISCRETE FOURIER TRANSFORMS)
S. Aguirre *In its* The Telecommunications and Data Acquisition Report 15 Aug. 1988 p 222-231 (For primary document see N89-10186 01-32)
Avail: NTIS HC A14/MF A01 CSCL 20N

An automatic frequency control (AFC) loop is introduced and analyzed in detail. The new scheme is a generalization of the well known Cross Product AFC loop that uses running overlapping discrete Fourier transforms (DFTs) to create a discriminator curve. Linear analysis is included and supported with computer simulations. The algorithm is tested in a low carrier to noise ratio (CNR) dynamic environment, and the probability of loss of lock is estimated via computer simulations. The algorithm discussed is a suboptimum tracking scheme with a larger frequency error variance compared to an optimum strategy, but offers simplicity of implementation and a very low operating threshold CNR. This technique can be applied during the carrier acquisition and re-acquisition process in the Advanced Receiver. Author

N89-10205*# Jet Propulsion Lab., California Inst. of Tech., Pasadena.
HEAT EXCHANGER EXPERT SYSTEM LOGIC c34
R. Cormier *In its* The Telecommunications and Data Acquisition Report 15 Aug. 1988 p 232-244 (For primary document see N89-10186 01-32)
Avail: NTIS HC A14/MF A01 CSCL 20D

The reduction is described of the operation and fault diagnostics of a Deep Space Network heat exchanger to a rule base by the application of propositional calculus to a set of logic statements. The value of this approach lies in the ease of converting the logic and subsequently implementing it on a computer as an expert system. The rule base was written in Process Intelligent Control software. Author

N89-10206*# Jet Propulsion Lab., California Inst. of Tech., Pasadena.
STORAGE AND COMPUTATIONALLY EFFICIENT PERMUTATIONS OF FACTORIZED COVARIANCE AND SQUARE-ROOT INFORMATION ARRAYS c64
R. J. Muellerschoen *In its* The Telecommunications and Data Acquisition Report 15 Aug. 1988 p 245-256 (For primary document see N89-10186 01-32)
Avail: NTIS HC A14/MF A01 CSCL 12A

A unified method to permute vector stored Upper triangular Diagonal factorized covariance and vector stored upper triangular Square Root Information arrays is presented. The method involves cyclic permutation of the rows and columns of the arrays and retriangularization with fast (slow) Givens rotations (reflections). Minimal computation is performed, and a one dimensional scratch array is required. To make the method efficient for large arrays on a virtual memory machine, computations are arranged so as to avoid expensive paging faults. This method is potentially important for processing large volumes of radio metric data in the Deep Space Network. Author

N89-10207*# Jet Propulsion Lab., California Inst. of Tech., Pasadena.
PHASING THE ANTENNAS OF THE VERY LARGE ARRAY (VLA) FOR RECEPTION OF TELEMETRY FROM VOYAGER 2 AT NEPTUNE ENCOUNTER c17
J. S. Ulvestad *In its* The Telecommunications and Data Acquisition Report 15 Aug. 1988 p 257-273 (For primary document see N89-10186 01-32)
Avail: NTIS HC A14/MF A01 CSCL 09F

The Very Large Array (VLA) radio telescope is being instrumented at 8.4 GHz to receive telemetry from Voyager 2 during its encounter with Neptune in 1989. The procedure in which the 27 antennas have their phases adjusted in near real time so that the signals from the individual elements of the array can be added coherently is examined. Calculations of the expected signal to noise ratio, tests of the autophasing process at the VLA, and off-line simulations of that process are all presented. Various possible procedures for adjusting the phases are considered. It is shown that the signal to noise ratio at the VLA is adequate for summing the signals from the individual antennas with less than 0.1 dB of loss caused by imperfect coherence among the antennas. Tropospheric variations during the summer of 1989 could cause enough loss of coherence to make the losses higher than 0.1 dB. Experiments show that the losses caused by the troposphere can probably be kept below 0.2 dB if the time delay inherent in the phase adjustment process is no longer than approx. 5 secs. This relatively small combining loss meets the goal estabished to minimize the bit error rate in the Voyager telemetry and implies adequate autophasing of the VLA. Author

N89-10208*# Jet Propulsion Lab., California Inst. of Tech., Pasadena.
PHOBOS LANDER CODING SYSTEM: SOFTWARE AND ANALYSIS c61
K.-M. Cheung and F. Pollara *In its* The Telecommunications and Data Acquisition Report 15 Aug. 1988 p 274-286 (For primary document see N89-10186 01-32)
Avail: NTIS HC A14/MF A01 CSCL 09B

The software developed for the decoding system used in the telemetry link of the Phobos Lander mission is described. Encoders and decoders are provided to cover the three possible telemetry configurations. The software can be used to decode actual data or to simulate the performance of the telemetry system. The theoretical properties of the codes chosen for this mission are analyzed and discussed. Author

N89-10209*# Jet Propulsion Lab., California Inst. of Tech., Pasadena.
RELATIVE PLANETARY RADAR SENSITIVITIES: ARECIBO AND GOLDSTONE
N. A. Renzetti, T. W. Thompson, and M. A. Slade *In its* The Telecommunications and Data Acquisition Report 15 Aug. 1988 p 287-293 (For primary document see N89-10186 01-32)
Avail: NTIS HC A14/MF A01 CSCL 20N

The increase of the Deep Space Network antennas from 64 meter to 70 meter diameter represents the first of several improvements that will be made over the next decade to enhance earth based radar sensitivity to solar system targets. The aperture increase at the Goldstone DSS-14 site, coupled with a proposed increase in transmitter power to 1000 kW, will improve the 3.5 cm radar by about one order of magnitude. Similarly, proposed Arecibo Observatory upgrades of a Gregorian feed structure and an increase of transmitter power to 1000 kW will increase the sensitivity of this radar about 20 fold. In addition, a Goldstone to Very Large Array bistatic observation with horizon to horizon tracking will have 3.5 times more sensitivity than will a Goldstone horizon to horizon monostatic observation. All of these

improvements, which should be in place within the next decade, will enrich an already fertile field of planetary exploration. Author

N89-10210*# Jet Propulsion Lab., California Inst. of Tech., Pasadena.
DSN 64-METER ANTENNA L-BAND (1668-MHz) MICROWAVE SYSTEM PERFORMANCE OVERVIEW
J. Withington *In its* The Telecommunications and Data Acquisition Report 15 Aug. 1988 p 294-300 (For primary document see N89-10186 01-32)
Avail: NTIS HC A14/MF A01 CSCL 20N

In 1985, L-band (1668 MHz) receive-only feed systems were installed on the three Deep Space Network 64 meter antennas to provide tracking support for two non-NASA spacecraft. The specifications, design approach, and operational test results are presented. The L-band microwave system met all of its tracking goals and is currently being upgraded to include a C-band (5000 MHz) uplink. Author

N89-10211*# Jet Propulsion Lab., California Inst. of Tech., Pasadena.
SUMMARY OF DSN (DEEP SPACE NETWORK) REIMBURSABLE LAUNCH SUPPORT **c14**
N. A. Fanelli and M. E. Wyatt *In its* The Telecommunications and Data Acquisition Report 15 Aug. 1988 p 301-306 (For primary document see N89-10186 01-32)
Avail: NTIS HC A14/MF A01 CSCL 14B

The Deep Space Network is providing ground support to space agencies of foreign governments as well as to NASA and other agencies of the Federal government which are involved in space activities. DSN funding for support of missions other than NASA are on either a cooperative or a reimbursable basis. Cooperative funding and support are accomplished in the same manner as NASA sponsored missions. Reimbursable launch funding and support methods are described. Author

N89-10212# National Aerospace Lab., Amsterdam (Netherlands).
DIGITAL RECORDING OF RADAR DATA IN AN AIRCRAFT
H. Pouwels 20 Jul. 1987 24 p In DUTCH; ENGLISH summary Presented at Lecture Course on Digital Signal Processing for Realtime Applications, Utrecht, Netherlands, 27 Feb. 1986; sponsored by NIRIA and KIVI
(PB88-209507; NLR-MP-86057-U) Avail: NTIS HC A03/MF A01 CSCL 17I

In the Netherlands, Side Looking Airborne Radar (SLAT) is operated with a digital recording of the data. A description is given of the airborne recording chain and of the ground based processing. The airborne electronics for the digitizing, formatting and recording of the radar data are described in detail. The system setup is tailored to the use of the SLAR as a research tool. GRA

N89-10213*# Ohio State Univ., Columbus. ElectroScience Lab.
CALCULATION OF THE EFFECTS OF ICE ON THE BACKSCATTER OF A GROUND PLANE
K. M. Lambert and L. Peters, Jr. Sep. 1988 55 p
(Grant NAG3-913)
(NASA-CR-183303; NAS 1.26:183303; ESL-TR-720964-1) Avail: NTIS HC A04/MF A01 CSCL 20N

Described is a technique for examining the effect of a rough ice layer on the backscatter of a ground plane. The technique is applied to the special case of a rough ice layer that is periodic in space. By assuming that the roughness is periodic, the backscatter of the ground plane can be found from the backscatter of a single period. Backscatter calculations are presented for a single period in which the thickness of the ice layer has a Gaussian shape. Author

N89-10214# Helsinki Univ. of Technology, Espoo (Finland). Electromagnetics Lab.
SPACE-HARMONIC ANALYSIS OF MULTI-DEPTH CORRUGATED WAVEGUIDES
Markku Iimari Oksanen Apr. 1988 27 p
(PB88-210059; Rept-27; ISBN-951-754-465-0) Avail: NTIS HC A03/MF A01 CSCL 20N

Multi-depth corrugated and ring-loaded waveguides are analyzed in terms of space-harmonics. A general eigenvalue equation for the corrugated waveguide with M different slot depths in one corrugation period is derived under the assumption of thin corrugations. The theory is then applied for corrugated waveguides possessing from one to four different slot depths. Dispersion curves for tri-depth corrugated guides are calculated, and propagation characteristics in dual-depth corrugated and ring-loaded guides are compared with each other. Frequency band properties of these guides and accuracies of some more approximate methods in tri-depth guide analysis are discussed. GRA

N89-10215*# National Aeronautics and Space Administration. Lewis Research Center, Cleveland, Ohio.
A METHOD FOR PRODUCING A SHAPED CONTOUR RADIATION PATTERN USING A SINGLE SHAPED REFLECTOR AND A SINGLE FEED
A. R. Cherrette, S. W. Lee (Illinois Univ., Urbana.), and R. J. Acosta Oct. 1988 45 p
(Grant NAG3-419)
(NASA-TM-101369; E-4408; NAS 1.15:101369) Avail: NTIS HC A03/MF A01 CSCL 20N

Eliminating the corporate feed network in shaped contour beam antennas will reduce the expense, weight, and RF loss of the antenna system. One way of producing a shaped contour beam without using a feed network is to use a single shaped reflector with a single feed element. For a prescribed contour beam and feed, an optimization method for designing the reflector shape is given. As a design example, a shaped reflector is designed to produce a continental U.S. coverage (CONUS) beam. The RF performance of the shaped reflector is then verified by physical optics. Author

N89-10216*# Stanford Univ., Calif. Electronics Lab.
HIGH SPEED FIBER OPTICS LOCAL AREA NETWORKS: DESIGN AND IMPLEMENTATION Final Report, 1 Jan. 1984 - 31 Dec. 1987
Fouad A. Tobagi 29 Sep. 1988 9 p
(Grant NAG2-292)
(NASA-CR-182432; NAS 1.26:182432) Avail: NTIS HC A02/MF A01 CSCL 17B

The design of high speed local area networks (HSLAN) for communication among distributed devices requires solving problems in three areas: (1) the network medium and its topology; (2) the medium access control; and (3) the network interface. Considerable progress has been made in all areas. Accomplishments are divided into two groups according to their theoretical or experimental nature. A brief summary is given in Section 2, including references to papers which appeared in the literature, as well as to Ph.D. dissertations and technical reports published at Stanford University. Author

N89-10217# Kansas Univ. Center for Research, Inc., Lawrence. Telecommunications and Information Sciences Lab.
EVALUATION OF HARDWARE ARCHITECTURES FOR HF ANTENNA ARRAYS Final Report, May 1986 - May 1987
R. K. Balasubramaniam, Victor Frost, Roger Spohn, Ryan Moates, and Stephen Fechtel Jan. 1988 232 p
(Contract F30602-81-C-0205)
(AD-A196204; TISL-5481-2; RADC-TR-87-240) Avail: NTIS HC A11/MF A01 CSCL 25B

A variety of hardware architectures can be used for the implementation of HF adaptive signal processing algorithms. The purpose of this study is to evaluate various hardware structures, enumerate their advantages and disadvantages relative to the HF adaptive array problem, and to recommend the architectures best suited to the adaptive HF array systems. The hardware structures are compared based upon complexity which is determined by issues such as computational bounds, input requirements and characteristics of hardware structures. This evaluation is performed

in a hierarchical manner. Application of general microprocessor technology is considered first. Integrated circuits tailored for digital signal processing applications is investigated next. Finally VLSI signal processing technology is considered. Included here are systolic and wavefront architectures. GRA

N89-10218# Materials Research Labs., Melbourne (Australia).
AN INTERACTIVE PROGRAM FOR ESTIMATING EXTINCTION AND SCATTERING PROPERTIES OF MOST PARTICULATE CLOUDS
B. T. N. Evans Jun. 1988 38 p
(MRL-R-1123; AR-005-237) Avail: NTIS HC A03/MF A01

An interactive computer program is described that enables the user to calculate the phase function, extinction, scattering, and absorption efficiencies, the mass extinction coefficient, and backscatter to extinction ratio for most clouds. These clouds may be composed of either mono- or polydispersed particles of the following geometries: sphere, coated sphere, infinite cylinder, coated infinite cylinder, finite cylinder, or various irregular shapes. The nonspherical regular shapes may be either oriented or have random orientation. Author

N89-10219# Instituto de Pesquisas Espaciais, Sao Jose dos Campos (Brazil).
S-BAND TRANSPONDER AND TELECOMMAND DECODER DESIGN AND DEVELOPMENT FOR MECB SATELLITES
Paulo MelloMarshall Aug. 1988 17 p Presented at the 6th Simposio Nipo-Brasileiro de Ciencia e Tecnologia, Sao Jose dos Campos, Brazil, Aug. 1988 Submitted for publication
(INPE-4659-PRE/1362) Avail: NTIS HC A03/MF A01

The main features and development status of the on-board S-band Transponder and Telecommand Dual Decoder equipment intended for use in the Telemetry, Tracking, and Command (TT and C) subsystem of the second data collection satellite (SDC-2) of the Brazilian Complete Space Mission (MECB) are described. The main features of the equipment are presented. The designs are validated by the results of tests performed on the engineering models. The projected work towards qualification models of the equipment is also presented. Author

N89-10220# National Telecommunications and Information Administration, Boulder, Colo. Inst. for Telecommunication Sciences.
MULTITIER SPECIFICATION APPLIED TO MODIFY THE HARDNESS OF AN ESSENTIAL NSEP (NATIONAL SECURITY/EMERGENCY PREPAREDNESS) FIBER OPTIC LINK
David F. Peach and Robert T. Adair Mar. 1988 156 p Sponsored by National Communications System, Washington, D.C.
(PB88-210778; NTIA-88-231; NCS-TIB-88-02) Avail: NTIS HC A08/MF A01 CSCL 17B

The Multitier Specification was developed to provide guidelines and recommendations for improving the durability of the communication installations necessary for National Security Emergency Preparedness (NSEP). The application of the Multitier Specification is considered beyond the installation and engineering requirements of typical commercial fiber optic systems. Five levels of hardness are defined. A link that could be important to the operation of the U.S. Space Command/NORAD was chosen as a candidate for the analysis. Based on the time critical nature of the telecommunication traffic carried on this link and the stress expected, the Level 4 (Maximum) hardness was chosen as the target level for upgrade of this link. The elements of the existing system are classified into levels using the Multitier Specification. The enhancements needed to mitigate the stress threat within the guidelines of the Multitier Specification and to raise the level of hardness to Level 4 are described. The cost associated with the installation of these enhancements is included. Solutions to problems peculiar to the path suggested for the link are described in terms of one suggested alternative. Author

N89-10221# Instituto de Pesquisas Espaciais, Sao Jose dos Campos (Brazil).
THEORETICAL AND EXPERIMENTAL ANALYSIS OF QUADRIFILAR ANTENNAS FOR THE FIRST BRAZILIAN SATELLITE
Carlos Alberto IennacoMiranda Jun. 1988 25 p Presented at the DFVLR/CTA Workshop on Antennas, Propagation and Scattering, 10-14 Aug. 1987
(INPE-4581-PRE/1315) Avail: NTIS HC A03/MF A01

Since its development the resonant quadrifilar helix has found application in a number of spacecraft programs. This presentation deals with the calculation of the radiation pattern for this type of antenna, mounted on a convex, polyhedral satellite, by means of the Geometrical Theory of Diffraction. The input filed is completely described either by a model of the quadrifilar helix, obtained from amplitude and phase measurements or by the solutions of the integral equations which describe the helix radiation characteristics. As a basis for these calculations, measurements were done with various quadrifilar helix models mounted on the RF mock-up of the first Brazilian satallite. The results have shown good agreement with the computed radiation patterns. Author

N89-10222# National Academy of Sciences - National Research Council, Washington, D. C.
ANTENNAS, SATELLITE BROADCASTING, AND EMERGENCY PREPAREDNESS FOR THE VOICE OF AMERICA Interim Report
May 1988 68 p Sponsored by Voice of America, Washington, D.C.
(PB88-209895) Avail: NTIS HC A04/MF A01 CSCL 17B

Long-term technical measures that should increase the extent and quality of Voice of America (VOA) broadcast quality are recommended. VOA should develop a U.S. program in DBS-A, including active participation in International Telecommunication Union deliberations and liaison with the receiver industry. VOA should also develop its emergency preparedness program consistant with existing national guidelines. Finally, attention is called to the desirability of an explicit and visible research and development program. GRA

N89-10223*# Ohio State Univ., Columbus. ElectroScience Lab.
MEASUREMENT OF THE PROPERTIES OF LOSSY MATERIALS INSIDE A FINITE CONDUCTING CYLINDER Final Report
R. Caldecott, A. Dominek, and A. Park Oct. 1988 30 p
(Grant NAG3-784)
(NASA-CR-182500; NAS 1.26:182500; FR-719300-4) Avail: NTIS HC A03/MF A01 CSCL 20N

A computer code was developed to automatically perform swept frequency reflection and transmission measurements using a HP5510B Network Analyzer and computer. This software is used in conjunction with a modified high temperature test rig to obtain reflection measurements from a flat material sample. The software allows data processing to eliminate measurement errors and to obtain a reflection coefficient in the frequency or time domain. A description of the program is presented. Author

N89-10224# Los Alamos National Lab., N. Mex.
LOSSES IN MAGNETIC FLUX COMPRESSION GENERATORS. PART 2: RADIATION LOSSES
C. M. Fowler Jun. 1988 50 p
(Contract W-7405-eng-36)
(DE88-015046; LA-9956-MS-Pt-2) Avail: NTIS HC A03/MF A01

An analysis of flux losses in explosive driven magnetic flux compression generators is given. Flux loss by radiation from the outer conductor walls is treated. Flux leakage rates through walls of finite thickness are first obtained by diffusion theory. It is shown, for normal wall thicknesses, that flux leakage is determined essentially by the wall conductance, defined as the product of wall thickness and wall conductivity. This remains true when the wall thickness is reduced to zero at unchanged conductance. In this case, the wall is said to be coalesced. Solutions for a cavity

bounded by a perfect conductor on one side and a coalesced wall on the other are then obtained using the complete Maxwell wave equations in both the cavity and free space beyond the coalesced wall. Several anomalies that arise from diffusion analysis are resolved by the wave treatment. Conditions for the validity of the diffusion treatment are noted, and an expression is obtained within the framework of diffusion theory for energy radiated into space from the cavity walls. DOE

N89-10225*# Ohio State Univ., Columbus. ElectroScience Lab.
MATERIAL PARAMETER DETERMINATION FROM SCATTERING MEASUREMENTS
A. Dominek, A. Park, and L. Peters, Jr. Sep. 1988 43 p
(Grant NAG3-784)
(NASA-CR-183312; NAS 1.26:183312; ESL-TR-719300-3) Avail: NTIS HC A03/MF A01 CSCL 20N

The electrical, macroscopic performance of isotropic material can generally be described through their constitutive scalar parameters, permittivity and permeability which are symbolically represented by epsilon and mu, respectively. These parameters relate the electric and magnetic flux densities to the electric and magnetic fields through the following relationships: (1) D=epsilonE; and (2) B=muH. It is through these parameters that the interaction of electromagnetic waves with material can be quantized in terms of reflection and transmission coefficients, and propagation and attenuation factors. Author

N89-10226# Alcatel Thomson Espace, Toulouse (France).
SPACEBORNE SAR IMAGING OF LAND, AN OPPORTUNITY FOR POLYPHASE CODE
Jean Rozes and Alain Pinel 29 Nov. 1987 2 p Presented at TGARSS 87
(ATES/DMA/RAD/002-86; ETN-88-93080) Avail: NTIS HC A02/MF A01

The performances of a polyphase code compression and an analog compression are compared. The interest in terms of performances, of block diagram simplicity, of weight, and of power comsumption are treated in a typical land SAR observation. Simulated pictures highlight the improvement of picture quality for land application in the case of classical analog chirp and in the case of proposed polyphase code. This comparison, significant at mission level, assumes similar requirements for critical units such as high power amplifier (in term of phase linearity) and such as pulse generation electronics. ESA

N89-10227# Centre National d'Etudes Spatiales, Toulouse (France).
PRELIMINARY PROJECT PASTEL: SYSTEM INTERFACE BETWEEN SPOT 4 AND THE PSDE'S PASSENGER
S. Potteck 3 Apr. 1987 13 p In FRENCH; ENGLISH summary
(CNES-87/088-CT/DRT/TIT/TR; ETN-88-93089) Avail: NTIS HC A03/MF A01

Problems on the optical data link between SPOT 4 and the GEO satellite which will relay its data, due to different bit rates, are discussed. While the SPOT 4 digital transmission rate is 2 x 24.68 Mbits/sec, the GEO reception rate should be 2 x 30 Mbits/sec, for standardization reasons. Adaptation of the geostationary terminal is economically attractive for clients who do not have to change their digital rate, but increases terminal development costs. Changing the SPOT rate puts the cost burden onto clients. No preference is stated. ESA

N89-10065*# Bendix Field Engineering Corp., Lanham, Md.
AN EXPERT SYSTEM FOR SCHEDULING REQUESTS FOR COMMUNICATIONS LINKS BETWEEN TDRSS AND ERBS
David R. McLean, Ronald G. Littlefield, and David S. Beyer *In* NASA, Goddard Space Flight Center, Proceedings of 1987 Goddard Conference on Space Applications of Artificial Intelligence (AI) and Robotics 1987 16 p Previously announced in IAA as A88-20485 (For primary document see N89-10063 01-12)
Avail: NTIS HC A99/MF E03 CSCL 17B

N89-10458# Electrical and Computer Engineering, Athens, Ohio.
ON A SURFACE MOUNTED TRANSMISSION LINE CONFIGURATION FOR APERTURE TESTING
C. D. Taylor, F. Marcum, C. C. Herrmann, and W. D. Prather (Air Force Weapons Lab., Kirtland AFB, N. Mex.) *In* NOAA, International Aerospace and Ground Conference on Lightning and Static Electricity Apr. 1988 p 197-20 (For primary document see N89-10429 01-47)
Avail: NTIS HC A23/MF A01 CSCL 20N

33 ELECTRONICS AND ELECTRICAL ENGINEERING

Includes test equipment and maintainability; components, e.g., tunnel diodes and transistors; microminiaturization; and integrated circuitry.

For related information see also *60 Computer Operations and Hardware* and *76 Solid-State Physics.*

N89-10228 Bath Univ. (England).
SINGLE-POLE SWITCHING SCHEMES FOR EHV TRANSMISSION SYSTEMS Ph.D. Thesis
Qais M. Alias 1986 291 p
Avail: Univ. Microfilms Order No. BRDX80822

The financial constraints that electric utilities face require new and innovative techniques to be used to minimize the installation of new power system facilities, while maintaining high reliability. Also, the enactment of siting regulations for transmission lines makes it more difficult to install new transmission facilities quickly. Recognizing that a high percentage of transmission line faults are single phase to earth and temporary, provides the impetus for considering single pole switching to enhance the reliability of EHV transmission systems. The effectiveness of single pole switching schemes, largely determined by the speed with which the secondary arcs extinguish, allow system restoration. Simulation techniques that enable better prediction of the faulted system response are very important to the design and assessment of the various single pole switching scheme applications. Digital methods are developed to enable the faulted response of EHV systems to be simulated for a variety of different single pole switching schemes. These include, conventional switching, autoreclosure, neutral switched reactor and High Speed Grounding Switch implementations.
Dissert. Abstr.

N89-10229# Los Alamos National Lab., N. Mex. Applied Theoretical Div.
SIMULATION OF PLASMA EROSION OPENING SWITCHES
Rodney J. Mason and Michael E. Jones 1988 7 p Presented at the 7th International Conference on High-Power Particle Beams, Karlsruhe, Fed. Republic of Germany, 4 Jul. 1988
(Contract W-7405-eng-36)
(DE88-014425; LA-UR-88-2029; CONF-880713-11) Avail: NTIS HC A02/MF A01

Recent progress in the modeling of Plasma Erosion Opening Switches is reviewed, and new results from both fluid and particle simulation compared. Three-fluid simulations with the ANTHEM code for switches on the NRL GAMBLE 1 machine and SNL PBFA 2 machine have shown strong dependence of the opening dynamics on the anode structure, the threshold for electron emission, on the possible presence of anomalous resistivity, and on advection of the magnetic field with cathode emitted electrons. Simulations with the implicit particle-in-cell code ISIS confirm these observations, but manifest broader current channels - in better agreement with GAMBLE 1 experimental results. DOE

N89-10230# Lawrence Livermore National Lab., Calif.
CROSSATRON SWITCH AS THYRATRON REPLACEMENT IN HIGH REPETITION RATE, HIGH AVERAGE POWER MODULATORS
J. S. Sullivan Jun. 1988 7 p Presented at the 18th Power Modulator Symposium, Hilton Head, S.C., 20 Jun. 1988

(Contract W-7405-eng-48)
(DE88-013706; UCRL-98072; CONF-880699-8) Avail: NTIS HC A02

The Crossatron is a cold cathode, low pressure, gas discharge switch with opening and closing capabilities. Due to its cold cathode operation, the Crossatron may offer lifetime advantages compared to the hydrogen thyratron. Unfortunately, little information regarding Crossatron lifetime and performance in high repetition rate, high average power, pulse modulators exists. Four prototype Crossatron devices, fabricated by Hughes Aircraft, were obtained to evaluate their performance and lifetime in high repetition rate, high average power, pulse modulators that had previously been equipped with hydrogen thyratrons. The prototype Crossatrons were evaluated over a range of operating parameters. Various grid drive, keep alive power levels and triggering schemes were employed in the tests. Switch parameters such as trigger time, anode fall time, jitter, recovery time, peak di/dt, switch efficiency, and the gas pumping effect of the discharge were observed. One Crossatron prototype was also subjected to lifetime tests that accumulated tens of billions of pulses. Lifetime data will be compared to various thyratron models tested similarly. DOE

N89-10231# Sandia National Labs., Albuquerque, N. Mex. Physical Chemistry and Mechanical Properties of Polymers Div.
HYDROGEN SORPTION STUDIES OF MATERIALS USED IN LI(SI)/FeS2 THERMAL BATTERIES
Roger A. Assink, Duane A. Schneider, and Ronald A. Guidotti Jun. 1988 21 p
(Contract DE-AC04-76DP-00789)
(DE88-013154; SAND-87-3149) Avail: NTIS HC A03/MF A01

Hydrogen formation occurs during long-term storage of Li(Si)/FeS2 thermal batteries as a result of residual moisture reacting with the Li(Si) anode. A study of the rates of hydrogen sorption by materials used in Li(Si)/FeS2 thermal batteries was undertaken in order to obtain a measure of their reactivity to hydrogen in the thermal battery environment. The sorption of hydrogen by pellets of the anode material, separator mix, catholyte mix, and heat powder was monitored for periods of up to a month at a temperature of 60 C. The anode material was 44 percent Li/56 percent Si alloy; the separator was 65 percent LiCl-KCl eutectic/35 percent MgO; the catholyte was 75 percent FeS2/25 percent electrolyte binder mix (with the composition 88 percent LiCl-KCl eutectic/12 percent SiO2; and the heat powder was 88 percent Fe/12 percent KClO4. Individual components of the mixes exhibiting significant sorption of hydrogen were examined, and the FeS2 was the only material found to be actively sorbing hydrogen. The kinetics of the sorption process were enhanced by a smaller particle size of FeS2, a higher hydrogen pressure, and a higher level of oxidized iron impurities. The hydrogen was not removed by vacuum heating at 200 C. A hydrogen sorption study of the insulation materials used in the battery showed the ceramic-fiber blanket to be a significant sorbent for hydrogen. DOE

N89-10232# Lawrence Livermore National Lab., Calif.
DESIGN AND PERFORMANCE OF THE SSVCO
P. Poulsen, J. J. Morrison, J. B. Chase, E. E. Domning, R. S. Hawke, H. T. Takemori, and G. E. Vogtlin 13 Jun. 1988 9 p Presented at the 4th National High Power Microwave Conference, Monterey, Calif., 9 May 1988
(Contract W-7405-eng-48)
(DE88-012435; UCRL-98910; CONF-8805132-10) Avail: NTIS HC A02/MF A01

A magnetized and tunable virtual cathode oscillator with radial extraction of RF power (SSVCO) has been constructed. The diagnostic chamber guides the RF power to an array of orthogonal sets of dipole antennas which provide accurate power measurement over a wide range of power, polarization, frequencies, and directions of the incident power. The vacuum chamber incorporates liquid nitrogen pumping which, in combination with prepulsing the beam, substantially extends the RF pulse duration and the delivered energy. The results indicate that ions formed at the anode surface will flow into the electron beam, causing space charge neutralization, and terminating the RF pulse. Cleaning the system by prepulsing and pumping decreases the rate of ion formation and extends the RF pulse. Conditions for which the reflexing and the beam frequency are equal have been found to produce instantaneous efficiencies of RF production as high as 20 percent. DOE

N89-10233# Keuring van Electrotechnische Materialen N.V., Arnhem (Netherlands). Physical Research Dept.
OPTICAL SENSORS FOR THE MEASUREMENT OF ELECTRIC CURRENT AND VOLTAGE
W. R. Rutgers, H. J. M. Hulshof, I. J. Laurensse, and A. H. vanderWey 1987 16 p Submitted for publication
(PB88-208467; ISBN-90-353-0058-0) Avail: NTIS HC A03/MF A01 CSCL 09C

Optical sensors for the measurement of electrical current and voltage were developed for application in electric power systems. The current sensor, based on the Faraday effect in a monomode glass fiber, and the voltage sensor, based on the transverse Pockels effect in a crystal, are demonstrated in wide-band (10 MHz) interference-free measurements of pulsed currents and impulse voltages. GRA

N89-10234# Los Alamos National Lab., N. Mex.
EFFECTS OF MODULATED ELECTRON BEAMS AND CAVITIES ON REDITRONS
T. J. T. Kwan, H. A. Davis, R. D. Fulton, and E. G. Sherwood 1988 8 p Presented at the 7th International Conference on High-Power Particle Beams, Karlsruhe, Fed. Republic of Germany, 4 Jul. 1988
(Contract W-7405-eng-36)
(DE88-014317; LA-UR-88-2189; CONF-880713-10) Avail: NTIS HC A02/MF A01

The virtual cathode, when formed in a cavity, can generate microwaves at different cavity modes depending on the geometry of the cavity. We found that the formation and the oscillation frequency of the virtual cathode in a reditron can be significantly influenced by cavity designs. The length of a cavity can play a role in frequency and mode selection. Our simulations showed that TM sub 012 and TM sub 033 were excited for cavity lengths of 15.0 cm and 22.5 cm, respectively. In addition to the cavity effects on reditrons, we discovered that highly modulated electron beams can be produced in reditrons. Full modulation (100 percent) of the transmitted electron beam current has been confirmed in our simulations. We further showed that incorporation of an inverse diode configuration can achieve microwave production efficiency of 26 percent. DOE

N89-10235*# National Aeronautics and Space Administration. Lewis Research Center, Cleveland, Ohio.
SEQUENTIALLY EVAPORATED THIN Y-Ba-Cu-O SUPERCONDUCTOR FILMS: COMPOSITION AND PROCESSING EFFECTS
George J. Valco, Norman J. Rohrer (Ohio State Univ., Columbus.), Joseph D. Warner, and Kul B. Bhasin Oct. 1988 10 p Presented at the 35th National Vacuum Symposium, Atlanta, Ga., 3-7 Oct. 1988; sponsored by the American Vacuum Society
(NASA-TM-101388; E-4448; NAS 1.15:101388) Avail: NTIS HC A02/MF A01 CSCL 09A

Thin films of YBa2Cu3O(7-beta) have been grown by sequential evaporation of Cu, Y, and BaF2 on SrTiO3 and MgO substrates. The onset temperatures were as high as 93 K while T sub c was 85 K. The Ba/Y ratio was varied from 1.9 to 4.0. The Cu/Y ratio was varied from 2.8 to 3.4. The films were then annealed at various times and temperatures. The times ranged from 15 min to 3 hr, while the annealing temperatures used ranged from 850 C to 900 C. A good correlation was found between transition temperature (T sub c) and the annealing conditions; the films annealed at 900 C on SrTiO3 had the best T sub c's. There was a weaker correlation between composition and T sub c. Barium poor films exhibitied semiconducting normal state resistance behavior while barium rich films were metallic. The films were

analyzed by resistance versus temperature measurements and scanning electron microscopy. The analysis of the films and the correlations are reported. Author

N89-10236# Centre National de la Recherche Scientifique, Toulouse (France). Lab. d'Automatique et d'Analyse des Systemes.
DYNAMIC PROPERTIES OF POWER MOS TRANSISTORS
Ph.D. Thesis - Toulouse Univ.
Mohammed Belabadia 1988 224 p In FRENCH; ENGLISH summary
(LAAS-88-162; ETN-88-92959) Avail: NTIS HC A10/MF A01

Power MOSFET's were modeled in dynamic high frequency and switching regimes, based on a theoretical analysis of the active region, taking into account the short channel effects and those related to structural configuration elements. The theoretical synthesis of intrinsic and parasitic elements leads to a complete nonlinear physical model compatible with electric simulators. The model is used for simulation and computer aided design of electric circuits which use power MOSFET's such as RF amplifiers, and frequency doublers. For the switching regime, a hierarchy of models for power V.DMOS transistors is developed. Two compact models consistent with SPICE-2 program and well suited for study and characterization of power V.DMOSFET, in switching condition under resistive and inductive loads, are proposed. They can describe low, medium, and high voltage structures. ESA

N89-10237# Centre National d'Etudes Spatiales, Toulouse (France).
COMMUNICATIONS TO NATIONAL MICROWAVE DAYS
J. Sombrin, J. Larroque, L. Lapierre, J. F. Sautereau, H. D. Park, M. Pyee, P. Jarry, C. Boschet, and C. Guichaoua 25 May 1987 11 p In FRENCH; ENGLISH summary
(CNES-CT/DRT/TIT/HY/87/130; ETN-88-93090) Avail: NTIS HC A03/MF A01

A microwave QPSK remodulating demodulator was designed and realized for the regeneration of telecommunication signals in a satellite. A wideband distributed amplifier was designed to add the power of microwave FET transistors. A hybrid ceramic quartz technology was used. A computer aided design program to compute the coupling coefficients necessary for a cavity filter with an assymetric amplitude response was produced. ESA

N89-10193*# Jet Propulsion Lab., California Inst. of Tech., Pasadena.
EVALUATION OF THE CHARACTERISTICS OF A FIELD EMISSION CATHODE FOR USE IN A MERCURY ION TRAP FREQUENCY STANDARD
J. M. Christman *In its* The Telecommunications and Data Acquisition Report 15 Aug. 1988 p 86-92 (For primary document see N89-10186 01-32)
Avail: NTIS HC A14/MF A01 CSCL 09A

N89-10199*# Jet Propulsion Lab., California Inst. of Tech., Pasadena.
AN 8.4-GHz CRYOGENICALLY COOLED HEMT AMPLIFIER FOR DSS 13
L. Tanida *In its* The Telecommunications and Data Acquisition Report 15 Aug. 1988 p 163-169 (For primary document see N89-10186 01-32)
Avail: NTIS HC A14/MF A01 CSCL 09A

N89-10473# National Research Council of Canada, Ottawa (Ontario). Div. of Electrical Engineering.
LIGHTNING STANDARDS FOR PROTECTION OF GROUND ELECTRONIC SYSTEMS
Andrew S. Podgorski and Elizabeth M. Podgorski (Radio Systems Engineering, Ottawa, Ontario) *In* NOAA, International Aerospace and Ground Conference on Lightning and Static Electricity Apr. 1988 p 324-32 (For primary document see N89-10429 01-47)
Avail: NTIS HC A23/MF A01 CSCL 04B

N89-10475# BDM Corp., Albuquerque, N. Mex.
COMPUTER SIMULATION OF THE EFFECTS OF LIGHTNING STROKE ATTACHMENT TO AN ELECTRIC POWER SUBSTATION
D. E. Thomas, C. M. Wiggins, and F. S. Nickel *In* NOAA, International Aerospace and Ground Conference on Lightning and Static Electricity Apr. 1988 p 338-34 (For primary document see N89-10429 01-47)
Avail: NTIS HC A23/MF A01 CSCL 09C

N89-10484# United Kingdom Atomic Energy Authority, Culham (England). Lightning Studies Unit.
A FILAMENTARY METHOD FOR CALCULATING INDUCED VOLTAGES WITHIN RESISTIVE STRUCTURES IN EITHER THE FREQUENCY OR TIME DOMAIN
C. J. Hardwick, S. J. Haigh, and B. J. C. Burrows *In* NOAA, International Aerospace and Ground Conference on Lightning and Static Electricity Apr. 1988 p 401-40 (For primary document see N89-10429 01-47)
Avail: NTIS HC A23/MF A01 CSCL 09C

N89-10493# Department of National Defence, Ottawa (Ontario). Quality Engineering Test Establishment.
ELECTROSTATIC DISCHARGE AND FIELD EFFECTS OF ELECTRONICS SYSTEMS
L. R. Dicks and G. Morin *In* NOAA, International Aerospace and Ground Conference on Lightning and Static Electricity Apr. 1988 p 481-48 (For primary document see N89-10429 01-47)
Avail: NTIS HC A23/MF A01 CSCL 09C

N89-10496# Electro Magnetic Applications, Inc., Lakewood, Colo.
THE INTERACTION BETWEEN LIGHTNING GROUNDING SYSTEMS AND BURIED CABLES
Richard S. Collier *In* NOAA, International Aerospace and Ground Conference on Lightning and Static Electricity Apr. 1988 p 499-50 (For primary document see N89-10429 01-47)
(Contract DAAH01-85-D-A015)
Avail: NTIS HC A23/MF A01 CSCL 09C

N89-10497# Westinghouse Electric Corp., Baltimore, Md.
SYSTEM PROTECTION FROM ATMOSPHERIC ELECTRICITY FOR AEROSTATS WITH CONDUCTING TETHERS
M. S. Wheeler, G. R. Beach, P. R. Jakubowski, and F. A. Fisher (Lightning Technologies, Inc., Pittsfield, Mass.) *In* NOAA, International Aerospace and Ground Conference on Lightning and Static Electricity Apr. 1988 p 505-51 (For primary document see N89-10429 01-47)
Avail: NTIS HC A23/MF A01 CSCL 09C

34 FLUID MECHANICS AND HEAT TRANSFER

Includes boundary layers; hydrodynamics; fluidics; mass transfer; and ablation cooling.

For related information see also *02 Aerodynamics* and *77 Thermodynamics and Statistical Physics.*

N89-10238# Oak Ridge National Lab., Tenn.
SOLUTION OF ILL-POSED PROBLEMS BY MEANS OF TRUNCATED SVD (SINGULAR VALUE DECOMPOSITION)
Per Christian Hansen Jun. 1988 18 p Prepared in cooperation with Copenhagen Observatory, Denmark
(Contract DE-AC05-84OR-21400)
(DE88-013510; ORNL/TM-10772) Avail: NTIS HC A03/MF A01

We investigate Truncated Singular Value Decomposition (TSVD) solutions to ill-posed least squares problems involving matrices with ill-determined as well as well-determined numerical rank. If a discrete Picard condition is satisfied, then in both cases the truncation parameter can be chosen such that the TSVD solution

is satisfactory. The appropriate truncation parameter, giving the optimal signal-to-noise ratio in the solution, is the minimizer of the generalized cross-validation. DOE

N89-10239# Ballistic Research Labs., Aberdeen Proving Ground, Md.
MOMENT EXERTED ON A CONING PROJECTILE BY A SPINNING LIQUID IN A CYLINDRICAL CAVITY CONTAINING A POROUS MEDIUM
Gene R. Cooper Jun. 1988 35 p
(AD-A195291; BRL-MR-3677) Avail: NTIS HC A03/MF A01 CSCL 19J

White Phosphorous (WP) impregnated felt wedges are used as a payload in the M825 improved smoke projectile. An assumption made in this work in that the WP is in a liquid state (i.e., temperature greater than 44 degrees C) where such payloads have been seen to cause flight instabilities. The analytical results given here formulate an initial effort to gain an understanding of the dynamics of a projectile interacting with a WP/felt payload. The analytical methods used here are a simple extension of previous methods used to describe bulk-filled liquid payloads. Moments are predicted due to an inviscid liquid moving through a ridged porous medium which is confined to a spinning cylindrical cavity undergoing coning motion. A drag term is added to the classical Stewartson theory which is used to describe the flow in the porous media. The cylindrical cavity is assumed to consist of several chambers of circular cross section and uniform height, each separated by solid endcaps. This porous media theory is used to calculate the total liquid side moments exerted by all the chambers in the cylinder. Results are presented for a range of coning frequencies, fineness ratios, and porous drag coefficients. GRA

N89-10240# Oak Ridge National Lab., Tenn.
AN ANALYTICAL STUDY OF HYBRID EJECTOR/INTERNAL COMBUSTION ENGINE-DRIVEN HEAT PUMPS
R. W. Murphy 1988 8 p Presented at the 2nd DOE/ORNL Heat Pump Conference: Research and Development on the Heat Pump for Space Conditioning Applications, Washington, D.C., 17 Apr. 1988
(Contract DE-AC05-84OR-21400)
(DE88-013242; CONF-8804100-4) Avail: NTIS HC A02/MF A01

Because ejectors can combine high reliability with low maintenance cost in a package requiring little capital investment, they may provide attractive heat pumping capability in situations where the importance of their inefficiencies is minimized. One such concept, a hybrid system in which an ejector driven by engine reject heat is used to increase the performance of an internal combustion engine-driven heat pump, was analyzed by modifying an existing ejector heat pump model and combining it with generic compressor and internal combustion engine models. Under the model assumptions for nominal cooling mode conditions, the results showed that hybrid systems could provide substantial performance augmentation, i.e., up to 17 pct increase in system coefficient of performance for a parallel arrangement of an enhanced ejector with the engine-driven compressor. DOE

N89-10241 Dayton Univ., Ohio.
MODIFICATION OF THE UNSTEADY FLOW FIELD PREDICTED BY TRANSONIC SMALL DISTRUBANCE EQUATIONS USING A NAVIER-STOKES SOLUTION OF THE STEADY FLOW FIELD Ph.D. Thesis
Don Winston Kinsey 1987 169 p
Avail: Univ. Microfilms Order No. DA8805029

The first part of this report describes a numerical solution of the Navier-Stokes equations for flow over a thick supercritical airfoil with strong shock-induced separation on upper and lower surfaces. The separated flow region extends from the shock (approx 50 pct chord) to the trailing edge on both surfaces. The solution algorithm employed was an explicit predictor-corrector method. An algebraic turbulence model was used to describe the turbulent Reynolds stresses. The treatment of the eddy-viscosity behavior through the shock, in the separated regions over the airfoil and in the near wake was the critical step for a successful solution. Many approaches have been used to extend the useful range of 2-D, unsteady transonic small disturbances (TSD) procedures. The second part of the report describes another such procedure. Modifications to the TSD procedure, LTRAN2, that allow the procedure to determine the geometry corresponding to the prescibed pressure distribution from experimental data or as predicted by a Navier-Stokes solver are described. The new geometry accounts for compressible and viscous effects and is a much improved starting point for unsteady calculations. The TSD governing equations and boundary equations are reviewed, and then the modifications required for the inverse geometry definition are described. Results for three different airfoils (NACA 0012, NACA 64A010 and NLR 7301) are presented and discussed. A summary of the results, and recommendations for additional work are provided. Dissert. Abstr.

N89-10242*# National Aeronautics and Space Administration. Lewis Research Center, Cleveland, Ohio.
DISCRETIZATION FORMULAS FOR UNSTRUCTURED GRIDS
Kenneth J. Baumeister 1988 12 p Proposed for presentation at the 2nd International Conference on Numerical Grid Generation in Computational Fluid Dynamics, Miami Beach, Fla., 5-8 Dec. 1988; sponsored by NASA, AFOSR and Miami Univ.
(NASA-TM-101298; E-4094; NAS 1.15:101298) Avail: NTIS HC A03/MF A01 CSCL 20D

The Galerkin weighted residual technique using linear triangular weight functions is employed to develop finite difference formula in cartesian coordinates for the Laplacian operator, first derivative operators and the function for unstructured triangular grids. The weighted residual coefficients associated with the weak formulation of the Laplacian operator are shown to agree with the Taylor series approach on a global average. In addition, a simple algorithm is presented to determine the Voronoi (finite difference) area of an unstructured grid. Author

N89-10243*# Lockheed Missiles and Space Co., Huntsville, Ala. Engineering Center.
FLOWFIELD VISUALIZATION FOR SSME HOT GAS MANIFOLD Final Report
Robert P. Roger 15 Jul. 1988 72 p
(Contract NAS8-36090)
(NASA-CR-179403; NAS 1.26:179403; LMSC-HEC-TR-F225988)
Avail: NTIS HC A04/MF A01 CSCL 20D

The objective of this research, as defined by NASA-Marshall Space Flight Center, was two-fold: (1) to numerically simulate viscous subsonic flow in a proposed elliptical two-duct version of the fuel side Hot Gas Manifold (HGM) for the Space Shuttle Main Engine (SSME), and (2) to provide analytical support for SSME related numerical computational experiments, being performed by the Computational Fluid Dynamics staff in the Aerophysics Division of the Structures and Dynamics Laboratory at NASA-MSFC. Numerical results of HGM were calculations to complement both water flow visualization experiments and air flow visualization experiments and air experiments in two-duct geometries performed at NASA-MSFC and Rocketdyne. In addition, code modification and improvement efforts were to strengthen the CFD capabilities of NASA-MSFC for producing reliable predictions of flow environments within the SSME. Author

N89-10244 Michigan State Univ., East Lansing.
SYSTEMS ANALYSIS OF THE INVERSE HEAT CONDUCTION PROBLEM Ph.D. Thesis
David Bruce Manner 1987 193 p
Avail: Univ. Microfilms Order No. DA8801840

The groundwork necessary for frequency domain analysis of solutions to the inverse heat conduction problem, using Laplace and z-transform techniques is presented. The solution is traced back through the direct solution methods used to generate the inverse solution, and draws heavily upon tranfer function concepts. Transformation methods from continuous time ladder network models to discrete time models are developed. The mathematical relationship between ladder network models and finite difference

models is derived. In addition, a new procedure for generating errorless discrete time models from Fourier series solutions is presented. The frequency response of direct discrete time solutions and the impact on the stability and noise performance of inverse algorithms arising from these direct solutions is presented. Inverse algorithm methods are generalized according to their frequency domain structure, rather than time domain, which effectively decouples the algorithm classification from a direct solution. Precompensation filter concepts are introduced, and a frequency domain test for inverse algorithm stability is developed. Examples of Stolz's method and Beck's method are included. Results are discussed. Dissert. Abstr.

N89-10245# Naval Postgraduate School, Monterey, Calif.
STEADY FLOW FIELD MEASUREMENTS USING LASER DOPPLER VELOCIMETRY M.S. Thesis
Ricky E. Wilson Dec. 1987 52 p
(AD-A195228) Avail: NTIS HC A04/MF A01 CSCL 20D

A computer-integrated LDV system utilizing a Helium-Neon laser was designed, assembled and tested for use in the study of steady flow field quantities. All system elements were integrated to include a traverse mechanism, signal processing and conditioning, computer interface and display. The system was initially calibrated utilizing a rotating wheel of known velocity. Experimental flow measurement tests of the system were conducted across a conventional free jet flow and in the Naval Postgraduate School low speed wind tunnel. The flow field velocity measurements made in the wind tunnel were verified usin an existing pressure data acquisition station and a standard pitot static probe. GRA

N89-10246*# National Aeronautics and Space Administration. Lewis Research Center, Cleveland, Ohio.
HIGH-RESOLUTION HEAT-TRANSFER-COEFFICIENT MAPS APPLICABLE TO COMPOUND-CURVE SURFACES USING LIQUID CRYSTALS IN A TRANSIENT WIND TUNNEL
Terry V. Jones (Oxford Univ., England) and Steven A. Hippensteele Aug. 1988 12 p Presented at the ASME National Heat Transfer Conference, Pittsburgh, Pa., 9-12 Aug. 1987
(NASA-TM-89855; E-3269; NAS 1.15:89855) Avail: NTIS HC A03/MF A01 CSCL 20D

Tests were performed in a transient heat transfer tunnel in which the model under test was preheated prior to allowing room temperature air to be suddenly drawn over the model. The resulting movement of isothermal contours on the model is revealed using a surface coating of thermochromic liquid crystals that display distinctive colors at particular temperatures. A video record is obtained of a temperature and time data pair for all points on the model during a single test. Experiments on a duct model are reported in which the model was preheated using a hot air stream. A manner in which initial model temperature nonuniformities could be taken into account was investigated. The duct model was also tested with a steady-state measurement technique and results were compared with the transient measurements, but recognizing that differences existed between the upstream thermal boundary conditions. The steady-state and transient measurements were shown to be consistent with predicted values. The main advantage of this transient heat transfer technique using liquid crystals is that since the test model need not be actively heated, high-resolution measurements on surfaces with complex shapes may be obtained. Author

N89-10247# Carrier Corp., Syracuse, N.Y.
DEVELOPMENT AND PROOF-TESTING OF ADVANCED ABSORPTION REFRIGERATION CYCLE CONCEPTS, PHASE 2
Robert C. Reimann and Gorken Melikian (United Technologies Research Center, East Hartford, Conn.) 1988 7 p Presented at the 2nd DOE/ORNL Heat Pump Conference: Research and Development on the Heat Pump for Space Conditioning Applications, Washington, D.C., 17 Apr. 1988 Prepared for ORNL, Tenn.
(Contract DE-AC05-84OR-21400)
(DE88-013239; CONF-8804100-7) Avail: NTIS HC A02

This paper summarizes the results of the work performed to date under Phase II of the DOE program. The Phase II objective is to design, fabricate, and proof-test a natural gas-fired absorption heat pump (AHP) with an efficiency level substantially higher than present day state-of-the-art equipment. To achieve these objectives, Carrier investigated the performance of the candidate Phase I fluids (lithium bromide:zinc bromide/methyl alcohol-MEOH or lithium bromide:water methylmine-MMA) as well as high concentration formulations of the conventional LiBr/H2O mixture for high temperature, upper loop use. These results were compared with several existing fluid candidates including ammonia/water. DOE

N89-10248*# National Aeronautics and Space Administration, Washington, D.C.
RESONANT EXCITATION OF SPATIAL PERTURBATIONS IN A BOUNDARY LAYER IN THE PRESENCE OF A PRESSURE GRADIENT
I. Maslennikova Aug. 1988 13 p Transl. into ENGLISH of Russian report (Novosibirsk, USSR, Academy of Sciences), 1987 p 46-52 Transl. by Scientific Translation Service, Santa Barbara, Calif.
(Contract NASw-4307)
(NASA-TT-20305; NAS 1.77:20305) Avail: NTIS HC A03/MF A01 CSCL 20D

The calculation results presented indicate that resonant interaction in triads in the presence of a pressure gradient is qualitatively similar to the case of nongradient flow. The amplitude of the plane wave is the primary factor determining mode discrimination and the evolution of the triplet. If the amplitude of the plane wave is greater than some sufficiently low threshold level, a broad spectrum of three-dimensional subharmonic perturbations will be excited in all the flows considered. In slower flows the amplitudes of the primary wave and subharmonic are equalized in a narrower range of Reynolds numbers and the rates of increase of both components are much higher. The above makes it possible to infer that a positive pressure gradient has a destabilizing effect on resonant interaction in triads, which makes the role of gradients decisive in subharmonic transitions on actual streamline bodies. Author

N89-10249# Oak Ridge National Lab., Tenn. Energy Div.
COMPUTER SIMULATION OF ABSORPTION HEAT PUMP USING AQUEOUS LITHIUM BROMIDE AND TERNARY NITRATE MIXTURES
Moonis R. Ally Jun. 1988 35 p
(Contract DE-AC05-84OR-21400)
(DE88-013353; ORNL/TM-10392) Avail: NTIS HC A03/MF A01

A new aqueous ternary mixture consisting of 53 wt percent LiNO3, 28 wt percent KNO3, and 19 wt percent NaNO3 is available for high-temperature heat pump applications. The pressure-composition-temperature and the specific enthalpy-concentration-temperature data in the form of correlated polynomial expressions are used in a computer program to simulate results of a temperature amplifier heat pump with LiBr/H2O and ternary nitrate/H2O mixtures as working fluids. In the absence of adequate thermophysical data for the fluids, the study serves as a best guess first approximation. The results show that the ternary nitrate mixture potentially has approximately a 10 percent advantage in COP and a 15 percent advantage in temperature lifts over aqueous LiBr at high temperatures. Ternary nitrates are hampered by crystallization at low waste heat temperatures and cannot operate competitively in the low lift and waste heat temperature regions. The potential performance advantage at high temperatures for the ternary nitrate mixture is sufficiently attractive to justify additional work to obtain adequate thermodynamic transport and corrosion data. DOE

N89-10250# Tokyo Univ. (Japan). Inst. of Space and Astronautical Science.
NUMERICAL STUDY OF THE ENTRANCE FLOW AND ITS TRANSITION IN A CURCULAR PIPE

Hidesada Kanda Mar. 1988 63 p
(ISAS-RN-626; ISSN-0285-6808) Avail: NTIS HC A04/MF A01

Experimental data and results of prior investigations led to defining the problem of the transition from laminar to turbulent flow in a circular pipe. The flow field of the circular pipe is examined with particular emphasis on the entrance and transition length. The transition lengths were experimentally determined for two inlet shapes without and with bellmouth. The transition point is the starting point of oscillation of color dye filament in the pipe. Two-dimensional, time dependent computational scheme was devised for determining the flow development and the corresponding pressure drop in the entrance region at Reynolds number based on the pipe diameter of 10, 100, 2000 and 10000. The stream function vorticity formulation and the Poisson equation were applied, using the Gauss Seidel iteration method. The velocity field, pressure drop, and the convective and viscous terms are compared with the experimental results and also with the previous analysis. Thus, it is numerically verified that the laminar solution for Hagen Poiseuille flow exists regardless of the Reynold number and it was experimentally observed that the real transition length is much shorter than the entrance length. Author

N89-10251# Case Western Reserve Univ., Cleveland, Ohio. Dept. of Mechanical and Aerospace Engineering.
LASER VELOCIMETER MEASUREMENTS OF SOLIDS IN MULTIPHASE FLOW Technical Progress Report, 1 Mar. - 31 May 1988
J. R. Kadambi 1988 8 p
(Contract DE-FG22-86PC-90961)
(DE88-011611; DOE/PC-90961/T7) Avail: NTIS HC A02/MF A01

Preliminary tests were conducted using water as the fluid in the refractive index matched multiphase flow loop. A Laser Doppler Velocimeter was used for measuring the fluid velocity along a horizontal diameter located 17 feet downstream of the pump. The tests were conducted in the Reynolds number range of 1000 to 3000. In addition to LDV velocity measurements, pressure drops as well as flow rates were also measured. Representative velocity profiles and pressure drop data are presented. The test loop was then filled with the refractive index matched fluid, 55 percent (by weight) sodium iodide solution in water. The velocity profile for a representative data point and pressure drop data is shown. DOE

N89-10252# Materials Research Labs., Melbourne (Australia).
AN ANALYSIS OF AN IMPLICIT FACTORED SCHEME FOR SIMULATING SHOCK WAVES
M. B. Tyndall May 1988 34 p
(AR-005-231; MRL-R-1117) Copyright Avail: NTIS HC A03/MF A01

A detailed derivation and analysis of an implicit factored scheme (Beam and Warming 1976) is given. A one-dimensional shock tube problem is solved numerically using the factored scheme. The results and exact solution are presented for this problem. An analysis of the features of the method is made and the limitations of this implict factored scheme for more general applications to shock waves in solids are discussed. An alternative approach which has been developed by Boris and Book (1976) appears to have wider applicability than the method studied here. Author

N89-10253*# Universities Space Research Association, Huntsville, Ala.
NUMERICAL ANALYSIS OF LAMINAR AND TURBULENT INCOMPRESSIBLE FLOWS USING THE FINITE ELEMENT FLUID DYNAMICS ANALYSIS PACKAGE (FIDAP) Final Report
Jeong L. Sohn Aug. 1988 60 p
(Contract NAS8-35918)
(NASA-CR-179390; NAS 1.26:179390) Avail: NTIS HC A04/MF A01 CSCL 20D

The purpose of the study is the evaluation of the numerical accuracy of FIDAP (Fluid Dynamics Analysis Package). Accordingly, four test problems in laminar and turbulent incompressible flows are selected and the computational results of these problems compared with other numerical solutions and/or experimental data. These problems include: (1) 2-D laminar flow inside a wall-driven cavity; (2) 2-D laminar flow over a backward-facing step; (3) 2-D turbulent flow over a backward-facing step; and (4) 2-D turbulent flow through a turn-around duct. Author

N89-10254# Sandia National Labs., Albuquerque, N. Mex.
A FINITE ELEMENT FORMULATION FOR INCOMPRESSIBLE, CONJUGATE, VISCOUS/POROUS FLOW PROBLEMS
D. K. Gartling 1988 8 p Presented at the 1st International Conference on Computational Methods in Flow Analysis, Okayama, Japan, 5 Sep. 1988
(Contract DE-AC04-76DP-00789)
(DE88-007113; SAND-87-2496C; CONF-880936-1) Avail: NTIS HC A02/MF A01

In previous work, the Brinkman equation was used to describe the flow in a porous region. The objective of the present study was to develop a general method for solving conjugate fluid and porous flow problems using a finite element method. In pursuing this goal several combinations of porous flow equations and interface conditions were examined and compared. DOE

N89-10255# Oak Ridge National Lab., Tenn.
OVERVIEW OF GROUND COUPLED HEAT PUMP RESEARCH AND TECHNOLOGY TRANSFER ACTIVITIES
V. D. Baxter and V. C. Mei 1988 9 p Presented at the 2nd DOE/ORNL Heat Pump Conference: Research and Development on the Heat Pump for Space Conditioning Applications, Washington, D.C., 17 Apr. 1988
(Contract DE-AC05-84OR-21400)
(DE88-012938; CONF-8804100-18) Avail: NTIS HC A02/MF A01

Highlights of DOE-sponsored ground coupled heat pump (GCHP) research at Oak Ridge National Laboratory (ORNL) are presented. ORNL, in cooperation with Niagara Mohawk Power Company, Climate Master, Inc., and Brookhaven National Laboratory developed and demonstrated an advanced GCHP design concept with shorter ground coils that can reduce installed costs for northern climates. In these areas it can also enhance the competitiveness of GCHP systems versus air-source heat pumps by lowering their payback from 6 to 7 years to 3 to 5 years. Ground coil heat exchanger models (based primarily on first principles) have been developed and used by others to generate less conservative ground coil sizing methods. An aggressive technology transfer initiative was undertaken to publicize results of this research and make it available to the industry. Included in this effort were an international workshop, trade press releases and articles, and participation in a live teleconference on GCHP technology. DOE

N89-10256# Edgerton, Germeshausen and Grier, Inc., Idaho Falls, Idaho.
DISCRETE MODELING CONSIDERATIONS IN MULTIPHASE FLUID DYNAMICS
V. H. Ransom and J. D. Ramshaw 1988 11 p Presented at the Japan-US Seminar on Two-phase Flow Dynamics, Kyoto, Japan, 15 Jul. 1988
(Contract DE-AC07-76ID-01570)
(DE88-015188; EGG-M-88219; CONF-880792-1) Avail: NTIS HC A03/MF A01

The modeling of multiphase flows play a fundamental role in light water reactor safety. The main ingredients in our discrete modeling Weltanschauung are the following considerations: (1) any physical model must be cast into discrete form for a digital computer; (2) the usual approach of formulating models in differential form and then discretizing them is potentially hazardous (it may be preferable to formulate the model in discrete terms from the outset); (3) computer time and storage constraints limit the resolution that can be employed in practical calculations; (4) practical resolution limits are generally so coarse that traditional convergence and truncation-error analyses become irrelevant; (5) a discrete model constitutes a reduced description of a physical system, from which fine-scale details are eliminated. This elimination creates a statistical closure problem. Methods from

statistical physics may therefore be useful in the formulation of discrete models. In Researchers elaborate on these themes and illustrate them with simple examples. DOE

N89-10257# Max-Planck-Institut fuer Stroemungsforschung, Goettingen (West Germany).
NUMERICAL INVESTIGATION OF THE DYNAMICS OF HETEROGENEOUS SHOCK-CAVITATION
Martin Rein and E.-A. Mueller, ed. 1987 101 p In GERMAN; ENGLISH summary
(MPIS-Mitt-86-1987; ISSN-0374-1257; ETN-88-93204) Avail: NTIS HC A06/MF A01

The variety of nuclei types in a liquid is described by a discrete spectrum of a finite number of gas bubble classes, having different equilibrium radii. The mixture of these bubbles and the liquid is modeled as a homogeneous fluid, having effective variables of state. The dynamics of the bubbles of the individual bubble classes are taken into account by a relation between the radius of a bubble and the pressure far away from this bubble. Using this model the dynamics of heterogeneous shock-cavitation is investigated by the method of characteristics. The dynamics of the individual gas bubbles plays an important role for heterogeneous shock-cavitation. The large tensions due to the expansion waves decrease quickly, and the gas bubbles grow violently. Relaxation effects produce pressure oscillation behind the expansion waves. The oscillations may result in the formation of several distinct regions with large bubbles and a void fraction. The influence of parameters such as expansion wave amplitude and the liquid's nuclei content on these events is discussed. The number density of the bubbles only and not their size, determines heterogeneous shock-cavitation within wide bounds. ESA

N89-10258# Max-Planck-Institut fuer Stroemungsforschung, Goettingen (West Germany).
EXPERIMENTS ON THE INFLUENCE OF THE GEOMETRY ON THE STABILITY OF TAYLOR-COUETTE FLOW
Arne Lorenzen and E.-A. Mueller, ed. 1987 87 p In GERMAN; ENGLISH summary
(MPIS-Mitt-87-1987; ISSN-0374-1257; ETN-88-93205) Avail: NTIS HC A05/MF A01

The influence of the container geometry on the stability of the Taylor-Couette flow was investigated. The length of the annular regime was varied and thus a variable vortex size produced. For long concentric cylinders, the occurrence of traveling waves on increasing Re is dependent on the vortex size, and different wave types are observed. Short cylinders have a stabilizing effect in that higher critical Re are found. Other wave types are also produced. For a system with a square outer cylinder stable stationary vortex flows are found as well. These tend to become asymmetric, but still stationary. On further increase in Re these flows become time dependent, at first almost periodic but soon and at comparatively low Re turbulent. The velocity spectra are similar to those for other flows, however none of the popular chaos models is sufficient to describe this way to turbulence. Anomalous vortex flows are found for both geometries and their stability limits were investigated. The measurements are in qualitative agreement with the theoretical predictions of Benjamin. ESA

N89-10259# Max-Planck-Institut fuer Stroemungsforschung, Goettingen (West Germany).
EXPERIMENTAL DETECTION OF HIGH SPEED FRONTS AND CLARIFICATION OF THEIR COHERENCE WITH LOW SPEED STREAKS AND STREAMWISE VORTICES IN A FULLY DEVELOPED TURBULENT CHANNEL
Michael Randolph and E.-A. Mueller, ed. 1987 99 p In GERMAN; ENGLISH summary
(MPIS-Mitt-88-1987; ISSN-0374-1257; ETN-88-93206) Avail: NTIS HC A05/MF A01

In a fully developed turbulent channel flow hot-film measurements of the streamwise spatial velocity gradient and the temporal velocity gradient were carried out. Large positive spatial and temporal gradients are strongly correlated. These events are found to be identical with the sweep events observed by Corino and Brodkey (1969) in visual studies. Through conditioned correlation, a detection criterion with which sweeps can be found in a turbulent flow by means of hot-film anemometry is stated. A mechanical probe is used to qualitatively determine the streamwise vorticity component. The coherence between streamwise vortices and sweeps was studied by measuring with the mechanical probe and the hot-films simultaneously. This was based on a vortex model which enables a uniform description of sweeps, streamwise vortices, and low and high speed streaks. ESA

N89-10205*# Jet Propulsion Lab., California Inst. of Tech., Pasadena.
HEAT EXCHANGER EXPERT SYSTEM LOGIC
R. Cormier *In its* The Telecommunications and Data Acquisition Report 15 Aug. 1988 p 232-244 (For primary document see N89-10186 01-32)
Avail: NTIS HC A14/MF A01 CSCL 20D

35 INSTRUMENTATION AND PHOTOGRAPHY

Includes remote sensors; measuring instruments and gages; detectors; cameras and photographic supplies; and holography.

For aerial photography see *43 Earth Resources and Remote Sensing.* For related information see also *06 Aircraft Instrumentation,* and *19 Spacecraft Instrumentation.*

N89-10260# Rome Univ. (Italy). Dipt. di Fisica.
AN ELECTROMAGNETIC CALORIMETER FOR A BEAUTY FACTORY
B. Borgia, F. Ferroni, and E. Longo 29 Jan. 1988 31 p Presented at the Workshop on Heavy Quarks Factory and Nuclear Physics Facility with Superconducting Linacs, Courmayeur, Italy, 14-18 Dec. 1987
(Nota-Interna-905; ETN-88-92625) Avail: NTIS HC A03/MF A01

The requirements of an electromagnetic calorimeter (EMC) for B physics were established. It is argued that BGO is the best candidate for an ultrafine EMC as its only disadvantage, the price, is compensated by the reduced volume required to obtain the best performances, even if the minimal r (50 cm) is incompatible with the volume of the inner detectors. A large size BGO calorimeter was designed for L3 collaboration at LEP. The first half barrel, consisting of 3840 crystals is already operating, and its performances were extensively tested on electron beams. Energy resolution and spatial resolution, particle, overlap, and pi(0) and heavy meson reconstruction considerations support this choice. An EMC design is presented. ESA

N89-10261# Sandia National Labs., Albuquerque, N. Mex.
SELECTION AND EVALUATION OF VIDEO TAPE RECORDERS FOR SURVEILLANCE APPLICATIONS
Robert L. Martinez 1988 5 p Presented at the 29th Annual Meeting of the Institute of Nuclear Materials Management, Las Vegas, Nev., 26 Jun. 1988
(Contract DE-AC04-76DP-00789)
(DE88-014240; SAND-88-1715C; CONF-880631-34) Avail: NTIS HC A02

Unattended surveillance places unique requirements on video recorders. One such requirement, extended operational reliability, often cannot be determined from the manufacturers' data. Subsequent to market surveys and preliminary testing, the Sony 8mm EVO-210 recorder was selected for use in the Modular Integrated Video System (MIVS), while concurrently undergoing extensive reliability testing. A microprocessor based controller was developed to life test and evaluate the performance of the video cassette recorders. The controller has the capability to insert a unique binary count in the vertical interval of the recorded video signal for each scene. This feature allows for automatic verification of the recorded data using a MIVS Review Station. Initially, twenty

recorders were subjected to the accelerated life test, which involves recording one scene (eight video frames) every 15 seconds. The recorders were operated in the exact manner in which they are utilized in the MIVS. This paper describes the results of the preliminary testing, accelerated life test and the extensive testing on 130 Sony EVO-210 recorders. DOE

N89-10262*# National Aeronautics and Space Administration, Washington, D.C.
THERMAL TRANSFER RECORDING MEDIA
T. Takei, M. Taniguchi, H. Fukushima, Y. Yamaguchi, M. Shinozuka, and K. K. Suwa Seikohsha Aug. 1988 11 p Transl. into ENGLISH of Japanese Patent no. SHO-62-87074 (7 Oct. 1985) p 437-440 Transl. by Scientific Translation Service, Santa Barbara, Calif.
(Contract NASw-4307)
(NASA-TT-20322; NAS 1.77:20322) Avail: NTIS HC A03/MF A01 CSCL 14B

The recording media consist of more than or one coloring layer and a layer containing a flame retardant to ensure noncombustibility and good thermal transfer. Thus, a PET film was coated on a side with a compound containing Vylon 290 (polyester resin), AFR-1021 (decabromodiphenyl oxide) 8 and Polysafe 60 (Sb oxide), and coated on the other side with a compound containing carnauba wax, HNP-9 (paraffin wax), EV-410 (ethylene-vinyl acetate copolymer), and Cu phthalocyanine to give a thermal transfer recording medium which showed good noncombustibility and antiblocking properties, and provided high quality images. Author

N89-10263 York Univ. (England).
AN OPTICAL SENSOR FOR THE NON-INTERACTIVE DETECTION OF WEAK ELECTRIC FIELDS Ph.D. Thesis
Colin R. Paton 1986 230 p
Avail: Univ. Microfilms Order No. BRDX80783

The linear electro-optic (Pockels) effect in certain piezo-electric crystals is used to detect and measure small electric fields, of the order of magnitude found in radio signals, while keeping the interaction of the detector with the field to a minimum. A study was made of two particular electro-optic materials, namely Lithium Niobate and Potassium di-Deuterium Phosphate (KD*D), and the relative merits of each are discussed. Various schemes for increasing the sensitivity of the device by having the light beam make multiple passes through the crystal were also investigated. Finally, a study was made of various methods for detecting the light modulated by the electro-optic effect, and these are discussed and compared. A sensor was constructed, using a crystal of KD*P, which has the capability to detect and measure, in unit bandwidth, fields of magnitude down to 5 m/Vm(-1). Dissert. Abstr.

N89-10264*# Alabama Univ., Huntsville. Dept. of Physics.
COMPACT IMAGING SPECTROMETER FOR INDUCED EMISSIONS Final Technical Report, 31 Mar. 1986 - 1 Feb. 1988
Douglas G. Torr Sep. 1988 20 p
(Grant NAG8-060)
(NASA-CR-183187; NAS 1.26:183187) Avail: NTIS HC A03/MF A01 CSCL 14B

On the basis of spectral measurements made from the Space Shuttle and on models of the possible Space Station external environment, it appears likely that, even at the planned altitudes of Space Station, photon emissions will be induced. These emissions will occur to some degree throughout the ultraviolet-visible-infrared spectrum. The emissions arise from a combination of processes including gas phase collisions between relatively energetic ambient and surface emitted or re-emitted atoms or molecules, where the surface raises some species to excited energy states. At the present time it is not possible to model these processes or the anticipated intensity levels with any accuracy, as a number of fundamental parameters needed for such calculations are still poorly known or unknown. However, it is possible that certain spectral line and band features will exceed the desired goal that concomitant emissions not exceed the natural zodiacal background. Also, in the near infrared and infrared, it appears that this level will be exceeded to a significant degree. Therefore it will be necessary to monitor emission levels in the vicinity of Space Station, both in order to establish the levels and to better model the environment. A small spectrometer is briefly described which is suitable for monitoring the spectrum from 1200 A to less than or equal to 12,000 A. The instrument uses focal plane array detectors to image this full spectral range simultaneously. The spectral resolution is 4 to 12 A, depending on the portion of the wavelength range. Author

N89-10265# Sandia National Labs., Albuquerque, N. Mex.
DESIGN STUDY FOR A REMOTE LASER WAVELENGTH SENSOR
Christopher Reiser Aug. 1988 51 p
(Contract DE-AC04-76DP-00789)
(DE88-015417; SAND-88-2077) Avail: NTIS HC A04

Design parameters and expected performance levels of a sensor that measures laser wavelength have been identified. The sensor may use either an Index Mismatched Interferometer (IMI) or a Girard Interferometer (GI). Suitable IMI materials for spanning the wavelength range of 0.3 to 10 microns are discussed, including KCl and KI:KCl. Many optical materials are suitable for GI construction. Quantitative results of modeling calculations relate wavelength reading accuracy to the direction and divergence of the incoming beam. Background blackbody light will not interfere with the wavelength determination unless it saturates the detector. It is found that the GI has wider performance and construction latitude than the IMI. DOE

N89-10266# Rome Univ. (Italy). Dipt. di Fisica.
VERTEX DETECTOR FOR A LINEAR BEAUTY FACTORY
G. Gratta and C. Zaccardelli 3 Feb. 1988 34 p Presented at the Workshop on Heavy Quarks Factory and Nuclear Physics Facility with Superconducting Linacs, Courmayeur, Italy, 14-18 Dec. 1987
(Nota-Interna-906; ETN-88-92626) Avail: NTIS HC A03/MF A01

A very high resolution vertex detector to help in B meson identification both tagging on the B decay length and antitagging on the D decay length; reduce the combinatorial problems for charged tracks; measure lifetimes study B(0) B bar (0) mixing as a function of time for both Bd and Bs systems; study time dependent asymmetries due to CP violation; look for DD bar mixing; and detect phenomena which could become reachable with the new regime of luminosity is proposed. The detector is based on 3 coaxial layers of silicon pixel devices, each made of 10 flat detectors arranged cylindrically. Mechanics and vacuum of the system are outlined, along with control electronics and alignment. ESA

N89-10267# Oak Ridge National Lab., Tenn.
SELECTION OF SENSORS FOR MEASUREMENT AND CONTROL
R. L. Anderson and G. N. Miller 1988 4 p Presented at the Sensors Expo, Chicago, Ill., 13 Sep. 1988
(Contract DE-AC05-84OR-21400)
(DE88-012936; CONF-8809106-1) Avail: NTIS HC A02

The factors that must be considered in selecting sensors for measurement and control are outlined and discussed: parameters to be measured, range, allowable uncertainty, the medium in contact with the sensor, environment outside the sensor, desired output, tried-and-true vs state-of-the-art, reliability and lifetime requirements, cost tradeoffs, application-specific considerations, failure modes, response time, and other considerations. DOE

N89-10268# Sandia National Labs., Albuquerque, N. Mex. Photometrics and Optical Development Div.
COMPARISON OF MECHANICAL AND ELECTRONIC HIGH-SPEED RECORDING SYSTEMS
W. C. Sweatt, G. S. Phipps, R. N. Shagam, and R. A. Hill 1988 26 p Presented at the 32d International Technical Symposium on Optical and Opto-electronic Applied Sciences and Engineering,

San Diego, Calif., 14 Aug. 1988
(Contract DE-AC04-76DP-00789)
(DE88-015264; SAND-88-1060C; CONF-880887-7) Avail: NTIS HC A03/MF A01

Commercially available mechanical, video, and electronic high-speed imaging systems are compared as part of an attempt to answer the question, will electronic cameras replace film cameras for high-speed recording. Of special interest is the relationship between spatial resolution and frame rate. Equally important is the compatability of the imaging systems for recording different types of experiments and tests. The resolution of a number of systems that represent various classes of framing cameras has been compared at their maximum framing rate. Included are several classes of mechanically advanced framing cameras, electronic streak cameras operated in a framing mode, and high-speed video systems. Likewise, the resolution of various classes of streak and image motion cameras has been compared at their maximum temporal resolution. The results: at frame rates up to 25 Mf/s, mechanical cameras can record from 10 to 100 times more data per frame and several times as many frames per run as existing electronic cameras, and from 100 to 1000 times more data per frame than existing video cameras. Video systems are limited in resolution and speed but provide instant access to data. Electronic cameras provide faster frame and streak rates than mechanical cameras (up to 600 Mf/s) but are limited in resolution. DOE

N89-10269*# National Aeronautics and Space Administration. Lewis Research Center, Cleveland, Ohio.
PERFORMANCE OF MULTIMIRROR QUARTZLINE LAMPS IN A HIGH-PRESSURE, UNDERWATER ENVIRONMENT
Howard A. Slater 1988 8 p Presented at the 32nd Annual International Symposium on Optical and Optoelectronic Applied Science and Engineering, San Diego, Calif., 14-19 Aug. 1988; sponsored by the Society of Photo-Optical Instrumentation Engineers
(NASA-TM-101374; E-4427; NAS 1.15:101374) Avail: NTIS HC A02/MF A01 CSCL 14B

Multimirror Quartzline Lamps are extremely versatile and effective for nonconventional imaging requirements such as high-speed photo and video instrumentation and high-magnification imaging. The lamps' versatility though, is not limited to conventional environments. Many research experiments and projects require a high pressure environment. Continuous photographic data acquisition in a high-pressure vessel requires wall penetrations and creates design problems as well as potential failure sites. Underwater photography adds the extra consideration of a liquid. This report expands upon the basic research presented in, Performance of Multimirror Quartzline Lamps in High-Pressure Environments, (NASA-TM-83793, Ernie Walker and Howard Slater, 1984). The report provides information to professional industrial, scientific, and technical photographers as well as research personnel on the survivability of lighting a multimirror quartzline lamp in a nonconventional high-pressure underwater environment. Test results of lighted ELH 300 W multimirror quartzline lamps under high-pressure conditions are documented and general information on the lamps' intensity (footcandle output), cone of light coverage, approximate color temperature is provided. Continuous lighting considerations in liquids are also discussed. Author

N89-10270# Deutsche Forschungs- und Versuchsanstalt fuer Luft- und Raumfahrt, Oberpfaffenhofen (West Germany). Abteilung Prozessortechnik.
IMAGE PROCESSING DOCUMENT: HALLEY MULTICOLOR CAMERA (GIOTTO MISSION)
Adelheid Craubner, Eberhard Mikusch, Kurt Schmidt, and Gottfried Schwartz Mar. 1988 423 p Original contains color illustrations
(DFVLR-FB-88-20; ISSN-0171-1342; ETN-88-93186) Avail: NTIS HC A18/MF A01; DFVLR, VB-PL-DO, 90 60 58, 5000 Cologne, Fed. Republic of Germany, 155 Deutsche marks

Scientific data evaluation of cometary images as recorded by the Halley Multicolor Camera and by ground based observations is described. Hardware structure of an image processing system, system software, and application programs are outlined. The result is a comfortable interactive image processing system for fast and reliable evaluation of physical phenomena without being limited by rigid menu structures. ESA

N89-10271# Deutsche Forschungs- und Versuchsanstalt fuer Luft- und Raumfahrt, Oberpfaffenhofen (West Germany). Abteilung Infrattotechnik.
INFRARED TEMPERATURE MEASUREMENT WITH INHERENT CONSIDERATION OF EMISSIVITY Ph.D. Thesis - Technische Univ., Munich
Volker Tank Mar. 1988 176 p In GERMAN; ENGLISH summary Report will also be announced as translation (ESA-TT-1131)
(DFVLR-FB-88-22; ISSN-0171-1342; ETN-88-93188) Avail: NTIS HC A09/MF A01; DFVLR, VB-PL-DO, 90 60 58, 5000 Cologne, Fed. Republic of Germany, 50.50 Deutsche marks

Development of a system for contactless infrared temperature measurement (filter spectrometer linked to a computer) is described, including investigations on components, data reduction, and calibration procedures. It uses a method which measures spectral radiances of an object in 10 narrow infrared bands. Applying a balancing calculation on these data, the temperatures of the object and its environment as well as the object's emissivity are computed. The method is feasible also for strongly reflecting objects (epsilon less than 0.2) below the temperature of glow (T less than 973 K), thereby extending and completing the range of conventional instruments. Examples of measurements are shown. ESA

N89-10487# Honeywell, Inc., Phoenix, Ariz.
LSZ-850 LIGHTNING SENSOR SYSTEM
Ernest W. Coleman *In* NOAA, International Aerospace and Ground Conference on Lightning and Static Electricity Apr. 1988 p 434-43 (For primary document see N89-10429 01-47)
Avail: NTIS HC A23/MF A01 CSCL 14B

N89-10491# University of Technology, Lae (Papua New Guinea). Electrical and Communication Engineering.
THE LIGHTNING FLASH COUNTER: PAPUA NEW GUINEAN EXPERIENCE
Feroze Coowar, Paul R. P. Hoole, and Peter Greenwood (Hydro-Electric Power Commission, Tasmania, Australia) *In* NOAA, International Aerospace and Ground Conference on Lightning and Static Electricity Apr. 1988 p 460-46 (For primary document see N89-10429 01-47)
Avail: NTIS HC A23/MF A01 CSCL 14B

N89-10494# Tokyo Univ. (Japan). Inst. of Industrial Science.
SITE ERRORS OF A MAGNETIC DIRECTION FINDER FOR LIGHTNING FLASHES
T. Kawamura, M. Ishii, and Y. Miyake (Sankosha Co. Ltd., Tokyo, Japan) *In* NOAA, International Aerospace and Ground Conference on Lightning and Static Electricity Apr. 1988 p 487-49 (For primary document see N89-10429 01-47)
Avail: NTIS HC A23/MF A01 CSCL 14B

36 LASERS AND MASERS

Includes parametric amplifiers.
For related information see also *76 Solid-State Physics.*

N89-10272# Sandia National Labs., Albuquerque, N. Mex.
LASER INTERFEROMETRIC DILATOMETER FOR LOW-EXPANSION MATERIALS
W. D. Drotning 1988 21 p Presented at the 10th Symposium on Thermophysical Properties, Gaithersburg, Md., 20 Jun. 1988
(Contract DE-AC04-76DP-00789)
(DE88-012329; SAND-87-2806C; CONF-880606-4) Avail: NTIS HC A03/MF A01

The development of a high-precision dilatometer based on interferometry presents a number of challenges. This paper

describes a laser interferometric dilatometer developed for high-precision thermal expansion measurements in the materials laboratory. The Sandia dilatometer uses dual-beam laser interferometry with a computer-controlled optical alignment feature to achieve high-precision length change measurements. This device has been modified to expand its measurement capabilities in a number of areas. A new thermal chamber has been incorporated which provides a range of measurement from 90 to 500 K while minimizing thermal effects on the optical portion of the instrument. A new specimen holder has been developed to cover this temperature range while accommodating a wider variety of specimen types. In particular, thin (1 mm) composites may be employed in the holder, which uses a single specimen, with only modest shape and preparation requirements, to provide absolute length change measurements. Tilt errors limit the overall performance of dilatometers based on dual-beam interferometry. Significant improvements in precision were demonstrated by incorporating a unique optical system which independently measures specimen holder tilt. DOE

N89-10273# Air Force Systems Command, Wright-Patterson AFB, Ohio. Foreign Technology Div.
VIBRATIONAL RELAXATION PROCESSES IN CO2-N2-H2O LASER SYSTEMS
Yan Haixing 9 Jun. 1988 20 p Transl. into ENGLISH from Jiguang (Peoples Republic of China), v. 8, no. 11, 1981 p 11-17
(AD-A196211; FTD-ID(RS)T-0258-88) Avail: NTIS HC A03/MF A01 CSCL 07D

This article discusses a number of important questions concerning relaxation processes: the V-V energy transfer mechanism inside CO2(v3) molecules; the mechanisms involved in the main reactions of water on relaxation processes; resonant energy transfer between nu1 and nu2 in CO2; similarities and differences in the relaxation rates for expansion and compression flows; and, possibilities of non-equilibrium existing between different levels of rotational energy and between different levels of vibrational energy within the same vibrational mode. The article points out that it is necessary to do more detailed research on these questions. The content of these discussions is also appropriate for use with other gas laser systems. GRA

N89-10274# Los Alamos National Lab., N. Mex.
FLUID DYNAMIC ISSUES IN CONTINUOUS WAVE SHORT WAVELENGTH CHEMICAL LASERS
R. R. Mikatarian, E. J. Jumper, and C. Woolhiser (Air Force Weapons Lab., Kirtland AFB, N. Mex.) 1988 35 p Presented at the Conference on Thermophysics, Plasma Dynamics and Lasers, San Antonio, Tex., 27 Jun. 1988
(Contract W-7405-eng-36)
(DE88-014428; LA-UR-88-2019; CONF-880676-2) Avail: NTIS HC A03/MF A01

This paper addresses fluid dynamic issues of concern in the design and development of Continuous Wave (CW) Short Wavelength Chemical Lasers (SWCLs). Short Wavelength Chemical Laser technology is in its research stage and SWCL concepts are in their evolving mode. Researchers are presently addressing candidate chemical systems and activation concepts. Since these lasers will be flowing systems, it is necessary to discuss both the probable fluid dynamics issues, because of the inherent complexities fluid dynamicist can support this activity. In addition to addressing the SWCL fluid dynamic issues, this paper will review past fluid dynamic activities in hign energy lasers and discuss additional research still required. This paper will also address the various levels of fluid dynamic modeling and how these models can be applied in studying the fluid dynamics of Short Wavelength Chemical Lasers. Where it is felt that specific fluid methodologies are not available, but are required in order to conduct specific analyses, they will be defined. DOE

N89-10275# Naval Postgraduate School, Monterey, Calif.
A TRANSITION RADIATION EXPERIMENT TO MEASURE THE ELECTRON BEAM MODULATION INDUCED BY THE FREE ELECTRON LASER: A DESIGN STUDY M.S. Thesis
Jack E. Joynson Dec. 1987 90 p
(AD-A195169) Avail: NTIS HC A05/MF A01 CSCL 09C

The modulated beam of the free electron laser when passed through a thin target should produce strong transition radiation. The measurement of the transition radiation is a direct measurement of the electron beam modulation in the free electron laser. A transition radiation experiment using the Stanford MK3 Infrared Free Electron Laser (IRFEL) has been proposed. The analysis has centered on TRANSPORT, a computer program used for designing charged particle beam systems. The MK3 IRFEL wiggler exit bending magnet system was modeled using TRANSPORT. Analysis reveals that the transverse emittance and momentum spread characteristics will cause the modulated beam to demodulate along the path of the central trajectory. A detector location 10 millimeters downstream of the first bending magnet is found suitable for the measurement of the electron beam modulation. For this case the thin foil must be rotated approximately 11.25 degrees about the y axis to yield a minimum effective picobunch extent as seen by the thin foil. Alternate FEL systems are suggested for investigation. GRA

N89-10276# Purdue Univ., West Lafayette, Ind.
NONLINEAR OPTICAL INTERACTIONS INVOLVING THE REAL GAUSSIAN FIELD Progress Report
1988 3 p
(Contract DE-FG02-86ER-13576)
(DE88-012399; DOE/ER-13576/2) Avail: NTIS HC A02

Development of a technique for generating a laser field known as the Real Gaussian field has been the major object of efforts to date. This field is characterized by a randomly fluctuating amplitude, epsilon(t), whose average value is zero, E(t) = epsilon(t)e(sup -iw.t). Application of this field to a number of nonlinear optical interactions will allow us to study the effect of laser field correlations on adsorption rates, widths, and other spectral features. The technique involves the application of a randomly fluctuating voltage to the electrodes of a pair of LiTaO3 Electro-optic crystals. DOE

N89-10277*# Washington Univ., Seattle. Aerospace and Energetics Research Program.
STUDIES OF BLACKBODY-PUMPED LASERS Semiannual Progress Report, 1 Jan. - 30 Jun. 1988
W. H. Christiansen, J. Chang, and M. Sirota 23 Sep. 1988 19 p
(Grant NAG1-176)
(NASA-CR-183214; NAS 1.26:183214) Avail: NTIS HC A03/MF A01 CSCL 20E

Laser action was achieved in a large-scale pulsed system and meaningful experiments were carried out in the axial flow facility to understand the physics of solar-pumped lasers. Studies of the variation of laser mixture composition were done for mixtures of CO2 and N2O additions. Theoretical analysis and modeling of the system were also performed based on a model including radiative pumping, diffusion and wall deactivation, and vibrational energy transfer between two optically active species. Qualitative agreement between predictions in the parameter variation and the experimental results were obtained with CO and N2O mixtures. Several experimental studies were performed to quantify the properties of carbon monoxide as absorber and storage of energy in the blackbody pumped system. Author

N89-10278# Berkeley Research Associates, Inc., Calif.
RESEARCH ON A TWO-STAGE FREE ELECTRON LASER OSCILLATOR Final Report
Mar. 1988 91 p
(Contract N00014-85-C-2069)
(AD-A195339; BRA-88-W034R) Avail: NTIS HC A05/MF A01 CSCL 09C

The research involved the theoretical and numerical analysis of the physics of free electron lasers using relativistic particle beams. The major emphasis of the research was to obtain design criteria for the development of a two-stage FEL oscillator operating

in the trapped particle mode. The present work was centered on the development of a fully relativistic, nonlinear analysis of the spatial and temporal evolution of multiple modes within a free electron laser oscillator and of a large amplitude, nonlinearly saturated state characteristic of trapped particle mode operation. The equations solved are the Maxwell equations of electrodynamics coupled with the collisionless Boltzmann equation that describes collisionless particles under influence of the electromagnetic fields. The electromagnetic fields include the radiation fields from the FEL and the self-electric fields from the longitudinal potential due to the space charge, i.e., the dominant component of the interparticle Coulomb forces. The particle dynamics transverse to the magnetic axis are included, but gradients in the radiation fields are ignored. The electron beam equilibrium is assumed to be spatially uniform and temporally stationary. Justification and probable impact of further approximations are discussed in the technical section of this report. The approximations employed are consistent with the purpose of obtaining experimentally implementable design criteria for the FEL oscillator. GRA

N89-10279# Los Alamos National Lab., N. Mex.
RECENT RESULTS FROM THE LOS ALAMOS FREE-ELECTRON LASER
D. W. Feldman, R. W. Warren, B. E. Carlsten, W. E. Stein, J. M. Watson, C. A. Brau, G. Spalek, L. M. Young, A. H. Lumpkin, and S. C. Bender 1988 39 p Presented at the Free Electron Laser Seminar, Beijing, China, 11 Aug. 1988
(Contract W-7405-eng-36)
(DE88-014409; LA-UR-88-2136; CONF-880888-9) Avail: NTIS HC A03/MF A01

In this paper we review the most recent experimental results of the Los Alamos free-electron laser program. Three major effects will be described: lasing at improved efficiency over that previously attained, electron beam improvement, and energy recovery. An extraction efficiency of 2 percent was achieved with a wiggler having a 12 percent wavelength taper. The beam has been improved so that limits to its quality are now caused, not by injector performance, but by wake fields related to the high peak currents achieved. Limits to optical power are set by mirror damage. Experiments are described that demonstrate the successful operation of an energy recovery system. DOE

37 MECHANICAL ENGINEERING

Includes auxiliary systems (nonpower); machine elements and processes; and mechanical equipment.

N89-10280# Brookhaven National Lab., Upton, N. Y.
DESIGN APPROACHES AND PARAMETERS FOR MAGNETICALLY LEVITATED TRANSPORT SYSTEMS
Gordon T. Danby and James R. Powell 1988 30 p Presented at the Conference on Superconductivity and Applications, Buffalo, N.Y., 18 Apr. 1988
(Contract DE-AC02-76CH-00016)
(DE88-014286; BNL-41434; CONF-880466-10) Avail: NTIS HC A03/MF A01

Mechanically levitated transport system approaches are assessed with regard to thrust power needs, track cost, suspension stability, and safety. The null flux suspension appears as the favored approach, having the least thrust power requirements, highest stability, and lowest amount of track material. Various null flux configurations are described together with their operating parameters. The Linear Synchronous Motor (LSM) propulsion system is also described for propelling the suspended vehicles. Cryogenics and superconductivity aspects are discussed and the effect of high T sub c superconductors evaluated. DOE

N89-10281# Oak Ridge National Lab., Tenn.
LASER WELDING OF STAINLESS STEEL WELD FILLER METALS AT HIGH COOLING RATES
John M. Vitek and Stan A. David 1988 15 p Presented at the 4th International Symposium on Welding and Melting by Electron and Laser Beams, Cannes, France, 26 Sep. 1988
(Contract DE-AC05-84OR-21400)
(DE88-002345; CONF-880922-1) Avail: NTIS HC A03/MF A01

Several stainless steels were laser welded under conditions resulting in high cooling rates of the welds. Significant changes in the microstructures, compared to those produced by conventional welding techniques, were found. For alloys 304, 308, 309, 316 and 347, a general decrease in ferrite content with increasing cooling rate was found. For three alloys (304, 308, 347), a fully austenitic structure was obtained at the highest cooling rates. For alloys 312 and 446, the high cooling rates retarded the formation of austenite, resulting in higher ferrite contents and fully ferritic structures at the highest cooling rates. Only for alloy 310 was the microstructure after laser welding comparable to that found after conventional welding. The results are discussed in terms of their impact on the Schaeffler diagram and its applicability to laser welding. DOE

N89-10282*# National Aeronautics and Space Administration. Lewis Research Center, Cleveland, Ohio.
GENERATION OF A CROWNED PINION TOOTH SURFACE BY A SURFACE OF REVOLUTION
F. L. Litvin, J. Zhang, and R. F. Handschuh (Army Aviation Systems Command, Cleveland, Ohio.) Sep. 1988 15 p
(Grant NAG3-655)
(NASA-TM-100260; E-3888; NAS 1.15:100260; AVSCOM-TR-87-C-34) Avail: NTIS HC A03/MF A01 CSCL 13I

A method of generating crowned pinion tooth surfaces using a surface of revolution is developed. The crowned pinion meshes with a regular involute gear and has a prescribed parabolic type of transmission errors when the gears operate in the aligned mode. When the gears are misaligned the transmission error remains parabolic with the maximum level still remaining very small (less than 0.34 arc sec for the numerical examples). Tooth contact analysis (TCA) is used to simulate the conditions of meshing, determine the transmission error, and determine the bearing contact. Author

N89-10283*# National Aeronautics and Space Administration. Lewis Research Center, Cleveland, Ohio.
GENERATION OF A CROWNED PINION TOOTH SURFACE BY A PLANE
F. L. Litvin, J. Zhang, and R. F. Handschuh (Army Aviation Systems Command, Cleveland, Ohio.) Sep. 1988 15 p
(Grant NAG3-655)
(NASA-TM-100259; E-3887; NAS 1.15:100259; AVSCOM-TR-87-C-33) Avail: NTIS HC A03/MF A01 CSCL 13I

The topology of a crowned spur pinion tooth surface that reduces the level of transmission errors due to misalignment is described. The geometry of the modified pinion tooth surface and of the regular involute gear tooth surface is discussed. The tooth contact analysis between the meshing surfaces is also described. Generating a modified pinion tooth surface by a plane whose motion is controlled by a 5-degree-of-freedom system is investigated. The numerical results included indicate that the transmission error remains low as the gears are misaligned. Author

N89-10284# Allied-Signal Aerospace Co., Kansas City, Mo. Kansas City Div.
RIVETING A CASE SECTION WITH BLIND, SELF-PLUGGING RIVETS Final Report
S. B. Smith Jun. 1988 18 p
(Contract DE-AC04-76DP-00613)
(DE88-013224; BDX-613-3949) Avail: NTIS HC A03/MF A01

Blind, self-plugging, flush-head rivets, NAS1721, were installed on a case section to determine compatibility with current product and process requirements. Shear strength properties compared favorably to the solid body rivet currently used. The blind rivet was found to be a more cost effective solution toward improving

riveting process time than buying upgraded riveting equipment to rivet solid body rivets. The effects of using blind rivets on secondary processes such as painting were also evaluated. DOE

N89-10285 Illinois Univ., Urbana-Champaign.
ON MOTION PLANNING AND CONTROL OF MULTI-LINK LIGHTWEIGHT ROBOTIC MANIPULATORS Ph.D. Thesis
Sabri Cetinkunt 1987 275 p
Avail: Univ. Microfilms Order No. DA8803697

A general gross and fine motion planning and control strategy is needed for lightweight robotic manipulator applications such as painting, welding, material handling, surface finishing, and spacecraft servicing. The control problem of lightweight manipulators is to perform fast, accurate, and robust motions despite the payload variations, structural flexibility, and other environmental disturbances. Performance of rigid manipulator model based computed torque and decoupled joint control methods are determined and simulated for the couterpart flexible manipulators. A counterpart flexible manipulator is one which has structural flexibility, along with the same inertial, geometric, and actuation properties of a rigid manipulator. An adaptive model following control (AMFC) algorithm is developed to improve the performance in speed, accuracy and robustness. It is found that the AMFC improves the speed performance by a factor of two over the nonadaptive control methods for accuracy requirements while proving to be more robust with respect to payload variations. Yet there are limitations on the performance of AMFC alone imposed by arm flexibility. A combined control strategy is developed to improve performance. Dissert. Abstr.

N89-10286# Mechanical Technology, Inc., Latham, N. Y.
FREE-PISTON STIRLING ENGINE DEVELOPMENT Final Report, 1 Jan. 1986 - 31 Dec. 1987
R. A. Ackermann Apr. 1988 165 p
(Contract GRI-5082-242-0721)
(PB88-220025; GRI-88/0037) Avail: NTIS HC A08/MF A01 CSCL 13I

The free-piston Stirling engine (FPSE) is being developed as a potential gas-fired prime mover for heat applications in the residential market. The heat pump features an advanced FPSE coupled to an advanced Rankine refrigerant compressor through a hermetically sealed diaphragm-activated hydraulic transmission. During the past two years, the program has concentrated on developing the engine and the compressor component to improve performance and reliability. The progress made during the period and the results of an independent test and evaluation performed on the Mark 1 heat pump module are discussed. GRA

N89-10287# Massachusetts Inst. of Tech., Cambridge. Artificial Intelligence Lab.
A DEXTERITY MEASURE FOR THE KINEMATIC CONTROL OF ROBOT MANIPULATOR WITH REDUNDANCY
Pyung H. Chang Feb. 1988 53 p
(Contract N00014-80-C-0505)
(AD-A196223; AI-M-1021) Avail: NTIS HC A04/MF A01 CSCL 12I

We have derived a new performance measure, product of minors of the Jacobian matrix, that tells how far kinematically redundant manipulators are from singularity. It was demonstrated that previously used performance measures, namely condition number and manipulability measure allowed to change configurations, causing repeatability problems and discontinuity effects. The new measure, on the other hand, assures that the arm solution remains in the same configuration, thus effectively preventing these problems. GRA

N89-10288 Case Western Reserve Univ., Cleveland, Ohio.
ROBOTIC ADAPTIVE GRASPING BASED ON VISION AND TACTILE SENSOR DATA Ph.D. Thesis
Dong Min Woo 1987 135 p
Avail: Univ. Microfilms Order No. DA8802462

How an intelligent sensor system can be utilized and controlled in an integrated manner to support robotic grasping is described. Visual sensing and proximity sensing was used to identify and locate parts and use tactile sensing and force torque sensing to ensure that the part is grasped correctly. For recognition, a new two-dimensional vision system is developed, which can identify a part as a generic shape. Matching between the object and generic shape is performed in the frequency domain. The DFT of the object contour is decomposed to estimate the orientation of the object and to evaluate the similarity between the object and generic shape. This approach has many advantages over the conventional correlation technique. With only a few uniformly sampled points, this method can estimate the orientation in an optimal manner. Another advantage is its robustness against noise, since the method is performed in the frequency domain and includes implicit noise filtering. No preprocessing of the contour is required. However, uncertainties in the identity and location of the object arise from the two-dimensional vision system. To resolve these uncertainties, a high level control mechanism is developed to provide verification. Dissert. Abstr.

N89-10289# Oak Ridge National Lab., Tenn. Instrumentation and Controls Div.
TELEROBOTIC CONTROL OF THE SEVEN-DEGREE-OF-FREEDOM CESAR MANIPULATOR
S. M. Babcock, R. V. Dubey (Tennessee Univ., Knoxville.), J. A. Euler, R. L. Glassell, R. L. Kress, and W. R. Hamel 1988 16 p Presented at the NATO Advanced Research Workshop on Robots With Redundancy: Design, Sensing, and Control, Salo, Italy, 27 Jun. 1988
(Contract DE-AC05-84OR-21400)
(DE88-012937; CONF-8806183-1) Avail: NTIS HC A03/MF A01

The application of a computationally efficient kinematic control scheme for manipulators with redundant degrees of freedom to the unilateral telerobotic control of seven-degree-of-freedom manipulator (CESARM) at the Oak Ridge National Laboratory Center for Engineering Systems Advanced Research is presented. The kinematic control scheme uses a gradient projection optimization method, which eliminates that need to determine the generalized inverse of the Jacobian when solving for joint velocities, given Cartesian end-effector velocities. A six-degree-of-freedom (nonreplica) master controller is used. Performance indices for redundancy resolution are discussed. DOE

38 QUALITY ASSURANCE AND RELIABILITY

Includes product sampling procedures and techniques; and quality control.

No abstracts in this category.

39 STRUCTURAL MECHANICS

Includes structural element design and weight analysis; fatigue; and thermal stress.

For applications see *05 Aircraft Design, Testing and Performance* and *18 Spacecraft Design, Testing and Performance.*

N89-10290# Sydney Univ. (Australia). School of Civil and Mining Engineering.
BUCKLING OF RINGS IN COLUMN-SUPPORTED BINS AND TANKS
J. G. Teng and J. M. Rotter Sep. 1987 38 p
(PB88-217336; R-552) Avail: NTIS HC A03/MF A01 CSCL 20K

Theories for the out-of-plane buckling of rings under uniform circumferential compression are well established. However these

theories are not applicable to rings in column supported bins where the circumferential stress in the ring varies significantly over the cross section and around the circumference. The out-of-plane buckling of annular plate rings in column supported bins and tanks are examined. The stress distribution in such rings are first studied using a finite element shell analysis. A closed form solution for the buckling of rings under nonuniform circumferential stresses is then derived. Results from the closed form solution are compared with those from a finite element shell buckling analysis, and close agreement is found. The significant effect of stress nonuniformity on the buckling predictions is demonstrated. Finally, simplified equations are given which are suitable for structural design purposes, and which closely model the predictions of the more rigorous solution. Author

N89-10291*# Virginia Polytechnic Inst. and State Univ., Blacksburg. Dept. of Engineering Science and Mechanics.
ON THE PROBLEM OF MODELING FOR PARAMETER IDENTIFICATION IN DISTRIBUTED STRUCTURES
Mark A. Norris and Leonard Meirovitch 1988 24 p
(Grant NAG1-225)
(NASA-CR-182739; NAS 1.26:182739) Avail: NTIS HC A03/MF A01 CSCL 20K

Structures are often characterized by parameters, such as mass and stiffness, that are spatially distributed. Parameter identification of distributed structures is subject to many of the difficulties involved in the modeling problem, and the choice of the model can greatly affect the results of the parameter identification process. Analogously to control spillover in the control of distributed-parameter systems, identification spillover is shown to exist as well and its effect is to degrade the parameter estimates. Moreover, as in modeling by the Rayleigh-Ritz method, it is shown that, for a Rayleigh-Ritz type identification algorithm, an inclusion principle exists in the identification of distributed-parameter systems as well, so that the identified natural frequencies approach the actual natural frequencies monotonically from above. Author

N89-10292# Sydney Univ. (Australia). School of Civil and Mining Engineering.
DEFORMATIONS AND RESIDUAL STRESSES INDUCED IN CHANNEL SECTION COLUMNS BY PRESETTING AND WELDING
K. J. R. Rasmussen and G. J. Hancock Aug. 1987 70 p
(PB88-199971; R-550) Avail: NTIS HC A04/MF A01 CSCL 20K

Deformations of fabricated mono-symmetric members caused by weld shrinkage forces eccentric from the section centroid were studied. A method of manufacture is presented which counteracts the deformation from weld shrinkage by presetting and subsequently clamping of the plate elements prior to welding. The method can also be used to produce a specified overall bow of the member. A theory is outlined for controling the deformation after fabrication by presetting, and expressions are stated for the residual stresses induced by the combined effects of presetting and weld shrinkage. The presetting method is applied to the fabrication of channel section members. Residual stresses are measured in a total of nine specimens and are compared with theoretically predicted stresses. The obtained straightness revealed that the presetting technique is an effective method for eliminating weld shrinkage deformation in fabricated monosymmetric members. GRA

N89-10293 Denver Univ., Colo.
AN INVESTIGATION OF THE ACOUSTIC EMISSION GENERATED BY VARIOUS CRACK PROPAGATION MODES IN 304 STAINLESS STEEL Ph.D. Thesis
Daniel Richard Smith, Jr. 1987 129 p
Avail: Univ. Microfilms Order No. DA8803350

The effectiveness of making careful acoustic emission measurements in conjunction with indepth metallographic analysis, in order to fully investigate and characterize the various crack propagation modes in 304 stainless steel, is shown. Acoustic emission measurements were made during different types of crack propagation in the 304 stainless steel. The crack propagation modes were changed by a combination of heat treating the material and cathodically charging it with hydrogen. The various crack propagation modes could be identified by their acoustic emission characteristics. The acoustic emission parameters which provided the most information were the acoustic energy and power spectra. A very significant result was obtained regarding the hydrogen degradation mechanism in 304 stainless steel. The result of the investigation indicates that the hydrogen degradation mechanism in 304 stainless steel is the lowering of cohesive energy.
Dissert. Abstr.

N89-10294# Defence Research Establishment Atlantic, Dartmouth (Nova Scotia).
INFLUENCE OF SPECIMEN SIZE ON FATIGUE CRACK INITIATION OF WELDED HY100 STEEL
Wolfgang Kreuzer Jan. 1988 72 p
(AD-A196219; DREA-TM-88/201) Avail: NTIS HC A04/MF A01 CSCL 11F

The assumption of a statistical distribution of the flaws in a component leads to a prediction of a correlation between crack initiation life and the size of a fatigue loaded part. The influence of the specimen size on the fatigue crack initiation behavior was analysed for two series of welded HY 100 steel plates of different widths. The weldments were prepared with E12018M2 electrodes. The prediction of the number of cycles to crack initiation and of the allowable stresses for samples of a different size agreed well with the experimental results. GRA

N89-10295# Sydney Univ. (Australia). School of Civil and Mining Engineering.
ELASTIC-PLASTIC LARGE DEFLECTION ANALYSIS OF AXISYMMETRIC SHELLS
J. G. Teng and J. M. Rotter Nov. 1987 87 p
(PB88-217344; R-556) Avail: NTIS HC A05/MF A01 CSCL 20K

A finite element formulation is presented for elastic-plastic large deflection analysis of axisymmetric shells. The doubly curved shell finite element used has been widely applied to linear elastic stress analyses and linear stability analyses by the author et al previously. Recently developed nonlinear shell strain displacement relations are used in place of the widely used relations of Donnell or Sanders. For plastic analysis, a multilayered approach is employed, employing the Prandtl-Reuss normal flow rule with isotropic hardening. An efficient and accurate state determination algorithm is adopted and demonstrated. The variable arc length method is realized in the formulation by assuming incremental reversibility for plastic behavior, which facilitates an efficient iterative procedure for tracing both the pre- and post-critical load deflection path. Several examples are included to show the accuracy, efficiency and capability of the present formulation. Author

N89-10296# Sydney Univ. (Australia). School of Civil and Mining Engineering.
GEOMETRIC IMPERFECTIONS IN PLATED STRUCTURES SUBJECT TO INTERACTION BETWEEN BUCKLING MODES
K. J. R. Rasmussen and G. J. Hancock Apr. 1987 47 p
(PB88-200902; R-541) Avail: NTIS HC A03/MF A01 CSCL 20K

An analytical technique is described for expanding a measured geometric imperfection surface in the buckling modes of a structure. The surface is expanded longitudinally as well as transversely. In the transverse expansion, the constituent plates are treated as a plate assembly so that the imperfections of the individual plates can be interrelated. The technique is applied to a channel section which buckles interactively in an overall flexural mode in the plane of symmetry and a primary local buckling mode. The imperfection components of these modes are determined, as are the components of the secondary local buckling modes which may be triggered as a result of the interaction between the overall and local modes. The imperfection components are determined approximately from imperfection measurements taken at six points

in each cross-section along the length of the column. The application of the technique to other cross-section types is mentioned. GRA

N89-10297*# North Carolina Agricultural and Technical State Univ., Greensboro. Dept. of Architectural Engineering.
DYNAMICS AND CONTROL OF THE ORBITING GRID STRUCTURES AND THE SYNCHRONOUSLY DEPLOYABLE BEAM Final Report
Elias G. Abu-Saba 28 Sep. 1988 62 p
(Grant NAG1-405)
(NASA-CR-183205; NAS 1.26:183205) Avail: NTIS HC A04/MF A01 CSCL 20K

Analytical models were provided for the orbiting grid structure and the joint dominated beam and computational procedures used in determining the eigen value characteristics. Author

N89-10298 Nebraska Univ., Lincoln.
NONLINEAR FINITE ELEMENT ANALYSIS FOR PLASTIC DEFORMATION BY LOCAL RANDOM YIELDING Ph.D. Thesis
Kuen-Nan Lin 1987 106 p
Avail: Univ. Microfilms Order No. DA8803759

A probabilistic local random yielding model has been developed in simulating the uniaxial stress-strain curve. Due to the mathematical existence of the microplastic strain at any loading level, a continuous expansion of random yielding surface is defined. A piecewise linearity assumption is applied in the nonlinear finite element analysis for plastic deformation. The elastic-plastic matrix for the incremental stress-strain relationship was continuously characterized by the hardening function using the local random yielding model. In determinig the elastic-plastic matrix for each element, the mathematical continuity of the hardening function eliminates the numerical iteration when an element is forced from the elastic to the plastic region. The numerical solution of stress, strain and displacement fields at each element node accumulates through each incremental step. The validity and accuracy of the nonlinear finite element method for plastic deformation has been demonstrated by comparing with the experimental results reported in the literature. Dissert. Abstr.

N89-10299# Sydney Univ. (Australia). School of Civil and Mining Engineering.
INELASTIC BUCKLING ANALYSES OF BEAMS, COLUMNS AND PLATES USING THE SPLINE FINITE STRIP METHOD
S. C. W. Lau and G. J. Hancock Oct. 1987 67 p
(PB88-214291; R-553) Avail: NTIS HC A04/MF A01 CSCL 20K

Inelastic buckling of thin-walled structural members and plates is studied using the spline finite strip method. The analysis takes into account the nonlinear material stress-strain properties, strain hardening, and residual stresses. The plastic theories studied are the flow theory of plasticity and the deformation theory of plasticity. The spline finite strip method of inelastic buckling analysis is applied to a variety of instability problems including plates, cold-formed columns, hot-rolled columns, and welded tee section beams. The buckling modes and loads computed are compared with theoretical values and test results. GRA

N89-10300*# National Aeronautics and Space Administration. Langley Research Center, Hampton, Va.
RECENT DEVELOPMENTS IN STRUCTURAL SENSITIVITY ANALYSIS
Raphael T. Haftka (Virginia Polytechnic Inst. and State Univ., Blacksburg.) and Howard M. Adelman Aug. 1988 32 p Presented at the 3rd ISPE International Conference on CAD/CAM, Robotics, and Factories of the Future, Southfield, Mich., 14-17 Aug. 1988
(NASA-TM-100668; NAS 1.15:100668) Avail: NTIS HC A03/MF A01 CSCL 20K

Recent developments are reviewed in two major areas of structural sensitivity analysis: sensitivity of static and transient response; and sensitivity of vibration and buckling eigenproblems. Recent developments from the standpoint of computational cost, accuracy, and ease of implementation are presented. In the area of static response, current interest is focused on sensitivity to shape variation and sensitivity of nonlinear response. Two general approaches are used for computing sensitivities: differentiation of the continuum equations followed by discretization, and the reverse approach of discretization followed by differentiation. It is shown that the choice of methods has important accuracy and implementation implications. In the area of eigenproblem sensitivity, there is a great deal of interest and significant progress in sensitivity of problems with repeated eigenvalues. In addition to reviewing recent contributions in this area, the paper raises the issue of differentiability and continuity associated with the occurrence of repeated eigenvalues. Author

N89-10301# KMS Fusion, Inc., Ann Arbor, Mich.
THE TENSILE STRENGTH OF GLASS SHELLS
M. A. Ebner, W. J. Miller, and J. L. Evans 1988 12 p Presented at the 6th Target Fabrication Specialist's Meeting, Los Alamos, N. Mex., 19 Jun. 1988
(Contract DE-AC03-87DP-10560)
(DE88-013011; KMSF-U-1975; CONF-8806170-7) Avail: NTIS HC A03/MF A01

Glass shells used as ICF fuel containers must withstand extreme external and internal pressure. A shell's resistance to external pressure (compressive strength) determines how rapidly it can be filled with fuel by permeation; its resistance to internal pressure (tensile strength) determines how much gaseous fuel it can ultimately hold. Tensile strength is difficult to study because it is a function of the history of the glass and does not have an inherent value. While the theoretical strength of glass is on the order of 1.38 to 3.44 x 10 to the 10th Pa, the actual strength of a particular glass object is usually several orders of magnitude lower, and is determined by the flaw population. Furthermore, tensile failure can occur either by stress intensification at the tips of surface flaws and defects, or by crack growth induced by stress corrosion (delayed failure or fatigue). Consequently, since flaws are generally produced on the surface of glass objects by handling and exposure to an abrasive or reactive environment, glass fracture is highly random in nature. These considerations have caused increasing concern in target fabrication as target sizes have increased and specifications become more stringent. We seek to determine the effects on tensile strength of the permeant gas, and of the geometric characteristics, surface area, and glass volume of the shells. As the failures have become more costly, greater target reliability (or predictability) has become increasingly desirable. We have therefore resumed studies to determine the effective tensile strength of glass shells. DOE

N89-10007# Imperial Coll. of Science and Technology, London (England). Dept. of Mechanical Engineering.
BASIC STRUCTURAL DYNAMICS
D. J. Ewins *In* AGARD, AGARD Manual on Aeroelasticity in Axial-Flow Turbo Machines. Volume 2: Structural Dynamics and Aeroelasticity Jun. 1988 14 p (For primary document see N89-10006 01-02)
Copyright Avail: NTIS HC A12/MF A01

N89-10016# Detroit Diesel Allison, Indianapolis, Ind.
FORCED VIBRATION AND FLUTTER DESIGN METHODOLOGY
Lynn E. Snyder and Donald W. Burns *In* AGARD, AGARD Manual on Aeroelasticity in Axial-Flow Turbo Machines. Volume 2: Structural Dynamics and Aeroelasticity Jun. 1988 28 p (For primary document see N89-10006 01-02)
Copyright Avail: NTIS HC A12/MF A01

42 GEOSCIENCES (GENERAL)

No abstracts in this category.

43 EARTH RESOURCES AND REMOTE SENSING

Includes remote sensing of earth resources by aircraft and spacecraft; photogrammetry; and aerial photography.

For instrumentation see *35 Instrumentation and Photography.*

N89-10302# Instituto de Pesquisas Espaciais, Sao Jose dos Campos (Brazil).

RELATIONSHIPS BETWEEN SPECTRAL REFLECTANCE AND PHYTOMASS OF THE GROUND LAYER COMMUNITY OF NEOTROPICAL SAVANNA (CERRADO)

Dalton deMorissonValeriano and Marisa Dantas BittencourtPereira (Sao Paulo Univ., Brazil) Aug. 1988 11 p Presented at the 16th Congress of International Society for Photogrammetry and Remote Sensing, Kyoto, Japan, 1-10 Jul. 1988 Submitted for publication

(INPE-4635-PRE/1347) Avail: NTIS HC A03/MF A01

Spectral reflectance measurements of 47 (1 m squared) plots of the ground layer of the Savanna of Central Brazil were obtained using a Kimoto PM-12A hand-held spectroradiometer at 13 visible bands and 4 near infrared bands of the electromagnetic spectrum. The above ground phytomass of each plot was clipped, weighed, oven dried and reweighed. An amount of the fresh phytomass (5 to 15 percent) was separated from the sample in order to estimate the proportion of the photosynthetically active phytomass. The correletion and regression relationships between the reflectance and phytomass data were examined. The results are: (1) fresh and dry total phytomass showed negative correlations for all spectral bands with highest r squared at delta = 575 nm; (2) fresh and dry green phytomass presented negative correlations for all visible bands and positive for near infrared bands; (3) fresh phytomass (both, total and green) showed higher r squared than dry phytomass; and (4) the bands that presented best positive and negative correlations with green phytomass were combined to generate vegetation indices. Improved r squared was achieved, with the best performance obtained by TVI. Author

N89-10303# Dornier-Werke G.m.b.H., Friedrichshafen (West Germany).

SOLID EARTH MISSION STUDY. VOLUME 2: TECHNICAL REPORT Final Report

R. Benz, H. Faulks, P. G. Hardtke, R. Klein, M. Langemann, U. Denskat, C. Etienne, P. Peyrot, A. Bernard, and A. Ciampolini (Aeritalia S.p.A., Turin, Italy) et al. Paris, France ESA Nov. 1987 387 p Prepared in cooperation with Matra Espace, Toulouse, France; ONERA, Paris, France; Aeritalia SpA, Turin, Italy; Fokker BV, Amsterdam, The Netherlands; BAe, Bristol, United Kingdom; LABEN Space Instrumentation and Systems, Milan, Italy (Contract ESTEC-7149/87-NL-JS)

(ESA-CR(P)-2626-Vol-2; ETN-88-93153) Avail: NTIS HC A17/MF A01

The Applications and Research Involving Space Techniques Observing The Earth field from Low Earth Satellite (ARISTOTELES) mission is introduced. The ARISTOTELES studies include gravity field measurements, magnetic field measurements, and geokinematics. Gravity anomalies are to be determined with better than 5 mGal accuracy at 100 km spatial resolution by a gravity gradiometer (GRADIO) made with a three axis assembly of microaccelerometers (design goal 0.001 EU accuracy). The satellite is to be launched by Ariane with ERS-2. A dawn-dusk orbit at 220 km is suggested. The most critical point is accommodation of GRADIO, but this is not insurmountable. Technical aspects of the mission are presented. ESA

N89-10304*# California Inst. of Tech., Pasadena. Seismological Lab.

DYNAMIC INTERPRETATION OF GEOID ANOMALIES Final Report, 15 Apr. 1983 - 14 Apr. 1988

Bradford H. Hager 24 Aug. 1988 9 p

(Grant NAG5-315)

(NASA-CR-183164; NAS 1.26:183164) Avail: NTIS HC A02/MF A01 CSCL 08B

The NASA Geodynamics program has as two of its missions precise determination of spatial variations in earth's geopotential (or geoid) and highly accurate monitoring of polar motion, including changes in the length of day (LOD). For the past several years, data sets provided by NASA, along with data and models from other areas of geophysic were used to place fundamental contraints on the large scale dynamics of earth and her sister planet Venus. The main approach was using fluid mechanical models of mantle flow to predict the long-wavelength variations in the geoid. Author

N89-10305# European Space Agency, Paris (France).

PROCEEDINGS OF THE 4TH INTERNATIONAL COLLOQUIUM ON SPECTRAL SIGNATURES IN REMOTE SENSING

T. D. Guyenne, ed. and J. J. Hunt, ed. Apr. 1988 535 p Partly in ENGLISH and FRENCH Proceedings held in Aussois, France, 18-22 Jan. 1988; sponsored in cooperation with Inst. National de la Recherche Agronomique, Montfavet, France, CNES, Toulouse, France, CNRS, Verrieres-le-Buisson, France, and ESA, Paris, France

(ESA-SP-287; ISSN-0379-6566; ETN-88-93044) Copyright Avail: NTIS HC A23/MF A01; ESA Publications Division, ESTEC, Noordwijk, Netherlands 80 Dutch guilders

Radar signatures of vegetation; microwave interaction with sea surface; models of spectral response of natural surfaces; emission of natural surfaces in the thermal infrared; laser active remote sensing; high spectral resolution; spectral characteristics of natural surfaces (MOMS program); and large scientific remote sensing programs were discussed. For individual titles, see N89-10306 through N89-10393.

N89-10306# Institut National de la Recherche Agronomique, Avignon (France). Station de Bioclimatologie.

EXTRACTING SOIL AND VEGETATION CHARACTERISTICS FROM MICROWAVE REMOTE SENSING DATA [EXTRACTION DES CARACTERISTIQUES DU SOL ET DE LA VEGETATION A PARTIR DE DONNEES DE TELEDETECTION HYPERFREQUENCES]

L. Prevot, I. Champion, and G. Guyot *In* ESA, Proceedings of the 4th International Colloquium on Spectral Signatures in Remote Sensing Apr. 1988 p 7-12 In FRENCH (For primary document see N89-10305 01-43)

Copyright Avail: NTIS HC A23/MF A01; ESA Publications Division, ESTEC, Noordwijk, Netherlands 80 Dutch guilders

Models for direct interpretation of active microwave remote sensing signals from under vegetation canopies are reviewed and the problem of introducing characteristic vegetation variables in semi-empirical water drop type models is discussed. The feasibility of operational inversion of these models is assessed, taking into account sensor accuracy and parameter variations from one crop to another. Use of the models to invert the data is shown to be possible, although limits to the technique are indicated. ESA

N89-10307# Karlsruhe Univ. (West Germany).

COHERENT POLARIMETRIC SIGNATURES OF CONIFEROUS TREES: A SURVEY

D. Kaehny, S. Riegger, G. Schoene, and W. Wiesbeck *In* ESA, Proceedings of the 4th International Colloquium on Spectral Signatures in Remote Sensing Apr. 1988 p 13-18 (For primary document see N89-10305 01-43)

(Contract JRC-3106-86-12-ED-ISP-D)

Copyright Avail: NTIS HC A23/MF A01; ESA Publications Division, ESTEC, Noordwijk, Netherlands 80 Dutch guilders

The state of the art in polarimetric signatures, their inherent ideas, and typical experimental results for coniferous tree parts are reviewed. Special types of signatures are evaluated for straight twigs of picea abies (spruce tree) and abies alba (silver fir) trees. Characteristics, resulting from the measurements, are discussed and interpreted. The radar cross section matrix is shown to reveal typical characteristics for similar parts of trees. ESA

N89-10308# Institut National de la Recherche Agronomique, Montfavet (France).
MEASURING IN-SITU SOIL SURFACE ROUGHNESS USING A LASER PROFILOMETER
P. Bertuzzi and J. M. Caussignac (Ecole Nationale des Ponts et Chaussees, Paris, France) *In* ESA, Proceedings of the 4th International Colloquium on Spectral Signatures in Remote Sensing Apr. 1988 p 19-24 Prepared in cooperation with Laboratoire Central des Ponts et Chaussees, Paris (France) (For primary document see N89-10305 01-43)
Copyright Avail: NTIS HC A23/MF A01; ESA Publications Division, ESTEC, Noordwijk, Netherlands 80 Dutch guilders

An optical technique for measuring field roughness characteristics of soil using a laser profilometer is described. The method is based on the defect-of-focus of a laser light beam. Laboratory and field tests were carried out in order to improve the method for field use and to compare the technique with a reference method. The technique is considerably quicker, and causes no disturbance to soil. The degree of resolution and accuracy are satisfactory. ESA

N89-10309# Centre for Agrobiological Research, Wageningen (Netherlands).
MICROWAVE BACKSCATTER FROM BEETS, PEAS AND POTATOES THROUGHOUT THE GROWING SEASON
B. A. M. Bouman *In* ESA, Proceedings of the 4th International Colloquium on Spectral Signatures in Remote Sensing Apr. 1988 p 25-30 Sponsored by Begeleidingscommissie Remote Sensing, Delft, The Netherlands (For primary document see N89-10305 01-43)
Copyright Avail: NTIS HC A23/MF A01; ESA Publications Division, ESTEC, Noordwijk, Netherlands 80 Dutch guilders

The X-band radar backscatter from beet, peas, and potatoes was analyzed in relation to crop growth, to changes in canopy morphology, and to meteorological data. The cloud model for microwave backscatter from vegetation is used to describe the backscatter during the growing season. The results for 1 yr are used to predict the backscatter in another year at another location. The general trend in X-band microwave backscatter from these crops can be fairly well described by the model. However large erratic fluctuations in the observed microwave backscatter remain unexplained. These are probably due to instantaneous changes in canopy geometry which can be caused by meteorological conditions. ESA

N89-10310# Institut National de la Recherche Agronomique, Montfavet (France). Station de Bioclimatologie.
COMPLEMENTARY OF MICROWAVE AND OPTICAL RANGE IN THE CHARACTERIZATION OF CROPS BY REMOTE SENSING [COMPLEMENTARITE DES HYPERFREQUENCES ET DU DOMAINE OPTIQUE DANS LA CARACTERISATION DES CULTURES PAR TELEDETECTION]
I. Champion, L. Prevot, G. Rondeaux, F. Baret, and G. Guyot *In* ESA, Proceedings of the 4th International Colloquium on Spectral Signatures in Remote Sensing Apr. 1988 p 31-36 In FRENCH (For primary document see N89-10305 01-43)
Copyright Avail: NTIS HC A23/MF A01; ESA Publications Division, ESTEC, Noordwijk, Netherlands 80 Dutch guilders

The possibility of using the SPOT optical (red and near infrared) and microwave (C and X) bands in a complementary manner for crop characterization was studied using data acquired for winter wheat over a 2 yr period. Simplified models of reflectance and backscatter in which the main variables are leaf area index and surface soil moisture are used to compare the sensitivity of each spectral band. Estimation accuracy for one variable when the uncertainty for the other is known is evaluated. The domain in which model inversion is also possible is defined for four measurement configurations (SPOT XS2 and XS3 and bands C and X). It is shown that leaf area index can be estimated with acceptable accuracy in an index range from 0.6 to 3 in the red channel, 1.25 to 6 in the near infrared, and from 2.5 in the X-band. Soil moisture is measured well in C-band. Strategies for using the measurements to complement each other, e.g., replacing optical sensors with X-band in cloudy conditions, are suggested. ESA

N89-10311# Institut National de la Recherche Agronomique, Montfavet (France). Station de Science du Sol.
USE OF MICROWAVE BACKSCATTER MEASUREMENTS AS BOUNDARY CONDITIONS IN SOIL/ATMOSPHERE WATER TRANSFER MODELING
H. Witono and L. Bruckler *In* ESA, Proceedings of the 4th International Colloquium on Spectral Signatures in Remote Sensing Apr. 1988 p 37-42 (For primary document see N89-10305 01-43)
Copyright Avail: NTIS HC A23/MF A01; ESA Publications Division, ESTEC, Noordwijk, Netherlands 80 Dutch guilders

Results derived from a numerical soil-atmosphere heat and mass flows model are compared to field data when soil surface water contents derived from microwave measurements are used. Field experiments were performed on a bare soil (27.2 percent clay) using a scatterometer to measure volumetric water content and temperature profiles. Results show that satisfactory estimates for actual evaporation and water contents are obtained when microwave measurements are used as boundary conditions, but simplified approaches are to be developed for practical uses. ESA

N89-10312# Centre National d'Etudes Spatiales, Toulouse (France).
A RADAR REFLECTOR FOR MICROWAVE REMOTE SENSING INSTRUMENTS EXTERNAL CALIBRATION
J.-M. Lopez, O. Llopis, and M. Perennes (Ecole Nationale Superieure des Telecommunications, Brest, France) *In* ESA, Proceedings of the 4th International Colloquium on Spectral Signatures in Remote Sensing Apr. 1988 p 43-46 (For primary document see N89-10305 01-43)
Copyright Avail: NTIS HC A23/MF A01; ESA Publications Division, ESTEC, Noordwijk, Netherlands 80 Dutch guilders

Software to predict the theoretical radar cross section (RCS) main pattern of trihedral reflectors is described. The software is usable for complex shape trihedral reflectors. The example of the compensated reflector is illustrated, with application to a medium angular coverage and a flat RCS pattern. The advantages of such reflectors are shown in comparison with the classical one. ESA

N89-10313# Paris VI Univ. (France).
EVALUATION OF VARAN DATA IN GEOLOGY AND GEOMORPHOLOGY IN THE SOUTHEAST OF FRANCE [EVALUATION DES DONNEES VARAN EN GEOLOGIE ET EN GEOMORPHOLOGIE SUR LE SUD-EST DE LA FRANCE]
J. P. Rudant, B. Cervelle, J. Chorowicz, P. Durand, P. Kamoun, S. Louahala, L. Polidori, S. Riazanoff, A. Simonin, and I. Tannous (Paris VII Univ., France) *In* ESA, Proceedings of the 4th International Colloquium on Spectral Signatures in Remote Sensing Apr. 1988 p 47-50 In FRENCH (For primary document see N89-10305 01-43)
Copyright Avail: NTIS HC A23/MF A01; ESA Publications Division, ESTEC, Noordwijk, Netherlands 80 Dutch guilders

The utility of synthetic aperture radar imagery for geology and geomorphology was assessed using the VARAN airborne system. Filtering, pattern recognition, multisource data superpositioning, and stereoscopy are discussed. Image interpretation and digital terrain models are considered. Advantages of the technique over traditional aerial photography and spaceborne imagery are shown. ESA

N89-10314# Universite Catholique de Louvain (Belgium). Lab. de Telecommunications et d'Hyperfrequences.
A THREE DEGREE-OF-FREEDOM DESCRIPTION OF THE OCEAN SURFACE FOR MICROWAVE REMOTE SENSING OF WAVE HEIGHT AND WIND FRICTION VELOCITY
C. Baufays, A. Guissard, and P. Sobieski *In* ESA, Proceedings of the 4th International Colloquium on Spectral Signatures in Remote Sensing Apr. 1988 p 55-61 (For primary document

see N89-10305 01-43)
Copyright Avail: NTIS HC A23/MF A01; ESA Publications Division, ESTEC, Noordwijk, Netherlands 80 Dutch guilders

A sea surface displacement spectral model which combines three components in a unique spectrum with three degrees of freedom is proposed. This spectral model is described through two internal parameters and the wind friction velocity. Comparisons are made with wind dependent models and with sea data gathered by McClain et al (1982). The application of this model for electromagnetic scattering calculation is under study, showing results nearest the reality in the parameters of propagation during a satellite-ship mobile link with grazing angles. ESA

N89-10315# Marconi Co. Ltd., Great Baddow (England).
THE USE OF THE COMPLEX CORRELATION FUNCTION IN THE RECOVERY OF OCEAN WAVE SPECTRA FROM SAR IMAGES
R. A. Cordey and J. T. Macklin *In* ESA, Proceedings of the 4th International Colloquium on Spectral Signatures in Remote Sensing Apr. 1988 p 63-67 (For primary document see N89-10305 01-43)
(Contract ESA-6878/87-HGE-I(SC))
Copyright Avail: NTIS HC A23/MF A01; ESA Publications Division, ESTEC, Noordwijk, Netherlands 80 Dutch guilders

A method to predict the wavenumber dependence of the speckle component in spectra of synthetic-aperture radar intensity images was tested using data from VARAN-S and Seasat systems. The method uses the correlation function of the corresponding complex images and assumes that pixel statistics are Gaussian. It is expected that such a technique will be of use in the routine recovery of ocean wave height spectra from SAR imagery. Results from the Agrisar campaign with VARAN-S over land and sea are good, with speckle spectra being well matched by their predicted forms. Ocean spectra from Seasat are, however, poorly matched in their dependence on azimuth wavenumber. This is not thought to be caused by any sea surface or propagation effect but rather to be an artifact of signal processing. ESA

N89-10316# Centre National d'Etudes Spatiales, Toulouse (France).
COMPARISON BETWEEN ACTIVE AND PASSIVE MICROWAVE MEASUREMENTS OVER ANTARCTICA
F. Remy, M. Anderson (Scripps Institution of Oceanography, La Jolla, Calif.), and J. F. Minster *In* ESA, Proceedings of the 4th International Colloquium on Spectral Signatures in Remote Sensing Apr. 1988 p 69-72 (For primary document see N89-10305 01-43)
Copyright Avail: NTIS HC A23/MF A01; ESA Publications Division, ESTEC, Noordwijk, Netherlands 80 Dutch guilders

The effects of wind on the snow grain size derived from passive microwave radiometer data above continental ice was examined. Wind speed is provided by the power return of the Seasat altimeter measurements. The grain size is derived from the emissivity estimated from 37 GHz NIMBUS-7 radiometer. All possible interactions between the retrieved parameters are reviewed. The role of the wind on the thermal history of ice grains seems to be a dominant factor, while other effects are either insignificant or account for less than 10 percent of the emissivity variance. ESA

N89-10317# State Univ. of New York, Binghamton.
A PERSPECTIVE ON VEGETATION CANOPY REFLECTANCE MODELS
N. S. Goel *In* ESA, Proceedings of the 4th International Colloquium on Spectral Signatures in Remote Sensing Apr. 1988 p 77-85 (For primary document see N89-10305 01-43)
Copyright Avail: NTIS HC A23/MF A01; ESA Publications Division, ESTEC, Noordwijk, Netherlands 80 Dutch guilders

Factors which affect the spectral signature of or reflectance from a vegetation canopy are delineated. Canopy reflectance models which attempt to incorporate these factors are reviewed. A technique for estimating important biophysical parameters like leaf area index, leaf angle distribution, and canopy architecture, through inversion of these models is reviewed. ESA

N89-10318*# National Aeronautics and Space Administration. Goddard Space Flight Center, Greenbelt, Md.
THE SPECTRAL BIDIRECTIONAL REFLECTANCE OF SNOW
J. Dozier, R. E. Davis (Sierra Nevada Aquatic Research Lab., Mammoth Lakes, Calif.), A. T. C. Chang, and K. Brown *In* ESA, Proceedings of the 4th International Colloquium on Spectral Signatures in Remote Sensing Apr. 1988 p 87-92 Sponsored in cooperation with JPL, Calif. Inst. of Technology, Pasadena; and California Univ., Santa Barbara (For primary document see N89-10305 01-43)
Copyright Avail: NTIS HC A23/MF A01; ESA Publications Division, ESTEC, Noordwijk, Netherlands 80 Dutch guilders CSCL 02F

A radiative transfer model for the bidirectional reflectance-distribution function (BRDF) shows that snow is moderately anisotropic in the near-infrared wavelengths. Although the directional-hemispherical albedo of snow decreases as the grains become larger, the forward scattering also increases, with the result that the illumination and viewing geometry must be considered when interpreting physical properties of the surface layer of the snow pack from remote sensing data. Measurements of the BRDF for a variety of snow conditions were made throughout the winter and spring seasons with a spectroradiometer, for wavelengths from 0.38 to 1.11 microns. Coincident with these the surface grain properties were analyzed by stereological methods. The data show that Mie scattering calculations using an equivalent spherical radius match the directional-hemispherical reflectance, but the BRDF usually shows a small peak in the backscattered direction that would not occur from spherical grains. The sphere with the same surface-to-volume ratio as the ice grains is used as the equivalent sphere. ESA

N89-10319# Institut National de la Recherche Agronomique, Montfavet (France). Station de Bioclimatologie.
SPECTRAL PROFILE AND BIOMASS ESTIMATION [PROFIL SPECTRAL ET ESTIMATION DE LA BIOMASSE]
F. Baret, G. Guyot, J. M. Teres, and D. Rigal *In* ESA, Proceedings of the 4th International Colloquium on Spectral Signatures in Remote Sensing Apr. 1988 p 93-98 In FRENCH (For primary document see N89-10305 01-43)
Copyright Avail: NTIS HC A23/MF A01; ESA Publications Division, ESTEC, Noordwijk, Netherlands 80 Dutch guilders

A procedure to estimate biomass production of a crop from the proportion of photosynthetic active energy (PAR) absorbed by the canopy (Sigma i) is outlined. It is shown that Sigma i is functionally linked to the radiometric response of the crop, and an analytic method to estimate it is outlined. It explicitly accounts for factors such as Sun position, canopy structure, and soil optical properties normally treated implicitly. Its use requires the inversion of reflectance models in order to deduce canopy parameters from radiometric data. These parameters can be input to a PAR absorptance model to estimate Sigma i. The data obtained can be used in a canopy function model to estimate crop yield. ESA

N89-10320# Rijkswaterstaat, Delft (Netherlands).
VALIDATION OF AN ATMOSPHERIC CORRECTION METHOD FOR SATELLITE BORNE IMAGERY
J. M. M. Kokke, H. T. C. vanStokkom, J. F. DeHaan, and J. W. Hovenier (Vrije Universiteit, Amsterdam, Netherlands) *In* ESA, Proceedings of the 4th International Colloquium on Spectral Signatures in Remote Sensing Apr. 1988 p 99-104 (For primary document see N89-10305 01-43)
Copyright Avail: NTIS HC A23/MF A01; ESA Publications Division, ESTEC, Noordwijk, Netherlands 80 Dutch guilders

In order to evaluate an atmospheric correction method for multispectral satellite borne imagery in the visible, validation experiments were carried out for the applied simplified radiative transfer method (SMART-method). This was performed by comparing the computed results and obtained correction parameters for a number of theoretical situations with those of an exact method which provides high quality data. It is concluded that the SMART-method is sufficiently accurate under the circumstances commonly to be expected. The ground-based

spectroradiometers used in the correction method were preliminary calibrated in an absolute sense by assessing the frequency characteristics of the spectral channels. ESA

N89-10321# Centre d'Etude Spatiale des Rayonnements, Toulouse (France).
RETRIEVING VEGETATION AND SOIL PARAMETERS FROM RADAR MEASUREMENTS
Alphonse LeToan and T LeToan *In* ESA, Proceedings of the 4th International Colloquium on Spectral Signatures in Remote Sensing Apr. 1988 p 105-111 (For primary document see N89-10305 01-43)
Copyright Avail: NTIS HC A23/MF A01; ESA Publications Division, ESTEC, Noordwijk, Netherlands 80 Dutch guilders

An approach for inverting radar measurements into soil and vegetation volumetric moisture content is presented. The approach consists in using a theoretical model (Eom and Fung, 1984) to simulate the radar responses to a wide range of vegetation and soil parameters. The simulated data are used in a sensitivity study to determine the validity conditions for inversion; and to derive fitting parameters of a semi-empirical model selected for inversion. The results obtained on soybean canopies at C-band and 20 deg of incidence are presented. Inversion is shown to be possible. ESA

N89-10322# Institut National de la Recherche Agronomique, Montfavet (France). Station de Bioclimatologie.
A SIMPLIFIED VEGETATION CANOPY REFLECTANCE AND ABSORPTION MODEL [UN MODELE SIMPLIFIE DE REFLECTANCE ET D'ABSORPTANCE D'UN COUVERT VEGETAL]
F. Baret *In* ESA, Proceedings of the 4th International Colloquium on Spectral Signatures in Remote Sensing Apr. 1988 p 113-120 In FRENCH (For primary document see N89-10305 01-43)
Copyright Avail: NTIS HC A23/MF A01; ESA Publications Division, ESTEC, Noordwijk, Netherlands 80 Dutch guilders

A model giving vegetation canopy reflectance and diffuse transmittance and reflectance for vertical view angles is outlined. It is based on a Beer's law type formalism. It takes explicitly into account characteristic canopy parameters and the optical properties of its elements, as well as Sun position. The model correctly reproduces data obtained from the Suits model, on which it was adjusted. The simplified formalism facilitates inversion and allows a clear interpretation of canopy spectral response in terms of amplitude and rate of variation of reflectance (or transmittance) as a function of the leaf area index. It also allows spectral reflectance in different spectral domains to be linked, and linking of reflectance to absorptance. ESA

N89-10323# Institut National de la Recherche Agronomique, Thiverval-Grignon (France). Station de Bioclimatologie et Teledetection.
POTENTIAL NUMBER OF WINTER WHEAT EARS ESTIMATION USING RADIOMETRY TECHNIQUES AT AN EARLY STAGE
P. Boissard, J.-G. Pointel, P. Leterme, and O. Buisson *In* ESA, Proceedings of the 4th International Colloquium on Spectral Signatures in Remote Sensing Apr. 1988 p 121-124 In FRENCH; ENGLISH summary (For primary document see N89-10305 01-43)
Copyright Avail: NTIS HC A23/MF A01; ESA Publications Division, ESTEC, Noordwijk, Netherlands 80 Dutch guilders

Agronomical studies showed that it is possible to estimate the potential number of winter wheat ears from dry biomass measurement at an early stage. The potential number of ears is reached without any stress condition (light excepted) and provides one of the yield components. Using radiometric measurements in SPOT bands, it is shown that dry biomass can be estimated in a range 0 to 200 g/sqm with r sq coefficient = 0.87 (+ or - 40 g/sqm at 95 percent confidence interval, corresponding to + or - 100 ears in the middle range of potential curves). Use of normalized difference to calculate a vegetation index must be discussed because this index is sensitive to incoming radiation variations. ESA

N89-10324# Institut National de la Recherche Agronomique, Montfavet (France). Station de Bioclimatologie.
INTRODUCING SPECTRAL DATA INTO A PLANT PROCESS MODEL FOR IMPROVING ITS PREDICTION ABILITY
R. Delecolle and M. Guerif *In* ESA, Proceedings of the 4th International Colloquium on Spectral Signatures in Remote Sensing Apr. 1988 p 125-127 (For primary document see N89-10305 01-43)
Copyright Avail: NTIS HC A23/MF A01; ESA Publications Division, ESTEC, Noordwijk, Netherlands 80 Dutch guilders

The feasibility of using vegetation index values from spectral data as inputs to AFRCWHEAT, a wheat simulation model, is studied. This is done by using an independent submodel of leaf area index (LAI) evolution which is iteratively corrected for each new LAI value estimated by normalized difference, and resuming the global simulation from sowing time. The prediction error is greatly decreased by the method, but the bias remains important. Constraining assumptions still remain like the robustness of the simulated development scale, which rules partitioning of assimilates and growth of vegetative organs. ESA

N89-10325# Los Alamos National Lab., N. Mex. Theoretical Div.
THE ANGULAR REFLECTANCE SIGNATURE OF THE CANOPY HOT SPOT IN THE OPTICAL REGIME
S. A. W. Gerstl *In* ESA, Proceedings of the 4th International Colloquium on Spectral Signatures in Remote Sensing Apr. 1988 p 129-132 (For primary document see N89-10305 01-43)
Copyright Avail: NTIS HC A23/MF A01; ESA Publications Division, ESTEC, Noordwijk, Netherlands 80 Dutch guilders

It is shown from experimental data and by modeling that the canopy hot spot angular reflectance signature carries information about plant stand architecture that is often more distinctive for different plant species than their spectral signatures. Model results show that the angular width of the hot spot reflectance distribution is highly correlated with the leaf size and canopy height. Atmospheric radiative transfer calculations indicate that such angular signatures are invariant to atmospheric perturbations. Thus, the hot spot of plant canopies is recognized as an angular reflectance signature that carries information about the plant stand architecture which may be useful for instant crop identification from off-nadir satellite measurements. ESA

N89-10326*# State Univ. of New York, Binghamton.
A MODEL FOR RADIATIVE TRANSFER IN HETEROGENEOUS THREE-DIMENSIONAL CANOPIES
N. S. Goel and T. Grier *In* ESA, Proceedings of the 4th International Colloquium on Spectral Signatures in Remote Sensing Apr. 1988 p 133-136 Sponsored by NASA (For primary document see N89-10305 01-43)
Copyright Avail: NTIS HC A23/MF A01; ESA Publications Division, ESTEC, Noordwijk, Netherlands 80 Dutch guilders CSCL 02F

A model, dubbed TRIM, for the interaction of electromagnetic radiation with inhomogeneous vegetation canopies is presented. It is based on the four flux theory for homogeneous canopies. The canopy is assumed to consist of ellipsoidal subcanopies located on the ground at periodic intervals. The model is inverted with field measured data for reflectance from corn canopies in the near infrared region. It is shown that TRIM correctly identifies the architecture of the canopy (homogeneous or row canopy, percentage of ground cover) and gives a good estimate of leaf area index. ESA

N89-10327# Institut National de la Recherche Agronomique, Montfavet (France).

BIOMASS AND WHEAT CROP YIELD ESTIMATION FROM SPOT VEGETATIVE INDEXES [ESTIMATION DE LA BIOMASSE DU RENDEMENT DE CULTURES DE BLE DUR A PARTIR DES INDICES DE VEGETATION SPOT]

M. Guerif, R. Delecolle, X. Gu, J. P. Guinot, M. Jappiot, and S. Steinmetz *In* ESA, Proceedings of the 4th International Colloquium on Spectral Signatures in Remote Sensing Apr. 1988 p 137-141 In FRENCH Sponsored by the Conseil General de la Region P.A.C.A., France (For primary document see N89-10305 01-43)

Copyright Avail: NTIS HC A23/MF A01; ESA Publications Division, ESTEC, Noordwijk, Netherlands 80 Dutch guilders

A two stage method for regional estimation of wheat crop yield from data is presented. Biomass is estimated from vegetative index using an extremely simplified formalism derived from models of the interaction of radiation with vegetation canopy and photosynthesis. Crop yield or its components are estimated from the biomass. The model was validated over a dozen plots, and improvements are suggested. The difficulty of treating the great variety of crop situations found at regional level is stressed. ESA

N89-10328# Centre National d'Etudes Spatiales, Toulouse (France).

SPECTRAL CHARACTERIZATION OF FOREST TARGETS IN MOUNTAINOUS ZONES ON THEMATIC MAPPER IMAGES [CARACTERISATION SPECTRALE DE CIBLES FORESTIERES EN ZONE DE MONTAGE SUR DES DONNEES DU THEMATIC MAPPER]

C. Leprieur, J.-M. Durand, and J.-L. Peyron *In* ESA, Proceedings of the 4th International Colloquium on Spectral Signatures in Remote Sensing Apr. 1988 p 143-146 In FRENCH (For primary document see N89-10305 01-43)

Copyright Avail: NTIS HC A23/MF A01; ESA Publications Division, ESTEC, Noordwijk, Netherlands 80 Dutch guilders

Analysis and representation of the evolution of the LANDSAT Thematic Mapper signal of forests were used to characterize the variability of the responses. The forests are representative of relief conditions in temperate European regions. The proportion of the variability explained by the nature of the target and that induced by modification of acquisition geometry are quantified for each spectral domain. Directional effects proper to each forest species are shown. It is concluded that the signal is relatively little dependent on observation conditions. The greatest part of signal variability is linked to thematic texture. ESA

N89-10329# Southampton Univ. (England). Dept. of Geography.

A SIMPLIFIED REFLECTANCE MODEL FOR SHRUB CANOPIES

E. J. Milton and E. M. Rollin *In* ESA, Proceedings of the 4th International Colloquium on Spectral Signatures in Remote Sensing Apr. 1988 p 147-150 (For primary document see N89-10305 01-43)

Copyright Avail: NTIS HC A23/MF A01; ESA Publications Division, ESTEC, Noordwijk, Netherlands 80 Dutch guilders

A simplified descriptive model of the angular reflectance of shrub canopies based on data from a spectroradiometer is presented. The directional reflectance observed at the solar zenith angle for a range of azimuth angles is discussed. A marked minimum in reflectance relative to nadir when viewing up-Sun and a localized peak (in visible wavelengths especially), when viewing down-Sun are both features characteristic of the heather (Calluna vulgaris) canopies studied. These relationships are encapsulated in a simple graphic device: that of an imaginary landscape. This is seen as a necessary first step towards an analytical model for shrub canopies. ESA

N89-10330# Sherbrooke Univ. (Quebec).

ANALYSIS OF THE CONTRIBUTION OF THE ATMOSPHERE TO WATER REFLECTANCE IN THE FIRST TWO CHANNELS OF THE NOAA SATELLITES AVHRR [ANALYSE DE LA CONTRIBUTION DE L'ATMOSPHERE A LA REFLECTANCE DE L'EAU DANS LES DEUX PREMIERS CANAUX AVHRR DES SATELLITES NOAA]

A. Royer, L. Chartier, and P. Cote *In* ESA, Proceedings of the 4th International Colloquium on Spectral Signatures in Remote Sensing Apr. 1988 p 151-156 In FRENCH (For primary document see N89-10305 01-43)

Copyright Avail: NTIS HC A23/MF A01; ESA Publications Division, ESTEC, Noordwijk, Netherlands 80 Dutch guilders

Optical thickness of aerosols was determined from water reflectance. The signal measured at the sensor is modeled according to four components: volumetric reflectance of water; diffuse specular reflectance; direct specular reflectance as a function of wind speed; and atmospheric reflectance. The contributions of these factors is analyzed in terms of view angle for different turbidity and wind conditions. It is shown that even outside critical zones, the relative terms of surface phenomena can be superior to other components. The amplitude of calculated variations compares well with those observed on three NOAA AVHRR image pairs for successive orbits. Model validation results using ground measurements, however, indicate an overestimation of optical thicknesses. ESA

N89-10331# National Aerospace Lab., Amsterdam (Netherlands).

NUMERICAL ACCURACY OF A TWO-STREAM RADIATIVE TRANSFER MODEL FROM COMPARISON WITH AN N-STREAM MODEL

W. Verhoef *In* ESA, Proceedings of the 4th International Colloquium on Spectral Signatures in Remote Sensing Apr. 1988 p 157-162 (For primary document see N89-10305 01-43)

Copyright Avail: NTIS HC A23/MF A01; ESA Publications Division, ESTEC, Noordwijk, Netherlands 80 Dutch guilders

A relatively simple radiative transfer model, based on scattering and extinction of two-isotropic diffuse fluxes and two direct fluxes (solar beam and radiance in the viewing direction), was applied to vegetation canopies and to the atmosphere. For comparison, a model, with vectorized Kubelka-Munk equations and with the two additional direct fluxes, was implemented for $N = 72$, which can be assumed accurate enough for remote sensing applications. Calculations were carried out for the scattering of light by atmospheric haze, which is a medium that is most difficult to model, in order to evaluate the accuracy of the simple model under a number of simulated circumstances, given by optical thickness and observation geometry. The results for the simple-model show that in the region of small off-nadir viewing angles (e.g., up to 30 deg) application is feasible if errors of up to 10 percent maximum are acceptable. ESA

N89-10332# Institut National de la Recherche Agronomique, Thiverval-Grignon (France). Station de Bioclimatologie.

ESTIMATION OF THE INTERCEPTION EFFICIENCY OF AN ALFALFA CANOPY FROM A VEGETATIVE INDEX [ESTIMATION DE L'EFFICIENCE DE L'INTERCEPTION D'UN COUVERT DE LUZERNE A PARTIR D'UN INDICE DE VEGETATION]

J. M. Allirand, M. Chartier, and G. Gosse *In* ESA, Proceedings of the 4th International Colloquium on Spectral Signatures in Remote Sensing Apr. 1988 p 163-166 In FRENCH (For primary document see N89-10305 01-43)

Copyright Avail: NTIS HC A23/MF A01; ESA Publications Division, ESTEC, Noordwijk, Netherlands 80 Dutch guilders

It is shown that the interception efficiency of an alfalfa canopy, needed to estimate yield, can be estimated from a combination of visible and near infrared reflectances obtained with sensors with a semihemispherical field of view, commonly used in agronomy. The obtained relationship depends essentially on soil optical properties. ESA

N89-10333# Institut National de la Recherche Agronomique, Thiverval-Grignon (France). Station de Bioclimatologie.
RELATION BETWEEN SUGAR BEET CROP YIELD AND VEGETATIVE INDEXES CALCULATED FROM LANDSAT MSS IMAGES [RELATION ENTRE LE RENDEMENT DE CULTURES DE BETTERAVE A SUCRE ET DES INDICES DE VEGETATION CALCULES A PARTIR D'IMAGES LANDSAT MSS]
B. Andrieu and J. Caneill *In* ESA, Proceedings of the 4th International Colloqium on Spectral Signatures in Remote Sensing Apr. 1988 p 167-170 In FRENCH Sponsored by CNES/CNRS, France (For primary document see N89-10305 01-43)
Copyright Avail: NTIS HC A23/MF A01; ESA Publications Division, ESTEC, Noordwijk, Netherlands 80 Dutch guilders

Images from LANDSAT MSS were used to calculate radiometric growth indexes for 42 sugar beet parcels on July 31 and Sept. 4, and soil radiance index on Jan. 1. Yield was estimated on the ground by geometric weighing at the end of October. The proportion of yield variance explained by radiometric indexes depends mainly on the number of pixels which could be taken into account for the radiometric characterization of the parcels. A bilinear regression using the growth index in September and the radiance index in January enables 86 percent of the variance in sugar yield to be explained for parcels containing at least 8 pure pixels. ESA

N89-10334# Sheffield Univ. (England). Dept. of Geography.
DEVELOPING A RADIOMETRIC LEAF AREA INDEX
P. J. Curran and N. W. Wardley *In* ESA, Proceedings of the 4th International Colloquium on Spectral Signatures in Remote Sensing Apr. 1988 p 171-173 Sponsored by the Natural Environment Research Council, London, England (For primary document see N89-10305 01-43)
Copyright Avail: NTIS HC A23/MF A01; ESA Publications Division, ESTEC, Noordwijk, Netherlands 80 Dutch guilders

A measure of vegetation amount that is sensitive to canopy geometry was developed. This measure, termed the radiometric leaf area index (RLAI), comprises measurements of LAI, leaf inclination or curvature and the area of the canopy visible to the sensor. The RLAI was evaluated on simulated data and proves to be sensitive to canopy geometry. ESA

N89-10335*# Scripps Institution of Oceanography, La Jolla, Calif. California Space Inst.
SENSITIVITY OF SATELLITE-DERIVED NET SHORTWAVE IRRADIANCE AT THE EARTH'S SURFACE TO RADIOMETRIC CALIBRATION
C. Gautier and R. Frouin *In* ESA, Proceedings of the 4th International Colloquium on Spectral Signatures in Remote Sensing Apr. 1988 p 179-184 (For primary document see N89-10305 01-43)
(Contract NAS1-4195-C; NA86AA-D-AC051)
Copyright Avail: NTIS HC A23/MF A01; ESA Publications Division, ESTEC, Noordwijk, Netherlands 80 Dutch guilders CSCL 02F

The effect of radiometric calibration uncertainties on satellite-derived net shortwave irradiance at the Earth's surface was examined. Net shortwave irradiance sensitivity to calibration is expressed as a function of two basic components that depend on surface and cloud albedo sensitivities, respectively. The analysis of these sensitivities for a wide range of atmospheric and surface conditions, as well as radiation geometries, shows that a 10 percent uncertainty in the calibration induces up to 40 W/sqm errors in instantaneous net shortwave irradiance (negative when the calibration uncertainty is positive). The maximum relative errors are obtained in overcast conditions when cloud albedos are high. On a monthly time scale, the induced error becomes typically 13 W/sqm in the tropics and 16 W/sqm in higher latitude regions during summer. The error almost vanishes at high latitudes during winter. A 10 percent positive uncertainty in the calibration gives a net shortwave irradiance error similar to that induced by the 3 hr sampling of the ISCCP Project. ESA

N89-10336# Groupement Scientifique de Teledetection de Strasbourg (France).
ATTEMPT AT ABSOLUTE DETERMINATION OF SPECTRAL SIGNATURES OF BARE SOILS IN THE THERMAL INFRARED, IN EMISSION AND REFLECTION [ESSAI DE DETERMINATION ABSOLUE DES SIGNATURES SPECTRALES DE SOLS NUS DANS L'INFRAROUGE THERMIQUE, EN EMISSION ET EN REFLEXION]
F. Nerry, J. Labed, and M. P. Stoll *In* ESA, Proceedings of the 4th International Colloquium on Spectral Signatures in Remote Sensing Apr. 1988 p 185-188 In FRENCH Sponsored by CNES, France (For primary document see N89-10305 01-43)
Copyright Avail: NTIS HC A23/MF A01; ESA Publications Division, ESTEC, Noordwijk, Netherlands 80 Dutch guilders

An autocalibration based method for estimating spectral emissivity signatures, without radiation temperature measurements, and without any a priori hypothesis, is discussed. Relative accuracy is + or - 0.6 percent. Measurement of spectral signatures in reflection confirm the emission results. Natural materials, minerals, and cultivated soils illustrate the measurement possibilities. ESA

N89-10337# Iceland Univ., Reykjavik. Lab. for Information Technology and Signal Processing.
STRENGTHS AND SHORTCOMINGS IN AIRBORNE THEMATIC MAPPER (ATM) TECHNOLOGY AS APPLIED TO VOLCANIC AND GEOTHERMAL AREAS IN ICELAND
S. Bjornsson and K. Arnason (Technische Univ., Munich, West Germany) *In* ESA, Proceedings of the 4th International Colloquium on Spectral Signatures in Remote Sensing Apr. 1988 p 189-191 (For primary document see N89-10305 01-43)
Copyright Avail: NTIS HC A23/MF A01; ESA Publications Division, ESTEC, Noordwijk, Netherlands 80 Dutch guilders

Experiments with an airborne thermal scanner of conventional design were conducted to test the applicability of airborne thematic mappers to geothermal research in Iceland. Results from two thermal areas which show strengths and shortcomings of the method as commonly applied are presented. The technology provides much better global data on the spatial distribution of surface temperatures than any other previously obtained. Sites of convective thermal output inside geothermal areas are readily discernible because of their relatively high temperatures, but in areas where heat conduction plays a primary role, subtle temperature differences can not be differentiated, in particular on surface materials with varying emissivities. Due to lack of radiometric resolution, discrimination of slight temperature variations especially in regions of low to moderate temperatures is insufficient. The result of the observations led to the development of an improved thermal scanner in the 8 to 14 micron wavelength range. ESA

N89-10338*# National Aeronautics and Space Administration. Goddard Space Flight Center, Greenbelt, Md.
ATMOSPHERIC EFFECT REMOVAL FROM SPACE IMAGERY
Hongsuk H. Kim *In* ESA, Proceedings of the 4th International Colloquium on Spectral Signatures in Remote Sensing Apr. 1988 p 193-196 (For primary document see N89-10305 01-43)
Copyright Avail: NTIS HC A23/MF A01; ESA Publications Division, ESTEC, Noordwijk, Netherlands 80 Dutch guilders CSCL 02F

A method to derive a ground reflectance scene from space imagery by removing the contribution of atmospheric radiance was developed. The method utilizes a multiple scattering radiative transfer code to model the Earth-atmosphere system and converts the output into a set of quadratic coefficients which best fit the relationships between the upwelling radiance reaching the sensor and the lower boundary conditions of the ground reflectance. Pixel by pixel correction of the atmospheric effects is done by invoking these coefficients. The algorithm was applied to a number of Thematic Mapper and CZCS data to generate interesting ground scenes and was used to simulate space imagery from ground reflectance scenes. ESA

N89-10339# Linkoeping Univ. (Sweden). Dept. of Electrical Engineering.

ATMOSPHERIC CORRECTION OF THERMAL INFRARED DATA FROM LANDSAT-5 FOR SURFACE TEMPERATURE ESTIMATION

S. Axelsson and B. Lunden (Stockholm Univ., Sweden) *In* ESA, Proceedings of the 4th International Colloquium on Spectral Signatures in Remote Sensing Apr. 1988 p 197-200 Sponsored by the Swedish Board for Space Activities, Stockholm, Sweden and the Swedish Natural Science Research Council, Stockholm, Sweden (For primary document see N89-10305 01-43)

Copyright Avail: NTIS HC A23/MF A01; ESA Publications Division, ESTEC, Noordwijk, Netherlands 80 Dutch guilders

The information of the LANDSAT-5 thermal channel was assessed using two satellite registrations over the Stockholm area. Atmospheric corrections are predicted from a multilayer radiative transfer model, in which the temperature and water vapor attenuation of each layer is estimated from radiosonde profiles of temperature, pressure, and specific humidity. The modeling of the water vapor attenuation, which dominates in the window 10.4 to 12.5 microns includes continuum and line absorption effects. The usefulness of the correction algorithm was verified by comparing water temperatures derived from TM band 6 data with in situ measurements. Another comparison was based on the temperature of conifers, which at moderate and high wind-speed is close to the air temperature. With access to radiosonde data and an atmospheric propagation model it seems possible to use LANDSAT TM band 6 for mapping of relative and absolute temperatures of natural surfaces. ESA

N89-10340# Groupement Scientifique de Teledetection de Strasbourg (France).

MULTISPECTRAL CHARACTERIZATION OF THE SPATIAL STRUCTURE OF REMOTELY SENSED SCENES [CARACTERISATION MULTISPECTRALE DE LA STRUCTURE SPATIALE DES SCENES TELEDETECTEES]

G. Ramstein and M. Raffy *In* ESA, Proceedings of the 4th International Colloquium on Spectral Signatures in Remote Sensing Apr. 1988 p 201-203 In FRENCH (For primary document see N89-10305 01-43)

Copyright Avail: NTIS HC A23/MF A01; ESA Publications Division, ESTEC, Noordwijk, Netherlands 80 Dutch guilders

The notion of regionalized variables used in geostatistics is applied to remote sensing to analyze the spatial organization of the image. The variogram concept is reviewed and it is shown that its modeling enables the structural parameters characterizing the different textures to be defined. The evolution of the variogram in the spectral domain translates the differentiation of textures according to wavelength. Modeling of the variogram also allows an optimal choice of spectral band for a textural classification. The covariogram widens the variogram concept and synthesizes the available spectral and spatial information. These notions lead to a resampling of the image based on the stochastic behavior of a scene in different spectral bands. ESA

N89-10341# Centre National d'Etudes Spatiales, Toulouse (France).

ANALYSIS OF DIRECTIONAL EFFECTS ON NOAA AVHRR

A. Begue, P. Y. Deschamps, A. Podaire, and D. Tanre (Universite des Sciences et Techniques de Lille, France) *In* ESA, Proceedings of the 4th International Colloquium on Spectral Signatures in Remote Sensing Apr. 1988 p 205-209 In FRENCH; ENGLISH summary (For primary document see N89-10305 01-43)

Copyright Avail: NTIS HC A23/MF A01; ESA Publications Division, ESTEC, Noordwijk, Netherlands 80 Dutch guilders

Using the NOAA AVHRR GAC data base for west Africa (a month of consecutive data for May 1985) and simultaneous measurements of atmospheric parameters, spectral response was analyzed according to imaging configuration (angles under which the target was viewed within a 130 deg range). This analysis was used to evaluate the importance of directional effects in raw data, extracted after sampling, on a target. The sensitivity of acquired measurements to an atmospheric correction (knowing the size and composition of aerosols) was studied. Interpretation of the results enables the possibility of inversing the signal after correction for atmospheric effects to be considered. ESA

N89-10342# Bonn Univ. (West Germany). Inst. fuer Pflanzenbau.

SPECTRAL REFLECTANCE OF SUGAR BEET AND WINTER WHEAT CANOPIES IN THE VISIBLE AND INFRARED DURING GROWTH

K. Dockter, J. Schellberg, W. Kuehbauch, C. vonRuesten, U. Tempelmann, and G. Kupfer *In* ESA, Proceedings of the 4th International Colloquium on Spectral Signatures in Remote Sensing Apr. 1988 p 211-216 (For primary document see N89-10305 01-43)

Copyright Avail: NTIS HC A23/MF A01; ESA Publications Division, ESTEC, Noordwijk, Netherlands 80 Dutch guilders

The spectral reflectivity of differently managed sugar beet and winter wheat crops was investigated during growth. Simultaneously plants were analyzed for parameters relevant to yield. Meteorological data were recorded to explain the effect of illumination conditions (e.g., cloudiness). Qualitative comparisons indicate typical relationships between plant parameters (leaf vitality, water stress and fungi impact, leaf inclination angle) and spectral response. Results of a plant model (hot spot, distribution and number of leaves) are presented. ESA

N89-10343# Valencia Univ. (Spain). Remote Sensing Group.

A THEORETICAL MODEL FOR INTERPRETING REMOTELY SENSED THERMAL INFRARED MEASUREMENTS OBTAINED OVER AGRICULTURAL AREAS

J. A. Sobrino, V. Caselles, and F. Becker (Groupement Scientifique de Teledetection de Strasbourg, France) *In* ESA, Proceedings of the 4th International Colloquium on Spectral Signatures in Remote Sensing Apr. 1988 p 217-220 (For primary document see N89-10305 01-43)

(Contract CAICyT-A-172/85)

Copyright Avail: NTIS HC A23/MF A01; ESA Publications Division, ESTEC, Noordwijk, Netherlands 80 Dutch guilders

A theoretical model to interpret remotely sensed thermal infrared measurements carried out over agricultural areas cultivated in rows was developed. Factors which take part in the definition of the effective emissivity and temperature (observation height, viewing angle, type of soil, dimensions and separation of vegetation) are analyzed. The model was validated in a citrus orchard during three typical nights of radiative cooling (clear sky and calmed wind). The model performs to an accuracy of 1 percent. ESA

N89-10344# Universite Catholique de Louvain (Belgium). Lab. de Telecommunications et d'Hyperfrequences.

AN APPROXIMATIVE MODEL FOR THE MICROWAVE BRIGHTNESS TEMPERATURE SCATTERED BY A ROUGH OPEN OCEAN SURFACE

P. Sobieski, A. Guissard, and C. Baufays *In* ESA, Proceedings of the 4th International Colloquium on Spectral Signatures in Remote Sensing Apr. 1988 p 221-224 (For primary document see N89-10305 01-43)

Copyright Avail: NTIS HC A23/MF A01; ESA Publications Division, ESTEC, Noordwijk, Netherlands 80 Dutch guilders

A modified two-scale model for scattering and emissivity calculations for the random rough sea surface is described. It produces a contracted approximated form of the radiative transfer equation including a scattering correction. This leads to a method simple and accurate enough for real-time inversion algorithms in microwave remote sensing. ESA

N89-10345# Deutsche Forschungs- und Versuchsanstalt fuer Luft- und Raumfahrt, Oberpfaffenhofen (West Germany). Inst. for Optoelectronics.

THERMAL INFRARED LASER SPECTROSCOPY: THE POTENTIAL OF DUAL ACTIVE/PASSIVE THERMAL INFRARED SENSORS FOR EARTH OBSERVATION

F. Lehmann and R. Richter *In* ESA, Proceedings of the 4th

International Colloquium on Spectral Signatures in Remote Sensing Apr. 1988 p 229-232 (For primary document see N89-10305 01-43)
Copyright Avail: NTIS HC A23/MF A01; ESA Publications Division, ESTEC, Noordwijk, Netherlands 80 Dutch guilders

Laboratory spectroscopic measurements and airborne campaigns to demonstrate the potential of CO2 laser systems for the discrimination and identification of natural and manmade materials are reviewed. The extremely high spectral resolution (0.1 nm) and multispectral reflectance measurement capability of CO2 laser spectrometers in the thermal infrared is a complementary, not competitive, method compared to passive thermal infrared sensors. The combination of multispectral active and passive sensors is a step to advanced thermal infrared remote sensing systems for the analysis and interpretation of spectral signatures, ground temperature estimation, and atmospheric effects. ESA

N89-10346# Joint Research Centre of the European Communities, Ispra (Italy).
TIME-RESOLVED LASER FLUORESCENSING: TRENDS AND APPLICATIONS
G. Bertolini, P. Camagni (Pavia Univ., Italy), C. Koechler, A. Pedrini, and A. Prosdocimi *In* ESA, Proceedings of the 4th International Colloquium on Spectral Signatures in Remote Sensing Apr. 1988 p 233-238 (For primary document see N89-10305 01-43)
Copyright Avail: NTIS HC A23/MF A01; ESA Publications Division, ESTEC, Noordwijk, Netherlands 80 Dutch guilders

Oil fluorosensing is reviewed. Fluorescent spectra from natural oil targets can be remotely sensed with available techniques of pulsed excitation and multispectral detection, so as to insure a consistent analysis of their time evolution, with sufficient sensitivity to follow simultaneously the time decay of separated spectral regions on the scale of nanoseconds. Therefore different classes of oils can be monitored in terms of specific signatures, linking decay times, wavelength, and emission efficiency of definite spectral components to the nature and composition of the oil in which they are contained. Criteria for fingerprinting can be derived on this basis. Monitoring of fluorescent and scattering phenomena in the water column are considered. ESA

N89-10347# Consiglio Nazionale delle Ricerche, Florence (Italy).
A NEW LIDAR SYSTEM FOR APPLICATIONS OVER LAND AND SEA
F. Castagnoli, G. Cecchi, L. Pantani, B. Radicati, P. Mazzinghi, A. Barbaro, and M. Romoli (Florence Univ., Italy) *In* ESA, Proceedings of the 4th International Colloquium on Spectral Signatures in Remote Sensing Apr. 1988 p 239-243 (For primary document see N89-10305 01-43)
Copyright Avail: NTIS HC A23/MF A01; ESA Publications Division, ESTEC, Noordwijk, Netherlands 80 Dutch guilders

The use of fluorescence lidars for environmental monitoring was studied. A sensor prototype was designed and built to operate as a fluorescence lidar and a passive spectrometer in the visible, in both cases with a high spectral resolution. Field experiments on sea and vegetation remote sensing show that the sensor can detect fluorescence and Raman spectra in different water conditions, and can be used to detect photosynthesis behavior. ESA

N89-10348# Karlsruhe Univ. (West Germany). Inst. of Botany.
CHANGES IN THE CHLOROPHYLL FLUORESCENCE SPECTRA DURING THE KAUTSKY INDUCTION KINETICS
H. K. Lichtenthaler and C. Buschmann *In* ESA, Proceedings of the 4th International Colloquium on Spectral Signatures in Remote Sensing Apr. 1988 p 245-250 (For primary document see N89-10305 01-43)
Copyright Avail: NTIS HC A23/MF A01; ESA Publications Division, ESTEC, Noordwijk, Netherlands 80 Dutch guilders

An optical multichannel analyzer was used to screen the in situ chlorophyll fluorescence signatures of vegetation. It permits the fast registration of fluorescence spectra during the Kautsky induction kinetic. From the digitized data the induction kinetics at any given wavelength-range can be traced and the ratio F690/F735 and the Rfd-values determined. Though the ratio F690/F735 changes during the fluorescence induction kinetics, the changes are small compared to the differences between leaves of different chlorophyll content and different photosynthetic activity of stressed or damaged plants. Results demonstrate that the ratio F690/F735 is a very suitable fluorescence parameter to develop an airborne system for the remote sensing of chlorophyll fluorescence of terrestrial plants. ESA

N89-10349# Karlsruhe Univ. (West Germany). Inst. of Botany.
CHLOROPHYLL FLUORESCENCE SPECTRA OF LEAVES AS INDUCED BY BLUE LIGHT AND RED LASER LIGHT
H. K. Lichtenthaler and U. Rinderle *In* ESA, Proceedings of the 4th International Colloquium on Spectral Signatures in Remote Sensing Apr. 1988 p 251-254 Sponsored by the Joint Research Center of the European Communities, Ispra, Italy (For primary document see N89-10305 01-43)
Copyright Avail: NTIS HC A23/MF A01; ESA Publications Division, ESTEC, Noordwijk, Netherlands 80 Dutch guilders

The dependence of the chlorophyll-fluorescence emission spectra of green plant tissue (leaves, needles) on the wavelength of the excitation light was determined and the differences in the spectra were quantified by the fluorescence ratio F690/F735. The differences in the ratio F690/F735, which can be taken as indicator of stress to plants, using either blue (470 + or - 30 nm) or red excitation light (620 + or - 20 nm or He/Ne-laser 632.8 nm) are listed for leaves with different chlorophyll content and photosynthetic activity. The application of the ratio F690/F735 in detecting stress to terrestrial vegetation via remote sensing of laser-induced chlorophyll fluorescence is discussed. ESA

N89-10350# Kisarazu National Coll. of Technology (Japan). Faculty of Engineering.
LASER-INDUCED FLUORESCENCE ON IN-VIVO CHLOROPHYLL OF A RICE PLANT: A TECHNIQUE FOR THE REMOTE DETECTION OF PLANT GROWTH
K. Takahashi, T. Nakamura, Y. Emori, and A. Kimura (Chiba Univ., Japan) *In* ESA, Proceedings of the 4th International Colloquium on Spectral Signatures in Remote Sensing Apr. 1988 p 255-258 (For primary document see N89-10305 01-43)
Copyright Avail: NTIS HC A23/MF A01; ESA Publications Division, ESTEC, Noordwijk, Netherlands 80 Dutch guilders

The laser-induced fluorescence (LIF) of a rice plant is evaluated as a means of remotely detecting leaf color and estimating plant growth. The leaf color is influenced by quantity of chlorophyll contained in the leaf. Fluorescence intensity of in-vivo chlorophyll is changed by the amount of fertilizer used. Leaf color was measured in a rice field using a color scale. There are differences in its observation owing to the observer's individual character. In the LIF system, the fluorescence spectra of in-vivo chlorophyll are excited with a nitrogen laser emitting at 337.1 nm. By detecting changes in fluorescence intensity at 684 nm and 740 nm concerned with photosynthesis, rice plant growth is estimated. ESA

N89-10351# Paris XI Univ., Orsay (France). Lab. pour l'Utilisation du Rayonnement Electromagnetique.
TECHNIQUES FOR REMOTE SENSING OF LIFE SPAN AND QUANTUM YIELD OF CHLOROPHYLL FLUORESCENCE IN VIVO [TECHNIQUES POUR LA TELEDETECTION DE LA DUREE DE VIE ET DU RENDEMENT QUANTIQUE DE LA FLUORESCENCE DE LA CHLOROPHYLLE IN VIVO]
I. Moya, Y. Goulas, and J. M. Briantis *In* ESA, Proceedings of the 4th International Colloquium on Spectral Signatures in Remote Sensing Apr. 1988 p 259-262 In FRENCH (For primary document see N89-10305 01-43)
Copyright Avail: NTIS HC A23/MF A01; ESA Publications Division, ESTEC, Noordwijk, Netherlands 80 Dutch guilders

Use of laser induced fluorescence for remote sensing of chlorophyll from flying platforms is discussed. By refining the sensing it may be possible to attain the average life span of the fluorescence. Laboratory measurements under widely varying

conditions show that the average life span is in proportion to the quantum yield of the fluorescence. Quantum yield can be used to predict the physiological state of chlorophylls, but it is inaccessible to direct measurement. Measurement techniques which could be adapted to remote sensing are presented, including photon counting, phase fluorimetry, and ultrarapid oscilloscope. ESA

N89-10352# GKSS-Forschungszentrum Geesthacht (West Germany).
HIGH-RESOLUTION SPECTROSCOPY FOR REMOTE SENSING OF OCEAN AND ATMOSPHERE
R. Doeffer, J. Fischer, and H. Grassl *In* ESA, Proceedings of the 4th International Colloquium on Spectral Signatures in Remote Sensing Apr. 1988 p 267-272 (For primary document see N89-10305 01-43)
Copyright Avail: NTIS HC A23/MF A01; ESA Publications Division, ESTEC, Noordwijk, Netherlands 80 Dutch guilders

The benefits of using narrow spectral features, like chlorophyll fluorescence for the detection of phytoplankton and oxygen A-band absorption for the retrieval of cloud heights are demonstrated. Radiative transfer calculations are used because of the advantage of a systematic analysis of possible measurement conditions. However, the results are transferable to real conditions as far as the assumptions of a plane-parallel atmosphere-cloud or atmosphere-ocean system and the optical properties used in the radiative transfer model are valid. Results show that retrieval of concentrations of water substances is improved if the Sun stimulated chlorophyll fluorescence at 685 nm is measured with a spectral resolution of at least 5 nm. Spectral absorption within the oxygen A-band in the near infrared can be used for cloud-top height detection. ESA

N89-10353# Institute of Ocean Sciences, Sidney (British Columbia).
THE FLUORESCENCE LINE IMAGER: HIGH-RESOLUTION IMAGING SPECTROSCOPY OVER WATER AND LAND
J. F. R. Gower, G. A. Borstad, L. H. Gray, and H. R. Edel (Department of Fisheries and Environment, Ottawa, Ontario) *In* ESA, Proceedings of the 4th International Colloquium on Spectral Signatures in Remote Sensing Apr. 1988 p 273-278 (For primary document see N89-10305 01-43)
Copyright Avail: NTIS HC A23/MF A01; ESA Publications Division, ESTEC, Noordwijk, Netherlands 80 Dutch guilders

The FLI (Fluorescence Line Imager) airborne imaging spectrometer was designed and constructed as the first stage in developing an advanced satellite sensor based on CCD cameras. It was flown on a wide variety of airborne test flights to evaluate the applications of its higher resolution and sensitivity. The primary goal of the FLI was to image the spatial distribution of naturally stimulated fluorescence emission from chlorophyll A in phytoplankton in near surface sea and lake water. Sensitivity limit is 0.2 to 0.3 mg/cu m. Results also demonstrate other uses over a wide variety of targets on land and water. ESA

N89-10354# Institut National de la Recherche Agronomique, Montfavet (France). Station de Bioclimatologie.
USE OF HIGH SPECTRAL RESOLUTION TO FOLLOW THE STATE OF VEGETATION CANOPIES [UTILISATION DE LA HAUTE RESOLUTION SPECTRALE POUR SUIVRE L'ETAT DES COUVERTS VEGETAUX]
G. Guyot and F. Baret *In* ESA, Proceedings of the 4th International Colloquium on Spectral Signatures in Remote Sensing Apr. 1988 p 279-286 In FRENCH (For primary document see N89-10305 01-43)
Copyright Avail: NTIS HC A23/MF A01; ESA Publications Division, ESTEC, Noordwijk, Netherlands 80 Dutch guilders

The action mechanisms of factors which control the movement of the wavelength of a point of inflection lambda i of the reflectance curve of vegetation between the red and near infrared regions are analyzed at leaf and vegetation canopy scales. Variations of lambda i seem to carry the same type of information as the combination of measurements in wide spectral bands (normalized difference, ND). However the introduction of atmospheric effects in satellite measurements reveals that the value of lambda i is much less dependent on atmospheric conditions than ND. Thus a set of four or five narrow spectral bands is proposed to determine lambda i from satellite measurements in order to determine and follow the state of vegetation canopies. ESA

N89-10355# Institute for Image Processing Computer Mapping, Graz (Austria).
STRESS DETECTION IN MIXED CONIFEROUS-BROADLEAVED FORESTS FROM AIRBORNE IMAGING SPECTROMETER (AIS) DATA
C. Banninger *In* ESA, Proceedings of the 4th International Colloquium on Spectral Signatures in Remote Sensing Apr. 1988 p 287-290 (For primary document see N89-10305 01-43)
Copyright Avail: NTIS HC A23/MF A01; ESA Publications Division, ESTEC, Noordwijk, Netherlands 80 Dutch guilders

The spectral response of forests was examined. Airborne imaging spectrometer data acquired from a metal-stressed spruce-broadleaved forest display changes in absorption features in the near to shortwave infrared region that coincide with canopy leaf tannin and starch absorption bands. These features, however, are often subdued or masked by the influence of stronger atmospheric water and carbon dioxide absorption bands present in this wavelength region, which must be removed to delineate or enhance the subtle leaf chemistry absorption features. ESA

N89-10356# Iceland Univ., Reykjavik. Lab. for Information Technology and Signal Processing.
A NARROW-BAND THERMAL IMAGER BASED ON MULTILINE REAL-TIME AVERAGING
S. Bjornsson, V. Thorvaldsson, and A. Eiriksson *In* ESA, Proceedings of the 4th International Colloquium on Spectral Signatures in Remote Sensing Apr. 1988 p 291-292 (For primary document see N89-10305 01-43)
Copyright Avail: NTIS HC A23/MF A01; ESA Publications Division, ESTEC, Noordwijk, Netherlands 80 Dutch guilders

A multichannel thermal imager for low temperatures is described. It is capable of high sensitivity in narrow bands (selective search mode), high thermal resolution in case of known or constant emissivity (thermal mapping), material selectivity in case of known or constant temperature, and wavelength dependent emissivity (thematic mapping); as well as allowing the customary method of measuring the total emissive power with much increased sensitivity. It is intended for research on volcanoes and geothermal areas. ESA

N89-10357*# Jet Propulsion Lab., California Inst. of Tech., Pasadena.
AIRBORNE VISIBLE/INFRARED IMAGING SPECTROMETER (AVIRIS): INFLIGHT RADIOMETRIC CALIBRATION AND THE DETERMINATION OF SURFACE REFLECTANCE
J. E. Conel, G. Vane, R. O. Green, R. E. Alley, V. Carere, A. Gabell, and C. J. Bruegge *In* ESA, Proceedings of the 4th International Colloquium on Spectral Signatures in Remote Sensing Apr. 1988 p 293-297 (For primary document see N89-10305 01-43)
Copyright Avail: NTIS HC A23/MF A01; ESA Publications Division, ESTEC, Noordwijk, Netherlands 80 Dutch guilders CSCL 02F

The inflight radiometric performance of AVIRIS is presented together with a comparison of methods of recovering surface spectral reflectance from the data. Performance is evaluated by comparing radiance predicted from AVIRIS with radiance generated from the LOWIRAN 6 atmospheric model and measured surface reflectance. Comparisons show apparent agreement to within a few percent between 1800 and 2450 nm. Between 600 and 1800 nm the response of AVIRIS is systematically low by as much as 70 percent, and between 400 and 600 nm it is higher than expected. These problems are traced to thermal distortions of the instrument, and to detachment during flight of optical fibers connecting foreoptics to two of four spectrometers in the instrument. Of three methods studied, an empirical one involving calibration curves

constructed from field reflectance measurements returns accurate predictions of the surface reflectance independent of the actual radiometric significance of the flight data. ESA

N89-10358# Nottingham Univ. (England). Dept. of Geography.
HIGH SPECTRAL RESOLUTION INDICES FOR MONITORING CROP GROWTH AND CHLOROSIS
T. H. Demetriades-Shah and M. D. Steven *In* ESA, Proceedings of the 4th International Colloquium on Spectral Signatures in Remote Sensing Apr. 1988 p 299-302 (For primary document see N89-10305 01-43)
(Contract NERC-GST/02/124)
Copyright Avail: NTIS HC A23/MF A01; ESA Publications Division, ESTEC, Noordwijk, Netherlands 80 Dutch guilders

Spectral reflectance of sugar beet in the 400 to 1100 nm region was examined in relation to chlorosis inducing stresses. Spectral indices to predict crop growth and condition unambiguously were tested. Canopy growth variables are most correlated with the first derivative at 940 nm and chlorosis with the second derivative at 636 nm although other derivative indices are also promising. Conventional near-infrared/red based indices and the wavelength of maximum slope of canopy reflectance (the red edge) proposed as an index for monitoring chlorosis are not found to be as good for monitoring stressed vegetation. ESA

N89-10359# Deutsche Forschungs- und Versuchsanstalt fuer Luft- und Raumfahrt, Oberpfaffenhofen (West Germany). Inst. of Optoelectronics.
OPTIMIZATION FOR CLASSIFICATION OF FOREST DAMAGE CLASSES
G. Kritikos, R. Mueller, and P. Reinartz *In* ESA, Proceedings of the 4th International Colloquium on Spectral Signatures in Remote Sensing Apr. 1988 p 303-309 (For primary document see N89-10305 01-43)
Copyright Avail: NTIS HC A23/MF A01; ESA Publications Division, ESTEC, Noordwijk, Netherlands 80 Dutch guilders

Using airborne scanner data of forest stands from different flight altitudes, damage classes are classified. In order to improve classification accuracy, the scanner data can be preprocessed due to the viewing angle dependance of the reflected signal using an empirical correction method. The damage classes have a natural overlap in their signatures. The calculation of the separability of the classes with the Jeffries-Matusita measure allows the optimization of channel and training area selections. Derived features can be checked for their information content in a classification. ESA

N89-10360# Paris VI Univ. (France). Lab. de Mineralogie-Cristallographie.
USEFULNESS OF HIGH SPECTRAL RESOLUTION RADIOMETRY FOR GEOLOGICAL MAPPING IN THE MEDITERRANEAN REGION [INTERET DE LA RADIOMETRIE A HAUTE RESOLUTION SPECTRALE POUR LA CARTOGRAPHIE GEOLOGIQUE EN REGION MEDITERRANEENE]
S. Louahala, B. Cervelle, J. Chorowicz, J.-P. Rudant, and J.-Y. Scanvic (Bureau de Recherches Geologiques et Minieres, Orleans, France) *In* ESA, Proceedings of the 4th International Colloquium on Spectral Signatures in Remote Sensing Apr. 1988 p 311-314 In FRENCH (For primary document see N89-10305 01-43)
Copyright Avail: NTIS HC A23/MF A01; ESA Publications Division, ESTEC, Noordwijk, Netherlands 80 Dutch guilders

Aborptance spectra between 470 and 910 nm were acquired on the ground, using a spectroradiometer, for 30 different lithologies representing 8 types representive of the Mediterranean area. Their form is mainly decided by the presence on the surface of iron in the form of oxide and chlorophyll micro-organisms on the surface of the rocks. The study shows that natural geological surfaces in the Mediterranean region have important spectral variations over short distances. Information contained in the ground spectra of these surfaces are only extremely roughly correlated with the underlying lithology. In favorable cases, positioning in the 540 to 600 band can restore the most important ferrous contrasts. Spectral resolution less than 20 nm does not improve discrimination between the rocks studied for such surfaces. ESA

N89-10361# Sherbrooke Univ. (Quebec).
IMAGING SPECTROMETRY APPLIED TO THE REMOTE SENSING OF SUBMERGED SEAWEED
N. T. ONeill, Y. Gauthier, E. Lambert (Montreal Univ., Quebec), L. Hubert, J. M. M. Dubois, and H. Edel *In* ESA, Proceedings of the 4th International Colloquium on Spectral Signatures in Remote Sensing Apr. 1988 p 315-318 Sponsored by the Department of Fisheries and Oceans, Ontario, Canada (For primary document see N89-10305 01-43)
Copyright Avail: NTIS HC A23/MF A01; ESA Publications Division, ESTEC, Noordwijk, Netherlands 80 Dutch guilders

The utility of imaging spectrometry data for the remote sensing of submerged seaweed is investigated by analyzing data collected by the fluorescence line imager (FLI) and comparing these results with ground based measurements and spectral reflectance models. Radiance differences referenced to the values of the deep water radiance are computed for the FLI data and the spectral models in order to analyze the spectral influence of the water turbidity and the reflectance of the seaweed species indigenous to the region of study (Laminaria sp). Comparisons of ground based spectral measurements and the computations of a spectral reflectance indicate a reasonable level of agreement when the free parameters of the model (chlorophyll concentration and depth) are adjusted to obtain the best spectral fit to the measured points. A method of radiance differences was employed to enhance a broad yellow-red peak in the FLI data which is believed to be related to the presence of submerged Laminaria sp seaweed canopies. The model employed to simulate the airborne signal yields a spectral feature which is narrower and whose peak is shifted relative to the FLI data. This discrepency may be related to a significant decrease in water turbidity in going from shallow to deep waters. ESA

N89-10362# Paris VI Univ. (France). Lab. Mineralogie-Cristallographie.
CHARACTERIZATION OF ROCKS BY VISIBLE AND INFRARED HIGH SPECTRAL RESOLUTION TERRAIN SPECTROSCOPY [CARACTERISATION DES ROCHES PAR SPECTROMETRIE DE TERRAIN A HAUTE RESOLUTION SPECTRALE VISIBLE ET INFRAROUGE PROCHE]
B. Cervelle, J. Chorowicz, J.-P. Rudant, G. Tamain, and E. M. Alem (Mohammed V Univ., Rabat, Morocco) *In* ESA, Proceedings of the 4th International Colloquium on Spectral Signatures in Remote Sensing Apr. 1988 p 319-322 In FRENCH (For primary document see N89-10305 01-43)
Copyright Avail: NTIS HC A23/MF A01; ESA Publications Division, ESTEC, Noordwijk, Netherlands 80 Dutch guilders

Two spectral signatures were derived from the analysis of 200 high spectral resolution spectra at 500 and 900 nm of rocky terrain in an arid region: those of ferrous iron and those of an acid/base character of the rocks. They are represented by indexes for the SPOT bands. However, surface alterations and roughness mask the fine spectral characteristics of the underlying lithology. Processing of SPOT data, given their geometrical quality, does nonetheless discriminate between and outline with precision, the various rock faces; spectral signatures appear to be amplified by morphological signatures. The case of remote sensing of heavenly bodies with no atmosphere, little subject to alteration, but bombarded by meteorites and cosmic rays is quoted. ESA

N89-10363# Institut Francais de Recherche pour l'Exploitation de la Mer, Brest (France).
COMPARATIVE ANALYSIS OF SPECTRAL RESPONSE IN THE OPTICAL DOMAIN OF TARGETS IN A TROPICAL SWAMP AT VARIOUS SPECTRAL AND SPATIAL RESOLUTIONS [ANALYSE COMPARATIVE DES REPONSES SPECTRALES DANS LE DOMAINE OPTIQUE DES CIBLES D'UN MARAIS TROPICAL A DIVERSES RESOLUTIONS SPATIALES ET SPECTRALES]

L. Loubersac, M. Viollier, and C. Lemasson (ENSAIA, Nancy, France) *In* ESA, Proceedings of the 4th International Colloquium on Spectral Signatures in Remote Sensing Apr. 1988 p 323-327 In FRENCH; ENGLISH summary (For primary document see N89-10305 01-43)
Copyright Avail: NTIS HC A23/MF A01; ESA Publications Division, ESTEC, Noordwijk, Netherlands 80 Dutch guilders

Spectral signatures of the same tropical salt marsh targets, acquired on the ground (Sept. 20, 1986) and from altitude (helicopter survey Sept. 17, 1986) with 3 look angles are compared to the SPOT HRV data of Sept. 18, 1986 and correlated to physical properties of the barren salt flats. Observations give coherent results but on dense vegetation the satellite response appears underestimated; on barren flats, it appears overestimated. An atmospheric environmental effect explanation is proposed. Significant correlations between vegetation and brightness indexes and humidity and organic matter content of soils are found. ESA

N89-10364*# National Aeronautics and Space Administration. Goddard Space Flight Center, Greenbelt, Md.
SPATIAL RESOLUTION REQUIREMENTS FOR MODIS-N
J. R. G. Townshend, C. O. Justice, B. L. Markham, and S. A. Briggs (Royal Aircraft Establishment, Farnborough, England) *In* ESA, Proceedings of the 4th International Colloquium on Spectral Signatures in Remote Sensing Apr. 1988 p 329-331 (For primary document see N89-10305 01-43)
(Grants NAGS-399; NERC-F60/G6/12; GFSC-Proj-415)
Copyright Avail: NTIS HC A23/MF A01; ESA Publications Division, ESTEC, Noordwijk, Netherlands 80 Dutch guilders CSCL 02F

An empirical investigation of the required spatial resolution for MODIS-N is outlined. It is based on 5 LANDSAT multispectral scanner system images of the normalized difference vegetation index degraded to resolutions between 250 m and 4000 m. Pairs of images from different dates were registered and difference images were generated. Fourier analysis indicates that resolutions finer than 1 km are highly desirable for change detection. A sensor with a resolution of 500 m is recommended as providing the best compromise between detail of changes detected and the size of the resultant data volume, but other options are also suggested. ESA

N89-10365# Institut Francais de Recherche pour l'Exploitation de la Mer, Brest (France).
HIGH RESOLUTION RADIOMETRIC MEASUREMENT OF INTERTIDAL MICROPHYTOBENTHOS [MESURES RADIOMETRIQUES HAUTE RESOLUTION DU MICROPHYTOBENTHOS INTERTIDAL]
B. Guillaumont, P. Gentien, and M. Viollier (Centre National de la Recherche Scientifique, Roscoff, France) *In* ESA, Proceedings of the 4th International Colloquium on Spectral Signatures in Remote Sensing Apr. 1988 p 333-336 In FRENCH (For primary document see N89-10305 01-43)
Copyright Avail: NTIS HC A23/MF A01; ESA Publications Division, ESTEC, Noordwijk, Netherlands 80 Dutch guilders

High resolution spectroradiometric measurements were used to show that spectral variations of the reflectance of intertidal sediments can be likened to spectrophotometric measurements of acetone extracts, a technique usually employed to estimate the microbenthic biomass. Analysis suggests that utilization of the normalized vegetative index calculated from SPOT channels should enable the importance of microflora zones to be determined. For more accurate quantitative estimates, a certain number of ground control points are necessary. ESA

N89-10366*# National Aeronautics and Space Administration. Goddard Space Flight Center, Greenbelt, Md.
THE BASIS FOR THE SPECTRAL BEHAVIOUR OF SILICATES IN THE THERMAL INFRARED AND APPLICATIONS TO REMOTE SENSING
L. S. Walter and J. W. Salisbury (Geological Survey, Reston, Va.) *In* ESA, Proceedings of the 4th International Colloquium on Spectral Signatures in Remote Sensing Apr. 1988 p 337-340 (For primary document see N89-10305 01-43)
Copyright Avail: NTIS HC A23/MF A01; ESA Publications Division, ESTEC, Noordwijk, Netherlands 80 Dutch guilders CSCL 02F

Variations in the thermal infrared (TIR) spectral response of silicate rocks is related to changes in the structures and divalent cation contents of the minerals which form the rocks. These considerations lead to a chemical parameter, SCFM, which reflects mineral structures, rock types, and their spectra. The parameter is the ratio of silica to the abundance of depolymerizing cations, defined as SCFM = SiO2/SiO2 + CaO + MgO + FeO. Parameter SCFM is therefore proposed for use in TIR remote sensing of igneous rocks. It is also demonstrated that two or three broad bands are sufficient for distinguishing among major rock types and the system noise has little effect on the quality of the results. These factors can be traded off against improved spatial resolution in instrument design. ESA

N89-10367# Laval Univ. (Quebec). Dept. des Sciences Geodesiques et de Teledetection.
TEXTURE ANALYSIS IN FOREST AREAS: HIGH SPECTRAL RESOLUTION SYNTHETIC APERTURE RADAR DATA [ANALYSE TEXTURALE EN MILIEU FORESTIER: DONNEES RADAR A OUVERTURE SYNTHETIQUE DE HAUTE RESOLUTION SPATIALE]
R. Landry, G. Edwards, K. P. B. Thomson, and P. Gilbert *In* ESA, Proceedings of the 4th International Colloquium on Spectral Signatures in Remote Sensing Apr. 1988 p 341-345 In FRENCH (For primary document see N89-10305 01-43)
Copyright Avail: NTIS HC A23/MF A01; ESA Publications Division, ESTEC, Noordwijk, Netherlands 80 Dutch guilders

Visual interpretation (spectral aspect) of SAR images of forests, supported by terrain data, is described. It is concluded that radar imagery can aid in planning clearings, in mapping roads, and in evaluating the density of vertical twigs and first leaves in clearing areas. The methodology and results of a quantitative analysis of the texture (spatial aspect) are summarized. It is concluded that texture enables covers that would otherwise be confounded to be distinguished. ESA

N89-10368# Institut National de la Recherche Agronomique, Thiverval-Grignon (France). Station de Bioclimatologie.
ESTIMATION OF LEAF SPECTRA FROM MEASUREMENTS IN WIDE SPECTRAL BANDS [ESTIMATION DE SPECTRES DE FEUILLES A PARTIR DE MESURES DANS DES BANDES SPECTRALES LARGES]
B. Andrieu, F. Baret, J. Schellberg, and U. Rinderle (Karlsruhe Univ., West Germany) *In* ESA, Proceedings of the 4th International Colloquium on Spectral Signatures in Remote Sensing Apr. 1988 p 351-356 In FRENCH (For primary document see N89-10305 01-43)
Copyright Avail: NTIS HC A23/MF A01; ESA Publications Division, ESTEC, Noordwijk, Netherlands 80 Dutch guilders

A simple reflectance model to simulate leaf spectra from chlorophyll concentration and infrared reflectance level is proposed. A derived model which only takes into account chlorophyll concentration enables leaf reflectance in the wide bands of a densitometer to be simulated. The inversion of the latter model gives precise estimates of chlorophyll concentration which can be used to reconstruct the complete reflectance spectrum of the leaf. Tests on wheat show that a rapid, but fine, characterization of the optical properties of canopy elements using a simple densitometer is possible. ESA

N89-10369# Institut National de la Recherche Agronomique, Thiverval-Grignon (France). Lab. de Pedologie.
MODELING OF SOIL COLOR BY REMOTE SENSING [MODELISATION DE LA COULEUR DES SOLS PAR TELEDETECTION]
D. Courault, M.-C. Girard, and R. Escadafal (Office de la Recherche Scientifique et Technique, Bondy, France) *In* ESA, Proceedings of the 4th International Colloquium on Spectral Signatures in Remote Sensing Apr. 1988 p 357-362 In FRENCH; ENGLISH

summary (For primary document see N89-10305 01-43)
Copyright Avail: NTIS HC A23/MF A01; ESA Publications Division, ESTEC, Noordwijk, Netherlands 80 Dutch guilders

Eighty-four very different soil samples were characterized in the laboratory with: reflectance curves from 350 to 2000 nm recorded with a spectrophotometer; physical and chemical analysis; and color from Munsell soil chart. Different types of curve shapes were related to the main constituents of the studied samples. Using colorimetric concepts, soil spectral characteristics were modeled from Munsell color. It is shown that the reflectance curve of a soil sample can be predicted from converting its Munsell coordinates into the trichromatic system RGB. The low occurrence of materism for soils allows the relation between spectral reflectance and color to be inverted. ESA

N89-10370# Ecole Polytechnique Federale de Lausanne (Switzerland). Inst. for Agricultural Engineering.
THE NORMALIZATION OF A SOIL BRIGHTNESS INDEX FOR THE STUDY OF CHANGES IN SOIL CONDITIONS
R. Caloz, B. Abednego, and C. Collet (Fribourg Univ., Switzerland) *In* ESA, Proceedings of the 4th International Colloquium on Spectral Signatures in Remote Sensing Apr. 1988 p 363-366 (For primary document see N89-10305 01-43)
Copyright Avail: NTIS HC A23/MF A01; ESA Publications Division, ESTEC, Noordwijk, Netherlands 80 Dutch guilders

A methodology for comparing soil surface characteristics from remotely sensed data acquired from orbital remote sensing systems at different dates is proposed. It is based on the normalization of the soil line index or soil brightness index computed from red and infrared band information. The normalization removes the influence of changes in illumination and atmospheric conditions as well as in detector system characteristics. Normalized index values can therefore be utilized to study changes in soil surface conditions throughout time. ESA

N89-10371# Centre National d'Etudes Spatiales, Toulouse (France). Lab. d'Etudes et de Recherches en Teledection Spatiale.
ESTIMATION OF PRIMARY MARINE PRODUCTION USING SPACEBORNE DATA ON OCEAN COLOR [ESTIMATION DE LA PRODUCTION PRIMAIRE MARINE A L'AIDE DE DONNEES SPATIALES DE COULEUR DE L'OCEAN]
B. Berthelot and P.-Y. Deschamps *In* ESA, Proceedings of the 4th International Colloquium on Spectral Signatures in Remote Sensing Apr. 1988 p 367-370 In FRENCH (For primary document see N89-10305 01-43)
Copyright Avail: NTIS HC A23/MF A01; ESA Publications Division, ESTEC, Noordwijk, Netherlands 80 Dutch guilders

An algorithm which directly determines the amount of photosynthetic available radiation absorbed by chlorophyll pigments from backscattered reflectance from sea water was developed. It assumes that the chemical output of the photosynthesis is known. The algorithm can be used in estimating primary marine production (PMP) from narrow or wideband satellite observations of ocean color, and establishes a linear relationship between PMP and backscattered reflectance. The algorithm was tested using simulated data from the NIMBUS-7 coastal zone color scanner and the SPOT 4 vegetation instrument. It was compared with an algorithm that uses the determination of the concentration of chlorophyll pigments. The superiority of the developed algorithm, especially given the noisy nature of satellite data, is shown. ESA

N89-10372# Grenoble-1 Univ. (France).
SATELLITE SURVEILLANCE OF ICE AND SNOW COVERED SURFACES IN THE FRENCH ALPS USING VISIBLE AND NEAR INFRARED REFLECTANCE MEASUREMENTS FROM THE SPOT AND LANDSAT THEMATIC MAPPER SENSORS [SURVEILLANCE SATELLITAIRE DES SURFACES ENGLACEES ET ENNEIGEES DANS LES ALPES FRANCAISES PAR MESURE DE REFLECTANCES VISIBLES ET PROCHE INFRAROUGE ISSUE DES CAPTEURS SPOT ET LANDSAT THEMATIC MAPPER]
J.-P. Dedieu and E. Elizechea (Groupement pour le Developpement de la Teledetection Aerospatiale, Toulouse, France) *In* ESA, Proceedings of the 4th International Colloquium on Spectral Signatures in Remote Sensing Apr. 1988 p 371-375 In FRENCH (For primary document see N89-10305 01-43)
Copyright Avail: NTIS HC A23/MF A01; ESA Publications Division, ESTEC, Noordwijk, Netherlands 80 Dutch guilders

The use of satellite imagery to monitor glacier mass balance was studied. Analysis of spectral signatures of snow and ice to discriminate between firm and moving ice zones is described. The analysis is based on the utilization of specific ratios in the visible and near infrared spectral domains, sensitive to the effects of snow grain and ice crystal size. Tests show the utility of combining SPOT panchromatic and multispectral images, with the 10m ground resolution of the panchromatic images allowing comparisons with terrain measurements, and the multispectral images giving a means for fine radiometric discrimination of snow and ice particles. ESA

N89-10373# Valencia Univ. (Spain). Dept. de Termodinamica.
SPECTRAL SIGNATURE OF CITRUS FRUITS AND ITS EVOLUTION: IDENTIFICATION OF THE VEGETATIVE INDEX OF LEAST TEMPORAL VARIATION [SIGNATURE SPECTRALE DES AGRUMES ET SON EVOLUTION: IDENTIFICATION D'INDEX DE VEGETATION DE MOINDRE VARIATION TEMPORELLE]
D. Segarra, A. Gilabert, S. Gandia, and J. Melia *In* ESA, Proceedings of the 4th International Colloquium on Spectral Signatures in Remote Sensing Apr. 1988 p 377-382 In FRENCH (For primary document see N89-10305 01-43)
(Contract CAICyT-A-172/85)
Copyright Avail: NTIS HC A23/MF A01; ESA Publications Division, ESTEC, Noordwijk, Netherlands 80 Dutch guilders

Images from LANDSAT 5 were used to monitor the evolution of the spectral signature of a citrus fruit growing area during a winter period. Results show that there is no seasonal spectral signature for citrus fruits, the variability within one season being as great as that between seasons, and there are significant differences in reflectance from one plot to another, depending on vegetation cover. A method to detect zones affected by frost and to assess the impact was developed. It is based on a multitemporal analysis of the vegetative index before and after the frost. ESA

N89-10374# Musee Royal de l'Afrique Centrale, Tervuren (Belgium).
ROCK AND SOIL DISCRIMINATION IN NATURAL TROPICAL CONDITIONS USING A SPOT-CALIBRATED RADIOMETER
J. Lavreau, J. P. Rudant (Paris VI Univ., France), and Philippe Trefois *In* ESA, Proceedings of the 4th International Colloquium on Spectral Signatures in Remote Sensing Apr. 1988 p 383-386 (For primary document see N89-10305 01-43)
Copyright Avail: NTIS HC A23/MF A01; ESA Publications Division, ESTEC, Noordwijk, Netherlands 80 Dutch guilders

A radiometry survey was executed in the western Tanzanian Karema area bordering lake Tanganyika. Spectral values in the SPOT bands were statistically analyzed. A discriminant analysis on different data sets concludes at the discriminability of the vegetal from the mineral objects, whereas the recognition of the soils, defined according to subsurface lithology, is usually less effective. A principal component and a cluster analysis of different groups shows the importance of non or less lithology-related parameters. A set of soils was submitted to a chemical analysis and a wide-range spectroradiometry. The analysis of the correlation matrix between chemical and spectral variables reveals that a better geochemical discrimination of the soils can be achieved when a greater number of spectral bands is taken into account. ESA

N89-10375# Office de la Recherche Scientifique et Technique Outre-Mer, Dakar (Senegal). Centre de Recherches Oceanographiques.
BATHYMETRY USING SPOT IMAGERY OF THE CASAMANCE (SENEGAL). FIRST RESULTS [BATHYMETRIE PAR IMAGERIE SPOT SUR LA CASAMANCE (SENEGAL). RESULTATS PRELIMINAIRES]
J. Pages, J. Citeau, and H. Demarcq *In* ESA, Proceedings of

the 4th International Colloqium on Spectral Signatures in Remote Sensing Apr. 1988 p 387-392 In FRENCH; ENGLISH summary (For primary document see N89-10305 01-43)
Copyright Avail: NTIS HC A23/MF A01; ESA Publications Division, ESTEC, Noordwijk, Netherlands 80 Dutch guilders

The bathymetry of Casamance river in Senegal was studied using SPOT images to help develop a model to predict salinity, which governs economic activities such as fishing and rice growing. Four campaigns for ground truth measurements were done with determination of the usual hydrobiological parameters. The use of a hand-borne radiometer with spectral windows identical to the 3 SPOT channels, used over various type of shallow waters, shows that the channel 3/channel 1 ratio correlates highly with chlorophyll content (C3/C1 = K.Ln(Chl.)) and with depth in the 0.8 to 0.02 m depth range (C3/c1 = K.Ln(z)). Using SPOT imagery for the end of rainy season, 4 water categories were determined: deep water (over 0.6 m), shallow water, partly emerged sludge, and land. Similarly to ground measurements results, the SPOT channel 3/channel 1 ratio was used to define semiquantitative scales of depths. On test areas bathymetry was determined by relative value. Preliminary results need to be refined, and the depth scale to be improved and extended to larger areas to take into account the shallow water areas in the salinity budget of Casamance River.
ESA

N89-10376# Sherbrooke Univ. (Quebec). Centre d'Applications et de Recherches en Teledetection.
DISCRIMINATION OF ZONES OF HIGH WATER EROSION RISK USING SPOT IMAGES [DISTINCTION DES ZONES A HAUT RISQUE D'EROSION HYDRIQUE A L'AIDE D'IMAGES SPOT]
S. Perras, D. Baril, A. Pesant (Agriculture Canada, Lennoxville, Quebec), and F. Bonn *In* ESA, Proceedings of the 4th International Colloquium on Spectral Signatures in Remote Sensing Apr. 1988 p 393-397 In FRENCH Sponsored in cooperation with the Centre des Recherches et des Services Agricoles, Quebec, Canada (For primary document see N89-10305 01-43)
(Contract Dossier-3B1-68400260-002)
Copyright Avail: NTIS HC A23/MF A01; ESA Publications Division, ESTEC, Noordwijk, Netherlands 80 Dutch guilders

Erosion risk of an arable farming area was assessed using SPOT imagery, a digitized pedological map, and soil erodability measurements. The potential of the SPOT images to discriminate between different soil series was examined. The SPOT images are incapable of classifying soil types. The digitized pedological map was superimposed on land use images to give bare soil area for each type of soil. These data, along with the rate of erodability, enable the quantity of soil eroded in the region to be estimated.
ESA

N89-10377*# National Aeronautics and Space Administration. Lyndon B. Johnson Space Center, Houston, Tex.
EMITTED SHORT WAVELENGTH INFRARED RADIATION FOR DETECTION AND MONITORING OF VOLCANIC ACTIVITY
D. A. Rothery, P. W. Francis (Open Univ., Milton, England), and C. A. Wood *In* ESA, Proceedings of the 4th International Colloquium on Spectral Signatures in Remote Sensing Apr. 1988 p 399-402 (For primary document see N89-10305 01-43)
(Contract NASw-4066)
Copyright Avail: NTIS HC A23/MF A01; ESA Publications Division, ESTEC, Noordwijk, Netherlands 80 Dutch guilders
CSCL 02F

Thematic Mapper images from LANDSAT were used to monitor volcanoes. Achievements include: (1) the discovery of a magmatic precursor to the 16 Sept. 1986 eruption of Lascar, northern Chile, on images from Mar. and July 1985 and of continuing fumarolic activity after the eruption; (2) the detection of unreported major changes in the distribution of lava lakes on Erta'Ale, Ethiopia; and (3) the mapping of a halo of still-hot spatter surrounding a vent on Mount Erebus, Antarctica, on an image acquired 5 min after a minor eruption otherwise known only from seismic records. A spaceborne short wavelength infrared sensor for observing hot phenomena of volcanoes is proposed. A polar orbit is suggested.
ESA

N89-10378*# Jet Propulsion Lab., California Inst. of Tech., Pasadena.
MONITORING SEASONAL VARIATIONS OF SOIL MOISTURE AND VEGETATION COVER USING SATELLITE MICROWAVE RADIOMETRY
Y. H. Kerr and E. G. Njoku *In* ESA, Proceedings of the 4th International Colloquium on Spectral Signatures in Remote Sensing Apr. 1988 p 403-406 Sponsored by NASA (For primary document see N89-10305 01-43)
Copyright Avail: NTIS HC A23/MF A01; ESA Publications Division, ESTEC, Noordwijk, Netherlands 80 Dutch guilders CSCL 02F

The NIMBUS-7 scanning multichannel microwave radiometer measured brightness temperatures at 5 frequencies (6.6, 10.7, 18, 21, 37 GHz), all dual-polarized with a 50 deg incidence angle over Africa since 1978. A 3 yr data set is being processed (1983 to 1985), and a theoretical model was developed, allowing investigation of the microwave emissivity of land features in the frequency range 6.6 to 37 GHz and of the extent to which vegetation and roughness can be determined in order to improve the soil moisture estimation.
ESA

N89-10379*# National Aeronautics and Space Administration. Goddard Space Flight Center, Greenbelt, Md.
COMPARATIVE POINT-SPREAD FUNCTION CALCULATIONS FOR THE MOMS-1, THEMATIC MAPPER AND SPOT-HRV INSTRUMENTS
V. V. Salomonson, J. E. Nickeson, J. Bodechtel, and J. Zilger (Technische Univ., Munich, West Germany) *In* ESA, Proceedings of the 4th International Colloquium on Spectral Signatures in Remote Sensing Apr. 1988 p 407-412 (For primary document see N89-10305 01-43)
Copyright Avail: NTIS HC A23/MF A01; ESA Publications Division, ESTEC, Noordwijk, Netherlands 80 Dutch guilders CSCL 02F

Point-spread functions (PSF) comparisons were made between the Modular Optoelectronic Multispectral Scanner (MOMS-01), the LANDSAT Thematic Mapper (TM) and the SPOT-HRV instruments, principally near Lake Nakuru, Kenya. The results, expressed in terms of the width of the point spread functions at the 50 percent power points as determined from the in-scene analysis show that the TM has a PSF equal to or narrower than the MOMS-01 instrument (50 to 55 for the TM versus 50 to 68 for the MOMS). The SPOT estimates of the PSF range from 36 to 40. When the MOMS results are adjusted for differences in edge scanning as compared to the TM and SPOT, they are nearer 40 in the 575 to 625 nm band.
ESA

N89-10380# Phillips Petroleum Co., Bartlesville, Okla.
THE RESULTS OF THE GEOSAT MOMS SUBCOMMITTEE'S DATA EVALUATION: PERFORMANCE AND APPLICABILITY OF THE MOMS-1 SENSOR FOR EXPLORATION GEOLOGY
G. I. Ballew and F. B. Henderson, III (Geosat Committee, Inc., Norman, Okla.) *In* ESA, Proceedings of the 4th International Colloquium on Spectral Signatures in Remote Sensing Apr. 1988 p 413-423 (For primary document see N89-10305 01-43)
Copyright Avail: NTIS HC A23/MF A01; ESA Publications Division, ESTEC, Noordwijk, Netherlands 80 Dutch guilders

Digital imagery from 14 sites in Africa, Asia, Australia, and South America acquired by the MOMS-01 sensor on Space Shuttle flight STS-4 (41-B) in February 1984 was analyzed to determine suitability for hydrocarbon energy and mineral exploration by comparison with geological maps and other satellite data. The MOMS two-band spectral data and 20m resolution display many geological and vegetation features discernable on LANDSAT and SPOT data. The MOMS limitations include striping, limited gray shades, non-map geometry, and large data size. On balance,

MOMS provides high resolution data useful for international energy and mineral exploration. ESA

N89-10381# Karlsruhe Univ. (West Germany). Dept. of Photogrammetry and Remote Sensing.
DESIGN OF SPECTRAL BANDS FOR THE GERMAN MOMS-2 SENSOR
H. Kaufmann, D. Meissner, J. Bodechtel (Commission of the European Communities, Ispra, Italy), F. J. Behr, R. Geerken, and K. Jung *In* ESA, Proceedings of the 4th International Colloquium on Spectral Signatures in Remote Sensing Apr. 1988 p 425-430 Sponsored by the Bundesministerium fuer Forschung und Technologie, Bonn, Fed. Republic of Germany (For primary document see N89-10305 01-43)
Copyright Avail: NTIS HC A23/MF A01; ESA Publications Division, ESTEC, Noordwijk, Netherlands 80 Dutch guilders

Spectral bands for the MOMS-02 instrument, designed as a pushbroom scanning device with on-track three channel stereo capability and four spectral bands in the visible and NIR range are discussed. For centering and defining the width of spectral bands in the 0.4 to 1 micron range, laboratory measurements, using spectrophotometer were performed. Various species of 3 yr old deciduous and coniferous trees as well as mineral standards, rocks, and soils containing Fe(2+/3+) ions were measured and analyzed. Band optimization is based on an iterative process including the spectral properties of distinct targets, atmospheric transmission (LOWTRAN 6), calibration standards and system parameters. The proposed spectral bands (435 to 510 nm; 530 to 575 nm; 655 to 685 nm; 830 to 890 nm) were calculated for 15.75 x 15.75 m ground pixel size (nominal altitude = 324 km at equator) and an internal dynamic range of 9-bit, whereby priority was given to vegetation targets. The wavelength range of the panchromatic nadir and off-nadir looking stereo modules is established at 625 nm + or - 125. ESA

N89-10382# Paris VI Univ. (France). Dept. de Geotectonique.
THE USE OF MOMS-1 DATA FOR GEOLOGICAL MAPPING OF THE ASWA LINEAMENT (EAST AFRICAN RIFT)
J. Chorowicz, M. Guezlane, J.-P. Rudant, and G. Vidal *In* ESA, Proceedings of the 4th International Colliquium on Spectral Signatures in Remote Sensing Apr. 1988 p 431-434 (For primary document see N89-10305 01-43)
Copyright Avail: NTIS HC A23/MF A01; ESA Publications Division, ESTEC, Noordwijk, Netherlands 80 Dutch guilders

The MOMS-01 characteristics (20 m ground resolution, two spectral bands, the yellow band expressing the drainage pattern, the infrared one giving geomorphology, and synoptic view) were exploited to produce a geological map of the large Aswa lineament zone. This zone appears to be a Late Proterozoic NW-SE fault zone due to the wrapping of the Mozambiquian belt around the Tanzanian shield. Frontal and lateral ramps developed in the belt were reworked respectively as normal and transcurrent faults of the East African Rift, responsible for virgation of the Gregory Rift. The NE trending fault direction expressed in the Archean basement, resulted in the Nyanza graben formation. ESA

N89-10383# Dundee Univ. (Scotland). Dept. of Applied Physics and Electronic and Manufacturing Engineering.
MOMS-1 DATA FOR BATHYMETRIC AND GEOLOGICAL STUDIES
A. K. Saraf, A. P. Cracknell, and M. Ibrahim *In* ESA, Proceedings of the 4th International Colloquium on Spectral Signatures in Remote Sensing Apr. 1988 p 435-438 (For primary document see N89-10305 01-43)
Copyright Avail: NTIS HC A23/MF A01; ESA Publications Division, ESTEC, Noordwijk, Netherlands 80 Dutch guilders-

The MOMS data from the Shuttle flights STS-7 and STS-11 were used to investigate water depths in the Red Sea and for geological studies in Burma, respectively. For the Red Sea an exponential relationship between pixel intensity and water depth is obtained but the root-mean-square deviation of the fit of the data to control points is 3.7 m which is far too large for operational bathymetric work. The main reason for this is the low sensitivity of the instrument for the typical intensities received from the water. The data for Burma are useful for structural mapping but for lithological mapping the spectral response of rocks is less sensitive. ESA

N89-10384# Open Univ., Milton (England). Dept. of Earth Sciences.
MOMS-1 USED SYNERGISTICALLY WITH LANDSAT TM
D. A. Rothery *In* ESA, Proceedings of the 4th International Colloquium on Spectral Signatures in Remote Sensing Apr. 1988 p 439-442 (For primary document see N89-10305 01-43)
Copyright Avail: NTIS HC A23/MF A01; ESA Publications Division, ESTEC, Noordwijk, Netherlands 80 Dutch guilders

It is shown how the best attributes of MOMS-01 imagery and LANDSAT TM can be combined to make an optimized image. For many geological applications, the important information within an image can be considered as comprising textural and spectral components. Because of the non-sun-synchronous orbit of the Space Shuttle, MOMS-01 acquired many images during low solar elevation which shows up topographic textural features very well. The TM records much more spectral information than MOMS-01, which can be emphasized by decorrelation stretching and related techniques. By modulating three enhanced TM channels by one of the MOMS-01 channels, a color composite can be produced which combines the spectral advantages of TM with the textural detail recorded by MOMS-01. ESA

N89-10385# Technische Univ., Munich (West Germany). Inst. for General and Applied Geology.
COMPARATIVE GEOLOGICAL EVOLUTION OF DIFFERENT REMOTE SENSING DATA OF THE HOGGAR MOUNTAINS (ALGERIA)
F. Jaskolla and M. Rast (European Space Agency. European Space Research and Technology Center, ESTEC, Noordwijk, Netherlands) *In* ESA, Proceedings of the 4th International Colloquium on Spectral Signatures in Remote Sensing Apr. 1988 p 443-450 (For primary document see N89-10305 01-43)
Copyright Avail: NTIS HC A23/MF A01; ESA Publications Division, ESTEC, Noordwijk, Netherlands 80 Dutch guilders

The suitability for geological mapping of spaceborne remote sensing data (LANDSAT-5 TM, MOMS-01, Metric Camera and SIR-A) of the Hoggar Mountains (Algeria) was assessed. The optoelectronic MOMS-01 data prove their suitability for the task. Qualitative differences with comparable LANDSAT TM bands are not significant. Additional data are of great importance, especially the availability of stereoscopic data for geological applications. They can provide information which can not be collected by multispectral scanning systems. Radar data offer distinct improvements especially in sand covered areas; however, the question must be put if the information gain is in relation to the enormous costs of a required multifrequency/multipolarization radar system. ESA

N89-10386# Technische Univ., Munich (West Germany). Inst. for General and Applied Geology.
DIGITAL ANALYSIS OF MOMS-1, LANDSAT TM, AND SPOT DATA OF THE NAKURU AREA (KENYA)
J. Henkel, U. Terhalle, and J. Zilger *In* ESA, Proceedings of the 4th International Colloquium on Spectral Signatures in Remote Sensing Apr. 1988 p 451-456 (For primary document see N89-10305 01-43)
Copyright Avail: NTIS HC A23/MF A01; ESA Publications Division, ESTEC, Noordwijk, Netherlands 80 Dutch guilders

Data from MOMS were compared with LANDSAT TM and SPOT for geoscientific thematic mapping. When operating in gain level 1, MOMS has a lower dynamic range than TM; switched to gain position 2, the dynamic ranges are comparable. The infrared band of MOMS-01, which was out of focus during the first mission, then tried to be corrected during the refurbishment, still is slightly out of focus; in processings where the visible channel is included, the overall detectability is not reduced, because it is controlled by

the highest resolving data set of the product. The radiometric correction procedures, though improved for the STS-11/41-B flight by introducing preflight calibration tables in dependence of the saturation (steps of 5 percent starting from 0 to 100 percent), still leaves sensor invariances, in flight and across flight direction; gray value variations are between 1 and 2. The optoelectronic concept provides for a high geometric accuracy. In terms of the SPOT/TM comparison, the spectral range presently available for optoelectronic systems (VIS to NIR) is not utilized optimally for applications, for geologic as for those of renewable resources.
ESA

N89-10387# Joint Research Centre of the European Communities, Ispra (Italy).
AGRISAR'86: CONTRIBUTING TO SIGNATURE RESEARCH
A. J. Sieber *In* ESA, Proceedings of the 4th International Colloquium on Spectral Signatures in Remote Sensing Apr. 1988 p 459-462 (For primary document see N89-10305 01-43)
Copyright Avail: NTIS HC A23/MF A01; ESA Publications Division, ESTEC, Noordwijk, Netherlands 80 Dutch guilders

Results of the evaluation of AGRISAR'86 image data are discussed as far as they may be used for signature research in microwave remote sensing. It is pointed out that such an airborne campaign includes too many problems to result in signatures based on physically meaningful model assumptions about the electromagnetic wave, target interaction. It is recommended first to undertake a dedicated calibration experiment and than a project for the investigation of the radar signatures of selected objects.
ESA

N89-10388# Department of Agriculture, Beltsville, Md. Hydrology Lab.
AIRCRAFT REMOTE SENSING IN HAPEX
T. Schmugge and L. Janssen (Wageningen Agricultural Univ., Netherlands) *In* ESA, Proceedings of the 4th International Colloquium on Spectral Signatures in Remote Sensing Apr. 1988 p 463-467 (For primary document see N89-10305 01-43)
Copyright Avail: NTIS HC A23/MF A01; ESA Publications Division, ESTEC, Noordwijk, Netherlands 80 Dutch guilders

A C-130 remote sensing aircraft was used in calculation of surface moisture and heat fluxes using combined aircraft observations of surface temperature and soil moisture with surface measurements of the fluxes; spatial integration of aircraft surface albedo and temperature observations for comparison with satellite data; and comparison of the fluxes estimated using the remotely sensed data with those determined from an eddy correlation aircraft. Sensors operating from the visible through the infrared into the microwave provided data over two small fresh water lakes. Thermal infrared multispectral scanner performance is discussed. The instrument can estimate surface temperature with 1 C accuracy if atmospheric effects are accounted for.
ESA

N89-10389# Centre National de Recherches Meteorologiques, Toulouse (France).
A STUDY OF THE VEGETATION COVER WITH AVHRR DURING HAPEX-MOBILHY
T. Phulpin and J. P. Jullien *In* ESA, Proceedings of the 4th International Colloquium on Spectral Signatures in Remote Sensing Apr. 1988 p 469-472 (For primary document see N89-10305 01-43)
Copyright Avail: NTIS HC A23/MF A01; ESA Publications Division, ESTEC, Noordwijk, Netherlands 80 Dutch guilders

The LANDSAT AVHRR vegetation index images were used to map the dominant vegetation types and study the vegetation state in the South-West of France. It is shown that artifacts due to haze, precipitations, or difference of anisotropy between AVHRR channels 1 and 2 could falsify the interpretation of the temporal variations of NDVI in terms of phenologic evolution. A compositing procedure allowing to keep a high time sampling rate is proposed.
ESA

N89-10390# Institut National de la Recherche Agronomique, Thiverval-Grignon (France).
A NEW METHOD FOR ESTIMATING REGIONAL EVAPORATION FROM THERMAL INFRARED SURFACE TEMPERATURE MEASUREMENTS [UNE NOUVELLE METHODE D'ESTIMATION DE L'EVAPORATION REGIONALE A PARTIR DE MESURES DE TEMPERATURE DE SURFACE DANS L'INFRAROUGE THERMIQUE]
Y. Brunet, J. P. Lagouarde, and M. Nunez (Hobart Univ., Australia) *In* ESA, Proceedings of the 4th International Colloquium on Spectral Signatures in Remote Sensing Apr. 1988 p 473-476 In FRENCH (For primary document see N89-10305 01-43)
Copyright Avail: NTIS HC A23/MF A01; ESA Publications Division, ESTEC, Noordwijk, Netherlands 80 Dutch guilders

A method to estimate evaporation at regional scale, on an hourly basis, based on a single measurement of surface temperature is presented. The algorithm is based on the coupling of a model of surface exchanges with a simple model of the planetary boundary layer. Climate data become dependent variables and the only surface parameters to be taken into account are albedo, emissivity, and roughness length. Model initialization requires radio sounding. The method is validated using three sets of micrometeorological data for dry, wet, and average conditions.
ESA

N89-10391# Joint Research Centre of the European Communities, Ispra (Italy).
DEVELOPMENT OF MOMS TO A FUTURE MULTIBAND AND STEREOSCOPIC SENSOR
J. Bodechtel, F. Ackermann, D. Meissner, H. Kauffmann, P. Seige, H. Winkenbach, and J. Zilger (Technische Univ., Munich, West Germany) *In* ESA, Proceedings of the 4th International Colloquium on Spectral Signatures in Remote Sensing Apr. 1988 p 479-482 (For primary document see N89-10305 01-43)
Copyright Avail: NTIS HC A23/MF A01; ESA Publications Division, ESTEC, Noordwijk, Netherlands 80 Dutch guilders

Based on the success of MOMS-01, flown twice on the Space Shuttle, the decision was made to construct an advanced instrument, which combines simultaneously multispectral and stereoscopic in-track data sampling capabilities, MOMS-02. It is scheduled for space test in connection with the German Spacelab D-2 mission. Scientific guidance of the development, missions, and data evaluation is provided by a team of project scientists, representing the requirements of the photogrammetric and geoscientific thematic user community.
ESA

N89-10392# Centre National d'Etudes Spatiales, Paris (France).
THE FRENCH SPACE PROGRAM FOR EARTH OBSERVATION [LE PROGRAMME SPATIAL FRANCAIS POUR L'OBSERVATION DE LA TERRE]
M. Chevrel *In* ESA, Proceedings of the 4th International Colloquium on Spectral Signatures in Remote Sensing Apr. 1988 p 483-486 In FRENCH (For primary document see N89-10305 01-43)
Copyright Avail: NTIS HC A23/MF A01; ESA Publications Division, ESTEC, Noordwijk, Netherlands 80 Dutch guilders

Earth observations from space (land, ocean, climate) are reviewed. The SPOT and TOPEX/POSEIDON programs are introduced. Instrumentation and systems of future space based programs, and an airplane for atmospheric research and remote sensing are mentioned.
ESA

N89-10393*# National Aeronautics and Space Administration, Washington, D.C.
NASA'S FUTURE LAND REMOTE SENSING PROGRAM
R. E. Murphy, M. Baltuck, M. Ruzek, and D. E. Wickland *In* ESA, Proceedings of the 4th International Colloquium on Spectral Signatures in Remote Sensing Apr. 1988 p 487-492 (For primary document see N89-10305 01-43)
Copyright Avail: NTIS HC A23/MF A01; ESA Publications Division, ESTEC, Noordwijk, Netherlands 80 Dutch guilders CSCL 02F

The NASA remote sensing plans for the Land Processes Program are reviewed in the context of the science driven programs in ecology, hydrology, and geology. The instrumental capabilities in place on airborne platforms, and those available on the Earth Observing System in the mid 1990s, are considered. Coordinated field experiments which are evolutionary from the First ISLSCP Field Experiment are discussed. ESA

N89-10394# Compagnie Internationale de Service en Informatique, Toulouse (France).
STUDY ON REPRESENTATION OF SURFACE COVERAGE BY IMAGING EXPERIMENTS Final Report
Georges Balmino and Veronique Lepine Paris, France ESA Nov. 1987 81 p
(Contract ESA-5211/82-D-JS(SC))
(ESA-CR(P)-2584; ETN-88-93029) Avail: NTIS HC A05/MF A01

A tool for remote sensing mission analysis, which represent the final coverage to be expected on the observed planet or natural satellite, was developed. The mission analysis methods only concern the final orbit, to obtain the best resolution on the observed body. However, classical methods of visibility studies are also available in the package. The methods and algorithms developed for the tasks proposed by the package, and the software organization around a user communication subsystem are described. The package may be used entirely in interactive mode for first stage evaluations, and in an interactive mode for defining the environment followed by a batch run to perform the computations. Preference is given to analytical algorithms. ESA

N89-10395*# Michigan State Univ., East Lansing. Center for Remote Sensing.
USE OF REMOTE SENSING FOR LAND USE POLICY FORMULATION Final Report, Jan. 1985 - May 1987
1987 101 p
(Grant NGL-23-004-083)
(NASA-CR-183148; NAS 1.26:183148) Avail: NTIS HC A06/MF A01 CSCL 08B

The overall objectives and strategies of the Center for Remote Sensing remain to provide a center for excellence for multidisciplinary scientific expertise to address land-related global habitability and earth observing systems scientific issues. Specific research projects that were underway during the final contract period include: digital classification of coniferous forest types in Michigan's northern lower peninsula; a physiographic ecosystem approach to remote classification and mapping; land surface change detection and inventory; analysis of radiant temperature data; and development of methodologies to assess possible impacts of man's changes of land surface on meteorological parameters. Significant progress in each of the five project areas has occurred. Summaries on each of the projects are provided.
Author

N89-10396# Instituto de Pesquisas Espaciais, Sao Jose dos Campos (Brazil).
IDENTIFYING THE REFORESTED AREAS UTILIZING THE SPOT SATELLITE DATA
Pedro HernandezFilho Jul. 1988 13 p In PORTUGUESE; ENGLISH summary Presented at the 69th Congresso Florestal Estadual, Nova Prata, Brazil, 24 Sep. 1988 Submitted for publication
(INPE-4624-PRE/1343) Avail: NTIS HC A03/MF A01

The objective of this work is to evaluate the application of the SPOT satellite data to the assessment of reforested areas. The study area (4,000 ha) is localized at the municipality of Mogi-Guacu in the state of Sao Paulo, Brazil, and is reforested by Pinus elliotti, P. taeda, P. patula, P. oocarpa, P. caribee (Campininha fram of the Forestry Institute of the state of Sao Paulo), and Eucalyptus grandis and E. salingna (Santa Terezinha Park - Champion Paper and Cellulose). The utilized image is the one acquired by the multispectral mode XS (714-374), 15 June 1986 hard copy, color composite 3, 2, 1, at the scale of 1:100,000. The procedure for visual interpretation of the image considered classical features of conventional photointerpretation such as tone, photographic texture, and shape, in order to identify the reforested areas. The mapped classes are Pinus-1 (P. elliottii, P. oocarpa), Pinus-2 (P. taeda, P. caribeae, P. patula) and Euca (Eucalyptus spp) and the overall classification accuracy reached circa 90 percent. The obtained results reveal that the SPOT images are very useful to the characterization and mapping of reforested areas. Author

N89-10397# Dornier-Werke G.m.b.H., Friedrichshafen (West Germany).
SOLID EARTH MISSION STUDY. VOLUME 1: EXECUTIVE SUMMARY Final Report
R. Benz, H. Faulks, P. G. Hardtke, R. Klein, M. Langemann, U. Denskat, C. Etienne, P. Peyrot, A. Bernard, and A. Ciampolini (Aeritalia S.p.A., Turin, Italy) et al. Paris, France ESA Nov. 1987 71 p Prepared in cooperation with Matra Espace, Toulouse, France; ONERA, Paris, France; Aeritalia SpA, Turin, Italy; Fokker BV, Amsterdam, The Netherlands: BAe, Bristol, United Kingdom; LABEN Space Instrumentation and Systems, Milan, Italy
(Contract ESTEC-7149/87-NL-JS)
(ESA-CR(P)-2626-Vol-1; ETN-88-93152) Avail: NTIS HC A04/MF A01

The Applications and Research involving Space Techniques Observing The Earth field from Low Earth Satellite (ARISTOTELES) mission is introduced. The ARISTOTELES studies include gravity field measurements, magnetic field measurements, and geokinematics. Gravity anomalies are to be determined with better than 5 mGal accuracy at 100 km spatial resolution by a gravity gradiometer (GRADIO) made with a three axis assembly of microaccelerometers (design goal 0.001 EU accuracy). The satellite is to be launched by Ariane with ERS-2. A dawn-dusk orbit at 220 km is suggested. The most critical point is accommodation of GRADIO, but this is not insurmountable. A summary is presented of the planned mission. ESA

N89-10398* National Aeronautics and Space Administration, Washington, D.C.
EARTH RESOURCES: A CONTINUING BIBLIOGRAPHY WITH INDEXES (ISSUE 58)
Aug. 1988 139 p
(NASA-SP-7041(58); NAS 1.21:7041(58)) Avail: NTIS HC A07; NTIS standing order as PB88-903800. $15.50 domestic, $31.00 foreign CSCL 08B

This bibliography lists 500 reports, articles, and other documents introduced into the NASA scientific and technical information system between April 1 and June 30, 1988. Emphasis is placed on the use of remote sensing and geophysical instrumentation in spacecraft and aircraft to survey and inventory natural resources and urban areas. Subject matter is grouped according to agriculture and forestry, environmental changes and cultural resources, geodesy and cartography, geology and mineral resources, hydrology and water management, data processing and distribution systems, instrumentation and sensors, and economic analysis.
Author

N89-10399# Dornier-Werke G.m.b.H., Friedrichshafen (West Germany).
SOLID EARTH MISSION STUDY. VOLUME 3: PROGRAM PLANNING REPORT Final Report
R. Benz, H. Faulks, P. G. Hardtke, R. Klein, M. Langemann, U. Denskat, C. Etienne, P. Peyrot, A. Bernard, and A. Ciampolini (Aeritalia S.p.A., Turin, Italy) et al. Paris, France ESA Nov. 1987 54 p Prepared in cooperation with Matra Espace, Toulouse, France; ONERA, Paris, France; Aeritalia SpA, Turin, Italy; Fokker BV, Amsterdam, The Netherlands; BAe, Bristol, United Kingdom; LABEN Space Instrumentation and Systems, Milan, Italy
(Contract ESTEC-7149/87-NL-JS)
(ESA-CR(P)-2626-Vol-3; ETN-88-93154) Avail: NTIS HC A04/MF A01

The Applications and Research Involving Space Techniques Observing the Earth field from Low Earth Satellite mission program planning is outlined. ESA

N89-10400# Instituto de Pesquisas Espaciais, Sao Jose dos Campos (Brazil).
THE TRANSFORMED VEGETATION INDEX (TVI) FOR ESTIMATION OF BRAZILIAN CERRADO'S PHYTOMASS
Joao Roberto dosSantos, Attilio Antonio Disperati, Antonio Jose deAraujo, and Roberto Tuyoshi Hosakawa (Universidade Federal de Parana, Curitiba, Brazil) Jun. 1988 11 p Presented at the Remote Sensing Workshop on Vegetation Indices and Their Interpretation, Nottingham, England, 25 May 1988
(INPE-4603-PRE/1326) Avail: NTIS HC A03/MF A01

The main objective of this study is to make an analysis of the relationship between the cerrado's foliar phytomass and the vegetation indices (TVI sub 4,3 and TVI sub 5,3) obtained by the Thematic Mapper/LANDSAT-5. The ground and remote sensing data were gathered in three selected areas: Roncador Ecological Reserve-IBGE, Experimental Station of Brazilia University-UnB, and CPAC/EMBRAPA Station, located at the central region of Brazil. The linear ($y = a + bx$) and exponential ($y = ae^{bx}$) were used to analyze the functional relationship between each of the vegetation indices (x) and cerrado's phytomass (y). From the results it can be inferred that the exponential regression model shows a better fit compared to the linear one although a significant difference was not obtained. Also, the results showed better performance of the TVI sub 4,3 to fit the cerrado's phytomass (dry weight). It explained 62 percent of the variation in the dependent variable (y). This study is part of the large project that is being carried out by INPE and CPAC/EMBRAPA, of the test the TM/LANDSAT data capability for phytomass estimation of the cerrado in order to support future monitoring of this ecosystem.
Author

N89-10401*# National Aeronautics and Space Administration, Washington, D.C.
SAPPING FEATURES OF THE COLORADO PLATEAU: A COMPARATIVE PLANETARY GEOLOGY FIELD GUIDE
Alan D. Howard, ed., R. Craig Kochel, ed., and Henry E. Holt, ed. (Geological Survey, Flagstaff, Ariz.) 1987 115 p Original contains color illustrations
(Grant NsG-7572)
(NASA-SP-491; NAS 1.21:491; LC-87-15305) Avail: NTIS HC A06/MF A01; also available SOD HC $6.00 as 003-000-01027-3 CSCL 08H

This book is an attempt to determine geomorphic criteria to be used to distinguish between channels formed predominantly by sapping and seepage erosion and those formed principally by surface runoff processes. The geologic nature of the Colorado Plateau has resulted in geomorphic features that show similarities to some areas on Mars, especially certain valley networks within thick sandstone formations. Where spring sapping is an effective process, the valleys that develop are unique in terms of their morphology and network pattern.
Author

N89-10402# Instituto de Pesquisas Espaciais, Sao Jose dos Campos (Brazil).
NATION-WIDE FOREST MAPPING AND TIMBER VOLUME ESTIMATION USING LANDSAT-5 TM IMAGERY
Rene Antonio Novaes, David Chung Liang Lee, Pedro HernandezFilho, Armando PachecodosSantos, and Flavio Jorge Ponzoni Aug. 1988 33 p Presented at the Simposio Latino-Americano de Sensoriamento Remoto, 7th Reunion Plenaria SELPER, Bogota, Colombia, 16-20 Nov. 1987
(INPE-4643-PRE/1354) Avail: NTIS HC A03/MF A01

The project described was supported by the United Nations Industrial Development Organization (UNIDO). The main objective of this project was to obtain basic forest information for development, promotion, and utilization of alternative sources of energy based on the use of the country's natural resources. A methodology is described which used LANDSAT TM data as a first segment of a two-stage sampling plan designed to produce typical forest information for the plantations and to map forest areas in Uruguay. From this project it can be concluded that the total forest area is about 3 percent of the total land area in Uruguay. The plantation forest, which has high productivity of woods, is about 23.7 percent of total forested areas. The overall interpretation and mapping accuracies werer 90.6 andn 83.3 percent, respectively. The total stand timber volume of pine and eucalypt plantation was estimated at 3,539,418.15 cubic meters and 24,231,118.83 cubic meters, respectively. From all the results obtained the project would conclude that LANDSAT-5 TM imagery, at a scale of 1:100,000, served well as the primary source of data from forest area mapping and timber inventory over a nation-wide level.
Author

N89-10403*# National Aeronautics and Space Administration. Lewis Research Center, Cleveland, Ohio.
DATA REPORT FOR THE SIPLE COAST (ANTARCTICA) PROJECT
R. A. Bindschadler, S. N. Stephenson, E. P. Roberts, D. R. MacAyeal, and D. R. Lindstrom (Chicago Univ., Ill.) Oct. 1988 108 p
(NASA-TM-100708; NAS 1.15:100708; Rept-88B-0214) Avail: NTIS HC A06/MF A01 CSCL 08B

This report presents data collected during three field seasons of glaciological studies in the Antarctica and describes the methods employed. The region investigated covers the mouths of Ice Streams B and C (the Siple Coast) and Crary Ice Rise on the Ross Ice Shelf. Measurements included in the report are as follows: surface velocity and deformation from repeated satellite geoceiver positions; surface topography from optical levelling; radar sounding of ice thickness; accumulation rates; near-surface densities and temperature profiles; and mapping from aerial photography.
Author

N89-10404# Deutsche Forschungs- und Versuchsanstalt fuer Luft- und Raumfahrt, Oberpfaffenhofen (West Germany). Abteilung Fernerkundung.
APPLICATIONS OF LANDSAT (TM AND MSS) DATA FOR AN ESTIMATION OF RANGELAND CONDITIONS IN SEMIARID AND ARID AREAS OF NORTHERN KENYA
Christoph Dreiser Dec. 1987 119 p In GERMAN; ENGLISH summary Original contains color illustrations
(DFVLR-FB-88-18; ISSN-0171-1342; ETN-88-93185) Avail: NTIS HC A06/MF A01; DFVLR, VB-PL-DO, 90 60 58, 5000 Cologne, Fed. Republic of Germany, 66 Deutsche marks

Digital multispectral data are analyzed to prove the applicability of LANDSAT 5 sensors, Thematic Mapper (TM) and Multispectral Scanner (MSS), to recognize variations of sparse vegetation coverage. The research area is a dwarf-shurb semidesert in Northern Kenya (Marsabit District). The size of the subscene is 1024 x 1024 pixels. Data were acquired in the dry season. Perpendicular vegetation index is used for tracing training areas. A maximum likelihood classification of TM channels, 3, 4, 5, and 7 gives acceptable results. Compared with the classification of MSS data, TM classification leads to much more exact results. Classification results are processed further to estimate the actual rangeland potential.
ESA

44 ENERGY PRODUCTION AND CONVERSION

Includes specific energy conversion systems, e.g., fuel cells; global sources of energy; geophysical conversion; and windpower.

For related information see also *07 Aircraft Propulsion and Power, 20 Spacecraft Propulsion and Power,* and *28 Propellants and Fuels.*

N89-10405*# National Aeronautics and Space Administration. Lewis Research Center, Cleveland, Ohio.
HYDROGEN-BROMINE FUEL CELL ADVANCE COMPONENT DEVELOPMENT
JoAnn Charleston and James Reed (Atlanta Univ., Ga.) 1988 16 p Presented at the National Technical Association Conference, Chicago, Ill., 13-16 Jul. 1988

(NASA-TM-101345; E-4368; NAS 1.15:101345) Avail: NTIS HC A03/MF A01 CSCL 10B

Advanced cell component development is performed by NASA Lewis to achieve improved performance and longer life for the hydrogen-bromine fuel cells system. The state-of-the-art hydrogen-bromine system utilizes the solid polymer electrolyte (SPE) technology, similar to the SPE technology developed for the hydrogen-oxygen fuel cell system. These studies are directed at exploring the potential for this system by assessing and evaluating various types of materials for cell parts and electrode materials for Bromine-hydrogen bromine environment and fabricating experimental membrane/electrode-catalysts by chemical deposition. Author

N89-10406# Midwest Research Inst., Golden, Colo. Solar Energy Research Inst.

ELECTRONIC STRUCTURE OF ELECTRODEPOSITED THIN FILM CdTe SOLAR CELLS

H. S. Ullal May 1988 16 p

(Contract DE-AC02-83CH-10093)

(DE88-001170; SERI/TP-211-3361) Avail: NTIS HC A03/MF A01

Independent experimental verification done at four research laboratories, namely, Ametek, Colorado State University (CSU), Institute of Energy Conversion (IEC), and Solar Energy Research Institute (SERI) confirm the n-i-p model proposed by Ametek. The experiments done for the verification of the n-i-p structure are the high frequency capacitance-voltage, light and voltage bias quantum efficiency, and EBIC measurements. All experimental evidence suggests that the n-i-p model is appropriate for the existing n-CdS/i-CdTe/p-ZnTe cell structure. From the C-V measurements, the depletion width has been estimated at 1.7 to 2.0 microns and corresponds to the thickness of the CdTe film. This unique thin films device design has resulted in improved stability and a SERI-verified world record single-junction total area AM1.5 global efficiency of 11 percent. Further refinements in device design and cell processing should result in 12 to 13 percent efficiencies for thin-film CdTe solar cells in the not-too-distant future. DOE

N89-10407*# Lockheed Missiles and Space Co., Sunnyvale, Calif.

ADVANCED PLANAR ARRAY DEVELOPMENT FOR SPACE STATION Final Report

19 May 1987 68 p

(Contract NAS8-36419)

(NASA-CR-179372; NAS 1.26:179372) Avail: NTIS HC A04/MF A01 CSCL 10A

The objectives are to develop a process for manufacturing superstrate assemblies; demonstrate superstrate technology through fabrication and testing; develop and analyze a preliminary solar array wing design; and fabricate a wing segment based on the wing design. The task description, project flow diagram, and schedule are outlined. The progress to date is presented.

Author

N89-10408# Oak Ridge National Lab., Tenn.

LABORATORY CAPACITY MODULATION EXPERIMENTS, ANALYSES AND VALIDATION

William A. Miller 1988 15 p Presented at the 2nd DOE/ORNL Heat Pump Conference: Research and Development on the Heat Pump for Space Conditioning Applications, Washington, D.C., 17 Apr. 1988

(Contract DE-AC05-84OR-21400)

(DE88-012930; CONF-8804100-17) Avail: NTIS HC A03

A combined experimental and analytical project was conducted on a breadboarded continuously variable speed air-to-air heat pump (CVSHP). The split-system residential unit of nominal 2.75-ton (9.7-kW) cooling capacity was instrumented and tested in environmental chambers. The steady-state, frosting/demand defrosting, and cycling efficiency characteristics of the CVSHP with first generation components (e.g., heat exchangers, compressor, and indoor blower, both having variable speed induction motors) were measured in the laboratory for compressor drive frequencies ranging from 15 through 90 Hz. Steady-state efficiency data were used to validate an initial version of the Oak Ridge National Laboratory steady-state modulating heat pump design program. Algorithms were developed from reduced dynamic loss data from which calculations were made of the seasonal losses for the test CVSHP. DOE

N89-10409*# National Aeronautics and Space Administration. Lewis Research Center, Cleveland, Ohio.

OXYGEN ELECTRODE BIFUNCTIONAL ELECTROCATALYST NiCo2O4 SPINEL

William L. Fielder and Joseph Singer Sep. 1988 22 p

(NASA-TM-100947; E-4238; NAS 1.15:100947) Avail: NTIS HC A03/MF A01 CSCL 10A

A significant increase in energy density may be possible if a two-unit alkaline regenerative H2-O2 fuel cell is replaced with a single-unit system that uses passive means for H2O transfer and thermal control. For this single-unit system, new electrocatalysts for the O2 electrode will be required which are not only bifunctionally active but also chemically and electrochemically stable between the voltage range of about 0.7 and 1.5 V. NiCo2O4 spinel is reported to have certain characteristics that make it useful for a study of electrode fabrication techniques. High surface area NiCo2O4 powder was fabricated into unsupported, bifunctional, PTFE-bonded, porous gas fuel cell electrodes by commercial sources using varying PTFE contents and sintering temperatures. The object of this study is to measure the bifunctional activities of these electrodes and to observe what performance differences might result from different commercial electrode fabricators. O2 evolution and O2 reduction data were obtained at 80 C (31 percent KOH). An irreversible reaction (i.e., aging) occurred during O2 evolution at potentials greater than about 1.5 V. Anodic Tafel slopes of 0.06 and 0.12 V/decade were obtained for the aged electrodes. Within the range of 15 to 25 percent, the PTFE content was not a critical parameter for optimizing the electrode for O2 evolution activity. Sintering temperatures between 300 and 340 C may be adequate but heating at 275 C may not be sufficient to properly sinter the PTFE-NiCo2O4 mixture. Electrode disintegration was observed during O2 reduction. Transport of O2 to the NiCo2O4 surface became prohibitive at greater than about -0.02 A/sq cm. Cathodic Tafel slopes of -0.6 and -0.12 V/decade were assumed for the O2 reduction process. A PTFE content of 25 percent (or greater) appears to be preferable for sintering the PTFE-NiCo2O4 mixture. Author

N89-10410# Midwest Research Inst., Golden, Colo. Solar Energy Research Inst.

SOLID STATE PHOTOVOLTAIC RESEARCH BRANCH Annual Report, FY 1987

Jun. 1988 252 p

(Contract DE-AC02-83CH-10093)

(DE88-001179; SERI/PR-212-3337) Avail: NTIS HC A12/MF A01

This report summarizes the progress of the Solid State Photovoltaic Research Branch of the Solar Energy Research Institute (SERI) from 1 October 1986 through 30 September 1987. Six technical sections of the report cover these main areas of SERI's in-house photovoltaic research: Semiconductor Crystal Growth, Amorphous Silicon Research, Polycrystalline Thin films, III-V High-efficiency Photovoltaic Cells, Solid State Theory, and Laser Raman and Luminescence Spectroscopy. In each section, the purposes and major accomplishments of this work are explained in the context of the U.S. Department of Energy's National Photovoltaic Program Plan goals. DOE

N89-10411# Honeywell, Inc., Bloomington, Minn. Physical Sciences Center.

MOCVD TECHNIQUES FOR CdTe SOLAR CELLS Final Report, 15 Feb. 1985 - 1 Apr. 1987

D. E. Schafer Feb. 1988 49 p

(Contract DE-AC02-83CH-10093)

(DE88-001163; SERI/STR-211-3218) Avail: NTIS HC A03/MF A01

This report summarizes the application of metal-organic chemical vapor deposition (MOCVD) film growth to two aspects of CdTe/ITO solar cell fabrication: (1) the growth of large-area CdTe films on ITO, and (2) the formation of low-resistance ohmic contacts to p-type CdTe. A reduced-temperature MOCVD process was developed for the deposition of CdTe films in order to minimize the potential for chemical and physical changes in the ITO layer during cell fabrication of ohmic contacts (opaque and long wavelength transparent, respectively) to the CdTe layer of the photovoltaic structure. This report details the MOCVD reactor geometries and process parameters used in the development of the CdTe, HgTe, and ZnTe layer growth, as well as the results of C-V analysis of the carrier concentration in the MOCVD CdTe layers and resistance characteristics of various interfaces formed by CdTe, HgTe, and ZnTe. DOE

45 ENVIRONMENT POLLUTION

Includes atmospheric, noise, thermal, and water pollution.

N89-10412# Lawrence Livermore National Lab., Calif.
APPLICATIONS OF A THREE-DIMENSIONAL FINITE ELEMENT MODEL TO MOUNTAIN-VALLEY FLOWS
Robert L. Lee and John M. Leone, Jr. Feb. 1988 8 p Presented at the 1st International Conference on Computational Methods in Flow Analysis, Okayama, Japan, 5 Sep. 1988
(Contract W-7405-eng-48)
(DE88-008898; UCRL-97389; CONF-880936-2) Avail: NTIS HC A02/MF A01

In this paper we will describe briefly a modified finite element procedure which we have developed to solve the non-hydrostatic planetary boundary layer equations. We have exploited several cost effective procedures such as a one-point quadrature scheme and mass lumping in conjunction with an explicit, modified forward Euler, time integration scheme. This simplified approach enables us to achieve computational efficiencies competitive with standard finite difference models. In addition we employ an iterative technique based on a preconditioned conjugate gradient alogrithm for the time-consuming pressure solution portion of the model. In order to realistically model the atmospheric flows of interest we have implemented a K-Theory (variable eddy diffusivity) model to parameterize the turbulent fluxes within the boundary layer. The K-model proposed by McNider and Pielke is used for application in nocturnal (stabie) situations. In this formulation, the vertical eddy diffusion coefficients are calculated as a function of the local Richardson number, a measure of the local stability an air parcel. In daytime (convective) situations, we employ an O'Brien cubic profile to model the vertical variation of the eddy diffusivities. DOE

N89-10413# Instituto de Pesquisas Espaciais, Sao Jose dos Campos (Brazil).
ENVIRONMENTAL IMPACT OF THE URBAN GROWTH ON THE WESTERN SAO PAULO METROPOLITAN AREA
Celina Foresti Aug. 1988 11 p Presented at the 16th Congress of International Society for Photogrammetry and Remote Sensing, Kyoto, Japan, 1-10 Jul. 1988 Submitted for publication
(INPE-4670-PRE/1370) Avail: NTIS HC A03/MF A01

Satellite-borne remote sensing data are useful for urban environment analysis owing to their improved spatial, spectral, and radiometric resolution. The present study assess the environmental impact of urban growth on the Western Sao Paulo Metropolitan Area from 1975 to 1985. Multidate digital data from MSS/LANDSAT, TM/LANDSAT, and HRV-SPOT were registered and urban structure changes within that period were detected. Color composite photographs of TM band 5, 3, and 4 were applied to map the urban land use for new urban areas. The HRV-SPOT panchromatic data, digitally enlarged to the scale of 1:10,000 were applied to urban structure mapping and environmental monitoring. Ground truth data collection and helicopter-borne data collection were used to complement the remote sensed data. Several environment degradation levels were determined and compared to the Physical Aptitude for Urban Settlement Chart. The results showed that environmental impacts are more related to the pattern of urban settlement than to the physiographic features. Vegetative cover proved to be the most important key, indicating environmental change as far as orbital remote sensing is concerned. Soil erosion is caused by the removal of vegetative cover, but the erosion rates are controlled by the different patterns of land use. Author

N89-10414# California Univ., Berkeley. Lawrence Berkeley Lab. Engineering Div.
FOURIER TRANSFORM INFRARED SPECTROMETRY OF AMBIENT AEROSOLS
M. Pollard and J. Jaklevic May 1988 82 p Sponsored by Environmental Monitoring Systems Lab., Research Triangle Park, N.C.
(PB88-213236; EPA-600/4-88-020) Avail: NTIS HC A05/MF A01 CSCL 13B

Fourier transform infrared (FTIR) spectrometry was evaluated as a method for determining the concentration of selected species present in ambient aerosols collected on Teflon filters. The filters are analyzed by transmission measurements after collection of the fine fraction of the ambient particles on 2 micrometers pore size Teflon filters. The spectra of the blank filters are subtracted from the spectra of the loaded filters and the area of the specific absorbance bands for ammonium, nitrate, and sulfate are measured and compared to calibration curves. The filter orientation must be maintained for all measured infrared spectra. GRA

N89-10415# Oak Ridge National Lab., Tenn. Environmental Sciences Div.
EVALUATING IMPACTS OF POLLUTANTS FROM THE ATMOSPHERE
D. F. Grigal (Minnesota Univ., Saint Paul.) and R. S. Turner 1988 27 p Presented at the International Interactive Workshop on Soil Resources: Their Inventory, Analysis and Interpretation for Use in the 1990s, Minneapolis, Minn., 22 Mar. 1988
(Contract DE-AC05-84OR-21400)
(DE88-014550; CONF-8803128-1) Avail: NTIS HC A03/MF A01

As a result of industrialization, concentrations of many compounds have increased in the atmosphere. Deposition of some of these compounds from the atmosphere to soil has been hypothesized to alter soil properties. These alterations may adversely affect plant growth and create conditions for movement of toxic materials from terrestrial to aquatic systems. Acidic deposition, in both wet and dry forms, can displace and hence remove nutrient cations from the rooting zone. Associated declines in pH can increase the solubility of toxic metals such as Al. In acid soils, increasing SO4(+2) concentrations in soil solution from atmospheric deposition can also mobilize Al. Atmospheric deposition can also increase the concentration of other toxic metals, such as Pb and Hg, in soil. Assessment of the impacts of deposition on soil may depend on before and-after sampling, whereby results of recent analyses are compared to results either from older reports or from reanalysis of archived samples. Changes in laboratory procedures and uncertainty about sampling location affect the first method, whereas limited numbers of archived samples and changes in properties during storage affect the second method. Assessment of impacts can also be made by field measurements of soil solution chemistry or by measurements of changes in soil chemical properties. Such measurements, however, are both expensive and difficult to obtain for many sites. DOE

46 GEOPHYSICS

Includes aeronomy; upper and lower atmosphere studies; ionospheric and magnetospheric physics; and geomagnetism.

For space radiation see *93 Space Radiation.*

N89-10416*# Johns Hopkins Univ., Baltimore, Md. Dept. of Earth and Planetary Sciences.
THE DELINEATION AND INTERPRETATION OF THE EARTH'S GRAVITY FIELD Annual Progress Report, 1 Jun. 1987 - 31 May 1988
Bruce D. Marsh 31 May 1988 27 p
(Grant NAG5-32)
(NASA-CR-183283; NAS 1.26:183283) Avail: NTIS HC A03/MF A01 CSCL 08G

A series of fluid dynamical experiments in variable viscosity fluid have been made and are in progress to study: (1) the onset of small scale convection relative to lithosphere growth rate; (2) the influence of paired fracture zones in modulating the horizontal scale of small scale convection; (3) the influence of the mantle vertical viscosity structure on determing the mode of small scale convection; and (4) the 3-D and temporal evolution of flows beneath a high viscosity lid. These experiments extend and amplify the present experimental work that has produced small scale convection beneath a downward-moving solidification front. Rapid growth of a high viscosity lid stifles the early onset of convection such that convection only begins once the lithosphere is older than a certain minimum age. The interplay of this convection with both the structure of the lithosphere and mantle provide a fertile field of investigation into the origin of geoid, gravity, and topographic anomalies in the central Pacific. These highly correlated fields of intermediate wavelength (approximately 200 to 2000 km), but not the larger wavelengths. It is the ultimate, dynamic origin of this class of anomalies that is sought in this investigation. Author

N89-10417*# Utah State Univ., Logan. Center for Atmospheric and Space Sciences.
DYNAMICS EXPLORER GUEST INVESTIGATOR Final Report, 15 Mar. 1986 - 30 Jun. 1988
J. J. Sojka 30 Aug. 1988 9 p
(Grant NAG5-748)
(NASA-CR-183163; NAS 1.26:183163) Avail: NTIS HC A02/MF A01 CSCL 04A

The research has focused on using the SAI auroral images as a high resolution auroral precipitation input to the USU global scale ionospheric model. From the global scale modeling viewpoint, these images offer unique spatial and temporal resolution since all prior studies have used empirical auroral models. These latter models are devoid of storm, substorm, or discrete oval features. The research focused on the problems in converting images to energy flux; using LAPU data to calibrate these energy fluxes; using the USU Time Dependent Ionospheric Model (TDIM) to look at the ionospheric consequences of this structure; and then using DE-2 in-situ observations to compare with the TDIM ionospheric parameters. In carrying out these studies, several additional investigations cropped up which were pursued to help meet the overall goals. The foremost difficulty in carrying out the TDIM modeling in conjunction with the high resolution DE auroral model was that of defining an appropriate ionospheric convection pattern. Under northward conditions this pattern is very complex. In order to study Theta aurora or in general northward IMF conditions, a new model was required. Hence, a study was completed to supply this new model to drive the TDIM as a function of the IMF. With the DE auroral model having adequate resolution to show structure on the 100's of km and all model electric fields being devoid of such structure, an investigation was pursued to find out the effects of structures in the electric field on the F-region. Author

N89-10418# Compagnie de Prospection Geophysique Francaise, Puteaux.
APPLICATION OF MICROGRAVITY TO THE ASSESSMENT OF EXISTING STRUCTURES AND STRUCTURAL FOUNDATIONS Final Report, Apr. 1986 - Apr. 1988
Jacques Lakshmanan 29 Apr. 1988 328 p
(Contract DAJA45-86-C-0022; DA Proj. 1L1-61102-BH-57)
(AD-A195599) Avail: NTIS HC A15/MF A01 CSCL 08E

The report evaluates microgravity and other geophysical techniques, applied to the detection of density anomalies in structures and in their foundations. Microgravity measurement and processing techniques, as well as in-situ density evaluation (including the Cheops pyramid) are described. The report summarizes microgravity techniques. After a description of field techniques, the main interpretation techniques, both conventional and innovative, are described. The report describes the application of microgravity to the direct in-situ measurements of embankment densities and to the assessment of foundations of existing structures, and includes the description of the Cheops survey. The report describes the use of microgravity for grouting control and other repeat surveys. The report compares microgravity with other geophysical methods in the fields of cavity detection and grout control. It describes the use of resistivity, electromagnetics, seismic methods and down-hole logging. The report compares current French practice in the field of cavity detection, with methods used in the rest of the world. GRA

N89-10419*# Houston Univ., Tex.
WILSON CYCLE STUDIES Semiannual Report, 14 Jan. - 15 Jul. 1988
Kevin Burke Jul. 1988 19 p Prepared in cooperation with Lunar and Planetary Inst., Houston, Tex.
(Grant NAG5-585)
(NASA-CR-183146; NAS 1.26:183146) Avail: NTIS HC A03/MF A01 CSCL 08G

Effort was concentrated in problems of continental evolution and a presentation was made to a workshop on the Deep Continental Growth of South India. An interpretation of the lithospheric structure of Africa as related to continental collision (together with its volcanism and topography) was prepared and a paper on this topic is about to be submitted. No expenditures were charged to the grant during this 6 month period. Author

N89-10420*# National Aeronautics and Space Administration. Langley Research Center, Hampton, Va.
COMPILATION OF METHODS IN ORBITAL MECHANICS AND SOLAR GEOMETRY
James J. Buglia Washington Oct. 1988 81 p
(NASA-RP-1204; L-16451; NAS 1.61:1204) Avail: NTIS HC A05/MF A01 CSCL 04A

This paper contains a collection of computational algorithms for determining geocentric ephemerides of Earth satellites, useful for both mission planning and data reduction applications. Special emphasis is placed on the computation of sidereal time, and on the determination of the geocentric coordinate of the center of the Sun, all to the accuracy found in the Astronomical Almanac. The report is completely self-contained in that no requirement is placed on any external source of information, and hence, these methods are ideal for computer application. Author

N89-10421 California Univ., San Diego.
VOID COLLAPSE AND VOID GROWTH IN CRYSTALLINE SOLIDS Ph.D. Thesis
Muneo Hori 1987 147 p
Avail: Univ. Microfilms Order No. DA8804728

It is commonly accepted that local plastic flow plays a major role in large deformation of pre-existing cavities in crystalline solids under high loading rates, and that the global failure can be caused by the coalescence of growing cavities, or their collapse. Effects of the loading rate and the plastic flow on this type of failure mechanisms are investigated. To this end, plastic constitutive relations, based on the rate dependent power law slip on crystallographic planes, are assumed. The problem is formulated in the rate form, and solved, taking the involved finite deformations into account. The mechanism of void deformation which involves large plastic flows is studied. Both the void deformation and the global material response are shown to be highly dependent on the loading rate. The slip induced anisotropy, which is not included

in the existing phenomenological models, is clearly shown to be an important controlling factor in determining the response and failure modes of crystalline solids. The overall failure of materials containing cavities under high loading rates is studied, the mechanism of fracturing caused by unstable collapse and/or growth of pre-existing cavities is examined. Dissert. Abstr.

N89-10422# Office National d'Etudes et de Recherches Aerospatiales, Paris (France).
LA RECHERCHE AEROSPATIALE, BIMONTHLY BULLETIN, NUMBER 1987-5, 240/SEPTEMBER-OCTOBER
ESA Jun. 1988 76 p Transl. into ENGLISH of La Recherche Aerospatiale, Bulletin Bimestriel (Paris, France, ONERA), no. 1987-5, 240/Sep.-Oct., 1987
(ESA-TT-1095; ETN-88-93054) Avail: NTIS HC A05/MF A01

Asymptotic analysis of the k-epsilon model for a turbulent boundary layer; detection of the OH radical in flames by resonance coherent anti-Stokes Raman spectroscopy; a wind tunnel study of the degradation of optical images by heterogeneous aerodynamic flows; optical imaging through atmospheric turbulence; and modeling mechanical subsystems by boundary impedance in the finite element method are discussed. For individual titles, see N89-10423 through N89-10423.

N89-10423# Office National d'Etudes et de Recherches Aerospatiales, Paris (France).
OPTICAL IMAGING THROUGH ATMOSPHERIC TURBULENCE
G. Rousset, J.-C. Fontanella, J. Primot, and A. Seve *In its* La Recherche Aerospatiale, Bimonthly Bulletin, Number 1987-5, 240/September-October Jun. 1988 p 47-58 Transl. into ENGLISH from La Recherche Aerospatiale, Bulletin Bimestriel (Paris, France, ONERA), no. 1987-5, 240/Sep.-Oct., 1987 Sponsored in part by Direction des Recherches, Etudes et Techniques (For primary document see N89-10422 01-46)
Avail: NTIS HC A05/MF A01

A review is first made of research done at ONERA in optical imaging through atmospheric turbulence. Several techniques previously proposed, by which images can be obtained with a resolution at the diffraction limit, are compared on the basis of their field of application, the expected signal-to-noise ratio, and the practical difficulties involved with these methods, which are: techniques involving off-line digital processing, based on a generalization of the speckle interferometry method proposed by A. Labeyrie; the deconvolution from wave-front sensing; and adaptive optics, which seems to be a very promising technique. Author

N89-10424 Alaska Univ., Fairbanks.
ELECTRON TRANSPORT AND OPTICAL EMISSIONS IN THE AURORA Ph.D. Thesis
Dirk Lummerzheim 1987 145 p
Avail: Univ. Microfilms Order No. DA8804158

A one-dimensional, steady state auroral model is developed based on a linear electron transport calculation. A set of cross sections for electron neutral collisions describing elastic scattering, energy loss, and photon emission is compiled and used in conjunction with a discrete ordinate transport code. Calculated electron intensities are compared with in situ rocket measurements. Auroral optical emissions that result from direct electron impact on neutrals are calculated for synthetic and observed electron spectra. A systematic dependence of the brightness of auroral features on energy flux, characteristic energy, and atmospheric composition is found and parameterized. A method for interpreting the brightness and the ratio of brightness of certain auroral emissions in terms of the energy flux, characteristic energy, and relative oxygen density is described. Application of this method to auroral images acquired by nadir viewing instruments aboard a satellite is discussed and the distribution of energy flux, characteristic energy, and ionospheric conductances over the auroral oval is determined. Emissions that are suitable for analysing auroral spectra in terms of the atomic oxygen abundance are identified. Dissert. Abstr.

N89-10425*# California Inst. of Tech., Pasadena. Seismological Lab.
EARTH ROTATION AND CORE TOPOGRAPHY Final Report, 15 Jul. 1986 - 14 Sep. 1987
Bradford H. Hager, Robert W. Clayton, and Mary Ann Spieth (Jet Propulsion Lab., California Inst. of Tech., Pasadena.) 20 Sep. 1988 10 p
(Grant NAG5-819)
(NASA-CR-183186; NAS 1.26:183186) Avail: NTIS HC A02/MF A01 CSCL 08G

The NASA Geodynamics program has as one of its missions highly accurate monitoring of polar motion, including changes in length of day (LOD). These observations place fundamental constraints on processes occurring in the atmosphere, in the mantle, and in the core of the planet. Short-timescale (t less than or approx 1 yr) variations in LOD are mainly the result of interaction between the atmosphere and the solid earth, while variations in LOD on decade timescales result from the exchange of angular momentum between the mantle and the fluid core. One mechanism for this exchange of angular momentum is through topographic coupling between pressure variations associated with flow in the core interacting with topography at the core-mantel boundary (CMB). Work done under another NASA grant addressing the origin of long-wavelength geoid anomalies as well as evidence from seismology, resulted in several models of CMB topography. The purpose of work supported by NAG5-819 was to study further the problem of CMB topography, using geodesy, fluid mechanics, geomagnetics, and seismology. This is a final report. Author

N89-10190*# Jet Propulsion Lab., California Inst. of Tech., Pasadena.
SPAIN 31-GHz OBSERVATIONS OF SKY BRIGHTNESS TEMPERATURES
B. L. Gary *In its* The Telecommunications and Data Acquisition Report 15 Aug. 1988 p 42-60 (For primary document see N89-10186 01-32)
Avail: NTIS HC A14/MF A01 CSCL 04A

N89-10191*# Jet Propulsion Lab., California Inst. of Tech., Pasadena.
AUSTRALIA 31-GHz BRIGHTNESS TEMPERATURE EXCEEDANCE STATISTICS
B. L. Gary *In its* The Telecommunications and Data Acquisition Report 15 Aug. 1988 p 61-74 (For primary document see N89-10186 01-32)
Avail: NTIS HC A14/MF A01 CSCL 04A

N89-10192*# Jet Propulsion Lab., California Inst. of Tech., Pasadena.
GRAVITATIONAL WAVE SEARCHES USING THE DSN (DEEP SPACE NETWORK)
S. J. Nelson and J. W. Armstrong *In its* The Telecommunications and Data Acquisition Report 15 Aug. 1988 p 75-85 (For primary document see N89-10186 01-32)
Avail: NTIS HC A14/MF A01 CSCL 04A

47 METEOROLOGY AND CLIMATOLOGY

Includes weather forecasting and modification.

N89-10426*# Florida State Univ., Tallahassee. Dept. of Meteorology.
ANALYSIS AND USE OF VAS SATELLITE DATA Final Report, 23 Aug. 1985 - 22 Aug. 1988
Henry E. Fuelberg, Mark J. Andrews, John L. Beven, II, Steven R. Moore, and Bradley M. Muller Aug. 1988 88 p
(Grant NAG8-033)
(NASA-CR-183184; NAS 1.26:183184) Avail: NTIS HC A05/MF A01 CSCL 04B

A series of interrelated investigations has examined the analysis and use of VAS (VISSR Atmospheric Sounder) satellite data. A case study of VAS-derived mesoscale stability parameters

suggested that they would have been a useful supplement to conventional data in the forecasting of thunderstorms on the day of interest. However, the meteorological significance of small or short lived stability features was uncertain. A second investigation examined the roles of first guess and VAS radiometric data in producing sounding retrievals. The radiance data often did not have a decisive influence on the final satellite soundings. Broad-scale patterns of the first guess, radiances, and retrievals frequently were similar, whereas small scale retrieval features, especially in the dew points, were often of uncertain origin.
Author

N89-10427# Control Data Corp., Minneapolis, Minn. Meteorology Research Center.
MEASUREMENT OF VERTICAL VELOCITY USING CLEAR-AIR DOPPLER RADARS
T. E. VanZandt, J. L. Green, G. D. Nastrom, K. S. Gage, and W. L. Clark 25 Mar. 1988 3 p Presented at the Symposium on Lower Tropospheric Profiling: Needs and Technologies, Boulder, Colo., 31 May - 3 Jun. 1988
(Contract F49620-86-C-0027)
(AD-A195344; AFOSR-88-0495TR) Avail: NTIS HC A02/MF A01 CSCL 17I

Since the development of the clear-air Doppler radar technique (also called the Wind-profiling or MST-radar technique) at Jicamarca, Peru (Woodman and Guillen, 1974), it has been applied to a wide range of meteorological problems (see, e.g., Liu and Kato, 1985). Despite this rapid progress, research on some important problems has been frustrated by the fact that most clear-air Doppler radars are near mountains. The resulting orographic effects act as geophysical noise on observations of other processes. These effects are especially serious for studies of the vertical component of motion. For example, Ecklund et al. (1982) found that when the wind flowed over the mountains, the variance of the vertical velocity was strongly correlated with the wind speed. Nastrom et al. (1985) found that they could extract the small synoptic-scale vertical velocity only when the horizontal wind was not from the direction of nearby mountains. Following their suggestion, we have constructed anew clear-air Doppler radar, called the Flatland radar, in very flat terrain near Champaign-Urbana, Illinois. We find that the vertical velocity field over very flat terrain is indeed quite different from that near rough terrain, and we present observations that suggest that the vertical velocity due to other processes, such as synoptic-scale motions and gravity waves, can be studied by clear-air Doppler radars in very flat terrain.
GRA

N89-10428# National Center for Atmospheric Research, Boulder, Colo. Climate and Global Dynamics Div.
CCM (COMMUNITY CLIMATE MODEL) MODULAR PROCESSOR USERS' GUIDE (VERSION PROC02)
R. J. Wolski Oct. 1987 257 p
(Grant NSF ATM-87-09659)
(PB88-216577; NCAR/TN-290/IA) Avail: NTIS HC A12/MF A01 CSCL 04B

A complete description is provided of the capabilities of the PROC02 version of the CCM Modular Processor, including all of the information needed to run the code on the Crays at NCAR. A few aspects of Processor design are discussed where appropriate, but there is no attempt to document the details of the code. This is a rewrite of the NCAR Tech Note TN-261+IA CCM Modular Processor Users' Guide (Version PROC01), January 1986. A short description of PROC02 relative to PROC01 is also available.
Author

N89-10429# National Oceanic and Atmospheric Administration, Rockville, Md.
INTERNATIONAL AEROSPACE AND GROUND CONFERENCE ON LIGHTNING AND STATIC ELECTRICITY
Apr. 1988 535 p Conference held in Oklahoma City, Okla., 19-22 Apr. 1988
(PB88-197439) Avail: NTIS HC A23/MF A01 CSCL 04B

Various topics related to lightning and static electricity are discussed. Aircraft strike statistics, lightning propagation models, aerospace vehicles, simulation, aircraft hazards rocket launch hazards, thunderstorms, lightning detection and protection, and mapping systems are among the topics covered. For individual titles, see N89-10430 through N89-10497.

N89-10430# Tohoku Univ., Sendai (Japan). Dept. of Electrical Engineering.
STATISTICS OF LIGHTNING INTERACTION WITH AIRCRAFT IN JAPAN
Yukihiro Goto and Yoshihiro Murooka (National Defence Academy, Yokosuka, Japan) *In* NOAA, International Aerospace and Ground Conference on Lightning and Static Electricity Apr. 1988 p 1-7 (For primary document see N89-10429 01-47)
Avail: NTIS HC A23/MF A01 CSCL 04B

A survey of lightning interaction with commercial aircraft in Japan for the past 10 years is given. Aircraft flight conditions during lightning strikes and concomitant synoptic weather which were reported by flight crews were correlated as a percentage of the total number of strikes reported in Japan.
Author

N89-10431# Chelton (Electrostatics) Ltd., Marlow (England).
ISRAEL AIR FORCE (IAF) IN-SERVICE AIRCRAFT LIGHTNING STRIKE AND DAMAGE SURVEY
Elya B. Joffe *In* NOAA, International Aerospace and Ground Conference on Lightning and Static Electricity Apr. 1988 p 8-12 (For primary document see N89-10429 01-47)
Avail: NTIS HC A23/MF A01 CSCL 04B

A survey of lightning strikes to aircraft, covering all types of aircraft (tactical fighters, transport aircraft and helicopters), is given. The survey results include descriptive data on each strike and the effects. A lightning strike in which an F-16 was struck while in flight is discussed. Some basic problems arising from new requirements for lightning protection are discussed.
Author

N89-10432# Computer Resource Management, Inc., Atlantic City, N.J.
LIGHTNING INFORMATION DATABASE
R. L. McDowall and Michael S. Glynn (Federal Aviation Agency, Atlantic City, N.J.) *In* NOAA, International Aerospace and Ground Conference on Lightning and Static Electricity Apr. 1988 p 13-15 (For primary document see N89-10429 01-47)
Avail: NTIS HC A23/MF A01 CSCL 04B

The Federal Aviation Administration (FAA) is creating a data base of electromagnetic information on lightning. A number of sources of information have been identified and an attempt to acquire and centrally locate the data is being pursued. The data will ultimately be available to general researchers. In certain cases on-line access to database peripheral information such as altitude, temperature, precipitation, turbulence, and peak and average electromagnetic values will be available. It is also anticipated that digitized waveforms will be available.
Author

N89-10433# Electro Magnetic Applications, Inc., Lakewood, Colo.
A STOCHASTIC MODEL FOR THE TORTUOUS PROPAGATION OF A LIGHTNING STEPPED LEADER
Robert W. Haupt and Dale A. Steffen *In* NOAA, International Aerospace and Ground Conference on Lightning and Static Electricity Apr. 1988 p 16-21 (For primary document see N89-10429 01-47)
Avail: NTIS HC A23/MF A01 CSCL 04B

A lightning discharge propagation model (LDPM) was developed to be integrated into the South Dakota School of Mines' Time-Dependent Storm Electrification Model. The LDPM approximates in three dimensions the tortuous path of a lightning channel in a thunderstorm environment. The channel is established as a series of connected stepped leader segments, each with a length of 50 meters, and propagates until specific termination conditions are met.
Author

N89-10434# Army Cold Regions Research and Engineering Lab., Hanover, N.H.

WHAT MAKES THUNDERBOLTS ZIG AND ZAG

Kazuhiko Itagaki *In* NOAA, International Aerospace and Ground Conference on Lightning and Static Electricity Apr. 1988 p 22-27 (For primary document see N89-10429 01-47)

Avail: NTIS HC A23/MF A01 CSCL 04B

It is well known that lightning bolts trace a zig-zag course between clouds or from cloud to ground. The course is apparently determined by the development of leader strokes through which the bolt advances. A model for the development of such a leader stroke is proposed. Monte Carlo simulation of such a model in two and three dimensions has produced patterns with a striking resemblance to published photographs of lightning bolts. By comparing the statistical analysis of lightning stroke shapes obtained from photographs with observed field conditions causing the strokes, various parameters such as field strength and cell size could be estimated. Author

N89-10435# University of Southern Illinois, Carbondale. Dept. of Electrical Engineering.

FRAMEWORK FOR LIGHTNING MODELING: COMPARING RESULTS

James G. Smith *In* NOAA, International Aerospace and Ground Conference on Lightning and Static Electricity Apr. 1988 p 28-35 (For primary document see N89-10429 01-47)

Avail: NTIS HC A23/MF A01 CSCL 04B

The development and use of a framework consisting of equations and a single curve set that permits those modeling lightning to develop system parameters and initial conditions that will permit meaningful comparisons between models of differing degrees of sophistication are discussed. This framework permits the use of models with any reasonable range of cloud charge, charge density, height, and inferred breakdown electric field strength. Example models are presented to illustrate the utility of this approach for both the examination of single-parameter details of a model, as well as the wide overview of the entire charge system and the discharge process. Author

N89-10436# Lanzhou Inst. of Plateau Atmospheric Physics (China).

THE CRITERION FOR THE PROPAGATION OF THE POSITIVE STREAMER AND ITS APPLICATION

Dachong Wang and Changming Guo *In* NOAA, International Aerospace and Ground Conference on Lightning and Static Electricity Apr. 1988 p 36-43 (For primary document see N89-10429 01-47)

Avail: NTIS HC A23/MF A01 CSCL 04B

Through analyzing the upward leader from tall structures under storm conditions, it is concluded that the intense electric field in a limited, small region provides the necessary condition for natural lightning discharge to occur. Such a local intense field could make it possible that a weak streamer grows and continues to travel in an ambient field of only several tens of kilovolts per meter, which otherwise would propagate only in the ambient field of several hundred kilovolts per meter. A criterion was deduced for determining whether the positive streamer propagates continuously or not. By using this criteria, researchers found the striking distance for tall structures, and the electric environment for artificially triggering lightning by rocket launching with grounding wire. Author

N89-10437# Nagoya Univ. (Japan). Research Inst. of Atmospherics.

NUMERICAL SIMULATIONS OF LIGHTNING BY MEANS OF THE LEADER PROPAGATION MODEL

Zen-Ichiro Kawasaki, Minoru Nakano, Tosio Takeuti, and Yasuhiro Iriyama *In* NOAA, International Aerospace and Ground Conference on Lightning and Static Electricity Apr. 1988 p 44-46 (For primary document see N89-10429 01-47)

Avail: NTIS HC A23/MF A01 CSCL 04B

Numerical simulations of a stepped leader near the ground surface are carried out by using the Leader Propagation Model. This model is composed of a thunder cloud, a stepped leader channel, an artificial construction on the ground, and the ground itself. The Poisson's equation must be solved numerically at every stage of the leader propagation successively. Both the finite element method and the finite difference method are applied. Author

N89-10438*# Electro Magnetic Applications, Inc., Lakewood, Colo.

TRIGGERING OF LIGHTNING BY THE ATLAS CENTAUR VEHICLE

Rodney A. Perala and Terence H. Rudolph *In* NOAA, International Aerospace and Ground Conference on Lightning and Static Electricity Apr. 1988 p 47-57 Previously announced in IAA as A88-22290 Sponsored in part by NASA. Langley Research Center (For primary document see N89-10429 01-47)

Avail: NTIS HC A23/MF A01 CSCL 04B

The triggering of lightning by in-flight vehicles is investigated. Specific attention is placed on the NASA F-106B Thunderstorm Research Aircraft and the Atlas-Centaur vehicle involved in the 1987 AC-67 failure. Thunderstorm and vehicle parameters relevant to triggered lightning initiation are identified. A numerical simulation technique suitable for application to triggered lightning events is discussed. Results from this model's use in the F-106B program are shown and compared to measured data from actual lightning strikes to the aircraft. Issues unique to the Atlas-Centaur incident are presented. The results consist of currents and current time derivatives on the vehicle as a function of time. Derived ambient electric fields at the altitude of the lightning incident are compared with ground based electric field measurements. Finally, questions still unresolved in the physics of triggered lightning are identified. Author

N89-10439*# Electro Magnetic Applications, Inc., Lakewood, Colo.

EVALUATION AND MITIGATION OF LIGHTNING HAZARDS TO THE SPACE SHUTTLE SOLID ROCKET MOTORS (SRM)

Gregory J. Rigden and Peter B. Papazian *In* NOAA, International Aerospace and Ground Conference on Lightning and Static Electricity Apr. 1988 p 58-67 Sponsored in part by Morton Thiokol, Inc., Brigham City, Utah (For primary document see N89-10429 01-47)

(Contract NAS8-30490)

Avail: NTIS HC A23/MF A01 CSCL 04B

The objective was to quantify electric field strengths in the Solid Rocket Motor (SRM) propellant in the event of a worst case lightning strike. Using transfer impedance measurements for selected lightning protection materials and 3D finite difference modeling, a retrofit design approach for the existing dielectric grain cover and railcar covers was evaluated and recommended for SRM segment transport. A safe level of 300 kV/m was determined for the propellant. The study indicated that a significant potential hazard exists for unprotected segments during rail transport. However, modified railcar covers and grain covers are expected to prevent lightning attachment to the SRM and to reduce the levels to several orders of magnitude below 300 kV/m. Author

N89-10440*# Electro Magnetic Applications, Inc., Lakewood, Colo.

TRANSFER IMPEDANCE MEASUREMENTS OF THE SPACE SHUTTLE SOLID ROCKET MOTOR (SRM) JOINTS, WIRE MESHES AND A CARBON GRAPHITE MOTOR CASE **c20**

Peter B. Papazian, Rodney A. Perala, John D. Curry, Alan B. Lankford, and J. David Keller *In* NOAA, International Aerospace and Ground Conference on Lightning and Static Electricity Apr. 1988 p 68-77 Sponsored in part by NASA Langley Research Center, and by Morton Thiokol, Inc., Brigham City, Utah (For primary document see N89-10429 01-47)

(Contract NAS8-30490)

Avail: NTIS HC A23/MF A01 CSCL 04B

Using three different current injection methods and a simple voltage probe, transfer impedances for Solid Rocket Motor (SRM) joints, wire meshes, aluminum foil, Thorstrand and a graphite

composite motor case were measured. In all cases, the surface current distribution for the particular current injection device was calculated analytically or by finite difference methods. The results of these calculations were used to generate a geometric factor which was the ratio of total injected current to surface current density. The results were validated in several ways. For wire mesh measurements, results showed good agreement with calculated results for a 14 by 18 Al screen. SRM joint impedances were independently verified. The filiment wound case measurement results were validated only to the extent that their curve shape agrees with the expected form of transfer impedance for a homogeneous slab excited by a plane wave source. Author

N89-10441# Tokyo Univ. (Japan). Inst. of Industrial Science.
ON THE STATISTICS OF FIELD WAVEFORMS ASSOCIATED WITH LIGHTNING RETURN STROKES
Masaru Ishii and Junichi Hojo *In* NOAA, International Aerospace and Ground Conference on Lightning and Static Electricity Apr. 1988 p 78-83 (For primary document see N89-10429 01-47)
Avail: NTIS HC A23/MF A01 CSCL 04B

Electromagnetic fields associated with lightning flashes were observed throughout the year by a waveform recording system and a wideband magnetic direction finding system. Parameters of electromagnetic waveforms originating from return strokes, such as the 0 to 100 percent rise time, the zero crossing time, etc., have been statistically studied. Variation in the distribution of these parameters depending on the polarity and the season is revealed. It results in the low detection efficiency of a magnetic direction finder for Japanese winter thunderstorms. Author

N89-10442# Nagoya Univ. (Japan). Research Inst. of Atmospherics.
MEASUREMENTS OF THE VELOCITY CHANGE OF A LIGHTNING RETURN STROKE WITH HEIGHT
M. Nakano, M. Nagatani, H. Nakada, T. Takeuti, and Z. Kawasaki *In* NOAA, International Aerospace and Ground Conference on Lightning and Static Electricity Apr. 1988 p 84-86 (For primary document see N89-10429 01-47)
Avail: NTIS HC A23/MF A01 CSCL 04B

A new system is developed to detect optical signals from return stroke channel segments at different heights. The system consists of an optical detector, electric amplifiers and analog to digital converters with 12 channels. Ten channels are used for optical signals, and two channels are used for the electric field charge and ultrahigh frequency radiation. A silicon photodiode array is used as an optical detector. An example in winter positive lightning shows that the two dimensional velocity of a return stroke is 2 times 10 to the 8th power m/s at the height of 310 m above sea level and decreases to 0.3 times 10 to the 8th power m/s at the height of 490 m. Author

N89-10443# SRI International Corp., Menlo Park, Calif.
AN AIRCRAFT-BORNE ELECTRIC FIELD MEASURING SYSTEM FOR ROCKET LAUNCH SUPPORT
Joseph E. Manevicz, Jeffrey S. Thayer, and Hugh Heritage (Aerospace Corp., Los Angeles, Calif.) *In* NOAA, International Aerospace and Ground Conference on Lightning and Static Electricity Apr. 1988 p 87-93 (For primary document see N89-10429 01-47)
Avail: NTIS HC A23/MF A01 CSCL 04B

A new field measuring system and associated instrumentation installed on a NASA 705 Learjet to be flown into a region of a rocket launch trajectory to verify meteorological and electric field conditions relative to lightning strike potential are discussed. The new system is based on an earlier system used for the support of the Apollo/Soyuz and Viking launches. The outputs from a set of four field meters installed in the skin of the vehicle are fed to a real-time analog processor that yields the three components of free-space electric field and aircraft potential. The system also records aircraft navigational parameters and time to permit the data to be correlated with other measurements. Author

N89-10444# Airborne Research Associates, Weston, Mass.
NEW ELECTRIC FIELD INSTRUMENTATION AND THE EFFECTS OF SPACE CHARGE AT KENNEDY SPACE CENTER
Ralph Markson and Bruce Anderson *In* NOAA, International Aerospace and Ground Conference on Lightning and Static Electricity Apr. 1988 p 94-102 (For primary document see N89-10429 01-47)
Avail: NTIS HC A23/MF A01 CSCL 04B

A program is being conducted to develop low power consumption electric field sensors for installation at remote sites, where there is no ac power, in order to expand the aerial coverage of the lightning warning network. Both radioactive probe and corona current instruments are being considered. In addition, the layer of space charge which develops over land (due to corona) and water (due to electrode effect) when thundercloud electric fields are present are being investigated since it strongly affects electric field measurements made close to the ground. The space charge layer is being studied through horizontal and vertical profiles obtained from an instrumented aircraft as well as an electrosonde which is raised and lowered through the space charge layer by a tethered balloon system. Author

N89-10445# Tohoku Electric Power Co., Inc., Sendai (Japan).
CURRENT MEASUREMENT OF LIGHTNING SUPERBOLT AT THE JAPAN SEA COAST
S. Sawada, H. Komuro, Y. Goto, and K. Narita (Miyagi Vocational Training Coll., Japan) *In* NOAA, International Aerospace and Ground Conference on Lightning and Static Electricity Apr. 1988 p 103-11 (For primary document see N89-10429 01-47)
Avail: NTIS HC A23/MF A01 CSCL 04B

The observation of winter lightning has been made on an isolated meteorological observation tower of which the height is about 150 m at Maki in Niigata Prefecture of Japan. It was discovered that the discharge energy of winter lightning is enormously large. The purpose of the research is to clarify the lightning characteristics in winter season and to get data for the protective design of power facilities and equipment. Of the 55 data recorded by magnetic links, 56.3 percent were negative polarity, 30.9 percent were positive, and 12.8 percent were too small to determine polarities or peak values. Three negative currents and four positive exceeded 100 KA. In October 1986, the positve peak value 322 KA was obtained and that was the largest one. The dissipated power in the channel due to the lightning discharge of 322 KA is 3.9 times 10 to the 12th power W. This confirms the real existance of lightning superbolts at Maki during a winter season. Author

N89-10446# University of Technology, Lae (Papua New Guinea). Electrical and Communication Engineering.
LIGHTNING RETURN STROKE VELOCITY
Paul R. P. Hoole *In* NOAA, International Aerospace and Ground Conference on Lightning and Static Electricity Apr. 1988 p 111-11 (For primary document see N89-10429 01-47)
Avail: NTIS HC A23/MF A01 CSCL 04B

The dispersion relations for the lightning return stroke obtained from the transmission line and directly derived from Maxwell's equations are examined. It is shown that signal velocity is in good agreement with the observed return stroke velocity. Hence, the transmission line model of the return stroke is shown to have a sound basis. Author

N89-10447# National Research Council of Canada, Ottawa (Ontario). Div. of Electrical Engineering.
A CASE FOR A UNIFIED LIGHTNING THREAT
Andrew S. Podgorski *In* NOAA, International Aerospace and Ground Conference on Lightning and Static Electricity Apr. 1988 p 118-12 (For primary document see N89-10429 01-47)
Avail: NTIS HC A23/MF A01 CSCL 04B

For the first time a unified set of lightning parameters that can describe the lightning measured at the ground or on towers or airplanes is proposed. This set of parameters can be used to accurately predict the electromagnetic fields generated by lightning. The new set of lightning parameters was obtained from the lightning

current measurements conducted at the CN Tower during the 1986 lightning seasons. The measured currents were compensated for the presence of the tower. Author

N89-10448# Toulouse Univ. (France). Lab. dAerologie.
ELECTROMAGNETIC RADIATIONS GENERATED BY MICRODISCHARGES FROM HYDROMETEORS
Khalil Kably and Serge Chauzy *In* NOAA, International Aerospace and Ground Conference on Lightning and Static Electricity Apr. 1988 p 123-12 (For primary document see N89-10429 01-47)
Avail: NTIS HC A23/MF A01 CSCL 04B

The presented preliminary measurements on individual microdischarges between hydrometeors indicate that this phenomenon is a powerful source of electromagnetic radiation from thunderclouds, especially within the VHF/UHF range. Even if the charge transfer by collision is not as powerful a source as the air discharge, its influence must be considered. In order to overcome the reflection problems that bias the electromagnetic detection, this work will be completed by direct measurements of the electric current and a more complex modelling taking into account the oscillatory current signature. The research aims at evaluating the overall signal emitted by a given volume of cloud holding a given concentration of charged or uncharged hydrometeors in an ambient field. More experiments and modeling will be necessary to achieve this task. Author

N89-10449# Office National d'Etudes et de Recherches Aeronautiques, Paris (France).
SUMMARY OF INFLIGHT DATA ON LIGHTNING CURRENTS AND FIELDS
J. P. Moreau, J. M. Reazer, and P. L. Rustan (Defense Nuclear Agency, Washington, D.C.) *In* NOAA, International Aerospace and Ground Conference on Lightning and Static Electricity Apr. 1988 p 129-13 (For primary document see N89-10429 01-47)
Avail: NTIS HC A23/MF A01 CSCL 04B

The peak amplitudes, risetimes and repetition rates of the current and electromagnetic field pulses measured during lightning strikes to a two-engine turbo prop CV-580 aircraft are discussed. The .5 Hz to 500 kHz electric field variations recorded in the aircraft during lightning strikes are summarized. Finally, the current and electric field variations measured in the aircraft are compared with those in the MIL-STD-1757A and the newly recommended draft advisory circular for the SAE committee AE4L-87-3. Author

N89-10450# Office National d'Etudes et de Recherches Aeronautiques, Paris (France).
ANALYSIS OF RECENT IN-FLIGHT LIGHTNING MEASUREMENTS ON DIFFERENT AIRCRAFT **c03**
J. L. Boulay, J. P. Moreau, A. Asselineau, and P. L. Rustan (Defense Nuclear Agency, Washington, D.C.) *In* NOAA, International Aerospace and Ground Conference on Lightning and Static Electricity Apr. 1988 p 136-14 (For primary document see N89-10429 01-47)
Avail: NTIS HC A23/MF A01 CSCL 01C

Two experimental programs have been conducted since 1984 in order to obtain in-situ measurements on lightning effects on aircraft. These two programs involve the CV-580 aircraft and the Transall aircraft. Researchers now have a large amount of information concerning typical parameter variations during a direct lightning stroke in flight: currents, electric and magnetic fields in several locations on the aircraft structures. One of the most important features of these measurements concerns the great similarity between parameter variations for the two experimental programs. After presentation of typical results obtained with the Transall, a comparative analysis is made of CV-580 and Transall data on I and H waveforms during the attachment phase of the lightning strike. A number of hypotheses aimed at giving physical explanations of the measurements detected in flight are discussed. Author

N89-10451*# Electro Magnetic Applications, Inc., Lakewood, Colo.
LINEAR AND NONLINEAR INTERPRETATION OF CV-580 LIGHTNING DATA **c03**
Poh H. Ng, Terence H. Rudolph, and Rodney A. Perala *In* NOAA, International Aerospace and Ground Conference on Lightning and Static Electricity Apr. 1988 p 145-15 Sponsored in part by FAA, Atlantic City, N.J. (For primary document see N89-10429 01-47)
(Contract NAS1-17748)
Avail: NTIS HC A23/MF A01 CSCL 01C

Numerical models developed for the study of lightning strike data acquired by in-flight aircraft are applied to the data measured on the CV-580. The basic technique used is the three dimensional time domain finite difference solution of Maxwell's equations. Both linear and nonlinear models are used in the analysis. In the linear model, the lightning channel and the aircraft are assumed to form a linear time invariant system. A transfer function technique can then be used to study the response of the aircraft to a given lightning strike current. Conversely, the lightning current can be inferred from the measured response. In the nonlinear model, the conductivity of air in the vicinity of the aircraft is calculated and incorporated into the solution of the Maxwell's equations. The nonlinear model thus simulates corona formation and air breakdown. Results obtained from the models are in reasonable agreement with the measured data. This study provides another validation of the models and increases confidence that the models may be used to predict aircraft response to any general lightning strike. Author

N89-10452# Boeing Advanced Systems Co., Seattle, Wash.
LIGHTNING TESTS ON AN ALL-COMPOSITE HELICOPTER **c03**
David B. Walen *In* NOAA, International Aerospace and Ground Conference on Lightning and Static Electricity Apr. 1988 p 152-15 (For primary document see N89-10429 01-47)
Avail: NTIS HC A23/MF A01 CSCL 01C

Lightning tests were performed on an all-composite helicopter to determine lightning-induced transient effects on the helicopter electrical and electronic systems. Results of the tests were used to assess the lightning simulation techniques. The helicopter incorporated graphite/epoxy, Kelvar, and fiberglass materials in the structure and skins. Swept continuous wave (CW) transfer function measurements and current pulse tests with drive currents ranging from 20 kA to 200 kA were used for the lightning tests. Transient voltage and current responses were measured on the helicopter avionics and wiring. The response waveform comparisons showed that the transformed transfer functions had similar shapes and amplitudes to the measured pulse responses. Within constraints of the pulse variations, scaling generally provided conservative response predictions. Author

N89-10453# Texas Technological Univ., Lubbock. Dept. of Electrical Engineering.
BREAKDOWN CHARACTERISTICS OF AN ISOLATED CONDUCTING OBJECT IN A UNIFORM ELECTRIC FIELD
Michael G. Grothaus and Thomas F. Trost *In* NOAA, International Aerospace and Ground Conference on Lightning and Static Electricity Apr. 1988 p 160-17 (For primary document see N89-10429 01-47)
Avail: NTIS HC A23/MF A01 CSCL 04B

A laboratory experiment was conducted to investigate the physical processes involved in the electrical breakdown of a particular type of spark-gap arrangement. The gap consists of an isolated conducting ellipsoid located midway between two large flat electrodes. Gradual increase of the applied electric field in the gap produces corona on the ellipsoid tips followed by flashover in a leader arc sequence. The leader phase consists of the formation of ionized channels which partially bridge the gap and then decay prior to the arc. Measurements of dE/dt and of current were made, and photographs were taken with an image converter camera. Author

N89-10454*# Electro Magnetic Applications, Inc., Huntsville, Ala.
ESTIMATING ELECTRIC FIELD ENHANCEMENT FACTORS ON AN AIRCRAFT UTILIZING A SMALL SCALE MODEL: A METHOD EVALUATION **c03**
Calvin C. Easterbrook, Terence Rudolph, and Kevin Easterbrook *In* NOAA, International Aerospace and Ground Conference on Lightning and Static Electricity Apr. 1988 p 171-17 (For primary document see N89-10429 01-47)
(Contract NAS1-17748)
Avail: NTIS HC A23/MF A01 CSCL 01C

A method for obtaining field enhancement factors at specific points on an aircraft utilizing a small scale model was evaluated by measuring several canonical shapes. Comparison of the form factors obtained by analytical means with measurements indicate that the experimental method has serious flaws. Errors of 200 to 300 percent were found between analytical values and measured values. As a result of the study, the analytical method is not recommended for calibration of field meters located on aircraft, and should not be relied upon in any application where the local spatial derivatives of the electric field on the model are large over the dimensions of the sensing probe. Author

N89-10455# AIRO, Inc., Colorado Springs, Colo.
A CHRONOLOGY OF IN-CLOUD ELECTRIC FIELD AND LIGHTNING STRIKES ON AN INSTRUMENTED RESEARCH AIRCRAFT **c03**
J. William Bullock and J. J. Jones (New Mexico State Bureau of Mines and Mineral Resources, Socorro.) *In* NOAA, International Aerospace and Ground Conference on Lightning and Static Electricity Apr. 1988 p 175-18 (For primary document see N89-10429 01-47)
Avail: NTIS HC A23/MF A01 CSCL 04B

The two lightning strikes to the aircraft in 1983 were identified. The strikes occurred when the aircraft was entering or leaving a region of strong vertical electric field. In both cases, the measured field subsequent to the strikes was greatly reduced from the pre-strike value, indicating that the strike removed the nearby charge which was the source of the pre-strike electric field. It appears that the aircraft triggered these strikes, and a possible triggering mechanism is proposed. The strikes also removed the pre-strike charge on the aircraft. Since both strikes occurred during cloud penetrations near zero degree isotherm and depleted a region of positive charge, it is believed that these were so-called Lower Position Charge Centers. Author

N89-10456*# National Severe Storms Lab., Norman, Okla.
LIGHTNING INITIATION ON AIRCRAFT IN THUNDERSTORMS **c03**
Vladislav Mazur *In* NOAA, International Aerospace and Ground Conference on Lightning and Static Electricity Apr. 1988 p 181-19 Previously announced as A88-22289 Sponsored in part by NASA (For primary document see N89-10429 01-47)
Avail: NTIS HC A23/MF A01 CSCL 01C

A physical model of the initiation of lightning flashes in thunderstorms is presented. The model is based on the bi-directional charged leader concept of Kasemir, and is verified with airborne data from lightning strikes to instrumented airplanes (NASA F-106B and FAA CV-580). The characteristics of electromagnetic processes during lightning attachment are identified by comparison with those studied in natural flashes, those triggered by wire trailing rockets, and laboratory discharges. A triggered flash starts with either a negative corona or a positive leader that depends on the ambient electric field vector and the airplane form factor. The positive leader with continuous current that increases with time is followed in a few milliseconds by the negative stepped leader with current pulses of a few kA. The two leaders develop in space simultaneously and bi-directionally from the oppositely charged extremities of the airplane. Author

N89-10457# De Havilland Aircraft Co. of Canada Ltd., Downsview (Ontario).
LIGHTNING TESTS TO MEASURE THE BULK CURRENT LEVELS ASSOCIATED WITH THE ELECTRONIC ENGINE CONTROL OF A TURBOPROP COMMUTER TRANSPORT **c03**
Peter Bootsma *In* NOAA, International Aerospace and Ground Conference on Lightning and Static Electricity Apr. 1988 p 192-19 (For primary document see N89-10429 01-47)
Avail: NTIS HC A23/MF A01 CSCL 01C

Impulse lightning tests were carried out as part of a development program to measure the cable current levels associated with the electronic engine control (EEC) of a turboprop commuter transport. Described here are two test programs, each utilizing full scale vehicles to measure the bulk current levels associated with the engine control cable harness. In the first test program, the tests were performed with the 1200 ampere unipolar test waveform. The second test program was carried out using a 15 kiloampere damped sinusoid test waveform. The latter program was extended for a period of several weeks in order to develop a method of diverting current from the engine to the surrounding nacelle, and improve the shielding of the engine control cable harness.
Author

N89-10458# Electrical and Computer Engineering, Athens, Ohio.
ON A SURFACE MOUNTED TRANSMISSION LINE CONFIGURATION FOR APERTURE TESTING **c32**
C. D. Taylor, F. Marcum, C. C. Herrmann, and W. D. Prather (Air Force Weapons Lab., Kirtland AFB, N. Mex.) *In* NOAA, International Aerospace and Ground Conference on Lightning and Static Electricity Apr. 1988 p 197-20 (For primary document see N89-10429 01-47)
Avail: NTIS HC A23/MF A01 CSCL 20N

An analysis of the performance of a surface mounted transmission line used as a localized aperture driver is presented. The fields illuminating the aperture are obtained via a finite difference solution technique, and multiconductor transmission line theory is used to determine the performance of the transmission line. Data are presented for the transmission line illuminator operating over a metal surface covered by a dielectric paint.
Author

N89-10459# Electro Magnetic Applications, Inc., Lakewood, Colo.
INTERFERENCE OF PRECIPITATION STATIC DISCHARGES WITH AIRCRAFT NAVIGATIONAL SYSTEMS **c03**
Gregory J. Rigden *In* NOAA, International Aerospace and Ground Conference on Lightning and Static Electricity Apr. 1988 p 205-21 Sponsored in part by FAA, Atlantic City, N.J.; Lightning and Transients Research Inst., St. Paul, Minn. (For primary document see N89-10429 01-47)
(Contract DTFA03-84-C-00066)
Avail: NTIS HC A23/MF A01 CSCL 01C

The objective was to address p-static problems by determining ways to reduce their effects. The Gates Learjet was used as a model for this study. The small size of the Learjet enabled an accurate numerical investigation utilizing a three dimensional finite difference approach to solving Maxwell's equations. The study included an analysis of the possible discharges, where they are likely to occur and how often, an examination of dischargers to determine the dependency of noise levels on discharger design, and a look at electromagnetic responses from different types of dischargers. Author

N89-10460# New Mexico Inst. of Mining and Technology, Socorro.
ELECTRIFICATION OF HOVERING HELICOPTERS **c03**
C. B. Moore, Marx Brock, and Clyde N. Richards (Atmospheric Physics, Inc., Peralta, N. Mex.) *In* NOAA, International Aerospace and Ground Conference on Lightning and Static Electricity Apr. 1988 p 213-21 (For primary document see N89-10429 01-47)
Avail: NTIS HC A23/MF A01 CSCL 01C

Helicopters hovering above the earth are often highly charged

with electricity and this causes operational problems for ground crew personnel when contact with the aircraft is required. The source of this charge is often attributed to elastic collisions of the rotor blades with dust particles in the surrounding air, but researchers found that appreciable charge transfers also occur through the hot, conductive engine exhaust gases acted on by local electric fields. Some control of the residue charge on hovering aircraft has been achieved by shielding the exhaust gases from electric fields and then varying the voltages applied to electrodes immersed in the hot gases so as to cause an export of the unwanted charge. Author

N89-10461# Naval Research Lab., Washington, D.C. Plasma Physics Div.
MEASUREMENT OF THE ELECTROSTATIC CHARGING ON LARGE HELICOPTERS AND CONTROL OF THE SHOCK HAZARD **c03**
R. E. Pechacek, D. P. Murphy, and J. R. Greig (G-T Devices, Inc., Springfield, Va.) *In* NOAA, International Aerospace and Ground Conference on Lightning and Static Electricity Apr. 1988 p 218-22 (For primary document see N89-10429 01-47)
Avail: NTIS HC A23/MF A01 CSCL 01C

This work was undertaken to ascertain the electrical hazard to ground personnel attaching cargo to hovering CH-53E helicopters. The hazard is severe, but a solution has been rediscovered. An approximately 10-megohm resister, replacing the stainless wire connected along the nylon cable from the helicopter to the cargo hook allows a man to discharge 200-KV, 1000-pF helicopter through his body with a barely perceptible shock. The system has been successfully field tested twice. Author

N89-10462# Naval Research Lab., Washington, D.C.
ELECTROSTATIC FIELDS OF GROUND TRIGGERED LIGHTNING
Lothar H. Ruhnke and Heinz W. Kasemir (Colorado Scientific Research Corp., Berthoud.) *In* NOAA, International Aerospace and Ground Conference on Lightning and Static Electricity Apr. 1988 p 228-23 (For primary document see N89-10429 01-47)
Avail: NTIS HC A23/MF A01 CSCL 04B

Electric fields of lightning triggered by wire rockets have been measured at several observation sites in Florida in 1986 and 1987 at distances of a few kilometers from the trigger location. Characteristic waveforms are described and show a continuous rise in electric fields for 200 milliseconds followed by a period of high variability and ending with several return stroke signals. Electric fields are related to currents, charges and velocities of the positive leader of the triggered lightning. The relationship is tested on a physical model of triggered lightning suggested earlier by Kasemir. Author

N89-10463# Queensland Univ., St. Lucia (Australia). Dept. of Electrical Engineering.
A REVIEW OF MEDICAL ASPECTS OF LIGHTNING INJURY **c52**
C. J. Andrews, M. Darveniza, and D. Mackerras *In* NOAA, International Aerospace and Ground Conference on Lightning and Static Electricity Apr. 1988 p 231-25 (For primary document see N89-10429 01-47)
Avail: NTIS HC A23/MF A01 CSCL 06P

Many disparate reports of the pathological and pathophysiological effects of lightning on an injured person are drawn together into a coherent review representing the current state of knowledge of the physico-medical effects of lightning. Special attention is paid to those effects of lightning which distinguish it from other electrical injuries. These include neurological and psychiatric syndromes, burns of specific types, cardio-respiratory signs of a particular nature and other, more general, effects. The nature of all of these injuries is given, with current theories of their genesis. The importance of the recognition of lightning injuries from the forensic viewpoint is presented, and a review of current treatment regimens is given with an emphasis on first aid. Finally, a formal review of 221 literature cases is given, placing in perspective the incidence of the varied injuries presented in the foregoing discussion. Author

N89-10464# Queensland Univ., St. Lucia (Australia). Dept. of Electrical Engineering.
A RETROSPECTIVE STUDY OF THE INJURIES SUSTAINED IN TELEPHONE-MEDIATED LIGHTNING STRIKE **c52**
C. J. Andrews, M. Darveniza, and D. Mackerras *In* NOAA, International Aerospace and Ground Conference on Lightning and Static Electricity Apr. 1988 p 251-27 (For primary document see N89-10429 01-47)
Avail: NTIS HC A23/MF A01 CSCL 06P

Injuries due to lightning impulses mediated by the public telephone system are discussed. The reported frequency of symptoms are compared with those previously presented for in-the-field strikes, as is the spectrum of injury sustained. The main thrust here is a retrospective study of 328 persons in Australia claiming telephone related injury in the period 1980 to 1985. The study aimed to obtain a complete medical history taken from these individuals with regard to their injury. The histories were analyzed and three distinct lightning strike syndromes were identified with their own clinical pictures and relative frequencies of occurrence. The histories of injury obtained in the survey were further compared with those obtained by the medical practitioners they consulted. A brief discussion is given of the physical mechanisms by which these injuries are thought to occur, together with hypotheses regarding those factors which are thought to have contributed to the recent upsurge in reports. Author

N89-10465# United Kingdom Atomic Energy Authority, Culham (England). Lightning Studies Unit.
FACTORS INFLUENCING THE DETECTION OF VOLTAGE SPARKS BY FLAMMABLE GAS AND OPTICAL TECHNIQUES **c25**
S. J. Haigh, R. E. Baldwin, and C. R. Banks *In* NOAA, International Aerospace and Ground Conference on Lightning and Static Electricity Apr. 1988 p 272-28 (For primary document see N89-10429 01-47)
Avail: NTIS HC A23/MF A01 CSCL 21B

Voltage and thermal sparks in fuel tanks are primarily detected photographically or by using flammable gas mixtures such as ethylene/air. To compare the sensitivities of these techniques, sparks of varying length and energy were detected by both methods and by a photomultiplier detector. For a 1.3 stoichiometric mixture of ethylene and air, the probability of ignition from sparks longer than the quenching distance was found to be closely related to the energy per unit length of the spark; a 1.5 mm 200 micro J spark has a 70 percent probability of causing ignition. The light output from the sparks correlated better with charge transmitted in the spark rather than its energy, although it was also dependent on the condition of the spark electrodes. The ability of the camera systems to detect such sparks was found to depend on the object distance and the focal length of the lens as well as lens f-stop and film speed. Author

N89-10466# Air Force Western Space and Missile Center, Vandenberg AFB, Calif. Office of Staff Meteorology.
LIGHTNING NEAR VANDENBERG AFB AS RELATED TO VARIOUS SYNOPTIC PATTERNS
Steven M. Hunter *In* NOAA, International Aerospace and Ground Conference on Lightning and Static Electricity Apr. 1988 p 281-28 (For primary document see N89-10429 01-47)
Avail: NTIS HC A23/MF A01 CSCL 04B

Researchers saw a correlation between decreasing 500 mb core temperatures and lightning frequency, especially at core temperatures -21 C. The correlation follows the direction implied by the -21 C rule-of-thumb, but is too rigid. Significant lightning can occur at core temperatures as warm as -12 C, although indications are that such instances are infrequent. Nevertheless, the forecaster should be wary of all vigorous storm systems, closely monitoring the Lightning Location System (LLS) for strikes. A more cautious rule-of-thumb is proposed: the potential for widespread

lightning (more than 40 strikes) is large for core temperatures -20 C. Author

N89-10467# New Mexico Inst. of Mining and Technology, Socorro. Geophysical Research Center.
LIGHTNING PROTECTION FOR HIGH EXPLOSIVES AND INSTRUMENTATION USING A FIELD MILL SYSTEM c28
William Rison and Gerald P. Chapman (Mission Research Corp., Albuquerque, N. Mex.) *In* NOAA, International Aerospace and Ground Conference on Lightning and Static Electricity Apr. 1988 p 289-29 (For primary document see N89-10429 01-47)
Avail: NTIS HC A23/MF A01 CSCL 21I

In May 1987, on the edge of the White Sands Missile Range in New Mexico, the Defense Nuclear Agency (DNA) sponsored a high explosive test using 4,545 metric tons of ammonium nitrate and fuel oil (ANFO) in a 26.8 meter diameter hemisphere. In a circular fashion about the ANFO container was an extensive experimental and data recording array. A field system was designed and built to assist in protecting personnel from explosions resulting from lightning. The details of the hardware, the system configuration, some data on the warning times, the warning threshold, the type of printed record provided, and comments upon the accuracy and merits of such a system are given. Author

N89-10468# Toulouse Univ. (France). Lab. dAerologie.
THE SURFACE ELECTRIC FIELD AS A WARNING CRITERION
Serge Soula, Serge Chauzy, and Alexandre Faizoun *In* NOAA, International Aerospace and Ground Conference on Lightning and Static Electricity Apr. 1988 p 294-29 (For primary document see N89-10429 01-47)
Avail: NTIS HC A23/MF A01 CSCL 04B

It is shown that the probability of triggering a lightning stroke is not essentially correlated to the sole instantaneous surface electric field value, but mostly to the history of this field. The corona charge layer generated at the surface is responsible for this observation. The influence of this layer is revealed by electric field measurements at various levels above ground. The modeling of corona ion production and evolution, as well as the influence of this mechanism on the electric field variations, is carried out. The results show that the stabilized value of the surface electric field depends on two major factors: the regeneration rate of the cloud charges and the field dependence of the corona current density. Finally, a method of clearing the surface field evolution of the effect of the corona local charge is proposed. It leads to the definition of the intrinsic electric field which is the field which would exist if no local charge were generated. Author

N89-10469# Lawrence Livermore National Lab., Calif.
AN INTERAGENCY WORKING GROUP ON LIGHTNING THREAT WARNING
R. T. Hasbrouck *In* NOAA, International Aerospace and Ground Conference on Lightning and Static Electricity Apr. 1988 p 300-30 (For primary document see N89-10429 01-47)
(Contract W-7405-eng-48)
Avail: NTIS HC A23/MF A01 CSCL 04B

Presently, the need for a lightning warning system can be met through the use of a cloud-to ground lightning detection and warning system. Several manufacturers are installing these systems and the Federal government is seeking to coordinate them into a nationwide network. However, these systems do not provide lightning threat (pre-first-strike) warning. Techniques and equipment for producing such warnings exist, but recently there has been no unified effort to consolidate the knowledge, standardize the requirements, and identify the problems of the various users. Described here is the formation of an interagency group which intends to specifically address such issues. Author

N89-10470# Mississippi Univ., University. Dept. of Physics.
THE ELECTRICAL STRUCTURE OF THUNDERSTORM ANVILS
Thomas C. Marshall, W. David Rust, William P. Winn, and Kenneth E. Gilbert (National Center for Physical Acoustics, University, Miss.) *In* NOAA, International Aerospace and Ground Conference on Lightning and Static Electricity Apr. 1988 p 303-30 (For primary document see N89-10429 01-47)
Avail: NTIS HC A23/MF A01 CSCL 04B

Two electric field soundings through thunderstorm anvil clouds show similar charge structures; negatively charged screening layers on top and bottom surfaces, a layer of positive charge on the interior, and one or two layers of zero charge. Both anvil clouds were strongly electrified; the peak magnitudes of the electric field in the two storms were 70 and 90 kV/m (so, aircraft penetrating anvil thunderstorms run no risk of triggering lightning flashes). The non-zero layers had charge densities comparable to those found in storm cores, ranging in magnitude from 0.4 to 2.7 nC/m cubed. The layers ranged in thickness from 300 to 2000m. The positive charge probably originated in the main positive charge region normally found at high altitudes in the core of thunderstorms. The removal of the positive charge from the storm's core to the anvil may influence the ratio of intra-cloud to cloud-to-ground lightning flashes and the rate of generation of charge in the core. The negatively conducting layers were probably screening layers resulting from the discontinuity in the electrical conductivity at the cloud boundaries. The lower negative screening layer appeared to be carried toward the storm's core by winds below and at the lower anvil boundary. Author

N89-10471# National Oceanic and Atmospheric Administration, Boulder, Colo. Weather Research Program.
LIGHTNING IN MESOSCALE CONVECTIVE COMPLEXES ON 3-5 JUNE 1985 IN OKLAHOMA AND KANSAS
Ronald L. Holle, Andrew I. Watson, Raul E. Lopez, and Donald R. MacGorman (National Severe Storms Lab., Norman, Okla.) *In* NOAA, International Aerospace and Ground Conference on Lightning and Static Electricity Apr. 1988 p 310-31 (For primary document see N89-10429 01-47)
Avail: NTIS HC A23/MF A01 CSCL 04B

Cloud to ground lightning data are described for four mesoscale convective complexes (MCCs) that occurred in a swarm on 3 to 5 June 1985 in Oklahoma and Kansas during the PRE-STORM program. Of 26,597 flashes to ground detected for the 4 MCCs, 95 percent were negative. Flashes were related to radar echoes that were objectively determined to be convective or stratiform. Altogether, 61 percent of the negatives and 42 percent of the positives were found to be in convective echoes. It was determined that during the life cycle of the storm, MCCs typically began with negative flashes in convective echoes, and that positive flashes and stratiform echoes became more frequent toward the end of the storm. For each MCC, both polarities of flashes are shown divided by area and rain volume. A relatively constant rate of flash production per convective rain volume was found for all storms after the initial third of the systems' lifetime. Author

N89-10472*# Arizona Univ., Tucson. Inst. of Atmospheric Physics.
SPATIAL DISTRIBUTION OF LIGHTNING STRIKES TO GROUND DURING SMALL THUNDERSTORMS IN FLORIDA
E. Philip Krider *In* NOAA, International Aerospace and Ground Conference on Lightning and Static Electricity Apr. 1988 p 318-32 (For primary document see N89-10429 01-47)
(Contracts NAS8-36477; NAS10-11390)
Avail: NTIS HC A23/MF A01 CSCL 04B

The spatial patterns of the strike points produced by cloud-to-ground lightning under three small thunderstorms have been analyzed to determine the area flash density as a function of radius from the storm center, the distribution of the nearest-neighbor distances, and the distribution of the horizontal distances between successive flashes. The storm average flash densities range from about 0.8 to 1.6 Fl/km squared, and the average lightning fluxes range from 0.03 to 0.05 Fl/km squared/min. The mean nearest-neighbor distances are about 0.7 km and smaller, but are still in good agreement with a theory that assumes an infinite and uniform flash density. The mean distance between successive flashes ranges from 3.2 to 4.2 km, and a sizable fraction of this variation could be due to channel geometry. Author

N89-10473# National Research Council of Canada, Ottawa (Ontario). Div. of Electrical Engineering.
LIGHTNING STANDARDS FOR PROTECTION OF GROUND ELECTRONIC SYSTEMS **c33**
Andrew S. Podgorski and Elizabeth M. Podgorski (Radio Systems Engineering, Ottawa, Ontario) *In* NOAA, International Aerospace and Ground Conference on Lightning and Static Electricity Apr. 1988 p 324-32 (For primary document see N89-10429 01-47)
Avail: NTIS HC A23/MF A01 CSCL 04B

A set of standards for the protection of electronic aviation equipment against lightning is proposed. These standards were established on the basis of lightning threat characterization determined with the use of a new 3-D lightning model and two years of current data collection at the 553 m tall tower in Toronto. Author

N89-10474# Stringfellow and Associates, Atlanta, Ga.
LIGHTNING AND SURGE PROTECTION OF LARGE GROUND FACILITIES **c31**
Michael F. Stringfellow *In* NOAA, International Aerospace and Ground Conference on Lightning and Static Electricity Apr. 1988 p 328-33 (For primary document see N89-10429 01-47)
Avail: NTIS HC A23/MF A01 CSCL 13B

The vulnerability of large ground facilities to direct lightning strikes and to lightning-induced overvoltages on the power distribution, telephone and data communication lines are discussed. Advanced electrogeometric modeling is used for the calculation of direct strikes to overhead power lines, buildings, vehicles and objects within the facility. Possible modes of damage, injury and loss are discussed. Some appropriate protection methods for overhead power lines, structures, vehicles and aircraft are suggested. Methods to mitigate the effects of transients on overhead and underground power systems as well as within buildings and other structures are recommended. The specification and location of low-voltage surge suppressors for the protection of vulnerable hardware such as computers, telecommunication equipment and radar installations are considered. The advantages and disadvantages of commonly used grounding techniques, such as single point, multiple and isolated grounds are compared. An example is given of the expected distribution of lightning flashes to a large airport, its buildings, structures and facilities, as well as to vehicles on the ground. Author

N89-10475# BDM Corp., Albuquerque, N. Mex.
COMPUTER SIMULATION OF THE EFFECTS OF LIGHTNING STROKE ATTACHMENT TO AN ELECTRIC POWER SUBSTATION **c33**
D. E. Thomas, C. M. Wiggins, and F. S. Nickel *In* NOAA, International Aerospace and Ground Conference on Lightning and Static Electricity Apr. 1988 p 338-34 (For primary document see N89-10429 01-47)
Avail: NTIS HC A23/MF A01 CSCL 09C

A model which has been used extensively for prediction of switching transients in electric power substations is applied to a hypothetical direct lightning attachment on such a substation. The model, which has been used primarily to investigate transients caused by disconnector and breaker switching operations in substations, is shown to have sufficient dynamic resolution to be useful for assessment of responses to the large bandwidth, long duration signal sources that are typically produced by lightning. Some predictions of predicted and measured bus current switching transients are presented for a typical 115 kilowatt substation; predictions for the transient currents caused by direct lightning attachment to the same substation are presented for various substation locations. The capabilities of the complete model to also predict near-zone radiated fields and their coupling to other circuits are briefly discussed. Author

N89-10476# Hydro-British Columbia, Vancouver.
A REVISED ELECTROGEOMETRIC MODEL FOR THE TERMINATION OF LIGHTNING STROKES ON GROUND OBJECTS
Abdul M. Mousa and K. D. Srivastava *In* NOAA, International Aerospace and Ground Conference on Lightning and Static Electricity Apr. 1988 p 342-35 (For primary document see N89-10429 01-47)
Avail: NTIS HC A23/MF A01 CSCL 04B

Discrepancies have been reported between field observations and the assumptions and predictions of the electrogeometric model (EGM). It is shown that the concepts of the EGM are valid and that the discrepancies are caused by: oversimplification of the representation of power lines; not taking the inequality of the striking distances into consideration; and using a value for the medium stroke current to flat ground that is significantly less than the actual value. A revised model is then presented with parameters based on available field observations and laboratory measurements. Author

N89-10477# Electro Magnetic Applications, Inc., Lakewood, Colo.
MODEL RESULTS FOR A PROPOSED TACTICAL MISSILE TRAINING SITE LIGHTNING PROTECTION SYSTEM **c31**
John D. Curry *In* NOAA, International Aerospace and Ground Conference on Lightning and Static Electricity Apr. 1988 p 353-35 (For primary document see N89-10429 01-47)
(Contract DAAH01-85-D-A015)
Avail: NTIS HC A23/MF A01 CSCL 13B

A three-dimensional finite-difference model of a tactical missile training site lightning protection system was modelled. The model, using a uniform grid size of one meter, is composed of six fifteen-meter high, ten-inch diameter posts placed in two rows of three each, with the two rows being 19 meters apart and thirty-six meters between the posts in each row, giving a nineteen meter by seventy-two meter protected area enclosed by the six posts. The three posts in each row are connected at the top by an aerial wire, and a counterpoise wire one meter deep in the soil connects the six posts along the perimeter of the training site. Two computer runs are presented: a strike to a corner post and a strike to one of the two middle posts. A worst case lightning waveform is used, having a two hundred kilo-ampere peak and a 0.2 microsecond risetime. Contours of the ground plane electric field magnitude are presented at various times during the strike, along with arrow plots giving the field direction. Also presented are currents induced on the lightning protection system and how they are absorbed by the conductive soil. Author

N89-10478*# National Aeronautics and Space Administration. Langley Research Center, Hampton, Va.
IMPLICATIONS OF A RECENT LIGHTNING STRIKE TO A NASA JET TRAINER **c03**
Bruce D. Fisher, Ralph J. Taeuber, and Keith E. Crouch (Lightning Technologies, Inc., Pittsfield, Mass.) *In* NOAA, International Aerospace and Ground Conference on Lightning and Static Electricity Apr. 1988 p 360-36 Previously announced in IAA as A88-22291 (For primary document see N89-10429 01-47)
Avail: NTIS HC A23/MF A01 CSCL 01C

On February 24, 1987, a NASA T-38A airplane experienced a lightning strike while approaching the Los Alamitos Army Aviation Facility in California. The airplane was landed safely at Los Alamitos with no injury to the crew members. However, the airplane suffered extensive fire damage in the center of the fuselage section. The NASA investigation board concluded that the airplane was struck by lightning, which resulted in an inflight explosion with subsequent fire. The implications of this mishap to aircraft lightning protection and the avoidance of those conditions conducive to lightning strikes to aircarft are discussed. Author

N89-10479# Office National d'Etudes et de Recherches Aeronautiques, Paris (France).
ELECTROMAGNETIC COUPLING THROUGH COMPOSITE MATERIALS **c24**
V. Gobin, G. Labaune, and F. Issac *In* NOAA, International Aerospace and Ground Conference on Lightning and Static Electricity Apr. 1988 p 370-37 Sponsored in part by DRET (Direction des Recherches, Etudes et Techniques), and AMD/BA

(Avions Marcel Dassault Breguet Aviation) (For primary document see N89-10429 01-47)
Avail: NTIS HC A23/MF A01 CSCL 11D

An overview of the accuracy of an integral equation formalism in the study of the effectiveness of conductive shielding is given. The solutions described are limited to materials that can be modeled by surface impedance, excluding the skin effect representation. The free and loaded apertures are analyzed theoretically and experimentally. The effect of a joint is pointed out in a configuration of practical interest. An example of a 3-D loaded structure is calculated numerically and the result is compared with the analytical solution. Author

N89-10480# Bonn Univ. (West Germany). Radioastronomical Inst.

MONITORING LIGHTNING ACTIVITY IN SOUTH AFRICA WITH A VLF SINGLE-STATION TECHNIQUE: COMPARISON WITH METEOSAT INFRARED DATA

C. Grandt and H. Volland *In* NOAA, International Aerospace and Ground Conference on Lightning and Static Electricity Apr. 1988 p 378-38 (For primary document see N89-10429 01-47)
Avail: NTIS HC A23/MF A01 CSCL 04B

A new semiempirical method to evaluate the location of distant thunderstorms with a single-station VLF technique is presented. The technique is based on the theoretically expected internal relationship between spectral amplitude ratio (SAR) and the group time delay difference (GDD) of an individual sferic. A statistical analysis allows one to separate the source characteristics of a mean lightning stroke from the propagation properties of the atmospheric waveguide. During daytime conditions, thunderstorm detection is possible for distances between about 700 and 4500 km. The daytime results during the observational period from November 1985 to February 1986 are presented as thunderstorm maps covering the wider environment of Pretoria and are compared with METEOSAT infrared data. It is shown that there is a correlation between the thunderstorm frequency and the cloud top temperature, the respective temperature values being a function of orographic features and of the latitude of the thunderstorm locations. Author

N89-10481# Office National d'Etudes et de Recherches Aeronautiques, Paris (France).

THE SAFIR LIGHTNING MONITORING AND WARNING SYSTEM, APPLICATIONS TO AEROSPACE ACTIVITIES **c31**

P. Richard, A. Soulage, P. Laroche, and J. Appel *In* NOAA, International Aerospace and Ground Conference on Lightning and Static Electricity Apr. 1988 p 383-39 (For primary document see N89-10429 01-47)
Avail: NTIS HC A23/MF A01 CSCL 13B

A real-time lightning monitoring and warning system developed on the bases of recent advances in the field of lightning characterization are described. Applications and perspectives of the system are discussed, particularly applications for the field of aerospace safety. Author

N89-10482# Electricity Council Research Centre, Capenhurst (England).

A LIGHTNING LOCATION SYSTEM FOR THE UK ELECTRICITY SUPPLY INDUSTRY **c31**

Laura Scott *In* NOAA, International Aerospace and Ground Conference on Lightning and Static Electricity Apr. 1988 p 391-39 (For primary document see N89-10429 01-47)
Avail: NTIS HC A23/MF A01 CSCL 13B

A short history is given of the development of a lightning location system based on a network of direction finding stations. The system makes use of the earth-ionosphere waveguide to greatly reduce the effect of anomalous waves on bearing accuracy. An improved direction finding loop antenna is described. Details of the system performance are given. Author

N89-10483# Saab-Scania, Linkoping (Sweden).

FINITE DIFFERENCE ANALYSIS OF EXTERNAL AND INTERNAL LIGHTNING RESPONSE OF THE JAS39 CFC WING **c03**

Bo I. Wahlgren and Jonas W. Rosen *In* NOAA, International Aerospace and Ground Conference on Lightning and Static Electricity Apr. 1988 p 396-40 (For primary document see N89-10429 01-47)
Avail: NTIS HC A23/MF A01 CSCL 01C

Analysis was carried out on a carbon fiber composite (CFC) wing for the JAS39 aircraft, using a 3-D finite difference technique in the time domain. The wing box was also subjected to extensive lightning testing which allowed researchers to compare test and analysis results. For both the wing and the wing box, the external configuration as well as the internal installations were modeled quite accurately. The model provided for the correct interaction between external and internal fields. The model is described in some detail and test results are given. Author

N89-10484# United Kingdom Atomic Energy Authority, Culham (England). Lightning Studies Unit.

A FILAMENTARY METHOD FOR CALCULATING INDUCED VOLTAGES WITHIN RESISTIVE STRUCTURES IN EITHER THE FREQUENCY OR TIME DOMAIN **c33**

C. J. Hardwick, S. J. Haigh, and B. J. C. Burrows *In* NOAA, International Aerospace and Ground Conference on Lightning and Static Electricity Apr. 1988 p 401-40 (For primary document see N89-10429 01-47)
Avail: NTIS HC A23/MF A01 CSCL 09C

A program was developed to predict current distributions resulting from a direct lightning strike to a structure of constant cross section consisting of both metallic and composite conductors. The structure is represented by a set of filaments which are assigned values of both resistance and self inductance. The current can be calculated in either the frequency or time domain; this current distribution then allows either the transfer impedance of wires located within the structure or the induced voltage on these wires as a function of time to be calculated. Author

N89-10485# Societe Nationale Industrielle Aerospatiale, Toulouse (France).

MODELLING OF COMMON MODE COUPLING BETWEEN AN AIRCRAFT WING TRAVERSED BY A LIGHTNING CURRENT AND WIRING INSTALLED IN THAT WING **c03**

Michel Crokaert *In* NOAA, International Aerospace and Ground Conference on Lightning and Static Electricity Apr. 1988 p 408-42 (For primary document see N89-10429 01-47)
Avail: NTIS HC A23/MF A01 CSCL 01C

A code for the calculation of lightning induced common mass voltage and current in wiring installed in a wing was developed on the basis of the experimental results of the tests on an Airbus A300 wing subjected to current pulses with very different shapes and amplitudes. The code uses conventional transmission line modelling by quadripole method for both internal and external fields. This model made it possible to explain how magnetic and electric coupling intervenes in time in the voltage and current in wiring. It also makes it possible to account for the loss coefficients of the two lines which make up the external and internal fields and to explain the limitation of certain overvoltages that can intervene. This enables researchers to use the similarity existing between lines and antennae to extrapolate the results to lightning striking an aircraft in flight. Author

N89-10486# Meteorological Office, Bracknell (England).

PRECISE LONG-RANGE LIGHTNING MAPPING WITH THE UK ARRIVAL TIME DIFFERENCE VLF TECHNIQUE

A. C. L. Lee *In* NOAA, International Aerospace and Ground Conference on Lightning and Static Electricity Apr. 1988 p 425-43 (For primary document see N89-10429 01-47)
Avail: NTIS HC A23/MF A01 CSCL 04B

The Meteorological Office is bringing its Arrival Time Difference (ATD) long-range lightning mapping system into formal operation; results will be distributed internationally on World Meteorological

Organization (WMO) data channels, with higher resolution data available for internal use. Two operational ATD cases are analyzed by non-operational algorithms that domonstrate consistent bias elimination over several hours in one day, and between days.
Author

N89-10487# Honeywell, Inc., Phoenix, Ariz.
LSZ-850 LIGHTNING SENSOR SYSTEM **c35**
Ernest W. Coleman *In* NOAA, International Aerospace and Ground Conference on Lightning and Static Electricity Apr. 1988 p 434-43 (For primary document see N89-10429 01-47)
Avail: NTIS HC A23/MF A01 CSCL 14B

The design and summary of test results of a new Honeywell Wideband Lightning Sensor System (LSZ-850) is presented. The unique method for identifying, direction-finding and ranging to a lightning stroke is discussed. The LSZ-850 Lightning Sensor System senses electrostatic and electromagnetic disturbances caused by lightning discharge activity. When a discharge occurs, the system carefully analyzes the lightning discharge and creates the proper symbol for display on the radar indicator. The system's computer determines the rate of lightning in a fixed geographical area and then displays the centroid of that area with the unique lightning rate symbol. Wide bandwidth, extensive signal processing and lightning stroke recognition algorithms are used. Tests on a number of lightning storms at distances to 100 nm indicate the angular resolution to be better than plus or minus 10 degrees, and may be in the range of less than 3 degrees with little or no systematic dependence on the number of active thunderstorm cells which are at different angles. Test results are presented which show the accuracy of the system in locating severe weather. Author

N89-10488# Lightning Location and Protection, Inc., Tucson, Ariz.
CONSIDERATIONS FOR USING LIGHTNING LOCATING SYSTEMS IN PERFORMANCE EVALUATIONS OF SINGLE-STATION LIGHTNING DETECTION SENSORS
W. T. Neumann, L. G. Byerley, A. E. Pifer, and W. Hiscox *In* NOAA, International Aerospace and Ground Conference on Lightning and Static Electricity Apr. 1988 p 439-44 (For primary document see N89-10429 01-47)
Avail: NTIS HC A23/MF A01 CSCL 04B

The fundamental and practical limitations of lightning location systems are reviewed, indicating how the locating system accuracy and efficiency depend on the shape and dimensions of the network. Also reviewed are the conventions that are used in these lightning locating systems for the discrimination, definition, and time-tagging of a reported flash. Author

N89-10489# Universidad Nacional de Mexico, Mexico City. Centro de Ciencias de la Atmosfera.
SOME OBSERVATIONS AND ANALYSIS OF ATMOSPHERIC ELECTRICITY OVER NON-UNIFORM HIGH TERRAIN
Oscar TroncosoLozada *In* NOAA, International Aerospace and Ground Conference on Lightning and Static Electricity Apr. 1988 p 450-45 (For primary document see N89-10429 01-47)
Avail: NTIS HC A23/MF A01 CSCL 04B

A series of measurements were made at CU-Electromagnetic Laboratory located in the Mexico Valley. The ground station was instrumented to measure electric field, radio noise at frequencies of 10 kHz and 27 kHz. Good electrical data are being obtained on the spatial and temporal structures of the lowest kilometers of the atmosphere that will refine knowledge of the earth's electrical field. The results for the period covered by the observations, particularly in local scale, warrent further detailed study. Special programs are planned to study relationships between thunderclouds and orography. Also being planned are studies to answer the questions of why thunderstorms produce more lightning on days when significant southerly wind is present and why flashes tend to develop in the afternoon over the southern mountainside of the Mexico Valley. Author

N89-10490# Massachusetts Inst. of Tech., Cambridge. Dept. of Earth, Atmospheric and Planetary Sciences.
INTRACLOUD LIGHTNING AS A PRECURSOR TO THUNDERSTORM MICROBURSTS
E. R. Williams and R. E. Orville (State Univ. of New York, Albany.) *In* NOAA, International Aerospace and Ground Conference on Lightning and Static Electricity Apr. 1988 p 454-45 (For primary document see N89-10429 01-47)
Avail: NTIS HC A23/MF A01 CSCL 04B

The intracloud lightning activity of microburst-producing thunderstorms is shown to be a systematic precurser to the maximum outflow velocity at ground level. The time of peak flash rate leads the time of maximum differential velocity by 5 to 10 minutes. The consistent temporal relationship between the electrical phenomenon (lightning rate) and the dynamical phenomenon (the microburst) is attributed to a common cause - ice particles aloft. Author

N89-10491# University of Technology, Lae (Papua New Guinea). Electrical and Communication Engineering.
THE LIGHTNING FLASH COUNTER: PAPUA NEW GUINEAN EXPERIENCE **c35**
Feroze Coowar, Paul R. P. Hoole, and Peter Greenwood (Hydro-Electric Power Commission, Tasmania, Australia) *In* NOAA, International Aerospace and Ground Conference on Lightning and Static Electricity Apr. 1988 p 460-46 (For primary document see N89-10429 01-47)
Avail: NTIS HC A23/MF A01 CSCL 14B

The main purpose was to contain information on the frequency of occurrence of lightning flashes to ground, since the risk of damage from lightning is obviously more related to this than to hearing thunder. Furthermore, it is hoped that the vastly varying climate and topography from region to region within Papua, New Guinea amd local lightning activity measurements will help to correlate thunderstorms with other meteorological data. Author

N89-10492# Messerschmitt-Boelkow-Blohm G.m.b.H., Munich (West Germany).
INDIRECT EFFECTS ON ELECTRONIC AND MECHANICAL SYSTEMS INSTALLED IN CARBON FIBRE COMPOUND AIRCRAFT STRUCTURES **c03**
Rainer Strauss *In* NOAA, International Aerospace and Ground Conference on Lightning and Static Electricity Apr. 1988 p 470-48 (For primary document see N89-10429 01-47)
Avail: NTIS HC A23/MF A01 CSCL 01C

A test program for indirect strike effects on electrical and mechanical systems installed in a carbon fiber compound aircraft structure is described. The test program was carried out on the front and center of a simulated fuselage of real size, unprotected and protected with aluminum mesh. The test results showed the differences of cable shielding standards and also the shielding effect of the aluminum mesh. Author

N89-10493# Department of National Defence, Ottawa (Ontario). Quality Engineering Test Establishment.
ELECTROSTATIC DISCHARGE AND FIELD EFFECTS OF ELECTRONICS SYSTEMS **c33**
L. R. Dicks and G. Morin *In* NOAA, International Aerospace and Ground Conference on Lightning and Static Electricity Apr. 1988 p 481-48 (For primary document see N89-10429 01-47)
Avail: NTIS HC A23/MF A01 CSCL 09C

The effects of static electricity on modern electronics are discussed, as well as a comprehensive approach to electrostatic discharge (ESD) protection measures in all phases of the life cycle of an electronic system. Static electricity has become a potential source of damage to electronic systems used in most applications, including aircraft, ground and shipboard installations. Author

N89-10494# Tokyo Univ. (Japan). Inst. of Industrial Science.
SITE ERRORS OF A MAGNETIC DIRECTION FINDER FOR LIGHTNING FLASHES **c35**
T. Kawamura, M. Ishii, and Y. Miyake (Sankosha Co. Ltd., Tokyo, Japan) *In* NOAA, International Aerospace and Ground

Conference on Lightning and Static Electricity Apr. 1988 p 487-49 (For primary document see N89-10429 01-47)
Avail: NTIS HC A23/MF A01 CSCL 14B

In Japan, several networks of magnetic direction finders (DFs) are operated by a university and several electric power utilities. These DF stations exhibit systematic errors which are a function of the bearing of the incident. Such errors are called site errors, and generally it is difficult to determine the causes of them. Among the sites of DF stations on the coast of the Sea of Japan, there are three spots where two DFs are installed closely on the same site. The difference between the bearings obtained by two DFs, installed within several tens of meters, has been measured. Two methods in estimating site errors are tested and the results are compared with measured differences of site errors. Estimated site errors are approximately in agreement with the measurement. Author

N89-10495# SRI International Corp., Menlo Park, Calif.
GROUNDING FOR SAFETY AND COMPATIBILITY c31
Edward F. Vance and Werner Graf *In* NOAA, International Aerospace and Ground Conference on Lightning and Static Electricity Apr. 1988 p 494-49 (For primary document see N89-10429 01-47)
Avail: NTIS HC A23/MF A01 CSCL 13B

In modern electronic systems, grounding must protect personnel and equipment without causing interference in sensitive electronic circuits. Thus, the grounding topology must be compatible with the shielding topology used to protect the circuits. Grounding conductors should not penetrate shield surfaces. The relation of cable shields and signal returns to grounding is defined. Author

N89-10496# Electro Magnetic Applications, Inc., Lakewood, Colo.
THE INTERACTION BETWEEN LIGHTNING GROUNDING SYSTEMS AND BURIED CABLES c33
Richard S. Collier *In* NOAA, International Aerospace and Ground Conference on Lightning and Static Electricity Apr. 1988 p 499-50 (For primary document see N89-10429 01-47)
(Contract DAAH01-85-D-A015)
Avail: NTIS HC A23/MF A01 CSCL 09C

Lightning protection systems for facilities often involve aerial terminals, down conductors and ground laid counterpoise systems. If lightning attaches to the protection system, there can be a significant interaction between the lightning grounding system and any incoming power or signal lines which may be entering the facility. A three dimensional finite difference formalism of Maxwell's equations has been used to model this interaction and to calculate currents and voltages on nearby buried cables. The cables are analyzed using a numerical transmission line formalism with driving fields along the line caused by the lightning induced ground currents. Results are obtained for horizontal buried cables near a single down conductor with a vertical grounding rod, and these results are compared with calculations involving more extensive grounding counterpoise systems. Rules are given for finding the peak currents and voltages induced on the cables for various relative geometric configurations between the cables and the counterpoise system. Author

N89-10497# Westinghouse Electric Corp., Baltimore, Md.
SYSTEM PROTECTION FROM ATMOSPHERIC ELECTRICITY FOR AEROSTATS WITH CONDUCTING TETHERS c33
M. S. Wheeler, G. R. Beach, P. R. Jakubowski, and F. A. Fisher (Lightning Technologies, Inc., Pittsfield, Mass.) *In* NOAA, International Aerospace and Ground Conference on Lightning and Static Electricity Apr. 1988 p 505-51 (For primary document see N89-10429 01-47)
Avail: NTIS HC A23/MF A01 CSCL 09C

Aerostat power tethers have demonstrated survival of lightning strikes, but they usually have to be reterminated or replaced afterward. Two requirements are given for the prevention of lightning damage to the tether to about 100 kA: installation of a metal-to-metal contact on the outer tether surface to ground the tether at the base flying sheave at typical flying positions; and installation of a shielding band within the outer tether jacket with a weight of about 0.05 lb/ft for a half-inch tether. This determination was made in part by high current tests and in part by electrical modeling. Author

N89-10498*# Alabama Univ., Huntsville. Atmospheric Science and Remote Sensing Lab.
ANALYSIS AND MODELING OF SUMMERTIME CONVECTIVE CLOUD AND PRECIPITATION STRUCTURE OVER THE SOUTHEASTERN UNITED STATES Semiannual Report, 15 Mar. - 15 Sep. 1988
Kevin R. Knupp 20 Sep. 1988 33 p
(Grant NAG8-654)
(NASA-CR-183192; NAS 1.26:183192) Avail: NTIS HC A03/MF A01 CSCL 04B

Described is work performed under NASA Grant NAG8-654 for the period 15 March to 15 September 1988. This work entails primarily data analysis and numerical modeling efforts related to the 1986 Satellite Precipitation and Cloud Experiment (SPACE). In the following, the SPACE acronym is used along with the acronym COHMEX, which represents the encompassing Cooperative Huntsville Meteorological Experiment. Progress made during the second half of the first year of the study included: (1) installation and testing of the RAMS numerical Modeling system on the Alabama CRAY X-MP/24; (2) a start on the analysis of the mesoscale convection system (MCS) of 13 July 1986 COHMEX case; and (3) a cursory examination of a small MCS that formed over the COHMEX region on 15 July 1986. Details of each of these individual tasks are given. Author

N89-10499# National Oceanic and Atmospheric Administration, Boulder, Colo. Environmental Sciences Group.
OKLAHOMA-KANSAS PRELIMINARY REGIONAL EXPERIMENT FOR STORM-CENTRAL (O-K PRE-STORM). VOLUME 3: AIRCRAFT MISSION SUMMARY
Jose G. Meitin, Jr. Feb. 1988 112 p
(PB88-205489; NOAA-TM-ERL-ESG-30-Vol-3) Avail: NTIS HC A06/MF A01 CSCL 04B

Researchers are provided with a synopsis of the flights taken during May and June of 1985 as part of the Oklahoma-Kansas Preliminary Regional Experiment for STORM-Central (PRE-STORM). This is the final report in a series which describes the activities and catalogs the data collected during the field phase of the PRE-STORM project. The principal goals of the aircraft subprogram were to: (1) gather aircraft data in the vicinity of developing and mature convective systems in order to better define their structure, evolution, and physical processes, and (2) develop and test observational strategies for optimal use of long range research aircraft in the mesoscale convective system (MCS) environment in order to help define measurement techniques, for example, the use of airborne Doppler radar in coordination with ground based Doppler radars. Author

N89-10500# Air Force Geophysics Lab., Hanscom AFB, Mass.
THE REMOTE ATMOSPHERIC PROBING INFORMATION DISPLAY (RAPID) SYSTEM Final Report, Sep. 1986 - Sep. 1987
P. A. Sadoski, D. Egerton, F. I. Harris (ST Systems Corp., Lexington, Mass.), and A. R. Bohne 15 Jan. 1988 26 p
(AF Proj. 6670)
(AD-A196314; AFGL-TR-88-0036; AFGL-ERP-997) Avail: NTIS HC A03/MF A01 CSCL 04B

The RAPID system has been developed to support short term forecasting of cloud and precipitation. RAPID was developed with the philosophy that the system should be easily maintained, user-friendly, yet powerful enough to perform both the analysis or radar and satellite data and generation of forecasts in real-time. The two major hardware components are a VAX host computer and an ADAGE RDS-3000 image processor. The RAPID user environment is structured to encourage user participation. Numerous standardization procedures are employed: a functional disk organization, standardized data and source file headers, extensive file documentation, and use of user developed RAPID

tools, and libraries of often used routines. Data management has been designed to maximize the potential for real time capability. Radar and satellite data are preprocessed on other computers before ingestion into RAPID. The bulk of these data and derived products are stored, and analysis and display are performed entirely within the image processor. GRA

N89-10501 Utah Univ., Salt Lake City.
THE ROLE OF CLOUDS IN SURFACE RADIATION BUDGETS Ph.D. Thesis
Michael K. Griffin 1987 345 p
Avail: Univ. Microfilms Order No. DA8802710

A one-dimensional radiative transfer model was used to derive the surface radiation budget over the U.S. and China for 2 months of the first GARP Global Experiment (FGGE) year. Time concurrent low, middle, and high cloud climatologies over the two regions were computed from the A.F. Global Weather Central Three-Dimensional Cloud Nephanalysis and were used in conjunction with FGGE atmospheric profiles and daily adjusted surface albedos in the analysis. Model tests were performed for a variety of cloud cases with reasonable comparisons of the outgoing solar and IR fluxes made with the Nimbus-7 Earth Radiation Budget measured product. A number of parameters were derived to isolate the effects of clouds on the transfer of radiation. Distributions of the surface, atmospheric, and cloud parameters were presented for both regions. Comparisons of the model derived surface solar insolation over the U.S. and China compared well with available data sources. The low cloud amount was found to correlate with the surface net infrared flux, while even small amounts of cloudiness were seen to have a significant effect on the transfer of solar radiation. Dissert. Abstr.

N89-10502# Instituto de Pesquisas Espaciais, Sao Jose dos Campos (Brazil).
METEOROLOGICAL MEASUREMENTS MADE USING BRAZILIAN DRIFTING BUOYS: TECHNICAL ASPECTS AND FIRST RESULTS
Merritt R. Stevenson and Pedro Rubens A. deCarvalho Aug. 1988 16 p Presented at the I Seminario Sobre Ciencias Atmosfericas e Espaciais do Programa Artartico Brasileiro, Sao Jose dos Campos, Brazil, 27-29 Apr. 1988
(INPE-4674-PRE/1372) Avail: NTIS HC A03/MF A01

Progress in the technical development and use of meteorological sensors fixed to a Brazilian drifting oceanographic buoy is presented. Research with thermistors to measure both air and water temperatures from buoys showed promise with regard to simplicity in their applications and the associated costs. These sensors were designed, tested, and used in Antarctica in March 1985 and 1986, and after being redesigned, used again during January to April of 1987. A significant advancement was made during 1987, with the construction of a compact tower to support meteorological sensors 2 m above the water line of the buoy. This instrumented buoy was used in the Polar Front of the Antarctic Circumpolar Current, in the Drake Passage during December 1987. The buoy's sensors included two each, for air and water temperature, an anemometer for wind speed and direction and an electronic compass within the buoy to compensate for the effects of buoy rotation on wind direction. Problems related to the development and use of these drifting buoys and their data are discussed and future expectations are noted. Author

N89-10503# National Oceanic and Atmospheric Administration, Boulder, Colo. Wave Propagation Lab.
COMPARISON OF TEMPERATURE PROFILES MEASURED BY THREE COLLOCATED MICROWAVE RADIOMETERS AND RADIOSONDE
J. B. Snider, M. D. Jacobson, M. J. Falls, and J. R. Jordon Jan. 1988 45 p
(PB88-212808; NOAA-TM-ERL-WPL-151) Avail: NTIS HC A03/MF A01 CSCL 04B

The results of a nine month intercomparison of the performance of three ground based, passive microwave temperature profiles of different design are reported. Temperature profiles measured by the remote sensors are compared with those measured at standard times by radiosondes launched from the National Weather Service Forecast Office at Denver, CO. Differences in instrument performance are considered in terms of design, operating mode, and calibration methods employed by the various systems. Implications of the results upon the design of future operational temperature profilers are discussed. Author

N89-10504# National Weather Service, Salt Lake City, Utah. Weather Service Forecast Office.
CLIMATE OF SAN FRANCISCO, REVISED
George T. Pericht Apr. 1988 53 p
(PB88-208624; NOAA-TM-NWS-WR-126-Rev-1) Avail: NTIS HC A04/MF A01 CSCL 04B

An earlier summary of the climate of San Francisco written by E. Jan is revised, updated, and expanded. In addition to the revision of tables to include data through 1987, the following changes were incorporated: (1) the geographical and climatological summary was revised to include more details of the microclimates of San Francisco and to include information on sea surface temperatures; (2) corrected data to replace erroneous data from the malfunctioning rain gage from 1973 to 1982; (3) reasons behind the move of the observing; and (4) revised normal temperatures. Author

N89-10505# Naval Postgraduate School, Monterey, Calif.
ONR TROPICAL CYCLONE MOTION RESEARCH INITIATIVE: FIRST-YEAR REVIEW, DISCUSSION AND TENTATIVE HYPOTHESES Interim Report, Oct. 1986 - Sep. 1987
Russell L. Elsberry Feb. 1988 91 p
(AD-A194902; NPS63-88-003) Avail: NTIS HC A05/MF A01 CSCL 04B

The ONR Tropical Cyclone Motion initiative is a five-year program to improve basic understanding of tropical cyclone motion. On 27-30 January 1988, a meeting was held in Monterey, Calif. to: (1) Review the first year's research activities; (2) Discuss issues and plan future research; and (3) Begin discussion of tentative hypotheses that might be explored in a field experiment in the western North Pacific region during summer 1990. Each of these topics is briefly discussed to indicate the progress and plans of the initiative. GRA

N89-10506# Naval Postgraduate School, Monterey, Calif.
MIZEX (MARGINAL ICE ZONE EXPERIMENT) 87 METEOROLOGY ATLAS Technical Report, 1 Oct. 1986 - 31 Sep. 1987
Peter S. Guest and Kenneth L. Davidson Feb. 1988 146 p
(AD-A195361; NPS-63-88-004) Avail: NTIS HC A07/MF A01 CSCL 04B

The 1987 Marginal Ice Zone Experiment (MIZEX 87) was a multi-national interdisciplinary project in the Fram Strait from 19 March to 11 April 1987. Surface and upper-level measurements of meteorological parameters were obtained from three ships, the R/V Polar Circle, the R/V Haakon Mosby and the R/V Valdivia. This atlas contains: (1) Time series of surface wind velocity, barometric pressure, relative humidity, and atmospheric temperature from the ships; (2) Maps showing six-hour averages of the locations of the ships and ice edge, and surface wind velocity vectors at the ships; (3) High-resolution profiles of wind, temperature and humidity up to 2500 m; and (4) Maps of sea-level pressure every 12 hours. GRA

N89-10507# Royal Aircraft Establishment, Farnborough (England).
UPPER-ATMOSPHERE ZONAL WINDS FROM SATELLITE ORBIT ANALYSIS: AN UPDATE
D. G. King-Hele and D. M. C. Walker Oct. 1987 24 p
(RAE-TR-87058; RAE-SS-3; BR105558; ETN-88-93139)
Copyright Avail: NTIS HC A03/MF A01; Defence Research Information Centre, 65 Brown Street, Glasgow, G2 8EX, United Kingdom

The rotation rate lambda of the upper atmosphere can be evaluated from the observed changes in satellite orbital inclination,

and in 1982 we reviewed the results then available. From the 85 values accepted for the review, it was possible to determine the variation with height (130-680 km), local time and season; but dependence on other parameters was not established. The present Report updates the previous review, incorporating 18 new values determined in the past 5 years and generally of better accuracy. The previous picture is strengthened by the new data but not significantly changed. After adding the new results, we find that the average value of lambda increases from 1.0 rev/day at 125 km height to about 1.2 at 300 km, and then decreases to about 0.9 at 500 km; lambda is higher in the evening (18 to 24 h), with a maximum value near 300 km which corresponds to a west-to-east wind of 150 m/s, and is lower in the morning (06 to 12 h), with east-to-west winds of order 50 m/s at heights of 200 to 400 km. The values of lambda are higher in winter than in summer for heights of 200 to 300 km, and there is an indication that lambda may vary with solar activity, being about 0.1 lower for medium solar activity than for high or low solar activity. Results for heights above 450 km are still sparse. ESA

N89-10508# Deutsche Forschungs- und Versuchsanstalt fuer Luft- und Raumfahrt, Oberpfaffenhofen (West Germany). Abteilung Meteorologische Modelle.
THE GERMAN FRONT EXPERIMENT 1987: OBSERVATIONS AND PRELIMINARY RESULTS
Klaus-Peter Hoinka, Hans Volkerts, and Dietrich Heimann May 1988 136 p Original contains color illustrations
(DFVLR-FB-88-21; ISSN-0171-1342; ETN-88-93187) Avail: NTIS HC A07/MF A01; DFVLR, VB-PL-DO, 90 60 58, 5000 Cologne, Fed. Republic of Germany, 49.50 Deutsche marks

The impact of the Alps on cold fronts was studied. The observational program was performed during five intensive observation periods when a cold front crossed central Europe. A reduced program was performed during one additional cold front event. An outline of the experiment, the collected data, and preliminary results are presented. ESA

48 OCEANOGRAPHY

Includes biological, dynamic, and physical oceanography; and marine resources.

For related information see also *43 Earth Resources and Remote Sensing.*

N89-10509# National Oceanic and Atmospheric Administration, Seattle, Wash. Marine Environmental Lab.
EPOCS (EQUATORIAL PACIFIC OCEAN CLIMATE STUDIES) MOORED TEMPERATURE, CURRENT AND WIND MEASUREMENTS: 0 DEG, 140 DEG W, MAY-JUNE, 1987
H. P. Freitag and M. J. McPhaden Apr. 1988 37 p
(PB88-219415; NOAA-DR-ERL-PMEL-23; CONTRIB-1033) Avail: NTIS HC A03/MF A01 CSCL 08C

Temperature, current and wind data measurement during May and June 1987, in the eastern equatorial Pacific are reported. Ocean current and temperature data were obtained from Equatorial Pacific Ocean Climate Studies (EPOCS) mooring EC65 located at 0 deg 0.2 min N, 139 deg 55.4 min W. These data were collected as part of a collaborative study involving EPOCS and TROPIC HEAT to examine the relationship of high frequency internal wave processes to vertical mixing and to large scale current and temperature variability. Author

N89-10510# Centre Univ. de Luminy, Marseilles (France). Inst. de Mecanique Statistique de la Turbulence.
FINAL SYNTHESIS ON RESEARCH DONE ON THE SUBJECT OF INTERACTIONS BETWEEN OBLIQUE SWELLS AND WINDS
A. Ramamonjiarisoa and C. Kharif Dec. 1986 54 p In FRENCH Sponsored by Direction des Recherches, Etudes et Techniques, Paris, France
(PB87-186961) Avail: NTIS HC E04/MF E04; copy not available from STI Facility CSCL 08C

The various physical phenomena manifesting themselves between a swell and a field of waves created by the wind are specified, taking into account the possibility that the propagation direction of the swell could be oblique with respect to the direction of the average wind. The study represents an extension of that undertaken within the framework of the DRET/IMST no 83/366 operation which was limited to the case of a swell and the disturbances to which it was exposed propagated in the same direction. Author

N89-10511# Battelle Ocean Sciences, Duxbury, Mass.
STUDY OF BIOLOGICAL PROCESSES ON THE US NORTH ATLANTIC SLOPE AND RISE, VOLUME 2 Final Report
N. Maciolek, J. F. Grassle, B. Hecker, B. Brown, and J. A. Blake 15 Dec. 1987 538 p Sponsored by Minerals Management Service, Vienna, Va. Prepared in cooperation with Woods Hole Oceanographic Inst., Mass. and Lamont-Doherty Geological Observatory, Palisades, N.Y.
(Contract DI-14-12-0001-30064)
(PB88-196514; OCS/MMS-87/0051-Vol-2) Avail: NTIS HC A23/MF A01 CSCL 08C

Temporal and spatial variations in infaunal community structure, sediment texture, and concentrations of total organic carbon, hydrogen, nitrogen, and hydrocarbons in sediments were sampled at 14 stations six times between Nov. 1984 and Jul. 1986. Megafaunal populations were studied along a transect near the U.S./Canadian boundary, a second transect to the west, and along the 2100 m isobath near Lydonia Canyon. The fauna appears to change along depth gradients. These stations are dominated by large bodied infaunal sipunculans and aplacophoran molluscs. Author

N89-10512# National Oceanic and Atmospheric Administration, Miami, Fla. Oceanographic and Meteorological Labs.
JOINT CGS-AOML (CHARTING AND GEODETIC SERVICE-ATLANTIC OCEANOGRAPHIC AND METEOROLOGICAL LABORATORY) ACOUSTICAL BOTTOM ECHO-FORMATION RESEARCH. 1: LITERATURE SEARCH AND INITIAL MODELLING RESULTS
T. L. Clarke, J. R. Proni, D. A. Seem, and J. J. Tsai Mar. 1988 80 p
(PB88-202007; NOAA-TM-ERL-AOML-66) Avail: NTIS HC A05/MF A01 CSCL 08C

A literature survey has found work dealing with the problem of echo-formation for rough sedimentary bottoms. The main attempts at practical application have been at frequencies lower than those used for echo sounding work. A model was formulated that includes the effect of surface scattering and volume scattering in a unified manner. The model draws on biot theory, multiple scattering theory, and rough surface scattering. This model was implemented on the AOML computer and exercised for a variety of bottom types and echo sounding frequencies. GRA

N89-10513# National Oceanic and Atmospheric Administration, Boulder, Colo. Wave Propagation Lab.
TURBULENT DIFFUSION OF OCEAN BUBBLES
G. B. Crawford Jan. 1988 18 p
(PB88-212816; NOAA-TM-ERL-WPL-150) Avail: NTIS HC A03/MF A01 CSCL 08C

Mean bubble concentration profiles were analyzed in terms of a turbulent diffusion process. Two of four cases which were studied exhibit regions where diffusion coefficient profiles vary roughly linearly with depth. These profiles are consistent with the concept of a constant stress layer. The layer starts at a depth of between 3 and 10 times the rms waveheight. Author

N89-10514# National Oceanic and Atmospheric Administration, Seattle, Wash. Marine Environmental Lab.
MODEL-DATA COMPARISONS FOR THE 1982-83 EL NINO: THE XBT TRACKS
D. E. Harrison, W. S. Kessler, and B. S. Giese May 1988 67 p Prepared in cooperation with Washington Univ., Seattle

(PB88-221668; NOAA-TM-ERL-PMEL-79; CONTRIB-1035) Avail: NTIS HC A04/MF A01 CSCL 08C

Five different analyses of 1982 to 1983 monthly average surface wind stress fields were used to force an ocean general circulation model of the tropical Pacific, in a series of El Nino hindcast experiments. The results of these hindcasts are compared with the variability of upper ocean dynamic height, sea surface temperature and subsurface temperature as observed from XBT data observed along the three main ship of opportunity tracks. During 1982 to 1983 there were prominent departures from climatology in the surface wind stress field. The ocean underwent several major changes during this period according to the XBT data; these changes are summarized. The model hindcasts are examined to determine the extent to which the observed major ocean changes were reproduced. Author

N89-10515# Vrije Universiteit, Amsterdam (Netherlands). Dept. of Mathematics.

REAL ALGEBRAIC MORPHISMS WITH VALUES IN THE UNIT CIRCLE

J. Bochnak and W. Kucharz (New Mexico Univ., Albuquerque.) Sep. 1987 11 p

(PB88-208921; Rept-329) Avail: NTIS HC A03/MF A01 CSCL 08C

Let X be a nonsingular compact connected real algebraic set and let (S sup 1) be the unit circle. The group Gamma(X) = (C sup infinity) (X,(S sup 1))/(C sup R, sup infinity)(X, (S sup 1)), where (C sup infinity) (X,(S sup1) is the group of (C sup infinity) mappings from X into (S sup 1) and (C sup R, sub infinity) (X,(S sup 1) is its subgroup of (C sug infinity) mappings approximable by regular mappings (i.e., real algebraic morphisms from X into (S sup 1) was studied. It was shown that Gamma(X) approximately = (Z/2) sup p for some nonnegative integer p, and compute precisely the exponent p for dim X = 2. GRA

N89-10516# National Oceanic and Atmospheric Administration, Miami, Fla. Oceanographic and Meteorological Labs.

DRIFTING BUOY DATA FROM THE EQUATORIAL PACIFIC FOR THE PERIOD JANUARY 1, 1984 THROUGH MAY 31, 1985

Mayra C. Pazos Mar. 1988 106 p

(PB88-212824; NOAA-DR-ERL-AOML-11) Avail: NTIS HC A06/MF A01 CSCL 08C

Satellite tracked drifting buoy Oceanographic data collected in the eastern tropical Pacific Ocean during the period of 1 January 1984 through 31 May 1985 is presented. Deployment times, locations and characteristics of each buoy is detailed. Author

N89-10517# Battelle Ocean Sciences, Duxbury, Mass.

STUDY OF BIOLOGICAL PROCESSES ON THE US NORTH ATLANTIC SLOPE AND RISE. VOLUME 1: EXECUTIVE SUMMARY Report, Nov. 1984 - Nov. 1986

N. Maciolek, J. F. Grassle, B. Hecker, B. Brown, and J. A. Blake 15 Dec. 1987 52 p Sponsored by Minerals Management Service, Vienna, Va. Prepared in cooperation with Woods Hole Oceanographic Inst., Mass. and Lamont-Doherty Geological Observatory, Palisades, N.Y.

(Contract DI-14-12-0001-30064)
(PB88-196522; OCS/MMS-87/0051-Vol-1) Avail: NTIS HC A04/MF A01 CSCL 08C

Temporal and spatial variations in infaunal community structure, sediment texture, and concentrations of total organic carbon, hydrogen, nitrogen, and hydrocarbons in sediments were sampled at 14 stations six times between Nov. 1984 and Jul. 1986. Megafaunal populations were studied along a transect near the U.S./Canadian boundary, a second transect to the west, and along the 2100 m isobath near Lydonia Canyon. The most distinct communities were seen on the upper slope, where sediments are coarse and currents presumably are strong. Recolonization experiments indicate slow rates of recovery of disturbed environments. Author

51 LIFE SCIENCES (GENERAL)

N89-10518*# State Univ. of New York, Stony Brook. Dept. of Biochemistry.

CHROMOSOMES AND PLANT CELL DIVISION IN SPACE Final Technical Report

A. D. Krikorian 1988 70 p

(Grant NAG10-35)
(NASA-CR-183213; NAS 1.26:183213) Avail: NTIS HC A04/MF A01 CSCL 06C

The objectives were: examination of chromosomal aberrations; development of an experimental system; and engineering design units (EDUs) evaluation. Evaluation criteria are presented. Procedures were developed for shuttle-based investigations which result in the procurement of plant root tips for subsequent cytological examination. Author

52 AEROSPACE MEDICINE

Includes physiological factors; biological effects of radiation; and effects of weightlessness on man and animals.

N89-10519# Army Research Inst. of Environmental Medicine, Natick, Mass.

MODULATION OF HUMAN PLASMA FIBRONECTIN LEVELS FOLLOWING EXERCISE

David A. DuBose, L. E. Armstrong, W. J. Kraemer, and M. Lukason Jan. 1988 23 p

(AD-A192674; USARIEM-M-18/88) Avail: NTIS HC A03/MF A01 CSCL 06J

Tissue and Plasma Fibronectin (PF) represent two forms of this large molecular weight (440 kilodaltons) glycoprotein. While the tissue type is cell-associated and important to cell adhesion and shape, PF circulates in the blood and serves as a nonspecific opsonin for the reticuloendothelial system (RES). Although it may not participate in all forms of RES clearance. PF is an important contributor to this RES function. It supports particulate clearance by binding to material released to the vascular space as the result of tissue injury and thereby enhances the engulfment of this debris by the phagocytic cells of the RES. In this way, PF influences blood vessel patency and continued blood flow. Augmentation of particulate clearance by PF is perhaps one explanation for the correlation between elevated RES function and increased survival after shock. RES function and PF are suppressed after shock and trauma. Trauma-induced organ failure correlates with reduced PF level. While PF concentration rapidly recovers in survivors that have experienced traumatic episodes, it remains suppresses in nonsurvivors. Immunoglobulin reduction of PF results in decreased phagocytosis and decreased resistance to shock. Moreover, experimental rat heat stress mortality rate is significantly lessened by increased RES clearance capacity and naturally occurring elevations in PF level. Hence, elevation of PF may influence the outcome of trauma and correlate with the degree of tolerance to environmental stress. GRA

N89-10463# Queensland Univ., St. Lucia (Australia). Dept. of Electrical Engineering.

A REVIEW OF MEDICAL ASPECTS OF LIGHTNING INJURY

C. J. Andrews, M. Darveniza, and D. Mackerras *In* NOAA, International Aerospace and Ground Conference on Lightning and Static Electricity Apr. 1988 p 231-25 (For primary document see N89-10429 01-47)

Avail: NTIS HC A23/MF A01 CSCL 06P

N89-10464# Queensland Univ., St. Lucia (Australia). Dept. of Electrical Engineering.

A RETROSPECTIVE STUDY OF THE INJURIES SUSTAINED IN TELEPHONE-MEDIATED LIGHTNING STRIKE

C. J. Andrews, M. Darveniza, and D. Mackerras *In* NOAA, International Aerospace and Ground Conference on Lightning and

Static Electricity Apr. 1988 p 251-27 (For primary document see N89-10429 01-47)
Avail: NTIS HC A23/MF A01 CSCL 06P

53 BEHAVIORAL SCIENCES

Includes psychological factors; individual and group behavior; crew training and evaluation; and psychiatric research.

N89-10520# Katholieke Universiteit, Nijmegen (Netherlands). Mathematical Psychology Group.
ORDMET3: AN IMPROVED ALGORITHM TO FIND THE MAXIMUM SOLUTION TO A SYSTEM OF LINEAR (in)EQUALITIES
E. E. Roskam 1987 35 p
(PB88-208970; Rept-87-MA-06) Avail: NTIS HC A03/MF A01 CSCL 05I

An improved algorithm, called ORDMET3, for psychological measurement and scaling data, is used to find both a set of solutions to a system of linear (in)equalities and the maximum r solution. As such, it improves on the algorithms of others. The present algorithm is faster and requires less storage capacity, is more robust in finding the maximum r solution, and can process linear equality constraints. GRA

N89-10521# Pacific Northwest Labs., Richland, Wash.
EFFECT OF A 12-HOUR/DAY SHIFT ON PERFORMANCE
Paul M. Lewis and Dan J. Swaim (Westinghouse Hanford Co., Richland, Wash.) Jun. 1988 11 p Presented at the 4th International Conference on Human Factors and Power Plants, Monterey, Calif., 5 Jun. 1988
(Contract DE-AC06-76RL-01830)
(DE88-013184; PNL-SA-15620; CONF-880633-7) Avail: NTIS HC A03/MF A01

The operating crews at the Fast Flux Facility near Richland, Washington, changed their rotating shift schedule from an 8- to 12- hour per day work schedule. The primary reason for the change was to reduce the attrition of operators by increasing their job satisfaction. Eighty-four percent of the operators favored the change. Plant performance and safety were not adversely affected. A statistical analysis of 53 operator-related, off-normal events in 28 months concluded that there was no significant difference in either the number or the severity of off-normal events on the 12-hour shift. A statistical analysis of 200,000 log entries concluded that the error rate in completing logs actually declined by 25 percent on the 12-hour shift. Alertness, which was measured using computerized tests of mathematics and logical reasoning, reach a nadir on the first night shift for the 8- and 12-hour schedules alike, which indicates that the primary cause of fatigue was sleep disruption, not cumulative hours of work. All supervisors and 52 percent of the operators believe their crews work more effectively on the 12-hour shift; only 12 percent of the operators believe that their crews work less effectively. The evaluation indicated that the 12-hour shift scheduled is a reasonable alternative to an 8-hour schedule at this facility. DOE

54 MAN/SYSTEM TECHNOLOGY AND LIFE SUPPORT

Includes human engineering; biotechnology; and space suits and protective clothing.

For related information see also *16 Space Transportation.*

N89-10522*# National Aeronautics and Space Administration, Washington, D.C.
LIVING IN SPACE, BOOK 2, LEVELS D, E, F
Sheila Briskin Andrews and Audrey Kirschenbaum 1987 70 p
Original document contains color illustrations
(NASA-EP-223; NAS 1.19:223) Avail: SOD HC $4.75 as 033-000-01001; NTIS MF A01 CSCL 06K

In June 1984, President Reagan announced a new NASA program, Operation Liftoff. For more than 25 years NASA has pioneered on the cutting edge of science and technology and has stimulated our young people to strive for excellence in all they do. This program is designed to encourage pupils in the nation's elementary schools to take a greater interest in mathematics and science. Areas addressed include: food, clothing, health, housing, communication, and working in space. B.G.

N89-10523# Illinois Univ., Urbana. Dept. of Physics.
PRESSURE STUDIES OF PROTEIN DYNAMICS Annual Report, 1 Mar. 1987 - 26 Feb. 1988
Hans Frauenfelder and Robert D. Young 26 Feb. 1988 20 p
(Contract N00014-86-K-0270; RR0-4106)
(AD-A192386) Avail: NTIS HC A03/MF A01 CSCL 06A

In this research we extend and deepen our studies of the relation between dynamic structure and function in proteins. We study protein dynamics using flash photolysis together with near ultraviolet, visible, and near and mid-infrared spectroscopies over wide ranges in time (50 ns to 10 ks), temperature (60 to 320 K), and pressure (0.1 to 100 MPa). Initially we study a simple biomolecular reaction -- carbon monoxide (CO) binding to myoglobin (Mb). We have greatly expanded knowledge of pressure effects on proteins by using the infrared CO stretching frequencies in MbCO as a probe. The combined pressure and temperature studies shed new light on various features of the hierarchical model of protein substates and motions. These studies also provide much information on the glass like behavior of proteins, including the slaved glass transition and glass-like relaxation processes near the transition temperature. GRA

N89-10088*# California Univ., Berkeley. Telerobotics Unit.
A UNIVERSITY TEACHING SIMULATION FACILITY
Lawrence Stark, Won-Soo Kim, Frank Tendick, Mitchell Tyler, Blake Hannaford, Wissam Barakat, Olaf Bergengruen, Louis Braddi, Joseph Eisenberg, and Stephen Ellis et al. *In* NASA, Goddard Space Flight Center, Proceedings of 1987 Goddard Conference on Space Applications of Artificial Intelligence (AI) and Robotics 1987 30 p (For primary document see N89-10063 01-12)
Avail: NTIS HC A99/MF E03 CSCL 05H

N89-10089*# Grumman Aerospace Corp., Bethpage, N.Y.
OPEN CONTROL/DISPLAY SYSTEM FOR A TELEROBOTICS WORK STATION
Saul Keslowitz *In* NASA, Goddard Space Flight Center, Proceedings of 1987 Goddard Conference on Space Applications of Artificial Intelligence (AI) and Robotics 1987 21 p (For primary document see N89-10063 01-12)
Avail: NTIS HC A99/MF E03 CSCL 05H

N89-10090*# Human Machine Interfaces, Inc., Knoxville, Tenn. Fuel Recycle Div.
CONSOLIDATED FUEL REPROSSING PROGRAM: THE IMPLICATIONS OF FORCE REFLECTION FOR TELEOPERATION IN SPACE
John V. Draper, Joseph N. Herndon, and Wendy E. Moore *In* NASA, Goddard Space Flight Center, Proceedings of 1987 Goddard Conference on Space Applications of Artificial Intelligence (AI) and Robotics 1987 16 p Previously announced as N87-27402 Prepared in cooperation with Martin Marietta Aerospace, Denver, Colo. (For primary document see N89-10063 01-12)
(Contract DE-AC05-84OR-21400)
Avail: NTIS HC A99/MF E03 CSCL 05H

N89-10091*# Martin Marietta Aerospace, Denver, Colo.
ISSUES, CONCERNS, AND INITIAL IMPLEMENTATION RESULTS FOR SPACE BASED TELEROBOTIC CONTROL
D. A. Lawrence, J. D. Chapel, and T. M. Depkovich *In* NASA, Goddard Space Flight Center, Proceedings of 1987 Goddard Conference on Space Applications of Artificial Intelligence (AI) and

Robotics 1987 18 p (For primary document see N89-10063 01-12)
Avail: NTIS HC A99/MF E03 CSCL 05H

N89-10092*# RCA Advanced Technology Labs., Moorestown, N.J.
A SHARED POSITION/FORCE CONTROL METHODOLOGY FOR TELEOPERATION
Jin S. Lee *In* NASA, Goddard Space Flight Center, Proceedings of 1987 Goddard Conference on Space Applications of Artificial Intelligence (AI) and Robotics 1987 12 p (For primary document see N89-10063 01-12)
Avail: NTIS HC A99/MF E03 CSCL 05H

N89-10093*# Jet Propulsion Lab., California Inst. of Tech., Pasadena.
MULTIPLE SENSOR SMART ROBOT HAND WITH FORCE CONTROL
Richard R. Killion, Lee R. Robinson, and Antal Bejczy *In* NASA, Goddard Space Flight Center, Proceedings of 1987 Goddard Conference on Space Applications of Artificial Intelligence (AI) and Robotics 1987 20 p (For primary document see N89-10063 01-12)
Avail: NTIS HC A99/MF E03 CSCL 05H

N89-10094*# McDonnell-Douglas Astronautics Co., Houston, Tex. Engineering Services.
AN OPTIMAL RESOLVED RATE LAW FOR KINDEMATICALLY REDUNDANT MANIPULATORS
B. J. Bourgeois *In* NASA, Goddard Space Flight Center, Proceedings of 1987 Goddard Conference on Space Applications of Artificial Intelligence (AI) and Robotics 1987 20 p Previously announced as N88-17268 (For primary document see N89-10063 01-12)
Avail: NTIS HC A99/MF E03 CSCL 05H

N89-10095*# Maryland Univ., College Park. Robotics Lab.
AN ADAPTIVE CONTROL SCHEME FOR A FLEXIBLE MANIPULATOR
T. C. Yang, J. C. S. Yang, and P. Kudva (Advanced Technology and Research, Inc., Burtonsville, Md.) *In* NASA, Goddard Space Flight Center, Proceedings of 1987 Goddard Conference on Space Applications of Artificial Intelligence (AI) and Robotics 1987 14 p (For primary document see N89-10063 01-12)
Avail: NTIS HC A99/MF E03 CSCL 05H

N89-10098*# Oak Ridge National Lab., Tenn. Center for Engineering Systems Advanced Research.
DYNAMIC TASK ALLOCATION FOR A MAN-MACHINE SYMBIOTIC SYSTEM
L. E. Parker and F. G. Pin *In* NASA, Goddard Space Flight Center, Proceedings of 1987 Goddard Conference on Space Applications of Artificial Intelligence (AI) and Robotics 1987 19 p Previously announced as N87-30070 Submitted for publication (For primary document see N89-10063 01-12)
(Contract DE-AC05-84OR-21400)
Avail: NTIS HC A99/MF E03 CSCL 05H

N89-10101*# Martin Marietta Aerospace, Denver, Colo. Advance Automation Technology (Robotics) Group.
ACTUATORS FOR A SPACE MANIPULATOR
W. Chun and P. Brunson *In* NASA, Goddard Space Flight Center, Proceedings of 1987 Goddard Conference on Space Applications of Artificial Intelligence (AI) and Robotics 1987 20 p (For primary document see N89-10063 01-12)
Avail: NTIS HC A99/MF E03 CSCL 05H

N89-10102*# National Aeronautics and Space Administration. Goddard Space Flight Center, Greenbelt, Md.
CABLE APPLICATIONS IN ROBOT COMPLIANT DEVICES
James J. Kerley *In its* Proceedings of 1987 Goddard Conference on Space Applications of Artificial Intelligence (AI) and Robotics 1987 11 p (For primary document see N89-10063 01-12)
Avail: NTIS HC A99/MF E03 CSCL 05H

N89-10104*# Jet Propulsion Lab., California Inst. of Tech., Pasadena.
TELEOPERATED POSITION CONTROL OF A PUMA ROBOT
Edmund Austin and Chung P. Fong *In* NASA, Goddard Space Flight Center, Proceedings of 1987 Goddard Conference on Space Applications of Artificial Intelligence (AI) and Robotics 1987 19 p (For primary document see N89-10063 01-12)
Avail: NTIS HC A99/MF E03 CSCL 05H

55 SPACE BIOLOGY

Includes exobiology; planetary biology; and extraterrestrial life.

No abstracts in this category.

59 MATHEMATICAL AND COMPUTER SCIENCES (GENERAL)

No abstracts in this category.

60 COMPUTER OPERATIONS AND HARDWARE

Includes hardware for computer graphics, firmware, and data processing.

For components see *33 Electronics and Electrical Engineering.*

N89-10524*# National Aeronautics and Space Administration. Langley Research Center, Hampton, Va.
ON THE DIAGNOSTIC EMULATION TECHNIQUE AND ITS USE IN THE AIRLAB
Gerard E. Migneault Oct. 1988 28 p
(NASA-TM-4027; L-16397; NAS 1.15:4027) Avail: NTIS HC A03/MF A01 CSCL 09B

An aid is presented for understanding and judging the relevance of the diagnostic emulation technique to studies of highly reliable, digital computing systems for aircraft. A short review is presented of the need for and the use of the technique as well as an explanation of its principles of operation and implementation. Details that would be needed for operational control or modification of existing versions of the technique are not described. Author

N89-10525# Office of Science and Technology, Washington, D.C.
FEDERAL COORDINATING COUNCIL ON SCIENCE, ENGINEERING AND TECHNOLOGY, COMMITTEE ON COMPUTER RESEARCH AND APPLICATIONS, SUBCOMMITTEE ON SCIENCE AND ENGINEERING COMPUTING Annual Report, 1987
Mar. 1988 13 p
(DE88-013228; DOE/ER-0368) Avail: NTIS HC A03/MF A01

In the past year the committee initiated efforts that resulted in the report A Research and Development Strategy for High Performance Computing and will presently provide a government-wide implementation plan to address the technological opportunities possible with the achievement of significantly enhanced supercomputer capability. The committee met on a regular basis to review government supported programs in research, development and application of new supercomputer technology. The Committee annually visits supercomputer manufacturers to

be briefed on their plans for future generation machines. Cray Research and ETA Systems continue to make progress toward developing more advanced supercomputers. Reports by the Defense Science Board and the National Security Council/Economic Policy Council, which addressed semiconductor issues, were completed during the year with advice and input from the Committee. IBM has re-entered the supercomputer marketplace. The current 3090 series with expandable vector processing capability has achieved a low end position in the supercomputer performance spectrum. Subsequent development and marketing by IBM of more powerful machines would have important and far reaching impact on the domestic and world supercomputer market. Computers with massively parallel architecture--thousands of processors--are entering the market place and are beginning to become more of a factor in the computational productivity scale. DOE

N89-10526*# Lockheed-Georgia Co., Marietta.
HARDWARE FAULT INSERTION AND INSTRUMENTATION SYSTEM: EXPERIMENTATION AND RESULTS
J. W. Benson, D. B. Mulcare, and W. E. Larson Mar. 1987 80 p Prepared for FAA, Atlantic City, N.J.
(Contract NAS2-11853)
(NASA-CR-182746; NAS 1.26:182746; AD-A189863; DOT/FAA/CT-86/34) Avail: NTIS HC A05/MF A01 CSCL 01D

This report describes the motivation, conduct, and analysis of some 2500 low-level hardware fault cases applied in automated testing at the NASA Ames Reconfigurable Digital Flight Control System (RDFCS) Facility. Fault detection was correlated with hardware and software fault monitoring, and in limited cases, with sensitivity to flight program execution modes. Results obtained have been statistically assessed to ascertain system-level reliability implications based on a model that is described herein. The overall methodology/facility itself has been critiqued and found to constitute a promising enhancement to current practice. GRA

N89-10096*# National Aeronautics and Space Administration. Ames Research Center, Moffett Field, Calif.
ADVANCED DATA MANAGEMENT DESIGN FOR AUTONOMOUS TELEROBOTIC SYSTEMS IN SPACE USING SPACEBORNE SYMBOLIC PROCESSORS
Andre Goforth *In* NASA, Goddard Space Flight Center, Proceedings of 1987 Goddard Conference on Space Applications of Artificial Intelligence (AI) and Robotics 1987 19 p (For primary document see N89-10063 01-12)
Avail: NTIS HC A99/MF E03 CSCL 09B

N89-10099*# National Bureau of Standards, Gaithersburg, Md. Robot Systems Div.
NASREN: STANDARD REFERENCE MODEL FOR TELEROBOT CONTROL
J. S. Albus, R. Lumia, and H. McCain *In* NASA, Goddard Space Flight Center, Proceedings of 1987 Goddard Conference on Space Applications of Artificial Intelligence (AI) and Robotics 1987 19 p (For primary document see N89-10063 01-12)
Avail: NTIS HC A99/MF E03 CSCL 09B

N89-10103*# National Aeronautics and Space Administration. John F. Kennedy Space Center, Cocoa Beach, Fla.
COMPUTER HARDWARE AND SOFTWARE FOR ROBOTIC CONTROL
Virgil Leon Davis *In* NASA, Goddard Space Flight Center, Proceedings of 1987 Goddard Conference on Space Applications of Artificial Intelligence (AI) and Robotics 1987 19 p (For primary document see N89-10063 01-12)
Avail: NTIS HC A99/MF E03 CSCL 09B

61 COMPUTER PROGRAMMING AND SOFTWARE

Includes computer programs, routines, alogorithms, and specific applications, e.g., CAD/CAM.

N89-10527# Naval Postgraduate School, Monterey, Calif.
SEGMENTATION OF NOISY IMAGES USING NONSTATIONARY MARKOV FIELDS M.S. Thesis
Kani Hacipasaoglu Dec. 1987 69 p
(AD-A195229) Avail: NTIS HC A04/MF A01 CSCL 12D

The purpose of this thesis is to develop an algorithm for segmenting images corrupted by a high level of noise with different characteristics. In particular the images considered are composed of several regions describing different objects and background. The algorithm described is based on a Markov Random Field model of the image and uses Kalman Filtering techniques and Dynamic Programming in order to smooth within the regions. The theoretical background for one dimensional and two dimensional data which have different characteristics and simulation results are presented, with examples of synthetic data and underwater images. GRA

N89-10528 Illinois Univ., Urbana-Champaign.
AN EXPERT SYSTEM FOR VLSI LAYOUT Ph.D. Thesis
Youn-Long Steve Lin 1987 133 p
Avail: Univ. Microfilms Order No. DA8803119

The problem of automatic layout generation for the random logic modules in a VLSI chip is addressed. A new top-down methodology that eliminates the weakness of a standard cell layout system is proposed. This methodology decomposes the module layout problem into a smaller leaf-cell layout problem and designs the leaf-cell exactly according to their environmental needs. The previous approaches to solving this problem was surveyed. The overview of LES, which implements this methodology is presented. The analysis subtask is described, which extracts some useful information from the input decription. The placement subtask is describe. The heuristics is able to produce a better initial placement compared with a random initial placement. The characterization subtasks are presented, which determines the leaf-cell specifications. A flexible cell generator is described, which is used as a replacement for the cell library. An optimizer is also described that improves LES's layout quality at the symbolic level. A set of benchmarks were collected to test out layout methodology. LES's results were compared with three standard cell system with different processing technologies. Dissert. Abstr.

N89-10529# Vrije Universiteit, Amsterdam (Netherlands). Subfaculteit Wiskunde en Informatica.
ORCA: A LANGUAGE FOR DISTRIBUTED OBJECT-BASED PROGRAMMING
Henri E. Bal and Andrew S. Tanenbaum Dec. 1987 15 p Sponsored in part by the Netherlands Organization for the Advancement of Pure Research, Amsterdam
(PB88-208533; IR-140) Avail: NTIS HC A03/MF A01 CSCL 09B

Although dozens of programming languages for distributed systems exist, only few of them are intended for general distribution applications programming. Most languages are strongly oriented toward systems programming and present a relatively low-level programming model, typically based on message passing. A much simpler model of shared objects is presented which extends the abstract data type model to support distributed programming. The model essentially provides shared address space semantics, rather than message-passing semantics, without requiring physical shared memory to be present in the target system. A new programming language, Orca, based on shared objects is also proposed. GRA

N89-10530# Instituto de Pesquisas Espaciais, Sao Jose dos Campos (Brazil).
SATELLITE IMAGE REGISTRATION THROUGH STRUCTURAL MATCHING

Leonardo SantAnnaBins and Flavio Roberto DiasVelasco May 1988 9 p Presented at the 16th Congress of International Society for Photogrammetry and Remote Sensing, Kyoto, Japan, 1-10 Jul. 1988 Submitted for publication
(INPE-4563-PRE/1304) Avail: NTIS HC A02/MF A01

A method is proposed for registration of satellite images based on the matching of their high-level symbolic description. The method consists of the following steps. First the images are segmented and the objects extracted are represented using a set of shape and grey-level descriptors. For each image, the spatial relations between the objects is computed and a description in the form of a directed graph is obtained. Finally the best match between the structures is computed using relaxation techniques. The advantages of the method are that it can be made insensitive to a large class of geometric and radiometric transformations. Through a proper choice of attribute descriptors and spatial relations, a matching can be found even in the presence of geometric distortions like scaling, rotation, and others. Radiometric distortions can also be handled in a similar way so it can be used to match images of very different natures such as images obtained with different sensors or even to match satellite images and maps. The method is illustrated with several examples using satellite images and images and maps. Author

N89-10531*# Colorado Univ., Boulder. Computer Systems Design Group.
MULTIPROGRAMMING AND THE PERFORMANCE OF PARALLEL PROGRAMS Interim Report
Muhammad S. Benten and Harry F. Jordan Jan. 1988 14 p
(Contract NAG1-640; N00014-86-K-0204)
(NASA-CR-183238; NAS 1.26:183238; AD-A193464; CSDG-88-2; ECE-TR-88-1-2) Avail: NTIS HC A03/MF A01 CSCL 09B

Tight synchronization in parallel programs executed on multiprogrammed multiprocessors may result in catastrophic performance losses as a result of the absence of swapped out processes. Our work introduces a programming methodology that utilizes computational synchronization and avoids tight control flow synchronization in parallel programs. In this methodology, each phase of the computation is assigned a stutus that can be ready, blocked or completed, and tasks in each computational phase are self-scheduled to ensure computational progress by the available executing processes. Results obtained indicate that this methodology avoids the catastrophic performance losses resulting from the swapping of processes in multiprogrammed multiprocessors. Author

N89-10532# Technische Hogeschool, Delft (Netherlands). Dept. of Industrial Design Engineering.
TOPOLOGICAL ATTRIBUTES FOR STEP CURVE AND SURFACE ENTITIES
J. S. M. Vergeest 2 Feb. 1987 20 p
(PB88-209630; MEMO-K145) Avail: NTIS HC A03/MF A01 CSCL 09B

The advantages and the need of including topological attributes in the definition of some curve and surface entities is emphasized. It is advertised that wireframe and surface models for STEP are constructed in a way strictly similar to the solid boundary definition, whichever STEP B-rep is going to be selected. Curve and surface entities are listed insofar as they are alternative with respect to the CAD*I proposal. Author

N89-10533# Los Alamos National Lab., N. Mex. Center for National Security Studies.
SUPERCOMPUTING: AN INDISPENSABLE COMPONENT OF APPLIED RESEARCH
W. F. Miller Jul. 1988 9 p
(Contract W-7405-eng-36)
(DE88-015363; LA-11392-MS) Avail: NTIS HC A02/MF A01

Computational science's part in scientific inquiry is discussed as well as developments in several aspects of scientific supercomputing. Also discussed are supercomputer applications and challenges in the future. DOE

N89-10534*# College of William and Mary, Williamsburg, Va. Dept. of Computer Science.
INFECTION AND PROPAGATION ANALYSIS: A FAULT-BASED APPROACH TO ESTIMATING SOFTWARE RELIABILITY
Larry J. Morell and Jeffrey M. Voas 1988 15 p
(Grant NAG1-824)
(NASA-CR-183276; NAS 1.26:183276; WM-88-2) Avail: NTIS HC A03/MF A01 CSCL 09B

A structure-based approach to analyzing software is presented which focuses on the impact faults have on reliability. To contribute to the failure rate of a program, a fault must be reached, it must adversely affect the succeeding data state, and that effect must persist to the output. The probability that a fault will infect its successor state is an infection rate. The probability an infected state will persist to output is called a propagation rate. Empirical methods are described for estimating the infection and propagation rate for each location in the program. These rates are then used to analyze testing complexity, the number of remaining faults, reliability, and confidence in reliability methods. Author

N89-10535# Argonne National Lab., Ill. Mathematics and Computer Science Div.
TOOLS TO AID IN THE ANALYSIS OF MEMORY ACCESS PATTERNS FOR FORTRAN PROGRAMS LAPACK Working Note No. 6
O. Brewer, J. Dongarra, and D. Sorensen Jun. 1988 16 p
(Contract W-31109-eng-38)
(DE88-013609; ANL/MCS-TM-120) Avail: NTIS HC A03/MF A01

The goals of this work is to assist in formulating correct algorithms for high-performance computers and to aid as much as possible the process of translating an algorithm into an efficient implementation on a specific machine. Over the past five years we have developed approaches in the design of certain numerical algorithms that allow both efficient and portability. Our current efforts emphasize three areas: environments for algorithm development, parallel programming methodologies, and advanced algorithm development. DOE

N89-10536# Rome Air Development Center, Griffiss AFB, N.Y.
SECOND ANNUAL KNOWLEDGE-BASED SOFTWARE ASSISTANT CONFERENCE
Kevin M. Benner, ed. Jan. 1988 306 p Conference held at Griffiss AFB, N.Y., 18-20 Aug. 1987
(AF Proj. 5581)
(AD-A189819; RADC-TR-87-243) Avail: NTIS HC A14/MF A01 CSCL 12E

The proceedings of the 2nd Annual Knowledge-Based Software Assistant Conference, held 18 to 20 August 1987 are given. Overviews are given in the areas of requirements and specifications. Planning, software design, technology transfer, performance estimation, knowledge integration and user interfaces are among the topics covered. For individual titles, see N89-10537 through N89-10555.

N89-10537# Honeywell Systems and Research Center, Minneapolis, Minn.
A COMMON FRAMEWORK FOR KNOWLEDGE-BASED PROGRAMMING
Steve Huseth and Tim King *In* RADC, Second Annual Knowledge-Based Software Assistant Conference Jan. 1988 p 25-37 (For primary document see N89-10536 01-61)
(Contract F30602-86-C-0074)
Avail: NTIS HC A14/MF A01 CSCL 12E

The requirements and motivations of a common knowledge-based software assistant (KBSA) framework which will provide services not available in the tool frameworks are described. An initial architecture for such a system is described, as is its implementation. The construction of advanced software engineering frameworks will borrow heavily from many other developing technologies of large data bases, distributed computing systems, programming languages, and natural language understanding. Author

N89-10538# Sanders Associates, Inc., Nashua, N. H.
AN OVERVIEW OF THE KNOWLEDGE-BASED REQUIREMENTS ASSISTANT
David R. Harris *In* RADC, Second Annual Knowledge-Based Software Assistant Conference Jan. 1988 p 38-47 (For primary document see N89-10536 01-61)
(Contract F30602-85-C-0267)
Avail: NTIS HC A14/MF A01 CSCL 12E

The Knowledge-Based Requirements Assistant (KBRA) is an intelligent assistant computer program designed to actively assist engineers in the requirements acquisition and analysis of complex computer systems. The KBRA addresses the Knowledge-Based Software Assistant (KBSA) requirements facet goals. These goals include formalization, knowledge-based editing and management of requirements, requirements review, and requirements testing. Here, the KBRA problem definition is indicated, the KBRA system is described, the knowledge representation approach is summarized, and the relationship of KBRA to related research is pointed out. Author

N89-10539# University of Southern California, Marina del Rey. Information Sciences Inst.
OVERVIEW OF THE KNOWLEDGE-BASED SPECIFICATION ASSISTANT
W. Lewis Johnson *In* RADC, Second Annual Knowledge-Based Software Assistant Conference Jan. 1988 p 48-79 (For primary document see N89-10536 01-61)
Avail: NTIS HC A14/MF A01 CSCL 12E

In order for specifications to be used effectively in software development, tools are needed that will do the following: (1) assist in developing the specification; (2) analyze and evaluate the specification; and (3) explain the specification. The Knowledge-Based Specification Assistant (KBSA) is designed to provide assistance along these three dimensions. This system aids people in specifying programs by allowing them to record their initial views of system requirements and to gradually transform them into complete specifications. Symbolic evaluation and simulation tools are provided so that unexpected implications of statements in the specification can be detected. Explanation facilities do retrievals from the specification database in response to user queries and generate natural language answers and summaries in response to the queries. An overview of each of these facilities is given. Author

N89-10540# Kestrel Inst., Palo Alto, Calif.
PERFORMANCE ESTIMATION FOR A KNOWLEDGE-BASED SOFTWARE ASSISTANT
Allen Goldberg and Douglas R. Smith *In* RADC, Second Annual Knowledge-Based Software Assistant Conference Jan. 1988 p 80-92 (For primary document see N89-10536 01-61)
(Contract F30602-86-C-0026)
Avail: NTIS HC A14/MF A01 CSCL 12E

The long-term goal of a Performance Estimator Assistant (PEA) is to aid in the creation and maintenance of programs that meet their performance requirements or are generally efficient in their use of computational resources. The principal function of the PEA is to guide implementation decisions that will effect the ultimate performance of the system by generating and reasoning about performance estimates for expressions ranging from very high-level specifications to low-level code. The short-term goals for PEA capabilities are identified as symbolic evaluation, data structure analysis and advice, and subroutine and module decomposition advice. Author

N89-10541# Boeing Computer Services Co., Seattle, Wash.
TECHNOLOGY TRANSFER AND THE KNOWLEDGE-BASED SOFTWARE ASSISTANT
R. W. Lawler *In* RADC, Second Annual Knowledge-Based Software Assistant Conference Jan. 1988 p 100-105 (For primary document see N89-10536 01-61)
Avail: NTIS HC A14/MF A01 CSCL 12E

A model for management of technology transfer relative to the Knowledge-Based Software Assistant (KBSA) is given in graphic form. Another figure represents an instance of this model in action for an application of artificial intelligence to maintenance and diagnosis. Author

N89-10542# Software Productivity Consortium, Reston, Va.
SELECTION OF INVESTMENT STRATEGIES WHICH ARE OPTIMAL FOR THE IMPLEMENTATION OF SOFTWARE SUPPORT ENVIRONMENTS Abstract Only
Kenneth E. Nidiffer *In* RADC, Second Annual Knowledge-Based Software Assistant Conference Jan. 1988 p 106-107 (For primary document see N89-10536 01-61)
Avail: NTIS HC A14/MF A01 CSCL 12E

The objective of the research was to further the depth of understanding of the variables that impact the problem solving process leading to the investment strategy decision. An investment strategy decision is made for almost every defense system acquired by the Department of Defense (DOD) with respect to the identification of what software support environment will be used in the development and support of the mission code associated with the defense system and what level of standardization will be employed by DOD with respect to the selected software support environment. This research was directed at answering two questions: what is the proper investment strategy decision process, and what is the proper investment strategy decision. The research answered these questions by developing an econometric model based on insights gained about the variables that impact the investment strategy decision process and by designing, building, verifying, evaluating and validating a program manager's decision support system. Author

N89-10543# Honeywell Systems and Research Center, Minneapolis, Minn.
KBSA COMMON FRAMEWORK IMPLEMENTATION
Aaron Larson and Steve Huseth *In* RADC, Second Annual Knowledge-Based Software Assistant Conference Jan. 1988 p 108-116 (For primary document see N89-10536 01-61)
Avail: NTIS HC A14/MF A01 CSCL 12E

The implementation details of the Knowledge-Based Software Assistant (KBSA) Common Framework are described. The system forms a distributed knowledge base for knowledge-base programming tools and executes on multiple Symbolics workstations. Within the system, researchers attemped to merge an object-oriented programming environment supporting the representation of project data with a logic programming environment to support data consistency and control of the programming process. The internal organization of the system and some implementation lessons are described. Author

N89-10544# Sanders Associates, Inc., Nashua, N. H.
WHERE'S THE INTELLIGENCE IN THE INTELLIGENT ASSISTANT REQUIREMENTS ANALYSIS: INFERENCE PROCESSES IN THE KBRA
Andrew J. Czuchry, Jr. *In* RADC, Second Annual Knowledge-Based Software Assistant Conference Jan. 1988 p 117-137 (For primary document see N89-10536 01-61)
(Contract F30602-85-C-0267)
Avail: NTIS HC A14/MF A01 CSCL 12E

The intent is to explain how a variety of artificial intelligence (AI) inference techniques have been used in the context of the Knowledge-Based Requirements Assistant (KBRA) and the resulting intelligent behavior of the KBRA system. The inferences processes used and how they support requirement characterization are discussed. Additionally, interesting examples of the manner in which inferences support the various characteristics of requirements characterization are presented. Author

N89-10545# University of Southern California, Marina del Rey. Information Sciences Inst.
TURNING IDEAS INTO SPECIFICATIONS
W. Lewis Johnson *In* RADC, Second Annual Knowledge-Based Software Assistant Conference Jan. 1988 p 138-153 (For primary document see N89-10536 01-61)

(Contract F30602-85-C-0221)
Avail: NTIS HC A14/MF A01 CSCL 12E

In the Knowledge-Based Specification Assistant project, the focus is on the steps that specifiers go through in developing detailed specifications from initial ideas of what the specification is supposed to do. The Specification Assistant aids in developing, evaluating, and explaining specifications. Here, the development aids in the Specification Assistant are discussed, and it is shown how they help in the transformation of requirements into specifications. Author

N89-10546# Defense Advanced Research Projects Agency, Arlington, Va.
SOFTWARE DESIGN RESEARCH AT DARPA
W. Scherlis *In* RADC, Second Annual Knowledge-Based Software Assistant Conference Jan. 1988 p 154-162 (For primary document see N89-10536 01-61)
Avail: NTIS HC A14/MF A01 CSCL 12E

Viewgraphs are given that present information on the technology focus, program goals, and funding for software systems design and life cycle management. Information is given on parallel computer architecture and management and transition strategy. R.J.F.

N89-10547# Massachusetts Univ., Amherst. Dept. of Computer and Information Science.
PLANS AND META-PLANS IN AN INTELLIGENT ASSISTANT FOR THE PROCESS OF PROGRAMMING
Karen E. Huff and Victor R. Lesser *In* RADC, Second Annual Knowledge-Based Software Assistant Conference Jan. 1988 p 163-184 (For primary document see N89-10536 01-61)
Avail: NTIS HC A14/MF A01 CSCL 12E

An architecture for providing intelligent assistance to the programmer carrying out the process of programming is described. The architecture, based on an artificial intelligence (AI) planning paradigm, can provide both passive and active assistance. Passive assistance, accomplished by plan recognition, is used to detect and avert process errors. Active assistance, accomplished by planning, is used to automate the programming process. A key issue in achieving appropriate levels of assistance is the ability to capture complex domain knowledge in a planning formalism. Several problems in traditional hierarchical formalisms are illustrated, and a solution based on the use of meta-plans that dynamically transform plans is proposed. Author

N89-10548# Kestrel Inst., Palo Alto, Calif.
TECHNICAL ISSUES FOR PERFORMANCE ESTIMATION
Allen Goldberg *In* RADC, Second Annual Knowledge-Based Software Assistant Conference Jan. 1988 p 185-195 (For primary document see N89-10536 01-61)
(Contract F30602-86-C-0026)
Avail: NTIS HC A14/MF A01 CSCL 12E

The plans and progress toward the construction of a prototype Performance Estimation Assistant (PEA) are discussed. Approaches to performance estimation, the generator that the PEA will use, the specification language, data types, refinement rules, the performance estimator and implementation status are discussed. Author

N89-10549# Honeywell Systems and Research Center, Minneapolis, Minn.
DESIGNING AN EFFECTIVE USER INTERFACE FOR A KNOWLEDGE-BASED DEVELOPMENT ENVIRONMENT
Tim King *In* RADC, Second Annual Knowlege-Based Software Assistant Conference Jan. 1988 p 196-206 (For primary document see N89-10536 01-61)
Avail: NTIS HC A14/MF A01 CSCL 12E

One of the chief factors in the success of transferring Knowledge-Based Software Assistant (KBSA) technology to industry will be the ability of users to interact efficiently and effectively with the KBSA system. As a result, the KBSA user interface must be carefully designed to provide a wide variety of users with easy access to a wide variety of information. Described here are design issues of an effective interface, the interface's required functionality, and possible approaches to providing that functionality. Author

N89-10550# IBM Federal Systems Div., Gaithersburg, Md. Artificial Intelligence Center.
KNOWLEDGE BASED TOOLS FOR KNOWLEDGE-BASED SYSTEMS
Lance A. Miller *In* RADC, Second Annual Knowledge-Based Software Assistant Conference Jan. 1988 p 207-219 (For primary document see N89-10536 01-61)
Avail: NTIS HC A14/MF A01 CSCL 12E

Three aspects of an approach to remedying problems with Artificial Intelligence (AI) systems are overviewed. A proposed life cycle for Knowledge-Based Systems (KBSs); techniques for knowledge-base verification; and representation and traceability of requirements are discussed. Author

N89-10551# Boeing Computer Services Co., Seattle, Wash. Advanced Technology Center for Computer Sciences.
THE KNOWLEDGE INTEGRATION TOOL: KNOWLEDGE INTERFACE (A KNOWLEDGE BASED SYSTEM DEVELOPMENT ENVIRONMENT)
Philip H. Newcomb *In* RADC, Second Annual Knowledge-Based Software Assistant Conference Jan. 1988 p 220-256 (For primary document see N89-10536 01-61)
Avail: NTIS HC A14/MF A01 CSCL 12E

The Knowledge Integration Tool (KIT) is a knowledge based environment for developing and using knowledge based systems. The KIT facilitates rapid construction of programming environments and end-user application software. Using the KIT, conceptional modes can be created, composed of conceptional primatives for agents, activities, causality, goals, methodologies, objects, resources, states and time. The KIT employs user profiles to construct highly specialized environments tailored to focus the user's attention upon just the knowledge and operations pertinent to his activities. The KIT possesses the rudiments of an architectural infrastructure which supports development and utilization of knowledge based systems and knowledge based environments within the knowledge based corporation. Author

N89-10552# Rome Air Development Center, Griffiss AFB, N.Y. Command and Control Software Technology Div.
PROJECT MANAGEMENT ASSISTANT: WHAT HAVE WE LEARNED
Kevin M. Benner and Louis J. Hoebel *In its* Second Annual Knowledge-Based Software Assistant Conference Jan. 1988 p 257-261 (For primary document see N89-10536 01-61)
Avail: NTIS HC A14/MF A01 CSCL 12E

The purpose is to explain what has been learned from the Product Management Assistant (PMA) facet of a Knowledge-Based Software Assistant (KBSA). A description of PMA and the supporting technologies is given, followed by an analysis of what was learned from the PMA effort both in terms of life cycle activities and supporting activities. Author

N89-10553*# Inference Corp., Los Angeles, Calif.
SIMPLIFYING THE CONSTRUCTION OF DOMAIN-SPECIFIC AUTOMATIC PROGRAMMING SYSTEMS: THE NASA AUTOMATED SOFTWARE DEVELOPMENT WORKSTATION PROJECT
Bradley P. Allen and Peter L. Holtzman *In* RADC, Second Annual Knowledge-Based Software Assistant Conference Jan. 1988 p 262-271 Previously announced as N88-17212 (For primary document see N89-10536 01-61)
(Contract NAS9-17766)
Avail: NTIS HC A14/MF A01 CSCL 09B

An overview is presented of the Automated Software Development Workstation Project, an effort to explore knowledge-based approaches to increasing software productivity. The project focuses on applying the concept of domain specific automatic programming systems (D-SAPSs) to application domains at NASA's Johnson Space Flight Center. A version of a D-SAPS

developed in Phase 1 of the project for the domain of space station momentum management is described. How problems encountered during its implementation led researchers to concentrate on simplifying the process of building and extending such systems is discussed. Researchers propose to do this by attacking three observed bottlenecks in the D-SAPS development process through the increased automation of the acquisition of programming knowledge and the use of an object oriented development methodology at all stages of the program design. How these ideas are being implemented in the Bauhaus, a prototype workstation for D-SAPS development is discussed.
Author

N89-10554# Mitre Corp., Bedford, Mass.
ASDL: AN INTELLIGENT ACQUISITION SUPPORT TOOL
Richard Adler and Terry Gleason *In* RADC, Second Annual Knowledge-Based Software Assistant Conference Jan. 1988 p 272-290 (For primary document see N89-10536 01-61)
Avail: NTIS HC A14/MF A01 CSCL 12E

The Automatic System Development Library (ASDL), an experimental prototype for an artificial intelligence (AI) based acquisition support environment is described. Acquisition analysts and systems engineers will employ ASDL to represent and maintain functional requirements and other aspects of system specifications in the form of symbolic models. These symbolic system descriptions are constructed by copying and adapting (historical) models of previous systems or elements from a library of generic function, component, and system templates. Analysis capabilities are under development to assist users in evaluating the economic and technical feasibility of system models. Specifically, facilities are being implemented to represent and dynamically simulate behavioral aspects of systems and to compute system sizing estimates.
Author

N89-10555# Massachusetts Univ., Amherst. Dept. of Computer and Information Science.
PLAN RECOGNITION IN GRAPPLE: AN INTELLIGENT ASSISTANT FOR THE PROCESS OF PROGRAMMING Abstract Only
Karen E. Huff and Victor R. Lesser *In* RADC, Second Annual Knowledge-Based Software Assistant Conference Jan. 1988 p 291 (For primary document see N89-10536 01-61)
Avail: NTIS HC A14/MF A01 CSCL 12E

A prototype system, called GRAPPLE, that provides intelligent assistance to the programmer carrying out the process of programming is discussed. The architecture, based on an artificial intelligence (AI) paradigm, can provide both passive and active assistance. Passive assistance, accomplished by plan recognition, is used to detect and avert process errors. Active assistance, accomplished by planning, is used to automate the programming process. The plan recognition facilities and the programmer assistance based upon plan recognition in the current prototype running on a Texas Instrument Explorer are discussed.
Author

N89-10556# Pacific Northwest Labs., Richland, Wash.
STATISTICAL EVALUATION OF PACSTAT RANDOM NUMBER GENERATION CAPABILITIES
G. F. Piepel, M. R. Toland, H. Harty, M. J. Budden, and C. L. Bartley May 1988 308 p
(Contract DE-AC06-76RL-01830)
(DE88-012754; PNL-6434) Avail: NTIS HC A14/MF A01

This report summarizes the work performed in verifying the general purpose Monte Carlo driver-program PACSTAT. The main objective of the work was to verify the performance of PACSTAT's random number generation capabilities. Secondary objectives were to document (using controlled configuration management procedures) changes made in PACSTAT at Pacific Northwest Laboratory, and to assure that PACSTAT input and output files satisfy quality assurance traceability constraints. Upon receipt of the PRIME version of the PACSTAT code from the Basalt Waste Isolation Project, Pacific Northwest Laboratory staff converted the code to run on Digital Equipment Corporation (DEC) VAXs. The modifications to PACSTAT were implemented using the WITNESS configuration management system, with the modifications themselves intended to make the code as portable as possible. Certain modifications were made to make the PACSTAT input and output files conform to quality assurance traceability constraints.
DOE

N89-10557# Total Army Personnel Agency (Provisional), Alexandria, Va.
THE EFFECT OF A GAP NONLINEARITY ON RECURSIVE PARAMETER IDENTIFICATION ALGORITHMS Final Report
Scott E. Schaffer 9 May 1988 89 p
(AD-A196020) Avail: NTIS HC A05/MF A01 CSCL 22B

This work examines the performance of the Recursive Least Squares (RLS) Algorithm, and derivative, the Recursive Lattice Least Squares (RLLS) Algorithm in matching a linear model to a simple nonlinear system. The response of a single degree of freedom mass-spring-dashpot system to continuous forcing is simulated, and estimates for the modal parameters are obtained. Nonlinearity is introduced by allowing the restoring spring to slide without friction in a gap of specified width. Such a nonlinearity is of interest since it is a simple model of the effect of loose joints in a deployable spacecraft restoring spring to slide without friction in a gap of specified width. Such a nonlinearity is of interest since it is a simple model of the effect of loose joints in a deployable spacecraft structure. The effect of the gap size on the algorithms is studied, and the noise level and sampling rate are adjusted to see how they influence these results. The RLS Algorithm is found to be the most reliable. Finally, the RLS Algorithm is extended to include an estimate for the gap width, and good results are obtained for the noise-free case. Additional conclusions are made on how to minimize the effect of such a gap nonlinearity on the identification process.
GRA

N89-10558# Colorado Univ., Boulder. Dept. of Computer Science.
CONCURRENT ALGORITHMS FOR NUMERICAL COMPUTATION ON HYPERCUBE COMPUTER Final Report, 1 Oct. 1986 - 30 Sep. 1987
R. Schnabel 22 Feb. 1988 3 p
(Grant AF-AFOSR-0055-87; AF Proj. 2304)
(AD-A195502; AFOSR-88-0587TR) Avail: NTIS HC A02/MF A01 CSCL 12F

The purpose of this grant was to purchase a hypercube computer to support DOD-sponsored research, and other research, in parallel numerical computation. The plans that were outlined in the proposal were followed very closely. We have purchased a 32-node Intel iPSC-D5 hypercube computer with the funds from this grant, and have used the matching University contribution to support the maintenance of this computer. This computer has been used, over the past year, for research in parallel numerical computation in areas including global optimization, VLSI design, large sparse systems of linear equations, and eigenvalue problems, as well as for research in the languages for parallel computation and in the debugging and measurement of parallel programs.
GRA

N89-10559# Sandia National Labs., Albuquerque, N. Mex.
FACTORING VERY LARGE NUMBERS USING A MASSIVELY PARALLEL COMPUTER
Diane B. Holdridge and James A. Davis 1988 9 p Presented at the Computational Number Theory Conference, Brunswick, Maine, 10 Jul. 1988
(Contract DE-AC04-76DP-00789)
(DE88-014247; SAND-88-1875C; CONF-880785-1) Avail: NTIS HC A02/MF A01

This paper discusses the Quadratic Sieve algorithms of factoring large numbers on parallel processors.
DOE

N89-10560*# National Aeronautics and Space Administration. Langley Research Center, Hampton, Va.
PROGRAMMING THE NAVIER-STOKES COMPUTER: AN ABSTRACT MACHINE MODEL AND A VISUAL EDITOR Final Interim Report No. 5

David Middleton, Tom Crockett, and Sherry Tomboulian Aug. 1988 31 p
(Contract NAS1-18107)
(NASA-CR-181691; NAS 1.26:181691) Avail: NTIS HC A03/MF A01 CSCL 09B

The Navier-Stokes computer is a parallel computer designed to solve Computational Fluid Dynamics problems. Each processor contains several floating point units which can be configured under program control to implement a vector pipeline with several inputs and outputs. Since the development of an effective compiler for this computer appears to be very difficult, machine level programming seems necessary and support tools for this process have been studied. These support tools are organized into a graphical program editor. A programming process is described by which appropriate computations may be efficiently implemented on the Navier-Stokes computer. The graphical editor would support this programming process, verifying various programmer choices for correctness and deducing values such as pipeline delays and network configurations. Step by step details are provided and demonstrated with two example programs. Author

N89-10561*# College of William and Mary, Williamsburg, Va. Dept. of Computer Science.
INCREMENTAL ASSESSMENT AND IMPROVEMENT OF SOFTWARE RELIABILITY Midterm Report
Larry J. Morell 27 Sep. 1988 10 p
(Grant NAG1-824)
(NASA-CR-183275; NAS 1.26:183275) Avail: NTIS HC A02/MF A01 CSCL 09B

The objectives of this research are: (1) to investigate the relationship between program faults and program failure rates, (2) to develop a method for improved assessment of reliability based on structural characteristics of the program, and (3) to help design and implement a long-range study of faults in a realistic program. Since January, all three goals have been pursued. A model was developed for analyzing the impact a potential fault may have on a program's failure rate. Based on this model, a method is developed for estimating the number of remaining faults and resultant reliability, and for determining the confidence bounds in those estimates. One version of the software to be used in a multi-version testing experiment has also been developed. The specific activities are described as follows. Section 2 discusses the model developed for assessing software. Section 3 discusses the potential application areas of the model. Section 4 gives the current status of the Guidance Control System under development. The last section describes future plans. Details may also be found in the appendices. Author

N89-10562# Argonne National Lab., Ill. Mathematics and Computer Science Div.
CONVERGENCE PROPERTIES OF TRUST REGION METHODS FOR LINEAR AND CONVEX CONSTRAINTS
James V. Burke, Jorge J. More, and Gerardo Toraldo Apr. 1988 32 p
(Contract W-31109-eng-38)
(DE88-013608; ANL/MCS-TM-116) Avail: NTIS HC A03/MF A01

We develop a convergence theory for convex and linearly constrained trust region methods which only requires that the step between iterates produce a sufficient reduction in the trust region subproblem. Global convergence is established for a general convex minimization problem while the local analysis is for linearly constrained problems. The main local result establishes that if the sequence converges to a nondegenerate stationary point then the active constraints at the solution are identified in a finite number of iterations. As a consequence of the identification properties, we develop rate of convergence results by assuming that the step is a truncated Newton method. Our development is mainly geometrical; this approach allows the development of a convergence theory without any linear independence assumptions. DOE

N89-10563# National Aerospace Lab., Tokyo (Japan).
[GENERATION OF A GRID FOR A FINITE DIFFERENCE CALCULATION OF FLOWS AROUND AN AIRCRAFT IN CARTESIAN COORDINATES]
1987 18 p In JAPANESE; ENGLISH summary
(NAL-TR-956; ISSN-0389-4010) Avail: NTIS HC A03/MF A01

The generation of a grid for an infinite difference calculation of flows around an aircraft in Cartesian coordinates is examined. The main equations governing the generation are plane and line equations in the three-dimensional field. The external form of the aircraft is shaped from a large number of small triangular planes. The grid is formed by three groups of lines perpendicularly intersecting each other. The quantitative relations between the external form of the aircraft and points of the grid are obtained by algebraic treatment of the plane and line equations. In the same manner, views of the aircraft are drawn using these equations. Author

N89-10564*# College of William and Mary, Williamsburg, Va. Dept. of Computer Science.
THEORETICAL INSIGHTS INTO FAULT-BASED TESTING
Larry J. Morell 1988 18 p
(Grant NAG1-824)
(NASA-CR-183277; NAS 1.26:183277) Avail: NTIS HC A03/MF A01 CSCL 09B

Testing is fault-based when its goal is to demonstrate the absence of prespecified faults. This paper presents a framework that characterizes fault-based testing schemes based on how many prespecified faults are considered and on the contextual information used to deduce the absence of those faults. Established methods of fault-based testing are placed within this framework. Most methods either are limited to finite fault classes, or focus on local effects of faults rather than global effects. A new method of fault-based testing called symbolic testing is presented by which infinitely many prespecified faults can be proven to be absent from a program based on the global effect faults would have if they were present. Circumstances are discussed as to when testing with a finite test set is sufficient to prove that infinitely many prespecified faults are not present in the program. Author

N89-10565# National Aerospace Lab., Tokyo (Japan).
PROGRAMMING TECHNIQUES FOR HIGH-SPEED PROCESSING ON THE SUPERCOMPUTER FUJITSU VP-SYSTEM
Masahiro Yoshida, Kinuyo Nakamura, Keiichiro Uchida, and Yoshiyuki Tanakura 1986 78 p In JAPANESE; ENGLISH summary
(NAL-TR-915; ISSN-0389-4010) Avail: NTIS HC A05/MF A01

Various methods of effective FORTRAN programming for supercomputers are presented. These programming methods are designed to increase vectorization rates and to facilitate high-speed processing of FORTRAN programs. The methods were used to improve the following NAL application software packages: the FVMCAS program for analyzing inviscid compressible flow through three-dimensional cascades and the USTF3 program for unsteady transonic potential flow over oscillating three-dimensional wings. The vectorized codes are executed on the supercomputer FUJITSU VP-400. Computing times compared with those of the original programs show the excellent usefulness of the vectorizing methods. Author

N89-10566# Sandia National Labs., Albuquerque, N. Mex.
A LINEAR PROGRAMMING APPROACH TO MAXIMUM ENTROPY SIGNAL RESTORATION
G. A. Mastin and D. C. Ghiglia 1988 8 p Presented at the 32nd International Technical Symposium on Optical and Opto-electronic Applied Sciences and Engineering, San Diego, Calif., 14 Aug. 1988
(Contract DE-AC04-76DP-00789)
(DE88-013021; SAND-88-0371C; CONF-880887-3) Avail: NTIS HC A02/MF A01

In future computing environments where computer resources are abundant, a linear programming (LP) approach to maximum

entropy signal/image restoration could have advantages over traditional techniques. A revised simplex LP algorithm with inequality constraints is presented. Dantzig's bounded-variable method is used to express the maximum entropy restoration problem as a LP problem. This is done by approximating the nonlinear objective function with piecewise linear segments, then bounding the variables as a function of the number of segments used. Linear inequality constraints may be used to assure a basic feasible solution. Experimental results with 512-point signals are presented. These include restorations of noisy signals. Problems with as many as 513 equations and 6144 unknowns are demonstrated. The complexity of the LP restoration approach is briefly addressed.
DOE

N89-10049# Raytheon Co., Bedford, Mass. Missile Systems Div.
COMPARISON OF STATISTICAL DIGITAL SIMULATION METHODS
Paul Zarchan *In* AGARD, Guidance and Control Systems Simulation and Validation Techniques Jul. 1988 16 p (For primary document see N89-10048 01-08)
Copyright Avail: NTIS HC A07/MF A01

N89-10050# Dynetics, Inc., Huntsville, Ala.
A GENERIC SEEKER SIMULATION FOR THE EVALUATION OF ACTIVE RF GUIDANCE SYSTEMS
Frank T. Campos *In* AGARD, Guidance and Control Systems Simulation and Validation Techniques Jul. 1988 9 p (For primary document see N89-10048 01-08)
(Contract F08635-83-C-0123)
Copyright Avail: NTIS HC A07/MF A01

N89-10051# Magnavox Electronic Systems Co., Fort Wayne, Ind. Control Systems Operation.
DIGITAL SIMULATION TECHNIQUES FOR END GAME PHENOMENA
Martin E. Tanenhaus and Duane J. Cart *In* AGARD, Guidance and Control Systems Simulation and Validation Techniques Jul. 1988 37 p (For primary document see N89-10048 01-08)
Copyright Avail: NTIS HC A07/MF A01

N89-10052# Raytheon Co., Bedford, Mass.
DESIGN CRITERIA FOR HARDWARE-IN-THE-LOOP SIMULATION FACILITIES
S. J. Powers and M. E. Sisle *In* AGARD, Guidance and Control Systems Simulation and Validation Techniques Jul. 1988 10 p (For primary document see N89-10048 01-08)
Copyright Avail: NTIS HC A07/MF A01

N89-10083*# Computer Sciences Corp., Baltimore, Md. Astronomy Programs.
A NATURAL LANGUAGE QUERY SYSTEM FOR HUBBLE SPACE TELESCOPE PROPOSAL SELECTION
Thomas Hornick, William Cohen, and Glenn Miller *In* NASA, Goddard Space Flight Center, Proceedings of 1987 Goddard Conference on SpaceApplications o f Artificial Intelligence (AI) and Robotics 1987 17 p Prepared in cooperation with Space Telescope Science Inst., Baltimore, Md. (For primary document see N89-10063 01-12)
Avail: NTIS HC A99/MF E03 CSCL 09B

N89-10085*# Ford Aerospace and Communications Corp., College Park, Md.
A LISP-Ada CONNECTION
Allan Jaworski, David Lavallee, and David Zoch *In* NASA, Goddard Space Flight Center, Proceedings of 1987 Goddard Conference on Space Applications of Artificial Intelligence (AI) and Robotics 1987 14 p (For primary document see N89-10063 01-12)
Avail: NTIS HC A99/MF E03 CSCL 09B

N89-10086*# Computer Sciences Corp., Baltimore, Md. Astronomy Programs.
EXPERT SYSTEMS BUILT BY THE EXPERT: AN EVALUATION OF OPS5
Robert Jackson *In* NASA, Goddard Space Flight Center, Proceedings of 1987 Goddard Conference on Space Applications of Artificial Intelligence (AI) and Robotics 1987 14 p Prepared in cooperation with Space Telescope Science Inst., Baltimore, Md. (For primary document see N89-10063 01-12)
Avail: NTIS HC A99/MF E03 CSCL 09B

N89-10202*# Jet Propulsion Lab., California Inst. of Tech., Pasadena.
NODE SYNCHRONIZATION OF VITERBI DECODERS USING STATE METRICS
U. Cheng *In its* The Telecommunications and Data Acquisition Report 15 Aug. 1988 p 201-209 (For primary document see N89-10186 01-32)
Avail: NTIS HC A14/MF A01 CSCL 09B

N89-10203*# Jet Propulsion Lab., California Inst. of Tech., Pasadena.
A SOFTWARE SIMULATION STUDY OF THE LONG CONSTRAINT LENGTH VLSI VITERBI DECODER
S. Arnold and F. Pollara *In its* The Telecommunications and Data Acquisition Report 15 Aug. 1988 p 210-221 (For primary document see N89-10186 01-32)
Avail: NTIS HC A14/MF A01 CSCL 09B

N89-10208*# Jet Propulsion Lab., California Inst. of Tech., Pasadena.
PHOBOS LANDER CODING SYSTEM: SOFTWARE AND ANALYSIS
K.-M. Cheung and F. Pollara *In its* The Telecommunications and Data Acquisition Report 15 Aug. 1988 p 274-286 (For primary document see N89-10186 01-32)
Avail: NTIS HC A14/MF A01 CSCL 09B

62 COMPUTER SYSTEMS

Includes computer networks and special application computer systems.

N89-10567 Illinois Univ., Urbana-Champaign.
INTEGRATED SWITCHING NETWORKS: A PERFORMANCE STUDY Ph.D. Thesis
Chong Kwon Kim 1987 142 p
Avail: Univ. Microfilms Order No. DA8803086

Voice, data and video traffic share the same transmission and switching facilities in integrated switching networks. Because resources are dynamically shared, integrated switching can support heterogeneous traffic cost effectively. In addition, integrated switching is flexible and access transparent. However, integrated networks have more dynamic traffic fluctuations than packet or circuit switching networks. Hence, it is necessary to use efficient routing algorithms to fully achieve the potential advantage of integrated switching. Five existing packet routing algorithms were selected for the performance study: NRCC, random, shortest queue, delta, and priority queue routing. In addition, a new hybrid technique called hybrid weighted routing was developed and included. In hybrid weighted routing, local nodes adjust the credit given to global and local information. Results from packet switching network simulation and integrated network simulation indicated the superiority of hybrid weighted routing. Especially, in a movable boundary integrated network, hybrid weighted routing supported a larger fraction of traffic, while still maintaining smaller packet delay. Dissert. Abstr.

N89-10568# Honeywell, Inc., Golden Valley, Minn. Corporate Systems Development Div.
VERY LARGE PARALLEL DATA FLOW Final Report, Dec. 1985 - Dec. 1987
R. Ramnarayan, C. Baker, H. Lu, K. Mikkilineni, and J. Richardson Mar. 1988 287 p
(Contract F30602-85-C-0215)
(AD-A196205; RADC-TR-88-42) Avail: NTIS HC A13/MF A01 CSCL 12F

This report describes a three-phase effort to investigate the use of parallel processing in very large data/knowledge database management systems (D/KBMS) as a means of attaining required performance levels. Phase one involved investigation of parallel processing techniques for inference processing, parallel processing techniques for very large database management and fault tolerant techniques for very large databases. During phase two, the results of investigation studies were combined to develop a methodology for specifying high performance, highly available D/KBMS computer architecture architectures for very large data/knowledge base (D/KB) environments. During phase three, a data/knowledge base management testbed was designed and implemented to serve both as a demonstration and performance measurement and evaluation platform. The testbed was used to perform several experiments designed to quantitatively measure D/KBMS performance and understand D/KBMS performance sensitivity and behavior with respect to various system paramounts. Several key results and conclusions have been identified from this work and directions for future work have been identified. GRA

N89-10569# Massachusetts Inst. of Tech., Cambridge. Microsystems Research Center.

SPACE-EFFICIENT QUEUE MANAGEMENT USING FIXED-CONNECTION NETWORKS

Tom Leighton and Eric Schwabe Nov. 1987 12 p
(Contract N00014-80-C-0622; AF-AFOSR-0076-86)
(AD-A195167; VLSI-Memo-87-426) Avail: NTIS HC A03/MF A01 CSCL 12D

On of the main difficulties in designing algorithms for large scale parallel machines is making sure that the capacities of the local memories are not exceeded. This paper presents a general scheme for dynamically reorganizing memory so that local memory constraints are never exceeded provided that global memory constraints are not exceeded. The scheme is simple, real-time, space-efficient, deterministic and transparent to the programmer. It requires only that the total hardware used (i.e., wires and total memory) exceed the number of local memories by a logarithmic factor. In return, the scheme guarantees an arbitrarily high percentage utilization of the total memory, independent of whatever local demands for memory arise. The authors analyze the behavior of our scheme in worst-case and average-case settings, and show that it is optimal in many respects, even when compared to randomized algorithms. GRA

N89-10570# Air Force Inst. of Tech., Wright-Patterson AFB, Ohio.

A META-PROTOCOL ARCHITECTURE FOR CONNECTING COMPUTER NETWORKS M.S. Thesis - Brigham Young Univ., Provo, Utah

Joel Brad Lindsey Dec. 1987 89 p
(AD-A196319; AFIT/CI/NR-88-135) Avail: NTIS HC A05/MF A01 CSCL 12E

Accompanying the proliferation of computer networks has been a movement to connect them into cooperating internets. However, when attempting to do so, the different protocols used to satisfy these once isolated networks are found to incompatible. Due to its reliable nature, the transport layer from ISO's OSI Reference Model is chosen as the point of attachment for subnets and internet gateways. In this role, it is expected to supply traditional transport and inherited services. A meta-protocol architecture is proposed to relay these services from one subnet to the next, until internet messages arrive at their destination. The architecture is based upon each subnet providing two conversion routines -- one from the subnet protocol to the meta- protocol, the other, back to its own protocol. A simulated internet, demonstrating the capabilities of the meta-protocol approach, is described. GRA

N89-10571# Stanford Univ., Calif. Systems Optimization Lab.

PARALLEL PROCESSORS FOR PLANNING UNDER UNCERTAINTY

George B. Dantzig and Peter W. Glynn Jun. 1988 19 p Sponsored in cooperation with the Center for Economic Policy Research at Stanford Univ.
(Contracts DE-FG03-87ER-25028; N00014-85-K-0343; NSF DMS-84-20623; NSF ECS-86-17905; NSF SES-85-18662; EPRI-RP2940-1)
(DE88-016184; SOL-88-8) Avail: NTIS HC A03/MF A01

In this paper we describe joint research under way by Mordecai Avriel, Robert Entriken, and the authors. Our goal is to demonstrate, for an important class of multistage stochastic models, that a variety of techniques for solving large-scale linear programs can be effectively mixed to attack this fundamental problem. The ideas involve nested primal and dual decomposition, combined with Monte Carol simulation, high speed importance sampling, and quadrature methods for numerical integration, together with the use parallel processors. DOE

N89-10572# Massachusetts Inst. of Tech., Cambridge. Microsystems Research Center.

OPTIMAL SIMULATIONS BY BUTTERFLY NETWORKS: EXTENDED ABSTRACT

Sandeep N. Bhatt, Fan R. Chung, Jia-Wei Hong, F. T. Leighton, and Arnold Rosenberg (Massachusetts Univ., Amherst.) Nov. 1987 13 p Sponsored in part by NSF, Washington, D.C., American Telephone and Telegraphy Co. and IBM Corp. Prepared in cooperation with New York Univ., N.Y.
(Contract N00014-80-C-0622; AF AFOSR-0076-86)
(AD-A195168) Avail: NTIS HC A03/MF A01 CSCL 25E

We investigate the power of the Butterfly network (which is the FFT network with inputs and outputs identified) relative to other proposed multicomputer interconnection networks, by considering how efficiently the Butterfly can simulate the other networks. Formally we ask, How efficiently can one embed the graph underlying the other network in the graph underlying the Butterfly? We measure the efficiency of an embedding of a graph G in a graph H in terms of: the dilation, or, the maximum amount that any edge of G is stretched by the embedding; the expansion, or, the ratio of the number of vertices of H to the number of vertices of G. We present three simulations that are optimal, to within constant factors: (1) any complete binary tree can be embedded in a Butterfly graph, with simultaneous dilation O(1) and expansion O(1); (2) the n-vertex X-tree can be embedded in a Butterfly graph with simultaneous dilation O(log log n) and expansion O(1); no embedding has better dilation, independent of expansion; (3) any embedding of the n x n mesh in the Butterfly graph must have dilation (log n), independent of expansion; any embedding of the mesh in the Butterfly graph achieves this dilation. Thus, we have simulations of complete-binary-tree machines, X-tree machines, and mesh computers on Butterfly machines, that are optimal in resource utilization (expansion) and delay (dilation), to within constant factors. GRA

N89-10573# Centre National d'Etudes Spatiales, Toulouse (France).

FAULT TOLERANCE COMPUTING: CONSTRAINTS IN USING MULTIPROCESSOR SYNCHRONIZATION BY STATIC PREPLANNED SCHEDULING

F. Bossard 13 Apr. 1988 8 p In FRENCH; ENGLISH summary
(CNES-CT/DRT/TIT/TB-096; ETN-88-93088) Avail: NTIS HC A02/MF A01

Synchronization in fault tolerant parallel architectures based on N-processors in redundancy is discussed. Solutions using preplanned scheduling, such as SIFT method, are reviewed. Constraints in the application software design and efficiency they bring are outlined. ESA

N89-10074*# National Aeronautics and Space Administration. Goddard Space Flight Center, Greenbelt, Md.

A LOCAL AREA COMPUTER NETWORK EXPERT SYSTEM FRAMEWORK

Robert Dominy *In its* Proceedings of 1987 Goddard Conference on Space Applications of Artificial Intelligence (AI) and Robotics 1987 5 p Prepared in cooperation with Bendix Field Engineering Corp., Greebelt, Md. (For primary document see N89-10063

01-12)
Avail: NTIS HC A99/MF E03 CSCL 09B

63 CYBERNETICS

Includes feedback and control theory, artificial intelligence, robotics and expert systems.

For related information see also *54 Man/System Technology and Life Support.*

N89-10574*# National Aeronautics and Space Administration, Washington, D.C.
SPOCK: A TOOL FOR REAL TIME ARTIFICIAL INTELLIGENCE
J. P. LaCroix, G. A. Berthon, F. Fages, and P. Repusseau Aug. 1988 17 p Transl. into ENGLISH of SPOCK, un Outil pour l'Intelligence Artificielle Temps Reel presented at AGARD 55th Meeting of the Avionics Panel of Software and Engineering and its Application to Avionics, 1988 Meeting held in Cesme, Turkey, 25-29 Apr. 1988 Transl. by Scientific Translation Service, Santa Barbara, Calif.
(Contract NASw-4307)
(NASA-TT-20357; NAS 1.77:20357) Avail: NTIS HC A03/MF A01 CSCL 09B

Airborne expert systems must take into account very harsh real time conditions which, when combined with the environmental conditions of the object computer, require the development of new solutions. The proceduralization obtained by compiling the RETE algorithm toward symbolic, procedural, or real time oriented target languages provides a solution to the primary problems of airborne applications: speed requirements, memory control, harmonization of symbolic parts with the traditional portions of the applications. This approach is supported by the SPOCK family of tools (-LISP, -C, LTR3, -ADA) developed by the Central Research Laboratory of Thomson-Csf which offers significant improvements over presently available products. One of the SPOCK applications in Thomson-Csf is a helicopter mission aid system which takes into consideration the threats and terrain, thanks to integration with an airborne cartographic data base. Author

N89-10105*# Advanced Technology and Research, Inc., Burtonsville, Md.
PERFORMANCE IMPROVEMENT OF ROBOTS USING A LEARNING CONTROL SCHEME
Ramuhalli Krishna, Pen-Tai Chiang, and Jackson C. S. Yang (Maryland Univ., College Park.) *In* NASA, Goddard Space Flight Center, Proceedings of 1987 Goddard Conference on Space Applications of Artificial Intelligence (AI) and Robotics 1987 20 p (For primary document see N89-10063 01-12)
Avail: NTIS HC A99/MF E03 CSCL 09B

64 NUMERICAL ANALYSIS

Includes iteration, difference equations, and numerical approximation.

N89-10575*# National Aeronautics and Space Administration. Lewis Research Center, Clevelanrd, Ohio.
AN ALGORITHM FOR UNSTEADY FLOWS WITH STRONG CONVECTION
Vallorie Peridier and J. David A. Walker Oct. 1988 15 p
(Contract C99066G; F49620-85-C-0033)
(NASA-TM-100828; E-4016; NAS 1.15:100828; ICOMP-88-5)
Avail: NTIS HC A03/MF A01 CSCL 12A

An implicit ADI numerical method for the calculation of 2-D unsteady flows with strong convection effects is described. The method is based on the conventional Crank-Nicholson approach for parabolic equations but an upwind-downwind differencing is used for the first order spatial derivatives associated with convection. The differencing is carried out in the current and previous time plane in such a way that the algorithm is second order accurate in both space and time. The difference equations are factored into sequential operators, one in each independent spatial variable; the solution at each time step may then be computed as a sequence of tridiagonal matrix problems. The method may be used in a noniterative manner although iteration at each time step is recommended in situations where the effects of convection are strong. Author

N89-10576# National Aerospace Lab., Tokyo (Japan).
DELTA SQUARE-CORRECTION SCHEME FOR UNSTEADY EULER EQUATIONS
Kenichi Matuno Oct. 1987 11 p In JAPANESE; ENGLISH summary
(NAL-TR-948; ISSN-0389-4010) Avail: NTIS HC A03/MF A01

An implicit finite-difference scheme for unsteady Euler equations is proposed. The quantities of the order of the square of the time-step are employed as unknowns of the scheme, which produces a delta squared form of the algorithm. The present scheme has second-order time accuracy without iteration. The iteration process in the algorithm, which the scheme has as an option, improves the numerical accuracy and robustness. Numerical experiments show that the present scheme is very good not only for an unsteady problem but also for a steady problem. Author

N89-10577*# National Aeronautics and Space Administration. Langley Research Center, Hampton, Va.
IMPROVING THE ACCURACY OF CENTRAL DIFFERENCE SCHEMES Final Report
Eli Turkel (Tel-Aviv Univ., Israel) Sep. 1988 15 p Submitted for publication
(Contract NAS1-18107)
(NASA-CR-181712; ICASE-88-53; NAS 1.26:181712) Avail: NTIS HC A03/MF A01 CSCL 12A

General difference approximations to the fluid dynamic equations require an artificial viscosity in order to converge to a steady state. This artificial viscosity serves two purposes. One is to suppress high frequency noise which is not damped by the central differences. The second purpose is to introduce an entropy-like condition so that shocks can be captured. These viscosities need a coefficient to measure the amount of viscosity to be added. In the standard scheme, a scalar coefficient is used based on the spectral radius of the Jacobian of the convective flux. However, this can add too much viscosity to the slower waves. Hence, it is suggested that a matrix viscosity be used. This gives an appropriate viscosity for each wave component. With this matrix valued coefficient, the central difference scheme becomes closer to upwind biased methods. Author

N89-10578# Helsinki Univ. of Technology, Espoo (Finland). Inst. of Mathematics.
ANALYSIS OF SOME LOW-ORDER FINITE ELEMENT SCHEMES FOR MINDLIN-REISSNER AND KIRCHHOFF PLATES
J. Pitkaeranta 1986 27 p
(PB87-175899; HTKK-MAT-A242; ISBN-951-753-960-6) Avail: NTIS HC E03/MF E01; copy not available from STI Facility
CSCL 12A

A framework was set up for analyzing mixed finite element methods for the plate problem using a mesh dependent energy norm which applies both to the Kirchhoff and the Mindlin-Reissner formulation of the problem. The analysis techniques are applied to some low order finite element schemes where three degrees of freedom are associated to each vertex of a triangulation of the domain. The schemes proceed from the Mindlin-Reissner formulation with modified shear energy. Author

N89-10579# Vrije Universiteit, Amsterdam (Netherlands). Subfaculteit Wiskunde en Informatica.
ABSTRACT, TOPOLOGICAL AND UNIFORM CONVEX STRUCTURES
M. vandeVel Jul. 1987 206 p
(PB88-202965; Rept-325) Avail: NTIS HC A10/MF A01
CSCL 12A

Abstract convex structures are covered. Specific topics include:

basic concepts; half-spaces and separation; base-point orders and geometry; classical convex invariants: invariants and product spaces; median convexity; and some other convex invariants.
GRA

N89-10580# Vrije Universiteit, Amsterdam (Netherlands). Dept. of Mathematics.
INTERACTIVE EDITING OF MATHEMATICAL FORMULAE
S. vanEgmond, F. C. Heeman, and J. C. vanVliet Aug. 1987 10 p
(PB88-203005; IR-131) Avail: NTIS HC A02/MF A01 CSCL 12A

INFORM is an interactive syntax-directed editor for mathematical formulae. In INFORM, the user manipulates a two-dimensional representation of a formula on the screen. The structure and lay-out of formulae is described in a grammar. The editor is completely generated from this grammar. GRA

N89-10581# National Aerospace Lab., Tokyo (Japan). Computational Sciences Div.
ON HIGH RESOLUTION SCHEMES FOR THREE-DIMENSIONAL EULER EQUATIONS
Tomiko Ishiguro, Satoru Ogawa, and Yoko Takakura (Fujitsu Ltd., Tokyo, Japan) Oct. 1987 21 p In JAPANESE; ENGLISH summary
(NAL-TR-950T; ISSN-0389-4010) Avail: NTIS HC A03/MF A01

Numerical estimations of TVD schemes (Yee-Harten's TVD and Chakravarthy-Osher's TVD) in three-dimensional general coordinate systems are performed by solving the Euler equations around the ONERA M6 wing. It is known that their TVD schemes do not give good solutions in curvilinear coordinate systems, and several modifications with regard to treatment of metrics are carried out. Compared with the solution of the Beam-Warming scheme, the modified TVD schemes yield excellent solutions with very few numerical oscillations for strong shock waves; and they have a high ability to capture the leading edge expansion. Further it is shown that the solutions of both TVD schemes almost perfectly coincide with each other when computations are made using an adaptive grid. Author

N89-10582*# National Aeronautics and Space Administration. Langley Research Center, Hampton, Va.
NON-OSCILLATORY CENTRAL DIFFERENCING FOR HYPERBOLIC CONSERVATION LAWS Final Report
Haim Nessyahu and Eitan Tadmor (Tel-Aviv Univ., Israel) Sep. 1988 53 p Submitted for publication
(Contracts NAS1-18107; NAS1-18605; BSF-85-00346; NSF DMS-85-03294)
(NASA-CR-181709; ICASE-88-51; NAS 1.26:181709) Avail: NTIS HC A04/MF A01 CSCL 12A

Many of the recently developed high resolution schemes for hyperbolic conservation laws are based on upwind differencing. The building block for these schemes is the averaging of an appropriate Godunov solver; its time consuming part involves the field-by-field decomposition which is required in order to identify the direction of the wind. Instead, the use of the more robust Lax-Friedrichs (LxF) solver is proposed. The main advantage is simplicity: no Riemann problems are solved and hence field-by-field decompositions are avoided. The main disadvantage is the excessive numerical viscosity typical to the LxF solver. This is compensated for by using high-resolution MUSCL-type interpolants. Numerical experiments show that the quality of results obtained by such convenient central differencing is comparable with those of the upwind schemes. Author

N89-10583*# National Aeronautics and Space Administration. Langley Research Center, Hampton, Va.
AN ADAPTIVE PSEUDOSPECTRAL METHOD FOR DISCONTINUOUS PROBLEMS Final Report
Jeffrey M. Augenbaum (Connecticut Univ., Storrs.) Sep. 1988 34 p Submitted for publication
(Contract NAS1-18107)
(NASA-CR-181717; ICASE-88-54; NAS 1.26:181717) Avail: NTIS HC A03/MF A01 CSCL 12A

The accuracy of adaptively chosen, mapped polynomial approximations is studied for functions with steep gradients or discontinuities. It is shown that, for steep gradient functions, one can obtain spectral accuracy in the original coordinate system by using polynomial approximations in a transformed coordinate system with substantially fewer collocation points than are necessary using polynomial expansion directly in the original, physical, coordinate system. It is also shown that one can avoid the usual Gibbs oscillation associated with steep gradient solutions of hyperbolic pde's by approximation in suitably chosen coordinate systems. Continuous, high gradient solutions are computed with spectral accuracy (as measured in the physical coordinate system). Discontinuous solutions associated with nonlinear hyperbolic equations can be accurately computed by using an artificial viscosity chosen to smooth out the solution in the mapped, computational domain. Thus, shocks can be effectively resolved on a scale that is subgrid to the resolution available with collocation only in the physical domain. Examples with Fourier and Chebyshev collocation are given. Author

N89-10584# National Aerospace Lab., Tokyo (Japan).
COMPARISON OF PLOTTING METHODS USED ON NORMAL PROBABILITY PAPER
Toshiyuki Shimokawa 1987 13 p In JAPANESE; ENGLISH summary
(NAL-TR-951; ISSN-0389-4010) Avail: NTIS HC A03/MF A01

The objective of this study is to compare eight kinds of plotting methods used on normal probability paper and to select appropriate methods for estimating the parameters when a personal computer is available. Suppose that the data from complete samples are plotted on the coordinates of normal probability paper by using each plotting method and the parameters are estimated by the least-squares methods with and without weights. As criteria for comparison this study uses expected values, mean square errors, and variances of the estimators of the population parameters, as well as the mean square difference of the parameter estimates derived by each graphical method and the moments method. These values are derived by analysis and Monte-Carlo simulation for samples of sizes two to twenty and are graphically illustrated. The eight kinds of plotting methods are compared on the basis of the obtained results. This study recommends the symmetrical sample cumulative distribution function and the cumulative probabilities corresponding to normal scores for practical use.
Author

N89-10585# Rome Univ. (Italy). Dipt. di Fisica.
DIMENSIONAL DEFORMATIONS OF INTEGRABLE SYSTEMS: AN APPROACH TO INTEGRABILITY IN MULTIDIMENSIONS, PART 1
P. M. Santini 10 Feb. 1988 22 p Sponsored in part by the Italian Ministry of Education
(Preprint-586; ETN-88-92635) Avail: NTIS HC A03/MF A01

An approach, the dimensional deformations of integrable systems, to generate in a natural, straightforward and unified manner, higher dimensional analogs of integrable systems is proposed. In this approach, based on the theory describing the algebraic aspects of integrability, the algebraic structure of given integrable systems is explored, to generate integrable generalizations in higher dimensions. This approach is illustrated by examples and known and novel integrable systems are derived. The simplicity of the method allows also to single out the theoretical and technical problems responsible for the almost total absence of integrable structures in multidimensions. ESA

N89-10586*# Rensselaer Polytechnic Inst., Troy, N.Y. Dept. of Mechanical Engineering.
AN INVESTIGATION OF NEW METHODS FOR ESTIMATING PARAMETER SENSITIVITIES
Todd J. Beltracchi and Gary A. Gabriele Aug. 1988 138 p

(Grant NAG1-752)
(NASA-CR-183195; NAS 1.26:183195) Avail: NTIS HC A07/MF A01 CSCL 12A

Parameter sensitivity is defined as the estimation of changes in the modeling functions and the design variables due to small changes in the fixed parameters of the formulation. There are currently several methods for estimating parameter sensitivities requiring either difficult to obtain second order information, or do not return reliable estimates for the derivatives. Additionally, all the methods assume that the set of active constraints does not change in a neighborhood of the estimation point. If the active set does in fact change, than any extrapolations based on these derivatives may be in error. The objective here is to investigate more efficient new methods for estimating parameter sensitivities when the active set changes. The new method is based on the recursive quadratic programming (RQP) method and in conjunction a differencing formula to produce estimates of the sensitivities. This is compared to existing methods and is shown to be very competitive in terms of the number of function evaluations required. In terms of accuracy, the method is shown to be equivalent to a modified version of the Kuhn-Tucker method, where the Hessian of the Lagrangian is estimated using the BFS method employed by the RPQ algorithm. Inital testing on a test set with known sensitivities demonstrates that the method can accurately calculate the parameter sensitivity. To handle changes in the active set, a deflection algorithm is proposed for those cases where the new set of active constraints remains linearly independent. For those cases where dependencies occur, a directional derivative is proposed. A few simple examples are included for the algorithm, but extensive testing has not yet been performed. Author

N89-10587# Vrije Universiteit, Amsterdam (Netherlands). Subfaculteit Wiskunde en Informatica.
BLOCK TOEPLITZ OPERATORS WITH RATIONAL SYMBOLS
I. Gohberg and M. A. Kaashoek Jul. 1987 58 p
(PB88-202890; Rept-327) Avail: NTIS HC A04/MF A01 CSCL 12A

Semi-infinite block Toeplitz operators with rational matrix symbols are inverted explicitly by using the factorizaiton method and by a method of reduction to singular systems with boundary conditions. The case of finite block Toeplitz matrices is also included. Fredholm characteristics are computed. All formulas are explicit and based on a realization of the symbol as a transfer function of a singular system. GRA

N89-10588# Vrije Universiteit, Amsterdam (Netherlands). Subfaculteit Wiskunde en Informatica.
FREE CHOICE PERMISSIONS AND ROSS'S PARADOX: INTERNAL VERSUS EXTERNAL NONDETERMINISM
J. J. C. Meyer Aug. 1987 13 p
(PB88-202874; Rept-130) Avail: NTIS HC A03/MF A01 CSCL 12A

It is shown how the well-known paradox of free choice permissions in deontic logic can be understood in terms of nondeterministic actions. Free and imposed permissions can be treated adequately by distinguishing between two kinds of nondeterministic choice operators: one that expresses an external choice, which cannot be influenced by the actor, and one that expresses an internal choice, on which the actor has an influence. Similar notions of nondeterminism are well-known in computer science where they are used in context of parallel execution of programs with the possibility of synchronization. Also applied are the insights gained by this approach in a discussion of the well-known paradox of Ross. GRA

N89-10589# Air Force Inst. of Tech., Wright-Patterson AFB, Ohio.
FINITE PRECISION ARITHMETIC IN SINGULAR VALUE DECOMPOSITION ARCHITECTURES Ph.D. Thesis
Robert A. Duryea Aug. 1987 234 p
(AD-A196188; AFIT/CI/NR-88-119) Avail: NTIS HC A11/MF A01 CSCL 12F

The Singular Value Decomposition (SVD) is an important matrix algorithm which has many applications in signal processing. However, its use has been limited due to its computational complexity. Several computer architectures have been proposed to compute the SVD using arrays of parallel processors. This thesis derives requirements for the precision of arithmetic units ;(AUs) used in SVD arrays and compare the resource requirements of several architectures. The results are based on the assumption that we are operating on matrices of quantized data. Since the matrices have quantization errors, it is shown that their singular values will have quantization errors which are as large as the data errors. To compute the number of bits needed in SVD AUs, it is required that the AUs have enough bits to keep the round-off errors of the SVD computation smaller than the quantization errors. This analysis shows that we need essentially the same number of bits for either the Hestenes or Jacobi SVD algorithms. If the matrix has been scaled to prevent overflows and if we use properly rounded arithmetic, CORDIC and fixed point AUs require 8 fewer bits than floating point AUs. Our computations indicate that 32 bit floating point AUs are useful only for small arrays of 8-bit data. For 100-by-100 arrays of 16 bit data we need 40-bit floating point AUs. 32-bit fixed point AUs can be used in SVD arrays for large 8-bit matrices or moderate size 16-bit arrays. GRA

N89-10590# Sandia National Labs., Albuquerque, N. Mex.
PROGRESS IN NODAL TRANSPORT METHODS
A. Badruzzaman 1988 18 p Presented at the 7th International Conference on Radiation Shielding, Bournemouth, England, 12 Sep. 1988
(Contract DE-AC04-76DP-00789)
(DE88-012416; SAND-88-0850C; CONF-880906-3) Avail: NTIS HC A03/MF A01

The state-of-the-art methods in nodal transport are discussed. Two major classes of these methods have been developed in multi-dimensional cartesian geometry. The first can be viewed as a set of general difference schemes of the discrete ordinates (S(sub N)) transport equation. In the second, the angular dependence of the cell-edge fluxes is treated by interface-current techniques of varying degrees of sophistication. Both methods are reviewed. Development of appropriate acceleration schemes and the recent extension of the nodal S(sub N) procedures to time-dependent and cylindrical geometry are discussed briefly. DOE

N89-10206*# Jet Propulsion Lab., California Inst. of Tech., Pasadena.
STORAGE AND COMPUTATIONALLY EFFICIENT PERMUTATIONS OF FACTORIZED COVARIANCE AND SQUARE-ROOT INFORMATION ARRAYS
R. J. Muellerschoen *In its* The Telecommunications and Data Acquisition Report 15 Aug. 1988 p 245-256 (For primary document see N89-10186 01-32)
Avail: NTIS HC A14/MF A01 CSCL 12A

65 STATISTICS AND PROBABILITY

Includes data sampling and smoothing; Monte Carlo method; and stochastic processes.

N89-10591# Centre National de la Recherche Scientifique, Grenoble (France). Tech. de l'Informatique, des Math., de la Microelectronique et de la Microscopie Quantitative.
A FAST MONTE-CARLO CROSS-VALIDATION PROCEDURE FOR LARGE LEAST SQUARES PROBLEMS WITH NOISY DATA
Didier Girard Dec. 1987 25 p
(RR-687-M; ETN-88-92752) Avail: NTIS HC A03/MF A01

A fast Mont-Carlo algorithm is proposed for calculating reliable estimates of the trace of the influence matrix A tau involved in regularization of linear equations (or data smoothing problems), where tau is the regularization (or smoothing) parameter: (1) generate n pseudo-random values w1,...,wn, from the standard normal distribution (where n is the number of data points) and let

w=(w1,...,wn) sup T; (2) compute the residual vector w-A tau wi; (3) calculate T asterisk (w)=(w sup T (w-A tau w)) / (w sup T w) (and consider T asterisk (w) as an approximation to (1/n)tr(I-A tau)). It is shown by theoretical bounds and by numerical simulations on typical problems, that the expected relative precision of these estimates is good when n is large enough, and that they can be used in the minimization with respect to tau of the generalized cross validation (GCV) function. This permits the use of the GCV method for choosing tau on large data sets, with only a similar amount of work as the standard residual method. Numerical applications of this procedure to optimal spline smoothing in one or two dimensions show its efficiency. In two dimension with n=1000 and using a conjugate gradient method for computing A tau y, given tau and y, the existing procedures for GCV are impractical. ESA

N89-10592# Stanford Linear Accelerator Center, Calif.
BOOTSTRAP CONFIDENCE INTERVALS IN A COMPLEX SITUATION: A SEQUENTIAL PAIRED CLINICAL TRIAL
Sally C. Morton Jun. 1988 25 p Presented at the Joint Statistical Meetings, New Orleans, La., 22 Aug. 1988
(Contract DE-AC03-76SF-00515)
(DE88-015338; SLAC-PUB-4665; CONF-880872-4) Avail: NTIS HC A03/MF A01

This paper considers the problem of determining a confidence interval for the difference between two treatments in a simplified sequential paired clinical trial, which is analogous to setting an interval for the drift of a random walk subject to a parabolic stopping boundary. Three bootstrap methods of construction are applied: Efron's accelerated bias-covered, the DiCiccio-Romano, and the bootstrap-t. The results are compared with a theoretical approximate interval due to Siegmund. Difficulties inherent in the use of these bootstrap methods in a complex situations are illustrated. The DiCiccio-Romano method is shown to be the easiest to apply and to work well. DOE

N89-10593# Naval Postgraduate School, Monterey, Calif.
SMOOTHING SPATIAL DATA BY ESTIMATING MEAN LOCAL VARIANCE
Laura D. Johnson Apr. 1988 36 p
(AD-A195302; NPS55-88-005) Avail: NTIS HC A03/MF A01 CSCL 24A

A nearest neighbor nonparametric regression method is used to estimate air pollution levels at other than measured points. The method requires an appropriate smoother. Cross-validation is used to determine the appropriate smoother. An alternative method is introduced to determine an appropriate level of smoothing which involves minimizing mean local variance. Mean local variance is a function of the size of a circular window. It is minimized for two pollutants in Ohio, New York and Florida. The smoother obtained by cross-validation using Ohio's data is compared to that obtained by minimizing mean local variance. GRA

N89-10594# Technische Hogeschool, Delft (Netherlands). Onderafdeling der Wiskunde en Informatica.
COMPARISON OF SOME ROBUST REGRESSION ESTIMATORS
B. C. vanZomeren 1986 15 p
(PB88-126289; Rept-86-54) Avail: NTIS HC E03/MF E01; copy not available from STI Facility CSCL 12A

Scientists have been using robust procedures for a long time. Most of the theory is about robust estimation of location and scale, and the most well-known robust estimators are Huber's M-estimators, which generalize the Maximum Likelihood principle. More recently, other robust estimators for regression have been proposed, with a breakdown point of 50 pct even in the presence of leverage points. Among them are the Least Median of Squares estimator and the Least Trimmed Squares estimator as well as the S-estimator. In the paper the performance of these estimators is studied using real data. The estimators are also compared with respect to their computation time. GRA

N89-10595# Los Alamos National Lab., N. Mex.
MEAN ESTIMATION IN HIGHLY SKEWED SAMPLES
S. Pederson and R. J. Beckman 1988 14 p Presented at the Joint Statistical Meetings, New Orleans, La., 22 Aug. 1988
(Contract W-7405-eng-36)
(DE88-010929; LA-UR-88-1590; CONF-880872-1) Avail: NTIS HC A03/MF A01

When data arise from an asymmetric population, and the center of such a population is of interest, many techniques are available to estimate this center. Most involve either developing an estimator robust to the asymmetry, or transforming the data to create a more symmetric distribution. In these cases the true mean of the underlying population is not preserved; rather, quantities such as the median are estimated. There are situations, however, in which the mean is really the quantity of interest. For example, in neutron transport problems the energies of individual particles are measured. Primary interest may be in total energy: this is merely a rescaling of mean energy per particle. This report details some efforts to develop mean estimation techniques in large samples of highly skewed data. DOE

66 SYSTEMS ANALYSIS

Includes mathematical modeling; network analysis; and operations research.

N89-10596# Los Alamos National Lab., N. Mex.
DIRECTED ENERGY CONCEPTS FOR STRATEGIC DEFENSE
Gregory H. Canavan Jun. 1988 70 p
(Contract W-7405-eng-36)
(DE88-015050; LA-11173-MS) Avail: NTIS HC A04/MF A01

Directed energy concepts can play unique roles in strategic defense because of their reaction time, speed of light engagement, and large geographic coverage. This report discusses the main directed energy concepts, engagements in which they could have significant leverage, and their expected performance in them. It covers both boost phase engagements and midcourse applications, and contrasts these results with those of earlier analyses. DOE

N89-10597# Los Alamos National Lab., N. Mex.
MILITARY USES OF SPACE
Gregory H. Canavan Aug. 1988 17 p
(Contract W-7405-eng-36)
(DE88-015053; LA-11344-MS) Avail: NTIS HC A03/MF A01

This report reviews the information gathering, offensive, and defensive uses of space. The report concludes that, while all defensive uses are likely to grow, the most important ones are warning, verification target relocation, and defense. DOE

N89-10598# Los Alamos National Lab., N. Mex.
SDI (STRATEGIC DEFENSE INITIATIVE): MYTH OR REALITY
Gregory H. Canavan Jun. 1988 20 p
(Contract W-7405-eng-36)
(DE88-015059; LA-11322-MS) Avail: NTIS HC A03/MF A01

This report reviews previous attempts to develop strategic defenses, the technologies currently under consideration by the Strategic Defense Initiative (SDI), their main unknowns, and the likely performance of strategic defense concepts against evolving threats. DOE

N89-10599# Lawrence Livermore National Lab., Calif.
CONTROL SYSTEM RESEARCH FOR DIRECTED ENERGY WEAPONS Annual Technical Report, FY 1987
K. David Young, ed. Dec. 1987 461 p Prepared in cooperation with Illinois Univ., Urbana; Univ. of Southern California, Los Angeles; Stanford Univ., Calif.; Ohio State Univ., Columbus; and Santa Clara Univ., Calif.
(Contract W-7405-eng-48)
(DE88-015371; UCID-20950-87) Avail: NTIS HC A20/MF A01

This paper discusses the different control systems that are being considered to direct directed- energy weapons. The control

methods discussed are: large scale systems control methods; robust control methods; decentralized/relegated control methods; multirate digital control; decentralized multirate control; and distributed finite element modeling and controls. DOE

67 THEORETICAL MATHEMATICS

Includes topology and number theory.

N89-10600# Rome Univ. (Italy). Dipt. di Fisica.
GENERALIZED LYAPUNOV EXPONENTS IN HIGH-DIMENSIONAL CHAOTIC DYNAMICS AND PRODUCTS OF LARGE RANDOM MATRICES
Andrea Crisanti, Giovanni Paladin, and Angelo Vulpiani 19 Apr. 1988 28 p
(Preprint-595; ETN-88-92642) Avail: NTIS HC A03/MF A01

The behavior of the generalized Lyapunov exponents for chaotic symplectic dynamical systems and products of random matrices in the limit of large dimensions D are studied. For products of random matrices without any particular structure the generalized Lyapunov exponents become equal in this limit and the value of one of the generalized Lyapunov exponents is obtained by simple arguments. However, for random symplectic matrices with peculiar structures and for chaotic symplectic maps the generalized Lyapunov exponents are different also for D tends to infinity indicating that high dimensionality cannot always destroy intermittency. ESA

70 PHYSICS (GENERAL)

For precision time and time interval (PTTI) see *35 Instrumentation and Photography;* for geophysics, astrophysics or solar physics see *46 Geophysics, 90 Astrophysics,* or *92 Solar Physics.*

No abstracts in this category.

71 ACOUSTICS

Includes sound generation, transmission and attenuation. For noise pollution see *45 Environmental Pollution.*

N89-10601*# Planning Research Corp., Hampton, Va.
ON THE APPROPRIATENESS OF APPLYING CHI-SQUARE DISTRIBUTION BASED CONFIDENCE INTERVALS TO SPECTRAL ESTIMATES OF HELICOPTER FLYOVER DATA
Charles K. Rutledge Aug. 1988 65 p
(Contract NAS1-18000)
(NASA-CR-181692; NAS 1.26:181692) Avail: NTIS HC A04/MF A01 CSCL 20A

The validity of applying chi-square based confidence intervals to far-field acoustic flyover spectral estimates was investigated. Simulated data, using a Kendall series and experimental acoustic data from the NASA/McDonnell Douglas 500E acoustics test, were analyzed. Statistical significance tests to determine the equality of distributions of the simulated and experimental data relative to theoretical chi-square distributions were performed. Bias and uncertainty errors associated with the spectral estimates were easily identified from the data sets. A model relating the uncertainty and bias errors to the estimates resulted, which aided in determining the appropriateness of the chi-square distribution based confidence intervals. Such confidence intervals were appropriate for nontonally associated frequencies of the experimental data but were inappropriate for tonally associated estimate distributions. The appropriateness at the tonally associated frequencies was indicated by the presence of bias error and noncomformity of the distributions to the theoretical chi-square distribution. A technique for determining appropriate confidence intervals at the tonally associated frequencies was suggested. Author

N89-10602 North Carolina State Univ., Raleigh.
ACOUSTIC RADIATION FROM PLATES DRIVEN BY MULTI-POINT RANDOM FORCES Ph.D. Thesis
Hong Peng 1987 133 p
Avail: Univ. Microfilms Order No. DA8804820

The problem of acoustic radiation from plates driven by multiple random point forces is analyzed. First, the formulation of the sound power radiated by infinite thin plates under the action of multiple random point forces is derived. The reaction of the acoustic medium on the vibratory response of plates is taken into account. With the input spectrum being assumed as band-limited white noise, the effects of input force correlation on the acoustic power levels are examined. The analysis is then extended to finite thin plates with four simply supported edges. The exact expressions for the surface acoustic intensity and the radiated sound power are also derived. By assuming the plates to be lightly damped and neglecting the fluid loading effect, approximate solutions for acoustic intensity and sound power are obtained. An experimental study is carried out to measure the surface acoustic intensity patterns and compare with the analytical results. The effects of input force correlation on the acoustic intensity pattern and the sound power level are also discussed. Dissert. Abstr.

N89-10603*# National Aeronautics and Space Administration. Lewis Research Center, Cleveland, Ohio.
THE EFFECT OF FRONT-TO-REAR PROPELLER SPACING ON THE INTERACTION NOISE AT CRUISE CONDITIONS OF A MODEL COUNTERROTATION PROPELLER HAVING A REDUCED DIAMETER AFT PROPELLER
James H. Dittmar, Eliott B. Gordon (Sverdrup Technology, Inc., Cleveland, Ohio.), and Robert J. Jeracki Oct. 1988 30 p
(NASA-TM-101329; E-4340; NAS 1.15:101329) Avail: NTIS HC A03/MF A01 CSCL 20A

The effect of forward-to-aft propeller spacing on the interaction noise of a counterrotation propeller with reduced aft diameter was measured at cruise conditions. In general, the tones at 100 percent speed decreased from close to nominal spacing as expected from a wake decay model. However, when the spacing was further increased to the far position, the noise did not decrease as expected and in some cases increased. The behavior at the far spacing was attributed to changing forward propeller performance, which produced larger wakes. The results of this experiment indicate that simple wake decay model is sufficient to describe the behavior of the interaction noise only if the aerodynamic coupling of the two propellers does not change with spacing. If significant coupling occurs such that the loading of the forward propeller is altered, the interaction noise does not necessarily decrease with larger forward-to-aft propeller spacing. Author

N89-10604# Max-Planck-Institut fuer Stroemungsforschung, Goettingen (West Germany).
A WATER SOUND GENERATOR FOR PRESSURE PULSES OF HIGH ENERGY
Andreas Laake and E.-A. Mueller, ed. 1987 95 p In GERMAN; ENGLISH summary
(MPIS-Mitt-85-1987; ISSN-0374-1257; ETN-88-93203) Avail: NTIS HC A05/MF A01

The watershock, a water sound generator for high energy pressure pulses, is presented. The design consists of a mechanical drive with an energy accumulator, a converter from mechanical to acoustic energy, and an acoustic coupler. The dimensions of these three parts enable one to adapt the pulse width, the main frequency, and the bandwidth of the power spectrum to different requirements. The peak-shaped pressure signal of the watershock results from the sound generation by inverse water hammer and from the sound damping by acoustic cavitation. The signal is almost unrestrained from distributing forward or back-runners, and thus the analysis of the seismograms is simplified because these noise arrivals may be disregarded. In comparison to conventional sound generation, the method of sound generation by inverse water hammer shows

high efficiency and large bandwidth of its power spectrum. The watershock may also be employed in investigations of frequency dependent attenuation. ESA

72 ATOMIC AND MOLECULAR PHYSICS

Includes atomic structure, electron properties, and molecular spectra.

N89-10605*# National Aeronautics and Space Administration. Ames Research Center, Moffett Field, Calif.
THE LOWEST IONIZATION POTENTIALS OF Al2
Charles W. Bauschlicher, Jr., Leslie A. Barnes, and Peter R. Taylor (Eloret Corp., Sunnyvale, Calif.) [1988] 16 p
(Contract NCC2-371)
(NASA-TM-101171; NAS 1.15:101171) Avail: NTIS HC A03/MF A01 CSCL 20H

Potential curves for the lowest two electronic states (X 2 sigma g + and A 2 pi u) of Al2(+) were computed using complete active space SCF/multireference CI wave functions and large Gaussian basis sets. The lowest observable vertical ionization potential (to Al2(+) X 2 sigma g +) of the Al2 X 3 pi u ground state is calculated to occur around 6.1 eV, in excellent agreement with the experimental range of 6.0 to 6.42 eV obtained in recent cluster ionization studies by Cox and co-workers. The second vertical ionization potential (to Al2(+) A 2 pi u) occurs near 6.4 eV, also within the experimental range. The adiabatic IP of 5.90 eV is in good agreement with the value of 5.8 to 6.1 eV deduced by Hanley and co-workers from the difference in thresholds between collision induced dissociation processes of Al3(+). The computed IP values are somewhat larger than those deduced from branching ratios in cluster fragmentation experiments by Jarrold and co-workers. The observation of an ionization threshold below 6.42 eV is shown to be incompatible with an Al2 ground electronic state assignment of 3 sigma g -, but the separation between the two lowest states of Al2 is so small that it is likely that both are populated in the experiments, so that this does not provide unambiguous support for the recent theoretical assignment of the ground state as 3 pi u. Author

N89-10606# Pacific Northwest Labs., Richland, Wash.
AN ION-OPTICAL BENCH FOR TESTING ION SOURCE LENSES
J. J. Stoffels and D. R. Ells Jun. 1988 9 p Presented at the 36th Annual Conference on Mass Spectrometry and Allied Topics, San Francisco, Calif., 6 Jun. 1988
(Contract DE-AC06-76RL-01830)
(DE88-013186; PNL-SA-15443; CONF-8806199-2) Avail: NTIS HC A02/MF A01

An ion-optical bench has been designed and constructed to obtain experimental data on the focusing properties of ion lenses in three dimensions. The heart of the apparatus is a position-sensitive detector (PSD) that gives output signals proportional to the x and y positions of each ion impact. The position signals can be displayed on an oscilloscope screen and analyzed by a two-parameter pulse-height analyzer, thereby giving a visual picture of the ion beam cross section and intensity distribution. The PSD itself is mounted on a track and is movable during operation from a position immediately following the ion lens to 30 cm away. This enables the rapid collection of accurate data on the intensity distribution and divergence angles of ions leaving the source lens. Examples of ion lens measurements are given. DOE

N89-10607# Oak Ridge National Lab., Tenn.
MULTIPHOTON IONIZATION OF TRANSIENT SPECIES IN SUPERSONIC JETS
John C. Miller and Charles S. Feigerle (Tennessee Univ., Knoxville.) 1988 5 p Presented at the 4th International Symposium on Resonance Ionization Spectroscopy and Its Applications, Gaithersburg, Md., 10-15 Apr. 1988
(Contract DE-AC05-84OR-21400)
(DE88-008366; CONF-880435-7) Avail: NTIS HC A02/MF A01

A series of experiments utilizing mass-resolved multiphoton ionization to study NO diluted into supersonic beams of rare gases is presented. The sensitivity of the technique is demonstrated by the detection of 10 to the 3d to 10 to the 4th molecules of the rare isotopic combination N(15)O(18) in its natural abundance. New results are given on the spectroscopy and photophysics of the Ar-NO, Kr-NO, and Xe-NO van der Waals molecules present in the beam. Finally, the addition of an electron beam or glow discharge at the orifice of the supersonic nozzle results in the formation of metastable rare gas atoms, sputtered metal atoms, and vibrationally hot NO molecules. DOE

N89-10608# Houston Univ., Tex. Dept. of Chemistry.
INELASTIC ION-SURFACE COLLISIONS. ION NEUTRALIZATION ON INTERMETALLIC SURFACES
J. W. Rabalais 1 Jun. 1988 17 p
(Contract F19628-86-K-0013)
(AD-A196322; AFGL-TR-88-0137; SR-2) Avail: NTIS HC A03/MF A01 CSCL 07B

Ion scattering and direct recoil spectrometries were used to investigate electronic excitation and charge transfer processes occurring during rare gas ion bombardment of CuLi alloy. Excitations in the close encounter appear to be governed by the degree of inner shell mixing between the colliding pair. Excitations in the outgoing trajectory are governed by the probabilities of Auger and resonant charge exchange between the scattered or recoiled particle and the surface. Measurements of the vacuum ultraviolet photon emission of the scattered and recoiled particles proved to be unsuccessful due to low photon yields. The ion induced surface damage to transition metal fluoroanions was investigated by XPS and UPS. Ion bombardment reduces the transition metal atom to lower oxidation states, in some cases all the way to the metal. These results are consistent with the thermal spike model of ion damage. GRA

N89-10609# Sandia National Labs., Albuquerque, N. Mex.
ANALYTICAL APPROXIMATIONS FOR X-RAY CROSS SECTIONS 3
Frank Biggs and Ruth Lighthill Aug. 1988 137 p
(Contract DE-AC04-76DP-00789)
(DE88-015366; SAND-87-0070) Avail: NTIS HC A07/MF A01

This report updates our previous work that provided analytical approximations to cross sections for both photoelectric absorption of photons by atoms and incoherent scattering of photons by atoms. This representation is convenient for use in programmable calculators and in computer programs to evaluate these cross sections numerically. The results apply to atoms of atomic numbers between 1 and 100 and for photon energies greater than or equal to 10 eV. The photoelectric cross sections are again approximated by four-term polynomials in reciprocal powers of the photon energy. There are now more fitting intervals, however, than were used previously. The incoherent-scattering cross sections are based on the Klein-Nishina relation, but use simpler approximate equations for efficient computer evaluation. We describe the averaging scheme for applying these atomic results to any composite material. The fitting coefficients are included in tables, and the cross sections are shown graphically. DOE

N89-10610*# National Aeronautics and Space Administration. Ames Research Center, Moffett Field, Calif.
THEORETICAL STUDY OF THE DISSOCIATION ENERGY AND THE RED AND VIOLET BAND SYSTEMS OF CN
Charles W. Bauschlicher, Jr., Stephen R. Langhoff, and Peter R. Taylor (Eloret Corp., Sunnyvale, Calif.) [1987] 28 p
(Contract NCC2-371)
(NASA-TM-101190; NAS 1.15:101190) Avail: NTIS HC A03/MF A01 CSCL 20H

The dissociation energy (D sub O) of CN is determined to be 7.65 + or - 0.06 eV. This corresponds to delta H sub f (CN) = 105.3 + or - 1.5 kcal/mole, in excellent agreement with Engleman and Rouse (1975), but considerably larger than the recent value

deduced from shock-tube studies by Colket (1984). The result is obtained not only from extensive ab initio MRCI calculations using a very large Gaussian basis set, but also from extrapolation of the directly computed value by comparison of computed and experimental results fo NO, C2, and N2. As an additional calibration of the methods, the D sub O value for CN was computed from the corresponding value for CN(-) using the experimental electron affinity data. The lifetime of the nu prime = 0 level of the violet (B 2 sigma + yields X 2 sigma +) system was computed to be 62.4 ns, in good agreement with both experiment and previous calculations. Lifetimes for the red (A 2 pi yields X 2 sigma +) system decrease with increasing nu prime, which is consistent both with the recent experiment and calculations. While the computed lifetimes are significantly longer that those obtained from the experiment, they are shorter than those deduced from an analysis of the solar spectrum. However the D sub O and f (sub OO) are consistent with Lambert's model for the solar spectrum.
Author

N89-10611 Max-Planck-Inst. fuer Physik und Astrophysik, Garching (West Germany). Werner-Heisenberg Inst. fuer Physik.
USE OF THE TIME PROJECTION CHAMBER FOR MEASURING HEAVY ION COLLISIONS
R. Settles Jun. 1988 13 p Presented at the International Conference on Physics and Astrophysics of Quark-Gluon Plasma, Bombay, India, 8-12 Feb. 1988 Submitted for publication
(MPE-PAE/Exp-EL-191; ETN-88-93192) Copyright Avail: Fachinformationszentrum Karlsruhe, 7514
Eggenstein-Leopoldshafen 2, Fed. Republic of Germany

The status of using time projection chambers as the central tracking detector for heavy-ion collision experiments is reviewed.
ESA

73 NUCLEAR AND HIGH-ENERGY PHYSICS

Includes elementary and nuclear particles; and reactor theory.

For space radiation see *93 Space Radiation.*

N89-10612*# National Aeronautics and Space Administration. Langley Research Center, Hampton, Va.
MULTIPLE NUCLEON KNOCKOUT BY COULOMB DISSOCIATION IN RELATIVISTIC HEAVY-ION COLLISIONS
Francis A. Cucinotta, John W. Norbury (Washington State Univ., Pullman.), and Lawrence W. Townsend Nov. 1988 7 p
(NASA-TM-4070; L-16466; NAS 1.15:4070) Avail: NTIS HC A02/MF A01 CSCL 20H

The Coulomb dissociation contributions to fragmentation cross sections in relativistic heavy ion collisions, where more than one nucleon is removed, are estimated using the Weizsacker-Williams method of virtual quanta. Photonuclear cross sections taken from experimental results were used to fold into target photon number spectra calculated with the Weizsacker-Williams method. Calculations for several projectile target combinations over a wide range of charge numbers, and a wide range of incident projectile energies, are reported. These results suggest that multiple nucleon knockout by the Coulomb field may be of negligible importance in galactic heavy ion studies for projectiles lighter than Fe-56.
Author

N89-10613# Continuous Electron Beam Accelerator Facility, Newport New, Va.
RELATIVISTIC NUCLEAR PHYSICS WITH THE SPECTATOR MODEL
Franz Gross 1988 24 p Presented at the Workshop on Nuclear and Particle Physics in the Light Cone, Los Alamos, N. Mex., 18-22 Jul. 1988 Prepared in cooperation with College of William and Mary, Williamsburg, Va.
(Contract DE-AC05-84ER-40150)
(CEBAF-PR-88-011) Avail: NTIS HC A03/MF A01

The spectator model, a general approach to the relativistic treatment of nuclear physics problems in which spectators to nuclear interactions are put on their mass-shell, will be defined and described. The approach grows out of the relativistic treatment of two and three body systems in which one particle is off-shell, and recent numerical results for the NN interaction will be presented. Two meson-exchange models, one with only 4 mesons (pi, sigma, rho, omega) but with a 25 percent admixture of gamma sub 5 coupling for the pion, and a second with 6 mesons (pi, sigma, gamma, delta, and eta) but a pure gamma sub 5 gamma sub mu pion coupling, are shown to give very good quantitative fits to NN scattering phase shifts below 400 MeV, and also a good description of the p C-40 alpha elastic scattering observables.
Author

N89-10614# Continuous Electron Beam Accelerator Facility, Newport New, Va.
NONLINEAR SPIN ACCEPTANCE IN ELECTRON STORAGE RINGS
Joerg Kewisch, Robert Rossmanith, and Torsten Limberg (Deutsches Elektronen-Synchrotron, Hamburg, West Germany) [1987] 8 p Submitted for publication
(Contract DE-AC05-84ER-40150)
(CEBAF-PR-88-009) Avail: NTIS HC A02/MF A01

It is shown that the degree of polarization of a beam in electron storage rings can be limited by nonlinear effects. The strength of a nonlinear effect depends on the amplitude of the particles. Particles performing synchrotron and betatron oscillations with high amplitudes can contribute over proportionally to depolarization. As a result, the emittance of a beam is not allowed to exceed certain boundaries, otherwise the beam will become more and more depleted. This limit is called nonlinear spin acceptance.
Author

74 OPTICS

Includes light phenomena; and optical devices.

For lasers see *36 Lasers and Masers.*

N89-10615*# EIC, Inc., Norwood, Mass.
PHOTOELECTROCHEMICAL FABRICATION OF SPECTROSCOPIC DIFFRACTION GRATINGS Final Report, 13 Feb. - 12 Aug. 1986
R. David Rauh, Michael M. Carrabba, and Nguyet M. Nguyen Sep. 1986 38 p
(Contract NAS5-29279)
(NASA-CR-180786; NAS 1.26:180786) Avail: NTIS HC A03/MF A01 CSCL 20F

Photoelectrochemical etching was demonstrated as a means of fabricating a variety of periodic structures in semiconductors. The semiconductor is used as an electrode in an electrochemical cell, and is in contact with a liquid electrolyte. When the crystal is held at a positive voltage and illuminated, etching occurs in only the illuminated regions to a depth proportional to the illumination intensity and exposure time. In Phase 1, it was determined that diffraction gratings could be produced in gallium arsenide crystals by this method, using either a scanned focused laser beam or by uniform illumination of a ruling mask defined in metal or photoresist on the crystal surface. The latter approach was determined to produce V-grooves if the mask is oriented along certain crystallographic directions. These V-grooves were produced with an exceedingly smooth crystal morphology due to the highly controllable nature of the process and the mild electrolytes involved. The results form the basis for photoelectrochemical fabrication of deep, low pitch Eschelle gratings for use in high orders in NASA spectrographic instrumentation such as the Space Telescope Imaging Spectrograph.
Author

N89-10616# California Univ., San Diego.
ARCHITECTURE STUDIES AND SYSTEM DEMONSTRATIONS FOR OPTICAL PARALLEL PROCESSOR FOR AI AND NI Semiannual Report, 1 Oct. 1987 - 31 Mar. 1988
Sing H. Lee 31 Mar. 1988 55 p

(Grant AF-AFOSR-0022-88; AF Proj. 6150)
(AD-A195480; AFOSR-88-0579TR) Avail: NTIS HC A04/MF A01 CSCL 20F

In solving deterministic AI problems the data search for matching the arguments of a PROLOG expression causes serious bottleneck when implemented sequentially by electronic systems. To overcome this bottleneck we have developed the concepts for an optical expert system based on matrix-algebraic formulation, which will be suitable for parallel optical implementation. The optical AI system based on matrix-algebraic formation will offer distinct advantages for parallel search, adult learning, etc. GRA

N89-10617 Arizona Univ., Tucson.
ANALYSIS OF METHODS FOR DETECTING FOCUS ERROR IN OPTICAL DATA STORAGE SYSTEMS Ph.D. Thesis
Donald Kenneth Cohen 1987 247 p
Avail: Univ. Microfilms Order No. DA8804168

Theoretical and experimental techniques are developed to study three common approaches to focus error signal generation for optical data storage applications. Specifically, the astigmatic, obstruction knife edge (a.k.a. shaded aperture), and critical angle prism systems are studied. These techniques are then applied to a new focus detection system, based on a lateral shearing interferometer. The sensitivity of a given optical system to the primary design point, alignment errors, aberrations and optical recording medium topology are presented. A new approach to constructing the focus error signal for the astigmatic and interferometric techniques is presented which greatly reduces the alignment sensitivity. Dissert. Abstr.

N89-10618# Lawrence Livermore National Lab., Calif.
DEFLECTION OF LIGHT BY USING TUNGSTEN BRONZE CRYSTALS
L. F. Jelsma, G. M. McWright, F. A. Schumacher, and R. R. Neurgaonkar (Rockwell International Corp., Thousand Oaks, Calif.) Jul. 1988 7 p Presented at the Optoelectronic Materials and Devices 2, Boston, Mass., 6 Sep. 1988
(Contract W-7405-eng-48)
(DE88-014151; UCRL-97782-Rev-1; CONF-8809111-1-Rev-1)
Avail: NTIS HC A02/MF A01

This paper reports our preliminary results on an electrooptical light deflector for streak camera applications that uses tungsten bronze SBN:60% crystals. We found the performance of these ferroelectric crystals to be an order of magnitude better than the best LiNbO sub 3 crystals currently available. We discuss the theory and performance of this crystal as well as other bronze crystals for application to the streak camera. DOE

N89-10619 New Mexico State Univ., University Park.
ADEQUACY OF THE TRANSMITTED NEAR-FIELD TECHNIQUES FOR MEASURING OPTICAL FIBER CORE DIAMETER Ph.D. Thesis
Ernest Makoto Kim 1987 243 p
Avail: Univ. Microfilms Order No. DA8803930

A computer-controlled system is described for measuring transmitted near-field (TNF) radiation patterns in two dimensions from optical fibers. The dependence of the TNF system on source wavelength and linewidth, fiber sample length, and launch position was studied. These studies showed that measurements made by the transmitted near-field method were not severely affected by these parameters. The transmitted near-field technique was also shown to be a viable method for determining optical fiber core diameter. The novel 2-D capability of the system was used to obtain an iso-intensity map of multimode optical fiber cores. The maps provided information on core noncircularity. Leaky modes were shown in theoretical studies to attenuate rapidly if the fiber core is noncircular. The core noncircularity data were used to confirm this theory experimentally. Innovative single-mode optical fiber measurements were also made with the system. These included mode cutoff, index profile by short wavelengths, mode-field diameter, and 2-D mode-field diameter measurements.
Dissert. Abstr.

N89-10620 Heriot-Watt Univ., Edinburgh (Scotland).
OPTICAL BISTABILITY IN SEMICONDUCTOR WAVEGUIDES Ph.D. Thesis
J. Stewart Aitchison 1987 258 p
Avail: Univ. Microfilms Order No. BRDX80159

Reported is an experimental investigation of optical nonlinearities in GaAlAs waveguides and in particular the observation of four distinct types of cw optical bistability (OB). In the high refractive index layer three types of OB were observed: (1) optothermal refractive OB occurring on a timescale of r approximately 100 ms for input powers below 20 mW; (2) induced absorption OB again with r approximately 100 ms and for input powers of approxiamately 5 mW; and (3) an induced absorption switch with r approximately 2 microns and P sub o approximately 25 mW. The difference between these latter two effects has been studied in some detail and attributed to the degree of localization of the optothermal response. The fourth type of OB was observed in a leaky waveguide and was due to a redistribution of power between the modes. The effect was again optothermal in origin with r approximately 100 ms and P sub o approximately 25 to 30 mW. Finally, the experimental observation of two photon absorption in a waveguide geometry, illuminated by 35 ps pulses of Nd:YAG radiation is also reported. Dissert. Abstr.

N89-10621# Lawrence Livermore National Lab., Calif.
A NOVEL ALIGNMENT TECHNIQUE FOR POINTING AND CENTERING OPTICAL COMPONENTS
R. J. Ellis Aug. 1988 4 p Presented at the 32d International Technical Symposium on Optical and Opto-electronic Applied Sciences and Engineering, San Diego, Calif., 14 Aug. 1988
(Contract W-7405-eng-48)
(DE88-015441; UCRL-99168; CONF-880887-9) Avail: NTIS HC A02/MF A01

A relatively simple technique was devised to precisely align the components of a diagnostic instrument which recorded the first neutron images of imploding laser fusion targets. Alignment was achieved using a laser, a 2 mm diameter glass sphere, and a pair of lenses. With this technique, a 6 cm long aperture was pointed with an accuracy of 68 microradians and coaxially aligned with a target and detector separated by 10.5 meters. The alignment technique is described and critical features are discussed. DOE

N89-10622 British Petroleum Co. Ltd., London (England).
PHASE CONJUGATE REFLECTING MEDIA Patent Application
Lucy Margaret Connors and Marion Rosemary Drury 28 Oct. 1987 13 p Filed 16 Apr. 1987 Priority 24 Apr. 1986 GB 8610027
(EP-Patent-0-243-130-A1; EP-Patent-Appl-87303437.5; Int-Patent-Class-G-02-F-1/35; ETN-88-93129) Avail: UK Patent Office, 25 Southampton Buildings, London WC2A 1AY, United Kingdom

The use of films of poly(acetylene) whether isotropic, of low crystallinity or oriented as a nonlinear phase conjugate reflecting medium is proposed. The principle can be applied to devices comprising phase conjugate mirrors, or use of such devices for degenerate four-wave mixing or for producing real time holograms. The resultant devices can be used in laser targetting, high speed image processing, optical communication, and for power and image transmission. ESA

N89-10623# Battelle Inst., Frankfurt am Main (West Germany).
DEVELOPMENT OF RADIATION HARDENED FAR IR DETECTOR ARRAYS. VOLUME 1: PHASE 2 Final Report
D. Engemann, R. Faymonville, D. Haschberger, O. Frenzel, and M. Ilgenstein Paris, France ESA Feb. 1986 43 p
(Contract ESTEC-5506/83-NL-GM)
(BF-R-65.641-2; ESA-CR(P)-2638-Vol-1; ETN-88-93168) Avail: NTIS HC A03/MF A01

A detector manufacturing method for the fabrication of radiation hardened detectors and detector arrays is presented. Different doping levels of the IR sensitive layer of the epitaxial double layer detectors were investigated leading to background radiation limited performance data of noise equivalent power = 10 to the

minus 16th power W/sq rt Hz at a current responsivity of 2 A/W. These improvements compared to the results of Phase 1 are obtained without enhancing the low sensitivity of these devices to ionizing radiation. Crosstalk reduction is found to be at least a factor of 1:35. Besides the improvement in the performance data, the detectors and the arrays are less sensitive to ionizing radiation than conventional Si:P detectors. ESA

N89-10624# Battelle Inst., Frankfurt am Main (West Germany).
DEVELOPMENT OF RADIATION HARDENED FAR IR DETECTOR ARRAYS. VOLUME 2: PHASE 3 Final Report
D. Engemann, R. Faymonville, D. Haschberger, O. Frenzel, and M. Ilgenstein Paris, France ESA Jan. 1987 43 p
(Contract ESTEC-5506/83-NL-GM)
(BF-R-65.641-3; ESA-CR(P)-2638-Vol-2; ETN-88-93169) Avail: NTIS HC A03/MF A01

A detector manufacturing method for the fabrication of radiation hardened detectors and detector arrays is presented. Different types of linear and area arrays were fabricated and measured. The best performance data are noise equivalent power = 5 times 10 to the minus 17th power W/sq rt Hz, and current responsivity = 6 A/W. These improvements compared to the results of Phase 2 are obtained without enhancing the low sensitivity of these devices to ionizing radiation, which remains an order of magnitude lower than that of conventional extrinsic photoconducting detectors. An upper limit of the crosstalk is calculated to be 5 percent. ESA

N89-10625# European Space Agency, Paris (France).
CONSIDERATIONS AND CALCULATIONS FOR APPLICATION OF AN OPTICAL AMPLIFIER AS AN END- AND PREAMPLIFIER
Friedrich Malota Jul. 1988 43 p Transl. into ENGLISH of Ueberlungungen und Rechnungen zur Andendung eines Optischen Verstaerkers als End- und Vorverstaerder (Oberpfaffenhofen, Fed. Republic of Germany, DFVLR) Original language document was anounced as N86-32734
(ESA-TT-1004; DFVLR-FB-86-11; ETN-88-93177) Avail: NTIS HC A03/MF A01; original German version available from DFVLR, VB-PL-DO, 90 60 58, 5000 Cologne, Fed. Republic of Germany 25.50 Deutsche marks

The simultaneous application of an optical amplifier for outgoing laser pulses and as a preamplifier for such pulses, which are reflected from a target are discussed. The calculations show that such application is possible, when definite time differences between outgoing pulses and reflected ones are kept. Calculations for the signal to noise ratio of preamplifiers are given. ESA

75 PLASMA PHYSICS

Includes magnetohydrodynamics and plasma fusion.

For ionospheric plasmas see *46 Geophysics*. For space plasmas see *90 Astrophysics*.

N89-10626# Purdue Univ., West Lafayette, Ind. School of Nuclear Engineering.
NON-LOCAL KINETIC TRANSPORT STUDIES OF A FIELD-REVERSED CONFIGURATION Annual Technical Report, 1 Jul. 1987 - 30 Jun. 1988
C. K. Choi 1988 63 p
(Contract DE-FG02-87ER-53250)
(DE88-012397; DOE/ER-13553/2) Avail: NTIS HC A04/MF A01

The Field Reversed Configuration (FRC) is a type of plasma experiment of current interest in fusion research. The life of an FRC can be divided into two periods, a highly dynamic formation phase followed by a quiescent equilibrium phase. The FRC can be a viable source of fusion energy only if the confinement properties of the equilibrium phase are sufficient for breakeven. The purpose of this report is to provide the FRC theory community with equilibrium models that have been found to be useful. Three equilibrium models are presented: a kinetic model, a rigidly rotating model, and an MHD model. DOE

N89-10627# Nagoya Univ. (Japan). Inst. of Plasma Physics.
NEOCLASSICAL RESONANT-PLATEAU TRANSPORT IN THE NONCIRCULAR EQUIPOTENTIAL SURFACE OF A TANDEM MIRROR
I. Katanuma, Y. Kiwamoto, K. Ishii, K. Yatsu, and S. Miyoshi (Tsukuba Univ., Ibaraki, Japan) Jul. 1988 15 p
(IPPJ-879; ISSN-0469-4732) Avail: NTIS HC A03/MF A01

Neoclassical resonant-plateau transport in a minimum-beta anchored tandem mirror is calculated in an experimentally observed case that a magnetic flux tube of an equipotential contours is not circular at the central cell. Author

N89-10628# Sandia National Labs., Albuquerque, N. Mex.
METALLIC MATERIALS AS PLASMA FACING COMPONENTS
J. B. Whitley, K. L. Wilson, and D. A. Buchenauer Mar. 1988 40 p Presented at the 3d International Conference on Fusion Reactor Materials, Karlsruhe, Fed. Republic of Germany, 4-8 Oct. 1987 Submitted for publication
(Contract DE-AC04-76DP-00789)
(DE88-010103; SAND-87-2308; CONF-871036-36) Avail: NTIS HC A03/MF A01

The design and fabrication of suitable plasma facing components for fusion devices are difficult tasks with often conflicting requirements. Most operating devices utilize stainless steel as the first wall material and graphite for the main limiters. There are potential problems with the extrapolation of graphite to power producing reactors and, hence, the evaluation of metallic alternatives is important. Prime candidate metals are beryllium and tungsten for plasma interactive components. There are several potential advantages to metallic components over graphite or ceramics. In general, metals have superior fracture toughness, are inert chemically to the hydrogen atmosphere, have a better developed fabrication and joining technology, and better resistance to neutron damage. Metals are limited, however, in their ability to withstand disruption damage and, with the exception of beryllium, require a very low edge temperature to avoid sputtering problems. The current status of research in the areas of erosion, tritium permeation and inventory, thermal stress and fatigue, off-normal events, neutron irradiation and fabrication on these and other metals is reviewed and compared to the prime non-metal choice of graphite. DOE

N89-10629# Nagoya Univ. (Japan). Inst. of Plasma Physics.
ADVENTURES IN MAGNETOHYDRODYNAMICS
John L. Johnson (Princeton Univ., N. J.) Mar. 1988 75 p
(IPPJ-862; ISSN-0469-4732) Avail: NTIS HC A04/MF A01

The material in the report was presented in a series of three lectures presented on two days, October 29 and 30, 1987, at Nagoya University. A survey of magnetohydrodynamic theory was given as it applies to toroidal confinement. The material was broken down into four sections: (1) the derivation and justification of the MHD equations; (2) the equilibrium problem; (3) linearized stability; and (4) comments on nonlinear evolution, magnetic islands and transport theory. Author

N89-10630# Instituto de Pesquisas Espaciais, Sao Jose dos Campos (Brazil). Lab. Associado de Plasma.
EXPERIMENTAL STUDIES ON THE SURFACE CONFINED QUIESCENT PLASMA AT INPE
Jose Leonardo Ferreira, Julia GuimaraesFerreira, Gilberto M. Sandonato, Maria Virginia Alves, Gerson Otto Ludwig, and Antonio Montes Jun. 1988 12 p Presented at the 6th Japan-Brazil Symposium on Science and Technology, Sao Paulo, Brazil, 10-12 Aug. 1988 Submitted for publication
(INPE-4605-PRE/1328) Avail: NTIS HC A03/MF A01

Quiescent plasma machines are being used in several experiments at the Associated Plasma Laboratory at INPE. The research activities comprises particle simulation studies on ion acoustic double layers, and studies on the plasma production and loss in surface confined magnetic multidipole thermionic discharges.

Recent results from these studies have shown a non-maxwellian plasma formed in most of the discharge conditions. The plasma leakage through the multidipole fields shows an anomalous diffusion process driven by ion acoustic turbulence in the magnetic sheath. The information derived from these studies are being used in the construction and characterization of ion sources for shallow ion implantation in semiconductors, in ion thrusters for space propulsion, and in the development of powerful ion sources for future use in neutral beam injection systems. Author

N89-10631# Nagoya Univ. (Japan). Inst. of Plasma Physics.
GAS-CONTACT COOLING FOR VUV LASER OSCILLATION IN RECOMBINING PLASMAS
Utaro Furukane, Kuninori Sato, and Toshiatsu Oda Jul. 1988 34 p
(IPPJ-881; ISSN-0469-4732) Avail: NTIS HC A03/MF A01

High potentiality leading to rapid cooling of a high temperature plasma is investigated in a gas contact cooling method in which the effect of finite time for mixing the plasma and the contact gas is considered. The calculation has shown that the cooling is much more rapid than the radiative loss cooling and that the gain per unit length of the He II 164 nm is approximately 2/cm for the laser oscillation under an optimum condition. Possibility of realizing a shorter wavelength laser is also discussed in a plasma with higher charge number Z. Author

N89-10632# Nagoya Univ. (Japan). Inst. of Plasma Physics.
NEON PUFFING EXPERIMENTS IN THE JIPP T-IIU TOKAMAK
E. Meservey, K. Toi, R. Ando, R. Bell, S. Hirokura, R. Hulse (Princeton Univ., N. J.), K. Kawahata, Y. Kawasumi, S. Morita, and I. Ogawa et al. May 1988 36 p
(IPPJ-870; ISSN-0469-4732) Avail: NTIS HC A03/MF A01

Large amounts of neon were puffed into the discharge of the JIPP T-IIU tokamak, producing values of effective ion charge, Z sub eff, as large as 6 or 7 at linear average electron density bar n sub e, up to 3.5 x 10 to the 13th/cu cm. Electron temperatures, T sub e, rise to about twice those obtained in hydrogen puffing discharges that have the same current and electron density time behavior. Energy containment times are about the same for the neon and hydrogen puffing cases. At high values of Z sub eff, there appears to be a difference between the value of Z sub eff calculated from the bar n sub e produced by neon puffing and the values calculated from Spitzer conductivity corrected for trapped electron effects. Brightness of Ne V, VIII, and IX lines and total radiated power were calculated from temperature and density profiles and the estimated amount of neon in the discharge. These calculations agree well with measured values, except at the highest values of bar n sub e and Z sub eff, where the calculated power is twice measured. Author

N89-10633# New York Univ., New York.
LASER DIAGNOSTICS OF GAS DISCHARGE TUBES Final Technical Report
H. H. Stroke 28 Mar. 1988 5 p
(Contract DE-AC03-84SF-11996)
(DE88-008124; DOE/SF-11996/T1) Avail: NTIS HC A02/MF A01

The project was set up to develop the basic instrumentation and methods for optical diagnostics of plasmas. Specifically, the work was to permit the measurement of the radial distribution of atomic and ionic species in gas discharge tubes as exemplified by household fluorescent lamps. The aim is obviously to attempt to increase the efficiency by control of the discharge parameters. This report describes the system and results. DOE

N89-10634# Nagoya Univ. (Japan). Inst. of Plasma Physics.
STUDY OF CRITICAL BETA NON-CIRCULAR TOKAMAK EQUILIBRIA SUSTAINED IN STEADY STATE BY BEAM DRIVEN CURRENTS
K. Okano, Y. Ogawa, and H. Naitou Jul. 1988 61 p
(IPPJ-878; ISSN-0469-4732) Avail: NTIS HC A04/MF A01

A MHD-equilibrium/current-drive analysis code was developed to analyze the high beta tokamak equilibria consistent with the beam drive current profiles. In this code, the critical beta equilibrium, which is stable against the ballooning, kink, and Mercier mode, is determined first using MHD equilibrium and stability analysis codes (EQLAUS/ERATO). Then, the current drive and plasma parameters, required to sustain this critical beta equilibrium, are determined by iterative calculations. The beam driven current profiles are evaluated by the Fokker-Planck calculations on individual flux surfaces, where the toroidal effects on the beam ion and plasma electron trajectories are considered. The pressure calculation takes into account the beam ion and fast alpha components. A peculiarity of the method is that the obtained solution is not only consistent with the MHD equilibrium but also consistent with the critical beta limit conditions, in the current profile and the pressure profile. Using the beta is approximately 21 percent bean and beta is approximately D-type critical beta equilibria were scanned for various parameters. It was found that the achievable Q value for the bean type was always about 30 percent larger than for the D-type cases, where Q = fusion power/beam power. With strong beanness, Q is approximately 6 for DEMO type tokamaks (approximately 500 MWth) and Q is approximately 20 for power reactor size (4.5 GWth) are achievable. On the other hand, the Q value would not exceed sixteen for the D-type machines. Author

N89-10635# Sydney Univ. (Australia). Dept. of Wills Plasma Physics.
[THE STUDY OF HYDROMAGNETIC WAVES AND RF HEATING USING THE TORTUS TOKAMAK AND THE DEVELOPMENT OF DIAGNOSTIC TECHNIQUES]
1986 69 p
Avail: NTIS HC A04/MF A01

The Wills Plasma Physics Department of the University of Sydney research program continues to have two major focuses: the study of hydromagnetic waves and RF heating using the TORTUS tokamak and the development of diagnostic techniques. Their gas discharge studies have been expanded to include work on the characteristics of metal vapor vacuum arcs, as well as on the magnetron sputtering discharge used in the production of selective surfaces for solar collectors. Author

N89-10636# Texas Univ., Austin. Inst. for Fusion Studies.
INITIAL EVOLUTION OF NONLINEAR MAGNETIC ISLANDS IN HIGH TEMPERATURE PLASMAS
M. Kotschenreuther Jun. 1988 14 p
(Contract DE-FG05-80ET-53088)
(DE88-012346; DOE/ET-53088/319) Avail: NTIS HC A03/MF A01

The evolution of nonlinear magnetic islands is computed in the kinetic collisionality regime called semicollisional, which is appropriate to present fusion confinement devices. Realistic effects are included, such as the presence of small external field errors, radial electric fields, and omega. When present simultaneously, these effects can greatly change the stability of small amplitude nonlinear islands. Islands with ' Delta' greater than 0 can sometimes be prevented from growing to macroscopic size; it is also possible to produce moderate mode-number nonlinear instabilities in the plasma edge. Furthermore, island growth can be prevented by application of external fields with suitably chosen amplitude and frequency. DOE

N89-10637# Lawrence Livermore National Lab., Calif.
TIME-RESOLVED X-RAY CONVERSION EFFICIENCIES OF LASER-HEATED PLASMAS
F. Ze, R. L. Kauffman, B. Lasinski, L. Suter, S. Langer, H. Kornblum, G. Tietbohl, T. Thiessen, D. Montgomery, and R. P. Drake et al. 1988 12 p Presented at the 7th Topical Conference on High Temperature Plasma Diagnostics, Napa, Calif., 13 May 1988
(Contract W-7405-eng-48)
(DE88-015456; UCRL-97044; CONF-880364-33) Avail: NTIS HC A03/MF A01

Experiments to obtain time-resolved, soft X-ray emission from laser-driven plasmas are succinctly described. The spectra (0.19 keV less than or equal to h nu 1.3 keV) at various times have been deconvolved and energy-integrated to obtain time-resolved

yields from Au disk targets. The temporal profiles of the total thermal X-ray output power follow the overall laser temporal shape but do not show the high frequency fluctuation observed in the laser pulse. The behavior of the ratio of the instantaneous X-ray yields over the laser absorption is studied. The studies were done at the LLNL Nova laser facility. Single-pulse and pulses in picket fence configuration were used to heat gold targets. DOE

N89-10638# Air Force Geophysics Lab., Hanscom AFB, Mass.
MARGINAL STABILITY OF ION-ACOUSTIC WAVES IN A WEAKLY COLLISIONAL TWO-TEMPERATURE PLASMA WITHOUT A CURRENT Environmental Research Papers, Jun. 1986 - Jun. 1987
Bamandas Basu and John R. Jasperse 6 Aug. 1987 16 p
(AD-A195840; AFGL-TR-87-0240; AFGL-ERP-982) Avail: NTIS HC A03/MF A01 CSCL 20I

This report presents two important results for a weakly collisional, current-free, two-temperature electron-ion plasma: (1) that e-i collisions have an undamping effect on ion acoustic waves, and (2) that, for appropriate values of the plasma parameters, ion-acoustic waves become marginally stable. The results are based on the closed form solution for the dielectric function for the linearized Balescu-Lenard-Poisson kinetic equations. The weakly collisional ordering is necessary to obtain an iterative solution for the collisional dielectric function, imposes two independent restrictions on the parameters that characterize the plasma. The linearized Balescu-Lenard-Poisson equations are solved in the weakly collisional limit to show that ion-acoustic waves in a current-free plasma, which are Landau-damped in the absence of collisions, can become marginally stable due to the undamping effect of electron-ion (e-i) collisions. For sq rt.(T sub e0/T sub i0) sup 1/2 much less than (5/16) sq rt. (m sub i/m sub e) sup 1/2, the e-i collisional undamping effect dominates the i-i, e-e, and i-e collisional effects, and marginal stability occurs when the collisional undamping rate balances the electron and ion Landau damping rates. GRA

N89-10639# National Aerospace Lab., Tokyo (Japan).
SPECTRAL CHARACTERISTICS OF ARC-HEATED LOW DENSITY PLASMA FLOWS (2) NITROGEN PLASMA
Y. Watanabe and N. Hirabayashi Nov. 1987 16 p In JAPANESE; ENGLISH summary
(NAL-TR-952; ISSN-0389-4010) Avail: NTIS HC A03/MF A01

Emissions from the nitrogen plasma flows produced in an arc-heated low-density wind tunnel were analyzed spectroscopically. The prominent emitters were identified as N2(+) first negative, N2 second positive, and N2 first positive systems. By measuring the rotational and vibrational intensity distributions in some bands of the N2(+) first negative system, temperatures in the plenum chamber were determined to be in the range between 5,500 and 6,900 K. Intensity distributions in the N2 first positive system seemed to be consistent with these temperatures. Molecular state populations of N2 and N2(+) showed deviations from those expected from LTE relations. In the low density test section flows, vibrational temperatures determined by the N2(+) first negative system bands showed a large difference from rotational temperatures. The N2 first positive system also showed nonequilibrium intensity distribution, which resembled those found in Lewis-Rayleigh afterglows. The possible excitation-emission mechanisms of these band-systems in the low density plasma flows are discussed. Author

N89-10640# Nagoya Univ. (Japan). Inst. of Plasma Physics.
EFFECT OF DOUBLE-SHELL STRUCTURE ON REDUCTION OF FIELD ERRORS IN THE STP-3(M) REVERSED-FIELD PINCH
S. Yamada, S. Masamune, H. Arimoto, H. Oshiyama, K. I. Sato, and A. Nagata Aug. 1988 19 p
(IPPJ-882; ISSN-0469-4732) Avail: NTIS HC A03/MF A01

Reversed-field pinch (RFP) operation on the STP-3(M) proved that the addition of a quasi-stationary vertical field B sub 1 together with a large reduction of irregular magnetic field at the shell gap could remarkably improve properties of the plasma confinement. Here, the gaps of a thick shell is wholely covered with the single primary coil having a shell shape. The measured field error at the gap is as small as 7.5 percent of the poloidal field. The application of B sub 1 sets the plasma at a more perfect equilibrium. In this operation, the plasma resistivity is decreased by a factor of 2 and the electron temperature rose up to 0.8 KeV. Author

N89-10641# Nagoya Univ. (Japan). Inst. of Plasma Physics.
ON THE GENERATION OF RUNAWAY ELECTRONS AND THEIR IMPACT TO PLASMA FACING COMPONENTS
Takaichi Kawamura, Haruo Obayashi, and Akira Miyahara Jun. 1988 14 p
(IPPJ-871; ISSN-0469-4732) Avail: NTIS HC A03/MF A01

Runaway electrons accompanied by inductive or noninductive plasma currents in a tokamak have severe interactions with plasma facing materials of a first wall, and influence the first wall structure due to activation and damage. Modeling of runaway electron generation near the wall in a tokamak is carried out. This includes the evaluation of acceleration along magnetic surfaces for relativistic electrons with energies larger than the runaway threshold. Penetration of runaway electrons of energy ranges from a few MeV to several ten MeV leads to gamma ray photon production by bremsstrahlung. One of the specific features of the impact on the first wall technology is that they give rise to activation due to giant resonance of the (gamma, n) nuclear reaction and, as a consequence, cause a requirement of remote maintenance. The other is that they bring energy deposition at brazing areas between low Z material and metal, or at a metal itself, and they result in melting, cracking and grain growth. The methods to estimate these effects using nuclear data and material data on the basis of runaway flux modeling are introduced and examples of estimation are given. Author

N89-10642# National Aerospace Lab., Tokyo (Japan).
SPECTRAL CHARACTERISTICS OF ARC-HEATED LOW DENSITY PLASMA FLOWS (1) ARGON PLASMA
Y. Watanabe and N. Hirabayashi Dec. 1987 20 p In JAPANESE; ENGLISH summary
(NAL-TR-954; ISSN-0389-4010) Avail: NTIS HC A03/MF A01

Argon plasma was investigated spectroscopically in the plenum chamber and the test section of the NAL arc-heated low density wind tunnel. The excitation temperature T sub ex, determined by relative intensity measurements of blue AI lines, and the electron density n sub e, derived from the Stark broadening of hydrogen Balmer lines, were used to examine the stagnation condition in the plenum chamber at a nondimensional enthalpy of up to 94 with pressure between 0.6 and 0.95 atm. The result showed that an LTE (Local Thermodynamic Equilibrium) state was attainable in the plenum chamber at a high enthalpy range. In the test section, the variation of T sub ex along a nozzle was measured and a large deviation of T sub ex from kinetic temperature was observed as predicted by nonequilibrium nozzle flow calculations. Molecular spectra excited in the flow were analyzed and the role of metastable atoms and recombination processes on long duration emission of jets was discussed. Author

N89-10643# Nagoya Univ. (Japan). Inst. of Plasma Physics.
STRUCTURAL INSTABILITY OF SHEATH POTENTIAL DISTRIBUTION AND ITS POSSIBLE IMPLICATIONS FOR THE L/H TRANSITION IN TOKAMAK PLASMAS
Zensho Yoshida and Hiroshi Yamada Jul. 1988 20 p
(IPPJ-877; ISSN-0469-4732) Avail: NTIS HC A03/MF A01

The Bohm equation of electrostatic potential distributions in one-dimensional plasmas was studied for various Mach numbers and plasma potentials. Solvability and structural stability were discussed using the Sagdeev potential. Implications of the structural stability for the L/H transitions in tokamak plasmas was also discussed. Author

N89-10644# Dartmouth Coll., Hanover, N.H. Dept. of Physics and Astronomy.
NONLINEAR MAGNETOHYDRODYNAMICS Progress Report, 1 Jan. 1987 - 30 Jun. 1988
David C. Montgomery Aug. 1988 11 p

(Contract DE-FG02-85ER-53194)
(DE88-015703; DOE/ER-53194/1) Avail: NTIS HC A03/MF A01

The results of a variety of 3-D numerical simulations of toroidal Z pinches are analyzed in which their relaxation to an MHD state which is force-free, but not minimum-energy, was followed. Analytical calculation, based on the principle of minimum energy dissipation rate, seems to account for many of the observed features. Tokamak temperature sawteeth about helical current channels have been observed in 3-D Strauss equations computations. An analytical theory of MHD turbulent density fluctuations has been presented and confirmed numerically. The report is structured as follows. The activity of the last two years is summarized. Abstracts of papers recently published and/or submitted are collected. DOE

N89-10645# Washington Univ., Seattle. Aerospace and Energetics Research Program.
CONFINEMENT AND HEATING OF HIGH BETA PLASMAS WITH EMPHASIS ON COMPACT TOROIDS Final Progress Report, period ending 15 Feb. 1987
G. C. Vlases and Z. A. Pietrzyk 1987 108 p
(Contract DE-AS06-72ET-53047)
(DE88-015777; DOE/ET-53047/26; UWAERP-14) Avail: NTIS HC A06

This report describes work performed at the University of Washington Aerospace and Energetics Research Program involving the compact toroid approach to magnetic confinement of plasmas. The five experiments comprising the effort are: the coaxial slow source experiment; the CSS project; the variable length experiment; the merging spheromak experiment; and the variable angle conical theta pinch experiment. DOE

76 SOLID-STATE PHYSICS

Includes superconductivity.

For related information, see also *33 Electronics and Electrical Engineering* and *36 Lasers and Masers.*

N89-10646# Technische Univ., Berlin (West Germany). Fachbereich fuer Physik.
INFLUENCE OF BOUNDARY SURFACE ROUGHNESS, ORDER EFFECTS AND DOPANTS ON OPTICAL PROPERTIES OF InP BASED METAL ORGANIC GAS PHASE EPITAXY (MOCVD) HETEROSTRUCTURE Ph.D. Thesis [EINFLUSS VON GRENZFLAECHENRAUHIGKEIT, ORDNUNGSEFFEKTEN UND DOTIERUNGEN AUF DIE OPTISCHE EIGENSCHAFTEN VON INP-BASIERTEN MOCVD-HETEROSTRUKTUREN]
Detlef Oertel 1987 122 p In GERMAN
(ETN-88-92986) Avail: NTIS HC A06/MF A01

Optical properties of AlInAs/GaInAs and GaInAsP/InP heterostructures in MOCVD were analyzed. Separation and quantification of the diffusion mechanism is studied in relation with growth mechanisms. Measurement methods and epitaxy procedures are explained and characterization methods of APMOCVD (by atmospheric pressure) are given. ESA

N89-10647# Argonne National Lab., Ill. Materials Science Div.
QUASIPERIODIC ORDERING IN GRAIN BOUNDARIES
N. Rivier and A. J. A. Lawrence (Heriot-Watt Univ., Edinburgh, Scotland) Apr. 1988 10 p Presented at the ILL/CODEST Workshop on Quasicrystalline Materials, Grenoble, France, 21 Mar. 1988 Prepared in cooperation with Heriot-Watt Univ., Edinburgh (UK). Dept. of Mathematics.
(Contract W-31-109-eng-38)
(DE88-012199; CONF-8803115-1) Avail: NTIS HC A02

The authors show that a general grain boundary consists of a quasiperiodic grid of topological dislocation lines, with the same golden or noble inflation coefficient in all directions. In some particular cases, the grid may be periodic in one or more directions along with translational symmetry then replaces inflation symmetry. DOE

N89-10648# Wisconsin Univ., Madison. Dept. of Metallurgical and Mineral Engineering.
THERMODYNAMICS AND KINETICS OF PHASE FORMATION OF THIN-FILM METAL ON GALLIUM ARSENIDE
Y. A. Chang 1988 6 p
(Contract DE-FG02-86ER-45274)
(DE88-015702; DOE/ER-45274/2) Avail: NTIS HC A02/MF A01

Objectives are to study the thermodynamics and kinetics of reactions between selected metals and GaAs in the bulk and thin-film forms. Even though micro-electronics devices are made of thin-films, their reactions cannot be rationalized without an understanding of the bulk phenomena. In fact, it is our belief that if we understand the thermodynamics and kinetics of the bulk reactions, we can forecast what may happen in thin-films, with perhaps the exception of epitaxial formations. In order to understand the bulk reactions between metals and GaAs, we need to know (1) the ternary phase diagram of Ga-As-M, (2) the diffusion path of GaAs/M in the bulk form and (3) reaction sequence between GaAs and M. Results obtained for items (2) and (3) in the bulk form are correlated with the results obtained for thin films. This paper summarizes the results obtained for several GaAs/M systems. DOE

N89-10649# Massachusetts Inst. of Tech., Cambridge.
SYNTHESIS AND STUDY OF MATERIALS FOR SUPERCONDUCTING ELECTRONICS Final Report, 1 Oct. 1984 - 30 Sep. 1987
P. M. Tedrow, R. Meservey, and T. P. Orlando 27 Mar. 1988 16 p
(Contract F49620-85-C-0005)
(AD-A195279; AFOSR-88-0453TR) Avail: NTIS HC A03/MF A01 CSCL 20C

Study of high-Tc superconductors in single-crystal and thin film form has begun. Investigation of semiconductor tunnel barriers has led to improvement of their theoretical description. Transport measurements of layered films of transition metal nitrides showed evidence of spin-orbit scattering and dimensional crossover effects. A technique for analyzing tunneling conductances to obtain the amount of Zeeman splitting using Fourier transforms has been developed and applied to V3Ga tunneling data. Spin-orbit scattering rates measured by two independent techniques, spin-polarized tunneling and magnetoresistance, have been shown to be similar. The strength of Fermi-liquid corrections on the effective magnetic moment of conduction electrons in vanadium and gallium has been found using spin-polarized tunneling. The effect of spin-orbit scattering on the density of states of superconducting thin films has been measured. The superconducting properties of ultra-thin niobium films were studied. GRA

N89-10650# Lawrence Livermore National Lab., Calif.
PRESSURE EFFECTS ON THE ELECTRONIC STRUCTURE OF 4f AND 5f MATERIALS
A. K. McMahan Jun. 1988 22 p Presented at the 18th Rare Earth Research Conference, Lake Geneva, Wis., 11 Sep. 1988
(Contract W-7405-eng-48)
(DE88-014149; UCRL-98881; CONF-880914-1) Avail: NTIS HC A03/MF A01

The gamma-alpha transition in Ce has been the focus of considerable theoretical effort. It has been attributed to a Mott-like transition of the 4f electrons from localized to itinerant character, as well as to volume sensitivity of the Kondo binding energy, to mention two of the competing explanations. Less attention has been directed towards analogous transitions observed at higher pressures in Pr, Nd, and Sm among the elemental 4f metals; and in Am, Cm, Bk, and Cf among the 5f metals. This paper reviews current theoretical understanding of the evolution in electronic structure which underlies these dramatic transitions in compressed 4f and 5f materials. DOE

N89-10651# Sandia National Labs., Albuquerque, N. Mex. Surface Chemistry and Analysis Div.
CHARACTERIZATION OF LAYERS CREATED USING SURFACE MODIFICATION TECHNIQUES
J. A. Borders 1988 11 p Presented at the Ion Implantation and Plasma Assisted Processes for Industrial Applications Conference, Atlanta, Ga., 21 May 1988
(Contract DE-AC04-76DP-00789)
(DE88-011918; SAND-87-2669C; CONF-8805134-4) Avail: NTIS HC A03/MF A01

Modern surface modification techniques, such as ion implantation, are capable of treating surface layers with properties very different from those of the bulk underlying material. By correlating measured chemical and structural changes, induced by a surface modification method, with the changes in the physical properties of interest, an understanding can be developed as to why a particular method of modification produces a surface layer with specific properties. There are a large number of modern analytical techniques capable of probing the chemical and structural properties of material surfaces. These methods are reviewed with emphasis on the techniques that are most commonly and commercially available. Examples of applications of these methods to surface-modified materials are given. DOE

N89-10652# Crystallume, Menlo Park, Calif.
PECVD (PLASMA ENHANCED CHEMICAL VAPOR DEPOSITION) DIAMOND THIN FILMS FOR RESEARCH INSTRUMENTATION Final Report, 9 Jan. 1987 - 30 Apr. 1988
M. G. Peters, J. M. Pinneo, K. V. Ravi, and L. S. Plano 1988 37 p
(Contract F49620-87-C-0102)
(AD-A195443; AFOSR-88-0647TR) Avail: NTIS HC A03/MF A01 CSCL 07B

Natural diamond exhibits several properties that indicate its utility as a semiconducting material. It is environmentally robust and an excellent thermal conductor, characteristics which would allow it to operate under temperature and radiation conditions that would render useless more commonly used semiconductors such as silicon and GaAs. In addition, it has optical properties that suggest its use as a short wavelength turnable laser. Several materials issues have prevented the development of diamond as a semi-conductor in device, laser and related applications. Natural diamond is expensive to obtain in useful sizes. The impurity and defect levels can vary dramatically from one sample to the next, making potential product reproducibility difficult to achieve. It is unavailable in thin film form. High pressure synthetic diamond is also unsuitable for the foregoing applications because of impurities and inability to produce thin films. GRA

N89-10653*# Roberts Associates, Inc., Vienna, Va.
CONVECTION EFFECTS IN PROTEIN CRYSTAL GROWTH Final Report, 28 Jul. 1986 - 26 Jun. 1988
Glyn O. Roberts 26 Jun. 1988 50 p
(Contract NAS8-36652)
(NASA-CR-179368; NAS 1.26:179368; RAI-87-P-4) Avail: NTIS HC A03/MF A01 CSCL 20L

Protein crystals for X-ray diffraction study are usually grown resting on the bottom of a hanging drop of a saturated protein solution, with slow evaporation to the air in a small enclosed cell. The evaporation rate is controlled by hanging the drop above a reservoir of water, with its saturation vapor pressure decreased by a low concentration of a passive solute. The drop has a lower solute concentration, and its volume shrinks by evaporation until the molecular concentrations match. Protein crystals can also be grown from a seed crystal suspended or supported in the interior of a supersaturated solution. The main analysis of this report concerns this case because it is less complicated than hanging-drop growth. Convection effects have been suggested as the reason for the apparent cessation of growth at a certain rather small crystal size. It seeems that as the crystal grows, the number of dislocations increases to a point where further growth is hindered. Growth in the microgravity environment of an orbiting space vehicle has been proposed as a method for obtaining larger crystals. Experimental observations of convection effects during the growth of protein crystals have been reported. Author

N89-10654# Washington Univ., St. Louis, Mo. Dept. of Physics.
STRUCTURE OF AMORPHOUS SILICON ALLOY FILMS Annual Report, 15 Jan. 1987 - 14 Jan. 1988
R. E. Norberg and P. A. Fedders May 1988 35 p Prepared in cooperation with Midwest Research Inst., Golden, Colo.
(Contract DE-AC02-83CH-10093)
(DE88-001167; SERI/STR-211-3352) Avail: NTIS HC A03/MF A01

The principal objective of the first year of this research program was to improve our understanding at the microscopic level of amorphous silicon--germanium alloy films deposited under various conditions to assist researchers in producing higher quality films. The method was a joint theoretical and experimental approach to the correlation of nuclear magnetic resonance (NMR), electron spin resonance (ESR), other characterizations, especially relating to rearrangements of hydrogen. Deuteron magnetic resonance reveals the presence of (and changes in) tightly bonded hydrogen (deuterium), weakly bonded hydrogen, molecular hydrogen, and rotating silyl groups. Ge-D configurations appear to be more varied than Si-D. It has been shown that ESR hyperfine structure results can be interpreted very well via dangling bonds, but not with floating bonds. The presence of fluorine correlates with the occurrence of larger microvoid dimensions. DOE

N89-10655# Colorado State Univ., Fort Collins.
BEAM ASSISTED FABRICATION OF 3-5/Si MONOLITHIC DEVICES Semiannual Report, 1 Oct. 1987 - 31 Mar. 1988
Gary Y. Robinson 31 Mar. 1988 10 p
(Contract F49620-86-K-0021)
(AD-A195479; AFOSR-88-0577TR) Avail: NTIS HC A02/MF A01 CSCL 20L

This research project is to explore two new methods for deposition of 3-5 semiconducting films on Si substrates. Using gas-source molecular beam epitaxy (MBE) and photo-beam and electron-beam assisted metal-organic chemical vapor deposition (MOCVD), GaAs and other 3-5 films with abrupt heterojunctions are being formed epitaxially on Si, and by means of optical and electrical characterization the suitability of the resulting 3-5/Si structures are being examined for use with monolithic devices. A well-confined hydrogen plasma of disk shape is employed both as a vacuum ultraviolet (VUV) lamp operating primarily at 121.5 nm and as a source of atomic hydrogen radicals. Both VUV photons and atomic hydrogen act to dissociate feedstock gases used in low-temperature (less than 400 C) metalorganic chemical vapor deposition (MOCVD). Thin films have been deposited both with the confined hydrogen plasma and with an excimer laser operating at 193 nm in order to compare the two methods. Preliminary chemical and electrical properties of the films deposited via the two methods indicate the superiority of the atomic hydrogen assisted MOCVD technique. GRA

N89-10656*# National Aeronautics and Space Administration. Marshall Space Flight Center, Huntsville, Ala.
A PRELIMINARY REVIEW OF ORGANIC MATERIALS SINGLE CRYSTAL GROWTH BY THE CZOCHRALSKI TECHNIQUE
B. G. Penn, A. W. Shields, and D. O. Frazier Sep. 1988 13 p
(NASA-TM-100341; NAS 1.15:100341) Avail: NTIS HC A03/MF A01 CSCL 20B

The growth of single crystals of organic compounds by the Czochralski method is reviewed. From the literature it is found that single crystals of benzil, a nonlinear optical material with a d sub 11 value of 11.2 + or - 1.5 x d sub 11 value of alpha quartz, has fewer dislocations than generally contained in Bridgman crystals. More perfect crystals were grown by repeated Czochralski growth. This consists of etching away the defect-containing portion of a Czochralski grown crystal and using it as a seed for further growth. Other compounds used to grow single crystals are benzophenone, 12-tricosanone (laurone), and salol. The physical properties, growth apparatus, and processing conditions presented

in the literature are discussed. Moreover, some of the possible advantages of growing single crystals of organic compounds in microgravity to obtain more perfect crystals than on Earth are reviewed. Author

N89-10657# Oak Ridge National Lab., Tenn.
THE DETECTION OF CONFORMATIONAL DISORDER BY THERMAL ANALYSIS
B. Wunderlich 1988 9 p Presented at the 9th International Congress on Thermal Analysis: ICTA 9, Jerusalem, Israel, 21 Aug. 1988 Prepared in cooperation with Tennessee Univ., Knoxville
(Contract DE-AC05-84OR-21400)
(DE88-012932; CONF-880813-2) Avail: NTIS HC A02/MF A01

Conformational disorder in crystals is found in many molecules that possess a plurality of conformational isomers. Typical examples are linear macromolecules such as polyethylene, polytetrafluoroethylene and trans-1,4-polybutadiene; and small molecules such as paraffins, cycloparaffins, soaps, lipids and many liquid-crystal forming molecules. Conformational motion is often coupled with the cooperative creation of disorder. In this case a heat and entropy of transition is observed by thermal analysis. Levels of transition entropies can be estimated, assuming most of the disorder can be traced to conformational isomerism. In case there is conformational disorder frozen-in at low temperature, thermal analysis can be used to find the glass transition of a condis crystal. An Advanced Thermal Analysis System has been developed, and will be described that permits a detailed interpretation of the thermal analysis traces. It rests with the establishment of high quality heat capacity for the rigid solid state (vibration only) and the mobile liquid state (vibrations and large amplitude cooperative motion). DOE

N89-10658# Los Alamos National Lab., N. Mex.
ELECTRONIC STRUCTURE OF THE QUENCHED SUPERCONDUCTIVITY OF MATERIALS Y(SUB 1-x)Pr(SUB x)Ba2Cu3O(SUB 7-DELTA)
J. S. Kang, J. W. Allen, Z. X. Shen, W. P. Ellis, J. J. Yeh, B. W. Lee, M. B. Maple, W. E. Spicer, and I. Lindau 1988 21 p Presented at the 18th Rare Earth Research Conference, Lake Geneva, Wisc., 11 Sep. 1988
(Contract W-7405-eng-36)
(DE88-014414; LA-UR-88-2112; CONF-880914-2) Avail: NTIS HC A03/MF A01

The superconductivity of the Y(sub 1-x)Pr(sub x)Ba2Cu3O(sub 7-delta) system is quenched as x increases. It has been speculated that Pr has valence 4+, resulting in extra charge in the Cu-O planes, and causing T sub c -quenching. To study the Pr electronic state, we have measured valence band resonant photoemission of the Y(sub 1-x)Pr(sub x Ba2Cu3O(sub 7- delta) system for x = 0, 0.2, 0.4, 0.6, 0.8, and 1.0. We find that the Pr valence is close to 3+ for all x and that the extracted Pr 4f spectral weight has a complex lineshape, implying extensive Pr 4f/O 2p hybridization which probably causes the T sub c -quenching by disrupting the electronic or magnetic structure of the x = 0 material, perhaps via a Pr-Cu superexchange interaction. DOE

77 THERMODYNAMICS AND STATISTICAL PHYSICS

Includes quantum mechanics; theoretical physics; and Bose and Fermi statistics.

For related information see also *25 Inorganic and Physical Chemistry* and *34 Fluid Mechanics and Heat Transfer.*

N89-10659# Lawrence Livermore National Lab., Calif. Dept. of Physics.
LOOPSPACE GENERAL COVARIANCE IN STRING FIELD THEORY
F. R. Klinkhamer May 1988 4 p Presented at the International Symposium on Spacetime Symmetries, College Park, Md., 24 May 1988
(Contract W-7405-eng-48)
(DE88-014170; UCRL-99090; CONF-880539-1) Avail: NTIS HC A02/MF A01

The prime goal in string physics today is to discover the underlying symmetries and derive the theory from first principles. Reported here is recent work by J. Greensite and author on how to make bosonic string field theory invariant under another enormous symmetry, namely loop-dependent general coordinate transformations. DOE

N89-10660# IIT Research Inst., Bartlesville, Okla. National Inst. for Petroleum and Energy Research.
THERMODYNAMIC PROPERTIES BY NON-CALORIMETRIC METHODS: PROGRESS REPORT
M. Michael Strube, R. D. Chirico, W. B. Collier, and W. V. Steele 1988 10 p
(Contract DE-FG05-87ER-13758)
(DE88-015422; DOE/ER-13758/1) Avail: NTIS HC A10/MF A01

This project for the Office of Energy Research focuses on the noncalorimetric determination of thermodynamic properties of polynuclear aromatic molecules through the extension of existing correlation methodologies and through molecular spectroscopy with statistical mechanics. This report highlights progress during the first third of the contract period. Important advances include: derivation of group-contribution parameters for estimation of thermodynamic properties for polycyclic hydrocarbon and nitrogen-containing compounds; calculation of thermodynamic properties for eight key monocyclic compounds based on new and literature spectra were completed for the derivation of 'ring-correction' property estimation parameters; design and construction of a long pathlength, far-infrared sample cell for the collection of vapor-phase spectra of low vapor-pressure compounds; development of a method to predict the vibrational frequencies of two- and three-ring polycyclic molecules to an accuracy sufficient for identifying the fundamental vibrations in experimental spectra; and development of a method to calculate the kinetic energy expansions as a function of the coordinate for the ring-puckering, ring-twisting (in-phase), and ring-twisting (out-of-phase) vibrations of 9,10-dihydroanthracene and related molecules. DOE

N89-10661# Florida Univ., Gainesville. Dept. of Physics.
GRAVITATIONAL TIME DELAY DUE TO A SPINNING STRING
Diego Harari and Alexios P. Polychronakos 1988 8 p
(Contract DE-FG05-86ER-40272)
(DE88-014733; DOE/ER-40272/57; UFTP-88-6) Avail: NTIS HC A02/MF A01

We show that gravity around a straight cosmic string that carries angular momentum per unit length (J) induces a delay between the arrival time of two particles that describe an arbitrary closed trajectory around the string with the same speed at each point but in opposite directions. The time delay is 16GJ, where G is Newton's constant. The particle delayed is the one that circles the closed path in the sense contrary to the angular momentum. As a consequence, double images of a star produced by the string acting as a gravitational lens will acquire a relative time delay, thus providing a mechanism, at least in principle, to measure the string angular momentum. We argue, however, that in any realistic model the time delay effect is negligible. We also discuss other possible implications of this effect in 2+1 dimensions. DOE

N89-10662# Yale Univ., New Haven, Conn. Dept. of Applied Physics.
INVESTIGATION OF SUPERRADIANT LDV MARKERS AND THREE-COMPONENT VELOCITY MAPPING Final Report, 1 Jan. 1985 - 31 Dec. 1987
Richard K. Chang, Marshall B. Long, and Roman Kuc 10 Mar. 1988 29 p
(Contract F49620-85-K-0002)
(AD-A195504; AFOSR-88-0641TR) Avail: NTIS HC A03/MF A01 CSCL 14B

Research areas were: (1) micrometer-size droplets; (2)

three-dimensional scalar mapping; and (3) three-dimensional velocity mapping. Nonlinear optical interactions in a droplet occur at remarkably low input intensity levels because the droplet acts as a lens to concentrate the input radiation at a location just within the shadow face and as an optical cavity to provide feedback for the internally generated radiation. The following nonlinear optical effects have been observed in single droplets: lasing; stimulated Raman scattering up to the 14th order; coherent Raman gain due to the presence of another input wave; phase-modulation broadening of the elastically scattered and stimulated Raman scattered radiation; delay time in generating the multiorder stimulated Raman scattering; and effective Q-factor of the droplet cavity based on a lifetime measurement of the radiation trapped within the droplet. Laser-induced breakdown within the droplet occurs when the rising portion of the input laser pulse causes multiphoton ionization, which is followed by cascade multiplication. The resultant plasma within the droplet transforms a nominally transparent droplet into an absorping droplet, and the remaining portion of the input laser pulse heats the droplet. Plasma is ejected from the droplet, first from the shadow face and then from the illuminated face. Once the plasma has been quenched, the droplet undergoes explosive vaporization. Three-dimensional scalar mapping was made possible by sweeping the laser illumination sheet and by recording scattering images on a high speed framing camera. GRA

N89-10663# Los Alamos National Lab., N. Mex.
THE INVERSE-SQUARE LAW AND QUANTUM GRAVITY
M. M. Nieto, T. Goldman, and R. J. Hughes 1988 4 p Presented at the Workshop on Relativistic Gravitation Experiments in Space, Annapolis, Md., 28 Jun. 1988
(Contract W-7405-eng-36)
(DE88-014332; LA-UR-88-2351; CONF-8806193-1) Avail: NTIS HC A02/MF A01

This paper briefly discusses a modification to central potential of gravity when antimatter is involved and the possible existence of quantum gravity and a fifth force of nature. DOE

80 SOCIAL SCIENCES (GENERAL)

Includes educational matters.

No abstracts in this category.

81 ADMINISTRATION AND MANAGEMENT

Includes management planning and research.

N89-10664# Metocean Consultancy Ltd., Haslemere (England).
REVIEW OF THE REQUIREMENTS FOR HIGHER LEVEL ERS-1 PRODUCTS WITHIN EUROPE
Norman H. Babbedge and Kevin R. Deeming Paris, France ESA Sep. 1987 64 p
(Contracts ESA-6877/87-HGE-1(SC); P73/1987)
(ESA-CR(P)-2586; ETN-88-93030) Avail: NTIS HC A04/MF A01

Potential users of ERS-1 ocean, ice, and land products were asked to define their needs. Low bit rate ocean products such as wind and wave data are proven products which should be available on a near operational basis. For these, users are able to be fairly specific about their requirements. For SAR products and most other land products, users are not yet in a position to specify formats for products because some are still experimental. For these products the attitude is much more one of wait and see. Nevertheless, considerable interest is expressed in their potential. Users are concerned that no details are available of the proposed costs of the data, and that no provisional mission plans are published. Recommendations are made for the production of marketing booklets to be distributed to the ERS-1 end user community in advance of the launch of the satellite; many potential users have either not heard of ERS-1, or have only vague ideas of its capabilities and potential. ESA

N89-10665*# National Aeronautics and Space Administration, Washington, D.C.
CIVIL SPACE TECHNOLOGY INITIATIVE: A FIRST STEP
1988 25 p Original contains color illustrations
(NASA-TM-100949; NAS 1.15:100949) Avail: NTIS HC A03/MF A01 CSCL 05A

This is the first published overview of OAST's focused program, the Civil Space Technology Initiative, (CSTI) which started in FY88. This publication describes the goals, technical approach, current status, and plans for CSTI. Periodic updates are planned. Author

N89-10666# Advisory Group for Aerospace Research and Development, Neuilly-Sur-Seine (France). Aerospace Medical Panel.
PERFORMANCE ASSESSMENT REGISTER
[1988] 152 p
(AGARD-R-763) Copyright Avail: NTIS HC A08/MF A01

This Report presents the results of the first phase of AGARD Aerospace Medical Panel Working Group 12 on Human Performance Assessment Methods. The major goal of Working Group 12 is to develop a standardized test battery, satisfying conventional psychometric criteria such as reliability, validity, and sensitivity, for which an extensive data base may be compiled. Each member of the Working Group sent a simple questionnaire to researchers in his own country who are active in performance testing. The responses have been collated in the form of this Report, which, it is hoped, will facilitate the communication between laboratories necessary for the success of the subsequent standardization program. Author

N89-10066*# Ford Aerospace and Communications Corp., College Park, Md. Space Station Programs.
THE MISSION OPERATIONS PLANNING ASSISTANT
James G. Schuetzle *In* NASA, Goddard Space Flight Center, Proceedings of 1987 Goddard Conference on Space Applications of Artificial Intelligence (AI) and Robotics 1987 16 p Previously announced in IAA as A88-20484 (For primary document see N89-10063 01-12)
Avail: NTIS HC A99/MF E03 CSCL 05A

N89-10069*# Contel Federal Systems, Inc., Gaithersburg, Md.
AN EXPERT SYSTEM THAT PERFORMS A SATELLITE STATION KEEPIMG MANEUVER
M. Kate LinesBrowning and John L. Stone, Jr. *In* NASA, Goddard Space Flight Center, Proceedings of 1987 Goddard Conference on Space Applications of Artificial Intelligence (AI) and Robotics 1987 13 p Previously announced in IAA as A88-20488 (For primary document see N89-10063 01-12)
Avail: NTIS HC A99/MF E03 CSCL 05A

N89-10070*# Jet Propulsion Lab., California Inst. of Tech., Pasadena.
DEEP SPACE NETWORK RESOURCE SCHEDULING APPROACH AND APPLICATION
William C. Eggemeyer and Alan Bowling *In* NASA, Goddard Space Flight Center, Proceedings of 1987 Goddard Conference on Space Applications of Artificial Intelligence (AI) and Robotics 1987 9 p (For primary document see N89-10063 01-12)
Avail: NTIS HC A99/MF E03 CSCL 05A

N89-10071*# Computer Sciences Corp., Beltsville, Md. System Sciences Div.
SPACE STATION PLATFORM MANAGEMENT SYSTEM (PMS) REPLANNING USING RESOURCE ENVELOPES
Joy Lee Bush, Anna Critchfield, and Audrey Loomis *In* NASA, Goddard Space Flight Center, Proceedings of 1987 Goddard Conference on Space Applications of Artificial Intelligence (AI) and

Robotics 1987 17 p (For primary document see N89-10063 01-12)
Avail: NTIS HC A99/MF E03 CSCL 05A

N89-10072*# National Aeronautics and Space Administration. Goddard Space Flight Center, Greenbelt, Md.
CLEAR: COMMUNICATIONS LINK EXPERT ASSISTANCE RESOURCE
Larry G. Hull and Peter M. Hughes *In its* Proceedings of 1987 Goddard Conference on Space Applications of Artificial Intelligence (AI) and Robotics 1987 12 p (For primary document see N89-10063 01-12)
Avail: NTIS HC A99/MF E03 CSCL 05A

N89-10073*# National Aeronautics and Space Administration. Goddard Space Flight Center, Greenbelt, Md.
THE LOAD SHEDDING ADVISOR: AN EXAMPLE OF A CRISIS-RESPONSE EXPERT SYSTEM
Terry B. Bollinger, Eric Lightner, John Laverty (Bendix Field Engineering Corp., Greenbelt, Md.), and Edward Ambrose *In its* Proceedings of 1987 Goddard Conference on Space Applications of Artificial Intelligence (AI) and Robotics 1987 11 p (For primary document see N89-10063 01-12)
Avail: NTIS HC A99/MF E03 CSCL 05A

N89-10075*# National Aeronautics and Space Administration. Goddard Space Flight Center, Greenbelt, Md.
FIESTA: AN OPERATIONAL DECISION AID FOR SPACE NETWORK FAULT ISOLATION
Dawn Lowe, Bob Quillin, Nadine Matteson, Bill Wilkinson, and Steve Miksell (Stanford Telecommunications, Inc., McLean, Va.) *In its* Proceedings of 1987 Goddard Conference on Space Applications of Artificial Intelligence (AI) and Robotics 1987 21 p Prepared in cooperation with Bendix Field Engineering Corp., Greenbelt, Md. (For primary document see N89-10063 01-12)
(Contract NAS5-27600)
Avail: NTIS HC A99/MF E03 CSCL 05A

N89-10076*# National Aeronautics and Space Administration. Goddard Space Flight Center, Greenbelt, Md.
EXPERT SYSTEM SUPPORT FOR HST OPERATIONS
Bryant Cruse (Lockheed Missiles and Space Co., Greenbelt, Md.) and Charles Wende *In its* Proceedings of 1987 Goddard Conference on Space Applications of Artificial Intelligence (AI) and Robotics 1987 11 p (For primary document see N89-10063 01-12)
Avail: NTIS HC A99/MF E03 CSCL 05A

N89-10077*# Stanford Telecommunications, Inc., McLean, Va.
A HIERARCHICALLY DISTRIBUTED ARCHITECTURE FOR FAULT ISOLATION EXPERT SYSTEMS ON THE SPACE STATION
Steve Miksell and Sue Coffer *In* NASA, Goddard Space Flight Center, Proceedings of 1987 Goddard Conference on Space Applications of Artificial Intelligence (AI) and Robotics 1987 9 p (For primary document see N89-10063 01-12)
(Contract NAS5-29280)
Avail: NTIS HC A99/MF E03 CSCL 05A

N89-10078*# National Aeronautics and Space Administration. Goddard Space Flight Center, Greenbelt, Md.
AUTOMATION OF SPACECRAFT CONTROL CENTERS
Robert Dutilly *In its* Proceedings of 1987 Goddard Conference on Space Applications of Artificial Intelligence (AI) and Robotics 1987 9 p (For primary document see N89-10063 01-12)
Avail: NTIS HC A99/MF E03 CSCL 05A

N89-10079*# National Aeronautics and Space Administration. Goddard Space Flight Center, Greenbelt, Md.
SPACELAB DATA PROCESSING FACILITY (SLDPF) QUALITY ASSURANCE EXPERT SYSTEMS DEVELOPMENT
Angelita C. Kelly, Lisa Basile, Troy Ames, Janice Watson, and William Dallam (Lockheed Missiles and Space Co., Greenbelt, Md.) *In* NASA, Goddard Space Flight Center, Proceedings of 1987 Goddard Conference on Space Applications of Artificial Intelligence (AI) and Robotics 1987 23 p Previously announced in IAA as A88-20490 (For primary document see N89-10063 01-12)
Avail: NTIS HC A99/MF E03 CSCL 05A

N89-10081*# National Aeronautics and Space Administration. Ames Research Center, Moffett Field, Calif.
EXPERT SYSTEMS TOOLS FOR HUBBLE SPACE TELESCOPE OBSERVATION SCHEDULING
Glenn Miller, Don Rosenthal, William Cohen, and Mark Johnston (Space Telescope Science Inst., Baltimore, Md.) *In* NASA, Goddard Space Flight Center, Proceedings of 1987 Goddard Conference on Space Applications of Artificial Intelligence (AI) and Robotics 1987 13 p Previously announced in IAA as A88-20489 (For primary document see N89-10063 01-12)
Avail: NTIS HC A99/MF E03 CSCL 05A

N89-10082*# George Washington Univ., Washington, D.C. Inst. for Artificial Intelligence.
TOWARD AN EXPERT PROJECT MANAGEMENT SYSTEM
Barry G. Silverman, Arthur Murray, Coty Diakite (Intellitek, Inc., Rockville, Md.), and Kostas Feggos *In* NASA, Goddard Space Flight Center, Proceedings of 1987 Goddard Conference on Space Applications of Artificial Intelligence (AI) and Robotics 1987 18 p (For primary document see N89-10063 01-12)
Avail: NTIS HC A99/MF E03 CSCL 05A

N89-10084*# Ford Aerospace and Communications Corp., College Park, Md. Space Missions Div.
MAINTAINING CONSISTENCY BETWEEN PLANNING HIERARCHIES: TECHNIQUES AND APPLICATIONS
David R. Zoch *In* NASA, Goddard Space Flight Center, Proceedings of 1987 Goddard Conference on Space Applications of Artificial Intelligence (AI) and Robotics 1987 18 p (For primary document see N89-10063 01-12)
Avail: NTIS HC A99/MF E03 CSCL 05A

82 DOCUMENTATION AND INFORMATION SCIENCE

Includes information management; information storage and retrieval technology; technical writing; graphic arts; and micrography.

For computer documentation see *61 Computer Programming and Software.*

N89-10667 Illinois Univ., Urbana-Champaign.
AN EVALUATION OF ONLINE DATABASE SELECTION BY A GATEWAY SYSTEM WITH ARTIFICIAL INTELLIGENCE TECHNIQUES Ph.D. Thesis
Chen-gren Hu 1987 277 p
Avail: Univ. Microfilms Order No. DA8803073

The tremendous growth of computer readable data bases makes automated data base selection very desirable in online services. Gateway systems as components in online networks convert information among online systems and aid the users in various ways including data base selection. An evaluation of online data base selection by an existing gateway system (InfoMaster, a version of EasyNet) was performed, comparing data base selections made by experienced reference librarians with those made by inexperienced searchers aided by InfoMaster for the same set of queries. The results show that automated data base selection by InfoMaster still heavily depends on a human decision concerning the broad subject area into which a query falls. When the gateway user properly selects the subject area for a particular query, InfoMaster can do automated data base selection as well as the human intermediaries. Artificial intelligence techniques for automated data base selection by gateway systems were studied and a framework of AI techniques for this particular function was outlined based on the analysis of the evaluation results. Author

N89-10668# Massachusetts Inst. of Tech., Cambridge.
INTEGRATING DISTRIBUTED HOMOGENEOUS AND HETEROGENEOUS DATABASES: PROTOTYPES, VOLUME 3 Final Report, Sep. 1986 - Jan. 1988
Amar Gupta and Stuart Madnick Dec. 1987 220 p
(Contract DTRS57-85-C-00083)
(AD-A195852; AD-E500978; MIT-KBIISE-3) Avail: NTIS HC A10/MF A01 CSCL 12G

This volume discusses key issues relating to distributed databases, and presents alternate methods for integrating them together. It is divided into four parts. The first part, Evolution Towards Strategic Applications of Databases Through Composite Information Systems, divides applications into four categories: intercorporate, inter-divisional, inter-product, and inter-model. The second part, Distributed Homogenous Database systems: A Comparison between Oracle and Ingres, compares commercial products in terms of the levels of transparency and independence supported by them. The third part, Achieving a Single Model for Integrating Heterogenous Databases attempts to come up with a single unified modified that encompasses both the database issue and the communication issue. In the communication area, there are two types of standards: connection-oriented and connectionless. In the database area there are multiple standards suited for different environments. The fourth part, A Technical Comparison of Distributed Heterogenous Database Management Systems, describes eight systems being developed around the world. Because of the added complexity involved in translating between multiple systems and multiple data models, distributed heterogenous database systems are more complex than equivalent homogenous ones. While all of these eight systems are able to do global retrieves, their ability to perform global updates and other capabilities is varied. GRA

N89-10669 Illinois Univ., Urbana-Champaign.
LOOK: IMPLEMENTATION OF AN EXPERT SYSTEM IN INFORMATION RETRIEVAL FOR DATABASE SELECTION Ph.D. Thesis
Gail Ellen Thornburg 1987 111 p
Avail: Univ. Microfilms Order No. DA8803222

This project was designed to construct an advisory or expert system in one area of online information retrieval, specifically, choice of online data base. Problems of this domain include proliferation of potentially expensive data bases, and the difficulty of predicting the specific data base most likely to yield optimum results in the climate of extreme information compartmentalization. This implementation made use of an integrated set of software tools developed recently. The system was designed to reflect as closely as possible the decision making expertise of academic online searchers in life sciences. The implemented system, LOOK (nonacronymic), represented general features of 18 online data bases, and its advice succeeded in satisfying the experts involved in its development. The system used a rule based representation, and advisory sessions were guided by an inference based algorithm featuring three phases of evaluation. Issues discussed here include the numbers of variables and values required to represent the domain with an adequacy, the levels of abstraction apparent in these variables, and the difficulty of separating domain from world knowledge in constructing an apt representation. Dissert. Abstr.

N89-10670# Loughborough Univ. of Technology (England). Dept. of Transport Technology.
ATTITUDES TO THE USE OF COMPUTERISED INFORMATION SYSTEMS FOR PRODUCTION MANAGEMENT IN MANUFACTURING INDUSTRY: A SURVEY
D. Gillingwater Aug. 1987 56 p
(TT-8706) Avail: NTIS HC A04/MF A01

The application of computers in production management is receiving considerable attention at the present time. A frequent claim from those supporting the adoption of such information technology is that it can help the production manager to make complex decisions about sequencing and timing production activities to satisfy competing priorities: for example, meeting delivery deadlines, using resources more efficiently, minimizing stock levels, and maintaining production quality. Until recently such claims were not treated to any systematic appraisal. This report seeks to get at the facts. It consists of the presentation of findings gleaned from a survey of 107 companies in manufacturing, together with case studies of two companies who have recently ventured into the application of computerized information systems for production management (CISPMs). The overall aim of the survey was to obtain as objective an assessment as possible of the level of CISPM applications in UK manufacturing and the attitudes of production managers to their use (and usefulness). Author

N89-10671 Southampton Univ. (England).
AUTOMATIC GENERATION OF DATABASE SCHEMA Ph.D. Thesis
L. M. Hobbs 1987 208 p
Avail: Univ. Microfilms Order No. BRD-80847

Designing a computer database is a very complex task. It is a lengthy and time consuming process which involves investigating the business thoroughly, understanding the transactions that will be applied against the database and then translating this into the physical design. One of the major problems with this task is that once the information has been collected, it must then be cross-referenced, collated, documented and then used to formulate the design. When a system comprises hundreds of data items and tens of transactions, this is a very difficult manual task. This research shows that it is possible to develop a computer system which performs all of these tasks. Using the Entity Model as the starting point for the design, the attributes are defined. Then the transactions are described as text and verified, using a natural language processor against the information already entered into the system. Finally the schemas for a CODASYL compliant database are created. The system is now described in detail, using as an example to illustrate how a database may be created, a simple system for processing policies in a Life Assurance Company. Dissert. Abstr.

N89-10672# Massachusetts Inst. of Tech., Cambridge.
OBJECT-ORIENTED APPROACH TO INTEGRATING DATABASE SEMANTICS, VOLUME 4 Final Report, Sep. 1986 - Jan. 1988
Amar Gupta and Stuart Madnick Dec. 1987 298 p
(Contract DTRS57-85-C-00083)
(AD-A195853; AD-E500978; MIT-KBIISE-4) Avail: NTIS HC A13/MF A01 CSCL 12G

This volume presents the idea of using an object-oriented rule-based approach to integrating database semantics. It is divided into three parts. The first part, An Actor's Role in Integrating Expert and Database Systems, presents arguments for various approaches for using expert system techniques in combination with database management systems and concludes by recommending an object-oriented approach. The second part, Interfacing Objects and Databases, describes the motivation, development, and usage of a prototype Knowledge Oriented Representation Language (KOREL) that uses an object-oriented approach for interfacing to existing database systems. KOREL is implemented in common LISP. One of the important features of KOREL is that it automatically retrieves data as needed from the underlying databases rather than snapshot the entire database. This improves performance and minimizes the impact of skew. The third part, A Knowledge-Based System for Resolving Semantic Conflicts: A Problem of Integrating Heterogeneous Database Management Systems, presents a comprehensive example of the integration of multiple databases. The application analyzed involves multiple tour guide databases which have overlapping information that is often ambiguous, contradictory, and incomplete. Various types of semantic conflicts are identified and approaches to their resolution are presented. A prototype system, based on the Knowledge Engineering Environment (KEE) software, is described. GRA

N89-10673 Durham Univ. (England).
RELATIONAL MULTIMEDIA DATABASES Ph.D. Thesis
Sylivano Chiluli Non Kitinya 1987 179 p
Avail: Univ. Microfilms Order No. BRD-80802

The design and implementation of a Relational Multimedia Database System, RMDBS, is studied. RMDBS is designed to efficiently use storage space and manipulate various kinds of data; attribute data, bit mapped pictures, and programs in binary code. RMDBS is an integrated system which enables the user to manage and control operations on the different forms of data in a user friendly manner. This means that even non-experienced users can work with the system. The research is novel in that a true multimedia database was implemented within the framework of a traditional relational DBMS. Previous work in this area has concentrated either in building database management systems for storing picture-based data or multimedia databases which are not true database management systems. RMDBS is implemented using the Revelation database management system. Dissert. Abstr.

N89-10674# Arinc Research Corp., Annapolis, Md.
DEVELOP AN AUTOMATED DATA BASE MANAGEMENT SYSTEM (DBMS): REPORT ON DBMS SOFTWARE AND USER'S GUIDE Final Report
Aug. 1987 55 p
(Contract DE-AC01-85DP-20133)
(DE88-015996; DOE/DP-20133/T1; ARINC-3067-01-01-4437)
Avail: NTIS HC A04/MF A01

This final report, prepared for the Department of Energy Office of Military Application (OMA), describes the Task Two efforts of Contract DE-AC01-85DP20133. It addresses the software packages that constitute the OMA automated data base management system (DBMS) developed by ARINC Research Corporation. Off-the-shelf software adapted for these efforts and the software written by ARINC Research specifically for the project are also described. In addition to providing details about the DBMS software, the report includes and OMA DBMS User's Guide to be employed as a reference manual by OMA. The report was prepared after an approximately ten-month period devoted to user evaluation of the system. DOE

N89-10675# Massachusetts Inst. of Tech., Cambridge. Artificial Intelligence Lab.
UNITRAN (UNIVERSAL TRANSLATOR): A PRINCIPLE-BASED APPROACH TO MACHINE TRANSLATION Technical Report, Sep. 1984 - May 1987
Bonnie J. Dorr Dec. 1987 314 p
(Contracts N00014-80-C-0505; N00014-85-K-0124)
(AD-A195281; ARI-TR-1000) Avail: NTIS HC A14/MF A01 CSCL 05G

This report presents an approach to natural language translation that relies on principle based descriptions of grammar rather than rule-oriented descriptions. The model that has been constructed is based on abstract principles as developed by Chomsky (1981) and several other researchers working within the Government and Binding (GB) framework. The approach taken is interlingual, i.e., the model is based on universal principles that hold across all languages; the distinctions among languages are then handled by settings of parameters associated with the universal principles. The design of the UNITRAN (UNIversal TRANslator) system is such that a language may be described by the same set of parameters that specify the language in linguistic theory. Because of the modular nature of the model, the interaction effects of universal principles are easily handled by the system; thus, the programmer does not need to specifically spell out the details of rule applications. Because only a small set of principles covers all languages, the unmanageable grammar size of alternative approaches is no longer a problem. GRA

N89-10676# Instituto de Pesquisas Espaciais, Sao Jose dos Campos (Brazil).
A GENERAL DATA MODEL FOR GEOGRAPHIC INFORMATION SYSTEMS
Guaraci Jose Erthal, Gilberto CamaraNeto, and Diogenes SalasAlves May 1988 11 p Presented at the 16th Congress of International Society for Photogrammetry and Remote Sensing, Kyoto, Japan, 1-10 Jul. 1988 Submitted for publication
(INPE-4560-PRE/1301) Avail: NTIS HC A03/MF A01

Recently, a major trend in Geographic Information Systems (GIS) is integrating remote sensing data in such an environment. This work presents a GIS to be used in remote sensing applications, together with an image processing system, enabling satellite imagery to be combined with thematic maps, DTMs, and tabular data. In designing an integrated system, vector and raster data must be treated on a common data base. In order to overcome such diversities, the design relied on abstract data types. The data base uses a geo-relational model. Author

N89-10080*# Space Telescope Science Inst., Baltimore, Md.
AN EXPERT SYSTEM APPROACH TO ASTRONOMICAL DATA ANALYSIS
Mark D. Johnston *In* NASA, Goddard Space Flight Center, Proceedings of 1987 Goddard Conference on Space Applications of Artificial Intelligence (AI) and Robotics 1987 17 p (For primary document see N89-10063 01-12)
Avail: NTIS HC A99/MF E03 CSCL 05B

83 ECONOMICS AND COST ANALYSIS

Includes cost effectiveness studies.

No abstracts in this category.

84 LAW, POLITICAL SCIENCE AND SPACE POLICY

Includes NASA appropriation hearings; aviation law; space law and policy; international law; international cooperation; and patent policy.

No abstracts in this category.

85 URBAN TECHNOLOGY AND TRANSPORTATION

Includes applications of space technology to urban problems; technology transfer; technology assessment; and surface and mass transportation.

For related information see also *03 Air Transportation and Safety, 16 Space Transportation,* and *44 Energy Production and Conversion.*

N89-10677# Commerce Dept., Washington, D.C.
SPACE COMMERCE: AN INDUSTRY ASSESSMENT
May 1988 138 p
(PB88-214069) Avail: NTIS HC A07/MF A01 CSCL 05A

Existing and potential worldwide markets are identified for space related goods and services, focusing on five major areas: (1) Space Transportation; (2) Satellite Communications; (3) Satellite Remote Sensing; (4) Space Based Industrial Facilities; and (5) Materials Research and Processing in Space. Aspects of Insurance and Finance relevant to commercial ventures in these markets are examined. Finally, assessments are presented from U.S. industry representatives on their ability to compete against foreign competition in each of the five major areas. GRA

88 SPACE SCIENCES (GENERAL)

N89-10678*# National Aeronautics and Space Administration. Goddard Space Flight Center, Greenbelt, Md.
INTERPLANETARY MEDIUM DATA BOOK: SUPPLEMENT 3A, 1977-1985
David A. Couzens and Joseph H. King Apr. 1986 312 p
(NASA-TM-89630; NAS 1.15:89630;
NSSDC/WDC-A-RS-86-04a-Suppl-3A) Avail: NTIS HC
A14/MF A01 CSCL 03B

Supplement 3 of the Interplanetary Medium Data Book contains a detailed discussion of a data set compilation of hourly averaged interplanetary plasma and magnetic field parameters. The discussion addresses data sources, systematic and random differences, time shifting of ISEE 3 data, and plasma normalizations. Supplement 3 also contains solar rotation plots of field and plasma parameters. Supplement 3A contains computer-generated listings of selected parameters from the composite data set. These parameters are bulk speed (km/sec), density (per cu cm), temperature (in units of 1000 K) and the IMF parameters: average magnitude, latitude and longitude angles of the vector made up of the average GSE components, GSM Cartesian components, and the vector standard deviation. The units of field magnitude, components, and standard deviation are gammas, while the units of field direction angles and degrees. Author

89 ASTRONOMY

Includes radio, gamma-ray, and infrared astronomy, and astrometry.

N89-10679 Durham Univ. (England).
A POLARISATION STUDY OF SPIRAL GALAXIES Ph.D. Thesis
Derek Ward-Thompson 1987 150 p
Avail: Univ. Microfilms Order No. BRD-80835

Optical polarimetry results are presented for four spiral galaxies: NGC 5194 (M51), NGC 1068, NGC 4565 and NGC 4594 (M104). M51 and NGC 1068 show spiral polarization patterns which are interpreted as indicating a spiral magnetic field in each case. NGC 4565 and M104 show polarizations in their dust lanes which are parallel to their galactic planes, and which are interpreted in terms of a magnetic field in the plane of each. It is hypothesized that the observed magnetic field may be linked to galactic shocks. A discussion of the origin of galactic magnetic fields concludes that there is no evidence which necessitates a primordial magnetic field. Dissert. Abstr.

N89-10680# Instituto de Pesquisas Espaciais, Sao Jose dos Campos (Brazil).
GAMMA-RAY OBSERVATIONS OF SUPERNOVA SN 1987A
C. A. W. Souza, J. A. C. F. Neri, and U. B. Jayanthi Jun. 1988 7 p Presented at the 6th Simposio Nipo-Brasileiro de Ciencia e Tecnologia, Sao Jose dos Campos
(INPE-4604-PRE/1327) Avail: NTIS HC A02/MF A01

Theoretical investigations of supernova explosions predict a high emission of gamma rays (approximately .01 photons/sq cm/s) beginning around 300 days after explosion. A balloon-borne experiment was flown in October, 1987, to observe this emission. The payload carried 4 phoswich detectors of BGO/CsI and NaI/CsI with areas 169 sq and 100 sq cm, respectively. The detectors' sensitivity (for 10,000 s at 3g/cu cm with error bar of 3 sigma) is about .001 to approximately .0001 photons/sq sm/s at energies above 200 KeV. The detectors mounted on a stabilized platform observed the supernova for about 2 hours. The data are being analyzed for pulsations (equal to or less than 0.5 ms) and gamma ray emission. Energy spectra and temporal analysis will be presented and discussed. Author

N89-10681# Instituto de Pesquisas Espaciais, Sao Jose dos Campos (Brazil).
PROFILES OF EMISSION LINES IN AGN. PART 3: ON THE BROAD Ha COMPONENT OF IC 5063, IC 5135 AND NGC 2992
I. C. Busko and J. E. Steiner Aug. 1988 7 p Presented at the 134th IAU Symposium on Active Galactic Nuclei, Santa Cruz, Calif., 15-18 Aug. 1988
(INPE-4678-PRE/1375) Avail: NTIS HC A02/MF A01

The southern Seyfert galaxies IC 5063, IC 5135, and NGC 2992 were observed with 0.55 A resolution at the H alpha. After deblending the N II lines, a broad H alpha component is seen in the spectra of IC 5063 and IC 5135. In the first case, the broad component, with FWZI = 3000 km/s has 40 percent of the total H alpha flux. In the second case, the broad component has FWZI = 3800 km/s and 60 percent of the flux. In NGC 2992, contrary to previous reports that found a broad H alpha that is similar in intensity to the narrow components, we found that it is, at least, 5 times weaker. This difference is probably due to the different instrumental resolution. Author

N89-10682# European Space Agency, Paris (France).
A DECADE OF UV ASTRONOMY WITH THE IUE SATELLITE, VOLUME 1
E. J. Rolfe, ed. Jun. 1988 442 p Symposium held in Greenbelt, Md., 12-15 Apr. 1988; sponsored by NASA, ESA, the United Kingdom Science and Engineering Research Council, and the American Astronomical Society
(ESA-SP-281-Vol-1; ISSN-0379-6566; ETN-88-93155) Avail: NTIS HC A19/MF A01; ESA Publications Div., ESTEC, Noordwijk, Netherlands, 140 Dutch guilders

The IUE contribution to studies of the solar system, supernovae and their remnants; X-ray and cataclysmic binary systems; binary stars, circumstellar matter, and mass transfer; white dwarf stars; stellar activity; and stellar atmospheres and variable stars was discussed. For individual titles, see N89-10683 through N89-10770.

N89-10683*# Harvard-Smithsonian Center for Astrophysics, Cambridge, Mass.
OBSERVING SN 1987A WITH IUE
Robert P. Kirshner *In* ESA, A Decade of UV Astronomy with the IUE Satellite, Volume 1 Jun. 1988 p 3-7 (For primary document see N89-10682 01-89)
(Grants NAG5-645; NAG5-841; NSF AST-85-16537)
Avail: NTIS HC A19/MF A01; ESA Publications Div., ESTEC, Noordwijk, Netherlands, 140 Dutch guilders CSCL 03A

Spectra from IUE were used to study SN 1987A in order to examine its progenitor and stellar evolution before the explosion. The B3 Ia blue supergiant is identified as progenitor. The narrow UV lines from the circumstellar shell are discussed. When the supernova turns transparent in the ultraviolet, the ultraviolet spectra can provide important chemical information about the interior of the massive star. ESA

N89-10684# European Space Agency. ESA Tracking Station, Madrid (Spain). IUE Observatory.
CATACLYSMIC VARIABLES
Angelo Cassatella and Pier Luigi Selvelli (Osservatorio Astronomico, Trieste, Italy) *In its* A Decade of UV Astronomy with the IUE Satellite, Volume 1 Jun. 1988 p 9-15 (For primary document see N89-10682 01-89)
Avail: NTIS HC A19/MF A01; ESA Publications Div., ESTEC, Noordwijk, Netherlands, 140 Dutch guilders

The IUE results for classical novae, old novae, and recurrent novae are reviewed. Classical novae in outburst and quiescence, and the recurrent novae RS Oph and T CrB are emphasized. ESA

N89-10685# Kiel Univ. (West Germany). Inst. fuer Theoretische Physik und Sternwarte.
WHITE DWARFS
Volker Weidemann *In* ESA, A Decade of UV Astronomy with the IUE Satellite, Volume 1 Jun. 1988 p 17-27 (For primary

document see N89-10682 01-89)
Avail: NTIS HC A19/MF A01; ESA Publications Div., ESTEC, Noordwijk, Netherlands, 140 Dutch guilders

The IUE contribution to the study of white dwarf stars is reviewed. Hot DA stars, calibration problems in the SWP range, the 1400/1600 A quasimolecular features in cool spectra, the helium-rich DB and DBA stars, and cooler non-DA stars with UV carbon lines of type DQ and metal lines of type DZ are discussed. It is shown that carbon abundances are only weakly dependent on T(eff). For dredge-up this implies helium-layers of different thickness. Hot white dwarfs with metal lines, especially the PG 1159 class, are mentioned. ESA

N89-10686# Iowa State Univ. of Science and Technology, Ames. Astronomy Program.
IUE OBSERVATIONS OF PULSATING STARS: ATMOSPHERIC STRUCTURE, SHOCK WAVES AND STELLAR WINDS
L. A. Willson *In* ESA, A Decade of UV Astronomy with the IUE Satellite, Volume 1 Jun. 1988 p 29-40 Sponsored by the IUE project (For primary document see N89-10682 01-89)
Avail: NTIS HC A19/MF A01; ESA Publications Div., ESTEC, Noordwijk, Netherlands, 140 Dutch guilders

Pulsating stars studied by IUE, including Miras and semiregular long period variables, Cepheids, RR Lyrae stars, delta Scuti stars, Beta Cep stars, Be stars, hot subdwarfs (PG1159 stars), and pulsating white dwarfs are discussed. The interpretation of IUE observations of obviously pulsating stars in terms of static model atmospheres, models applicable to similar but nonpulsating stars, or models applicable to stars with different pulsation properties is always fundamentally wrong. The atmospheric temperature, density, and velocity structure of a star is very much altered by the presence of radial (or large amplitude nonradial) pulsation, and the structure depends strongly on the pulsation period and on the efficiency of mechanisms driving a stellar wind. For the well-studied radially pulsating stars (Beta Cep variables, Cepheids of all types, and long period variables) IUE observations are all at least qualitatively consistent with the predictions of models and analytic theory based on the assumption that pulsation is the dominant factor. ESA

N89-10687# Observatoire de Paris-Meudon (France).
IUE OBSERVATIONS OF PLANETARY ATMOSPHERES
Therese Encrenaz *In* ESA, A Decade of UV Astronomy with the IUE Satellite, Volume 1 Jun. 1988 p 41-46 (For primary document see N89-10682 01-89)
Avail: NTIS HC A19/MF A01; ESA Publications Div., ESTEC, Noordwijk, Netherlands, 140 Dutch guilders

The UV observations of planetary atmospheres were used to study the upper parts of the atmospheres, below and above the homopause. The IUE observations significantly contribute to knowledge of the aeronomy and photochemistry of planetary atmospheres. On Venus, SO2 is detected; ozone is observed on Mars; C2H2 and NH3 are detected in the Jovian upper atmosphere; acetylene is detected also on Saturn and Uranus; aurorae are detected and mapped on Jupiter and Saturn; Lyman alpha excess, interpreted by Voyager as electroglow, is observed on Uranus. The IUE can be useful for monitoring programs such as ozone on Mars and aurorae on giant planets. ESA

N89-10688*# Maryland Univ., College Park. Astronomy Program.
COMETS
Michael F. AHearn *In* ESA, A Decade of UV Astronomy with the IUE Satellite, Volume 1 Jun. 1988 p 47-58 Sponsored by NASA, Washington, D.C. (For primary document see N89-10682 01-89)
Avail: NTIS HC A19/MF A01; ESA Publications Div., ESTEC, Noordwijk, Netherlands, 140 Dutch guilders CSCL 03A

The IUE was used to study comets including the first dynamically new comet to approach closer than 3 AU. Differences between old and new comets are studied. Results relevant to the nature of cometary nuclei are discussed. Identification of species in the spectra; relative abundances; variability of comets; and comet mass are considered. ESA

N89-10689# Harvard-Smithsonian Center for Astrophysics, Cambridge, Mass.
SOME RECENT RESULTS FROM THE STUDY OF COOL STARS
A. K. Dupree *In* ESA, A Decade of UV Astronomy with the IUE Satellite, Volume 1 Jun. 1988 p 59-65 (For primary document see N89-10682 01-89)
Avail: NTIS HC A19/MF A01; ESA Publications Div., ESTEC, Noordwijk, Netherlands, 140 Dutch guilders

The IUE observations of circumstellar disks around low mass stars; extended atmospheric structures on cool dwarf stars; pulsation as a common phenomenon in luminous cool stars; and magnetic activity cycles in dwarf stars are reviewed. The results illustrate the unique and scientifically rewarding use of IUE, and the pressing need for multifrequency measurements and continuous measurements of cool stars in order to explore stellar evolution and atmospheric structure. ESA

N89-10690# New Mexico Inst. of Mining and Technology, Socorro. Astrophysics Research Center.
IUE OBSERVATIONS AND PHYSICAL PROCESSES OF INTERACTING BINARY STARS
Steven N. Shore *In* ESA, A Decade of UV Astronomy with the IUE Satellite, Volume 1 Jun. 1988 p 67-76 (For primary document see N89-10682 01-89)
Avail: NTIS HC A19/MF A01; ESA Publications Div., ESTEC, Noordwijk, Netherlands, 140 Dutch guilders

The IUE was used to study processes connected with accretion disk structure and stability, wind accretion and wind-wind collisions, contact systems, and stellar activity in close binary stars. Time dependent phenomena already known from optical studies appear to be even more important in the ultraviolet. The systems show flows which are unstable on timescales of single orbits, variable winds, tidally-induced phenomena, and unstable stellar components. Given that many of the physical processes in interacting binary systems may be nonlinear and highly dependent on the specific details of individual systems, and even on specific times of observation, the reliability of single object analyses and short timescale studies is called into question. Conservative models for mass transfer between components, steady or otherwise, are wrong and need to be corrected in order to properly understand binary star evolution. ESA

N89-10691*# Johns Hopkins Univ., Baltimore, Md.
Io: IUE OBSERVATIONS OF ITS ATMOSPHERE AND THE PLASMA TORUS
G. E. Ballester, H. W. Moos, P. D. Feldman, D. F. Strobel, T. E. Skinner, J.-L. Bertaux, and M. C. Festou (Observatoire de Besancon, France) *In* ESA, A Decade of UV Astronomy with the IUE Satellite, Volume 1 Jun. 1988 p 79-83 (For primary document see N89-10682 01-89)
(Grant NsG-5393)
Avail: NTIS HC A19/MF A01; ESA Publications Div., ESTEC, Noordwijk, Netherlands, 140 Dutch guilders CSCL 03A

Two of the main components of the atmosphere of Io, neutral oxygen and sulfur, were detected with the IUE. Four observations yield brightnesses that are similar, regardless of whether the upstream or the downstream sides of the torus plasma flow around Io is observed. A simple model requires the emissions to be produced by the interaction of O and S columns in the exospheric range with 2 eV electrons. Cooling of the 5 eV torus electrons is required prior to their interaction with the atmosphere of Io. Inconsistencies in the characteristics of the spectra that cannot be accounted for in this model require further analysis with improved atomic data. The Io plasma torus was monitored with the IUE. The long-term stability of the warm torus is established. The observed brightnesses were analyzed using a model of the torus, and variations of less than 30 percent in the composition are observed, the quantitative results being model dependent. ESA

N89-10692# State Univ. of New York, Stony Brook. Astronomy Program.
ON THE ABUNDANCE OF MICRON-SIZED PARTICLES IN SATURN'S A AND B RINGS
R. Wagener and J. Caldwell (York Univ., Ontario) *In* ESA, A Decade of UV Astronomy with the IUE Satellite, Volume 1 Jun. 1988 p 85-88 (For primary document see N89-10682 01-89)
Avail: NTIS HC A19/MF A01; ESA Publications Div., ESTEC, Noordwijk, Netherlands, 140 Dutch guilders

A set of 12 IUE spectra of Saturn's rings was obtained between July 1982 and Feb. 1985. The large aperture was positioned on the Cassini division at the western ansa and the size of the aperture was such that the A and B rings contributed equally to the total area inside the aperture. The IUE data are complemented at wavelength below 1600 A by Voyager 2 UVS data. The most obvious feature of the combined spectrum, which covers the wavelength range from 500 to 3000 A, is the water ice absorption edge between 1650 and 1700 A. Three different modeling approaches were used to interpret the data: multiple Rayleigh scattering approximation for extremely small particles (r = 0.003 microns); single Mie scattering for power law size distributions (r = 0.01 to 40 microns); and Hapke geometrical optics approximation for very large ring particles (r larger than 100 microns). The most satisfactory fits can be obtained with the Mie scattering approach and the Hapke approximation. However, the available data are not sufficient to uniquely determine a particle size distribution.
ESA

N89-10693*# Johns Hopkins Univ., Baltimore, Md.
JOVIAN EQUATORIAL H2 EMISSION FROM 1979-1987
M. A. McGrath, H. W. Moos, G. E. Ballester, and K. A. Coplin *In* ESA, A Decade of UV Astronomy with the IUE Satellite, Volume 1 Jun. 1988 p 89-92 (For primary document see N89-10682 01-89)
(Grant NsG-5393)
Avail: NTIS HC A19/MF A01; ESA Publications Div., ESTEC, Noordwijk, Netherlands, 140 Dutch guilders CSCL 03A

Ninety two IUE observations of the Jovian equatorial region taken between 2 Dec. 1978 and 1 Feb. 1988 were averaged together by date of observation, resulting in 22 averaged spectra which were fit with a model to determine the amount of H2 Lyman band emission in the region 1552 to 1624A. The data suggest that the H2 emission may vary with time. Especially suggestive is the marked downward trend of the emission between 1983 and 1987, during which time the strength of the emission in the 1552 to 1624A region decreases by a factor of 10. Uncertainty in the existing data and a gap in the data in 1980 and 1981 preclude a positive identification of a correlation between the brightness of the H2 emission and the major solar cycle.
ESA

N89-10694*# Arizona Univ., Tucson. Lunar and Planetary Lab.
LARGE TIME SCALE VARIATION IN HYDROGEN EMISSION FROM JUPITER AND SATURN
D. E. Shemansky, D. T. Hall, and J. B. Holberg *In* ESA, A Decade of UV Astronomy with the IUE Satellite, Volume 1 Jun. 1988 p 93-96 (For primary document see N89-10682 01-89)
(Grant NsG-5560)
Avail: NTIS HC A19/MF A01; ESA Publications Div., ESTEC, Noordwijk, Netherlands, 140 Dutch guilders CSCL 03A

The IUE and Voyager spacecraft observations of Jupiter and Saturn were combined to obtain a consistent measurement of temporal variation of the equatorial subsolar hydrogen emission. The outer planets appear to have rather independent behavior over time scales of the order of 10 yr, particularly in emission from the H Ly alpha line. The time interval from 1978 to the present shows variation of mean equatorial H Ly alpha brightness of 2 at Jupiter and 5 at Saturn. The relative magnitudes of the variations is sufficiently different to suggest that response to input from the Sun is at least nonlinear. The brightness of H2 band emission appears to be relatively more stable than H Ly alpha. There is evidence in IUE observations of a moderate increase in H2 band brightness with increasing time at Jupiter, in opposition to the variation in H Ly alpha.
ESA

N89-10695# Johns Hopkins Univ., Baltimore, Md. Dept. of Physics and Astronomy.
PHENOMENOLOGICAL ANALYSIS OF JOVIAN NORTH AURORAL H2 LYMAN BAND EMISSIONS
T. A. Livengood, H. W. Moos, and G. E. Ballester *In* ESA, A Decade of UV Astronomy with the IUE Satellite, Volume 1 Jun. 1988 p 97-100 (For primary document see N89-10682 01-89)
Avail: NTIS HC A19/MF A01; ESA Publications Div., ESTEC, Noordwijk, Netherlands, 140 Dutch guilders

Low-dispersion spectra taken with the IUE SWP from 1981 to 1988 are examined for gross longitudinal features in Jovian north auroral emission activity and for evidence of long-term trends in auroral characteristics. Integrated photon flux in the H2 Lyman-band region is extracted from each of the spectra, characterizing auroral emission strength at time of exposure. A plot of flux vs Jovian central meridian longitude (System III) corroborates an enhanced emission region centered at 180 deg reported by Skinner et al., (1984). Curves fit to fluxes grouped as scans (consecutive exposures made over a single Jovian rotation) vs longitude characterize width, position, and intensity of the enhanced region. Long-term variation in auroral peak intensity and width of the enhanced region vs time, as well as possible correlation of the light curve integrated over longitude as a measure of total power emitted, vs the longitudinal position of the intensity peak were studied. More energetic aurorae appear to peak at values of central meridian longitude lower than the previously reported 180 deg. Longitudinal dependence in the ratio of photon flux in the Lyman and Werner bands, an indicator of primary particle energy, is analyzed.
ESA

N89-10696# Space Telescope Science Inst., Baltimore, Md.
OBSERVATIONS OF SN 1987A: THE NARROW EMISSION LINES
Nino Panagia *In* ESA, A Decade of UV Astronomy with the IUE Satellite, Volume 1 Jun. 1988 p 103-106 (For primary document see N89-10682 01-89)
Avail: NTIS HC A19/MF A01; ESA Publications Div., ESTEC, Noordwijk, Netherlands, 140 Dutch guilders

The IUE observations of narrow emission lines of He2, CIII, NIII, NIV, NV, and OIII in the short wavelength spectrum of SN 1987A are presented. It is shown that they originate from a circumstellar shell, which is at least a light year in size and whose nitrogen abundance relative to both carbon and oxygen is greatly enhanced as compared with cosmic values. Because of its characteristics, this shell is likely to be the remnant of the wind ejected by the progenitor star when it was a red supergiant.
ESA

N89-10697*# National Aeronautics and Space Administration. Goddard Space Flight Center, Greenbelt, Md. Astronomy Programs.
THE PROGENITOR OF SN 1987A
G. Sonneborn *In* ESA, A Decade of UV Astronomy with the IUE Satellite, Volume 1 Jun. 1988 p 107-110 (For primary document see N89-10682 01-89)
Avail: NTIS HC A19/MF A01; ESA Publications Div., ESTEC, Noordwijk, Netherlands, 140 Dutch guilders CSCL 03A

Spatially resolved IUE spectra (1150 to 2000 A) taken at the position of SN 1987A in March 1987 show that the 12th mag B3 I star Sk -69 deg 202 disappeared. Only the fainter companion stars (Star 2 and Star 3) are present near the site of the supernova. It is concluded that Sk -69 deg 202 exploded to produce SN 1987A. The known characteristics of Sk -69 deg 202 are consistent with the interpretation that the progenitor was a relatively compact star, having a high-velocity low-density stellar wind prior to the outburst. Recent IUE spectra of SN 1987A (May 1988) show no evidence that Sk -69 deg 202 still exists inside the expanding ejecta.
ESA

N89-10698*# National Aeronautics and Space Administration. Goddard Space Flight Center, Greenbelt, Md. Astronomy Programs.

THE COMPLETE VISUAL LIGHT CURVE OF SN 1987A: THIRTEEN MONTHS OF FES OBSERVATIONS

G. Sonneborn *In* ESA, A Decade of UV Astronomy with the IUE Satellite, Volume 1 Jun. 1988 p 111-113 (For primary document see N89-10682 01-89)

Avail: NTIS HC A19/MF A01; ESA Publications Div., ESTEC, Noordwijk, Netherlands, 140 Dutch guilders CSCL 03A

Visual brightness measurements of SN 1987A are being obtained with the IUE acquisition camera and star tracker Fine Error Sensor, (FES) as part of each ultraviolet observation. Due to IUE's around-the-clock operation and lack of clouds, the FES record of SN 1987A provides the most complete set of visual photometry of the supernova made by any single instrument. The data illustrate the photometric limitations of the FES (+ or - 0.03 mag). Use of differential photometric methods are recommended for IUE observers desiring accurate photometry from FES measurements made during their observing shifts. ESA

N89-10699*# Johns Hopkins Univ., Baltimore, Md.

IUE OBSERVATIONS OF OXYGEN-RICH SUPERNOVA REMNANTS

W. P. Blair, J. C. Raymond, J. Danziger, and F. Matteucci (European Southern Observatory, Garching, West Germany) *In* ESA, A Decade of UV Astronomy with the IUE Satellite, Volume 1 Jun. 1988 p 117-120 (For primary document see N89-10682 01-89)

(Grants NAG5-701; NAG5-988; NAG5-87)

Avail: NTIS HC A19/MF A01; ESA Publications Div., ESTEC, Noordwijk, Netherlands, 140 Dutch guilders CSCL 03A

The IUE observations were used to determine the composition of the ejecta (especially C and Si abundances) and to test models for the ionization and excitation of the ejecta of two oxygen-rich supernova remnants (N132D in the Large Magellanic Cloud and 1E 0102-7219 in the Small Magellanic Cloud). Time-dependent photoionization by the EUV and X-ray radiation from 1E 0102-7219 can qualitatively explain its UV and optical line emission, but the density and ionization structures are complex and prevent a unique model from being specified. Many model parameters are poorly constrained, including the time dependence and shape of the ionizing spectrum. Moreover, the models presented are not self-consistent in that the volumes and densities of the optically emitting gas imply optical depths of order unity in the EUV, but absorption of the ionizing radiation was ignored. It is possible that these shortcomings reflect a more fundamental limitation of the model assumptions. It is assumed that the electron velocity distribution is Maxwellian and that the energy deposited by photoionization heats the electrons directly. The 500 eV electrons produced by the Auger process may excite or ionize other ions before they slow down enough to share their energy with other electrons. Many of the excitations would produce photons that could ionize lower ionization stages. ESA

N89-10700*# Colorado Univ., Boulder. Center for Astrophysics and Space Astronomy.

EJECTA IN SN 1006: THE KNOTTY ISSUE

Robert A. Fesen and Andrew J. S. Hamilton (Joint Inst. for Lab. Astrophysics, Boulder, Colo.) *In* ESA, A Decade of UV Astronomy with the IUE Satellite, Volume 1 Jun. 1988 p 121-124 (For primary document see N89-10682 01-89)

(Contract NAS5-31436)

Avail: NTIS HC A19/MF A01; ESA Publications Div., ESTEC, Noordwijk, Netherlands, 140 Dutch guilders CSCL 03A

The 1988 IUE SWP observations of a faint sdOB star situated behind the remnant of the supernova of AD 1006 are presented. These spectra along with IUE spectra of the star taken between 1982 and 1986 provide a detailed look at the elemental composition and dynamical properties of the SN 1006 remnant. Over the 6 years there were no significant changes in the absorption features associated with the remnant at 1281, 1330, or 1420 A. While the lack of variability in these absorption lines makes it impossible to decide whether the ejecta is distributed smoothly or in knots, it is clear that the 1281 A feature is a blend, requiring either S II absorption redshifted at 6000 km/sec plus Si II 1260 at 5200 km/sec, or else 2 individual Si absorbing regions. ESA

N89-10701# Milan Univ. (Italy). Dipt. di Fisica.

FAR UV OBSERVATIONS OF BLACK HOLE CANDIDATES: THE CASE OF LMC X-3

A. Treves, T. Belloni, P. Bouchet, L. Chiappetti, R. Falomo (Osservatorio Astronomico, Padova, Italy), L. Maraschi, and E. G. Tanzi *In* ESA, A Decade of UV Astronomy with the IUE Satellite, Volume 1 Jun. 1988 p 127-131 (For primary document see N89-10682 01-89)

Avail: NTIS HC A19/MF A01; ESA Publications Div., ESTEC, Noordwijk, Netherlands, 140 Dutch guilders

Stellar mass black hole candidates observed in the far UV are reported. All of them, except SS 433, which is heavily reddened, were detected in the far UV; A0620-00, was observed with the ANS satellite during X-ray flaring. For Cyg X-1, LMC X-1, LMC X-3 the data derive from 10 yr of IUE observations. Observations of 2 sources which have a massive non collapsed component, namely Cyg X-1 and LMC X-1 are reviewed, and A0620-00 and LMC X-3, whose visible component is much less luminous are discussed. The latter object is emphasized, because of its nontransient nature, and the important role of UV observations in clarifying the nature of the accretion disk around the hole. The UV observations yield information of the accretion onto black hole mainly because the UV radiation is produced by the interaction of the X-rays with the accretion material. As from variability studies, the dynamics of the accretion process can be reconstructed. Simultaneous monitoring at UV, optical, and X-ray frequencies is of the utmost importance. ESA

N89-10702# University Coll., London (England). Dept. of Physics and Astronomy.

IUE SPECTROPHOTOMETRY OF THE ACCRETION DISK OF HZ HER/HER X-1

Stephen J. Boyle and Ian D. Howarth *In* ESA, A Decade of UV Astronomy with the IUE Satellite, Volume 1 Jun. 1988 p 133-136 Sponsored in part by the United Kingdom Science and Engineering Research Council (For primary document see N89-10682 01-89)

Avail: NTIS HC A19/MF A01; ESA Publications Div., ESTEC, Noordwijk, Netherlands, 140 Dutch guilders

Low resolution IUE spectra of the accretion disk of the X-ray binary HZ Her/Her X-1 are presented. The UV flux contribution from the sub-giant companion HZ Her was predicted, using a model constrained by fits to B-magnitude photometry, and subtracted from the observed IUE spectra to leave accretion disk spectra. The observed disk UV fluxes are compared with those predicted by a simple model of the disk emission based on X-ray reprocessing. ESA

N89-10703*# National Aeronautics and Space Administration. Goddard Space Flight Center, Greenbelt, Md.

SIMULTANEOUS IUE, EXOSAT AND OPTICAL OBSERVATIONS OF THE UNUSUAL AM HER TYPE VARIABLE H058+608

C. R. Shrader, J. E. McClintock, R. Remillard, A. Silber, and D. Q. Lamb (Chicago Univ., Ill.) *In* ESA, A Decade of UV Astronomy with the IUE Satellite, Volume 1 Jun. 1988 p 137-140 (For primary document see N89-10682 01-89)

Avail: NTIS HC A19/MF A01; ESA Publications Div., ESTEC, Noordwijk, Netherlands, 140 Dutch guilders CSCL 03A

Simultaneous observations of the AM Her type variable H0538+608 made with IUE, EXOSAT, and a 1.3 m ground based telescope, and subsequent optical spectrophotometry at high and low resolution are discussed. The X-ray and optical data show clear evidence of a 3.30 + or - 0.03 hr period. Three SWP spectra were taken outside of eclipse and during overlapping phase intervals. The UV spectra contain strong emission lines characteristic of this class of objects and a flat continuum which appears to be deficient, given the brightness of source at optical

and X-ray wavelengths. There is evidence for intensity variations in emission lines, particularly C IV. The X-ray light curves for H0538+608 reveal behavior which may be related to irregularities in its accretion flow. ESA

N89-10704# Consiglio Nazionale delle Ricerche, Frascati (Italy). Istituto di Astrofisica.
A 0535+26/HDE 245770: A TYPICAL Be/X-RAY TRANSIENT SYSTEM: COORDINATED MULTIWAVELENGTH TWELVE YEARS MONITOR
F. Giovannelli, M. Burger, E. L. vanDessel, C. Bartolini, A. Guarnieri, A. Piccioni, V. G. Kurt (Academy of Sciences, USSR, Moscow), and E. K. Sheffer *In* ESA, A Decade of UV Astronomy with the IUE Satellite, Volume 1 Jun. 1988 p 141-144 (For primary document see N89-10682 01-89)
Avail: NTIS HC A19/MF A01; ESA Publications Div., ESTEC, Noordwijk, Netherlands, 140 Dutch guilders

The transient X-ray binary system A 0535+26/HDE 245770 was monitored at different wavelengths since its discovery as X-ray emitter. These coordinated observations reveal correlations in the variability of the optical and X-ray emissions. During activity periods of the system, UV discrete absorption components in Si IV and C IV resonance lines whose velocities vary between -300 and -600 km/sec were detected. The study of the narrow absorption components at the expected activity epochs (periastron passages of the neutron star) simultaneously with X-ray, optical, and IR observations is essential for a better knowledge of the wind structure of the Be star and its interaction with the neutron star. The physics and dynamics of mass transfer at periastron and subsequent X-ray flaring, are emphasized. ESA

N89-10705# Osservatorio Astronomico, Turin (Italy).
IUE AND OPTICAL OBSERVATIONS OF X-RAY SOURCES IN THE LARGE MARGELLANIC CLOUD (LMC)
Luciana Bianchi and Manfred Pakull (Observatoire de Besancon, France) *In* ESA, A Decade of UV Astronomy with the IUE Satellite, Volume 1 Jun. 1988 p 145-148 (For primary document see N89-10682 01-89)
Avail: NTIS HC A19/MF A01; ESA Publications Div., ESTEC, Noordwijk, Netherlands, 140 Dutch guilders

The optical counterparts of LMC X-6 (star Wo564) and of LHG-8 (HV5542) were observed with IUE and with optical instruments on the ground. The analysis of the UV spectral features and continuum flux, from which the values of the effective temperature and bolometric luminosity of the stars are derived, is outlined. Ultraviolet and optical observations of the source LHG-83, obtained over a 3 yr period, are also analyzed. ESA

N89-10706*# Arizona State Univ., Tempe. Dept. of Physics.
THE ANALYSIS OF SPECTRA OF NOVAE TAKEN NEAR MAXIMUM
L. L. Stryker, J. Hestand, S. Starrfield, R. Wehrse, P. Hauschildt, W. Spies, B. Baschek, and G. Shaviv (Technion - Israel Inst. of Tech., Haifa.) *In* ESA, A Decade of UV Astronomy with the IUE Satellite, Volume 1 Jun. 1988 p 149-152 Sponsored by NASA, Washington, D.C., NSF, Washington, D.C. and DOE, Washington, D.C. (For primary document see N89-10682 01-89)
Avail: NTIS HC A19/MF A01; ESA Publications Div., ESTEC, Noordwijk, Netherlands, 140 Dutch guilders CSCL 03A

A project to analyze ultraviolet spectra of novae obtained at or near maximum optical light is presented. These spectra are characterized by a relatively cool continuum with superimposed permitted emission lines from ions such as Fe II, Mg II, and Si II. Spectra obtained late in the outburst show only emission lines from highly ionized species and in many cases these are forbidden lines. The ultraviolet data will be used with calculations of spherical, expanding, stellar atmospheres for novae to determine elemental abundances by spectral line synthesis. This method is extremely sensitive to the abundances and completely independent of the nebular analyses usually used to obtain novae abundances. ESA

N89-10707*# National Aeronautics and Space Administration. Goddard Space Flight Center, Greenbelt, Md.
THE 1981 OUTBURST OF THE OLD NOVA GK PERSEI
C.-C. Wu, R. J. Panek, A. V. Holm, J. C. Raymond, L. W. Hartmann (Harvard-Smithsonian Center for Astrophysics, Cambridge, Mass.), and J. H. Swank *In* ESA, A Decade of UV Astronomy with the IUE Satellite, Volume 1 Jun. 1988 p 155-157 (For primary document see N89-10682 01-89)
Avail: NTIS HC A19/MF A01; ESA Publications Div., ESTEC, Noordwijk, Netherlands, 140 Dutch guilders CSCL 03A

Old nova GK Per was observed in 1981 with the IUE, during its rise, maximum, and subsequent return to minimum. In outburst, GK Per is luminous but much redder than dwarf novae or standard model accretion disks. The observed spectrum can be explained qualitatively with the Ghosh and Lamb (1979) model for the interaction of an accretion disk with the magnetic field of the accreting white dwarf. The N V and He2 are enhanced relative to other emission lines during outburst. This can be understood with photoionization by very soft X-rays having a luminosity comparable to that of the hard X-rays. ESA

N89-10708*# National Aeronautics and Space Administration. Goddard Space Flight Center, Greenbelt, Md.
OBSERVATIONS OF CLASSICAL NOVAE IN OUTBURST
S. Starrfield, L. L. Stryker, G. Sonneborn, Warren M. Sparks, Gary Ferland, R. M. Wagner, R. E. Williams, Robert D. Gehrz, Edward P. Ney, and Scott Kenyon (Harvard Univ., Boston, Mass.) et al. *In* ESA, A Decade of UV Astronomy with the IUE Satellite, Volume 1 Jun. 1988 p 159-161 Sponsored by NASA, Washington, D.C., NSF, Washington, D.C. and DOE, Washington, D.C. (For primary document see N89-10682 01-89)
Avail: NTIS HC A19/MF A01; ESA Publications Div., ESTEC, Noordwijk, Netherlands, 140 Dutch guilders CSCL 03A

The IUE obtained ultraviolet data on novae in outburst. The characteristics of every one of the outbursts are different. Optical and infrared data on many of the same novae were also obtained. Three members of the carbon-oxygen class of novae are presented. ESA

N89-10709*# National Aeronautics and Space Administration. Goddard Space Flight Center, Greenbelt, Md.
OBSERVATIONS AND SIMULATIONS OF NOVA Vul 1984 NO. 2: A NOVA WITH EJECTA RICH IN OXYGEN, NEON, AND MAGNESIUM
S. Starrfield, G. Sonneborn, L. L. Stryker, Warren M. Sparks, James W. Truran, Gary Ferland, R. M. Wagner, J. S. Gallagher, R. Wade, and R. E. Williams (Cerro Tololo Inter-American Observatory, La Serena, Chile) et al. *In* ESA, A Decade of UV Astronomy with the IUE Satellite, Volume 1 Jun. 1988 p 163-166 Sponsored by NASA, Washington, D.C., NSF, Washington, D.C. and DOE, Washington, D.C. (For primary document see N89-10682 01-89)
Avail: NTIS HC A19/MF A01; ESA Publications Div., ESTEC, Noordwijk, Netherlands, 140 Dutch guilders CSCL 03A

Nova Vul 1984 no. 2 was observed with IUE from Dec. 1984 through Nov. 1987. The spectra are characterized by strong lines from Mg, Ne, C, Si, O, N, and other elements. Data obtained in the ultraviolet, infrared, and optical show that this nova is ejecting material rich in oxygen, neon, and magnesium. ESA

N89-10710*# National Aeronautics and Space Administration. Goddard Space Flight Center, Greenbelt, Md.
OBSERVATIONS AND SIMULATIONS OF RECURRENT NOVAE: U Sco AND V394 CrA
S. Starrfield, G. Sonneborn, Warren M. Sparks, G. Shaviv, R. E. Williams, S. Heathcote, Gary Ferland, Robert D. Gehrz, Edward P. Ney, and Scott Kenyon (Minnesota Univ., Minneapolis.) et al. *In* ESA, A Decade of UV Astronomy with the IUE Satellite, Volume 1 Jun. 1988 p 167-170 Sponsored by NASA, Washington, D.C., NSF, Washington, D.C. and DOE, Washington, D.C. (For primary document see N89-10682 01-89)
Avail: NTIS HC A19/MF A01; ESA Publications Div., ESTEC, Noordwijk, Netherlands, 140 Dutch guilders CSCL 03A

Observations and analysis of the Aug. 1987 outburst of the

recurrent nova V394 CrA are presented. This nova is extremely fast and its outburst characteristics closely resemble those of the recurrent nova U Sco. Hydrodynamic simulations of the outbursts of recurrent novae were performed. Results as applied to the outbursts of V394 CrA and U Sco are summarized. ESA

N89-10711*# National Aeronautics and Space Administration. Goddard Space Flight Center, Greenbelt, Md.
OPTICAL AND ULTRAVIOLET OBSERVATIONS OF NOVA Vul 1987
S. Starrfield, L. L. Stryker, G. Sonneborn, Warren M. Sparks, R. M. Wagner, Gary Ferland, J. S. Gallagher, R. Wade, R. E. Williams, and Robert D. Gehrz (Minnesota Univ., Minneapolis.) et al. *In* ESA, A Decade of UV Astronomy with the IUE Satellite, Volume 1 Jun. 1988 p 171-173 Sponsored by NASA, Washington, D.C., NSF, Washington, D.C. and DOE, Washington, D.C. (For primary document see N89-10682 01-89)
Avail: NTIS HC A19/MF A01; ESA Publications Div., ESTEC, Noordwijk, Netherlands, 140 Dutch guilders CSCL 03A

The outburst for a nova discovered in Nov. 1987 and followed since then is summarized. Although it was possible to observe it with the IUE at maximum, its ultraviolet energy faded rapidly, and after the first 2 weeks it was impossible to observe it at IUE wavelengths. It is observed to form a thick dust shell and is in the nebular stage. ESA

N89-10712*# National Aeronautics and Space Administration. Goddard Space Flight Center, Greenbelt, Md.
ULTRAVIOLET OBSERVATIONS OF LMC NOVA 1988
S. Starrfield, L. L. Stryker, G. Sonneborn, Warren M. Sparks, E. M. Sion, R. M. Wagner, Gary Ferland, J. S. Gallagher, R. Wade, and R. E. Williams (Cerro Tololo Inter-American Observatory, La Serena, Chile) et al. *In* ESA, A Decade of UV Astronomy with the IUE Satellite, Volume 1 Jun. 1988 p 175-177 Sponsored by NASA, Washington, D.C., NSF, Washington, D.C. and DOE, Washington, D.C. (For primary document see N89-10682 01-89)
Avail: NTIS HC A19/MF A01; ESA Publications Div., ESTEC, Noordwijk, Netherlands, 140 Dutch guilders CSCL 03A

The IUE obtained ultraviolet spectra of a nova in an external galaxy. The spectral features do not seem unusual for a nova at maximum but it is hoped to be able to follow it for a long enough time to be able to study the high ionization lines that appear when the density drops to lower values (the nebular stage). A high dispersion spectrum was also obtained to assist in the line identification and to study the line of sight to the LMC 1 deg of arc away from SN 1987A. ESA

N89-10713# Computer Sciences Corp., Silver Spring, Md. Astronomy Operations.
SS CYGNI IN QUIESCENCE
Albert V. Holm and Ronald S. Polidan (Arizona Univ., Tucson.) *In* ESA, A Decade of UV Astronomy with the IUE Satellite, Volume 1 Jun. 1988 p 179-181 (For primary document see N89-10682 01-89)
Avail: NTIS HC A19/MF A01; ESA Publications Div., ESTEC, Noordwijk, Netherlands, 140 Dutch guilders

Low reslution IUE spectra of SS Cygni obtained near quiescence show a strong absorption feature near 1225A. If this feature is interpreted as the red wing of the Lyman alpha absorption in the spectrum of the white dwarf component, then the star has an effective temperature of 34,000 + or - 5000 K. This information is used to derive limits on the distance. Observations obtained in outburst are used to determine an E(B-V) estimate of 0.04 + or - 0.02. While these observations are consistent with the detection of the white dwarf primary they also show that the disk itself can produce Lyman alpha absorption resembling that of a white dwarf and that the existence of the feature is not proof that the white dwarf is detected. ESA

N89-10714# Preston Polytechnic (England). School of Physics and Astronomy.
UV AND OPTICAL LINE EMISSION FROM THE SHELL OF THE OLD NOVA GK PERSEI
M. F. Bode, H. W. Duerbeck, W. C. Seitter, J. S. Albinson, and A. Evans (University Coll. of North Staffordshire, Keele, England) *In* ESA, A Decade of UV Astronomy with the IUE Satellite, Volume 1 Jun. 1988 p 183-185 Sponsored by the United Kingdom Science and Engineering Research Council and Deutsche Forschungsgemeinschaft, Bonn, Fed. Republic of Germany (For primary document see N89-10682 01-89)
Avail: NTIS HC A19/MF A01; ESA Publications Div., ESTEC, Noordwijk, Netherlands, 140 Dutch guilders

Ultraviolet line emission is found in IUE spectra taken of the brightest region (bar) of the shell of GK Per in 1987. This makes the remnant of the nova of 1901 the first classical nova nebula to be detected in wavelengths from the radio region to the ultraviolet. Results suggest that the spectral line ratios can be fitted by a shock model assuming an underabundance of hydrogen and an overabundance of nitrogen. The observed shock velocities in the range 100 to 200 km/sec are characteristic of reverse shocks entering the nova ejecta. ESA

N89-10715*# National Aeronautics and Space Administration. Goddard Space Flight Center, Greenbelt, Md.
IUE OBSERVATIONS OF THE 1987 SUPEROUTBURST OF THE DWARF NOVA Z Cha
E. Harlaftis, B. J. M. Hassall, G. Sonneborn, T. Naylor (European Space Agency. ESA Tracking Station, Madrid, Spain), and P. A. Charles *In* ESA, A Decade of UV Astronomy with the IUE Satellite, Volume 1 Jun. 1988 p 187-190 (For primary document see N89-10682 01-89)
Avail: NTIS HC A19/MF A01; ESA Publications Div., ESTEC, Noordwijk, Netherlands, 140 Dutch guilders CSCL 03A

Low resolution IUE observations of the dwarf nova Z Cha during superoutburst are presented. These cover most of the development of the outburst and have sufficient time resolution to probe continuum and line behavior on orbital phase. The observed modulation on this phase is very similar to that observed in the related object OY Car. The results imply the presence of a cool spot on the edge of the edge of the accretion disk, which periodically occults the brighter inner disk. Details of the line behavior suggest that the line originated in an extended wind-emitting region. In contrast to archive spectra obtained in normal outburst, the continuum is fainter and redder, indicating that the entire superoutburst disk may be geometrically thicker than during a normal outburst. ESA

N89-10716# Los Alamos National Lab., N. Mex.
OBSERVATIONS OF GALACTIC WC + O BINARY SYSTEMS: HD 97152 AND HD 152270
L. H. Auer, C. Colome, and G. Koenigsberger (Universidad Autonoma de Madrid, Cantoblanco, Spain) *In* ESA, A Decade of UV Astronomy with the IUE Satellite, Volume 1 Jun. 1988 p 193-195 Sponsored in part by DOE, Washington, D.C. (For primary document see N89-10682 01-89)
Avail: NTIS HC A19/MF A01; ESA Publications Div., ESTEC, Noordwijk, Netherlands, 140 Dutch guilders

The IUE observations of the Wolf-Rayet binary systems HD 97152 and HD 152270 are presented. Both systems contain a WC7 component, and both have relatively small orbital inclinations. Weak atmospheric eclipses at emission line wavelengths are detected in HD 97152, the system for which a more suitable phase coverage is available. ESA

N89-10717# Universidad Autonoma de Madrid, Cantoblanco (Spain). Inst. de Astronomia.
ATMOSPHERIC ECLIPSE EFFECTS IN WOLF-RAYET BINARIES IN THE SMALL MAGELLANIC CLOUD
Gloria Koenigsberger, Anthony F. J. Moffat, and Lawrence H. Auer (Los Alamos National Lab., N. Mex.) *In* ESA, A Decade of UV Astronomy with the IUE Satellite, Volume 1 Jun. 1988 p 197-199 Sponsored by the Canadian Natural Sciences and Engineering Research Council and DOE, Washington, D.C. (For primary document see N89-10682 01-89)
Avail: NTIS HC A19/MF A01; ESA Publications Div., ESTEC, Noordwijk, Netherlands, 140 Dutch guilders

Results of IUE observations of three SMC W-R binary systems are presented. Selective atmospheric eclipse effects are evident in HD5980 (WN4+06I) and Sk 188 (W04+04V), and are very weak, or absent in Sk 108 (WN3+06I). The difference in heavy-metal content between the SMC and Galactic objects is clearly manifest in the lack of atmospheric eclipse effects in the wavelength range 1360 to 1470 A in HD5980 and Sk 188. ESA

N89-10718*# National Aeronautics and Space Administration. Goddard Space Flight Center, Greenbelt, Md.
MASS FLOW IN THE INTERACTING BINARY TX URSAE MAJORIS
G. E. McCluskey, Jr., C. P. S. McCluskey (Pennsylvania State Univ., University Park.), and Y. Kondo *In* ESA, A Decade of UV Astronomy with the IUE Satellite, Volume 1 Jun. 1988 p 201-203 (For primary document see N89-10682 01-89)
(Grant NsG-5386)
Avail: NTIS HC A19/MF A01; ESA Publications Div., ESTEC, Noordwijk, Netherlands, 140 Dutch guilders CSCL 03A

Twenty-two far-ultraviolet and 23 near-ultraviolet high resolution IUE spectra of the interactive Algol-type binary TX Ursae Majoris (B8 V + F-K III-IV) were analyzed in order to determine the nature of the mass flow occurring in this system. Absorption features due to high-temperature ions of Si IV, C IV, and N V are always present. The resonance lines of Al III, Fe II, Mg II and Si IV show strong phase and secular variations indicative of gas streaming and circumstellar/circumbinary material. Radial velocities as high as 500 to 600 km/sec are present. The gas flow is particularly prominent in 1985 between phases 0.7 and 0.0. The system is more active than U Sagittae and as active as U Cephei. ESA

N89-10719*# Arizona Univ., Tucson. Lunar and Planetary Lab.
A NEW STUDY OF THE INTERACTING BINARY STAR V356 Sgr
R. S. Polidan *In* ESA, A Decade of UV Astronomy with the IUE Satellite, Volume 1 Jun. 1988 p 205-208 (For primary document see N89-10682 01-89)
(Grants NAGw-587; NAG5-441)
Avail: NTIS HC A19/MF A01; ESA Publications Div., ESTEC, Noordwijk, Netherlands, 140 Dutch guilders CSCL 03A

Results on V356 Sgr from IUE and Voyager ultraviolet (500 to 3200 A) observations obtained in 1986 and 1987, primarily during 2 total eclipses are presented. The eclipse of Aug. 15, 1986 was fully covered with IUE low dispersion images and 9 hr of Voyager UVS data. The eclipse of Mar. 25, 1987 was covered with IUE low dispersion images and 1 high dispersion SWP image. During both eclipses the total strength of the emission lines is found to be invariant. An uneclipsed UV continuum is detected at wavelengths shorter than 1500 A. The high dispersion SWP spectrum reveals that the emission lines are extremely broad, almost symmetrical emissions with weak, slightly blue shifted absorption components. No evidence of carbon, C I, C II, C III, or C IV, is seen in the emission or absorption spectrum of V356 Sgr in eclipse. Models for this binary system are presented. ESA

N89-10720# University Coll., London (England).
MATTER STREAMS IN SEMI-DETACHED BINARY SYSTEMS
D. Wonnacott *In* ESA, A Decade of UV Astronomy with the IUE Satellite, Volume 1 Jun. 1988 p 209-212 (For primary document see N89-10682 01-89)
Avail: NTIS HC A19/MF A01; ESA Publications Div., ESTEC, Noordwijk, Netherlands, 140 Dutch guilders

The gas stream between the two components of CX Draconis was observed in the UV and modeled using a simple ballistic code. To scale the model to the data, an inclination of 15 deg is required. A jet of high velocity material is also present but cannot be accounted for with the model. It is conjectured that viscosity causes the infalling stream to spread to the extent that it can avoid collision with the photosphere of the primary and escape from the system by a gravitational slingshot effect. ESA

N89-10721*# Space Telescope Science Inst., Baltimore, Md. Astronomy Programs.
THE NOVEMBER 1987 ECLIPSE OF THE ZETA-Aur SYSTEM HR 2554
Thomas B. Ake, III and Sidney B. Parsons *In* ESA, A Decade of UV Astronomy with the IUE Satellite, Volume 1 Jun. 1988 p 213-215 (For primary document see N89-10682 01-89)
(Grant NAS5-28749)
Avail: NTIS HC A19/MF A01; ESA Publications Div., ESTEC, Noordwijk, Netherlands, 140 Dutch guilders CSCL 03A

It is confirmed that HR 2554 (G6 II + A0 V) is an atmospheric eclipsing system of the zeta-Aur type. The IUE observations of the Nov. 1987 eclipse indicate that the eclipse of the A star lasts 4 days and is not total. Absorption lines due to the extended atmosphere of the primary can be seen a day before and after the eclipse and are missing 2 days from first and 4th contact. Thus the outer envelope of the primary extends to less than 1 stellar radius beyond the photosphere. Compared to 22 Vul (G3 Ib-II + B9 V), where the absorption can be traced to a few stellar radii, HR 2554 is a more moderate case of mass outflow, which implies there is reduced interaction of the secondary within the wind from the primary as is seen in the other zeta-Aur systems. ESA

N89-10722*# Imad ad Dean, Inc., Bethesda, Md.
ASYMMETRY IN ZETA AURIAGE CHROMOSPHERES
I. A. Ahmad *In* ESA, A Decade of UV Astronomy with the IUE Satellite, Volume 1 Jun. 1988 p 217-220 (For primary document see N89-10682 01-89)
(Contract NAS5-29381)
Avail: NTIS HC A19/MF A01; ESA Publications Div., ESTEC, Noordwijk, Netherlands, 140 Dutch guilders CSCL 03A

Asymmetry in the ultraviolet spectra of zeta-Aur, similar to that reported in optical observations, was studied using IUE data. A plot of the integrated flux of zeta Aurigae from 1625 to 1675 A as a function of absolute phase shows no significant difference between the ingress and egress phases. A plot of the integrated flux from 1625 to 1675 A for 22 Vul as a function of absolute phase for both ingress and egress confirms that the atmospheric eclipse is asymmetric in 22 Vul. The eclipse in 22 Vul begins symmetrically but departs from symmetry at a phase greater than 0.05. The pronounced dip at ingress suggests a feature in the chromosphere. ESA

N89-10723# California Univ., Los Angeles. Dept. of Astronomy.
SUPERIONIZED PLASMAS IN ALGOL BINARIES
Mirek J. Plavec *In* ESA, A Decade of UV Astronomy with the IUE Satellite, Volume 1 Jun. 1988 p 221-224 (For primary document see N89-10682 01-89)
Avail: NTIS HC A19/MF A01; ESA Publications Div., ESTEC, Noordwijk, Netherlands, 140 Dutch guilders

Outflowing gas is studied for semidetached binaries of the Algol type. A survey of 11 systems observed during the total primary eclipse shows that the same type of emission-line spectrum appears, but that important differences exist, correlated with the character of the mass-accreting star, although it is not clear if the correlation is with spectral type or with mass. The line emitting plasma is specified, but the dominant electron temperature varies from system to system and determines the relative line strengths. Evidence for CNO processing, affecting the abundance ratios C/N, is also present. ESA

N89-10724# Space Telescope Science Inst., Baltimore, Md. Astronomy Programs.
HD 207739 AND OTHER F + BE VARIABLES
S. B. Parsons, R. C. Dempsey, and B. W. Bopp (Ritter Observatory, Toledo, Ohio.) *In* ESA, A Decade of UV Astronomy with the IUE Satellite, Volume 1 Jun. 1988 p 225-227 (For primary document see N89-10682 01-89)
Avail: NTIS HC A19/MF A01; ESA Publications Div., ESTEC, Noordwijk, Netherlands, 140 Dutch guilders

Characteristics for a group of composite spectrum stars which have strong H alpha emission and peculiar satellite UV spectra

are compared. Spectroscopic periods and photometric variability are discussed. Compared with normal noninteracting composite spectrum binaries, they exhibit excess flux in the middle UV region. This is believed to indicate the presence of an accretion disk.
ESA

N89-10725# Computer Sciences Corp., Silver Spring, Md. Astronomy Operations.
SEARCHING FOR THE WHITE DWARF IN WZ SAGITTAE
Albert V. Holm *In* ESA, A Decade of UV Astronomy with the IUE Satellite, Volume 1 Jun. 1988 p 229-231 (For primary document see N89-10682 01-89)
Avail: NTIS HC A19/MF A01; ESA Publications Div., ESTEC, Noordwijk, Netherlands, 140 Dutch guilders

Far ultraviolet IUE spectra of WZ Sge from July 1979 through Nov. 1981 were studied to search for the spectroscopic signature of the white dwarf primary. The ultraviolet fluxes continue to decline throughout this period. The ultraviolet spectrum of WZ Sge near minimum is not completely consistent with the hypothesis that the white dwarf is visible, although the ultraviolet energy distribution can be matched by a DA-type white dwarf. This does not explain the behavior of the absorption spectrum. However, the accretion on the top of the atmosphere of material having normal metal abundances might greatly alter the appearance of the spectrum. Development of model atmospheres having solar abundances for white dwarfs is recommended to investigate this possibility. Models of white dwarfs heated by a bright accretion disk are also needed to determine whether this mechanism could cause the surface temperature to be high for several years after the outburst. ESA

N89-10726# Oxford Univ. (England). Dept. of Theoretical Physics.
MODEL CHROMOSPHERE AND TRANSITION REGION FOR 56 Peg (K0 IIp + wd): A PRELIMINARY STUDY
M. G. Munday *In* ESA, A Decade of UV Astronomy with the IUE Satellite, Volume 1 Jun. 1988 p 233-236 (For primary document see N89-10682 01-89)
Avail: NTIS HC A19/MF A01; ESA Publications Div., ESTEC, Noordwijk, Netherlands, 140 Dutch guilders

Observations by IUE of 56 Peg (K0 IIp + wd) show the presence of ultraviolet emission lines associated with warm (100,000 K) material. Although it was suggested that this emission comes from an ionized region in a cool wind around the secondary, the characteristics of the emission indicate that the lines are formed in a transition region around the late-type supergiant. A self-consistent model chromosphere and transition region are presented as further evidence. A satisfactory model, taking into account the transition region material, the variable asymmetry in Mg II, and the X-ray emission might be possible in terms of a hybrid supergiant with an X-ray illuminated cool wind. ESA

N89-10727*# Toronto Univ. (Ontario). Dept. of Astronomy.
CEPHEID BINARIES WITH LARGE MASS RATIOS (M1/M2)
Nancy Remage Evans *In* ESA, A Decade of UV Astronomy with the IUE Satellite, Volume 1 Jun. 1988 p 237-239 Sponsored in cooperation with the Canadian Natural Sciences and Engineering Council (For primary document see N89-10682 01-89)
(Grant NAS5-28749)
Avail: NTIS HC A19/MF A01; ESA Publications Div., ESTEC, Noordwijk, Netherlands, 140 Dutch guilders CSCL 03A

The IUE observations of 3 Cepheid systems (Polaris, FF Aql, and S Sge) are used to derive, or set limits on, the temperatures and masses of the companions. Light from the companions of FF Aql and S Sge from 1700 to 2000 A is consistent with an A5 to A7 main sequence companion for both Cepheids, with a mass of 1.8 solar mass. This mass for the companion of S Sge is smaller than required by the orbital mass function and an evolutionary mass of the Cepheid, suggesting that the companion may itself be a binary. For Polaris, the mass of the companion must be less than 1.8 solar mass. ESA

N89-10728*# Toronto Univ. (Ontario). Dept. of Astronomy.
THE ORBIT OF THE CEPHEID AW Per
Nancy Remage Evans and Douglas L. Welch *In* ESA, A Decade of UV Astronomy with the IUE Satellite, Volume 1 Jun. 1988 p 241-243 Sponsored in cooperation with the Canadian Natural Sciences and Engineering Council (For primary document see N89-10682 01-89)
(Grant NAS5-28749)
Avail: NTIS HC A19/MF A01; ESA Publications Div., ESTEC, Noordwijk, Netherlands, 140 Dutch guilders CSCL 03A

An orbit for the classical Cepheid AW Per was derived. Phase residuals from the light curve are consistent with the light-time effect from the orbit. The companion was studied using IUE spectra. The flux distribution from 1300 to 1700 A is unusual, probably an extreme PbSi star, comparable to a B7V or B8V star. The flux of the composite spectrum from 1200 A through V is well matched by F7Ib and B8V standard stars with Delta M(sub upsilon) = 3(m) multiplied by 1. The mass function from the orbit indicates that the mass of the Cepheid must be greater that 4.7 solar mass if it is the more massive component. A B7V to B8V companion is compatible with the 1 sigma lower limit (3.5 solar mass) from the mass function. This implies that the Cepheid has the same mass, but the large magnitude difference rules this out. It is likely that the companion is itself a binary. ESA

N89-10729*# Space Telescope Science Inst., Baltimore, Md. Astronomy Programs.
COMPANIONS TO PECULIAR RED GIANTS: HR 363 AND HR 1105
Thomas B. Ake, III, Hollis R. Johnson, and Benjamin F. Perry, Jr. (Howard Univ., Washington, D. C.) *In* ESA, A Decade of UV Astronomy with the IUE Satellite, Volume 1 Jun. 1988 p 245-248 (For primary document see N89-10682 01-89)
(Grant NAS5-28749)
Avail: NTIS HC A19/MF A01; ESA Publications Div., ESTEC, Noordwijk, Netherlands, 140 Dutch guilders CSCL 03A

Recent IUE observations of two Tc-deficient S-type peculiar red giants that are also spectroscopic binaries, HR 363 and HR 1105 are reported. A 675 min SWP exposure of HR 363 shows emission lines of O I 1304 and Si II 1812 and a trace of continuum. Compared to the M giants, the far UV flux may be relatively larger, indicating a possible contribution from a white dwarf companion, but no high temperature emission lines are seen to indicate that this is an interacting system where mass-transfer recently occurred. However, HR 1105 appears to have a highly variable UV companion. In 1982, no UV flux was discerned for this system, but by 1986 C IV was strong, increasing by a factor of 3 in 1987 with prominent lines of Si III, C III, O III, Si IV, and N V. Using orbital parameters, these observations are consistent with high activity occuring when the side of the S-star primary illuminated by the companion faces the Earth, but since the IUE data were taken over 3 orbits, a secular change in the UV component cannot be excluded. ESA

N89-10730*# Colorado Univ., Boulder. Center for Astrophysics and Space Astronomy.
DIRECT UV OBSERVATIONS OF THE CIRCUMSTELLAR ENVELOPE OF ALPHA ORIONIS
R. E. Stencel, K. G. Carpenter, J. E. Pesce, S. Skinner, A. Brown, and P. Judge (Joint Inst. for Lab. Astrophysics, Boulder, Colo.) *In* ESA, A Decade of UV Astronomy with the IUE Satellite, Volume 1 Jun. 1988 p 249-252 (For primary document see N89-10682 01-89)
(Grant NAG5-816)
Avail: NTIS HC A19/MF A01; ESA Publications Div., ESTEC, Noordwijk, Netherlands, 140 Dutch guilders CSCL 03A

Observations were made in the IUE LWP camera, low dispersion mode, with alpha Ori being offset various distances from the center of the Long Wavelength Large Aperture along its major axis. Signal was acquired at all offset positions and is comprised of unequal components of background/dark counts, telescope-scattered light, and scattered light emanating from the extended circumstellar shell. The star is known from optical and infrared observations to possess an extended, arc-minute sized, shell of cool material. Attempts to

observe this shell with the IUE are described, although the deconvolution of the stellar signal from the telescope scattered light requires further calibration effort. ESA

N89-10731*# Colorado Univ., Boulder. Center for Astrophysics and Space Astronomy.
MULTI-WAVELENGTH OBSERVATIONS OF THE PECULIAR RED GIANT HR 3126
Joseph E. Pesce, Robert E. Stencel, Frederick M. Walter, Jesse Doggett, Joachim Dachs, Patricia A. Whitelock, and Reinhard Mundt (Max-Planck-Inst. fuer Astronomie, Heidelberg, West Germany) *In* ESA, A Decade of UV Astronomy with the IUE Satellite, Volume 1 Jun. 1988 p 253-256 (For primary document see N89-10682 01-89)
(Contract JPL-957632; NAG5-816; NGT-700052)
Avail: NTIS HC A19/MF A01; ESA Publications Div., ESTEC, Noordwijk, Netherlands, 140 Dutch guilders CSCL 03A

Ultraviolet observations of the red giant HR 3126 are combined with multi-wavelength data in order to provide a firmer basis for explaining the arc-minute sized nebula surrounding the object. Possibilities as to the location of HR 3126 on the Hertzsprung-Russel diagram, and to the formation mechanisms of the reflection nebula IC 2220 associated with it, are summarized. ESA

N89-10732*# National Aeronautics and Space Administration. Goddard Space Flight Center, Greenbelt, Md.
RECURRENT SHELL INFALL EVENTS IN A B0.5e STAR: HD 58978 1979-1988
C. A. Grady, G. J. Peters, K. S. Bjorkman, and H. F. Henrichs (Amsterdam Univ., Netherlands) *In* ESA, A Decade of UV Astronomy with the IUE Satellite, Volume 1 Jun. 1988 p 257-260 (For primary document see N89-10682 01-89)
Avail: NTIS HC A19/MF A01; ESA Publications Div., ESTEC, Noordwijk, Netherlands, 140 Dutch guilders

Infall from the circumstellar envelope onto the bright B0.5 IVe star, HD 58978 was studied. The IUE data indicate that the star was surrounded by a low and moderately ionized circumstellar shell at least 12 times between 1979 and 1988. During 6 of these episodes, the signatures of cool circumstellar material were redshifted with respect to the photosphere by 20 to 80 km/sec. The data indicate that the transition from infall to minimal shell absorption can occur in under 10 days, and are consistent either with infall phases lasting up to 6 months, or with infall episodes shorter than 10 to 15 days. The long term behavior of the shell episodes is compared with variability in the stellar wind. ESA

N89-10733*# Arizona Univ., Tucson. Lunar and Planetary Lab.
IUE OBSERVATIONS OF A HOT DAO WHITE DWARF: IMPLICATIONS FOR DIFFUSION THEORY AND PHOTOSPHERIC STRATIFICATION
J. B. Holberg, E. M. Sion, J. Liebert, and Gerard Vauclair (Observatoire du Pic-du-Midi, Bagneres de Bigorre, France) *In* ESA, A Decade of UV Astronomy with the IUE Satellite, Volume 1 Jun. 1988 p 263-265 (For primary document see N89-10682 01-89) .
(Grants NAG5-434; NAG5-343)
Avail: NTIS HC A19/MF A01; ESA Publications Div., ESTEC, Noordwijk, Netherlands, 140 Dutch guilders CSCL 03A

Observations of the DAO white dwarf PG1210+533, including the first high dispersion spectrum of a hybrid H-He object of this nature were obtained by IUE. In contrast with hot DAs in the 50,000 K temperature range, PG1210+533 shows no narrow interstellar-like metal lines, in spite of an optically observed He/H abundance of 0.1. This lack of metal makes accretion from the ISM an unlikely source for the He in the PG1210+533 photosphere. A significant discovery in the high dispersion spectrum is the existence of a sharp, non-LTE like, core seen in the He II 1640 line. Such features are detected in DO white dwarfs. A small aperture SWP low dispersion observation reveals the Lyman alpha profile of PG1210+533 to be surprisingly weak and narrow. Fits of this profile using pure H models yielded a T(eff) = 56,000 K. Fits of the Balmer H gamma profile however, yield T(eff) = 42,300 K and log g = 8.5 + or - 0.5 for the same models. It is unlikely that homogeneously mixed H-He atmospheres can resolve the inconsistency between the Lyman alpha and H gamma features in this star. Stratified models involving thin H photospheres may be necessary to explain these results. ESA

N89-10734*# California Univ., Berkeley. Space Sciences Lab.
TEMPERATURE DETERMINATIONS OF HOT DA WHITE DWARFS USING IUE CONTINUUM FLUXES
David Finley, Gibor Basri, and Stuart Bowyer *In* ESA, A Decade of UV Astronomy with the IUE Satellite, Volume 1 Jun. 1988 p 267-270 (For primary document see N89-10682 01-89)
(Contract NAS5-29298)
Avail: NTIS HC A19/MF A01; ESA Publications Div., ESTEC, Noordwijk, Netherlands, 140 Dutch guilders CSCL 03A

Effective temperatures of 15 DA white dwarfs hotter than 20,000 K were derived from low-dispersion far ultraviolet spectra obtained with IUE. The analysis was carried out by comparing the observed far ultraviolet fluxes with model fluxes scaled to the V-band flux. Accurate calibration of the IUE spectra is critical for this analysis. Observations at all epochs were corrected to the 1980 IUE calibration using the time-dependent corrections of Bohlin (1988). Taking advantage of the smooth and well-defined continuum fluxes provided by DA white dwarfs, seven white dwarfs for which accurate, independent temperature determinations were made from line profile analyses were used to improve the accuracy of the IUE flux calibration. The correction to the original calibration is as great as 20 percent in individual 5 A wavelength bins, while the average over the IUE wavelength range is 5 percent. The final calibration correction and the temperatures for the hot white dwarfs are presented. ESA

N89-10735# Commissariat a l'Energie Atomique, Saclay (France). Centre d'Etudes Nucleaires.
THE ULTRAVIOLET EMISSION OF ACCRETING MAGNETIC WHITE DWARFS
Jean-Marc Bonnet-Bidaud and Martine Mouchet (Observatoire de Paris-Meudon, France) *In* ESA, A Decade of UV Astronomy with the IUE Satellite, Volume 1 Jun. 1988 p 271-276 (For primary document see N89-10682 01-89)
Avail: NTIS HC A19/MF A01; ESA Publications Div., ESTEC, Noordwijk, Netherlands, 140 Dutch guilders

The ultraviolet continuum and emission line characteristics of AM Her (polars) and DQ Her (intermediate polars) were analyzed. The UV energy distribution is compared to different emitting contributions: the UV flux most probably results from X-ray heating of the column and of the surface of the white dwarf but cannot be explained by cyclotron radiation. The emission line intensities of the different systems are compared. The resonance line intensity ratios are similar for both classes and are generally in accordance with what is expected from photoionization by soft X-rays. However two of these systems exhibit anomalous ratios, tentatively interpreted as due to abnormal abundances of carbon and nitrogen. ESA

N89-10736# Hawaii Univ., Honolulu. Inst. of Astronomy.
IUE OBSERVATIONS OF RAPIDLY ROTATING K DWARFS IN THE PLEIADES
Theodore Simon *In* ESA, A Decade of UV Astronomy with the IUE Satellite, Volume 1 Jun. 1988 p 279-282 (For primary document see N89-10682 01-89)
Avail: NTIS HC A19/MF A01; ESA Publications Div., ESTEC, Noordwijk, Netherlands, 140 Dutch guilders

Low-resolution Mg II spectra were obtained with the IUE for rapidly rotating, spotted K dwarf stars in the Pleiades cluster. The observations show an order of magnitude spread in the chromospheric emission of presumably coeval members of the cluster. The emission is correlated with the stellar rotation rate, being strongest for stars having periods of less than 1 day and weakest for more slowly rotating stars. The strength of the emission of the rapid rotators lies well above the emission levels that characterize the most active solar-type stars in the field and is significant stronger than the Mg II emission observed for low-mass

pre-main sequence stars. The observations indicate that the decay of stellar chromospheric activity with age does not follow any simple rule, such as the square-root law or an exponential decay law. ESA

N89-10737# Oxford Univ. (England). Dept. of Theoretical Physics.
ON THE FLUX-PERIOD AND FLUX-FLUX CORRELATIONS IN LATE TYPE STARS
B. Montesinos and C. Jordan *In* ESA, A Decade of UV Astronomy with the IUE Satellite, Volume 1 Jun. 1988 p 283-286 (For primary document see N89-10682 01-89)
Avail: NTIS HC A19/MF A01; ESA Publications Div., ESTEC, Noordwijk, Netherlands, 140 Dutch guilders

The analysis of a wide sample of stars including both main-sequence and evolved stars shows that while flux-flux correlations are the same for the whole sample, the flux-period relations show a lower dependence on period for evolved stars. A gravity dependence also enters the flux-period relation for evolved stars. The flux-flux and flux-period relations are combined with coronal parameters to express Pc, Tc, and Bc in terms of the period. All increase with decreasing period, as expected if dynamo action controls activity. Specific relations between observable quantities are found which could be tested from further observations. Calculations of the convective zone fields in mildly evolved stars suggest that a larger convective zone field results which could explain the greater emission from evolved stars for a given period. ESA

N89-10738# Osservatorio Astrofisico di Arcetri, Florence (Italy).
ULTRAVIOLET EMISSION FROM THE SUN AND STARS: A COMPARISON OF IUE AND SKYLAB SPECTRA
A. Cappelli, M. Cerruti-Sola, C. C. Cheng (Hulburt, E. O. Center for Space Research, Washington, D.C), and R. Pallavicini *In* ESA, A Decade of UV Astronomy with the IUE Satellite, Volume 1 Jun. 1988 p 287-290 (For primary document see N89-10682 01-89)
Avail: NTIS HC A19/MF A01; ESA Publications Div., ESTEC, Noordwijk, Netherlands, 140 Dutch guilders

Low-resolution IUE SWP spectra of late-type stars and high-resolution Skylab spectra of spatially-resolved solar regions of various degrees of magnetic activity (quiet areas, plages, flares) are compared. The high-resolution solar spectra are degraded to the same resolution of IUE and the solar and stellar data are analyzed in exactly the same way. It is shown that the different levels of chromospheric and transition region emission observed in stars of similar spectral types are paralleled by a similar behavior displayed by solar regions of different magnetic activity. Spatially-resolved solar data obey the same flux-flux relationships as the stellar data over more than three orders of magnitude, with virtually the same slope and similar scatter. The similar behavior of the solar and stellar UV line fluxes, together with the dependence of the stellar fluxes on rotation, are indirect evidence that stellar activity is of magnetic origin and likely results from a dynamo process. The contribution of blends, under different activity conditions, to line fluxes derived from IUE low-reslution spectra varies depending on the activity level, and may be substantial for the lines of O I at 1304 A and He II at 1640 A. ESA

N89-10739*# National Aeronautics and Space Administration. Goddard Space Flight Center, Greenbelt, Md.
SPECTRAL IMAGES OF HD 199178
J. E. Neff, O. Vilhu, and F. M. Walter (Colorado Univ., Boulder.) *In* ESA, A Decade of UV Astronomy with the IUE Satellite, Volume 1 Jun. 1988 p 291-293 (For primary document see N89-10682 01-89)
Avail: NTIS HC A19/MF A01; ESA Publications Div., ESTEC, Noordwijk, Netherlands, 140 Dutch guilders

High-resolution IUE spectra of the Mg II k line of HD 199178 were analyzed, applying spectral imaging techniques to derive an image of the chromospheric structure and to study the transient behavior of the chromosphere. All spectra in the IUE archives were uniformly reduced and analyzed. Results are compared with ground-based observations of the photosphere. Four ultraviolet flares on HD 199178 are observed; 3 of these occurred at roughly the same rotational phase. There is no clear phase-dependence of the SWP line fluxes, but there is for the Mg II k flux. The emission centroid of the Mg II k line varies in a quasi-sinusoidal fashion, presumably due to the rotation of a nonuniform chromosphere. ESA

N89-10740*# Colorado Univ., Boulder. Center for Astrophysics and Space Astronomy.
DOPPLER IMAGING OF AR LACERTAE AT THREE EPOCHS
Frederick M. Walter, James E. Neff, Jeffrey L. Linsky, and Marcello Rodono (Catania Univ., Italy) *In* ESA, A Decade of UV Astronomy with the IUE Satellite, Volume 1 Jun. 1988 p 295-297 Sponsored in cooperation with CNR, Italy and the Italian Ministry of Public Education (For primary document see N89-10682 01-89)
(Grants NAG5-429; NAG5-82)
Avail: NTIS HC A19/MF A01; ESA Publications Div., ESTEC, Noordwijk, Netherlands, 140 Dutch guilders CSCL 03A

Observations from IUE were used to study the structure of the lower chromosphere of AR Lacertae in the light of Mg II k. Sequences of LWR/P-HI images distributed around the binary period at three epochs were obtained. Discrete plage-like regions of enhanced Mg II surface flux in this system are identified. There are temporal variations in the Mg II flux on timescales of hours as well as substantial changes in chromospheric morphology on timescales of years. Even with the limited S/N attainable with the IUE, one can map the gross structures of active stellar atmospheres. With such information, one can begin to study the true 3-D structure of the atmospheres of late-type stars. ESA

N89-10741*# Helsinki Univ. of Technology, Espoo (Finland). Observatory.
ROTATIONAL MODULATION OF HYDROGEN LYMAN ALPHA FLUX FROM 44II BOOTIS
O. Vilhu, J. E. Neff (Joint Inst. for Lab. Astrophysics, Boulder, Colo.), and T. Rahunen *In* ESA, A Decade of UV Astronomy with the IUE Satellite, Volume 1 Jun. 1988 p 299-302 (For primary document see N89-10682 01-89)
(Grant NAG5-82)
Avail: NTIS HC A19/MF A01; ESA Publications Div., ESTEC, Noordwijk, Netherlands, 140 Dutch guilders CSCL 03A

Observations with IUE that cover the entire 6.4 hr orbital cycle of the late-type contact binary 44i Bootis are presented. Intrinsic stellar hydrogen Lyman alpha emission flux was determined from low-resolution IUE spectra, compensating for geocoronal emission and for interstellar absorption. The variation of the stellar Lyman alpha emission flux correlates well with the variation of the C II and C IV emission fluxes, and shows orbital modulation in phase with the visual light curve. The ratio of Lyman alpha to CII flux (15 to 20) is similar to that observed in solar active regions. Hydrogen Lyman alpha emission is thus one of the most important cooling channels in the outer atmosphere of 44i Boo. A high-resolution spectrum of the Lyman alpha line was obtained between orbital phases 0.0 and 0.6. The integrated flux in the observed high-resolution Lyman alpha profile is consistent with the fluxes determined using low-resolution spectra, and the composite profile indicates that both components of this binary have equally active chromospheres and transition regions. The uncertainty in the interstellar hydrogen column density cannot mimic the observed variation in the integrated Lyman alpha flux, because the stellar line is very much broader than the interstellar absorption. ESA

N89-10742*# Villanova Univ., Pa. Dept. of Astronomy and Astrophysics.
MAPPING OF SURFACE ACTIVITY ON THE W UMa-TYPE SYSTEM VW CEPHEI
David H. Bradstreet and Edward F. Guinan *In* ESA, A Decade of UV Astronomy with the IUE Satellite, Volume 1 Jun. 1988 p 303-306 Sponsored in part by NASA, Washington, D.C. (For primary document see N89-10682 01-89)

Avail: NTIS HC A19/MF A01; ESA Publications Div., ESTEC, Noordwijk, Netherlands, 140 Dutch guilders CSCL 03A

After multifilter photometry of the W UMa-type contact binary VW Cep (P = 6.67 hr; G5V + K0V) in 1986/87 revealed large asymmetries in the light curves believed to be caused by large, cool starspot regions on the surface of the larger stars, in Apr. 1987 it was observed with IUE to study the chromospheres and transition regions of the components. During one complete orbital cycle, three SWP and four LWP low dispersion spectra were obtained, including and then excluding the suspected active region. Phase dependent TR line emission strengths were found, most notably C IV, which is 50 percent stronger when the spot region is most visible. The results could be important because VW Cep represents an extreme case for studying stellar dynamo theory and observations can play a crucial role in the unterstanding of magnetic fields and activity cycles in rapidly rotating solar-like stars. ESA

N89-10743# Armagh Observatory (Northern Ireland).
ULTRAVIOLET FLARES ON 2 Peg
J. G. Doyle and P. B. Byrne *In* ESA, A Decade of UV Astronomy with the IUE Satellite, Volume 1 Jun. 1988 p 307-309 (For primary document see N89-10682 01-89)
Avail: NTIS HC A19/MF A01; ESA Publications Div., ESTEC, Noordwijk, Netherlands, 140 Dutch guilders

Observations by IUE of the RS CVn star II Peg in the upper chromospheric and transition regions lines Mg II k, C IV, and He II in Feb. 1983 show evidence for flare activity. The electron pressure derived from the mean of two different line ratios produces good agreement between the allowed and intersystem lines in the differential emission measure curves. The total radiative losses from the chromosphere and transition region for the first flare on Feb. 2 is 2.46 times 10 to the 35th power erg, and at least 1.91 times 10 to the 34th power erg, for the flare on Feb. 4. ESA

N89-10744# Rutherford High Energy Lab., Chilton (England). Astrophysics Group.
CHROMOSPHERIC MASS MOTIONS DURING A FLARE ON UV CETI
K. J. H. Phillips, G. E. Bromage, P. L. Dufton, F. P. Keenan, and A. E. Kingston (Queens Univ., Belfast, Northern Ireland) *In* ESA, A Decade of UV Astronomy with the IUE Satellite, Volume 1 Jun. 1988 p 311-313 (For primary document see N89-10682 01-89)
Avail: NTIS HC A19/MF A01; ESA Publications Div., ESTEC, Noordwijk, Netherlands, 140 Dutch guilders

Simultaneous optical and IUE observations of a flare on UV Ceti in 1980 are reported. The IUE spectra show only slight increase of C IV line emission. The optical spectrophotometric observations show, from Balmer line profiles, turbulent broadening in quiescent and flare spectra, and downward-directed flow (of 100 km/sec) during the flare. The latter is particularly reminiscent of solar flares, and probably arises from the formation of a chromospheric condensation, as modeled for solar flares. ESA

N89-10745*# Washington Univ., Seattle. Dept. of Astronomy.
THE ENERGY INPUT MECHANISM INTO THE LOWER TRANSITION REGIONS BETWEEN STELLAR CHROMOSPHERES AND CORONAE
Erika Boehm-Vitense *In* ESA, A Decade of UV Astronomy with the IUE Satellite, Volume 1 Jun. 1988 p 315-317 (For primary document see N89-10682 01-89)
(Grant NsG-5398)
Avail: NTIS HC A19/MF A01; ESA Publications Div., ESTEC, Noordwijk, Netherlands, 140 Dutch guilders CSCL 03A

The ratio of the emission line fluxes for the C II and C IV lines in the lower transition regions (T = 30,000 to 100,000 K) between stellar chromospheres and transition layers is shown to depend mainly on the temperature gradient in the line emitting regions which can therefore be determined from this line ratio. From the observed constant (within the limits of observational error) ratio of the emission line fluxes of the C II (1335 A) and C IV (1550 A) lines it is concluded that the temperature gradients in the lower transition layers are similar for the large majority of stars independently of T sub eff, L, and degree of activity. This means that the temperature dependence of the damping length for the mechanical flux must be the same for all these stars. Since for different kinds of mechanical fluxes the dependence of the damping length on gas pressure and temperature is quite different, it is concluded that the same heating mechanism must be responsible for the heating of all the lower transition layers of these stars, regardless of their chromospheric activity. Only the amount of mechanical flux changes. The T Tauri stars are exceptions: their emission lines are probably mainly due to circumstellar material. ESA

N89-10746# Armagh Observatory (Northern Ireland).
TRANSITION REGIONS OF dM STARS
P. B. Byrne and J. G. Doyle *In* ESA, A Decade of UV Astronomy with the IUE Satellite, Volume 1 Jun. 1988 p 319-322 (For primary document see N89-10682 01-89)
Avail: NTIS HC A19/MF A01; ESA Publications Div., ESTEC, Noordwijk, Netherlands, 140 Dutch guilders

Weak upper-chromospheric and transition region (TR) emission from two dM stars (Gl784 and Gl825) were observed using deep IUE SWP exposures. In addition to the usual TR lines, Lyman alpha fluxes for the two stars were also determined. The relative importance of Lyman alpha and Mg II as chromospheric coolants in the M dwarfs and the status of the X-ray/He II (1640A) relationship in the light of these results are discussed. ESA

N89-10747*# Colorado Univ., Boulder. Center for Astrophysics and Space Astronomy.
TRANSITION REGION FLUXES IN A-F DWARFS: BASAL FLUXES AND DYNAMO ACTIVITY
Frederick M. Walter, Carolus J. Schrijver (Joint Inst. for Lab. Astrophysics, Boulder, Colo.), and William Boyd *In* ESA, A Decade of UV Astronomy with the IUE Satellite, Volume 1 Jun. 1988 p 323-326 (For primary document see N89-10682 01-89)
(Contract NAG5-429)
Avail: NTIS HC A19/MF A01; ESA Publications Div., ESTEC, Noordwijk, Netherlands, 140 Dutch guilders CSCL 03A

The transition region spectra of 87 late A and early F dwarfs and subgiants were analyzed. The emission line fluxes are uniformly strong in the early F stars, and drop off rapidly among the late A stars. The basal flux level in the F stars is consistent with an extrapolation of that observed among the G stars, while the magnetic component displays the same flux-flux relations seen among solar-like stars. Despite the steep decrease in transition region emission flux for B-V less than 0.28, C II emission is detected in alpha Aql (B-V = 0.22). The dropoff in emission is inconsistent with models of the mechanically generated acoustic flux available. It is concluded that, although the nonmagnetic basal heating is an increasingly important source of atmospheric heating among the early F stars, magnetic heating occurs in any star which has a sufficiently thick convective zone to generate acoustic heating. ESA

N89-10748# Indiana Univ., Indianapolis. Center for Astrophysics.
LINE FORMATION OF COOL CARBON STAR CHROMOSPHERES
Donald G. Luttermoser, Hollis R. Johnson, and Eugene H. Avrett *In* ESA, A Decade of UV Astronomy with the IUE Satellite, Volume 1 Jun. 1988 p 327-330 (For primary document see N89-10682 01-89)
Avail: NTIS HC A19/MF A01; ESA Publications Div., ESTEC, Noordwijk, Netherlands, 140 Dutch guilders

Based on adopted photospheric plus chromospheric models, synthetic fluxes of the C II (UV 0.01) and fluxes and profiles for the Mg II (UV 1) lines in complete (CRD) and partial (PRD) redistribution are generated and compared to IUE spectra of the carbon star TX Psc. Non-LTE calculations with the program PANDORA are made for H, C, Na, Mg, and Ca. For CRD and a well constrained chromospheric model, the best fit to the Mg II

line profiles gives a flux in the C II lines (produced at the same depth as the Mg II lines) 2.6 times too great and produces too much emission in the Mg II line wings. The PRD in the Mg II h and k lines in an expanding chromosphere with an adjusted temperature structure produces the observed Mg II emission. The reduction in temperature produces C II fluxes that matches the IUE low resolution spectra. ESA

N89-10749*# Vanderbilt Univ., Nashville, Tenn.
LITHIUM AND CHROMOSPHERICALLY ACTIVE SINGLE GIANTS
Francis C. Fekel *In* ESA, A Decade of UV Astronomy with the IUE Satellite, Volume 1 Jun. 1988 p 331-334 Sponsored in part by NASA, Washington, D.C. (For primary document see N89-10682 01-89)
Avail: NTIS HC A19/MF A01; ESA Publications Div., ESTEC, Noordwijk, Netherlands, 140 Dutch guilders CSCL 03A

Nine chromospherically active single K giants were identified from surveys of chromospherically active stars. The stars have v sin i's ranging from 6 to 46 km/sec. Such large velocities are not explained by scenarios of main sequence to giant star evolution. Fluxes of the ultraviolet emission lines of these stars are substantially less than those of FK Comae. Many of these giants have a moderate or strong lithium line strongly suggesting that these stars recently evolved from rapidly rotating A or early F stars as is suggested by their space motions. Thus, they are not spun down FK Com stars. The characteristics of these stars are such that they may be confused with pre-main sequence stars. The primary difference may be that the post main sequence stars have strong H alpha absorption lines while the pre-main sequence stars appear to have a weak H alpha absorption line or possibly H alpha in emission above the continuum. ESA

N89-10750*# Joint Inst. for Lab. Astrophysics, Boulder, Colo.
Mg II FLUX AND PROFILE VARIABILITY OF HYBRID-CHROMOSPHERE STARS
Anthony Veale and Alexander Brown *In* ESA, A Decade of UV Astronomy with the IUE Satellite, Volume 1 Jun. 1988 p 335-338 (For primary document see N89-10682 01-89)
(Grants NAG5-82; NAG5-985)
Avail: NTIS HC A19/MF A01; ESA Publications Div., ESTEC, Noordwijk, Netherlands, 140 Dutch guilders CSCL 03A

Results from an IUE investigation of the variability seen in the Mg II emission line fluxes and wind absorption components of hybrid-chromosphere stars are presented. Real Mg II flux variability is shown with most of the variation being long-term. This variability appears to be due to global changes in the Mg II surface activity. Major changes in the wind absorption component are not seen. ESA

N89-10751# New Mexico Inst. of Mining and Technology, Socorro. Astrophysics Research Center.
THE DISCOVERY OF A CO-ROTATING MAGNETOSPHERE IN A HELIUM WEAK STAR: HD5737 = ALPHA Scl
S. N. Shore, D. N. Brown, and G. Sonneborn (Computer Sciences Corp., Greenbelt, Md.) *In* ESA, A Decade of UV Astronomy with the IUE Satellite, Volume 1 Jun. 1988 p 339-342 (For primary document see N89-10682 01-89)
Avail: NTIS HC A19/MF A01; ESA Publications Div., ESTEC, Noordwijk, Netherlands, 140 Dutch guilders

The discovery, using combined IUE spectroscopy and Zeeman polarimetric magnetic field measurements, of a magnetosphere in a helium weak star is reported. The star, HD 5737 = alpha Scl, is one of the extreme He weak stars in its He deficiency, but is otherwise quite similar to the other sn stars HD 21699 and HD 79158. A period for the magnetic and C IV and Si IV variations of 21.65 days, a factor of 10 longer than the other variable sn stars is indicated. The effective (longitudinal) field nulls correspond extremely well to C IV line strength maxima. The magnetic field and equatorial magnetosphere are highly oblique (70 deg) and the line variations appear to be stable. ESA

N89-10752*# Colorado Univ., Boulder. Center for Astrophysics and Space Astronomy.
OBSERVATIONS OF ULTRAVIOLET VARIABILITY IN RV TAURI STARS
Edward W. Brugel and Jason A. Cardelli *In* ESA, A Decade of UV Astronomy with the IUE Satellite, Volume 1 Jun. 1988 p 343-346 (For primary document see N89-10682 01-89)
(Contract NAG5-350)
Avail: NTIS HC A19/MF A01; ESA Publications Div., ESTEC, Noordwijk, Netherlands, 140 Dutch guilders CSCL 03A

An IUE program to monitor the ultraviolet variability in RV Tauri stars was initiated. The Mg II region was investigated as a potential probe of atmospheric shocks, which are believed to be associated with the pulsational variability of this class of objects. Observations, a description of the spectra, and findings for V Vul and AC Her are presented. The Mg II emission does vary significantly during the cycle; major changes in the emission line strength occur on a time scale much less than 0.2 in phase; and as the UV (and optical) continuum flux increases, the Mg II lines decrease and increased emission may be seen at 2823, 2844, and 2900 A. ESA

N89-10753*# National Aeronautics and Space Administration. Goddard Space Flight Center, Greenbelt, Md.
FLUORESCENCE PROCESSES AND LINE IDENTIFICATIONS IN THE UV SPECTRA OF COOL STARS
Kenneth G. Carpenter and Sveneric Johansson *In* ESA, A Decade of UV Astronomy with the IUE Satellite, Volume 1 Jun. 1988 p 349-356 (For primary document see N89-10682 01-89)
(Grants NAG5-797; NAS5-29337)
Avail: NTIS HC A19/MF A01; ESA Publications Div., ESTEC, Noordwijk, Netherlands, 140 Dutch guilders CSCL 03A

Fluorescence processes active in the outer atmospheres of noncoronal cool stars and the UV lines they produce are summarized. Eight pumping processes and 21 fluorescent line products are discussed. The processes, which produce 12 lines, involves energy levels not previously known to be radiatively populated. Four of these are examples of self-fluorescence, whereby one or more lines of Fe II photo-excite through coincident lines the upper levels of other Fe II lines lines seen in emission, while two others explain the selective excitation of solitary Ni II and Si I lines. Nine of the line products are decays from levels in Fe I and Fe II already known to be radiatively populated. ESA

N89-10754# Consiglio Nazionale delle Ricerche, Frascati (Italy). Istituto Astrofisica Spaziale.
Fe II LEVEL POPULATION IN LUMINOUS VARIABLE STARS
R. Viotti, C. Rossi, G. Muratorio, M. Friedjung, and G. B. Baratta (Osservatorio Astronomico, Rome, Italy) *In* ESA, A Decade of UV Astronomy with the IUE Satellite, Volume 1 Jun. 1988 p 357-359 (For primary document see N89-10682 01-89)
Avail: NTIS HC A19/MF A01; ESA Publications Div., ESTEC, Noordwijk, Netherlands, 140 Dutch guilders

The overall FeII level population in the luminous variable stars KQ Pup and AG Car was derived using the self absorption curve method of analysis of the optical and UV Fe II emission lines. Most levels are nearly populated according a Boltzmann-type law with excitation temperatures of 6500 and 7500 K for KQ Pup and AG Car respectively. For KQ Pup there is evidence of selective excitation processes and dielectronic recombination in the level population. The importance of the study of the Fe II spectrum as diagnostics of the physical processes in astrophysical objects, from stellar chromospheres to distant galaxies, is discussed. ESA

N89-10755*# National Aeronautics and Space Administration. Goddard Space Flight Center, Greenbelt, Md.
IDENTIFICATION OF NEW FLUORESCENCE PROCESSES IN THE UV SPECTRA OF COOL STARS FROM NEW ENERGY LEVELS OF Fe II AND Cr II
Sveneric Johansson and Kenneth G. Carpenter (Colorado Univ., Boulder.) *In* ESA, A Decade of UV Astronomy with the IUE Satellite, Volume 1 Jun. 1988 p 361-363 (For primary document

see N89-10682 01-89)
Avail: NTIS HC A19/MF A01; ESA Publications Div., ESTEC, Noordwijk, Netherlands, 140 Dutch guilders

Two fluorescence processes operating in atmospheres of cool stars, symbiotic stars, and the Sun are presented. Two emission lines, at 1347.03 and 1360.17 A, are identified as fluorescence lines of Cr II and Fe II. The lines are due to transitions from highly excited levels, which are populated radiatively by the hydrogen Lyman alpha line due to accidental wavelength coincidences. Three energy levels, one in Cr II and two in Fe II, are reported. ESA

N89-10756*# National Aeronautics and Space Administration. Goddard Space Flight Center, Greenbelt, Md.
PERIODIC MODULATION OF THE ATMOSPHERE OF ALPHA ORIONIS
A. K. Dupree, S. L. Baliunas, E. F. Guinan, L. Hartmann, G. E. Nassiopoulos (Harvard-Smithsonian Center for Astrophysics, Cambridge, Mass.), and G. Sonneborn *In* ESA, A Decade of UV Astronomy with the IUE Satellite, Volume 1 Jun. 1988 p 365-368 (For primary document see N89-10682 01-89)
Avail: NTIS HC A19/MF A01; ESA Publications Div., ESTEC, Noordwijk, Netherlands, 140 Dutch guilders CSCL 03A

Alpha Orionis (Betelgeuse; M2 lab) was monitored with IUE since 1984. Discovery of a 420-day periodic modulation of the flux in the optical and ultraviolet continua, and in the Mg II h and k line emission cores suggests that periodic photospheric pulsations were present from 1984 to 1986. This behavior continues through 1987. However, the general flux level of the ultraviolet continuum and the Mg II lines is decreasing, and the amplitude of the variation may be reduced. These decreases may be the emerging signature of an additional longer period. The density sensitive C II diagnostic, 2325.4/2328.1, indicates the chromospheric densities range between log N(sub e) (cm-3) = 8.7 and 9.5, but periodicities are not evident. ESA

N89-10757*# Colorado Univ., Boulder. Center for Astrophysics and Space Astronomy.
Mg II LINE PROFILES OF THE MIRA S CARINAE
Edward W. Brugel, Jay A. Bookbinder, and Alexander Brown (Joint Inst. for Lab. Astrophysics, Boulder, Colo.) *In* ESA, A Decade of UV Astronomy with the IUE Satellite, Volume 1 Jun. 1988 p 369-372 (For primary document see N89-10682 01-89)
(Contracts NAG5-82; NAG5-350)
Avail: NTIS HC A19/MF A01; ESA Publications Div., ESTEC, Noordwijk, Netherlands, 140 Dutch guilders CSCL 03A

High-dispersion IUE observations obtained to investigate the evolution of the shock structure of the Mira S Carinae (S Car) produced, despite very limited phase coverage, a set of five spectra of the Mg II h and k lines. There is significant emission from both the h and k lines at velocities of -150 km/sec relative to the stellar photosphere. The h-to-k ratio of the Mg II doublet remains below the theoretically predicated values of 2:1 to 1:1, and shows a smooth dependence on the optical phase. Archival studies of other Miras (e.g., R Car) indicate that S Car is not unique in possessing unusual and highly variable Mg II h and k line profiles. ESA

N89-10758# European Space Agency. ESA Tracking Station, Madrid (Spain).
THE VARIABILITY OF THE UV SPECTRUM OF THE SYMBIOTIC STAR BF CYGNI
R. Gonzalez-Riestra, A. Cassatella, and T. Fernandez-Castro *In its* A Decade of UV Astronomy with the IUE Satellite, Volume 1 Jun. 1988 p 373-376 (For primary document see N89-10682 01-89)
Avail: NTIS HC A19/MF A01; ESA Publications Div., ESTEC, Noordwijk, Netherlands, 140 Dutch guilders

The symbiotic star BF Cygni was monitored by IUE in low and high resolution since July 1986 to cover a full photometric period. In order to study the long-term UV variability of the system, spectra were used with archive data taken during the period 1979 to 1981. During the IUE lifetime, BF Cygni underwent dramatic changes in the UV continuum and emission line fluxes. Most of the emission lines vary in phase with the continuum with deep eclipses near photometric phase 0. All the observational evidence supports a model in which the variability of the system could be mainly due to occultations of the different emitting regions during the orbital motion. ESA

N89-10759# Centre National de la Recherche Scientifique, Verrieres-Le Buisson (France). Lab. de Physique Stellaire et Planetaire.
ABUNDANCE AND f VALUES NEEDED TO INTERPRET ADEQUATELY THE HIGH RESOLUTION IUE SPECTRA
R. FreireFerrero *In* ESA, A Decade of UV Astronomy with the IUE Satellite, Volume 1 Jun. 1988 p 377-379 (For primary document see N89-10682 01-89)
Avail: NTIS HC A19/MF A01; ESA Publications Div., ESTEC, Noordwijk, Netherlands, 140 Dutch guilders

To establish the real needs to interpret correctly a high resolution IUE spectrum, a rough estimate of what would be the abundance or the f minimal values that correspond to isolated lines in the limit of detection given by instrumental resolution is made. The need to develop the determination or calculation of atomic data concerning very weak spectral lines is stressed. Thus, with more complete and reliable atomic data, systematic synthetic spectra calculations could lead to better understanding of physical conditions of stellar atmospheres. ESA

N89-10760*# Washington Univ., Seattle. Dept. of Astronomy.
CARBON AND NITROGEN ABUNDANCE DETERMINATIONS FROM TRANSITION LAYER LINES
Erika Boehm-Vitense and Jose Mena-Werth *In* ESA, A Decade of UV Astronomy with the IUE Satellite, Volume 1 Jun. 1988 p 381-384 (For primary document see N89-10682 01-89)
(Grant NsG-5398)
Avail: NTIS HC A19/MF A01; ESA Publications Div., ESTEC, Noordwijk, Netherlands, 140 Dutch guilders CSCL 03A

For red giants a smooth increase in the nitrogen to carbon abundance ratio for increasing B-V as is expected for the first dredge up phase when the outer convection zone deepens is found. An average increase in the nitrogen to silicon ratio for B-V = 0.6 which goes back to almost solar values for cool giants with B - V approximately 1.0 is reported. It looks as if Si would be enriched for deeper mixing contrary to expectations from standard evolution theory. ESA

N89-10761*# National Aeronautics and Space Administration. Goddard Space Flight Center, Greenbelt, Md.
THE ANOMALOUS C 4 INTENSITY RATIO IN SYMBIOTIC STARS
A. G. Michalitsianos, M. Kafatos (George Mason Univ., Fairfax, Va.), and R. P. Fahey *In* ESA, A Decade of UV Astronomy with the IUE Satellite, Volume 1 Jun. 1988 p 385-388 (For primary document see N89-10682 01-89)
Avail: NTIS HC A19/MF A01; ESA Publications Div., ESTEC, Noordwijk, Netherlands, 140 Dutch guilders CSCL 03A

The C IV lambda lambda 1548.2,1550.8 resonance doublet in a symbiotic stars was shown to exhibit anomalous line intensity ratios in which I (lambda 1548.2)/I(lambda 1550.8) less than 1, or less than the optically-thick limit of unity. The R Aquarii-central HII region and RX Puppis exhibit this phenomena. The I(lambda 1548.2)/I(lambda 1550.8) ratio in RX Puppis is found to vary inversely with the total C IV line intensity, and with the FES-visual light, as the object declined over a 5 yr period following a brightening in UV and optical emission which peaked in 1982. This doublet intensity behavior could be explained by a wind which has a narrow velocity range of 600 approx. less than sup v wind approx. less than 1000 km/sec, or by the pumping of the Fe II (mul. 45.01) transition a sup 4 F sub 9/2 - y sup 4 H(o) sub 11/2 by C IV lambda 1548.2, which effectively scatters C IV photons into the Fe II spectrum in these objects. ESA

N89-10762# Observatoire de Paris-Meudon (France).
THE IUE SPECTRAL ATLAS OF TWO NORMAL B STARS: pi Cet AND nu Cap (125 TO 200 nm)
M.-C. Artru, J. Borsenberger (Lausanne Univ., Switzerland), and T. Lanz *In* ESA, A Decade of UV Astronomy with the IUE Satellite, Volume 1 Jun. 1988 p 389-391 (For primary document see N89-10682 01-89)
Avail: NTIS HC A19/MF A01; ESA Publications Div., ESTEC, Noordwijk, Netherlands, 140 Dutch guilders

An atlas for B stars pi Cet (HD17081, B7V) and nu Cap (HD192432, B9.5V) was prepared in the range 125 to 200 nm. By means of an improved software to process the IUE images and by the coaddition of 10 high-resolution images, the best possible resolution and signal to noise ratio are obtained. The identification of the lines is based on updated laboratory lists with a selection of the dominant contributors for each absorption line. About 80 percent of the measured lines have a definite identification. ESA

N89-10763# Applied Research Corp., Landover, Md.
THE UV SILICON SPECTRA OF EARLY B STARS
Derck Massa *In* ESA, A Decade of UV Astronomy with the IUE Satellite, Volume 1 Jun. 1988 p 393-396 (For primary document see N89-10682 01-89)
Avail: NTIS HC A19/MF A01; ESA Publications Div., ESTEC, Noordwijk, Netherlands, 140 Dutch guilders

The UV silicon spectra of mid to early B stars are examined and compared to models. It is found that lines are extremely sensitive to stellar temperature and luminosity. Although the models fail to predict the quantitative behavior of the line strengths, they do, in most instances, describe their qualitative behavior. ESA

N89-10764*# National Aeronautics and Space Administration. Goddard Space Flight Center, Greenbelt, Md.
C IV AND Si IV IN IUE SPECTRA OF NORMAL B8-A0 STARS: UV IDENTIFIED Be/Ae STARS
Weihsueh A. Chiu, C. A. Grady, and Frederick C. Bruhweiler (Catholic Univ. of America, Washington, D.C.) *In* ESA, A Decade of UV Astronomy with the IUE Satellite, Volume 1 Jun. 1988 p 397-400 (For primary document see N89-10682 01-89)
Avail: NTIS HC A19/MF A01; ESA Publications Div., ESTEC, Noordwijk, Netherlands, 140 Dutch guilders CSCL 03A

Archival IUE high dispersion spectra of 42 B6-A2 stars within 200 pc were surveyed. Five of the program stars show significant C IV and Si IV absorption. All of the stars with detected C IV have v sin i less than or = 190 km/sec. Sharp absorption cores are present in Si II lambda 1533 in 3 of the objects, indicating that these are previously unrecognized shell stars. Three of the stars have variable or asymmetric C IV profiles which are consistent with the C IV and Si IV being produced in stellar winds. One star has C IV in the form of a shortward-shifted discrete absorption component, similar to those observed in Be stars. The data are compared with similar data for Be and B shell stars. ESA

N89-10765*# Colorado Univ., Boulder. Center for Astrophysics and Space Astronomy.
ULTRAVIOLET PROPERTIES OF IRAS-SELECTED Be STARS
Karen S. Bjorkman and Theodore P. Snow *In* ESA, A Decade of UV Astronomy with the IUE Satellite, Volume 1 Jun. 1988 p 401-404 (For primary document see N89-10682 01-89)
(Grant NsG-5300)
Avail: NTIS HC A19/MF A01; ESA Publications Div., ESTEC, Noordwijk, Netherlands, 140 Dutch guilders CSCL 03A

New IUE observations were obtained of 35 Be stars from a list of stars which show excess infrared fluxes in IRAS data. The IRAS-selected Be stars show larger C IV and Si IV equivalent widths than other Be stars. Excess C IV and Si IV absorption seems to be independent of spectral type for IRAS-selected Be stars later than spectral type B4. This is interpreted as evidence for a possible second mechanism acting in conjunction with radiation pressure for producing the winds in Be stars. No clear correlation of IR excess of v sin i with C IV or Si IV equivalent widths is seen, although a threshold for the occurrence of excess C IV and Si IV absorption appears at a v sin i of 150 km/sec. ESA

N89-10766# Goettingen Univ. (West Germany).
Au II IN IUE SPECTRA OF CHEMICALLY PECULIAR STARS
K. Fuhrmann *In* ESA, A Decade of UV Astronomy with the IUE Satellite, Volume 1 Jun. 1988 p 405-408 (For primary document see N89-10682 01-89)
Avail: NTIS HC A19/MF A01; ESA Publications Div., ESTEC, Noordwijk, Netherlands, 140 Dutch guilders

From work on HR 465, the identification of the odd-Z element gold (Z=79) in the spectra of magnetic (CP2) as well as nonmagnetic (CP3) stars is reported. The importance of quantitative abundance analyses of the Pt-Au-Hg elemental sequence is pointed out, as well as a closer relationship between CP2 and CP3 stars than generally assumed. ESA

N89-10767# Dominion Astrophysical Observatory, Victoria (British Columbia).
VALIDITY OF THE CLASSIFICATION OF UV GALLIUM STARS
M. Takada-Hidai and K. Sadakane *In* ESA, A Decade of UV Astronomy with the IUE Satellite, Volume 1 Jun. 1988 p 409-412 Sponsored by Itoh Science Foundation, Japan and the Japan Cultural Inst. (For primary document see N89-10682 01-89)
Avail: NTIS HC A19/MF A01; ESA Publications Div., ESTEC, Noordwijk, Netherlands, 140 Dutch guilders

Line intensities of Ga II at 1414 A and Ga III at 1495 A are surveyed on high-dispersion IUE spectra of 7 stars classified as UV gallium stars on low dispersion IUE spectra. The Ga II line intensity in HD 124224 is found to be weaker in all 11 high dispersion spectra than that expected from the spectral classification criteria. The remaining six stars show the strong Ga II line consistent with the classification criteria. A cross-check with the help of high dispersion spectra must be effective in classification based on low dispersion spectra. ESA

N89-10768# Centre National de la Recherche Scientifique, Verrieres-Le Buisson (France). Lab. de Physique Stellaire et Planetaire.
DETECTED UV VARIABILITY IN THE IUE SPECTRA OF THE Ap-Si STAR HD 25823
R. FreireFerrero and M.-C. Artru (Observatoire de Paris-Meudon, France) *In* ESA, A Decade of UV Astronomy with the IUE Satellite, Volume 1 Jun. 1988 p 413-415 (For primary document see N89-10682 01-89)
Avail: NTIS HC A19/MF A01; ESA Publications Div., ESTEC, Noordwijk, Netherlands, 140 Dutch guilders

Spectral UV variabilities for the Ap-Si star HD 25823 are detected from 5 SWP IUE images. This peculiar and magnetic star presents also an uncommon overabundance of gallium. From the observations, it seems that silicon and gallium (and also other) abundance varies according to the rotational period of the star, as does the magnetic field. The anticorrelation observed between periodic variations of silicon and gallium confirms the predictions of diffusion theory. ESA

N89-10769*# New Mexico Inst. of Mining and Technology, Socorro. Astrophysics Research Dept.
THE GALATIC AND LMC EXTREME LINE SUPERGIANTS COMPARED: IUE OBSERVATIONS OF THE HENIZE-CARLSON AND ZOO STAR SAMPLES OF MASSIVE SUPERGIANTS
S. N. Shore, N. Sanduleak, D. N. Brown, G. Sonneborn, B. W. Bopp, and C. R. Robinson (Toledo Univ., Ohio.) *In* ESA, A Decade of UV Astronomy with the IUE Satellite, Volume 1 Jun. 1988 p 417-420 Sponsored by NASA, Washington, D.C. (For primary document see N89-10682 01-89)
Avail: NTIS HC A19/MF A01; ESA Publications Div., ESTEC, Noordwijk, Netherlands, 140 Dutch guilders CSCL 03A

The Henize-Carlson sample of galactic massive supergiants, and a comparison between the Galactic and LMC samples are discussed. Several of the stars, notably He3-395 and S 127/LMC, have very similar shell characteristics. There appears to be little

difference, other than luminosity, between the LMC and Galactic samples. One star, He3-1482, was detected with the Very Large Array at 6 cm. The UV data is combined with IRAS and optical information. ESA

N89-10770# Delaware Univ., Newark. Bartol Research Inst.
MASS LOSS FROM THE K DWARF IN V471 TAURI
D. J. Mullan, F. Bruhweiler, and E. M. Sion (Villanova Univ., Pa.) *In* ESA, A Decade of UV Astronomy with the IUE Satellite, Volume 1 Jun. 1988 p 423-424 (For primary document see N89-10682 01-89)
Avail: NTIS HC A19/MF A01; ESA Publications Div., ESTEC, Noordwijk, Netherlands, 140 Dutch guilders

Spectra of Mg II h and k were obtained for V471 Tau at phases zero (K dwarf in front) and 0.5 (white dwarf in front). At phase zero, strong blueshifted absorption is present, suggestive of a wind from the K dwarf with terminal velocity 600 to 400 km/sec and mass loss rate at least 3 orders of magnitude greater than solar. Discrete blue-shifted absorption features occur at velocities of 200 and 500 km/sec. At phase 0.5, the blueshifted absorption is much weaker, although still detectable. ESA

N89-10064*# National Aeronautics and Space Administration. Ames Research Center, Moffett Field, Calif.
MAINTAINING AN EXPERT SYSTEM FOR THE HUBBLE SPACE TELESCOPE GROUND SUPPORT
Kelly Lindenmayer, Shon Vick (Space Telescope Science Inst., Baltimore, Md.), and Don Rosenthal *In* NASA, Goddard Space Flight Center, Proceedings of 1987 Goddard Conference on Space Applications of Artificial Intelligence (AI) and Robotics 1987 p 1-1 (For primary document see N89-10063 01-12)
Avail: NTIS HC A99/MF E03 CSCL 03A

90 ASTROPHYSICS

Includes cosmology; celestial mechanics; space plasmas; and interstellar and interplanetary gases and dust.
For related information see also *75 Plasma Physics*.

N89-10771 Durham Univ. (England).
SUPERNOVA REMNANTS' INTERACTIONS WITH THE INTER-STELLAR MEDIUM Ph.D. Thesis
Michael Lawrence Parkinson 1987 283 p
Avail: Univ. Microfilms Order No. BRD-80799

All sky data at a number of different wavelengths are used to examine the Giant Radio Loops. The X-ray emission of Loop 1 is modeled as being due to a Supernova Remnant that has evolved in a hot, homogeneous, quasi-isotropic medium. The shock is found to weaken towards higher latitudes, and this is attributed to an increase in the ambient gas temperature away from the galactic plane. Other evolutionary possibilities are examined. Radio spectral index maps from 38 to 1420 MHz of the northern celestrial hemisphere are produced, and the spectra of Loops 1 and 3 are modeled on the assumption that the energy distribution of electrons accelerated in the shocks will have an upper energy cut-off due to the finite age of the remnants. It is found that the steepening spectra can be fitted by such a model. The electron distribution below the cut-off or order 10 GeV is found to fit best if a flatter spectrum than predicted by simple shock theory is assumed. The idea that shocks interacting with clouds can explain this flatter spectrum and enhance the soft X-ray emission is put forward as an alternative evolutionary possibility, bringing together the two seperate X-ray and radio emission mechanisms. Dissert. Abstr.

N89-10772*# National Aeronautics and Space Administration. Goddard Space Flight Center, Greenbelt, Md.
INTERPLANETARY MEDIUM DATA BOOK. SUPPLEMENT 3: 1977-1985
David A. Couzens and Joseph H. King Apr. 1986 246 p Supersedes N83-19657
(NASA-TM-89660; NSSDC/WDC-A-R/S-86-04-Suppl-3; NAS 1.15:89660) Avail: NTIS HC A11/MF A01 CSCL 03B

The updating of the hourly resolution, near-Earth solar wind data compilation is discussed. Data plots and listings are then presented. In the text, the time shifting of ISEE 3 fine-scale magnetic field and and plasma data, using corotation delay, and the normalization of IMP-MIT and ISEE densities and temperatures to equivalent IMP-LANL values, are discussed in detail. The levels of arbitrariness in combining data sets, and of random differences between data sets, are elucidated. Author

N89-10773# Lawrence Livermore National Lab., Calif.
PROSPECTS FOR UNDERSTANDING THE ASTROPHYSICAL r-PROCESS
G. J. Mathews and J. J. Cowan (Oklahoma Univ., Norman.) Jul. 1988 6 p Presented at the Tokyo Symposium on Heavy-ion and Nuclear Astrophysical Problems, Tokyo, Japan, 19 Jul. 1988
(Contract W-7405-eng-48)
(DE88-015449; UCRL-99326; CONF-880795-1) Avail: NTIS HC A02/MF A01

This paper discusses several recent advances toward a deeper understanding of the still unknown astrophysical site for rapid (r-process) neutron capture nucleosynthesis. The physical constraints on the r-process from the input nuclear data are highlighted and the particular importance of the recent measurements of beta-decay lifetimes along the r-process path is discussed. Astronomical observations of s- and r-process elemental abundances on metal poor halo stars are also discussed, in the context of models for the galactic chemical evolution of heavy-element abundances, as a constraint on the nature of the r-process. On the basis of these constraints it is suggested that the most likely source for the r-process may be from the ejection of core material from low-mass type II supernovae. DOE

N89-10774*# New Hampshire Univ., Durham. Gamma-Ray Astronomy Group.
A SUMMARY OF MAJOR ACTIVITIES OF THE UNH AND NRL GROUPS Annual Progress Report, 15 Nov. 1987 - 14 May 1988
E. L. Chupp 15 Aug. 1988 22 p
(Grant NAG5-720)
(NASA-CR-180949; NAS 1.26:180949) Avail: NTIS HC A03/MF A01 CSCL 03B

The major activities of the SMM GRS team members at the University of New Hampshire and the Naval Research Laboratory since the last semi-annual report are summarized. An updated list of published papers and invited papers or contributed papers presented at scientific meetings is provided. Author

N89-10775# Los Alamos National Lab., N. Mex.
COSMOGENIC (SUP 36)Cl PRODUCTION RATES IN METEORITES AND THE LUNAR SURFACE
K. Nishiizumi, P. W. Kubik, D. Elmore, R. C. Reedy, and J. R. Arnold (California Univ., San Diego.) 1988 30 p Presented at GEOTIMES: 19th Lunar and Planetary Science Conference, Houston, Tex., 14 Mar. 1988
(Contracts W-7405-eng-36; W-31-109-eng-38)
(DE88-014452; LA-UR-88-1878; CONF-880391-2) Avail: NTIS HC A03/MF A01

Activity vs. depth profiles of cosmic ray produced Cl-36 were measured in metal from two cores each in the St. Severin and Jilin chondrites and in lunar core 15008. Production of Cl-36 in these samples range from high-energy reactions with Fe and Ni to low-energy reactions with Ca and K and possibly neutron-capture reactions with Cl-36. The cross sections used in the Reedy-Arnold model for neutron-induced reactions were adjusted to get production rates that fit the measured Cl-36 activities in St. Severin metal and in the lunar soil of core 15008. The Cl-36 in metal from St. Severin has a fairly flat activity-vs-depth profile, unlike most other cosmogenic nuclides in bulk samples from St. Severin, which increase in concentration with depth. In metal from Jilin, a decrease in Cl-36 was observed near its center. The length of Jilin's most recent cosmic-ray exposure was approximately 0.5 My. Lunar core 15008 has an excess in Cl-36 of about 4 dpm/kg

near its surface that was produced by solar-proton-induced reactions. The calculated production rates are consistent with these measured trends in 15008. DOE

N89-10776 Arizona Univ., Tucson.
GLOBAL PROPERTIES OF MOLECULAR CLOUDS AND THE INTERSTELLAR MEDIUM IN GALAXIES Ph.D. Thesis
Philip Richard Maloney 1987 332 p
Avail: Univ. Microfilms Order No. DA8804180

Molecular gas in other galaxies is generally studied by observations of CO emission; a conversion from CO integrated intensity to H(sub2) column density must be made. Modeling of the emission from an ensemble of molecular clouds shows that these conversion factors are sensitive to temperature, so that molecular gas masses in galaxies with high star formation rates have probably been overestimated. Conversely, models of molecular clouds in low metallicity systems demonstrate the molecular gas abundance. The observed properties of dark clouds and high latitude clouds are consistent with clouds in equilibrium with an intercloud pressure of P/kappa approx. = 10000. Detailed comparison of the CO and 170 micron emission from the disks of NGC 6946 and M51 shows that the far infrared flux must rise from dust in molecular clouds, not atomic clouds; this emission may be powered by embedded young stars or by the interstellar radiation field. The interpretation of the ratio of infrared to CO luminosities as a star formation efficiency is of dubious validity. Modeling of the observed CO and far infrared emission from a sample of galactic nuclei shows that roughly half of the CO flux is produced by very active star forming clouds. Dissert. Abstr.

N89-10777 California Univ., Los Angeles.
ACCRETION DISK MODELS OF QUASARS AND ACTIVE GALACTIC NUCLEI Ph.D. Thesis
Wei-Hsin Sun 1987 216 p
Avail: Univ. Microfilms Order No. DA8802513

Calculations are presented of the spectra of black hole accretion disks which may power quasars and active galactic nuclei. The effects of electron scattering opacity and general relativistic corrections at different disk inclinations on the observed spectra are included. Low gravity non-LTE stellar atmospheres are used in order to account for the dominance of electron scattering opacity. Alternative disks with a series of blackbodies at different temperatures are also modeled. Both Kerr and Schwarzschild geometries are considered. The relativistic correction is much more significant in the Kerr case than that in the Schwarzschild case. The atmosphere disk predicts a spectrum harder than that of the blackbody disk. When the disk is viewed at higher inclinations, the apparent disk spectrum also becomes harder. The Kerr disks are fitted to the multi-wavelength continua of a sample of 60 QSOs and AGNs. The disk spectra using atmospheres do not predict the observations as well as the blackbody disks. In both Kerr and Schwarzschild cases, it was found that the low redshift Seyfert galaxies have relatively low accretion rates while the most luminous quasars are accreting near their Eddington limit.
Dissert. Abstr.

N89-10778# State Univ. of New York, Stony Brook. Dept. of Earth and Space Sciences.
RESEARCH IN NUCLEAR ASTROPHYSICS: STELLAR COLLAPSE AND SUPERNOVAE Annual Performance Report, 1 Dec. 1987 - 30 Nov. 1988
James M. Lattimer and A. Yahil 1988 12 p
(Contract DE-FG02-87ER-40317)
(DE88-015267; DOE/ER-40317/2) Avail: NTIS HC A03/MF A01

This annual performance report summarizes the activity in the nuclear astrophysics research program in the Earth and Space Scienes Department at Stony Brook. The central themes in the projects that comprise this program are supernovae, neutron star formation, and the equation of state of hot, dense metter. There is a close coupling between the physics of nuclear matter and weak interactions on the one hand, and supernovae and neutron stars on the other. The properties of nuclear matter might at present best be delineated by astrophysical considerations. We have been active in researching both the nuclear physics of the equation of state and the astrophysics of stellar collapse, neutrino emission, and neutron star formation. DOE

91 LUNAR AND PLANETARY EXPLORATION

Includes planetology; and manned and unmanned flights. For spacecraft design or space stations see *18 Spacecraft Design, Testing and Performance.*

N89-10779*# Utah State Univ., Logan. Center for Atmospheric and Space Sciences.
THE DYNAMICS OF THE VENUS IONOSPHERE Final Technical Report, 1 Jan. 1985 - 31 May 1988
K. L. Miller 1988 31 p
(Grant NAGw-689)
(NASA-CR-183167; NAS 1.26:183167) Avail: NTIS HC A03/MF A01 CSCL 03B

Data from the Pioneer-Venus orbiter has demonstrated the importance of understanding ion dynamics in the Venus ionosphere. The analysis of the data has shown that during solar maximum the topside Venus ionosphere in the dark hemisphere is generated almost entirely on the dayside of the planet during solar maximum, and flows with supersonic velocities across the terminator into the nightside. The flow field in the ionosphere is mainly axially-symmetric about the sun-Venus axis, as are most measured ionospheric quantities. The primary data base used consisted of the ion velocity measurements made by the RPA during three years that periapsis of the orbiter was maintained in the Venus ionosphere. Examples of ion velocities were published and modeled. This research examined the planetary flow patterns measured in the Venus ionosphere, and the physical implications of departures from the mean flow. Author

N89-10780*# Lunar and Planetary Inst., Houston, Tex.
MECA SYMPOSIUM ON MARS: EVOLUTION OF ITS CLIMATE AND ATMOSPHERE
Victor Baker, ed., Michael Carr, ed., Fraser Fanale, ed., Ronald Greeley, ed., Robert Haberle, ed., Conway Leovy, ed., and Ted Maxwell, ed. 1987 135 p Symposium held in Washington, D.C., 17-19 Jul. 1986; sponsored by National Air and Space Museum Previously announced in IAA as A88-11426
(Contract NASw-4066)
(NASA-CR-182872; NAS 1.26:182872; LPI-TR-87-01) Avail: NTIS HC A07/MF A01 CSCL 03B

The geological, atmospheric, and climatic history of Mars is explored in reviews and reports of recent observational and interpretive investigations. Topics addressed include evidence for a warm wet climate on early Mars, volatiles on Earth and on Mars, CO2 adsorption on palagonite and its implications for Martian regolith partitioning, and the effect of spatial resolution on interpretations of Martian subsurface volatiles. Consideration is given to high resolution observations of rampart craters, ring furrows in highland terrains, the interannual variability of the south polar cap, telescopic observations of the north polar cap and circumpolar clouds, and dynamical modeling of a planetary wave polar warming mechanism. For individual titles, see N89-10781 through N89-10825.

N89-10781*# Texas A&M Univ., College Station.
EVIDENCE FOR GLACIATION IN ELYSIUM Abstract Only
Duwayne M. Anderson and Gary W. Brandstrom *In* Lunar and Planetary Inst., MECA Symposium on Mars: Evolution of its Climate and Atmosphere 1987 p 15-17 (For primary document see N89-10780 01-91)
Avail: NTIS HC A07/MF A01 CSCL 03B

It is suggested that certain landforms in the Elysium region of Mars provide strong evidence for glaciation. Landscapes related to subglacial volcanism suggest that ice was a primary agent in the development of Elysium. E.R.

N89-10782*# Oregon State Univ., Corvallis. Dept. of Atmospheric Sciences.
NUMERICAL SIMULATIONS OF DUST TRANSPORT INTO NORTHERN HIGH LATITUDES DURING A MARTIAN POLAR WARMING
J. R. Barnes and J. L. Hollingsworth *In* Lunar and Planetary Inst., MECA Symposium on Mars: Evolution of its Climate and Atmosphere 1987 p 18-19 (For primary document see N89-10780 01-91)
Avail: NTIS HC A07/MF A01 CSCL 03B

The formation and evolution of the polar laminated terrain depends on rates of dust transport to the polar caps. A simplified dynamical model is shown similar to models used to simulate terrestrial stratospheric polar warmings could simulate certain observed features of the circulation during Martian global dust storms. Model simulations of dust transport showed that substantial quantities of dust, enough to produce optical depths of approx. 1, could reach the pole during these storms. E.R.

N89-10783*# Mission Research Corp., Alexandria, Va. Mars Research.
THE PALEO-OCEAN OF MARS Abstract Only
John E. Brandenburg *In* Lunar and Planetary Inst., MECA Symposium on Mars: Evolution of its Climate and Atmosphere 1987 p 20-22 (For primary document see N89-10780 01-91)
Avail: NTIS HC A07/MF A01 CSCL 03B

A Paleo-ocean on the northern plains of Mars is proposed. The hypothetical ocean would have formed very early in Mars' history, during the early period of rapid outgassing and cratering. As the ocean froze and receded, bursting of aquifers along the shoreline would create catastrophic flooding. Analysis of soil at the two Viking landing sites, both of which occur on the floor of the hypothetical ocean, is not inconsistent with an oceanic clay rich in water soluble salts. E.R.

N89-10784*# Geological Survey, Menlo Park, Calif.
MARS: A WATER-RICH PLANET Abstract Only
Michael H. Carr *In* Lunar and Planetary Inst., MECA Symposium on Mars: Evolution of its Climate and Atmosphere 1987 p 23-25 (For primary document see N89-10780 01-91)
Avail: NTIS HC A07/MF A01 CSCL 03B

Good geomorphic evidence is presented for a planet that was once water rich, and that a lower limit on the amount of water available for a given Martian watershed may be estimated by assuming that the volume of material eroded was equal to the volume of water available. This estimate, coupled with high latitude water estimates of 50 to 100 m gives a global inventory of about 500 m total water in the subsurface. It was emphasized that this is a lower limit as considerable water may be bound in weathered debris and in primary minerals. E.R.

N89-10785*# Geological Survey, Menlo Park, Calif.
MARTIAN VOLCANISM: A REVIEW Abstract Only
Michael H. Carr *In* Lunar and Planetary Inst., MECA Symposium on Mars: Evolution of its Climate and Atmosphere 1987 p 26-28 (For primary document see N89-10780 01-91)
Avail: NTIS HC A07/MF A01 CSCL 03B

Martian volcanism is reviewed. It is emphasized that lava plains constitute the major type of effusive flow, and can be differentiated by morphologic characteristics. Shield volcanoes, domes, and patera constitute the major constructional landforms, and recent work has suggested that explosive activity and resulting pyroclastic deposits may have been involved with formation of some of the small shields. Analysis of morphology, presumed composition, and spectroscopic data all indicate that Martian volcanism was dominantly basaltic in composition. E.R.

N89-10786*# Martin Marietta Aerospace, Denver, Colo. Planetary Sciences Lab.
COMETS, VOLCANISM, THE SALT RICH REGOLITH AND CYCLING OF VOLATILES ON MARS Abstract Only
Benton C. Clark *In* Lunar and Planetary Inst., MECA Symposium on Mars: Evolution of its Climate and Atmosphere 1987 p 29-31 Previously announced in IAA as A88-11430 (For primary document see N89-10780 01-91)
Avail: NTIS HC A07/MF A01 CSCL 03B

The composition of the Martian surface and its evolution are examined, reviewing the results of recent theoretical models and composition estimates based on Viking lander analyses. The data are compiled in tables and characterized in detail, and a high degree of variation among the predictions is noted. The discussion centers on the possible roles of comets (as sources of volatiles), the salt rich regolith (as an important water sink), and volcanic activity (interfering with volatile-recycling processes and eventually producing a volatile depleted surface layer). E.R.

N89-10787*# Lunar and Planetary Inst., Houston, Tex.
MARS: CRUSTAL PORE VOLUME, CRYOSPHERIC DEPTH, AND THE GLOBAL OCCURRENCE OF GROUNDWATER
Stephen M. Clifford *In its* MECA Symposium on Mars: Evolution of its Climate and Atmosphere 1987 p 32-34 (For primary document see N89-10780 01-91)
Avail: NTIS HC A07/MF A01 CSCL 03B

It is argued that most of the Martian hydrosphere resides in a porous outer layer of crust that, based on a lunar analogy, appears to extend to a depth of about 10 km. The total pore volume of this layer is sufficient to store the equivalent of a global ocean of water some 500 to 1500 m deep. Thermal modeling suggests that about 300 to 500 m of water could be stored as ice within the crust. Any excess must exist as groundwater. E.R.

N89-10788*# Hawaii Univ., Honolulu. Hawaii Inst. of Geophysics.
IS REGOLITH ABSORBTION THE EXPLANATION FOR THE TRANSITION FROM EARLY TO PRESENT MARS CLIMATE
F. P. Fanale, S. Postawko, A. P. Zent, and J. R. Salvail *In* Lunar and Planetary Inst., MECA Symposium on Mars: Evolution of its Climate and Atmosphere 1987 p 35-36 (For primary document see N89-10780 01-91)
Avail: NTIS HC A07/MF A01 CSCL 03B

Experimental data is presented for CO2 adsorption on palagonites (now thought to provide the most acceptable spectral match to Mars weathering products). When corrected for great differences in specific surface area, the adsorptive behavior exhibited by palogonites, nontronite, and basalt with respect to CO2 can be (approx.) described by the same generic equation. Using this relationship normalized to a Mars soil surface area, and the dependence of subsurface temperatures on latitude and depth, the current inventory of regolith absorbed CO2 was estimated. E.R.

N89-10789*# National Aeronautics and Space Administration. Goddard Space Flight Center, Greenbelt, Md.
MARTIAN SURFACE PHYSICAL PROPERTIES TO BE DERIVED BY RADAR ALTIMETER ON THE MARS OBSERVER SPACECRAFT
J. B. Garvin, F. T. Ulaby, D. E. Smith, H. V. Frey, S. Solomon (Massachusetts Inst. of Tech., Cambridge.), and H. J. Zwally *In* Lunar and Planetary Inst., MECA Symposium on Mars: Evolution of its Climate and Atmosphere 1987 p 37-39 (For primary document see N89-10780 01-91)
Avail: NTIS HC A07/MF A01 CSCL 03B

The potential is described of a candidate Mars Observer altimeter for determining dielectric properties of Mars regolith. It is pointed out that it is straightforward to use the time between altimeter pulse trains for passive radiometry (hence dielectric properties) and roughness can be derived. Given the mission plan the whole surface can be mapped at least three times, yielding data on seasonal variability. E.R.

N89-10790*# Arizona State Univ., Tempe. Dept. of Geology.
RELEASE OF MAGMATIC WATER ON MARS: ESTIMATED TIMING AND VOLUMES
R. Greeley *In* Lunar and Planetary Inst., MECA Symposium on Mars: Evolution of its Climate and Atmosphere 1987 p 40-42

(For primary document see N89-10780 01-91)
Avail: NTIS HC A07/MF A01 CSCL 03B

By estimating the total amount of water released by volcanic processes on Mars, the abundance of H2O at 10 m was estimated. This value was based on mapping volcanic units, estimating thicknesses and volumes, and using a 10 wt. percent value H2O from terrestrial analogs. By combining such estimates with crater count ages, it is also possible to estimate the timing of water release through Martian history. E.R.

N89-10791*# Arizona State Univ., Tempe. Dept. of Geology.
THE MARTIAN DUST CYCLE: A PROPOSED MODEL
Ronald Greeley *In* Lunar and Planetary Inst., MECA Symposium on Mars: Evolution of its Climate and Atmosphere 1987 p 43-45 (For primary document see N89-10780 01-91)
Avail: NTIS HC A07/MF A01 CSCL 03B

Despite more than a decade of study of martian dust storms, many of their characteristics and associated processes remain enigmatic, including the mechanisms for dust raising, modes of settling, and the nature of dust deposits. However, observations of Mars dust, considerations of terrestrial analogs, theoretical models, and laboratory simulations permit the formulation of a Martian Dust Cycle Model, which consists of three main processes: (1) suspension threshold, (2) transportation, and (3) deposition; two associated processes are also included: (4) dust removal and (5) the addition of new dust to the cycle. Although definitions vary, dust includes particles less than 4 to approx. 60 microns in diameter, which by terrestrial usage includes silt, loess, clay, and aerosolic dust particles. The dust cycle model is explained.
Author

N89-10792*# National Aeronautics and Space Administration. Ames Research Center, Moffett Field, Calif.
INTERANNUAL VARIABILITY OF GLOBAL DUST STORMS ON MARS Abstract Only
R. M. Haberle *In* Lunar and Planetary Inst., MECA Symposium on Mars: Evolution of its Climate and Atmosphere 1987 p 46 (For primary document see N89-10780 01-91)
Avail: NTIS HC A07/MF A01 CSCL 03B

Global dust storms on Mars occur in some years but not in others. In years with global dust storms, dust is raised in the Southern Hemisphere and spread over much of the planet by an intensified Hadley circulation. In years without global dust storms, dust is raised in the Northern Hemisphere by relatively active midlatitude storm systems, but does not spread globally. In both cases the dusty season is winter in the north. It is shown from numerical simulations that a Northern Hemisphere dust haze weakens the intensity of the cross equatorial Hadley circulation and the contribution it makes to the surface stress in the Southern Hemisphere. This, in turn, reduces the possibility of global dust storm development. The interannual variability is the result either of a competition between circulation in opposite hemispheres, in which case the variability has a random component; or it is the result of the cycling of dust between hemispheres, in which case the variability is related to the characteristics of global dust storms themselves.
Author

N89-10793*# Massachusetts Univ., Amherst. Geology/Geography.
CHEMICAL FROST WEATHERING OF OLIVINE: EXPERIMENTAL STUDY AND IMPLICATIONS Abstract Only
S. L. Harris and R. L. Huguenin *In* Lunar and Planetary Inst., MECA Symposium on Mars: Evolution of its Climate and Atmosphere 1987 p 47-49 (For primary document see N89-10780 01-91)
Avail: NTIS HC A07/MF A01 CSCL 03B

New experimental results are reported on the frost weathering of olivine. After first weathering, a decrease in Fe sup 2(+)M(2) absorption bands were noted. This decrease is related to the protonation of O(+) in the mineral. It is contented that this reaction may result in the regolith storage of 100 to 1000 m of H(sub 2) over the history of Mars. E.R.

N89-10794*# Massachusetts Univ., Amherst. Geology/Geography.
MARS LOW ALBEDO REGIONS: POSSIBLE MAP OF NEAR-SURFACE Abstract Only
R. L. Huguenin *In* Lunar and Planetary Inst., MECA Symposium on Mars: Evolution of its Climate and Atmosphere 1987 p 50-52 (For primary document see N89-10780 01-91)
Avail: NTIS HC A07/MF A01 CSCL 03B

A freeze/thaw desorption mechanism is proposed in certain low albedo areas which could be the factor that instigated dust storms. It is widely accepted that the bulk of the episodic gas evolution (not necessarily the oxygen release) experienced during the humidification process in the Viking Gas Exhange Experiment (GEX) was caused by a familiar process in which more polar H2O molecules replace large quantities of other preadsorbed gas molecules on adsorption sites. The author suggests that a similar process could produce high pore pressures in soil that could disrupt the soil and eject dust at high velocity. The author also argued that association of sites of dust storms initiated with high thermal inertial areas may simply reflect repeated dust depletion. E.R.

N89-10795*# Massachusetts Univ., Amherst. Geology/Geography.
PHOTOCHEMICAL WEATHERING AND CONTEMPORARY VOLATILE LOSS ON MARS
R. L. Huguenin *In* Lunar and Planetary Inst., MECA Symposium on Mars: Evolution of its Climate and Atmosphere 1987 p 53-56 (For primary document see N89-10780 01-91)
Avail: NTIS HC A07/MF A01 CSCL 03B

In an earlier series of papers by the author it was proposed that photochemical weathering of Fe(2+) in magnetite and in mafic silicates may be occurring in the contemporary surface environment with a resultant loss of O2 from the atmosphere. Morris and Lauer challenged the photochemical weathering model, proposing that oxidation by radiant heating rather than UV photoelectron emission induced oxidation may have dominated in the authors experiments. Subsequent laboratory studies of photochemical weathering of magnetite described here support the authors original proposal that UV illunimation can indeed drive the oxidation of magnetite under contemporary Martian surface conditions. The negative results of the Morris and Lauer study can now be explained.
Author

N89-10796*# Kyoto Univ. (Japan).
INTERANNUAL DIFFERENCES IN THE REGRESSIONS OF THE POLAR CAPS OF MARS
K. Iwasaki, Y. Saito, and T. Akabane (Kyoto Univ., Kamitakara, Japan) *In* Lunar and Planetary Inst., MECA Symposium on Mars: Evolution of its Climate and Atmosphere 1987 p 57-59 (For primary document see N89-10780 01-91)
Avail: NTIS HC A07/MF A01 CSCL 03B

Analyses of the behavior of the Martian polar caps in the recent spacecraft and ground based observations seem to reveal the existence of year to year variations on their regressions. In order to investigate the interannual differences in the regressions of the polar caps, the earlier data by Fischbacher et al., were reexamined, which were based on the measurements of the large number of high quality photographic plates and films collected from 1905 to 1965 at the Lowell Observatory. The results are reported and discussed.
Author

N89-10797*# Jet Propulsion Lab., California Inst. of Tech., Pasadena.
THE OBSERVED DAY-TO-DAY VARIABILITY OF MARS WATER VAPOR
Bruce M. Jakosky, Michael R. LaPointe (Colorado Univ., Boulder.), and Richard W. Zurek *In* Lunar and Planetary Inst., MECA Symposium on Mars: Evolution of its Climate and Atmosphere 1987 p 60-61 (For primary document see N89-10780 01-91)
Avail: NTIS HC A07/MF A01 CSCL 03B

The diurnal variability of atmospheric water vapor as derived from the Viking MAWD data is discussed. The detection of day to day variability of atmospheric water would be a significant finding

since it would place constraints on the nature of surface reservoirs. Unfortunately, the diurnal variability seen by the MAWD experiment is well correlated with the occurrence of dust and/or ice hazes, making it difficult to separate real variations from observational effects. Analysis of the day to day variability of water vapor in the Martian atmosphere suggests that the observations are, at certain locations and seasons, significantly affected by the presence of water-ice hazes. Because such effects are generally limited to specific locations, such as Tharsis, Lunae Planum, and the polar cap edge during the spring, the seasonal and latitudinal trends in water vapor that have been previously reported are not significantly affected. E.R.

N89-10798*# Missouri Univ., St. Louis. Dept. of Physics.
THE DIRECTION OF WATER TRANSPORT ON MARS: A POSSIBLE PUMPING MECHANISM Abstract Only
P. B. James *In* Lunar and Planetary Inst., MECA Symposium on Mars: Evolution of its Climate and Atmosphere 1987 p 62-63 (For primary document see N89-10780 01-91)
Avail: NTIS HC A07/MF A01 CSCL 03B

It is suggested that an atmospheric pumping mechanism might be at work in which water is preferentially transported into the north by a mass outflow wind (due to sublimation from polar cap) that is stronger during southern spring than it is during northern spring. The mechanism is provided by the asymmetric seasonal temperature distribution produced by the eccentric martial orbit and by the associated seasonal asymmetry in the carbon dioxide cycle. The alternating condensation and sublimation of CO2 at the poles produces condensation winds which, in turn, contribute to the meridional transport of water vapor. E.R.

N89-10799*# National Aeronautics and Space Administration. Ames Research Center, Moffett Field, Calif.
CLIMATIC EFFECTS OF ENHANCED CO2 LEVELS IN MARS EARLY ATMOSPHERE
James F. Kasting *In* Lunar and Planetary Inst., MECA Symposium on Mars: Evolution of its Climate and Atmosphere 1987 p 64-66 (For primary document see N89-10780 01-91)
Avail: NTIS HC A07/MF A01 CSCL 03B

Results are presented of one-dimensional radiation convection modeling of the early Mars atmosphere. Up to 5 bars of CO2 would have been required to raise the surface temperature (orbitally and globally averaged) above the freezing point, although at the equator at perihelion, 1 bar would have sufficed. Such an atmospheric CO2 invertory, the author argued, is not inconsistent with any known constraint on Mars' degassed volatile inventory. E.R.

N89-10800*# Academy of Sciences (USSR), Leningrad. Planetology Section.
AREAL AND TIME DISTRIBUTIONS OF VOLCANIC FORMATIONS ON MARS Abstract Only
G. N. Katterfeld and V. I. Vityaz *In* Lunar and Planetary Inst., MECA Symposium on Mars: Evolution of its Climate and Atmosphere 1987 p 67-68 (For primary document see N89-10780 01-91)
Avail: NTIS HC A07/MF A01 CSCL 03B

The analysis of igneous rock distribution has been fulfilled on the basis of the geomorphological map of Mars at scale 1:5,000,000, according to data obtained from interpretation of 1:2,000,000 scale pictures of Mariner 9, Mars 4, Mars 5, Viking 1 and 2. Areological areas are listed as having been distinguished as the stratigraphic basis for a martian time scale. The area of volcanic eruptions and the number of eruptive centers are calculated on 10 x 10 deg cells and for each areological eras. The largest area of eruptive happening at different times is related with Tharsis tectonic uplift. The study of distribution of igneous rock area and volcanic centers number on 10 deg sectors and zones revealed the concentration belts of volcanic formations. Author

N89-10801*# Jet Propulsion Lab., California Inst. of Tech., Pasadena.
INFLUENCE OF POLAR-CAP ALBEDO ON PAST AND CURRENT MARTIAN CLIMATE Abstract Only
Hugh H. Kieffer (Geological Survey, Flagstaff, Ariz.) and David A. Paige *In* Lunar and Planetary Inst., MECA Symposium on Mars: Evolution of its Climate and Atmosphere 1987 p 69-70 (For primary document see N89-10780 01-91)
Avail: NTIS HC A07/MF A01 CSCL 03B

The finding that the observed albedo of the Martian polar caps increase with increasing isolation is reviewed. Models of the Martian climate system are greatly stabilized when an insolation-dependent frost albedo instead of a constant albedo is used in the energy budget. The authors views on microphysics of the process is then presented. Long term climate models must account for the variability of CO2 frost albedo. E.R.

N89-10802*# Arizona State Univ., Tempe. Dept. of Geology.
REGIONAL SOURCES AND SINKS OF DUST ON MARS: VIKING OBSERVATIONS OF CERBERUS, SOLIS PLANUM, AND SYRTIS MAJOR Abstract Only
Steven W. Lee *In* Lunar and Planetary Inst., MECA Symposium on Mars: Evolution of its Climate and Atmosphere 1987 p 71-72 Previously announced as N87-23450 (For primary document see N89-10780 01-91)
Avail: NTIS HC A07/MF A01 CSCL 03B

A study of seasonal variation of albedo features in the Cerberus, Solis Planum, and Syrtis Major regions was based on Viking Orbiter data obtained over more than one complete Martian year. Contour maps of Lambert albedo and single point thermal inertia were constructed from the Infrared Thermal Mapper experiment data, and Orbiter images were used to determine the pattern and variability of regional winds (inferred from wind streak orientations). Coupled with ground based radar data, these data allow the regional sediment transport direction, surface properties (texture, morphology, and roughness), and the implications of the observed seasonal and longer term dust redistribution to be investigated. Results are outlined. E.R.

N89-10803*# Geological Survey, Flagstaff, Ariz.
WATER AND ICE ON MARS: EVIDENCE FROM VALLES MARINERIS Abstract Only
B. K. Lucchitta *In* Lunar and Planetary Inst., MECA Symposium on Mars: Evolution of its Climate and Atmosphere 1987 p 73-75 Previously announced as N87-23469 (For primary document see N89-10780 01-91)
Avail: NTIS HC A07/MF A01 CSCL 03B

An important contribution to the volatile history of Mars comes from a study of Valles Marineris, where stereoimages and a 3-D view of the upper Martian crust permit unusual insights. The evidence that ground water and ice existed until relatively recently or still exist in the equatorial area comes from observations of landslides, wall rock, and dark volcanic vents. Valles Marineris landslides are different in efficiency from large catastrophic landslides on Earth. One explanation for the difference might be that the Martian slides are lubricated by water. A comparison of landslide speeds also suggests that the Martian slides contain water. That Valles Marineris wall rock contained water or ice is further suggested by its difference from the interior layered deposits. Faults and fault zones in Valles Marineris also shed light on the problem of water content in the walls. Because the main evidence for water and ice in the wall rock comes from slides, their time of emplacement is important. The slides in Valles Marineris date from the time of late eruptions of the Tharsis volcanoes and thus were emplaced after the major activity of Martian outflow channels. E.R.

N89-10804*# Lowell Observatory, Flagstaff, Ariz. Planetary Research Center.
THE GREAT DUST STORM OF 1986
L. J. Martin and P. B. James *In* Lunar and Planetary Inst., MECA Symposium on Mars: Evolution of its Climate and Atmosphere 1987 p 76-77 Prepared in cooperation with

Missouri Univ., St. Louis (For primary document see N89-10780 01-91)
Avail: NTIS HC A07/MF A01 CSCL 03B

It is reported that on the global scale, no major dust storm activity was seen during telescopic observations of Mars during the several months or so preceeding this conference. However, the corresponding season on Mars was early fall, which is at the beginning of the dust storm season. It was too early to tell, therefore, if a great dust storm was going to occur that year. Current observations and what they show about present atmospheric conditions and the recession of the South Polar Cap is discussed. E.R.

N89-10805*# Geological Survey, Menlo Park, Calif.
ABLATION OF MARTIAN GLACIERS
Henry J. Moore and Philip A. Davis (Geological Survey, Flagstaff, Ariz.) *In* Lunar and Planetary Inst., MECA Symposium on Mars: Evolution of its Climate and Atmosphere 1987 p 78-80 (For primary document see N89-10780 01-91)
Avail: NTIS HC A07/MF A01 CSCL 03B

Glacier like landforms are observed in the fretted terrain of Mars in the latitude belts near + or - 42 deg. It was suggested that sublimation or accumulation-ablation rates could be estimated for these glaciers if their shapes were known. To this end, photoclinometric profiles were obtained of a number of these landforms. On the basis of analyses of these profiles, it was concluded that ice is chiefly ablating from these landforms that either are inactive rock-glaciers or have materials within them that are moving exceedingly slowly at this time. These conclusions are consistent with other geologic information. The analyses were performed using a two-dimensional model of an isothermal glacier. Author

N89-10806*# Hawaii Univ., Honolulu. Planetary Geosciences Div.
ICE OR LIQUID WATER IN THE MARTIAN REGOLITH. MORPHOLOGIC INDICATORS FROM RAMPART CRATERS
P. J. MouginisMark *In* Lunar and Planetary Inst., MECA Symposium on Mars: Evolution of its Climate and Atmosphere 1987 p 81-83 (For primary document see N89-10780 01-91)
Avail: NTIS HC A07/MF A01 CSCL 03B

The morphology of ejecta blankets around certain Martian craters carries implications for volatiles in either the Martian crust or the atmosphere or both. The evidence that rampart crater ejecta can be used to infer the physical condition of volatiles in target rocks at the time of impact is reviewed. It was concluded that ice, and not liquid water, was the main volatile state, although rare examples also suggest the presence of liquid water at the time the craters were formed. E.R.

N89-10807*# Washington Univ., Seattle. Dept. of Atmospheric Sciences.
SEASONAL WIND VARIATIONS IN THE MARTIAN SUBTROPICS Abstract Only
James Murphy, Conway Leovy, and James Tillman *In* Lunar and Planetary Inst., MECA Symposium on Mars: Evolution of its Climate and Atmosphere 1987 p 84 (For primary document see N89-10780 01-91)
Avail: NTIS HC A07/MF A01 CSCL 03B

A possible initiation mechanism for global dust storms was raised by describing a new analysis of winds at Viking Lander I, the Mutch Memorial Station, at 28 deg N latitude. It was shown that strong winds associated with an eastward propagation planetary wave coincided with the onset of a major dust storm at that site, and it was speculated that these high latitude winter systems may sometimes contribute to the initiation of Martian global dust storms. E.R.

N89-10808*# Tokai Univ., Kumamoto (Japan).
OPTICAL THICKNESS OF THE OLYMPUS CLOUD
Y. Narumi *In* Lunar and Planetary Inst., MECA Symposium on Mars: Evolution of its Climate and Atmosphere 1987 p 85-87 (For primary document see N89-10780 01-91)
Avail: NTIS HC A07/MF A01 CSCL 03B

Results are presented from a model of telescope observations that indicate a diurnal cycle exist, at least at one location, in the Martian atmosphere. By comparing calculated intensities with observed intensities of reflected sunlight, the diurnal variations in the optical thickness of the Olympus cloud that forms near the summit of Olympus Mons during summer was estimated. The results indicate that the optical depth at 0.4 microns rises sharply from near zero in late morning to about 0.8 in the early afternoon. E.R.

N89-10809*# National Aeronautics and Space Administration. Ames Research Center, Moffett Field, Calif.
FORMATION OF THE LAYERED DEPOSITS IN THE VALLES MARINERIS, MARS
S. S. Nedell (San Jose State Univ., Calif.) and S. W. Squyres *In* Lunar and Planetary Inst., MECA Symposium on Mars: Evolution of its Climate and Atmosphere 1987 p 88-90 (For primary document see N89-10780 01-91)
Avail: NTIS HC A07/MF A01 CSCL 03B

Evidence is presented for large standing bodies of water on Mars during past epochs. It is noted that the origin of the horizontally-layered deposits in the Valles Marineris can be best explained by formation in standing bodies of water. These lakes, if they existed, were most likely covered by ice. There are several geologically feasible mechanisms that could have led to formation to thick deposits in ice covered paleolakes in the Valles Marineris. Present data are insufficient to choose conclusively among the various possibilities. E.R.

N89-10810*# State Univ. of New York, Stony Brook. Dept. of Earth and Space Sciences.
COULD ICY IMPACTS RECONCILE VENUS WITH EARTH AND MARS Abstract Only
T. Owen *In* Lunar and Planetary Inst., MECA Symposium on Mars: Evolution of its Climate and Atmosphere 1987 p 91 (For primary document see N89-10780 01-91)
Avail: NTIS HC A07/MF A01 CSCL 03B

The problem of volatile sources in the martian atomosphere was studied. It is suggested that a combination of an impact by an icy planetesimal (radius about 150 km) and solar wind implantation of neon could explain the noble gas abundances on Venus. Early solar wind would supply the right amount of neon with the correct Ne-20/Ne-22 as compared with lunar soils. However, observations of noble gases in a fresh comet are needed to test this hypothesis. E.R.

N89-10811*# National Aeronautics and Space Administration. Lyndon B. Johnson Space Center, Houston, Tex.
SEISMIC EXPLORATION FOR WATER ON MARS Abstract Only
Thornton Page *In* Lunar and Planetary Inst., MECA Symposium on Mars: Evolution of its Climate and Atmosphere 1987 p 92 (For primary document see N89-10780 01-91)
Avail: NTIS HC A07/MF A01 CSCL 03B

It is proposed to soft-land three seismometers in the Utopia-Elysium region and three or more radio controlled explosive charges at nearby sites that can be accurately located by an orbiter. Seismic signatures of timed explosions, to be telemetered to the orbiter, will be used to detect present surface layers, including those saturated by volatiles such as water and/or ice. The Viking Landers included seismometers that showed that at present Mars is seismically quiet, and that the mean crustal thickness at the site is about 14 to 18 km. The new seismic landers must be designed to minimize wind vibration noise, and the landing sites selected so that each is well formed on the regolith, not on rock outcrops or in craters. The explosive charges might be mounted on penetrators aimed at nearby smooth areas. They must be equipped with radio emitters for accurate location and radio receivers for timed detonation. Author

N89-10812*# Jet Propulsion Lab., California Inst. of Tech., Pasadena.
THE THERMAL PROPERTIES OF MARTIAN SURFACE MATERIALS AT HIGH LATTITUDES: POSSIBLE EVIDENCE FOR PERMAFROST
D. A. Paige and H. H. Kieffer (Geological Survey, Flagstaff, Ariz.) *In* Lunar and Planetary Inst., MECA Symposium on Mars: Evolution of its Climate and Atmosphere 1987 p 93-95 (For primary document see N89-10780 01-91)
Avail: NTIS HC A07/MF A01 CSCL 03B

Evidence is presented from analysis of Viking thermal mapping results that suggests a transition to high thermal inertial material at a depth of approx. 12 cm at +75 deg latitude. This was interpreted as reflecting the transition from ice poor soil to hard frozen permafrost. It was pointed out that such a transition would be expected on the basis of theoretical models of hard frozen permafrost distribution. Although permafrost is not the only plausible martian surface material with high thermal inertia, polar thermal mapping may turn out to be a powerful tool for determining the distribution of permafrost deposits and understanding their behavior. At this point, the circumstantial case for permafrost deposits in the north pole region of Mars is very strong. E.R.

N89-10813*# Jet Propulsion Lab., California Inst. of Tech., Pasadena.
GEOMORPHIC EVIDENCE FOR ANCIENT SEAS ON MARS
Timothy J. Parker, Dale M. Schneeberger, David C. Pieri, and R. Stephen Saunders *In* Lunar and Planetary Inst., MECA Symposium on Mars: Evolution of its Climate and Atmosphere 1987 p 96-98 (For primary document see N89-10780 01-91)
Avail: NTIS HC A07/MF A01 CSCL 03B

Geomorphic evidence is presented for ancient seas on Mars. Several features, similar to terrestrial lacustrine and coastal features, were identified along the northern plains periphery from Viking images. The nature of these features argues for formation in a predominantly liquid, shallow body of standing water. Such a shallow sea would require either relatively rapid development of shoreline morphologies or a warmer than present climate at the time of outflow channel formation. E.R.

N89-10814*# Minnesota Univ., Minneapolis. School of Physics and Astronomy.
VOLATILE INVENTORY OF MARS-2: PRIMORDIAL SOURCES AND FRACTIONATING PROCESSES
R. O. Pepin *In* Lunar and Planetary Inst., MECA Symposium on Mars: Evolution of its Climate and Atmosphere 1987 p 99-101 (For primary document see N89-10780 01-91)
Avail: NTIS HC A07/MF A01 CSCL 03B

The total volatile inventory of Mars has been modeled using meteoritic and presumed primordial abundances in the early solar system. Evidence is presented which indicates that the elemental abundances of the noble gases on Earth and Mars are similar, and their ratios are comparable to those in average carbonaceous chondrites with the exception of xenon and krypton. In order to account for presently observed variations in gas abundances, two primordial sources were used. One was the solar composition similar to the solar wind, and the other of carbonaceous grains that were the source for trace exotic components. For Mars, a model in which the early, high solar EUV flux with continued hydrogen production by differentiation results in mass fractionation of the primordial atmosphere, early depletion of xenon, and later depletion of gases lighter than krypton. The result is that the primordial Mars water inventory may have been on the order of 20 to 30 km if spread over the planet. E.R.

N89-10815*# Southern Methodist Univ., Dallas, Tex. Dept. of Geological Sciences.
MARTIAN TECTONICS: A REVIEW Abstract Only
R. J. Phillips *In* Lunar and Planetary Inst., MECA Symposium on Mars: Evolution of its Climate and Atmosphere 1987 p 102-103 (For primary document see N89-10780 01-91)
Avail: NTIS HC A07/MF A01 CSCL 03B

It is concluded that Mars was dominated by vertical tectonism more than any of the other terrestrial planets. The structural imprint of the Tharsis and Elysium provinces extends over half the planet, and despite 15 years of debate over the cause of the elevation, volcanic activity, and tectonic style of Tharsis, no uniform theory of Tharsis evolution has been generally agreed upon. Although several theories have been suggested for the origin of the north-south planetary dichotomy, there is also a lack of a testable, plausible model for that major unknown in Mars' evolution. E.R.

N89-10816*# National Aeronautics and Space Administration. Ames Research Center, Moffett Field, Calif.
PARTITIONING OF CARBON DIOXIDE BETWEEN THE ATMOSPHERE AND LITHOSPHERE ON EARLY MARS Abstract Only
J. B. Pollack, J. Kasting, and S. Richardson (Iowa State Univ. of Science and Technology, Ames.) *In* Lunar and Planetary Inst., MECA Symposium on Mars: Evolution of its Climate and Atmosphere 1987 p 104-105 (For primary document see N89-10780 01-91)
Avail: NTIS HC A07/MF A01 CSCL 03B

It is pointed out that in addition to the 1 to 5 bar CO2 total inventory, a high level of global volcanism was needed to keep the CO2 from being drawn away permanently by weathering of igneous rocks; the volcanism would continually decompose the carbonate resulting in steady efficient recycling. E.R.

N89-10817*# Osmania Univ., Hyderabad (India). Dept. of Geology.
IMPLICATIONS OF ISOTOPIC SIGNATURES OF NOBLE GASES FOR THE ORIGIN AND EVOLUTION OF TERRESTRIAL ATMOSPHERES
A. S. P. Rao *In* Lunar and Planetary Inst., MECA Symposium on Mars: Evolution of its Climate and Atmosphere 1987 p 106-108 (For primary document see N89-10780 01-91)
Avail: NTIS HC A07/MF A01 CSCL 03B

It is contented that the initial quantities of noble gases present in planetesimals were controlled by the sizes and masses of the planets, and fit with a model of successive accretion. The successive accretion model proposed for the origin of terrestrial planets is based upon: (1) the sequence of zones of condensation of solar nebula, (2) the condensation sequence of minerals, iron and nickel in different P-T regimes of the solar nebula, and (3) the sequence in the nucleation of iron cores of the terrestrial planets. Author

N89-10818*# Brown Univ., Providence, R. I. Dept. of Geological Sciences.
CRATER EJECTA MORPHOLOGY AND THE PRESENCE OF WATER ON MARS
P. H. Schultz *In* Lunar and Planetary Inst., MECA Symposium on Mars: Evolution of its Climate and Atmosphere 1987 p 109-111 Previously announced as N87-23508 (For primary document see N89-10780 01-91)
Avail: NTIS HC A07/MF A01 CSCL 03B

The possible effects of projectile, target, and environment on the cratering process is reviewed. It is suggested that contradictions in interpreting Martian crater ejecta morphologies reflect over simplifying the process as a singular consequence of buried water. It seem entirely possible that most ejecta facies could be produced without the presence of liquid water. However, the combination of extraordinary ejecta fluidity, absence of secondaries, and high ejection angles all would point to the combined effects of atmosphere and fluid rich substrates. Moreover, recent experiments revealing the broad scour zone associated with rapid vapor expansion may account for numerous craters in the circumpolar regions with subtle radial grooving extending 10 crater radii away with faint distal ramparts. Thus certain crater ejecta morphologies may yet provide fundamental clues for the presence of unbound water. Author

N89-10819*# George Mason Univ., Fairfax, Va.
PHOBOS AND DEIMOS: A BASE FOR SAMPLING THE MARTIAN PAST Abstract Only

S. F. Singer *In* Lunar and Planetary Inst., MECA Symposium on Mars: Evolution of its Climate and Atmosphere 1987 p 112 (For primary document see N89-10780 01-91)
Avail: NTIS HC A07/MF A01 CSCL 03B

Future exploration of Mars is summed up by the proposal that the Martian satellites provide an ideal base for exploring the surface of Mars. For example, a manned base on Deimos could direct a series of unmanned rovers and sample recovery operations, providing an immediate feedback to the operation. Samples analyzed in such an environment would be fresh, and most importantly, would not require quarantine. E.R.

N89-10820*# Washington Univ., Seattle. Dept. of Atmospheric Sciences.
MARS GLOBAL ATMOSPHERIC OSCILLATIONS: TRANSIENTS AND DUST STORM RELATIONS Abstract Only
James E. Tillman *In* Lunar and Planetary Inst., MECA Symposium on Mars: Evolution of its Climate and Atmosphere 1987 p 113 (For primary document see N89-10780 01-91)
Avail: NTIS HC A07/MF A01 CSCL 03B

It is showed that periods of enhanced quasitidal pressure oscillations occur during the season preceding the global dust storm season during every Martian year. Periods of these oscillations often differ slightly from the diurnal and semidiurnal, and the oscillations may correspond to atmospheric normal modes excited by solar heating. They may also contribute to the initiation of some global dust storms. E.R.

N89-10821*# Arizona Univ., Tucson. Lunar and Planetary Lab.
VERTICAL O(SUB 3) DISTRIBUTION AS A DIAGNOSTIC FOR EDDY DIFFUSION PROFILE
A. L. Tyler and D. M. Hunten *In* Lunar and Planetary Inst., MECA Symposium on Mars: Evolution of its Climate and Atmosphere 1987 p 114-116 (For primary document see N89-10780 01-91)
Avail: NTIS HC A07/MF A01 CSCL 03B

A model study of the distribution of ozone on Mars is presented. It is showed that knowledge of the vertical ozone distribution, such as could be obtained from ultraviolet measurements from an orbiter, could be used to infer vertical transport rates at various levels in the atmosphere. The dependence of the vertical distribution of O(sub 3) on the height variation of eddy diffusion coefficient is illustrated. Ozone abundance is a valuable diagnostic for other climatological parameters. In addition, the sensitivity of O(sub 3) distribution to eddy diffusion may aid in determining the role of surface oxidation and recombination processes and lead to a better understanding of the volatiles released or adsorbed cyclically in the Martian regolith. E.R.

N89-10822*# Max-Planck-Inst. fuer Chemie, Mainz (West Germany).
WATER ON MARS
H. Waenke and G. Dreibus *In* Lunar and Planetary Inst., MECA Symposium on Mars: Evolution of its Climate and Atmosphere 1987 p 117-119 (For primary document see N89-10780 01-91)
Avail: NTIS HC A07/MF A01 CSCL 03B

It is reported that the SNC meteorites are a factor of 2 richer in moderately volatile elements (Na, K, P, etc.) and some volatile elements (Cl, Br, I, S) compared to the Earth and Mars. It is proposed that Mars accreted homogeneously, with the result that all the water except trace amounts (on reaction with metallic Fe) was converted to H(sub 2) and escaped. This model predicts a total Mars H(sub 2)O inventory of 18 ppm (equivalent to an ocean 80 m deep on the planet), and a value for Earth of 300 ppm, close to the actual abundance. E.R.

N89-10823*# California Univ., Los Angeles. Inst. of Geophysics.
MARS REGOLITH VERSUS SNC METEORITES: EVIDENCE FOR ABUNDANT CRUSTAL CARBONATES
Paul H. Warren *In* Lunar and Planetary Inst., MECA Symposium on Mars: Evolution of its Climate and Atmosphere 1987 p 120-122 (For primary document see N89-10780 01-91)
Avail: NTIS HC A07/MF A01 CSCL 03B

Viking XRF analyses are compared with those for terrestrial and lunar basalt samples, and eucritic meteorites (of possible Mars origin). The comparison indicates depletion of Ca relative to Si in the Mars regolith. It is suggested that carbonate formation during a warmer, wetter epoch early in Mars' history could have been responsible. E.R.

N89-10824*# Hawaii Univ., Honolulu. Planetary Geosciences Div.
ABSORPTION OF THE MARTIAN REGOLITH: SPECIFIC SURFACE AREA AND MISSING CO(SUB 2)
A. P. Zent, F. P. Fanale, and S. E. Postawko *In* Lunar and Planetary Inst., MECA Symposium on Mars: Evolution of its Climate and Atmosphere 1987 p 123-125 (For primary document see N89-10780 01-91)
Avail: NTIS HC A07/MF A01 CSCL 03B

For most estimates of available regolith and initial degassed CO(sub 2) inventories, it appears that any initial inventory must have been lost to space or incorporated into carbonates. Most estimates of the total available degassed CO(sub 2) inventory are only marginally sufficient to allow for a major early greenhouse effect. It is suggested that the requirements for greenhouse warming to produce old dessicated terrain would be greatly lessened if groundwater brines rather than rainfall were involved and if a higher internal gradient were involved to raise the water (brine) table, leading to more frequent sapping. E.R.

N89-10825*# Lunar and Planetary Inst., Houston, Tex.
THERMAL PROPERTIES OF CHANNELS IN THE AEOLIS QUADRANGLE: TOPOGRAPHIC TRAPS FOR AEOLIAN MATERIALS
James R. Zimbelman *In its* MECA Symposium on Mars: Evolution of its Climate and Atmosphere 1987 p 126-128 (For primary document see N89-10780 01-91)
Avail: NTIS HC A07/MF A01 CSCL 03B

Analysis of high spatial resolution (down to 2 to 5 km) thermal data that shows the presence of aeolian debris mantling in topographic traps such as some channels is presented. In cases where this occurs, even if the mantle is thin, it can prevent remote sensing analysis of actual compositional differences that may characterize the true floors of the features. E.R.

N89-10826*# Arkansas Coll., Batesville.
METHODS OF EXTRACTING HYDROGEN FROM LUNAR SOIL Final Technical Report, 1 Apr. - 31 Oct. 1988
Roberta Bustin 31 Oct. 1988 8 p
(Grant NAG9-272)
(NASA-CR-180465; NAS 1.26:180465) Avail: NTIS HC A02/MF A01 CSCL 03B

Increasing interest in establishing a lunar base has generated considerable study on the utilization of lunar resources. Because of its importance in producing water, reducing oxides, and serving as a fuel for orbital tranfer vehicles, hydrogen is of prime importance as a resource. Lowman (1985) states that hydrogen would greatly facilitate the establishment of an autonomous permanent colony, and he calls hydrogen the most valuable lunar resource. Through the centuries, hydrogen has been embedded in lunar soil by the solar wind. The hydrogen can be extracted by heating the soil to 900 C (Carr et al, 1987). In order to obtain hydrogen on the lunar surface, an extraction method must be developed which will not only be reliable but also economically feasible. Three heating methods are examined for possible use in extracting hydrogen from lunar soil. Author

92 SOLAR PHYSICS

Includes solar activity, solar flares, solar radiation and sunspots.

For related information see *93 Space Radiation.*

N89-10827*# Joint Inst. for Lab. Astrophysics, Boulder, Colo.
C 4 FLUXES FROM THE SUN AS A STAR AND THE CORRELATION WITH MAGNETIC FLUX Final Report
C. J. Schrijver, J. L. Linsky, J. Bennett, A. Brown, and S. H. Saar 30 Aug. 1988 13 p Prepared in cooperation with NBS, Boulder, Colo.
(Grant NAG5-932)
(NASA-CR-183156; NAS 1.26:183156; UCB-153-1213) Avail: NTIS HC A03/MF A01 CSCL 03B

A total of 144 C 4 wavelength 1548 SMM-UVSP spectroheliograms of solar plages were analyzed, some of which are series of exposures of the same region on the same day. Also analyzed were C 4 wavelength 1551 rasters of plages and C 4 1548 rasters of the quiet sun. The sample contains data on 17 different plages, observed on 50 different days. The center-to-limb variations of the active regions show that the optical thickness effects in the C 4 wavelength 1548 line can be neglected in the conversion from intensity to flux density. As expected for the nearly optically thin situation, the C 4 1548 line is twice as bright as the C 4 wavelength 1551 line. The average C 4 wavelength 1548 flux density for a quiet is 2700 erg/cm/s and, with surprisingly little scatter, 18,000 erg/cm/s for plages. The intensity histograms of rasters obtained at disk centers can be separated into characteristic plage and quiet-sun contributions with variable relative filling factors. The disk-averaged flux density in the C 4 doublet and the disk-averaged magnitude of the magnetic flux density are related. The relationship between the C 4 and magnetic flux densities for spatially resolved data is inferred to be almost the same, with only an additional factor of order unity in the constant of proportionality. Author

N89-10828# National Geophysical Data Center, Boulder, Colo.
SOLAR-GEOPHYSICAL DATA NUMBER 524, APRIL 1988. PART 2: (PROMPT REPORTS). DATA FOR OCTOBER 1987 AND MISCELLANEA
Helen E. Coffey, ed. and John A. McKinnon, ed. Apr. 1988 54 p
(Contract N00014-86-F-0049)
(PB88-217401; SGD-524-Pt-2; ISSN-0038-0911; LC-79-640375)
Avail: NTIS HC A04/MF A01 CSCL 03B

Solar geophysical data for October 1987 is presented. The data includes Meudon carte synoptique, solar flares, solar radio bursts at fixed frequencies, solar x ray radiation from GOES satellite, mass ejections for the sun, active prominences and filaments. Author

N89-10829# National Geophysical Data Center, Boulder, Colo.
SOLAR-GEOPHYSICAL DATA NUMBER 524, APRIL 1988. PART 1: (PROMPT REPORTS). DATA FOR MARCH, FEBRUARY 1988 AND LATE DATA
Helen E. Coffey, ed. and John A. McKinnon, ed. Apr. 1988 135 p
(Contract N00014-86-F-0049)
(PB88-217393; SGD-524-Pt-1; ISSN-0038-0911; LC-79-640375)
Avail: NTIS HC A07/MF A01 CSCL 03B

Solar geophysical data is presented with a detailed index for 1987 and 1988. Data for March 1988 includes: IUWDS alert periods (advance and worldwide), solar flares, solar radio emission, Stanford mean solar magnetic field, and Vostok inferred interplanetary magnetic field. Data for February 1988 include: solar active regions, sudden ionospheric disturbances, solar radio spectral observations, geomagnetic indices, and radio propagation indices. Late data includes: Pioneer 12 interplanetary magnetic field for July through September 1987, cosmic ray measurements by neutron monitor, and geomagnetic sudden commencements/ solar flare effects. Author

93 SPACE RADIATION

Includes cosmic radiation; and inner and outer earth's radiation belts.

For biological effects of radiation see *52 Aerospace Medicine.* For theory see *73 Nuclear and High-Energy Physics.*

No abstracts in this category.

99 GENERAL

No abstracts in this category.

Typical Subject Index Listing

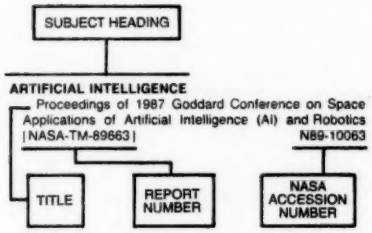

The subject heading is the key to the subject content of the document. Titles, report numbers, and accession numbers of pertinent documents are provided under each subject heading. When the title is insufficiently descriptive of the document content, a title extension has been added, separated from the title by three hyphens. The report number helps to indicate the type of document cited (e.g., NASA report, NASA translation, NASA contractor report). The NASA accession number is the number by which the document abstracts are arranged in this journal and by which the document is sold or requested. The titles, with title extensions if present, are arranged under each subject heading in ascending accession number order. The subject headings have been selected from the latest revision of the *NASA Thesaurus* (NASA SP-7064).

A

ABLATION
Standardization of the carbon-phenolic materials and processes. Vol. 2: Test methods and specifications
[NASA-CR-183227] N89-10033
Ablation of Martian glaciers N89-10805

ABSORPTANCE
A simplified vegetation canopy reflectance and absorption model N89-10322

ABSORPTION COOLING
Development and proof-testing of advanced absorption refrigeration cycle concepts, phase 2
[DE88-013239] N89-10247

ABSORPTION SPECTROSCOPY
High-resolution spectroscopy for remote sensing of ocean and atmosphere N89-10352

ABSORPTIVITY
An interactive program for estimating extinction and scattering properties of most particulate clouds
[MRL-R-1123] N89-10218

ABUNDANCE
Abundance and f values needed to interpret adequately the high resolution IUE spectra N89-10759
Carbon and nitrogen abundance determinations from transition layer lines --- giant stars N89-10760
Volatile inventory of Mars-2: Primordial sources and fractionating processes N89-10814

ACCELEROMETERS
La Recherche Aerospatiale, Bimonthly Bulletin, number 1987-6, 241/November-December
[ESA-TT-1102] N89-10030

ACCESS CONTROL
Tools to aid in the analysis of memory access patterns for FORTRAN programs
[DE88-013609] N89-10535

ACCRETION DISKS
IUE spectrophotometry of the accretion disk of HZ Her/Her X-1 N89-10702
Accretion disk models of quasars and active galactic nuclei N89-10777

ACCURACY
Improving the accuracy of central difference schemes
[NASA-CR-181712] N89-10577

ACID BASE EQUILIBRIUM
A new method of determining acid base strength distribution and a new acidity-basicity scale for solid catalysts: The strongest point, HO
[NASA-TT-20334] N89-10141

ACOUSTIC EMISSION
An investigation of the acoustic emission generated by various crack propagation modes in 304 stainless steel N89-10293

ACOUSTIC MEASUREMENT
An investigation of the acoustic emission generated by various crack propagation modes in 304 stainless steel N89-10293
On the appropriateness of applying chi-square distribution based confidence intervals to spectral estimates of helicopter flyover data
[NASA-CR-181692] N89-10601

ACTIVE GALACTIC NUCLEI
Profiles of emission lines in AGN. Part 3: On the broad Ha component of IC 5063, IC 5135 and NGC 2992
[INPE-4678-PRE/1375] N89-10681
Accretion disk models of quasars and active galactic nuclei N89-10777

ACTUATORS
Actuators for a space manipulator N89-10101

ADA (PROGRAMMING LANGUAGE)
A LISP-Ada connection N89-10085

ADAPTIVE CONTROL
An adaptive control scheme for a flexible manipulator N89-10095
Computer hardware and software for robotic control N89-10103
On motion planning and control of multi-link lightweight robotic manipulators N89-10285
Robotic adaptive grasping based on vision and tactile sensor data N89-10288
An adaptive pseudospectral method for discontinuous problems
[NASA-CR-181717] N89-10583

ADDITIVES
The effect of Al2O3, CaO, Cr2O3 and MgO on devitrification of silica
[NASA-TM-101335] N89-10124

ADHESIVES
Adhesive blends and multi-layered structures comprising the adhesive blends
[EP-PATENT-0-258-990-A1] N89-10174

ADSORPTION
Is regolith absorbtion the explanation for the transition from early to present Mars climate N89-10788
Absorption of the Martian regolith: Specific surface area and missing CO(sub 2) N89-10824

AERIAL PHOTOGRAPHY
Aircraft remote sensing in HAPEX --- hydrology N89-10388

AERIAL RECONNAISSANCE
Unmanned air vehicles - real time intelligence without the risk
[AD-A195199] N89-10039

AERODYNAMIC CHARACTERISTICS
Hellfire system model validation N89-10057

AERODYNAMIC STALLING
Unsteady three-dimensional stall on a rectangular wing N89-10027

AERODYNAMICS
Aeronautical engineering: A continuing bibliography with indexes (supplement 231)
[NASA-SP-7037(231)] N89-10002
Validation of a pair of computer codes for estimation and optimization of subsonic aerodynamic performance of simple hinged-flap systems for thin swept wings
[NASA-TP-2828] N89-10024

AEROELASTICITY
Measurement of aerodynamic characteristics of a hang-glider-wing by ground run tests using a test vehicle
[NAL-TR-953] N89-10004
AGARD manual on aeroelasticity in axial-flow turbomachines. Volume 2: Structural dynamics and aeroelasticity
[AGARD-AG-298-VOL-2] N89-10006
Aeroelastic coupling: An elementary approach N89-10012
Aeroelastic formulation for tuned and mistuned rotors N89-10013
Fan flutter test N89-10014
Aeroelastic thermal effects N89-10015
Forced vibration and flutter design methodology N89-10016
La Recherche Aerospatiale, Bimonthly Bulletin, Number 1987-4, 239/July-August
[ESA-TT-1088] N89-10026
The pros and cons of code validation
[NASA-TM-100657] N89-10034
Vibration, performance, flutter and forced response characteristics of a large-scale propfan and its aeroelastic model
[NASA-TM-101322] N89-10043

AERONAUTICAL ENGINEERING
Aeronautical engineering: A continuing bibliography with indexes (supplement 231)
[NASA-SP-7037(231)] N89-10002

AEROSOLS
Analysis of the contribution of the atmosphere to water reflectance in the first two channels of the NOAA satellites AVHRR N89-10330
Numerical accuracy of a two-stream radiative transfer model from comparison with an N-stream model N89-10331
Fourier transform infrared spectrometry of ambient aerosols
[PB88-213236] N89-10414

AEROSPACE ENGINEERING
Aerospace systems and technology: The role of the RAE
[RAE-TR-88042] N89-10003

AEROSPACE ENVIRONMENTS
Compact imaging spectrometer for induced emissions
[NASA-CR-183187] N89-10264
Chromosomes and plant cell division in space
[NASA-CR-183213] N89-10518

AEROSPACE INDUSTRY
Technical evaluation report on the Flight Mechanics Panel Symposium on Flight Vehicle Development Time and Cost Reduction
[AGARD-AR-244] N89-10001
Civil Space Technology Initiative: A first step
[NASA-TM-100949] N89-10665
Space commerce: An industry assessment
[PB88-214069] N89-10677

AEROSPACE MEDICINE
Living in space, book 2, levels D, E, F
[NASA-EP-223] N89-10522

AEROSPACE PLANES
Technology issues associated with fueling the national aerospace plane with slush hydrogen
[NASA-TM-101386] N89-10123

AEROSPACE SYSTEMS
Aerospace systems and technology: The role of the RAE
[RAE-TR-88042] N89-10003

AEROSPACE VEHICLES
Triggering of lightning by the Atlas Centaur vehicle N89-10438

AFRICA
The use of MOMS-1 data for geological mapping of the Aswa lineament (East African rift) N89-10382

AGRICULTURE
AGRISAR'86: Contributing to signature research N89-10387

AIR
Turbulent diffusion of ocean bubbles
[PB88-212816] N89-10513

AIR LAND INTERACTIONS
Use of microwave backscatter measurements as boundary conditions in soil/atmosphere water transfer modeling N89-10311

AIR NAVIGATION
Interference of precipitation static discharges with aircraft navigational systems N89-10459
AIR POLLUTION
Contamination of environmental control systems in Hercules aircraft [MRL-R-1116] N89-10040
Evaluating impacts of pollutants from the atmosphere [DE88-014550] N89-10415
Smoothing spatial data by estimating mean local variance [AD-A195302] N89-10593
AIR QUALITY
Smoothing spatial data by estimating mean local variance [AD-A195302] N89-10593
AIR TRAFFIC CONTROL
Terminal control area design and air traffic loadings [DOT/FAA/DS-88/11] N89-10038
AIR TRANSPORTATION
Using full-mission simulation for human factors research in air transport operations [NASA-TM-88330] N89-10037
AIR WATER INTERACTIONS
A three degree-of-freedom description of the ocean surface for microwave remote sensing of wave height and wind friction velocity N89-10314
Model-data comparisons for the 1982-83 El Nino: The XBT tracks [PB88-221668] N89-10514
Crater ejecta morphology and the presence of water on Mars N89-10818
AIRBORNE EQUIPMENT
Digital recording of radar data in an aircraft [PB88-209507] N89-10212
Strengths and shortcomings in Airborne Thematic Mapper (ATM) technology as applied to volcanic and geothermal areas in Iceland N89-10337
The fluorescence line imager: High-resolution imaging spectroscopy over water and land N89-10353
Stress detection in mixed coniferous-broadleaved forests from Airborne Imaging Spectrometer (AIS) data N89-10355
An aircraft-borne electric field measuring system for rocket launch support N89-10443
Estimating electric field enhancement factors on an aircraft utilizing a small scale model: A method evaluation N89-10454
AIRBORNE/SPACEBORNE COMPUTERS
On the diagnostic emulation technique and its use in the AIRLAB [NASA-TM-4027] N89-10524
AIRCRAFT ACCIDENT INVESTIGATION
Aircraft accident reports, brief format, US civil and foreign aviation, issue number 10 of 1987 accidents [PB88-916905] N89-10035
Aircraft accident reports, brief format, US civil and foreign aviation, issue number 12 of 1986 accidents [PB88-916903] N89-10036
AIRCRAFT ACCIDENTS
Aircraft accident reports, brief format, US civil and foreign aviation, issue number 10 of 1987 accidents [PB88-916905] N89-10035
Aircraft accident reports, brief format, US civil and foreign aviation, issue number 12 of 1986 accidents [PB88-916903] N89-10036
AIRCRAFT COMPARTMENTS
Contamination of environmental control systems in Hercules aircraft [MRL-R-1116] N89-10040
AIRCRAFT CONSTRUCTION MATERIALS
Indirect effects on electronic and mechanical systems installed in carbon fibre compound aircraft structures N89-10492
AIRCRAFT CONTROL
Design and evaluation of dynamic flight test manoeuvres [PB88-210760] N89-10042
AIRCRAFT DESIGN
Wheel performance evaluation. Phase 1: Analysis [DOT/FAA/CT-88/16] N89-10041
Generation of a grid for a finite difference calculation of flows around an aircraft in Cartesian coordinates [NAL-TR-956] N89-10563
AIRCRAFT ENGINES
Alternate fuels for General Aviation aircraft with spark ignition engines [DOT/FAA/CT-88/05] N89-10179
AIRCRAFT EQUIPMENT
On the diagnostic emulation technique and its use in the AIRLAB [NASA-TM-4027] N89-10524
AIRCRAFT FUELS
The performance of alternate fuels in general aviation aircraft [DOT/FAA/CT-88/13] N89-10175
AIRCRAFT HAZARDS
Statistics of lightning interaction with aircraft in Japan N89-10430
Israel Air Force (IAF) in-service aircraft lightning strike and damage survey N89-10431
Lightning information database N89-10432
Triggering of lightning by the Atlas Centaur vehicle N89-10438
Evaluation and mitigation of lightning hazards to the space shuttle Solid Rocket Motors (SRM) N89-10439
AIRCRAFT INSTRUMENTS
A case for a unified lightning threat N89-10447
AIRCRAFT MANEUVERS
Design and evaluation of dynamic flight test manoeuvres [PB88-210760] N89-10042
AIRCRAFT MODELS
Estimating electric field enhancement factors on an aircraft utilizing a small scale model: A method evaluation N89-10454
AIRCRAFT NOISE
The effect of front-to-rear propeller spacing on the interaction noise at cruise conditions of a model counterrotation propeller having a reduced diameter aft propeller [NASA-TM-101329] N89-10603
AIRCRAFT PERFORMANCE
Wave drag and high-speed performance of supersonic STOVL fighter configuration [NASA-TM-100061] N89-10017
AIRCRAFT PRODUCTION
Technical evaluation report on the Flight Mechanics Panel Symposium on Flight Vehicle Development Time and Cost Reduction [AGARD-AR-244] N89-10001
AIRCRAFT RELIABILITY
Functional mock-up tests of the flight control system of the NAL QSTOL research aircraft: Planning and mechanical system test [NAL-TR-944] N89-10047
AIRCRAFT SAFETY
Terminal control area design and air traffic loadings [DOT/FAA/DS-88/11] N89-10038
International Aerospace and Ground Conference on Lightning and Static Electricity [PB88-197439] N89-10429
Summary of inflight data on lightning currents and fields N89-10449
Analysis of recent in-flight lightning measurements on different aircraft N89-10450
Linear and nonlinear interpretation of CV-580 lightning data N89-10451
A chronology of in-cloud electric field and lightning strikes on an instrumented research aircraft N89-10455
Lightning initiation on aircraft in thunderstorms N89-10456
Factors influencing the detection of voltage sparks by flammable gas and optical techniques N89-10465
The SAFIR lightning monitoring and warning system, applications to aerospace activities N89-10481
Modelling of common mode coupling between an aircraft wing traversed by a lightning current and wiring installed in that wing N89-10485
AIRCRAFT STABILITY
Design and evaluation of dynamic flight test manoeuvres [PB88-210760] N89-10042
AIRCRAFT STRUCTURES
Fracture criteria for discontinuously reinforced metal matrix composites [NASA-CR-181175] N89-10125
Analysis of recent in-flight lightning measurements on different aircraft N89-10450
Lightning tests on an all-composite helicopter N89-10452
A filamentary method for calculating induced voltages within resistive structures in either the frequency or time domain N89-10484
AIRFOILS
A potential theory for the steady separated flow about an aerofoil section [ARL-AERO-R-176] N89-10005
Aeroelastic thermal effects N89-10015
AIRFRAMES
Fracture criteria for discontinuously reinforced metal matrix composites [NASA-CR-181175] N89-10125
AIRPORT PLANNING
Terminal control area design and air traffic loadings [DOT/FAA/DS-88/11] N89-10038
AIRPORTS
Lightning and surge protection of large ground facilities N89-10474
AIRSHIPS
System protection from atmospheric electricity for aerostats with conducting tethers N89-10497
ALBEDO
Mars low albedo regions: Possible map of near-surface N89-10794
Influence of polar-cap albedo on past and current Martian climate N89-10801
Regional sources and sinks of dust on Mars: Viking observations of Cerberus, Solis Planum, and Syrtis Major N89-10802
ALFALFA
Estimation of the interception efficiency of an alfalfa canopy from a vegetative index N89-10332
ALGEBRA
Real algebraic morphisms with values in the unit circle [PB88-208921] N89-10515
ALGORITHMS
Comparison of Euler algorithms for two-dimensional shock calculations [PB88-210372] N89-10032
AUTOPLAN: A PC-based automated mission planning tool N89-10067
Solution of ill-posed problems by means of truncated SVD (Singular Value Decomposition) [DE88-013510] N89-10238
Systems analysis of the inverse heat conduction problem N89-10244
Atmospheric effect removal from space imagery N89-10338
A new method for estimating regional evaporation from thermal infrared surface temperature measurements N89-10390
ORDMET3: An improved algorithm to find the maximum solution to a system of linear (in)Equalities [PB88-208970] N89-10520
Segmentation of noisy images using nonstationary Markov fields [AD-A195229] N89-10527
Tools to aid in the analysis of memory access patterns for FORTRAN programs [DE88-013609] N89-10535
The effect of a gap nonlinearity on recursive parameter identification algorithms [AD-A196020] N89-10557
Concurrent algorithms for numerical computation on hypercube computer [AD-A195502] N89-10558
Factoring very large numbers using a massively parallel computer [DE88-014247] N89-10559
Convergence properties of trust region methods for linear and convex constraints [DE88-013608] N89-10562
A linear programming approach to maximum entropy signal restoration [DE88-013021] N89-10566
Integrated switching networks A performance study N89-10567
Space-efficient queue management using fixed-connection networks [AD-A195167] N89-10569
An algorithm for unsteady flows with strong convection [NASA-TM-100828] N89-10575
Finite precision arithmetic in singular value decomposition architectures [AD-A196188] N89-10589
Progress in NODAL transport methods [DE88-012416] N89-10590
LOOK: Implementation of an expert system in information retrieval for database selection N89-10669
ALIGNMENT
A novel alignment technique for pointing and centering optical components [DE88-015441] N89-10621
ALLOCATIONS
Dynamic task allocation for a man-machine symbiotic system N89-10098
ALLOYS
A compendium of sources of fracture toughness and fatigue crack growth data for metallic alloys, part 3 [NASA-TM-100675] N89-10165
ALPS MOUNTAINS (EUROPE)
The German Front Experiment 1987: Observations and preliminary results [DFVLR-FB-88-21] N89-10508
ALUMINIDES
Thermodynamic analysis of compatibility of several reinforcement materials with beta phase NiAl alloys [NASA-CR-4171] N89-10131
Recent developments in aluminides and silicides [DE88-012926] N89-10155
Engineering processing and properties of nickel aluminides [DE88-011019] N89-10164

ALUMINUM
Indirect effects on electronic and mechanical systems installed in carbon fibre compound aircraft structures N89-10492
The lowest ionization potentials of Al2 [NASA-TM-101171] N89-10605
ALUMINUM ALLOYS
Thermodynamic analysis of compatibility of several reinforcement materials with FeAl alloys [NASA-CR-4172] N89-10128
Tensile properties of commercial aluminum-lithium alloys at cryogenic temperatures [DE88-014857] N89-10153
Premartensitic microstructures as seen in the high-resolution electron microscope: A study of a NiAl alloy [DE88-008042] N89-10160
ALUMINUM COMPOUNDS
Theoretical studies of grain boundaries in Ni, Al and Ni3Al with and without boron [DE88-014323] N89-10152
AMMONIUM NITRATES
HAN (hydroxylammonium nitrate density)-based liquid gun propellants: Physical properties [AD-A195246] N89-10180
Lightning protection for high explosives and instrumentation using a field mill system N89-10467
AMPLIFIER DESIGN
Communications to National Microwave Days [CNES-CT/DRT/TIT/HY/87/130] N89-10237
Considerations and calculations for application of an optical amplifier as an end- and preamplifier [ESA-TT-1004] N89-10625
ANGULAR MOMENTUM
Gravitational time delay due to a spinning string [DE88-014733] N89-10661
ANNUAL VARIATIONS
Monitoring seasonal variations of soil moisture and vegetation cover using satellite microwave radiometry N89-10378
Interannual variability of global dust storms on Mars N89-10792
Interannual differences in the regressions of the polar caps of Mars N89-10796
Regional sources and sinks of dust on Mars: Viking observations of Cerberus, Solis Planum, and Syrtis Major N89-10802
Seasonal wind variations in the Martian subtropics N89-10807
ANOMALIES
Expert system support for HST operations N89-10076
Dynamic interpretation of geoid anomalies [NASA-CR-183164] N89-10304
Application of microgravity to the assessment of existing structures and structural foundations [AD-A195599] N89-10418
ANTARCTIC REGIONS
Data report for the Siple Coast (Antarctica) project [NASA-TM-100708] N89-10403
Meteorological measurements made using Brazilian drifting buoys: Technical aspects and first results [INPE-4674-PRE/1372] N89-10502
ANTENNA ARRAYS
Evaluation of hardware architectures for HF antenna arrays [AD-A196204] N89-10217
ANTENNA DESIGN
Relative planetary radar sensitivities: Arecibo and Goldstone N89-10209
Theoretical and experimental analysis of quadrifilar antennas for the first Brazilian satellite [INPE-4581-PRE/1315] N89-10221
ANTENNA FEEDS
X/X/Ka-band prime focus feed antenna for the Mars Observer beacon spacecraft N89-10195
ANTENNA RADIATION PATTERNS
Antenna pointing compensation based on precision optical measurement techniques N89-10197
A method for producing a shaped contour radiation pattern using a single shaped reflector and a single feed [NASA-TM-101369] N89-10215
ANTENNAS
Design and performance of the SSVCO [DE88-012435] N89-10232
ANTIMATTER
The inverse-square law and quantum gravity [DE88-014332] N89-10663
ANTISHIP MISSILES
Simulation with real elements of Exocet anti-ship missiles N89-10056
ANVIL CLOUDS
The electrical structure of thunderstorm anvils N89-10470
APERTURES
On a surface mounted transmission line configuration for aperture testing N89-10458
APPROXIMATION
Analytical approximations for X-ray cross sections 3 [DE88-015366] N89-10609
ARC HEATING
Spectral characteristics of arc-heated low density plasma flows (2) nitrogen plasma [NAL-TR-952] N89-10639
Spectral characteristics of arc-heated low density plasma flows (1) argon plasma [NAL-TR-954] N89-10642
ARCHITECTURE
Quadruplex digital flight control system assessment [NASA-CR-182741] N89-10058
ARCHITECTURE (COMPUTERS)
A hierarchically distributed architecture for fault isolation expert systems on the space station N89-10077
NASREN: Standard reference model for telerobot control N89-10099
Teleoperated position control of a PUMA robot N89-10104
A software simulation study of the long constraint length VLSI Viterbi decoder N89-10203
Evaluation of hardware architectures for HF antenna arrays [AD-A196204] N89-10217
Supercomputing: An indispensable component of applied research [DE88-015363] N89-10533
Software design research at DARPA N89-10546
Plans and meta-plans in an intelligent assistant for the process of programming N89-10547
The knowledge integration tool: Knowledge interface (a knowledge based system development environment) N89-10551
A meta-protocol architecture for connecting computer networks [AD-A196319] N89-10570
Finite precision arithmetic in singular value decomposition architectures [AD-A196188] N89-10589
Architecture studies and system demonstrations for optical parallel processor for AI and NI [AD-A195480] N89-10616
ARCTIC REGIONS
MIZEX (marginal ice zone experiment) 87 meteorology atlas [AD-A195361] N89-10506
ARGON PLASMA
Spectral characteristics of arc-heated low density plasma flows (1) argon plasma [NAL-TR-954] N89-10642
ARIANE LAUNCH VEHICLE
Means for testing aerospace launcher structures [ETN-88-93082] N89-10110
Choice of coating and surface behavior of the hydrogen turbopump of the Vulcain engine [ETN-88-93084] N89-10173
ARID LANDS
Applications of LANDSAT (TM and MSS) data for an estimation of rangeland conditions in semiarid and arid areas of northern Kenya [DFVLR-FB-88-18] N89-10404
ARITHMETIC AND LOGIC UNITS
Finite precision arithmetic in singular value decomposition architectures [AD-A196188] N89-10589
ARTIFICIAL INTELLIGENCE
Proceedings of 1987 Goddard Conference on Space Applications of Artificial Intelligence (AI) and Robotics [NASA-TM-89663] N89-10063
Maintaining an expert system for the Hubble Space Telescope ground support N89-10064
PLAN-IT: Scheduling assistant for solar system exploration N89-10068
Deep space network resource scheduling approach and application N89-10070
Space station Platform Management System (PMS) replanning using resource envelopes N89-10071
The load shedding advisor: An example of a crisis-response expert system N89-10073
FIESTA: An operational decision aid for space network fault isolation N89-10075
Expert system support for HST operations N89-10076
Toward an expert project management system N89-10082
Expert systems built by the Expert: An evaluation of OPS5 N89-10086
Issues, concerns, and initial implementation results for space based telerobotic control N89-10091
Computer hardware and software for robotic control N89-10103
Knowledge based tools for knowledge-based systems N89-10550
The knowledge integration tool: Knowledge interface (a knowledge based system development environment) N89-10551
Plan recognition in GRAPPLE: An intelligent assistant for the process of programming N89-10555
Architecture studies and system demonstrations for optical parallel processor for AI and NI [AD-A195480] N89-10616
An evaluation of online database selection by a gateway system with artificial intelligence techniques N89-10667
ARTIFICIAL SATELLITES
Compilation of methods in orbital mechanics and solar geometry [NASA-RP-1204] N89-10420
ASTRONOMICAL CATALOGS
The IUE spectral atlas of two normal B stars: pi Cet and nu Cap (125 to 200 nm) N89-10762
ASTRONOMICAL MODELS
Accretion disk models of quasars and active galactic nuclei N89-10777
ASTRONOMICAL OBSERVATORIES
The Telecommunications and Data Acquisition Report --- Deep Space Network [NASA-CR-183243] N89-10186
Relative planetary radar sensitivities: Arecibo and Goldstone N89-10209
ASTRONOMY
An expert system approach to astronomical data analysis N89-10080
Expert systems built by the Expert: An evaluation of OPS5 N89-10086
ASTROPHYSICS
Prospects for understanding the astrophysical r-process [DE88-015449] N89-10773
A summary of major activities of the UNH and NRL groups [NASA-CR-180949] N89-10774
ASYMMETRY
Asymmetry in zeta Aurigae chromospheres N89-10722
ATMOSPHERIC CHEMISTRY
Multiphoton ionization of transient species in supersonic jets [DE88-008366] N89-10607
ATMOSPHERIC CIRCULATION
ONR tropical cyclone motion research initiative: First-year review, discussion and tentative hypotheses [AD-A194902] N89-10505
Upper-atmosphere zonal winds from satellite orbit analysis: An update [RAE-TR-87058] N89-10507
The Martian dust cycle: A proposed model N89-10791
Interannual variability of global dust storms on Mars N89-10792
ATMOSPHERIC COMPOSITION
Climatic effects of enhanced CO2 levels in Mars early atmosphere N89-10799
Vertical O(sub 3) distribution as a diagnostic for eddy diffusion profile N89-10821
ATMOSPHERIC CORRECTION
Validation of an atmospheric correction method for satellite borne imagery N89-10320
Atmospheric correction of thermal infrared data from LANDSAT-5 for surface temperature estimation N89-10339
ATMOSPHERIC EFFECTS
Atmospheric propagation effects relevant to optical communications N89-10201
Analysis of the contribution of the atmosphere to water reflectance in the first two channels of the NOAA satellites AVHRR N89-10330
Atmospheric effect removal from space imagery N89-10338
ATMOSPHERIC HEATING
Numerical simulations of dust transport into northern high latitudes during a Martian polar warming N89-10782
ATMOSPHERIC MODELS
Use of microwave backscatter measurements as boundary conditions in soil/atmosphere water transfer modeling N89-10311
Dynamics Explorer guest investigator [NASA-CR-183163] N89-10417
Analysis and modeling of summertime convective cloud and precipitation structure over the southeastern United States [NASA-CR-183192] N89-10498
ATMOSPHERIC MOISTURE
Use of microwave backscatter measurements as boundary conditions in soil/atmosphere water transfer modeling N89-10311

Analysis of the contribution of the atmosphere to water reflectance in the first two channels of the NOAA satellites AVHRR N89-10330

ATMOSPHERIC OPTICS
Analysis of the contribution of the atmosphere to water reflectance in the first two channels of the NOAA satellites AVHRR N89-10330
La Recherche Aerospatiale, Bimonthly Bulletin, number 1987-5, 240/September-October [ESA-TT-1095] N89-10422
Optical imaging through atmospheric turbulence N89-10423

ATMOSPHERIC PHYSICS
The Martian dust cycle: A proposed model N89-10791

ATMOSPHERIC REFRACTION
Atmospheric effect removal from space imagery N89-10338

ATMOSPHERIC SOUNDING
High-resolution spectroscopy for remote sensing of ocean and atmosphere N89-10352
Analysis and use of VAS satellite data [NASA-CR-183184] N89-10426
IUE observations of planetary atmospheres N89-10667

ATMOSPHERIC STRATIFICATION
IUE observations of a hot DAO white dwarf: Implications for diffusion theory and photospheric stratification N89-10733

ATMOSPHERIC TEMPERATURE
Lightning near Vandenberg AFB as related to various synoptic patterns N89-10466
Comparison of temperature profiles measured by three collocated microwave radiometers and radiosonde [PB88-212606] N89-10503

ATMOSPHERIC TIDES
Mars global atmospheric oscillations: Transients and dust storm relations N89-10820

ATMOSPHERICS
International Aerospace and Ground Conference on Lightning and Static Electricity [PB88-197439] N89-10429
Monitoring lightning activity in South Africa with a VLF single-station technique: Comparison with meteosat infrared data N89-10480

ATOMIC SPECTRA
The anomalous C 4 intensity ratio in symbiotic stars N89-10751

ATOMIC STRUCTURE
Electronic structure of electrodeposited thin film CdTe solar cells [DE88-001170] N89-10406
Theoretical study of the dissociation energy and the red and violet band systems of CN [NASA-TM-101190] N89-10610
Pressure effects on the electronic structure of 4f and 5f materials [DE88-014149] N89-10650
Beam assisted fabrication of 3-5/Si monolithic devices [AD-A195479] N89-10655
Electronic structure of the quenched superconductivity of materials Y(sub 1-x)Pr(sub x)Ba2Cu3O(sub 7-delta) [DE88-014414] N89-10658

ATTITUDE (INCLINATION)
Measurement of infrared horizon profiles from TT-500A sounding rocket [NAL-TR-947] N89-10121

AUGER SPECTROSCOPY
Characterization of layers created using surface modification techniques [DE88-011918] N89-10651

AUGMENTATION
Turbofan forced mixer lobe flow modeling. Part 3: Application to augment engines [NASA-CR-4147] N89-10025

AURORAS
Dynamics Explorer guest investigator [NASA-CR-183163] N89-10417
Electron transport and optical emissions in the aurora N89-10424
Phenomenological analysis of Jovian north auroral H2 Lyman band emissions -- IUE N89-10695

AUTOMATIC CONTROL
Space truss assembly using teleoperated manipulators N89-10087
Lightning tests to measure the bulk current levels associated with the electronic engine control of a turboprop commuter transport N89-10457

AUTOMATIC FLIGHT CONTROL
Hardware fault insertion and instrumentation system: Experimentation and results [NASA-CR-182746] N89-10526

AUTOMATIC FREQUENCY CONTROL
An automatic frequency control loop using overlapping DFTs (Discrete Fourier Transforms) N89-10204

AUTOMOBILES
Estimation of up-wash distribution around an automobile by three-dimensional smoke wind tunnel test [NAL-TR-921] N89-10023

AXIAL MODES
Investigation of the flame-acoustic wave interaction during axial solid rocket instabilities N89-10120

AXIAL STRAIN
Characterization of dynamic fracture in copper under uniaxial stress and uniaxial strain [DE88-007824] N89-10162

AXIAL STRESS
Characterization of dynamic fracture in copper under uniaxial stress and uniaxial strain [DE88-007824] N89-10162

AXISYMMETRIC BODIES
Elastic-plastic large deflection analysis of axisymmetric shells [PB88-217344] N89-10295

B

B STARS
The discovery of a co-rotating magnetosphere in a helium weak star: HD5737 = alpha Scl N89-10751
The IUE spectral atlas of two normal B stars: pi Cet and nu Cap (125 to 200 nm) N89-10762
The UV silicon spectra of early B stars N89-10763
C IV and Si IV in IUE spectra of normal B8-A0 stars: UV identified Be/Ae stars N89-10764
Ultraviolet properties of IRAS-selected Be stars N89-10765

BACKGROUND RADIATION
A summary of major activities of the UNH and NRL groups [NASA-CR-180949] N89-10774

BACKSCATTERING
Calculation of the effects of ice on the backscatter of a ground plane [NASA-CR-183303] N89-10213
Microwave backscatter from beets, peas and potatoes throughout the growing season N89-10309
Use of microwave backscatter measurements as boundary conditions in soil/atmosphere water transfer modeling N89-10311

BAINITIC STEEL
Graded structure composites [EP-PATENT-0-260-850-A2] N89-10135

BALLOON-BORNE INSTRUMENTS
Scientific ballooning in Brazil [INPE-4602-PRE/1325] N89-10018

BARIUM OXIDES
Electronic structure of the quenched superconductivity of materials Y(sub 1-x)Pr(sub x)Ba2Cu3O(sub 7-delta) [DE88-014414] N89-10658

BASALT
Martian volcanism: A review N89-10785

BATHYMETERS
Bathymetry using SPOT imagery of the Casamance (Senegal). First results N89-10375
MOMS-1 data for bathymetric and geological studies N89-10383

BEAM SWITCHING
Simulation of plasma erosion opening switches [DE88-014425] N89-10229

BEAMS (SUPPORTS)
Structural dynamic characteristics of bladed assemblies N89-10009
Dynamics and control of the orbiting grid structures and the synchronously deployable beam [NASA-CR-183205] N89-10297

BEARING (DIRECTION)
Site errors of a magnetic direction finder for lightning flashes N89-10494

BENDING FATIGUE
Flexural fatigue of a 2-D carbon/carbon composite material [DE88-010501] N89-10133

BIBLIOGRAPHIES
Aeronautical engineering: A continuing bibliography with indexes (supplement 231) [NASA-SP-7037(231)] N89-10002
Earth resources: A continuing bibliography with indexes (issue 58) [NASA-SP-7041(58)] N89-10398

BINARY ALLOYS
Metastable alloy phases prepared by solid state reactions and ball milling [DE88-009156] N89-10163

BINARY FLUIDS
Reports of investigations on: Derivation of an infinite-dilution activity coefficient model and application to two-component vapor/liquid equilibria data [DE88-007517] N89-10147

BINARY STARS
IUE observations and physical processes of interacting binary stars N89-10690
Observations of galactic WC + O binary systems: HD 97152 and HD 152270 N89-10716
Matter streams in semi-detached binary systems N89-10720
HD 207739 and other F + Be variables N89-10724
Model chromosphere and transition region for 56 Peg (K0 IIp + wd): A preliminary study N89-10726
Rotational modulation of hydrogen Lyman alpha flux from 44i Bootis N89-10741

BIODYNAMICS
Pressure studies of protein dynamics [AD-A192386] N89-10523

BIOMASS
Spectral profile and biomass estimation N89-10319

BIT ERROR RATE
Node synchronization of viterbi decoders using state metrics N89-10202

BIT SYNCHRONIZATION
Preliminary project PASTEL: System interface between SPOT 4 and the PSDE's passenger [CNES-87/088-CT/DRT/TIT/TR] N89-10227
Fault tolerance computing: Constraints in using multiprocessor synchronization by static preplanned scheduling [CNES-CT/DRT/TIT/TB-096] N89-10573

BLACK HOLES (ASTRONOMY)
Far UV observations of black hole candidates: The case of LMC X-3 N89-10701
Accretion disk models of quasars and active galactic nuclei N89-10777

BLOOD CIRCULATION
Modulation of human plasma fibronectin levels following exercise [AD-A192674] N89-10519

BLOOD PRESSURE
Modulation of human plasma fibronectin levels following exercise [AD-A192674] N89-10519

BOATTAILS
Normal force coefficient of supersonic flows over conical flare, cone-cylinder and conical boattails [NAL-TR-949] N89-10021

BOOMS (EQUIPMENT)
Development in helicopter tail boom strake applications in the US [NASA-TM-101496] N89-10059

BORESIGHT ERROR
Antenna pointing compensation based on precision optical measurement techniques N89-10197

BORON
Theoretical studies of grain boundaries in Ni, Al and Ni3Al with and without boron [DE88-014323] N89-10152

BOUNDARY LAYER EQUATIONS
Applications of a three-dimensional finite element model to mountain-valley flows [DE88-008898] N89-10412

BOUNDARY LAYER FLOW
A transonic interactive boundary-layer theory for laminar and turbulent flow over swept wings [NASA-CR-4185] N89-10029
La Recherche Aerospatiale, Bimonthly Bulletin, number 1987-5, 240/September-October [ESA-TT-1095] N89-10422

BOUNDARY LAYER TRANSITION
Resonant excitation of spatial perturbations in a boundary layer in the presence of a pressure gradient [NASA-TT-20305] N89-10248
Numerical study of the entrance flow and its transition in a curcular pipe [ISAS-RN-626] N89-10250

BOUNDARY VALUE PROBLEMS
Solution of two-point boundary value problems in optimal maneuvers of flexible vehicles N89-10114
Progress in NODAL transport methods [DE88-012416] N89-10590

BRASSES
The influence of texture on strain hardening [DE88-009157] N89-10158

BRAZIL
Relationships between spectral reflectance and phytomass of the ground layer community of neotropical savanna (CERRADO) [INPE-4635-PRE/1347] N89-10302
Environmental impact of the urban growth on the Western Sao Paulo metropolitan area [INPE-4670-PRE/1370] N89-10413

BRIDGMAN METHOD
Theoretical model for the solute distribution of a PbSnTe growth by VMS in microgravity environment [INPE-4664-PRE/1365] N89-10183

BRIGHTNESS
The normalization of a soil brightness index for the study of changes in soil conditions N89-10370
BRIGHTNESS TEMPERATURE
Spain 31-GHz observations of sky brightness temperatures N89-10190
Australia 31-GHz brightness temperature exceedance statistics N89-10191
An approximative model for the microwave brightness temperature scattered by a rough open ocean surface N89-10344
BROADBAND AMPLIFIERS
A 32-GHz reflected-wave maser amplifier with wide instantaneous bandwidth N89-10198
BROADCASTING
Antennas, satellite broadcasting, and emergency preparedness for the Voice of America
[PB88-209895] N89-10222
BROMIDES
Hydrogen-bromine fuel cell advance component development
[NASA-TM-101345] N89-10405
BROMINE
Hydrogen-bromine fuel cell advance component development
[NASA-TM-101345] N89-10405
BRONZES
Deflection of light by using tungsten bronze crystals
[DE88-014151] N89-10618
BUBBLES
Numerical investigation of the dynamics of heterogeneous shock-cavitation
[MPIS-MITT-86-1987] N89-10257
Turbulent diffusion of ocean bubbles
[PB88-212816] N89-10513
BUCKLING
Buckling of rings in column-supported bins and tanks
[PB88-217336] N89-10290
Geometric imperfections in plated structures subject to interaction between buckling modes
[PB88-200902] N89-10296
Inelastic buckling analyses of beams, columns and plates using the spline finite strip method
[PB88-214291] N89-10299
BUDGETING
Summary of DSN (Deep Space Network) reimbursable launch support N89-10211
BUOYS
Meteorological measurements made using Brazilian drifting buoys: Technical aspects and first results
[INPE-4674-PRE/1372] N89-10502
Drifting buoy data from the Equatorial Pacific for the period January 1, 1984 through May 31, 1985
[PB88-212824] N89-10516
BURSTS
Observations of classical novae in outburst N89-10708
IUE observations of the 1987 superoutburst of the dwarf nova Z Cha N89-10715
BUS CONDUCTORS
Computer simulation of the effects of lightning stroke attachment to an electric power substation N89-10475

C

C BAND
Complementary of microwave and optical range in the characterization of crops by remote sensing N89-10310
C-130 AIRCRAFT
Contamination of environmental control systems in Hercules aircraft
[MRL-R-1116] N89-10040
CABLES (ROPES)
Cable applications in robot compliant devices N89-10102
CADMIUM TELLURIDES
Electronic structure of electrodeposited thin film CdTe solar cells
[DE88-001170] N89-10406
MOCVD techniques for CdTe solar cells
[DE88-001163] N89-10411
CALIBRATING
An investigation into force-moment calibration techniques applicable to a magnetic suspension and balance system
[NASA-CR-181695] N89-10061
Effects of switch leakages upon Nimbus-7 SMMR calibration
[NASA-CR-180792] N89-10115
A radar reflector for microwave remote sensing instruments external calibration N89-10312
Sensitivity of satellite-derived net shortwave irradiance at the Earth's surface to radiometric calibration N89-10335
Airborne Visible/Infrared Imaging Spectrometer (AVIRIS): Inflight radiometric calibration and the determination of surface reflectance N89-10357
Estimating electric field enhancement factors on an aircraft utilizing a small scale model: A method evaluation N89-10454
CALORIMETERS
An electromagnetic calorimeter for a beauty factory
[NOTA-INTERNA-905] N89-10260
CAMERAS
Comparison of mechanical and electronic high-speed recording systems
[DE88-015264] N89-10268
CANOPIES (VEGETATION)
Relationships between spectral reflectance and phytomass of the ground layer community of neotropical savanna (CERRADO)
[INPE-4635-PRE/1347] N89-10302
A perspective on vegetation canopy reflectance models N89-10317
A simplified vegetation canopy reflectance and absorption model N89-10322
The angular reflectance signature of the canopy hot spot in the optical regime N89-10325
A model for radiative transfer in heterogeneous three-dimensional canopies N89-10326
A simplified reflectance model for shrub canopies N89-10329
Numerical accuracy of a two-stream radiative transfer model from comparison with an N-stream model N89-10331
Estimation of the interception efficiency of an alfalfa canopy from a vegetative index N89-10332
Developing a radiometric leaf area index N89-10334
Spectral reflectance of sugar beet and winter wheat canopies in the visible and infrared during growth N89-10342
Use of high spectral resolution to follow the state of vegetation canopies N89-10354
Environmental impact of the urban growth on the Western Sao Paulo metropolitan area
[INPE-4670-PRE/1370] N89-10413
CARBON
Transfer impedance measurements of the space shuttle Solid Rocket Motor (SRM) joints, wire meshes and a carbon graphite motor case N89-10440
The anomalous C 4 intensity ratio in symbiotic stars N89-10761
CARBON DIOXIDE
High resolution infrared spectroscopy of carbon dioxide and nitrous oxide at elevated temperatures
[AD-A196317] N89-10146
CARBON DIOXIDE CONCENTRATION
Climatic effects of enhanced CO2 levels in Mars early atmosphere N89-10799
Partitioning of carbon dioxide between the atmosphere and lithosphere on early Mars N89-10816
Absorption of the Martian regolith: Specific surface area and missing CO(sub 2) N89-10824
CARBON DIOXIDE LASERS
Considerations and calculations for application of an optical amplifier as an end- and preamplifier
[ESA-TT-1004] N89-10625
CARBON FIBERS
Standardization of the carbon-phenolic materials and processes. Vol. 2: Test methods and specifications
[NASA-CR-183227] N89-10033
Standardization of the carbon-phenolic materials and processes. Vol. 1: Experimental studies
[NASA-CR-183226] N89-10127
Finite difference analysis of external and internal lightning response of the JAS39 CFC wing N89-10483
Indirect effects on electronic and mechanical systems installed in carbon fibre compound aircraft structures N89-10492
CARBON STARS
Line formation of cool carbon star chromospheres N89-10748
CARBON STEELS
Graded structure composites
[EP-PATENT-0-260-850-A2] N89-10135
CARBON-CARBON COMPOSITES
Fabrication and test of a carbon-carbon composite combustion chamber for a low thrust storable engine
[NAL-TR-946] N89-10118
Flexural fatigue of a 2-D carbon/carbon composite material
[DE88-010501] N89-10133
CARBONATES
Mars regolith versus SNC meteorites: Evidence for abundant crustal carbonates N89-10823
CARTESIAN COORDINATES
Generation of a grid for a finite difference calculation of flows around an aircraft in Cartesian coordinates
[NAL-TR-956] N89-10563
CASTING
Engineering processing and properties of nickel aluminides
[DE88-011019] N89-10164
Directional spectral emissivity measurements on a ceramic mold material
[DE88-015407] N89-10167
CATACLYSMIC VARIABLES
Cataclysmic variables N89-10684
Simultaneous IUE, EXOSAT and optical observations of the unusual AM Her type variable H058+608 N89-10703
SS Cygni in quiescence --- IUE N89-10713
Searching for the white dwarf in WZ Sagittae N89-10725
CATALYSTS
A new method of determining acid base strength distribution and a new acidity-basicity scale for solid catalysts: The strongest point, HO
[NASA-TT-20334] N89-10141
Basic research on natural gas combustion phenomena-catalytic combustion
[PB88-214806] N89-10142
CATHODES
Design and performance of the SSVCO
[DE88-012435] N89-10232
CAVITATION FLOW
Numerical investigation of the dynamics of heterogeneous shock-cavitation
[MPIS-MITT-86-1987] N89-10257
CAVITIES
Effects of modulated electron beams and cavities on reditrons
[DE88-014317] N89-10234
Application of microgravity to the assessment of existing structures and structural foundations
[AD-A195599] N89-10418
CAVITY RESONATORS
Effects of modulated electron beams and cavities on reditrons
[DE88-014317] N89-10234
CEPHEID VARIABLES
The orbit of the Cepheid AW Per N89-10728
CERAMIC FIBERS
Properties of silicon carbide fiber-reinforced silicon nitride matrix composites
[NASA-TM-101356] N89-10130
CERAMIC MATRIX COMPOSITES
Thermal effects on the mechanical properties of SiC fiber reinforced reaction bonded silicon nitride matrix (SiC/RBSN) composites
[NASA-TM-101348] N89-10134
Development of ceramic matrix composites for application in the ceramic technology for advanced heat engines
[DE88-015329] N89-10168
CERAMICS
A sintering model for SiC(sub)w/Si3N4 composites
[NASA-TM-101336] N89-10166
Directional spectral emissivity measurements on a ceramic mold material
[DE88-015407] N89-10167
Development of a theory of wear of ceramics
[DE88-015327] N89-10170
Time-dependent mechanical behavior of partially stabilized zirconia for diesel engine applications
[DE88-015330] N89-10171
CHANNEL FLOW
Experimental detection of high speed fronts and clarification of their coherence with low speed streaks and streamwise vortices in a fully developed turbulent channel
[MPIS-MITT-88-1987] N89-10259
CHAOS
Generalized Lyapunov exponents in high-dimensional chaotic dynamics and products of large random matrices
[PREPRINT-595] N89-10600
CHARACTERIZATION
Multispectral characterization of the spatial structure of remotely sensed scenes N89-10340
CHEMICAL ANALYSIS
Physics and technology for the in-situ investigation of properties of materials
[AD-A195498] N89-10145
Engineering processing and properties of nickel aluminides
[DE88-011019] N89-10164
CHEMICAL BONDS
Ab initio studies of transition-metal dihydrogen chemistry
[DE88-014467] N89-10139
CHEMICAL COMPOSITION
Sequentially evaporated thin Y-Ba-Cu-O superconductor films: Composition and processing effects
[NASA-TM-101388] N89-10235

CHEMICAL LASERS
Fluid dynamic issues in continuous wave short wavelength chemical lasers
[DE88-014428] N89-10274
Directed energy concepts for strategic defense
[DE88-015050] N89-10596
CHEMICAL PROPERTIES
Beam assisted fabrication of 3-5/Si monolithic devices
[AD-A195479] N89-10655
CHEMICAL REACTIONS
Chemoviscosity modeling for thermosetting resin systems, part 3
[NASA-CR-181718] N89-10132
Ab initio studies of transition-metal dihydrogen chemistry
[DE88-014467] N89-10139
Direct Numerical Simulations (DNS) of an unpremixed turbulent jet flame
[AD-A196128] N89-10149
Beam assisted fabrication of 3-5/Si monolithic devices
[AD-A195479] N89-10655
CHIPS (ELECTRONICS)
An expert system for VLSI layout N89-10528
CHLOROPHYLLS
Changes in the chlorophyll fluorescence spectra during the Kautsky induction kinetics N89-10348
Chlorophyll fluorescence spectra of leaves as induced by blue light and red laser light N89-10349
Laser-induced fluorescence on in-vivo chlorophyll of a rice plant: A technique for the remote detection of plant growth N89-10350
Techniques for remote sensing of life span and quantum yield of chlorophyll fluorescence in vivo N89-10351
Estimation of leaf spectra from measurements in wide spectral bands N89-10368
CHONDRITES
Cosmogenic (sup 36)Cl production rates in meteorites and the lunar surface
[DE88-014452] N89-10775
CHROMOSOMES
Chromosomes and plant cell division in space
[NASA-CR-183213] N89-10518
CHROMOSPHERE
Asymmetry in zeta Aurigae chromospheres N89-10722
Model chromosphere and transition region for 56 Peg (K0 IIp + wd): A preliminary study N89-10726
Doppler imaging of AR Lacertae at three epochs N89-10740
Chromospheric mass motions during a flare on UV Ceti N89-10744
The energy input mechanism into the lower transition regions between stellar chromospheres and coronae N89-10745
Line formation of cool carbon star chromospheres N89-10748
Lithium and chromospherically active single giants N89-10749
Mg II flux and profile variability of hybrid-chromosphere stars N89-10750
Fluorescence processes and line identifications in the UV spectra of cool stars N89-10753
CHRONOLOGY
Areal and time distributions of volcanic formations on Mars N89-10800
CIRCUIT BREAKERS
Computer simulation of the effects of lightning stroke attachment to an electric power substation N89-10475
CIRCUIT DIAGRAMS
An expert system for VLSI layout N89-10528
CIRCUIT PROTECTION
International Aerospace and Ground Conference on Lightning and Static Electricity
[PB88-197439] N89-10429
Grounding for safety and compatibility N89-10495
CITRUS TREES
Spectral signature of citrus fruits and its evolution: Identification of the vegetative index of least temporal variation N89-10373
CLASSIFICATIONS
Optimization for classification of forest damage classes N89-10359
Use of remote sensing for land use policy formulation
[NASA-CR-183148] N89-10395
Validity of the classification of UV gallium stars N89-10767
CLEAN ROOMS
The Radiation-Hardened Integrated Circuit (RHIC) Laboratory: Pursuit of Class 1
[DE88-006640] N89-10062
CLEAR AIR TURBULENCE
Atmospheric propagation effects relevant to optical communications N89-10201
Measurement of vertical velocity using clear-air Doppler radars
[AD-A195344] N89-10427
CLIMATE
CCM (Community Climate Model) modular processor users' guide (version PROC02)
[PB88-216577] N89-10428
Climate of San Francisco, revised
[PB88-208624] N89-10504
CLIMATOLOGY
MECA Symposium on Mars: Evolution of its Climate and Atmosphere
[NASA-CR-182872] N89-10780
CLOUD COVER
The role of clouds in surface radiation budgets N89-10501
CLOUDS
An interactive program for estimating extinction and scattering properties of most particulate clouds
[MRL-R-1123] N89-10218
Optical thickness of the Olympus cloud N89-10808
CLOUDS (METEOROLOGY)
Electromagnetic radiations generated by microdischarges from hydrometeors N89-10448
Intracloud lightning as a precursor to thunderstorm microbursts N89-10490
The role of clouds in surface radiation budgets N89-10501
COASTS
Current measurement of lightning superbolt at the Japan sea coast N89-10445
COBALT
Oxygen electrode bifunctional electrocatalyst NiCo2O4 spinel
[NASA-TM-100847] N89-10409
CODING
Spaceborne SAR imaging of land, an opportunity for polyphase code
[ATES/DMA/RAD/002-86] N89-10226
Study of critical beta non-circular tokamak equilibria sustained in steady state by beam driven currents
[IPPJ-878] N89-10634
COHESION
Structure of grain boundaries in iron
[DE88-014412] N89-10154
COLD CATHODE TUBES
Crossatron switch as thyratron replacement in high repetition rate, high average power modulators
[DE88-013706] N89-10230
COLD FRONTS
The German Front Experiment 1987: Observations and preliminary results
[DFVLR-FB-88-21] N89-10508
COLLISION PARAMETERS
Marginal stability of ion-acoustic waves in a weakly collisional two-temperature plasma without a current
[AD-A195840] N89-10638
COLLISIONAL PLASMAS
Marginal stability of ion-acoustic waves in a weakly collisional two-temperature plasma without a current
[AD-A195840] N89-10638
COLLISIONLESS PLASMAS
Non-local kinetic transport studies of a field-reversed configuration
[DE88-012397] N89-10626
COLOR PHOTOGRAPHY
Image processing document: Halley multicolor camera (Giotto Mission)
[DFVLR-FB-88-20] N89-10270
Environmental impact of the urban growth on the Western Sao Paulo metropolitan area
[INPE-4670-PRE/1370] N89-10413
COLORADO
Sapping features of the Colorado Plateau: A comparative planetary geology field guide
[NASA-SP-491] N89-10401
COLORIMETRY
Modeling of soil color by remote sensing N89-10369
COLUMNS (SUPPORTS)
Buckling of rings in column-supported bins and tanks
[PB88-217336] N89-10290
Inelastic buckling analyses of beams, columns and plates using the spline finite strip method
[PB88-214291] N89-10299
COMBUSTIBLE FLOW
Direct Numerical Simulations (DNS) of an unpremixed turbulent jet flame
[AD-A196128] N89-10149
COMBUSTION CHAMBERS
Turbofan forced mixer lobe flow modeling. Part 3: Application to augment engines
[NASA-CR-4147] N89-10025
Fabrication and test of a carbon-carbon composite combustion chamber for a low thrust storable engine
[NAL-TR-946] N89-10118
Study on twin valveless pulse burner: Combustion stability and mixing patterns
[NAL-TR-955] N89-10144
Pulse combustor modeling: One dimensional wave-dynamic model utilizing dynamic injection and energy release submodels
[DE88-005369] N89-10150
COMBUSTION STABILITY
Study on twin valveless pulse burner: Combustion stability and mixing patterns
[NAL-TR-955] N89-10144
COMET NUCLEI
Comets --- IUE N89-10688
COMETS
Comets --- IUE N89-10688
Comets, volcanism, the salt rich regolith and cycling of volatiles on Mars N89-10786
COMMAND AND CONTROL
FIESTA: An operational decision aid for space network fault isolation N89-10075
Automation of spacecraft control centers N89-10078
COMMERCE
Integrating distributed homogeneous and heterogeneous databases: Prototypes, volume 3
[AD-A195852] N89-10668
Space commerce: An industry assessment
[PB88-214069] N89-10677
COMMUNICATION
Living in space, book 2, levels D, E, F
[NASA-EP-223] N89-10522
COMMUNICATION CABLES
Lightning tests to measure the bulk current levels associated with the electronic engine control of a turboprop commuter transport N89-10457
Lightning and surge protection of large ground facilities N89-10474
Grounding for safety and compatibility N89-10495
COMMUNICATION EQUIPMENT
Lightning standards for protection of ground electronic systems N89-10473
COMMUNICATION SATELLITES
Antennas, satellite broadcasting, and emergency preparedness for the Voice of America
[PB88-209895] N89-10222
COMPANION STARS
Cepheid binaries with large mass ratios (M1/M2) N89-10727
Companions to peculiar red giants: HR 363 and HR 1105 N89-10729
COMPARISON
Sapping features of the Colorado Plateau: A comparative planetary geology field guide
[NASA-SP-491] N89-10401
Finite difference analysis of external and internal lightning response of the JAS39 CFC wing N89-10483
Comparison of some robust regression estimators
[PB88-126289] N89-10594
COMPATIBILITY
Thermodynamic analysis of compatibility of several reinforcement materials with FeAl alloys
[NASA-CR-4172] N89-10128
Thermodynamic analysis of compatibility of several reinforcement materials with beta phase NiAl alloys
[NASA-CR-4171] N89-10131
COMPLEX COMPOUNDS
Ab initio studies of transition-metal dihydrogen chemistry
[DE88-014467] N89-10139
COMPONENT RELIABILITY
Forced vibration and flutter design methodology N89-10016
A digital simulation method of cumulative fatigue damage evaluation for spacecraft components
[NAL-TR-957] N89-10113
COMPOSITE MATERIALS
Standardization of the carbon-phenolic materials and processes. Vol. 2: Test methods and specifications
[NASA-CR-183227] N89-10033
Standardization of the carbon-phenolic materials and processes. Vol. 1: Experimental studies
[NASA-CR-183226] N89-10127
A sintering model for SiC(sub)w/Si3N4 composites
[NASA-TM-101336] N89-10166
Laser interferometric dilatometer for low-expansion materials
[DE88-012329] N89-10272
Electromagnetic coupling through composite materials N89-10479
COMPOSITE STRUCTURES
Fabrication and test of a carbon-carbon composite combustion chamber for a low thrust storable engine
[NAL-TR-946] N89-10118
Evaluation and control of residual states in curved, composite panels
[DE88-012103] N89-10126
Graded structure composites
[EP-PATENT-0-260-850-A2] N89-10135

Adhesive blends and multi-layered structures comprising the adhesive blends
[EP-PATENT-0-258-990-A1] N89-10174
Lightning tests on an all-composite helicopter N89-10452
Finite difference analysis of external and internal lightning response of the JAS39 CFC wing N89-10483
Indirect effects on electronic and mechanical systems installed in carbon fibre compound aircraft structures N89-10492

COMPRESSING
Losses in magnetic flux compression generators. Part 2: Radiation losses
[DE88-015046] N89-10224

COMPRESSORS
T55-L-712 turbine engine compressor housing refurbishment-plasma spray project
[NASA-TM-101310] N89-10156
Free-piston Stirling engine development
[PB88-220025] N89-10286
Laboratory capacity modulation experiments, analyses and validation
[DE88-012930] N89-10408

COMPUTATION
Comparison of Euler algorithms for two-dimensional shock calculations
[PB88-210372] N89-10032

COMPUTATIONAL FLUID DYNAMICS
The pros and cons of code validation
[NASA-TM-100657] N89-10034
Numerical analysis of laminar and turbulent incompressible flows using the finite element Fluid Dynamics Analysis Package (FIDAP)
[NASA-CR-179390] N89-10253
Numerical investigation of the dynamics of heterogeneous shock-cavitation
[MPIS-MITT-86-1987] N89-10257
Programming the Navier-Stokes computer: An abstract machine model and a visual editor
[NASA-CR-181691] N89-10560
On high resolution schemes for three-dimensional Euler equations
[NAL-TR-950T] N89-10581

COMPUTATIONAL GRIDS
Navier-Stokes simulation of transonic wing flow fields using a zonal grid approach
[NASA-TM-100039] N89-10022
Discretization formulas for unstructured grids
[NASA-TM-101298] N89-10242
Generation of a grid for a finite difference calculation of flows around an aircraft in Cartesian coordinates
[NAL-TR-956] N89-10563

COMPUTER AIDED DESIGN
Study on conceptual design of spacecraft using computer-aided engineering techniques
[ESA-CR(P)-2615] N89-10116
Communications to National Microwave Days
[CNES-CT/DRT/TIT/HY/87/130] N89-10237

COMPUTER DESIGN
Federal Coordinating Council on Science, Engineering and Technology, Committee on Computer Research and Applications, Subcommittee on Science and Engineering Computing
[DE88-013228] N89-10525

COMPUTER GRAPHICS
Digital simulation techniques for end game phenomena N89-10051
Open control/display system for a telerobotics work station N89-10089
An interactive program for estimating extinction and scattering properties of most particulate clouds
[MRL-R-1123] N89-10218
Comparison of plotting methods used on normal probability paper
[NAL-TR-951] N89-10584
A general data model for geographic information systems
[INPE-4560-PRE/1301] N89-10676

COMPUTER NETWORKS
A meta-protocol architecture for connecting computer networks
[AD-A196319] N89-10570

COMPUTER PROGRAM INTEGRITY
Theoretical insights into fault-based testing
[NASA-CR-183277] N89-10564

COMPUTER PROGRAMMING
Expert systems built by the Expert: An evaluation of OPS5 N89-10086
Tools to aid in the analysis of memory access patterns for FORTRAN programs
[DE88-013609] N89-10535
Second Annual Knowledge-Based Software Assistant Conference
[AD-A189819] N89-10536
A common framework for knowledge-based programming N89-10537
An overview of the knowledge-based requirements assistant N89-10538
Technology transfer and the knowledge-based software assistant N89-10541
KBSA common framework implementation N89-10543
Plans and meta-plans in an intelligent assistant for the process of programming N89-10547
Technical issues for performance estimation N89-10548
The knowledge integration tool: Knowledge interface (a knowledge based system development environment) N89-10551
Simplifying the construction of domain-specific automatic programming systems: The NASA automated software development workstation project N89-10553
ASDL: An intelligent acquisition support tool N89-10554
Plan recognition in GRAPPLE: An intelligent assistant for the process of programming N89-10555
Programming techniques for high-speed processing on the supercomputer FUJITSU VP-system
[NAL-TR-915] N89-10565
Object-oriented approach to integrating database semantics, volume 4
[AD-A195853] N89-10672

COMPUTER PROGRAMS
Validation of a pair of computer codes for estimation and optimization of subsonic aerodynamic performance of simple hinged-flap systems for thin swept wings
[NASA-TP-2828] N89-10024
A generic seeker simulation for the evaluation of active RF guidance systems N89-10050
PSA: A program to streamline orbit determination for launch support operations N89-10189
Design of an optical PPM communication link in the presence of component tolerances N89-10200
Phobos lander coding system: Software and analysis N89-10208
An interactive program for estimating extinction and scattering properties of most particulate clouds
[MRL-R-1123] N89-10218
Measurement of the properties of lossy materials inside a finite conducting cylinder
[NASA-CR-182500] N89-10223
Dynamics and control of the orbiting grid structures and the synchronously deployable beam
[NASA-CR-183205] N89-10297
CCM (Community Climate Model) modular processor users' guide (version PROC02)
[PB88-216577] N89-10428
Model results for a proposed tactical missile training site lightning protection system N89-10477
A filamentary method for calculating induced voltages within resistive structures in either the frequency or time domain N89-10484
Hardware fault insertion and instrumentation system: Experimentation and results
[NASA-CR-182746] N89-10526
Multiprogramming and the performance of parallel programs
[NASA-CR-183238] N89-10531
An overview of the knowledge-based requirements assistant N89-10538
Overview of the knowledge-based specification assistant N89-10539
Turning ideas into specifications N89-10545
Programming techniques for high-speed processing on the supercomputer FUJITSU VP-system
[NAL-TR-915] N89-10565
Develop an automated Data Base Management System (DBMS): Report on DBMS software and user's guide
[DE88-015996] N89-10674

COMPUTER STORAGE DEVICES
Space-efficient queue management using fixed-connection networks
[AD-A195167] N89-10569

COMPUTER SYSTEMS DESIGN
A natural language query system for Hubble Space Telescope proposal selection N89-10083
Study on conceptual design of spacecraft using computer-aided engineering techniques
[ESA-CR(P)-2615] N89-10116
Automatic generation of database schema N89-10671
Relational multimedia databases N89-10673

COMPUTER SYSTEMS PERFORMANCE
Technical issues for performance estimation N89-10548
Theoretical insights into fault-based testing
[NASA-CR-183277] N89-10564
Relational multimedia databases N89-10673

COMPUTER SYSTEMS PROGRAMS
Expert systems tools for Hubble Space Telescope observation scheduling N89-10081
PRIMORB: Preliminary orbit with two positions
[CNES-CT/DTI/MS/AE/072] N89-10107

COMPUTER TECHNIQUES
Storage and computationally efficient permutations of factorized covariance and square-root information arrays N89-10206
The Remote Atmospheric Probing Information Display (RAPID) system
[AD-A196314] N89-10500

COMPUTERIZED SIMULATION
A generic seeker simulation for the evaluation of active RF guidance systems N89-10050
Range delay techniques for radar target simulators N89-10054
Simulation validation experience: PATRIOT guidance system N89-10055
Hellfire system model validation N89-10057
Performance improvement of robots using a learning control scheme N89-10105
Numerical simulation of the explosives effects of two closely spaced pyrotechnic pods
[MRL-R-1095] N89-10177
A software simulation study of the long constraint length VLSI Viterbi decoder N89-10203
Computer simulation of absorption heat pump using aqueous lithium bromide and ternary nitrate mixtures
[DE88-013353] N89-10249
Discrete modeling considerations in multiphase fluid dynamics
[DE88-015188] N89-10256
Applications of a three-dimensional finite element model to mountain-valley flows
[DE88-008898] N89-10412
Computer simulation of the effects of lightning stroke attachment to an electric power substation N89-10475
Joint CGS-AOML (Charting and Geodetic Service-Atlantic Oceanographic and Meteorological Laboratory) acoustical bottom echo-formation research. 1: Literature search and initial modelling results
[PB88-202007] N89-10512
On the diagnostic emulation technique and its use in the AIRLAB
[NASA-TM-4027] N89-10524

COMPUTERS
The Remote Atmospheric Probing Information Display (RAPID) system
[AD-A196314] N89-10500

CONCENTRATION (COMPOSITION)
Fourier transform infrared spectrometry of ambient aerosols
[PB88-213236] N89-10414

CONCENTRIC CYLINDERS
Experiments on the influence of the geometry on the stability of Taylor-Couette flow
[MPIS-MITT-87-1987] N89-10258

CONCURRENT PROCESSING
Concurrent algorithms for numerical computation on hypercube computer
[AD-A195502] N89-10558

CONDUCTION
Measurement of the properties of lossy materials inside a finite conducting cylinder
[NASA-CR-182500] N89-10223

CONDUCTIVE HEAT TRANSFER
Systems analysis of the inverse heat conduction problem N89-10244

CONES
Normal force coefficient of supersonic flows over conical flare, cone-cylinder and conical boattails
[NAL-TR-949] N89-10021

CONFERENCES
Technical evaluation report on the Flight Mechanics Panel Symposium on Flight Vehicle Development Time and Cost Reduction
[AGARD-AR-244] N89-10001
Proceedings of 1987 Goddard Conference on Space Applications of Artificial Intelligence (AI) and Robotics
[NASA-TM-89663] N89-10083
Recent results from the Los Alamos free-electron laser
[DE88-014409] N89-10279
International Aerospace and Ground Conference on Lightning and Static Electricity
[PB88-197439] N89-10429
Second Annual Knowledge-Based Software Assistant Conference
[AD-A189819] N89-10536
MECA Symposium on Mars: Evolution of its Climate and Atmosphere
[NASA-CR-182872] N89-10780

CONFIDENCE
Bootstrap confidence intervals in a complex situation: A sequential paired clinical trial
[DE88-015338] N89-10592

On the appropriateness of applying chi-square distribution based confidence intervals to spectral estimates of helicopter flyover data
[NASA-CR-181692] N89-10601
CONFIDENCE LIMITS
Incremental assessment and improvement of software reliability
[NASA-CR-183275] N89-10561
CONFINEMENT
Confinement and heating of high beta plasmas with emphasis on compact toroids
[DE88-015777] N89-10645
CONIFERS
Coherent polarimetric signatures of coniferous trees: A survey N89-10307
CONSERVATION LAWS
Non-oscillatory central differencing for hyperbolic conservation laws
[NASA-CR-181709] N89-10582
CONSTITUTIVE EQUATIONS
Material parameter determination from scattering measurements
[NASA-CR-183312] N89-10225
CONTAMINANTS
Contamination of environmental control systems in Hercules aircraft
[MRL-R-1116] N89-10040
Evaluating impacts of pollutants from the atmosphere
[DE88-014550] N89-10415
CONTAMINATION
A comparative evaluation of RPD (Rotary Particle Depositor) and ferrographic diagnostic methods for turbine engine lubricant samples
[AD-A196207] N89-10044
CONTINENTAL SHELVES
Study of biological processes on the US North Atlantic slope and rise, volume 2
[PB88-196514] N89-10511
Study of biological processes on the US North Atlantic slope and rise. Volume 1: Executive summary
[PB88-196522] N89-10517
CONTINENTS
Wilson cycle studies
[NASA-CR-183146] N89-10419
CONTINUOUS WAVE LASERS
Fluid dynamic issues in continuous wave short wavelength chemical lasers
[DE88-014426] N89-10274
CONTOURS
A method for producing a shaped contour radiation pattern using a single shaped reflector and a single feed
[NASA-TM-101359] N89-10215
CONTROL SIMULATION
Simulation validation experience: PATRIOT guidance system N89-10055
CONTROL SYSTEMS DESIGN
Design and evaluation of dynamic flight test manoeuvres
[PB88-210760] N89-10042
Functional mock-up tests of the flight control system of the NAL QSTOL research aircraft: Planning and mechanical system test
[NAL-TR-944] N89-10047
Issues, concerns, and initial implementation results for space based telerobotic control N89-10091
A shared position/force control methodology for teleoperation N89-10092
Multiple sensor smart robot hand with force control N89-10093
An adaptive control scheme for a flexible manipulator N89-10095
NASREN: Standard reference model for telerobot control N89-10099
Computer hardware and software for robotic control N89-10103
Teleoperated position control of a PUMA robot N89-10104
Performance improvement of robots using a learning control scheme N89-10105
Selection of sensors for measurement and control
[DE88-012936] N89-10267
CONTROL THEORY
A dexterity measure for the kinematic control of robot manipulator with redundancy
[AD-A196223] N89-10287
CONTROLLERS
A university teaching simulation facility N89-10088
Control System Research for Directed Energy Weapons
[DE88-015371] N89-10599
CONVECTION
The delineation and interpretation of the earth's gravity field
[NASA-CR-183283] N89-10416
Lightning in mesoscale convective complexes on 3-5 June 1985 in Oklahoma and Kansas N89-10471
An algorithm for unsteady flows with strong convection
[NASA-TM-100828] N89-10575
Convection effects in protein crystal growth
[NASA-CR-179368] N89-10653
CONVECTION CLOUDS
Analysis and modeling of summertime convective cloud and precipitation structure over the southeastern United States
[NASA-CR-183192] N89-10498
CONVECTION CURRENTS
Oklahoma-Kansas preliminary regional experiment for storm-central (O-K pre-storm). Volume 3: Aircraft mission summary
[PB88-205489] N89-10499
CONVECTIVE HEAT TRANSFER
Climatic effects of enhanced CO2 levels in Mars early atmosphere N89-10799
CONVERGENCE
Convergence properties of trust region methods for linear and convex constraints
[DE88-013608] N89-10562
CONVEXITY
Convergence properties of trust region methods for linear and convex constraints
[DE88-013608] N89-10562
Abstract, topological and uniform convex structures
[PB88-202965] N89-10579
COOL STARS
Some recent results from the study of cool stars --- IUE N89-10689
IUE observations of rapidly rotating K dwarfs in the Pleiades N89-10736
Mapping of surface activity on the W UMa-type system VW Cephei N89-10742
Fluorescence processes and line identifications in the UV spectra of cool stars N89-10753
Identification of new fluorescence processes in the UV spectra of cool stars from new energy levels of Fe II and Cr II N89-10755
COOLING
Laser welding of stainless steel weld filler metals at high cooling rates
[DE88-002345] N89-10281
Gas-contact cooling for VUV laser oscillation in recombining plasmas
[IPPJ-881] N89-10631
COPPER
The influence of texture on strain hardening
[DE88-009157] N89-10158
Characterization of dynamic fracture in copper under uniaxial stress and uniaxial strain
[DE88-007824] N89-10162
COPPER ALLOYS
Micromechanisms of deformation and fracture in ordered intermetallic alloys. 1: Strengthening mechanisms
[DE88-015382] N89-10159
CORE SAMPLING
Cosmogenic (sup 36)Cl production rates in meteorites and the lunar surface
[DE88-014452] N89-10775
CORES
Adequacy of the transmitted near-field techniques for measuring optical fiber core diameter N89-10619
COROTATION
The discovery of a co-rotating magnetosphere in a helium weak star: HD5737 = alpha Scl N89-10751
CORROSION
Sulfide corrosion of silver contacts during satellite storage
[AD-A196217] N89-10112
Engineering processing and properties of nickel aluminides
[DE88-011019] N89-10164
COSMIC BACKGROUND EXPLORER SATELLITE
CLEAR: Communications Link Expert Assistance Resource N89-10072
COSMIC RAYS
Cosmogenic (sup 36)Cl production rates in meteorites and the lunar surface
[DE88-014452] N89-10775
Solar-geophysical data number 524, April 1988. Part 1: (Prompt reports). Data for March, February 1988 and late data
[PB88-217393] N89-10829
COSMOLOGY
Cosmogenic (sup 36)Cl production rates in meteorites and the lunar surface
[DE88-014452] N89-10775
COST EFFECTIVENESS
Cost effective simulation for millimeter wave guidance systems N89-10053
Riveting a case section with blind, self-plugging rivets
[DE88-013224] N89-10284
COUETTE FLOW
Experiments on the influence of the geometry on the stability of Taylor-Couette flow
[MPIS-MITT-87-1987] N89-10258
COULOMB COLLISIONS
Multiple nucleon knockout by Coulomb dissociation in relativistic heavy-ion collisions
[NASA-TM-4070] N89-10612
COUNTER ROTATION
The effect of front-to-rear propeller spacing on the interaction noise at cruise conditions of a model counterrotation propeller having a reduced diameter aft propeller
[NASA-TM-101329] N89-10603
COUNTERFLOW
Weak-wave analysis of shock interaction with a slipstream
[NASA-TP-2848] N89-10020
COUNTERMEASURES
Range delay techniques for radar target simulators N89-10054
COUNTERS
The lightning flash counter: Papua New Guinean experience N89-10491
COUPLING
Electromagnetic coupling through composite materials N89-10479
COUPLINGS
Aeroelastic coupling: An elementary approach N89-10012
COVARIANCE
Storage and computationally efficient permutations of factorized covariance and square-root information arrays N89-10206
Loopspace general covariance in string field theory
[DE88-014170] N89-10659
COVERINGS
Evaluation and mitigation of lightning hazards to the space shuttle Solid Rocket Motors (SRM) N89-10439
CRACK INITIATION
La Recherche Aerospatiale, Bimonthly Bulletin, number 1987-6, 241/November-December
[ESA-TT-1102] N89-10030
Influence of specimen size on fatigue crack initiation of welded HY100 steel
[AD-A196219] N89-10294
CRACK PROPAGATION
Fatigue and assessment methods of blade vibration N89-10010
Wheel performance evaluation. Phase 1: Analysis
[DOT/FAA/CT-88/16] N89-10041
A study of the fatigue behavior of small cracks in nickel-base superalloys
[AD-A195489] N89-10161
A compendium of sources of fracture toughness and fatigue crack growth data for metallic alloys, part 3
[NASA-TM-100675] N89-10165
An investigation of the acoustic emission generated by various crack propagation modes in 304 stainless steel N89-10293
CREEP PROPERTIES
Life time prediction: Synthesis on ONERA's research in viscoplasticity and continuous damage mechanics, applied to engine materials and structures N89-10011
CRITERIA
Design criteria for hardware-in-the-loop simulation facilities N89-10052
CROP GROWTH
Microwave backscatter from beets, peas and potatoes throughout the growing season N89-10309
Laser-induced fluorescence on in-vivo chlorophyll of a rice plant: A technique for the remote detection of plant growth N89-10350
High spectral resolution indices for monitoring crop growth and chlorosis N89-10358
CROP INVENTORIES
Complementary of microwave and optical range in the characterization of crops by remote sensing N89-10310
Potential number of winter wheat ears estimation using radiometry techniques at an early stage N89-10323
CROP VIGOR
Spectral profile and biomass estimation N89-10319
Biomass and wheat crop yield estimation from SPOT vegetative indexes N89-10327
Relation between sugar beet crop yield and vegetative indexes calculated from LANDSAT MSS images N89-10333
CRUISING FLIGHT
Supersonic missile air intakes: Design and development criteria N89-10031
The effect of front-to-rear propeller spacing on the interaction noise at cruise conditions of a model counterrotation propeller having a reduced diameter aft propeller
[NASA-TM-101329] N89-10603

CRYOGENIC COOLING
An 8.4-GHz cryogenically cooled HEMT amplifier for DSS 13 N89-10199
CRYOGENIC ROCKET PROPELLANTS
Technology issues associated with fueling the national aerospace plane with slush hydrogen [NASA-TM-101386] N89-10123
CRYOGENIC WIND TUNNELS
Highlights of experience with a flexible walled test section in the NASA Langley 0.3-meter transonic cryogenic tunnel [NASA-TM-101491] N89-10060
CRYOGENICS
Tensile properties of commercial aluminum-lithium alloys at cryogenic temperatures [DE88-014857] N89-10153
Design approaches and parameters for magnetically levitated transport systems [DE88-014286] N89-10280
CRYSTAL DEFECTS
Characterization of layers created using surface modification techniques [DE88-011918] N89-10651
CRYSTAL GROWTH
Solid State Photovoltaic Research Branch [DE88-001179] N89-10410
MOCVD techniques for CdTe solar cells [DE88-001163] N89-10411
Convection effects in protein crystal growth [NASA-CR-179368] N89-10653
A preliminary review of organic materials single crystal growth by the Czochralski technique [NASA-TM-100341] N89-10656
CRYSTAL STRUCTURE
Structure of grain boundaries in iron [DE88-014412] N89-10154
Void collapse and void growth in crystalline solids N89-10421
Quasiperiodic ordering in grain boundaries [DE88-012199] N89-10647
Pressure effects on the electronic structure of 4f and 5f materials [DE88-014149] N89-10650
Structure of amorphous silicon alloy films [DE88-001167] N89-10654
CRYSTALLIZATION
The effect of Al2O3, CaO, Cr2O3 and MgO on devitrification of silica [NASA-TM-101335] N89-10124
CRYSTALS
The detection of conformational disorder by thermal analysis [DE88-012932] N89-10657
CURRENT DENSITY
The surface electric field as a warning criterion N89-10468
CURVED PANELS
Evaluation and control of residual states in curved, composite panels [DE88-012103] N89-10126
CURVES (GEOMETRY)
Topological attributes for STEP curve and surface entities [PB88-209630] N89-10532
CYANIDES
Theoretical study of the dissociation energy and the red and violet band systems of CN [NASA-TM-101190] N89-10610
CYCLIC LOADS
Flexural fatigue of a 2-D carbon/carbon composite material [DE88-010501] N89-10133
CYCLONES
ONR tropical cyclone motion research initiative: First-year review, discussion and tentative hypotheses [AD-A194902] N89-10505
CYLINDERS
Measurement of the properties of lossy materials inside a finite conducting cylinder [NASA-CR-182500] N89-10223
CYTOLOGY
Chromosomes and plant cell division in space [NASA-CR-183213] N89-10518
CZOCHRALSKI METHOD
A preliminary review of organic materials single crystal growth by the Czochralski technique [NASA-TM-100341] N89-10656

D

DAMAGE
Life time prediction: Synthesis on ONERA's research in viscoplasticity and continuous damage mechanics, applied to engine materials and structures N89-10011
Wheel performance evaluation. Phase 1: Analysis [DOT/FAA/CT-88/16] N89-10041
Israel Air Force (IAF) in-service aircraft lightning strike and damage survey N89-10431
The interaction between lightning grounding systems and buried cables N89-10496
DAMAGE ASSESSMENT
A digital simulation method of cumulative fatigue damage evaluation for spacecraft components [NAL-TR-957] N89-10113
Optimization for classification of forest damage classes N89-10359
DAMPING
Marginal stability of ion-acoustic waves in a weakly collisional two-temperature plasma without a current [AD-A195840] N89-10638
DATA ACQUISITION
Lightning information database N89-10432
Lightning in mesoscale convective complexes on 3-5 June 1985 in Oklahoma and Kansas N89-10471
ASDL: An intelligent acquisition support tool N89-10554
DATA BASE MANAGEMENT SYSTEMS
Very large parallel data flow [AD-A196205] N89-10568
Integrating distributed homogeneous and heterogeneous databases: Prototypes, volume 3 [AD-A195852] N89-10668
Automatic generation of database schema N89-10671
Object-oriented approach to integrating database semantics, volume 4 [AD-A195853] N89-10672
Relational multimedia databases N89-10673
Develop an automated Data Base Management System (DBMS): Report on DBMS software and user's guide [DE88-015996] N89-10674
Interplanetary medium data book: Supplement 3A, 1977-1985 [NASA-TM-89630] N89-10678
DATA BASES
Lightning information database N89-10432
A common framework for knowledge-based programming N89-10537
Designing an effective user interface for a knowledge-based development environment N89-10549
An evaluation of online database selection by a gateway system with artificial intelligence techniques N89-10667
LOOK: Implementation of an expert system in information retrieval for database selection N89-10669
Automatic generation of database schema N89-10671
Relational multimedia databases N89-10673
Develop an automated Data Base Management System (DBMS): Report on DBMS software and user's guide [DE88-015996] N89-10674
A general data model for geographic information systems [INPE-4560-PRE/1301] N89-10676
DATA CORRELATION
Statistics of lightning interaction with aircraft in Japan N89-10430
DATA LINKS
Design of an optical PPM communication link in the presence of component tolerances N89-10200
Multitier specification applied to modify the hardness of an essential NSEP (National Security/Emergency Preparedness) fiber optic link [PB88-210778] N89-10220
Preliminary project PASTEL: System interface between SPOT 4 and the PSDE's passenger [CNES-87/088-CT/DRT/TIT/TR] N89-10227
DATA MANAGEMENT
Advanced data management design for autonomous telerobotic systems in space using spaceborne symbolic processors N89-10096
The Remote Atmospheric Probing Information Display (RAPID) system [AD-A196314] N89-10500
Finite precision arithmetic in singular value decomposition architectures [AD-A196188] N89-10589
DATA PROCESSING
Proceedings of 1987 Goddard Conference on Space Applications of Artificial Intelligence (AI) and Robotics [NASA-TM-89663] N89-10063
An expert system approach to astronomical data analysis N89-10080
Linear and nonlinear interpretation of CV-580 lightning data N89-10451
DATA REDUCTION
Storage and computationally efficient permutations of factorized covariance and square-root information arrays N89-10206
Gamma-ray observations of supernova SN 1987A [INPE-4604-PRE/1327] N89-10680
DATA SMOOTHING
A fast Monte-Carlo cross-validation procedure for large least squares problems with noisy data [RR-687-M] N89-10591
Smoothing spatial data by estimating mean local variance [AD-A195302] N89-10593
DATA STORAGE
Storage and computationally efficient permutations of factorized covariance and square-root information arrays N89-10206
DATA STRUCTURES
Technical issues for performance estimation N89-10548
DATA TRANSMISSION
Preliminary project PASTEL: System interface between SPOT 4 and the PSDE's passenger [CNES-87/088-CT/DRT/TIT/TR] N89-10227
DEBRIS
A comparative evaluation of RPD (Rotary Particle Depositor) and ferrographic diagnostic methods for turbine engine lubricant samples [AD-A196207] N89-10044
DECISION MAKING
FIESTA: An operational decision aid for space network fault isolation N89-10075
Automation of spacecraft control centers N89-10078
Performance estimation for a knowledge-based software assistant N89-10540
Selection of investment strategies which are optimal for the implementation of software support environments N89-10542
Free choice permissions and Ross's paradox: Internal versus external nondeterminism [PB88-202874] N89-10588
Attitudes to the use of computerised information systems for production management in manufacturing industry: A survey [TT-8706] N89-10670
DECODING
S-band transponder and telecommand decoder design and development for MECB satellites [INPE-4659-PRE/1362] N89-10219
DECOMPOSITION
Single crystal orientation effects in shock initiation of PETN explosive [DE88-014406] N89-10182
DEEP SPACE NETWORK
Deep space network resource scheduling approach and application N89-10070
The Telecommunications and Data Acquisition Report --- Deep Space Network [NASA-CR-183243] N89-10186
Deep space tracking in local reference frames N89-10187
Spain 31-GHz observations of sky brightness temperatures N89-10190
Gravitational wave searches using the DSN (Deep Space Network) N89-10192
Dual passband dichroic plate for X-band N89-10196
Antenna pointing compensation based on precision optical measurement techniques N89-10197
An 8.4-GHz cryogenically cooled HEMT amplifier for DSS 13 N89-10199
Heat exchanger expert system logic N89-10205
Relative planetary radar sensitivities: Arecibo and Goldstone N89-10209
DSN 64-meter antenna L-band (1668-MHz) microwave system performance overview N89-10210
Summary of DSN (Deep Space Network) reimbursable launch support N89-10211
DEFENSE PROGRAM
Selection of investment strategies which are optimal for the implementation of software support environments N89-10542
Military uses of space [DE88-015053] N89-10597
DEFLAGRATION
Numerical simulation of the explosives effects of two closely spaced pyrotechnic pods [MRL-R-1095] N89-10177
DEFLECTION
Elastic-plastic large deflection analysis of axisymmetric shells [PB88-217344] N89-10295
DEFORMATION
Micromechanisms of deformation and fracture in ordered intermetallic alloys. 1: Strengthening mechanisms [DE88-015382] N89-10159
Deformations and residual stresses induced in channel section columns by presetting and welding [PB88-199971] N89-10292

Inelastic buckling analyses of beams, columns and plates using the spline finite strip method
[PB88-214291] N89-10299

DEGREES OF FREEDOM
Telerobotic control of the seven-degree-of-freedom CESAR manipulator
[DE88-012937] N89-10289

DEIMOS
Phobos and Deimos: A base for sampling the Martian past N89-10819

DENSITY MEASUREMENT
Application of microgravity to the assessment of existing structures and structural foundations
[AD-A195599] N89-10418

DESIGN ANALYSIS
Quadruplex digital flight control system assessment
[NASA-CR-182741] N89-10058
The mission operations planning assistant N89-10066
Robot hands and extravehicular activity N89-10097
Design and performance of the SSVCO
[DE88-012435] N89-10232
Design study for a remote laser wavelength sensor
[DE88-015417] N89-10265
Design approaches and parameters for magnetically levitated transport systems
[DE88-014286] N89-10280

DESORPTION
Mars low albedo regions: Possible map of near-surface N89-10794

DETECTION
Application of microgravity to the assessment of existing structures and structural foundations
[AD-A195599] N89-10418
Electromagnetic radiations generated by microdischarges from hydrometeors N89-10448
Factors influencing the detection of voltage sparks by flammable gas and optical techniques N89-10465
An interagency working group on lightning threat warning N89-10469
Monitoring lightning activity in South Africa with a VLF single-station technique: Comparison with meteosat infrared data N89-10480
LSZ-850 lightning sensor system N89-10487
Considerations for using lightning locating systems in performance evaluations of single-station lightning detection sensors N89-10488

DETECTORS
Use of the time projection chamber for measuring heavy ion collisions
[MPE-PAE/EXP-EL-191] N89-10611

DETONATION
Single crystal orientation effects in shock initiation of PETN explosive
[DE88-014406] N89-10182

DEUTERIUM
Ab initio studies of transition-metal dihydrogen chemistry
[DE88-014467] N89-10139
Jovian equatorial H2 emission from 1979-1987 N89-10693
Phenomenological analysis of Jovian north auroral H2 Lyman band emissions — IUE N89-10695

DIAMETERS
Adequacy of the transmitted near-field techniques for measuring optical fiber core diameter N89-10619

DIAMONDS
New diamond
[NASA-TT-20325] N89-10169
PECVD (Plasma Enhanced Chemical Vapor Deposition) diamond thin films for research instrumentation
[AD-A195443] N89-10652

DICHROISM
Dual passband dichroic plate for X-band N89-10196

DIELECTRIC POLARIZATION
Dual passband dichroic plate for X-band N89-10196

DIELECTRIC PROPERTIES
Deflection of light by using tungsten bronze crystals
[DE88-014151] N89-10618
Martian surface physical properties to be derived by radar altimeter on the Mars observer spacecraft N89-10789

DIELECTRICS
On a surface mounted transmission line configuration for aperture testing N89-10458

DIESEL ENGINES
Time-dependent mechanical behavior of partially stabilized zirconia for diesel engine applications
[DE88-015330] N89-10171
Final review of US Army fire-resistant fuel program
[AD-A194304] N89-10176

DIESEL FUELS
Final review of US Army fire-resistant fuel program
[AD-A194304] N89-10176

DIFFERENCE EQUATIONS
Improving the accuracy of central difference schemes
[NASA-CR-181712] N89-10577
Non-oscillatory central differencing for hyperbolic conservation laws
[NASA-CR-181709] N89-10582

DIFFUSION
Metastable alloy phases prepared by solid state reactions and ball milling
[DE88-009156] N89-10163
Losses in magnetic flux compression generators. Part 2: Radiation losses
[DE88-015046] N89-10224

DIFFUSION THEORY
IUE observations of a hot DAO white dwarf: Implications for diffusion theory and photospheric stratification N89-10733

DIGITAL COMPUTERS
Hardware fault insertion and instrumentation system: Experimentation and results
[NASA-CR-182746] N89-10526

DIGITAL DATA
Digital recording of radar data in an aircraft
[PB88-209507] N89-10212

DIGITAL SIMULATION
Guidance and control systems simulation and validation techniques
[AGARD-AG-273] N89-10048
Comparison of statistical digital simulation methods N89-10049
Digital simulation techniques for end game phenomena N89-10051
A digital simulation method of cumulative fatigue damage evaluation for spacecraft components
[NAL-TR-957] N89-10113
Numerical simulations of dust transport into northern high latitudes during a Martian polar warming N89-10782

DIGITAL SYSTEMS
Quadruplex digital flight control system assessment
[NASA-CR-182741] N89-10058
Hardware fault insertion and instrumentation system: Experimentation and results
[NASA-CR-182746] N89-10526

DIHYDRIDES
Ab initio studies of transition-metal dihydrogen chemistry
[DE88-014467] N89-10139

DILUTION
Physics and technology for the in-situ investigation of properties of materials
[AD-A195498] N89-10145
Reports of investigations on: Derivation of an infinite-dilution activity coefficient model and application to two-component vapor/liquid equilibria data
[DE88-007517] N89-10147

DIRECTION FINDING
On the statistics of field waveforms associated with lightning return strokes N89-10441
A lightning location system for the UK electricity supply industry N89-10482
LSZ-850 lightning sensor system N89-10487
Considerations for using lightning locating systems in performance evaluations of single-station lightning detection sensors N89-10488
Site errors of a magnetic direction finder for lightning flashes N89-10494

DISCONTINUITY
An adaptive pseudospectral method for discontinuous problems
[NASA-CR-181717] N89-10583

DISCRETE FUNCTIONS
Discretization formulas for unstructured grids
[NASA-TM-101298] N89-10242

DISK GALAXIES
Global properties of molecular clouds and the interstellar medium in galaxies N89-10776

DISORDERS
The detection of conformational disorder by thermal analysis
[DE88-012932] N89-10657

DISPLAY DEVICES
Open control/display system for a telerobotics work station N89-10089
The Remote Atmospheric Probing Information Display (RAPID) system
[AD-A196314] N89-10500

DISSOCIATION
Theoretical study of the dissociation energy and the red and violet band systems of CN
[NASA-TM-101190] N89-10610

DISTRIBUTED PARAMETER SYSTEMS
On the problem of modeling for parameter identification in distributed structures
[NASA-CR-182739] N89-10291

DISTRIBUTED PROCESSING
A hierarchically distributed architecture for fault isolation expert systems on the space station N89-10077
Advanced data management design for autonomous telerobotic systems in space using spaceborne symbolic processors N89-10096
Orca: A language for distributed object-based programming
[PB88-208533] N89-10529
Integrating distributed homogeneous and heterogeneous databases: Prototypes, volume 3
[AD-A195852] N89-10668

DISTRIBUTION (PROPERTY)
A filamentary method for calculating induced voltages within resistive structures in either the frequency or time domain N89-10484

DISTRIBUTION FUNCTIONS
Mean estimation in highly skewed samples
[DE88-010929] N89-10595
C 4 fluxes from the sun as a star and the correlation with magnetic flux
[NASA-CR-183156] N89-10827

DIURNAL VARIATIONS
The observed day-to-day variability of Mars water vapor N89-10797
Optical thickness of the Olympus cloud N89-10808

DOPED CRYSTALS
Influence of boundary surface roughness, order effects and dopants on optical properties of InP based metal organic gas phase epitaxy (MOCVD) heterostructure
[ETN-88-92986] N89-10646

DOPPLER RADAR
Gravitational wave searches using the DSN (Deep Space Network) N89-10192
Measurement of vertical velocity using clear-air Doppler radars
[AD-A195344] N89-10427
Intracloud lightning as a precursor to thunderstorm microbursts N89-10490

DOWNLINKING
Simultaneous S- and X-band uplink-downlink performance at DSS 13 N89-10194

DRAINAGE PATTERNS
Sapping features of the Colorado Plateau: A comparative planetary geology field guide
[NASA-SP-491] N89-10401

DROPS (LIQUIDS)
Investigation of superradiant LDV markers and three-component velocity mapping
[AD-A195504] N89-10662

DUCTILITY
Recent developments in aluminides and silicides
[DE88-012926] N89-10155
Engineering processing and properties of nickel aluminides
[DE88-011019] N89-10164

DURABILITY
Multitier specification applied to modify the hardness of an essential NSEP (National Security/Emergency Preparedness) fiber optic link
[PB88-210778] N89-10220

DUST
A comparative evaluation of RPD (Rotary Particle Depositor) and ferrographic diagnostic methods for turbine engine lubricant samples
[AD-A196207] N89-10044
Electrification of hovering helicopters N89-10460
Regional sources and sinks of dust on Mars: Viking observations of Cerberus, Solis Planum, and Syrtis Major N89-10802

DUST STORMS
Numerical simulations of dust transport into northern high latitudes during a Martian polar warming N89-10782
The Martian dust cycle: A proposed model N89-10791
Interannual variability of global dust storms on Mars N89-10792
Mars low albedo regions: Possible map of near-surface N89-10794
The great dust storm of 1986 N89-10804
Mars global atmospheric oscillations: Transients and dust storm relations N89-10820

DWARF NOVAE
The 1981 outburst of the old nova GK Persei N89-10707
IUE observations of the 1987 superoutburst of the dwarf nova Z Cha N89-10715

DWARF STARS
IUE observations of rapidly rotating K dwarfs in the Pleiades N89-10736
Transition region fluxes in A-F Dwarfs: Basal fluxes and dynamo activity N89-10747
Mass loss from the K dwarf in V471 Tauri N89-10770

DYE LASERS
Laser diagnostics of gas discharge tubes
[DE88-008124] N89-10633
DYNAMIC MODELS
An adaptive control scheme for a flexible manipulator N89-10095
Dynamic properties of power MOS transistors
[LAAS-88-162] N89-10236
Pressure studies of protein dynamics
[AD-A192386] N89-10523
DYNAMIC RESPONSE
Design and evaluation of dynamic flight test manoeuveres
[PB88-210760] N89-10042
Vibration, performance, flutter and forced response characteristics of a large-scale propfan and its aeroelastic model
[NASA-TM-101322] N89-10043
DYNAMIC STRUCTURAL ANALYSIS
AGARD manual on aeroelasticity in axial-flow turbomachines. Volume 2: Structural dynamics and aeroelasticity
[AGARD-AG-298-VOL-2] N89-10006
Basic structural dynamics N89-10007
Structural dynamic characteristics of individual blades N89-10008
Structural dynamic characteristics of bladed assemblies N89-10009
Aeroelastic coupling: An elementary approach N89-10012
Aeroelastic formulation for tuned and mistuned rotors N89-10013
Means for testing aerospace launcher structures
[ETN-88-93082] N89-10110
Buckling of rings in column-supported bins and tanks
[PB88-217336] N89-10290
Elastic-plastic large deflection analysis of axisymmetric shells
[PB88-217344] N89-10295
Recent developments in structural sensitivity analysis
[NASA-TM-100668] N89-10300
DYNAMICAL SYSTEMS
Pulse combustor modeling: One dimensional wave-dynamic model utilizing dynamic injection and energy release submodels
[DE88-005369] N89-10150
Dimensional deformations of integrable systems: An approach to integrability in multidimensions, part 1
[PREPRINT-586] N89-10585
Generalized Lyapunov exponents in high-dimensional chaotic dynamics and products of large random matrices
[PREPRINT-595] N89-10600
DYNAMICS EXPLORER SATELLITES
Dynamics Explorer guest investigator
[NASA-CR-183163] N89-10417

E

EARTH CORE
Earth rotation and core topography
[NASA-CR-183186] N89-10425
EARTH GRAVITATION
The delineation and interpretation of the earth's gravity field
[NASA-CR-183283] N89-10416
EARTH OBSERVATIONS (FROM SPACE)
Solid earth mission study. Volume 2: Technical report
[ESA-CR(P)-2626-VOL-2] N89-10303
Thermal infrared laser spectroscopy: The potential of dual active/passive thermal infrared sensors for Earth observation N89-10345
The French space program for Earth observation N89-10392
NASA's future land remote sensing program N89-10393
Solid Earth mission study. Volume 1: Executive summary
[ESA-CR(P)-2626-VOL-1] N89-10397
Solid earth mission study. Volume 3: Program planning report
[ESA-CR(P)-2626-VOL-3] N89-10399
EARTH OBSERVING SYSTEM (EOS)
Precise orbit determination for NASA's earth observing system using GPS (Global Positioning System) N89-10188
EARTH RADIATION BUDGET
The role of clouds in surface radiation budgets N89-10501
EARTH RADIATION BUDGET EXPERIMENT
An expert system for scheduling requests for communications Links between TDRSS and ERBS N89-10065
EARTH RESOURCES
Earth resources: A continuing bibliography with indexes (issue 58)
[NASA-SP-7041(58)] N89-10398
EARTH ROTATION
Earth rotation and core topography
[NASA-CR-183186] N89-10425
EARTH SURFACE
Sensitivity of satellite-derived net shortwave irradiance at the Earth's surface to radiometric calibration N89-10335
Airborne Visible/Infrared Imaging Spectrometer (AVIRIS): Inflight radiometric calibration and the determination of surface reflectance N89-10357
A new method for estimating regional evaporation from thermal infrared surface temperature measurements N89-10390
The surface electric field as a warning criterion N89-10468
Spatial distribution of lightning strikes to ground during small thunderstorms in Florida N89-10472
A revised electrogeometric model for the termination of lightning strokes on ground objects N89-10476
ECHELLE GRATINGS
Photoelectrochemical fabrication of spectroscopic diffraction gratings
[NASA-CR-180786] N89-10615
ECHO SOUNDING
Joint CGS-AOML (Charting and Geodetic Service-Atlantic Oceanographic and Meteorological Laboratory) acoustical bottom echo-formation research. 1: Literature search and initial modelling results
[PB88-202007] N89-10512
ECLIPSES
The November 1987 eclipse of the zeta-Aur system HR 2554 N89-10721
ECLIPSING BINARY STARS
Atmospheric eclipse effects in Wolf-Rayet binaries in the Small Magellanic Cloud N89-10717
Mass flow in the interacting binary TX Ursae Majoris N89-10718
A new study of the interacting binary star V356 Sgr N89-10719
The November 1987 eclipse of the zeta-Aur system HR 2554 N89-10721
Asymmetry in zeta Auriage chromospheres N89-10722
Superionized plasmas in Algol binaries N89-10723
ECONOMICS
Hydrogen supply over long distances using chemicals description and evaluation of a technical system
[DE88-012630] N89-10178
Selection of investment strategies which are optimal for the implementation of software support environments N89-10542
ECOSYSTEMS
Use of remote sensing for land use policy formulation
[NASA-CR-183148] N89-10395
EDITING
Interactive editing of mathematical formulae
[PB88-203005] N89-10580
EDUCATION
Model results for a proposed tactical missile training site lightning protection system N89-10477
EFFICIENCY
Laser diagnostics of gas discharge tubes
[DE88-008124] N89-10633
EJECTA
Ejecta in SN 1006: The knotty issue --- supernova remnant N89-10700
Observations and simulations of nova Vul 1984 no. 2: A nova with ejecta rich in oxygen, neon, and magnesium N89-10709
Ice or liquid water in the Martian regolith. Morphologic indicators from rampart craters N89-10806
Crater ejecta morphology and the presence of water on Mars N89-10818
EL NINO
Model-data comparisons for the 1982-83 El Nino: The XBT tracks
[PB88-221668] N89-10514
ELASTIC PROPERTIES
Inelastic buckling analyses of beams, columns and plates using the spline finite strip method
[PB88-214291] N89-10299
ELASTIC SCATTERING
Electron transport and optical emissions in the aurora N89-10424
ELASTIC SHELLS
Elastic-plastic large deflection analysis of axisymmetric shells
[PB88-217344] N89-10295
ELASTOPLASTICITY
Elastic-plastic large deflection analysis of axisymmetric shells
[PB88-217344] N89-10295
ELECTRIC ARCS
Breakdown characteristics of an isolated conducting object in a uniform electric field N89-10453
ELECTRIC BRIDGES
Semiconductor Bridge (SCB): A new method for the ignition of explosives and pyrotechnics
[DE88-011246] N89-10151
ELECTRIC CHARGE
Framework for lightning modeling: Comparing results N89-10435
A chronology of in-cloud electric field and lightning strikes on an instrumented research aircraft N89-10455
Lightning initiation on aircraft in thunderstorms N89-10456
Electrification of hovering helicopters N89-10460
Measurement of the electrostatic charging on large helicopters and control of the shock hazard N89-10461
The electrical structure of thunderstorm anvils N89-10470
ELECTRIC CONDUCTORS
The interaction between lightning grounding systems and buried cables N89-10496
ELECTRIC CONNECTORS
Optimal simulations by butterfly networks: Extended abstract
[AD-A195168] N89-10572
ELECTRIC CORONA
Lightning initiation on aircraft in thunderstorms N89-10456
The surface electric field as a warning criterion N89-10468
ELECTRIC CURRENT
Optical sensors for the measurement of electric current and voltage
[PB88-208467] N89-10233
A filamentary method for calculating induced voltages within resistive structures in either the frequency or time domain N89-10484
Modelling of common mode coupling between an aircraft wing traversed by a lightning current and wiring installed in that wing N89-10485
The interaction between lightning grounding systems and buried cables N89-10496
ELECTRIC DISCHARGES
Electrostatic discharge and field effects of electronics systems N89-10493
ELECTRIC FIELD STRENGTH
An optical sensor for the non-interactive detection of weak electric fields N89-10263
ELECTRIC FIELDS
An optical sensor for the non-interactive detection of weak electric fields N89-10263
What makes thunderbolts zig and zag N89-10434
The criterion for the propagation of the positive streamer and its application N89-10436
Numerical simulations of lightning by means of the leader propagation model N89-10437
An aircraft-borne electric field measuring system for rocket launch support N89-10443
New electric field instrumentation and the effects of space charge at Kennedy Space Center N89-10444
Summary of inflight data on lightning currents and fields N89-10449
Estimating electric field enhancement factors on an aircraft utilizing a small scale model: A method evaluation N89-10454
A chronology of in-cloud electric field and lightning strikes on an instrumented research aircraft N89-10455
The surface electric field as a warning criterion N89-10468
The electrical structure of thunderstorm anvils N89-10470
Some observations and analysis of atmospheric electricity over non-uniform high terrain N89-10489
The interaction between lightning grounding systems and buried cables N89-10496
ELECTRIC GENERATORS
Losses in magnetic flux compression generators. Part 2: Radiation losses
[DE88-015046] N89-10224
ELECTRIC POTENTIAL
Optical sensors for the measurement of electric current and voltage
[PB88-208467] N89-10233
Factors influencing the detection of voltage sparks by flammable gas and optical techniques N89-10465
A filamentary method for calculating induced voltages within resistive structures in either the frequency or time domain N89-10484
Neoclassical resonant-plateau transport in the noncircular equipotential surface of a tandem mirror
[IPPJ-879] N89-10627
Structural instability of sheath potential distribution and its possible implications for the L/H transition in tokamak plasmas
[IPPJ-877] N89-10643

ELECTRIC POWER TRANSMISSION
Single-pole switching schemes for EHV transmission systems N89-10228
Computer simulation of the effects of lightning stroke attachment to an electric power substation N89-10475
A lightning location system for the UK electricity supply industry N89-10482
Modelling of common mode coupling between an aircraft wing traversed by a lightning current and wiring installed in that wing N89-10485
ELECTRIC SPARKS
Factors influencing the detection of voltage sparks by flammable gas and optical techniques N89-10465
ELECTRIC SWITCHES
Computer simulation of the effects of lightning stroke attachment to an electric power substation N89-10475
ELECTRIC WIRE
Modelling of common mode coupling between an aircraft wing traversed by a lightning current and wiring installed in that wing N89-10485
ELECTRICAL FAULTS
Breakdown characteristics of an isolated conducting object in a uniform electric field N89-10453
ELECTRICAL GROUNDING
Measurement of the electrostatic charging on large helicopters and control of the shock hazard N89-10461
Lightning and surge protection of large ground facilities N89-10474
Grounding for safety and compatibility N89-10495
System protection from atmospheric electricity for aerostats with conducting tethers N89-10497
ELECTRICAL MEASUREMENT
International Aerospace and Ground Conference on Lightning and Static Electricity
[PB88-197439] N89-10429
An aircraft-borne electric field measuring system for rocket launch support N89-10443
New electric field instrumentation and the effects of space charge at Kennedy Space Center N89-10444
Current measurement of lightning superbolt at the Japan sea coast N89-10445
A case for a unified lightning threat N89-10447
Electromagnetic radiations generated by microdischarges from hydrometeors N89-10448
Summary of inflight data on lightning currents and fields N89-10449
Analysis of recent in-flight lightning measurements on different aircraft N89-10450
Estimating electric field enhancement factors on an aircraft utilizing a small scale model: A method evaluation N89-10454
A chronology of in-cloud electric field and lightning strikes on an instrumented research aircraft N89-10455
Lightning tests to measure the bulk current levels associated with the electronic engine control of a turboprop commuter transport N89-10457
Measurement of the electrostatic charging on large helicopters and control of the shock hazard N89-10461
Electrostatic fields of ground triggered lightning N89-10462
Lightning protection for high explosives and instrumentation using a field mill system N89-10467
The surface electric field as a warning criterion N89-10468
Model results for a proposed tactical missile training site lightning protection system N89-10477
Some observations and analysis of atmospheric electricity over non-uniform high terrain N89-10489
ELECTRICAL PROPERTIES
Structure of amorphous silicon alloy films
[DE88-001167] N89-10654
Beam assisted fabrication of 3-5/Si monolithic devices
[AD-A195479] N89-10655
ELECTRICAL RESISTIVITY
Linear and nonlinear interpretation of CV-580 lightning data N89-10451
Breakdown characteristics of an isolated conducting object in a uniform electric field N89-10453
Estimating electric field enhancement factors on an aircraft utilizing a small scale model: A method evaluation N89-10454
Electromagnetic coupling through composite materials N89-10479
ELECTRO-OPTICAL PHOTOGRAPHY
The results of the Geosat MOMS subcommittee's data evaluation: Performance and applicability of the MOMS-1 sensor for exploration geology N89-10380
Design of spectral bands for the German MOMS-2 sensor N89-10381
The use of MOMS-1 data for geological mapping of the Aswa lineament (East African rift) N89-10382
MOMS-1 data for bathymetric and geological studies N89-10383
MOMS-1 used synergistically with LANDSAT TM N89-10384
Digital analysis of MOMS-1, LANDSAT TM, and SPOT data of the Nakuru area (Kenya) N89-10386
Development of MOMS to a future multiband and stereoscopic sensor N89-10391
ELECTRO-OPTICS
An optical sensor for the non-interactive detection of weak electric fields N89-10263
Considerations and calculations for application of an optical amplifier as an end- and preamplifier
[ESA-TT-1004] N89-10625
ELECTROCATALYSTS
Oxygen electrode bifunctional electrocatalyst NiCo2O4 spinel
[NASA-TM-100947] N89-10409
ELECTRODEPOSITION
Electronic structure of electrodeposited thin film CdTe solar cells
[DE88-001170] N89-10406
ELECTRODES
Oxygen electrode bifunctional electrocatalyst NiCo2O4 spinel
[NASA-TM-100947] N89-10409
Breakdown characteristics of an isolated conducting object in a uniform electric field N89-10453
ELECTROKINETICS
Changes in the chlorophyll fluorescence spectra during the Kautsky induction kinetics N89-10348
ELECTROMAGNETIC FIELDS
Losses in magnetic flux compression generators. Part 2: Radiation losses
[DE88-015046] N89-10224
Computer simulation of the effects of lightning stroke attachment to an electric power substation N89-10475
Site errors of a magnetic direction finder for lightning flashes N89-10494
ELECTROMAGNETIC INTERFERENCE
Grounding for safety and compatibility N89-10495
ELECTROMAGNETIC NOISE
Interference of precipitation static discharges with aircraft navigational systems N89-10459
Some observations and analysis of atmospheric electricity over non-uniform high terrain N89-10489
ELECTROMAGNETIC PULSES
Transfer impedance measurements of the space shuttle Solid Rocket Motor (SRM) joints, wire meshes and a carbon graphite motor case N89-10440
Electromagnetic radiations generated by microdischarges from hydrometeors N89-10448
Lightning standards for protection of ground electronic systems N89-10473
ELECTROMAGNETIC RADIATION
Compact imaging spectrometer for induced emissions
[NASA-CR-183187] N89-10264
On the statistics of field waveforms associated with lightning return strokes N89-10441
Interference of precipitation static discharges with aircraft navigational systems N89-10459
ELECTROMAGNETIC SCATTERING
Material parameter determination from scattering measurements
[NASA-CR-183312] N89-10225
ELECTROMAGNETIC SHIELDING
On a surface mounted transmission line configuration for aperture testing N89-10458
A revised electrogeometric model for the termination of lightning strokes on ground objects N89-10476
Electromagnetic coupling through composite materials N89-10479
ELECTRON BEAMS
Design and performance of the SSVCO
[DE88-012435] N89-10232
Effects of modulated electron beams and cavities on reditrons
[DE88-014317] N89-10234
A transition radiation experiment to measure the electron beam modulation induced by the free electron laser: A design study
[AD-A195169] N89-10275
Recent results from the Los Alamos free-electron laser
[DE88-014409] N89-10279
ELECTRON DENSITY (CONCENTRATION)
Neon puffing experiments in the JIPP T-IIU tokamak
[IPPJ-870] N89-10632
ELECTRON ENERGY
Neon puffing experiments in the JIPP T-IIU tokamak
[IPPJ-870] N89-10632
ELECTRON MICROSCOPY
Background modelling alternatives in electron energy-loss spectroscopy and their implications on microanalysis
[DE88-010361] N89-10140
Premartensitic microstructures as seen in the high-resolution electron microscope: A study of a NiAl alloy
[DE88-008042] N89-10160
ELECTRON PARAMAGNETIC RESONANCE
Structure of amorphous silicon alloy films
[DE88-001167] N89-10654
ELECTRON PRECIPITATION
Dynamics Explorer guest investigator
[NASA-CR-183163] N89-10417
ELECTRON RUNAWAY (PLASMA PHYSICS)
On the generation of runaway electrons and their impact to plasma facing components
[IPPJ-871] N89-10641
ELECTRON SOURCES
Evaluation of the characteristics of a field emission cathode for use in a Mercury ion trap frequency standard N89-10193
ELECTRON SPECTROSCOPY
Background modelling alternatives in electron energy-loss spectroscopy and their implications on microanalysis
[DE88-010361] N89-10140
Electron transport and optical emissions in the aurora N89-10424
Characterization of layers created using surface modification techniques
[DE88-011918] N89-10651
ELECTRON STATES
The lowest ionization potentials of Al2
[NASA-TM-101171] N89-10605
ELECTRON TRANSFER
Electron transport and optical emissions in the aurora N89-10424
ELECTRON TRANSITIONS
Pressure effects on the electronic structure of 4f and 5f materials
[DE88-014149] N89-10650
ELECTRONIC EQUIPMENT
Lightning standards for protection of ground electronic systems N89-10473
Electrostatic discharge and field effects of electronics systems N89-10493
Hardware fault insertion and instrumentation system: Experimentation and results
[NASA-CR-182746] N89-10526
ELECTRONIC RECORDING SYSTEMS
Comparison of mechanical and electronic high-speed recording systems
[DE88-015264] N89-10268
ELECTRONS
A stochastic model for the tortuous propagation of a lightning stepped leader N89-10433
Nonlinear spin acceptance in electron storage rings
[CEBAF-PR-88-009] N89-10614
Electronic structure of the quenched superconductivity of materials Y(sub 1-x)Pr(sub x)Ba2Cu3O(sub 7-delta)
[DE88-014414] N89-10658
ELECTROPHORESIS
Electrospray ionization phenomena and the interface of capillary electrophoresis and mass spectrometry
[DE88-014080] N89-10143
An improved interface for capillary zone electrophoresis-mass spectrometry
[DE88-014079] N89-10148
ELECTROSTATIC CHARGE
Measurement of the electrostatic charging on large helicopters and control of the shock hazard N89-10461
Electrostatic fields of ground triggered lightning N89-10462
ELECTROSTATICS
Electrostatic discharge and field effects of electronics systems N89-10493
EMBEDDED COMPUTER SYSTEMS
Optimal simulations by butterfly networks: Extended abstract
[AD-A195168] N89-10572
EMBRITTLEMENT
Recent developments in aluminides and silicides
[DE88-012926] N89-10155
EMERGENCIES
Antennas, satellite broadcasting, and emergency preparedness for the Voice of America
[PB88-209895] N89-10222
EMISSION
Spectral characteristics of arc-heated low density plasma flows (2) nitrogen plasma
[NAL-TR-952] N89-10639
EMISSION SPECTRA
Attempt at absolute determination of spectral signatures of bare soils in the thermal infrared, in emission and reflection N89-10336
Observations of SN 1987A: The narrow emission lines --- IUE N89-10696
Lithium and chromospherically active single giants N89-10749
Fe II level population in luminous variable stars N89-10754

EMISSIVITY
Infrared temperature measurement with inherent consideration of emissivity
[DFVLR-FB-88-22] N89-10271
EMULSIONS
Final review of US Army fire-resistant fuel program
[AD-A194304] N89-10176
ENERGY CONSERVATION
Impacts of advanced refrigerator insulation
[DE88-001180] N89-10185
ENERGY CONVERSION
Direct methane conversion: An assessment
[DE88-010225] N89-10181
ENERGY CONVERSION EFFICIENCY
Direct methane conversion: An assessment
[DE88-010225] N89-10181
ENERGY DISSIPATION
Losses in magnetic flux compression generators. Part 2: Radiation losses
[DE88-015046] N89-10224
ENERGY METHODS
Analysis of some low-order finite element schemes for Mindlin-Reissner and Kirchhoff plates
[PB87-175899] N89-10578
ENERGY TRANSFER
Vibrational relaxation processes in CO2-N2-H2O laser systems
[AD-A196211] N89-10273
Fluid dynamic issues in continuous wave short wavelength chemical lasers
[DE88-014428] N89-10274
Studies of blackbody-pumped lasers
[NASA-CR-183214] N89-10277
Analytical approximations for X-ray cross sections 3
[DE88-015366] N89-10609
The energy input mechanism into the lower transition regions between stellar chromospheres and coronae N89-10745
ENGINE CONTROL
Lightning tests to measure the bulk current levels associated with the electronic engine control of a turboprop commuter transport N89-10457
ENGINE TESTS
Aeroelastic thermal effects N89-10015
Shock tunnel studies of scramjet phenomena
[NASA-CR-181721] N89-10045
Alternate fuels for General Aviation aircraft with spark ignition engines
[DOT/FAA/CT-88/05] N89-10179
ENGINES
Development of ceramic matrix composites for application in the ceramic technology for advanced heat engines
[DE88-015329] N89-10168
ENTHALPY
Computer simulation of absorption heat pump using aqueous lithium bromide and ternary nitrate mixtures
[DE88-013353] N89-10249
ENVIRONMENT EFFECTS
Environmental impact of the urban growth on the Western Sao Paulo metropolitan area
[INPE-4670-PRE/1370] N89-10413
ENVIRONMENTAL MONITORING
Contamination of environmental control systems in Hercules aircraft
[MRL-R-1116] N89-10040
A new lidar system for applications over land and sea N89-10347
ENVIRONMENTS
The load shedding advisor: An example of a crisis-response expert system N89-10073
Performance of multimirror quartzline lamps in a high-pressure, underwater environment
[NASA-TM-101374] N89-10269
EPHEMERIDES
Compilation of methods in orbital mechanics and solar geometry
[NASA-RP-1204] N89-10420
EPITAXY
Influence of boundary surface roughness, order effects and dopants on optical properties of InP based metal organic gas phase epitaxy (MOCVD) heterostructure
[ETN-88-92986] N89-10646
EPOXY RESINS
Lightning tests on an all-composite helicopter N89-10452
EQUATIONS OF MOTION
Dynamics and control of the orbiting grid structures and the synchronously deployable beam
[NASA-CR-183205] N89-10297
EQUATIONS OF STATE
Research in nuclear astrophysics: Stellar collapse and supernovae
[DE88-015267] N89-10778
EQUATORIAL REGIONS
EPOCS (Equatorial Pacific Ocean Climate Studies) moored temperature, current and wind measurements: 0 deg, 140 deg W, May-June, 1987
[PB88-219415] N89-10509
Drifting buoy data from the Equatorial Pacific for the period January 1, 1984 through May 31, 1985
[PB88-212824] N89-10516
EROSION
Simulation of plasma erosion opening switches
[DE88-014425] N89-10229
ERROR ANALYSIS
The pros and cons of code validation
[NASA-TM-100657] N89-10034
Hellfire system model validation N89-10057
ERROR SIGNALS
Analysis of methods for detecting focus error in optical data storage systems N89-10617
ERRORS
Estimating electric field enhancement factors on an aircraft utilizing a small scale model: A method evaluation N89-10454
Effect of double-shell structure on reduction of field errors in the STP-3(M) reversed-field pinch
[IPPJ-882] N89-10640
ERS-1 (ESA SATELLITE)
Review of the requirements for higher level ERS-1 products within Europe
[ESA-CR(P)-2586] N89-10664
ESTIMATES
Estimating electric field enhancement factors on an aircraft utilizing a small scale model: A method evaluation N89-10454
Performance estimation for a knowledge-based software assistant N89-10540
Technical issues for performance estimation N89-10548
An investigation of new methods for estimating parameter sensitivities
[NASA-CR-183195] N89-10586
ESTIMATORS
Comparison of some robust regression estimators
[PB88-126289] N89-10594
ETCHING
Photoelectrochemical fabrication of spectroscopic diffraction gratings
[NASA-CR-180786] N89-10615
ETHYL ALCOHOL
HAN (hydroxylammonium nitrate density)-based liquid gun propellants: Physical properties
[AD-A195246] N89-10180
EULER EQUATIONS OF MOTION
Delta square-correction scheme for unsteady Euler equations
[NAL-TR-948] N89-10576
Improving the accuracy of central difference schemes
[NASA-CR-181712] N89-10577
On high resolution schemes for three-dimensional Euler equations
[NAL-TR-950T] N89-10581
EUROPE
Review of the requirements for higher level ERS-1 products within Europe
[ESA-CR(P)-2586] N89-10664
EUROPEAN SPACE PROGRAMS
Solid earth mission study. Volume 2: Technical report
[ESA-CR(P)-2626-VOL-2] N89-10303
Solid Earth mission study. Volume 1: Executive summary
[ESA-CR(P)-2626-VOL-1] N89-10397
Solid earth mission study. Volume 3: Program planning report
[ESA-CR(P)-2626-VOL-3] N89-10399
EVALUATION
Evaluating impacts of pollutants from the atmosphere
[DE88-014550] N89-10415
Considerations for using lightning locating systems in performance evaluations of single-station lightning detection sensors N89-10488
Performance assessment register
[AGARD-R-763] N89-10666
EVAPORATION
Sequentially evaporated thin Y-Ba-Cu-O superconductor films: Composition and processing effects
[NASA-TM-101388] N89-10235
A new method for estimating regional evaporation from thermal infrared surface temperature measurements N89-10390
EVOLUTION
Initial evolution of nonlinear magnetic islands in high temperature plasmas
[DE88-012346] N89-10636
EVOLUTION (DEVELOPMENT)
Wilson cycle studies
[NASA-CR-183146] N89-10419
EXCITATION
Resonant excitation of spatial perturbations in a boundary layer in the presence of a pressure gradient
[NASA-TT-20305] N89-10248
Spectral characteristics of arc-heated low density plasma flows (1) argon plasma
[NAL-TR-954] N89-10642
EXHAUST GASES
Electrification of hovering helicopters N89-10460
EXPERIMENT DESIGN
Bootstrap confidence intervals in a complex situation: A sequential paired clinical trial
[DE88-015338] N89-10592
EXPERT SYSTEMS
Proceedings of 1987 Goddard Conference on Space Applications of Artificial Intelligence (AI) and Robotics
[NASA-TM-89663] N89-10063
Maintaining an expert system for the Hubble Space Telescope ground support N89-10064
An expert system for scheduling requests for communications Links between TDRSS and ERBS N89-10065
The mission operations planning assistant N89-10066
PLAN-IT: Scheduling assistant for solar system exploration N89-10068
An expert system that performs a satellite station keeping maneuver N89-10069
Space station Platform Management System (PMS) replanning using resource envelopes N89-10071
CLEAR: Communications Link Expert Assistance Resource N89-10072
The load shedding advisor: An example of a crisis-response expert system N89-10073
A local area computer network expert system framework N89-10074
FIESTA: An operational decision aid for space network fault isolation N89-10075
Expert system support for HST operations N89-10076
A hierarchically distributed architecture for fault isolation expert systems on the space station N89-10077
Automation of spacecraft control centers N89-10078
Spacelab Data Processing Facility (SLDPF) quality assurance expert systems development N89-10079
An expert system approach to astronomical data analysis N89-10080
Expert systems tools for Hubble Space Telescope observation scheduling N89-10081
Toward an expert project management system N89-10082
A LISP-Ada connection N89-10085
Expert systems built by the Expert: An evaluation of OPS5 N89-10086
Open control/display system for a telerobotics work station N89-10089
Advanced data management design for autonomous telerobotic systems in space using spaceborne symbolic processors N89-10096
Heat exchanger expert system logic N89-10205
An expert system for VLSI layout N89-10528
Second Annual Knowledge-Based Software Assistant Conference
[AD-A189819] N89-10536
An overview of the knowledge-based requirements assistant N89-10538
Overview of the knowledge-based specification assistant N89-10539
Performance estimation for a knowledge-based software assistant N89-10540
Technology transfer and the knowledge-based software assistant N89-10541
Selection of investment strategies which are optimal for the implementation of software support environments N89-10542
KBSA common framework implementation N89-10543
Where's the intelligence in the intelligent assistant requirements analysis: Inference processes in the KBRA N89-10544
Plans and meta-plans in an intelligent assistant for the process of programming N89-10547
Technical issues for performance estimation N89-10548
Designing an effective user interface for a knowledge-based development environment N89-10549
Project management assistant: What have we learned N89-10552
Simplifying the construction of domain-specific automatic programming systems: The NASA automated software development workstation project N89-10553
ASDL: An intelligent acquisition support tool N89-10554
SPOCK: A tool for real time artificial intelligence
[NASA-TT-20357] N89-10574

Architecture studies and system demonstrations for optical parallel processor for Al and Ni
[AD-A195480] N89-10616
LOOK: Implementation of an expert system in information retrieval for database selection N89-10669
Object-oriented approach to integrating database semantics, volume 4
[AD-A195853] N89-10672

EXPLOSIONS
Gamma-ray observations of supernova SN 1987A
[INPE-4604-PRE/1327] N89-10680

EXPLOSIVES
Semiconductor Bridge (SCB): A new method for the ignition of explosives and pyrotechnics
[DE88-011246] N89-10151
Single crystal orientation effects in shock initiation of PETN explosive
[DE88-014406] N89-10182
Lightning protection for high explosives and instrumentation using a field mill system N89-10467

EXPONENTS
Generalized Lyapunov exponents in high-dimensional chaotic dynamics and products of large random matrices
[PREPRINT-595] N89-10600

EXTENSOMETERS
Laser interferometric dilatometer for low-expansion materials
[DE88-012329] N89-10272

EXTINCTION
An interactive program for estimating extinction and scattering properties of most particulate clouds
[MRL-R-1123] N89-10218

EXTRAVEHICULAR ACTIVITY
Robot hands and extravehicular activity N89-10097

EXTREMELY HIGH FREQUENCIES
X/X/Ka-band prime focus feed antenna for the Mars Observer beacon spacecraft N89-10195

F

F REGION
Dynamics Explorer guest investigator
[NASA-CR-183163] N89-10417

F-16 AIRCRAFT
Israel Air Force (IAF) in-service aircraft lightning strike and damage survey N89-10431

FABRICATION
Fabrication and test of a carbon-carbon composite combustion chamber for a low thrust storable engine
[NAL-TR-946] N89-10118
Evaluation and control of residual states in curved, composite panels
[DE88-012103] N89-10126
Deformations and residual stresses induced in channel section columns by presetting and welding
[PB88-199971] N89-10292
The tensile strength of glass shells
[DE88-013011] N89-10301
Hydrogen-bromine fuel cell advance component development
[NASA-TM-101345] N89-10405
Electronic structure of electrodeposited thin film CdTe solar cells
[DE88-001170] N89-10406
Advanced planar array development for space station
[NASA-CR-179372] N89-10407
Development of radiation hardened far IR detector arrays. Volume 1: Phase 2
[BF-R-65.641-2] N89-10623
Development of radiation hardened far IR detector arrays. Volume 2: Phase 3
[BF-R-65.641-3] N89-10624
Metallic materials as plasma facing components
[DE88-010103] N89-10628
Beam assisted fabrication of 3-5/Si monolithic devices
[AD-A195479] N89-10655

FABRICS
Standardization of the carbon-phenolic materials and processes. Vol. 2: Test methods and specifications
[NASA-CR-183227] N89-10033
Standardization of the carbon-phenolic materials and processes. Vol. 1: Experimental studies
[NASA-CR-183226] N89-10127

FACTOR ANALYSIS
Storage and computationally efficient permutations of factorized covariance and square-root information arrays N89-10206
An analysis of an implicit factored scheme for simulating shock waves
[AR-005-231] N89-10252
Factoring very large numbers using a massively parallel computer
[DE88-014247] N89-10559

FACULAE
Doppler imaging of AR Lacertae at three epochs N89-10740
C 4 fluxes from the sun as a star and the correlation with magnetic flux
[NASA-CR-183156] N89-10827

FAILURE ANALYSIS
Fatigue and assessment methods of blade vibration N89-10010
Expert system support for HST operations N89-10076
The tensile strength of glass shells
[DE88-013011] N89-10301
On the diagnostic emulation technique and its use in the AIRLAB
[NASA-TM-4027] N89-10524

FAILURE MODES
Selection of sensors for measurement and control
[DE88-012936] N89-10267

FANS
Fan flutter test N89-10014

FAR INFRARED RADIATION
Development of radiation hardened far IR detector arrays. Volume 1: Phase 2
[BF-R-65.641-2] N89-10623
Development of radiation hardened far IR detector arrays. Volume 2: Phase 3
[BF-R-65.641-3] N89-10624

FAR ULTRAVIOLET RADIATION
Beam assisted fabrication of 3-5/Si monolithic devices
[AD-A195479] N89-10655

FARADAY EFFECT
Optical sensors for the measurement of electric current and voltage
[PB88-208467] N89-10233

FARMLANDS
A theoretical model for interpreting remotely sensed thermal infrared measurements obtained over agricultural areas N89-10343
Discrimination of zones of high water erosion risk using SPOT images N89-10376

FATIGUE (MATERIALS)
Forced vibration and flutter design methodology N89-10016
Wheel performance evaluation. Phase 1: Analysis
[DOT/FAA/CT-88/16] N89-10041
A digital simulation method of cumulative fatigue damage evaluation for spacecraft components
[NAL-TR-957] N89-10113

FATIGUE LIFE
A compendium of sources of fracture toughness and fatigue crack growth data for metallic alloys, part 3
[NASA-TM-100675] N89-10165

FATIGUE TESTS
Flexural fatigue of a 2-D carbon/carbon composite material
[DE88-010501] N89-10133
A study of the fatigue behavior of small cracks in nickel-base superalloys
[AD-A195489] N89-10161

FAULT TOLERANCE
Proceedings of 1987 Goddard Conference on Space Applications of Artificial Intelligence (AI) and Robotics
[NASA-TM-89663] N89-10063
A local area computer network expert system framework N89-10074
FIESTA: An operational decision aid for space network fault isolation N89-10075
A hierarchically distributed architecture for fault isolation expert systems on the space station N89-10077
Heat exchanger expert system logic N89-10205
Infection and propagation analysis: A fault-based approach to estimating software reliability
[NASA-CR-183276] N89-10534
Theoretical insights into fault-based testing
[NASA-CR-183277] N89-10564
Fault tolerance computing: Constraints in using multiprocessor synchronization by static preplanned scheduling
[CNES-CT/DRT/TIT/TB-096] N89-10573

FEEDBACK
Consolidated fuel reprossing program: The implications of force reflection for teleoperation in space N89-10090

FEEDBACK CONTROL
Computer hardware and software for robotic control N89-10103
An automatic frequency control loop using overlapping DFTs (Discrete Fourier Transforms) N89-10204

FERROELECTRICITY
Deflection of light by using tungsten bronze crystals
[DE88-014151] N89-10618

FERROMAGNETISM
A comparative evaluation of RPD (Rotary Particle Depositor) and ferrographic diagnostic methods for turbine engine lubricant samples
[AD-A196207] N89-10044

FIBER COMPOSITES
Thermodynamic analysis of compatibility of several reinforcement materials with FeAl alloys
[NASA-CR-4172] N89-10128
Properties of silicon carbide fiber-reinforced silicon nitride matrix composites
[NASA-TM-101356] N89-10130
Leaf spring
[EP-PATENT-0-253-574-A1] N89-10136

FIBER OPTICS
High speed fiber optics local area networks: Design and implementation
[NASA-CR-182432] N89-10216
Multitier specification applied to modify the hardness of an essential NSEP (National Security/Emergency Preparedness) fiber optic link
[PB88-210778] N89-10220

FIBERS
Thermodynamic analysis of compatibility of several reinforcement materials with beta phase NiAl alloys
[NASA-CR-4171] N89-10131
Thermal effects on the mechanical properties of SiC fiber reinforced reaction bonded silicon nitride matrix (SiC/RBSN) composites
[NASA-TM-101348] N89-10134

FIBRIN
Modulation of human plasma fibronectin levels following exercise
[AD-A192674] N89-10519

FIELD EFFECT TRANSISTORS
Dynamic properties of power MOS transistors
[LAAS-88-162] N89-10236

FIELD EMISSION
Evaluation of the characteristics of a field emission cathode for use in a Mercury ion trap frequency standard N89-10193

FIELD INTENSITY METERS
An optical sensor for the non-interactive detection of weak electric fields N89-10263

FIELD THEORY (PHYSICS)
The inverse-square law and quantum gravity
[DE88-014332] N89-10663

FIGHTER AIRCRAFT
Wave drag and high-speed performance of supersonic STOVL fighter configuration
[NASA-TM-100061] N89-10017

FILAMENT WINDING
Transfer impedance measurements of the space shuttle Solid Rocket Motor (SRM) joints, wire meshes and a carbon graphite motor case N89-10440

FILLERS
Laser welding of stainless steel weld filler metals at high cooling rates
[DE88-002345] N89-10281

FINANCE
Space commerce: An industry assessment
[PB88-214069] N89-10677

FINITE DIFFERENCE THEORY
On a surface mounted transmission line configuration for aperture testing N89-10458
Model results for a proposed tactical missile training site lightning protection system N89-10477
Finite difference analysis of external and internal lightning response of the JAS39 CFC wing N89-10483
The interaction between lightning grounding systems and buried cables N89-10496
Generation of a grid for a finite difference calculation of flows around an aircraft in Cartesian coordinates
[NAL-TR-956] N89-10563

FINITE ELEMENT METHOD
Basic structural dynamics N89-10007
Direct Numerical Simulations (DNS) of an unpremixed turbulent jet flame
[AD-A196128] N89-10149
Numerical analysis of laminar and turbulent incompressible flows using the finite element Fluid Dynamics Analysis Package (FIDAP)
[NASA-CR-179390] N89-10253
A finite element formulation for incompressible, conjugate, viscous/porous flow problems
[DE88-007113] N89-10254
Nonlinear finite element analysis for plastic deformation by local random yielding N89-10298
Applications of a three-dimensional finite element model to mountain-valley flows
[DE88-008898] N89-10412
Analysis of some low-order finite element schemes for Mindlin-Reissner and Kirchhoff plates
[PB87-175899] N89-10578

FIRE PREVENTION
Fire behavior and risk analysis in spacecraft
[NASA-TM-100944] N89-10111
FIRES
Final review of US Army fire-resistant fuel program
[AD-A194304] N89-10176
FLAME PROPAGATION
Investigation of the flame-acoustic wave interaction during axial solid rocket instabilities N89-10120
FLAME RETARDANTS
Thermal transfer recording media
[NASA-TT-20322] N89-10262
FLAME STABILITY
Investigation of the flame-acoustic wave interaction during axial solid rocket instabilities N89-10120
FLAMES
Direct Numerical Simulations (DNS) of an unpremixed turbulent jet flame
[AD-A196128] N89-10149
FLAMMABILITY
Thermal transfer recording media
[NASA-TT-20322] N89-10262
FLAPPING HINGES
Validation of a pair of computer codes for estimation and optimization of subsonic aerodynamic performance of simple hinged-flap systems for thin swept wings
[NASA-TP-2828] N89-10024
FLARE STARS
Transition regions of dM stars N89-10746
FLARED BODIES
Normal force coefficient of supersonic flows over conical flare, cone-cylinder and conical boattails
[NAL-TR-949] N89-10021
FLEXIBILITY
On motion planning and control of multi-link lightweight robotic manipulators N89-10285
FLEXIBLE BODIES
Dynamics and control of the orbiting grid structures and the synchronously deployable beam
[NASA-CR-183205] N89-10297
FLEXIBLE SPACECRAFT
Solution of two-point boundary value problems in optimal maneuvers of flexible vehicles N89-10114
FLEXING
Flexural fatigue of a 2-D carbon/carbon composite material
[DE88-010501] N89-10133
FLIGHT CONDITIONS
Aircraft accident reports, brief format, US civil and foreign aviation, issue number 10 of 1987 accidents
[PB88-916905] N89-10035
Aircraft accident reports, brief format, US civil and foreign aviation, issue number 12 of 1986 accidents
[PB88-916903] N89-10036
FLIGHT CONTROL
Functional mock-up tests of the flight control system of the NAL QSTOL research aircraft: Planning and mechanical system test
[NAL-TR-944] N89-10047
Quadruplex digital flight control system assessment
[NASA-CR-182741] N89-10058
FLIGHT INSTRUMENTS
International Aerospace and Ground Conference on Lightning and Static Electricity
[PB88-197439] N89-10429
FLIGHT TESTS
Design and evaluation of dynamic flight test manoeuveres
[PB88-210760] N89-10042
FLORIDA
Spatial distribution of lightning strikes to ground during small thunderstorms in Florida N89-10472
FLOW DISTRIBUTION
Estimation of up-wash distribution around an automobile by three-dimensional smoke wind tunnel test
[NAL-TR-921] N89-10023
Modification of the unsteady flow field predicted by transonic small distrubance equations using a Navier-Stokes solution of the steady flow field N89-10241
Flowfield visualization for SSME hot gas manifold
[NASA-CR-179403] N89-10243
Steady flow field measurements using laser Doppler velocimetry
[AD-A195228] N89-10245
Numerical study of the entrance flow and its transition in a curcular pipe
[ISAS-RN-626] N89-10250
Generation of a grid for a finite difference calculation of flows around an aircraft in Cartesian coordinates
[NAL-TR-956] N89-10563
The dynamics of the Venus ionosphere
[NASA-CR-183167] N89-10779
The direction of water transport on Mars: A possible pumping mechanism N89-10798
FLOW EQUATIONS
Direct Numerical Simulations (DNS) of an unpremixed turbulent jet flame
[AD-A196128] N89-10149
FLOW MEASUREMENT
Steady flow field measurements using laser Doppler velocimetry
[AD-A195228] N89-10245
Experimental detection of high speed fronts and clarification of their coherence with low speed streaks and streamwise vortices in a fully developed turbulent channel
[MPIS-MITT-88-1987] N89-10259
FLOW STABILITY
Experiments on the influence of the geometry on the stability of Taylor-Couette flow
[MPIS-MITT-87-1987] N89-10258
FLOW VELOCITY
Laser velocimeter measurements of solids in multiphase flow
[DE88-011611] N89-10251
FLOW VISUALIZATION
Flowfield visualization for SSME hot gas manifold
[NASA-CR-179403] N89-10243
Experimental detection of high speed fronts and clarification of their coherence with low speed streaks and streamwise vortices in a fully developed turbulent channel
[MPIS-MITT-88-1987] N89-10259
FLUID DYNAMICS
Discrete modeling considerations in multiphase fluid dynamics
[DE88-015188] N89-10256
Fluid dynamic issues in continuous wave short wavelength chemical lasers
[DE88-014428] N89-10274
The delineation and interpretation of the earth's gravity field
[NASA-CR-183283] N89-10416
Improving the accuracy of central difference schemes
[NASA-CR-181712] N89-10577
FLUID FLOW
Turbofan forced mixer lobe flow modeling. Part 3: Application to augment engines
[NASA-CR-4147] N89-10025
A comparative evaluation of RPD (Rotary Particle Depositor) and ferrographic diagnostic methods for turbine engine lubricant samples
[AD-A196207] N89-10044
An improved interface for capillary zone electrophoresis-mass spectrometry
[DE88-014079] N89-10148
Vibrational relaxation processes in CO2-N2-H2O laser systems
[AD-A196211] N89-10273
FLUID MECHANICS
A finite element formulation for incompressible, conjugate, viscous/porous flow problems
[DE88-007113] N89-10254
Fluid dynamic issues in continuous wave short wavelength chemical lasers
[DE88-014428] N89-10274
Dynamic interpretation of geoid anomalies
[NASA-CR-183164] N89-10304
FLUORESCENCE
The fluorescence line imager: High-resolution imaging spectroscopy over water and land N89-10353
Fluorescence processes and line identifications in the UV spectra of cool stars N89-10753
Identification of new fluorescence processes in the UV spectra of cool stars from new energy levels of Fe II and Cr II N89-10755
FLUTTER
AGARD manual on aeroelasticity in axial-flow turbomachines. Volume 2: Structural dynamics and aeroelasticity
[AGARD-AG-298-VOL-2] N89-10006
Fan flutter test N89-10014
Aeroelastic thermal effects N89-10015
Forced vibration and flutter design methodology N89-10016
FLUTTER ANALYSIS
Vibration, performance, flutter and forced response characteristics of a large-scale propfan and its aeroelastic model
[NASA-TM-101322] N89-10043
FLUX (RATE)
On the flux-period and flux-flux correlations in late type stars N89-10737
FOCUSING
An ion-optical bench for testing ion source lenses
[DE88-013186] N89-10606
Analysis of methods for detecting focus error in optical data storage systems N89-10617
FORCE DISTRIBUTION
Normal force coefficient of supersonic flows over conical flare, cone-cylinder and conical boattails
[NAL-TR-949] N89-10021
An investigation into force-moment calibration techniques applicable to a magnetic suspension and balance system
[NASA-CR-181695] N89-10061
FORCED VIBRATION
AGARD manual on aeroelasticity in axial-flow turbomachines. Volume 2: Structural dynamics and aeroelasticity
[AGARD-AG-298-VOL-2] N89-10006
Structural dynamic characteristics of individual blades N89-10008
Fatigue and assessment methods of blade vibration N89-10010
Aeroelastic coupling: An elementary approach N89-10012
Forced vibration and flutter design methodology N89-10016
Vibration, performance, flutter and forced response characteristics of a large-scale propfan and its aeroelastic model
[NASA-TM-101322] N89-10043
FORESTS
Spectral characterization of forest targets in mountainous zones on Thematic Mapper images N89-10328
Stress detection in mixed coniferous-broadleaved forests from Airborne Imaging Spectrometer (AIS) data N89-10355
Optimization for classification of forest damage classes N89-10359
Texture analysis in forest areas: High spectral resolution synthetic aperture radar data N89-10367
Use of remote sensing for land use policy formulation
[NASA-CR-183148] N89-10395
Identifying the reforested areas utilizing the SPOT satellite data
[INPE-4624-PRE/1343] N89-10396
Nation-wide forest mapping and timber volume estimation using LANDSAT-5 TM imagery
[INPE-4643-PRE/1354] N89-10402
FORMULAS (MATHEMATICS)
Interactive editing of mathematical formulae
[PB88-203005] N89-10580
FORTRAN
Programming techniques for high-speed processing on the supercomputer FUJITSU VP-system
[NAL-TR-915] N89-10565
FOUNDATIONS
Application of microgravity to the assessment of existing structures and structural foundations
[AD-A195599] N89-10418
FOURIER TRANSFORMATION
An automatic frequency control loop using overlapping DFTs (Discrete Fourier Transforms) N89-10204
Fourier transform infrared spectrometry of ambient aerosols
[PB88-213236] N89-10414
FRACTURE STRENGTH
Fracture criteria for discontinuously reinforced metal matrix composites
[NASA-CR-181175] N89-10125
Characterization of dynamic fracture in copper under uniaxial stress and uniaxial strain
[DE88-007824] N89-10162
A compendium of sources of fracture toughness and fatigue crack growth data for metallic alloys, part 3
[NASA-TM-100675] N89-10165
FRACTURING
Micromechanisms of deformation and fracture in ordered intermetallic alloys. 1: Strengthening mechanisms
[DE88-015382] N89-10159
FRAGMENTATION
Multiple nucleon knockout by Coulomb dissociation in relativistic heavy-ion collisions
[NASA-TM-4070] N89-10612
FRANCK-CONDON PRINCIPLE
The lowest ionization potentials of Al2
[NASA-TM-101171] N89-10605
FREDHOLM EQUATIONS
Block Toeplitz operators with rational symbols
[PB88-202890] N89-10587
FREE ELECTRON LASERS
A transition radiation experiment to measure the electron beam modulation induced by the free electron laser: A design study
[AD-A195169] N89-10275
Research on a two-stage free electron laser oscillator
[AD-A195339] N89-10278
Recent results from the Los Alamos free-electron laser
[DE88-014409] N89-10279

Directed energy concepts for strategic defense [DE88-015050] N89-10596

FRENCH SPACE PROGRAMS
The French space program for Earth observation N89-10392

FREQUENCIES
A filamentary method for calculating induced voltages within resistive structures in either the frequency or time domain N89-10484

FREQUENCY DISCRIMINATORS
An automatic frequency control loop using overlapping DFTs (Discrete Fourier Transforms) N89-10204

FREQUENCY MODULATION
Effects of modulated electron beams and cavities on reditrons [DE88-014317] N89-10234

FREQUENCY STABILITY
Evaluation of the characteristics of a field emission cathode for use in a Mercury ion trap frequency standard N89-10193

FREQUENCY STANDARDS
Evaluation of the characteristics of a field emission cathode for use in a Mercury ion trap frequency standard N89-10193

FREQUENCY SYNCHRONIZATION
Node synchronization of viterbi decoders using state metrics N89-10202

FRICTION
Development of a theory of wear of ceramics [DE88-015327] N89-10170

FRICTION FACTOR
A three degree-of-freedom description of the ocean surface for microwave remote sensing of wave height and wind friction velocity N89-10314

FROST
Spectral signature of citrus fruits and its evolution: Identification of the vegetative index of least temporal variation N89-10373
Chemical frost weathering of olivine: Experimental study and implications N89-10793
Influence of polar-cap albedo on past and current Martian climate N89-10801

FUEL COMBUSTION
Basic research on natural gas combustion phenomena-catalytic combustion [PB88-214606] N89-10142

FUEL INJECTION
Turbofan forced mixer lobe flow modeling. Part 3: Application to augment engines [NASA-CR-4147] N89-10025

FUEL OILS
Lightning protection for high explosives and instrumentation using a field mill system N89-10467

FUEL SYSTEMS
Final review of US Army fire-resistant fuel program [AD-A194304] N89-10176

FUEL TANKS
Factors influencing the detection of voltage sparks by flammable gas and optical techniques N89-10465

FUNCTIONAL DESIGN SPECIFICATIONS
Spatial resolution requirements for MODIS-N --- Polar Platform Moderate Resolution Imaging Spectrometer (MODIS) N89-10364

FUNCTIONS (MATHEMATICS)
Space-efficient queue management using fixed-connection networks [AD-A195167] N89-10569

FUSELAGES
Indirect effects on electronic and mechanical systems installed in carbon fibre compound aircraft structures N89-10492

FUSION REACTORS
Metallic materials as plasma facing components [DE88-010103] N89-10628
The study of hydromagnetic waves and RF heating using the TORTUS tokamak and the development of diagnostic techniques N89-10635

G

GALERKIN METHOD
Discretization formulas for unstructured grids [NASA-TM-101298] N89-10242

GALLIUM
Validity of the classification of UV gallium stars N89-10767

GALLIUM ARSENIDES
Thermodynamics and kinetics of phase formation of thin-film metal on gallium arsenide [DE88-015702] N89-10648

GAMMA RAYS
Gamma-ray observations of supernova SN 1987A [INPE-4604-PRE/1327] N89-10680

GAPS
The effect of a gap nonlinearity on recursive parameter identification algorithms [AD-A196020] N89-10557

GAS IONIZATION
Superionized plasmas in Algol binaries N89-10723

GAS MIXTURES
Factors influencing the detection of voltage sparks by flammable gas and optical techniques N89-10465

GAS STREAMS
Matter streams in semi-detached binary systems N89-10720

GASEOUS DIFFUSION
Turbulent diffusion of ocean bubbles [PB88-212816] N89-10513

GEAR TEETH
Generation of a crowned pinion tooth surface by a surface of revolution [NASA-TM-100260] N89-10282

GEARS
Generation of a crowned pinion tooth surface by a plane [NASA-TM-100259] N89-10283

GENERAL AVIATION AIRCRAFT
Alternate fuels for General Aviation aircraft with spark ignition engines [DOT/FAA/CT-88/05] N89-10179

GEOCENTRIC COORDINATES
Compilation of methods in orbital mechanics and solar geometry [NASA-RP-1204] N89-10420

GEODESY
Solid earth mission study. Volume 2: Technical report [ESA-CR(P)-2626-VOL-2] N89-10303
Solid Earth mission study. Volume 1: Executive summary [ESA-CR(P)-2626-VOL-1] N89-10397
Solid earth mission study. Volume 3: Program planning report [ESA-CR(P)-2626-VOL-3] N89-10399

GEODYNAMICS
Solid earth mission study. Volume 2: Technical report [ESA-CR(P)-2626-VOL-2] N89-10303
Solid Earth mission study. Volume 1: Executive summary [ESA-CR(P)-2626-VOL-1] N89-10397
Solid earth mission study. Volume 3: Program planning report [ESA-CR(P)-2626-VOL-3] N89-10399
Earth rotation and core topography [NASA-CR-183186] N89-10425

GEOGRAPHIC INFORMATION SYSTEMS
A general data model for geographic information systems [INPE-4560-PRE/1301] N89-10676

GEOGRAPHY
Climate of San Francisco, revised [PB88-208624] N89-10504

GEOIDS
Dynamic interpretation of geoid anomalies [NASA-CR-183164] N89-10304

GEOLOGICAL FAULTS
The use of MOMS-1 data for geological mapping of the Aswa lineament (East African rift) N89-10382
Martian tectonics: A review N89-10815

GEOLOGICAL SURVEYS
Evaluation of VARAN data in geology and geomorphology in the southeast of France N89-10313
Usefulness of high spectral resolution radiometry for geological mapping in the Mediterranean region N89-10360
The results of the Geosat MOMS subcommittee's data evaluation: Performance and applicability of the MOMS-1 sensor for exploration geology N89-10380
The use of MOMS-1 data for geological mapping of the Aswa lineament (East African rift) N89-10382
MOMS-1 data for bathymetric and geological studies N89-10383
MOMS-1 used synergistically with LANDSAT TM N89-10384
Comparative geological evolution of different remote sensing data of the Hoggar Mountains (Algeria) N89-10385

GEOMAGNETISM
Solid earth mission study. Volume 2: Technical report [ESA-CR(P)-2626-VOL-2] N89-10303
Solid Earth mission study. Volume 1: Executive summary [ESA-CR(P)-2626-VOL-1] N89-10397
Solid earth mission study. Volume 3: Program planning report [ESA-CR(P)-2626-VOL-3] N89-10399

GEOMETRICAL THEORY OF DIFFRACTION
Theoretical and experimental analysis of quadrifilar antennas for the first Brazilian satellite [INPE-4581-PRE/1315] N89-10221

GEOMETRY
Geometric imperfections in plated structures subject to interaction between buckling modes [PB88-200902] N89-10296

GEOMORPHOLOGY
Evaluation of VARAN data in geology and geomorphology in the southeast of France N89-10313
Sapping features of the Colorado Plateau: A comparative planetary geology field guide [NASA-SP-491] N89-10401
Mars: A water-rich planet N89-10784
Martian volcanism: A review N89-10785
Mars: Crustal pore volume, cryospheric depth, and the global occurrence of groundwater N89-10787
Ice or liquid water in the Martian regolith. Morphologic indicators from rampart craters N89-10806
Geomorphic evidence for ancient seas on Mars N89-10813
Crater ejecta morphology and the presence of water on Mars N89-10818

GEOPHYSICS
Dynamic interpretation of geoid anomalies [NASA-CR-183164] N89-10304
Wilson cycle studies [NASA-CR-183146] N89-10419
Measurement of vertical velocity using clear-air Doppler radars [AD-A195344] N89-10427
Solar-geophysical data number 524, April 1988. Part 2: (Prompt reports). Data for October 1987 and miscellanea [PB88-217401] N89-10828
Solar-geophysical data number 524, April 1988. Part 1: (Prompt reports). Data for March, February 1988 and late data [PB88-217393] N89-10829

GEOPOTENTIAL
Solid earth mission study. Volume 2: Technical report [ESA-CR(P)-2626-VOL-2] N89-10303
Solid Earth mission study. Volume 1: Executive summary [ESA-CR(P)-2626-VOL-1] N89-10397
Solid earth mission study. Volume 3: Program planning report [ESA-CR(P)-2626-VOL-3] N89-10399

GEOTEMPERATURE
Strengths and shortcomings in Airborne Thematic Mapper (ATM) technology as applied to volcanic and geothermal areas in Iceland N89-10337

GIANT STARS
Spectral images of HD 199178 N89-10739
Lithium and chromospherically active single giants N89-10749
Carbon and nitrogen abundance determinations from transition layer lines --- giant stars N89-10760

GIBBS PHENOMENON
An adaptive pseudospectral method for discontinuous problems [NASA-CR-181717] N89-10583

GIOTTO MISSION
Image processing document: Halley multicolor camera (Giotto Mission) [DFVLR-FB-88-20] N89-10270

GLACIERS
Ablation of Martian glaciers N89-10805

GLACIOLOGY
Data report for the Siple Coast (Antarctica) project [NASA-TM-100708] N89-10403
Evidence for glaciation in Elysium N89-10781

GLASS FIBERS
Optical sensors for the measurement of electric current and voltage [PB88-208467] N89-10233

GLOBAL POSITIONING SYSTEM
Precise orbit determination for NASA's earth observing system using GPS (Global Positioning System) N89-10188

GLOW DISCHARGES
Multiphoton ionization of transient species in supersonic jets [DE88-008366] N89-10607

GOALS
Civil Space Technology Initiative: A first step [NASA-TM-100949] N89-10665

GOLD
Au II in IUE spectra of chemically peculiar stars N89-10766

GRAIN BOUNDARIES
Theoretical studies of grain boundaries in Ni, Al and Ni3Al with and without boron [DE88-014323] N89-10152
Structure of grain boundaries in iron [DE88-014412] N89-10154
Quasiperiodic ordering in grain boundaries [DE88-012199] N89-10647

GRAIN SIZE
Comparison between active and passive microwave measurements over Antarctica N89-10316
GRAMMARS
UNITRAN (universal translator): A principle-based approach to machine translation
[AD-A195281] N89-10675
GRAPHITE
Transfer impedance measurements of the space shuttle Solid Rocket Motor (SRM) joints, wire meshes and a carbon graphite motor case N89-10440
GRASSLANDS
Relationships between spectral reflectance and phytomass of the ground layer community of neotropical savanna (CERRADO)
[INPE-4635-PRE/1347] N89-10302
The Transformed Vegetation Index (TVI) for estimation of Brazilian cerrado's phytomass
[INPE-4603-PRE/1326] N89-10400
GRAVITATION THEORY
The inverse-square law and quantum gravity
[DE88-014332] N89-10663
GRAVITATIONAL FIELDS
The delineation and interpretation of the earth's gravity field
[NASA-CR-183283] N89-10416
Gravitational time delay due to a spinning string
[DE88-014733] N89-10661
GRAVITATIONAL WAVES
Gravitational wave searches using the DSN (Deep Space Network) N89-10192
GRAVITY WAVES
Measurement of vertical velocity using clear-air Doppler radars
[AD-A195344] N89-10427
GREENHOUSE EFFECT
High resolution infrared spectroscopy of carbon dioxide and nitrous oxide at elevated temperatures
[AD-A196317] N89-10146
GREGORIAN ANTENNAS
Relative planetary radar sensitivities: Arecibo and Goldstone N89-10209
GRINDING (COMMINUTION)
Metastable alloy phases prepared by solid state reactions and ball milling
[DE88-009156] N89-10163
GROUND CREWS
Measurement of the electrostatic charging on large helicopters and control of the shock hazard N89-10461
GROUND SUPPORT EQUIPMENT
Maintaining an expert system for the Hubble Space Telescope ground support N89-10064
Lightning standards for protection of ground electronic systems N89-10473
GROUND SUPPORT SYSTEMS
Summary of DSN (Deep Space Network) reimbursable launch support N89-10211
GROUND TRUTH
The Transformed Vegetation Index (TVI) for estimation of Brazilian cerrado's phytomass
[INPE-4603-PRE/1326] N89-10400
GROUND WATER
Sapping features of the Colorado Plateau: A comparative planetary geology field guide
[NASA-SP-491] N89-10401
Mars: Crustal pore volume, cryospheric depth, and the global occurrence of groundwater N89-10787
Water and ice on Mars: Evidence from Valles Marineris N89-10803
Formation of the layered deposits in the Valles Marineris, Mars N89-10809
The thermal properties of Martian surface materials at high latitudes: Possible evidence for permafrost N89-10812
Geomorphic evidence for ancient seas on Mars N89-10813
GROWTH
Initial evolution of nonlinear magnetic islands in high temperature plasmas
[DE88-012346] N89-10636
GUN PROPELLANTS
HAN (hydroxylammonium nitrate density)-based liquid gun propellants: Physical properties
[AD-A195246] N89-10180
GUNS (ORDNANCE)
HAN (hydroxylammonium nitrate density)-based liquid gun propellants: Physical properties
[AD-A195246] N89-10180

H

H LINES
Jovian equatorial H2 emission from 1979-1987 N89-10693
H-53 HELICOPTER
Measurement of the electrostatic charging on large helicopters and control of the shock hazard N89-10461
HALF SPACES
Abstract, topological and uniform convex structures
[PB88-202965] N89-10579
HALLEY'S COMET
Image processing document: Halley multicolor camera (Giotto Mission)
[DFVLR-FB-88-20] N89-10270
HANDBOOKS
Interplanetary medium data book: Supplement 3A, 1977-1985
[NASA-TM-89630] N89-10678
HANG GLIDERS
Measurement of aerodynamic characteristics of a hang-glider-wing by ground run tests using a test vehicle
[NAL-TR-953] N89-10004
HARDENING (SYSTEMS)
Multitier specification applied to modify the hardness of an essential NSEP (National Security/Emergency Preparedness) fiber optic link
[PB88-210778] N89-10220
HARMONICS
Space-harmonic analysis of multi-depth corrugated waveguides
[PB88-210059] N89-10214
HARNESSES
Lightning tests to measure the bulk current levels associated with the electronic engine control of a turboprop commuter transport N89-10457
HAZARDS
Measurement of the electrostatic charging on large helicopters and control of the shock hazard N89-10461
Implications of a recent lightning strike to a NASA jet trainer N89-10478
HEAT EXCHANGERS
Heat exchanger expert system logic N89-10205
Overview of ground coupled heat pump research and technology transfer activities
[DE88-012938] N89-10255
Laboratory capacity modulation experiments, analyses and validation
[DE88-012930] N89-10408
HEAT PUMPS
Solution of ill-posed problems by means of truncated SVD (Singular Value Decomposition)
[DE88-013510] N89-10238
An analytical study of hybrid ejector/internal combustion engine-driven heat pumps
[DE88-013242] N89-10240
Development and proof-testing of advanced absorption refrigeration cycle concepts, phase 2
[DE88-013239] N89-10247
Computer simulation of absorption heat pump using aqueous lithium bromide and ternary nitrate mixtures
[DE88-013353] N89-10249
Overview of ground coupled heat pump research and technology transfer activities
[DE88-012938] N89-10255
Free-piston Stirling engine development
[PB88-220025] N89-10286
Laboratory capacity modulation experiments, analyses and validation
[DE88-012930] N89-10408
HEAT RADIATORS
The solar dynamic radiator with a historical perspective
[NASA-TM-100972] N89-10117
HEAT RESISTANT ALLOYS
Life time prediction: Synthesis on ONERA's research in viscoplasticity and continuous damage mechanics, applied to engine materials and structures N89-10011
Applications of process modelling to heat treatment of superalloys
[DE88-015445] N89-10157
A study of the fatigue behavior of small cracks in nickel-base superalloys
[AD-A195489] N89-10161
HEAT TRANSFER
Development and proof-testing of advanced absorption refrigeration cycle concepts, phase 2
[DE88-013239] N89-10247
Computer simulation of absorption heat pump using aqueous lithium bromide and ternary nitrate mixtures
[DE88-013353] N89-10249
Thermal transfer recording media
[NASA-TT-20322] N89-10262
HEAT TRANSFER COEFFICIENTS
High-resolution heat-transfer-coefficient maps applicable to compound-curve surfaces using liquid crystals in a transient wind tunnel
[NASA-TM-89855] N89-10246
HEAT TREATMENT
Applications of process modelling to heat treatment of superalloys
[DE88-015445] N89-10157
HEATING
Confinement and heating of high beta plasmas with emphasis on compact toroids
[DE88-015777] N89-10645
HEAVY IONS
Use of the time projection chamber for measuring heavy ion collisions
[MPE-PAE/EXP-EL-191] N89-10611
Multiple nucleon knockout by Coulomb dissociation in relativistic heavy-ion collisions
[NASA-TM-4070] N89-10612
HEIGHT
Measurements of the velocity change of a lightning return stroke with height N89-10442
HELICOPTER DESIGN
Helicopter roll control effectiveness criteria program summary
[NASA-CR-177477] N89-10046
HELICOPTERS
Development in helicopter tail boom strake applications in the US
[NASA-TM-101496] N89-10059
Lightning tests on an all-composite helicopter N89-10452
Electrification of hovering helicopters N89-10460
On the appropriateness of applying chi-square distribution based confidence intervals to spectral estimates of helicopter flyover data
[NASA-CR-181692] N89-10601
HELIUM
The discovery of a co-rotating magnetosphere in a helium weak star: HD5737 = alpha Sci N89-10751
HEMATOPOIETIC SYSTEM
Modulation of human plasma fibronectin levels following exercise
[AD-A192674] N89-10519
HEMOGLOBIN
Pressure studies of protein dynamics
[AD-A192386] N89-10523
HIERARCHIES
A hierarchically distributed architecture for fault isolation expert systems on the space station N89-10077
Maintaining consistency between planning hierarchies: Techniques and applications N89-10084
NASREN: Standard reference model for telerobot control N89-10099
HIGH ELECTRON MOBILITY TRANSISTORS
An 8.4-GHz cryogenically cooled HEMT amplifier for DSS 13 N89-10199
HIGH FREQUENCIES
Evaluation of hardware architectures for HF antenna arrays
[AD-A196204] N89-10217
HIGH PRESSURE
Performance of multimirror quartzline lamps in a high-pressure, underwater environment
[NASA-TM-101374] N89-10269
HIGH RESOLUTION
High-resolution heat-transfer-coefficient maps applicable to compound-curve surfaces using liquid crystals in a transient wind tunnel
[NASA-TM-89855] N89-10246
Use of high spectral resolution to follow the state of vegetation canopies N89-10354
High spectral resolution indices for monitoring crop growth and chlorosis N89-10358
Usefulness of high spectral resolution radiometry for geological mapping in the Mediterranean region N89-10360
High resolution radiometric measurement of intertidal microphytobenthos N89-10365
On high resolution schemes for three-dimensional Euler equations
[NAL-TR-950T] N89-10581
HIGH SPEED
High speed fiber optics local area networks: Design and implementation
[NASA-CR-182432] N89-10216
HIGH STRENGTH STEELS
Structure of grain boundaries in iron
[DE88-014412] N89-10154
HIGH TEMPERATURE
Solution of ill-posed problems by means of truncated SVD (Singular Value Decomposition)
[DE88-013510] N89-10238
HIGH TEMPERATURE GASES
High resolution infrared spectroscopy of carbon dioxide and nitrous oxide at elevated temperatures
[AD-A196317] N89-10146
Flowfield visualization for SSME hot gas manifold
[NASA-CR-179403] N89-10243

HIGH TEMPERATURE PLASMAS
Gas-contact cooling for VUV laser oscillation in recombining plasmas
[IPPJ-881] N89-10631
Initial evolution of nonlinear magnetic islands in high temperature plasmas
[DE88-012346] N89-10636
HIGH TEMPERATURE SUPERCONDUCTORS
Synthesis and study of materials for superconducting electronics
[AD-A195279] N89-10649
HIGH VOLTAGES
Single-pole switching schemes for EHV transmission systems N89-10228
HOMING
Comparison of statistical digital simulation methods N89-10049
A generic seeker simulation for the evaluation of active RF guidance systems N89-10050
Cost effective simulation for millimeter wave guidance systems N89-10053
HOMOGENEOUS TURBULENCE
Direct Numerical Simulations (DNS) of an unpremixed turbulent jet flame
[AD-A196128] N89-10149
HOMOMORPHISMS
Real algebraic morphisms with values in the unit circle
[PB88-206921] N89-10515
HOT SURFACES
The angular reflectance signature of the canopy hot spot in the optical regime N89-10325
HOT-FILM ANEMOMETERS
Experimental detection of high speed fronts and clarification of their coherence with low speed streaks and streamwise vortices in a fully developed turbulent channel
[MPIS-MITT-88-1987] N89-10259
HOT-WIRE ANEMOMETERS
The pros and cons of code validation
[NASA-TM-100657] N89-10034
HOUSINGS
T55-L-712 turbine engine compressor housing refurbishment-plasma spray project
[NASA-TM-101310] N89-10156
HOVERING
Measurement of the electrostatic charging on large helicopters and control of the shock hazard N89-10461
HUBBLE SPACE TELESCOPE
Expert system support for HST operations N89-10076
Expert systems tools for Hubble Space Telescope observation scheduling N89-10081
HUMAN FACTORS ENGINEERING
Using full-mission simulation for human factors research in air transport operations
[NASA-TM-88330] N89-10037
HUMAN PERFORMANCE
Performance assessment register
[AGARD-R-763] N89-10666
HYBRID PROPELLANT ROCKET ENGINES
An analytical study of hybrid ejector/internal combustion engine-driven heat pumps
[DE88-013242] N89-10240
HYDROCARBONS
Thermodynamic properties by non-calorimetric methods: Progress report
[DE88-015422] N89-10660
HYDROGEN
Rechargeable metal hydrides for spacecraft application
[NASA-TM-4076] N89-10184
Hydrogen sorption studies of materials used in Li(Si)/FeS2 thermal batteries
[DE88-013154] N89-10231
Large time scale variation in hydrogen emission from Jupiter and Saturn N89-10694
HYDROGEN FUELS
Technology issues associated with fueling the national aerospace plane with slush hydrogen
[NASA-TM-101386] N89-10123
Choice of coating and surface behavior of the hydrogen turbopump of the Vulcain engine
[ETN-88-93084] N89-10173
HYDROGEN OXYGEN ENGINES
Orbit transfer rocket engine technology program. Phase 2: Advanced engine study
[NASA-CR-179602] N89-10119
HYDROGEN OXYGEN FUEL CELLS
Hydrogen-bromine fuel cell advance component development
[NASA-TM-101345] N89-10405
Oxygen electrode bifunctional electrocatalyst NiCo2O4 spinel
[NASA-TM-100947] N89-10409
HYDROGEN PRODUCTION
Hydrogen supply over long distances using chemicals description and evaluation of a technical system
[DE88-012630] N89-10178
Methods of extracting hydrogen from lunar soil
[NASA-CR-180465] N89-10826
HYDROGENATION
Hydrogen supply over long distances using chemicals description and evaluation of a technical system
[DE88-012630] N89-10178
HYDROLOGICAL CYCLE
The direction of water transport on Mars: A possible pumping mechanism N89-10798
HYDROLOGY
Aircraft remote sensing in HAPEX --- hydrology N89-10388
HYDROMETEOROLOGY
Electromagnetic radiations generated by microdischarges from hydrometeors N89-10448
HYDROXYL COMPOUNDS
HAN (hydroxylammonium nitrate density)-based liquid gun propellants: Physical properties
[AD-A195246] N89-10180
HYDROXYL RADICALS
La Recherche Aerospatiale, Bimonthly Bulletin, number 1987-5, 240/September-October
[ESA-TT-1095] N89-10422
HYPERBOLIC FUNCTIONS
Non-oscillatory central differencing for hyperbolic conservation laws
[NASA-CR-181709] N89-10582
HYPERCUBE MULTIPROCESSORS
Concurrent algorithms for numerical computation on hypercube computer
[AD-A195502] N89-10558

I

ICE
Calculation of the effects of ice on the backscatter of a ground plane
[NASA-CR-183303] N89-10213
Intracloud lightning as a precursor to thunderstorm microbursts N89-10490
Water and ice on Mars: Evidence from Valles Marineris N89-10803
Could icy impacts reconcile Venus with Earth and Mars N89-10810
Seismic exploration for water on Mars N89-10811
ICE REPORTING
Satellite surveillance of ice and snow covered surfaces in the French Alps using visible and near infrared reflectance measurements from the SPOT and LANDSAT Thematic Mapper sensors N89-10372
IGNEOUS ROCKS
The basis for the spectral behaviour of silicates in the thermal infrared and applications to remote sensing N89-10366
IMAGE ANALYSIS
Multispectral characterization of the spatial structure of remotely sensed scenes N89-10340
A study of the vegetation cover with AVHRR during HAPEX-MOBILHY N89-10389
IMAGE PROCESSING
Comparison of mechanical and electronic high-speed recording systems
[DE88-015264] N89-10268
Image processing document: Halley multicolor camera (Giotto Mission)
[DFVLR-FB-88-20] N89-10270
Analysis of directional effects on NOAA AVHRR N89-10341
Applications of LANDSAT (TM and MSS) data for an estimation of rangeland conditions in semiarid and arid areas of northern Kenya
[DFVLR-FB-88-18] N89-10404
The Remote Atmospheric Probing Information Display (RAPID) system
[AD-A196314] N89-10500
Segmentation of noisy images using nonstationary Markov fields
[AD-A195229] N89-10527
A general data model for geographic information systems
[INPE-4560-PRE/1301] N89-10676
IMAGE RESOLUTION
Study on representation of surface coverage by imaging experiments
[ESA-CR(P)-2584] N89-10394
IMAGE TRANSDUCERS
La Recherche Aerospatiale, Bimonthly Bulletin, Number 1987-4, 239/July-August
[ESA-TT-1088] N89-10026
IMAGES
La Recherche Aerospatiale, Bimonthly Bulletin, number 1987-5, 240/September-October
[ESA-TT-1095] N89-10422
IMAGING SPECTROMETERS
Compact imaging spectrometer for induced emissions
[NASA-CR-183187] N89-10264
IMAGING TECHNIQUES
The fluorescence line imager: High-resolution imaging spectroscopy over water and land N89-10353
Optical imaging through atmospheric turbulence N89-10423
Satellite image registration through structural matching
[INPE-4563-PRE/1304] N89-10530
IMPACT
Evaluating impacts of pollutants from the atmosphere
[DE88-014550] N89-10415
IMPACT DAMAGE
Could icy impacts reconcile Venus with Earth and Mars N89-10810
IMPEDANCE MEASUREMENT
Transfer impedance measurements of the space shuttle Solid Rocket Motor (SRM) joints, wire meshes and a carbon graphite motor case N89-10440
INCOMPRESSIBLE FLOW
Numerical analysis of laminar and turbulent incompressible flows using the finite element Fluid Dynamics Analysis Package (FIDAP)
[NASA-CR-179390] N89-10253
A finite element formulation for incompressible, conjugate, viscous/porous flow problems
[DE88-007113] N89-10254
INDUSTRIES
Designing an effective user interface for a knowledge-based development environment N89-10549
Attitudes to the use of computerised information systems for production management in manufacturing industry: A survey
[TT-8706] N89-10670
INELASTIC COLLISIONS
Inelastic ion-surface collisions. Ion neutralization on intermetallic surfaces
[AD-A196322] N89-10608
INEQUALITIES
ORDMET3: An improved algorithm to find the maximum solution to a system of linear (in)Equalities
[PB88-208970] N89-10520
INERTIAL CONFINEMENT FUSION
Adventures in magnetohydrodynamics
[IPPJ-862] N89-10629
INFERENCE
Where's the intelligence in the intelligent assistant requirements analysis: Inference processes in the KBRA N89-10544
INFORMATION DISSEMINATION
Lightning information database N89-10432
INFORMATION FLOW
Very large parallel data flow
[AD-A196205] N89-10568
INFORMATION RETRIEVAL
Architecture studies and system demonstrations for optical parallel processor for AI and NI
[AD-A195480] N89-10616
An evaluation of online database selection by a gateway system with artificial intelligence techniques N89-10667
LOOK: Implementation of an expert system in information retrieval for database selection N89-10669
INFORMATION SYSTEMS
A LISP-Ada connection N89-10085
Use of remote sensing for land use policy formulation
[NASA-CR-183148] N89-10395
The Remote Atmospheric Probing Information Display (RAPID) system
[AD-A196314] N89-10500
Integrating distributed homogeneous and heterogeneous databases: Prototypes, volume 3
[AD-A195852] N89-10668
Attitudes to the use of computerised information systems for production management in manufacturing industry: A survey
[TT-8706] N89-10670
INFRARED ABSORPTION
Estimation of the interception efficiency of an alfalfa canopy from a vegetative index N89-10332
INFRARED ASTRONOMY SATELLITE
Ultraviolet properties of IRAS-selected Be stars N89-10765
INFRARED DETECTORS
Infrared temperature measurement with inherent consideration of emissivity
[DFVLR-FB-88-22] N89-10271
Development of radiation hardened far IR detector arrays. Volume 1: Phase 2
[BF-R-65.641-2] N89-10623

Development of radiation hardened far IR detector arrays. Volume 2: Phase 3
[BF-R-65.641-3] N89-10624

INFRARED IMAGERY
A new method for estimating regional evaporation from thermal infrared surface temperature measurements N89-10390

INFRARED RADIATION
Monitoring lightning activity in South Africa with a VLF single-station technique: Comparison with meteosat infrared data N89-10480

INFRARED RADIOMETERS
Airborne Visible/Infrared Imaging Spectrometer (AVIRIS): Inflight radiometric calibration and the determination of surface reflectance N89-10357
Rock and soil discrimination in natural tropical conditions using a spot-calibrated radiometer N89-10374

INFRARED SCANNERS
A narrow-band thermal imager based on multiline real-time averaging N89-10356
Emitted short wavelength infrared radiation for detection and monitoring of volcanic activity N89-10377
Aircraft remote sensing in HAPEX --- hydrology N89-10388

INFRARED SPECTRA
Complementary of microwave and optical range in the characterization of crops by remote sensing N89-10310
Attempt at absolute determination of spectral signatures of bare soils in the thermal infrared, in emission and reflection N89-10336
Atmospheric correction of thermal infrared data from LANDSAT-5 for surface temperature estimation N89-10339
A theoretical model for interpreting remotely sensed thermal infrared measurements obtained over agricultural areas N89-10343
The basis for the spectral behaviour of silicates in the thermal infrared and applications to remote sensing N89-10366
Thermodynamic properties by non-calorimetric methods: Progress report
[DE88-015422] N89-10660

INFRARED SPECTROMETERS
Thermal infrared laser spectroscopy: The potential of dual active/passive thermal infrared sensors for Earth observation N89-10345
Stress detection in mixed coniferous-broadleaved forests from Airborne Imaging Spectrometer (AIS) data N89-10355
Airborne Visible/Infrared Imaging Spectrometer (AVIRIS): Inflight radiometric calibration and the determination of surface reflectance N89-10357
Imaging spectrometry applied to the remote sensing of submerged seaweed N89-10361
Spatial resolution requirements for MODIS-N --- Polar Platform Moderate Resolution Imaging Spectrometer (MODIS) N89-10364

INFRARED SPECTROSCOPY
Characterization of rocks by visible and infrared high spectral resolution terrain spectroscopy N89-10362
Fourier transform infrared spectrometry of ambient aerosols
[PB88-213236] N89-10414

INJECTION
Pulse combustor modeling: One dimensional wave-dynamic model utilizing dynamic injection and energy release submodels
[DE88-005369] N89-10150

INJURIES
A review of medical aspects of lightning injury N89-10463
A retrospective study of the injuries sustained in telephone-mediated lightning strike N89-10464

INSERTION
Hardware fault insertion and instrumentation system: Experimentation and results
[NASA-CR-182746] N89-10526

INSTRUMENT COMPENSATION
Antenna pointing compensation based on precision optical measurement techniques N89-10197

INSTRUMENT ERRORS
Site errors of a magnetic direction finder for lightning flashes N89-10494

INSTRUMENTS
The mission operations planning assistant N89-10066

INTAKE SYSTEMS
Supersonic missile air intakes: Design and development criteria N89-10031

INTEGRAL EQUATIONS
Solution of ill-posed problems by means of truncated SVD (Singular Value Decomposition)
[DE88-013510] N89-10238
Electromagnetic coupling through composite materials N89-10479
Dimensional deformations of integrable systems: An approach to integrability in multidimensions, part 1
[PREPRINT-586] N89-10585

INTEGRATED CIRCUITS
The Radiation-Hardened Integrated Circuit (RHIC) Laboratory: Pursuit of Class 1
[DE88-006640] N89-10062
Integrated switching networks: A performance study N89-10567

INTELLIGENCE
Unmanned air vehicles - real time intelligence without the risk
[AD-A195199] N89-10039

INTERACTIONAL AERODYNAMICS
A transonic interactive boundary-layer theory for laminar and turbulent flow over swept wings
[NASA-CR-4185] N89-10029

INTERFACES
Electrospray ionization phenomena and the interface of capillary electrophoresis and mass spectrometry
[DE88-014080] N89-10143
An improved interface for capillary zone electrophoresis-mass spectrometry
[DE88-014079] N89-10148
Designing an effective user interface for a knowledge-based development environment N89-10549

INTERFEROMETERS
Design study for a remote laser wavelength sensor
[DE88-015417] N89-10265

INTERFEROMETRY
Laser interferometric dilatometer for low-expansion materials
[DE88-012329] N89-10272

INTERMETALLICS
Micromechanisms of deformation and fracture in ordered intermetallic alloys. 1: Strengthening mechanisms
[DE88-015382] N89-10159
Metastable alloy phases prepared by solid state reactions and ball milling
[DE88-009156] N89-10163
Engineering processing and properties of nickel aluminides
[DE88-011019] N89-10164

INTERNAL COMBUSTION ENGINES
Alternate fuels for General Aviation aircraft with spark ignition engines
[DOT/FAA/CT-88/05] N89-10179
An analytical study of hybrid ejector/internal combustion engine-driven heat pumps
[DE88-013242] N89-10240

INTERPLANETARY MAGNETIC FIELDS
Interplanetary medium data book. Supplement 3: 1977-1985
[NASA-TM-89660] N89-10772

INTERPLANETARY MEDIUM
Interplanetary medium data book: Supplement 3A, 1977-1985
[NASA-TM-89630] N89-10678
Interplanetary medium data book. Supplement 3: 1977-1985
[NASA-TM-89660] N89-10772

INTERPROCESSOR COMMUNICATION
Teleoperated position control of a PUMA robot N89-10104

INTERSTELLAR GAS
Global properties of molecular clouds and the interstellar medium in galaxies N89-10776

INTERSTELLAR MATTER
Ejecta in SN 1006: The knotty issue --- supernova remnant N89-10700
Supernova remnants' interactions with the inter-stellar medium N89-10771
Global properties of molecular clouds and the interstellar medium in galaxies N89-10776

INTERVALS
Bootstrap confidence intervals in a complex situation: A sequential paired clinical trial
[DE88-015338] N89-10592
On the appropriateness of applying chi-square distribution based confidence intervals to spectral estimates of helicopter flyover data
[NASA-CR-181692] N89-10601

INVESTMENT
Selection of investment strategies which are optimal for the implementation of software support environments N89-10542

IO
Io: IUE observations of its atmosphere and the plasma torus N89-10691

ION ACOUSTIC WAVES
Experimental studies on the surface confined quiescent plasma at INPE
[INPE-4605-PRE/1328] N89-10630
Marginal stability of ion-acoustic waves in a weakly collisional two-temperature plasma without a current
[AD-A195840] N89-10638

ION DENSITY (CONCENTRATION)
The dynamics of the Venus ionosphere
[NASA-CR-183167] N89-10779

ION IMPLANTATION
Characterization of layers created using surface modification techniques
[DE88-011918] N89-10651

ION SOURCES
An ion-optical bench for testing ion source lenses
[DE88-013186] N89-10606

ION TRAPS (INSTRUMENTATION)
Evaluation of the characteristics of a field emission cathode for use in a Mercury ion trap frequency standard N89-10193

IONIZATION
Electrospray ionization phenomena and the interface of capillary electrophoresis and mass spectrometry
[DE88-014080] N89-10143
Multiphoton ionization of transient species in supersonic jets
[DE88-008366] N89-10607

IONIZATION CROSS SECTIONS
Background modelling alternatives in electron energy-loss spectroscopy and their implications on microanalysis
[DE88-010361] N89-10140

IONIZATION POTENTIALS
The lowest ionization potentials of Al2
[NASA-TM-101171] N89-10605

IONOSPHERES
The dynamics of the Venus ionosphere
[NASA-CR-183167] N89-10779

IRON
Thermodynamic analysis of compatibility of several reinforcement materials with FeAl alloys
[NASA-CR-4172] N89-10128
Fe II level population in luminous variable stars N89-10754

IRON ALLOYS
Structure of grain boundaries in iron
[DE88-014412] N89-10154

IRRADIANCE
Sensitivity of satellite-derived net shortwave irradiance at the Earth's surface to radiometric calibration N89-10335

ISLANDS
Initial evolution of nonlinear magnetic islands in high temperature plasmas
[DE88-012346] N89-10636

ISOMERS
The detection of conformational disorder by thermal analysis
[DE88-012932] N89-10657

ISOTOPIC LABELING
Implications of isotopic signatures of noble gases for the origin and evolution of terrestrial atmospheres N89-10817

ISOTROPIC MEDIA
Material parameter determination from scattering measurements
[NASA-CR-183312] N89-10225

ITERATION
Delta square-correction scheme for unsteady Euler equations
[NAL-TR-948] N89-10576

IUE
A Decade of UV Astronomy with the IUE Satellite, volume 1
[ESA-SP-281-VOL-1] N89-10682
Observing SN 1987A with IUE N89-10683
Cataclysmic variables N89-10684
White dwarfs N89-10685
IUE observations of pulsating stars: Atmospheric structure, shock waves and stellar winds N89-10686
IUE observations of planetary atmospheres N89-10687
Comets --- IUE N89-10688
Some recent results from the study of cool stars --- IUE N89-10689
IUE observations and physical processes of interacting binary stars N89-10690
Io: IUE observations of its atmosphere and the plasma torus N89-10691
On the abundance of micron-sized particles in Saturn's A and B rings N89-10692
Jovian equatorial H2 emission from 1979-1987 N89-10693
Large time scale variation in hydrogen emission from Jupiter and Saturn N89-10694
Phenomenological analysis of Jovian north auroral H2 Lyman band emissions --- IUE N89-10695
Observations of SN 1987A: The narrow emission lines --- IUE N89-10696

The Progenitor of SN 1987A --- IUE N89-10697
The complete visual light curve of SN 1987A: Thirteen months of FES observations --- IUE Fine Error Sensor (FES) N89-10698
IUE observations of oxygen-rich supernova remnants N89-10699
Ejecta in SN 1006: The knotty issue --- supernova remnant N89-10700
Far UV observations of black hole candidates: The case of LMC X-3 N89-10701
IUE spectrophotometry of the accretion disk of HZ Her/Her X-1 N89-10702
Simultaneous IUE, EXOSAT and optical observations of the unusual AM Her type variable H058+608 N89-10703
A 0535+26/HDE 245770: A typical Be/X-ray transient system: Coordinated multiwavelength twelve years monitor N89-10704
IUE and optical observations of X-ray sources in the Large Margellanic Cloud (LMC) N89-10705
The analysis of spectra of novae taken near maximum N89-10706
The 1981 outburst of the old nova GK Persei N89-10707
Observations of classical novae in outburst N89-10708
Observations and simulations of nova Vul 1984 no. 2: A nova with ejecta rich in oxygen, neon, and magnesium N89-10709
Observations and simulations of recurrent novae: U Sco and V394 CrA N89-10710
Optical and ultraviolet observations of nova Vul 1987 N89-10711
Ultraviolet observations of LMC nova 1988 N89-10712
SS Cygni in quiescence --- IUE N89-10713
UV and optical line emission from the shell of the old nova GK Persei N89-10714
IUE observations of the 1987 superoutburst of the dwarf nova Z Cha N89-10715
Observations of galactic WC + O binary systems: HD 97152 and HD 152270 N89-10716
Atmospheric eclipse effects in Wolf-Rayet binaries in the Small Magellanic Cloud N89-10717
Mass flow in the interacting binary TX Ursae Majoris N89-10718
A new study of the interacting binary star V356 Sgr N89-10719
Matter streams in semi-detached binary systems N89-10720
The November 1987 eclipse of the zeta-Aur system HR 2554 N89-10721
Asymmetry in zeta Auriage chromospheres N89-10722
Superionized plasmas in Algol binaries N89-10723
HD 207739 and other F + Be variables N89-10724
Searching for the white dwarf in WZ Sagittae N89-10725
Model chromosphere and transition region for 56 Peg (K0 IIp + wd): A preliminary study N89-10726
Cepheid binaries with large mass ratios (M1/M2) N89-10727
The orbit of the Cepheid AW Per N89-10728
Companions to peculiar red giants: HR 363 and HR 1105 N89-10729
Direct UV observations of the circumstellar envelope of alpha Orionis N89-10730
Multi-wavelength observations of the peculiar red giant HR 3126 N89-10731
Recurrent shell infall events in a B0.5e star: HD 58978 1979-1988 N89-10732
IUE observations of a hot DAO white dwarf: Implications for diffusion theory and photospheric stratification N89-10733
Temperature determinations of hot DA white dwarfs using IUE continuum fluxes N89-10734
The ultraviolet emission of accreting magnetic white dwarfs N89-10735
IUE observations of rapidly rotating K dwarfs in the Pleiades N89-10736
On the flux-period and flux-flux correlations in late type stars N89-10737
Ultraviolet emission from the sun and stars: A comparison of IUE and Skylab spectra N89-10738
Spectral images of HD 199178 N89-10739
Doppler imaging of AR Lacertae at three epochs N89-10740
Rotational modulation of hydrogen Lyman alpha flux from 44i Bootis N89-10741
Mapping of surface activity on the W UMa-type system VW Cephei N89-10742
Ultraviolet flares on 2 Peg N89-10743
Chromospheric mass motions during a flare on UV Ceti N89-10744
The energy input mechanism into the lower transition regions between stellar chromospheres and coronae N89-10745
Transition regions of dM stars N89-10746
Transition region fluxes in A-F Dwarfs: Basal fluxes and dynamo activity N89-10747
Line formation of cool carbon star chromospheres N89-10748
Lithium and chromospherically active single giants N89-10749
Mg II flux and profile variability of hybrid-chromosphere stars N89-10750
The discovery of a co-rotating magnetosphere in a helium weak star: HD5737 = alpha Scl N89-10751
Observations of ultraviolet variability in RV Tauri stars N89-10752
Fluorescence processes and line identifications in the UV spectra of cool stars N89-10753
Fe II level population in luminous variable stars N89-10754
Identification of new fluorescence processes in the UV spectra of cool stars from new energy levels of Fe II and Cr II N89-10755
Periodic modulation of the atmosphere of Alpha Orionis N89-10756
Mg II line profiles of the Mira S Carinae N89-10757
The variability of the UV spectrum of the symbiotic star BF Cygni N89-10758
Abundance and f values needed to interpret adequately the high resolution IUE spectra N89-10759
Carbon and nitrogen abundance determinations from transition layer lines --- giant stars N89-10760
The anomalous C 4 intensity ratio in symbiotic stars N89-10761
The IUE spectral atlas of two normal B stars: pi Cet and nu Cap (125 to 200 nm) N89-10762
The UV silicon spectra of early B stars N89-10763
C IV and Si IV in IUE spectra of normal B8-A0 stars: UV identified Be/Ae stars N89-10764
Ultraviolet properties of IRAS-selected Be stars N89-10765
Au II in IUE spectra of chemically peculiar stars N89-10766
Validity of the classification of UV gallium stars N89-10767
Detected UV variability in the IUE spectra of the Ap-Si star HD 25823 N89-10768
The galatic and LMC extreme line supergiants compared: IUE observations of the Henize-Carlson and Zoo star samples of massive supergiants --- Large Magellanic cloud (LMC) N89-10769
Mass loss from the K dwarf in V471 Tauri N89-10770

J

J-97 ENGINE
Phase 4 static tests of the J-97 powered, external augmentor V/STOL model at the NASA, Ames Research Center, November 1983
[NASA-CR-177395] N89-10028
JACOBI MATRIX METHOD
A dexterity measure for the kinematic control of robot manipulator with redundancy
[AD-A196223] N89-10287
JAPAN
On the statistics of field waveforms associated with lightning return strokes N89-10441
Current measurement of lightning superbolt at the Japan sea coast N89-10445
JET FLOW
Direct Numerical Simulations (DNS) of an unpremixed turbulent jet flame
[AD-A196128] N89-10149
JOINTS (JUNCTIONS)
Transfer impedance measurements of the space shuttle Solid Rocket Motor (SRM) joints, wire meshes and a carbon graphite motor case N89-10440
Electromagnetic coupling through composite materials N89-10479
The effect of a gap nonlinearity on recursive parameter identification algorithms
[AD-A196020] N89-10557
JUPITER ATMOSPHERE
Jovian equatorial H2 emission from 1979-1987 N89-10693
Large time scale variation in hydrogen emission from Jupiter and Saturn N89-10694
Phenomenological analysis of Jovian north auroral H2 Lyman band emissions --- IUE N89-10695

K

KALMAN FILTERS
Segmentation of noisy images using nonstationary Markov fields
[AD-A195229] N89-10527
KANSAS
Lightning in mesoscale convective complexes on 3-5 June 1985 in Oklahoma and Kansas N89-10471
KEVLAR (TRADEMARK)
Lightning tests on an all-composite helicopter N89-10452
KINEMATICS
An optimal resolved rate law for kindematically redundant manipulators N89-10094
Kinematic study of flight telerobotic servicer configuration issues N89-10100
A dexterity measure for the kinematic control of robot manipulator with redundancy
[AD-A196223] N89-10287
Optical imaging through atmospheric turbulence N89-10423
KINETIC ENERGY
The dynamics of the Venus ionosphere
[NASA-CR-183167] N89-10779
KINETICS
Non-local kinetic transport studies of a field-reversed configuration
[DE88-012397] N89-10626
KNOWLEDGE
Second Annual Knowledge-Based Software Assistant Conference
[AD-A189819] N89-10536
A common framework for knowledge-based programming N89-10537
An overview of the knowledge-based requirements assistant N89-10538
Knowledge based tools for knowledge-based systems N89-10550
The knowledge integration tool: Knowledge interface (a knowledge based system development environment) N89-10551
Simplifying the construction of domain-specific automatic programming systems: The NASA automated software development workstation project N89-10553

L

LABORATORY EQUIPMENT
An electromagnetic calorimeter for a beauty factory
[NOTA-INTERNA-905] N89-10260
Electrostatic fields of ground triggered lightning N89-10462
LAMINAR FLOW
A transonic interactive boundary-layer theory for laminar and turbulent flow over swept wings
[NASA-CR-4185] N89-10029
Numerical analysis of laminar and turbulent incompressible flows using the finite element Fluid Dynamics Analysis Package (FIDAP)
[NASA-CR-179390] N89-10253
LAMINATES
Physical principles of ultrasonic non-destructive evaluation of advanced composites
[NASA-CR-180225] N89-10129
LAND
A new lidar system for applications over land and sea N89-10347
NASA's future land remote sensing program N89-10393
LAND ICE
Data report for the Siple Coast (Antarctica) project
[NASA-TM-100708] N89-10403
Mars: Crustal pore volume, cryospheric depth, and the global occurrence of groundwater N89-10787
Ice or liquid water in the Martian regolith. Morphologic indicators from rampart craters N89-10806
Formation of the layered deposits in the Valles Marineris, Mars N89-10809
Crater ejecta morphology and the presence of water on Mars N89-10818
LANDFORMS
Evidence for glaciation in Elysium N89-10781
LANDING MODULES
Phobos lander coding system: Software and analysis N89-10208
LANDSAT SATELLITES
A study of the vegetation cover with AVHRR during HAPEX-MOBILHY N89-10389
LANDSLIDES
Water and ice on Mars: Evidence from Valles Marineris N89-10803

LARGE SPACE STRUCTURES
Dynamics and control of the orbiting grid structures and the synchronously deployable beam
[NASA-CR-183205] N89-10297
LASER APPLICATIONS
Measuring in-situ soil surface roughness using a laser profilometer N89-10308
LASER DOPPLER VELOCIMETERS
Steady flow field measurements using laser Doppler velocimetry
[AD-A195228] N89-10245
Laser velocimeter measurements of solids in multiphase flow
[DE88-011611] N89-10251
Investigation of superradiant LDV markers and three-component velocity mapping
[AD-A195504] N89-10662
LASER HEATING
Time-resolved X-ray conversion efficiencies of laser-heated plasmas
[DE88-015456] N89-10637
LASER INDUCED FLUORESCENCE
Time-resolved laser fluorescensing: Trends and applications N89-10346
A new lidar system for applications over land and sea N89-10347
Changes in the chlorophyll fluorescence spectra during the Kautsky induction kinetics N89-10348
Chlorophyll fluorescence spectra of leaves as induced by blue light and red laser light N89-10349
Laser-induced fluorescence on in-vivo chlorophyll of a rice plant: A technique for the remote detection of plant growth N89-10350
Techniques for remote sensing of life span and quantum yield of chlorophyll fluorescence in vivo N89-10351
LASER MATERIALS
Laser interferometric dilatometer for low-expansion materials
[DE88-012329] N89-10272
LASER OUTPUTS
Nonlinear optical interactions involving the real Gaussian field
[DE88-012399] N89-10276
Studies of blackbody-pumped lasers
[NASA-CR-183214] N89-10277
Laser diagnostics of gas discharge tubes
[DE88-008124] N89-10633
LASER PLASMA INTERACTIONS
Investigation of superradiant LDV markers and three-component velocity mapping
[AD-A195504] N89-10662
LASER PLASMAS
Investigation of superradiant LDV markers and three-component velocity mapping
[AD-A195504] N89-10662
LASER PUMPING
Laser diagnostics of gas discharge tubes
[DE88-008124] N89-10633
LASER TARGETS
The tensile strength of glass shells
[DE88-013011] N89-10301
A novel alignment technique for pointing and centering optical components
[DE88-015441] N89-10621
LASER WELDING
Laser welding of stainless steel weld filler metals at high cooling rates
[DE88-002345] N89-10281
LASERS
Design study for a remote laser wavelength sensor
[DE88-015417] N89-10265
PECVD (Plasma Enhanced Chemical Vapor Deposition) diamond thin films for research instrumentation
[AD-A195443] N89-10652
LASING
Studies of blackbody-pumped lasers
[NASA-CR-183214] N89-10277
LATE STARS
On the flux-period and flux-flux correlations in late type stars N89-10737
LATERAL CONTROL
Helicopter roll control effectiveness criteria program summary
[NASA-CR-177477] N89-10046
LAUNCH VEHICLE CONFIGURATIONS
Space shuttle phase B wind tunnel model and test information. Volume 3: Launch configuration
[NASA-CR-178416-VOL-3-PT-1] N89-10019
LAUNCH VEHICLES
An aircraft-borne electric field measuring system for rocket launch support N89-10443
LAUNCHING
Scientific ballooning in Brazil
[INPE-4602-PRE/1325] N89-10018
LEAF AREA INDEX
Developing a radiometric leaf area index N89-10334
LEAKAGE
Effects of switch leakages upon Nimbus-7 SMMR calibration
[NASA-CR-180792] N89-10115
LEAR JET AIRCRAFT
Interference of precipitation static discharges with aircraft navigational systems N89-10459
LEARNING
Performance improvement of robots using a learning control scheme N89-10105
LEAST SQUARES METHOD
ZOOM orbitography software: On the Givens method. Presentation and software implementation evaluation for least square problems
[CNES-CT/DTI/MS/AE/219] N89-10109
Solution of ill-posed problems by means of truncated SVD (Singular Value Decomposition)
[DE88-013510] N89-10238
The effect of a gap nonlinearity on recursive parameter identification algorithms
[AD-A196020] N89-10557
Comparison of plotting methods used on normal probability paper
[NAL-TR-951] N89-10584
A fast Monte-Carlo cross-validation procedure for large least squares problems with noisy data
[RR-687-M] N89-10591
LEAVES
Chlorophyll fluorescence spectra of leaves as induced by blue light and red laser light N89-10349
Estimation of leaf spectra from measurements in wide spectral bands N89-10368
LENSES
An ion-optical bench for testing ion source lenses
[DE88-013186] N89-10606
A novel alignment technique for pointing and centering optical components
[DE88-015441] N89-10621
LEVITATION
Design approaches and parameters for magnetically levitated transport systems
[DE88-014286] N89-10260
LIAPUNOV FUNCTIONS
Generalized Lyapunov exponents in high-dimensional chaotic dynamics and products of large random matrices
[PREPRINT-595] N89-10600
LIFE (DURABILITY)
Life time prediction: Synthesis on ONERA's research in viscoplasticity and continuous damage mechanics, applied to engine materials and structures N89-10011
Selection of sensors for measurement and control
[DE88-012936] N89-10267
LIFE SUPPORT SYSTEMS
Living in space, book 2, levels D, E, F
[NASA-EP-223] N89-10522
LIFT AUGMENTATION
Phase 4 static tests of the J-97 powered, external augmentor V/STOL model at the NASA, Ames Research Center, November 1983
[NASA-CR-177395] N89-10028
LIGHT CURVE
The complete visual light curve of SN 1987A: Thirteen months of FES observations --- IUE Fine Error Sensor (FES) N89-10698
LIGHT SCATTERING
Electron transport and optical emissions in the aurora N89-10424
LIGHT TRANSMISSION
Atmospheric propagation effects relevant to optical communications N89-10201
LIGHT WATER REACTORS
Discrete modeling considerations in multiphase fluid dynamics
[DE88-015188] N89-10256
LIGHTNING
International Aerospace and Ground Conference on Lightning and Static Electricity
[PB88-197439] N89-10429
Statistics of lightning interaction with aircraft in Japan N89-10430
Israel Air Force (IAF) in-service aircraft lightning strike and damage survey N89-10431
Lightning information database N89-10432
A stochastic model for the tortuous propagation of a lightning stepped leader N89-10433
What makes thunderbolts zig and zag N89-10434
Framework for lightning modeling: Comparing results N89-10435
The criterion for the propagation of the positive streamer and its application N89-10436
Numerical simulations of lightning by means of the leader propagation model N89-10437
Triggering of lightning by the Atlas Centaur vehicle N89-10438
Evaluation and mitigation of lightning hazards to the space shuttle Solid Rocket Motors (SRM) N89-10439
Transfer impedance measurements of the space shuttle Solid Rocket Motor (SRM) joints, wire meshes and a carbon graphite motor case N89-10440
On the statistics of field waveforms associated with lightning return strokes N89-10441
Measurements of the velocity change of a lightning return stroke with height N89-10442
An aircraft-borne electric field measuring system for rocket launch support N89-10443
New electric field instrumentation and the effects of space charge at Kennedy Space Center N89-10444
Current measurement of lightning superbolt at the Japan sea coast N89-10445
Lightning return stroke velocity N89-10446
A case for a unified lightning threat N89-10447
Electromagnetic radiations generated by microdischarges from hydrometeors N89-10448
Summary of inflight data on lightning currents and fields N89-10449
Analysis of recent in-flight lightning measurements on different aircraft N89-10450
Linear and nonlinear interpretation of CV-580 lightning data N89-10451
Lightning tests on an all-composite helicopter N89-10452
A chronology of in-cloud electric field and lightning strikes on an instrumented research aircraft N89-10455
Lightning initiation on aircraft in thunderstorms N89-10456
Lightning tests to measure the bulk current levels associated with the electronic engine control of a turboprop commuter transport N89-10457
Electrostatic fields of ground triggered lightning N89-10462
A review of medical aspects of lightning injury N89-10463
A retrospective study of the injuries sustained in telephone-mediated lightning strike N89-10464
Factors influencing the detection of voltage sparks by flammable gas and optical techniques N89-10465
Lightning near Vandenberg AFB as related to various synoptic patterns N89-10466
Lightning protection for high explosives and instrumentation using a field mill system N89-10467
An interagency working group on lightning threat warning N89-10469
The electrical structure of thunderstorm anvils N89-10470
Lightning in mesoscale convective complexes on 3-5 June 1985 in Oklahoma and Kansas N89-10471
Spatial distribution of lightning strikes to ground during small thunderstorms in Florida N89-10472
Lightning standards for protection of ground electronic systems N89-10473
Lightning and surge protection of large ground facilities N89-10474
Computer simulation of the effects of lightning stroke attachment to an electric power substation N89-10475
A revised electrogeometric model for the termination of lightning strokes on ground objects N89-10476
Model results for a proposed tactical missile training site lightning protection system N89-10477
Implications of a recent lightning strike to a NASA jet trainer N89-10478
Electromagnetic coupling through composite materials N89-10479
Monitoring lightning activity in South Africa with a VLF single-station technique: Comparison with meteosat infrared data N89-10480
The SAFIR lightning monitoring and warning system, applications to aerospace activities N89-10481
A lightning location system for the UK electricity supply industry N89-10482
Finite difference analysis of external and internal lightning response of the JAS39 CFC wing N89-10483
A filamentary method for calculating induced voltages within resistive structures in either the frequency or time domain N89-10484
Modelling of common mode coupling between an aircraft wing traversed by a lightning current and wiring installed in that wing N89-10485
Precise long-range lightning mapping with the UK arrival time difference VLF technique N89-10486
LSZ-850 lightning sensor system N89-10487
Considerations for using lightning locating systems in performance evaluations of single-station lightning detection sensors N89-10488
Some observations and analysis of atmospheric electricity over non-uniform high terrain N89-10489
Intracloud lightning as a precursor to thunderstorm microbursts N89-10490
The lightning flash counter: Papua New Guinean experience N89-10491
Indirect effects on electronic and mechanical systems installed in carbon fibre compound aircraft structures N89-10492

Site errors of a magnetic direction finder for lightning flashes N89-10494
The interaction between lightning grounding systems and buried cables N89-10496
System protection from atmospheric electricity for aerostats with conducting tethers N89-10497

LINE SPECTRA
Line formation of cool carbon star chromospheres N89-10748
Mg II flux and profile variability of hybrid-chromosphere stars N89-10750
Mg II line profiles of the Mira S Carinae N89-10757

LINEAR PROGRAMMING
A linear programming approach to maximum entropy signal restoration [DE88-013021] N89-10566
Parallel processors for planning under uncertainty [DE88-016184] N89-10571

LINEAR SYSTEMS
The effect of a gap nonlinearity on recursive parameter identification algorithms [AD-A196020] N89-10557

LININGS
Standardization of the carbon-phenolic materials and processes. Vol. 2: Test methods and specifications [NASA-CR-183227] N89-10033
Standardization of the carbon-phenolic materials and processes. Vol. 1: Experimental studies [NASA-CR-183226] N89-10127
Metallic materials as plasma facing components [DE88-010103] N89-10628

LIQUID CRYSTALS
High-resolution heat-transfer-coefficient maps applicable to compound-curve surfaces using liquid crystals in a transient wind tunnel [NASA-TM-89855] N89-10246

LIQUID FILLED SHELLS
Moment exerted on a coning projectile by a spinning liquid in a cylindrical cavity containing a porous medium [AD-A195291] N89-10239

LIQUID FUELS
HAN (hydroxylammonium nitrate density)-based liquid gun propellants: Physical properties [AD-A195246] N89-10180

LIQUID PROPELLANT ROCKET ENGINES
Choice of coating and surface behavior of the hydrogen turbopump of the Vulcain engine [ETN-88-93064] N89-10173

LIQUIDS
An improved interface for capillary zone electrophoresis-mass spectrometry [DE88-014079] N89-10148

LISP (PROGRAMMING LANGUAGE)
A LISP-Ada connection N89-10085

LITHIUM
Lithium and chromospherically active single giants N89-10749

LITHIUM ALLOYS
Tensile properties of commercial aluminum-lithium alloys at cryogenic temperatures [DE88-014857] N89-10153

LITHIUM SULFUR BATTERIES
Hydrogen sorption studies of materials used in Li(Si)/FeS2 thermal batteries [DE88-013154] N89-10231

LITHOLOGY
Usefulness of high spectral resolution radiometry for geological mapping in the Mediterranean region N89-10360
Characterization of rocks by visible and infrared high spectral resolution terrain spectroscopy N89-10362

LITHOSPHERE
Wilson cycle studies [NASA-CR-183146] N89-10419
Partitioning of carbon dioxide between the atmosphere and lithosphere on early Mars N89-10616

LOADING RATE
Void collapse and void growth in crystalline solids N89-10421

LOADS (FORCES)
Measurement of aerodynamic characteristics of a hang-glider-wing by ground run tests using a test vehicle [NAL-TR-953] N89-10004
Consolidated fuel reprossing program: The implications of force reflection for teleoperation in space N89-10090
A shared position/force control methodology for teleoperation N89-10092
Multiple sensor smart robot hand with force control N89-10093
Inelastic buckling analyses of beams, columns and plates using the spline finite strip method [PB88-214291] N89-10299

LOCAL AREA NETWORKS
A local area computer network expert system framework N89-10074
High speed fiber optics local area networks: Design and implementation [NASA-CR-182432] N89-10216

LOGIC CIRCUITS
Heat exchanger expert system logic N89-10205
An expert system for VLSI layout N89-10528

LOOK ANGLES (ELECTRONICS)
Analysis of directional effects on NOAA AVHRR N89-10341

LOOP ANTENNAS
A lightning location system for the UK electricity supply industry N89-10482

LOOPS
Loopspace general covariance in string field theory [DE88-014170] N89-10659

LOSSY MEDIA
Measurement of the properties of lossy materials inside a finite conducting cylinder [NASA-CR-182500] N89-10223

LOW GRAVITY MANUFACTURING
Theoretical model for the solute distribution of a PbSnTe growth by VMS in microgravity environment [INPE-4664-PRE/1365] N89-10183

LOW TEMPERATURE
Tensile properties of commercial aluminum-lithium alloys at cryogenic temperatures [DE88-014857] N89-10153

LOW TEMPERATURE ENVIRONMENTS
A narrow-band thermal imager based on multiline real-time averaging N89-10356

LUBRICANTS
A comparative evaluation of RPD (Rotary Particle Depositor) and ferrographic diagnostic methods for turbine engine lubricant samples [AD-A196207] N89-10044

LUNAR BASES
Methods of extracting hydrogen from lunar soil [NASA-CR-180465] N89-10826

LUNAR SOIL
Methods of extracting hydrogen from lunar soil [NASA-CR-180465] N89-10826

LUNAR SURFACE
Cosmogenic (sup 36)Cl production rates in meteorites and the lunar surface [DE88-014452] N89-10775
Methods of extracting hydrogen from lunar soil [NASA-CR-180465] N89-10826

LYMAN ALPHA RADIATION
Large time scale variation in hydrogen emission from Jupiter and Saturn N89-10694
Phenomenological analysis of Jovian north auroral H2 Lyman band emissions --- IUE N89-10695
Rotational modulation of hydrogen Lyman alpha flux from 44i Bootis N89-10741

LYMAN SPECTRA
Jovian equatorial H2 emission from 1979-1987 N89-10693

M

MACHINE TRANSLATION
UNITRAN (universal translator): A principle-based approach to machine translation [AD-A195281] N89-10675

MACHINING
Generation of a crowned pinion tooth surface by a surface of revolution [NASA-TM-100260] N89-10282
Generation of a crowned pinion tooth surface by a plane [NASA-TM-100259] N89-10283

MAGELLANIC CLOUDS
IUE observations of oxygen-rich supernova remnants N89-10699
Far UV observations of black hole candidates: The case of LMC X-3 N89-10701
IUE and optical observations of X-ray sources in the Large Margellanic Cloud (LMC) N89-10705
Ultraviolet observations of LMC nova 1988 N89-10712
Atmospheric eclipse effects in Wolf-Rayet binaries in the Small Magellanic Cloud N89-10717
The galatic and LMC extreme line supergiants compared: IUE observations of the Henize-Carlson and Zoo star samples of massive supergiants --- Large Magellanic cloud (LMC) N89-10769

MAGMA
Release of magmatic water on Mars: Estimated timing and volumes N89-10790

MAGNESIUM
The influence of texture on strain hardening [DE88-009157] N89-10158
Mg II flux and profile variability of hybrid-chromosphere stars N89-10750
Mg II line profiles of the Mira S Carinae N89-10757

MAGNETIC CHARGE DENSITY
Material parameter determination from scattering measurements [NASA-CR-183312] N89-10225

MAGNETIC FIELD CONFIGURATIONS
Non-local kinetic transport studies of a field-reversed configuration [DE88-012397] N89-10626

MAGNETIC FIELDS
An investigation into force-moment calibration techniques applicable to a magnetic suspension and balance system [NASA-CR-181695] N89-10061
Physics and technology for the in-situ investigation of properties of materials [AD-A195498] N89-10145
Initial evolution of nonlinear magnetic islands in high temperature plasmas [DE88-012346] N89-10636
Confinement and heating of high beta plasmas with emphasis on compact toroids [DE88-015777] N89-10645
A polarisation study of spiral galaxies N89-10679

MAGNETIC FLUX
Losses in magnetic flux compression generators. Part 2: Radiation losses [DE88-015046] N89-10224
C 4 fluxes from the sun as a star and the correlation with magnetic flux [NASA-CR-183156] N89-10827

MAGNETIC LEVITATION VEHICLES
Design approaches and parameters for magnetically levitated transport systems [DE88-014286] N89-10280

MAGNETIC STARS
Detected UV variability in the IUE spectra of the Ap-Si star HD 25823 N89-10768

MAGNETIC SURVEYS
Solid earth mission study. Volume 2: Technical report [ESA-CR(P)-2626-VOL-2] N89-10303
Solid Earth mission study. Volume 1: Executive summary [ESA-CR(P)-2626-VOL-1] N89-10397
Solid earth mission study. Volume 3: Program planning report [ESA-CR(P)-2626-VOL-3] N89-10399

MAGNETIC SUSPENSION
An investigation into force-moment calibration techniques applicable to a magnetic suspension and balance system [NASA-CR-181695] N89-10061

MAGNETOHYDRODYNAMIC TURBULENCE
Nonlinear magnetohydrodynamics [DE88-015703] N89-10644

MAGNETOHYDRODYNAMIC WAVES
The study of hydromagnetic waves and RF heating using the TORTUS tokamak and the development of diagnostic techniques N89-10635

MAGNETOHYDRODYNAMICS
Adventures in magnetohydrodynamics [IPPJ-862] N89-10629
Study of critical beta non-circular tokamak equilibria sustained in steady state by beam driven currents [IPPJ-878] N89-10634
Nonlinear magnetohydrodynamics [DE88-015703] N89-10644

MAGNETOSPHERES
The discovery of a co-rotating magnetosphere in a helium weak star: HD5737 = alpha Scl N89-10751

MAINTENANCE
Maintaining an expert system for the Hubble Space Telescope ground support N89-10064

MAN ENVIRONMENT INTERACTIONS
Use of remote sensing for land use policy formulation [NASA-CR-183148] N89-10395

MAN MACHINE SYSTEMS
Dynamic task allocation for a man-machine symbiotic system N89-10098

MANAGEMENT
Software design research at DARPA N89-10546

MANIFOLDS
Flowfield visualization for SSME hot gas manifold [NASA-CR-179403] N89-10243

MANIPULATORS
Consolidated fuel reprossing program: The implications of force reflection for teleoperation in space N89-10090
Multiple sensor smart robot hand with force control N89-10093
An optimal resolved rate law for kinematically redundant manipulators N89-10094
An adaptive control scheme for a flexible manipulator N89-10095
Robot hands and extravehicular activity N89-10097
Actuators for a space manipulator N89-10101

On motion planning and control of multi-link lightweight robotic manipulators N89-10285
A dexterity measure for the kinematic control of robot manipulator with redundancy [AD-A196223] N89-10287

MAPPING
Use of remote sensing for land use policy formulation [NASA-CR-183148] N89-10395
Precise long-range lightning mapping with the UK arrival time difference VLF technique N89-10486
Real algebraic morphisms with values in the unit circle [PB88-208921] N89-10515
A general data model for geographic information systems [INPE-4560-PRE/1301] N89-10676

MARINE BIOLOGY
Study of biological processes on the US North Atlantic slope and rise, volume 2 [PB88-196514] N89-10511
Study of biological processes on the US North Atlantic slope and rise. Volume 1: Executive summary [PB88-196522] N89-10517

MARINE METEOROLOGY
MIZEX (marginal ice zone experiment) 87 meteorology atlas [AD-A195361] N89-10506

MARINE RESOURCES
Estimation of primary marine production using spaceborne data on ocean color N89-10371

MARKERS
Investigation of superradiant LDV markers and three-component velocity mapping [AD-A195504] N89-10662

MARKET RESEARCH
Review of the requirements for higher level ERS-1 products within Europe [ESA-CR(P)-2586] N89-10664

MARKOV PROCESSES
Segmentation of noisy images using nonstationary Markov fields [AD-A195229] N89-10527

MARS (PLANET)
MECA Symposium on Mars: Evolution of its Climate and Atmosphere [NASA-CR-182872] N89-10780

MARS ATMOSPHERE
MECA Symposium on Mars: Evolution of its Climate and Atmosphere [NASA-CR-182872] N89-10780
Numerical simulations of dust transport into northern high latitudes during a Martian polar warming N89-10782
The Martian dust cycle: A proposed model N89-10791
Interannual variability of global dust storms on Mars N89-10792
Photochemical weathering and contemporary volatile loss on Mars N89-10795
The observed day-to-day variability of Mars water vapor N89-10797
The direction of water transport on Mars: A possible pumping mechanism N89-10798
Climatic effects of enhanced CO2 levels in Mars early atmosphere N89-10799
Influence of polar-cap albedo on past and current Martian climate N89-10801
The great dust storm of 1986 N89-10804
Seasonal wind variations in the Martian subtropics N89-10807
Optical thickness of the Olympus cloud N89-10808
Volatile inventory of Mars-2: Primordial sources and fractionating processes N89-10814
Partitioning of carbon dioxide between the atmosphere and lithosphere on early Mars N89-10816
Implications of isotopic signatures of noble gases for the origin and evolution of terrestrial atmospheres N89-10817
Mars global atmospheric oscillations: Transients and dust storm relations N89-10820
Vertical O(sub 3) distribution as a diagnostic for eddy diffusion profile N89-10821
Water on Mars N89-10822
Absorption of the Martian regolith: Specific surface area and missing CO(sub 2) N89-10824

MARS CRATERS
Ice or liquid water in the Martian regolith. Morphologic indicators from rampart craters N89-10806
Could icy impacts reconcile Venus with Earth and Mars N89-10810
Crater ejecta morphology and the presence of water on Mars N89-10818

MARS OBSERVER
X/X/Ka-band prime focus feed antenna for the Mars Observer beacon spacecraft N89-10195

MARS SURFACE
Sapping features of the Colorado Plateau: A comparative planetary geology field guide [NASA-SP-491] N89-10401
Evidence for glaciation in Elysium N89-10781
The Paleo-ocean of Mars N89-10783
Mars: A water-rich planet N89-10784
Martian volcanism: A review N89-10785
Comets, volcanism, the salt rich regolith and cycling of volatiles on Mars N89-10786
Mars: Crustal pore volume, cryospheric depth, and the global occurrence of groundwater N89-10787
Is regolith absorbtion the explanation for the transition from early to present Mars climate N89-10788
Martian surface physical properties to be derived by radar altimeter on the Mars observer spacecraft N89-10789
Release of magmatic water on Mars: Estimated timing and volumes N89-10790
The Martian dust cycle: A proposed model N89-10791
Chemical frost weathering of olivine: Experimental study and implications N89-10793
Mars low albedo regions: Possible map of near-surface N89-10794
Interannual differences in the regressions of the polar caps of Mars N89-10796
Regional sources and sinks of dust on Mars: Viking observations of Cerberus, Solis Planum, and Syrtis Major N89-10802
Water and ice on Mars: Evidence from Valles Marineris N89-10803
The great dust storm of 1986 N89-10804
Ablation of Martian glaciers N89-10805
Formation of the layered deposits in the Valles Marineris, Mars N89-10809
Seismic exploration for water on Mars N89-10811
The thermal properties of Martian surface materials at high lattitudes: Possible evidence for permafrost N89-10812
Geomorphic evidence for ancient seas on Mars N89-10813
Martian tectonics: A review N89-10815
Crater ejecta morphology and the presence of water on Mars N89-10818
Phobos and Deimos: A base for sampling the Martian past N89-10819
Water on Mars N89-10822
Mars regolith versus SNC meteorites: Evidence for abundant crustal carbonates N89-10823
Thermal properties of channels in the Aeolis Quadrangle: Topographic traps for Aeolian materials N89-10825

MARS VOLCANOES
Martian volcanism: A review N89-10785
Comets, volcanism, the salt rich regolith and cycling of volatiles on Mars N89-10786
Release of magmatic water on Mars: Estimated timing and volumes N89-10790
Areal and time distributions of volcanic formations on Mars N89-10800
Martian tectonics: A review N89-10815
Partitioning of carbon dioxide between the atmosphere and lithosphere on early Mars N89-10816

MARSHLANDS
Comparative analysis of spectral response in the optical domain of targets in a tropical swamp at various spectral and spatial resolutions N89-10363

MASERS
A 32-GHz reflected-wave maser amplifier with wide instantaneous bandwidth N89-10198

MASS FLOW
Mass flow in the interacting binary TX Ursae Majoris N89-10718

MASS RATIOS
Cepheid binaries with large mass ratios (M1/M2) N89-10727

MASS SPECTRA
Multiphoton ionization of transient species in supersonic jets [DE88-008366] N89-10607

MASS SPECTROSCOPY
Electrospray ionization phenomena and the interface of capillary electrophoresis and mass spectrometry [DE88-014080] N89-10143
An improved interface for capillary zone electrophoresis-mass spectrometry [DE88-014079] N89-10148

MASS TRANSFER
Matter streams in semi-detached binary systems N89-10720
Recurrent shell infall events in a B0.5e star: HD 58978 1979-1988 N89-10732

MATCHING
Satellite image registration through structural matching [INPE-4563-PRE/1304] N89-10530

MATHEMATICAL MODELS
Basic structural dynamics N89-10007
Structural dynamic characteristics of individual blades N89-10008
Structural dynamic characteristics of bladed assemblies N89-10009
Simulation validation experience: PATRIOT guidance system N89-10055
Reports of investigations on: Derivation of an infinite-dilution activity coefficient model and application to two-component vapor/liquid equilibria data [DE88-007517] N89-10147
Pulse combustor modeling: One dimensional wave-dynamic model utilizing dynamic injection and energy release submodels [DE88-005369] N89-10150
Systems analysis of the inverse heat conduction problem N89-10244
Numerical investigation of the dynamics of heterogeneous shock-cavitation [MPIS-MITT-86-1987] N89-10257
Studies of blackbody-pumped lasers [NASA-CR-183214] N89-10277
On the problem of modeling for parameter identification in distributed structures [NASA-CR-182739] N89-10291
Dynamics and control of the orbiting grid structures and the synchronously deployable beam [NASA-CR-183205] N89-10297
Dynamic interpretation of geoid anomalies [NASA-CR-183164] N89-10304
Use of microwave backscatter measurements as boundary conditions in soil/atmosphere water transfer modeling N89-10311
A perspective on vegetation canopy reflectance models N89-10317
A model for radiative transfer in heterogeneous three-dimensional canopies N89-10326
Numerical accuracy of a two-stream radiative transfer model from comparison with an N-stream model N89-10331
A theoretical model for interpreting remotely sensed thermal infrared measurements obtained over agricultural areas N89-10343
CCM (Community Climate Model) modular processor users' guide (version PROC02) [PB88-216577] N89-10428
Framework for lightning modeling: Comparing results N89-10435
Numerical simulations of lightning by means of the leader propagation model N89-10437
Lightning return stroke velocity N89-10446
A case for a unified lightning threat N89-10447
Linear and nonlinear interpretation of CV-580 lightning data N89-10451
A revised electrogeometric model for the termination of lightning strokes on ground objects N89-10476
Model results for a proposed tactical missile training site lightning protection system N89-10477
Modelling of common mode coupling between an aircraft wing traversed by a lightning current and wiring installed in that wing N89-10485
The role of clouds in surface radiation budgets N89-10501
Joint CGS-AOML (Charting and Geodetic Service-Atlantic Oceanographic and Meteorological Laboratory) acoustical bottom echo-formation research. 1: Literature search and initial modelling results [PB88-202007] N89-10512
Model-data comparisons for the 1982-83 El Nino: The XBT tracks [PB88-221668] N89-10514
Progress in NODAL transport methods [DE88-012416] N89-10590
Relativistic nuclear physics with the spectator model [CEBAF-PR-88-011] N89-10613
Gas-contact cooling for VUV laser oscillation in recombining plasmas [IPPJ-881] N89-10631
Structural instability of sheath potential distribution and its possible implications for the L/H transition in tokamak plasmas [IPPJ-877] N89-10643

MATRICES (MATHEMATICS)
Block Toeplitz operators with rational symbols [PB88-202890] N89-10587
Generalized Lyapunov exponents in high-dimensional chaotic dynamics and products of large random matrices [PREPRINT-595] N89-10600
Theoretical study of the dissociation energy and the red and violet band systems of CN [NASA-TM-101190] N89-10610

MAXIMUM ENTROPY METHOD
A linear programming approach to maximum entropy signal restoration [DE88-013021] N89-10566

MAXWELL EQUATION
The interaction between lightning grounding systems and buried cables N89-10496
MEAN
Mean estimation in highly skewed samples [DE88-010929] N89-10595
MEASURING INSTRUMENTS
Selection of sensors for measurement and control [DE88-012936] N89-10267
MECHANICAL PROPERTIES
Fracture criteria for discontinuously reinforced metal matrix composites [NASA-CR-181175] N89-10125
Properties of silicon carbide fiber-reinforced silicon nitride matrix composites [NASA-TM-101356] N89-10130
Thermal effects on the mechanical properties of SiC fiber reinforced reaction bonded silicon nitride matrix (SiC/RBSN) composites [NASA-TM-101348] N89-10134
Recent developments in aluminides and silicides [DE88-012926] N89-10155
Engineering processing and properties of nickel aluminides [DE88-011019] N89-10164
Computer simulation of absorption heat pump using aqueous lithium bromide and ternary nitrate mixtures [DE88-013353] N89-10249
MEDITERRANEAN SEA
Usefulness of high spectral resolution radiometry for geological mapping in the Mediterranean region N89-10360
MEMORY (COMPUTERS)
Tools to aid in the analysis of memory access patterns for FORTRAN programs [DE88-013609] N89-10535
Relational multimedia databases N89-10673
MESH
Transfer impedance measurements of the space shuttle Solid Rocket Motor (SRM) joints, wire meshes and a carbon graphite motor case N89-10440
Indirect effects on electronic and mechanical systems installed in carbon fibre compound aircraft structures N89-10492
Optimal simulations by butterfly networks: Extended abstract [AD-A195168] N89-10572
MESON-MESON INTERACTIONS
Vertex detector for a linear beauty factory [NOTA-INTERNA-906] N89-10266
MESONS
An electromagnetic calorimeter for a beauty factory [NOTA-INTERNA-905] N89-10260
Relativistic nuclear physics with the spectator model [CEBAF-PR-88-011] N89-10613
MESOSCALE PHENOMENA
Lightning in mesoscale convective complexes on 3-5 June 1985 in Oklahoma and Kansas N89-10471
Analysis and modeling of summertime convective cloud and precipitation structure over the southeastern United States [NASA-CR-183192] N89-10498
MESSAGE PROCESSING
Orca: A language for distributed object-based programming [PB88-208533] N89-10529
METAL CRYSTALS
Deflection of light by using tungsten bronze crystals [DE88-014151] N89-10618
METAL FATIGUE
Fatigue and assessment methods of blade vibration N89-10010
Life time prediction: Synthesis on ONERA's research in viscoplasticity and continuous damage mechanics, applied to engine materials and structures N89-10011
A study of the fatigue behavior of small cracks in nickel-base superalloys [AD-A195489] N89-10161
Influence of specimen size on fatigue crack initiation of welded HY100 steel [AD-A196219] N89-10294
METAL FILMS
Thermodynamics and kinetics of phase formation of thin-film metal on gallium arsenide [DE88-015702] N89-10648
METAL HYDRIDES
Rechargeable metal hydrides for spacecraft application [NASA-TM-4076] N89-10184
METAL MATRIX COMPOSITES
Fracture criteria for discontinuously reinforced metal matrix composites [NASA-CR-181175] N89-10125
METAL OXIDE SEMICONDUCTORS
Dynamic properties of power MOS transistors [LAAS-88-162] N89-10236
METAL PLATES
Dual passband dichroic plate for X-band N89-10196
METAL SURFACES
On a surface mounted transmission line configuration for aperture testing N89-10458
METALLIC GLASSES
Metastable alloy phases prepared by solid state reactions and ball milling [DE88-009156] N89-10163
METALLOGRAPHY
Influence of specimen size on fatigue crack initiation of welded HY100 steel [AD-A196219] N89-10294
METALS
A compendium of sources of fracture toughness and fatigue crack growth data for metallic alloys, part 3 [NASA-TM-100675] N89-10165
Laser welding of stainless steel weld filler metals at high cooling rates [DE88-002345] N89-10281
Metallic materials as plasma facing components [DE88-010103] N89-10628
METASTABLE STATE
Metastable alloy phases prepared by solid state reactions and ball milling [DE88-009156] N89-10163
METEORITES
Mars regolith versus SNC meteorites: Evidence for abundant crustal carbonates N89-10823
METEOROLOGICAL PARAMETERS
The lightning flash counter: Papua New Guinean experience N89-10491
MIZEX (marginal ice zone experiment) 87 meteorology atlas [AD-A195361] N89-10506
METEOROLOGICAL RADAR
The Remote Atmospheric Probing Information Display (RAPID) system [AD-A196314] N89-10500
METEOROLOGICAL SATELLITES
The Remote Atmospheric Probing Information Display (RAPID) system [AD-A196314] N89-10500
METEOROLOGY
An aircraft-borne electric field measuring system for rocket launch support N89-10443
METEOSAT SATELLITE
Monitoring lightning activity in South Africa with a VLF single-station technique: Comparison with meteosat infrared data N89-10480
METHANE
Basic research on natural gas combustion phenomena-catalytic combustion [PB88-214606] N89-10142
Direct methane conversion: An assessment [DE88-010225] N89-10181
METHYL ALCOHOL
Direct methane conversion: An assessment [DE88-010225] N89-10181
METRIC PHOTOGRAPHY
Comparative geological evolution of different remote sensing data of the Hoggar Mountains (Algeria) N89-10385
MEXICO
Some observations and analysis of atmospheric electricity over non-uniform high terrain N89-10489
MICROANALYSIS
Background modelling alternatives in electron energy-loss spectroscopy and their implications on microanalysis [DE88-010361] N89-10140
MICROMECHANICS
Micromechanisms of deformation and fracture in ordered intermetallic alloys. 1: Strengthening mechanisms [DE88-015382] N89-10159
MICROORGANISMS
High resolution radiometric measurement of intertidal microphytobenthos N89-10365
MICROSTRUCTURE
Micromechanisms of deformation and fracture in ordered intermetallic alloys. 1: Strengthening mechanisms [DE88-015382] N89-10159
Premartensitic microstructures as seen in the high-resolution electron microscope: A study of a NiAl alloy [DE88-008042] N89-10160
MICROWAVE ANTENNAS
DSN 64-meter antenna L-band (1668-MHz) microwave system performance overview N89-10210
MICROWAVE EQUIPMENT
Effects of modulated electron beams and cavities on reditrons [DE88-014317] N89-10234
MICROWAVE RADIOMETERS
Effects of switch leakages upon Nimbus-7 SMMR calibration [NASA-CR-180792] N89-10115
Potential number of winter wheat ears estimation using radiometry techniques at an early stage N89-10323
Analysis of the contribution of the atmosphere to water reflectance in the first two channels of the NOAA satellites AVHRR N89-10330
Monitoring seasonal variations of soil moisture and vegetation cover using satellite microwave radiometry N89-10378
Comparison of temperature profiles measured by three collocated microwave radiometers and radiosonde [PB88-212808] N89-10503
MICROWAVE SCATTERING
An approximative model for the microwave brightness temperature scattered by a rough open ocean surface N89-10344
MICROWAVES
Effects of modulated electron beams and cavities on reditrons [DE88-014317] N89-10234
MILITARY AIR FACILITIES
Lightning near Vandenberg AFB as related to various synoptic patterns N89-10466
MILITARY HELICOPTERS
Helicopter roll control effectiveness criteria program summary [NASA-CR-177477] N89-10046
MILLIMETER WAVES
Cost effective simulation for millimeter wave guidance systems N89-10053
MINERAL EXPLORATION
The results of the Geosat MOMS subcommittee's data evaluation: Performance and applicability of the MOMS-1 sensor for exploration geology N89-10380
MIRRORS
Sulfide corrosion of silver contacts during satellite storage [AD-A196217] N89-10112
Performance of multimirror quartzline lamps in a high-pressure, underwater environment [NASA-TM-101374] N89-10269
MISSILE CONTROL
Guidance and control systems simulation and validation techniques [AGARD-AG-273] N89-10048
Comparison of statistical digital simulation methods N89-10049
A generic seeker simulation for the evaluation of active RF guidance systems N89-10050
Cost effective simulation for millimeter wave guidance systems N89-10053
Simulation validation experience: PATRIOT guidance system N89-10055
MISSILE DEFENSE
Directed energy concepts for strategic defense [DE88-015050] N89-10596
Military uses of space [DE88-015053] N89-10597
SDI (Strategic Defense Initiative): Myth or reality [DE88-015059] N89-10598
Control System Research for Directed Energy Weapons [DE88-015371] N89-10599
MISSILE DESIGN
Supersonic missile air intakes: Design and development criteria N89-10031
Guidance and control systems simulation and validation techniques [AGARD-AG-273] N89-10048
Comparison of statistical digital simulation methods N89-10049
A generic seeker simulation for the evaluation of active RF guidance systems N89-10050
Hellfire system model validation N89-10057
MISSILES
Model results for a proposed tactical missile training site lightning protection system N89-10477
MISSION PLANNING
Using full-mission simulation for human factors research in air transport operations [NASA-TM-88330] N89-10037
The mission operations planning assistant N89-10066
AUTOPLAN: A PC-based automated mission planning tool N89-10067
Expert systems tools for Hubble Space Telescope observation scheduling N89-10081
Maintaining consistency between planning hierarchies: Techniques and applications N89-10084
Summary of DSN (Deep Space Network) reimbursable launch support N89-10211

Solid earth mission study. Volume 3: Program planning report
[ESA-CR(P)-2626-VOL-3] N89-10399

MIXING
Turbofan forced mixer lobe flow modeling. Part 3: Application to augment engines
[NASA-CR-4147] N89-10025
Physics and technology for the in-situ investigation of properties of materials
[AD-A195498] N89-10145

MIXTURES
Adhesive blends and multi-layered structures comprising the adhesive blends
[EP-PATENT-0-258-990-A1] N89-10174
Computer simulation of absorption heat pump using aqueous lithium bromide and ternary nitrate mixtures
[DE88-013353] N89-10249

MODELS
Phase 4 static tests of the J-97 powered, external augmentor V/STOL model at the NASA, Ames Research Center, November 1983
[NASA-CR-177395] N89-10028
Vibration, performance, flutter and forced response characteristics of a large-scale propfan and its aeroelastic model
[NASA-TM-101322] N89-10043
Chemoviscosity modeling for thermosetting resin systems, part 3
[NASA-CR-181718] N89-10132
A sintering model for SiC(sub)w/Si3N4 composites
[NASA-TM-101336] N89-10166
Integrating distributed homogeneous and heterogeneous databases: Prototypes, volume 3
[AD-A195852] N89-10668

MODULATION
A transition radiation experiment to measure the electron beam modulation induced by the free electron laser: A design study
[AD-A195169] N89-10275
Laboratory capacity modulation experiments, analyses and validation
[DE88-012930] N89-10408

MODULATORS
Crossatron switch as thyratron replacement in high repetition rate, high average power modulators
[DE88-013706] N89-10230

MOLDING MATERIALS
Directional spectral emissivity measurements on a ceramic mold material
[DE88-015407] N89-10167

MOLECULAR CLOUDS
Global properties of molecular clouds and the interstellar medium in galaxies N89-10776

MOLECULAR RELAXATION
Vibrational relaxation processes in CO2-N2-H2O laser systems
[AD-A196211] N89-10273

MOLECULAR STRUCTURE
High resolution infrared spectroscopy of carbon dioxide and nitrous oxide at elevated temperatures
[AD-A196317] N89-10146
Pressure studies of protein dynamics
[AD-A192386] N89-10523

MOLECULES
Thermodynamic properties by non-calorimetric methods: Progress report
[DE88-015422] N89-10660

MOMENT DISTRIBUTION
An investigation into force-moment calibration techniques applicable to a magnetic suspension and balance system
[NASA-CR-181695] N89-10061
Moment exerted on a coning projectile by a spinning liquid in a cylindrical cavity containing a porous medium
[AD-A195291] N89-10239

MOMENTS
Moment exerted on a coning projectile by a spinning liquid in a cylindrical cavity containing a porous medium
[AD-A195291] N89-10239

MONITORS
The load shedding advisor: An example of a crisis-response expert system N89-10073
Monitoring lightning activity in South Africa with a VLF single-station technique: Comparison with meteosat infrared data N89-10480
The SAFIR lightning monitoring and warning system, applications to aerospace activities N89-10481

MONTE CARLO METHOD
What makes thunderbolts zig and zag N89-10434
Statistical evaluation of PACSTAT random number generation capabilities
[DE88-012754] N89-10556
Parallel processors for planning under uncertainty
[DE88-016184] N89-10571
Comparison of plotting methods used on normal probability paper
[NAL-TR-951] N89-10584
A fast Monte-Carlo cross-validation procedure for large least squares problems with noisy data
[RR-687-M] N89-10591

MORPHOLOGY
Characterization of layers created using surface modification techniques
[DE88-011918] N89-10651

MOUNTAINS
Spectral characterization of forest targets in mountainous zones on Thematic Mapper images N89-10328
Applications of a three-dimensional finite element model to mountain-valley flows
[DE88-008898] N89-10412
Some observations and analysis of atmospheric electricity over non-uniform high terrain N89-10489

MULTICHANNEL COMMUNICATION
Effects of switch leakages upon Nimbus-7 SMMR calibration
[NASA-CR-180792] N89-10115

MULTIPHASE FLOW
Laser velocimeter measurements of solids in multiphase flow
[DE88-011611] N89-10251
Discrete modeling considerations in multiphase fluid dynamics
[DE88-015188] N89-10256

MULTIPROCESSING (COMPUTERS)
Multiprogramming and the performance of parallel programs
[NASA-CR-183238] N89-10531
Fault tolerance computing: Constraints in using multiprocessor synchronization by static preplanned scheduling
[CNES-CT/DRT/TIT/TB-096] N89-10573

MULTIPROGRAMMING
Multiprogramming and the performance of parallel programs
[NASA-CR-183238] N89-10531

MULTISPECTRAL BAND SCANNERS
Effects of switch leakages upon Nimbus-7 SMMR calibration
[NASA-CR-180792] N89-10115
Applications of LANDSAT (TM and MSS) data for an estimation of rangeland conditions in semiarid and arid areas of northern Kenya
[DFVLR-FB-88-18] N89-10404

MULTISPECTRAL PHOTOGRAPHY
Development of MOMS to a future multiband and stereoscopic sensor N89-10391
Applications of LANDSAT (TM and MSS) data for an estimation of rangeland conditions in semiarid and arid areas of northern Kenya
[DFVLR-FB-88-18] N89-10404

MYOGLOBIN
Pressure studies of protein dynamics
[AD-A192386] N89-10523

N

NACELLES
Lightning tests to measure the bulk current levels associated with the electronic engine control of a turboprop commuter transport N89-10457

NASA PROGRAMS
Living in space, book 2, levels D, E, F
[NASA-EP-223] N89-10522

NASA SPACE PROGRAMS
NASA's future land remote sensing program N89-10393

NATURAL GAS
Basic research on natural gas combustion phenomena-catalytic combustion
[PB88-214606] N89-10142

NATURAL LANGUAGE (COMPUTERS)
A natural language query system for Hubble Space Telescope proposal selection N89-10083
UNITRAN (universal translator): A principle-based approach to machine translation
[AD-A195281] N89-10675

NAVIER-STOKES EQUATION
Navier-Stokes simulation of transonic wing flow fields using a zonal grid approach
[NASA-TM-100039] N89-10022
La Recherche Aerospatiale, Bimonthly Bulletin, Number 1987-4, 239/July-August
[ESA-TT-1088] N89-10026
La Recherche Aerospatiale, Bimonthly Bulletin, number 1987-6, 241/November-December
[ESA-TT-1102] N89-10030
Modification of the unsteady flow field predicted by transonic small distrubance equations using a Navier-Stokes solution of the steady flow field N89-10241
A finite element formulation for incompressible, conjugate, viscous/porous flow problems
[DE88-007113] N89-10254
Programming the Navier-Stokes computer: An abstract machine model and a visual editor
[NASA-CR-181691] N89-10560

NAVIGATION AIDS
PSA: A program to streamline orbit determination for launch support operations N89-10189

NEAR FIELDS
Adequacy of the transmitted near-field techniques for measuring optical fiber core diameter N89-10619

NEGATIVE RESISTANCE DEVICES
A 32-GHz reflected-wave maser amplifier with wide instantaneous bandwidth N89-10198

NEON
Neon puffing experiments in the JIPP T-IIU tokamak
[IPPJ-870] N89-10632

NEUTRON STARS
Research in nuclear astrophysics: Stellar collapse and supernovae
[DE88-015267] N89-10778

NEW GUINEA (ISLAND)
The lightning flash counter: Papua New Guinean experience N89-10491

NICKEL
Oxygen electrode bifunctional electrocatalyst NiCo2O4 spinel
[NASA-TM-100947] N89-10409

NICKEL ALLOYS
Thermodynamic analysis of compatibility of several reinforcement materials with beta phase NiAl alloys
[NASA-CR-4171] N89-10131
Micromechanisms of deformation and fracture in ordered intermetallic alloys. 1: Strengthening mechanisms
[DE88-015382] N89-10159
Premartensitic microstructures as seen in the high-resolution electron microscope: A study of a NiAl alloy
[DE88-008042] N89-10160
A study of the fatigue behavior of small cracks in nickel-base superalloys
[AD-A195489] N89-10161
Engineering processing and properties of nickel aluminides
[DE88-011019] N89-10164

NICKEL COMPOUNDS
Theoretical studies of grain boundaries in Ni, Al and Ni3Al with and without boron
[DE88-014323] N89-10152

NIMBUS 7 SATELLITE
Effects of switch leakages upon Nimbus-7 SMMR calibration
[NASA-CR-180792] N89-10115
Monitoring seasonal variations of soil moisture and vegetation cover using satellite microwave radiometry N89-10378

NIOBIUM
Synthesis and study of materials for superconducting electronics
[AD-A195279] N89-10649

NITROGEN PLASMA
Spectral characteristics of arc-heated low density plasma flows (2) nitrogen plasma
[NAL-TR-952] N89-10639

NOAA SATELLITES
Analysis of the contribution of the atmosphere to water reflectance in the first two channels of the NOAA satellites AVHRR N89-10330
Analysis of directional effects on NOAA AVHRR N89-10341

NOISE GENERATORS
Numerical simulation of the explosives effects of two closely spaced pyrotechnic pods
[MRL-R-1095] N89-10177

NOISE MEASUREMENT
Measurement of vertical velocity using clear-air Doppler radars
[AD-A195344] N89-10427

NOISE REDUCTION
Simultaneous S- and X-band uplink-downlink performance at DSS 13 N89-10194

NOISE TEMPERATURE
A 32-GHz reflected-wave maser amplifier with wide instantaneous bandwidth N89-10198

NONDESTRUCTIVE TESTS
Wheel performance evaluation. Phase 1: Analysis
[DOT/FAA/CT-88/16] N89-10041
Physical principles of ultrasonic non-destructive evaluation of advanced composites
[NASA-CR-180225] N89-10129

NONFLAMMABLE MATERIALS
Final review of US Army fire-resistant fuel program
[AD-A194304] N89-10176
NONLINEAR EVOLUTION EQUATIONS
Dimensional deformations of integrable systems: An approach to integrability in multidimensions, part 1
[PREPRINT-586] N89-10585
NONLINEAR OPTICS
Nonlinear optical interactions involving the real Gaussian field
[DE88-012399] N89-10276
NONLINEAR SYSTEMS
Recent developments in structural sensitivity analysis
[NASA-TM-100668] N89-10300
The effect of a gap nonlinearity on recursive parameter identification algorithms
[AD-A196020] N89-10557
Initial evolution of nonlinear magnetic islands in high temperature plasmas
[DE88-012346] N89-10636
NONLINEARITY
Nonlinear finite element analysis for plastic deformation by local random yielding N89-10298
The effect of a gap nonlinearity on recursive parameter identification algorithms
[AD-A196020] N89-10557
Nonlinear spin acceptance in electron storage rings
[CEBAF-PR-88-009] N89-10614
Nonlinear magnetohydrodynamics
[DE88-015703] N89-10644
NONOSCILLATORY ACTION
Non-oscillatory central differencing for hyperbolic conservation laws
[NASA-CR-181709] N89-10582
NONPARAMETRIC STATISTICS
Smoothing spatial data by estimating mean local variance
[AD-A195302] N89-10593
NORMALIZING (STATISTICS)
The normalization of a soil brightness index for the study of changes in soil conditions N89-10370
NOVAE
Observations of classical novae in outburst N89-10708
Observations and simulations of nova Vul 1984 no. 2: A nova with ejecta rich in oxygen, neon, and magnesium N89-10709
Observations and simulations of recurrent novae: U Sco and V394 CrA N89-10710
Optical and ultraviolet observations of nova Vul 1987 N89-10711
Ultraviolet observations of LMC nova 1988 N89-10712
UV and optical line emission from the shell of the old nova GK Persei N89-10714
NOZZLE DESIGN
Normal force coefficient of supersonic flows over conical flare, cone-cylinder and conical boattails
[NAL-TR-949] N89-10021
Standardization of the carbon-phenolic materials and processes. Vol. 2: Test methods and specifications
[NASA-CR-183227] N89-10033
Standardization of the carbon-phenolic materials and processes. Vol. 1: Experimental studies
[NASA-CR-183226] N89-10127
NOZZLE FLOW
Spectral characteristics of arc-heated low density plasma flows (1) argon plasma
[NAL-TR-954] N89-10642
NUCLEAR ASTROPHYSICS
Research in nuclear astrophysics: Stellar collapse and supernovae
[DE88-015267] N89-10778
NUCLEAR FUSION
Adventures in magnetohydrodynamics
[IPPJ-862] N89-10629
NUCLEAR MAGNETIC RESONANCE
Structure of amorphous silicon alloy films
[DE88-001167] N89-10654
NUCLEAR POWER PLANTS
Effect of a 12-hour/day shift on performance
[DE88-013184] N89-10521
NUCLEAR RESEARCH
An electromagnetic calorimeter for a beauty factory
[NOTA-INTERNA-905] N89-10260
NUCLEAR WEAPONS
Military uses of space
[DE88-015053] N89-10597
SDI (Strategic Defense Initiative): Myth or reality
[DE88-015059] N89-10598
NUMERICAL ANALYSIS
Direct Numerical Simulations (DNS) of an unpremixed turbulent jet flame
[AD-A196128] N89-10149
An analysis of an implicit factored scheme for simulating shock waves
[AR-005-231] N89-10252
Numerical analysis of laminar and turbulent incompressible flows using the finite element Fluid Dynamics Analysis Package (FIDAP)
[NASA-CR-179390] N89-10253
Geometric imperfections in plated structures subject to interaction between buckling modes
[PB88-200902] N89-10296
An algorithm for unsteady flows with strong convection
[NASA-TM-100828] N89-10575
On high resolution schemes for three-dimensional Euler equations
[NAL-TR-950T] N89-10581
NUMERICAL CONTROL
Issues, concerns, and initial implementation results for space based telerobotic control N89-10091
A shared position/force control methodology for teleoperation N89-10092
NUTRITION
Living in space, book 2, levels D, E, F
[NASA-EP-223] N89-10522

O

OBJECT PROGRAMS
Orca: A language for distributed object-based programming
[PB88-208533] N89-10529
Object-oriented approach to integrating database semantics, volume 4
[AD-A195853] N89-10672
OCEAN BOTTOM
Study of biological processes on the US North Atlantic slope and rise, volume 2
[PB88-196514] N89-10511
Joint CGS-AOML (Charting and Geodetic Service-Atlantic Oceanographic and Meteorological Laboratory) acoustical bottom echo-formation research. 1: Literature search and initial modelling results
[PB88-202007] N89-10512
Study of biological processes on the US North Atlantic slope and rise. Volume 1: Executive summary
[PB88-196522] N89-10517
The Paleo-ocean of Mars N89-10783
OCEAN CURRENTS
EPOCS (Equatorial Pacific Ocean Climate Studies) moored temperature, current and wind measurements: 0 deg, 140 deg W, May-June, 1987
[PB88-219415] N89-10509
Turbulent diffusion of ocean bubbles
[PB88-212816] N89-10513
OCEAN DATA ACQUISITIONS SYSTEMS
A new lidar system for applications over land and sea N89-10347
OCEAN SURFACE
A three degree-of-freedom description of the ocean surface for microwave remote sensing of wave height and wind friction velocity N89-10314
The use of the complex correlation function in the recovery of ocean wave spectra from SAR images N89-10315
An approximative model for the microwave brightness temperature scattered by a rough open ocean surface N89-10344
OCEAN TEMPERATURE
EPOCS (Equatorial Pacific Ocean Climate Studies) moored temperature, current and wind measurements: 0 deg, 140 deg W, May-June, 1987
[PB88-219415] N89-10509
OCEANOGRAPHY
High-resolution spectroscopy for remote sensing of ocean and atmosphere N89-10352
Study of biological processes on the US North Atlantic slope and rise, volume 2
[PB88-196514] N89-10511
Model-data comparisons for the 1982-83 El Nino: The XBT tracks
[PB88-221668] N89-10514
Drifting buoy data from the Equatorial Pacific for the period January 1, 1984 through May 31, 1985
[PB88-212824] N89-10516
Study of biological processes on the US North Atlantic slope and rise. Volume 1: Executive summary
[PB88-196522] N89-10517
OIL POLLUTION
Time-resolved laser fluorescensing: Trends and applications N89-10346
OKLAHOMA
Lightning in mesoscale convective complexes on 3-5 June 1985 in Oklahoma and Kansas N89-10471
OLIVINE
Chemical frost weathering of olivine: Experimental study and implications N89-10793
OMEGA NAVIGATION SYSTEM
Scientific ballooning in Brazil
[INPE-4602-PRE/1325] N89-10018
ON-LINE SYSTEMS
An evaluation of online database selection by a gateway system with artificial intelligence techniques N89-10667
ONBOARD DATA PROCESSING
Spacelab Data Processing Facility (SLDPF) quality assurance expert systems development N89-10079
OPERATING SYSTEMS (COMPUTERS)
Open control/display system for a telerobotics work station N89-10089
OPERATOR PERFORMANCE
A university teaching simulation facility N89-10088
Effect of a 12-hour/day shift on performance
[DE88-013184] N89-10521
OPERATORS (MATHEMATICS)
Block Toeplitz operators with rational symbols
[PB88-202890] N89-10587
OPTICAL BISTABILITY
Optical bistability in semiconductor waveguides N89-10620
OPTICAL COMMUNICATION
Design of an optical PPM communication link in the presence of component tolerances N89-10200
Atmospheric propagation effects relevant to optical communications N89-10201
OPTICAL COMPUTERS
Architecture studies and system demonstrations for optical parallel processor for Al and Nl
[AD-A195480] N89-10616
OPTICAL DATA STORAGE MATERIALS
Analysis of methods for detecting focus error in optical data storage systems N89-10617
OPTICAL EMISSION SPECTROSCOPY
High-resolution spectroscopy for remote sensing of ocean and atmosphere N89-10352
OPTICAL EQUIPMENT
An ion-optical bench for testing ion source lenses
[DE88-013186] N89-10606
OPTICAL FIBERS
Adequacy of the transmitted near-field techniques for measuring optical fiber core diameter N89-10619
OPTICAL MEASUREMENT
Antenna pointing compensation based on precision optical measurement techniques N89-10197
OPTICAL MEASURING INSTRUMENTS
Optical sensors for the measurement of electric current and voltage
[PB88-208467] N89-10233
An optical sensor for the non-interactive detection of weak electric fields N89-10263
Measurements of the velocity change of a lightning return stroke with height N89-10442
OPTICAL MEMORY (DATA STORAGE)
Analysis of methods for detecting focus error in optical data storage systems N89-10617
OPTICAL POLARIZATION
Nonlinear optical interactions involving the real Gaussian field
[DE88-012399] N89-10276
A polarisation study of spiral galaxies N89-10679
OPTICAL PROPERTIES
Influence of boundary surface roughness, order effects and dopants on optical properties of InP based metal organic gas phase epitaxy (MOCVD) heterostructure
[ETN-88-92986] N89-10646
PECVD (Plasma Enhanced Chemical Vapor Deposition) diamond thin films for research instrumentation
[AD-A195443] N89-10652
OPTICAL RADAR
A new lidar system for applications over land and sea N89-10347
OPTICAL REFLECTION
Phase conjugate reflecting media
[EP-PATENT-0-243-130-A1] N89-10622
OPTICAL THICKNESS
Analysis of the contribution of the atmosphere to water reflectance in the first two channels of the NOAA satellites AVHRR N89-10330
Optical thickness of the Olympus cloud N89-10808
OPTIMAL CONTROL
Solution of two-point boundary value problems in optimal maneuvers of flexible vehicles N89-10114
OPTIMIZATION
Validation of a pair of computer codes for estimation and optimization of subsonic aerodynamic performance of simple hinged-flap systems for thin swept wings
[NASA-TP-2828] N89-10024
Parallel processors for planning under uncertainty
[DE88-016184] N89-10571

Optimal simulations by butterfly networks: Extended abstract
[AD-A195168] N89-10572

ORBIT CALCULATION
PRIMORB: Preliminary orbit with two positions
[CNES-CT/DTI/MS/AE/072] N89-10107
CARTEL: A method to calibrate S-band ranges with geostationary satellites. Results of orbit determination
[CNES-CT/DTI/MS/AE/124] N89-10108
ZOOM orbitography software: On the Givens method. Presentation and software implementation evaluation for least square problems
[CNES-CT/DTI/MS/AE/219] N89-10109
Precise orbit determination for NASA's earth observing system using GPS (Global Positioning System)
N89-10188
PSA: A program to streamline orbit determination for launch support operations N89-10189

ORBIT TRANSFER VEHICLES
Orbit transfer rocket engine technology program. Phase 2: Advanced engine study
[NASA-CR-179602] N89-10119

ORBITAL MANEUVERS
Orbit transfer rocket engine technology program. Phase 2: Advanced engine study
[NASA-CR-179602] N89-10119

ORBITAL MECHANICS
PRIMORB: Preliminary orbit with two positions
[CNES-CT/DTI/MS/AE/072] N89-10107
Compilation of methods in orbital mechanics and solar geometry
[NASA-RP-1204] N89-10420
Upper-atmosphere zonal winds from satellite orbit analysis: An update
[RAE-TR-87058] N89-10507

ORBITAL POSITION ESTIMATION
Precise orbit determination for NASA's earth observing system using GPS (Global Positioning System)
N89-10188

ORBITAL SERVICING
Orbit transfer rocket engine technology program. Phase 2: Advanced engine study
[NASA-CR-179602] N89-10119
Rechargeable metal hydrides for spacecraft application
[NASA-TM-4076] N89-10184

ORBITAL VELOCITY
Technology issues associated with fueling the national aerospace plane with slush hydrogen
[NASA-TM-101386] N89-10123

ORGANIC COMPOUNDS
Thermodynamic properties by non-calorimetric methods: Progress report
[DE88-015422] N89-10660

ORGANIC MATERIALS
A preliminary review of organic materials single crystal growth by the Czochralski technique
[NASA-TM-100341] N89-10856

ORIFICE FLOW
Numerical study of the entrance flow and its transition in a curcular pipe
[ISAS-RN-626] N89-10250

OROGRAPHY
The German Front Experiment 1987: Observations and preliminary results
[DFVLR-FB-88-21] N89-10508

OSCILLATIONS
An adaptive pseudospectral method for discontinuous problems
[NASA-CR-181717] N89-10583
Gas-contact cooling for VUV laser oscillation in recombining plasmas
[IPPJ-881] N89-10631

OSCILLATORS
Design and performance of the SSVCO
[DE88-012435] N89-10232
Research on a two-stage free electron laser oscillator
[AD-A195339] N89-10278

OVERVOLTAGE
Lightning and surge protection of large ground facilities N89-10474

OXYGEN
Oxygen electrode bifunctional electrocatalyst NiCo2O4 spinel
[NASA-TM-100947] N89-10409

OXYGEN SPECTRA
IUE observations of oxygen-rich supernova remnants
N89-10699

OZONE
Vertical O(sub 3) distribution as a diagnostic for eddy diffusion profile N89-10821

P

PACIFIC OCEAN
EPOCS (Equatorial Pacific Ocean Climate Studies) moored temperature, current and wind measurements: 0 deg, 140 deg W, May-June, 1987
[PB88-219415] N89-10509
Drifting buoy data from the Equatorial Pacific for the period January 1, 1984 through May 31, 1985
[PB88-212824] N89-10516

PACKET SWITCHING
Integrated switching networks: A performance study
N89-10567

PAINTS
On a surface mounted transmission line configuration for aperture testing N89-10458

PALEOCLIMATOLOGY
Is regolith absorbtion the explanation for the transition from early to present Mars climate N89-10788
Release of magmatic water on Mars: Estimated timing and volumes N89-10790
The direction of water transport on Mars: A possible pumping mechanism N89-10798
Climatic effects of enhanced CO2 levels in Mars early atmosphere N89-10799
Influence of polar-cap albedo on past and current Martian climate N89-10801
Geomorphic evidence for ancient seas on Mars
N89-10813
Partitioning of carbon dioxide between the atmosphere and lithosphere on early Mars N89-10816
Implications of isotopic signatures of noble gases for the origin and evolution of terrestrial atmospheres
N89-10817

PARADOXES
Free choice permissions and Ross's paradox: Internal versus external nondeterminism
[PB88-202874] N89-10588

PARALLEL PROCESSING (COMPUTERS)
Concurrent algorithms for numerical computation on hypercube computer
[AD-A195502] N89-10558
Factoring very large numbers using a massively parallel computer
[DE88-014247] N89-10559
Programming the Navier-Stokes computer: An abstract machine model and a visual editor
[NASA-CR-181691] N89-10560
Very large parallel data flow
[AD-A196205] N89-10568
Parallel processors for planning under uncertainty
[DE88-016184] N89-10571
Fault tolerance computing: Constraints in using multiprocessor synchronization by static preplanned scheduling
[CNES-CT/DRT/TIT/TB-096] N89-10573
Free choice permissions and Ross's paradox: Internal versus external nondeterminism
[PB88-202874] N89-10588
Architecture studies and system demonstrations for optical parallel processor for Al and Nl
[AD-A195480] N89-10616

PARALLEL PROGRAMMING
Multiprogramming and the performance of parallel programs
[NASA-CR-183238] N89-10531
Software design research at DARPA N89-10546

PARAMETER IDENTIFICATION
Deep space tracking in local reference frames
N89-10187
On the problem of modeling for parameter identification in distributed structures
[NASA-CR-182739] N89-10291
The effect of a gap nonlinearity on recursive parameter identification algorithms
[AD-A196020] N89-10557
An investigation of new methods for estimating parameter sensitivities
[NASA-CR-183195] N89-10586

PARAMETERIZATION
Retrieving vegetation and soil parameters from radar measurements N89-10321

PARSING ALGORITHMS
UNITRAN (universal translator): A principle-based approach to machine translation
[AD-A195281] N89-10675

PARTICLE BEAMS
Simulation of plasma erosion opening switches
[DE88-014425] N89-10229
Research on a two-stage free electron laser oscillator
[AD-A195339] N89-10278
Directed energy concepts for strategic defense
[DE88-015050] N89-10596

PARTICLE COLLISIONS
Use of the time projection chamber for measuring heavy ion collisions
[MPE-PAE/EXP-EL-191] N89-10611

PARTICLE SIZE DISTRIBUTION
On the abundance of micron-sized particles in Saturn's A and B rings N89-10692

PARTICLES
An interactive program for estimating extinction and scattering properties of most particulate clouds
[MRL-R-1123] N89-10218

PAYLOADS
AUTOPLAN: A PC-based automated mission planning tool N89-10067

PECULIAR STARS
Au II in IUE spectra of chemically peculiar stars
N89-10766
Validity of the classification of UV gallium stars
N89-10767
Detected UV variability in the IUE spectra of the Ap-Si star HD 25823 N89-10768

PERFORMANCE PREDICTION
AGARD manual on aeroelasticity in axial-flow turbomachines. Volume 2: Structural dynamics and aeroelasticity
[AGARD-AG-298-VOL-2] N89-10006
Guidance and control systems simulation and validation techniques
[AGARD-AG-273] N89-10048
Simulation validation experience: PATRIOT guidance system N89-10055
Design of an optical PPM communication link in the presence of component tolerances N89-10200

PERFORMANCE TESTS
Fan flutter test N89-10014
Vibration, performance, flutter and forced response characteristics of a large-scale propfan and its aeroelastic model
[NASA-TM-101322] N89-10043
A comparative evaluation of RPD (Rotary Particle Depositor) and ferrographic diagnostic methods for turbine engine lubricant samples
[AD-A196207] N89-10044
Functional mock-up tests of the flight control system of the NAL QSTOL research aircraft: Planning and mechanical system test
[NAL-TR-944] N89-10047
Digital simulation techniques for end game phenomena N89-10051
Fabrication and test of a carbon-carbon composite combustion chamber for a low thrust storable engine
[NAL-TR-946] N89-10118
The performance of alternate fuels in general aviation aircraft
[DOT/FAA/CT-88/13] N89-10175
Free-piston Stirling engine development
[PB88-220025] N89-10286
Lightning tests on an all-composite helicopter
N89-10452
LSZ-850 lightning sensor system N89-10487
Statistical evaluation of PACSTAT random number generation capabilities
[DE88-012754] N89-10556

PERMAFROST
Evidence for glaciation in Elysium N89-10781
The thermal properties of Martian surface materials at high lattitudes: Possible evidence for permafrost
N89-10812

PERMUTATIONS
Storage and computationally efficient permutations of factorized covariance and square-root information arrays
N89-10206

PEROVSKITES
Basic research on natural gas combustion phenomena-catalytic combustion
[PB88-214606] N89-10142

PERSONAL COMPUTERS
AUTOPLAN: A PC-based automated mission planning tool N89-10067

PERSONNEL
Effect of a 12-hour/day shift on performance
[DE88-013184] N89-10521

PERTURBATION
Resonant excitation of spatial perturbations in a boundary layer in the presence of a pressure gradient
[NASA-TT-20305] N89-10248

PERTURBATION THEORY
Solution of ill-posed problems by means of truncated SVD (Singular Value Decomposition)
[DE88-013510] N89-10238

PETN
Single crystal orientation effects in shock initiation of PETN explosive
[DE88-014406] N89-10182

PH FACTOR
A new method of determining acid base strength distribution and a new acidity-basicity scale for solid catalysts: The strongest point, HO
[NASA-TT-20334] N89-10141

PHASE CONJUGATION
Phase conjugate reflecting media
[EP-PATENT-0-243-130-A1] N89-10622

PHASE DEMODULATORS
Communications to National Microwave Days
[CNES-CT/DRT/TIT/HY/87/130] N89-10237

PHASE TRANSFORMATIONS
Two-dimensional spatially resolved Raman spectroscopy of solid materials
[DE88-014867] N89-10138
Premartensitic microstructures as seen in the high-resolution electron microscope: A study of a NiAl alloy
[DE88-008042] N89-10160
Influence of boundary surface roughness, order effects and dopants on optical properties of InP based metal organic gas phase epitaxy (MOCVD) heterostructure
[ETN-88-92986] N89-10646
The detection of conformational disorder by thermal analysis
[DE88-012932] N89-10657

PHASED ARRAYS
Phasing the antennas of the Very Large Array (VLA) for reception of telemetry from Voyager 2 at Neptune encounter N89-10207

PHENOLIC RESINS
Standardization of the carbon-phenolic materials and processes. Vol. 2: Test methods and specifications
[NASA-CR-183227] N89-10033
Standardization of the carbon-phenolic materials and processes. Vol. 1: Experimental studies
[NASA-CR-183226] N89-10127

PHOBOS
Phobos lander coding system: Software and analysis N89-10208
Phobos and Deimos: A base for sampling the Martian past N89-10819

PHOTOCHEMICAL REACTIONS
Photochemical weathering and contemporary volatile loss on Mars N89-10795

PHOTOELECTROCHEMICAL DEVICES
Photoelectrochemical fabrication of spectroscopic diffraction gratings
[NASA-CR-180786] N89-10615

PHOTOELECTROCHEMISTRY
Photoelectrochemical fabrication of spectroscopic diffraction gratings
[NASA-CR-180786] N89-10615

PHOTOGEOLOGY
Comparative geological evolution of different remote sensing data of the Hoggar Mountains (Algeria) N89-10385
Digital analysis of MOMS-1, LANDSAT TM, and SPOT data of the Nakuru area (Kenya) N89-10386

PHOTOGRAPHS
What makes thunderbolts zig and zag N89-10434

PHOTOGRAPHY
Factors influencing the detection of voltage sparks by flammable gas and optical techniques N89-10465

PHOTOINTERPRETATION
Identifying the reforested areas utilizing the SPOT satellite data
[INPE-4624-PRE/1343] N89-10396
What makes thunderbolts zig and zag N89-10434

PHOTONS
Compact imaging spectrometer for induced emissions
[NASA-CR-183187] N89-10264

PHOTOSPHERE
IUE observations of a hot DAO white dwarf: Implications for diffusion theory and photospheric stratification N89-10733

PHOTOVOLTAIC CELLS
Solid State Photovoltaic Research Branch
[DE88-001179] N89-10410

PHOTOVOLTAIC EFFECT
Photovoltaics for high capacity space power systems
[NASA-TM-101341] N89-10122

PHYSICAL EXERCISE
Modulation of human plasma fibronectin levels following exercise
[AD-A192674] N89-10519

PHYSIOLOGICAL EFFECTS
A review of medical aspects of lightning injury N89-10463

PIPE FLOW
Numerical study of the entrance flow and its transition in a curcular pipe
[ISAS-RN-626] N89-10250

PISTONS
Free-piston Stirling engine development
[PB88-220025] N89-10286

PITCHING MOMENTS
Measurement of aerodynamic characteristics of a hang-glider-wing by ground run tests using a test vehicle
[NAL-TR-953] N89-10004

PLANE WAVES
Resonant excitation of spatial perturbations in a boundary layer in the presence of a pressure gradient
[NASA-TT-20305] N89-10248

PLANETARY ATMOSPHERES
IUE observations of planetary atmospheres N89-10687

PLANETARY COMPOSITION
Martian volcanism: A review N89-10785
Volatile inventory of Mars-2: Primordial sources and fractionating processes N89-10814
Water on Mars N89-10822
Mars regolith versus SNC meteorites: Evidence for abundant crustal carbonates N89-10823
Absorption of the Martian regolith: Specific surface area and missing CO(sub 2) N89-10824
Thermal properties of channels in the Aeolis Quadrangle: Topographic traps for Aeolian materials N89-10825

PLANETARY CRUSTS
Mars: Crustal pore volume, cryospheric depth, and the global occurrence of groundwater N89-10787

PLANETARY EVOLUTION
MECA Symposium on Mars: Evolution of its Climate and Atmosphere
[NASA-CR-182872] N89-10780
Evidence for glaciation in Elysium N89-10781
The Paleo-ocean of Mars N89-10783
Comets, volcanism, the salt rich regolith and cycling of volatiles on Mars N89-10786
Photochemical weathering and contemporary volatile loss on Mars N89-10795
Interannual differences in the regressions of the polar caps of Mars N89-10796
The observed day-to-day variability of Mars water vapor N89-10797
Areal and time distributions of volcanic formations on Mars N89-10800
Implications of isotopic signatures of noble gases for the origin and evolution of terrestrial atmospheres N89-10817
Phobos and Deimos: A base for sampling the Martian past N89-10819

PLANETARY MANTLES
Partitioning of carbon dioxide between the atmosphere and lithosphere on early Mars N89-10816
Thermal properties of channels in the Aeolis Quadrangle: Topographic traps for Aeolian materials N89-10825

PLANETARY MAPPING
Martian surface physical properties to be derived by radar altimeter on the Mars observer spacecraft N89-10789

PLANETARY WAVES
Seasonal wind variations in the Martian subtropics N89-10807

PLANNING
Plan recognition in GRAPPLE: An intelligent assistant for the process of programming N89-10555
Parallel processors for planning under uncertainty
[DE88-016184] N89-10571

PLANT STRESS
Stress detection in mixed coniferous-broadleaved forests from Airborne Imaging Spectrometer (AIS) data N89-10355

PLANTS (BOTANY)
Chromosomes and plant cell division in space
[NASA-CR-183213] N89-10516

PLASMA CONTROL
Neoclassical resonant-plateau transport in the noncircular equipotential surface of a tandem mirror
[IPPJ-879] N89-10627
Effect of double-shell structure on reduction of field errors in the STP-3(M) reversed-field pinch
[IPPJ-882] N89-10640
Confinement and heating of high beta plasmas with emphasis on compact toroids
[DE88-015777] N89-10645
Beam assisted fabrication of 3-5/Si monolithic devices
[AD-A195479] N89-10655

PLASMA CURRENTS
Simulation of plasma erosion opening switches
[DE88-014425] N89-10229
Study of critical beta non-circular tokamak equilibria sustained in steady state by beam driven currents
[IPPJ-878] N89-10634
Marginal stability of ion-acoustic waves in a weakly collisional two-temperature plasma without a current
[AD-A195840] N89-10638
On the generation of runaway electrons and their impact to plasma facing components
[IPPJ-871] N89-10641

PLASMA DENSITY
Spectral characteristics of arc-heated low density plasma flows (1) argon plasma
[NAL-TR-954] N89-10642

PLASMA DIAGNOSTICS
A novel alignment technique for pointing and centering optical components
[DE88-015441] N89-10621
Laser diagnostics of gas discharge tubes
[DE88-008124] N89-10633
Confinement and heating of high beta plasmas with emphasis on compact toroids
[DE88-015777] N89-10645

PLASMA DYNAMICS
Simulation of plasma erosion opening switches
[DE88-014425] N89-10229

PLASMA HEATING
Time-resolved X-ray conversion efficiencies of laser-heated plasmas
[DE88-015456] N89-10637

PLASMA LAYERS
Experimental studies on the surface confined quiescent plasma at INPE
[INPE-4605-PRE/1328] N89-10630

PLASMA POTENTIALS
Structural instability of sheath potential distribution and its possible implications for the L/H transition in tokamak plasmas
[IPPJ-877] N89-10643

PLASMA RADIATION
Investigation of superradiant LDV markers and three-component velocity mapping
[AD-A195504] N89-10662

PLASMAS (PHYSICS)
Metallic materials as plasma facing components
[DE88-010103] N89-10628
Time-resolved X-ray conversion efficiencies of laser-heated plasmas
[DE88-015456] N89-10637
Effect of double-shell structure on reduction of field errors in the STP-3(M) reversed-field pinch
[IPPJ-882] N89-10640
Structural instability of sheath potential distribution and its possible implications for the L/H transition in tokamak plasmas
[IPPJ-877] N89-10643
PECVD (Plasma Enhanced Chemical Vapor Deposition) diamond thin films for research instrumentation
[AD-A195443] N89-10652

PLASTIC DEFORMATION
Nonlinear finite element analysis for plastic deformation by local random yielding N89-10298
Void collapse and void growth in crystalline solids N89-10421

PLASTIC FLOW
Void collapse and void growth in crystalline solids N89-10421

PLATEAUS
Sapping features of the Colorado Plateau: A comparative planetary geology field guide
[NASA-SP-491] N89-10401

PLATES (STRUCTURAL MEMBERS)
Structural dynamic characteristics of bladed assemblies N89-10009
Deformations and residual stresses induced in channel section columns by presetting and welding
[PB88-199971] N89-10292
Geometric imperfections in plated structures subject to interaction between buckling modes
[PB88-200902] N89-10296
Inelastic buckling analyses of beams, columns and plates using the spline finite strip method
[PB88-214291] N89-10299
Analysis of some low-order finite element schemes for Mindlin-Reissner and Kirchhoff plates
[PB87-175899] N89-10578

PLATES (TECTONICS)
Wilson cycle studies
[NASA-CR-183146] N89-10419

PLOTTING
Comparison of plotting methods used on normal probability paper
[NAL-TR-951] N89-10584

PODS (EXTERNAL STORES)
Numerical simulation of the explosives effects of two closely spaced pyrotechnic pods
[MRL-R-1095] N89-10177

POINT SPREAD FUNCTIONS
Comparative point-spread function calculations for the MOMS-1, Thematic Mapper and SPOT-HRV instruments N89-10379

POINTING CONTROL SYSTEMS
Antenna pointing compensation based on precision optical measurement techniques N89-10197

POLAR CAPS
Interannual differences in the regressions of the polar caps of Mars N89-10796
The direction of water transport on Mars: A possible pumping mechanism N89-10798
Influence of polar-cap albedo on past and current Martian climate N89-10801
The great dust storm of 1986 N89-10804
POLAR METEOROLOGY
MIZEX (marginal ice zone experiment) 87 meteorology atlas
[AD-A195361] N89-10506
POLARIMETERS
Coherent polarimetric signatures of coniferous trees: A survey N89-10307
POLARIZATION (SPIN ALIGNMENT)
Nonlinear spin acceptance in electron storage rings
[CEBAF-PR-88-009] N89-10614
POLLUTION MONITORING
Time-resolved laser fluorescensing: Trends and applications N89-10346
POLOIDAL FLUX
Effect of double-shell structure on reduction of field errors in the STP-3(M) reversed-field pinch
[IPPJ-882] N89-10640
POLYACETYLENE
Phase conjugate reflecting media
[EP-PATENT-0-243-130-A1] N89-10622
POLYETHER RESINS
Comparison of surface modifications of poly(ether urethanes) by chemical infusion and graft polymerization
[DE88-007887] N89-10172
POLYETHYLENE TEREPHTHALATE
Thermal transfer recording media
[NASA-TT-20322] N89-10262
POLYMER CHEMISTRY
Comparison of surface modifications of poly(ether urethanes) by chemical infusion and graft polymerization
[DE88-007887] N89-10172
POLYMER MATRIX COMPOSITES
Polymer composites
[EP-PATENT-0-232-138-A2] N89-10137
POLYMERIC FILMS
Thermal transfer recording media
[NASA-TT-20322] N89-10262
Phase conjugate reflecting media
[EP-PATENT-0-243-130-A1] N89-10622
POLYMERIZATION
Comparison of surface modifications of poly(ether urethanes) by chemical infusion and graft polymerization
[DE88-007887] N89-10172
POLYURETHANE RESINS
Comparison of surface modifications of poly(ether urethanes) by chemical infusion and graft polymerization
[DE88-007887] N89-10172
POROSITY
Physical principles of ultrasonic non-destructive evaluation of advanced composites
[NASA-CR-180225] N89-10129
POROUS MATERIALS
A finite element formulation for incompressible, conjugate, viscous/porous flow problems
[DE88-007113] N89-10254
POSITION (LOCATION)
Deep space tracking in local reference frames N89-10187
Breakdown characteristics of an isolated conducting object in a uniform electric field N89-10453
A lightning location system for the UK electricity supply industry N89-10482
Considerations for using lightning locating systems in performance evaluations of single-station lightning detection sensors N89-10488
Site errors of a magnetic direction finder for lightning flashes N89-10494
POSITION ERRORS
CARTEL: A method to calibrate S-band ranges with geostationary satellites. Results of orbit determination
[CNES-CT/DTI/MS/AE/124] N89-10108
POTATOES
Microwave backscatter from beets, peas and potatoes throughout the growing season N89-10309
POTENTIAL FLOW
Unsteady three-dimensional stall on a rectangular wing N89-10027
POTENTIAL THEORY
A potential theory for the steady separated flow about an aerofoil section
[ARL-AERO-R-176] N89-10005
POWDER METALLURGY
Engineering processing and properties of nickel aluminides
[DE88-011019] N89-10164
POWER LINES
Lightning and surge protection of large ground facilities N89-10474
A revised electrogeometric model for the termination of lightning strokes on ground objects N89-10476
PRASEODYMIUM
Electronic structure of the quenched superconductivity of materials Y(sub 1-x)Pr(sub x)Ba2Cu3O(sub 7-delta)
[DE88-014414] N89-10658
PRECIPITATION (METEOROLOGY)
Analysis and modeling of summertime convective cloud and precipitation structure over the southeastern United States
[NASA-CR-183192] N89-10498
PRECISION
Finite precision arithmetic in singular value decomposition architectures
[AD-A196188] N89-10589
PREDICTION ANALYSIS TECHNIQUES
An interactive program for estimating extinction and scattering properties of most particulate clouds
[MRL-R-1123] N89-10218
Introducing spectral data into a plant process model for improving its prediction ability N89-10324
PREDICTIONS
Digital simulation techniques for end game phenomena N89-10051
A filamentary method for calculating induced voltages within resistive structures in either the frequency or time domain N89-10484
PRESSURE DEPENDENCE
The tensile strength of glass shells
[DE88-013011] N89-10301
PRESSURE EFFECTS
Measurement of aerodynamic characteristics of a hang-glider-wing by ground run tests using a test vehicle
[NAL-TR-953] N89-10004
Normal force coefficient of supersonic flows over conical flare, cone-cylinder and conical boattails
[NAL-TR-949] N89-10021
Study on twin valveless pulse burner: Combustion stability and mixing patterns
[NAL-TR-955] N89-10144
The performance of alternate fuels in general aviation aircraft
[DOT/FAA/CT-88/13] N89-10175
Pressure studies of protein dynamics
[AD-A192386] N89-10523
Pressure effects on the electronic structure of 4f and 5f materials
[DE88-014149] N89-10650
PRESSURE GRADIENTS
Resonant excitation of spatial perturbations in a boundary layer in the presence of a pressure gradient
[NASA-TT-20305] N89-10248
PRESSURE OSCILLATIONS
Mars global atmospheric oscillations: Transients and dust storm relations N89-10820
PRESSURE PULSES
A water sound generator for pressure pulses of high energy
[MPIS-MITT-85-1987] N89-10604
PROBABILITY THEORY
Comparison of plotting methods used on normal probability paper
[NAL-TR-951] N89-10584
Inelastic ion-surface collisions. Ion neutralization on intermetallic surfaces
[AD-A196322] N89-10608
PROBLEM SOLVING
The load shedding advisor: An example of a crisis-response expert system N89-10073
Selection of investment strategies which are optimal for the implementation of software support environments N89-10542
PROCESS CONTROL (INDUSTRY)
Applications of process modelling to heat treatment of superalloys
[DE88-015445] N89-10157
PROCESS HEAT
Applications of process modelling to heat treatment of superalloys
[DE88-015445] N89-10157
PRODUCT DEVELOPMENT
Technical evaluation report on the Flight Mechanics Panel Symposium on Flight Vehicle Development Time and Cost Reduction
[AGARD-AR-244] N89-10001
PRODUCTION MANAGEMENT
Attitudes to the use of computerised information systems for production management in manufacturing industry: A survey
[TT-8706] N89-10670
PROFILOMETERS
Measuring in-situ soil surface roughness using a laser profilometer N89-10308
PROGRAM VERIFICATION (COMPUTERS)
ZOOM orbitography software: On the Givens method. Presentation and software implementation evaluation for least square problems
[CNES-CT/DTI/MS/AE/219] N89-10109
PROGRAMMING LANGUAGES
SPOCK: A tool for real time artificial intelligence
[NASA-TT-20357] N89-10574
Object-oriented approach to integrating database semantics, volume 4
[AD-A195853] N89-10672
PROJECT MANAGEMENT
Helicopter roll control effectiveness criteria program summary
[NASA-CR-177477] N89-10046
Deep space network resource scheduling approach and application N89-10070
Toward an expert project management system N89-10082
Project management assistant: What have we learned N89-10552
PROJECTILES
Moment exerted on a coning projectile by a spinning liquid in a cylindrical cavity containing a porous medium
[AD-A195291] N89-10239
PROLOG (PROGRAMMING LANGUAGE)
The load shedding advisor: An example of a crisis-response expert system N89-10073
PROPAGATION MODES
An investigation of the acoustic emission generated by various crack propagation modes in 304 stainless steel N89-10293
PROPELLANT COMBUSTION
Evaluation and mitigation of lightning hazards to the space shuttle Solid Rocket Motors (SRM) N89-10439
Transfer impedance measurements of the space shuttle Solid Rocket Motor (SRM) joints, wire meshes and a carbon graphite motor case N89-10440
PROPELLER BLADES
Vibration, performance, flutter and forced response characteristics of a large-scale propfan and its aeroelastic model
[NASA-TM-101322] N89-10043
PROPELLERS
The effect of front-to-rear propeller spacing on the interaction noise at cruise conditions of a model counterrotation propeller having a reduced diameter aft propeller
[NASA-TM-101329] N89-10603
PROPULSION
Design approaches and parameters for magnetically levitated transport systems
[DE88-014286] N89-10280
PROPULSION SYSTEM PERFORMANCE
Means for testing aerospace launcher structures
[ETN-88-93082] N89-10110
PROTECTION
Lightning standards for protection of ground electronic systems N89-10473
The interaction between lightning grounding systems and buried cables N89-10496
System protection from atmospheric electricity for aerostats with conducting tethers N89-10497
PROTECTIVE COATINGS
Fabrication and test of a carbon-carbon composite combustion chamber for a low thrust storable engine
[NAL-TR-946] N89-10118
Choice of coating and surface behavior of the hydrogen turbopump of the Vulcain engine
[ETN-88-93084] N89-10173
PROTEINS
Pressure studies of protein dynamics
[AD-A192386] N89-10523
Convection effects in protein crystal growth
[NASA-CR-179368] N89-10653
PROTOCOL (COMPUTERS)
A local area computer network expert system framework N89-10074
A meta-protocol architecture for connecting computer networks
[AD-A196319] N89-10570
PROTOPLANETS
Could icy impacts reconcile Venus with Earth and Mars N89-10810
PROTOTYPES
An expert system approach to astronomical data analysis N89-10080
Toward an expert project management system N89-10082
PROVING
Quadruplex digital flight control system assessment
[NASA-CR-182741] N89-10058
Knowledge based tools for knowledge-based systems N89-10550

A fast Monte-Carlo cross-validation procedure for large least squares problems with noisy data
[RR-687-M] N89-10591
PSYCHOLOGICAL EFFECTS
A review of medical aspects of lightning injury N89-10463
PSYCHOMETRICS
ORDMET3: An improved algorithm to find the maximum solution to a system of linear (in)Equalities
[PB88-208970] N89-10520
Performance assessment register
[AGARD-R-763] N89-10666
PULSE POSITION MODULATION
Design of an optical PPM communication link in the presence of component tolerances N89-10200
PULSES
Pulse combustor modeling: One dimensional wave-dynamic model utilizing dynamic injection and energy release submodels
[DE88-005369] N89-10150
PUMPS
Laser velocimeter measurements of solids in multiphase flow
[DE88-011611] N89-10251
PURITY
Sulfide corrosion of silver contacts during satellite storage
[AD-A196217] N89-10112
PUSHBROOM SENSOR MODES
Design of spectral bands for the German MOMS-2 sensor N89-10361
PYROTECHNICS
Semiconductor Bridge (SCB): A new method for the ignition of explosives and pyrotechnics
[DE88-011246] N89-10151
Numerical simulation of the explosives effects of two closely spaced pyrotechnic pods
[MRL-R-1095] N89-10177

Q

Q SWITCHED LASERS
Considerations and calculations for application of an optical amplifier as an end- and preamplifier
[ESA-TT-1004] N89-10625
QUADRATIC PROGRAMMING
An investigation of new methods for estimating parameter sensitivities
[NASA-CR-183195] N89-10586
QUALITY CONTROL
Spacelab Data Processing Facility (SLDPF) quality assurance expert systems development N89-10079
Statistical evaluation of PACSTAT random number generation capabilities
[DE88-012754] N89-10556
QUANTUM CHEMISTRY
Theoretical study of the dissociation energy and the red and violet band systems of CN
[NASA-TM-101190] N89-10610
QUANTUM EFFICIENCY
Techniques for remote sensing of life span and quantum yield of chlorophyll fluorescence in vivo N89-10351
QUANTUM ELECTRONICS
Studies of blackbody-pumped lasers
[NASA-CR-183214] N89-10277
QUANTUM THEORY
The inverse-square law and quantum gravity
[DE88-014332] N89-10663
QUARTZ LAMPS
Performance of multimirror quartzline lamps in a high-pressure, underwater environment
[NASA-TM-101374] N89-10269
QUASARS
Accretion disk models of quasars and active galactic nuclei N89-10777
QUENCHING
Electronic structure of the quenched superconductivity of materials Y(sub 1-x)Pr(sub x)Ba2Cu3O(sub 7-delta)
[DE88-014414] N89-10658
QUERY LANGUAGES
A natural language query system for Hubble Space Telescope proposal selection N89-10083

R

RADAR ANTENNAS
The Telecommunications and Data Acquisition Report --- Deep Space Network
[NASA-CR-183243] N89-10186
Relative planetary radar sensitivities: Arecibo and Goldstone N89-10209
RADAR CROSS SECTIONS
A radar reflector for microwave remote sensing instruments external calibration N89-10312
RADAR DATA
Digital recording of radar data in an aircraft
[PB88-209507] N89-10212
Evaluation of VARAN data in geology and geomorphology in the southeast of France N89-10313
RADAR DETECTION
Intracloud lightning as a precursor to thunderstorm microbursts N89-10490
RADAR HOMING MISSILES
Guidance and control systems simulation and validation techniques
[AGARD-AG-273] N89-10048
Range delay techniques for radar target simulators N89-10054
RADAR IMAGERY
Spaceborne SAR imaging of land, an opportunity for polyphase code
[ATES/DMA/RAD/002-86] N89-10226
Texture analysis in forest areas: High spectral resolution synthetic aperture radar data N89-10367
The Remote Atmospheric Probing Information Display (RAPID) system
[AD-A196314] N89-10500
RADAR MEASUREMENT
Retrieving vegetation and soil parameters from radar measurements N89-10321
RADAR REFLECTORS
A radar reflector for microwave remote sensing instruments external calibration N89-10312
RADAR SCATTERING
Microwave backscatter from beets, peas and potatoes throughout the growing season N89-10309
RADAR SIGNATURES
Proceedings of the 4th International Colloquium on Spectral Signatures in Remote Sensing
[ESA-SP-287] N89-10305
Evaluation of VARAN data in geology and geomorphology in the southeast of France N89-10313
AGRISAR'86: Contributing to signature research N89-10387
RADIANT FLUX DENSITY
Gravitational wave searches using the DSN (Deep Space Network) N89-10192
RADIATION DETECTORS
Gravitational wave searches using the DSN (Deep Space Network) N89-10192
RADIATION DISTRIBUTION
Acoustic radiation from plates driven by multi-point random forces N89-10602
RADIATION EFFECTS
Metallic materials as plasma facing components
[DE88-010103] N89-10628
RADIATION HARDENING
The Radiation-Hardened Integrated Circuit (RHIC) Laboratory: Pursuit of Class 1
[DE88-006640] N89-10062
Development of radiation hardened far IR detector arrays. Volume 1: Phase 2
[BF-R-65.641-2] N89-10623
Development of radiation hardened far IR detector arrays. Volume 2: Phase 3
[BF-R-65.641-3] N89-10624
RADIATION MEASUREMENT
Measurement of infrared horizon profiles from TT-500A sounding rocket
[NAL-TR-947] N89-10121
A transition radiation experiment to measure the electron beam modulation induced by the free electron laser: A design study
[AD-A195169] N89-10275
RADIATION PYROMETERS
Infrared temperature measurement with inherent consideration of emissivity
[DFVLR-FB-88-22] N89-10271
RADIATIVE TRANSFER
The spectral bidirectional reflectance of snow N89-10318
A model for radiative transfer in heterogeneous three-dimensional canopies N89-10326
Numerical accuracy of a two-stream radiative transfer model from comparison with an N-stream model N89-10331
The role of clouds in surface radiation budgets N89-10501
Theoretical study of the dissociation energy and the red and violet band systems of CN
[NASA-TM-101190] N89-10610
RADICALS
Theoretical study of the dissociation energy and the red and violet band systems of CN
[NASA-TM-101190] N89-10610
RADIO ASTRONOMY
The Telecommunications and Data Acquisition Report --- Deep Space Network
[NASA-CR-183243] N89-10186
RADIO COMMUNICATION
Antennas, satellite broadcasting, and emergency preparedness for the Voice of America
[PB88-209895] N89-10222
RADIO FREQUENCIES
A generic seeker simulation for the evaluation of active RF guidance systems N89-10050
RADIO FREQUENCY HEATING
The study of hydromagnetic waves and RF heating using the TORTUS tokamak and the development of diagnostic techniques N89-10635
RADIO FREQUENCY INTERFERENCE
Electrification of hovering helicopters N89-10460
RADIO SIGNALS
Deep space tracking in local reference frames N89-10187
RADIO SPECTRA
Supernova remnants' interactions with the inter-stellar medium N89-10771
RADIO TELEMETRY
Phasing the antennas of the Very Large Array (VLA) for reception of telemetry from Voyager 2 at Neptune encounter N89-10207
RADIO TELESCOPES
Phasing the antennas of the Very Large Array (VLA) for reception of telemetry from Voyager 2 at Neptune encounter N89-10207
RADIOACTIVE DECAY
Prospects for understanding the astrophysical r-process
[DE88-015449] N89-10773
RADIOMETRIC CORRECTION
Sensitivity of satellite-derived net shortwave irradiance at the Earth's surface to radiometric calibration N89-10335
RADIOMETRIC RESOLUTION
High resolution radiometric measurement of intertidal microphytobenthos N89-10365
RADIOSONDES
Comparison of temperature profiles measured by three collocated microwave radiometers and radiosonde
[PB88-212808] N89-10503
RAIL TRANSPORTATION
Design approaches and parameters for magnetically levitated transport systems
[DE88-014286] N89-10280
RAIN
Lightning in mesoscale convective complexes on 3-5 June 1985 in Oklahoma and Kansas N89-10471
The Remote Atmospheric Probing Information Display (RAPID) system
[AD-A196314] N89-10500
RAMAN SPECTROSCOPY
Two-dimensional spatially resolved Raman spectroscopy of solid materials
[DE88-014867] N89-10138
RAMJET ENGINES
Supersonic missile air intakes: Design and development criteria N89-10031
RANDOM PROCESSES
Generalized Lyapunov exponents in high-dimensional chaotic dynamics and products of large random matrices
[PREPRINT-595] N89-10600
RANGEFINDING
LSZ-850 lightning sensor system N89-10487
RANGELANDS
Applications of LANDSAT (TM and MSS) data for an estimation of rangeland conditions in semiarid and arid areas of northern Kenya
[DFVLR-FB-88-18] N89-10404
RANKINE CYCLE
Free-piston Stirling engine development
[PB88-220025] N89-10286
RARE GASES
Volatile inventory of Mars-2: Primordial sources and fractionating processes N89-10814
Implications of isotopic signatures of noble gases for the origin and evolution of terrestrial atmospheres N89-10817
RATES (PER TIME)
Intracloud lightning as a precursor to thunderstorm microbursts N89-10490
REACTION BONDING
Thermal effects on the mechanical properties of SiC fiber reinforced reaction bonded silicon nitride matrix (SiC/RBSN) composites
[NASA-TM-101348] N89-10134
REACTION KINETICS
Direct Numerical Simulations (DNS) of an unpremixed turbulent jet flame
[AD-A196128] N89-10149
Thermodynamics and kinetics of phase formation of thin-film metal on gallium arsenide
[DE88-015702] N89-10648

REACTOR SAFETY
Discrete modeling considerations in multiphase fluid dynamics
[DE88-015188] N89-10256
REAL TIME OPERATION
Unmanned air vehicles - real time intelligence without the risk
[AD-A195199] N89-10039
SPOCK: A tool for real time artificial intelligence
[NASA-TT-20357] N89-10574
RECEIVERS
An 8.4-GHz cryogenically cooled HEMT amplifier for DSS 13 N89-10199
RECLAMATION
T55-L-712 turbine engine compressor housing refurbishment-plasma spray project
[NASA-TM-101310] N89-10156
RECOIL IONS
Inelastic ion-surface collisions. Ion neutralization on intermetallic surfaces
[AD-A196322] N89-10608
RECORDING
Digital recording of radar data in an aircraft
[PB88-209507] N89-10212
RECTANGULAR WINGS
Unsteady three-dimensional stall on a rectangular wing N89-10027
RECURSIVE FUNCTIONS
The effect of a gap nonlinearity on recursive parameter identification algorithms
[AD-A196020] N89-10557
An investigation of new methods for estimating parameter sensitivities
[NASA-CR-183195] N89-10586
RED GIANT STARS
Companions to peculiar red giants: HR 363 and HR 1105 N89-10729
Multi-wavelength observations of the peculiar red giant HR 3126 N89-10731
REDUCED GRAVITY
Application of microgravity to the assessment of existing structures and structural foundations
[AD-A195599] N89-10418
REFLECTANCE
Dual passband dichroic plate for X-band N89-10196
A perspective on vegetation canopy reflectance models N89-10317
The spectral bidirectional reflectance of snow N89-10318
A simplified vegetation canopy reflectance and absorption model N89-10322
The angular reflectance signature of the canopy hot spot in the optical regime N89-10325
A simplified reflectance model for shrub canopies N89-10329
Analysis of the contribution of the atmosphere to water reflectance in the first two channels of the NOAA satellites AVHRR N89-10330
Developing a radiometric leaf area index N89-10334
Spectral reflectance of sugar beet and winter wheat canopies in the visible and infrared during growth N89-10342
REFLECTED WAVES
A 32-GHz reflected-wave maser amplifier with wide instantaneous bandwidth N89-10198
REFLECTION
Consolidated fuel reprossing program: The implications of force reflection for teleoperation in space N89-10090
REFLECTION NEBULAE
Multi-wavelength observations of the peculiar red giant HR 3126 N89-10731
REFLECTOR ANTENNAS
X/X/Ka-band prime focus feed antenna for the Mars Observer beacon spacecraft N89-10195
REFLECTORS
A method for producing a shaped contour radiation pattern using a single shaped reflector and a single feed
[NASA-TM-101369] N89-10215
REFORESTATION
Identifying the reforested areas utilizing the SPOT satellite data
[INPE-4624-PRE/1343] N89-10396
REFRIGERATING
Development and proof-testing of advanced absorption refrigeration cycle concepts, phase 2
[DE88-013239] N89-10247
REFRIGERATORS
Impacts of advanced refrigerator insulation
[DE88-001180] N89-10185
An 8.4-GHz cryogenically cooled HEMT amplifier for DSS 13 N89-10199
REGOLITH
Comets, volcanism, the salt rich regolith and cycling of volatiles on Mars N89-10786
Is regolith absorbtion the explanation for the transition from early to present Mars climate N89-10788
Martian surface physical properties to be derived by radar altimeter on the Mars observer spacecraft N89-10789
Chemical frost weathering of olivine: Experimental study and implications N89-10793
Ice or liquid water in the Martian regolith. Morphologic indicators from rampart craters N89-10806
Mars regolith versus SNC meteorites: Evidence for abundant crustal carbonates N89-10823
Absorption of the Martian regolith: Specific surface area and missing CO(sub 2) N89-10824
REGRESSION ANALYSIS
Relationships between spectral reflectance and phytomass of the ground layer community of neotropical savanna (CERRADO)
[INPE-4635-PRE/1347] N89-10302
The Transformed Vegetation Index (TVI) for estimation of Brazilian cerrado's phytomass
[INPE-4603-PRE/1326] N89-10400
Smoothing spatial data by estimating mean local variance
[AD-A195302] N89-10593
REGRESSION COEFFICIENTS
Comparison of some robust regression estimators
[PB88-126289] N89-10594
REISSNER THEORY
Analysis of some low-order finite element schemes for Mindlin-Reissner and Kirchhoff plates
[PB87-175899] N89-10578
RELATIVISTIC PARTICLES
Research on a two-stage free electron laser oscillator
[AD-A195339] N89-10278
Multiple nucleon knockout by Coulomb dissociation in relativistic heavy-ion collisions
[NASA-TM-4070] N89-10612
Relativistic nuclear physics with the spectator model
[CEBAF-PR-88-011] N89-10613
RELIABILITY
Selection and evaluation of video tape recorders for surveillance applications
[DE88-014240] N89-10261
Infection and propagation analysis: A fault-based approach to estimating software reliability
[NASA-CR-183276] N89-10534
Incremental assessment and improvement of software reliability
[NASA-CR-183275] N89-10561
RELIABILITY ANALYSIS
On the diagnostic emulation technique and its use in the AIRLAB
[NASA-TM-4027] N89-10524
REMOTE CONTROL
Space truss assembly using teleoperated manipulators N89-10087
REMOTE MANIPULATOR SYSTEM
Telerobotic control of the seven-degree-of-freedom CESAR manipulator
[DE88-012937] N89-10289
REMOTE SENSING
Proceedings of the 4th International Colloquium on Spectral Signatures in Remote Sensing
[ESA-SP-287] N89-10305
Extracting soil and vegetation characteristics from microwave remote sensing data N89-10306
Coherent polarimetric signatures of coniferous trees: A survey N89-10307
Measuring in-situ soil surface roughness using a laser profilometer N89-10308
Microwave backscatter from beets, peas and potatoes throughout the growing season N89-10309
Complementary of microwave and optical range in the characterization of crops by remote sensing N89-10310
A radar reflector for microwave remote sensing instruments external calibration N89-10312
Evaluation of VARAN data in geology and geomorphology in the southeast of France N89-10313
A three degree-of-freedom description of the ocean surface for microwave remote sensing of wave height and wind friction velocity N89-10314
The use of the complex correlation function in the recovery of ocean wave spectra from SAR images N89-10315
Comparison between active and passive microwave measurements over Antarctica N89-10316
A perspective on vegetation canopy reflectance models N89-10317
The spectral bidirectional reflectance of snow N89-10318
Spectral profile and biomass estimation N89-10319
Validation of an atmospheric correction method for satellite borne imagery N89-10320
Retrieving vegetation and soil parameters from radar measurements N89-10321
A simplified vegetation canopy reflectance and absorption model N89-10322
Potential number of winter wheat ears estimation using radiometry techniques at an early stage N89-10323
Introducing spectral data into a plant process model for improving its prediction ability N89-10324
The angular reflectance signature of the canopy hot spot in the optical regime N89-10325
A model for radiative transfer in heterogeneous three-dimensional canopies N89-10326
A simplified reflectance model for shrub canopies N89-10329
Numerical accuracy of a two-stream radiative transfer model from comparison with an N-stream model N89-10331
Developing a radiometric leaf area index N89-10334
Attempt at absolute determination of spectral signatures of bare soils in the thermal infrared, in emission and reflection N89-10336
Strengths and shortcomings in Airborne Thematic Mapper (ATM) technology as applied to volcanic and geothermal areas in Iceland N89-10337
Atmospheric correction of thermal infrared data from LANDSAT-5 for surface temperature estimation N89-10339
Spectral reflectance of sugar beet and winter wheat canopies in the visible and infrared during growth N89-10342
A theoretical model for interpreting remotely sensed thermal infrared measurements obtained over agricultural areas N89-10343
An approximative model for the microwave brightness temperature scattered by a rough open ocean surface N89-10344
Thermal infrared laser spectroscopy: The potential of dual active/passive thermal infrared sensors for Earth observation N89-10345
Time-resolved laser fluorescensing: Trends and applications N89-10346
A new lidar system for applications over land and sea N89-10347
Changes in the chlorophyll fluorescence spectra during the Kautsky induction kinetics N89-10348
Chlorophyll fluorescence spectra of leaves as induced by blue light and red laser light N89-10349
Laser-induced fluorescence on in-vivo chlorophyll of a rice plant: A technique for the remote detection of plant growth N89-10350
Techniques for remote sensing of life span and quantum yield of chlorophyll fluorescence in vivo N89-10351
High-resolution spectroscopy for remote sensing of ocean and atmosphere N89-10352
The fluorescence line imager: High-resolution imaging spectroscopy over water and land N89-10353
Use of high spectral resolution to follow the state of vegetation canopies N89-10354
Stress detection in mixed coniferous-broadleaved forests from Airborne Imaging Spectrometer (AIS) data N89-10355
A narrow-band thermal imager based on multiline real-time averaging N89-10356
High spectral resolution indices for monitoring crop growth and chlorosis N89-10358
Usefulness of high spectral resolution radiometry for geological mapping in the Mediterranean region N89-10360
Imaging spectrometry applied to the remote sensing of submerged seaweed N89-10361
Characterization of rocks by visible and infrared high spectral resolution terrain spectroscopy N89-10362
Comparative analysis of spectral response in the optical domain of targets in a tropical swamp at various spectral and spatial resolutions N89-10363
Spatial resolution requirements for MODIS-N --- Polar Platform Moderate Resolution Imaging Spectrometer (MODIS) N89-10364
High resolution radiometric measurement of intertidal microphytobenthos N89-10365
The basis for the spectral behaviour of silicates in the thermal infrared and applications to remote sensing N89-10366
Texture analysis in forest areas: High spectral resolution synthetic aperture radar data N89-10367
Estimation of leaf spectra from measurements in wide spectral bands N89-10368
Modeling of soil color by remote sensing N89-10369
The normalization of a soil brightness index for the study of changes in soil conditions N89-10370
Estimation of primary marine production using spaceborne data on ocean color N89-10371
Satellite surveillance of ice and snow covered surfaces in the French Alps using visible and near infrared reflectance measurements from the SPOT and LANDSAT Thematic Mapper sensors N89-10372

Spectral signature of citrus fruits and its evolution: Identification of the vegetative index of least temporal variation N89-10373
Rock and soil discrimination in natural tropical conditions using a spot-calibrated radiometer N89-10374
Bathymetry using SPOT imagery of the Casamance (Senegal). First results N89-10375
Discrimination of zones of high water erosion risk using SPOT images N89-10376
Emitted short wavelength infrared radiation for detection and monitoring of volcanic activity N89-10377
Monitoring seasonal variations of soil moisture and vegetation cover using satellite microwave radiometry N89-10378
Comparative point-spread function calculations for the MOMS-1, Thematic Mapper and SPOT-HRV instruments N89-10379
The results of the Geosat MOMS subcommittee's data evaluation: Performance and applicability of the MOMS-1 sensor for exploration geology N89-10380
Design of spectral bands for the German MOMS-2 sensor N89-10381
The use of MOMS-1 data for geological mapping of the Aswa lineament (East African rift) N89-10382
MOMS-1 data for bathymetric and geological studies N89-10383
MOMS-1 used synergistically with LANDSAT TM N89-10384
Comparative geological evolution of different remote sensing data of the Hoggar Mountains (Algeria) N89-10385
AGRISAR'86: Contributing to signature research N89-10387
Aircraft remote sensing in HAPEX --- hydrology N89-10388
A study of the vegetation cover with AVHRR during HAPEX-MOBILHY N89-10389
Development of MOMS to a future multiband and stereoscopic sensor N89-10391
The French space program for Earth observation N89-10392
NASA's future land remote sensing program N89-10393
Study on representation of surface coverage by imaging experiments [ESA-CR(P)-2584] N89-10394
Use of remote sensing for land use policy formulation [NASA-CR-183148] N89-10395

REMOTE SENSORS
Design study for a remote laser wavelength sensor [DE88-015417] N89-10265
Robotic adaptive grasping based on vision and tactile sensor data N89-10288
Atmospheric effect removal from space imagery N89-10338
Multispectral characterization of the spatial structure of remotely sensed scenes N89-10340
Optimization for classification of forest damage classes N89-10359
Study on representation of surface coverage by imaging experiments [ESA-CR(P)-2584] N89-10394
Earth resources: A continuing bibliography with indexes (issue 58) [NASA-SP-7041(58)] N89-10398

REMOTELY PILOTED VEHICLES
Unmanned air vehicles - real time intelligence without the risk [AD-A195199] N89-10039

REPUBLIC OF SOUTH AFRICA
Monitoring lightning activity in South Africa with a VLF single-station technique: Comparison with meteosat infrared data N89-10480

REQUIREMENTS
Actuators for a space manipulator N89-10101
An overview of the knowledge-based requirements assistant N89-10538
Performance estimation for a knowledge-based software assistant N89-10540
Where's the intelligence in the intelligent assistant requirements analysis: Inference processes in the KBRA N89-10544
Turning ideas into specifications N89-10545
Technical issues for performance estimation N89-10548
Knowledge based tools for knowledge-based systems N89-10550

RESEARCH AND DEVELOPMENT
Guidance and control systems simulation and validation techniques [AGARD-AG-273] N89-10048
Federal Coordinating Council on Science, Engineering and Technology, Committee on Computer Research and Applications, Subcommittee on Science and Engineering Computing [DE88-013228] N89-10525
Civil Space Technology Initiative: A first step [NASA-TM-100949] N89-10665

RESEARCH FACILITIES
The Radiation-Hardened Integrated Circuit (RHIC) Laboratory: Pursuit of Class 1 [DE88-006640] N89-10062

RESIDUAL STRESS
Evaluation and control of residual states in curved, composite panels [DE88-012103] N89-10126
Deformations and residual stresses induced in channel section columns by presetting and welding [PB88-199971] N89-10292

RESONANCE
Resonant excitation of spatial perturbations in a boundary layer in the presence of a pressure gradient [NASA-TT-20305] N89-10248
Neoclassical resonant-plateau transport in the noncircular equipotential surface of a tandem mirror [IPPJ-879] N89-10627

RESONANCE CHARGE EXCHANGE
Inelastic ion-surface collisions. Ion neutralization on intermetallic surfaces [AD-A196322] N89-10608

RESONANT VIBRATION
Vibrational relaxation processes in CO2-N2-H2O laser systems [AD-A196211] N89-10273

RESOURCES MANAGEMENT
Space station Platform Management System (PMS) replanning using resource envelopes N89-10071
Automation of spacecraft control centers N89-10078
Estimation of primary marine production using spaceborne data on ocean color N89-10371

RESTORATION
A linear programming approach to maximum entropy signal restoration [DE88-013021] N89-10566

REVERSE FIELD PINCH
Non-local kinetic transport studies of a field-reversed configuration [DE88-012397] N89-10626
Effect of double-shell structure on reduction of field errors in the STP-3(M) reversed-field pinch [IPPJ-882] N89-10640

REVOLVING
Generation of a crowned pinion tooth surface by a surface of revolution [NASA-TM-100260] N89-10282

RICE
Laser-induced fluorescence on in-vivo chlorophyll of a rice plant: A technique for the remote detection of plant growth N89-10350

RING STRUCTURES
Buckling of rings in column-supported bins and tanks [PB88-217336] N89-10290

RISK
Unmanned air vehicles - real time intelligence without the risk [AD-A195199] N89-10039
Fire behavior and risk analysis in spacecraft [NASA-TM-100944] N89-10111

RIVERS
Bathymetry using SPOT imagery of the Casamance (Senegal). First results N89-10375
Sapping features of the Colorado Plateau: A comparative planetary geology field guide [NASA-SP-491] N89-10401

RIVETING
Riveting a case section with blind, self-plugging rivets [DE88-013224] N89-10284

RIVETS
Riveting a case section with blind, self-plugging rivets [DE88-013224] N89-10284

ROBOTICS
Proceedings of 1987 Goddard Conference on Space Applications of Artificial Intelligence (AI) and Robotics [NASA-TM-89663] N89-10063
Space truss assembly using teleoperated manipulators N89-10087
A university teaching simulation facility N89-10088
Open control/display system for a telerobotics work station N89-10089
Issues, concerns, and initial implementation results for space based telerobotic control N89-10091
A shared position/force control methodology for teleoperation N89-10092
Multiple sensor smart robot hand with force control N89-10093
Advanced data management design for autonomous telerobotic systems in space using spaceborne symbolic processors N89-10096
NASREN: Standard reference model for telerobot control N89-10099
Kinematic study of flight telerobotic servicer configuration issues N89-10100
Actuators for a space manipulator N89-10101
Cable applications in robot compliant devices N89-10102
Computer hardware and software for robotic control N89-10103
On motion planning and control of multi-link lightweight robotic manipulators N89-10285
Robotic adaptive grasping based on vision and tactile sensor data N89-10288

ROBOTS
An optimal resolved rate law for kinematically redundant manipulators N89-10094
Teleoperated position control of a PUMA robot N89-10104
Performance improvement of robots using a learning control scheme N89-10105
A dexterity measure for the kinematic control of robot manipulator with redundancy [AD-A196223] N89-10287

ROBUSTNESS (MATHEMATICS)
Comparison of some robust regression estimators [PB88-126269] N89-10594

ROCKET LAUNCHING
An aircraft-borne electric field measuring system for rocket launch support N89-10443

ROCKS
Characterization of rocks by visible and infrared high spectral resolution terrain spectroscopy N89-10362
Rock and soil discrimination in natural tropical conditions using a spot-calibrated radiometer N89-10374
Ablation of Martian glaciers N89-10805

ROTARY ENGINES
A comparative evaluation of RPD (Rotary Particle Depositor) and ferrographic diagnostic methods for turbine engine lubricant samples [AD-A196207] N89-10044

ROTARY WING AIRCRAFT
Helicopter roll control effectiveness criteria program summary [NASA-CR-177477] N89-10046

ROTATING LIQUIDS
Moment exerted on a coning projectile by a spinning liquid in a cylindrical cavity containing a porous medium [AD-A195291] N89-10239

ROTOR BLADES
Electrification of hovering helicopters N89-10460

ROTOR BLADES (TURBOMACHINERY)
AGARD manual on aeroelasticity in axial-flow turbomachines. Volume 2: Structural dynamics and aeroelasticity [AGARD-AG-298-VOL-2] N89-10006
Basic structural dynamics N89-10007
Structural dynamic characteristics of individual blades N89-10008
Structural dynamic characteristics of bladed assemblies N89-10009
Fatigue and assessment methods of blade vibration N89-10010
Aeroelastic coupling: An elementary approach N89-10012
Aeroelastic formulation for tuned and mistuned rotors N89-10013
Unsteady three-dimensional stall on a rectangular wing N89-10027

ROUTES
Integrated switching networks: A performance study N89-10567

RUN TIME (COMPUTERS)
SPOCK: A tool for real time artificial intelligence [NASA-TT-20357] N89-10574

RUNGE-KUTTA METHOD
Improving the accuracy of central difference schemes [NASA-CR-181712] N89-10577

S

SAFETY
Final review of US Army fire-resistant fuel program [AD-A194304] N89-10176
Grounding for safety and compatibility N89-10495

SAFETY MANAGEMENT
Fire behavior and risk analysis in spacecraft [NASA-TM-100944] N89-10111

SAMPLING
Physics and technology for the in-situ investigation of properties of materials [AD-A195498] N89-10145

SAN FRANCISCO (CA)
Climate of San Francisco, revised [PB88-208624] N89-10504

SATELLITE ANTENNAS
Phasing the antennas of the Very Large Array (VLA) for reception of telemetry from Voyager 2 at Neptune encounter N89-10207

SATELLITE ATMOSPHERES
Io: IUE observations of its atmosphere and the plasma torus N89-10691
SATELLITE COMMUNICATION
An expert system for scheduling requests for communications Links between TDRSS and ERBS N89-10065
SATELLITE CONTROL
An expert system that performs a satellite station keeping maneuver N89-10069
SATELLITE IMAGERY
Validation of an atmospheric correction method for satellite borne imagery N89-10320
Relation between sugar beet crop yield and vegetative indexes calculated from LANDSAT MSS images N89-10333
Atmospheric effect removal from space imagery N89-10338
Analysis of directional effects on NOAA AVHRR N89-10341
Estimation of primary marine production using spaceborne data on ocean color N89-10371
Satellite surveillance of ice and snow covered surfaces in the French Alps using visible and near infrared reflectance measurements from the SPOT and LANDSAT Thematic Mapper sensors N89-10372
A study of the vegetation cover with AVHRR during HAPEX-MOBILHY N89-10389
Use of remote sensing for land use policy formulation [NASA-CR-183148] N89-10395
Identifying the reforested areas utilizing the SPOT satellite data [INPE-4624-PRE/1343] N89-10396
Nation-wide forest mapping and timber volume estimation using LANDSAT-5 TM imagery [INPE-4643-PRE/1354] N89-10402
Applications of LANDSAT (TM and MSS) data for an estimation of rangeland conditions in semiarid and arid areas of northern Kenya [DFVLR-FB-88-18] N89-10404
Dynamics Explorer guest investigator [NASA-CR-183163] N89-10417
Analysis and use of VAS satellite data [NASA-CR-183184] N89-10426
Satellite image registration through structural matching [INPE-4563-PRE/1304] N89-10530
A general data model for geographic information systems [INPE-4560-PRE/1301] N89-10676
SATELLITE ORBITS
An expert system that performs a satellite station keeping maneuver N89-10069
ZOOM orbitography software: On the Givens method. Presentation and software implementation evaluation for least square problems [CNES-CT/DTI/MS/AE/219] N89-10109
Upper-atmosphere zonal winds from satellite orbit analysis: An update [RAE-TR-87058] N89-10507
SATELLITE TRACKING
CARTEL: A method to calibrate S-band ranges with geostationary satellites. Results of orbit determination [CNES-CT/DTI/MS/AE/124] N89-10108
SATELLITE-BORNE RADAR
Spaceborne SAR imaging of land, an opportunity for polyphase code [ATES/DMA/RAD/002-86] N89-10226
SATURN ATMOSPHERE
Large time scale variation in hydrogen emission from Jupiter and Saturn N89-10694
SATURN RINGS
On the abundance of micron-sized particles in Saturn's A and B rings N89-10692
SCALARS
Investigation of superradiant LDV markers and three-component velocity mapping [AD-A195504] N89-10662
SCALE MODELS
Estimating electric field enhancement factors on an aircraft utilizing a small scale model: A method evaluation N89-10454
SCATTERING
An interactive program for estimating extinction and scattering properties of most particulate clouds [MRL-R-1123] N89-10218
SCATTERING CROSS SECTIONS
Electron transport and optical emissions in the aurora N89-10424
Analytical approximations for X-ray cross sections 3 [DE88-015366] N89-10609
SCENE ANALYSIS
Multispectral characterization of the spatial structure of remotely sensed scenes N89-10340
SCHEDULES
Effect of a 12-hour/day shift on performance [DE88-013184] N89-10521
SCHEDULING
An expert system for scheduling requests for communications Links between TDRSS and ERBS N89-10065
PLAN-IT: Scheduling assistant for solar system exploration N89-10068
Deep space network resource scheduling approach and application N89-10070
Space station Platform Management System (PMS) replanning using resource envelopes N89-10071
Expert systems tools for Hubble Space Telescope observation scheduling N89-10081
Maintaining consistency between planning hierarchies: Techniques and applications N89-10084
Fault tolerance computing: Constraints in using multiprocessor synchronization by static preplanned scheduling [CNES-CT/DRT/TIT/TB-096] N89-10573
SCHOOLS
Living in space, book 2, levels D, E, F [NASA-EP-223] N89-10522
SEA ICE
Data report for the Siple Coast (Antarctica) project [NASA-TM-100708] N89-10403
MIZEX (marginal ice zone experiment) 87 meteorology atlas [AD-A195361] N89-10506
SEARCHING
Expert systems built by the Expert: An evaluation of OPS5 N89-10086
SEAS
Geomorphic evidence for ancient seas on Mars N89-10813
SEAWEEDS
Imaging spectrometry applied to the remote sensing of submerged seaweed N89-10361
SEDIMENT TRANSPORT
Regional sources and sinks of dust on Mars: Viking observations of Cerberus, Solis Planum, and Syrtis Major N89-10802
Formation of the layered deposits in the Valles Marineris, Mars N89-10809
SEDIMENTS
High resolution radiometric measurement of intertidal microphytobenthos N89-10365
Study of biological processes on the US North Atlantic slope and rise, volume 2 [PB88-196514] N89-10511
Study of biological processes on the US North Atlantic slope and rise. Volume 1: Executive summary [PB88-196522] N89-10517
SEEPAGE
Sapping features of the Colorado Plateau: A comparative planetary geology field guide [NASA-SP-491] N89-10401
SEGMENTS
Segmentation of noisy images using nonstationary Markov fields [AD-A195229] N89-10527
SEISMOGRAPHS
Seismic exploration for water on Mars N89-10811
SEISMOLOGY
Application of microgravity to the assessment of existing structures and structural foundations [AD-A195599] N89-10418
SEMANTICS
Orca: A language for distributed object-based programming [PB86-208533] N89-10529
SEMICONDUCTOR DEVICES
Semiconductor Bridge (SCB): A new method for the ignition of explosives and pyrotechnics [DE88-011246] N89-10151
Photoelectrochemical fabrication of spectroscopic diffraction gratings [NASA-CR-180786] N89-10615
SEMICONDUCTORS (MATERIALS)
Solid State Photovoltaic Research Branch [DE88-001179] N89-10410
Optical bistability in semiconductor waveguides N89-10620
PECVD (Plasma Enhanced Chemical Vapor Deposition) diamond thin films for research instrumentation [AD-A195443] N89-10652
SENEGAL
Bathymetry using SPOT imagery of the Casamance (Senegal). First results N89-10375
SENSITIVITY
Recent developments in structural sensitivity analysis [NASA-TM-100668] N89-10300
An investigation of new methods for estimating parameter sensitivities [NASA-CR-183195] N89-10586
SEPARATED FLOW
A potential theory for the steady separated flow about an aerofoil section [ARL-AERO-R-176] N89-10005
Estimation of up-wash distribution around an automobile by three-dimensional smoke wind tunnel test [NAL-TR-921] N89-10023
SEQUENCING
Hardware fault insertion and instrumentation system: Experimentation and results [NASA-CR-182746] N89-10526
SEQUENTIAL CONTROL
Dynamic task allocation for a man-machine symbiotic system N89-10098
SEYFERT GALAXIES
Profiles of emission lines in AGN. Part 3: On the broad Ha component of IC 5063, IC 5135 and NGC 2992 [INPE-4678-PRE/1375] N89-10681
SHAPE CONTROL
A method for producing a shaped contour radiation pattern using a single shaped reflector and a single feed [NASA-TM-101369] N89-10215
SHAPES
What makes thunderbolts zig and zag N89-10434
SHELLS (STRUCTURAL FORMS)
The tensile strength of glass shells [DE88-013011] N89-10301
SHIELDING
Transfer impedance measurements of the space shuttle Solid Rocket Motor (SRM) joints, wire meshes and a carbon graphite motor case N89-10440
Lightning tests to measure the bulk current levels associated with the electronic engine control of a turboprop commuter transport N89-10457
Electrification of hovering helicopters N89-10460
Indirect effects on electronic and mechanical systems installed in carbon fibre compound aircraft structures N89-10492
Grounding for safety and compatibility N89-10495
System protection from atmospheric electricity for aerostats with conducting tethers N89-10497
SHOCK (PHYSIOLOGY)
Modulation of human plasma fibronectin levels following exercise [AD-A192674] N89-10519
SHOCK TUNNELS
Shock tunnel studies of scramjet phenomena [NASA-CR-181721] N89-10045
SHOCK WAVE INTERACTION
Weak-wave analysis of shock interaction with a slipstream [NASA-TP-2848] N89-10020
Numerical investigation of the dynamics of heterogeneous shock-cavitation [MPIS-MITT-86-1987] N89-10257
SHOCK WAVES
Comparison of Euler algorithms for two-dimensional shock calculations [PB88-210372] N89-10032
Single crystal orientation effects in shock initiation of PETN explosive [DE88-014406] N89-10182
An analysis of an implicit factored scheme for simulating shock waves [AR-005-231] N89-10252
IUE observations of pulsating stars: Atmospheric structure, shock waves and stellar winds N89-10686
SHORT WAVE RADIATION
Sensitivity of satellite-derived net shortwave irradiance at the Earth's surface to radiometric calibration N89-10335
SHUTTLE IMAGING RADAR
Comparative geological evolution of different remote sensing data of the Hoggar Mountains (Algeria) N89-10385
SIDE-LOOKING RADAR
Digital recording of radar data in an aircraft [PB88-209507] N89-10212
SIGNAL ANALYSIS
The use of the complex correlation function in the recovery of ocean wave spectra from SAR images N89-10315
SIGNAL DETECTION
Node synchronization of viterbi decoders using state metrics N89-10202
SIGNAL PROCESSING
Digital simulation techniques for end game phenomena N89-10051
Range delay techniques for radar target simulators N89-10054
FIESTA: An operational decision aid for space network fault isolation N89-10075
Evaluation of hardware architectures for HF antenna arrays [AD-A196204] N89-10217

Optical imaging through atmospheric turbulence N89-10423
A linear programming approach to maximum entropy signal restoration
[DE88-013021] N89-10566
Finite precision arithmetic in singular value decomposition architectures
[AD-A196188] N89-10589

SIGNAL RECEPTION
Simultaneous S- and X-band uplink-downlink performance at DSS 13 N89-10194
Phasing the antennas of the Very Large Array (VLA) for reception of telemetry from Voyager 2 at Neptune encounter N89-10207

SIGNAL TRANSMISSION
Simultaneous S- and X-band uplink-downlink performance at DSS 13 N89-10194

SIGNATURES
Electromagnetic radiations generated by microdischarges from hydrometeors N89-10448

SIGNS AND SYMPTOMS
A review of medical aspects of lightning injury N89-10463

SILICATES
The basis for the spectral behaviour of silicates in the thermal infrared and applications to remote sensing N89-10366

SILICIDES
Recent developments in aluminides and silicides
[DE88-012926] N89-10155

SILICON
The UV silicon spectra of early B stars N89-10763

SILICON ALLOYS
Structure of amorphous silicon alloy films
[DE88-001167] N89-10654

SILICON CARBIDES
Properties of silicon carbide fiber-reinforced silicon nitride matrix composites
[NASA-TM-101356] N89-10130
Thermal effects on the mechanical properties of SiC fiber reinforced reaction bonded silicon nitride matrix (SiC/RBSN) composites
[NASA-TM-101348] N89-10134
A sintering model for SiC(sub)w/Si3N4 composites
[NASA-TM-101336] N89-10166
Development of ceramic matrix composites for application in the ceramic technology for advanced heat engines
[DE88-015329] N89-10168

SILICON DIOXIDE
The effect of Al2O3, CaO, Cr2O3 and MgO on devitrification of silica
[NASA-TM-101335] N89-10124

SILICON NITRIDES
Properties of silicon carbide fiber-reinforced silicon nitride matrix composites
[NASA-TM-101356] N89-10130
A sintering model for SiC(sub)w/Si3N4 composites
[NASA-TM-101336] N89-10166
Development of ceramic matrix composites for application in the ceramic technology for advanced heat engines
[DE88-015329] N89-10168

SILICON RADIATION DETECTORS
Vertex detector for a linear beauty factory
[NOTA-INTERNA-906] N89-10266

SILVER
The influence of texture on strain hardening
[DE88-009157] N89-10158

SIMULATION
Navier-Stokes simulation of transonic wing flow fields using a zonal grid approach
[NASA-TM-100039] N89-10022
Using full-mission simulation for human factors research in air transport operations
[NASA-TM-88330] N89-10037
Design criteria for hardware-in-the-loop simulation facilities N89-10052
Cost effective simulation for millimeter wave guidance systems N89-10053
Simulation with real elements of Exocet anti-ship missiles N89-10056
An adaptive control scheme for a flexible manipulator N89-10095
Direct Numerical Simulations (DNS) of an unpremixed turbulent jet flame
[AD-A196128] N89-10149
An analysis of an implicit factored scheme for simulating shock waves
[AR-005-231] N89-10252
Numerical simulations of lightning by means of the leader propagation model N89-10437
Linear and nonlinear interpretation of CV-580 lightning data N89-10451
Lightning tests on an all-composite helicopter N89-10452
Optimal simulations by butterfly networks: Extended abstract
[AD-A195168] N89-10572
Experimental studies on the surface confined quiescent plasma at INPE
[INPE-4605-PRE/1328] N89-10630
Observations and simulations of recurrent novae: U Sco and V394 CrA N89-10710

SIMULATORS
A comparative evaluation of RPD (Rotary Particle Depositor) and ferrographic diagnostic methods for turbine engine lubricant samples
[AD-A196207] N89-10044
A university teaching simulation facility N89-10088

SINGLE CRYSTALS
Polymer composites
[EP-PATENT-0-232-138-A2] N89-10137
Single crystal orientation effects in shock initiation of PETN explosive
[DE88-014406] N89-10182
Synthesis and study of materials for superconducting electronics
[AD-A195279] N89-10649
A preliminary review of organic materials single crystal growth by the Czochralski technique
[NASA-TM-100341] N89-10656

SINTERING
A sintering model for SiC(sub)w/Si3N4 composites
[NASA-TM-101336] N89-10166

SKIN (STRUCTURAL MEMBER)
Lightning tests on an all-composite helicopter N89-10452

SKY BRIGHTNESS
Spain 31-GHz observations of sky brightness temperatures N89-10190
Australia 31-GHz brightness temperature exceedance statistics N89-10191

SKYLAB PROGRAM
Ultraviolet emission from the sun and stars: A comparison of IUE and Skylab spectra N89-10738

SLIPSTREAMS
Weak-wave analysis of shock interaction with a slipstream
[NASA-TP-2848] N89-10020

SMALL PERTURBATION FLOW
Modification of the unsteady flow field predicted by transonic small distrubance equations using a Navier-Stokes solution of the steady flow field N89-10241

SNOW
Comparison between active and passive microwave measurements over Antarctica N89-10316
The spectral bidirectional reflectance of snow N89-10318

SNOW COVER
Satellite surveillance of ice and snow covered surfaces in the French Alps using visible and near infrared reflectance measurements from the SPOT and LANDSAT Thematic Mapper sensors N89-10372

SOFTWARE ENGINEERING
Study on conceptual design of spacecraft using computer-aided engineering techniques
[ESA-CR(P)-2615] N89-10116
Second Annual Knowledge-Based Software Assistant Conference
[AD-A189819] N89-10536
A common framework for knowledge-based programming N89-10537
An overview of the knowledge-based requirements assistant N89-10538
Overview of the knowledge-based specification assistant N89-10539
Performance estimation for a knowledge-based software assistant N89-10540
Technology transfer and the knowledge-based software assistant N89-10541
Selection of investment strategies which are optimal for the implementation of software support environments N89-10542
KBSA common framework implementation N89-10543
Turning ideas into specifications N89-10545
Software design research at DARPA N89-10546
Plans and meta-plans in an intelligent assistant for the process of programming N89-10547
The knowledge integration tool: Knowledge interface (a knowledge based system development environment) N89-10551
Project management assistant: What have we learned N89-10552
Simplifying the construction of domain-specific automatic programming systems: The NASA automated software development workstation project N89-10553
ASDL: An intelligent acquisition support tool N89-10554
Plan recognition in GRAPPLE: An intelligent assistant for the process of programming N89-10555

SOFTWARE TOOLS
Study on conceptual design of spacecraft using computer-aided engineering techniques
[ESA-CR(P)-2615] N89-10116
Measurement of the properties of lossy materials inside a finite conducting cylinder
[NASA-CR-182500] N89-10223
The Remote Atmospheric Probing Information Display (RAPID) system
[AD-A196314] N89-10500
Infection and propagation analysis: A fault-based approach to estimating software reliability
[NASA-CR-183276] N89-10534
Second Annual Knowledge-Based Software Assistant Conference
[AD-A189819] N89-10536
A common framework for knowledge-based programming N89-10537
Overview of the knowledge-based specification assistant N89-10539
Technology transfer and the knowledge-based software assistant N89-10541
KBSA common framework implementation N89-10543
Software design research at DARPA N89-10546
Plans and meta-plans in an intelligent assistant for the process of programming N89-10547
Designing an effective user interface for a knowledge-based development environment N89-10549
Knowledge based tools for knowledge-based systems N89-10550
The knowledge integration tool: Knowledge interface (a knowledge based system development environment) N89-10551
ASDL: An intelligent acquisition support tool N89-10554
Incremental assessment and improvement of software reliability
[NASA-CR-183275] N89-10561
SPOCK: A tool for real time artificial intelligence
[NASA-TT-20357] N89-10574

SOIL MOISTURE
Use of microwave backscatter measurements as boundary conditions in soil/atmosphere water transfer modeling N89-10311
Monitoring seasonal variations of soil moisture and vegetation cover using satellite microwave radiometry N89-10378

SOIL SCIENCE
Extracting soil and vegetation characteristics from microwave remote sensing data N89-10306
Modeling of soil color by remote sensing N89-10369

SOILS
Measuring in-situ soil surface roughness using a laser profilometer N89-10308
Retrieving vegetation and soil parameters from radar measurements N89-10321
Attempt at absolute determination of spectral signatures of bare soils in the thermal infrared, in emission and reflection N89-10336
The normalization of a soil brightness index for the study of changes in soil conditions N89-10370
Rock and soil discrimination in natural tropical conditions using a spot-calibrated radiometer N89-10374

SOLAR ARRAYS
Photovoltaics for high capacity space power systems
[NASA-TM-101341] N89-10122
Advanced planar array development for space station
[NASA-CR-179372] N89-10407

SOLAR CELLS
Electronic structure of electrodeposited thin film CdTe solar cells
[DE88-001170] N89-10406
Advanced planar array development for space station
[NASA-CR-179372] N89-10407
MOCVD techniques for CdTe solar cells
[DE88-001163] N89-10411

SOLAR DYNAMIC POWER SYSTEMS
The solar dynamic radiator with a historical perspective
[NASA-TM-100972] N89-10117
Photovoltaics for high capacity space power systems
[NASA-TM-101341] N89-10122

SOLAR FLARES
A summary of major activities of the UNH and NRL groups
[NASA-CR-180949] N89-10774
Solar-geophysical data number 524, April 1988. Part 2: (Prompt reports). Data for October 1987 and miscellanea
[PB88-217401] N89-10828

Solar-geophysical data number 524, April 1988. Part 1: (Prompt reports). Data for March, February 1988 and late data
[PB88-217393] N89-10829

SOLAR MAGNETIC FIELD
Solar-geophysical data number 524, April 1988. Part 1: (Prompt reports). Data for March, February 1988 and late data
[PB88-217393] N89-10829

SOLAR PHYSICS
A summary of major activities of the UNH and NRL groups
[NASA-CR-180949] N89-10774

SOLAR PROMINENCES
Solar-geophysical data number 524, April 1988. Part 2: (Prompt reports). Data for October 1987 and miscellanea
[PB88-217401] N89-10828

SOLAR RADIATION
Ultraviolet emission from the sun and stars: A comparison of IUE and Skylab spectra N89-10738

SOLAR RADIO BURSTS
Solar-geophysical data number 524, April 1988. Part 2: (Prompt reports). Data for October 1987 and miscellanea
[PB88-217401] N89-10828

SOLAR RADIO EMISSION
Solar-geophysical data number 524, April 1988. Part 1: (Prompt reports). Data for March, February 1988 and late data
[PB88-217393] N89-10829

SOLAR WIND
Interplanetary medium data book. Supplement 3: 1977-1985
[NASA-TM-89660] N89-10772

SOLID PROPELLANT COMBUSTION
Investigation of the flame-acoustic wave interaction during axial solid rocket instabilities N89-10120

SOLID PROPELLANT ROCKET ENGINES
Evaluation and mitigation of lightning hazards to the space shuttle Solid Rocket Motors (SRM) N89-10439
Transfer impedance measurements of the space shuttle Solid Rocket Motor (SRM) joints, wire meshes and a carbon graphite motor case N89-10440

SOLID ROCKET PROPELLANTS
Evaluation and mitigation of lightning hazards to the space shuttle Solid Rocket Motors (SRM) N89-10439

SOLID STATE
Metastable alloy phases prepared by solid state reactions and ball milling
[DE88-009156] N89-10163
Solid State Photovoltaic Research Branch
[DE88-001179] N89-10410

SOLIDS
Two-dimensional spatially resolved Raman spectroscopy of solid materials
[DE88-014867] N89-10138
A new method of determining acid base strength distribution and a new acidity-basicity scale for solid catalysts: The strongest point, HO
[NASA-TT-20334] N89-10141
An analysis of an implicit factored scheme for simulating shock waves
[AR-005-231] N89-10252

SOLIDS FLOW
Laser velocimeter measurements of solids in multiphase flow
[DE88-011611] N89-10251

SORPTION
Hydrogen sorption studies of materials used in Li(Si)/FeS2 thermal batteries
[DE88-013154] N89-10231

SOUND GENERATORS
A water sound generator for pressure pulses of high energy
[MPIS-MITT-85-1987] N89-10604

SOUND INTENSITY
Acoustic radiation from plates driven by multi-point random forces N89-10602

SOUND TRANSMISSION
Acoustic radiation from plates driven by multi-point random forces N89-10602

SOUND WAVES
Investigation of the flame-acoustic wave interaction during axial solid rocket instabilities N89-10120
Acoustic radiation from plates driven by multi-point random forces N89-10602

SOUND-SOUND INTERACTIONS
The effect of front-to-rear propeller spacing on the interaction noise at cruise conditions of a model counterrotation propeller having a reduced diameter aft propeller
[NASA-TM-101329] N89-10603

SOUNDING
The electrical structure of thunderstorm anvils N89-10470

SOUNDING ROCKETS
Measurement of infrared horizon profiles from TT-500A sounding rocket
[NAL-TR-947] N89-10121

SPACE CHARGE
New electric field instrumentation and the effects of space charge at Kennedy Space Center N89-10444

SPACE COMMERCIALIZATION
Multimegawatt power sources for commercial space operations
[DE88-015119] N89-10106
Review of the requirements for higher level ERS-1 products within Europe
[ESA-CR(P)-2586] N89-10664

SPACE COMMUNICATION
The Telecommunications and Data Acquisition Report --- Deep Space Network
[NASA-CR-183243] N89-10186

SPACE EXPLORATION
PLAN-IT: Scheduling assistant for solar system exploration N89-10068

SPACE INDUSTRIALIZATION
Space commerce: An industry assessment
[PB88-214069] N89-10677

SPACE MISSIONS
PLAN-IT: Scheduling assistant for solar system exploration N89-10068
Civil Space Technology Initiative: A first step
[NASA-TM-100949] N89-10665

SPACE PLASMAS
Io: IUE observations of its atmosphere and the plasma torus N89-10691
Superionized plasmas in Algol binaries N89-10723
Interplanetary medium data book. Supplement 3: 1977-1985
[NASA-TM-89660] N89-10772

SPACE POWER REACTORS
Multimegawatt power sources for commercial space operations
[DE88-015119] N89-10106

SPACE SHUTTLE MAIN ENGINE
Standardization of the carbon-phenolic materials and processes. Vol. 2: Test methods and specifications
[NASA-CR-183227] N89-10033
Standardization of the carbon-phenolic materials and processes. Vol. 1: Experimental studies
[NASA-CR-183226] N89-10127
Flowfield visualization for SSME hot gas manifold
[NASA-CR-179403] N89-10243

SPACE SHUTTLE MISSION 41-B
The results of the Geosat MOMS subcommittee's data evaluation: Performance and applicability of the MOMS-1 sensor for exploration geology N89-10380

SPACE SHUTTLE PAYLOADS
Comparative point-spread function calculations for the MOMS-1, Thematic Mapper and SPOT-HRV instruments N89-10379
Design of spectral bands for the German MOMS-2 sensor N89-10381
MOMS-1 data for bathymetric and geological studies N89-10383
MOMS-1 used synergistically with LANDSAT TM N89-10384

SPACE SHUTTLES
Space shuttle phase B wind tunnel model and test information. Volume 3: Launch configuration
[NASA-CR-178416-VOL-3-PT-1] N89-10019
Evaluation and mitigation of lightning hazards to the space shuttle Solid Rocket Motors (SRM) N89-10439
Transfer impedance measurements of the space shuttle Solid Rocket Motor (SRM) joints, wire meshes and a carbon graphite motor case N89-10440

SPACE STATION PAYLOADS
Maintaining consistency between planning hierarchies: Techniques and applications N89-10084

SPACE STATION POLAR PLATFORMS
Spatial resolution requirements for MODIS-N --- Polar Platform Moderate Resolution Imaging Spectrometer (MODIS) N89-10364

SPACE STATION STRUCTURES
Space station Platform Management System (PMS) replanning using resource envelopes N89-10071
Advanced planar array development for space station
[NASA-CR-179372] N89-10407

SPACE STATIONS
AUTOPLAN: A PC-based automated mission planning tool N89-10067
The solar dynamic radiator with a historical perspective
[NASA-TM-100972] N89-10117
Rechargeable metal hydrides for spacecraft application
[NASA-TM-4076] N89-10184
Compact imaging spectrometer for induced emissions
[NASA-CR-183187] N89-10264

SPACE SUITS
Living in space, book 2, levels D, E, F
[NASA-EP-223] N89-10522

SPACE WEAPONS
Directed energy concepts for strategic defense
[DE88-015050] N89-10596
Military uses of space
[DE88-015053] N89-10597
SDI (Strategic Defense Initiative): Myth or reality
[DE88-015059] N89-10598

SPACEBORNE ASTRONOMY
A Decade of UV Astronomy with the IUE Satellite, volume 1
[ESA-SP-281-VOL-1] N89-10682
Observing SN 1987A with IUE N89-10683
Cataclysmic variables N89-10684
White dwarfs N89-10685
IUE observations of pulsating stars: Atmospheric structure, shock waves and stellar winds N89-10686
IUE observations of planetary atmospheres N89-10687
Comets --- IUE N89-10688
Some recent results from the study of cool stars --- IUE N89-10689
IUE observations and physical processes of interacting binary stars N89-10690
Io: IUE observations of its atmosphere and the plasma torus N89-10691
On the abundance of micron-sized particles in Saturn's A and B rings N89-10692
Jovian equatorial H2 emission from 1979-1987 N89-10693
Large time scale variation in hydrogen emission from Jupiter and Saturn N89-10694
Phenomenological analysis of Jovian north auroral H2 Lyman band emissions --- IUE N89-10695
Observations of SN 1987A: The narrow emission lines --- IUE N89-10696
The Progenitor of SN 1987A --- IUE N89-10697
The complete visual light curve of SN 1987A: Thirteen months of FES observations --- IUE Fine Error Sensor (FES) N89-10698
IUE observations of oxygen-rich supernova remnants N89-10699
Ejecta in SN 1006: The knotty issue --- supernova remnant N89-10700
Far UV observations of black hole candidates: The case of LMC X-3 N89-10701
IUE spectrophotometry of the accretion disk of HZ Her/Her X-1 N89-10702
Simultaneous IUE, EXOSAT and optical observations of the unusual AM Her type variable H058+608 N89-10703
A 0535+26/HDE 245770: A typical Be/X-ray transient system: Coordinated multiwavelength twelve years monitor N89-10704
IUE and optical observations of X-ray sources in the Large Margellanic Cloud (LMC) N89-10705
The analysis of spectra of novae taken near maximum N89-10706
The 1981 outburst of the old nova GK Persei N89-10707
Observations of classical novae in outburst N89-10708
Observations and simulations of nova Vul 1984 no. 2: A nova with ejecta rich in oxygen, neon, and magnesium N89-10709
Observations and simulations of recurrent novae: U Sco and V394 CrA N89-10710
Optical and ultraviolet observations of nova Vul 1987 N89-10711
Ultraviolet observations of LMC nova 1988 N89-10712
SS Cygni in quiescence --- IUE N89-10713
UV and optical line emission from the shell of the old nova GK Persei N89-10714
IUE observations of the 1987 superoutburst of the dwarf nova Z Cha N89-10715
Observations of galactic WC + O binary systems: HD 97152 and HD 152270 N89-10716
Atmospheric eclipse effects in Wolf-Rayet binaries in the Small Magellanic Cloud N89-10717
Mass flow in the interacting binary TX Ursae Majoris N89-10718
A new study of the interacting binary star V356 Sgr N89-10719
Matter streams in semi-detached binary systems N89-10720
The November 1987 eclipse of the zeta-Aur system HR 2554 N89-10721
Asymmetry in zeta Auriage chromospheres N89-10722
Superionized plasmas in Algol binaries N89-10723
HD 207739 and other F + Be variables N89-10724
Searching for the white dwarf in WZ Sagittae N89-10725

Model chromosphere and transition region for 56 Peg (K0 IIp + wd): A preliminary study N89-10726
Cepheid binaries with large mass ratios (M1/M2) N89-10727
The orbit of the Cepheid AW Per N89-10728
Companions to peculiar red giants: HR 363 and HR 1105 N89-10729
Direct UV observations of the circumstellar envelope of alpha Orionis N89-10730
Multi-wavelength observations of the peculiar red giant HR 3126 N89-10731
Recurrent shell infall events in a B0.5e star: HD 58978 1979-1988 N89-10732
IUE observations of a hot DAO white dwarf: Implications for diffusion theory and photospheric stratification N89-10733
Temperature determinations of hot DA white dwarfs using IUE continuum fluxes N89-10734
The ultraviolet emission of accreting magnetic white dwarfs N89-10735
IUE observations of rapidly rotating K dwarfs in the Pleiades N89-10736
On the flux-period and flux-flux correlations in late type stars N89-10737
Ultraviolet emission from the sun and stars: A comparison of IUE and Skylab spectra N89-10738
Spectral images of HD 199178 N89-10739
Doppler imaging of AR Lacertae at three epochs N89-10740
Rotational modulation of hydrogen Lyman alpha flux from 44i Bootis N89-10741
Mapping of surface activity on the W UMa-type system VW Cephei N89-10742
Ultraviolet flares on 2 Peg N89-10743
Chromospheric mass motions during a flare on UV Ceti N89-10744
The energy input mechanism into the lower transition regions between stellar chromospheres and coronae N89-10745
Transition regions of dM stars N89-10746
Transition region fluxes in A-F Dwarfs: Basal fluxes and dynamo activity N89-10747
Line formation of cool carbon star chromospheres N89-10748
Lithium and chromospherically active single giants N89-10749
Mg II flux and profile variability of hybrid-chromosphere stars N89-10750
The discovery of a co-rotating magnetosphere in a helium weak star: HD5737 = alpha Scl N89-10751
Observations of ultraviolet variability in RV Tauri stars N89-10752
Fluorescence processes and line identifications in the UV spectra of cool stars N89-10753
Fe II level population in luminous variable stars N89-10754
Identification of new fluorescence processes in the UV spectra of cool stars from new energy levels of Fe II and Cr II N89-10755
Periodic modulation of the atmosphere of Alpha Orionis N89-10756
Mg II line profiles of the Mira S Carinae N89-10757
The variability of the UV spectrum of the symbiotic star BF Cygni N89-10758
Abundance and f values needed to interpret adequately the high resolution IUE spectra N89-10759
Carbon and nitrogen abundance determinations from transition layer lines — giant stars N89-10760
The anomalous C 4 intensity ratio in symbiotic stars N89-10761
The IUE spectral atlas of two normal B stars: pi Cet and nu Cap (125 to 200 nm) N89-10762
The UV silicon spectra of early B stars N89-10763
C IV and Si IV in IUE spectra of normal B8-A0 stars: UV identified Be/Ae stars N89-10764
Ultraviolet properties of IRAS-selected Be stars N89-10765
Au II in IUE spectra of chemically peculiar stars N89-10766
Validity of the classification of UV gallium stars N89-10767
Detected UV variability in the IUE spectra of the Ap-Si star HD 25823 N89-10768
The galatic and LMC extreme line supergiants compared: IUE observations of the Henize-Carlson and Zoo star samples of massive supergiants — Large Magellanic cloud (LMC) N89-10769
Mass loss from the K dwarf in V471 Tauri N89-10770

SPACEBORNE PHOTOGRAPHY
Image processing document: Halley multicolor camera (Giotto Mission) [DFVLR-FB-88-20] N89-10270
The use of MOMS-1 data for geological mapping of the Aswa lineament (East African rift) N89-10382
MOMS-1 data for bathymetric and geological studies N89-10383
Comparative geological evolution of different remote sensing data of the Hoggar Mountains (Algeria) N89-10385
Digital analysis of MOMS-1, LANDSAT TM, and SPOT data of the Nakuru area (Kenya) N89-10386
Development of MOMS to a future multiband and stereoscopic sensor N89-10391

SPACECRAFT ANTENNAS
Theoretical and experimental analysis of quadrifilar antennas for the first Brazilian satellite [INPE-4581-PRE/1315] N89-10221

SPACECRAFT CHARGING
Triggering of lightning by the Atlas Centaur vehicle N89-10438

SPACECRAFT COMMUNICATION
CLEAR: Communications Link Expert Assistance Resource N89-10072
Spain 31-GHz observations of sky brightness temperatures N89-10190
Space commerce: An industry assessment [PB88-214069] N89-10677

SPACECRAFT CONTROL
Solution of two-point boundary value problems in optimal maneuvers of flexible vehicles N89-10114

SPACECRAFT DESIGN
A digital simulation method of cumulative fatigue damage evaluation for spacecraft components [NAL-TR-957] N89-10113
Study on conceptual design of spacecraft using computer-aided engineering techniques [ESA-CR(P)-2615] N89-10116

SPACECRAFT LAUNCHING
Sulfide corrosion of silver contacts during satellite storage [AD-A196217] N89-10112
PSA: A program to streamline orbit determination for launch support operations N89-10189
Summary of DSN (Deep Space Network) reimbursable launch support N89-10211

SPACECRAFT MANEUVERS
An expert system that performs a satellite station keeping maneuver N89-10069
Solution of two-point boundary value problems in optimal maneuvers of flexible vehicles N89-10114

SPACECRAFT POWER SUPPLIES
Photovoltaics for high capacity space power systems [NASA-TM-101341] N89-10122

SPACECRAFT STRUCTURES
Means for testing aerospace launcher structures [ETN-88-93082] N89-10110

SPACECRAFT SURVIVABILITY
Fire behavior and risk analysis in spacecraft [NASA-TM-100944] N89-10111

SPACECRAFT TRACKING
Deep space tracking in local reference frames N89-10187
PSA: A program to streamline orbit determination for launch support operations N89-10189
DSN 64-meter antenna L-band (1668-MHz) microwave system performance overview N89-10210

SPACECRAFT TRAJECTORIES
Precise orbit determination for NASA's earth observing system using GPS (Global Positioning System) N89-10188
PSA: A program to streamline orbit determination for launch support operations N89-10189

SPACELAB
Spacelab Data Processing Facility (SLDPF) quality assurance expert systems development N89-10079

SPARK GAPS
Breakdown characteristics of an isolated conducting object in a uniform electric field N89-10453

SPARK IGNITION
Alternate fuels for General Aviation aircraft with spark ignition engines [DOT/FAA/CT-88/05] N89-10179

SPATIAL DISTRIBUTION
Dynamic interpretation of geoid anomalies [NASA-CR-183164] N89-10304
Spatial distribution of lightning strikes to ground during small thunderstorms in Florida N89-10472

SPATIAL RESOLUTION
Two-dimensional spatially resolved Raman spectroscopy of solid materials [DE88-014867] N89-10138
Spatial resolution requirements for MODIS-N — Polar Platform Moderate Resolution Imaging Spectrometer (MODIS) N89-10364

SPECIFICATIONS
Sulfide corrosion of silver contacts during satellite storage [AD-A196217] N89-10112
Multitier specification applied to modify the hardness of an essential NSEP (National Security/Emergency Preparedness) fiber optic link [PB88-210778] N89-10220
An interagency working group on lightning threat warning N89-10469
Meteorological measurements made using Brazilian drifting buoys: Technical aspects and first results [INPE-4674-PRE/1372] N89-10502
Overview of the knowledge-based specification assistant N89-10539
Turning ideas into specifications N89-10545

SPECTRA
Multiphoton ionization of transient species in supersonic jets [DE88-008366] N89-10607

SPECTRAL BANDS
Design of spectral bands for the German MOMS-2 sensor N89-10381

SPECTRAL EMISSION
Directional spectral emissivity measurements on a ceramic mold material [DE88-015407] N89-10167
Supernova remnants' interactions with the inter-stellar medium N89-10771
Global properties of molecular clouds and the interstellar medium in galaxies N89-10776

SPECTRAL METHODS
An adaptive pseudospectral method for discontinuous problems [NASA-CR-181717] N89-10583

SPECTRAL REFLECTANCE
Relationships between spectral reflectance and phytomass of the ground layer community of neotropical savanna (CERRADO) [INPE-4635-PRE/1347] N89-10302
Proceedings of the 4th International Colloquium on Spectral Signatures in Remote Sensing [ESA-SP-287] N89-10305
Airborne Visible/Infrared Imaging Spectrometer (AVIRIS): Inflight radiometric calibration and the determination of surface reflectance N89-10357
Comparative analysis of spectral response in the optical domain of targets in a tropical swamp at various spectral and spatial resolutions N89-10363
Estimation of leaf spectra from measurements in wide spectral bands N89-10368
Satellite surveillance of ice and snow covered surfaces in the French Alps using visible and near infrared reflectance measurements from the SPOT and LANDSAT Thematic Mapper sensors N89-10372
Regional sources and sinks of dust on Mars: Viking observations of Cerberus, Solis Planum, and Syrtis Major N89-10802

SPECTRAL RESOLUTION
Use of high spectral resolution to follow the state of vegetation canopies N89-10354
High spectral resolution indices for monitoring crop growth and chlorosis N89-10358
Usefulness of high spectral resolution radiometry for geological mapping in the Mediterranean region N89-10360

SPECTRAL SIGNATURES
Proceedings of the 4th International Colloquium on Spectral Signatures in Remote Sensing [ESA-SP-287] N89-10305
Extracting soil and vegetation characteristics from microwave remote sensing data N89-10306
Coherent polarimetric signatures of coniferous trees: A survey N89-10307
Measuring in-situ soil surface roughness using a laser profilometer N89-10308
Complementary of microwave and optical range in the characterization of crops by remote sensing N89-10310
A radar reflector for microwave remote sensing instruments external calibration N89-10312
Evaluation of VARAN data in geology and geomorphology in the southeast of France N89-10313
A three degree-of-freedom description of the ocean surface for microwave remote sensing of wave height and wind friction velocity N89-10314
The use of the complex correlation function in the recovery of ocean wave spectra from SAR images N89-10315
Comparison between active and passive microwave measurements over Antarctica N89-10316
A perspective on vegetation canopy reflectance models N89-10317
The spectral bidirectional reflectance of snow N89-10318
Spectral profile and biomass estimation N89-10319
Validation of an atmospheric correction method for satellite borne imagery N89-10320
Retrieving vegetation and soil parameters from radar measurements N89-10321

Potential number of winter wheat ears estimation using radiometry techniques at an early stage N89-10323
Introducing spectral data into a plant process model for improving its prediction ability N89-10324
The angular reflectance signature of the canopy hot spot in the optical regime N89-10325
A model for radiative transfer in heterogeneous three-dimensional canopies N89-10326
Spectral characterization of forest targets in mountainous zones on Thematic Mapper images N89-10328
A simplified reflectance model for shrub canopies N89-10329
Numerical accuracy of a two-stream radiative transfer model from comparison with an N-stream model N89-10331
Developing a radiometric leaf area index N89-10334
Attempt at absolute determination of spectral signatures of bare soils in the thermal infrared, in emission and reflection N89-10336
Strengths and shortcomings in Airborne Thematic Mapper (ATM) technology as applied to volcanic and geothermal areas in Iceland N89-10337
Atmospheric effect removal from space imagery N89-10338
Atmospheric correction of thermal infrared data from LANDSAT-5 for surface temperature estimation N89-10339
Analysis of directional effects on NOAA AVHRR N89-10341
Spectral reflectance of sugar beet and winter wheat canopies in the visible and infrared during growth N89-10342
A theoretical model for interpreting remotely sensed thermal infrared measurements obtained over agricultural areas N89-10343
An approximative model for the microwave brightness temperature scattered by a rough open ocean surface N89-10344
Thermal infrared laser spectroscopy: The potential of dual active/passive thermal infrared sensors for Earth observation N89-10345
Time-resolved laser fluorescensing: Trends and applications N89-10346
A new lidar system for applications over land and sea N89-10347
Changes in the chlorophyll fluorescence spectra during the Kautsky induction kinetics N89-10348
Chlorophyll fluorescence spectra of leaves as induced by blue light and red laser light N89-10349
Techniques for remote sensing of life span and quantum yield of chlorophyll fluorescence in vivo N89-10351
High-resolution spectroscopy for remote sensing of ocean and atmosphere N89-10352
The fluorescence line imager: High-resolution imaging spectroscopy over water and land N89-10353
Use of high spectral resolution to follow the state of vegetation canopies N89-10354
Stress detection in mixed coniferous-broadleaved forests from Airborne Imaging Spectrometer (AIS) data N89-10355
A narrow-band thermal imager based on multiline real-time averaging N89-10356
Airborne Visible/Infrared Imaging Spectrometer (AVIRIS): Inflight radiometric calibration and the determination of surface reflectance N89-10357
High spectral resolution indices for monitoring crop growth and chlorosis N89-10358
Optimization for classification of forest damage classes N89-10359
Usefulness of high spectral resolution radiometry for geological mapping in the Mediterranean region N89-10360
Imaging spectrometry applied to the remote sensing of submerged seaweed N89-10361
Characterization of rocks by visible and infrared high spectral resolution terrain spectroscopy N89-10362
Comparative analysis of spectral response in the optical domain of targets in a tropical swamp at various spectral and spatial resolutions N89-10363
Spatial resolution requirements for MODIS-N --- Polar Platform Moderate Resolution Imaging Spectrometer (MODIS) N89-10364
High resolution radiometric measurement of intertidal microphytobenthos N89-10365
The basis for the spectral behaviour of silicates in the thermal infrared and applications to remote sensing N89-10366
Texture analysis in forest areas: High spectral resolution synthetic aperture radar data N89-10367
Estimation of leaf spectra from measurements in wide spectral bands N89-10368
Modeling of soil color by remote sensing N89-10369
The normalization of a soil brightness index for the study of changes in soil conditions N89-10370
Estimation of primary marine production using spaceborne data on ocean color N89-10371
Satellite surveillance of ice and snow covered surfaces in the French Alps using visible and near infrared reflectance measurements from the SPOT and LANDSAT Thematic Mapper sensors N89-10372
Spectral signature of citrus fruits and its evolution: Identification of the vegetative index of least temporal variation N89-10373
Rock and soil discrimination in natural tropical conditions using a spot-calibrated radiometer N89-10374
Bathymetry using SPOT imagery of the Casamance (Senegal). First results N89-10375
Discrimination of zones of high water erosion risk using SPOT images N89-10376
Emitted short wavelength infrared radiation for detection and monitoring of volcanic activity N89-10377
Monitoring seasonal variations of soil moisture and vegetation cover using satellite microwave radiometry N89-10378
Comparative point-spread function calculations for the MOMS-1, Thematic Mapper and SPOT-HRV instruments N89-10379
The results of the Geosat MOMS subcommittee's data evaluation: Performance and applicability of the MOMS-1 sensor for exploration geology N89-10380
MOMS-1 used synergistically with LANDSAT TM N89-10384
Comparative geological evolution of different remote sensing data of the Hoggar Mountains (Algeria) N89-10385
AGRISAR'86: Contributing to signature research N89-10387
Aircraft remote sensing in HAPEX --- hydrology N89-10388
A study of the vegetation cover with AVHRR during HAPEX-MOBILHY N89-10389
Development of MOMS to a future multiband and stereoscopic sensor N89-10391
The French space program for Earth observation N89-10392

SPECTROMETERS
An improved interface for capillary zone electrophoresis-mass spectrometry [DE88-014079] N89-10148

SPECTROSCOPY
Thermodynamic properties by non-calorimetric methods: Progress report [DE88-015422] N89-10660
Profiles of emission lines in AGN. Part 3: On the broad Ha component of IC 5063, IC 5135 and NGC 2992 [INPE-4678-PRE/1375] N89-10681
A summary of major activities of the UNH and NRL groups [NASA-CR-180949] N89-10774

SPECTRUM ANALYSIS
Compact imaging spectrometer for induced emissions [NASA-CR-183187] N89-10264
The use of the complex correlation function in the recovery of ocean wave spectra from SAR images N89-10315
Interference of precipitation static discharges with aircraft navigational systems N89-10459
On the appropriateness of applying chi-square distribution based confidence intervals to spectral estimates of helicopter flyover data [NASA-CR-181692] N89-10601
The analysis of spectra of novae taken near maximum N89-10706
C 4 fluxes from the sun as a star and the correlation with magnetic flux [NASA-CR-183156] N89-10827

SPHERICAL COORDINATES
Compilation of methods in orbital mechanics and solar geometry [NASA-RP-1204] N89-10420

SPHERICAL HARMONICS
Progress in NODAL transport methods [DE88-012416] N89-10590

SPIN DYNAMICS
Moment exerted on a coning projectile by a spinning liquid in a cylindrical cavity containing a porous medium [AD-A195291] N89-10239
Gravitational time delay due to a spinning string [DE88-014733] N89-10661

SPINEL
Oxygen electrode bifunctional electrocatalyst NiCo2O4 spinel [NASA-TM-100947] N89-10409

SPIRAL GALAXIES
A polarisation study of spiral galaxies N89-10679

SPLINE FUNCTIONS
A fast Monte-Carlo cross-validation procedure for large least squares problems with noisy data [RR-687-M] N89-10591

SPOT (FRENCH SATELLITE)
Preliminary project PASTEL: System interface between SPOT 4 and the PSDE's passenger [CNES-87/088-CT/DRT/TIT/TR] N89-10227
Complementary of microwave and optical range in the characterization of crops by remote sensing N89-10310
Biomass and wheat crop yield estimation from SPOT vegetative indexes N89-10327
Rock and soil discrimination in natural tropical conditions using a spot-calibrated radiometer N89-10374
Bathymetry using SPOT imagery of the Casamance (Senegal). First results N89-10375
Discrimination of zones of high water erosion risk using SPOT images N89-10376
Comparative point-spread function calculations for the MOMS-1, Thematic Mapper and SPOT-HRV instruments N89-10379
Digital analysis of MOMS-1, LANDSAT TM, and SPOT data of the Nakuru area (Kenya) N89-10386

SPRAYERS
Electrospray ionization phenomena and the interface of capillary electrophoresis and mass spectrometry [DE88-014080] N89-10143
An improved interface for capillary zone electrophoresis-mass spectrometry [DE88-014079] N89-10148

SPRINGS (ELASTIC)
Leaf spring [EP-PATENT-0-253-574-A1] N89-10136

STABILITY
Study of critical beta non-circular tokamak equilibria sustained in steady state by beam driven currents [IPPJ-878] N89-10634
Marginal stability of ion-acoustic waves in a weakly collisional two-temperature plasma without a current [AD-A195840] N89-10638

STAINLESS STEELS
Laser welding of stainless steel weld filler metals at high cooling rates [DE88-002345] N89-10281
An investigation of the acoustic emission generated by various crack propagation modes in 304 stainless steel N89-10293

STANDARDS
Lightning standards for protection of ground electronic systems N89-10473

STAR TRACKERS
The complete visual light curve of SN 1987A: Thirteen months of FES observations --- IUE Fine Error Sensor (FES) N89-10698

STARSPOTS
Mapping of surface activity on the W UMa-type system VW Cephei N89-10742

STATIC CHARACTERISTICS
Recent developments in structural sensitivity analysis [NASA-TM-100668] N89-10300

STATIC DISCHARGERS
Interference of precipitation static discharges with aircraft navigational systems N89-10459

STATIC ELECTRICITY
International Aerospace and Ground Conference on Lightning and Static Electricity [PB88-197439] N89-10429
Electrostatic discharge and field effects of electronics systems N89-10493

STATIC TESTS
Phase 4 static tests of the J-97 powered, external augmentor V/STOL model at the NASA, Ames Research Center, November 1983 [NASA-CR-177395] N89-10028

STATIONKEEPING
An expert system that performs a satellite station keeping maneuver N89-10069

STATISTICAL ANALYSIS
Comparison of statistical digital simulation methods N89-10049
Australia 31-GHz brightness temperature exceedance statistics N89-10191
Multispectral characterization of the spatial structure of remotely sensed scenes N89-10340
Statistics of lightning interaction with aircraft in Japan N89-10430
What makes thunderbolts zig and zag N89-10434
On the statistics of field waveforms associated with lightning return strokes N89-10441
Monitoring lightning activity in South Africa with a VLF single-station technique: Comparison with meteosat infrared data N89-10480
Statistical evaluation of PACSTAT random number generation capabilities [DE88-012754] N89-10556
Bootstrap confidence intervals in a complex situation: A sequential paired clinical trial [DE88-015338] N89-10592

Mean estimation in highly skewed samples [DE88-010929] N89-10595

STATISTICAL MECHANICS
Thermodynamic properties by non-calorimetric methods: Progress report [DE88-015422] N89-10660

STEADY FLOW
A potential theory for the steady separated flow about an aerofoil section [ARL-AERO-R-176] N89-10005
Modification of the unsteady flow field predicted by transonic small distrubance equations using a Navier-Stokes solution of the steady flow field N89-10241
Steady flow field measurements using laser Doppler velocimetry [AD-A195228] N89-10245

STELLAR ACTIVITY
On the flux-period and flux-flux correlations in late type stars N89-10737
Ultraviolet emission from the sun and stars: A comparison of IUE and Skylab spectra N89-10738
Rotational modulation of hydrogen Lyman alpha flux from 44i Bootis N89-10741
Transition region fluxes in A-F Dwarfs: Basal fluxes and dynamo activity N89-10747

STELLAR ATMOSPHERES
IUE observations of pulsating stars: Atmospheric structure, shock waves and stellar winds N89-10686
IUE observations of a hot DAO white dwarf: Implications for diffusion theory and photospheric stratification N89-10733
Periodic modulation of the atmosphere of Alpha Orionis N89-10756
Abundance and f values needed to interpret adequately the high resolution IUE spectra N89-10759

STELLAR CORONAS
The energy input mechanism into the lower transition regions between stellar chromospheres and coronae N89-10745

STELLAR ENVELOPES
UV and optical line emission from the shell of the old nova GK Persei N89-10714
Direct UV observations of the circumstellar envelope of alpha Orionis N89-10730
Recurrent shell infall events in a B0.5e star: HD 58978 1979-1988 N89-10732

STELLAR EVOLUTION
The Progenitor of SN 1987A — IUE N89-10697
Research in nuclear astrophysics: Stellar collapse and supernovae [DE88-015267] N89-10778

STELLAR FLARES
Spectral images of HD 199178 N89-10739
Ultraviolet flares on 2 Peg N89-10743
Chromospheric mass motions during a flare on UV Ceti N89-10744

STELLAR MASS
Mass flow in the interacting binary TX Ursae Majoris N89-10718
Cepheid binaries with large mass ratios (M1/M2) N89-10727

STELLAR MASS ACCRETION
The ultraviolet emission of accreting magnetic white dwarfs N89-10735

STELLAR MASS EJECTION
IUE observations of pulsating stars: Atmospheric structure, shock waves and stellar winds N89-10686
Mass loss from the K dwarf in V471 Tauri N89-10770

STELLAR MODELS
Model chromosphere and transition region for 56 Peg (K0 IIp + wd): A preliminary study N89-10726

STELLAR ORBITS
The orbit of the Cepheid AW Per N89-10728

STELLAR RADIATION
Ultraviolet emission from the sun and stars: A comparison of IUE and Skylab spectra N89-10738

STELLAR ROTATION
IUE observations of rapidly rotating K dwarfs in the Pleiades N89-10736
Rotational modulation of hydrogen Lyman alpha flux from 44i Bootis N89-10741
The discovery of a co-rotating magnetosphere in a helium weak star: HD5737 = alpha Scl N89-10751

STELLAR SPECTRA
A Decade of UV Astronomy with the IUE Satellite, volume 1 [ESA-SP-281-VOL-1] N89-10682
The analysis of spectra of novae taken near maximum N89-10706
The UV silicon spectra of early B stars N89-10763
C IV and Si IV in IUE spectra of normal B8-A0 stars: UV identified Be/Ae stars N89-10764
Au II in IUE spectra of chemically peculiar stars N89-10766
Validity of the classification of UV gallium stars N89-10767
The galatic and LMC extreme line supergiants compared: IUE observations of the Henize-Carlson and Zoo star samples of massive supergiants — Large Magellanic cloud (LMC) N89-10769
Accretion disk models of quasars and active galactic nuclei N89-10777

STELLAR SPECTROPHOTOMETRY
IUE spectrophotometry of the accretion disk of HZ Her/Her X-1 N89-10702

STELLAR TEMPERATURE
Temperature determinations of hot DA white dwarfs using IUE continuum fluxes N89-10734

STELLAR WINDS
IUE observations of pulsating stars: Atmospheric structure, shock waves and stellar winds N89-10686
Mg II flux and profile variability of hybrid-chromosphere stars N89-10750

STEREOPHOTOGRAPHY
Development of MOMS to a future multiband and stereoscopic sensor N89-10391

STIRLING CYCLE
Free-piston Stirling engine development [PB88-220025] N89-10286

STOCHASTIC PROCESSES
A stochastic model for the tortuous propagation of a lightning stepped leader N89-10433
Parallel processors for planning under uncertainty [DE88-016184] N89-10571

STORAGE RINGS (PARTICLE ACCELERATORS)
Nonlinear spin acceptance in electron storage rings [CEBAF-PR-88-009] N89-10614

STORMS (METEOROLOGY)
Oklahoma-Kansas preliminary regional experiment for storm-central (O-K pre-storm). Volume 3: Aircraft mission summary [PB88-205489] N89-10499

STRAIN HARDENING
The influence of texture on strain hardening [DE88-009157] N89-10158

STRAKES
Development in helicopter tail boom strake applications in the US [NASA-TM-101496] N89-10059

STREAK CAMERAS
Deflection of light by using tungsten bronze crystals [DE88-014151] N89-10618

STRESS (PHYSIOLOGY)
Modulation of human plasma fibronectin levels following exercise [AD-A192674] N89-10519

STRESS ANALYSIS
Flexural fatigue of a 2-D carbon/carbon composite material [DE88-010501] N89-10133
Leaf spring [EP-PATENT-0-253-574-A1] N89-10136
Characterization of dynamic fracture in copper under uniaxial stress and uniaxial strain [DE88-007824] N89-10162
Time-dependent mechanical behavior of partially stabilized zirconia for diesel engine applications [DE88-015330] N89-10171
Buckling of rings in column-supported bins and tanks [PB88-217336] N89-10290
Elastic-plastic large deflection analysis of axisymmetric shells [PB88-217344] N89-10295

STRESS-STRAIN RELATIONSHIPS
Inelastic buckling analyses of beams, columns and plates using the spline finite strip method [PB88-214291] N89-10299

STRESSES
Influence of specimen size on fatigue crack initiation of welded HY100 steel [AD-A196219] N89-10294

STRING THEORY
Loopspace general covariance in string field theory [DE88-014170] N89-10659
Gravitational time delay due to a spinning string [DE88-014733] N89-10661

STRUCTURAL ANALYSIS
La Recherche Aerospatiale, Bimonthly Bulletin, Number 1987-4, 239/July-August [ESA-TT-1088] N89-10026
On the problem of modeling for parameter identification in distributed structures [NASA-CR-182739] N89-10291
Geometric imperfections in plated structures subject to interaction between buckling modes [PB88-200902] N89-10296
Multispectral characterization of the spatial structure of remotely sensed scenes N89-10340

STRUCTURAL DESIGN
Kinematic study of flight telerobotic servicer configuration issues N89-10100
Actuators for a space manipulator N89-10101
Semiconductor Bridge (SCB): A new method for the ignition of explosives and pyrotechnics [DE88-011246] N89-10151
S-band transponder and telecommand decoder design and development for MECB satellites [INPE-4659-PRE/1362] N89-10219
Overview of ground coupled heat pump research and technology transfer activities [DE88-012938] N89-10255
Advanced planar array development for space station [NASA-CR-179372] N89-10407
Meteorological measurements made using Brazilian drifting buoys: Technical aspects and first results [INPE-4674-PRE/1372] N89-10502
Abstract, topological and uniform convex structures [PB88-202965] N89-10579

STRUCTURAL PROPERTIES (GEOLOGY)
The Paleo-ocean of Mars N89-10783
Mars: A water-rich planet N89-10784
Martian volcanism: A review N89-10785
Mars: Crustal pore volume, cryospheric depth, and the global occurrence of groundwater N89-10787
Is regolith absorbtion the explanation for the transition from early to present Mars climate N89-10788
Martian surface physical properties to be derived by radar altimeter on the Mars observer spacecraft N89-10789
Water and ice on Mars: Evidence from Valles Marineris N89-10803
Ablation of Martian glaciers N89-10805
Formation of the layered deposits in the Valles Marineris, Mars N89-10809
Could icy impacts reconcile Venus with Earth and Mars N89-10810
Seismic exploration for water on Mars N89-10811
The thermal properties of Martian surface materials at high lattitudes: Possible evidence for permafrost N89-10812
Martian tectonics: A review N89-10815
Thermal properties of channels in the Aeolis Quadrangle: Topographic traps for Aeolian materials N89-10825

STRUCTURAL STABILITY
Structural instability of sheath potential distribution and its possible implications for the L/H transition in tokamak plasmas [IPPJ-877] N89-10643

SUBSONIC FLOW
Validation of a pair of computer codes for estimation and optimization of subsonic aerodynamic performance of simple hinged-flap systems for thin swept wings [NASA-TP-2828] N89-10024

SUGAR BEETS
Microwave backscatter from beets, peas and potatoes throughout the growing season N89-10309
Relation between sugar beet crop yield and vegetative indexes calculated from LANDSAT MSS images N89-10333
Spectral reflectance of sugar beet and winter wheat canopies in the visible and infrared during growth N89-10342

SUMMER
Analysis and modeling of summertime convective cloud and precipitation structure over the southeastern United States [NASA-CR-183192] N89-10498

SUN
Compilation of methods in orbital mechanics and solar geometry [NASA-RP-1204] N89-10420

SUPERCOMPUTERS
Federal Coordinating Council on Science, Engineering and Technology, Committee on Computer Research and Applications, Subcommittee on Science and Engineering Computing [DE88-013228] N89-10525
Supercomputing: An indispensable component of applied research [DE88-015363] N89-10533
Tools to aid in the analysis of memory access patterns for FORTRAN programs [DE88-013609] N89-10535
Programming techniques for high-speed processing on the supercomputer FUJITSU VP-system [NAL-TR-915] N89-10565

SUPERCONDUCTIVITY
Physics and technology for the in-situ investigation of properties of materials [AD-A195498] N89-10145
Design approaches and parameters for magnetically levitated transport systems [DE88-014285] N89-10280

Synthesis and study of materials for superconducting electronics
[AD-A195279] N89-10649
Electronic structure of the quenched superconductivity of materials Y(sub 1-x)Pr(sub x)Ba2Cu3O(sub 7-delta)
[DE88-014414] N89-10658

SUPERCONDUCTORS
Sequentially evaporated thin Y-Ba-Cu-O superconductor films: Composition and processing effects
[NASA-TM-101388] N89-10235

SUPERGIANT STARS
Direct UV observations of the circumstellar envelope of alpha Orionis N89-10730
Periodic modulation of the atmosphere of Alpha Orionis N89-10756
The galatic and LMC extreme line supergiants compared: IUE observations of the Henize-Carlson and Zoo star samples of massive supergiants --- Large Magellanic cloud (LMC) N89-10769

SUPERHIGH FREQUENCIES
CARTEL: A method to calibrate S-band ranges with geostationary satellites. Results of orbit determination
[CNES-CT/DTI/MS/AE/124] N89-10108
Simultaneous S- and X-band uplink-downlink performance at DSS 13 N89-10194
X/X/Ka-band prime focus feed antenna for the Mars Observer beacon spacecraft N89-10195
Dual passband dichroic plate for X-band N89-10196
S-band transponder and telecommand decoder design and development for MECB satellites
[INPE-4659-PRE/1362] N89-10219
Complementary of microwave and optical range in the characterization of crops by remote sensing N89-10310

SUPERNOVA REMNANTS
IUE observations of oxygen-rich supernova remnants N89-10699
Ejecta in SN 1006: The knotty issue --- supernova remnant N89-10700
Supernova remnants' interactions with the inter-stellar medium N89-10771

SUPERNOVA 1987A
Observing SN 1987A with IUE N89-10683
Observations of SN 1987A: The narrow emission lines --- IUE N89-10696
The Progenitor of SN 1987A --- IUE N89-10697
The complete visual light curve of SN 1987A: Thirteen months of FES observations --- IUE Fine Error Sensor (FES) N89-10698

SUPERNOVAE
Gamma-ray observations of supernova SN 1987A
[INPE-4604-PRE/1327] N89-10680
Prospects for understanding the astrophysical r-process
[DE88-015449] N89-10773
A summary of major activities of the UNH and NRL groups
[NASA-CR-180949] N89-10774
Research in nuclear astrophysics: Stellar collapse and supernovae
[DE88-015267] N89-10778

SUPERSONIC AIRCRAFT
Wave drag and high-speed performance of supersonic STOVL fighter configuration
[NASA-TM-100061] N89-10017

SUPERSONIC COMBUSTION RAMJET ENGINES
Shock tunnel studies of scramjet phenomena
[NASA-CR-181721] N89-10045

SUPERSONIC FLOW
Normal force coefficient of supersonic flows over conical flare, cone-cylinder and conical boattails
[NAL-TR-949] N89-10021
Multiphoton ionization of transient species in supersonic jets
[DE88-008366] N89-10607
The dynamics of the Venus ionosphere
[NASA-CR-183167] N89-10779

SUPERSONIC SPEED
Supersonic missile air intakes: Design and development criteria N89-10031
Multiphoton ionization of transient species in supersonic jets
[DE88-008366] N89-10607

SUPPLEMENTS
Interplanetary medium data book: Supplement 3A, 1977-1985
[NASA-TM-89630] N89-10678

SURFACE FINISHING
Comparison of surface modifications of poly(ether urethanes) by chemical infusion and graft polymerization
[DE88-007887] N89-10172
Choice of coating and surface behavior of the hydrogen turbopump of the Vulcain engine
[ETN-88-93084] N89-10173

SURFACE GEOMETRY
Generation of a crowned pinion tooth surface by a surface of revolution
[NASA-TM-100260] N89-10282

SURFACE LAYERS
Characterization of layers created using surface modification techniques
[DE88-011918] N89-10651

SURFACE PROPERTIES
Physical principles of ultrasonic non-destructive evaluation of advanced composites
[NASA-CR-180225] N89-10129
Topological attributes for STEP curve and surface entities
[PB88-209630] N89-10532
Neoclassical resonant-plateau transport in the noncircular equipotential surface of a tandem mirror
[IPPJ-879] N89-10627

SURFACE ROUGHNESS
Calculation of the effects of ice on the backscatter of a ground plane
[NASA-CR-183303] N89-10213
Measuring in-situ soil surface roughness using a laser profilometer N89-10308

SURFACE ROUGHNESS EFFECTS
An approximative model for the microwave brightness temperature scattered by a rough open ocean surface N89-10344

SURFACE TEMPERATURE
Atmospheric correction of thermal infrared data from LANDSAT-5 for surface temperature estimation N89-10339
A new method for estimating regional evaporation from thermal infrared surface temperature measurements N89-10390

SURGES
Lightning and surge protection of large ground facilities N89-10474
Computer simulation of the effects of lightning stroke attachment to an electric power substation N89-10475
Modelling of common mode coupling between an aircraft wing traversed by a lightning current and wiring installed in that wing N89-10485

SURVEILLANCE
Selection and evaluation of video tape recorders for surveillance applications
[DE88-014240] N89-10261

SURVEYS
Israel Air Force (IAF) in-service aircraft lightning strike and damage survey N89-10431
Performance assessment register
[AGARD-R-763] N89-10666
Attitudes to the use of computerised information systems for production management in manufacturing industry: A survey
[TT-8706] N89-10670

SUSPENSION SYSTEMS (VEHICLES)
Leaf spring
[EP-PATENT-0-253-574-A1] N89-10136

SWEPT WINGS
Validation of a pair of computer codes for estimation and optimization of subsonic aerodynamic performance of simple hinged-flap systems for thin swept wings
[NASA-TP-2828] N89-10024
A transonic interactive boundary-layer theory for laminar and turbulent flow over swept wings
[NASA-CR-4185] N89-10029

SWITCHES
Effects of switch leakages upon Nimbus-7 SMMR calibration
[NASA-CR-180792] N89-10115
Simulation of plasma erosion opening switches
[DE88-014425] N89-10229
Crossatron switch as thyratron replacement in high repetition rate, high average power modulators
[DE88-013706] N89-10230

SWITCHING
Single-pole switching schemes for EHV transmission systems N89-10228

SWITCHING CIRCUITS
Dynamic properties of power MOS transistors
[LAAS-88-162] N89-10236
Integrated switching networks: A performance study N89-10567

SYMBIOTIC STARS
The variability of the UV spectrum of the symbiotic star BF Cygni N89-10758
The anomalous C 4 intensity ratio in symbiotic stars N89-10761

SYMBOLIC PROGRAMMING
Advanced data management design for autonomous telerobotic systems in space using spaceborne symbolic processors N89-10096

SYMBOLS
Block Toeplitz operators with rational symbols
[PB88-202890] N89-10587

SYNCHRONOUS SATELLITES
CARTEL: A method to calibrate S-band ranges with geostationary satellites. Results of orbit determination
[CNES-CT/DTI/MS/AE/124] N89-10108

SYNOPTIC METEOROLOGY
Lightning near Vandenberg AFB as related to various synoptic patterns N89-10486

SYNTAX
Interactive editing of mathematical formulae
[PB88-203005] N89-10580

SYNTHESIS (CHEMISTRY)
New diamond
[NASA-TT-20325] N89-10169
Direct methane conversion: An assessment
[DE88-010225] N89-10181

SYNTHETIC APERTURE RADAR
Spaceborne SAR imaging of land, an opportunity for polyphase code
[ATES/DMA/RAD/002-86] N89-10226
The use of the complex correlation function in the recovery of ocean wave spectra from SAR images N89-10315
Texture analysis in forest areas: High spectral resolution synthetic aperture radar data N89-10367
AGRISAR'86: Contributing to signature research N89-10387

SYNTHETIC FUELS
Alternate fuels for General Aviation aircraft with spark ignition engines
[DOT/FAA/CT-88/05] N89-10179

SYSTEM FAILURES
Electrostatic discharge and field effects of electronics systems N89-10493

SYSTEMS ANALYSIS
Quadruplex digital flight control system assessment
[NASA-CR-182741] N89-10058
Systems analysis of the inverse heat conduction problem N89-10244
Study on representation of surface coverage by imaging experiments
[ESA-CR(P)-2584] N89-10394
Second Annual Knowledge-Based Software Assistant Conference
[AD-A189819] N89-10536
Where's the intelligence in the intelligent assistant requirements analysis: Inference processes in the KBRA N89-10544
ASDL: An intelligent acquisition support tool N89-10554
Object-oriented approach to integrating database semantics, volume 4
[AD-A195853] N89-10672

SYSTEMS ENGINEERING
Multimegawatt power sources for commercial space operations
[DE88-015119] N89-10106
An electromagnetic calorimeter for a beauty factory
[NOTA-INTERNA-905] N89-10260
Vertex detector for a linear beauty factory
[NOTA-INTERNA-906] N89-10266

SYSTEMS INTEGRATION
Design criteria for hardware-in-the-loop simulation facilities N89-10052
Project management assistant: What have we learned N89-10552

SYSTEMS SIMULATION
Study on representation of surface coverage by imaging experiments
[ESA-CR(P)-2584] N89-10394

T

T-38 AIRCRAFT
Implications of a recent lightning strike to a NASA jet trainer N89-10478

TACTILE DISCRIMINATION
Robotic adaptive grasping based on vision and tactile sensor data N89-10288

TAIL ASSEMBLIES
Development in helicopter tail boom strake applications in the US
[NASA-TM-101496] N89-10059

TAIL ROTORS
Development in helicopter tail boom strake applications in the US
[NASA-TM-101496] N89-10059

TANDEM MIRRORS
Neoclassical resonant-plateau transport in the noncircular equipotential surface of a tandem mirror
[IPPJ-879] N89-10627

TAPE RECORDERS
Selection and evaluation of video tape recorders for surveillance applications
[DE88-014240] N89-10261

TASKS
Space truss assembly using teleoperated manipulators N89-10087
Dynamic task allocation for a man-machine symbiotic system N89-10098
TAYLOR INSTABILITY
Experiments on the influence of the geometry on the stability of Taylor-Couette flow [MPIS-MITT-87-1987] N89-10258
TDR SATELLITES
An expert system for scheduling requests for communications Links between TDRSS and ERBS N89-10065
An expert system that performs a satellite station keeping maneuver N89-10069
Preliminary project PASTEL: System interface between SPOT 4 and the PSDE's passenger [CNES-87/088-CT/DRT/TIT/TR] N89-10227
TECHNOLOGY ASSESSMENT
Actuators for a space manipulator N89-10101
TECHNOLOGY TRANSFER
Overview of ground coupled heat pump research and technology transfer activities [DE88-012938] N89-10255
Technology transfer and the knowledge-based software assistant N89-10541
Designing an effective user interface for a knowledge-based development environment N89-10549
TECTONICS
Areal and time distributions of volcanic formations on Mars N89-10800
Martian tectonics: A review N89-10815
TELECOMMUNICATION
Integrating distributed homogeneous and heterogeneous databases: Prototypes, volume 3 [AD-A195852] N89-10668
TELEMETRY
Scientific ballooning in Brazil [INPE-4602-PRE/1325] N89-10018
Range delay techniques for radar target simulators N89-10054
The Remote Atmospheric Probing Information Display (RAPID) system [AD-A196314] N89-10500
TELEOPERATORS
Space truss assembly using teleoperated manipulators N89-10087
A university teaching simulation facility N89-10088
Open control/display system for a telerobotics work station N89-10089
Consolidated fuel reprossing program: The implications of force reflection for teleoperation in space N89-10090
Issues, concerns, and initial implementation results for space based telerobotic control N89-10091
A shared position/force control methodology for teleoperation N89-10092
Advanced data management design for autonomous telerobotic systems in space using spaceborne symbolic processors N89-10096
NASREN: Standard reference model for telerobot control N89-10099
Kinematic study of flight telerobotic servicer configuration issues N89-10100
Teleoperated position control of a PUMA robot N89-10104
Telerobotic control of the seven-degree-of-freedom CESAR manipulator [DE88-012937] N89-10289
TELEPHONES
A retrospective study of the injuries sustained in telephone-mediated lightning strike N89-10464
TEMPERATURE DEPENDENCE
Lightning near Vandenberg AFB as related to various synoptic patterns N89-10466
TEMPERATURE EFFECTS
Aeroelastic thermal effects N89-10015
Thermal effects on the mechanical properties of SiC fiber reinforced reaction bonded silicon nitride matrix (SiC/RBSN) composites [NASA-TM-101348] N89-10134
Basic research on natural gas combustion phenomena-catalytic combustion [PB88-214606] N89-10142
TEMPERATURE MEASUREMENT
Infrared temperature measurement with inherent consideration of emissivity [DFVLR-FB-88-22] N89-10271
Atmospheric correction of thermal infrared data from LANDSAT-5 for surface temperature estimation N89-10339
Emitted short wavelength infrared radiation for detection and monitoring of volcanic activity N89-10377
A new method for estimating regional evaporation from thermal infrared surface temperature measurements N89-10390
TEMPERATURE PROFILES
Comparison of temperature profiles measured by three collocated microwave radiometers and radiosonde [PB88-212808] N89-10503
TENSILE PROPERTIES
Tensile properties of commercial aluminum-lithium alloys at cryogenic temperatures [DE88-014857] N89-10153
Riveting a case section with blind, self-plugging rivets [DE88-013224] N89-10284
The tensile strength of glass shells [DE88-013011] N89-10301
TERMINAL FACILITIES
Terminal control area design and air traffic loadings [DOT/FAA/DS-88/11] N89-10038
TERNARY ALLOYS
Theoretical model for the solute distribution of a PbSnTe growth by VMS in microgravity environment [INPE-4664-PRE/1365] N89-10183
TERRESTRIAL RADIATION
The role of clouds in surface radiation budgets N89-10501
TEST EQUIPMENT
An ion-optical bench for testing ion source lenses [DE88-013186] N89-10606
TEST FACILITIES
Design criteria for hardware-in-the-loop simulation facilities N89-10052
Simulation with real elements of Exocet anti-ship missiles N89-10056
Hellfire system model validation N89-10057
Laser velocimeter measurements of solids in multiphase flow [DE88-011611] N89-10251
TETHERING
System protection from atmospheric electricity for aerostats with conducting tethers N89-10497
TEXTURES
The influence of texture on strain hardening [DE88-009157] N89-10158
Texture analysis in forest areas: High spectral resolution synthetic aperture radar data N89-10367
THEMATIC MAPPERS (LANDSAT)
Spectral characterization of forest targets in mountainous zones on Thematic Mapper images N89-10328
Atmospheric correction of thermal infrared data from LANDSAT-5 for surface temperature estimation N89-10339
Comparative point-spread function calculations for the MOMS-1, Thematic Mapper and SPOT-HRV instruments N89-10379
MOMS-1 used synergistically with LANDSAT TM N89-10384
Comparative geological evolution of different remote sensing data of the Hoggar Mountains (Algeria) N89-10385
Digital analysis of MOMS-1, LANDSAT TM, and SPOT data of the Nakuru area (Kenya) N89-10386
Applications of LANDSAT (TM and MSS) data for an estimation of rangeland conditions in semiarid and arid areas of northern Kenya [DFVLR-FB-88-18] N89-10404
THEMATIC MAPPING
Strengths and shortcomings in Airborne Thematic Mapper (ATM) technology as applied to volcanic and geothermal areas in Iceland N89-10337
Nation-wide forest mapping and timber volume estimation using LANDSAT-5 TM imagery [INPE-4643-PRE/1354] N89-10402
Investigation of superradiant LDV markers and three-component velocity mapping [AD-A195504] N89-10662
THERMAL ANALYSIS
The detection of conformational disorder by thermal analysis [DE88-012932] N89-10657
THERMAL BATTERIES
Hydrogen sorption studies of materials used in Li(Si)/FeS2 thermal batteries [DE88-013154] N89-10231
THERMAL CONDUCTIVITY
Impacts of advanced refrigerator insulation [DE88-001180] N89-10185
THERMAL EXPANSION
Laser interferometric dilatometer for low-expansion materials [DE88-012329] N89-10272
THERMAL FATIGUE
Time-dependent mechanical behavior of partially stabilized zirconia for diesel engine applications [DE88-015330] N89-10171
THERMAL INSULATION
Impacts of advanced refrigerator insulation [DE88-001180] N89-10185
THERMAL PLASMAS
The dynamics of the Venus ionosphere [NASA-CR-183167] N89-10779
THERMAL RADIATION
Climatic effects of enhanced CO2 levels in Mars early atmosphere N89-10799
THERMIONIC CATHODES
Evaluation of the characteristics of a field emission cathode for use in a Mercury ion trap frequency standard N89-10193
THERMIONIC EMISSION
Experimental studies on the surface confined quiescent plasma at INPE [INPE-4605-PRE/1328] N89-10630
THERMODYNAMIC PROPERTIES
Thermodynamic analysis of compatibility of several reinforcement materials with beta phase NiAl alloys [NASA-CR-4171] N89-10131
Reports of investigations on: Derivation of an infinite-dilution activity coefficient model and application to two-component vapor/liquid equilibria data [DE88-007517] N89-10147
Inelastic ion-surface collisions. Ion neutralization on intermetallic surfaces [AD-A196322] N89-10608
Thermodynamic properties by non-calorimetric methods: Progress report [DE88-015422] N89-10660
The thermal properties of Martian surface materials at high lattitudes: Possible evidence for permafrost N89-10812
Thermal properties of channels in the Aeolis Quadrangle: Topographic traps for Aeolian materials N89-10825
THERMODYNAMICS
Thermodynamic analysis of compatibility of several reinforcement materials with FeAl alloys [NASA-CR-4172] N89-10128
Reports of investigations on: Derivation of an infinite-dilution activity coefficient model and application to two-component vapor/liquid equilibria data [DE88-007517] N89-10147
Thermodynamics and kinetics of phase formation of thin-film metal on gallium arsenide [DE88-015702] N89-10648
THERMOSETTING RESINS
Chemoviscosity modeling for thermosetting resin systems, part 3 [NASA-CR-181718] N89-10132
THIN FILMS
Sequentially evaporated thin Y-Ba-Cu-O superconductor films: Composition and processing effects [NASA-TM-101388] N89-10235
Electronic structure of electrodeposited thin film CdTe solar cells [DE88-001170] N89-10406
Solid State Photovoltaic Research Branch [DE88-001179] N89-10410
Thermodynamics and kinetics of phase formation of thin-film metal on gallium arsenide [DE88-015702] N89-10648
Synthesis and study of materials for superconducting electronics [AD-A195279] N89-10649
PECVD (Plasma Enhanced Chemical Vapor Deposition) diamond thin films for research instrumentation [AD-A195443] N89-10652
Structure of amorphous silicon alloy films [DE88-001167] N89-10654
Beam assisted fabrication of 3-5/Si monolithic devices [AD-A195479] N89-10655
THIN PLATES
Acoustic radiation from plates driven by multi-point random forces N89-10602
THREE DIMENSIONAL FLOW
Applications of a three-dimensional finite element model to mountain-valley flows [DE88-008898] N89-10412
On high resolution schemes for three-dimensional Euler equations [NAL-TR-950T] N89-10581
THRUST
Turbofan forced mixer lobe flow modeling. Part 3: Application to augment engines [NASA-CR-4147] N89-10025
THUNDERSTORMS
International Aerospace and Ground Conference on Lightning and Static Electricity [PB88-197439] N89-10429
Triggering of lightning by the Atlas Centaur vehicle N89-10438
Electromagnetic radiations generated by microdischarges from hydrometeors N89-10448

Lightning initiation on aircraft in thunderstorms N89-10456
The electrical structure of thunderstorm anvils N89-10470
Lightning in mesoscale convective complexes on 3-5 June 1985 in Oklahoma and Kansas N89-10471
Spatial distribution of lightning strikes to ground during small thunderstorms in Florida N89-10472
Monitoring lightning activity in South Africa with a VLF single-station technique: Comparison with meteosat infrared data N89-10480
Some observations and analysis of atmospheric electricity over non-uniform high terrain N89-10489
Intracloud lightning as a precursor to thunderstorm microbursts N89-10490
The lightning flash counter: Papua New Guinean experience N89-10491

THYRATRONS
Crossatron switch as thyratron replacement in high repetition rate, high average power modulators [DE88-013706] N89-10230

TIMBER INVENTORY
Nation-wide forest mapping and timber volume estimation using LANDSAT-5 TM imagery [INPE-4643-PRE/1354] N89-10402

TIME
A filamentary method for calculating induced voltages within resistive structures in either the frequency or time domain N89-10484

TIME DEPENDENCE
Time-dependent mechanical behavior of partially stabilized zirconia for diesel engine applications [DE88-015330] N89-10171
A stochastic model for the tortuous propagation of a lightning stepped leader N89-10433

TIME LAG
Gravitational time delay due to a spinning string [DE88-014733] N89-10661

TOKAMAK DEVICES
Neon puffing experiments in the JIPP T-IIU tokamak [IPPJ-870] N89-10632
The study of hydromagnetic waves and RF heating using the TORTUS tokamak and the development of diagnostic techniques N89-10635
On the generation of runaway electrons and their impact to plasma facing components [IPPJ-871] N89-10641
Structural instability of sheath potential distribution and its possible implications for the L/H transition in tokamak plasmas [IPPJ-877] N89-10643

TOLLMEIN-SCHLICHTING WAVES
Resonant excitation of spatial perturbations in a boundary layer in the presence of a pressure gradient [NASA-TT-20305] N89-10248

TOOLS
Cable applications in robot compliant devices N89-10102

TOPOGRAPHY
Wilson cycle studies [NASA-CR-183146] N89-10419
Earth rotation and core topography [NASA-CR-183186] N89-10425

TOPOLOGY
Topological attributes for STEP curve and surface entities [PB88-209630] N89-10532
Abstract, topological and uniform convex structures [PB88-202965] N89-10579
Quasiperiodic ordering in grain boundaries [DE88-012199] N89-10647

TOROIDAL PLASMAS
Adventures in magnetohydrodynamics [IPPJ-862] N89-10629

TOROIDS
Confinement and heating of high beta plasmas with emphasis on compact toroids [DE88-015777] N89-10645

TORUSES
Io: IUE observations of its atmosphere and the plasma torus N89-10691

TOUGHNESS
A compendium of sources of fracture toughness and fatigue crack growth data for metallic alloys, part 3 [NASA-TM-100675] N89-10165

TOWERS
A case for a unified lightning threat N89-10447
A revised electrogeometric model for the termination of lightning strokes on ground objects N89-10476

TRAFFIC
Integrated switching networks: A performance study N89-10567

TRAJECTORIES
Inelastic ion-surface collisions. Ion neutralization on intermetallic surfaces [AD-A196322] N89-10608

TRANSFORMERS
Computer simulation of the effects of lightning stroke attachment to an electric power substation N89-10475

TRANSIENT HEATING
High-resolution heat-transfer-coefficient maps applicable to compound-curve surfaces using liquid crystals in a transient wind tunnel [NASA-TM-89855] N89-10246

TRANSIENT RESPONSE
Recent developments in structural sensitivity analysis [NASA-TM-100668] N89-10300

TRANSISTOR AMPLIFIERS
An 8.4-GHz cryogenically cooled HEMT amplifier for DSS 13 N89-10199

TRANSISTOR CIRCUITS
Dynamic properties of power MOS transistors [LAAS-88-162] N89-10236

TRANSITION FLOW
Numerical study of the entrance flow and its transition in a curcular pipe [ISAS-RN-626] N89-10250

TRANSITION METALS
Ab initio studies of transition-metal dihydrogen chemistry [DE88-014467] N89-10139
Inelastic ion-surface collisions. Ion neutralization on intermetallic surfaces [AD-A196322] N89-10608

TRANSITION TEMPERATURE
Physics and technology for the in-situ investigation of properties of materials [AD-A195498] N89-10145

TRANSMISSION LINES
Single-pole switching schemes for EHV transmission systems N89-10228
Lightning return stroke velocity N89-10446
On a surface mounted transmission line configuration for aperture testing N89-10458

TRANSMISSIONS (MACHINE ELEMENTS)
Generation of a crowned pinion tooth surface by a plane [NASA-TM-100259] N89-10283

TRANSONIC FLOW
Navier-Stokes simulation of transonic wing flow fields using a zonal grid approach [NASA-TM-100039] N89-10022
Modification of the unsteady flow field predicted by transonic small distrubance equations using a Navier-Stokes solution of the steady flow field N89-10241

TRANSONIC SPEED
A transonic interactive boundary-layer theory for laminar and turbulent flow over swept wings [NASA-CR-4185] N89-10029

TRANSONIC WIND TUNNELS
Highlights of experience with a flexible walled test section in the NASA Langley 0.3-meter transonic cryogenic tunnel [NASA-TM-101491] N89-10060

TRANSPONDERS
S-band transponder and telecommand decoder design and development for MECB satellites [INPE-4659-PRE/1362] N89-10219

TRANSPORT AIRCRAFT
Using full-mission simulation for human factors research in air transport operations [NASA-TM-88330] N89-10037
Contamination of environmental control systems in Hercules aircraft [MRL-R-1116] N89-10040

TRANSPORT PROPERTIES
Direct Numerical Simulations (DNS) of an unpremixed turbulent jet flame [AD-A196128] N89-10149

TRANSPORT THEORY
Progress in NODAL transport methods [DE88-012416] N89-10590
Numerical simulations of dust transport into northern high latitudes during a Martian polar warming N89-10782

TRANSPORTATION
Hydrogen supply over long distances using chemicals description and evaluation of a technical system [DE88-012630] N89-10178

TRAPPED MAGNETIC FIELDS
Research on a two-stage free electron laser oscillator [AD-A195339] N89-10278

TRAPPED PARTICLES
Research on a two-stage free electron laser oscillator [AD-A195339] N89-10278

TROPICAL METEOROLOGY
ONR tropical cyclone motion research initiative: First-year review, discussion and tentative hypotheses [AD-A194902] N89-10505
Model-data comparisons for the 1982-83 El Nino: The XBT tracks [PB88-221668] N89-10514

TROPICAL REGIONS
Comparative analysis of spectral response in the optical domain of targets in a tropical swamp at various spectral and spatial resolutions N89-10363
Rock and soil discrimination in natural tropical conditions using a spot-calibrated radiometer N89-10374
Seasonal wind variations in the Martian subtropics N89-10807

TRUSSES
Dynamics and control of the orbiting grid structures and the synchronously deployable beam [NASA-CR-183205] N89-10297

TUNGSTEN CARBIDES
Graded structure composites [EP-PATENT-0-260-850-A2] N89-10135

TUNING
Aeroelastic formulation for tuned and mistuned rotors N89-10013

TURBIDITY
Atmospheric propagation effects relevant to optical communications N89-10201

TURBINE ENGINES
A comparative evaluation of RPD (Rotary Particle Depositor) and ferrographic diagnostic methods for turbine engine lubricant samples [AD-A196207] N89-10044
T55-L-712 turbine engine compressor housing refurbishment-plasma spray project [NASA-TM-101310] N89-10156

TURBINE PUMPS
Choice of coating and surface behavior of the hydrogen turbopump of the Vulcain engine [ETN-88-93084] N89-10173

TURBINES
Development of ceramic matrix composites for application in the ceramic technology for advanced heat engines [DE88-015329] N89-10168

TURBOFAN ENGINES
Turbofan forced mixer lobe flow modeling. Part 3: Application to augment engines [NASA-CR-4147] N89-10025

TURBOMACHINERY
Forced vibration and flutter design methodology N89-10016

TURBULENCE
Resonant excitation of spatial perturbations in a boundary layer in the presence of a pressure gradient [NASA-TT-20305] N89-10248
Optical imaging through atmospheric turbulence N89-10423
Experimental studies on the surface confined quiescent plasma at INPE [INPE-4605-PRE/1328] N89-10630

TURBULENT DIFFUSION
Turbulent diffusion of ocean bubbles [PB88-212816] N89-10513
Vertical O(sub 3) distribution as a diagnostic for eddy diffusion profile N89-10821

TURBULENT FLOW
A transonic interactive boundary-layer theory for laminar and turbulent flow over swept wings [NASA-CR-4185] N89-10029
La Recherche Aerospatiale, Bimonthly Bulletin, number 1987-6, 241/November-December [ESA-TT-1102] N89-10030
Numerical analysis of laminar and turbulent incompressible flows using the finite element Fluid Dynamics Analysis Package (FIDAP) [NASA-CR-179390] N89-10253
Experimental detection of high speed fronts and clarification of their coherence with low speed streaks and streamwise vortices in a fully developed turbulent channel [MPIS-MITT-88-1987] N89-10259

TWO DIMENSIONAL FLOW
Highlights of experience with a flexible walled test section in the NASA Langley 0.3-meter transonic cryogenic tunnel [NASA-TM-101491] N89-10060

U

ULTRAHIGH FREQUENCIES
CARTEL: A method to calibrate S-band ranges with geostationary satellites. Results of orbit determination [CNES-CT/DTI/MS/AE/124] N89-10108
DSN 64-meter antenna L-band (1668-MHz) microwave system performance overview N89-10210
S-band transponder and telecommand decoder design and development for MECB satellites [INPE-4659-PRE/1362] N89-10219

ULTRASONIC TESTS
Physical principles of ultrasonic non-destructive evaluation of advanced composites [NASA-CR-180225] N89-10129
ULTRAVIOLET ASTRONOMY
A Decade of UV Astronomy with the IUE Satellite, volume 1 [ESA-SP-281-VOL-1] N89-10682
Observing SN 1987A with IUE N89-10683
Cataclysmic variables N89-10684
White dwarfs N89-10685
IUE observations of pulsating stars: Atmospheric structure, shock waves and stellar winds N89-10686
IUE observations of planetary atmospheres N89-10687
Comets --- IUE N89-10688
Some recent results from the study of cool stars --- IUE N89-10689
IUE observations and physical processes of interacting binary stars N89-10690
Io: IUE observations of its atmosphere and the plasma torus N89-10691
On the abundance of micron-sized particles in Saturn's A and B rings N89-10692
Jovian equatorial H2 emission from 1979-1987 N89-10693
Large time scale variation in hydrogen emission from Jupiter and Saturn N89-10694
Phenomenological analysis of Jovian north auroral H2 Lyman band emissions --- IUE N89-10695
Observations of SN 1987A: The narrow emission lines --- IUE N89-10696
The Progenitor of SN 1987A --- IUE N89-10697
The complete visual light curve of SN 1987A: Thirteen months of FES observations --- IUE Fine Error Sensor (FES) N89-10698
IUE observations of oxygen-rich supernova remnants N89-10699
Ejecta in SN 1006: The knotty issue --- supernova remnant N89-10700
Far UV observations of black hole candidates: The case of LMC X-3 N89-10701
IUE spectrophotometry of the accretion disk of HZ Her/Her X-1 N89-10702
Simultaneous IUE, EXOSAT and optical observations of the unusual AM Her type variable H058+608 N89-10703
A 0535+26/HDE 245770: A typical Be/X-ray transient system: Coordinated multiwavelength twelve years monitor N89-10704
IUE and optical observations of X-ray sources in the Large Margellanic Cloud (LMC) N89-10705
The analysis of spectra of novae taken near maximum N89-10706
The 1981 outburst of the old nova GK Persei N89-10707
Observations of classical novae in outburst N89-10708
Observations and simulations of nova Vul 1984 no. 2: A nova with ejecta rich in oxygen, neon, and magnesium N89-10709
Observations and simulations of recurrent novae: U Sco and V394 CrA N89-10710
Optical and ultraviolet observations of nova Vul 1987 N89-10711
Ultraviolet observations of LMC nova 1988 N89-10712
SS Cygni in quiescence --- IUE N89-10713
UV and optical line emission from the shell of the old nova GK Persei N89-10714
IUE observations of the 1987 superoutburst of the dwarf nova Z Cha N89-10715
Observations of galactic WC + O binary systems: HD 97152 and HD 152270 N89-10716
Atmospheric eclipse effects in Wolf-Rayet binaries in the Small Magellanic Cloud N89-10717
Mass flow in the interacting binary TX Ursae Majoris N89-10718
A new study of the interacting binary star V356 Sgr N89-10719
Matter streams in semi-detached binary systems N89-10720
The November 1987 eclipse of the zeta-Aur system HR 2554 N89-10721
Asymmetry in zeta Auriage chromospheres N89-10722
Superionized plasmas in Algol binaries N89-10723
HD 207739 and other F + Be variables N89-10724
Searching for the white dwarf in WZ Sagittae N89-10725
Model chromosphere and transition region for 56 Peg (K0 IIp + wd): A preliminary study N89-10726
Cepheid binaries with large mass ratios (M1/M2) N89-10727
The orbit of the Cepheid AW Per N89-10728
Companions to peculiar red giants: HR 363 and HR 1105 N89-10729
Direct UV observations of the circumstellar envelope of alpha Orionis N89-10730
Multi-wavelength observations of the peculiar red giant HR 3126 N89-10731
Recurrent shell infall events in a B0.5e star: HD 58978 1979-1988 N89-10732
IUE observations of a hot DAO white dwarf: Implications for diffusion theory and photospheric stratification N89-10733
Temperature determinations of hot DA white dwarfs using IUE continuum fluxes N89-10734
The ultraviolet emission of accreting magnetic white dwarfs N89-10735
IUE observations of rapidly rotating K dwarfs in the Pleiades N89-10736
On the flux-period and flux-flux correlations in late type stars N89-10737
Ultraviolet emission from the sun and stars: A comparison of IUE and Skylab spectra N89-10738
Doppler imaging of AR Lacertae at three epochs N89-10740
Rotational modulation of hydrogen Lyman alpha flux from 44i Bootis N89-10741
Mapping of surface activity on the W UMa-type system VW Cephei N89-10742
Ultraviolet flares on 2 Peg N89-10743
Chromospheric mass motions during a flare on UV Ceti N89-10744
The energy input mechanism into the lower transition regions between stellar chromospheres and coronae N89-10745
Transition regions of dM stars N89-10746
Transition region fluxes in A-F Dwarfs: Basal fluxes and dynamo activity N89-10747
Line formation of cool carbon star chromospheres N89-10748
Lithium and chromospherically active single giants N89-10749
Mg II flux and profile variability of hybrid-chromosphere stars N89-10750
The discovery of a co-rotating magnetosphere in a helium weak star: HD5737 = alpha Scl N89-10751
Observations of ultraviolet variability in RV Tauri stars N89-10752
Fluorescence processes and line identifications in the UV spectra of cool stars N89-10753
Fe II level population in luminous variable stars N89-10754
Identification of new fluorescence processes in the UV spectra of cool stars from new energy levels of Fe II and Cr II N89-10755
Periodic modulation of the atmosphere of Alpha Orionis N89-10756
Mg II line profiles of the Mira S Carinae N89-10757
The variability of the UV spectrum of the symbiotic star BF Cygni N89-10758
Abundance and f values needed to interpret adequately the high resolution IUE spectra N89-10759
Carbon and nitrogen abundance determinations from transition layer lines --- giant stars N89-10760
The anomalous C 4 intensity ratio in symbiotic stars N89-10761
The IUE spectral atlas of two normal B stars: pi Cet and nu Cap (125 to 200 nm) N89-10762
The UV silicon spectra of early B stars N89-10763
C IV and Si IV in IUE spectra of normal B8-A0 stars: UV identified Be/Ae stars N89-10764
Ultraviolet properties of IRAS-selected Be stars N89-10765
Au II in IUE spectra of chemically peculiar stars N89-10766
Validity of the classification of UV gallium stars N89-10767
Detected UV variability in the IUE spectra of the Ap-Si star HD 25823 N89-10768
The galatic and LMC extreme line supergiants compared: IUE observations of the Henize-Carlson and Zoo star samples of massive supergiants --- Large Magellanic cloud (LMC) N89-10769
Mass loss from the K dwarf in V471 Tauri N89-10770
ULTRAVIOLET LASERS
Gas-contact cooling for VUV laser oscillation in recombining plasmas [IPPJ-881] N89-10631
ULTRAVIOLET SPECTRA
A Decade of UV Astronomy with the IUE Satellite, volume 1 [ESA-SP-281-VOL-1] N89-10682
Observations of galactic WC + O binary systems: HD 97152 and HD 152270 N89-10716
Atmospheric eclipse effects in Wolf-Rayet binaries in the Small Magellanic Cloud N89-10717
Mass flow in the interacting binary TX Ursae Majoris N89-10718
A new study of the interacting binary star V356 Sgr N89-10719
Matter streams in semi-detached binary systems N89-10720
The November 1987 eclipse of the zeta-Aur system HR 2554 N89-10721
Asymmetry in zeta Auriage chromospheres N89-10722
Superionized plasmas in Algol binaries N89-10723
HD 207739 and other F + Be variables N89-10724
Searching for the white dwarf in WZ Sagittae N89-10725
Model chromosphere and transition region for 56 Peg (K0 IIp + wd): A preliminary study N89-10726
Cepheid binaries with large mass ratios (M1/M2) N89-10727
The orbit of the Cepheid AW Per N89-10728
Companions to peculiar red giants: HR 363 and HR 1105 N89-10729
Direct UV observations of the circumstellar envelope of alpha Orionis N89-10730
Multi-wavelength observations of the peculiar red giant HR 3126 N89-10731
Recurrent shell infall events in a B0.5e star: HD 58978 1979-1988 N89-10732
IUE observations of a hot DAO white dwarf: Implications for diffusion theory and photospheric stratification N89-10733
Temperature determinations of hot DA white dwarfs using IUE continuum fluxes N89-10734
The ultraviolet emission of accreting magnetic white dwarfs N89-10735
IUE observations of rapidly rotating K dwarfs in the Pleiades N89-10736
On the flux-period and flux-flux correlations in late type stars N89-10737
Ultraviolet emission from the sun and stars: A comparison of IUE and Skylab spectra N89-10738
Spectral images of HD 199178 N89-10739
Doppler imaging of AR Lacertae at three epochs N89-10740
Rotational modulation of hydrogen Lyman alpha flux from 44i Bootis N89-10741
Mapping of surface activity on the W UMa-type system VW Cephei N89-10742
Ultraviolet flares on 2 Peg N89-10743
Chromospheric mass motions during a flare on UV Ceti N89-10744
The energy input mechanism into the lower transition regions between stellar chromospheres and coronae N89-10745
Transition regions of dM stars N89-10746
Transition region fluxes in A-F Dwarfs: Basal fluxes and dynamo activity N89-10747
Line formation of cool carbon star chromospheres N89-10748
Lithium and chromospherically active single giants N89-10749
Mg II flux and profile variability of hybrid-chromosphere stars N89-10750
The discovery of a co-rotating magnetosphere in a helium weak star: HD5737 = alpha Scl N89-10751
Observations of ultraviolet variability in RV Tauri stars N89-10752
Fluorescence processes and line identifications in the UV spectra of cool stars N89-10753
Fe II level population in luminous variable stars N89-10754
Identification of new fluorescence processes in the UV spectra of cool stars from new energy levels of Fe II and Cr II N89-10755
Periodic modulation of the atmosphere of Alpha Orionis N89-10756
Mg II line profiles of the Mira S Carinae N89-10757
The variability of the UV spectrum of the symbiotic star BF Cygni N89-10758
Abundance and f values needed to interpret adequately the high resolution IUE spectra N89-10759
Carbon and nitrogen abundance determinations from transition layer lines --- giant stars N89-10760
The anomalous C 4 intensity ratio in symbiotic stars N89-10761
The IUE spectral atlas of two normal B stars: pi Cet and nu Cap (125 to 200 nm) N89-10762
The UV silicon spectra of early B stars N89-10763
C IV and Si IV in IUE spectra of normal B8-A0 stars: UV identified Be/Ae stars N89-10764
Ultraviolet properties of IRAS-selected Be stars N89-10765
Au II in IUE spectra of chemically peculiar stars N89-10766
Detected UV variability in the IUE spectra of the Ap-Si star HD 25823 N89-10768

UNDERGROUND TRANSMISSION LINES
The interaction between lightning grounding systems and buried cables N89-10496
UNDERWATER ACOUSTICS
Joint CGS-AOML (Charting and Geodetic Service-Atlantic Oceanographic and Meteorological Laboratory) acoustical bottom echo-formation research. 1: Literature search and initial modelling results
[PB88-202007] N89-10512
UNDERWATER RESOURCES
Imaging spectrometry applied to the remote sensing of submerged seaweed N89-10361
UNITED STATES
Development in helicopter tail boom strake applications in the US
[NASA-TM-101496] N89-10059
UNIVERSITIES
Civil Space Technology Initiative: A first step
[NASA-TM-100949] N89-10665
UNSTEADY AERODYNAMICS
AGARD manual on aeroelasticity in axial-flow turbomachines. Volume 2: Structural dynamics and aeroelasticity
[AGARD-AG-298-VOL-2] N89-10006
Aeroelastic formulation for tuned and mistuned rotors N89-10013
Fan flutter test N89-10014
UNSTEADY FLOW
Unsteady three-dimensional stall on a rectangular wing N89-10027
Modification of the unsteady flow field predicted by transonic small distrubance equations using a Navier-Stokes solution of the steady flow field N89-10241
An algorithm for unsteady flows with strong convection
[NASA-TM-100828] N89-10575
Delta square-correction scheme for unsteady Euler equations
[NAL-TR-948] N89-10576
UPLINKING
Simultaneous S- and X-band uplink-downlink performance at DSS 13 N89-10194
UPPER ATMOSPHERE
Upper-atmosphere zonal winds from satellite orbit analysis: An update
[RAE-TR-87058] N89-10507
URBAN DEVELOPMENT
Environmental impact of the urban growth on the Western Sao Paulo metropolitan area
[INPE-4670-PRE/1370] N89-10413
USER MANUALS (COMPUTER PROGRAMS)
CCM (Community Climate Model) modular processor users' guide (version PROC02)
[PB88-216577] N89-10428
Develop an automated Data Base Management System (DBMS): Report on DBMS software and user's guide
[DE88-015996] N89-10674
USER REQUIREMENTS
CLEAR: Communications Link Expert Assistance Resource N89-10072
Robot hands and extravehicular activity N89-10097
Designing an effective user interface for a knowledge-based development environment N89-10549
Review of the requirements for higher level ERS-1 products within Europe
[ESA-CR(P)-2586] N89-10664

V

V/STOL AIRCRAFT
Wave drag and high-speed performance of supersonic STOVL fighter configuration
[NASA-TM-100061] N89-10017
Phase 4 static tests of the J-97 powered, external augmentor V/STOL model at the NASA, Ames Research Center, November 1983
[NASA-CR-177395] N89-10028
VALLEYS
Applications of a three-dimensional finite element model to mountain-valley flows
[DE88-008898] N89-10412
Some observations and analysis of atmospheric electricity over non-uniform high terrain N89-10489
Water and ice on Mars: Evidence from Valles Marineris N89-10803
VAPOR DEPOSITION
PECVD (Plasma Enhanced Chemical Vapor Deposition) diamond thin films for research instrumentation
[AD-A195443] N89-10652
Beam assisted fabrication of 3-5/Si monolithic devices
[AD-A195479] N89-10655
VAPOR PHASE EPITAXY
New diamond
[NASA-TT-20325] N89-10169
VAPOR PHASES
Theoretical model for the solute distribution of a PbSnTe growth by VMS in microgravity environment
[INPE-4664-PRE/1365] N89-10183
VAPOR PRESSURE
Reports of investigations on: Derivation of an infinite-dilution activity coefficient model and application to two-component vapor/liquid equilibria data
[DE88-007517] N89-10147
VARIABILITY
Detected UV variability in the IUE spectra of the Ap-Si star HD 25823 N89-10768
VARIABLE STARS
IUE observations of pulsating stars: Atmospheric structure, shock waves and stellar winds N89-10686
Observations of ultraviolet variability in RV Tauri stars N89-10752
Fe II level population in luminous variable stars N89-10754
VECTORS (MATHEMATICS)
Programming techniques for high-speed processing on the supercomputer FUJITSU VP-system
[NAL-TR-915] N89-10565
VEGETATION
Extracting soil and vegetation characteristics from microwave remote sensing data N89-10306
Retrieving vegetation and soil parameters from radar measurements N89-10321
Monitoring seasonal variations of soil moisture and vegetation cover using satellite microwave radiometry N89-10378
VEGETATIVE INDEX
Introducing spectral data into a plant process model for improving its prediction ability N89-10324
Biomass and wheat crop yield estimation from SPOT vegetative indexes N89-10327
Estimation of the interception efficiency of an alfalfa canopy from a vegetative index N89-10332
Relation between sugar beet crop yield and vegetative indexes calculated from LANDSAT MSS images N89-10333
Spectral signature of citrus fruits and its evolution: Identification of the vegetative index of least temporal variation N89-10373
A study of the vegetation cover with AVHRR during HAPEX-MOBILHY N89-10389
The Transformed Vegetation Index (TVI) for estimation of Brazilian cerrado's phytomass
[INPE-4603-PRE/1326] N89-10400
VELOCITY MEASUREMENT
Steady flow field measurements using laser Doppler velocimetry
[AD-A195228] N89-10245
Measurement of vertical velocity using clear-air Doppler radars
[AD-A195344] N89-10427
Measurements of the velocity change of a lightning return stroke with height N89-10442
Lightning return stroke velocity N89-10446
VENUS ATMOSPHERE
The dynamics of the Venus ionosphere
[NASA-CR-183167] N89-10779
VERTICAL DISTRIBUTION
Vertical O(sub 3) distribution as a diagnostic for eddy diffusion profile N89-10821
VERTICAL TAKEOFF AIRCRAFT
Wave drag and high-speed performance of supersonic STOVL fighter configuration
[NASA-TM-100061] N89-10017
VERY LARGE ARRAY (VLA)
Phasing the antennas of the Very Large Array (VLA) for reception of telemetry from Voyager 2 at Neptune encounter N89-10207
VERY LARGE SCALE INTEGRATION
A software simulation study of the long constraint length VLSI Viterbi decoder N89-10203
An expert system for VLSI layout N89-10528
VERY LONG BASE INTERFEROMETRY
Deep space tracking in local reference frames N89-10187
VERY LOW FREQUENCIES
Precise long-range lightning mapping with the UK arrival time difference VLF technique N89-10486
VIDEO DATA
Selection and evaluation of video tape recorders for surveillance applications
[DE88-014240] N89-10261
VISCOELASTICITY
Life time prediction: Synthesis on ONERA's research in viscoplasticity and continuous damage mechanics, applied to engine materials and structures N89-10011
VISCOSITY
Chemoviscosity modeling for thermosetting resin systems, part 3
[NASA-CR-181718] N89-10132
The delineation and interpretation of the earth's gravity field
[NASA-CR-183283] N89-10416
VISCOUS FLOW
A finite element formulation for incompressible, conjugate, viscous/porous flow problems
[DE88-007113] N89-10254
VISIBILITY
Study on representation of surface coverage by imaging experiments
[ESA-CR(P)-2584] N89-10394
VISIBLE INFRARED SPIN SCAN RADIOMETER
Analysis and use of VAS satellite data
[NASA-CR-183184] N89-10426
VISUAL DISCRIMINATION
Robotic adaptive grasping based on vision and tactile sensor data N89-10288
VITERBI DECODERS
Node synchronization of viterbi decoders using state metrics N89-10202
A software simulation study of the long constraint length VLSI Viterbi decoder N89-10203
Phobos lander coding system: Software and analysis N89-10208
VOID RATIO
Void collapse and void growth in crystalline solids N89-10421
VOLATILITY
Photochemical weathering and contemporary volatile loss on Mars N89-10795
Seismic exploration for water on Mars N89-10811
Volatile inventory of Mars-2: Primordial sources and fractionating processes N89-10814
VOLCANOLOGY
Strengths and shortcomings in Airborne Thematic Mapper (ATM) technology as applied to volcanic and geothermal areas in Iceland N89-10337
Emitted short wavelength infrared radiation for detection and monitoring of volcanic activity N89-10377
Wilson cycle studies
[NASA-CR-183146] N89-10419

W

WAKES
Estimation of up-wash distribution around an automobile by three-dimensional smoke wind tunnel test
[NAL-TR-921] N89-10023
WARNING SYSTEMS
New electric field instrumentation and the effects of space charge at Kennedy Space Center N89-10444
Lightning protection for high explosives and instrumentation using a field mill system N89-10467
The surface electric field as a warning criterion N89-10468
An interagency working group on lightning threat warning N89-10469
The SAFIR lightning monitoring and warning system, applications to aerospace activities N89-10481
Considerations for using lightning locating systems in performance evaluations of single-station lightning detection sensors N89-10488
WASTE DISPOSAL
Living in space, book 2, levels D, E, F
[NASA-EP-223] N89-10522
WATER
Laser velocimeter measurements of solids in multiphase flow
[DE88-011611] N89-10251
Mars: A water-rich planet N89-10784
Release of magmatic water on Mars: Estimated timing and volumes N89-10790
Mars low albedo regions: Possible map of near-surface N89-10794
Ice or liquid water in the Martian regolith. Morphologic indicators from rampart craters N89-10806
Seismic exploration for water on Mars N89-10811
Water on Mars N89-10822
WATER COLOR
Estimation of primary marine production using spaceborne data on ocean color N89-10371
WATER COOLED REACTORS
Progress in NODAL transport methods
[DE88-012416] N89-10590
WATER EROSION
Discrimination of zones of high water erosion risk using SPOT images N89-10376
WATER HAMMER
A water sound generator for pressure pulses of high energy
[MPIS-MITT-85-1987] N89-10604

WATER VAPOR
Australia 31-GHz brightness temperature exceedance statistics N89-10191
The observed day-to-day variability of Mars water vapor N89-10797
WATER WAVES
A three degree-of-freedom description of the ocean surface for microwave remote sensing of wave height and wind friction velocity N89-10314
The use of the complex correlation function in the recovery of ocean wave spectra from SAR images N89-10315
Final synthesis on research done on the subject of interactions between oblique swells and winds [PB87-186961] N89-10510
WAVE DRAG
Wave drag and high-speed performance of supersonic STOVL fighter configuration [NASA-TM-100061] N89-10017
WAVE EQUATIONS
Relativistic nuclear physics with the spectator model [CEBAF-PR-88-011] N89-10613
WAVE FRONTS
Optical imaging through atmospheric turbulence N89-10423
WAVE FUNCTIONS
The lowest ionization potentials of Al2 [NASA-TM-101171] N89-10605
WAVE INTERACTION
Investigation of the flame-acoustic wave interaction during axial solid rocket instabilities N89-10120
WAVE PROPAGATION
Atmospheric propagation effects relevant to optical communications N89-10201
Space-harmonic analysis of multi-depth corrugated waveguides [PB88-210059] N89-10214
Optical imaging through atmospheric turbulence N89-10423
A stochastic model for the tortuous propagation of a lightning stepped leader N89-10433
The criterion for the propagation of the positive streamer and its application N89-10436
Numerical simulations of lightning by means of the leader propagation model N89-10437
Final synthesis on research done on the subject of interactions between oblique swells and winds [PB87-186961] N89-10510
Seasonal wind variations in the Martian subtropics N89-10807
WAVEGUIDES
Space-harmonic analysis of multi-depth corrugated waveguides [PB88-210059] N89-10214
Optical bistability in semiconductor waveguides N89-10620
WAVELENGTHS
Design study for a remote laser wavelength sensor [DE88-015417] N89-10265
WEAPON SYSTEMS
Digital simulation techniques for end game phenomena N89-10051
Design criteria for hardware-in-the-loop simulation facilities N89-10052
Military uses of space [DE88-015053] N89-10597
SDI (Strategic Defense Initiative): Myth or reality [DE88-015059] N89-10598
WEAPONS
Control System Research for Directed Energy Weapons [DE88-015371] N89-10599
WEAR
Development of a theory of wear of ceramics [DE88-015327] N89-10170
WEAR RESISTANCE
Graded structure composites [EP-PATENT-0-260-850-A2] N89-10135
WEATHER
Aircraft accident reports, brief format, US civil and foreign aviation, issue number 10 of 1987 accidents [PB88-916905] N89-10035
Aircraft accident reports, brief format, US civil and foreign aviation, issue number 12 of 1986 accidents [PB88-916903] N89-10036
Australia 31-GHz brightness temperature exceedance statistics N89-10191
Statistics of lightning interaction with aircraft in Japan N89-10430
Climate of San Francisco, revised [PB88-208624] N89-10504
WEATHER FORECASTING
Lightning near Vandenberg AFB as related to various synoptic patterns N89-10486
Oklahoma-Kansas preliminary regional experiment for storm-central (O-K pre-storm). Volume 3: Aircraft mission summary [PB88-205489] N89-10499
The Remote Atmospheric Probing Information Display (RAPID) system [AD-A196314] N89-10500
WEATHER RECONNAISSANCE AIRCRAFT
Oklahoma-Kansas preliminary regional experiment for storm-central (O-K pre-storm). Volume 3: Aircraft mission summary [PB88-205489] N89-10499
WEATHERING
The performance of alternate fuels in general aviation aircraft [DOT/FAA/CT-88/13] N89-10175
Chemical frost weathering of olivine: Experimental study and implications N89-10793
Photochemical weathering and contemporary volatile loss on Mars N89-10795
WEIGHTING FUNCTIONS
Discretization formulas for unstructured grids [NASA-TM-101298] N89-10242
WELDED STRUCTURES
Influence of specimen size on fatigue crack initiation of welded HY100 steel [AD-A196219] N89-10294
WELDING
Deformations and residual stresses induced in channel section columns by presetting and welding [PB88-199971] N89-10292
Influence of specimen size on fatigue crack initiation of welded HY100 steel [AD-A196219] N89-10294
WHEAT
Potential number of winter wheat ears estimation using radiometry techniques at an early stage N89-10323
Biomass and wheat crop yield estimation from SPOT vegetative indexes N89-10327
Spectral reflectance of sugar beet and winter wheat canopies in the visible and infrared during growth N89-10342
WHEELS
Wheel performance evaluation. Phase 1: Analysis [DOT/FAA/CT-88/16] N89-10041
WHISKER COMPOSITES
Development of ceramic matrix composites for application in the ceramic technology for advanced heat engines [DE88-015329] N89-10168
WHITE DWARF STARS
White dwarfs N89-10685
SS Cygni in quiescence --- IUE N89-10713
Searching for the white dwarf in WZ Sagittae N89-10725
IUE observations of a hot DAO white dwarf: Implications for diffusion theory and photospheric stratification N89-10733
Temperature determinations of hot DA white dwarfs using IUE continuum fluxes N89-10734
The ultraviolet emission of accreting magnetic white dwarfs N89-10735
WIND (METEOROLOGY)
Measurement of vertical velocity using clear-air Doppler radars [AD-A195344] N89-10427
Oklahoma-Kansas preliminary regional experiment for storm-central (O-K pre-storm). Volume 3: Aircraft mission summary [PB88-205489] N89-10499
WIND DIRECTION
Final synthesis on research done on the subject of interactions between oblique swells and winds [PB87-186961] N89-10510
WIND EFFECTS
Comparison between active and passive microwave measurements over Antarctica N89-10316
Final synthesis on research done on the subject of interactions between oblique swells and winds [PB87-186961] N89-10510
Regional sources and sinks of dust on Mars: Viking observations of Cerberus, Solis Planum, and Syrtis Major N89-10802
WIND MEASUREMENT
A three degree-of-freedom description of the ocean surface for microwave remote sensing of wave height and wind friction velocity N89-10314
EPOCS (Equatorial Pacific Ocean Climate Studies) moored temperature, current and wind measurements: 0 deg, 140 deg W, May-June, 1987 [PB88-219415] N89-10509
WIND PRESSURE
Model-data comparisons for the 1982-83 El Nino: The XBT tracks [PB88-221668] N89-10514
WIND TUNNEL MODELS
Space shuttle phase B wind tunnel model and test information. Volume 3: Launch configuration [NASA-CR-178416-VOL-3-PT-1] N89-10019
An investigation into force-moment calibration techniques applicable to a magnetic suspension and balance system [NASA-CR-181695] N89-10061
WIND TUNNEL TESTS
Measurement of aerodynamic characteristics of a hang-glider-wing by ground run tests using a test vehicle [NAL-TR-953] N89-10004
Space shuttle phase B wind tunnel model and test information. Volume 3: Launch configuration [NASA-CR-178416-VOL-3-PT-1] N89-10019
Estimation of up-wash distribution around an automobile by three-dimensional smoke wind tunnel test [NAL-TR-921] N89-10023
The pros and cons of code validation [NASA-TM-100657] N89-10034
Shock tunnel studies of scramjet phenomena [NASA-CR-181721] N89-10045
Highlights of experience with a flexible walled test section in the NASA Langley 0.3-meter transonic cryogenic tunnel [NASA-TM-101491] N89-10060
High-resolution heat-transfer-coefficient maps applicable to compound-curve surfaces using liquid crystals in a transient wind tunnel [NASA-TM-89855] N89-10248
WIND TUNNEL WALLS
Highlights of experience with a flexible walled test section in the NASA Langley 0.3-meter transonic cryogenic tunnel [NASA-TM-101491] N89-10060
WIND VARIATIONS
Seasonal wind variations in the Martian subtropics N89-10807
WINDS ALOFT
Upper-atmosphere zonal winds from satellite orbit analysis: An update [RAE-TR-87058] N89-10507
WINGS
Navier-Stokes simulation of transonic wing flow fields using a zonal grid approach [NASA-TM-100039] N89-10022
Finite difference analysis of external and internal lightning response of the JAS39 CFC wing N89-10483
Modelling of common mode coupling between an aircraft wing traversed by a lightning current and wiring installed in that wing N89-10485
WINTER
On the statistics of field waveforms associated with lightning return strokes N89-10441
Current measurement of lightning superbolt at the Japan sea coast N89-10445
WIRE
Transfer impedance measurements of the space shuttle Solid Rocket Motor (SRM) joints, wire meshes and a carbon graphite motor case N89-10440
WOLF-RAYET STARS
Observations of galactic WC + O binary systems: HD 97152 and HD 152270 N89-10716
WORKSTATIONS
Open control/display system for a telerobotics work station N89-10089
Simplifying the construction of domain-specific automatic programming systems: The NASA automated software development workstation project N89-10553

X

X RAY BINARIES
IUE spectrophotometry of the accretion disk of HZ Her/Her X-1 N89-10702
Simultaneous IUE, EXOSAT and optical observations of the unusual AM Her type variable H058+608 N89-10703
A 0535+26/HDE 245770: A typical Be/X-ray transient system: Coordinated multiwavelength twelve years monitor N89-10704
X RAY SOURCES
IUE and optical observations of X-ray sources in the Large Margellanic Cloud (LMC) N89-10705
X RAYS
Analytical approximations for X-ray cross sections 3 [DE88-015366] N89-10609
Time-resolved X-ray conversion efficiencies of laser-heated plasmas [DE88-015456] N89-10837

Y

YTTRIUM OXIDES
Electronic structure of the quenched superconductivity of materials Y(sub 1-x)Pr(sub x)Ba2Cu3O(sub 7-delta)
[DE88-014414] N89-10658

Z

ZEEMAN EFFECT
Synthesis and study of materials for superconducting electronics
[AD-A195279] N89-10649
ZINC ALLOYS
Micromechanisms of deformation and fracture in ordered intermetallic alloys. 1: Strengthening mechanisms
[DE88-015382] N89-10159
ZINC TELLURIDES
MOCVD techniques for CdTe solar cells
[DE88-001163] N89-10411
ZIRCONIUM OXIDES
Time-dependent mechanical behavior of partially stabilized zirconia for diesel engine applications
[DE88-015330] N89-10171

Typical Personal Author Index Listing

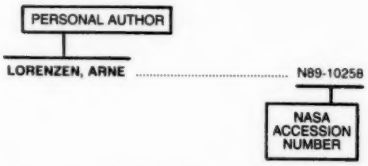

Listings in this index are arranged alphabetically by personal author. The NASA accession number denotes the number by which the citation is identified.

A

ABE, NOBORU N89-10118
ABEDNEGO, B. N89-10370
ABU-SABA, ELIAS G. N89-10297
ACKERMANN, F. N89-10391
ACKERMANN, R. A. N89-10286
ACOSTA, R. J. N89-10215
ADAIR, ROBERT T. N89-10220
ADELMAN, HOWARD M. N89-10300
ADLER, RICHARD N89-10554
AGUIRRE, S. N89-10204
AHEARN, MICHAEL F. N89-10688
AHMAD, I. A. N89-10722
AITCHISON, J. STEWART N89-10620
AKABANE, T. N89-10796
AKE, THOMAS B., III N89-10721
N89-10729
AKIMOTO, TOSHIO N89-10121
ALBA, J. J. N89-10116
ALBERS, R. C. N89-10152
ALBINSON, J. S. N89-10714
ALBRITTON, J. N89-10125
ALBRITTON, WILLIAM P., JR. N89-10048
ALBUS, J. S. N89-10099
ALEM, E. M. N89-10362
ALIAS, QAIS M. N89-10228
ALLEN, BRADLEY P. N89-10553
ALLEN, J. W. N89-10658
ALLEN, MARC S. N89-10067
ALLEY, R. E. N89-10357
ALLIRAND, J. M. N89-10332
ALLY, MOONIS R. N89-10249
ALVES, MARIA VIRGINIA N89-10630
AMBROSE, EDWARD N89-10073
AMES, TROY N89-10079
ANDERSON, BRUCE N89-10444
ANDERSON, DUWAYNE M. N89-10781
ANDERSON, M. N89-10316
ANDERSON, R. L. N89-10267
ANDO, R. N89-10632
ANDREWS, C. J. N89-10463
N89-10464
ANDREWS, MARK J. N89-10426
ANDREWS, SHEILA BRISKIN N89-10522
ANDRIEU, B. N89-10333
N89-10368
ANGULO, M. N89-10116
APPEL, J. N89-10481
ARIMOTO, H. N89-10640
ARMSTRONG, E. K. N89-10010
ARMSTRONG, J. W. N89-10192
ARMSTRONG, L. E. N89-10519
ARNASON, K. N89-10337
ARNOLD, J. R. N89-10775
ARNOLD, S. N89-10203
ARTRU, M.-C. N89-10762
N89-10768
ASSELINEAU, A. N89-10450
ASSINK, ROGER A. N89-10231
AUBERT, C. N89-10107
AUER, L. H. N89-10716
AUER, LAWRENCE H. N89-10717
AUGENBAUM, JEFFREY M. N89-10583
AUGUST, RICHARD N89-10043
AUSTIN, EDMUND N89-10104
AVRETT, EUGENE H. N89-10748
AXELSSON, S. N89-10339

B

BABBEDGE, NORMAN H. N89-10664
BABCOCK, S. M. N89-10289
BADRUZZAMAN, A. N89-10590
BAI, J. M. N89-10132
BAKER, C. N89-10568
BAKER, VICTOR N89-10780
BAKOW, L. N89-10041
BAL, HENRI E. N89-10529
BALASUBRAMANIAM, R. K. N89-10217
BALDWIN, R. E. N89-10465
BALIUNAS, S. L. N89-10756
BALLESTER, G. E. N89-10691
N89-10693
N89-10695
BALLEW, G. I. N89-10380
BALMINO, GEORGES N89-10394
BALTEAS, N. N89-10116
BALTUCK, M. N89-10393
BANDEIRA, IRAJA N. N89-10183
BANKS, C. R. N89-10465
BANNINGER, C. N89-10355
BARAKAT, WISSAM N89-10088
BARATTA, G. B. N89-10754
BARBARO, A. N89-10347
BARBER, T. N89-10025
BARET, F. N89-10310
N89-10319
N89-10322
N89-10354
N89-10368
BARGER, RAYMOND L. N89-10020
BARIL, D. N89-10376
BARINAGA, C. J. N89-10148
BARINAGA, CHARLES J. N89-10143
BARNES, J. R. N89-10782
BARNES, LESLIE A. N89-10605
BAROWY, WILLIAM M. N89-10146
BARR, P. K. N89-10150
BARTLEY, C. L. N89-10556
BARTOLINI, C. N89-10704
BASCHEK, B. N89-10706
BASILE, LISA N89-10079
BASRI, GIBOR N89-10734
BASU, BAMANDAS N89-10638
BAUER, REINHOLD N89-10112
BAUFAYS, C. N89-10314
N89-10344
BAUMEISTER, KENNETH J. N89-10242
BAUSCHLICHER, CHARLES W., JR. N89-10605
N89-10610
BAXTER, V. D. N89-10255
BEACH, G. R. N89-10497
BECKER, F. N89-10343
BECKMAN, R. J. N89-10595
BEGG, ALAN ROBERT N89-10135
BEGUE, A. N89-10341
BEHR, F. J. N89-10381
BEJCZY, ANTAL N89-10093
BELABADIA, MOHAMMED N89-10236
BELL, R. N89-10632
BELLONI, T. N89-10701
BELTRACCHI, TODD J. N89-10586
BENDER, S. C. N89-10279
BENNER, KEVIN M. N89-10536
N89-10552
BENNETT, J. N89-10827
BENSON, D. K. N89-10185
BENSON, J. W. N89-10526
BENTEN, MUHAMMAD S. N89-10531
BENZ, R. N89-10303
N89-10397
N89-10399
BERGENGRUEN, OLAF N89-10088
BERNARD, A. N89-10303
N89-10397
N89-10399
BERTAUX, J.-L. N89-10691
BERTHELOT, B. N89-10371
BERTHON, G. A. N89-10574
BERTOLINI, G. N89-10346
BERTUZZI, P. N89-10308
BEVEN, JOHN L., II N89-10426
BEYER, DAVID S. N89-10063
N89-10065
BHASIN, KUL B. N89-10235
BHATT, R. T. N89-10134
BHATT, RAMAKRISHNA T. N89-10130
BHATT, SANDEEP N. N89-10572
BIAD, NADIA N89-10109
BIANCHI, LUCIANA N89-10705
BICKES, R. W., JR. N89-10151
BIGGS, FRANK N89-10809
BINDSCHADLER, R. A. N89-10403
BITTENCOURTPEREIRA, MARISA DANTAS N89-10302
BJORKMAN, K. S. N89-10732
BJORKMAN, KAREN S. N89-10765
BJORNSSON, S. N89-10337
N89-10356
BLAIR, W. P. N89-10699
BLAKE, J. A. N89-10511
N89-10517
BLATT, J. R. N89-10025
BOBBITT, PERCY J. N89-10034
BOCHNAK, J. N89-10515
BODE, M. F. N89-10714
BODECHTEL, J. N89-10379
N89-10381
N89-10391
BOEHM-VITENSE, ERIKA N89-10745
N89-10760
BOHNE, A. R. N89-10500
BOISSARD, P. N89-10323
BOLLINGER, TERRY B. N89-10073
BONN, F. N89-10376
BONNET-BIDAUD, JEAN-MARC N89-10735
BOOKBINDER, JAY A. N89-10757
BOOTSMA, PETER N89-10457
BOPP, B. W. N89-10724
N89-10769
BORDERS, J. A. N89-10651
BORGIA, B. N89-10260
BORING, A. M. N89-10152
BORSENBERGER, J. N89-10762
BORSTAD, G. A. N89-10353
BOSCHET, C. N89-10237
BOSSARD, F. N89-10573
BOUCHET, P. N89-10701
BOULAY, J. L. N89-10450
BOUMAN, B. A. M. N89-10309
BOURGEOIS, B. J. N89-10094
BOURNE, SIMON M. N89-10046
BOWLING, ALAN N89-10070
BOWYER, STUART N89-10734
BOYD, WILLIAM N89-10747
BOYLE, STEPHEN J. N89-10702
BRADDI, LOUIS N89-10088
BRADLEY, S. N89-10168
BRADSTREET, DAVID H. N89-10742
BRAMLETTE, T. T. N89-10150
BRANDENBURG, JOHN E. N89-10783
BRANDSTROM, GARY W. N89-10781
BRAU, C. A. N89-10279
BRESCIANINI, C. N89-10045
BREWER, O. N89-10535
BRIANTIS, J. M. N89-10351
BRIGGS, S. A. N89-10364
BROCK, MARX N89-10460
BROMAGE, G. E. N89-10744
BROWN, A. N89-10730
N89-10827
BROWN, ALEXANDER N89-10750
N89-10757
BROWN, B. N89-10511
N89-10517
BROWN, COLIN WILLIAM N89-10135
BROWN, D. N. N89-10751
N89-10769

BROWN, K. N89-10318
BRUCKLER, L. N89-10311
BRUEGGE, C. J. N89-10357
BRUGEL, EDWARD W. N89-10752
N89-10757
BRUHWEILER, F. N89-10770
BRUHWEILER, FREDERICK C. N89-10764
BRUNET, Y. N89-10390
BRUNSON, P. N89-10101
BRUSSAT, T. R. N89-10041
BUCHENAUER, D. A. N89-10628
BUDDEN, M. J. N89-10556
BUGLIA, JAMES J. N89-10420
BUISSON, O. N89-10323
BULLOCK, J. WILLIAM N89-10455
BURGER, M. N89-10704
BURGESS, THOMAS W. N89-10087
BURKE, JAMES V. N89-10562
BURKE, KEVIN N89-10419
BURNS, DONALD W. N89-10016
BURROWS, B. J. C. N89-10484
BUSCHMANN, C. N89-10348
BUSE, LELAND C. N89-10054
BUSH, JOY LEE N89-10071
BUSKO, I. C. N89-10681
BUSTIN, ROBERTA N89-10826
BYERLEY, L. G. N89-10488
BYRNE, P. B. N89-10743
N89-10746

C

CALDECOTT, R. N89-10223
CALDWELL, J. N89-10592
CALOZ, R. N89-10370
CALVERT, PAUL DAVISON N89-10137
CAMAGNI, P. N89-10346
CAMARANETO, GILBERTO N89-10676
CAMPOS, FRANK T. N89-10050
CANAVAN, GREGORY H. N89-10596
N89-10597
N89-10598
CANEILL, J. N89-10333
CAPPELLI, A. N89-10738
CARDELLI, JASON A. N89-10752
CARERE, V. N89-10357
CARLSON, HARRY W. N89-10024
CARLSTEN, B. E. N89-10279
CARPENTER, K. G. N89-10730
CARPENTER, KENNETH G. N89-10753
N89-10755
CARR, MICHAEL N89-10780
CARR, MICHAEL H. N89-10784
N89-10785
CARRABBA, MICHAEL M. N89-10615
CART, DUANE J. N89-10051
CARTA, FRANKLIN O. N89-10006
N89-10012
CASELLES, V. N89-10343
CASH, D. L. N89-10172
CASSATELLA, A. N89-10758
CASSATELLA, ANGELO N89-10684
CASTAGNOLI, F. N89-10347
CAUSSIGNAC, J. M. N89-10308
CECCHI, G. N89-10347
CERRUTI-SOLA, M. N89-10738
CERVELLE, B. N89-10313
N89-10360
N89-10362
CETINKUNT, SABRI N89-10285
CHADERJIAN, NEAL M. N89-10022
CHAMPION, I. N89-10306
N89-10310
CHANG, A. T. C. N89-10318
CHANG, J. N89-10277
CHANG, PYUNG H. N89-10287
CHANG, RICHARD K. N89-10662
CHANG, Y. A. N89-10648
CHAPEL, J. D. N89-10091
CHAPMAN, GERALD P. N89-10467
CHARLES, P. A. N89-10715
CHARLESTON, JOANN N89-10405
CHARLESWORTH, J. M. N89-10040
CHARMAN, NEIL EDWARD SETH N89-10135
CHARTIER, L. N89-10330
CHARTIER, M. N89-10332
CHASE, J. B. N89-10232
CHAUZY, SERGE N89-10448
N89-10468
CHEN, C.-C. N89-10200
CHEN, S. P. N89-10152
CHEN, SHAO-PING N89-10154
CHENG, C. C. N89-10738
CHENG, U. N89-10202
CHERRETTE, A. R. N89-10215
CHEUNG, K.-M. N89-10208
CHEVREL, M. N89-10392
CHIANG, PEN-TAI N89-10105
CHIAPPETTI, L. N89-10701
CHIRICO, R. D. N89-10660
CHIU, WEIHSUEH A. N89-10764
CHOI, C. K. N89-10626
CHOROWICZ, J. N89-10313
N89-10360
N89-10362
N89-10382
CHRISTIANSEN, W. H. N89-10277
CHRISTMAN, J. M. N89-10193
CHUN, W. N89-10101
CHUNG, FAN R. N89-10572
CHUPP, E. L. N89-10774
CIAMPOLINI, A. N89-10303
N89-10397
N89-10399
CITEAU, J. N89-10375
CLARK, BENTON C. N89-10786
CLARK, W. L. N89-10427
CLARKE, T. L. N89-10512
CLAYTON, ROBERT W. N89-10425
CLIFFORD, STEPHEN M. N89-10787
COFFER, SUE N89-10077
COFFEY, HELEN E. N89-10828
N89-10829
COHEN, DONALD KENNETH N89-10617
COHEN, WILLIAM N89-10081
N89-10083
COLEMAN, ERNEST W. N89-10487
COLLET, C. N89-10370
COLLIER, RICHARD S. N89-10496
COLLIER, W. B. N89-10660
COLOME, C. N89-10716
CONEL, J. E. N89-10357
CONNORS, LUCY MARGARET N89-10622
COOPER, GENE R. N89-10239
COOWAR, FEROZE N89-10491
COPLIN, K. A. N89-10693
CORDEY, R. A. N89-10315
CORMIER, R. N89-10205
COSTES, J. J. N89-10027
COTE, P. N89-10330
COURAULT, D. N89-10369
COUZENS, DAVID A. N89-10678
N89-10772
COWAN, J. J. N89-10773
CRACKNELL, A. P. N89-10383
CRAUBNER, ADELHEID N89-10270
CRAWFORD, G. B. N89-10513
CRAWLEY, EDWARD F. N89-10013
CRISANTI, ANDREA N89-10600
CRITCHFIELD, ANNA N89-10071
CROCKETT, TOM N89-10560
CROKAERT, MICHEL N89-10485
CROUCH, KEITH E. N89-10478
CRUSE, BRYANT N89-10076
CUADRA, F. N89-10116
CUCINOTTA, FRANCIS A. N89-10612
CURRAN, P. J. N89-10334
CURRY, JOHN D. N89-10440
N89-10477
CZUCHRY, ANDREW J., JR. N89-10544

D

DACHS, JOACHIM N89-10731
DALLAM, WILLIAM N89-10079
DANBY, GORDON T. N89-10280
DANTZIG, GEORGE B. N89-10571
DANZIGER, J. N89-10699
DARDEN, CHRISTINE M. N89-10024
DARVENIZA, M. N89-10463
N89-10464
DAUSKARDT, R. H. N89-10138
DAVID, STAN A. N89-10281
DAVIDSON, KENNETH L. N89-10506
DAVIS, H. A. N89-10234
DAVIS, JAMES A. N89-10559
DAVIS, PHILIP A. N89-10805
DAVIS, R. E. N89-10318
DAVIS, VIRGIL LEON N89-10103
DEARAUJO, ANTONIO JOSE N89-10400
DEARIEN, JOHN A. N89-10106
DECARVALHO, PEDRO RUBENS A. N89-10502
DECKER, MADELYN M. N89-10180
DEDIEU, J.-P. N89-10372
DEEMING, KEVIN R. N89-10664
DEHAAN, J. F. N89-10320
DEJARNETTE, FRED R. N89-10029
DELECOLLE, R. N89-10324
N89-10327
DEMARCQ, H. N89-10375
DEMETRIADES-SHAH, T. H. N89-10358
DEMORISSONVALERIANO, DALTON N89-10302
DEMPSEY, R. C. N89-10724
DENSKAT, U. N89-10303
N89-10397
N89-10399
DEPKOVICH, T. M. N89-10091
DESCHAMPS, P. Y. N89-10341
DESCHAMPS, P.-Y. N89-10371
DEWITTE, M. N89-10062
DIAKITE, COTY N89-10082
DIAS, WILLIAM C. N89-10068
DIASVELASCO, FLAVIO ROBERTO N89-10530
DICK, J. J. N89-10182
DICKS, L. R. N89-10493
DISPERATI, ATTILIO ANTONIO N89-10400
DITTMAR, JAMES H. N89-10603
DOCKTER, K. N89-10342
DODGE, LEE G. N89-10176
DOEFFER, R. N89-10352
DOGGETT, JESSE N89-10731
DOMINEK, A. N89-10223
N89-10225
DOMINY, ROBERT N89-10074
DOMNING, E. E. N89-10232
DONAHUE, CYNTHIA C. N89-10059
DONGARRA, J. N89-10535
DORR, BONNIE J. N89-10675
DOSSANTOS, JOAO ROBERTO N89-10400
DOWNING, L. E. N89-10058
DOYLE, J. G. N89-10743
N89-10746
DOZIER, J. N89-10318
DRAKE, R. P. N89-10637
DRAPER, JOHN V. N89-10090
DREIBUS, G. N89-10822
DREISER, CHRISTOPH N89-10404
DROTNING, W. D. N89-10272
DRURY, MARION ROSEMARY N89-10622
DUBEY, R. V. N89-10289
DUBOIS, J. M. M. N89-10361
DUBOSE, DAVID A. N89-10519
DUERBECK, H. W. N89-10714
DUFTON, P. L. N89-10744
DUPREE, A. K. N89-10689
N89-10756
DURAND, J.-M. N89-10328
DURAND, P. N89-10313
DURSTON, DONALD A. N89-10017
DURUP, P. C. N89-10041
DURYEA, ROBERT A. N89-10589
DUTILLY, ROBERT N89-10078

E

EASTERBROOK, CALVIN C. N89-10454
EASTERBROOK, KEVIN N89-10454
EASTMAN, GEORGE A. N89-10053
EBNER, M. A. N89-10301
EDEL, H. N89-10361
EDEL, H. R. N89-10353
EDWARDS, G. N89-10367
EGERTON, D. N89-10500
EGGEMEYER, WILLIAM C. N89-10070
EIRIKSSON, A. N89-10356
EISENBERG, JOSEPH N89-10088
ELIZECHEA, E. N89-10372
ELLIS, R. J. N89-10621
ELLIS, STEPHEN N89-10088
ELLIS, W. P. N89-10658
ELLS, D. R. N89-10606
ELLUL, RAYMOND MARIO N89-10137
ELMORE, D. N89-10775
ELSBERRY, RUSSELL L. N89-10505
EMORI, Y. N89-10350
ENCRENAZ, THERESE N89-10687
ENGEMANN, D. N89-10623
N89-10624
ERICKSON, C. N89-10119
ERTHAL, GUARACI JOSE N89-10676
ESCADAFAL, R. N89-10369
ESKINS, JONATHAN N89-10061
ESPLIN, MARK P. N89-10146
ESQUIVEL, M. N89-10195
ETIENNE, C. N89-10303
N89-10397
N89-10399
EULER, J. A. N89-10289
EVANS, A. N89-10714
EVANS, B. T. N. N89-10218
EVANS, J. L. N89-10301
EVANS, NANCY REMAGE N89-10727
N89-10728
EWINS, D. J. N89-10007
N89-10008
N89-10009

F

FABBRI, MAURICIO N89-10183
FAGES, F. N89-10574
FAHEY, R. P. N89-10761
FAIZOUN, ALEXANDRE N89-10468
FALLS, M. J. N89-10503
FALOMO, R. N89-10701
FANALE, F. P. N89-10788
N89-10824
FANALE, FRASER N89-10780
FANELLI, N. A. N89-10211
FAULKS, H. N89-10303
N89-10397
N89-10399
FAYMONVILLE, R. N89-10623
N89-10624
FECHTEL, STEPHEN N89-10217
FEDDERS, P. A. N89-10654
FEGGOS, KOSTAS N89-10082
FEIGERLE, CHARLES S. N89-10607
FEKEL, FRANCIS C. N89-10749
FELDMAN, D. W. N89-10279
FELDMAN, P. D. N89-10691
FENG, JUN N89-10161
FERBER, M. K. N89-10171
FERLAND, GARY N89-10708
N89-10709
N89-10710
N89-10711
N89-10712
FERNANDEZ-CASTRO, T. N89-10758
FERRARA, AUGUSTO M. N89-10175
N89-10179
FERREIRA, JOSE LEONARDO N89-10630
FERRONI, F. N89-10260
FESEN, ROBERT A. N89-10700
FESTOU, M. C. N89-10691
FIELDER, WILLIAM L. N89-10409
FINLEY, DAVID N89-10734
FISCHER, J. N89-10352
FISHER, BRUCE D. N89-10478
FISHER, F. A. N89-10497
FLEMING, M. L. N89-10117
FLOOD, DENNIS J. N89-10122
FODOR, GEORGE E. N89-10176
FONG, CHUNG P. N89-10104
FONTANELLA, J.-C. N89-10423
FORESTI, CELINA N89-10413
FOWLER, C. M. N89-10224
FRANCIS, P. W. N89-10377
FRANCO, M. M. N89-10196
FRANTZ, C. E. N89-10162
FRAUENFELDER, HANS N89-10523
FRAZIER, D. O. N89-10656
FREEDMAN, ELI N89-10180
FREEDMAN, MARC R. N89-10166
FREILEY, A. J. N89-10194
FREIREFERRERO, R. N89-10759
N89-10768
FREITAG, H. P. N89-10509
FRENZEL, O. N89-10623
N89-10624
FREY, H. V. N89-10789
FRIEDJUNG, M. N89-10754
FRIEDMAN, ROBERT N89-10111
FROST, VICTOR N89-10217
FROUIN, R. N89-10335
FUELBERG, HENRY E. N89-10426
FUHRMANN, K. N89-10766
FUKUSHIMA, H. N89-10262
FULTON, R. D. N89-10234
FURUKANE, UTARO N89-10631

G

GABELL, A. N89-10357
GABRIELE, GARY A. N89-10586
GAGE, K. S. N89-10427
GALLAGHER, J. S. N89-10709
N89-10711
N89-10712
GANDIA, S. N89-10373
GARLAND, D. B. N89-10028
GARTLING, D. K. N89-10254
GARVIN, J. B. N89-10789
GARY, B. L. N89-10190
N89-10191
GAUTHIER, Y. N89-10361
GAUTIER, C. N89-10335
GAZAVE, ROBERT N89-10110
GEERKEN, R. N89-10381
GEHRZ, ROBERT D. N89-10708
N89-10710
N89-10711
GENTIEN, P. N89-10365
GEORGE, E. P. N89-10155
GERSTL, S. A. W. N89-10325
GHIGLIA, D. C. N89-10566
GIACOMAZZI, G. N89-10178
GIESE, B. S. N89-10514
GILABERT, A. N89-10373
GILBERT, KENNETH E. N89-10470
GILBERT, P. N89-10367
GILLINGWATER, D. N89-10670
GIOVANNELLI, F. N89-10704
GIRARD, DIDIER N89-10591
GIRARD, M.-C. N89-10369
GIVI, P. N89-10149
GLASSELL, R. L. N89-10289
GLAZER, J. N89-10153
GLEASON, TERRY N89-10554
GLYNN, J. L. N89-10019
GLYNN, MICHAEL S. N89-10432
GLYNN, PETER W. N89-10571
GOBIN, V. N89-10479
GOEL, N. S. N89-10317
N89-10326
GOFORTH, ANDRE N89-10096
GOHBERG, I. N89-10587
GOLDBERG, ALLEN N89-10540
N89-10548
GOLDMAN, T. N89-10663
GONZALEZ-RIESTRA, R. N89-10758
GORDON, ELIOTT B. N89-10603
GOREE, J. G. N89-10125
GOSSE, G. N89-10332
GOTO, Y. N89-10445
GOTO, YUKIHIRO N89-10430
GOULAS, Y. N89-10351
GOWER, J. F. R. N89-10353
GRADY, C. A. N89-10732
N89-10764
GRAF, WERNER N89-10495
GRANDT, C. N89-10480
GRASSL, H. N89-10352
GRASSLE, J. F. N89-10511
N89-10517
GRATTA, G. N89-10266
GRAY, D. N89-10181
GRAY, L. H. N89-10353
GREELEY, R. N89-10790
GREELEY, RONALD N89-10780
N89-10791
GREEN, J. L. N89-10427
GREEN, R. O. N89-10357
GREENWOOD, PETER N89-10491
GREIG, J. R. N89-10461
GRIER, T. N89-10326
GRIFFIN, MICHAEL K. N89-10501
GRIGAL, D. F. N89-10415
GROSS, FRANZ N89-10613
GROTHAUS, MICHAEL G. N89-10453
GU, X. N89-10327
GUARNIERI, A. N89-10704
GUERIF, M. N89-10324
N89-10327
GUESS, T. R. N89-10133
GUEST, PETER S. N89-10506
GUEZLANE, M. N89-10382
GUICHAOUA, C. N89-10237
GUIDOTTI, RONALD A. N89-10231
GUILLAUMONT, B. N89-10365
GUIMARAESFERREIRA, JULIA N89-10630
GUINAN, E. F. N89-10756
GUINAN, EDWARD F. N89-10742
GUINOT, J. P. N89-10327
GUISSARD, A. N89-10314
N89-10344
GUITART, A. N89-10108
GUO, CHANGMING N89-10436
GUPTA, AMAR N89-10668
N89-10672
GUYENNE, T. D. N89-10305
GUYOT, G. N89-10306
N89-10310
N89-10319
N89-10354

H

HABERLE, R. M. N89-10792
HABERLE, ROBERT N89-10780
HACIPASAOGLU, KANI N89-10527
HAFTKA, RAPHAEL T. N89-10300
HAGER, BRADFORD H. N89-10304
N89-10425
HAIGH, S. J. N89-10485
N89-10484
HAIXING, YAN N89-10273
HALL, D. T. N89-10694
HALL, WILLIAM B. N89-10033
N89-10127
HAMEL, W. R. N89-10289
HAMILTON, ANDREW J. S. N89-10700
HAN, DAESOO N89-10115
HANCOCK, G. J. N89-10292
N89-10296
N89-10299
HANDSCHUH, R. F. N89-10282
N89-10283
HANKINS, WALTER W., III N89-10087
HANNAFORD, BLAKE N89-10088
HANNUM, NED P. N89-10123
HANSEN, PER CHRISTIAN N89-10238
HARARI, DIEGO N89-10661
HARDTKE, P. G. N89-10303
N89-10397
N89-10399
HARDWICK, C. J. N89-10484
HARLAFTIS, E. N89-10715
HARRIS, DAVID R. N89-10538
HARRIS, F. I. N89-10500
HARRIS, S. L. N89-10793
HARRISON, D. E. N89-10514
HARRISON, RALPH J. N89-10154
HARTMANN, L. N89-10756
HARTMANN, L. W. N89-10707
HARTY, H. N89-10556
HASBROUCK, R. T. N89-10469
HASCHBERGER, D. N89-10623
N89-10624
HASSALL, B. J. M. N89-10715
HAUPT, ROBERT W. N89-10433
HAUSCHILDT, P. N89-10706
HAVSTAD, MARK A. N89-10167
HAWKE, R. S. N89-10232
HAY, P. J. N89-10152
HAY, P. JEFFREY N89-10139
HEATHCOTE, S. N89-10710
HECKER, B. N89-10511
N89-10517
HEEMAN, F. C. N89-10580
HEFFLEY, ROBERT K. N89-10046
HEIMANN, DIETRICH N89-10508
HENDERSON, F. B., III N89-10380
HENKEL, J. N89-10386
HENNESSY, ROBERT W. N89-10037
HENRICHS, H. F. N89-10732
HENRICKS, JULIA A. N89-10068
HENRY, R. N89-10008
HERITAGE, HUGH N89-10443
HERMES, R. E. N89-10172
HERNANDEZFILHO, PEDRO N89-10396
N89-10402
HERNDON, JOSEPH N. N89-10090
HERRMANN, C. C. N89-10458
HESTAND, J. N89-10706
HIGGINS, THOMAS H. N89-10038
HILL, R. A. N89-10268
HINE, T. N89-10171
HINES, B. N89-10119
HIPPENSTEELE, STEVEN A. N89-10246
HIRABAYASHI, N. N89-10639
N89-10642
HIROKURA, S. N89-10632
HISCOX, W. N89-10488
HOBBS, L. M. N89-10671
HOEBEL, LOUIS J. N89-10552
HOEHN, F. W. N89-10117
HOINKA, KLAUS-PETER N89-10508
HOJO, JUNICHI N89-10441
HOLBERG, J. B. N89-10694
N89-10733
HOLDRIDGE, DIANE B. N89-10559
HOLLE, RONALD L. N89-10471
HOLLINGSWORTH, J. L. N89-10782
HOLM, A. V. N89-10707
HOLM, ALBERT V. N89-10713
N89-10725
HOLT, HENRY E. N89-10401
HOLTZMAN, PETER L. N89-10553
HONG, JIA-WEI N89-10572
HOOLE, PAUL R. P. N89-10446
N89-10491
HOPE, PHILIP STEPHEN N89-10174
HOPE, STEPHEN ALEXANDER N89-10136
HORI, MUNEO N89-10421
HORNICK, THOMAS N89-10083
HORTON, J. A. N89-10159
HOSAKAWA, ROBERTO TUYOSHI N89-10400
HOU, T. H. N89-10132
HOVENIER, J. W. N89-10320
HOWARD, ALAN D. N89-10401
HOWARD, W. S. N89-10100
HOWARTH, IAN D. N89-10702

HOWERTON, R. L. N89-10117
HOZUMI, KOKI N89-10004
N89-10023
HU, CHEN-GREN N89-10667
HUBERT, L. N89-10361
HUDSON, C. MICHAEL N89-10165
HUFF, KAREN E. N89-10547
N89-10555
HUGHES, PETER M. N89-10072
HUGHES, R. J. N89-10663
HUGUENIN, R. L. N89-10793
N89-10794
N89-10795
HULL, LARRY G. N89-10072
HULSE, R. N89-10632
HULSHOF, H. J. M. N89-10233
HUNT, J. J. N89-10305
HUNTEN, D. M. N89-10821
HUNTER, STEVEN M. N89-10466
HUPP, R. V. N89-10057
HUPPI, RONALD J. N89-10146
HUSETH, STEVE N89-10537
N89-10543

I

IBRAHIM, M. N89-10383
IENNACOMIRANDA, CARLOS ALBERTO N89-10221
ILGENSTEIN, M. N89-10623
N89-10624
IRIYAMA, YASUHIRO N89-10437
ISHIGURO, TOMIKO N89-10581
ISHII, K. N89-10627
ISHII, M. N89-10494
ISHII, MASARU N89-10441
ISSAC, F. N89-10479
ITAGAKI, KAZUHIKO N89-10434
IWASAKI, K. N89-10796

J

JACKSON, ROBERT N89-10086
JACOBS, P. N89-10045
JACOBSON, M. D. N89-10503
JAKLEVIC, J. N89-10414
JAKOSKY, BRUCE M. N89-10797
JAKUBOWSKI, P. R. N89-10497
JAMES, P. B. N89-10798
N89-10804
JANSSEN, L. N89-10388
JAPPIOT, M. N89-10327
JARRY, P. N89-10237
JASKOLLA, F. N89-10385
JASPERSE, JOHN R. N89-10638
JAWORSKI, ALLAN N89-10085
JAYANTHI, U. B. N89-10680
JEFFERS, JAMES D., III N89-10015
JELSMA, L. F. N89-10618
JERACKI, ROBERT J. N89-10603
JOFFE, ELYA B. N89-10431
JOHANSSON, SVENERIC N89-10753
N89-10755
JOHNSON, HOLLIS R. N89-10729
N89-10748
JOHNSON, J. N. N89-10162
JOHNSON, JOHN L. N89-10629
JOHNSON, LAURA D. N89-10593
JOHNSON, W. LEWIS N89-10539
N89-10545
JOHNSTON, MARK N89-10081
JOHNSTON, MARK D. N89-10080
JONES, HOWARD C. N89-10087
JONES, J. J. N89-10455
JONES, MICHAEL E. N89-10229
JONES, TERRY V. N89-10246
JORDAN, C. N89-10737
JORDAN, HARRY F. N89-10531
JORDON, J. R. N89-10503
JOU, W.-H. N89-10149
JOYNSON, JACK E. N89-10275
JUDGE, P. N89-10730
JULLIEN, J. P. N89-10389
JUMPER, E. J. N89-10274
JUNG, K. N89-10381
JUSTICE, C. O. N89-10364

K

KAASHOEK, M. A. N89-10587
KABLY, KHALIL N89-10448
KADAMBI, J. R. N89-10251
KAEHNY, D. N89-10307
KAFATOS, M. N89-10761
KAMOUN, P. N89-10313
KANAKIA, MIKE D. N89-10176
KANDA, HIDESADA N89-10250
KANG, J. S. N89-10658
KARASEK, K. N89-10168
KASEMIR, HEINZ W. N89-10462
KASTING, J. N89-10816
KASTING, JAMES F. N89-10799
KATANUMA, I. N89-10627
KATTERFELD, G. N. N89-10800
KAUFFMAN, R. L. N89-10637
KAUFFMANN, H. N89-10391
KAUFMANN, H. N89-10381
KAWAHATA, K. N89-10632
KAWAMURA, T. N89-10494
KAWAMURA, TAKAICHI N89-10641
KAWASAKI, Z. N89-10442
KAWASAKI, ZEN-ICHIRO N89-10437
KAWASUMI, Y. N89-10632
KAYTEN, GERALD G. N89-10001
KAZA, KRISHNA RAO V. N89-10043
KEENAN, F. P. N89-10744
KELLER, J. DAVID N89-10440
KELLER, J. O. N89-10150
KELLEY, HENRY L. N89-10059
KELLY, ANGELITA C. N89-10079
KELSO, A. G. N89-10040
KENYON, SCOTT N89-10708
N89-10710
KERLEY, JAMES J. N89-10102
KERR, Y. H. N89-10378
KESLOWITZ, SAUL N89-10089
KESSLER, W. S. N89-10514
KEWISCH, JOERG N89-10614
KHARIF, C. N89-10510
KIDA, TAKASHI N89-10121
KIEFFER, H. H. N89-10812
KIEFFER, HUGH H. N89-10801
KILLION, RICHARD R. N89-10093
KIM, CHONG KWON N89-10567
KIM, ERNEST MAKOTO N89-10619
KIM, HONGSUK H. N89-10338
KIM, SEUNG T. N89-10115
KIM, WON-SOO N89-10088
KIMURA, A. N89-10350
KING-HELE, D. G. N89-10507
KING, JOSEPH H. N89-10678
N89-10772
KING, TIM N89-10537
N89-10549
KINGSTON, A. E. N89-10744
KINSEY, DON WINSTON N89-10241
KIRSCHENBAUM, AUDREY N89-10522
KIRSHNER, ROBERT P. N89-10683
KISER, JAMES D. N89-10166
KITABATAKE, M. N89-10169
KITINYA, SYLIVANO CHILULI NONGA N89-10673
KIWAMOTO, Y. N89-10627
KLEIN, NATHAN N89-10180
KLEIN, R. N89-10303
N89-10397
N89-10399
KLINKHAMER, F. R. N89-10659
KNUPP, KEVIN R. N89-10498
KOBAYASHI, RIKI N89-10147
KOBER, EDWARD M. N89-10139
KOCHEL, R. CRAIG N89-10401
KOCKS, U. F. N89-10158
KOECHLER, C. N89-10346
KOENIGSBERGER, G. N89-10716
KOENIGSBERGER, GLORIA N89-10717
KOKKE, J. M. M. N89-10320
KOMODA, MASAKI N89-10004
KOMURO, H. N89-10445
KONDO, Y. N89-10718
KORNBLUM, H. N89-10637
KOSAKA, KATSUAKI N89-10118
KOTSCHENREUTHER, M. N89-10636
KRAEMER, W. J. N89-10519
KRESS, R. L. N89-10289
KREUZER, WOLFGANG N89-10294
KRIDER, E. PHILIP N89-10472
KRIKORIAN, A. D. N89-10516
KRISHNA, RAMUHALLI N89-10105
KRISHNAN, KANNAN M. N89-10140
KRITIKOS, G. N89-10359
KUBIK, P. W. N89-10775
KUC, ROMAN N89-10662
KUCHARZ, W. N89-10515
KUDVA, P. N89-10095
KUEHBAUCH, W. N89-10342
KUPFER, G. N89-10342
KURT, V. G. N89-10704
KUSAKA, KAZUO N89-10118
KUWAHARA, TAKUO N89-10118
KWAN, T. J. T. N89-10234

L

LAAKE, ANDREAS N89-10604
LABAUNE, G. N89-10479
LABED, J. N89-10336
LABOURDETTE, R. N89-10011
LACROIX, J. P. N89-10574
LAGOUARDE, J. P. N89-10390
LAKSHMANAN, JACQUES N89-10418
LAMB, D. Q. N89-10703
LAMBERT, E. N89-10361
LAMBERT, K. M. N89-10213
LANDRY, R. N89-10367
LANGEMANN, M. N89-10303
N89-10397
N89-10399
LANGER, S. N89-10637
LANGHOFF, STEPHEN R. N89-10610
LANKFORD, ALAN B. N89-10440
LANZ, T. N89-10762
LAPIERRE, L. N89-10237
LAPOINTE, MICHAEL R. N89-10797
LAROCHE, P. N89-10481
LARROQUE, J. N89-10237
LARSON, AARON N89-10543
LARSON, W. E. N89-10526
LARUELLE, G. N89-10031
LASINSKI, B. N89-10637
LATTIMER, JAMES M. N89-10778
LAU, S. C. W. N89-10299
LAURENSSE, I. J. N89-10233
LAVALLEE, DAVID N89-10085
LAVERTY, JOHN N89-10073
LAVREAU, J. N89-10374
LAWLER, R. W. N89-10541
LAWRENCE, A. J. A. N89-10647
LAWRENCE, D. A. N89-10091
LAWRENCE, GEORGE F. N89-10067
LEE, A. C. L. N89-10486
LEE, B. W. N89-10658
LEE, DAVID CHUNG LIANG N89-10402
LEE, JIN S. N89-10092
LEE, ROBERT L. N89-10412
LEE, S. W. N89-10215
LEE, SING H. N89-10616
LEE, STEVEN W. N89-10802
LEGALLO, GUY N89-10056
LEGERTON, V. N. N89-10189
LEHMANN, F. N89-10345
LEIGHTON, F. T. N89-10572
LEIGHTON, TOM N89-10569
LEISSLER, GEORGE W. N89-10156
LEMASSON, C. N89-10363
LEONE, JOHN M., JR. N89-10412
LEOVY, CONWAY N89-10780
N89-10807
LEPINE, VERONIQUE N89-10394
LEPRIEUR, C. N89-10328
LESSER, VICTOR R. N89-10547
N89-10555
LETERME, P. N89-10323
LETOAN, ALPHONSE N89-10321
LETOAN, T N89-10321
LEVERITT, CHARLES S. N89-10180
LEWIS, PAUL M. N89-10521
LEWIS, R. H. N89-10100
LICHTENTHALER, H. K. N89-10348
N89-10349
LIEBERT, J. N89-10733
LIGHTHILL, RUTH N89-10609
LIGHTNER, ERIC N89-10073
LIMBERG, TORSTEN N89-10614
LIN, KUEN-NAN N89-10298
LIN, YOUN-LONG STEVE N89-10528
LINDAU, I. N89-10658
LINDENMAYER, KELLY N89-10064
LINDSEY, JOEL BRAD N89-10570
LINDSTROM, D. R. N89-10403
LINESBROWNING, M. KATE N89-10069
LINSKY, J. L. N89-10827
LINSKY, JEFFREY L. N89-10740
LITTLEFIELD, RONALD G. N89-10063
N89-10065
LITVIN, F. L. N89-10282
N89-10283
LIU, C. T. N89-10155
N89-10159
LIVENGOOD, T. A. N89-10695
LLOPIS, O. N89-10312
LONG, MARSHALL B. N89-10662
LONGO, E. N89-10260
LOO, J. A. N89-10148
LOOMIS, AUDREY N89-10071
LOPEZ, J.-M. N89-10312
LOPEZ, RAUL E. N89-10471

LORENZEN, ARNE N89-10258
LOUAHALA, S. N89-10313
N89-10360
LOUBERSAC, L. N89-10363
LOWE, DAWN N89-10075
LU, H. N89-10568
LUCCHITTA, B. K. N89-10803
LUDWIG, GERSON OTTO N89-10630
LUKASON, M. N89-10519
LUMIA, R. N89-10099
LUMMERZHEIM, DIRK N89-10424
LUMPKIN, A. H. N89-10279
LUNDEN, B. N89-10339
LUTTERMOSER, DONALD G. N89-10748

M

MACAYEAL, D. R. N89-10403
MACGORMAN, DONALD R. N89-10471
MACIOLEK, N. N89-10511
N89-10517
MACKERRAS, D. N89-10463
N89-10464
MACKLIN, J. T. N89-10315
MADNICK, STUART N89-10668
N89-10672
MALLEY, PETER JOHN N89-10174
MALONEY, PHILIP RICHARD N89-10776
MALOTA, FRIEDRICH N89-10625
MANEVICZ, JOSEPH E. N89-10443
MANNER, DAVID BRUCE N89-10244
MAPLE, M. B. N89-10658
MAPLES, VANCE H. N89-10053
MARASCHI, L. N89-10701
MARCUM, F. N89-10458
MARCUS, BETH N89-10097
MARKHAM, B. L. N89-10364
MARKSON, RALPH N89-10444
MARSH, BRUCE D. N89-10416
MARSHALL, THOMAS C. N89-10470
MARTIN, L. J. N89-10804
MARTINELL, JOHN S. N89-10105
MARTINEZ, A. N89-10119
MARTINEZ, ROBERT L. N89-10261
MASAMUNE, S. N89-10640
MASLENNIKOVA, I. N89-10248
MASON, RODNEY J. N89-10229
MASSA, DERCK N89-10763
MASTIN, G. A. N89-10566
MATHEWS, G. J. N89-10773
MATTESON, NADINE N89-10075
MATTEUCCI, F. N89-10699
MATUNO, KENICHI N89-10576
MAXWELL, TED N89-10780
MAZUR, VLADISLAV N89-10456
MAZZINGHI, P. N89-10347
MCCAIN, H. N89-10099
MCCARTY, J. G. N89-10142
MCCLINTOCK, J. E. N89-10703
MCCLUSKEY, C. P. S. N89-10718
MCCLUSKEY, G. E., JR. N89-10718
MCDOWALL, R. L. N89-10432
MCGRATH, M. A. N89-10693
MCKAMEY, C. G. N89-10155
MCKINNON, JOHN A. N89-10828
N89-10829
MCLALLIN, K. L. N89-10117
MCLEAN, DAVID R. N89-10065
MCLEAN, WILLIAM N89-10167
MCMAHAN, A. K. N89-10650
MCMURTRY, P. A. N89-10149
MCPHADEN, M. J. N89-10509
MCVEA, G. G. N89-10040
MCWRIGHT, G. M. N89-10618
MEI, V. C. N89-10255
MEIROVITCH, LEONARD N89-10291
MEISSNER, D. N89-10381
N89-10391
MEITIN, JOSE G., JR. N89-10499
MELIA, J. N89-10373
MELIKIAN, GORKEN N89-10247
MELLOMARSHALL, PAULO N89-10219
MENA-WERTH, JOSE N89-10760
MESERVEY, E. N89-10632
MESERVEY, R. N89-10649
MESNARD, B. N89-10108
METCALFE, R. W. N89-10149
MEYER, J. J. C. N89-10588
MICHALITSIANOS, A. G. N89-10761
MIDDLETON, DAVID N89-10560
MIGNEAULT, GERARD E. N89-10524
MIKATARIAN, R. R. N89-10274
MIKKILINENI, K. N89-10568
MIKSELL, STEVE N89-10075
N89-10077
MIKUSCH, EBERHARD N89-10270
MILLER, G. N. N89-10267
MILLER, GLENN N89-10081
N89-10083
MILLER, JAMES B. N89-10039
MILLER, JAMES G. N89-10129
MILLER, JOHN C. N89-10607
MILLER, K. L. N89-10779
MILLER, LANCE A. N89-10550
MILLER, W. F. N89-10533
MILLER, W. J. N89-10301
MILLER, WILLIAM A. N89-10408
MILTON, E. J. N89-10329
MINSTER, J. F. N89-10316
MIRANDA, LUIZ C. M. N89-10183
MISRA, AJAY K. N89-10128
N89-10131
MIXON, RANDOLPH W. N89-10087
MIYAHARA, AKIRA N89-10641
MIYAJIMA, HIROSHI N89-10118
MIYAKE, Y. N89-10494
MIYOSHI, S. N89-10627
MNICH, MARC A. N89-10046
MOATES, RYAN N89-10217
MOFFAT, ANTHONY F. J. N89-10717
MONTES, ANTONIO N89-10630
MONTESINOS, B. N89-10737
MONTGOMERY, D. N89-10637
MONTGOMERY, DAVID C. N89-10644
MOORE, C. B. N89-10460
MOORE, G. C. N89-10025
MOORE, HENRY J. N89-10805
MOORE, STEVEN R. N89-10426
MOORE, WENDY E. N89-10090
MOOS, H. W. N89-10691
N89-10693
N89-10695
MORE, JORGE J. N89-10562
MOREAU, J. P. N89-10449
N89-10450
MORELL, LARRY J. N89-10534
N89-10561
N89-10564
MORGAN, R. G. N89-10045
MORIN, G. N89-10493
MORITA, S. N89-10632
MORRIS, J. W., JR. N89-10153
MORRIS, N. N89-10045
MORRISON, J. J. N89-10232
MORTON, SALLY C. N89-10592
MORTON, WILLIAM C. N89-10055
MOTTINGER, N. A. N89-10189
MOUCHET, MARTINE N89-10735
MOUGINISMARK, P. J. N89-10806
MOUSA, ABDUL M. N89-10476
MOYA, I. N89-10351
MUELLER, E.-A. N89-10257
N89-10258
N89-10259
N89-10604
MUELLER, R. N89-10359
MUELLERSCHOEN, R. J. N89-10206
MULCARE, D. B. N89-10058
N89-10526
MULDER, J. A. N89-10042
MULLAN, D. J. N89-10770
MULLER, BRADLEY M. N89-10426
MUNDAY, M. G. N89-10726
MUNDT, REINHARD N89-10731
MURATORIO, G. N89-10754
MUROOKA, YOSHIHIRO N89-10430
MURPHY, D. P. N89-10461
MURPHY, JAMES N89-10807
MURPHY, MILES R. N89-10037
MURPHY, R. E. N89-10393
MURPHY, R. W. N89-10240
MURRAY, ARTHUR N89-10082

N

NAGASHIMA, RYUICHI N89-10118
NAGATA, A. N89-10640
NAGATANI, M. N89-10442
NAITOU, H. N89-10634
NAKADA, H. N89-10442
NAKAMURA, KINUYO N89-10565
NAKAMURA, T. N89-10350
NAKANO, M. N89-10442
NAKANO, MINORU N89-10437
NARITA, K. N89-10445
NARUMI, Y. N89-10808
NASSIOPOULOS, G. E. N89-10756
NASTROM, G. D. N89-10427
NAYLOR, T. N89-10715
NEDELL, S. S. N89-10809
NEFF, D. N89-10198
NEFF, J. E. N89-10739
N89-10741
NEFF, JAMES E. N89-10740
NELSON, S. J. N89-10192
NERI, J. A. C. F. N89-10680
NERRY, F. N89-10336
NESSYAHU, HAIM N89-10582
NEUMANN, W. T. N89-10488
NEURGAONKAR, R. R. N89-10618
NEWCOMB, PHILIP H. N89-10551
NEY, EDWARD P. N89-10708
N89-10710
NG, POH H. N89-10451
NGUYEN, NGUYET M. N89-10615
NICKEL, F. S. N89-10475
NICKESON, J. E. N89-10379
NIDIFFER, KENNETH E. N89-10542
NIETO, M. M. N89-10663
NISHIIZUMI, K. N89-10775
NJOKU, E. G. N89-10378
NOMIZO, KUNIO N89-10021
NORBERG, R. E. N89-10654
NORBURY, JOHN W. N89-10612
NORRIS, MARK A. N89-10291
NOUEL, F. N89-10107
NOVAES, RENE ANTONIO N89-10402
NUNEZ, M. N89-10390

O

OBAYASHI, HARUO N89-10641
OBERMAYER, RICHARD N89-10037
ODA, TOSHIATSU N89-10631
OERTEL, DETLEF N89-10646
OGAWA, I. N89-10632
OGAWA, SATORU N89-10581
OGAWA, Y. N89-10634
OHKAMI, YOSHIAKI N89-10121
OKAMOTO, OSAMU N89-10121
OKANO, K. N89-10634
OKSANEN, MARKKU ILMARI N89-10214
OLIVER, W. C. N89-10155
ONEILL, N. T. N89-10361
ONO, TAKATSUGU N89-10004
ORLADY, HARRY W. N89-10037
ORLANDO, T. P. N89-10649
ORVILLE, R. E. N89-10490
OSHIYAMA, H. N89-10640
OTOSHI, T. Y. N89-10196
OWEN, T. N89-10810

P

PACHECODOSSANTOS, ARMANDO N89-10402
PAGE, THORNTON N89-10811
PAGES, J. N89-10375
PAIGE, D. A. N89-10812
PAIGE, DAVID A. N89-10801
PAKULL, MANFRED N89-10705
PALADIN, GIOVANNI N89-10600
PALLAVICINI, R. N89-10738
PANAGIA, NINO N89-10696
PANEK, R. J. N89-10707
PANTANI, L. N89-10347
PAPAZIAN, PETER B. N89-10439
N89-10440
PARK, A. N89-10223
N89-10225
PARK, H. D. N89-10237
PARKER, L. E. N89-10098
PARKER, TIMOTHY J. N89-10813
PARKINSON, MICHAEL LAWRENCE N89-10771
PARPIA, J. M. N89-10145
PARSONS, S. B. N89-10724
PARSONS, SIDNEY B. N89-10721
PATERRA, FRANK C. N89-10067
PATON, COLIN R. N89-10263
PAULL, A. N89-10045
PAZOS, MAYRA C. N89-10516
PEACH, DAVID F. N89-10220
PECHACEK, R. E. N89-10461
PEDERSON, S. N89-10595
PEDRINI, A. N89-10346
PELLOUX, REGIS M. N89-10161
PENG, HONG N89-10602
PENN, B. G. N89-10656
PEPIN, R. O. N89-10814
PERALA, RODNEY A. N89-10438
N89-10440
N89-10451
PERENNES, M. N89-10312
PEREZ-ARRIAGA, I. J. N89-10116
PERICHT, GEORGE T. N89-10504

PERIDIER, VALLORIE N89-10575
PERRAS, S. N89-10376
PERRY, BENJAMIN F., JR. N89-10729
PERRY, J. L. N89-10184
PESANT, A. N89-10376
PESCE, J. E. N89-10730
PESCE, JOSEPH E. N89-10731
PETERS, G. J. N89-10732
PETERS, L., JR. N89-10213
N89-10225
PETERS, M. G. N89-10652
PEYRON, J.-L. N89-10326
PEYROT, P. N89-10303
N89-10397
N89-10399
PHILLIPS, K. J. H. N89-10744
PHILLIPS, R. E. N89-10134
PHILLIPS, R. J. N89-10815
PHIPPS, G. S. N89-10268
PHULPIN, T. N89-10389
PICCIONI, A. N89-10704
PIEPEL, G. F. N89-10556
PIERI, DAVID C. N89-10813
PIETRZYK, Z. A. N89-10645
PIFER, A. E. N89-10488
PIN, F. G. N89-10098
PINEL, ALAIN N89-10226
PINNEO, J. M. N89-10652
PITKAERANTA, J. N89-10578
PLANO, L. S. N89-10652
PLATZER, MAX F. N89-10006
PLAVEC, MIREK J. N89-10723
PODAIRE, A. N89-10341
PODGORSKI, ANDREW S. N89-10447
N89-10473
PODGORSKI, ELIZABETH M. N89-10473
POINTEL, J.-G. N89-10323
POLIDAN, R. S. N89-10719
POLIDAN, RONALD S. N89-10713
POLIDORI, L. N89-10313
POLLACK, J. B. N89-10816
POLLARA, F. N89-10203
N89-10208
POLLARD, M. N89-10414
POLYCHRONAKOS, ALEXIOS P. N89-10661
PONZONI, FLAVIO JORGE N89-10402
POPE, G. G. N89-10003
PORTER, W. D. N89-10155
POSNER, E. C. N89-10186
POSTAWKO, S. N89-10788
POSTAWKO, S. E. N89-10824
POTTECK, S. N89-10227
POTTER, T. F. N89-10185
POUCHER, D. E. N89-10019
POULSEN, P. N89-10232
POUWELS, H. N89-10212
POWELL, JAMES R. N89-10280
POWERS, S. J. N89-10052
PRATHER, W. D. N89-10458
PREVOT, L. N89-10306
N89-10310
PRIMOT, J. N89-10423
PRONI, J. R. N89-10512
PROSDOCIMI, A. N89-10346
PYEE, M. N89-10237

Q

QUILLIN, BOB N89-10075
QUINLAN, M. A. N89-10142

R

RABALAIS, J. W. N89-10608
RACK, H. J. N89-10125
RADICATI, B. N89-10347
RAFFY, M. N89-10340
RAHUNEN, T. N89-10741
RAMAMONJIARISOA, A. N89-10510
RAMNARAYAN, R. N89-10568
RAMSHAW, J. D. N89-10256
RAMSTEIN, G. N89-10340
RANDOLPH, MICHAEL N89-10259
RANSOM, V. H. N89-10256
RAO, A. S. P. N89-10817
RASMUSSEN, K. J. R. N89-10292
N89-10296
RAST, M. N89-10385
RATNAPARKHI, P. N89-10125
RAUH, R. DAVID N89-10615
RAVI, K. V. N89-10652
RAY, EDWARD J. N89-10060
RAYMOND, J. C. N89-10699
N89-10707
REAZER, J. M. N89-10449
REED, JAMES N89-10405
REEDY, R. C. N89-10775
REILLY, H. N89-10195
REIMANN, ROBERT C. N89-10247
REIN, MARTIN N89-10257
REINARTZ, P. N89-10359
REISER, CHRISTOPHER N89-10265
REMILLARD, R. N89-10703
REMY, F. N89-10316
RENON, CHRISTIANE N89-10056
RENZETTI, N. A. N89-10209
REPUSSEAU, P. N89-10574
REUTER, R. C., JR. N89-10126
RIAZANOFF, S. N89-10313
RICHARD, P. N89-10481
RICHARDS, CLYDE N. N89-10460
RICHARDSON, J. N89-10568
RICHARDSON, R. C. N89-10145
RICHARDSON, S. N89-10616
RICHTER, R. N89-10345
RIEGGER, S. N89-10307
RIGAL, D. N89-10319
RIGDEN, GREGORY J. N89-10439
N89-10459
RINDERLE, U. N89-10349
N89-10368
RISON, WILLIAM N89-10467
RITCHIE, R. O. N89-10138
RIVIER, N. N89-10647
ROBERTS, E. P. N89-10403
ROBERTS, GLYN O. N89-10653
ROBINSON, C. R. N89-10769
ROBINSON, GARY Y. N89-10655
ROBINSON, LEE R. N89-10093
RODONO, MARCELLO N89-10740
ROGER, ROBERT P. N89-10243
ROHRER, NORMAN J. N89-10235
ROLFE, E. J. N89-10682
ROLLETT, A. D. N89-10158
ROLLIN, E. M. N89-10329
ROMANOSKI, GLENN N89-10161
ROMOLI, M. N89-10347
RONDEAUX, G. N89-10310
ROPER, VAUGHAN P. N89-10147
ROSEN, JONAS W. N89-10483
ROSENBERG, ARNOLD N89-10572
ROSENBLATT, G. M. N89-10138
ROSENTHAL, DON N89-10064
N89-10081
ROSKAM, E. E. N89-10520
ROSSI, C. N89-10754
ROSSMANITH, ROBERT N89-10614
ROTHERY, D. A. N89-10377
N89-10384
ROTHMAN, LAURENCE S. N89-10146
ROTTER, J. M. N89-10290
N89-10295
ROUSSET, G. N89-10423
ROYER, A. N89-10330
ROZES, JEAN N89-10226
RUDANT, J. P. N89-10313
N89-10374
RUDANT, J.-P. N89-10360
N89-10362
N89-10382
RUDOLPH, TERENCE N89-10454
RUDOLPH, TERENCE H. N89-10438
N89-10451
RUHNKE, LOTHAR H. N89-10462
RUST, W. DAVID N89-10470
RUSTAN, P. L. N89-10449
N89-10450
RUTGERS, W. R. N89-10233
RUTLEDGE, CHARLES K. N89-10601
RUZEK, M. N89-10393

S

SAAR, S. H. N89-10827
SAARINEN, TUOMO N89-10032
SACKSTEDER, KURT R. N89-10111
SADAKANE, K. N89-10767
SADOSKI, P. A. N89-10500
SAITO, Y. N89-10796
SALASALVES, DIOGENES N89-10676
SALISBURY, J. W. N89-10366
SALOMONSON, V. V. N89-10379
SALVAIL, J. R. N89-10788
SANDERS, WILLIAM A. N89-10166
SANDONATO, GILBERTO M. N89-10630
SANDULEAK, N. N89-10769
SANGIL, J. J. N89-10116
SANKAR, SUBRAMANIAN V. N89-10120
SANTANNABINS, LEONARDO N89-10530
SANTINI, P. M. N89-10585
SARAF, A. K. N89-10383
SATO, K. I. N89-10640
SATO, KUNINORI N89-10631
SAUNDERS, R. STEPHEN N89-10813
SAUTEREAU, J. F. N89-10237
SAWADA, S. N89-10445
SCANVIC, J.-Y. N89-10360
SCHAFER, D. E. N89-10411
SCHAFFER, SCOTT E. N89-10557
SCHELLBERG, J. N89-10342
N89-10368
SCHERLIS, W. N89-10546
SCHIENLE, J. N89-10168
SCHMIDT, KURT N89-10270
SCHMUGGE, T. N89-10388
SCHNABEL, R. N89-10558
SCHNEEBERGER, DALE M. N89-10813
SCHNEIDER, DUANE A. N89-10231
SCHOENE, G. N89-10307
SCHRIJVER, C. J. N89-10827
SCHRIJVER, CAROLUS J. N89-10747
SCHRYVERS, D. N89-10160
SCHUETZLE, JAMES G. N89-10066
SCHULTZ, P. H. N89-10818
SCHUMACHER, F. A. N89-10618
SCHUMACHER, L. L. N89-10197
SCHWABE, ERIC N89-10569
SCHWARTZ, GOTTFRIED N89-10270
SCHWARZ, R. B. N89-10163
SCOTT, LAURA N89-10482
SCOTT, R. D. N89-10100
SEEM, D. A. N89-10512
SEGARRA, D. N89-10373
SEIGE, P. N89-10391
SEIKOHSHA, K. K. SUWA N89-10262
SEITTER, W. C. N89-10714
SELINCE, GERARD N89-10056
SELVELLI, PIER LUIGI N89-10684
SETTLES, R. N89-10611
SEVE, A. N89-10423
SEWARD, SUE K. N89-10165
SHAGAM, R. N. N89-10268
SHAIK, K. S. N89-10201
SHAPIRO, ARTHUR B. N89-10157
SHAVIV, G. N89-10706
N89-10710
SHEFFER, E. K. N89-10704
SHELL, J. N89-10198
SHEMANSKY, D. E. N89-10694
SHEN, J. N89-10181
SHEN, Z. X. N89-10658
SHERWOOD, E. G. N89-10234
SHIELDS, A. W. N89-10656
SHIMOKAWA, TOSHIYUKI N89-10584
SHINOZUKA, M. N89-10262
SHORE, S. N. N89-10751
N89-10769
SHORE, STEVEN N. N89-10690
SHRADER, C. R. N89-10703
SIEBER, A. J. N89-10387
SIIKONEN, TIMO N89-10032
SIKKA, V. K. N89-10164
SILBER, A. N89-10703
SILVERMAN, BARRY G. N89-10082
SIMON, THEODORE N89-10736
SIMONIN, A. N89-10313
SINGER, JOSEPH N89-10409
SINGER, S. F. N89-10819
SION, E. M. N89-10712
N89-10733
N89-10770
SIROTA, M. N89-10277
SISLE, M. E. N89-10052
SKINNER, S. N89-10730
SKINNER, T. E. N89-10691
SLADE, M. A. N89-10209
SLATER, HOWARD A. N89-10269
SMITH, D. E. N89-10789
SMITH, DANIEL RICHARD, JR. N89-10293
SMITH, DOUGLAS R. N89-10540
SMITH, JAMES G. N89-10435
SMITH, L. K. N89-10185
SMITH, M. K. N89-10058
SMITH, R. D. N89-10148
SMITH, RICHARD D. N89-10143
SMITH, S. B. N89-10284
SNIDER, J. B. N89-10503
SNOW, THEODORE P. N89-10765
SNYDER, LYNN E. N89-10016
SOBIESKI, P. N89-10314
N89-10344
SOBRINO, J. A. N89-10343
SOHN, JEONG L. N89-10253
SOJKA, J. J. N89-10417
SOLOMON, S. N89-10789

SOMBRIN, J. N89-10237
SONNEBORN, G. N89-10697
N89-10698
N89-10708
N89-10709
N89-10710
N89-10711
N89-10712
N89-10715
N89-10751
N89-10756
N89-10769
SORENSEN, D. N89-10535
SOULA, SERGE N89-10468
SOULAGE, A. N89-10481
SOUZA, C. A. W. N89-10680
SPAEPEN, FRANS N89-10154
SPALEK, G. N89-10279
SPARKS, WARREN M. N89-10708
N89-10709
N89-10710
N89-10711
N89-10712
SPICER, W. E. N89-10658
SPIES, W. N89-10706
SPIETH, MARY ANN N89-10425
SPOHN, ROGER N89-10217
SQUYRES, S. W. N89-10809
SRIVASTAVA, K. D. N89-10476
STALKER, R. J. N89-10045
STAMPFER, M. T. N89-10140
STANTON, P. N89-10195
STARGARDTER, HANS N89-10014
STARK, LAWRENCE N89-10088
STARRFIELD, S. N89-10706
N89-10708
N89-10709
N89-10710
N89-10711
N89-10712
STEELE, W. V. N89-10660
STEFFEN, DALE A. N89-10433
STEIN, W. E. N89-10279
STEINER, J. E. N89-10681
STEINMETZ, S. N89-10327
STENCEL, R. E. N89-10730
STENCEL, ROBERT E. N89-10731
STEPHENSON, S. N. N89-10403
STEVEN, M. D. N89-10358
STEVENSON, MERRITT R. N89-10502
STOFFELS, J. J. N89-10606
STOLARIK, ELLEN G. N89-10063
STOLL, M. P. N89-10336
STONE, JOHN L., JR. N89-10069
STONUM, RONALD K. N89-10017
STOUT, M. G. N89-10158
STRAUSS, RAINER N89-10492
STRINGER, I. N89-10045
STRINGFELLOW, MICHAEL F. N89-10474
STROBEL, D. F. N89-10691
STROKE, H. H. N89-10633
STRUBE, M. MICHAEL N89-10660
STRYKER, L. L. N89-10706
N89-10708
N89-10709
N89-10711
N89-10712
SULLIVAN, J. S. N89-10230
SUN, WEI-HSIN N89-10777
SUTER, L. N89-10637
SWAIM, DAN J. N89-10521
SWANK, J. H. N89-10707
SWEATT, W. C. N89-10268
SYLVESTRE, J. C. N89-10173

T

TADMOR, EITAN N89-10582
TAEUBER, RALPH J. N89-10478
TAKADA-HIDAI, M. N89-10767
TAKAHASHI, K. N89-10350
TAKAKURA, YOKO N89-10581
TAKEI, T. N89-10262
TAKEMORI, H. T. N89-10232
TAKEUTI, T. N89-10442
TAKEUTI, TOSIO N89-10437
TAMAIN, G. N89-10362
TANABE, K. N89-10141
TANAKURA, YOSHIYUKI N89-10565
TANENBAUM, ANDREW S. N89-10529
TANENHAUS, MARTIN E. N89-10051
TANIDA, L. N89-10199
TANIGUCHI, M. N89-10262
TANK, VOLKER N89-10271
TANNER, L. N89-10160
TANNOUS, I. N89-10313
TANRE, D. N89-10341
TANZI, E. G. N89-10701
TAYLOR, C. D. N89-10458
TAYLOR, PETER R. N89-10605
N89-10610
TEDROW, P. M. N89-10649
TEMPELMANN, U. N89-10342
TENDICK, FRANK N89-10088
TENG, J. G. N89-10290
N89-10295
TERES, J. M. N89-10319
TERHALLE, U. N89-10386
THAYER, JEFFREY S. N89-10443
THIESSEN, T. N89-10637
THOMAS, D. E. N89-10475
THOMPSON, ROGER CLIFTON N89-10114
THOMPSON, T. W. N89-10209
THOMSON, K. P. B. N89-10367
THORNBURG, GAIL ELLEN N89-10669
THORVALDSSON, V. N89-10356
TIETBOHL, G. N89-10637
TILLMAN, JAMES N89-10807
TILLMAN, JAMES E. N89-10820
TING, B.-Y. N89-10170
TOBAGI, FOUAD A. N89-10216
TOI, K. N89-10632
TOLAND, M. R. N89-10556
TOMBOULIAN, SHERRY N89-10560
TOMLINSON, G. N89-10181
TON, TRAN-CONG N89-10005
TORALDO, GERARDO N89-10562
TORR, DOUGLAS G. N89-10264
TOWNSEND, LAWRENCE W. N89-10612
TOWNSHEND, J. R. G. N89-10364
TREFOIS, PHILIPPE N89-10374
TREUHAFT, R. N. N89-10187
TREVES, A. N89-10701
TRONCOSOLOZADA, OSCAR N89-10489
TROST, THOMAS F. N89-10453
TRURAN, JAMES W. N89-10709
TSAI, J. J. N89-10512
TSUKANO, YUKICHI N89-10004
TURKEL, ELI N89-10577
TURNER, R. S. N89-10415
TYLER, A. L. N89-10821
TYLER, MITCHELL N89-10088
TYNDALL, M. B. N89-10252

U

UCHIDA, KEIICHIRO N89-10565
UDSETH, H. R. N89-10148
UDSETH, HAROLD R. N89-10143
UEDA, SHUICHI N89-10118
ULABY, F. T. N89-10789
ULLAL, H. S. N89-10406
ULVESTAD, J. S. N89-10207

V

VALCO, GEORGE J. N89-10235
VANASSE, GEORGE A. N89-10146
VANCE, EDWARD F. N89-10495
VANDERWEY, A. H. N89-10233
VANDESSEL, E. L. N89-10704
VANDEVEL, M. N89-10579
VANE, G. N89-10357
VANEGMOND, S. N89-10580
VANSTOKKOM, H. T. C. N89-10320
VANTENDELOO, G. N89-10160
VANVLIET, J. C. N89-10580
VANZANDT, T. E. N89-10427
VANZOMEREN, B. C. N89-10594
VARELACORREA, RICARDO N89-10018
VAUCLAIR, GERARD N89-10733
VEALE, ANTHONY N89-10750
VEIRS, D. K. N89-10138
VERGEEST, J. S. M. N89-10532
VERHOEF, W. N89-10331
VICK, SHON N89-10064
VIDAL, G. N89-10382
VILHU, O. N89-10739
N89-10741
VINCENT, M. N89-10107
VINOT, JEAN-CLAUDE N89-10110
VIOLLIER, M. N89-10363
N89-10365
VIOTTI, R. N89-10754
VITEK, JOHN M. N89-10281
VITYAZ, V. I. N89-10800
VIVIAN, H. C. N89-10197
VLASES, G. C. N89-10645
VOAS, JEFFREY M. N89-10534
VOGTLIN, G. E. N89-10232
VOLKERTS, HANS N89-10508
VOLLAND, H. N89-10480
VONRUESTEN, C. N89-10342
VOTER, A. F. N89-10152
VOTER, ARTHUR FORD N89-10154
VREULS, DONALD N89-10037
VULPIANI, ANGELO N89-10600

W

WADE, R. N89-10709
N89-10711
N89-10712
WAENKE, H. N89-10822
WAGENER, R. N89-10692
WAGNER, R. M. N89-10708
N89-10709
N89-10711
N89-10712
WAHLGREN, BO I. N89-10483
WAKABAYASHI, YASUHUMI N89-10121
WALEN, DAVID B. N89-10452
WALKER, D. M. C. N89-10507
WALKER, J. DAVID A. N89-10575
WALLIS, R. N89-10157
WALTER, F. M. N89-10739
WALTER, FREDERICK M. N89-10731
N89-10740
N89-10747
WALTER, L. S. N89-10366
WANG, DACHONG N89-10436
WARD-THOMPSON, DEREK N89-10679
WARDLEY, N. W. N89-10334
WARES, RICHARD N89-10175
WARNER, JOSEPH D. N89-10235
WARREN, PAUL H. N89-10823
WARREN, R. W. N89-10279
WASA, K. N89-10169
WASCHL, J. A. N89-10177
WATANABE, Y. N89-10639
N89-10642
WATSON, ANDREW I. N89-10471
WATSON, J. M. N89-10279
WATSON, JANICE N89-10079
WEHRSE, R. N89-10706
WEIDEMANN, VOLKER N89-10685
WELCH, DOUGLAS L. N89-10728
WENDE, CHARLES N89-10076
WESTBROOK, C. K. N89-10150
WHEELER, M. S. N89-10497
WHITELOCK, PATRICIA A. N89-10731
WHITLEY, J. B. N89-10628
WICKLAND, D. E. N89-10393
WIESBECK, W. N89-10307
WIGGINS, C. M. N89-10475
WILKINSON, BILL N89-10075
WILLIAMS, B. G. N89-10188
WILLIAMS, E. R. N89-10490
WILLIAMS, R. E. N89-10708
N89-10709
N89-10710
N89-10711
N89-10712
WILLSON, L. A. N89-10686
WILSON, JOHN C. N89-10059
WILSON, K. L. N89-10628
WILSON, RICKY E. N89-10245
WINER, W. O. N89-10170
WINKENBACH, H. N89-10391
WINN, WILLIAM P. N89-10470
WISE, H. N89-10142
WITHINGTON, J. N89-10210
WITONO, H. N89-10311
WOJCIECHOWSKI, JOSEPHINE Q. N89-10180
WOLF, STEPHEN W. D. N89-10060
WOLSKI, R. J. N89-10428
WONG, JENNIFER C. N89-10068
WONNACOTT, D. N89-10720
WOO, DONG MIN N89-10288
WOOD, C. A. N89-10377
WOODSON, SHAWN H. N89-10029
WOOLHISER, C. N89-10274
WRIGHT, DERNARD R. N89-10176
WRIGHT, ROBERT L. N89-10044
WROBLESKI, D. A. N89-10172
WU, C.-C. N89-10707
WUNDERLICH, B. N89-10657
WYATT, M. E. N89-10211

Y

YAHIL, A. N89-10778
YAMADA, HIROSHI N89-10643

YAMADA, S. N89-10640
YAMAGUCHI, ISAO N89-10121
YAMAGUCHI, Y. N89-10262
YAMANAKA, T. N89-10141
YANG, J. C. S. N89-10095
YANG, JACKSON C. S. N89-10105
YANG, T. C. N89-10095
YATSU, K. N89-10627
YEH, H. C. N89-10168
YEH, J. J. N89-10658
YENNI, KENNETH R. N89-10059
YOO, M. H. N89-10159
YOSHIDA, MASAHIRO N89-10585
YOSHIDA, ZENSHO N89-10643
YOUNG, K. DAVID N89-10599
YOUNG, L. M. N89-10279
YOUNG, ROBERT D. N89-10523
YUHAS, JOHN S. N89-10156

Z

ZACCARDELLI, C. N89-10266
ZAPLATYNSKY, ISIDOR N89-10124
ZARCHAN, PAUL N89-10049
ZE, F. N89-10637
ZENT, A. P. N89-10788
N89-10824
ZHANG, J. N89-10282
N89-10283
ZILGER, J. N89-10379
N89-10386
N89-10391
ZIMBELMAN, JAMES R. N89-10825
ZOCH, DAVID N89-10085
ZOCH, DAVID R. N89-10084
ZUREK, A. K. N89-10162
ZUREK, RICHARD W. N89-10797
ZWALLY, H. J. N89-10789

Typical Corporate Source Index Listing

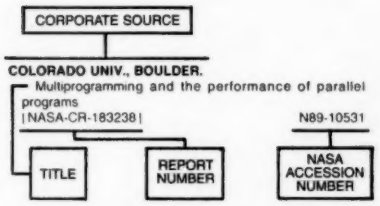

Listings in this index are arranged alphabetically by corporate source. The title of the document provides the user with a brief description of the subject matter. The report number helps to indicate the type of document cited (e.g., NASA report, translation, NASA contractor report). The NASA accession number denotes the number by which the citation is identified. The titles are arranged under each corporate source in ascending accession number order.

A

ACADEMY OF SCIENCES (USSR), LENINGRAD.
Areal and time distributions of volcanic formations on Mars N89-10800

ADVANCED TECHNOLOGY AND RESEARCH, INC., BURTONSVILLE, MD.
Performance improvement of robots using a learning control scheme N89-10105

ADVISORY GROUP FOR AEROSPACE RESEARCH AND DEVELOPMENT, NEUILLY-SUR-SEINE (FRANCE).
Technical evaluation report on the Flight Mechanics Panel Symposium on Flight Vehicle Development Time and Cost Reduction
[AGARD-AR-244] N89-10001
AGARD manual on aeroelasticity in axial-flow turbomachines. Volume 2: Structural dynamics and aeroelasticity
[AGARD-AG-298-VOL-2] N89-10006
Guidance and control systems simulation and validation techniques
[AGARD-AG-273] N89-10048
Performance assessment register
[AGARD-R-763] N89-10666

AERITALIA S.P.A., TURIN (ITALY).
Solid earth mission study. Volume 2: Technical report
[ESA-CR(P)-2626-VOL-2] N89-10303
Solid Earth mission study. Volume 1: Executive summary
[ESA-CR(P)-2626-VOL-1] N89-10397
Solid earth mission study. Volume 3: Program planning report
[ESA-CR(P)-2626-VOL-3] N89-10399

AERONAUTICAL RESEARCH LABS., MELBOURNE (AUSTRALIA).
A potential theory for the steady separated flow about an aerofoil section
[ARL-AERO-R-176] N89-10005

AEROSPACE CORP., EL SEGUNDO, CALIF.
Sulfide corrosion of silver contacts during satellite storage
[AD-A196217] N89-10112

AIR FORCE GEOPHYSICS LAB., HANSCOM AFB, MASS.
The Remote Atmospheric Probing Information Display (RAPID) system
[AD-A196314] N89-10500
Marginal stability of ion-acoustic waves in a weakly collisional two-temperature plasma without a current
[AD-A195840] N89-10638

AIR FORCE INST. OF TECH., WRIGHT-PATTERSON AFB, OHIO.
A meta-protocol architecture for connecting computer networks
[AD-A196319] N89-10570
Finite precision arithmetic in singular value decomposition architectures
[AD-A196188] N89-10589

AIR FORCE SYSTEMS COMMAND, WRIGHT-PATTERSON AFB, OHIO.
Vibrational relaxation processes in CO2-N2-H2O laser systems
[AD-A196211] N89-10273

AIR FORCE WESTERN SPACE AND MISSILE CENTER, VANDENBERG AFB, CALIF.
Lightning near Vandenberg AFB as related to various synoptic patterns N89-10466

AIR FORCE WRIGHT AERONAUTICAL LABS., WRIGHT-PATTERSON AFB, OHIO.
A comparative evaluation of RPD (Rotary Particle Depositor) and ferrographic diagnostic methods for turbine engine lubricant samples
[AD-A196207] N89-10044

AIRBORNE RESEARCH ASSOCIATES, WESTON, MASS.
New electric field instrumentation and the effects of space charge at Kennedy Space Center N89-10444

AIRO, INC., COLORADO SPRINGS, COLO.
A chronology of in-cloud electric field and lightning strikes on an instrumented research aircraft N89-10455

ALABAMA UNIV., HUNTSVILLE.
Compact imaging spectrometer for induced emissions
[NASA-CR-183187] N89-10264
Analysis and modeling of summertime convective cloud and precipitation structure over the southeastern United States
[NASA-CR-183192] N89-10498

ALASKA UNIV., FAIRBANKS.
Electron transport and optical emissions in the aurora N89-10424

ALCATEL THOMSON ESPACE, TOULOUSE (FRANCE).
Spaceborne SAR imaging of land, an opportunity for polyphase code
[ATES/DMA/RAD/002-86] N89-10226

ALLIED-SIGNAL AEROSPACE CO., KANSAS CITY, MO.
Riveting a case section with blind, self-plugging rivets
[DE88-013224] N89-10284

APPLIED RESEARCH CORP., LANDOVER, MD.
The UV silicon spectra of early B stars N89-10763

ARGONNE NATIONAL LAB., ILL.
Tools to aid in the analysis of memory access patterns for FORTRAN programs
[DE88-013609] N89-10535
Convergence properties of trust region methods for linear and convex constraints
[DE88-013608] N89-10562
Quasiperiodic ordering in grain boundaries
[DE88-012199] N89-10647

ARINC RESEARCH CORP., ANNAPOLIS, MD.
Develop an automated Data Base Management System (DBMS): Report on DBMS software and user's guide
[DE88-015996] N89-10674

ARIZONA STATE UNIV., TEMPE.
The analysis of spectra of novae taken near maximum N89-10706
Release of magmatic water on Mars: Estimated timing and volumes N89-10790
The Martian dust cycle: A proposed model N89-10791
Regional sources and sinks of dust on Mars: Viking observations of Cerberus, Solis Planum, and Syrtis Major N89-10802

ARIZONA UNIV., TUCSON.
Spatial distribution of lightning strikes to ground during small thunderstorms in Florida N89-10472
Analysis of methods for detecting focus error in optical data storage systems N89-10617
Large time scale variation in hydrogen emission from Jupiter and Saturn N89-10694
A new study of the interacting binary star V356 Sgr N89-10719
IUE observations of a hot DAO white dwarf: Implications for diffusion theory and photospheric stratification N89-10733
Global properties of molecular clouds and the interstellar medium in galaxies N89-10776
Vertical O(sub 3) distribution as a diagnostic for eddy diffusion profile N89-10821

ARKANSAS COLL., BATESVILLE.
Methods of extracting hydrogen from lunar soil
[NASA-CR-180465] N89-10826

ARMAGH OBSERVATORY (NORTHERN IRELAND).
Ultraviolet flares on 2 Peg N89-10743
Transition regions of dM stars N89-10746

ARMY COLD REGIONS RESEARCH AND ENGINEERING LAB., HANOVER, N.H.
What makes thunderbolts zig and zag N89-10434

ARMY MATERIALS RESEARCH AGENCY, WATERTOWN, MASS.
Structure of grain boundaries in iron
[DE88-014412] N89-10154

ARMY RESEARCH AND TECHNOLOGY LABS., MOFFETT FIELD, CALIF.
Helicopter roll control effectiveness criteria program summary
[NASA-CR-177477] N89-10046

ARMY RESEARCH INST. OF ENVIRONMENTAL MEDICINE, NATICK, MASS.
Modulation of human plasma fibronectin levels following exercise
[AD-A192674] N89-10519

B

BALLISTIC RESEARCH LABS., ABERDEEN PROVING GROUND, MD.
HAN (hydroxylammonium nitrate density)-based liquid gun propellants: Physical properties
[AD-A195246] N89-10180
Moment exerted on a coning projectile by a spinning liquid in a cylindrical cavity containing a porous medium
[AD-A195291] N89-10239

BATH UNIV. (ENGLAND).
Single-pole switching schemes for EHV transmission systems N89-10228

BATTELLE INST., FRANKFURT AM MAIN (WEST GERMANY).
Development of radiation hardened far IR detector arrays. Volume 1: Phase 2
[BF-R-65.641-2] N89-10623
Development of radiation hardened far IR detector arrays. Volume 2: Phase 3
[BF-R-65.641-3] N89-10624

BATTELLE OCEAN SCIENCES, DUXBURY, MASS.
Study of biological processes on the US North Atlantic slope and rise, volume 2
[PB88-196514] N89-10511
Study of biological processes on the US North Atlantic slope and rise. Volume 1: Executive summary
[PB88-196522] N89-10517

BDM CORP., ALBUQUERQUE, N. MEX.
Computer simulation of the effects of lightning stroke attachment to an electric power substation N89-10475

BENDIX FIELD ENGINEERING CORP., GREENBELT, MD.
FIESTA: An operational decision aid for space network fault isolation N89-10075

BENDIX FIELD ENGINEERING CORP., LANHAM, MD.
An expert system for scheduling requests for communications Links between TDRSS and ERBS N89-10065

BERKELEY RESEARCH ASSOCIATES, INC., CALIF.
Research on a two-stage free electron laser oscillator
[AD-A195339] N89-10278

BOEING ADVANCED SYSTEMS CO., SEATTLE, WASH.
Lightning tests on an all-composite helicopter N89-10452

BOEING AEROSPACE CO., SEATTLE, WASH.
Cost effective simulation for millimeter wave guidance systems N89-10053
Range delay techniques for radar target simulators N89-10054

BOEING COMPUTER SERVICES CO., SEATTLE, WASH.
Technology transfer and the knowledge-based software assistant N89-10541
The knowledge integration tool: Knowledge interface (a knowledge based system development environment) N89-10551

BONN UNIV. (WEST GERMANY).
Spectral reflectance of sugar beet and winter wheat canopies in the visible and infrared during growth
N89-10342
Monitoring lightning activity in South Africa with a VLF single-station technique: Comparison with meteosat infrared data
N89-10480
BRITISH AEROSPACE PUBLIC LTD. CO., BRISTOL (ENGLAND).
Solid earth mission study. Volume 2: Technical report
[ESA-CR(P)-2626-VOL-2] N89-10303
Solid Earth mission study. Volume 1: Executive summary
[ESA-CR(P)-2626-VOL-1] N89-10397
Solid earth mission study. Volume 3: Program planning report
[ESA-CR(P)-2626-VOL-3] N89-10399
BRITISH PETROLEUM CO. LTD., LONDON (ENGLAND).
Graded structure composites
[EP-PATENT-0-260-850-A2] N89-10135
Leaf spring
[EP-PATENT-0-253-574-A1] N89-10136
Polymer composites
[EP-PATENT-0-232-138-A2] N89-10137
Adhesive blends and multi-layered structures comprising the adhesive blends
[EP-PATENT-0-258-990-A1] N89-10174
Phase conjugate reflecting media
[EP-PATENT-0-243-130-A1] N89-10622
BROOKHAVEN NATIONAL LAB., UPTON, N. Y.
Design approaches and parameters for magnetically levitated transport systems
[DE88-014286] N89-10280
BROWN UNIV., PROVIDENCE, R. I.
Crater ejecta morphology and the presence of water on Mars
N89-10818

C

CALIFORNIA INST. OF TECH., PASADENA.
Dynamic interpretation of geoid anomalies
[NASA-CR-183164] N89-10304
Earth rotation and core topography
[NASA-CR-183186] N89-10425
CALIFORNIA UNIV., BERKELEY.
A university teaching simulation facility N89-10088
Temperature determinations of hot DA white dwarfs using IUE continuum fluxes N89-10734
CALIFORNIA UNIV., BERKELEY. LAWRENCE BERKELEY LAB.
Two-dimensional spatially resolved Raman spectroscopy of solid materials
[DE88-014867] N89-10138
Background modelling alternatives in electron energy-loss spectroscopy and their implications on microanalysis
[DE88-010361] N89-10140
Tensile properties of commercial aluminum-lithium alloys at cryogenic temperatures
[DE88-014857] N89-10153
Premartensitic microstructures as seen in the high-resolution electron microscope: A study of a NiAl alloy
[DE88-008042] N89-10160
Fourier transform infrared spectrometry of ambient aerosols
[PB88-213236] N89-10414
CALIFORNIA UNIV., LOS ANGELES.
Superionized plasmas in Algol binaries N89-10723
Accretion disk models of quasars and active galactic nuclei N89-10777
Mars regolith versus SNC meteorites: Evidence for abundant crustal carbonates N89-10823
CALIFORNIA UNIV., SAN DIEGO.
Void collapse and void growth in crystalline solids
N89-10421
Architecture studies and system demonstrations for optical parallel processor for Al and NI
[AD-A195480] N89-10616
CALIFORNIA UNIV., SANTA BARBARA.
The spectral bidirectional reflectance of snow
N89-10318
CAMERON IRON WORKS, INC., HOUSTON, TEX.
Applications of process modelling to heat treatment of superalloys
[DE88-015445] N89-10157
CARRIER CORP., SYRACUSE, N.Y.
Development and proof-testing of advanced absorption refrigeration cycle concepts, phase 2
[DE88-013239] N89-10247
CASE WESTERN RESERVE UNIV., CLEVELAND, OHIO.
Thermodynamic analysis of compatibility of several reinforcement materials with FeAl alloys
[NASA-CR-4172] N89-10128
Thermodynamic analysis of compatibility of several reinforcement materials with beta phase NiAl alloys
[NASA-CR-4171] N89-10131
Laser velocimeter measurements of solids in multiphase flow
[DE88-011611] N89-10251
Robotic adaptive grasping based on vision and tactile sensor data N89-10288
CENTRE D'ETUDE SPATIALE DES RAYONNEMENTS, TOULOUSE (FRANCE).
Retrieving vegetation and soil parameters from radar measurements N89-10321
CENTRE FOR AGROBIOLOGICAL RESEARCH, WAGENINGEN (NETHERLANDS).
Microwave backscatter from beets, peas and potatoes throughout the growing season N89-10309
CENTRE NATIONAL D'ETUDES SPATIALES, PARIS (FRANCE).
The French space program for Earth observation
N89-10392
CENTRE NATIONAL D'ETUDES SPATIALES, TOULOUSE (FRANCE).
PRIMORB: Preliminary orbit with two positions
[CNES-CT/DTI/MS/AE/072] N89-10107
CARTEL: A method to calibrate S-band ranges with geostationary satellites. Results of orbit determination
[CNES-CT/DTI/MS/AE/124] N89-10108
ZOOM orbitography software: On the Givens method. Presentation and software implementation evaluation for least square problems
[CNES-CT/DTI/MS/AE/219] N89-10109
Preliminary project PASTEL: System interface between SPOT 4 and the PSDE's passenger
[CNES-87/088-CT/DRT/TIT/TR] N89-10227
Communications to National Microwave Days
[CNES-CT/DRT/TIT/HY/87/130] N89-10237
A radar reflector for microwave remote sensing instruments external calibration N89-10312
Comparison between active and passive microwave measurements over Antarctica N89-10316
Spectral characterization of forest targets in mountainous zones on Thematic Mapper images
N89-10328
Analysis of directional effects on NOAA AVHRR
N89-10341
Estimation of primary marine production using spaceborne data on ocean color N89-10371
Fault tolerance computing: Constraints in using multiprocessor synchronization by static preplanned scheduling
[CNES-CT/DRT/TIT/TB-096] N89-10573
CENTRE NATIONAL DE LA RECHERCHE SCIENTIFIQUE, GRENOBLE (FRANCE).
A fast Monte-Carlo cross-validation procedure for large least squares problems with noisy data
[RR-687-M] N89-10591
CENTRE NATIONAL DE LA RECHERCHE SCIENTIFIQUE, TOULOUSE (FRANCE).
Dynamic properties of power MOS transistors
[LAAS-88-162] N89-10236
CENTRE NATIONAL DE LA RECHERCHE SCIENTIFIQUE, VERRIERES-LE BUISSON (FRANCE).
Abundance and f values needed to interpret adequately the high resolution IUE spectra N89-10759
Detected UV variability in the IUE spectra of the Ap-Si star HD 25823 N89-10768
CENTRE NATIONAL DE RECHERCHES METEOROLOGIQUES, TOULOUSE (FRANCE).
A study of the vegetation cover with AVHRR during HAPEX-MOBILHY N89-10389
CENTRE UNIV. DE LUMINY, MARSEILLES (FRANCE).
Final synthesis on research done on the subject of interactions between oblique swells and winds
[PB87-186961] N89-10510
CHELTON (ELECTROSTATICS) LTD., MARLOW (ENGLAND).
Israel Air Force (IAF) in-service aircraft lightning strike and damage survey N89-10431
CHRYSLER CORP., NEW ORLEANS, LA.
Space shuttle phase B wind tunnel model and test information. Volume 3: Launch configuration
[NASA-CR-178416-VOL-3-PT-1] N89-10019
CLEMSON UNIV., S.C.
Fracture criteria for discontinuously reinforced metal matrix composites
[NASA-CR-181175] N89-10125
COLLEGE OF WILLIAM AND MARY, WILLIAMSBURG, VA.
Infection and propagation analysis: A fault-based approach to estimating software reliability
[NASA-CR-183276] N89-10534
Incremental assessment and improvement of software reliability
[NASA-CR-183275] N89-10561
Theoretical insights into fault-based testing
[NASA-CR-183277] N89-10564
Relativistic nuclear physics with the spectator model
[CEBAF-PR-88-011] N89-10613
COLORADO STATE UNIV., FORT COLLINS.
Beam assisted fabrication of 3-5/Si monolithic devices
[AD-A195479] N89-10655
COLORADO UNIV., BOULDER.
Multiprogramming and the performance of parallel programs
[NASA-CR-183238] N89-10531
Concurrent algorithms for numerical computation on hypercube computer
[AD-A195502] N89-10558
Ejecta in SN 1006: The knotty issue N89-10700
Direct UV observations of the circumstellar envelope of alpha Orionis N89-10730
Multi-wavelength observations of the peculiar red giant HR 3126 N89-10731
Doppler imaging of AR Lacertae at three epochs
N89-10740
Transition region fluxes in A-F Dwarfs: Basal fluxes and dynamo activity N89-10747
Observations of ultraviolet variability in RV Tauri stars
N89-10752
Mg II line profiles of the Mira S Carinae N89-10757
Ultraviolet properties of IRAS-selected Be stars
N89-10765
COMMERCE DEPT., WASHINGTON, D.C.
Space commerce: An industry assessment
[PB88-214069] N89-10677
COMMISSARIAT A L'ENERGIE ATOMIQUE, SACLAY (FRANCE).
The ultraviolet emission of accreting magnetic white dwarfs N89-10735
COMMISSION OF THE EUROPEAN COMMUNITIES, ISPRA (ITALY).
Hydrogen supply over long distances using chemicals description and evaluation of a technical system
[DE88-012630] N89-10178
COMPAGNIE DE PROSPECTION GEOPHYSIQUE FRANCAISE, PUTEAUX.
Application of microgravity to the assessment of existing structures and structural foundations
[AD-A195599] N89-10418
COMPAGNIE INTERNATIONALE DE SERVICE EN INFORMATIQUE, TOULOUSE (FRANCE).
Study on representation of surface coverage by imaging experiments
[ESA-CR(P)-2584] N89-10394
COMPUTER RESOURCE MANAGEMENT, INC., ATLANTIC CITY, N.J.
Lightning information database N89-10432
COMPUTER SCIENCES CORP., BALTIMORE, MD.
A natural language query system for Hubble Space Telescope proposal selection N89-10083
Expert systems built by the Expert: An evaluation of OPS5 N89-10086
COMPUTER SCIENCES CORP., BELTSVILLE, MD.
Space station Platform Management System (PMS) replanning using resource envelopes N89-10071
COMPUTER SCIENCES CORP., SILVER SPRING, MD.
SS Cygni in quiescence N89-10713
Searching for the white dwarf in WZ Sagittae
N89-10725
CONSIGLIO NAZIONALE DELLE RICERCHE, FLORENCE (ITALY).
A new lidar system for applications over land and sea
N89-10347
CONSIGLIO NAZIONALE DELLE RICERCHE, FRASCATI (ITALY).
A 0535+26/HDE 245770: A typical Be/X-ray transient system: Coordinated multiwavelength twelve years monitor N89-10704
Fe II level population in luminous variable stars
N89-10754
CONTEL FEDERAL SYSTEMS, INC., GAITHERSBURG, MD.
An expert system that performs a satellite station keeping maneuver N89-10069
CONTINUOUS ELECTRON BEAM ACCELERATOR FACILITY, NEWPORT NEW, VA.
Relativistic nuclear physics with the spectator model
[CEBAF-PR-88-011] N89-10613
Nonlinear spin acceptance in electron storage rings
[CEBAF-PR-88-009] N89-10614
CONTROL DATA CORP., MINNEAPOLIS, MINN.
Measurement of vertical velocity using clear-air Doppler radars
[AD-A195344] N89-10427
COPENHAGEN OBSERVATORY (DENMARK).
Solution of ill-posed problems by means of truncated SVD (Singular Value Decomposition)
[DE88-013510] N89-10238
CORNELL UNIV., ITHACA, N.Y.
Physics and technology for the in-situ investigation of properties of materials
[AD-A195498] N89-10145

CRYSTALLUME, MENLO PARK, CALIF.
PECVD (Plasma Enhanced Chemical Vapor Deposition) diamond thin films for research instrumentation [AD-A195443] N89-10652

D

DARTMOUTH COLL., HANOVER, N.H.
Nonlinear magnetohydrodynamics [DE88-015703] N89-10644
DAYTON UNIV., OHIO.
Modification of the unsteady flow field predicted by transonic small distrubance equations using a Navier-Stokes solution of the steady flow field N89-10241
DE HAVILLAND AIRCRAFT CO. OF CANADA LTD., DOWNSVIEW (ONTARIO).
Phase 4 static tests of the J-97 powered, external augmentor V/STOL model at the NASA, Ames Research Center, November 1983 [NASA-CR-177395] N89-10028
Lightning tests to measure the bulk current levels associated with the electronic engine control of a turboprop commuter transport N89-10457
DEFENCE RESEARCH ESTABLISHMENT ATLANTIC, DARTMOUTH (NOVA SCOTIA).
Influence of specimen size on fatigue crack initiation of welded HY100 steel [AD-A196219] N89-10294
DEFENSE ADVANCED RESEARCH PROJECTS AGENCY, ARLINGTON, VA.
Software design research at DARPA N89-10546
DELAWARE UNIV., NEWARK.
Mass loss from the K dwarf in V471 Tauri N89-10770
DENVER UNIV., COLO.
An investigation of the acoustic emission generated by various crack propagation modes in 304 stainless steel N89-10293
DEPARTMENT OF AGRICULTURE, BELTSVILLE, MD.
Aircraft remote sensing in HAPEX N89-10388
DEPARTMENT OF NATIONAL DEFENCE, OTTAWA (ONTARIO).
Electrostatic discharge and field effects of electronics systems N89-10493
DETROIT DIESEL ALLISON, INDIANAPOLIS, IND.
Forced vibration and flutter design methodology N89-10016
DEUTSCHE FORSCHUNGS- UND VERSUCHSANSTALT FUER LUFT- UND RAUMFAHRT, OBERPFAFFENHOFEN (WEST GERMANY).
Image processing document: Halley multicolor camera (Giotto Mission) [DFVLR-FB-88-20] N89-10270
Infrared temperature measurement with inherent consideration of emissivity [DFVLR-FB-88-22] N89-10271
Thermal infrared laser spectroscopy: The potential of dual active/passive thermal infrared sensors for Earth observation N89-10345
Optimization for classification of forest damage classes N89-10359
Applications of LANDSAT (TM and MSS) data for an estimation of rangeland conditions in semiarid and arid areas of northern Kenya [DFVLR-FB-88-18] N89-10404
The German Front Experiment 1987: Observations and preliminary results [DFVLR-FB-88-21] N89-10508
DOMINION ASTROPHYSICAL OBSERVATORY, VICTORIA (BRITISH COLUMBIA).
Validity of the classification of UV gallium stars N89-10767
DORNIER-WERKE G.M.B.H., FRIEDRICHSHAFEN (WEST GERMANY).
Solid earth mission study. Volume 2: Technical report [ESA-CR(P)-2626-VOL-2] N89-10303
Solid Earth mission study. Volume 1: Executive summary [ESA-CR(P)-2626-VOL-1] N89-10397
Solid earth mission study. Volume 3: Program planning report [ESA-CR(P)-2626-VOL-3] N89-10399
DUNDEE UNIV. (SCOTLAND).
MOMS-1 data for bathymetric and geological studies N89-10383
DURHAM UNIV. (ENGLAND).
Relational multimedia databases N89-10673
A polarisation study of spiral galaxies N89-10679
Supernova remnants' interactions with the inter-stellar medium N89-10771
DYNETICS, INC., HUNTSVILLE, ALA.
A generic seeker simulation for the evaluation of active RF guidance systems N89-10050

E

ECOLE POLYTECHNIQUE FEDERALE DE LAUSANNE (SWITZERLAND).
The normalization of a soil brightness index for the study of changes in soil conditions N89-10370
EDGERTON, GERMESHAUSEN AND GRIER, INC., IDAHO FALLS, IDAHO.
Multimegawatt power sources for commercial space operations [DE88-015119] N89-10106
Discrete modeling considerations in multiphase fluid dynamics [DE88-015168] N89-10256
EIC, INC., NORWOOD, MASS.
Photoelectrochemical fabrication of spectroscopic diffraction gratings [NASA-CR-180786] N89-10615
ELECTRICAL AND COMPUTER ENGINEERING, ATHENS, OHIO.
On a surface mounted transmission line configuration for aperture testing N89-10458
ELECTRICITY COUNCIL RESEARCH CENTRE, CAPENHURST (ENGLAND).
A lightning location system for the UK electricity supply industry N89-10482
ELECTRO MAGNETIC APPLICATIONS, INC., HUNTSVILLE, ALA.
Estimating electric field enhancement factors on an aircraft utilizing a small scale model: A method evaluation N89-10454
ELECTRO MAGNETIC APPLICATIONS, INC., LAKEWOOD, COLO.
A stochastic model for the tortuous propagation of a lightning stepped leader N89-10433
Triggering of lightning by the Atlas Centaur vehicle N89-10438
Evaluation and mitigation of lightning hazards to the space shuttle Solid Rocket Motors (SRM) N89-10439
Transfer impedance measurements of the space shuttle Solid Rocket Motor (SRM) joints, wire meshes and a carbon graphite motor case N89-10440
Linear and nonlinear interpretation of CV-580 lightning data N89-10451
Interference of precipitation static discharges with aircraft navigational systems N89-10459
Model results for a proposed tactical missile training site lightning protection system N89-10477
The interaction between lightning grounding systems and buried cables N89-10496
EUROPEAN SPACE AGENCY, PARIS (FRANCE).
Proceedings of the 4th International Colloquium on Spectral Signatures in Remote Sensing [ESA-SP-287] N89-10305
Considerations and calculations for application of an optical amplifier as an end- and preamplifier [ESA-TT-1004] N89-10625
A Decade of UV Astronomy with the IUE Satellite, volume 1 [ESA-SP-281-VOL-1] N89-10682
EUROPEAN SPACE AGENCY. ESA TRACKING STATION, MADRID (SPAIN).
Cataclysmic variables N89-10684
The variability of the UV spectrum of the symbiotic star BF Cygni N89-10758

F

FEDERAL AVIATION ADMINISTRATION, ATLANTIC CITY, N.J.
Hardware fault insertion and instrumentation system: Experimentation and results [NASA-CR-182746] N89-10526
FEDERAL AVIATION ADMINISTRATION, WASHINGTON, D.C.
Terminal control area design and air traffic loadings [DOT/FAA/DS-88/11] N89-10038
FEDERAL AVIATION AGENCY, ATLANTIC CITY, N.J.
The performance of alternate fuels in general aviation aircraft [DOT/FAA/CT-88/13] N89-10175
Alternate fuels for General Aviation aircraft with spark ignition engines [DOT/FAA/CT-88/05] N89-10179
FLORIDA STATE UNIV., TALLAHASSEE.
Analysis and use of VAS satellite data [NASA-CR-183184] N89-10426
FLORIDA UNIV., GAINESVILLE.
Gravitational time delay due to a spinning string [DE88-014733] N89-10661
FLOW RESEARCH, INC., KENT, WASH.
Direct Numerical Simulations (DNS) of an unpremixed turbulent jet flame [AD-A196128] N89-10149
FOKKER B.V., AMSTERDAM (NETHERLANDS).
Solid earth mission study. Volume 2: Technical report [ESA-CR(P)-2626-VOL-2] N89-10303
Solid Earth mission study. Volume 1: Executive summary [ESA-CR(P)-2626-VOL-1] N89-10397
Solid earth mission study. Volume 3: Program planning report [ESA-CR(P)-2626-VOL-3] N89-10399
FORD AEROSPACE AND COMMUNICATIONS CORP., COLLEGE PARK, MD.
The mission operations planning assistant N89-10066
Maintaining consistency between planning hierarchies: Techniques and applications N89-10084
A LISP-Ada connection N89-10085

G

GARRETT CORP., TORRANCE, CALIF.
Development of ceramic matrix composites for application in the ceramic technology for advanced heat engines [DE88-015329] N89-10168
GEOLOGICAL SURVEY, FLAGSTAFF, ARIZ.
Water and ice on Mars: Evidence from Valles Marineris N89-10803
GEOLOGICAL SURVEY, MENLO PARK, CALIF.
Mars: A water-rich planet N89-10784
Martian volcanism: A review N89-10785
Ablation of Martian glaciers N89-10805
GEORGE MASON UNIV., FAIRFAX, VA.
Phobos and Deimos: A base for sampling the Martian past N89-10819
GEORGE WASHINGTON UNIV., WASHINGTON, D.C.
Toward an expert project management system N89-10082
GEORGIA INST. OF TECH., ATLANTA.
Investigation of the flame-acoustic wave interaction during axial solid rocket instabilities N89-10120
Development of a theory of wear of ceramics [DE88-015327] N89-10170
GKSS-FORSCHUNGSZENTRUM GEESTHACHT (WEST GERMANY).
High-resolution spectroscopy for remote sensing of ocean and atmosphere N89-10352
GOETTINGEN UNIV. (WEST GERMANY).
Au II in IUE spectra of chemically peculiar stars N89-10766
GRENOBLE-1 UNIV. (FRANCE).
Satellite surveillance of ice and snow covered surfaces in the French Alps using visible and near infrared reflectance measurements from the SPOT and LANDSAT Thematic Mapper sensors N89-10372
GROUPEMENT SCIENTIFIQUE DE TELEDETECTION DE STRASBOURG (FRANCE).
Attempt at absolute determination of spectral signatures of bare soils in the thermal infrared, in emission and reflection N89-10336
Multispectral characterization of the spatial structure of remotely sensed scenes N89-10340
GRUMMAN AEROSPACE CORP., BETHPAGE, N.Y.
Open control/display system for a telerobotics work station N89-10089

H

HARVARD-SMITHSONIAN CENTER FOR ASTROPHYSICS, CAMBRIDGE, MASS.
Observing SN 1987A with IUE N89-10683
Some recent results from the study of cool stars N89-10689
HAWAII UNIV., HONOLULU.
IUE observations of rapidly rotating K dwarfs in the Pleiades N89-10738
Is regolith absorbtion the explanation for the transition from early to present Mars climate N89-10788
Ice or liquid water in the Martian regolith. Morphologic indicators from rampart craters N89-10806
Absorption of the Martian regolith: Specific surface area and missing CO(sub 2) N89-10824
HELSINKI UNIV. OF TECHNOLOGY, ESPOO (FINLAND).
Space-harmonic analysis of multi-depth corrugated waveguides [PB88-210059] N89-10214
Analysis of some low-order finite element schemes for Mindlin-Reissner and Kirchhoff plates [PB87-175899] N89-10578
Rotational modulation of hydrogen Lyman alpha flux from 44i Bootis N89-10741
HELSINKI UNIV. TECHNOLOGY, OTANIEMI (FINLAND).
Comparison of Euler algorithms for two-dimensional shock calculations [PB88-210372] N89-10032

HERIOT-WATT UNIV., EDINBURGH (SCOTLAND).
Optical bistability in semiconductor waveguides N89-10620
HONEYWELL, INC., BLOOMINGTON, MINN.
MOCVD techniques for CdTe solar cells [DE88-001163] N89-10411
HONEYWELL, INC., GOLDEN VALLEY, MINN.
Very large parallel data flow [AD-A196205] N89-10566
HONEYWELL, INC., PHOENIX, ARIZ.
LSZ-850 lightning sensor system N89-10487
HONEYWELL SYSTEMS AND RESEARCH CENTER, MINNEAPOLIS, MINN.
A common framework for knowledge-based programming N89-10537
KBSA common framework implementation N89-10543
Designing an effective user interface for a knowledge-based development environment N89-10549
HOUSTON UNIV., TEX.
Wilson cycle studies [NASA-CR-183146] N89-10419
Inelastic ion-surface collisions. Ion neutralization on intermetallic surfaces [AD-A196322] N89-10608
HUMAN MACHINE INTERFACES, INC., KNOXVILLE, TENN.
Consolidated fuel reprosing program: The implications of force reflection for teleoperation in space N89-10090
HYDRO-BRITISH COLUMBIA, VANCOUVER.
A revised electrogeometric model for the termination of lightning strokes on ground objects N89-10476

I

IBM FEDERAL SYSTEMS DIV., GAITHERSBURG, MD.
Knowledge based tools for knowledge-based systems N89-10550
ICELAND UNIV., REYKJAVIK.
Strengths and shortcomings in Airborne Thematic Mapper (ATM) technology as applied to volcanic and geothermal areas in Iceland N89-10337
A narrow-band thermal imager based on multiline real-time averaging N89-10356
IIT RESEARCH INST., BARTLESVILLE, OKLA.
Thermodynamic properties by non-calorimetric methods: Progress report [DE88-015422] N89-10660
ILLINOIS UNIV., URBANA.
Time-dependent mechanical behavior of partially stabilized zirconia for diesel engine applications [DE88-015330] N89-10171
Pressure studies of protein dynamics [AD-A192386] N89-10523
Control System Research for Directed Energy Weapons [DE88-015371] N89-10599
ILLINOIS UNIV., URBANA-CHAMPAIGN.
On motion planning and control of multi-link lightweight robotic manipulators N89-10285
An expert system for VLSI layout N89-10528
Integrated switching networks: A performance study N89-10567
An evaluation of online database selection by a gateway system with artificial intelligence techniques N89-10667
LOOK: Implementation of an expert system in information retrieval for database selection N89-10669
IMAD AD DEAN, INC., BETHESDA, MD.
Asymmetry in zeta Auriage chromospheres N89-10722
IMPERIAL COLL. OF SCIENCE AND TECHNOLOGY, LONDON (ENGLAND).
Basic structural dynamics N89-10007
Structural dynamic characteristics of individual blades N89-10008
Structural dynamic characteristics of bladed assemblies N89-10009
INDIANA UNIV., INDIANAPOLIS.
Line formation of cool carbon star chromospheres N89-10748
INFERENCE CORP., LOS ANGELES, CALIF.
Simplifying the construction of domain-specific automatic programming systems: The NASA automated software development workstation project N89-10553
INSTITUT FRANCAIS DE RECHERCHE POUR L'EXPLOITATION DE LA MER, BREST (FRANCE).
Comparative analysis of spectral response in the optical domain of targets in a tropical swamp at various spectral and spatial resolutions N89-10363
High resolution radiometric measurement of intertidal microphytobenthos N89-10365
INSTITUT NATIONAL DE LA RECHERCHE AGRONOMIQUE, AVIGNON (FRANCE).
Extracting soil and vegetation characteristics from microwave remote sensing data N89-10306
INSTITUT NATIONAL DE LA RECHERCHE AGRONOMIQUE, MONTFAVET (FRANCE).
Measuring in-situ soil surface roughness using a laser profilometer N89-10308
Complementary of microwave and optical range in the characterization of crops by remote sensing N89-10310
Use of microwave backscatter measurements as boundary conditions in soil/atmosphere water transfer modeling N89-10311
Spectral profile and biomass estimation N89-10319
A simplified vegetation canopy reflectance and absorption model N89-10322
Introducing spectral data into a plant process model for improving its prediction ability N89-10324
Biomass and wheat crop yield estimation from SPOT vegetative indexes N89-10327
Use of high spectral resolution to follow the state of vegetation canopies N89-10354
INSTITUT NATIONAL DE LA RECHERCHE AGRONOMIQUE, THIVERVAL-GRIGNON (FRANCE).
Potential number of winter wheat ears estimation using radiometry techniques at an early stage N89-10323
Estimation of the interception efficiency of an alfalfa canopy from a vegetative index N89-10332
Relation between sugar beet crop yield and vegetative indexes calculated from LANDSAT MSS images N89-10333
Estimation of leaf spectra from measurements in wide spectral bands N89-10368
Modeling of soil color by remote sensing N89-10369
A new method for estimating regional evaporation from thermal infrared surface temperature measurements N89-10390
INSTITUTE FOR IMAGE PROCESSING COMPUTER MAPPING, GRAZ (AUSTRIA).
Stress detection in mixed coniferous-broadleaved forests from Airborne Imaging Spectrometer (AIS) data N89-10355
INSTITUTE OF OCEAN SCIENCES, SIDNEY (BRITISH COLUMBIA).
The fluorescence line imager: High-resolution imaging spectroscopy over water and land N89-10353
INSTITUTO DE INVESTIGACION TECNOLOGIA, MADRID (SPAIN).
Study on conceptual design of spacecraft using computer-aided engineering techniques [ESA-CR(P)-2615] N89-10116
INSTITUTO DE PESQUISAS ESPACIAIS, SAO JOSE DOS CAMPOS (BRAZIL).
Scientific ballooning in Brazil [INPE-4602-PRE/1325] N89-10018
Theoretical model for the solute distribution of a PbSnTe growth by VMS in microgravity environment [INPE-4664-PRE/1365] N89-10183
S-band transponder and telecommand decoder design and development for MECB satellites [INPE-4659-PRE/1362] N89-10219
Theoretical and experimental analysis of quadrifilar antennas for the first Brazilian satellite [INPE-4581-PRE/1315] N89-10221
Relationships between spectral reflectance and phytomass of the ground layer community of neotropical savanna (CERRADO) [INPE-4635-PRE/1347] N89-10302
Identifying the reforested areas utilizing the SPOT satellite data [INPE-4624-PRE/1343] N89-10396
The Transformed Vegetation Index (TVI) for estimation of Brazilian cerrado's phytomass [INPE-4603-PRE/1326] N89-10400
Nation-wide forest mapping and timber volume estimation using LANDSAT-5 TM imagery [INPE-4643-PRE/1354] N89-10402
Environmental impact of the urban growth on the Western Sao Paulo metropolitan area [INPE-4670-PRE/1370] N89-10413
Meteorological measurements made using Brazilian drifting buoys: Technical aspects and first results [INPE-4674-PRE/1372] N89-10502
Satellite image registration through structural matching [INPE-4563-PRE/1304] N89-10530
Experimental studies on the surface confined quiescent plasma at INPE [INPE-4605-PRE/1328] N89-10630
A general data model for geographic information systems [INPE-4560-PRE/1301] N89-10676
Gamma-ray observations of supernova SN 1987A [INPE-4604-PRE/1327] N89-10680
Profiles of emission lines in AGN. Part 3: On the broad Ha component of IC 5063, IC 5135 and NGC 2992 [INPE-4678-PRE/1375] N89-10681
IOWA STATE UNIV. OF SCIENCE AND TECHNOLOGY, AMES.
IUE observations of pulsating stars: Atmospheric structure, shock waves and stellar winds N89-10686

J

JEFFERS (JAMES D., III), TAMPA, FLA.
Aeroelastic thermal effects N89-10015
JET PROPULSION LAB., CALIFORNIA INST. OF TECH., PASADENA.
PLAN-IT: Scheduling assistant for solar system exploration N89-10068
Deep space network resource scheduling approach and application N89-10070
Multiple sensor smart robot hand with force control N89-10093
Teleoperated position control of a PUMA robot N89-10104
The Telecommunications and Data Acquisition Report [NASA-CR-183243] N89-10186
Deep space tracking in local reference frames N89-10187
Precise orbit determination for NASA's earth observing system using GPS (Global Positioning System) N89-10188
PSA: A program to streamline orbit determination for launch support operations N89-10189
Spain 31-GHz observations of sky brightness temperatures N89-10190
Australia 31-GHz brightness temperature exceedance statistics N89-10191
Gravitational wave searches using the DSN (Deep Space Network) N89-10192
Evaluation of the characteristics of a field emission cathode for use in a Mercury ion trap frequency standard N89-10193
Simultaneous S- and X-band uplink-downlink performance at DSS 13 N89-10194
X/X/Ka-band prime focus feed antenna for the Mars Observer beacon spacecraft N89-10195
Dual passband dichroic plate for X-band N89-10196
Antenna pointing compensation based on precision optical measurement techniques N89-10197
A 32-GHz reflected-wave maser amplifier with wide instantaneous bandwidth N89-10198
An 8.4-GHz cryogenically cooled HEMT amplifier for DSS 13 N89-10199
Design of an optical PPM communication link in the presence of component tolerances N89-10200
Atmospheric propagation effects relevant to optical communications N89-10201
Node synchronization of viterbi decoders using state metrics N89-10202
A software simulation study of the long constraint length VLSI Viterbi decoder N89-10203
An automatic frequency control loop using overlapping DFTs (Discrete Fourier Transforms) N89-10204
Heat exchanger expert system logic N89-10205
Storage and computationally efficient permutations of factorized covariance and square-root information arrays N89-10206
Phasing the antennas of the Very Large Array (VLA) for reception of telemetry from Voyager 2 at Neptune encounter N89-10207
Phobos lander coding system: Software and analysis N89-10208
Relative planetary radar sensitivities: Arecibo and Goldstone N89-10209
DSN 64-meter antenna L-band (1668-MHz) microwave system performance overview N89-10210
Summary of DSN (Deep Space Network) reimbursable launch support N89-10211
The spectral bidirectional reflectance of snow N89-10318
Airborne Visible/Infrared Imaging Spectrometer (AVIRIS): Inflight radiometric calibration and the determination of surface reflectance N89-10357
Monitoring seasonal variations of soil moisture and vegetation cover using satellite microwave radiometry N89-10378
The observed day-to-day variability of Mars water vapor N89-10797
Influence of polar-cap albedo on past and current Martian climate N89-10801
The thermal properties of Martian surface materials at high lattitudes: Possible evidence for permafrost N89-10812
Geomorphic evidence for ancient seas on Mars N89-10813

JOHNS HOPKINS UNIV., BALTIMORE, MD.
The delineation and interpretation of the earth's gravity field
[NASA-CR-183283] N89-10416
Io: IUE observations of its atmosphere and the plasma torus N89-10691
Jovian equatorial H2 emission from 1979-1987 N89-10693
Phenomenological analysis of Jovian north auroral H2 Lyman band emissions N89-10695
IUE observations of oxygen-rich supernova remnants N89-10699

JOINT INST. FOR LAB. ASTROPHYSICS, BOULDER, COLO.
Mg II flux and profile variability of hybrid-chromosphere stars N89-10750
C 4 fluxes from the sun as a star and the correlation with magnetic flux
[NASA-CR-183156] N89-10827

JOINT RESEARCH CENTRE OF THE EUROPEAN COMMUNITIES, ISPRA (ITALY).
Time-resolved laser fluorescensing: Trends and applications N89-10346
AGRISAR'86: Contributing to signature research N89-10387
Development of MOMS to a future multiband and stereoscopic sensor N89-10391

K

KANSAS UNIV. CENTER FOR RESEARCH, INC., LAWRENCE.
Evaluation of hardware architectures for HF antenna arrays
[AD-A196204] N89-10217

KARLSRUHE UNIV. (WEST GERMANY).
Coherent polarimetric signatures of coniferous trees: A survey N89-10307
Changes in the chlorophyll fluorescence spectra during the Kautsky induction kinetics N89-10348
Chlorophyll fluorescence spectra of leaves as induced by blue light and red laser light N89-10349
Design of spectral bands for the German MOMS-2 sensor N89-10381

KATHOLIEKE UNIVERSITEIT, NIJMEGEN (NETHERLANDS).
ORDMET3: An improved algorithm to find the maximum solution to a system of linear (in)Equalities
[PB88-208970] N89-10520

KESTREL INST., PALO ALTO, CALIF.
Performance estimation for a knowledge-based software assistant N89-10540
Technical issues for performance estimation N89-10548

KEURING VAN ELECTROTECHNISCHE MATERIALEN N.V., ARNHEM (NETHERLANDS).
Optical sensors for the measurement of electric current and voltage
[PB88-208467] N89-10233

KIEL UNIV. (WEST GERMANY).
White dwarfs N89-10685

KISARAZU NATIONAL COLL. OF TECHNOLOGY (JAPAN).
Laser-induced fluorescence on in-vivo chlorophyll of a rice plant: A technique for the remote detection of plant growth N89-10350

KMS FUSION, INC., ANN ARBOR, MICH.
The tensile strength of glass shells
[DE88-013011] N89-10301

KYOTO UNIV. (JAPAN).
Interannual differences in the regressions of the polar caps of Mars N89-10796

L

LABEN SPACE INSTRUMENTATION AND SYSTEMS, MILAN (ITALY).
Solid earth mission study. Volume 2: Technical report
[ESA-CR(P)-2626-VOL-2] N89-10303
Solid Earth mission study Volume 1: Executive summary
[ESA-CR(P)-2626-VOL-1] N89-10397
Solid earth mission study. Volume 3: Program planning report
[ESA-CR(P)-2626-VOL-3] N89-10399

LABORATOIRE CENTRAL DES PONTS ET CHAUSSEES, PARIS (FRANCE).
Measuring in-situ soil surface roughness using a laser profilometer N89-10308

LAMONT-DOHERTY GEOLOGICAL OBSERVATORY, PALISADES, N.Y.
Study of biological processes on the US North Atlantic slope and rise, volume 2
[PB88-196514] N89-10511
Study of biological processes on the US North Atlantic slope and rise. Volume 1: Executive summary
[PB88-196522] N89-10517

LANZHOU INST. OF PLATEAU ATMOSPHERIC PHYSICS (CHINA).
The criterion for the propagation of the positive streamer and its application N89-10436

LAVAL UNIV. (QUEBEC).
Texture analysis in forest areas: High spectral resolution synthetic aperture radar data N89-10367

LAWRENCE LIVERMORE NATIONAL LAB., CALIF.
Pulse combustor modeling: One dimensional wave-dynamic model utilizing dynamic injection and energy release submodels
[DE88-005369] N89-10150
Premartensitic microstructures as seen in the high-resolution electron microscope: A study of a NiAl alloy
[DE88-008042] N89-10160
Directional spectral emissivity measurements on a ceramic mold material
[DE88-015407] N89-10167
Crossatron switch as thyratron replacement in high repetition rate, high average power modulators
[DE88-013706] N89-10230
Design and performance of the SSVCO
[DE88-012435] N89-10232
Applications of a three-dimensional finite element model to mountain-valley flows
[DE88-008898] N89-10412
An interagency working group on lightning threat warning N89-10469
Control System Research for Directed Energy Weapons
[DE88-015371] N89-10599
Deflection of light by using tungsten bronze crystals
[DE88-014151] N89-10618
A novel alignment technique for pointing and centering optical components
[DE88-015441] N89-10621
Time-resolved X-ray conversion efficiencies of laser-heated plasmas
[DE88-015456] N89-10637
Pressure effects on the electronic structure of 4f and 5f materials
[DE88-014149] N89-10650
Loopspace general covariance in string field theory
[DE88-014170] N89-10659
Prospects for understanding the astrophysical r-process
[DE88-015449] N89-10773

LIGHTNING LOCATION AND PROTECTION, INC., TUCSON, ARIZ.
Considerations for using lightning locating systems in performance evaluations of single-station lightning detection sensors N89-10488

LINKOEPING UNIV. (SWEDEN).
Atmospheric correction of thermal infrared data from LANDSAT-5 for surface temperature estimation N89-10339

LITTLE (ARTHUR D.), INC., CAMBRIDGE, MASS.
Robot hands and extravehicular activity N89-10097

LOCKHEED AERONAUTICAL SYSTEMS CO., BURBANK, CALIF.
Wheel performance evaluation. Phase 1: Analysis
[DOT/FAA/CT-88/16] N89-10041

LOCKHEED-GEORGIA CO., MARIETTA.
Quadruplex digital flight control system assessment
[NASA-CR-182741] N89-10058
Hardware fault insertion and instrumentation system: Experimentation and results
[NASA-CR-182746] N89-10526

LOCKHEED MISSILES AND SPACE CO., HUNTSVILLE, ALA.
Flowfield visualization for SSME hot gas manifold
[NASA-CR-179403] N89-10243

LOCKHEED MISSILES AND SPACE CO., SUNNYVALE, CALIF.
Advanced planar array development for space station
[NASA-CR-179372] N89-10407

LOS ALAMOS NATIONAL LAB., N. MEX.
Ab initio studies of transition-metal dihydrogen chemistry
[DE88-014467] N89-10139
Theoretical studies of grain boundaries in Ni, Al and Ni3Al with and without boron
[DE88-014323] N89-10152
The influence of texture on strain hardening
[DE88-009157] N89-10158
Characterization of dynamic fracture in copper under uniaxial stress and uniaxial strain
[DE88-007824] N89-10162
Metastable alloy phases prepared by solid state reactions and ball milling
[DE88-009156] N89-10163
Comparison of surface modifications of poly(ether urethanes) by chemical infusion and graft polymerization
[DE88-007887] N89-10172
Single crystal orientation effects in shock initiation of PETN explosive
[DE88-014406] N89-10182
Losses in magnetic flux compression generators. Part 2: Radiation losses
[DE88-015046] N89-10224
Simulation of plasma erosion opening switches
[DE88-014425] N89-10229
Effects of modulated electron beams and cavities on reditrons
[DE88-014317] N89-10234
Fluid dynamic issues in continuous wave short wavelength chemical lasers
[DE88-014428] N89-10274
Recent results from the Los Alamos free-electron laser
[DE88-014409] N89-10279
The angular reflectance signature of the canopy hot spot in the optical regime N89-10325
Supercomputing: An indispensable component of applied research
[DE88-015363] N89-10533
Mean estimation in highly skewed samples
[DE88-010929] N89-10595
Directed energy concepts for strategic defense
[DE88-015050] N89-10596
Military uses of space
[DE88-015053] N89-10597
SDI (Strategic Defense Initiative): Myth or reality
[DE88-015059] N89-10598
Electronic structure of the quenched superconductivity of materials Y(sub 1-x)Pr(sub x)Ba2Cu3O(sub 7-delta)
[DE88-014414] N89-10658
The inverse-square law and quantum gravity
[DE88-014332] N89-10663
Observations of galactic WC + O binary systems: HD 97152 and HD 152270 N89-10716
Cosmogenic (sup 36)Cl production rates in meteorites and the lunar surface
[DE88-014452] N89-10775

LOUGHBOROUGH UNIV. OF TECHNOLOGY (ENGLAND).
Attitudes to the use of computerised information systems for production management in manufacturing industry: A survey
[TT-8706] N89-10670

LOWELL OBSERVATORY, FLAGSTAFF, ARIZ.
The great dust storm of 1986 N89-10804

LUNAR AND PLANETARY INST., HOUSTON, TEX.
Wilson cycle studies
[NASA-CR-183146] N89-10419
MECA Symposium on Mars: Evolution of its Climate and Atmosphere
[NASA-CR-182872] N89-10780
Mars: Crustal pore volume, cryospheric depth, and the global occurrence of groundwater N89-10787
Thermal properties of channels in the Aeolis Quadrangle: Topographic traps for Aeolian materials N89-10825

M

MAGNAVOX ELECTRONIC SYSTEMS CO., FORT WAYNE, IND.
Digital simulation techniques for end game phenomena N89-10051

MANUDYNE SYSTEMS, INC., LOS ALTOS, CALIF.
Helicopter roll control effectiveness criteria program summary
[NASA-CR-177477] N89-10046

MARCONI CO. LTD., GREAT BADDOW (ENGLAND).
The use of the complex correlation function in the recovery of ocean wave spectra from SAR images N89-10315

MARTIN MARIETTA AEROSPACE, DENVER, COLO.
Consolidated fuel reprossing program: The implications of force reflection for teleoperation in space N89-10090
Issues, concerns, and initial implementation results for space based telerobotic control N89-10091
Actuators for a space manipulator N89-10101
Comets, volcanism, the salt rich regolith and cycling of volatiles on Mars N89-10786

MARYLAND UNIV., COLLEGE PARK.
An adaptive control scheme for a flexible manipulator N89-10095
Comets N89-10688

MASSACHUSETTS INST. OF TECH., CAMBRIDGE.
Aeroelastic formulation for tuned and mistuned rotors N89-10013
A study of the fatigue behavior of small cracks in nickel-base superalloys
[AD-A195489] N89-10161

A dexterity measure for the kinematic control of robot manipulator with redundancy
[AD-A196223] N89-10287
Intracloud lightning as a precursor to thunderstorm microbursts N89-10490
Space-efficient queue management using fixed-connection networks
[AD-A195167] N89-10569
Optimal simulations by butterfly networks: Extended abstract
[AD-A195168] N89-10572
Synthesis and study of materials for superconducting electronics
[AD-A195279] N89-10649
Integrating distributed homogeneous and heterogeneous databases: Prototypes, volume 3
[AD-A195852] N89-10668
Object-oriented approach to integrating database semantics, volume 4
[AD-A195853] N89-10672
UNITRAN (universal translator): A principle-based approach to machine translation
[AD-A195281] N89-10675

MASSACHUSETTS UNIV., AMHERST.
Plans and meta-plans in an intelligent assistant for the process of programming N89-10547
Plan recognition in GRAPPLE: An intelligent assistant for the process of programming N89-10555
Chemical frost weathering of olivine: Experimental study and implications N89-10793
Mars low albedo regions: Possible map of near-surface N89-10794
Photochemical weathering and contemporary volatile loss on Mars N89-10795

MATERIALS RESEARCH LABS., MELBOURNE (AUSTRALIA).
Contamination of environmental control systems in Hercules aircraft
[MRL-R-1116] N89-10040
Numerical simulation of the explosives effects of two closely spaced pyrotechnic pods
[MRL-R-1095] N89-10177
An interactive program for estimating extinction and scattering properties of most particulate clouds
[MRL-R-1123] N89-10216
An analysis of an implicit factored scheme for simulating shock waves
[AR-005-231] N89-10252

MATRA ESPACE, TOULOUSE (FRANCE).
Solid earth mission study. Volume 2: Technical report
[ESA-CR(P)-2626-VOL-2] N89-10303
Solid Earth mission study. Volume 1: Executive summary
[ESA-CR(P)-2626-VOL-1] N89-10397
Solid earth mission study. Volume 3: Program planning report
[ESA-CR(P)-2626-VOL-3] N89-10399

MAX-PLANCK-INST. FUER CHEMIE, MAINZ (WEST GERMANY).
Water on Mars N89-10822

MAX-PLANCK-INST. FUER PHYSIK UND ASTROPHYSIK, GARCHING (WEST GERMANY).
Use of the time projection chamber for measuring heavy ion collisions
[MPE-PAE/EXP-EL-191] N89-10611

MAX-PLANCK-INSTITUT FUER STROEMUNGSFORSCHUNG, GOETTINGEN (WEST GERMANY).
Numerical investigation of the dynamics of heterogeneous shock-cavitation
[MPIS-MITT-86-1987] N89-10257
Experiments on the influence of the geometry on the stability of Taylor-Couette flow
[MPIS-MITT-87-1987] N89-10258
Experimental detection of high speed fronts and clarification of their coherence with low speed streaks and streamwise vortices in a fully developed turbulent channel
[MPIS-MITT-88-1987] N89-10259
A water sound generator for pressure pulses of high energy
[MPIS-MITT-85-1987] N89-10604

MCDONNELL-DOUGLAS ASTRONAUTICS CO., HOUSTON, TEX.
An optimal resolved rate law for kinematically redundant manipulators N89-10094

MECHANICAL TECHNOLOGY, INC., LATHAM, N. Y.
Free-piston Stirling engine development
[PB88-220025] N89-10286

MESSERSCHMITT-BOELKOW-BLOHM G.M.B.H., MUNICH (WEST GERMANY).
Indirect effects on electronic and mechanical systems installed in carbon fibre compound aircraft structures N89-10492

METEOROLOGICAL OFFICE, BRACKNELL (ENGLAND).
Precise long-range lightning mapping with the UK arrival time difference VLF technique N89-10486

METOCEAN CONSULTANCY LTD., HASLEMERE (ENGLAND).
Review of the requirements for higher level ERS-1 products within Europe
[ESA-CR(P)-2586] N89-10664

MICHIGAN STATE UNIV., EAST LANSING.
Systems analysis of the inverse heat conduction problem N89-10244
Use of remote sensing for land use policy formulation
[NASA-CR-183148] N89-10395

MIDWEST RESEARCH INST., GOLDEN, COLO.
Impacts of advanced refrigerator insulation
[DE88-001180] N89-10185
Electronic structure of electrodeposited thin film CdTe solar cells
[DE88-001170] N89-10406
Solid State Photovoltaic Research Branch
[DE88-001179] N89-10410
Structure of amorphous silicon alloy films
[DE88-001167] N89-10554

MILAN UNIV. (ITALY).
Far UV observations of black hole candidates: The case of LMC X-3 N89-10701

MINNESOTA UNIV., MINNEAPOLIS.
Volatile inventory of Mars-2: Primordial sources and fractionating processes N89-10814

MISSION RESEARCH CORP., ALEXANDRIA, VA.
The Paleo-ocean of Mars N89-10783

MISSISSIPPI STATE UNIV., MISSISSIPPI STATE.
Standardization of the carbon-phenolic materials and processes. Vol. 2: Test methods and specifications
[NASA-CR-183227] N89-10033
Standardization of the carbon-phenolic materials and processes. Vol. 1: Experimental studies
[NASA-CR-183226] N89-10127

MISSISSIPPI UNIV., UNIVERSITY.
The electrical structure of thunderstorm anvils N89-10470

MISSOURI UNIV., ST. LOUIS.
The direction of water transport on Mars: A possible pumping mechanism N89-10798
The great dust storm of 1986 N89-10804

MITRE CORP., BEDFORD, MASS.
ASDL: An intelligent acquisition support tool N89-10554

MITRE CORP., MCLEAN, VA.
Direct methane conversion: An assessment
[DE88-010225] N89-10181

MUSEE ROYAL DE L'AFRIQUE CENTRALE, TERVUREN (BELGIUM).
Rock and soil discrimination in natural tropical conditions using a spot-calibrated radiometer N89-10374

N

NAGOYA UNIV. (JAPAN).
Numerical simulations of lightning by means of the leader propagation model N89-10437
Measurements of the velocity change of a lightning return stroke with height N89-10442
Neoclassical resonant-plateau transport in the noncircular equipotential surface of a tandem mirror
[IPPJ-879] N89-10627
Adventures in magnetohydrodynamics
[IPPJ-862] N89-10629
Gas-contact cooling for VUV laser oscillation in recombining plasmas
[IPPJ-881] N89-10631
Neon puffing experiments in the JIPP T-IIU tokamak
[IPPJ-870] N89-10632
Study of critical beta non-circular tokamak equilibria sustained in steady state by beam driven currents
[IPPJ-878] N89-10634
Effect of double-shell structure on reduction of field errors in the STP-3(M) reversed-field pinch
[IPPJ-882] N89-10640
On the generation of runaway electrons and their impact to plasma facing components
[IPPJ-871] N89-10641
Structural instability of sheath potential distribution and its possible implications for the L/H transition in tokamak plasmas
[IPPJ-877] N89-10643

NATIONAL ACADEMY OF SCIENCES - NATIONAL RESEARCH COUNCIL, WASHINGTON, D. C.
Antennas, satellite broadcasting, and emergency preparedness for the Voice of America
[PB88-209895] N89-10222

NATIONAL AERONAUTICS AND SPACE ADMINISTRATION, WASHINGTON, D.C.
Aeronautical engineering: A continuing bibliography with indexes (supplement 231)
[NASA-SP-7037(231)] N89-10002
A new method of determining acid base strength distribution and a new acidity-basicity scale for solid catalysts: The strongest point, HO
[NASA-TT-20334] N89-10141
New diamond
[NASA-TT-20325] N89-10169
Resonant excitation of spatial perturbations in a boundary layer in the presence of a pressure gradient
[NASA-TT-20305] N89-10248
Thermal transfer recording media
[NASA-TT-20322] N89-10262
NASA's future land remote sensing program N89-10393
Earth resources: A continuing bibliography with indexes (issue 58)
[NASA-SP-7041(58)] N89-10398
Sapping features of the Colorado Plateau: A comparative planetary geology field guide
[NASA-SP-491] N89-10401
Living in space, book 2, levels D, E, F
[NASA-EP-223] N89-10522
SPOCK: A tool for real time artificial intelligence
[NASA-TT-20357] N89-10574
Civil Space Technology Initiative: A first step
[NASA-TM-100949] N89-10665

NATIONAL AERONAUTICS AND SPACE ADMINISTRATION. AMES RESEARCH CENTER, MOFFETT FIELD, CALIF.
Wave drag and high-speed performance of supersonic STOVL fighter configuration
[NASA-TM-100061] N89-10017
Navier-Stokes simulation of transonic wing flow fields using a zonal grid approach
[NASA-TM-100039] N89-10022
Using full-mission simulation for human factors research in air transport operations
[NASA-TM-88330] N89-10037
Maintaining an expert system for the Hubble Space Telescope ground support N89-10064
Expert systems tools for Hubble Space Telescope observation scheduling N89-10081
Advanced data management design for autonomous telerobotic systems in space using spaceborne symbolic processors N89-10096
The lowest ionization potentials of Al2
[NASA-TM-101171] N89-10605
Theoretical study of the dissociation energy and the red and violet band systems of CN
[NASA-TM-101190] N89-10610
Interannual variability of global dust storms on Mars N89-10792
Climatic effects of enhanced CO2 levels in Mars early atmosphere N89-10799
Formation of the layered deposits in the Valles Marineris, Mars N89-10809
Partitioning of carbon dioxide between the atmosphere and lithosphere on early Mars N89-10816

NATIONAL AERONAUTICS AND SPACE ADMINISTRATION. GODDARD SPACE FLIGHT CENTER, GREENBELT, MD.
Proceedings of 1987 Goddard Conference on Space Applications of Artificial Intelligence (AI) and Robotics
[NASA-TM-89663] N89-10063
CLEAR: Communications Link Expert Assistance Resource N89-10072
The load shedding advisor: An example of a crisis-response expert system N89-10073
A local area computer network expert system framework N89-10074
FIESTA: An operational decision aid for space network fault isolation N89-10075
Expert system support for HST operations N89-10076
Automation of spacecraft control centers N89-10078
Spacelab Data Processing Facility (SLDPF) quality assurance expert systems development N89-10079
Cable applications in robot compliant devices N89-10102
Effects of switch leakages upon Nimbus-7 SMMR calibration
[NASA-CR-180792] N89-10115
The spectral bidirectional reflectance of snow N89-10318
Atmospheric effect removal from space imagery N89-10338
Spatial resolution requirements for MODIS-N N89-10364
The basis for the spectral behaviour of silicates in the thermal infrared and applications to remote sensing N89-10366

Comparative point-spread function calculations for the MOMS-1, Thematic Mapper and SPOT-HRV instruments
N89-10379
Interplanetary medium data book: Supplement 3A, 1977-1985
[NASA-TM-89630] N89-10678
The Progenitor of SN 1987A N89-10697
The complete visual light curve of SN 1987A: Thirteen months of FES observations N89-10698
Simultaneous IUE, EXOSAT and optical observations of the unusual AM Her type variable H058+608
N89-10703
The 1981 outburst of the old nova GK Persei
N89-10707
Observations of classical novae in outburst
N89-10708
Observations and simulations of nova Vul 1984 no. 2: A nova with ejecta rich in oxygen, neon, and magnesium
N89-10709
Observations and simulations of recurrent novae: U Sco and V394 CrA N89-10710
Optical and ultraviolet observations of nova Vul 1987
N89-10711
Ultraviolet observations of LMC nova 1988
N89-10712
IUE observations of the 1987 superoutburst of the dwarf nova Z Cha N89-10715
Mass flow in the interacting binary TX Ursae Majoris
N89-10718
Recurrent shell infall events in a B0.5e star: HD 58978 1979-1988 N89-10732
Spectral images of HD 199178 N89-10739
Fluorescence processes and line identifications in the UV spectra of cool stars N89-10753
Identification of new fluorescence processes in the UV spectra of cool stars from new energy levels of Fe II and Cr II N89-10755
Periodic modulation of the atmosphere of Alpha Orionis N89-10756
The anomalous C 4 intensity ratio in symbiotic stars
N89-10761
C IV and Si IV in IUE spectra of normal B8-A0 stars: UV identified Be/Ae stars N89-10764
Interplanetary medium data book. Supplement 3: 1977-1985
[NASA-TM-89660] N89-10772
Martian surface physical properties to be derived by radar altimeter on the Mars observer spacecraft
N89-10789

NATIONAL AERONAUTICS AND SPACE ADMINISTRATION. JOHN F. KENNEDY SPACE CENTER, COCOA BEACH, FLA.
Computer hardware and software for robotic control
N89-10103

NATIONAL AERONAUTICS AND SPACE ADMINISTRATION. LYNDON B. JOHNSON SPACE CENTER, HOUSTON, TEX.
Emitted short wavelength infrared radiation for detection and monitoring of volcanic activity N89-10377
Seismic exploration for water on Mars N89-10811

NATIONAL AERONAUTICS AND SPACE ADMINISTRATION. LANGLEY RESEARCH CENTER, HAMPTON, VA.
Weak-wave analysis of shock interaction with a slipstream
[NASA-TP-2848] N89-10020
Validation of a pair of computer codes for estimation and optimization of subsonic aerodynamic performance of simple hinged-flap systems for thin swept wings
[NASA-TP-2828] N89-10024
The pros and cons of code validation
[NASA-TM-100657] N89-10034
Development in helicopter tail boom strake applications in the US
[NASA-TM-101496] N89-10059
Highlights of experience with a flexible walled test section in the NASA Langley 0.3-meter transonic cryogenic tunnel
[NASA-TM-101491] N89-10060
AUTOPLAN: A PC-based automated mission planning tool N89-10067
Space truss assembly using teleoperated manipulators
N89-10087
A compendium of sources of fracture toughness and fatigue crack growth data for metallic alloys, part 3
[NASA-TM-100675] N89-10165
Recent developments in structural sensitivity analysis
[NASA-TM-100668] N89-10300
Compilation of methods in orbital mechanics and solar geometry
[NASA-RP-1204] N89-10420
Implications of a recent lightning strike to a NASA jet trainer N89-10478
On the diagnostic emulation technique and its use in the AIRLAB
[NASA-TM-4027] N89-10524
Programming the Navier-Stokes computer: An abstract machine model and a visual editor
[NASA-CR-181691] N89-10560
Improving the accuracy of central difference schemes
[NASA-CR-181712] N89-10577
Non-oscillatory central differencing for hyperbolic conservation laws
[NASA-CR-181709] N89-10582
An adaptive pseudospectral method for discontinuous problems
[NASA-CR-181717] N89-10583
Multiple nucleon knockout by Coulomb dissociation in relativistic heavy-ion collisions
[NASA-TM-4070] N89-10612

NATIONAL AERONAUTICS AND SPACE ADMINISTRATION. LEWIS RESEARCH CENTER, CLEVELAND, OHIO.
Vibration, performance, flutter and forced response characteristics of a large-scale propfan and its aeroelastic model
[NASA-TM-101322] N89-10043
Fire behavior and risk analysis in spacecraft
[NASA-TM-100944] N89-10111
The solar dynamic radiator with a historical perspective
[NASA-TM-100972] N89-10117
Photovoltaics for high capacity space power systems
[NASA-TM-101341] N89-10122
Technology issues associated with fueling the national aerospace plane with slush hydrogen
[NASA-TM-101386] N89-10123
The effect of Al2O3, CaO, Cr2O3 and MgO on devitrification of silica
[NASA-TM-101335] N89-10124
Properties of silicon carbide fiber-reinforced silicon nitride matrix composites
[NASA-TM-101356] N89-10130
Thermal effects on the mechanical properties of SiC fiber reinforced reaction bonded silicon nitride matrix (SiC/RBSN) composites
[NASA-TM-101348] N89-10134
T55-L-712 turbine engine compressor housing refurbishment-plasma spray project
[NASA-TM-101310] N89-10156
A sintering model for SiC(sub)w/Si3N4 composites
[NASA-TM-101336] N89-10166
A method for producing a shaped contour radiation pattern using a single shaped reflector and a single feed
[NASA-TM-101369] N89-10215
Sequentially evaporated thin Y-Ba-Cu-O superconductor films: Composition and processing effects
[NASA-TM-101388] N89-10235
Discretization formulas for unstructured grids
[NASA-TM-101298] N89-10242
High-resolution heat-transfer-coefficient maps applicable to compound-curve surfaces using liquid crystals in a transient wind tunnel
[NASA-TM-89855] N89-10246
Performance of multimirror quartzline lamps in a high-pressure, underwater environment
[NASA-TM-101374] N89-10269
Generation of a crowned pinion tooth surface by a surface of revolution
[NASA-TM-100260] N89-10282
Generation of a crowned pinion tooth surface by a plane
[NASA-TM-100259] N89-10283
Data report for the Siple Coast (Antarctica) project
[NASA-TM-100708] N89-10403
Hydrogen-bromine fuel cell advance component development
[NASA-TM-101345] N89-10405
Oxygen electrode bifunctional electrocatalyst NiCo2O4 spinel
[NASA-TM-100947] N89-10409
An algorithm for unsteady flows with strong convection
[NASA-TM-100828] N89-10575
The effect of front-to-rear propeller spacing on the interaction noise at cruise conditions of a model counterrotation propeller having a reduced diameter aft propeller
[NASA-TM-101329] N89-10603

NATIONAL AERONAUTICS AND SPACE ADMINISTRATION. MARSHALL SPACE FLIGHT CENTER, HUNTSVILLE, ALA.
Rechargeable metal hydrides for spacecraft application
[NASA-TM-4076] N89-10184
A preliminary review of organic materials single crystal growth by the Czochralski technique
[NASA-TM-100341] N89-10656

NATIONAL AEROSPACE LAB., AMSTERDAM (NETHERLANDS).
Digital recording of radar data in an aircraft
[PB88-209507] N89-10212
Numerical accuracy of a two-stream radiative transfer model from comparison with an N-stream model
N89-10331

NATIONAL AEROSPACE LAB., TOKYO (JAPAN).
Measurement of aerodynamic characteristics of a hang-glider-wing by ground run tests using a test vehicle
[NAL-TR-953] N89-10004
Normal force coefficient of supersonic flows over conical flare, cone-cylinder and conical boattails
[NAL-TR-949] N89-10021
Estimation of up-wash distribution around an automobile by three-dimensional smoke wind tunnel test
[NAL-TR-921] N89-10023
Functional mock-up tests of the flight control system of the NAL QSTOL research aircraft: Planning and mechanical system test
[NAL-TR-944] N89-10047
A digital simulation method of cumulative fatigue damage evaluation for spacecraft components
[NAL-TR-957] N89-10113
Fabrication and test of a carbon-carbon composite combustion chamber for a low thrust storable engine
[NAL-TR-946] N89-10118
Measurement of infrared horizon profiles from TT-500A sounding rocket
[NAL-TR-947] N89-10121
Study on twin valveless pulse burner: Combustion stability and mixing patterns
[NAL-TR-955] N89-10144
Generation of a grid for a finite difference calculation of flows around an aircraft in Cartesian coordinates
[NAL-TR-956] N89-10563
Programming techniques for high-speed processing on the supercomputer FUJITSU VP-system
[NAL-TR-915] N89-10565
Delta square-correction scheme for unsteady Euler equations
[NAL-TR-948] N89-10576
On high resolution schemes for three-dimensional Euler equations
[NAL-TR-950T] N89-10581
Comparison of plotting methods used on normal probability paper
[NAL-TR-951] N89-10584
Spectral characteristics of arc-heated low density plasma flows (2) nitrogen plasma
[NAL-TR-952] N89-10639
Spectral characteristics of arc-heated low density plasma flows (1) argon plasma
[NAL-TR-954] N89-10642

NATIONAL BUREAU OF STANDARDS, BOULDER, COLO.
C 4 fluxes from the sun as a star and the correlation with magnetic flux
[NASA-CR-183156] N89-10827

NATIONAL BUREAU OF STANDARDS, GAITHERSBURG, MD.
NASREN: Standard reference model for telerobot control N89-10099

NATIONAL CENTER FOR ATMOSPHERIC RESEARCH, BOULDER, COLO.
CCM (Community Climate Model) modular processor users' guide (version PROC02)
[PB88-216577] N89-10428

NATIONAL GEOPHYSICAL DATA CENTER, BOULDER, COLO.
Solar-geophysical data number 524, April 1988. Part 2: (Prompt reports). Data for October 1987 and miscellanea
[PB88-217401] N89-10828
Solar-geophysical data number 524, April 1988. Part 1: (Prompt reports). Data for March, February 1988 and late data
[PB88-217393] N89-10829

NATIONAL OCEANIC AND ATMOSPHERIC ADMINISTRATION, BOULDER, COLO.
Lightning in mesoscale convective complexes on 3-5 June 1985 in Oklahoma and Kansas N89-10471
Oklahoma-Kansas preliminary regional experiment for storm-central (O-K pre-storm). Volume 3: Aircraft mission summary
[PB88-205489] N89-10499
Comparison of temperature profiles measured by three collocated microwave radiometers and radiosonde
[PB88-212808] N89-10503
Turbulent diffusion of ocean bubbles
[PB88-212816] N89-10513

NATIONAL OCEANIC AND ATMOSPHERIC ADMINISTRATION, MIAMI, FLA.
Joint CGS-AOML (Charting and Geodetic Service-Atlantic Oceanographic and Meteorological Laboratory) acoustical bottom echo-formation research. 1: Literature search and initial modelling results
[PB88-202007] N89-10512

Drifting buoy data from the Equatorial Pacific for the period January 1, 1984 through May 31, 1985
[PB88-212824] N89-10516

NATIONAL OCEANIC AND ATMOSPHERIC ADMINISTRATION, ROCKVILLE, MD.
International Aerospace and Ground Conference on Lightning and Static Electricity
[PB88-197439] N89-10429

NATIONAL OCEANIC AND ATMOSPHERIC ADMINISTRATION, SEATTLE, WASH.
EPOCS (Equatorial Pacific Ocean Climate Studies) moored temperature, current and wind measurements: 0 deg, 140 deg W, May-June, 1987
[PB88-219415] N89-10509
Model-data comparisons for the 1982-83 El Nino: The XBT tracks
[PB88-221668] N89-10514

NATIONAL RESEARCH COUNCIL OF CANADA, OTTAWA (ONTARIO).
A case for a unified lightning threat N89-10447
Lightning standards for protection of ground electronic systems N89-10473

NATIONAL SEVERE STORMS LAB., NORMAN, OKLA.
Lightning initiation on aircraft in thunderstorms N89-10456

NATIONAL TELECOMMUNICATIONS AND INFORMATION ADMINISTRATION, BOULDER, COLO.
Multitier specification applied to modify the hardness of an essential NSEP (National Security/Emergency Preparedness) fiber optic link
[PB88-210778] N89-10220

NATIONAL TRANSPORTATION SAFETY BOARD, WASHINGTON, D. C.
Aircraft accident reports, brief format, US civil and foreign aviation, issue number 10 of 1987 accidents
[PB88-916905] N89-10035
Aircraft accident reports, brief format, US civil and foreign aviation, issue number 12 of 1986 accidents
[PB88-916903] N89-10036

NATIONAL WEATHER SERVICE, SALT LAKE CITY, UTAH.
Climate of San Francisco, revised
[PB88-208624] N89-10504

NAVAL POSTGRADUATE SCHOOL, MONTEREY, CALIF.
Unmanned air vehicles - real time intelligence without the risk
[AD-A195190] N89-10039
Steady flow field measurements using laser Doppler velocimetry
[AD-A195228] N89-10245
A transition radiation experiment to measure the electron beam modulation induced by the free electron laser: A design study
[AD-A195169] N89-10275
ONR tropical cyclone motion research initiative: First-year review, discussion and tentative hypotheses
[AD-A194902] N89-10505
MIZEX (marginal ice zone experiment) 87 meteorology atlas
[AD-A195361] N89-10506
Segmentation of noisy images using nonstationary Markov fields
[AD-A195229] N89-10527
Smoothing spatial data by estimating mean local variance
[AD-A195302] N89-10593

NAVAL RESEARCH LAB., WASHINGTON, D.C.
Measurement of the electrostatic charging on large helicopters and control of the shock hazard N89-10461
Electrostatic fields of ground triggered lightning N89-10462

NEBRASKA UNIV., LINCOLN.
Nonlinear finite element analysis for plastic deformation by local random yielding N89-10298

NEW HAMPSHIRE UNIV., DURHAM.
A summary of major activities of the UNH and NRL groups
[NASA-CR-180949] N89-10774

NEW MEXICO INST. OF MINING AND TECHNOLOGY, SOCORRO.
Electrification of hovering helicopters N89-10460
Lightning protection for high explosives and instrumentation using a field mill system N89-10467
IUE observations and physical processes of interacting binary stars N89-10690
The discovery of a co-rotating magnetosphere in a helium weak star: HD5737 = alpha Sc! N89-10751
The galatic and LMC extreme line supergiants compared: IUE observations of the Henize-Carlson and Zoo star samples of massive supergiants N89-10769

NEW MEXICO STATE UNIV., UNIVERSITY PARK.
Adequacy of the transmitted near-field techniques for measuring optical fiber core diameter N89-10619

NEW YORK UNIV., NEW YORK.
Optimal simulations by butterfly networks: Extended abstract
[AD-A195168] N89-10572
Laser diagnostics of gas discharge tubes
[DE88-008124] N89-10633

NORTH CAROLINA AGRICULTURAL AND TECHNICAL STATE UNIV., GREENSBORO.
Dynamics and control of the orbiting grid structures and the synchronously deployable beam
[NASA-CR-183205] N89-10297

NORTH CAROLINA STATE UNIV., RALEIGH.
A transonic interactive boundary-layer theory for laminar and turbulent flow over swept wings
[NASA-CR-4185] N89-10029
Acoustic radiation from plates driven by multi-point random forces N89-10602

NOTTINGHAM UNIV. (ENGLAND).
High spectral resolution indices for monitoring crop growth and chlorosis N89-10358

O

OAK RIDGE NATIONAL LAB., TENN.
Dynamic task allocation for a man-machine symbiotic system N89-10098
Recent developments in aluminides and silicides
[DE88-012926] N89-10155
Micromechanisms of deformation and fracture in ordered intermetallic alloys. 1: Strengthening mechanisms
[DE88-015382] N89-10159
Engineering processing and properties of nickel aluminides
[DE88-011019] N89-10164
Development of ceramic matrix composites for application in the ceramic technology for advanced heat engines
[DE88-015329] N89-10168
Time-dependent mechanical behavior of partially stabilized zirconia for diesel engine applications
[DE88-015330] N89-10171
Solution of ill-posed problems by means of truncated SVD (Singular Value Decomposition)
[DE88-013510] N89-10238
An analytical study of hybrid ejector/internal combustion engine-driven heat pumps
[DE88-013242] N89-10240
Development and proof-testing of advanced absorption refrigeration cycle concepts, phase 2
[DE88-013239] N89-10247
Computer simulation of absorption heat pump using aqueous lithium bromide and ternary nitrate mixtures
[DE88-013353] N89-10249
Overview of ground coupled heat pump research and technology transfer activities
[DE88-012938] N89-10255
Selection of sensors for measurement and control
[DE88-012936] N89-10267
Laser welding of stainless steel weld filler metals at high cooling rates
[DE88-002345] N89-10281
Telerobotic control of the seven-degree-of-freedom CESAR manipulator
[DE88-012937] N89-10289
Laboratory capacity modulation experiments, analyses and validation
[DE88-012930] N89-10408
Evaluating impacts of pollutants from the atmosphere
[DE88-014550] N89-10415
Multiphoton ionization of transient species in supersonic jets
[DE88-008366] N89-10607
The detection of conformational disorder by thermal analysis
[DE88-012932] N89-10657

OBSERVATOIRE DE PARIS-MEUDON (FRANCE).
IUE observations of planetary atmospheres N89-10687
The IUE spectral atlas of two normal B stars: pi Cet and nu Cap (125 to 200 nm) N89-10762

OFFICE DE LA RECHERCHE SCIENTIFIQUE ET TECHNIQUE OUTRE-MER, DAKAR (SENEGAL).
Bathymetry using SPOT imagery of the Casamance (Senegal). First results N89-10375

OFFICE NATIONAL D'ETUDES ET DE RECHERCHES AERONAUTIQUES, PARIS (FRANCE).
Life time prediction: Synthesis on ONERA's research in viscoplasticity and continuous damage mechanics, applied to engine materials and structures N89-10011
Summary of inflight data on lightning currents and fields N89-10449
Analysis of recent in-flight lightning measurements on different aircraft N89-10450
Electromagnetic coupling through composite materials N89-10479
The SAFIR lightning monitoring and warning system, applications to aerospace activities N89-10481

OFFICE NATIONAL D'ETUDES ET DE RECHERCHES AEROSPATIALES, PARIS (FRANCE).
La Recherche Aerospatiale, Bimonthly Bulletin, Number 1987-4, 239/July-August
[ESA-TT-1068] N89-10026
Unsteady three-dimensional stall on a rectangular wing N89-10027
La Recherche Aerospatiale, Bimonthly Bulletin, number 1987-6, 241/November-December
[ESA-TT-1102] N89-10030
Supersonic missile air intakes: Design and development criteria N89-10031
Solid earth mission study. Volume 2: Technical report
[ESA-CR(P)-2626-VOL-2] N89-10303
Solid Earth mission study. Volume 1: Executive summary
[ESA-CR(P)-2626-VOL-1] N89-10397
Solid earth mission study. Volume 3: Program planning report
[ESA-CR(P)-2626-VOL-3] N89-10399
La Recherche Aerospatiale, Bimonthly Bulletin, number 1987-5, 240/September-October
[ESA-TT-1095] N89-10422
Optical imaging through atmospheric turbulence N89-10423

OFFICE OF SCIENCE AND TECHNOLOGY, WASHINGTON, D. C.
Federal Coordinating Council on Science, Engineering and Technology, Committee on Computer Research and Applications, Subcommittee on Science and Engineering Computing
[DE88-013228] N89-10525

OHIO STATE UNIV., COLUMBUS.
Calculation of the effects of ice on the backscatter of a ground plane
[NASA-CR-183303] N89-10213
Measurement of the properties of lossy materials inside a finite conducting cylinder
[NASA-CR-182500] N89-10223
Material parameter determination from scattering measurements
[NASA-CR-183312] N89-10225
Control System Research for Directed Energy Weapons
[DE88-015371] N89-10599

OPEN UNIV., MILTON (ENGLAND).
MOMS-1 used synergistically with LANDSAT TM N89-10384

OREGON STATE UNIV., CORVALLIS.
Numerical simulations of dust transport into northern high latitudes during a Martian polar warming N89-10782

OSMANIA UNIV., HYDERABAD (INDIA).
Implications of isotopic signatures of noble gases for the origin and evolution of terrestrial atmospheres N89-10817

OSSERVATORIO ASTROFISICO DI ARCETRI, FLORENCE (ITALY).
Ultraviolet emission from the sun and stars: A comparison of IUE and Skylab spectra N89-10738

OSSERVATORIO ASTRONOMICO, TURIN (ITALY).
IUE and optical observations of X-ray sources in the Large Margellanic Cloud (LMC) N89-10705

OXFORD UNIV. (ENGLAND).
Model chromosphere and transition region for 56 Peg (K0 IIp + wd): A preliminary study N89-10726
On the flux-period and flux-flux correlations in late type stars N89-10737

P

PACIFIC NORTHWEST LABS., RICHLAND, WASH.
Electrospray ionization phenomena and the interface of capillary electrophoresis and mass spectrometry
[DE88-014080] N89-10143
An improved interface for capillary zone electrophoresis-mass spectrometry
[DE88-014079] N89-10148
Effect of a 12-hour/day shift on performance
[DE88-013184] N89-10521
Statistical evaluation of PACSTAT random number generation capabilities
[DE88-012754] N89-10556
An ion-optical bench for testing ion source lenses
[DE88-013186] N89-10606

PARIS VI UNIV. (FRANCE).
Evaluation of VARAN data in geology and geomorphology in the southeast of France N89-10313
Usefulness of high spectral resolution radiometry for geological mapping in the Mediterranean region N89-10360
Characterization of rocks by visible and infrared high spectral resolution terrain spectroscopy N89-10362

The use of MOMS-1 data for geological mapping of the Aswa lineament (East African rift) N89-10382
PARIS XI UNIV., ORSAY (FRANCE).
Techniques for remote sensing of life span and quantum yield of chlorophyll fluorescence in vivo N89-10351
PHILLIPS PETROLEUM CO., BARTLESVILLE, OKLA.
The results of the Geosat MOMS subcommittee's data evaluation: Performance and applicability of the MOMS-1 sensor for exploration geology N89-10380
PLANNING RESEARCH CORP., HAMPTON, VA.
On the appropriateness of applying chi-square distribution based confidence intervals to spectral estimates of helicopter flyover data
[NASA-CR-181692] N89-10601
PRATT AND WHITNEY AIRCRAFT, EAST HARTFORD, CONN.
Fan flutter test N89-10014
Turbofan forced mixer lobe flow modeling. Part 3: Application to augment engines
[NASA-CR-4147] N89-10025
PRC SYSTEMS SERVICES CO., HAMPTON, VA.
Chemoviscosity modeling for thermosetting resin systems, part 3
[NASA-CR-181718] N89-10132
PRESTON POLYTECHNIC (ENGLAND).
UV and optical line emission from the shell of the old nova GK Persei N89-10714
PURDUE UNIV., WEST LAFAYETTE, IND.
Nonlinear optical interactions involving the real Gaussian field
[DE88-012399] N89-10276
Non-local kinetic transport studies of a field-reversed configuration
[DE88-012397] N89-10626

Q

QUEENSLAND UNIV., ST. LUCIA (AUSTRALIA).
Shock tunnel studies of scramjet phenomena
[NASA-CR-181721] N89-10045
A review of medical aspects of lightning injury N89-10463
A retrospective study of the injuries sustained in telephone-mediated lightning strike N89-10464

R

RAYTHEON CO., BEDFORD, MASS.
Comparison of statistical digital simulation methods N89-10049
Design criteria for hardware-in-the-loop simulation facilities N89-10052
Simulation validation experience: PATRIOT guidance system N89-10055
RCA ADVANCED TECHNOLOGY LABS., MOORESTOWN, N.J.
A shared position/force control methodology for teleoperation N89-10092
RCA ASTRO-ELECTRONICS DIV., PRINCETON, N. J.
Kinematic study of flight telerobotic servicer configuration issues N89-10100
RENSSELAER POLYTECHNIC INST., TROY, N.Y.
An investigation of new methods for estimating parameter sensitivities
[NASA-CR-183195] N89-10586
RICE UNIV., HOUSTON, TEX.
Reports of investigations on: Derivation of an infinite-dilution activity coefficient model and application to two-component vapor/liquid equilibria data
[DE88-007517] N89-10147
RIJKSWATERSTAAT, DELFT (NETHERLANDS).
Validation of an atmospheric correction method for satellite borne imagery N89-10320
ROBERTS ASSOCIATES, INC., VIENNA, VA.
Convection effects in protein crystal growth
[NASA-CR-179368] N89-10653
ROCKWELL INTERNATIONAL CORP., CANOGA PARK, CALIF.
Orbit transfer rocket engine technology program. Phase 2: Advanced engine study
[NASA-CR-179602] N89-10119
ROCKWELL INTERNATIONAL CORP., COLUMBUS, OHIO.
Hellfire system model validation N89-10057
ROLLS-ROYCE LTD., BRISTOL (ENGLAND).
Fatigue and assessment methods of blade vibration N89-10010
ROME AIR DEVELOPMENT CENTER, GRIFFISS AFB, N.Y.
Second Annual Knowledge-Based Software Assistant Conference
[AD-A189819] N89-10536
Project management assistant: What have we learned N89-10552
ROME UNIV. (ITALY).
An electromagnetic calorimeter for a beauty factory
[NOTA-INTERNA-905] N89-10260
Vertex detector for a linear beauty factory
[NOTA-INTERNA-906] N89-10266
Dimensional deformations of integrable systems: An approach to integrability in multidimensions, part 1
[PREPRINT-586] N89-10585
Generalized Lyapunov exponents in high-dimensional chaotic dynamics and products of large random matrices
[PREPRINT-595] N89-10600
ROYAL AEROSPACE ESTABLISHMENT, FARNBOROUGH (ENGLAND).
Aerospace systems and technology: The role of the RAE
[RAE-TR-88042] N89-10003
ROYAL AIRCRAFT ESTABLISHMENT, FARNBOROUGH (ENGLAND).
Upper-atmosphere zonal winds from satellite orbit analysis: An update
[RAE-TR-87058] N89-10507
RUTHERFORD HIGH ENERGY LAB., CHILTON (ENGLAND).
Chromospheric mass motions during a flare on UV Ceti N89-10744

S

SAAB-SCANIA, LINKOPING (SWEDEN).
Finite difference analysis of external and internal lightning response of the JAS39 CFC wing N89-10483
SANDERS ASSOCIATES, INC., NASHUA, N. H.
An overview of the knowledge-based requirements assistant N89-10538
Where's the intelligence in the intelligent assistant requirements analysis: Inference processes in the KBRA N89-10544
SANDIA NATIONAL LABS., ALBUQUERQUE, N. MEX.
The Radiation-Hardened Integrated Circuit (RHIC) Laboratory: Pursuit of Class 1
[DE88-006640] N89-10062
Evaluation and control of residual states in curved, composite panels
[DE88-012103] N89-10126
Flexural fatigue of a 2-D carbon/carbon composite material
[DE88-010501] N89-10133
Semiconductor Bridge (SCB): A new method for the ignition of explosives and pyrotechnics
[DE88-011246] N89-10151
Hydrogen sorption studies of materials used in Li(Si)/FeS2 thermal batteries
[DE88-013154] N89-10231
A finite element formulation for incompressible, conjugate, viscous/porous flow problems
[DE88-007113] N89-10254
Selection and evaluation of video tape recorders for surveillance applications
[DE88-014240] N89-10261
Design study for a remote laser wavelength sensor
[DE88-015417] N89-10265
Comparison of mechanical and electronic high-speed recording systems
[DE88-015264] N89-10268
Laser interferometric dilatometer for low-expansion materials
[DE88-012329] N89-10272
Factoring very large numbers using a massively parallel computer
[DE88-014247] N89-10559
A linear programming approach to maximum entropy signal restoration
[DE88-013021] N89-10566
Progress in NODAL transport methods
[DE88-012416] N89-10590
Analytical approximations for X-ray cross sections 3
[DE88-015366] N89-10609
Metallic materials as plasma facing components
[DE88-010103] N89-10628
Characterization of layers created using surface modification techniques
[DE88-011918] N89-10651
SANTA CLARA UNIV., CALIF.
Control System Research for Directed Energy Weapons
[DE88-015371] N89-10599
SATELLITE INTERNATIONAL LTD., DIDCOT (ENGLAND).
Solid earth mission study. Volume 2: Technical report
[ESA-CR(P)-2626-VOL-2] N89-10303
Solid Earth mission study. Volume 1: Executive summary
[ESA-CR(P)-2626-VOL-1] N89-10397

Solid earth mission study. Volume 3: Program planning report
[ESA-CR(P)-2626-VOL-3] N89-10399
SCRIPPS INSTITUTION OF OCEANOGRAPHY, LA JOLLA, CALIF.
Sensitivity of satellite-derived net shortwave irradiance at the Earth's surface to radiometric calibration N89-10335
SHEFFIELD UNIV. (ENGLAND).
Developing a radiometric leaf area index N89-10334
SHERBROOKE UNIV. (QUEBEC).
Analysis of the contribution of the atmosphere to water reflectance in the first two channels of the NOAA satellites AVHRR N89-10330
Imaging spectrometry applied to the remote sensing of submerged seaweed N89-10361
Discrimination of zones of high water erosion risk using SPOT images N89-10376
SOCIETE EUROPEENNE DE PROPULSION, VERNON (FRANCE).
Means for testing aerospace launcher structures
[ETN-88-93082] N89-10110
Choice of coating and surface behavior of the hydrogen turbopump of the Vulcain engine
[ETN-88-93084] N89-10173
SOCIETE NATIONALE INDUSTRIELLE AEROSPATIALE, PARIS (FRANCE).
Simulation with real elements of Exocet anti-ship missiles N89-10056
SOCIETE NATIONALE INDUSTRIELLE AEROSPATIALE, TOULOUSE (FRANCE).
Modelling of common mode coupling between an aircraft wing traversed by a lightning current and wiring installed in that wing N89-10485
SOFTWARE PRODUCTIVITY CONSORTIUM, RESTON, VA.
Selection of investment strategies which are optimal for the implementation of software support environments N89-10542
SOUTHAMPTON UNIV. (ENGLAND).
An investigation into force-moment calibration techniques applicable to a magnetic suspension and balance system
[NASA-CR-181695] N89-10061
A simplified reflectance model for shrub canopies N89-10329
Automatic generation of database schema N89-10671
SOUTHERN METHODIST UNIV., DALLAS, TEX.
Martian tectonics: A review N89-10815
SOUTHWEST RESEARCH INST., SAN ANTONIO, TEX.
Final review of US Army fire-resistant fuel program
[AD-A194304] N89-10176
SPACE TELESCOPE SCIENCE INST., BALTIMORE, MD.
An expert system approach to astronomical data analysis N89-10080
A natural language query system for Hubble Space Telescope proposal selection N89-10083
Expert systems built by the Expert: An evaluation of OPS5 N89-10086
Observations of SN 1987A: The narrow emission lines N89-10696
The November 1987 eclipse of the zeta-Aur system HR 2554 N89-10721
HD 207739 and other F + Be variables N89-10724
Companions to peculiar red giants: HR 363 and HR 1105 N89-10729
SRI INTERNATIONAL CORP., MENLO PARK, CALIF.
Basic research on natural gas combustion phenomena-catalytic combustion
[PB88-214606] N89-10142
An aircraft-borne electric field measuring system for rocket launch support N89-10443
Grounding for safety and compatibility N89-10495
STANFORD LINEAR ACCELERATOR CENTER, CALIF.
Bootstrap confidence intervals in a complex situation: A sequential paired clinical trial
[DE88-015338] N89-10592
STANFORD TELECOMMUNICATIONS, INC., MCLEAN, VA.
A hierarchically distributed architecture for fault isolation expert systems on the space station N89-10077
STANFORD UNIV., CALIF.
High speed fiber optics local area networks: Design and implementation
[NASA-CR-182432] N89-10216
Parallel processors for planning under uncertainty
[DE88-016184] N89-10571
Control System Research for Directed Energy Weapons
[DE88-015371] N89-10599
STATE UNIV. OF NEW YORK, BINGHAMTON.
A perspective on vegetation canopy reflectance models N89-10317
A model for radiative transfer in heterogeneous three-dimensional canopies N89-10326

STATE UNIV. OF NEW YORK, STONY BROOK.
Chromosomes and plant cell division in space
[NASA-CR-183213] N89-10518
On the abundance of micron-sized particles in Saturn's A and B rings N89-10692
Research in nuclear astrophysics: Stellar collapse and supernovae
[DE88-015267] N89-10778
Could icy impacts reconcile Venus with Earth and Mars N89-10810
STRINGFELLOW AND ASSOCIATES, ATLANTA, GA.
Lightning and surge protection of large ground facilities N89-10474
SYDNEY UNIV. (AUSTRALIA).
Buckling of rings in column-supported bins and tanks
[PB88-217336] N89-10290
Deformations and residual stresses induced in channel section columns by presetting and welding
[PB88-199971] N89-10292
Elastic-plastic large deflection analysis of axisymmetric shells
[PB88-217344] N89-10295
Geometric imperfections in plated structures subject to interaction between buckling modes
[PB88-200902] N89-10296
Inelastic buckling analyses of beams, columns and plates using the spline finite strip method
[PB88-214291] N89-10299
The study of hydromagnetic waves and RF heating using the TORTUS tokamak and the development of diagnostic techniques N89-10635

T

TECHNISCHE HOGESCHOOL, DELFT (NETHERLANDS).
Design and evaluation of dynamic flight test manoeuvres
[PB88-210760] N89-10042
Topological attributes for STEP curve and surface entities
[PB88-209630] N89-10532
Comparison of some robust regression estimators
[PB88-126289] N89-10594
TECHNISCHE UNIV., BERLIN (WEST GERMANY).
Influence of boundary surface roughness, order effects and dopants on optical properties of InP based metal organic gas phase epitaxy (MOCVD) heterostructure
[ETN-88-92986] N89-10646
TECHNISCHE UNIV., MUNICH (WEST GERMANY).
Comparative geological evolution of different remote sensing data of the Hoggar Mountains (Algeria) N89-10385
Digital analysis of MOMS-1, LANDSAT TM, and SPOT data of the Nakuru area (Kenya) N89-10386
TENNESSEE UNIV., KNOXVILLE.
The detection of conformational disorder by thermal analysis
[DE88-012932] N89-10657
TEXAS A&M UNIV., COLLEGE STATION.
Evidence for glaciation in Elysium N89-10781
TEXAS TECHNOLOGICAL UNIV., LUBBOCK.
Breakdown characteristics of an isolated conducting object in a uniform electric field N89-10453
TEXAS UNIV., AUSTIN.
Initial evolution of nonlinear magnetic islands in high temperature plasmas
[DE88-012346] N89-10636
TOHOKU ELECTRIC POWER CO., INC., SENDAI (JAPAN).
Current measurement of lightning superbolt at the Japan sea coast N89-10445
TOHOKU UNIV., SENDAI (JAPAN).
Statistics of lightning interaction with aircraft in Japan N89-10430
TOKAI UNIV., KUMAMOTO (JAPAN).
Optical thickness of the Olympus cloud N89-10808
TOKYO UNIV. (JAPAN).
Numerical study of the entrance flow and its transition in a curcular pipe
[ISAS-RN-626] N89-10250
On the statistics of field waveforms associated with lightning return strokes N89-10441
Site errors of a magnetic direction finder for lightning flashes N89-10494
TORONTO UNIV. (ONTARIO).
Cepheid binaries with large mass ratios (M1/M2) N89-10727
The orbit of the Cepheid AW Per N89-10728
TOTAL ARMY PERSONNEL AGENCY (PROVISIONAL), ALEXANDRIA, VA.
The effect of a gap nonlinearity on recursive parameter identification algorithms
[AD-A196020] N89-10557
TOULOUSE UNIV. (FRANCE).
Electromagnetic radiations generated by microdischarges from hydrometeors N89-10448
The surface electric field as a warning criterion N89-10468

U

UNITED KINGDOM ATOMIC ENERGY AUTHORITY, CULHAM (ENGLAND).
Factors influencing the detection of voltage sparks by flammable gas and optical techniques N89-10465
A filamentary method for calculating induced voltages within resistive structures in either the frequency or time domain N89-10484
UNITED TECHNOLOGIES RESEARCH CENTER, EAST HARTFORD, CONN.
Aeroelastic coupling: An elementary approach N89-10012
UNIVERSIDAD AUTONOMA DE MADRID, CANTOBLANCO (SPAIN).
Atmospheric eclipse effects in Wolf-Rayet binaries in the Small Magellanic Cloud N89-10717
UNIVERSIDAD NACIONAL DE MEXICO, MEXICO CITY.
Some observations and analysis of atmospheric electricity over non-uniform high terrain N89-10489
UNIVERSITE CATHOLIQUE DE LOUVAIN (BELGIUM).
A three degree-of-freedom description of the ocean surface for microwave remote sensing of wave height and wind friction velocity N89-10314
An approximative model for the microwave brightness temperature scattered by a rough open ocean surface N89-10344
UNIVERSITIES SPACE RESEARCH ASSOCIATION, HUNTSVILLE, ALA.
Numerical analysis of laminar and turbulent incompressible flows using the finite element Fluid Dynamics Analysis Package (FIDAP)
[NASA-CR-179390] N89-10253
UNIVERSITY COLL., LONDON (ENGLAND).
IUE spectrophotometry of the accretion disk of HZ Her/Her X-1 N89-10702
Matter streams in semi-detached binary systems N89-10720
UNIVERSITY OF SOUTHERN CALIFORNIA, LOS ANGELES.
Control System Research for Directed Energy Weapons
[DE88-015371] N89-10599
UNIVERSITY OF SOUTHERN CALIFORNIA, MARINA DEL REY.
Overview of the knowledge-based specification assistant N89-10539
Turning ideas into specifications N89-10545
UNIVERSITY OF SOUTHERN ILLINOIS, CARBONDALE.
Framework for lightning modeling: Comparing results N89-10435
UNIVERSITY OF TECHNOLOGY, LAE (PAPUA NEW GUINEA).
Lightning return stroke velocity N89-10446
The lightning flash counter: Papua New Guinean experience N89-10491
UTAH STATE UNIV., BEDFORD, MASS.
High resolution infrared spectroscopy of carbon dioxide and nitrous oxide at elevated temperatures
[AD-A196317] N89-10146
UTAH STATE UNIV., LOGAN.
Dynamics Explorer guest investigator
[NASA-CR-183163] N89-10417
The dynamics of the Venus ionosphere
[NASA-CR-183167] N89-10779
UTAH UNIV., SALT LAKE CITY.
The role of clouds in surface radiation budgets N89-10501

V

VALENCIA UNIV. (SPAIN).
A theoretical model for interpreting remotely sensed thermal infrared measurements obtained over agricultural areas N89-10343
Spectral signature of citrus fruits and its evolution: Identification of the vegetative index of least temporal variation N89-10373
VANDERBILT UNIV., NASHVILLE, TENN.
Lithium and chromospherically active single giants N89-10749
VILLANOVA UNIV., PA.
Mapping of surface activity on the W UMa-type system VW Cephei N89-10742
VIRGINIA POLYTECHNIC INST. AND STATE UNIV., BLACKSBURG.
Solution of two-point boundary value problems in optimal maneuvers of flexible vehicles N89-10114
On the problem of modeling for parameter identification in distributed structures
[NASA-CR-182739] N89-10291
VRIJE UNIVERSITEIT, AMSTERDAM (NETHERLANDS).
Real algebraic morphisms with values in the unit circle
[PB88-208921] N89-10515
Orca: A language for distributed object-based programming
[PB88-208533] N89-10529
Abstract, topological and uniform convex structures
[PB88-202965] N89-10579
Interactive editing of mathematical formulae
[PB88-203005] N89-10580
Block Toeplitz operators with rational symbols
[PB88-202890] N89-10587
Free choice permissions and Ross's paradox: Internal versus external nondeterminism
[PB88-202874] N89-10588

W

WASHINGTON UNIV., SEATTLE.
Studies of blackbody-pumped lasers
[NASA-CR-183214] N89-10277
Model-data comparisons for the 1982-83 El Nino: The XBT tracks
[PB88-221668] N89-10514
Confinement and heating of high beta plasmas with emphasis on compact toroids
[DE88-015777] N89-10645
The energy input mechanism into the lower transition regions between stellar chromospheres and coronae N89-10745
Carbon and nitrogen abundance determinations from transition layer lines N89-10760
Seasonal wind variations in the Martian subtropics N89-10807
Mars global atmospheric oscillations: Transients and dust storm relations N89-10820
WASHINGTON UNIV., ST. LOUIS, MO.
Physical principles of ultrasonic non-destructive evaluation of advanced composites
[NASA-CR-180225] N89-10129
Structure of amorphous silicon alloy films
[DE88-001167] N89-10654
WESTINGHOUSE ELECTRIC CORP., BALTIMORE, MD.
System protection from atmospheric electricity for aerostats with conducting tethers N89-10497
WISCONSIN UNIV., MADISON.
Thermodynamics and kinetics of phase formation of thin-film metal on gallium arsenide
[DE88-015702] N89-10648
WOODS HOLE OCEANOGRAPHIC INSTITUTION, MASS.
Study of biological processes on the US North Atlantic slope and rise, volume 2
[PB88-196514] N89-10511
Study of biological processes on the US North Atlantic slope and rise. Volume 1: Executive summary
[PB88-196522] N89-10517

Y

YALE UNIV., NEW HAVEN, CONN.
Investigation of superradiant LDV markers and three-component velocity mapping
[AD-A195504] N89-10662
YORK UNIV. (ENGLAND).
An optical sensor for the non-interactive detection of weak electric fields N89-10263

Typical Contract Number Index Listing

Listings in this index are arranged alphanumerically by contract number. Under each contract number the NASA accession numbers denoting documents that have been produced as a result of research done under that contract are arranged in ascending order. The NASA accession number denotes the number by which the citation is identified.

AF AFOSR-0075-84 ..... N89-10161
AF AFOSR-0076-86 ..... N89-10572
AF PROJ. 2304 ..... N89-10558
AF PROJ. 2306 ..... N89-10145
N89-10161
AF PROJ. 5581 ..... N89-10536
AF PROJ. 6150 ..... N89-10616
AF PROJ. 6670 ..... N89-10500
AF-AFOSR-0022-88 ..... N89-10616
AF-AFOSR-0055-87 ..... N89-10558
AF-AFOSR-0076-86 ..... N89-10569
AF-AFOSR-0148-87 ..... N89-10145
BSF-85-00346 ..... N89-10582
CAICYT-A-172/85 ..... N89-10343
N89-10373
C99066G N89-10575
DA PROJ. 1L1-61102-BH-57 ..... N89-10418
DA PROJ. 1L1-62209-AH-76 ..... N89-10156
DA PROJ. 1L7-62733-AH-20 ..... N89-10176
DAAH01-85-D-A015 ..... N89-10477
N89-10496
DAAK70-85-C-0007 ..... N89-10176
DAAK70-87-C-0043 ..... N89-10176
DAJA45-86-C-0022 ..... N89-10418
DE-AC01-85DP-20133 ..... N89-10674
DE-AC02-76CH-00016 ..... N89-10280
DE-AC02-83CH-10093 ..... N89-10185
N89-10406
N89-10410
N89-10411
N89-10654
DE-AC03-76SF-00098 ..... N89-10138
N89-10140
N89-10153
DE-AC03-76SF-00515 ..... N89-10592
DE-AC03-84SF-11996 ..... N89-10633
DE-AC03-87DP-10560 ..... N89-10301
DE-AC04-76DP-00613 ..... N89-10284
DE-AC04-76DP-00789 ..... N89-10062
N89-10126
N89-10133
N89-10151
N89-10181
N89-10231
N89-10254
N89-10261
N89-10265
N89-10268
N89-10272
N89-10559
N89-10566
N89-10590
N89-10609
N89-10628
N89-10651
DE-AC05-84ER-40150 ..... N89-10613
N89-10614
DE-AC05-84OR-21400 ..... N89-10090
N89-10098
N89-10155
N89-10159
N89-10164
N89-10168
N89-10170
N89-10171
N89-10238
N89-10240
N89-10247
N89-10249
N89-10255
N89-10267
N89-10281
N89-10289
N89-10408
N89-10415
N89-10607
N89-10657
DE-AC06-76RL-01830 ..... N89-10143
N89-10148
N89-10521
N89-10556
N89-10606
DE-AC07-76ID-01570 ..... N89-10106
N89-10256
DE-AS06-72ET-53047 ..... N89-10645
DE-FG02-85ER-53194 ..... N89-10644
DE-FG02-86ER-13576 ..... N89-10276
DE-FG02-86ER-45274 ..... N89-10648
DE-FG02-87ER-40317 ..... N89-10778
DE-FG02-87ER-53250 ..... N89-10626
DE-FG03-87ER-25028 ..... N89-10571
DE-FG05-80ET-53088 ..... N89-10636
DE-FG05-86ER-40272 ..... N89-10661
DE-FG05-87ER-13758 ..... N89-10660
DE-FG22-83PC-60037 ..... N89-10147
DE-FG22-86PC-90961 ..... N89-10251
DI-14-12-0001-30064 ..... N89-10511
N89-10517
DOSSIER-3B1-68400260-002 ..... N89-10376
DTFA03-84-C-00066 ..... N89-10459
DTRS57-85-C-00083 ..... N89-10668
N89-10672
EPRI-RP2940-1 ..... N89-10571
ESA-5211/82-D-JS(SC) N89-10394
ESA-6877/87-HGE-1(SC) N89-10664
ESA-6878/87-HGE-I(SC) N89-10315
ESTEC-5506/83-NL-GM N89-10623
N89-10624
ESTEC-6886/85-NL-PP N89-10116
ESTEC-7149/87-NL-JS N89-10303
N89-10397
N89-10399
F04701-85-C-0086 ..... N89-10112
F08635-83-C-0123 ..... N89-10050
F19628-83-C-0056 ..... N89-10146
F19628-86-K-0013 ..... N89-10608
F30602-81-C-0205 ..... N89-10217
F30602-85-C-0215 ..... N89-10568
F30602-85-C-0221 ..... N89-10545
F30602-85-C-0267 ..... N89-10538
N89-10544
F30602-86-C-0026 ..... N89-10540
N89-10548
F30602-86-C-0074 ..... N89-10537
F49620-85-C-0005 ..... N89-10649
F49620-85-C-0033 ..... N89-10575
F49620-85-C-0067 ..... N89-10149
F49620-85-K-0002 ..... N89-10662
F49620-86-C-0027 ..... N89-10427
F49620-86-K-0021 ..... N89-10655
F49620-87-C-0102 ..... N89-10652
GFSC-PROJ-415 ..... N89-10364
GRI-5082-242-0721 ..... N89-10286
GRI-5086-260-1245 ..... N89-10142
JPL-957632 ..... N89-10731
JRC-3106-86-12-ED-ISP-D N89-10307
NAGS-399 ..... N89-10364
NAGW-587 ..... N89-10719
NAGW-674 ..... N89-10045
NAGW-889 ..... N89-10779
NAG1-176 ..... N89-10277
NAG1-225 ..... N89-10291
NAG1-405 ..... N89-10297
NAG1-640 ..... N89-10531
NAG1-724 ..... N89-10125
NAG1-752 ..... N89-10586
NAG1-824 ..... N89-10534
N89-10561
N89-10564
NAG2-282 ..... N89-10216
NAG3-419 ..... N89-10215
NAG3-655 ..... N89-10282
N89-10283
NAG3-784 ..... N89-10223
N89-10225
NAG3-913 ..... N89-10213
NAG5-32 ..... N89-10416
NAG5-82 ..... N89-10740
N89-10741
N89-10750
N89-10757
NAG5-87 ..... N89-10699
NAG5-315 ..... N89-10304
NAG5-343 ..... N89-10733
NAG5-350 ..... N89-10752
N89-10757
NAG5-429 ..... N89-10740
N89-10747
NAG5-434 ..... N89-10733
NAG5-441 ..... N89-10719
NAG5-585 ..... N89-10419
NAG5-645 ..... N89-10683
NAG5-701 ..... N89-10699
NAG5-720 ..... N89-10774
NAG5-748 ..... N89-10417
NAG5-797 ..... N89-10753
NAG5-816 ..... N89-10730
N89-10731
NAG5-819 ..... N89-10425
NAG5-841 ..... N89-10683
NAG5-932 ..... N89-10827
NAG5-985 ..... N89-10750
NAG5-988 ..... N89-10699
NAG8-033 ..... N89-10426
NAG8-060 ..... N89-10264
NAG8-545 ..... N89-10033
N89-10127
NAG8-654 ..... N89-10498
NAG9-272 ..... N89-10826
NAG10-35 ..... N89-10518
NASW-2797 ..... N89-10028
NASW-4066 ..... N89-10377
N89-10780
NASW-4307 ..... N89-10141
N89-10169
N89-10248
N89-10262
N89-10574
NAS1-4195-C N89-10335
NAS1-17748 ..... N89-10451
N89-10454
NAS1-18000 ..... N89-10132
N89-10601
NAS1-18107 ..... N89-10560
N89-10577
N89-10582
N89-10583
NAS1-18276 ..... N89-10019
NAS1-18605 ..... N89-10582
NAS2-11665 ..... N89-10046
NAS2-11853 ..... N89-10058
N89-10526
NAS3-23039 ..... N89-10025
NAS3-23773 ..... N89-10119
NAS5-27600 ..... N89-10075
NAS5-28749 ..... N89-10721
N89-10727
N89-10728
N89-10729
NAS5-29279 ..... N89-10815
NAS5-29280 ..... N89-10077
NAS5-29298 ..... N89-10734
NAS5-29337 ..... N89-10753
NAS5-29381 ..... N89-10722
NAS5-29386 ..... N89-10115
NAS5-31436 ..... N89-10700
NAS8-30490 ..... N89-10439

N89-10440
NAS8-35918 ..... N89-10253
NAS8-36090 ..... N89-10243
NAS8-36419 ..... N89-10407
NAS8-36477 ..... N89-10472
NAS8-36652 ..... N89-10653
NAS9-17766 ..... N89-10553
NAS10-11390 ..... N89-10472
NA86AA-D-AC051 ..... N89-10335
NCC1-22 ..... N89-10029
NCC2-371 ..... N89-10805
N89-10610
NCC3-43 ..... N89-10128
N89-10131
NERC-F60/G6/12 ..... N89-10364
NERC-GST/02/124 ..... N89-10358
NGL-23-004-083 ..... N89-10395
NGT-700052 ..... N89-10731
NSF AST-85-16537 ..... N89-10683
NSF ATM-87-09659 ..... N89-10428
NSF DMS-84-20623 ..... N89-10571
NSF DMS-85-03294 ..... N89-10582
NSF ECS-86-17905 ..... N89-10571
NSF SES-85-18662 ..... N89-10571
NSG-1601 ..... N89-10129
NSG-5300 ..... N89-10765
NSG-5386 ..... N89-10718
NSG-5393 ..... N89-10691
N89-10693
NSG-5398 ..... N89-10745
N89-10760
NSG-5560 ..... N89-10694
NSG-7523 ..... N89-10061
NSG-7572 ..... N89-10401
N00014-80-C-0505 ..... N89-10287
N89-10675
N00014-80-C-0622 ..... N89-10569
N89-10572
N00014-85-C-2069 ..... N89-10278
N00014-85-K-0124 ..... N89-10675
N00014-85-K-0343 ..... N89-10571
N00014-86-F-0049 ..... N89-10828
N89-10829
N00014-86-K-0204 ..... N89-10531
N00014-86-K-0270 ..... N89-10523
ORNL-19B-07802C N89-10170
P73/1987 ..... N89-10664
RR0-4106 ..... N89-10523
W-31-109-ENG-38 ..... N89-10647
N89-10775
W-7405-ENG-36 ..... N89-10139
N89-10152
N89-10154
N89-10158
N89-10162
N89-10163
N89-10172
N89-10182
N89-10224
N89-10229
N89-10234
N89-10274
N89-10279
N89-10533
N89-10595
N89-10596
N89-10597
N89-10598
N89-10658
N89-10663
N89-10775
W-7405-ENG-48 ..... N89-10150
N89-10157
N89-10160
N89-10167
N89-10230
N89-10232
N89-10412
N89-10469
N89-10599
N89-10618
N89-10621
N89-10637
N89-10650
N89-10659
N89-10773
W-31109-ENG-38 ..... N89-10535
N89-10562
199-22-76-01 ..... N89-10612
323-53-6X N89-10111
471-42 ..... N89-10184
474-52-10 ..... N89-10117
505-43-01 ..... N89-10028
505-60-01-02 ..... N89-10020
505-60-21-02 ..... N89-10029
505-61-01-01 ..... N89-10034
505-61-01-02 ..... N89-10060
N89-10061
505-61-51-10 ..... N89-10059
505-61-71 ..... N89-10017
505-61-71-05 ..... N89-10024
505-62-OK N89-10156
505-62-21 ..... N89-10025
N89-10242
N89-10246
N89-10575
505-62-81-61 ..... N89-10045
505-63-1A N89-10124
N89-10166
505-63-1B N89-10043
505-63-01-01 ..... N89-10132
505-63-01-05 ..... N89-10165
505-63-51 ..... N89-10282
N89-10283
505-63-51-07 ..... N89-10601
505-63-81 ..... N89-10134
505-66-21-03 ..... N89-10524
505-67-11 ..... N89-10037
505-90-21-01 ..... N89-10560
N89-10577
N89-10582
N89-10583
506-40-11-08 ..... N89-10019
506-41-11 ..... N89-10122
506-41-21 ..... N89-10405
N89-10409
506-42-21 ..... N89-10119
506-43-41-01 ..... N89-10300
506-44-21 ..... N89-10235
535-03-01 ..... N89-10603
535-07-01 ..... N89-10128
N89-10130
N89-10131
650-60-20 ..... N89-10215
665-45-30-21 ..... N89-10420
763-01-21 ..... N89-10123

Typical Report Number Index Listing

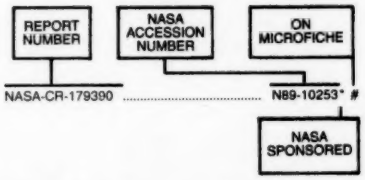

Listings in this index are arranged alphanumerically by report number. The NASA accession number denotes the number by which the citation is identified. An asterisk (*) indicates that the item is a NASA report. A pound sign (#) indicates that the item is available on microfiche.

A-86320 ..... N89-10037* #
A-88020 ..... N89-10022* #
A-88072 ..... N89-10017* #

AASU-88/4 ..... N89-10061* #

AD-A189819 ..... N89-10536 #
AD-A189863 ..... N89-10526* #
AD-A192386 ..... N89-10523 #
AD-A192674 ..... N89-10519 #
AD-A193464 ..... N89-10531* #
AD-A194304 ..... N89-10176 #
AD-A194902 ..... N89-10505 #
AD-A195167 ..... N89-10569 #
AD-A195168 ..... N89-10572 #
AD-A195169 ..... N89-10275 #
AD-A195199 ..... N89-10039 #
AD-A195228 ..... N89-10245 #
AD-A195229 ..... N89-10527 #
AD-A195246 ..... N89-10180 #
AD-A195279 ..... N89-10649 #
AD-A195281 ..... N89-10675 #
AD-A195291 ..... N89-10239 #
AD-A195302 ..... N89-10593 #
AD-A195339 ..... N89-10278 #
AD-A195344 ..... N89-10427 #
AD-A195361 ..... N89-10506 #
AD-A195443 ..... N89-10652 #
AD-A195479 ..... N89-10655 #
AD-A195480 ..... N89-10616 #
AD-A195489 ..... N89-10161 #
AD-A195498 ..... N89-10145 #
AD-A195502 ..... N89-10558 #
AD-A195504 ..... N89-10662 #
AD-A195599 ..... N89-10418 #
AD-A195840 ..... N89-10638 #
AD-A195852 ..... N89-10668 #
AD-A195853 ..... N89-10672 #
AD-A19[illegible]020 ..... N89-10557 #
AD-A196128 ..... N89-10149 #
AD-A196188 ..... N89-10589 #
AD-A196204 ..... N89-10217 #
AD-A196205 ..... N89-10568 #
AD-A196207 ..... N89-10044 #
AD-A196211 ..... N89-10273 #
AD-A196217 ..... N89-10112 #
AD-A196219 ..... N89-10294 #
AD-A196223 ..... N89-10287 #
AD-A196314 ..... N89-10500 #
AD-A196317 ..... N89-10146 #
AD-A196319 ..... N89-10570 #
AD-A196322 ..... N89-10608 #

AD-E500978 ..... N89-10668 #
AD-E500978 ..... N89-10672 #

AFGL-ERP-962 ..... N89-10638 #
AFGL-ERP-997 ..... N89-10500 #
AFGL-ERP-999 ..... N89-10146 #

AFGL-TR-87-0240 ..... N89-10638 #
AFGL-TR-88-0036 ..... N89-10500 #
AFGL-TR-88-0067 ..... N89-10146 #
AFGL-TR-88-0137 ..... N89-10608 #

AFIT/CI/NR-88-119 ..... N89-10589 #
AFIT/CI/NR-88-135 ..... N89-10570 #

AFOSR-88-0453TR ..... N89-10649 #
AFOSR-88-0457TR ..... N89-10161 #
AFOSR-88-0495TR ..... N89-10427 #
AFOSR-88-0577TR ..... N89-10655 #
AFOSR-88-0579TR ..... N89-10616 #
AFOSR-88-0587TR ..... N89-10558 #
AFOSR-88-0611TR ..... N89-10145 #
AFOSR-88-0641TR ..... N89-10662 #
AFOSR-88-0646TR ..... N89-10149 #
AFOSR-88-0647TR ..... N89-10652 #

AFWAL-TR-88-2020 ..... N89-10044 #

AGARD-AG-273 ..... N89-10048 #
AGARD-AG-298-VOL-2 ..... N89-10006 #

AGARD-AR-244 ..... N89-10001 #

AGARD-R-763 ..... N89-10666 #

AI-M-1021 ..... N89-10287 #

AIAA-PAPER-88-2535 ..... N89-10034* #

AIAA-88-3155 ..... N89-10043* #

ANL/MCS-TM-116 ..... N89-10562 #
ANL/MCS-TM-120 ..... N89-10535 #

AR-004-596 ..... N89-10005 #
AR-005-191 ..... N89-10177 #
AR-005-230 ..... N89-10040 #
AR-005-231 ..... N89-10252 #
AR-005-237 ..... N89-10218 #

ARI-TR-1000 ..... N89-10675 #

ARINC-3067-01-01-4437 ..... N89-10674 #

ARL-AERO-R-176 ..... N89-10005 #

ATES/DMA/RAD/002-86 ..... N89-10226 #

AVSCOM-TM-88-B-014 ..... N89-10059* #

AVSCOM-TR-87-C-33 ..... N89-10283* #
AVSCOM-TR-87-C-34 ..... N89-10282* #
AVSCOM-TR-88-C-027 ..... N89-10130* #
AVSCOM-TR-88-C-028 ..... N89-10134* #

BDX-613-3949 ..... N89-10284 #

BF-R-65.641-2 ..... N89-10623 #
BF-R-65.641-3 ..... N89-10624 #

BFLRF-244 ..... N89-10176 #

BNL-41434 ..... N89-10280 #

BRA-88-W034R ..... N89-10278 #

BRL-MR-3677 ..... N89-10239 #

BRL-TR-2864 ..... N89-10180 #

BR105558 ..... N89-10507 #

CEBAF-PR-88-009 ..... N89-10614 #
CEBAF-PR-88-011 ..... N89-10613 #

CNES-CT/DRT/TIT/HY/87/130 ..... N89-10237 #

CNES-CT/DRT/TIT/TB-096 ..... N89-10573 #

CNES-CT/DTI/MS/AE/072 ..... N89-10107 #
CNES-CT/DTI/MS/AE/124 ..... N89-10108 #
CNES-CT/DTI/MS/AE/219 ..... N89-10109 #

CNES-87/088-CT/DRT/TIT/TR ..... N89-10227 #

CONF-871036-36 ..... N89-10628 #
CONF-880259-2 ..... N89-10157 #
CONF-880364-33 ..... N89-10637 #
CONF-880391-2 ..... N89-10775 #
CONF-880408-34 ..... N89-10152 #
CONF-880435-7 ..... N89-10607 #
CONF-880466-10 ..... N89-10280 #
CONF-880539-1 ..... N89-10659 #
CONF-880606-4 ..... N89-10272 #
CONF-880631-34 ..... N89-10261 #
CONF-880633-7 ..... N89-10521 #
CONF-880676-2 ..... N89-10274 #
CONF-880699-8 ..... N89-10230 #
CONF-880713-10 ..... N89-10234 #
CONF-880713-11 ..... N89-10229 #
CONF-880785-1 ..... N89-10559 #
CONF-880792-1 ..... N89-10256 #
CONF-880795-1 ..... N89-10773 #
CONF-880802-1 ..... N89-10150 #
CONF-880813-2 ..... N89-10657 #
CONF-880814-5 ..... N89-10185 #
CONF-880841-14 ..... N89-10140 #
CONF-880841-18 ..... N89-10138 #
CONF-880844-2 ..... N89-10158 #
CONF-880844-3 ..... N89-10163 #
CONF-880855-3 ..... N89-10164 #
CONF-880855-4 ..... N89-10155 #
CONF-880872-1 ..... N89-10595 #
CONF-880872-4 ..... N89-10592 #
CONF-880887-3 ..... N89-10566 #
CONF-880887-7 ..... N89-10268 #
CONF-880887-9 ..... N89-10621 #
CONF-880888-9 ..... N89-10279 #
CONF-880906-3 ..... N89-10590 #
CONF-880909-1 ..... N89-10133 #
CONF-880912-1 ..... N89-10172 #
CONF-880912-6 ..... N89-10181 #
CONF-880914-1 ..... N89-10650 #
CONF-880914-2 ..... N89-10658 #
CONF-880922-1 ..... N89-10281 #
CONF-880933-1 ..... N89-10062 #
CONF-880936-1 ..... N89-10254 #
CONF-880936-2 ..... N89-10412 #
CONF-880940-1 ..... N89-10162 #
CONF-880976-1 ..... N89-10151 #
CONF-8706103-9 ..... N89-10160 #
CONF-8708268-1 ..... N89-10154 #
CONF-8803115-1 ..... N89-10647 #
CONF-8803128-1 ..... N89-10415 #
CONF-8803135-1 ..... N89-10153 #
CONF-8804100-4 ..... N89-10240 #
CONF-8804100-7 ..... N89-10247 #
CONF-8804100-17 ..... N89-10408 #
CONF-8804100-18 ..... N89-10255 #
CONF-8804176-1 ..... N89-10106 #
CONF-8805132-10 ..... N89-10232 #
CONF-8805134-4 ..... N89-10651 #
CONF-8806164-1 ..... N89-10126 #
CONF-8806170-7 ..... N89-10301 #
CONF-8806182-1 ..... N89-10139 #
CONF-8806183-1 ..... N89-10289 #
CONF-8806193-1 ..... N89-10663 #
CONF-8806199-2 ..... N89-10606 #
CONF-8806199-4 ..... N89-10143 #
CONF-8806199-5 ..... N89-10148 #
CONF-8809106-1 ..... N89-10267 #
CONF-8809109-1 ..... N89-10182 #
CONF-8809111-1-REV-1 ..... N89-10618 #

CONTRIB-1033 ..... N89-10509 #
CONTRIB-1035 ..... N89-10514 #

CSDG-88-2 ..... N89-10531* #

DE88-001163 ..... N89-10411 #
DE88-001167 ..... N89-10654 #
DE88-001170 ..... N89-10406 #
DE88-001179 ..... N89-10410 #
DE88-001180 ..... N89-10185 #

DE88-002345 ..... N89-10281 #
DE88-005369 ..... N89-10150 #
DE88-006640 ..... N89-10062 #
DE88-007113 ..... N89-10254 #
DE88-007517 ..... N89-10147 #
DE88-007824 ..... N89-10162 #
DE88-007887 ..... N89-10172 #
DE88-008042 ..... N89-10160 #
DE88-008124 ..... N89-10633 #
DE88-008366 ..... N89-10607 #
DE88-008898 ..... N89-10412 #
DE88-009156 ..... N89-10163 #
DE88-009157 ..... N89-10158 #
DE88-010103 ..... N89-10626 #
DE88-010225 ..... N89-10181 #
DE88-010361 ..... N89-10140 #
DE88-010501 ..... N89-10133 #
DE88-010929 ..... N89-10595 #
DE88-011019 ..... N89-10164 #
DE88-011246 ..... N89-10151 #
DE88-011611 ..... N89-10251 #
DE88-011918 ..... N89-10651 #
DE88-012103 ..... N89-10126 #
DE88-012199 ..... N89-10647 #
DE88-012329 ..... N89-10272 #
DE88-012346 ..... N89-10636 #
DE88-012397 ..... N89-10626 #
DE88-012399 ..... N89-10276 #
DE88-012416 ..... N89-10590 #
DE88-012435 ..... N89-10232 #
DE88-012630 ..... N89-10176 #
DE88-012754 ..... N89-10556 #
DE88-012926 ..... N89-10155 #
DE88-012930 ..... N89-10408 #
DE88-012932 ..... N89-10657 #
DE88-012936 ..... N89-10267 #
DE88-012937 ..... N89-10269 #
DE88-012938 ..... N89-10255 #
DE88-013011 ..... N89-10301 #
DE88-013021 ..... N89-10566 #
DE88-013154 ..... N89-10231 #
DE88-013184 ..... N89-10521 #
DE88-013186 ..... N89-10606 #
DE88-013224 ..... N89-10284 #
DE88-013228 ..... N89-10525 #
DE88-013239 ..... N89-10247 #
DE88-013242 ..... N89-10240 #
DE88-013353 ..... N89-10249 #
DE88-013510 ..... N89-10238 #
DE88-013608 ..... N89-10562 #
DE88-013609 ..... N89-10535 #
DE88-013706 ..... N89-10230 #
DE88-014079 ..... N89-10148 #
DE88-014080 ..... N89-10143 #
DE88-014149 ..... N89-10650 #
DE88-014151 ..... N89-10618 #
DE88-014170 ..... N89-10659 #
DE88-014240 ..... N89-10261 #
DE88-014247 ..... N89-10559 #
DE88-014286 ..... N89-10280 #
DE88-014317 ..... N89-10234 #
DE88-014323 ..... N89-10152 #
DE88-014332 ..... N89-10663 #
DE88-014406 ..... N89-10182 #
DE88-014409 ..... N89-10279 #
DE88-014412 ..... N89-10154 #
DE88-014414 ..... N89-10658 #
DE88-014425 ..... N89-10229 #
DE88-014428 ..... N89-10274 #
DE88-014452 ..... N89-10775 #
DE88-014467 ..... N89-10139 #
DE88-014550 ..... N89-10415 #
DE88-014733 ..... N89-10661 #
DE88-014857 ..... N89-10153 #
DE88-014867 ..... N89-10138 #
DE88-015046 ..... N89-10224 #
DE88-015050 ..... N89-10596 #
DE88-015053 ..... N89-10597 #
DE88-015059 ..... N89-10598 #
DE88-015119 ..... N89-10106 #
DE88-015188 ..... N89-10256 #
DE88-015264 ..... N89-10268 #
DE88-015287 ..... N89-10778 #
DE88-015327 ..... N89-10170 #
DE88-015329 ..... N89-10168 #
DE88-015330 ..... N89-10171 #
DE88-015330 ..... N89-10592 #
DE88-015363 ..... N89-10533 #
DE88-015366 ..... N89-10609 #
DE88-015371 ..... N89-10599 #
DE88-015382 ..... N89-10159 #
DE88-015407 ..... N89-10167 #
DE88-015417 ..... N89-10285 #
DE88-015422 ..... N89-10660 #
DE88-015441 ..... N89-10821 #
DE88-015445 ..... N89-10157 #
DE88-015449 ..... N89-10773 #
DE88-015456 ..... N89-10637 #
DE88-015702 ..... N89-10648 #
DE88-015703 ..... N89-10644 #
DE88-015777 ..... N89-10645 #
DE88-015996 ..... N89-10674 #
DE88-016184 ..... N89-10571 #

DFVLR-FB-86-11 ..... N89-10625 #
DFVLR-FB-88-18 ..... N89-10404 #
DFVLR-FB-88-20 ..... N89-10270 #
DFVLR-FB-88-21 ..... N89-10508 #
DFVLR-FB-88-22 ..... N89-10271 #

DMS-DB-02-VOL-3-PT-1 ..... N89-10019* #

DOE/DP-20133/T1 ..... N89-10674 #

DOE/ER-0368 ..... N89-10525 #
DOE/ER-13553/2 ..... N89-10626 #
DOE/ER-13576/2 ..... N89-10276 #
DOE/ER-13758/1 ..... N89-10660 #
DOE/ER-40272/57 ..... N89-10681 #
DOE/ER-40317/2 ..... N89-10778 #
DOE/ER-45274/2 ..... N89-10648 #
DOE/ER-53194/1 ..... N89-10644 #

DOE/ET-53047/26 ..... N89-10645 #
DOE/ET-53088/319 ..... N89-10636 #

DOE/PC-60037/T8 ..... N89-10147 #
DOE/PC-90961/T7 ..... N89-10251 #

DOE/SF-11996/T1 ..... N89-10633 #

DOT/FAA/CT-86/30-REV ..... N89-10058* #
DOT/FAA/CT-86/34 ..... N89-10526* #
DOT/FAA/CT-88/05 ..... N89-10179 #
DOT/FAA/CT-88/13 ..... N89-10175 #
DOT/FAA/CT-88/16 ..... N89-10041 #

DOT/FAA/DS-88/11 ..... N89-10038 #

DREA-TM-88/201 ..... N89-10294 #

E-3269 ..... N89-10246* #
E-3887 ..... N89-10283* #
E-3888 ..... N89-10282* #
E-4016 ..... N89-10575* #
E-4085 ..... N89-10025* #
E-4094 ..... N89-10242* #
E-4232 ..... N89-10111* #
E-4238 ..... N89-10409* #
E-4260 ..... N89-10043* #
E-4265 ..... N89-10117* #
E-4299 ..... N89-10131* #
E-4301 ..... N89-10156* #
E-4340 ..... N89-10603* #
E-4350 ..... N89-10124* #
E-4354 ..... N89-10166* #
E-4360 ..... N89-10122* #
E-4368 ..... N89-10405* #
E-4375 ..... N89-10134* #
E-4386 ..... N89-10130* #
E-4408 ..... N89-10215* #
E-4427 ..... N89-10269* #
E-4445 ..... N89-10123* #
E-4448 ..... N89-10235* #

ECE-TR-88-1-2 ..... N89-10531* #

EGG-M-88088 ..... N89-10106 #
EGG-M-88219 ..... N89-10256 #

EP-PATENT-APPL-87300809.8 ..... N89-10137
EP-PATENT-APPL-87303437.5 ..... N89-10622
EP-PATENT-APPL-87306071.9 ..... N89-10136
EP-PATENT-APPL-87306543.7 ..... N89-10174
EP-PATENT-APPL-87307826.5 ..... N89-10135

EP-PATENT-0-232-136-A2 ..... N89-10137
EP-PATENT-0-243-130-A1 ..... N89-10622
EP-PATENT-0-253-574-A1 ..... N89-10136
EP-PATENT-0-258-990-A1 ..... N89-10174
EP-PATENT-0-260-850-A2 ..... N89-10135

EPA-600/4-88-020 ..... N89-10414 #

ESA-CR(P)-2584 ..... N89-10394 #
ESA-CR(P)-2586 ..... N89-10664 #
ESA-CR(P)-2615 ..... N89-10116 #
ESA-CR(P)-2626-VOL-1 ..... N89-10397 #
ESA-CR(P)-2626-VOL-2 ..... N89-10303 #
ESA-CR(P)-2626-VOL-3 ..... N89-10399 #
ESA-CR(P)-2638-VOL-1 ..... N89-10623 #
ESA-CR(P)-2638-VOL-2 ..... N89-10624 #
ESA-SP-281-VOL-1 ..... N89-10682 #
ESA-SP-287 ..... N89-10305 #

ESA-TT-1004 ..... N89-10625 #
ESA-TT-1088 ..... N89-10026 #
ESA-TT-1095 ..... N89-10422 #
ESA-TT-1102 ..... N89-10030 #

ESL-TR-719300-3 ..... N89-10225* #
ESL-TR-720964-1 ..... N89-10213* #

ETN-88-92625 ..... N89-10260 #
ETN-88-92626 ..... N89-10286 #
ETN-88-92635 ..... N89-10585 #
ETN-88-92642 ..... N89-10600 #
ETN-88-92752 ..... N89-10591 #
ETN-88-92959 ..... N89-10236 #
ETN-88-92986 ..... N89-10646 #
ETN-88-93029 ..... N89-10394 #
ETN-88-93030 ..... N89-10664 #
ETN-88-93044 ..... N89-10305 #
ETN-88-93051 ..... N89-10026 #
ETN-88-93054 ..... N89-10422 #
ETN-88-93056 ..... N89-10030 #
ETN-88-93080 ..... N89-10226 #
ETN-88-93082 ..... N89-10110 #
ETN-88-93084 ..... N89-10173 #
ETN-88-93085 ..... N89-10107 #
ETN-88-93086 ..... N89-10108 #
ETN-88-93087 ..... N89-10109 #
ETN-88-93088 ..... N89-10573 #
ETN-88-93089 ..... N89-10227 #
ETN-88-93090 ..... N89-10237 #
ETN-88-93126 ..... N89-10135
ETN-88-93127 ..... N89-10174
ETN-88-93128 ..... N89-10136
ETN-88-93129 ..... N89-10622
ETN-88-93130 ..... N89-10137
ETN-88-93139 ..... N89-10507 #
ETN-88-93140 ..... N89-10003 #
ETN-88-93149 ..... N89-10116 #
ETN-88-93152 ..... N89-10397 #
ETN-88-93153 ..... N89-10303 #
ETN-88-93154 ..... N89-10399 #
ETN-88-93155 ..... N89-10682 #
ETN-88-93168 ..... N89-10823 #
ETN-88-93169 ..... N89-10624 #
ETN-88-93177 ..... N89-10625 #
ETN-88-93185 ..... N89-10404 #
ETN-88-93186 ..... N89-10270 #
ETN-88-93187 ..... N89-10508 #
ETN-88-93188 ..... N89-10271 #
ETN-88-93192 ..... N89-10611
ETN-88-93203 ..... N89-10604 #
ETN-88-93204 ..... N89-10257 #
ETN-88-93205 ..... N89-10258 #
ETN-88-93206 ..... N89-10259 #

EUR-11329 ..... N89-10178 #

FLOW-RR-440 ..... N89-10149 #

FR-719300-4 ..... N89-10223* #

FTD-ID(RS)T-0258-88 ..... N89-10273 #

GRI-88/0037 ..... N89-10286 #
GRI-88/0096 ..... N89-10142 #

HTKK-MAT-A242 ..... N89-10578 #

ICASE-88-51 ..... N89-10582* #
ICASE-88-53 ..... N89-10577* #
ICASE-88-54 ..... N89-10583* #

ICOMP-88-5 ..... N89-10575* #

INPE-4560-PRE/1301 ..... N89-10676 #
INPE-4563-PRE/1304 ..... N89-10530 #
INPE-4581-PRE/1315 ..... N89-10221 #
INPE-4602-PRE/1325 ..... N89-10018 #
INPE-4603-PRE/1326 ..... N89-10400 #
INPE-4604-PRE/1327 ..... N89-10680 #
INPE-4605-PRE/1328 ..... N89-10530 #
INPE-4624-PRE/1343 ..... N89-10396 #
INPE-4635-PRE/1347 ..... N89-10302 #
INPE-4643-PRE/1354 ..... N89-10402 #
INPE-4659-PRE/1362 ..... N89-10219 #
INPE-4664-PRE/1365 ..... N89-10183 #
INPE-4670-PRE/1370 ..... N89-10413 #
INPE-4674-PRE/1372 ..... N89-10502 #
INPE-4678-PRE/1375 ..... N89-10581 #

INT-PATENT-CLASS-B22F-7/02 ..... N89-10135

INT-PATENT-CLASS-C-08-K-3/00 ..... N89-10137

INT-PATENT-CLASS-C08L-23/10 ..... N89-10174

INT-PATENT-CLASS-F16F-1/36 ..... N89-10136

INT-PATENT-CLASS-G-02-F-1/35 ..... N89-10622

IPPJ-862 ..... N89-10629 #
IPPJ-870 ..... N89-10632 #
IPPJ-871 ..... N89-10641 #
IPPJ-877 ..... N89-10643 #
IPPJ-878 ..... N89-10634 #
IPPJ-879 ..... N89-10627 #
IPPJ-881 ..... N89-10631 #
IPPJ-882 ..... N89-10640 #

IR-131 ..... N89-10580 #
IR-140 ..... N89-10529 #

ISAS-RN-626 ..... N89-10250 #

ISBN-90-353-0058-0 ..... N89-10233 #
ISBN-92-835-0467-4 ..... N89-10006 #
ISBN-92-835-0472-0 ..... N89-10048 #
ISBN-92-835-0473-9 ..... N89-10001 #
ISBN-951-753-960-6 ..... N89-10578 #
ISBN-951-754-458-8 ..... N89-10032 #
ISBN-951-754-465-0 ..... N89-10214 #

ISSN-0038-0911 ..... N89-10828 #
ISSN-0038-0911 ..... N89-10829 #
ISSN-0171-1342 ..... N89-10270 #
ISSN-0171-1342 ..... N89-10271 #
ISSN-0171-1342 ..... N89-10404 #
ISSN-0171-1342 ..... N89-10508 #
ISSN-0285-6808 ..... N89-10250 #
ISSN-0374-1257 ..... N89-10257 #
ISSN-0374-1257 ..... N89-10258 #
ISSN-0374-1257 ..... N89-10259 #
ISSN-0374-1257 ..... N89-10604 #
ISSN-0379-6566 ..... N89-10305 #
ISSN-0379-6566 ..... N89-10682 #
ISSN-0389-4010 ..... N89-10004 #
ISSN-0389-4010 ..... N89-10021 #
ISSN-0389-4010 ..... N89-10023 #
ISSN-0389-4010 ..... N89-10047 #
ISSN-0389-4010 ..... N89-10113 #
ISSN-0389-4010 ..... N89-10118 #
ISSN-0389-4010 ..... N89-10121 #
ISSN-0389-4010 ..... N89-10144 #
ISSN-0389-4010 ..... N89-10563 #
ISSN-0389-4010 ..... N89-10565 #
ISSN-0389-4010 ..... N89-10576 #
ISSN-0389-4010 ..... N89-10581 #
ISSN-0389-4010 ..... N89-10584 #
ISSN-0389-4010 ..... N89-10639 #
ISSN-0389-4010 ..... N89-10642 #
ISSN-0469-4732 ..... N89-10627 #
ISSN-0469-4732 ..... N89-10629 #
ISSN-0469-4732 ..... N89-10631 #
ISSN-0469-4732 ..... N89-10632 #
ISSN-0469-4732 ..... N89-10634 #
ISSN-0469-4732 ..... N89-10640 #
ISSN-0469-4732 ..... N89-10641 #
ISSN-0469-4732 ..... N89-10643 #

JPL-TDA-PR-42-94 ..... N89-10186* #

KMSF-U-1975 ..... N89-10301 #

L-16397 ..... N89-10524* #
L-16428 ..... N89-10024* #
L-16451 ..... N89-10420* #
L-16466 ..... N89-10612* #
L-16469 ..... N89-10020* #

LA-UR-88-869 ..... N89-10172 #
LA-UR-88-1001 ..... N89-10162 #
LA-UR-88-1167 ..... N89-10163 #
LA-UR-88-1168 ..... N89-10158 #
LA-UR-88-1590 ..... N89-10595 #
LA-UR-88-1791 ..... N89-10139 #
LA-UR-88-1878 ..... N89-10775 #
LA-UR-88-2019 ..... N89-10274 #
LA-UR-88-2029 ..... N89-10229 #
LA-UR-88-2112 ..... N89-10658 #
LA-UR-88-2128 ..... N89-10154 #
LA-UR-88-2136 ..... N89-10279 #
LA-UR-88-2189 ..... N89-10234 #
LA-UR-88-2260 ..... N89-10152 #
LA-UR-88-2351 ..... N89-10663 #
LA-UR-88-2523 ..... N89-10182 #

LA-9956-MS-PT-2 ..... N89-10224 #
LA-11173-MS ..... N89-10596 #
LA-11322-MS ..... N89-10598 #
LA-11344-MS ..... N89-10597 #

LA-11392-MS ..... N89-10533 #

LAAS-88-162 ..... N89-10236 #

LBL-24971 ..... N89-10138 #
LBL-24987 ..... N89-10153 #
LBL-25203 ..... N89-10140 #

LC-79-640375 ..... N89-10828 #
LC-79-640375 ..... N89-10829 #
LC-87-15305 ..... N89-10401* #

LMSC-HEC-TR-F225988 ..... N89-10243* #

LPI-TR-87-01 ..... N89-10780* #

LR-497 ..... N89-10042 #

M-598 ..... N89-10184* #

MEMO-K145 ..... N89-10532 #

MIT-KBIISE-3 ..... N89-10668 #
MIT-KBIISE-4 ..... N89-10672 #

MPE-PAE/EXP-EL-191 ..... N89-10611

MPIS-MITT-85-1987 ..... N89-10604 #
MPIS-MITT-86-1987 ..... N89-10257 #
MPIS-MITT-87-1987 ..... N89-10258 #
MPIS-MITT-88-1987 ..... N89-10259 #

MRL-R-1095 ..... N89-10177 #
MRL-R-1116 ..... N89-10040 #
MRL-R-1117 ..... N89-10252 #
MRL-R-1123 ..... N89-10216 #

NAL-TR-915 ..... N89-10565 #
NAL-TR-921 ..... N89-10023 #
NAL-TR-944 ..... N89-10047 #
NAL-TR-946 ..... N89-10118 #
NAL-TR-947 ..... N89-10121 #
NAL-TR-948 ..... N89-10576 #
NAL-TR-949 ..... N89-10021 #
NAL-TR-950T ..... N89-10581 #
NAL-TR-951 ..... N89-10584 #
NAL-TR-952 ..... N89-10639 #
NAL-TR-953 ..... N89-10004 #
NAL-TR-954 ..... N89-10642 #
NAL-TR-955 ..... N89-10144 #
NAL-TR-956 ..... N89-10563 #
NAL-TR-957 ..... N89-10113 #

NAS 1.15:4027 ..... N89-10524* #
NAS 1.15:4070 ..... N89-10612* #
NAS 1.15:4076 ..... N89-10184* #
NAS 1.15:88330 ..... N89-10037* #
NAS 1.15:89630 ..... N89-10678* #
NAS 1.15:89660 ..... N89-10772* #
NAS 1.15:89663 ..... N89-10063* #
NAS 1.15:89855 ..... N89-10246* #
NAS 1.15:100039 ..... N89-10022* #
NAS 1.15:100061 ..... N89-10017* #
NAS 1.15:100259 ..... N89-10283* #
NAS 1.15:100260 ..... N89-10282* #
NAS 1.15:100341 ..... N89-10656* #
NAS 1.15:100657 ..... N89-10034* #
NAS 1.15:100668 ..... N89-10300* #
NAS 1.15:100675 ..... N89-10165* #
NAS 1.15:100708 ..... N89-10403* #
NAS 1.15:100828 ..... N89-10575* #
NAS 1.15:100944 ..... N89-10111* #
NAS 1.15:100947 ..... N89-10409* #
NAS 1.15:100949 ..... N89-10665* #
NAS 1.15:100972 ..... N89-10117* #
NAS 1.15:101171 ..... N89-10605* #
NAS 1.15:101190 ..... N89-10610* #
NAS 1.15:101298 ..... N89-10242* #
NAS 1.15:101310 ..... N89-10156* #
NAS 1.15:101322 ..... N89-10043* #
NAS 1.15:101329 ..... N89-10603* #
NAS 1.15:101335 ..... N89-10124* #
NAS 1.15:101336 ..... N89-10166* #
NAS 1.15:101341 ..... N89-10122* #
NAS 1.15:101345 ..... N89-10405* #
NAS 1.15:101348 ..... N89-10134* #
NAS 1.15:101356 ..... N89-10130* #
NAS 1.15:101369 ..... N89-10215* #
NAS 1.15:101374 ..... N89-10269* #
NAS 1.15:101386 ..... N89-10123* #
NAS 1.15:101388 ..... N89-10235* #
NAS 1.15:101491 ..... N89-10060* #
NAS 1.15:101496 ..... N89-10059* #
NAS 1.19:223 ..... N89-10522* #
NAS 1.21:491 ..... N89-10401* #
NAS 1.21:7037(231) N89-10002*

NAS 1.21:7041(58) N89-10398*
NAS 1.26:4147 ..... N89-10025* #
NAS 1.26:4171 ..... N89-10131* #
NAS 1.26:4172 ..... N89-10126* #
NAS 1.26:4185 ..... N89-10029* #
NAS 1.26:177395 ..... N89-10028* #
NAS 1.26:177477 ..... N89-10046* #
NAS 1.26:178416-VOL-3-PT-1 ..... N89-10019* #
NAS 1.26:179368 ..... N89-10653* #
NAS 1.26:179372 ..... N89-10407* #
NAS 1.26:179390 ..... N89-10253* #
NAS 1.26:179403 ..... N89-10243* #
NAS 1.26:179602 ..... N89-10119* #
NAS 1.26:180225 ..... N89-10129* #
NAS 1.26:180465 ..... N89-10826* #
NAS 1.26:180786 ..... N89-10615* #
NAS 1.26:180792 ..... N89-10115* #
NAS 1.26:180949 ..... N89-10774* #
NAS 1.26:181175 ..... N89-10125* #
NAS 1.26:181691 ..... N89-10560* #
NAS 1.26:181692 ..... N89-10601* #
NAS 1.26:181695 ..... N89-10061* #
NAS 1.26:181709 ..... N89-10582* #
NAS 1.26:181712 ..... N89-10577* #
NAS 1.26:181717 ..... N89-10583* #
NAS 1.26:181718 ..... N89-10132* #
NAS 1.26:181721 ..... N89-10045* #
NAS 1.26:182432 ..... N89-10216* #
NAS 1.26:182500 ..... N89-10223* #
NAS 1.26:182739 ..... N89-10291* #
NAS 1.26:182741 ..... N89-10058* #
NAS 1.26:182746 ..... N89-10526* #
NAS 1.26:182872 ..... N89-10780* #
NAS 1.26:183146 ..... N89-10419* #
NAS 1.26:183148 ..... N89-10395* #
NAS 1.26:183156 ..... N89-10827* #
NAS 1.26:183163 ..... N89-10417* #
NAS 1.26:183164 ..... N89-10304* #
NAS 1.26:183167 ..... N89-10779* #
NAS 1.26:183184 ..... N89-10426* #
NAS 1.26:183186 ..... N89-10425* #
NAS 1.26:183187 ..... N89-10264* #
NAS 1.26:183192 ..... N89-10498* #
NAS 1.26:183195 ..... N89-10586* #
NAS 1.26:183205 ..... N89-10297* #
NAS 1.26:183213 ..... N89-10518* #
NAS 1.26:183214 ..... N89-10277* #
NAS 1.26:183226 ..... N89-10127* #
NAS 1.26:183227 ..... N89-10033* #
NAS 1.26:183238 ..... N89-10531* #
NAS 1.26:183243 ..... N89-10186* #
NAS 1.26:183275 ..... N89-10561* #
NAS 1.26:183276 ..... N89-10534* #
NAS 1.26:183277 ..... N89-10564* #
NAS 1.26:183283 ..... N89-10416* #
NAS 1.26:183303 ..... N89-10213* #
NAS 1.26:183312 ..... N89-10225* #
NAS 1.60:2828 ..... N89-10024* #
NAS 1.60:2848 ..... N89-10020* #
NAS 1.61:1204 ..... N89-10420* #
NAS 1.77:20305 ..... N89-10248* #
NAS 1.77:20322 ..... N89-10262* #
NAS 1.77:20325 ..... N89-10169* #
NAS 1.77:20334 ..... N89-10141* #
NAS 1.77:20357 ..... N89-10574* #

NASA-CR-4147 ..... N89-10025* #
NASA-CR-4171 ..... N89-10131* #
NASA-CR-4172 ..... N89-10126* #
NASA-CR-4185 ..... N89-10029* #
NASA-CR-177395 ..... N89-10028* #
NASA-CR-177477 ..... N89-10046* #
NASA-CR-178416-VOL-3-PT-1 ..... N89-10019* #
NASA-CR-179368 ..... N89-10653* #
NASA-CR-179372 ..... N89-10407* #
NASA-CR-179390 ..... N89-10253* #
NASA-CR-179403 ..... N89-10243* #
NASA-CR-179602 ..... N89-10119* #
NASA-CR-180225 ..... N89-10129* #
NASA-CR-180465 ..... N89-10826* #
NASA-CR-180786 ..... N89-10615* #
NASA-CR-180792 ..... N89-10115* #
NASA-CR-180949 ..... N89-10774* #
NASA-CR-181175 ..... N89-10125* #
NASA-CR-181691 ..... N89-10560* #
NASA-CR-181692 ..... N89-10601* #
NASA-CR-181695 ..... N89-10061* #
NASA-CR-181709 ..... N89-10582* #
NASA-CR-181712 ..... N89-10577* #
NASA-CR-181717 ..... N89-10583* #
NASA-CR-181718 ..... N89-10132* #
NASA-CR-181721 ..... N89-10045* #
NASA-CR-182432 ..... N89-10216* #
NASA-CR-182500 ..... N89-10223* #
NASA-CR-182739 ..... N89-10291* #
NASA-CR-182741 ..... N89-10058* #

NASA-CR-182746 ..... N89-10526* #
NASA-CR-182872 ..... N89-10780* #
NASA-CR-183146 ..... N89-10419* #
NASA-CR-183148 ..... N89-10395* #
NASA-CR-183156 ..... N89-10827* #
NASA-CR-183163 ..... N89-10417* #
NASA-CR-183164 ..... N89-10304* #
NASA-CR-183167 ..... N89-10779* #
NASA-CR-183184 ..... N89-10426* #
NASA-CR-183186 ..... N89-10425* #
NASA-CR-183187 ..... N89-10264* #
NASA-CR-183192 ..... N89-10498* #
NASA-CR-183195 ..... N89-10586* #
NASA-CR-183205 ..... N89-10297* #
NASA-CR-183213 ..... N89-10518* #
NASA-CR-183214 ..... N89-10277* #
NASA-CR-183226 ..... N89-10127* #
NASA-CR-183227 ..... N89-10033* #
NASA-CR-183238 ..... N89-10531* #
NASA-CR-183243 ..... N89-10186* #
NASA-CR-183275 ..... N89-10561* #
NASA-CR-183276 ..... N89-10534* #
NASA-CR-183277 ..... N89-10564* #
NASA-CR-183283 ..... N89-10416* #
NASA-CR-183303 ..... N89-10213* #
NASA-CR-183312 ..... N89-10225* #

NASA-EP-223 ..... N89-10522* #

NASA-RP-1204 ..... N89-10420* #

NASA-SP-491 ..... N89-10401* #
NASA-SP-7037(231) N89-10002*
NASA-SP-7041(58) N89-10398*

NASA-TM-4027 ..... N89-10524* #
NASA-TM-4070 ..... N89-10612* #
NASA-TM-4076 ..... N89-10184* #
NASA-TM-88330 ..... N89-10037* #
NASA-TM-89630 ..... N89-10678* #
NASA-TM-89660 ..... N89-10772* #
NASA-TM-89663 ..... N89-10063* #
NASA-TM-89855 ..... N89-10246* #
NASA-TM-100039 ..... N89-10022* #
NASA-TM-100061 ..... N89-10017* #
NASA-TM-100259 ..... N89-10263* #
NASA-TM-100260 ..... N89-10282* #
NASA-TM-100341 ..... N89-10656* #
NASA-TM-100657 ..... N89-10034* #
NASA-TM-100668 ..... N89-10300* #
NASA-TM-100675 ..... N89-10165* #
NASA-TM-100708 ..... N89-10403* #
NASA-TM-100828 ..... N89-10575* #
NASA-TM-100944 ..... N89-10111* #
NASA-TM-100947 ..... N89-10409* #
NASA-TM-100949 ..... N89-10665* #
NASA-TM-100972 ..... N89-10117* #
NASA-TM-101171 ..... N89-10605* #
NASA-TM-101190 ..... N89-10610* #
NASA-TM-101298 ..... N89-10242* #
NASA-TM-101310 ..... N89-10156* #
NASA-TM-101322 ..... N89-10043* #
NASA-TM-101329 ..... N89-10603* #
NASA-TM-101335 ..... N89-10124* #
NASA-TM-101336 ..... N89-10166* #
NASA-TM-101341 ..... N89-10122* #
NASA-TM-101345 ..... N89-10405* #
NASA-TM-101348 ..... N89-10134* #
NASA-TM-101356 ..... N89-10130* #
NASA-TM-101369 ..... N89-10215* #
NASA-TM-101374 ..... N89-10269* #
NASA-TM-101386 ..... N89-10123* #
NASA-TM-101388 ..... N89-10235* #
NASA-TM-101491 ..... N89-10080* #
NASA-TM-101496 ..... N89-10059* #

NASA-TP-2828 ..... N89-10024* #
NASA-TP-2848 ..... N89-10020* #

NASA-TT-20305 ..... N89-10246* #
NASA-TT-20322 ..... N89-10262* #
NASA-TT-20325 ..... N89-10169* #
NASA-TT-20334 ..... N89-10141* #
NASA-TT-20357 ..... N89-10574* #

NCAR/TN-290/IA ..... N89-10428 #

NCS-TIB-88-02 ..... N89-10220 #

NLR-MP-88057-U ..... N89-10212 #

NOAA-DR-ERL-AOML-11 ..... N89-10516 #

NOAA-DR-ERL-PMEL-23 ..... N89-10509 #

NOAA-TM-ERL-AOML-66 ..... N89-10512 #

NOAA-TM-ERL-ESG-30-VOL-3 ..... N89-10499 #

NOAA-TM-ERL-PMEL-79 ..... N89-10514 #

NOAA-TM-ERL-WPL-150 ..... N89-10513 #
NOAA-TM-ERL-WPL-151 ..... N89-10503 #

NOAA-TM-NWS-WR-126-REV-1 ..... N89-10504 #

NOTA-INTERNA-905 ..... N89-10260 #
NOTA-INTERNA-906 ..... N89-10266 #

NPS-63-88-004 ..... N89-10506 #

NPS55-88-005 ..... N89-10593 #
NPS63-88-003 ..... N89-10505 #

NSSDC/WDC-A-R/S-86-04-SUPPL-3 ..... N89-10772* #

NSSDC/WDC-A-RS-86-04A-SUPPL-3A .... N89-10678* #

NTIA-88-231 ..... N89-10220 #

NTSB/AAB-88/03 ..... N89-10036 #
NTSB/AAB-88/05 ..... N89-10035 #

OCS/MMS-87/0051-VOL-1 ..... N89-10517 #
OCS/MMS-87/0051-VOL-2 ..... N89-10511 #

ORNL/SUB-84-7802/1 ..... N89-10170 #
ORNL/SUB-85-22008/1 ..... N89-10168 #
ORNL/SUB-85-27416/1 ..... N89-10171 #

ORNL/TM-10392 ..... N89-10249 #
ORNL/TM-10709-PT-1 ..... N89-10159 #
ORNL/TM-10772 ..... N89-10238 #

PB87-175899 ..... N89-10578 #
PB87-186961 ..... N89-10510 #
PB88-126289 ..... N89-10594 #
PB88-196514 ..... N89-10511 #
PB88-196522 ..... N89-10517 #
PB88-197439 ..... N89-10429 #
PB88-199971 ..... N89-10292 #
PB88-200902 ..... N89-10296 #
PB88-202007 ..... N89-10512 #
PB88-202874 ..... N89-10588 #
PB88-202890 ..... N89-10587 #
PB88-202965 ..... N89-10579 #
PB88-203005 ..... N89-10580 #
PB88-205489 ..... N89-10499 #
PB88-208467 ..... N89-10233 #
PB88-208533 ..... N89-10529 #
PB88-208624 ..... N89-10504 #
PB88-208921 ..... N89-10515 #
PB88-208970 ..... N89-10520 #
PB88-209507 ..... N89-10212 #
PB88-209630 ..... N89-10532 #
PB88-209895 ..... N89-10222 #
PB88-210059 ..... N89-10214 #
PB88-210372 ..... N89-10032 #
PB88-210760 ..... N89-10042 #
PB88-210778 ..... N89-10220 #
PB88-212808 ..... N89-10503 #
PB88-212816 ..... N89-10513 #
PB88-212824 ..... N89-10516 #
PB88-213236 ..... N89-10414 #
PB88-214069 ..... N89-10677 #
PB88-214291 ..... N89-10299 #
PB88-214606 ..... N89-10142 #
PB88-216577 ..... N89-10428 #
PB88-217336 ..... N89-10290 #
PB88-217344 ..... N89-10295 #
PB88-217393 ..... N89-10829 #
PB88-217401 ..... N89-10828 #
PB88-219415 ..... N89-10509 #
PB88-220025 ..... N89-10288 #
PB88-221668 ..... N89-10514 #
PB88-916903 ..... N89-10036 #
PB88-916905 ..... N89-10035 #

PNL-SA-15443 ..... N89-10606 #
PNL-SA-15620 ..... N89-10521 #
PNL-SA-15664 ..... N89-10143 #
PNL-SA-15730 ..... N89-10148 #

PNL-6434 ..... N89-10556 #

PREPRINT-586 ..... N89-10585 #
PREPRINT-595 ..... N89-10600 #

R-541 ..... N89-10296 #
R-550 ..... N89-10292 #
R-552 ..... N89-10290 #
R-553 ..... N89-10299 #
R-556 ..... N89-10295 #

RADC-TR-87-240 ..... N89-10217 #
RADC-TR-87-243 ..... N89-10536 #
RADC-TR-88-42 ..... N89-10568 #

RAE-DR/55/07 ..... N89-10003 #

RAE-SS-3 ..... N89-10507 #

RAE-TR-87058 ..... N89-10507 #
RAE-TR-88042 ..... N89-10003 #

RAI-87-P-4 ..... N89-10653* #

REPT-B-12 ..... N89-10032 #

REPT-27 ..... N89-10214 #
REPT-86-54 ..... N89-10594 #
REPT-87-MA-06 ..... N89-10520 #
REPT-88B-0214 ..... N89-10403* #
REPT-130 ..... N89-10588 #
REPT-325 ..... N89-10579 #
REPT-327 ..... N89-10587 #
REPT-329 ..... N89-10515 #

RI/RD-87-126 ..... N89-10119* #

RR-687-M ..... N89-10591 #

SAND-87-0070 ..... N89-10609 #
SAND-87-2294C ..... N89-10126 #
SAND-87-2308 ..... N89-10628 #
SAND-87-2496C ..... N89-10254 #
SAND-87-2669C ..... N89-10651 #
SAND-87-2808C ..... N89-10272 #
SAND-87-3040C ..... N89-10133 #
SAND-87-3149 ..... N89-10231 #
SAND-88-0371C ..... N89-10566 #
SAND-88-0545C ..... N89-10062 #
SAND-88-0679C ..... N89-10151 #
SAND-88-0850C ..... N89-10590 #
SAND-88-1060C ..... N89-10268 #
SAND-88-1715C ..... N89-10261 #
SAND-88-1875C ..... N89-10559 #
SAND-88-2077 ..... N89-10265 #
SAND-88-7092C ..... N89-10181 #

SD-TR-88-53 ..... N89-10112 #

SERI/PR-212-3337 ..... N89-10410 #

SERI/STR-211-3218 ..... N89-10411 #
SERI/STR-211-3352 ..... N89-10654 #

SERI/TP-211-3361 ..... N89-10406 #
SERI/TP-254-3380 ..... N89-10185 #

SGD-524-PT-1 ..... N89-10829 #
SGD-524-PT-2 ..... N89-10828 #

SLAC-PUB-4665 ..... N89-10592 #

SOL-88-8 ..... N89-10571 #

SR-2 ..... N89-10608 #

TISL-5481-2 ..... N89-10217 #

TR-0086A(2945-03)-7 ..... N89-10112 #

TT-8706 ..... N89-10670 #

UCB-153-1213 ..... N89-10827* #

UCID-20950-87 ..... N89-10599 #
UCID-21385 ..... N89-10167 #

UCRL-97044 ..... N89-10637 #
UCRL-97389 ..... N89-10412 #
UCRL-97782-REV-1 ..... N89-10618 #
UCRL-98039 ..... N89-10150 #
UCRL-98072 ..... N89-10230 #
UCRL-98126 ..... N89-10157 #
UCRL-98231 ..... N89-10160 #
UCRL-98881 ..... N89-10650 #
UCRL-98910 ..... N89-10232 #
UCRL-99090 ..... N89-10659 #
UCRL-99168 ..... N89-10621 #
UCRL-99326 ..... N89-10773 #

UFTP-88-6 ..... N89-10661 #

USAAVSCOM-TR-87-A-13 ..... N89-10046* #

USARIEM-M-18/88 ..... N89-10519 #

UWAERP-14 ..... N89-10645 #

VLSI-MEMO-87-426 ..... N89-10569 #

WM-88-2 ..... N89-10534* #

☆ U.S. GOVERNMENT PRINTING OFFICE: 1988—241-445/80023

FEDERAL REGIONAL DEPOSITORY LIBRARIES

ALABAMA

AUBURN UNIV. AT MONTGOMERY LIBRARY
Documents Department
Montgomery, AL 36193
(205) 271-9650

UNIV. OF ALABAMA LIBRARY
Documents Dept.-Box S
University, AL 35486
(205) 348-6046

ARIZONA

DEPT. OF LIBRARY, ARCHIVES AND PUBLIC RECORDS
Third Floor—State Cap.
1700 West Washington
Phoenix, AZ 85007
(602) 255-4121

UNIVERSITY OF ARIZONA LIB.
Government Documents Dept.
Tucson, AZ 85721
(602) 621-6433

ARKANSAS

ARKANSAS STATE LIBRARY
One Capitol Mall
Little Rock, AR 72201
(501) 371-2326

CALIFORNIA

CALIFORNIA STATE LIBRARY
Govt. Publications Section
P.O. Box 2037
Sacramento, CA 95809
(916) 324-4863

COLORADO

UNIV OF COLORADO LIB.
Government Pub. Division
Campus Box 184
Boulder, CO 80309
(303) 492-8834

DENVER PUBLIC LIBRARY
Govt. Pub. Department
1357 Broadway
Denver, CO 80203
(303) 571-2131

CONNECTICUT

CONNECTICUT STATE LIBRARY
Government Documents Unit
231 Capitol Avenue
Hartford, CT 06106
(203) 566-7029

FLORIDA

UNIV. OF FLORIDA LIBRARIES
Library West
Documents Department
Gainesville, FL 32611
(904) 392-0367

GEORGIA

UNIV. OF GEORGIA LIBRARIES
Government Reference Dept.
Athens, GA 30602
(404) 542-8949

HAWAII

UNIV. OF HAWAII LIBRARY
Govt. Documents Collection
2550 The Mall
Honolulu, HI 96822
(808) 948-8230

IDAHO

UNIV. OF IDAHO LIBRARY
Documents Section
Moscow, ID 83843
(208) 885-6344

ILLINOIS

ILLINOIS STATE LIBRARY
Information Services Branch
Centennial Building
Springfield, IL 62756
(217) 782-5185

INDIANA

INDIANA STATE LIBRARY
Serials Documents Section
140 North Senate Avenue
Indianapolis, IN 46204
(317) 232-3686

IOWA

UNIV. OF IOWA LIBRARIES
Govt. Documents Department
Iowa City, IA 52242
(319) 353-3318

KANSAS

UNIVERSITY OF KANSAS
Doc. Collect—Spencer Lib.
Lawrence, KS 66045-2800
(913) 864-4662

KENTUCKY

UNIV. OF KENTUCKY LIBRARIES
Govt. Pub. Department
Lexington, KY 40506-0039
(606) 257-3139

LOUISIANA

LOUISIANA STATE UNIVERSITY
Middleton Library
Govt. Docs. Dept.
Baton Rouge, LA 70803
(504) 388-2570

LOUISIANA TECHNICAL UNIV. LIBRARY
Documents Department
Ruston, LA 71272-0046
(318) 257-4962

MAINE

UNIVERSITY OF MAINE
Raymond H. Fogler Library
Tri-State Regional Documents Depository
Orono, ME 04469
(207) 581-1680

MARYLAND

UNIVERSITY OF MARYLAND
McKeldin Lib.—Doc. Div.
College Park, MD 20742
(301) 454-3034

MASSACHUSETTS

BOSTON PUBLIC LIBRARY
Government Docs. Dept.
Boston, MA 02117
(617) 536-5400 ext.226

MICHIGAN

DETROIT PUBLIC LIBRARY
Sociology Department
5201 Woodward Avenue
Detroit, MI 48202-4093
(313) 833-1409

MICHIGAN STATE LIBRARY
P.O. Box 30007
Lansing, MI 48909
(517) 373-1593

MINNESOTA

UNIVERSITY OF MINNESOTA
Government Pubs. Division
409 Wilson Library
309 19th Avenue South
Minneapolis, MN 55455
(612) 373-7870

MISSISSIPPI

UNIV. OF MISSISSIPPI LIB.
Documents Department
University, MS 38677
(601) 232-5857

MONTANA

UNIV. OF MONTANA
Mansfield Library
Documents Division
Missoula, MT 59812
(406) 243-6700

NEBRASKA

UNIVERSITY OF NEBRASKA - LINCOLN
Love Library
Documents Department
Lincoln, NE 68588-0410
(402) 472-2562

NEVADA

UNIVERSITY OF NEVADA LIB.
Govt. Pub. Department
Reno, NV 89557-0044
(702) 784-6579

NEW JERSEY

NEWARK PUBLIC LIBRARY
5 Washington Street
Newark, NJ 07101-0630
(201) 733-7812

NEW MEXICO

UNIVERSITY OF NEW MEXICO
Zimmerman Library
Government Pub. Dept.
Albuquerque, NM 87131
(505) 277-5441

NEW MEXICO STATE LIBRARY
Reference Department
325 Don Gaspar Avenue
Santa Fe, NM 87503
(505) 827-3826

NEW YORK

NEW YORK STATE LIBRARY
Empire State Plaza
Albany, NY 12230
(518) 474-5563

NORTH CAROLINA

UNIVERSITY OF NORTH CAROLINA AT CHAPEL HILL
Davis Library
BA/SS Documents Division
Chapel Hill, NC 27515
(919) 962-1151

NORTH DAKOTA

UNIVERSITY OF NORTH DAKOTA
Chester Fritz Library
Documents Department
Grand Forks, ND 58202
(701) 777-4629
In cooperation with North Dakota State Univ. Library

OHIO

STATE LIBRARY OF OHIO
Documents Department
65 South Front Street
Columbus, OH 43266-0334
(614) 462-7051

OKLAHOMA

OKLAHOMA DEPT. OF LIB.
Government Documents
200 NE 18th Street
Oklahoma City, OK 73105
(405) 521-2502, ext. 252

OKLAHOMA STATE UNIV. LIB.
Documents Department
Stillwater, OK 74078
(405) 624-6546

OREGON

PORTLAND STATE UNIV. LIB.
Documents Department
P.O. Box 1151
Portland, OR 97207
(503) 229-3673

PENNSYLVANIA

STATE LIBRARY OF PENN.
Government Pub. Section
P.O. Box 1601
Harrisburg, PA 17105
(717) 787-3752

TEXAS

TEXAS STATE LIBRARY
Public Services Department
P.O. Box 12927—Cap. Sta.
Austin, TX 78711
(512) 475-2996

TEXAS TECH. UNIV. LIBRARY
Govt. Documents Department
Lubbock, TX 79409
(806) 742-2268

UTAH

UTAH STATE UNIVERSITY
Merrill Library, U.M.C. 30
Logan, UT 84322
(801) 750-2682

VIRGINIA

UNIVERSITY OF VIRGINIA
Alderman Lib.—Public Doc.
Charlottesville, VA 22903-2498
(804) 924-3133

WASHINGTON

WASHINGTON STATE LIBRARY
Documents Section
Olympia, WA 98504
(206) 753-4027

WEST VIRGINIA

WEST VIRGINIA UNIV. LIB.
Documents Department
Morgantown, WV 26506-6069
(304) 293-3640

WISCONSIN

MILWAUKEE PUBLIC LIBRARY
814 West Wisconsin Avenue
Milwaukee, WI 53233
(414) 278-3065

ST. HIST LIB. OF WISCONSIN
Government Pub. Section
816 State Street
Madison, WI 53706
(608) 262-4347

WYOMING

WYOMING STATE LIBRARY
Supreme Ct. & Library Bld.
Cheyenne, WY 82002
(307) 777-5919

National Aeronautics and
Space Administration
Code NTT-4
Washington, D.C.
20546
Official Business
Penalty for Private Use, $300

SPECIAL FOURTH-CLASS RATE
POSTAGE & FEES PAID
NASA
PERMIT No. G 27

POSTMASTER: If Undeliverable (Section 158
Postal Manual) Do Not Return